Upper Salmon Subbasin Habitat Integrated Rehabilitation Assessment

June 2019

This page intentionally left blank.

Acronyms and Abbreviations

Acronym or Abbreviation	Description
BLM	Bureau of Land Management
CHaMP	Columbia Habitat Monitoring Program
CWA	Clean Water Act
Chinook salmon	Snake River spring/summer Chinook salmon
ESA	Endangered Species Act
GIS	Geographical Information System
HUC	Hydrologic unit code
IDEQ	Idaho Department of Environmental Quality
IDWR	Idaho Department of Water Resources
IRA	Integrated Rehabilitation Assessment
ISEMP	Integrated Status and Effectiveness Monitoring Program
LiDAR	Light Detection and Ranging
MAT	Minimum abundance threshold
MPG	Major population group
NOAA	National Oceanic and Atmospheric Administration
NOAA Fisheries	NOAA National Marine Fisheries Service
NPCC	Northwest Power and Conservation Council
NRCS	Natural Resources Conservation Service
OSC	Office of Species Conservation
PBF	Physical and Biological Feature
QRF	Quantile Regression Forest
Reclamation	Bureau of Reclamation
RM	River mile
Science Team	Upper Salmon Assessment Team
SNF	Sawtooth National Forest
SNRA	Sawtooth National Recreation Area
TA	Tributary Assessment
TMDL	Total Maximum Daily Load
USFS	U.S. Forest Service
USFWS	U.S. Fish and Wildlife Service
USGS	U.S. Geological Survey

This page intentionally left blank.

Executive Summary

Large-scale changes to aquatic ecosystems in the Pacific Northwest began with the fur trade, long before settlement and territorial governance. When beavers were removed from the landscape, the resiliency of the ecosystems diminished as channels became simplified and floodplain connectivity was reduced. As European settlement occurred, arable lands adjacent to water sources were homesteaded first, and the development of water for irrigation started a series of changes with cascading effects through the ecosystem. Natural resource extraction increased, placing additional pressures on the aquatic ecosystems. An exponential increase in the Columbia River Basin human population directly correlates with decreased salmon (and steelhead) available for harvest. Human influences have exerted significant changes in the freshwater, estuary, and ocean conditions under which salmon historically flourished. That change, which occurred on a relatively short time scale, is perhaps most apparent in tributary habitat, which has become degraded over time.

In response to dwindling Chinook salmon populations and loss of habitat, the Idaho Governor's Office of Species Conservation (OSC) and an interdisciplinary team of partners have created a biologically based evaluation called the Integrated Rehabilitation Assessment (IRA) to further the recovery of Endangered Species Act-listed Chinook salmon and steelhead populations in the Upper Salmon River Subbasin. The IRA uses empirically based quantile regression forest (QRF) models to estimate the number of redds and the number of juveniles that tributary habitat can support during summer (parr) and winter (presmolt) rearing, based on the quantity and quality of available habitat. These capacity estimates are compared to (1) current population capacity requirements, and (2) recovery plan goals. At a coarse scale, the resulting deficits are used to identify the magnitude, types, and generalized locations of habitat rehabilitation actions that will be most beneficial to help achieve recovery targets within a given watershed. Using guidance on restoration action types and locations provided by QRF models, a geomorphic analysis is employed to identify reaches within a given watershed that offer the opportunity to effectively and cost-efficiently implement restoration actions to increase capacity.

After completion of the IRA, the next step is the Multiple Reach Assessment (MRA) reports. There will be one report each for the Upper Lemhi River Basin, Lower Lemhi River Basin, Lower Pahsimeroi River Basin, and Upper Salmon River Basin above Redfish Lake Creek. The MRA will build upon the IRA to develop more detailed biologic and geomorphic characterization at the sub-reach and channel unit scale and directly tie into upcoming project work.

Recommended actions in all three watersheds from the IRA include increasing juvenile rearing capacity during summer and winter months by focusing on hydraulic diversity with instream velocity gradients, ample concealment cover, and complex habitat structure, accompanied by fine sediment reduction, especially in locations downstream of spawning areas. Complimentary actions would also address moderating water temperatures and instream flows by increasing floodplain connectivity, hyporheic flow, and the alluvial aquifer connection; improving riparian habitat; and reducing the stream width-to-depth ratio without increasing in-stream velocity. Actions specific to the three watersheds are detailed within watershed-specific chapters in the IRA, and will be further addressed in upcoming MRA reports.

This page intentionally left blank.

Table of Contents

Executive Summary i
Section 1: Introduction, Background, and Approach 1
Introduction 1
Rationale 4
Study Area 6
Document Structure 8
Attribute Definitions 8
Background 9
Integrated Rehabilitation Assessment 9
Salmonid Life History 10
    Chinook Salmon Life-Stages and Habitat Preferences 11
Historical Habitat Conditions 14
Human Impacts 17
Climate Change 20
Past Projects 23
    Lemhi River 23
    Pahsimeroi River 24
    Upper Salmon River 25
Assessment Approach 26
Biologic Assessment 26
    Required Habitat Capacity 27
    Available Habitat Capacity 27
    Habitat Capacity Deficits 29
Geomorphic Assessment 29
    Channel Units 30
    Reach Delineation 33
    Hydraulics 33
Temperature and Climate Change Assessment 36
Biologic and Geomorphic Assessment Integration 36
Next Steps 39
Section 2: Upper Salmon Subbasin Key Conclusions and Recommendations 40
Habitat Enhancement Recommendations Summary 40

Basin-wide Actions..40
Chinook Salmon Capacity Limitations..40
Steelhead Capacity Limitations...42
General Recommendations and Actions...45
The Lemhi River Watershed..46
Limiting Physical and Biological Features..46
Priority Areas..46
Recommendations..47
Biological and Geomorphic Assessment Integration...48
The Pahsimeroi River Watershed...50
Limiting Physical and Biological Features..50
Priority Areas..50
Recommendations..50
Biological and Geomorphic Assessment Integration...52
The Upper Salmon River (Headwaters) Watershed...54
Limiting Physical and Biological Features..54
Priority Areas..54
Recommendations..54
Biological and Geomorphic Assessment Integration...56
Sections 1 and 2 References...58
Section 3: Watershed-Level Results..60
Chapter 1 – Lemhi River Watershed..60
Location and Watershed Description...60
Biological Assessment...62
Habitat Capacity..62
Geomorphic Assessment..67
Historical Watershed Conditions...68
Existing Watershed Conditions...73
Watershed Impacts...89
Data Gaps..90
Lemhi Valley Segments and Geomorphic Reaches...90
Temperature and Climate Change Assessment..146
Chinook salmon...146

Steelhead....148
Results and Discussion....150
Limiting Physical and Biological Features....151
Priority Areas....151
References....152
Chapter 2 – Pahsimeroi River Watershed....154
Location and Watershed Description....154
Biological Assessment....156
Habitat Capacity....156
Geomorphic Assessment....162
Historical Watershed Conditions....162
Existing Watershed Conditions....166
Watershed Impacts....182
Data Gaps....183
Pahsimeroi Valley Segments and Geomorphic Reaches....183
Temperature and Climate Change Assessment....214
Chinook salmon....214
Steelhead....215
Results and Discussion....217
Limiting Physical and Biological Features....217
Priority Areas....218
References....219
Chapter 3 – Upper Salmon River Watershed (Above Redfish Lake Creek)....222
Location and Watershed Description....222
Biological Assessment....224
Habitat Capacity....224
Geomorphic Assessment....230
Historical Watershed Conditions....230
Existing Watershed Conditions....235
Watershed Impacts....251
Data Gaps....253
Upper Salmon Valley Segments and Geomorphic Reaches....253
Temperature and Climate Change Assessment....280

Chinook salmon 280
Steelhead....281
Results and Discussion....283
Limiting Physical and Biological Features 283
Priority Areas 284
References 285
Appendices 287

Appendices

Appendix A – Temperature Modeling and Climate Change

Appendix B – Habitat Capacity Estimation

Appendix C – Habitat Capacity Requirements

Appendix D – Hydraulics and Hydrologic Assessment (Lemhi, Pahsimeroi, Upper Salmon Rivers)

List of Tables

Table 1. Geomorphic characterization and description. 30

Table 2. Estimated current life stage specific capacity requirement versus estimated available capacity for Chinook salmon in the Lemhi River. 62

Table 3. Estimated life stage specific capacity requirements to accommodate ESA delisting and estimated available capacity for Chinook salmon in the Lemhi River. 63

Table 4. Estimated current life-stage-specific capacity requirements versus estimated available capacity for steelhead salmon in the Lemhi River. 65

Table 5. Estimate life-stage-specific capacity requirements to accommodate ESA delisting and estimated available capacity for steelhead in the Lemhi River. 66

Table 6. Summary of Lemhi River hydrology. 74

Table 7. Geomorphic features along the valley bottoms and margins, and associated soils. 84

Table 8. Streams and pollutants listed in the 1999 and 2012 reports with TMDLs 85

Table 9. Lemhi River watershed valley segment delineations and sub-watersheds. 91

Table 10. Summary of geomorphic reach characteristics for the Lemhi watershed. 93

Table 11. Upper Lemhi Valley Segment watershed hydrologic units and areas. 102

Table 12. Summary of attributes for Geomorphic Reach GR-1. 106

Table 13. Summary of attributes for Geomorphic Reach GR-2 108

Table 14. Summary of attributes for Geomorphic Reach GR-3 110

Table 15. Summary of attributes for Geomorphic Reach GR-4 112

Table 16. Summary of attributes for Geomorphic Reach GR-5 114

Table 17. Summary of attributes for Geomorphic Reach GR-6 116

Table 18. Summary of attributes for Geomorphic Reach GR-7 118

Table 19. Summary of attributes for Geomorphic Reach GR-8. 120

Table 20. Lemhi watershed hydrologic units and areas 122

Table 21. Middle Lemhi sub-watershed tributaries 122

Table 22. Summary of attributes for Geomorphic Reach GR-9 126

Table 23. Summary of attributes for Geomorphic Reach GR-10. 128

Table 24. Summary of attributes for Geomorphic Reach GR-11 130

Table 25. Summary of attributes for Geomorphic Reach GR-12. 132

Table 26. Lemhi watershed hydrologic units and areas. 135

Table 27. Lower Lemhi sub-watershed tributaries. 135

Table 28. Summary of attributes for Geomorphic Reach GR-13. 138

Table 29. Summary of attributes for Geomorphic Reach GR-14. 140

Table 30. Summary of attributes for Geomorphic Reach GR-15 142
Table 31. Summary of attributes for Geomorphic Reach GR-16 144
Table 32. Estimated current life-stage-specific capacity requirements versus estimated available capacity for Chinook salmon in the Pahsimeroi River. 156
Table 33. Estimated life-stage-specific capacity requirements to accommodate ESA de-listing and estimated available capacity for Chinook salmon in the Pahsimeroi River. 157
Table 34. Estimated current life-stage-specific capacity requirements versus estimated available capacity for steelhead in the Pahsimeroi River. 159
Table 35. Estimated life-stage-specific capacity requirements to accommodate ESA de-listing and estimated available capacity for steelhead in the Pahsimeroi River. 160
Table 36. Pahsimeroi River hydrology. 166
Table 37. Streams and pollutants for which TMDLs were developed 173
Table 38. Geomorphic features along the valley bottoms and margins, and associated soils..176
Table 39. Pahsimeroi River watershed valley segments delineations and sub-watersheds.....184
Table 40. Summary of geomorphic conditions for the Pahsimeroi River watershed 186
Table 41. Summary of attributes for Geomorphic Reach GR-1. 190
Table 42. Summary of attributes for Geomorphic Reach GR-2. 192
Table 43. Summary of attributes for Geomorphic Reach GR-3. 194
Table 44. Summary of attributes for Geomorphic Reach GR-4 198
Table 45. Summary of attributes for Geomorphic Reach GR-5. 200
Table 46. Summary of attributes for Geomorphic Reach GR-6. 202
Table 47. Summary of attributes for Geomorphic Reach GR-7. 204
Table 48. Summary of attributes for Geomorphic Reach GR-8. 208
Table 49. Summary of attributes for Geomorphic Reach GR-9. 210
Table 50. Summary of attributes for Geomorphic Reach GR-10. 212
Table 51. Estimated current life-stage-specific capacity requirements versus estimated available capacity for Chinook salmon in the Upper Salmon River. 224
Table 52. Estimated life-stage-specific capacity requirements to accommodate ESA de-listing and estimated available capacity for Chinook salmon in the Upper Salmon River. 225
Table 53. Estimated current life-stage-specific capacity requirements versus estimated available capacity for steelhead in the Upper Salmon River. 227
Table 54. Estimated life-stage-specific capacity requirements to accommodate ESA de-listing and estimated available capacity for steelhead in the Upper Salmon River. 228
Table 55. Upper Salmon River hydrology. 235
Table 56. Streams and pollutants listed in the 2016 Addendum (IDEQ 2016). 242

Table 57. Geomorphic features along the valley bottoms and margins, and associated soils..245
Table 58. Upper Salmon River watershed valley segment delineations and sub-watersheds..254
Table 59. Summary of geomorphic reach characteristics for the Upper Salmon watershed. ...256
Table 60. Summary of attributes for Geomorphic Reach GR-1. 258
Table 61. Summary of attributes for Geomorphic Reach GR-2. 260
Table 62. Summary of attributes for Geomorphic Reach GR-3. 262
Table 63. Summary of attributes for Geomorphic Reach GR-4. 264
Table 64. Summary of attributes for Geomorphic Reach GR-5. 266
Table 65. Summary of attributes for Geomorphic Reach GR-6. 268
Table 66. Summary of attributes for Geomorphic Reach GR-7. 272
Table 67. Summary of attributes for Geomorphic Reach GR-8. 274
Table 68. Summary of attributes for Geomorphic Reach GR-9. 276
Table 69. Summary of attributes for Geomorphic Reach GR-10. 278

List of Figures

Figure 1. Flow chart illustrating the relationship of the Integrated Rehabilitation Assessment (IRA) and Multiple Reach Assessments (MRAs), including inputs and goals for the overall assessment framework. 3

Figure 2. Human activities have had a dramatic effect on aquatic resources and in particular anadromous salmonids. The Y-axis above depicts harvest of salmon and steelhead in the Columbia as a surrogate for escapement due its long period of record. The Y2-axis depicts various activities, with the darker potion of the bar graph representing the peak of the activity. ..5

Figure 3. Upper Salmon subbasin (upstream of the Middle Fork Salmon River) vicinity map illustrating the three watersheds assessed in this report – Lemhi, Pahsimeroi, and Upper Salmon (upstream of Redfish Lake Creek)....7

Figure 4. The chart above depicts an ideal scenario on the left with no limiting factors, while the graphic on the right depicts a river with significant limiting factors resulting in less habitat capacity and less production. 11

Figure 5. Summary of Chinook salmon life stages and key physical attributes associated with known habitat preferences. 11

Figure 6. Generic basin-and-range faulting with valley fill sediment, illustrating how the Lemhi, Pahsimeroi, and Upper Salmon River headwaters have formed and partially filled with alluvial sediment. 14

Figure 7. Representative example from the Upper Lemhi River illustrating groundwater-influenced characteristics, including a highly sinuous, multi-threaded channel with multiple spring-fed side channels and a diversity of riparian vegetation all occupying the same floodplain. Flow direction in the aerial photo is from right to left, and from the bottom of the image to the top in the surface photos....16

Figure 8. Representative example from the Upper Salmon River headwaters illustrating characteristics typical of a snowmelt-influenced (peak flow) hydrology, including a moderate to low sinuosity, single-thread channel, active point bars driving channel migration, and a predominantly plane-bed morphology. Flow direction is from the right side of the image to the left in the aerial photos and away from the photographer in the surface photos. 17

Figure 9. Box-and-whisker plot showing the distribution of regionalized average monthly and annual streamflow (cubic feet per second; cfs) during the (a) historical and (b) future periods for each of the 97 projection members. (c) Box-and-whisker plot showing the distribution of regionalized average monthly and annual percent changes in streamflow between the two periods (future-historical) for the same 97 projection members. The horizontal blue line in (c) demarks a 0 percent change....22

Figure 10. Geomorphic characterization and associated response potential as used to map individual channel units to differentiate and categorize reaches within the Lemhi, Pahsimeroi, and Upper Salmon Rivers. 30

Figure 11. Summary of the habitat rehabilitation effort based on the relationship between geomorphic characterization and preferred habitat conditions per life stage. In general, more complex geomorphic character naturally yields conditions preferred by more life stages.

Rehabilitation efforts may be undertaken within an area defined by any geomorphic character, but the level of effort required to elicit and/or maintain the desired channel response will vary, as illustrated in this figure. 38

Figure 12. Estimates of available spawning (redd) capacity for Chinook salmon given current habitat conditions, made using quantile regression and random forest models (black bars) versus the capacity required to support contemporary abundance and minimum abundance thresholds (MATs) needed for ESA de-listing (blue bars). 41

Figure 13. Estimates of available summer juvenile (parr) rearing capacity for Chinook salmon given current habitat conditions, made using quantile regression and random forest models (black bars) versus the capacity required to support contemporary abundance and minimum abundance thresholds (MATs) needed for ESA de-listing (blue bars). 41

Figure 14. Estimates of available winter juvenile (presmolt) rearing capacity for Chinook salmon given current habitat conditions, made using quantile regression and random forest models (black bars) versus the capacity required to support contemporary abundance and minimum abundance thresholds (MATs) needed for ESA de-listing (blue bars). 42

Figure 15. Estimates of available spawning (redd) capacity for steelhead given current habitat conditions, made using quantile regression random forest models (black bars) versus the capacity required to support contemporary abundance and minimum abundance thresholds (MATs) needed for ESA de-listing (green bars). 43

Figure 16. Estimates of available summer juvenile (parr) rearing capacity for steelhead given current habitat conditions, made using quantile regression random forest models (black bars) versus the capacity required to support contemporary abundance and minimum abundance thresholds (MATs) needed for ESA de-listing (green bars). 44

Figure 17. Estimates of available winter juvenile (presmolt) rearing capacity for steelhead given current habitat conditions, made using quantile regression random forest models (black bars) versus the capacity required to support contemporary abundance and minimum abundance thresholds (MATs) needed for ESA de-listing (green bars). 44

Figure 18. Lemhi River map spatially illustrating geomorphic character per reach (pie charts) and predicted existing capacity for Chinook salmon parr (graded orange to yellow dots). 48

Figure 19. Lemhi River map spatially illustrating geomorphic character per reach (pie charts) and predicted existing capacity for steelhead parr (graded orange to yellow dots). 49

Figure 20. Pahsimeroi River map spatially illustrating geomorphic character per reach (pie charts) and predicted existing capacity for Chinook salmon parr (graded orange to yellow dots). 52

Figure 21. Pahsimeroi River map spatially illustrating geomorphic character per reach (pie charts) and predicted existing capacity for steelhead parr (graded orange to yellow dots). 53

Figure 22. Upper Salmon River headwaters map spatially illustrating geomorphic character per reach (pie charts) and predicted existing capacity for Chinook salmon parr (graded orange to yellow dots). 56

Figure 23. Upper Salmon River headwaters map spatially illustrating geomorphic character per reach (pie charts) and predicted existing capacity for steelhead parr (graded orange to yellow dots)....57

Figure 24. Location of the Lemhi River watershed within the Upper Salmon River subbasin.....61

Figure 25. Estimates of available spawning (redd) capacity given current habitat conditions for Chinook salmon in the Lemhi River watershed, made using quantile regression forest models (black bars) versus the capacity required to support contemporary abundance and minimum abundance thresholds (MATs) needed for ESA de-listing (blue bars). 64

Figure 26. Estimates of available summer juvenile (parr) rearing capacity given current habitat conditions for Chinook salmon in the Lemhi River watershed, made using quantile regression forest models (black bars) versus the capacity required to support contemporary abundance and minimum abundance thresholds (MATs) needed for ESA de-listing (blue bars). 64

Figure 27. Estimates of available winter juvenile (presmolt) rearing capacity given current habitat conditions for Chinook salmon in the Lemhi River watershed, made using quantile regression forest models (black bars) versus the capacity required to support contemporary abundance and minimum abundance thresholds (MATs) needed for ESA de-listing (blue bars). 65

Figure 28. Estimates of available spawning (redd) capacity given current habitat conditions for steelhead in the Lemhi River watershed, made using quantile regression forest models (black bars) versus the capacity required to support contemporary abundance and minimum abundance thresholds (MATs) needed for ESA de-listing (green bars). 66

Figure 29. Estimates of available summer juvenile (parr) rearing capacity given current habitat conditions for steelhead in the Lemhi River watershed, made using quantile regression forest models (black bars) versus the capacity required to support contemporary abundance and minimum abundance thresholds (MATs) needed for ESA de-listing (green bars)....67

Figure 30. Estimates of available winter juvenile (presmolt) rearing capacity given current habitat conditions for steelhead in the Lemhi River watershed, made using quantile regression forest models (black bars) versus the capacity required to support contemporary abundance and minimum abundance thresholds (MATs) needed for ESA de-listing (green bars)....67

Figure 31. Map showing delineation between the upper and lower Lemhi River....69

Figure 32. Lewis and Clark map (Moulton 1983) illustrating the lower Lemhi River (called the East Fork of the Lewis River by Lewis and Clark). The modern towns of Tendoy and Salmon are shown for reference. 71

Figure 33. Idaho Power diversion dam on the lower Lemhi River (Source: Oregon State University, downloaded March 14, 2017, from https://oregondigital.org/sets/streamsurvey/oregondigital:df66q392q) 72

Figure 34. Estimation of discharge lost to irrigation. 74

Figure 35. Comparison of actual and natural hydrographs for a dry year on the Lemhi River at Cottom Lane. 75

Figure 36. Comparison of actual and natural hydrographs for a wet year on the Lemhi River at Cottom Lane. 75

Figure 37. 1997 Lemhi River groundwater discharge graph, illustrating groundwater volume (solid lines) and percent of total discharge (dashed lines) for August during the peak of irrigation (blue lines) and October after irrigation season (orange lines) (interpreted from Donato 1998). 76

Figure 38. 2014 Lemhi River groundwater discharge graph illustrating groundwater volume (solid lines) and percent of total discharge (dashed lines) for August during the peak of irrigation (blue lines) and October after irrigation season (orange lines) (interpreted from IDWR 2017). ..77

Figure 39. Summary of representative hydraulic conditions at Site 1. 78

Figure 40. Summary of representative hydraulic conditions at Site 2. 79

Figure 41. Summary of representative hydraulic conditions at Site 3. 80

Figure 42. Locations of sediment domains within a typical watershed (Cluer and Thorne 2013). Unlike typical watersheds, a pronounced, low-gradient deposition zone occurs immediately below the alluvial fan zone on the Lemhi River resulting from a mid-valley bedrock grade control near the confluence of Hayden Creek (RM 32.9), followed by a transfer zone characterized by greater sediment availability and transport. 82

Figure 43. Lemhi River longitudinal profile (blue line) and average reach slope (dashed orange lines) by river mile. The gradient is generally lower upstream of an area of shallow bedrock that coincides with the Hayden Creek confluence near RM 32.9. 83

Figure 44. Lemhi River watershed valley segment locations. 92

Figure 45. Location of Lemhi Headwaters Valley Segment (VS-1) comprising Hawley Creek, Eighteenmile Creek, and Texas Creek. 95

Figure 46. Location of Texas Creek sub-watershed with the Lemhi Range and alluvial fans along the west that have seeps and springs that drain into a wetland complex that maintains perennial flows in Texas Creek. 97

Figure 47. Location of the Hawley Creek sub-watershed. 99

Figure 48. Location of the Eighteenmile Creek sub-watershed...101

Figure 49. Upper Lemhi Valley Segment (VS-2) and associated geomorphic reaches (GR-2 through GR-8). 103

Figure 50. Location of the Timber Creek sub-watershed. 105

Figure 51. GR-1 overview map illustrating the approximate floodplain, geomorphic characterization, and human alterations to the floodplain. 107

Figure 52. GR-2 overview map illustrating the approximate floodplain, geomorphic characterization, and human alterations to the floodplain 109

Figure 53. GR-3 overview map illustrating the approximate floodplain, geomorphic characterization, and human alterations to the floodplain. 111

Figure 54. GR-4 overview map illustrating the approximate floodplain, geomorphic characterization, and human alterations to the floodplain. 113

Figure 55. GR-5 overview map illustrating the approximate floodplain, geomorphic characterization, and human alterations to the floodplain. 115

Figure 56. GR-6 overview map illustrating the approximate floodplain, geomorphic characterization, and human alterations to the floodplain. 117

Figure 57. GR-7 overview map illustrating approximate floodplain, geomorphic characterization, and human alterations to floodplain..119

Figure 58. GR-8 overview map illustrating the approximate floodplain, geomorphic characterization, and human alterations to the floodplain. 121

Figure 59. Middle Lemhi Valley Segment (VS-3) and geomorphic reaches (GR-9 through GR-12). 123

Figure 60. Aerial image of Hayden Creek sub-watershed. 125

Figure 61. GR-9 overview map illustrating the approximate floodplain, geomorphic characterization, and human alterations to the floodplain. 127

Figure 62. GR-10 overview map illustrating the approximate floodplain, geomorphic characterization, and human alterations to the floodplain. 129

Figure 63. GR-11 overview map illustrating the approximate floodplain, geomorphic characterization, and human alterations to the floodplain. 131

Figure 64. GR-12 overview map illustrating the approximate floodplain, geomorphic characterization, and human alterations to the floodplain. 134

Figure 65. Lower Lemhi Valley Segment (VS-4) and geomorphic reaches (GR-13 through GR-16). 137

Figure 66. GR-13 overview map illustrating the approximate floodplain, geomorphic characterization, and human alterations to the floodplain. 139

Figure 67. GR-14 overview map illustrating the approximate floodplain, geomorphic characterization, and human alterations to the floodplain. 141

Figure 68. GR-15 overview map illustrating the approximate floodplain, geomorphic characterization, and human alterations to the floodplain. 143

Figure 69. GR-16 overview map illustrating the approximate floodplain, geomorphic characterization, and human alterations to the floodplain. 145

Figure 70. The percentage of time that Lemhi River watershed water temperatures were below, within, or above a given temperature threshold (Carter 2005) for seven Chinook salmon life stages. Water temperatures were averaged across years for which complete modeled temperature data were available (2012-2015). 147

Figure 71. The percentage of time that Lemhi River watershed water temperatures may potentially be below, within, or above a given temperature threshold (Carter 2005) for seven Chinook salmon life stages, assuming a potential climate change scenario. 148

Figure 72. The percentage of time that Lemhi River watershed water temperatures were below, within, or above a given temperature threshold (Carter 2005) for seven steelhead life-stages. Water temperatures were averaged across years for which complete modeled temperature data were available (2012-2015)...149

Figure 73. The percentage of time that Lemhi River watershed water temperatures may potentially be below, within, or above a given temperature threshold (Carter 2005) for seven steelhead life stages, assuming a potential climate change scenario. 150

Figure 74. Location map of the Pahsimeroi River watershed...155

Figure 75. Estimates of available spawning (redd) capacity given current habitat conditions for Chinook salmon in the Pahsimeroi River watershed, made using quantile regression forest models (black bars) versus the capacity required to support contemporary abundance and minimum abundance thresholds (MATs) needed for ESA de-listing (blue bars). 158

Figure 76. Estimates of available summer juvenile (parr) rearing capacity given current habitat conditions for Chinook salmon in the Pahsimeroi River watershed, made using quantile regression forest models (black bars) versus the capacity required to support contemporary abundance and minimum abundance thresholds (MATs) needed for ESA de-listing (blue bars). 158

Figure 77. Estimates of available winter juvenile (presmolt) rearing capacity given current habitat conditions for Chinook salmon in the Pahsimeroi River watershed, made using quantile regression forest models (black bars) versus the capacity required to support contemporary abundance and minimum abundance thresholds (MATs) needed for ESA de-listing (blue bars). 159

Figure 78. Estimates of available spawning (redd) capacity given current habitat conditions for steelhead in the Pahsimeroi River watershed, made using quantile regression forest models (black bars) versus the capacity required to support contemporary abundance and minimum abundance thresholds (MATs) needed for ESA de-listing (green bars). 161

Figure 79. Estimates of available summer juvenile (parr) rearing capacity given current habitat conditions for steelhead in the Pahsimeroi River watershed, made using quantile regression forest models (black bars) versus the capacity required to support contemporary abundance and minimum abundance thresholds (MATs) needed for ESA de-listing (green bars). 161

Figure 80. Estimates of available winter juvenile (presmolt) rearing capacity given current habitat conditions for steelhead in the Pahsimeroi River watershed, made using quantile regression forest models (black bars) versus the capacity required to support contemporary abundance and minimum abundance thresholds (MATs) needed for ESA de-listing (green bars). 162

Figure 81. Map of the Pahsimeroi River watershed illustrating the approximate boundary between the upper, middle, and lower valleys. 163

Figure 82. Representative Pahsimeroi River groundwater discharge, as interpreted from Williams et al (2006)...167

Figure 83. Summary of representative hydraulic conditions at Site 1. 169

Figure 84. Summary of representative hydraulic conditions at Site 2. 170

Figure 85. Summary of representative hydraulic conditions at Site 3. 171

Figure 86. Locations of sediment domains within a typical watershed (Cluer and Thorne 2013). 174

Figure 87. Pahsimeroi River longitudinal profile by geomorphic reach. The channel exhibits a typical concave curve with generally decreasing slopes in the downstream direction. 174

Figure 88. Pahsimeroi River watershed valley segment locations. 185

Figure 89. Location of Pahsimeroi Headwaters Valley Segment, comprising the West Fork and the East Fork drainages. 187

Figure 90. The Upper Pahsimeroi Valley Segment and associated geomorphic reaches (GR-1 through GR-3). 189

Figure 91. GR-1 overview map illustrating the approximate floodplain, geomorphic characterization, and human alterations to the floodplain. 191

Figure 92. GR-2 overview map illustrating the approximate floodplain, geomorphic characterization, and human alterations to the floodplain. 193

Figure 93. GR-3 overview map illustrating the approximate floodplain, geomorphic characterization, and human alterations to the floodplain. 195

Figure 94. Middle Pahsimeroi Valley Segment and associated geomorphic reaches (GR-4 through GR-7). 197

Figure 95. GR-4 overview map illustrating the approximate floodplain, geomorphic characterization, and human alterations to the floodplain. 199

Figure 96. GR-5 overview map illustrating the approximate floodplain, geomorphic characterization, and human alterations to the floodplain. 201

Figure 97. GR-6 overview map illustrating the approximate floodplain, geomorphic characterization, and human alterations to the floodplain. 203

Figure 98. GR-7 overview map illustrating the approximate floodplain, geomorphic characterization, and human alterations to the floodplain. 205

Figure 99. Lower Pahsimeroi Valley Segment and associated geomorphic reaches (GR-8 through GR-10). 207

Figure 100. GR-8 overview map illustrating the approximate floodplain, geomorphic characterization, and human alterations to the floodplain. 209

Figure 101. GR-9 overview map illustrating the approximate floodplain, geomorphic characterization, and human alterations to the floodplain. 211

Figure 102. GR-10 overview map illustrating the approximate floodplain, geomorphic characterization, and human alterations to the floodplain. 213

Figure 103. The percentage of time that Pahsimeroi River watershed water temperatures were below, within, or above a given temperature threshold (Carter 2005) for five Chinook salmon life stages. Water temperatures were averaged across years for which complete modeled temperature data were available (2011 and 2013). 214

Figure 104. The percentage of time that Pahsimeroi River watershed water temperatures may potentially be below, within, or above a given temperature threshold (Carter 2005) for five Chinook salmon life-stages assuming a potential climate change scenario. 215

Figure 105. The percentage of time that Pahsimeroi River watershed water temperatures in 2013 were below, within, or above a given temperature threshold (Carter 2005) for five steelhead life stages. Water temperatures were averaged across years for which complete modeled temperature data were available (2011 and 2013). 216

Figure 106. The percentage of time that Pahsimeroi River watershed water temperatures may potentially be below, within, or above a given temperature threshold (Carter 2005) for five steelhead life-stages, assuming a potential climate change scenario. 217

Figure 107. Map of location of the Upper Salmon River subbasin. 223

Figure 108. Estimates of available spawning (redd) capacity given current habitat conditions for Chinook salmon in the Upper Salmon River watershed, made using quantile regression forest models (black bars), versus the capacity required to support contemporary abundance and minimum abundance thresholds (MATs) needed for ESA de-listing (blue bars). 226

Figure 109. Estimates of available summer juvenile (parr) rearing capacity given current habitat conditions for Chinook salmon in the Pahsimeroi River watershed, made using quantile regression forest models (black bars), versus the capacity required to support contemporary abundance and minimum abundance thresholds (MATs) needed for ESA de-listing (blue bars). 226

Figure 110. Estimates of available winter juvenile (presmolt) rearing capacity given current habitat conditions for Chinook salmon in the Pahsimeroi River watershed, made using quantile regression forest models (black bars), versus the capacity required to support contemporary abundance and minimum abundance thresholds (MATs) needed for ESA de-listing (blue bars). 227

Figure 111. Estimates of available spawning (redd) capacity given current habitat conditions for steelhead in the Upper Salmon River watershed, made using quantile regression forest models (black bars) versus the capacity required to support contemporary abundance and minimum abundance thresholds (MATs) needed for ESA de-listing (green bars). 229

Figure 112. Estimates of available summer juvenile (parr) rearing capacity given current habitat conditions for steelhead in the Upper Salmon River watershed made using quantile regression forest models (black bars) versus the capacity required to support contemporary abundance and minimum abundance thresholds (MATs) needed for ESA de-listing (green bars). 229

Figure 113. Estimates of available winter juvenile (presmolt) rearing capacity given current habitat conditions for steelhead in the Upper Salmon River watershed made using quantile regression forest models (black bars) versus the capacity required to support contemporary abundance and minimum abundance thresholds (MATs) needed for ESA de-listing (green bars). 230

Figure 114. Ten-meter digital elevation model hill shade map illustrating the approximate terminal extent of Pleistocene glacial moraines. 232

Figure 115. Aerial photo of the Sawtooth Valley identifying areas of known and expected groundwater influence, based on past seepage runs and visible green floodplains relative to surrounding areas. 236

Figure 116. Summary of representative hydraulic conditions at Site 1. 238

Figure 117. Summary of representative hydraulic conditions at Site 1. 239

Figure 118. Summary of representative hydraulic conditions at Site 1. 240

Figure 119. Locations of sediment domains within a typical watershed (Cluer and Thorne 2013). 243

Figure 120. Upper Salmon River longitudinal profile and slope by geomorphic reach (Reach 1 slope is 6.94 percent and has been omitted from the figure to maintain a more legible scale).243

Figure 121. Illustration of valley constrictions and grade controls associated with glacial moraines and glacial outwash in the Upper Salmon River headwaters. The red lines illustrate the approximate edge of valley constrictions formed by glacial deposition on one or both sides of the valley, while the yellow lines illustrate the approximate edge of relatively unconfined valley areas...244

Figure 122. Simplified graphic illustrating the difference between lateral and downstream channel migration...248

Figure 123. Upper Salmon River watershed valley segment locations. 255

Figure 124. Location of Pole Creek Valley Segment and associated geomorphic reaches (GR-1 through GR-6). 257

Figure 125. GR-1 overview map illustrating the approximate floodplain, geomorphic characterization, and human alterations to the floodplain. 259

Figure 126. GR-2 overview map illustrating the approximate floodplain, geomorphic characterization, and human alterations to the floodplain. 261

Figure 127. GR-3 overview map illustrating the approximate floodplain, geomorphic characterization, and human alterations to the floodplain. 263

Figure 128. GR-4 overview map illustrating the approximate floodplain, geomorphic characterization, and human alterations to the floodplain. 265

Figure 129. GR-5 overview map illustrating the approximate floodplain, geomorphic characterization, and human alterations to the floodplain. 267

Figure 130. GR-6 overview map illustrating the approximate floodplain, geomorphic characterization, and human alterations to the floodplain. 269

Figure 131. Location of Redfish Lake Creek Valley Segment and associated geomorphic reaches (GR-7 through GR-10). 271

Figure 132. GR-7 overview map illustrating the approximate floodplain, geomorphic characterization, and human alterations to the floodplain. 273

Figure 133. GR-8 overview map illustrating the approximate floodplain, geomorphic characterization, and human alterations to the floodplain. 275

Figure 134. GR-9 overview map illustrating the approximate floodplain, geomorphic characterization, and human alterations to the floodplain. 277

Figure 135. GR-10 overview map illustrating the approximate floodplain, geomorphic characterization, and human alterations to the floodplain. 279

Figure 136. The percentage of time that Upper Salmon River watershed water temperatures were below, within, or above a given temperature threshold (Carter 2005) for five Chinook salmon life stages. Water temperatures were averaged across years for which complete modeled temperature data were available (2011 and 2013). 280

Figure 137. The percentage of time that Upper Salmon River watershed water temperatures may potentially be below, within, or above a given temperature threshold (Carter 2005) for five Chinook salmon life stages, assuming a potential climate change scenario. 281

Figure 138. The percentage of time that Upper Salmon River watershed water temperatures were below, within, or above a given temperature threshold (Carter 2005) for five steelhead life stages. Water temperatures were averaged across years for which complete modeled temperature data were available (2011 and 2013). 282

Figure 139. The percentage of time that Upper Salmon River watershed water temperatures may potentially be below, within, or above a given temperature threshold (Carter 2005) for five steelhead life stages, assuming a potential climate change scenario. 283

List of Photographs

Photograph 1. Examples of preferred habitat conditions for Chinook salmon adults (summer) holding and spawning, including appropriate cover and substrate accumulated in conjunction with instream woody material and healthy riparian vegetation. The left photograph is from the Middle Entiat River, Washington, and the right photograph is from the Upper Yankee Fork Salmon River. 12

Photograph 2. Example of preferred habitat conditions for Chinook salmon fry (spring) rearing with very low velocity and abundant cover. Photographs are from the Upper Yankee Fork (left) and Upper South Fork of the Salmon River (right). 12

Photograph 3. Example of preferred habitat conditions, including split flow, instream cover and hydraulic variability, which support Chinook salmon parr (summer) rearing. Photograph is from a constructed project in Catherine Creek in the Grande Ronde River watershed, Oregon. 13

Photograph 4. Examples of preferred habitat conditions for Chinook salmon pre-smolt (winter) rearing. Note large substrate (left) and dense woody material (right), both with significant interstitial space providing concealment cover for overwinter rearing. Photographs are from the Secesh River (left) and Catherine Creek in the Grande Ronde basin (right). 13

Photograph 5. Examples of irrigation diversions from the Upper Salmon River headwaters illustrating impacts to in-stream flow and fish passage. 18

Photograph 6. Examples from the Upper Lemhi (left) and Middle Pahsimeroi (right) Rivers illustrating impacts associated with riparian vegetation removal. 19

Photograph 7. Example from Lower Hayden Creek illustrating grazing impacts and associated lack of riparian vegetation. 19

Photograph 8. Oblique aerial photograph example of a straightened and armored section of the Upper Lemhi River just upstream of the Hayden Creek confluence. 20

Photograph 9. Example from a completed side-channel and bank/riparian improvement project from the Lower Lemhi River (Eagle Valley Ranch Phase 2, completed in 2016). 24

Photograph 10. Overview of mainstem Lemhi River habitat enhancement (Amonson Ranch) immediately following construction (left aerial photograph) and 5 years following construction (right photograph). 24

Photograph 11. Large woody debris installed to provide bank habitat and improve pool scour on the Pahsimeroi River as part of the P-16 irrigation improvement project completed in 2016. 25

Photograph 12. The Pole Creek Diversion Replacement in the Upper Salmon watershed included improvements to an irrigation system and fish screen, providing increased instream flow for Pole Creek and the Salmon River. In addition, a diversion structure (left) that blocked fish passage was replaced with a fish-passable low-head rock weir and improved channel geometry (right). 25

Photograph 13. Example of complex geomorphic character exemplified by the Upper Lemhi River with extensive riparian vegetation and sinuosity (left) and a larger channel in the Upper Salmon River with split flow and undercut banks. Photograph is looking downstream (right). 31

Photograph 14. Examples of mixed geomorphic character with excellent riparian structure in some areas but limited riparian vegetation in other areas due to land use activities, resulting in bank erosion and unnatural channel widening (Upper Pahsimeroi River on left and Upper Texas Creek, tributary to Lemhi River, on right). 31

Photograph 15. Examples of simplified geomorphic character on the Lower Lemhi River, where the channel has been historically straightened and armored and riparian vegetation removed. 32

Photograph 16. Pre- and post-habitat construction project improving simplified geomorphic condition on Catherine Creek, Oregon. 32

Photograph 17. Pre- and post-habitat construction project improving simplified geomorphic condition on the Lower Pahsimeroi River, with multiple rootwad structures installed along the bank to reduce unnatural rates of bank erosion and provide fish habitat. 33

Photograph 18. Photograph illustrating how anchor ice can fill interstitial space and alter channel geometry. (Source: www.monolake.org/today/2008/12/18/hydrology-update-for-121808/) 35

Photograph 19. Hummocks observed on the floodplain of the upper Lemhi River reveal 2 to 3 feet of fine sediment erosion (area between hummocks) associated with historic cattle grazing. Similar hummocks are common throughout large areas of the Lemhi River floodplain. 73

Photograph 20. Example of significant channel widening in the upper Lemhi River (Reach 2). Photograph is looking upstream, where the channel width exceeds 100 feet. Estimated historic and existing reference widths for this reach are on the order of 20 to 30 feet. 87

Photograph 21. Island-braided channel network along the lower Lemhi River within Reach 15 from RM 3.5 to RM 4.5. Although the area has been impacted by land use, irrigation, and other human activities, it represents the best reference condition for an island-braided reach in the lower Lemhi River watershed. 88

Photograph 22. Example of eroding bank in the Lower Pahsimeroi. This bank has subsequently been improved with multiple rootwad structures to reduce excessive bank erosion, reduce the over-widened width-to-depth ratio of the channel, and to provide habitat and cover for juvenile salmonids. 178

Photograph 23. Mature willow clump providing instream structure and splitting flow in a groundwater-influenced channel (Big Springs Creek in the Lemhi watershed). 179

Photograph 24. Forced pool-riffle morphology due to riparian plant structure on the bank of the lower Pahsimeroi River. 180

Photograph 25. Photograph illustrating a straightened channel and plane-bed morphology in the lower Pahsimeroi River. 181

Photograph 26. Plane-bed morphology in Big Creek in the upper Pahsimeroi River valley. 181

Photograph 27. Aerial photograph example of relic channel scars, oxbows, and meander scrolls in a response reach of the Upper Salmon River headwaters. 234

Photograph 28. Plane-bed stretch of the Upper Salmon River in Geomorphic Reach 8. 250

Photograph 29. Photograph example from Reach 9 illustrating a sinuous channel segment with deep scour pools along the outside of each bend, with riffles in between and woody debris associated with both..250

Photograph 30. Beaver dam located in a perennial side channel within a multi-threaded, groundwater-influenced portion of Reach 8. 251

Photograph 31. Historic oblique aerial photograph of the dewatered section of channel immediately downstream of the Busterback diversion prior to its removal. 252

Section 1: Introduction, Background, and Approach

Introduction

The Idaho Governor's Office of Species Conservation (OSC) and an interdisciplinary team of partners have created this Upper Salmon Subbasin Habitat Integrated Rehabilitation Assessment (IRA). The IRA is a biologically based assessment of habitat conditions in the Upper Salmon River subbasin in central Idaho for spring/summer run Chinook salmon (*Oncorhynchus tshawytscha*; hereafter Chinook salmon) and summer run steelhead (*O. mykiss*; hereafter steelhead) listed under the Endangered Species Act (ESA). This assessment leverages estimates of tributary habitat capacity, a summary of watershed-scale geomorphic conditions, hydrologic and hydraulic analyses, and information on current and projected water temperatures to build a framework for describing the status of habitat conditions. Moreover, estimates of available habitat capacity and potential habitat capacity limitations relative to current conditions are compared to estimates of capacity requirements necessary to support National Oceanic and Atmospheric Administration (NOAA; 2017) delisting. This IRA framework is used to evaluate capacity limitations and associated geomorphic character to facilitate habitat rehabilitation planning efforts for Chinook salmon and steelhead populations in the Upper Salmon River subbasin. The IRA is a watershed-scale assessment intended to identify the problem, or life-stage-specific capacity limitations, in the Upper Salmon River subbasin. Future Multiple Reach Assessments (MRAs) will be developed to identify potential reach-scale, geomorphically appropriate target conditions and enhancement actions to inform the prioritization and development of specific enhancement projects.

This IRA is a collaborative, interdisciplinary effort intended to guide the development of habitat improvement actions in coordination with local objectives and constraints. It is not intended to be a stand-alone document that directs the design and implementation of projects in the Upper Salmon subbasin; rather, it is the first step in a science-based approach that identifies priorities and data gaps in existing knowledge that will be useful for future analysis and implementation. Based on the data and results presented in this document and the accompanying technical appendices, stakeholders can better plan both smaller-scale projects that can be implemented as opportunities arise, and larger, more complex projects that will require further assessment at a reach scale. This watershed-scale IRA was developed largely from existing data with limited field validation and was guided by previous assessments completed by the Bureau of Reclamation (Reclamation) in Columbia River tributaries and processes developed by the Northwest Fisheries Science Center. The next step will be to perform reach-scale assessments (e.g., MRAs) in high-priority areas identified by the IRA. Future MRAs are intended to refine analyses from the IRA by incorporating finer-resolution data, field work, and reach-specific rehabilitation targets, which will inform future habitat actions.

Both the IRA and MRA benefit from, and build on, the considerable knowledge accumulated by the work of research biologists, and capitalize on the observational wisdom of biologists, Tribes, and landowners. The IRA provides initial efforts to quantify necessary increases in available habitat capacity to support NOAA recovery plan goals. Additionally, these efforts build upon the well-established platform of the 1995 Model Watershed Plan (Idaho Soil Conservation Commission 1995) and process, the 2002

Northwest Power and Conservation Council Salmon Subbasin Plan, and a large suite of successful habitat implementation actions since the early 1990s. Additionally, this report builds on a continuing history of collaborative effort in the Upper Salmon Subbasin among landowners, irrigators, agricultural interests, community members, funders, and technical specialists from government and conservation entities who are instrumental for applying the concepts presented in this assessment. This IRA document is intended to engage a diverse audience including landowners, habitat rehabilitation practitioners, and regulatory agencies. It is our hope that this structure enables readers to engage at whichever levels of contextual and quantitative content interest them and that the IRA contributes to ongoing conversations to recover listed Chinook salmon and steelhead in the Upper Salmon River subbasin.

The IRA focuses primarily on Chinook salmon, and secondarily on steelhead; additional existing data are available for Chinook salmon beyond that available for steelhead, and therefore, allows for a more thorough assessment. Additionally, given the similarities in habitat needs for Chinook salmon and steelhead, the IRA framework assumes that any habitat rehabilitation actions that occur to improve conditions for Chinook salmon will also improve steelhead habitat. Within the Upper Salmon River subbasin, the IRA focuses on three tributaries: the Lemhi River, Pahsimeroi River, and Upper Salmon River upstream of the confluence with Redfish Lake Creek (Salmon River headwaters). These locations are emphasized because their populations are critical to Chinook salmon recovery (NOAA 2017), and they are identified as designated strongholds in the Nez Perce Fishery Management Plan 2013-2028 (Nez Perce Tribe 2013). However, the IRA additionally provides preliminary assessments and life-stage-specific habitat capacity evaluations for the other five watersheds in the Upper Salmon River subbasin (Valley Creek, Yankee Fork Salmon River, East Fork Salmon River, North Fork Salmon River, and Panther Creek) in the appendices. Due to limited available data, bull trout (*Salvelinus confluentus*) are outside of the scope of the IRA. Habitat rehabilitation actions to benefit Chinook salmon (and steelhead) would likely benefit (or do no harm to) existing bull trout populations in the Upper Salmon River subbasin.

After completion of the IRA, the next steps include completing the MRA reports. There will be one MRA report each for the Upper Lemhi Basin, Lower Lemhi Basin, Pahsimeroi Basin, and Upper Salmon Basin above Redfish Lake Creek. The MRA reports will build upon the IRA to develop more detailed biologic and geomorphic characterization at the reach, sub-reach, and channel unit scale and directly tie into upcoming project work (Figure 1). Additional MRAs may be completed at a later date.

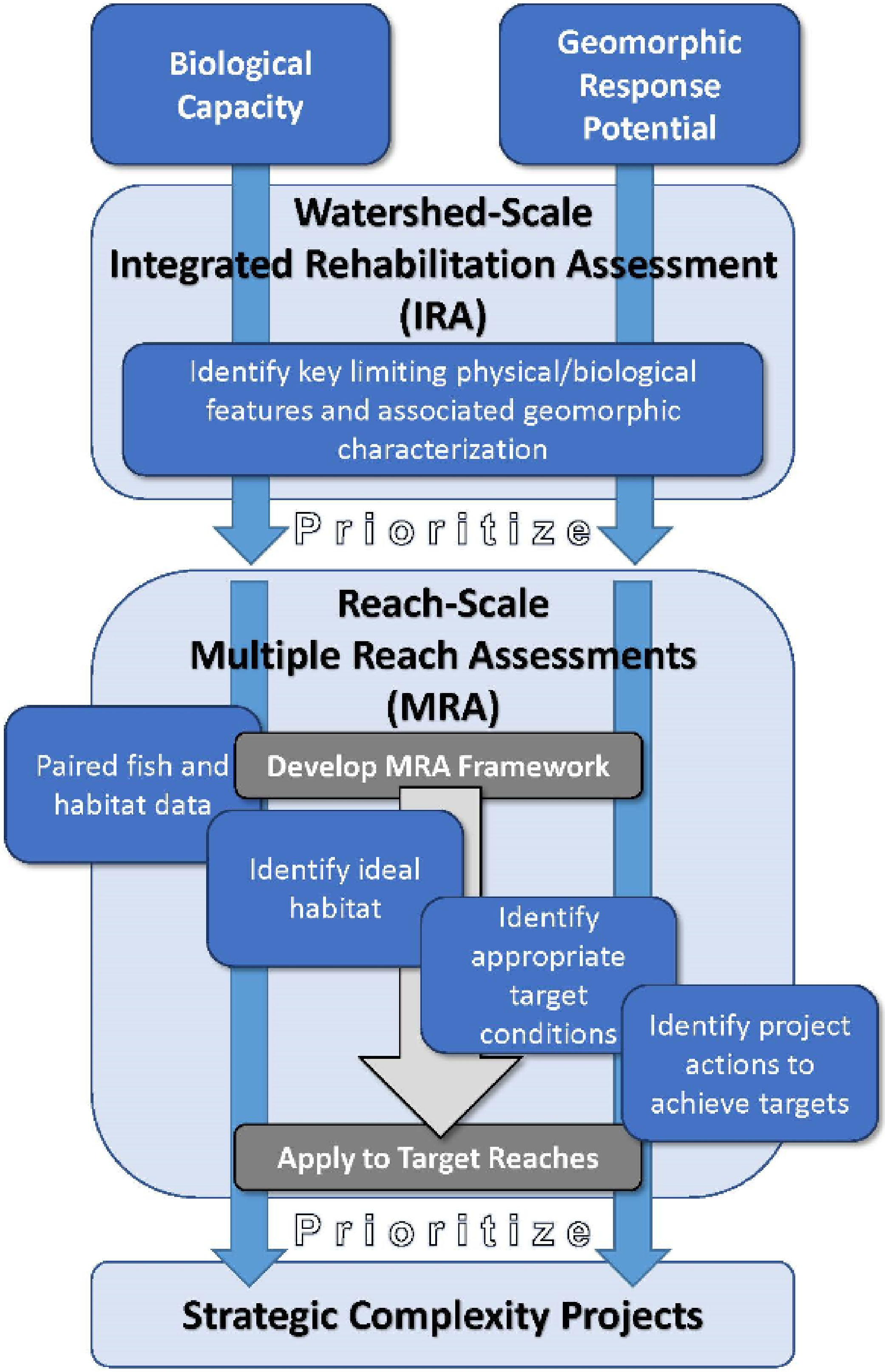

Figure 1. Flow chart illustrating the relationship of the Integrated Rehabilitation Assessment (IRA) and Multiple Reach Assessments (MRAs), including inputs and goals for the overall assessment framework.

Rationale

The life-history of anadromous salmonids can be usefully defined by two stages: 1) smolt to adult, describing the period when juveniles emigrate from freshwater to the ocean and subsequently return to freshwater as adults, and 2) adult to smolt, describing the period when adults enter tributary habitat for spawning, and encompassing the period of juvenile rearing in tributary habitat. The focus of the IRA framework is the latter, the period of the life cycle that occurs in tributary habitat. This focus is motivated by the fact that recovery, as presented in recently released Snake River recovery plans (NOAA 2017), requires that populations must be self-sustaining without reliance on hatchery production. As such, recovery necessarily requires the availability of suitable freshwater habitat to support all the physical and biological features (PBFs) for a species to complete all the freshwater life stages required of tributary habitat. PBFs are specific physical or biological features that provide for a species' life-history processes and are essential to the conservation and recovery of the species.

In completing habitat rehabilitation, our goal is to increase the capacity of the habitat to allow the productivity of target species to increase by identifying and addressing the most limiting PBFs by life-stage. This effort was initiated as a result of a combination of three events:

1. Interest on the part of the Bureau of Reclamation (Reclamation) in funding a Tributary Assessment (TA) of one major watershed in the upper-Salmon River subbasin.
2. Recently released recovery plans for spring/summer Chinook salmon and steelhead populations in the upper-Salmon River subbasin.
3. The advent of fish/habitat relationships from the Integrated Status and Effectiveness Monitoring Program (ISEMP) and Columbia River Habitat Monitoring Program (CHaMP) programs capable of estimating life-stage-specific habitat capacity across populations comprising a Major Population Group (MPG) and Distinct Population Segment (DPS).

Using the adult-to-smolt portion of the salmon/steelhead life-cycle model, we can identify needed habitat characteristics for each life stage (adult, egg, fry, parr, presmolt, etc.) to ensure the individual completes the life stage and transitions to the next successfully and in abundance to meet biological goals. Using fish-habitat models, we have identified capacity deficits for key life stages and bottlenecks in the quantity and quality of available connected habitats. Habitat available prior to European influence produced fish well in excess of our stated goals, as documented by numerous accounts of early explorers and fur traders. However, attempting to restore habitat to its exact pre-European-settlement condition is likely unrealistic.

Anthropogenic influences have exerted significant changes in the freshwater, estuary, and ocean ecosystems under which salmon historically flourished. Changes to tributary ecosystems in the Pacific Northwest began with the fur trade, long before settlement and territorial governance. Specifically, as beavers were removed from the landscape, the resiliency of ecosystems were diminished as channels became simplified and floodplain connectivity was reduced. As settlement occurred, arable lands adjacent to water sources were homesteaded first. As settlement continued, the development of water for irrigation started a series of changes with cascading effects through the ecosystem. Natural resource extraction increased over time, placing additional pressures on the aquatic ecosystems. Harvest records of Columbia River Basin salmon and steelhead stocks, because of their long period of data, are an indicator of ecosystem and stock health. Exponential increases in human population size in the Columbia River Basin are inversely correlated with the ability to harvest salmon and steelhead in the region (Figure 2).

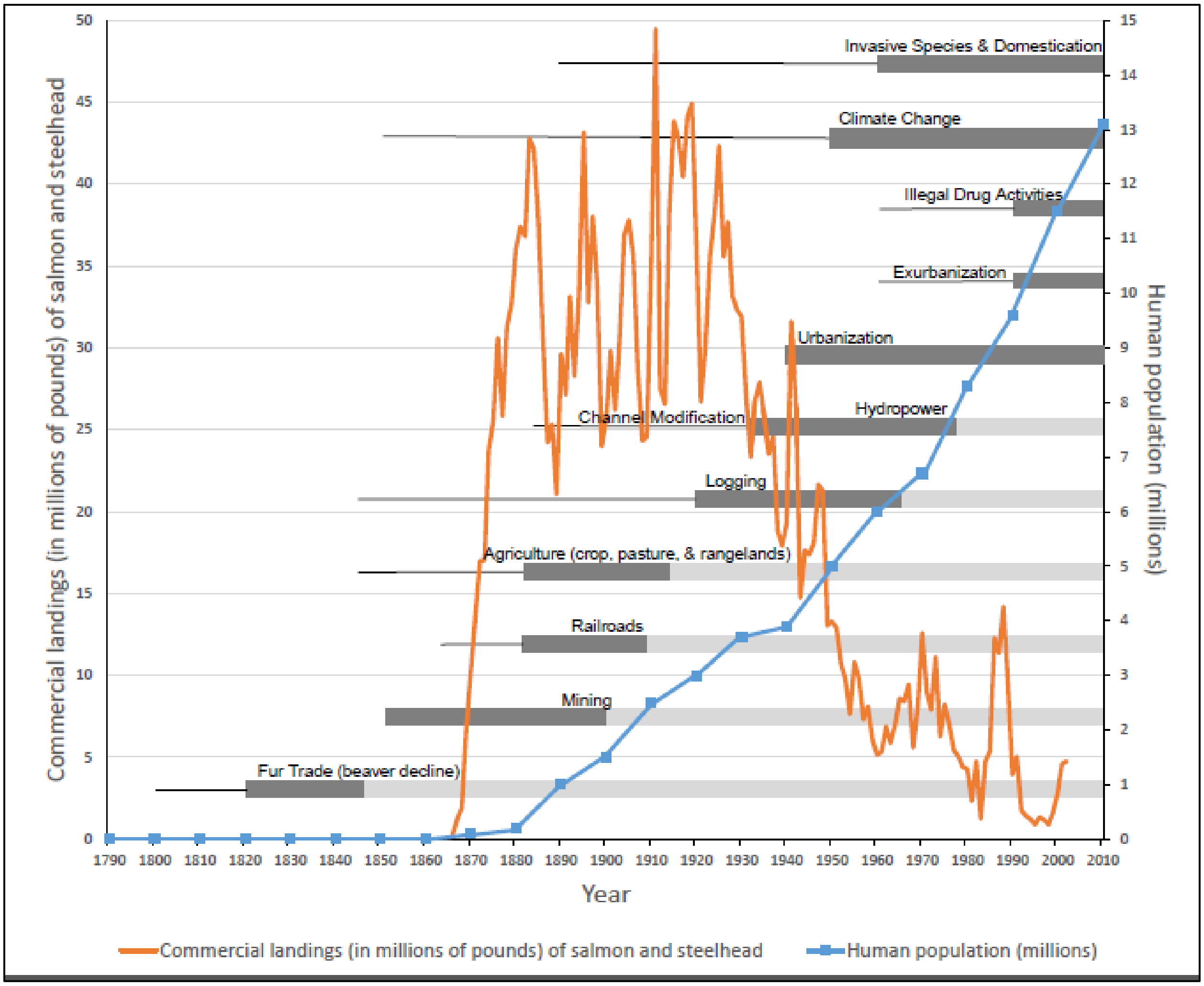

Figure 2. Human activities have had a dramatic effect on aquatic resources and in particular anadromous salmonids. The Y-axis above depicts harvest of salmon and steelhead in the Columbia as a surrogate for escapement due its long period of record. The Y2-axis depicts various activities, with the darker potion of the bar graph representing the peak of the activity.

In recent years, efforts to restore Chinook salmon and steelhead populations to historical conditions have shifted toward increasing the production and capacity in tributary spawning and rearing habitats, but project funders and policymakers have been frustrated over a lack of connection between habitat improvement and increases in adult salmon returns. However, a closer look at data reveals that habitat improvement efforts have benefited local populations in terms of increasing productivity and increasing abundance of juveniles and resident fish. Moving forward, monitoring programs should focus on collecting data to detect these increases in abundance in cohorts from life stage to life stage. As is discussed in further detail below, the efforts to date have benefited certain life stages of juvenile salmonids but either have not been enough to achieve recovery goals, or another subsequent life stage is further limiting the local population in question. Monitoring efforts such as ISEMP and CHaMP have begun to produce results that have helped to quantify the habitat deficiencies from life stage to life stage. This document further examines those deficiencies with the goal of focusing future efforts to increase the probability of sustainably improving adult salmon returns. Connecting implemented projects with quantitative estimates of their improvements in both physical habitat and fish population dynamics is key to addressing the concerns of project funders and policy makers – ultimately supporting accountability for taxpayers and providing a roadmap to sustainable and profitable fisheries in concert with other valuable land management and agricultural requirements.

The IRA team and many other partners in the Upper Salmon subbasin recognize the need to improve communication of the successes and challenges facing anadromous fish recovery in this MPG with project funders and policymakers. Data collected throughout the MPG demonstrate that populations are currently density-dependent, and hatchery supplementation will not necessarily result in a sustained increase of smolts or returning adults (Venditti et al. 2018). To better understand this issue and what can be done to reverse this trend, project partners have worked to implement a new approach – including the IRA and subsequent MRAs.

Study Area

The Upper Salmon River subbasin includes the Salmon River watershed upstream of the Middle Fork of the Salmon River (Figure 3). This area includes approximately 6,334 square miles located within the Northern Rocky Mountain System physiographic region that comprises extensive parallel mountain ranges, intermontane valleys, and plateaus. Elevations in the watershed range from a low of 3020 feet at the confluence of the Middle Fork Salmon River to the numerous high mountain ranges in the headwater areas, climbing to around 11000 feet. The eastern part of the subbasin (Lemhi and Pahsimeroi watersheds) falls within the Middle Rockies Level III Ecoregion, which is characterized by linear mountain ranges of mixed lithology with large intermontane valleys. Land use includes logging, mining, and livestock grazing. Land cover includes spruce and fir in the uplands and predominantly shrub and grass-covered valleys. The western part of the subbasin (Panther Creek, Valley Creek, East Fork, and Upper Salmon River headwaters) falls within the Idaho Batholith Level III Ecoregion, which is characterized by dissected, partially glaciated, mountainous plateau with granitic lithology and deeply weathered acidic soils. Land use includes logging and grazing. Land cover includes spruce and fir in the uplands and pine, shrubs, and grasses in the valleys.

Major tributaries within the Upper Salmon River subbasin include the Upper Salmon River (above Redfish Lake Creek), Valley Creek, Yankee Fork Salmon River, East Fork Salmon River, Pahsimeroi River, Lemhi River, North Fork Salmon River, and Panther Creek. This IRA report includes high-level hydrologic, biologic, and geomorphic assessments for three of the watersheds: Lemhi River, Pahsimeroi River, and the Upper Salmon River upstream of Redfish Lake Creek.

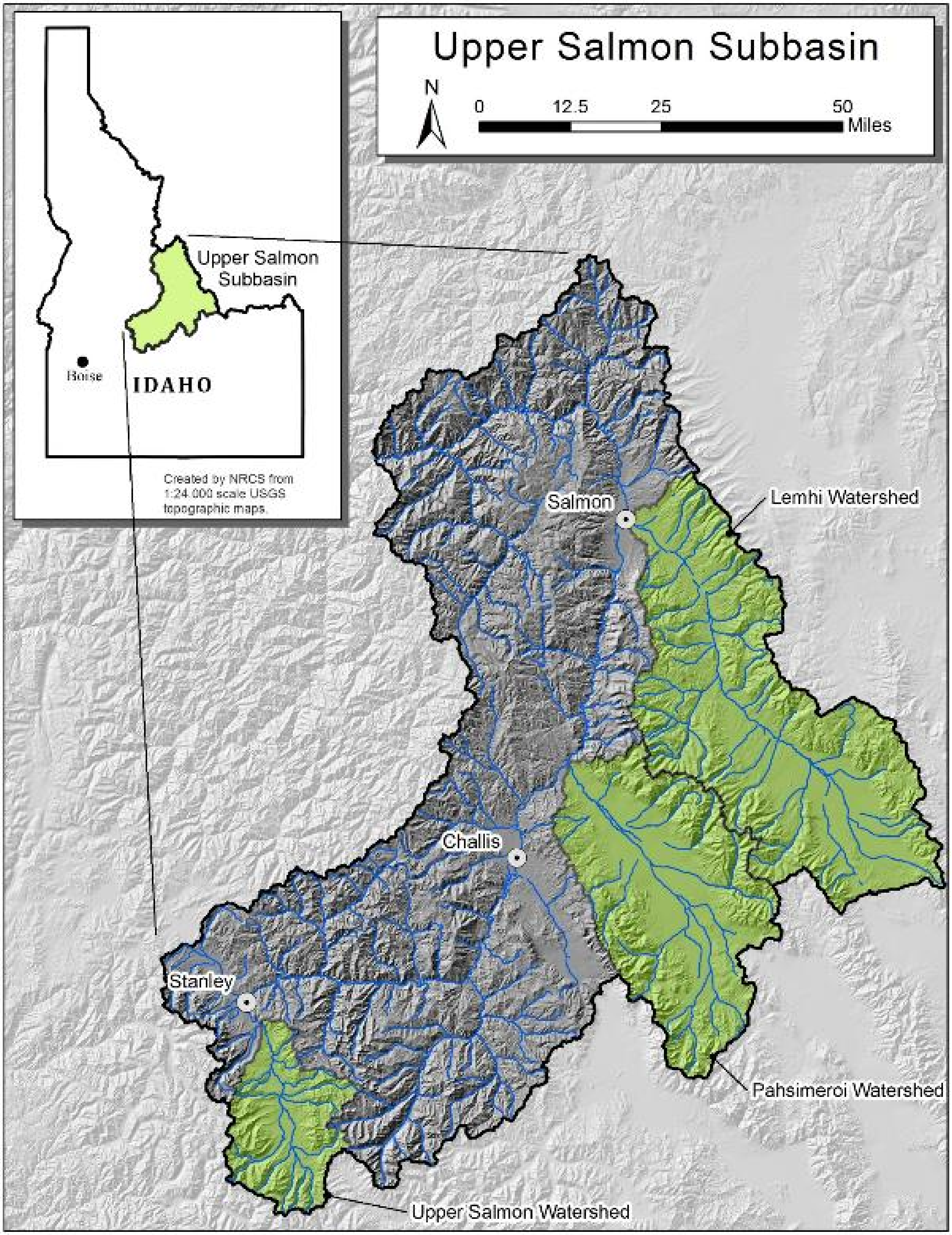

Figure 3. Upper Salmon subbasin (upstream of the Middle Fork Salmon River) vicinity map illustrating the three watersheds assessed in this report – Lemhi, Pahsimeroi, and Upper Salmon (upstream of Redfish Lake Creek).

Document Structure

The IRA document is structured as follows:

- **Section 1**: **Introduction, Background, and Approach.** Section 1 provides a high-level context for the IRA approach. Section 1 also provides rationale and relevant background for the IRA and an explanation of the overall assessment approach.
- **Section 2**: **Upper Salmon Basin Key Conclusions and Recommendations.** Section 2 provides high-level results from the IRA for focus populations and also for the Upper Salmon MPG (Chinook salmon) as a whole.
- **Section 3**: **Watershed-Level Results.** Section 3 provides more detailed results for the focus watersheds and is presented as three chapters, one for each of watershed (Lemhi River, Pahsimeroi River, Upper Salmon River above Redfish Lake Creek).
- **Appendices**: Appendices contain the greatest level of technical detail included in this document. Appendices provide additional context and background and are excluded from the main document for brevity. Four appendices are provided, including:
  - **Appendix A**: Detailed description of the spatially and temporally continuous temperature model used to evaluate potential temperature impediments at the watershed scale.
  - **Appendix B**: Detailed information on Quantile Regression and Random Forest (QRF) models developed for the spawning (redd), summer (parr), and winter (presmolt) life stages of Chinook salmon and steelhead. QRF models were used to estimated available habitat.
  - **Appendix C**: Detailed descriptions of habitat capacity requirement models used to estimate the amount of habitat necessary to support various levels of adult escapement, including escapement required for delisting (NOAA 2017) and recovery.
  - **Appendix D:** Detailed evaluation of watershed hydrology including peak flow frequency estimates, stream power assessments, discharge and water surface elevation measurements, and bottom sediment characteristics for the Lemhi, Pahsimeroi, and Upper Salmon watersheds.

Attribute Definitions

Summarized below are the geomorphic attribute definitions used to characterize the three watersheds in subsequent chapters. These definitions are listed one time here to provide context for the remainder of the report and to reduce potential redundancy within each of the three watershed chapters that follow.

- Valley Segment: spatial units delineated by HUC-10 confluences.
- Reach: spatial units delineated based on changes in measured valley confinement (entrenchment ratio), significant grade controls, and observed channel response characteristics.
- River Miles: measured along the centerline of the channel as interpreted from aerial photos from downstream to upstream.
- Valley Slope (ft/ft): change in elevation of reach divided by the centerline valley length.

- Average Valley Width (ft): approximation of valley width determined by taking the average of characteristic cross-sections of the assumed floodplain area interpreted from aerial photos.
- Average Constrained Valley Width: approximation of valley width (after accounting for road embankments and/or levees) determined by taking the average of characteristic cross-sections of the assumed floodplain area interpreted from aerial photos.
- Channel Slope: change in elevation of reach divided by the centerline river length.
- Average Channel Width: approximation of channel width determined by taking the average of characteristic cross-sections of the in-channel flow area interpreted from aerial photos.
- Sinuosity: channel centerline length divided by valley centerline length.
- Entrenchment Ratio: average valley width divided by average channel width.
- Constrained Entrenchment Ratio: average constrained valley width divided by average channel width.
- Human Disturbance Ratio (%): linear feet of mapped human features within 50 feet of the channel centerline, divided by the linear feet of mainstem channel per reach.
- Groundwater Characteristics: defines whether the reach is gaining, neutral, or losing surface flows due to groundwater seepage/springs, based on measured seepage runs, where available.
- Geomorphic Characterization: linear feet of mapped channel unit length (including side channels, main stem, and split-flow channels) characterized as Complex, Mixed, or Simplified, divided by total mapped linear feet of reach length (including side channels, mainstem, and split-flow channels).

Background

Integrated Rehabilitation Assessment

In 2015, Reclamation approached the Upper-Salmon Basin Watershed Program (USBWP) with the desire to collaborate on the completion of a TA for one watershed in the Upper Salmon River with goal of subsequent Reach Assessments (RAs) within that tributary to support more beneficial investments in tributary habitat enhancements. This was similar to the recent effort completed in the Yankee Fork of the Salmon River with Reclamation, the Shoshone-Bannock Tribe, Bonneville Power Administration (BPA), Trout Unlimited (TU), the U.S. Forest Service (USFS), OSC and others. After discussion, the USBWP concluded that the TA approach would benefit from the inclusion of newly developed fish/habitat relationships, clearly stated biological goals, and the application of these techniques to an entire MPG/DPS. A Request for Proposals was subsequently released by Reclamation to support the development and implementation of this new habitat assessment framework.

It was clear early in the proposal process that most partners in the USBWP were working at capacity; therefore, multiple contractors partnered with elements of the USBWP in proposal development. The Idaho Governor's OSC and the interdisciplinary team of Rio Applied Sciences and Engineering (Rio ASE), Quantitative Consultants Inc. (QCI), the Nature Conservancy (TNC), and TU (collectively the IRA Team) successfully competed for the development of the new habitat assessment framework and were awarded a Cooperative Agreement with Reclamation. The scope of the Reclamation Cooperative

Agreement included both the concept of a biologically enhanced TA known as the Integrated Rehabilitation Assessment (IRA) and multiple RAs now referred to as Multiple Reach Assessments (MRAs) across the entire Upper Salmon MPG/DPS over a 5-year period. The publication of this document marks the completion of the IRA and initiation of the MRAs. The high-level findings of the IRA process presented here are intended to guide current habitat enhancement efforts and the development of the MRAs, and will be broadly communicated to stakeholders, funders, and practitioners. The development of the MRAs marks the initiation of direct participation by the aforementioned groups through local technical teams in the Lemhi and Pahsimeroi River watersheds, and through the newly established Upper Salmon technical team subcommittee.

Salmonid Life History

Chinook salmon and steelhead are anadromous salmonids that emigrate from freshwater to the ocean as juveniles, returning to freshwater tributary habitat as adults for spawning. The life history stages of Chinook salmon and steelhead occurring in tributary habitat can be described briefly as spawning (redd construction), summer juvenile rearing (parr), overwinter juvenile rearing (presmolt), and emigration from tributary habitat in the spring (smolt). Chinook salmon in the Upper Salmon River MPG are stream-type, in which juveniles emigrate from tributary habitat to the ocean in the spring after the overwinter (presmolt) period. Similarly, steelhead within the Salmon River DPS, which includes the Upper Salmon Subbasin, may spend multiple years in tributary habitat, and most commonly emigrate from tributary habitat to the ocean in the spring. Although the tributary requirements for redd construction, summer rearing, and overwinter rearing share some commonalities, they occur over different seasons and spatial extents within tributary habitat.

This life history pattern can be described using a cone diagram (Figure 4), in which the width of the cone reflects the volume of habitat used by a given life stage. As juveniles transition from one life stage to the next, there is sufficient habitat capacity to provide the necessary PBFs for surviving juveniles under ideal conditions (Figure 4, optimal). Habitat degradation, or a reduction in habitat capacity, decreases the number of juveniles surviving to a subsequent life stage, and fewer juveniles survive to emigrate as smolts (Figure 4, actual).

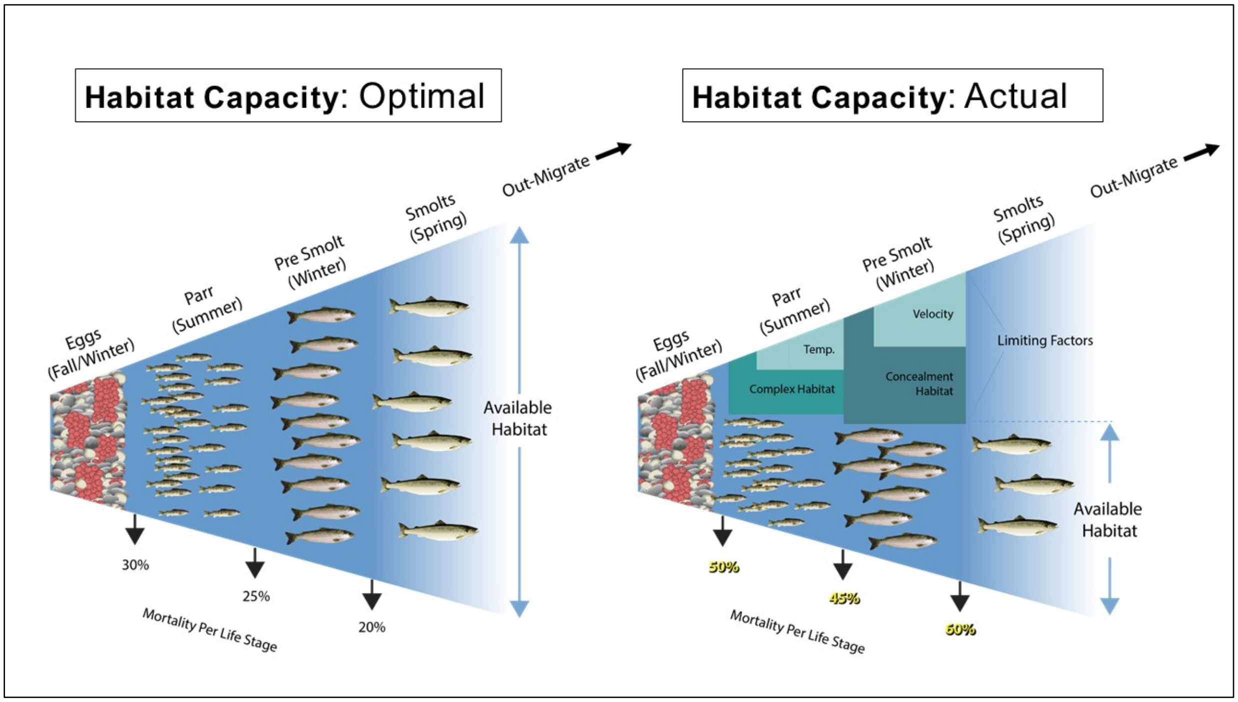

Figure 4. The chart above depicts an ideal scenario on the left with no limiting factors, while the graphic on the right depicts a river with significant limiting factors resulting in less habitat capacity and less production.

Here, the IRA focuses on Chinook salmon life stages and habitat preferences for those life stages. However, the framework assumes that any habitat rehabilitation actions aimed to improve conditions for a Chinook salmon life stage will also improve habitat for similar steelhead life stages. Steelhead life stages will be further explored in future assessments.

Chinook Salmon Life-Stages and Habitat Preferences

The geomorphic character defining the physical conditions also influence aquatic habitat. Some characteristics affect local habitat conditions (i.e., pool formation, bed armoring, and lack of cover) and others are more systemic (i.e., fine sediment and temperature) (Figure 5). Generally preferred habitat characteristics for key life-stages of spring/summer Chinook salmon are briefly described here.

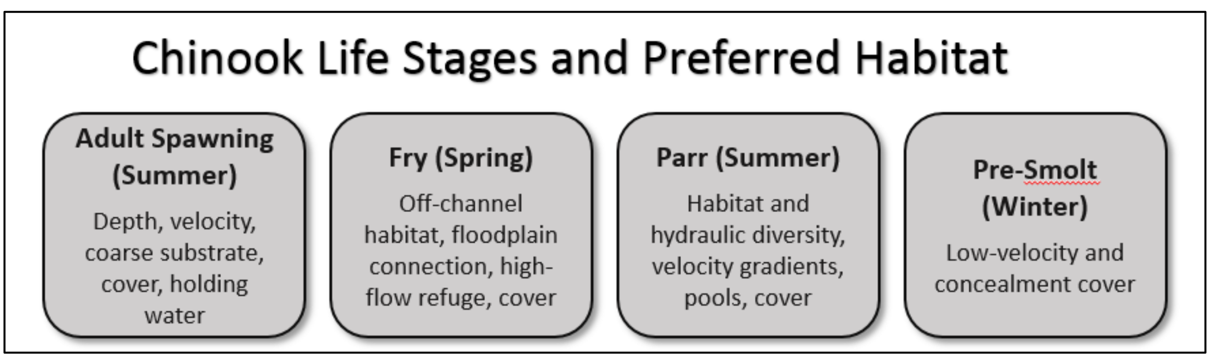

Figure 5. Summary of Chinook salmon life stages and key physical attributes associated with known habitat preferences.

Adult Spawning (Summer): Loose gravel/small cobble substrate, hyporheic flow to provide oxygen for eggs, water temperatures within stressful/lethal thresholds, pool/riffle complexes, proximity to cover or holding water, large woody debris, undercut banks, adequate depth and velocity (Photograph 1).

Photograph 1. Examples of preferred habitat conditions for Chinook salmon adults (summer) holding and spawning, including appropriate cover and substrate accumulated in conjunction with instream woody material and healthy riparian vegetation. The left photograph is from the Middle Entiat River, Washington, and the right photograph is from the Upper Yankee Fork Salmon River.

Fry (Spring): Low- to zero-velocity streamflow, off-channel habitat, floodplain connection, low-velocity refugia, overhanging vegetation cover, presence of aquatic vegetation, large woody debris, interstitial spaces (Photograph 2).

Photograph 2. Example of preferred habitat conditions for Chinook salmon fry (spring) rearing with very low velocity and abundant cover. Photographs are from the Upper Yankee Fork (left) and Upper South Fork of the Salmon River (right).

Parr (Summer): Hydraulic diversity and habitat heterogeneity, velocity gradients, frequent pools, vegetation and large woody debris cover, undercut banks, summer temperatures below stressful/lethal thresholds, velocity refugia (Photograph 3).

Photograph 3. Example of preferred habitat conditions, including split flow, instream cover and hydraulic variability, which support Chinook salmon parr (summer) rearing. Photograph is from a constructed project in Catherine Creek in the Grande Ronde River watershed, Oregon.

Pre-smolt (Winter): Interstitial spaces for concealment, additional concealment cover (e.g., vegetation, large woody debris), deep pools, low velocity, coarse substrate (Photograph 4).

Photograph 4. Examples of preferred habitat conditions for Chinook salmon pre-smolt (winter) rearing. Note large substrate (left) and dense woody material (right), both with significant interstitial space providing concealment cover for overwinter rearing. Photographs are from the Secesh River (left) and Catherine Creek in the Grande Ronde basin (right).

Historical Habitat Conditions

The existing Upper Salmon River subbasin was formed by a complex series of geologic events spanning more than 1 billion years. Prior to the formation of the Pacific Ocean, approximately 1.5 billion years ago, thick layers of sedimentary rock (Belt Supergroup) were deposited within a vast inland lake that spanned much of Idaho, Montana, and parts of eastern Asia (Winston and Link 1993). As the Pacific Ocean formed between Asia and North America, subsequent layers of sedimentary rock were deposited more than 100 million years ago along the continental margin, which covered much of Idaho, since the Oregon and Washington land mass had not yet formed (Link and Janecke 1999). These sedimentary rocks were uplifted and severely folded and faulted about 60 million years ago during the formation of the ancestral Rocky Mountains (Link and Janecke 1999). At roughly the same time, the subduction of the ancestral oceanic tectonic plate beneath the continental tectonic plate resulted in the emplacement of the granitic Idaho batholith, a large body of igneous granitic rock that comprises much of central Idaho (Johnson et al. 1988). Displacing and covering portions of the Idaho Batholith along its eastern margin were layers of volcanic rock deposited by a series of caldera-forming eruptions that created the Challis Volcanic Group about 45 million years ago (Moye et al. 1988).

Over the past several million years, the continental crust has expanded in parts of central and eastern Idaho due to the nearby Yellowstone hotspot (Pierce et al. 2007). Extensional faulting associated with the expansion has lowered some blocks of the crust, creating valleys, and raised others, forming mountain ranges (Simpson and Anders 1992). The previously deposited rock formations were faulted along roughly northwest-trending lines forming the Sawtooth, Pahsimeroi and Lemhi valleys (lowered blocks) and Sawtooth, Lost River, Pahsimeroi, Lemhi, and Beaverhead mountain ranges (raised blocks). The valleys have since partially filled with thick deposits of alluvial sediment from multiple episodes of hillslope erosion, mass wasting, stream deposition, and glacial deposition prior to and during the last ice age (Figure 6) (Meinzer 1924; Ungate 1988; Pierce and Scott 1982; Breckenridge et al. 1988). These thick alluvial deposits generally permit the presence of a local aquifer. Over the past several thousand years, streams have incised through surficial deposits of the alluvial valley fill, intercepting the aquifer in several locations and creating terraces with inset floodplains.

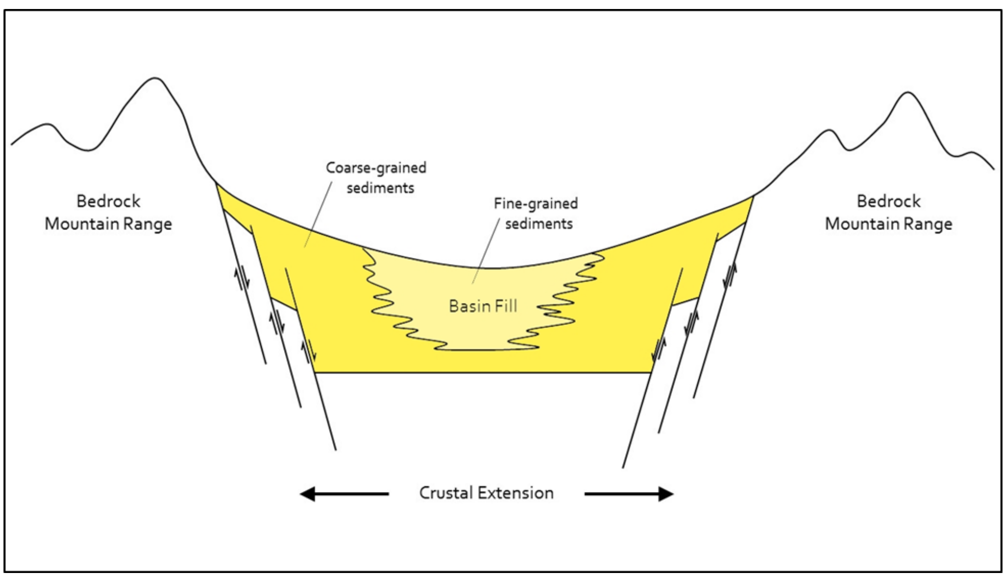

Figure 6. Generic basin-and-range faulting with valley fill sediment, illustrating how the Lemhi, Pahsimeroi, and Upper Salmon River headwaters have formed and partially filled with alluvial sediment.

In addition to the formation of the mountains and valleys in the Upper Salmon River subbasin, specific geologic features influence the existing channel character within each watershed uniquely. A prominent bedrock constriction roughly in the center of the Lemhi Valley provides local grade control, reducing upstream gradients and generally forcing greater groundwater contributions to the system upstream of that point. The depth of valley-fill alluvium in the Pahsimeroi Valley drives large shifts in surface-groundwater interactions throughout the watershed, with significant losses to the aquifer in the upper valley and large gains occurring in the lower valley. The Upper Salmon River headwaters are heavily influenced by glacial moraine deposits that extend well onto the valley floor, constricting the valley and creating moderately low gradient reaches, gaining from groundwater upstream of each constriction.

Common geomorphic characteristics associated with surface and groundwater interactions influence each of the watersheds assessed in this report. River reaches gaining flow from groundwater tend to exhibit similar traits, driven by geologic controls forcing groundwater to the surface, that also typically provide grade control, reducing upstream channel gradients. Prior to large-scale human disturbance, these heavily groundwater-influenced reaches were generally characterized by a highly sinuous, commonly multi-threaded (anastomosing) channel with multiple side channels and spring-fed tributary channels all occupying the same broad floodplain (Figure 7). The sediment regime was likely depositional (transport-limited), with varying amounts of coarse sediment, depending on the proximity to steeper reaches and tributaries supplying coarse sediment. Relic topographic variation from channel migration, occasional avulsions (the rapid abandonment of a river channel and the formation of a new river channel), beaver dams, and disturbance from grazing animals (bison, elk, and deer) likely created a mosaic of open water, emergent wetland, floodplain, and upland. The riparian community would have mirrored this diversity with areas of wetland meadow (rushes and sedges), floodplain shrubs (willow) and upland vegetation (sage and grass). The sinuous and multi-threaded channels likely exhibited a pool-riffle morphology (based on Montgomery and Buffington 1998) driven by sediment deposition, bank structure from willow vegetation, and in-stream woody structure (including beaver dams) where present (Figure 7).

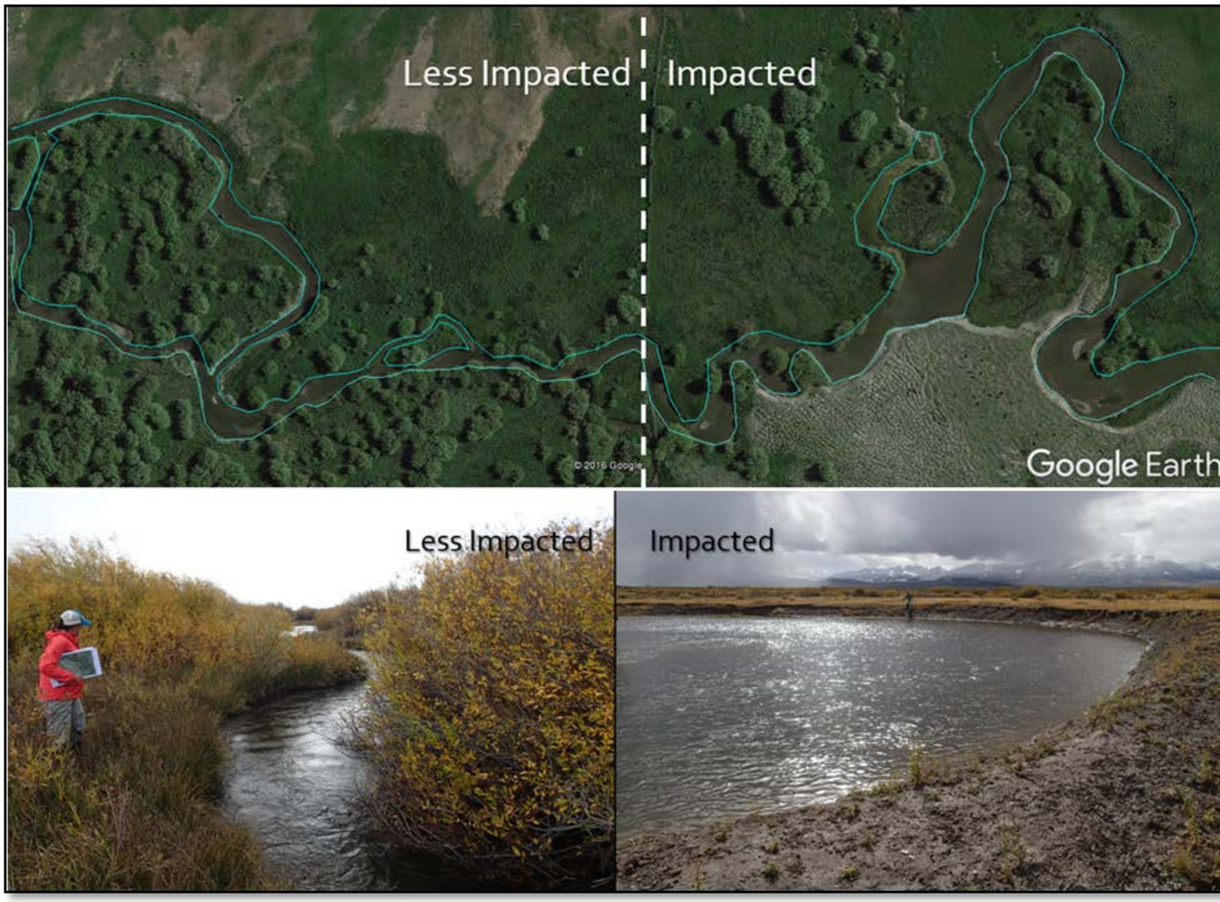

Figure 7. Representative example from the Upper Lemhi River illustrating groundwater-influenced characteristics, including a highly sinuous, multi-threaded channel with multiple spring-fed side channels and a diversity of riparian vegetation all occupying the same floodplain. Flow direction in the aerial photo is from right to left, and from the bottom of the image to the top in the surface photos.

Alternatively, river reaches that are either losing flow to the aquifer or are generally characterized by a predominantly snowmelt-influenced (i.e., peak flow) hydrology tend to exhibit different traits. Prior to large-scale human disturbance, these areas were generally characterized by a single-thread channel with active point bars, a seasonally active floodplain, and localized areas of island braiding where the stream is unconfined and in association with in-channel obstructions (i.e., log jams and/or stands of dense riparian vegetation) (Figure 8). The sediment regime was likely transport-dominated, with sufficient gradient and discharge to mobilize sediment and slowly incise the bed over thousands of years, creating a narrow, inset floodplain bound by relic terraces. The primarily single-threaded channel within the terraces was characterized by a relatively low sinuosity and a predominantly plane-bed morphology, although a forced pool-riffle morphology may have formed over small areas, given sufficient bank structure and/or woody debris loading (based on Montgomery and Buffington 1998). Areas that have been impacted by human activity, land use, and development are generally less sinuous, more incised, predominantly plain-bed, lacking in-stream structure, and no longer exhibit areas of complex island-braiding (Figure 8).

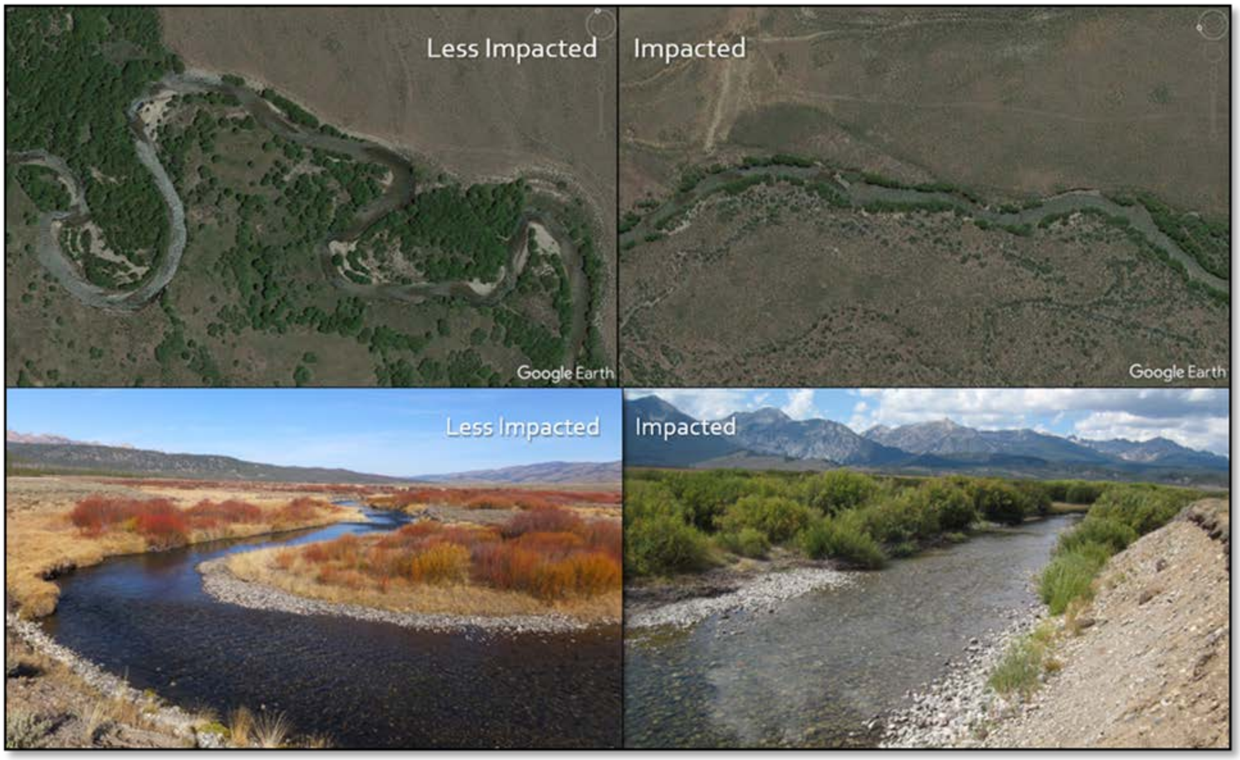

Figure 8. Representative example from the Upper Salmon River headwaters illustrating characteristics typical of a snowmelt-influenced (peak flow) hydrology, including a moderate to low sinuosity, single-thread channel, active point bars driving channel migration, and a predominantly plane-bed morphology. Flow direction is from the right side of the image to the left in the aerial photos and away from the photographer in the surface photos.

These generalized reach conditions, represented by the presence or absence of groundwater-influenced hydrology, exemplify the geomorphic character within each of the three watersheds assessed in this report. The Lemhi River is roughly split in half, with the Upper Lemhi (upstream of Hayden Creek) heavily influenced by the traits associated with groundwater hydrology, while the Lower Lemhi (below Hayden Creek) is more heavily influenced by traits associated with predominantly snowmelt-influenced hydrology. The Pahsimeroi River is the reverse of the Lemhi, with the Upper Pahsimeroi losing significant flow to the local aquifer and exhibiting primarily snowmelt-influenced characteristics, while the Lower Pahsimeroi is heavily groundwater-influenced. The Upper Salmon River headwaters is characterized by a predominantly snowmelt-influenced hydrology, with discrete areas of groundwater influence shaping individual reaches and sub-reaches, primarily upstream of prominent valley constrictions formed by glacial moraines.

Human Impacts

Relic and ongoing human impacts have significantly influenced channel character in all three watersheds. Many human-related impacts associated with visible features and/or relic or ongoing actions result in a less-complex, or more-simplified, geomorphic character. Overall, the physical and ecological processes in the upper tributary reaches are generally intact and functioning properly. However, there are localized impacts at mid- and lower elevations in all three watersheds that have negatively affected riverine process and form. These impacts include, but are not limited to, flow alteration from irrigation diversions, loss of riparian vegetation, excessive fine sediment, and areas of channel and floodplain alteration from roads and infrastructure.

Irrigation diversions significantly reduce instream flows by diverting tributaries away from, and flow out of, the mainstem rivers (Photograph 5). The many irrigation diversions in each watershed reduce the frequency and magnitude of peak flows, as well as the quantity of instream habitat through isolation (i.e., disconnected tributaries) and volume (i.e., linear feet of stream with adequate surface water). Irrigation diversions also alter the timing and spatial distribution of groundwater recharge. Diversions redistribute river water onto the floodplain during the summer months, artificially increasing groundwater levels in those locations. In some instances, the entire river has been diverted, leaving a dry, uninhabitable river bed that disconnects biologic and geomorphic processes between upper and lower river sections.

Photograph 5. Examples of irrigation diversions from the Upper Salmon River headwaters illustrating impacts to in-stream flow and fish passage.

Riparian vegetation has been removed to accommodate agriculture or lost due to overgrazing by livestock in many areas (Photograph 6). Where dense riparian vegetation (primarily willow) has been lost, the channel commonly exhibits an over-widened and homogenous channel character. Dense riparian vegetation on the outside of bends stabilizes the bank and obstructs flow, forcing contraction and resulting in pool scour and a narrow width-to-depth ratio, often with undercut banks. Dense riparian vegetation also promotes channel response via side-channel formation and avulsion around the structure provided by the vegetation, rather than bank erosion and widening when vegetation is lacking. A reduction in the amount of bank and instream structure has resulted in a simplified, homogenous channel in several areas, characterized by an over-widened, predominantly plane-bed morphology. The over-widened condition also expands the cross-sectional area of the channel between the banks, enabling more water to pass between the banks during floods, reducing floodplain connection frequency and duration. Finally, in all areas where woody riparian vegetation has been lost, the channel is exposed to greater solar radiation and thermal heating from the loss of shade.

Photograph 6. Examples from the Upper Lemhi (left) and Middle Pahsimeroi (right) Rivers illustrating impacts associated with riparian vegetation removal.

Grazing and agricultural practices, as well as the development of dirt roads and trails, have had a cumulative effect on fine sediment accumulation within each watershed (Photograph 7). Sheetwash erosion and excessive bank erosion associated with lost riparian vegetation contribute elevated levels of fine sediment to the system from spring snowmelt and summer rainstorm runoff. Similarly, sheetwash and wind-blown fine sediment from roads and trails add to the amount of fine sediment contribution from the watershed. Fine sediment fills interstitial spaces between gravels and cobbles, eliminating concealment cover for overwintering juvenile fish and reducing bed- and pool-scour potential through substrate embeddedness.

Photograph 7. Example from Lower Hayden Creek illustrating grazing impacts and associated lack of riparian vegetation.

Finally, channel and floodplain alterations from roads and infrastructure are prevalent throughout several reaches in each watershed. In many instances, portions of the channel have been straightened and confined to accommodate the infrastructure, and large portions of the floodplain have been disconnected from channel interactions (Photograph 8). Bridges commonly constrict bankfull and floodplain flow, often forcing contraction scour and incision, as well as a single-thread channel morphology. Channel-spanning weirs commonly obstruct the natural passage of fish and sediment. Bank armoring (i.e., riprap) prohibits natural channel migration and often concentrates flow along a hydraulically smooth surface, increasing rates of bank erosion and incision farther downstream.

Photograph 8. Oblique aerial photograph example of a straightened and armored section of the Upper Lemhi River just upstream of the Hayden Creek confluence.

Climate Change

The quantity, quality, and availability of tributary habitat is non-stationary, owing to natural and anthropogenic influences (e.g., as discussed in Budy and Schaller 2007). Thus, when considering the amount and/or types of restoration required to achieve long-term population stability, it would be shortsighted to assume that background conditions will remain static. For example, Dalton et al. (2013) documented a roughly 0.7° C increase in Pacific Northwest air temperature since 1900. Mantua et al. (2010) suggest that increases in air temperature may be accelerating and estimate a less than 1° C increase by 2020 and a 2 to 8° C increase by 2080. Even if water temperature currently does not impose an ecological limitation on the freshwater productivity of salmonids, anticipated changes in water temperatures could limit productivity. Processes that result in increased water temperature, and restoration to mitigate those processes, are often complex, typically relying on the reestablishment of riparian zones and reconnection of surface water and the alluvial aquifer (Poole and Berman 2001). Given that these restoration processes may require decades to achieve full effectiveness, early identification of future impairments is crucial.

Air and water temperatures in central Idaho are predicted to increase over time. While changes in air temperature can be somewhat reliably modeled, changes in precipitation are less predictable, ranging from a 4.7 percent reduction to a 13.5 percent increase (Mantua et al. 2010). The timing of snowmelt, and subsequently the seasonal availability of water, is expected to change substantially. Within the Snake River basin, a 3° C increase in air temperature would be anticipated to result in a decrease of 15 to 20 percent in spring stream flow, a 10 to 40 percent decrease in summer streamflow, and a substantial increase in winter streamflow (Tang et al. 2012).

Historical average streamflow projections (1950-1999) in Figure 9 (top panel) suggest that these sites are characterized by a late-spring/early-summer peak (April through July), with the largest average monthly values observed during June. Average monthly streamflows outside of the warm season (April through July) are typically lower in magnitude. Future streamflow projections (2000-2049) (middle panel of Figure 9) suggest that the average seasonal cycle across these sights is somewhat similar to historical conditions. The largest median percent increase is projected to occur in May (with a median increase from February through May), with the largest negative percent change projected to occur in June (with a median decrease from June through August).

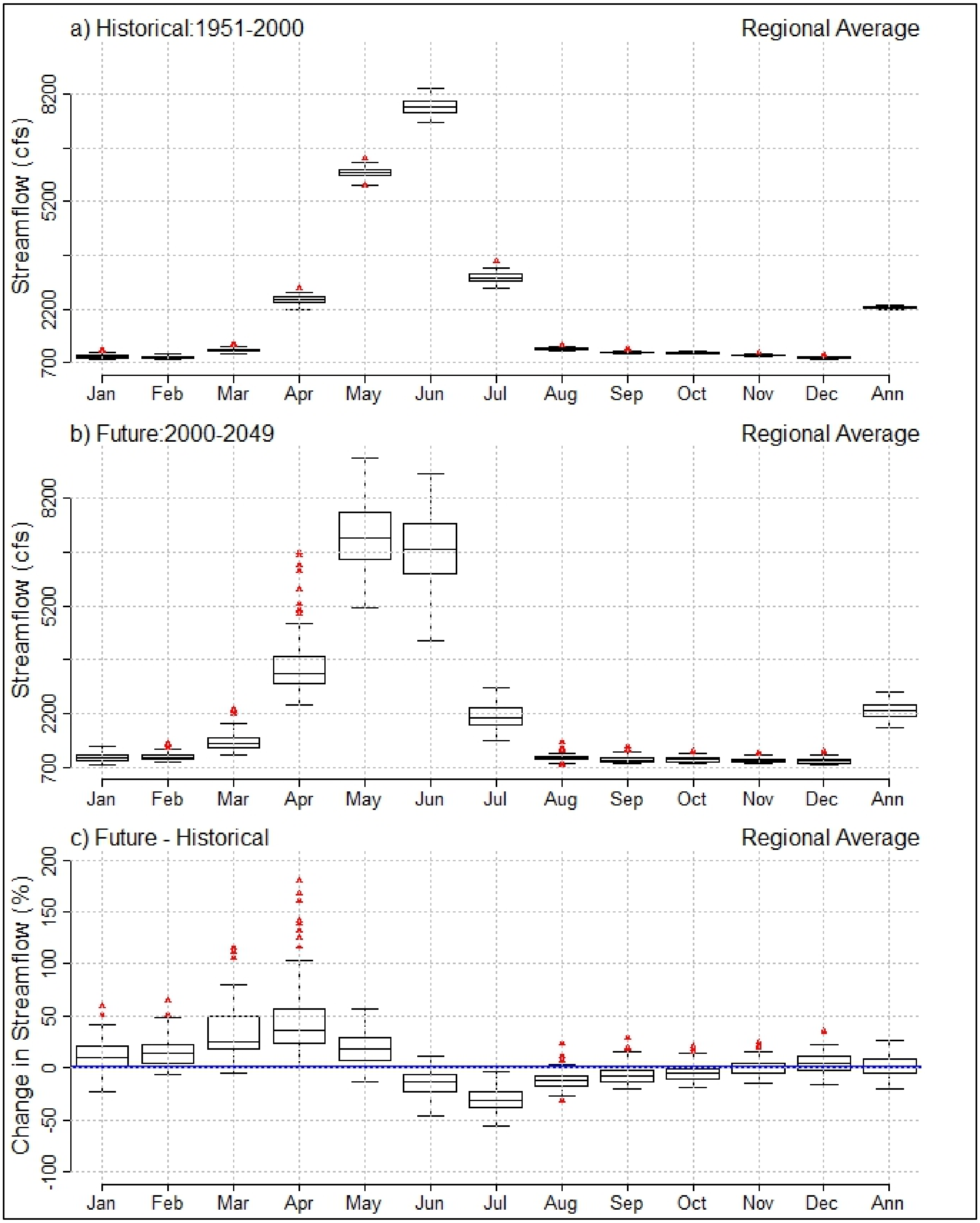

Figure 9. Box-and-whisker plot showing the distribution of regionalized average monthly and annual streamflow (cubic feet per second; cfs) during the (a) historical and (b) future periods for each of the 97 projection members. (c) Box-and-whisker plot showing the distribution of regionalized average monthly and annual percent changes in streamflow between the two periods (future-historical) for the same 97 projection members. The horizontal blue line in (c) demarks a 0 percent change.

Historical maximum streamflow projections (1950-1999) in Figure 9 (top panel) suggest these sites are characterized by a late-spring/early-summer peak (April through July), with the largest maximum monthly values observed during June. Maximum monthly streamflows outside of the warm season (April through July) are typically lower in magnitude.

Future streamflow projections (2000-2049) (middle panel of Figure 9) suggest that the maximum seasonal cycle across these sites is somewhat similar to historical conditions. Maximum monthly streamflow values for the future period peak during the same time of the year (April through July), while monthly streamflow values outside of this warm season remain relatively low.

Projected percent changes in regionalized maximum streamflow (bottom panel in Figure 9) show a combination of increases and decreases throughout the year. The largest median percent increase is projected to occur in March (with a median increase from January through May and December), with the largest negative percent change projected to occur in July (with a median decrease from June through August).

Past Projects

Habitat improvement work with a variety of agencies, landowners, and partners in the Upper Salmon subbasin has been ongoing since before the 1980s. These actions are categorized as 1) screening irrigation diversions, 2) improving spawning and rearing habitat access by removing barriers, 3) adding habitat complexity (quantity and quality), 4) increasing instream flow, and 5) improving riparian habitat, mostly by reducing grazing impacts from livestock. Over this time period, more than 200 improvement actions and 100 screening actions have been completed in the Lemhi River watershed. About 70 habitat improvement actions and 20 screening actions have been completed in the Pahsimeroi River watershed. More than 75 habitat improvement actions and about 20 screening actions have been completed in the Upper Salmon headwaters.

Below are examples of implemented actions that have occurred in select reaches of the Lemhi River, Pahsimeroi River, and the Upper Salmon River in recent years.

Lemhi River

Lower Lemhi River actions have focused on improving instream flow during the irrigation season, as well as irrigation diversion consolidation screening, barrier removal for habitat access and tributary flow reconnection, and increasing floodplain and habitat complexity (Photograph 9).

Photograph 9. Example from a completed side-channel and bank/riparian improvement project from the Lower Lemhi River (Eagle Valley Ranch Phase 2, completed in 2016).

Upper Lemhi River actions have focused on grazing management to improve riparian habitat, irrigation diversion consolidation screening, barrier removal for habitat access and tributary flow reconnection, and increasing floodplain and habitat complexity (Photograph 10).

Photograph 10. Overview of mainstem Lemhi River habitat enhancement (Amonson Ranch) immediately following construction (left aerial photograph) and 5 years following construction (right photograph).

Pahsimeroi River

Pahsimeroi River actions have focused on instream flow improvement during the irrigation season, grazing management to improve riparian habitat, irrigation diversion consolidation screening, barrier removal for habitat access and tributary flow reconnection, and increasing floodplain and habitat complexity (Photograph 11).

Photograph 11. Large woody debris installed to provide bank habitat and improve pool scour on the Pahsimeroi River as part of the P-16 irrigation improvement project completed in 2016.

Upper Salmon River

Upper Salmon River headwaters actions have focused on diversion consolidation screening, barrier removal for habitat access and tributary flow reconnection, instream flow improvement during the irrigation season, grazing management to improve riparian habitat, irrigation, and increasing floodplain and habitat complexity (Photograph 12).

Photograph 12. The Pole Creek Diversion Replacement in the Upper Salmon watershed included improvements to an irrigation system and fish screen, providing increased instream flow for Pole Creek and the Salmon River. In addition, a diversion structure (left) that blocked fish passage was replaced with a fish-passable low-head rock weir and improved channel geometry (right).

Assessment Approach

From a biological standpoint, two overarching themes drive the thought process within the IRA framework: density dependence and the degraded status of fish habitat found in the Upper Salmon River subbasin. Notably, there has been a shifting baseline of perception of what good habitat is and what range of juvenile densities can be supported by good habitat. By the time Chinook salmon and steelhead were listed as threatened under the Endangered Species Act, many tributaries in the Upper Salmon River subbasin, and elsewhere, were disconnected from the mainstems of rivers; furthermore, the mainstem of many rivers did not provide complete connectivity. Massive amounts of effort and funding have since been put into reconnecting tributaries and providing flow for functional passage. After the herculean effort to re-water and reconnect tributary habitat, it is timely to look at the quality of the habitat. The question then becomes *"What does the habitat need to look like to support the Minimum Abundance Threshold (MAT) goals and how much of this habitat does there need to be?"* This IRA document aims to first identify the problem by identifying limiting life stages for Chinook salmon and steelhead in the Upper Salmon subbasin, and then identify capacity deficits in habitat. Future MRAs will attempt to identify broad solutions by further describing what the habitat should look like to support MAT goals.

The overall approach of the IRA is to integrate biological assessment results, including the habitat capacity modeling, with high-level geomorphic (hydrology, hydraulics) and temperature assessments, to form applicable results and conclusions. The intended outcomes include actions that capitalize on local expertise to improve implementation. These can then guide understanding of current conditions and future habitat enhancement activities. Following, we provide additional details for each the biological, geomorphic, and temperature assessments. We then provide overall conclusions and recommendations for the Upper Salmon subbasin as a whole, as well as more detailed results, conclusions, and recommendations for each of the three target tributaries (Lemhi River, Pahsimeroi River, and Upper Salmon River above Redfish Lake Creek).

Biologic Assessment

Snake River Chinook salmon and steelhead have been ESA-listed since 1992 and 1997, respectively. The State of Idaho and partners have since worked with the National Marine Fisheries Service (NOAA Fisheries) to develop the 2017 Recovery Plan (NOAA 2017). The plan develops MATs for extant populations across the Snake River basin that provide an easily adoptable biological target to guide tributary habitat enhancement. Because the MATs set forth in NOAA (2017) are assessed using a 10-year geometric mean, it is necessary to ensure that adult escapement into each tributary equals or exceeds MAT. To accommodate this, the IRA team included a 25 percent buffer (MAT + 25%) to ensure goals will be met or exceeded. A margin of safety also provides a buffer due to variability in ocean conditions, conditions in the downstream migration corridor, and potential climate change scenarios.

The biological assessment focuses primarily on Chinook salmon and secondarily on steelhead. The Lemhi and Pahsimeroi River Chinook salmon populations are included because those populations have had extensive habitat enhancement in the past 20 years and are critical to salmon recovery. The Upper Salmon population is also critical to recovery efforts and has different physical attributes compared to the other two watersheds.

Potential capacity deficits due to potential limitations in habitat quantity and quality were assessed at three life stages for both Chinook salmon and steelhead: spawning (redd) capacity, and juvenile rearing capacity during both summer (parr) and winter (presmolt) months. First, life-stage-specific capacity required to support both contemporary adult abundance and adult abundance to achieve recovery goals was estimated using Generalized Capacity Models (described in Appendix C). Following, currently available redd and juvenile rearing capacity were estimated using recently developed quantile regression and random forest (QRF) models (described in Appendix B). Finally, life-stage-specific required capacities were compared to available habitat capacities to identify capacity deficits for both Chinook salmon and steelhead.

Required Habitat Capacity

Having identified population-specific adult escapement goals, including MAT and a buffer (MAT + 25%), the framework uses population-specific empirical data, where available, to estimate the number of redds, summer parr, and winter presmolts expected or required to achieve those goals. For those species and/or populations/tributaries lacking empirical and/or juvenile abundance and survival data, we relied on information from neighboring populations or regions. The models used to estimate required capacity are described in detail in Appendix C; namely, we use the Generalized Capacity Model described therein. Our approach explicitly assumed that tributary habitat must be capable of supporting redd and juvenile abundance accompanying MAT + 25% to sustainably support and maintain that level of escapement. Ultimately, the required capacity model leads to an estimate of the number of redds, summer parr, and winter presmolt that the tributary habitat occupied by a given population must support.

In addition, the IRA evaluated whether currently available habitat is sufficient to support contemporary estimates of life-stage-specific requirements based on recent adult abundance. Required capacity was calculated using both the mean and maximum observed adult abundance from the target tributaries; similar to above, those adult escapements were propagated across life stages using a combination of empirical and literature values (Appendix C). Observed abundance data were available for the following:

- **Lemhi River:** Chinook salmon (2000-2016); steelhead (2010-2015)
- **Pahsimeroi River:** Chinook salmon (2000-2015); steelhead (2011-2015)
- **Upper Salmon River:** Chinook salmon (2011, 2013); steelhead (2011, 2013)

Available Habitat Capacity

The IRA uses recently developed QRF models that enable spatially continuous estimates of available habitat capacity given existing conditions and for key life history stages of Chinook salmon and steelhead. Currently, available QRF models allow evaluation of three anadromous life stages: 1) spawning capacity (i.e., the number of redds that can be supported), 2) summer juvenile rearing capacity (i.e., the number of parr that can be supported during summer months), and 3) winter juvenile rearing capacity (i.e., the number of presmolts that can be supported during winter months). The QRF models that estimate available habitat capacity using available habitat data with more detailed results are described in Appendix B.

We define habitat (carrying) capacity as the maximal abundance or load the habitat can support for a given species and life stage given current resources and habitat quantity and quality. The QRF models predict carrying capacity using empirically derived fish-habitat relationships, recently collected habitat data, and globally available attribute (GAA) data. The juvenile QRF models pertain to juvenile rearing in wadeable streams during both summer (parr) and winter (presmolt) months; the adult model assesses fish-habitat relationships for spawning areas and predicts habitat capacity to support redds. The habitat data used in the QRF model are from the Columbia Habitat Monitoring Program (CHaMP;

https://www.champmonitoring.org), and fish and habitat data were paired at CHaMP sites (e.g., 200 to 500 m) where fish survey data were available. Importantly, the QRF models place no constraints on fish-habitat relationships; instead, relationships are estimated from the data regardless of being positive, negative, linear, non-linear, etc. Based on the observed fish-habitat relationships, we then predict habitat capacity at any location using measurements of the same habitat covariates used to populate the model (i.e., at all CHaMP sites). Finally, predictions at CHaMP sites can be extrapolated across larger scales using an extrapolation model and GAA data.

In summary, inputs to the QRF models to estimate available habitat capacity include (additional details in Appendix B):

- **Paired fish and habitat data:** Habitat data used in the QRF models are available from CHaMP; paired fish abundance/density information from CHaMP sites are available from the Integrated Status and Effectiveness Monitoring Program (ISEMP). Paired fish-habitat data are used to identify habitat covariates most highly associated with observed fish densities at CHaMP sites. Fish-habitat relationships are then developed for select habitat covariates used in the QRF models.

- **Spatial extent information:** Predictions of available habitat capacity can be extrapolated to larger spatial scales (e.g., watershed, population). However, a spatial extent must be provided that determines the scale at which total available capacity will be extrapolated and predicted. The QRF model uses shapefiles of a list of Generalized Random Tesselation Stratified (Stevens and Olsen 1999, 2004) master sample sites that CHaMP sites were initially selected from. Shapefiles can then be trimmed for any given watershed to a domain used by Chinook salmon or steelhead. The domain for any given watershed was determined either by StreamNet (http://www.streamnet.org) or using expert opinion from location biologists. For the IRA, the Upper Salmon spatial extents were determined using local expert opinion (Mark Moulton, personal communication) based on observed distributions across recent decades. Lemhi River spatial extents were available from recent juvenile fish surveys (Braden Lott, personal communication); all other watershed extents were from StreamNet. The spatial extent of model extrapolation is an important consideration when estimating total available capacity in a watershed. Extrapolation to too large or small of a spatial extent can lead to overestimates or underestimates, respectively, of available capacity.

- **Globally available attribute data:** The QRF models can be used to estimate available capacity an any location where the habitat covariates used in the model are available (i.e., at all CHaMP sites). However, in the case of the IRA, the goal was to estimate total capacity for all watersheds in the Upper Salmon River subbasin. Therefore, an extrapolation model was used that leverages GAA data to make predictions at all master sample sites within the determined spatial extent.

The IRA provides estimates of available habitat capacity for two species (Chinook salmon and steelhead), three life stages (redds, summer parr, winter presmolts), and three watersheds (Lemhi, Pahsimeroi, Upper Salmon River above Redfish Lake). Additionally, Appendix B provides results for the remaining five watersheds in the Upper Salmon River subbasin, including: Valley Creek, Yankee Fork Salmon River, East Fork Salmon River, North Fork Salmon River, and Panther Creek.

Habitat Capacity Deficits

Finally, species and life-stage-specific habitat capacity requirements, described above, are then compared to estimated available habitat capacity (assuming existing conditions) via QRF models. This comparison identifies 1) the life stages that may be limited for a given species and watershed under current conditions and to achieve recovery, and 2) the relative amount of capacity deficit that exists as MAT + 25% is approached. Adult escapement served as the starting value to maintain consistency with delisting criteria, which are expressed as an adult escapement goal.

Geomorphic Assessment

All streams evolve over time, and human impacts have, in some instances, altered the rate, magnitude, and form of that evolution, potentially impacting instream and off-channel habitat. A geomorphic assessment measures and compares various channel characteristics over time to better understand past channel evolution and associated human influences to develop predictions regarding future channel evolution and possible enhancement opportunities. In an alluvial system, channel processes are continually working to maintain a fairly stable condition by adjusting numerous variables that are mutually interdependent. For example, channel geometry and shape change in response to fluctuations in peak flow and/or sediment supply, which in turn controls the amount and timing of erosion and deposition. Erosion occurs in portions of the channel where velocity increases enough to scour bed/bank material and transport it downstream. Meanwhile, deposition results in other portions of the channel where velocity decreases to a point where sediment cannot be maintained in transport. Defining the channel character as it relates to habitat, then identifying the geomorphic processes that shape and maintain those habitat features, informs the type, location, and relative level of effort for potential rehabilitation actions.

Channel character generally refers to the shape (form) of the channel and processes responsible for the creation and maintenance of those forms (e.g., sediment transport, large wood recruitment, channel migration, etc.). For the geomorphic assessment, channel forms were remotely mapped using a geographical information system (GIS), aerial photography, and available digital elevation models (10-meter and/or LiDAR where available). Available past reports and data regarding groundwater hydrology, irrigation diversions, fish habitat, riparian conditions, and geologic features were synthesized to expand the team's understanding of the geomorphic character. Hydrology information and associated hydraulic calculations provided further explanation regarding channel process with regard to flooding and sediment transport. Limited on-site observations and measurements were made in select locations to field-verify remotely mapped features, to document site-specific features not visible in remote data (pools, under-cut banks, bed and bank composition, riparian vegetation, etc.), and to observe the most recent changes in channel form. Individual stream segments were then divided into distinct geomorphic reaches and channel units based on the observed differences and/or similarities in channel form and process, as interpreted from the available data. Specific channel segments were further broken down into three geomorphic categories of Complex, Mixed, and Simplified and further described based on typical channel responses.

In an effort to consistently and systematically compare the diverse and variable geomorphic character within each assessed river, the dominant geomorphic character associated with each reach (thousands of feet) was mapped at the channel unit scale (hundreds of feet). Geomorphic character was divided among three categories (Table 1, Figure 10) and further described based on typical channel response.

Channel Units

Channel units were remotely mapped using GIS, the NAIP September 10, 2015, aerial photography, and with limited field observations. Similar geomorphic characteristics were grouped based on observed channel forms and interpreted channel response (Table 1). This channel assessment method was developed specifically for the high-level analysis of the IRA, understanding the limitations of available data and the upcoming refined reach-scale assessments in future MRAs. The goal of the channel unit evaluation was to compare overall channel character and likely response potential between reaches to inform high-level decision-making and future MRA prioritization.

Table 1. Geomorphic characterization and description.

Geomorphic Characterization	Description
Complex	Characterized by a sinuous, low-gradient, unconfined channel(s) with dense riparian vegetation. Typical channel response is **dynamic,** including split flow, avulsion, lateral channel migration, pool scour, riffle deposition, and floodplain connection.
Mixed	Characterized by a moderate sinuosity, variable width and confinement, often lacking dense riparian vegetation. Typical channel response is **variable,** including lateral and downstream channel migration, widening, pool scour, riffle deposition, and moderate floodplain connection.
Simplified	Characterized by a straight, high-gradient, confined channel with sparse riparian vegetation. Channel response is **minimal,** including bed armoring, incisions, bank erosion, and poor floodplain connection.

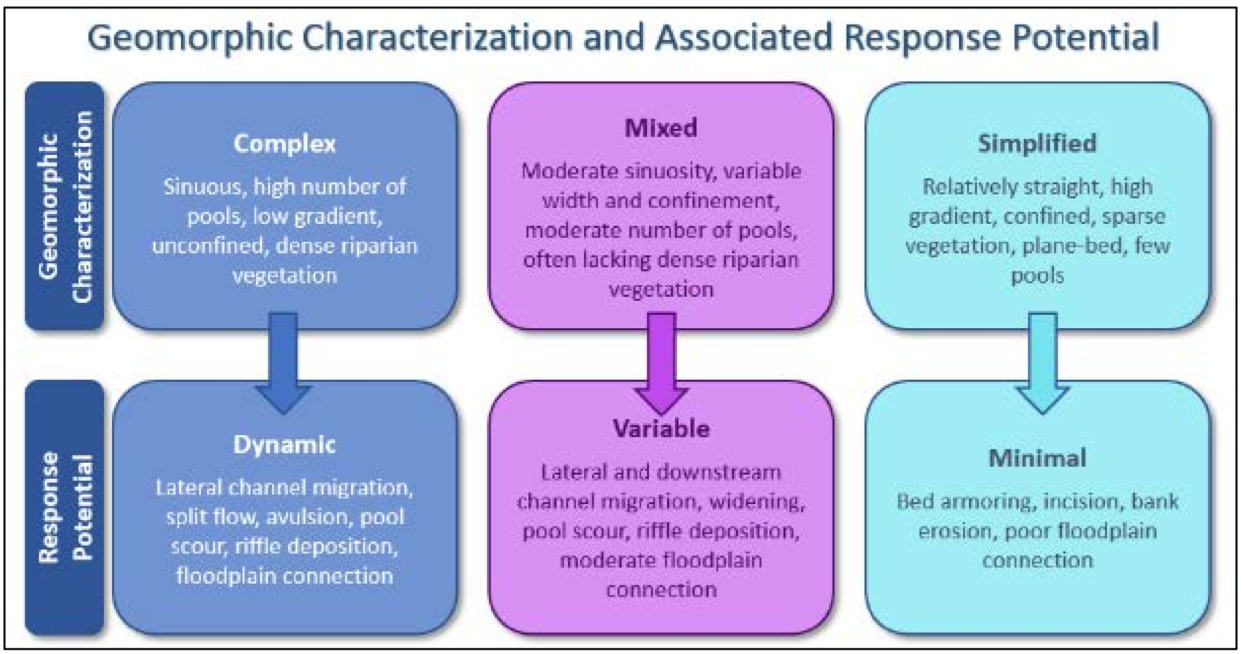

Figure 10. Geomorphic characterization and associated response potential as used to map individual channel units to differentiate and categorize reaches within the Lemhi, Pahsimeroi, and Upper Salmon Rivers.

A **complex** geomorphic character was assigned to channel units exhibiting two or more of the following characteristics: high sinuosity, multiple side channels, observable instream variability (including pools and riffles), moderately dense riparian vegetation, and an unconfined floodplain. The observed channel character in these areas suggest a **dynamic** geomorphic response potential when disturbed by high flow, significant sediment inputs, and/or channel obstruction. Dynamic channel response tends to increase channel complexity via lateral channel migration, split flow and avulsion, pool scour, sediment deposition, and floodplain activation (Photograph 13).

Photograph 13. Example of complex geomorphic character exemplified by the Upper Lemhi River with extensive riparian vegetation and sinuosity (left) and a larger channel in the Upper Salmon River with split flow and undercut banks. Photograph is looking downstream (right).

A **mixed** geomorphic character was assigned to channel units exhibiting two or more of the following characteristics: moderate sinuosity, primarily single-thread, variable width and confinement, comparatively few pools, and lack of dense riparian vegetation. The observed channel character in these areas suggests a **variable** geomorphic response potential when disturbed by high flow, significant sediment inputs, and/or channel obstruction. Variable channel response can either increase or decrease channel complexity via channel migration (lateral or downstream), channel widening, scour, deposition, and moderate floodplain activation (Photograph 14).

Photograph 14. Examples of mixed geomorphic character with excellent riparian structure in some areas but limited riparian vegetation in other areas due to land use activities, resulting in bank erosion and unnatural channel widening (Upper Pahsimeroi River on left and Upper Texas Creek, tributary to Lemhi River, on right).

A **simplified** geomorphic character was assigned to channel units exhibiting two or more of the following characteristics: fairly straight channel, high gradient, confined, lack of dense riparian vegetation, and minimal instream variability, including pools (i.e., plane-bed morphology). Simplified character was commonly associated with anthropogenic channel modification, including channel straightening, confinement, and bank armoring, although some channel units are naturally simplified, typically in high-gradient, confined reaches. The observed channel character in these areas suggests a **minimal** geomorphic response potential when disturbed by high flow, significant sediment inputs, and/or channel obstruction. Simplified reaches are typically sediment-transport dominated and often require much larger disturbances to evoke a significant response. Common channel response to disturbance includes incision followed by bed armoring, bank erosion, and poor floodplain activation (Photograph 15). Photograph 16 and Photograph 17 provide regional examples of pre- and post-habitat construction projects to improve simplified geomorphic conditions.

Photograph 15. Examples of simplified geomorphic character on the Lower Lemhi River, where the channel has been historically straightened and armored and riparian vegetation removed.

Photograph 16. Pre- and post-habitat construction project improving simplified geomorphic condition on Catherine Creek, Oregon.

Photograph 17. Pre- and post-habitat construction project improving simplified geomorphic condition on the Lower Pahsimeroi River, with multiple rootwad structures installed along the bank to reduce unnatural rates of bank erosion and provide fish habitat.

Reach Delineation

Reach delineation enables the categorization of similar attributes across a relatively broad spatial scale to facilitate data collection and analysis, providing consistency and efficiency in reporting, and ultimately, treatment. Areas exhibiting similar physical conditions are typically formed in the same way and therefore exhibit similar channel response character. Evaluating site-specific characteristics at one location within the reach can generally be extrapolated to the remainder of the reach, thereby greatly improving evaluation efficiency. Similarly, trends in channel response character can be assessed by comparing variation within the reach associated with site-specific disturbance. The response to a disturbance at a singular site represents likely response conditions to a similar disturbance at other sites within the reach. Additionally, systemic channel responses, such as incision, sediment transport, and flooding, tend to operate differently between reaches and may be controlled by reach-defining geologic or human grade controls (e.g., bridge, culvert, bedrock exposure).

Reaches were delineated within the project area by changes in measured valley confinement (entrenchment ratio) and observed channel response character (transport-limited response reaches versus supply-limited transport reaches). Response segments have a lower gradient in which significant morphologic adjustment occurs in response to increased sediment supply (Montgomery and Buffington 1998).

Hydraulics

Cross-sections were measured using a combination of LiDAR data (both land- and bathymetry-based, where available) and survey data from 2015 and 2016. Cross-sections were located in areas that were representative of the local reach based on aerial image interpretation. Cross-sections were obtained across the entire floodplain to assess existing conditions and observe potential historical differences. Cross-sectional elevation data were replaced with channel stage data, with a starting stage at the minimum elevation of the channel bed.

The cross-sections were analyzed using normal-depth water surface calculations for various flood frequency discharges at each site, based on the hydrologic methods described in Appendix D, to develop an approximate rating curve for the cross-section and to assess channel bed mobility. Normal-depth calculations were estimated using Manning’s equation, which is shown in Equation 1 below.

Equation (1)

$$Q = \frac{1.49}{n} A \left(\frac{A}{P}\right)^{\frac{2}{3}} S^{\frac{1}{2}}$$

Where: Q = Discharge (cfs)

n = Manning's Roughness

A= Cross-sectional Area (ft^2)

P = Wetted Perimeter (ft)

S = Channel Slope (ft/ft)

Cross-sections were assigned various Manning's n-values to represent the approximate channel and floodplain roughness at each site. A range of n-values was typically assigned within the channel and floodplain, while the average n-values were used in the reported hydraulic results. Local channel slope was estimated from approximate digital elevation model topographic slopes at each location. Cross-sectional area and wetter perimeter were calculated for each discharge estimate.

Hydraulic parameters estimated at these locations include top width, average channel velocity, average channel shear, average channel stream power, the approximate D_{50} mobilization discharge based on channel shear (i.e., incipient motion), the approximate entrenchment ratio, and the estimation of an armored or unarmored bed. Entrenchment ratio was approximated by dividing the 100-year water surface top width by the 1.25-year water surface top width. The bed was assumed to be armored if it took greater than a 5- to 10-year event to begin mobilizing the D_{50} sediment size determined from Wolman-style pebble counts (see Figures 39-41, 83-85, and 116-118 for specific cross-sectional information from the Lemhi, Pahsimeroi, and Upper Salmon Rivers, respectively).

Icing and Surface Water Interactions

River ice can be a powerful geomorphic forcing agent that influences channel-floodplain interactions, avulsions, and bed scour. River ice is generally composed of three phases: ice formation, growth, and break-up. Each phase is driven by several factors, including but not limited to, water and air temperatures, water depth and velocity, discharge, and ice transport or retention and jamming. During the winter months, low overall discharge and cold temperatures favor ice formation in turbulent areas that are not thermally buffered by major groundwater inputs. In these areas, anchor ice can form when the air temperature is well below freezing and the water temperatures quickly drop to the freezing point. Turbulent heat exchange draws bubbles of super-cooled air below the water surface, freezing the water around each bubble and creating small platelets of ice called frazil ice. These small platelets can collect in calm water, occupying the interstitial space between grains of cobbles and boulders on the river bed and banks, creating a progressively larger ice surface, which grows into blocks of anchor ice (Hammar and Shen 1995). Anchor ice can become large enough that the combination of shear and buoyancy can dislodge the ice, often disturbing the bed and/or banks in the process. Anchor ice also obstructs flow by occupying space within the cross-sectional area of the channel, increasing the potential for over-bank flow. Anchor ice is less frequently formed in deeper, less-turbulent areas, and/or areas influenced by warmer groundwater.

In addition to anchor ice, surface ice may also form on portions of the Lemhi River in areas of low water velocity, particularly along the banks. Surface ice accumulation can become significant, creating ice dams when broken apart at the end of the cycle during high flows. Surface ice sheets start growing across the tailouts of pools and runs, where flow velocities decrease to less than 1 ft/s. Once bank-to-bank ice cover forms, a process known as ice cover progression lengthens the cover in the upstream direction as arriving ice accumulates. Arriving frazil ice floes and slush can be drawn beneath the upstream edge of the ice cover to deposit in the form of a freeze-up ice jam. Flow conduits beneath the jams can become ice-clogged, forcing flow onto the surface of the ice cover and/or onto the floodplain.

Gradual ice break-up in the spring can extend over weeks, with minimal effect on the channel bed, banks, floodplains, and instream structures. Conversely, break-up ice runs can happen rapidly when the concentration of the moving ice floes exceeds the hydraulic conveyance capacity of the channel. These break-up ice runs can scour and erode the channel bed and banks, damage or destroy instream structures, and/or result in sudden flooding.

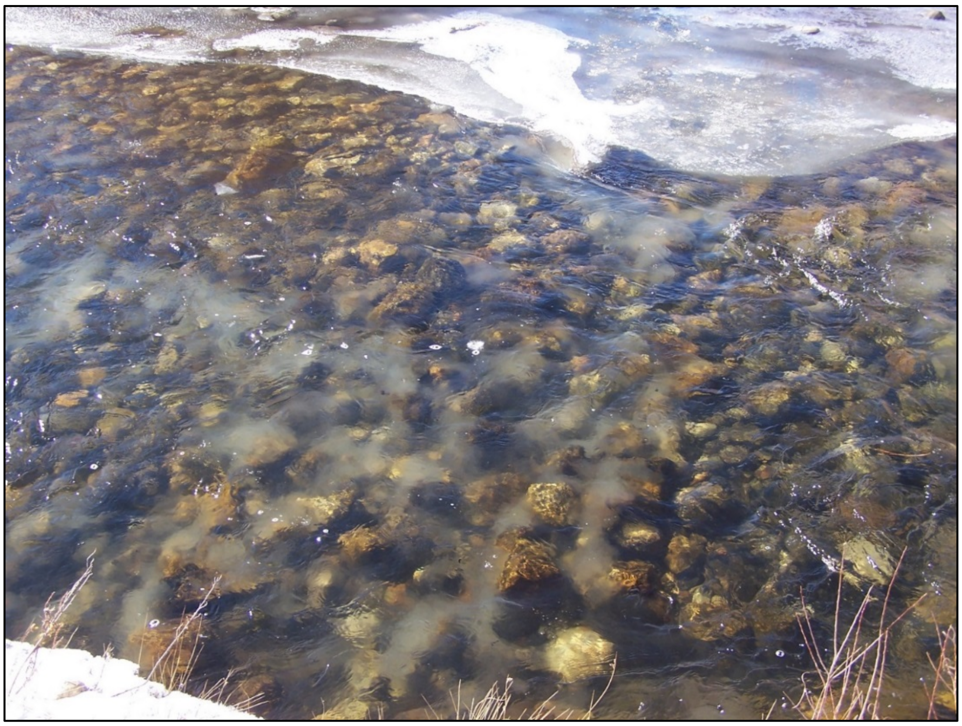

Photograph 18. Photograph illustrating how anchor ice can fill interstitial space and alter channel geometry. (Source: www.monolake.org/today/2008/12/18/hydrology-update-for-121808/)

Water Quality

Surface water quality standards apply to a waterbody, depending on its designated uses and/or existing uses. Pursuant to the Clean Water Act (CWA), Idaho recognizes existing uses, which are uses present or attained in a water body on or after November 28, 1975. When water bodies do not have designated beneficial uses, they are assigned a presumed use protection. All water bodies are classified for more than one beneficial use and must meet the fishable/swimmable intent of the CWA.

Under Idaho’s water quality standards, beneficial uses are categorized as aquatic life, recreation, water supply, wildlife habitat, and aesthetics. For the Upper Salmon River watershed, beneficial uses that are not fully supported are: (1) aquatic life, which includes salmonid spawning and cold-water aquatic life beneficial uses, and (2) and contact recreation that includes primary and secondary contact recreation.

The Idaho Department of Environmental Quality (IDEQ) completed a subbasin assessment for the Upper Salmon River watershed in 2003 (IDEQ 2003). Total maximum daily loads (TMDLs) were developed for water bodies not supporting their beneficial uses and impaired by a pollutant. In Idaho's 2002 Integrated Report (September 30, 2005), streams were converted from water-quality-limited segments to assessment units (AUs) based on Strahler Stream Order within a Waterbody ID.

Temperature and Climate Change Assessment

Temporally and spatially continuous water temperature models were developed for each of the target tributaries (Lemhi River, Pahsimeroi River, and Upper Salmon River above Redfish Lake Creek) to assess whether seasonal temperatures may limit the use of specific stream reaches for one or more life stages of anadromous salmonids. A combination of modeled temperature predictions and predictions of life-stage-specific temperature thresholds were used to evaluate whether current water temperatures might limit the ability of Chinook salmon or steelhead to use available habitat. Further, a simple warming scenario describing potential increases in stream temperature expected to result from climate change was used to assess whether the implementation of restoration actions to reduce temperatures may be necessary. The temperature model and species-specific temperature thresholds are described in more detail in Appendix A. Spatially and temporally continuous modeled water temperature data (McNyset et al. 2015) were available for the following:

- Lemhi River: 2011-2015
- Pahsimeroi River: 2011 and 2013
- Upper Salmon River: 2011 and 2013

Average modeled water temperatures (across years) for each of the watersheds were then compared to minimum, maximum, and acute temperature criteria adopted for various life stages of Chinook salmon and steelhead (Carter 2005) to identify seasons and life stages where temperature may be limiting.

Finally, an assessment was made to evaluate potential future limitations resulting from a climate change scenario. Although climate change could lead to a change in stream temperature, published estimates of anticipated changes in the Salmon River subbasin have not been found. However, by the year 2100, water temperature models for the Cook Inlet Basin, Alaska, suggest that water temperatures could increase by 1.2 to 7.1° C (Kyle and Brabets 2001). As an initial assessment, 3° C (a median value based on scenarios from Kyle and Brabets 2001) were added to average temperatures to evaluate how a potential climate change scenario might influence the vitality of Chinook salmon and steelhead. Combined with changes in the timing of water availability, increased temperature can be expected to exert a substantial influence on the timing of juvenile emergence, among other traits.

Biologic and Geomorphic Assessment Integration

The Upper Salmon River Subbasin IRA is a biologically driven assessment intended to guide the development of future assessments (e.g., MRAs) or habitat enhancement project development and implementation. To be actionable, however, the biological results provided herein must be integrated with a geomorphic assessment. First, the biological assessment identifies key Chinook salmon and steelhead life stages within each watershed that are limited. Potential effects to those life stages resulting from increased water temperatures associated with climate change are also acknowledged. Next, the geomorphic assessment identified physical forms and processes within each watershed and categorizes the relative geomorphic character as complex, mixed, or simplified. The biologic and geomorphic assessments are integrated by identifying the geomorphic character of preferred habitat for key life stages and identifying the relative level of rehabilitation effort required to improve habitat of an existing geomorphic character. The IRA team further applied fluvial geomorphology concepts to identify the most appropriate locations to focus future efforts (assessments and/or projects) to address factors or processes that limit these local fish populations. The biological and geomorphic analyses were closely coordinated with local professionals and stakeholders to leverage local knowledge and maximize local support. As a result of this work and planned follow-on, refined analyses (MRAs), designs and implementation efforts can be scientifically supported and strategically coordinated among local watershed teams and landowners.

Habitat rehabilitation actions can be undertaken to address identified limiting PBFs in priority areas, as discussed in Section 2 below. The level of rehabilitation effort will depend in part on the geomorphic character of the stream reach and the desired habitat conditions relative to capacity limitations within that reach. Depending on the intrinsic geomorphic character associated with each area, rehabilitation efforts may enhance or expedite existing geomorphic trends (passive treatments requiring less effort) or create new conditions otherwise unlikely to occur given existing impacts (active treatments requiring more effort). Generally, less rehabilitation effort is required in order to improve habitat in areas currently defined by complex geomorphic character, and greater rehabilitation effort is required in areas defined by simplified geomorphic character (Figure 11). An evaluation of the relative level of effort (i.e., cost) should always be contrasted with the likely potential benefit of a particular action when considering project identification and prioritization. Additional reach- and site-scale analysis may also be necessary, along with political, social, and funding considerations, in order to most appropriately prioritize and develop potential rehabilitation efforts.

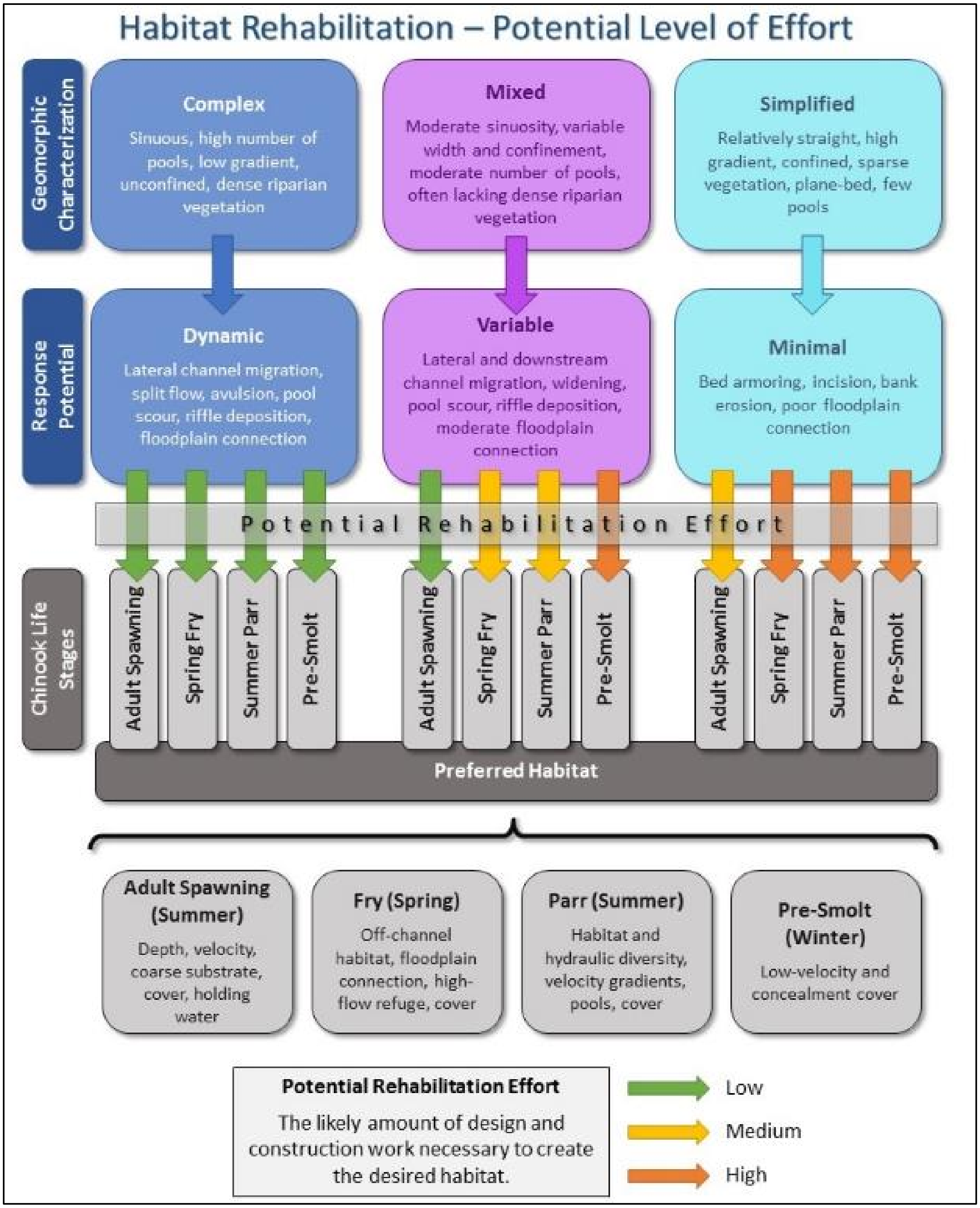

Figure 11. Summary of the habitat rehabilitation effort based on the relationship between geomorphic characterization and preferred habitat conditions per life stage. In general, more complex geomorphic character naturally yields conditions preferred by more life stages. Rehabilitation efforts may be undertaken within an area defined by any geomorphic character, but the level of effort required to elicit and/or maintain the desired channel response will vary, as illustrated in this figure.

Next Steps

The next steps will facilitate the transition from basin-wide efforts in this document to fill data gaps and provide higher-resolution information that informs future recovery efforts, including:

- Address data gaps using LiDAR; a juvenile salmon tracking study; and reach-scale geomorphic, hydraulic, and instream habitat data collection and evaluation;
- Expand capacity modeling to encompass the entire MPG; and
- Collaborate with local stakeholders to fill data gaps, share knowledge, and plan future efforts.

The above efforts are intended to help local practitioners and scientists identify and implement projects that maximize fish benefits and expedite recovery of ESA-listed species moving forward in the Upper Salmon River subbasin.

Section 2: Upper Salmon Subbasin Key Conclusions and Recommendations

Habitat Enhancement Recommendations Summary

This section includes a summary of key conclusions and recommendations associated with the Upper Salmon River subbasin as a whole, as well as for the Lemhi River, Pahsimeroi River, and Upper Salmon River headwaters, respectively. General and/or common conclusions and recommendations are summarized for the subbasin, while more specific details and recommendations are summarized for each respective watershed. In all instances, the conclusions and recommendations are supported by data and other information discussed in the following watershed-specific chapters and appendices.

Basin-wide Actions

Chinook Salmon Capacity Limitations

Across the Upper Salmon River spring/summer Chinook salmon MPG, we conclude that deficits in available summer and winter juvenile rearing capacity are the primary factor limiting growth of populations. As expected, estimates of available rearing capacity are sufficient to support contemporary mean escapements for the three watersheds (with the exception of Pahsimeroi winter rearing) (Figure 13 and Figure 14); however, available rearing habitat is not sufficient to support recent high escapement ,and the issue is exacerbated when evaluating requirements to support MAT and MAT + 25%. In contrast, our estimates of spawning (redd) capacity suggest that the adult spawning life stage is likely not limiting in the Upper Salmon River subbasin (Figure 12). Lastly, we conclude that seasonal variation in temperature is extreme, likely limiting growth in particular life stages and contributing to mortality.

Figure 12, Figure 13, and Figure 14 show comparisons of available habitat capacity from QRF versus capacity required to support various levels of adult abundance, including mean and maximum recent escapement, MAT, and MAT + 25% for the redd, summer (parr) rearing, and juvenile (presmolt) rearing life stages, respectively. Comparisons are for Chinook salmon and the three focal watersheds. Comparisons for the remaining five watersheds in the Upper Salmon River subbasin are provided in Appendix B.

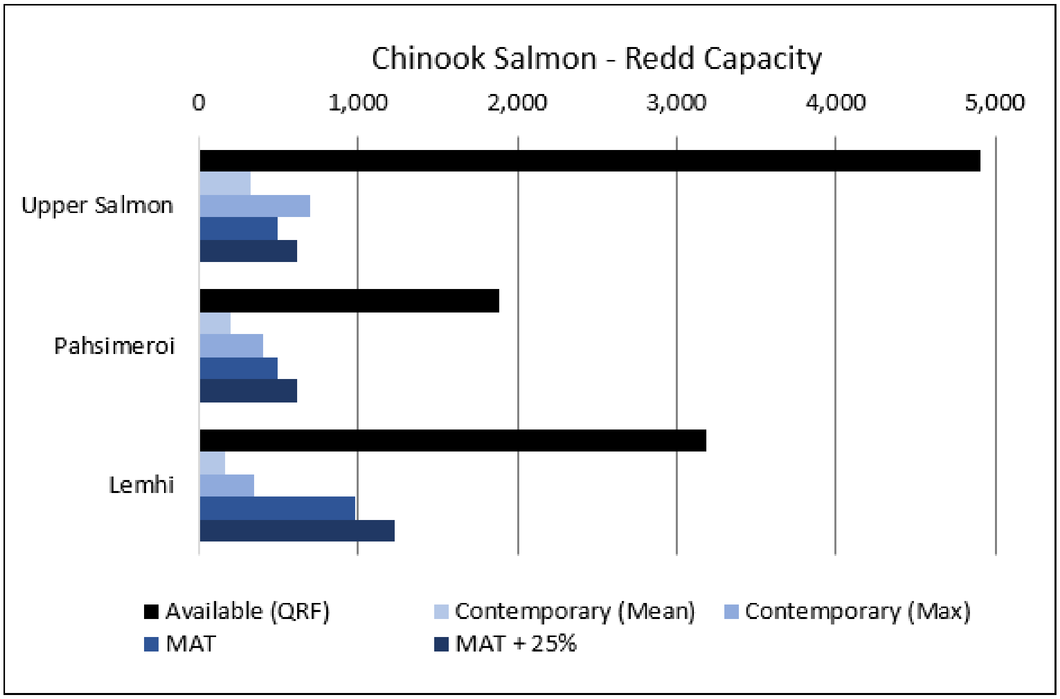

Figure 12. Estimates of available spawning (redd) capacity for Chinook salmon given current habitat conditions, made using quantile regression and random forest models (black bars) versus the capacity required to support contemporary abundance and minimum abundance thresholds (MATs) needed for ESA de-listing (blue bars).

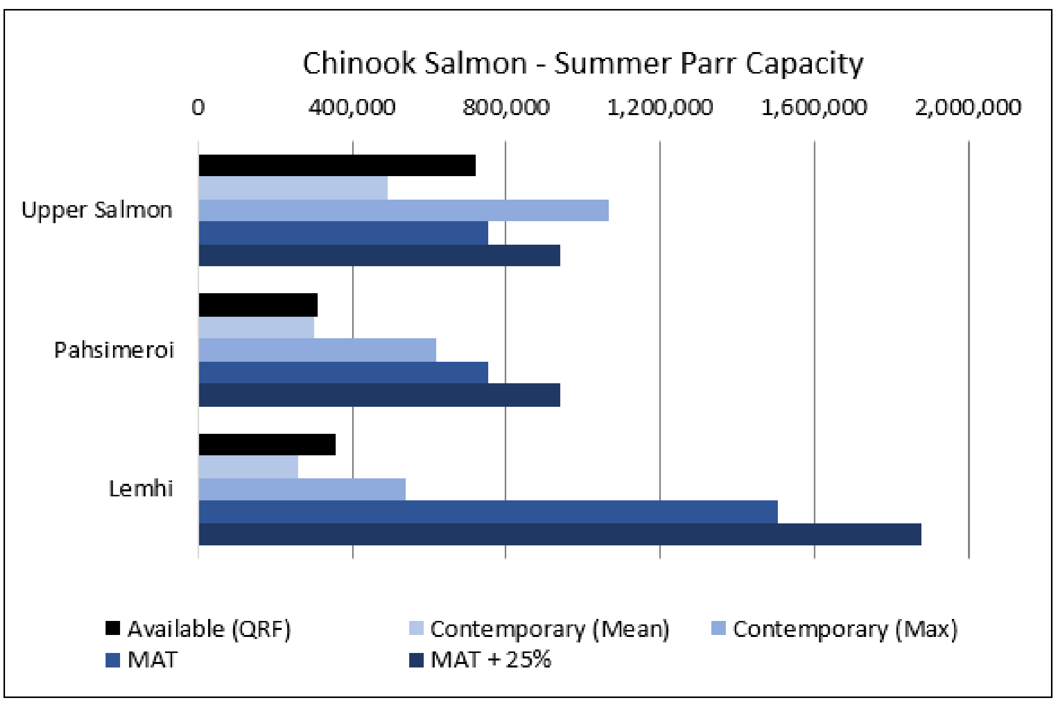

Figure 13. Estimates of available summer juvenile (parr) rearing capacity for Chinook salmon given current habitat conditions, made using quantile regression and random forest models (black bars) versus the capacity required to support contemporary abundance and minimum abundance thresholds (MATs) needed for ESA de-listing (blue bars).

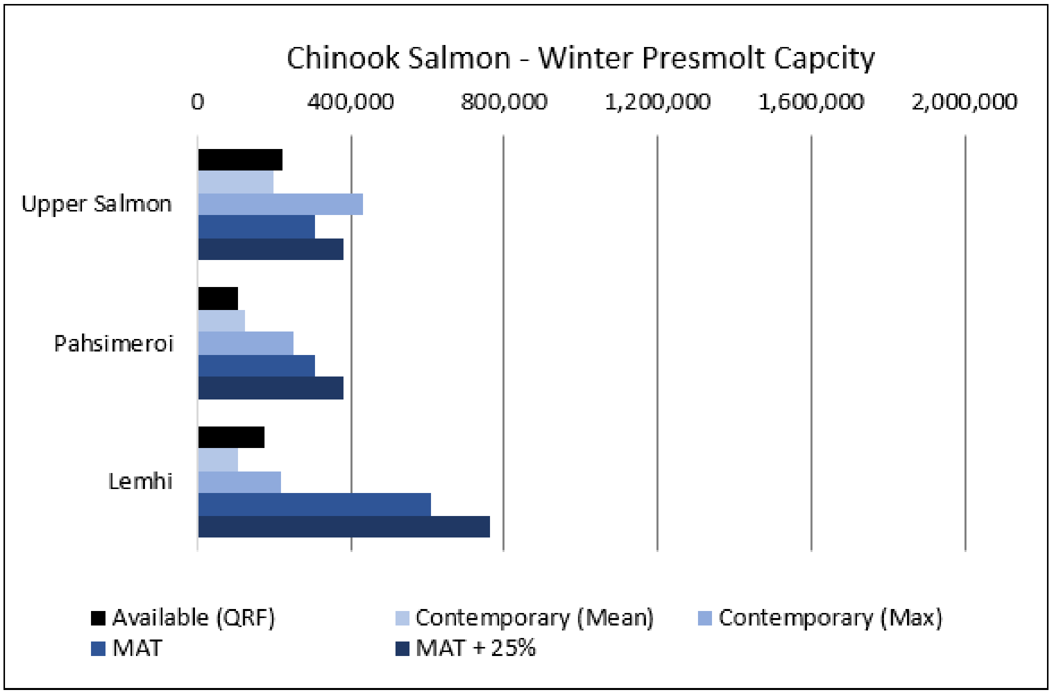

Figure 14. Estimates of available winter juvenile (presmolt) rearing capacity for Chinook salmon given current habitat conditions, made using quantile regression and random forest models (black bars) versus the capacity required to support contemporary abundance and minimum abundance thresholds (MATs) needed for ESA de-listing (blue bars).

Steelhead Capacity Limitations

Results for the steelhead available capacity estimates are considered preliminary. Models to estimate available habitat capacity for spawning (redds) and summer (parr) and winter (presmolt) rearing were completed in 2018 and are available. However, two considerations should be made when interpreting results from the juvenile steelhead models:

1. Juvenile steelhead may rear in natal tributaries for multiple years, whereas juvenile Chinook only rear in freshwater for a single year before emigration to the ocean. In addition, steelhead populations can contain a considerable number of residualized individuals.
2. All spatial modeling extents for the QRF and extrapolation models were done using StreamNet domains, and in initial discussions with local biologists, it appears the StreamNet domain may, in cases, overestimate the spatial extent of habitat available for steelhead spawning and rearing. Modeling too large of a spatial domain can result in overestimates of available capacity, and in turn, portray that capacity deficits do not exist when, in fact, they may.

Due to these considerations, steelhead results should be interpreted with caution. We hope to improve the spatial extents for the steelhead QRF models in the near future with collaboration from local biologists and experts. Improved model results can be incorporated into future reach-scale assessments.

For populations of steelhead across the Upper Salmon River subbasin, we conclude that sufficient available habitat exists for both the spawning (redd) and juvenile (presmolt) rearing life stages in each of the three target watersheds (Lemhi River, Pashimeroi River, and Upper Salmon River above Redfish Lake

Creek) (Figure 15 and Figure 17). However, we did conclude that summer (parr) rearing is limiting in at least the Pahsimeroi River watershed to support contemporary escapement and escapement necessary for delisting (Figure 16). Finally, of note, we conclude that water temperatures during the summer are above the optimum range for *O. mykiss* for at least a portion of the season for each of the three target watersheds, and the issue is exacerbated by the climate change scenario that we present.

Figure 15, Figure 16, and Figure 17 show comparisons of available habitat capacity from QRF versus capacity required to support various levels of adult abundance, including mean and maximum recent escapement, MAT, and MAT + 25% for the redd, summer (parr) rearing, and juvenile (presmolt) rearing life stages, respectively. Comparisons are for steelhead and the three focal watersheds. Comparisons for the remaining five watersheds in the Upper Salmon River subbasin are provided in Appendix B.

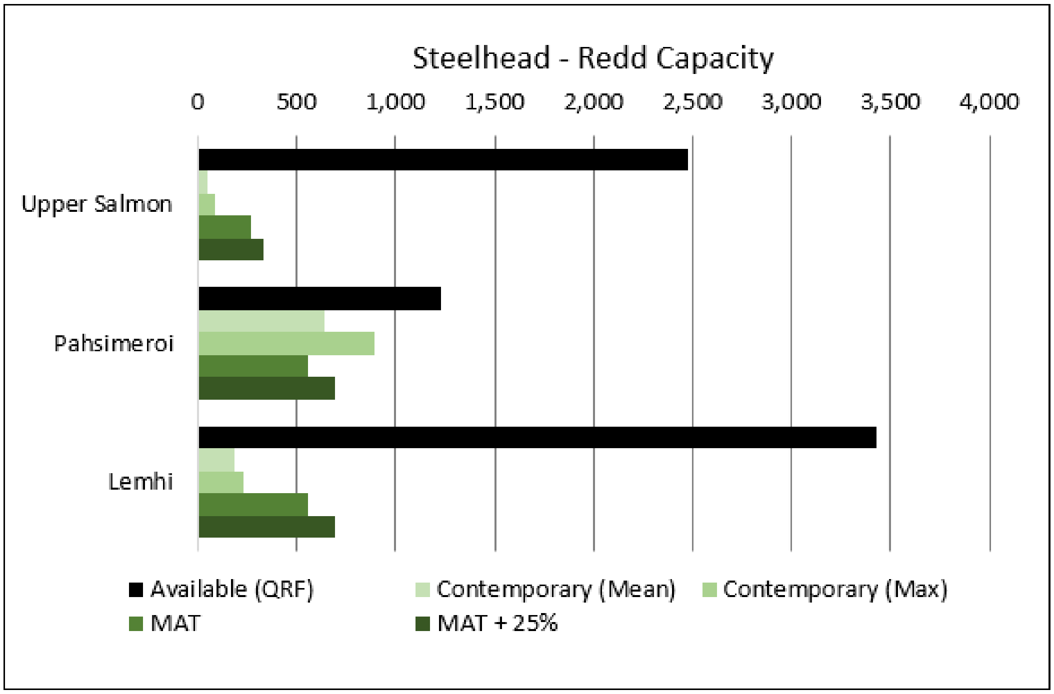

Figure 15. Estimates of available spawning (redd) capacity for steelhead given current habitat conditions, made using quantile regression random forest models (black bars) versus the capacity required to support contemporary abundance and minimum abundance thresholds (MATs) needed for ESA de-listing (green bars).

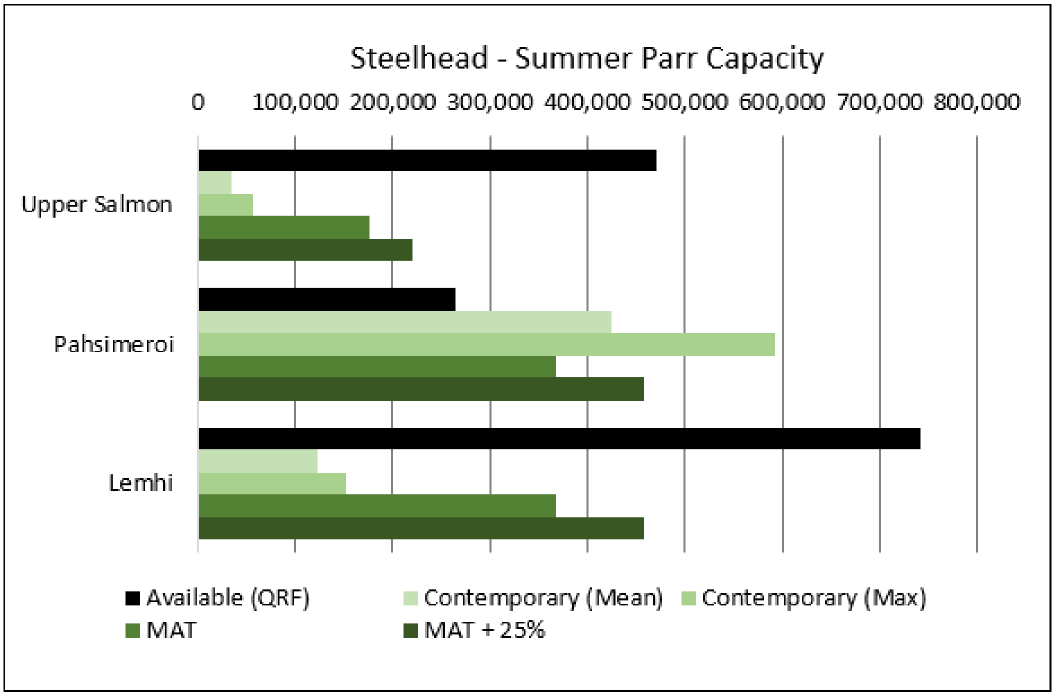

Figure 16. Estimates of available summer juvenile (parr) rearing capacity for steelhead given current habitat conditions, made using quantile regression random forest models (black bars) versus the capacity required to support contemporary abundance and minimum abundance thresholds (MATs) needed for ESA de-listing (green bars).

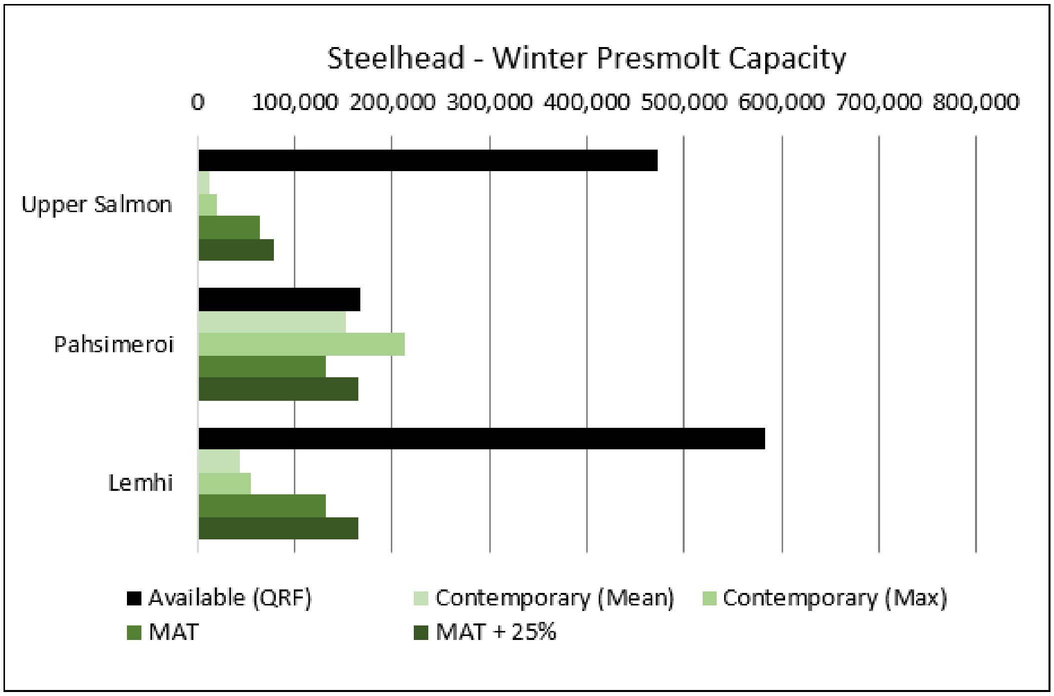

Figure 17. Estimates of available winter juvenile (presmolt) rearing capacity for steelhead given current habitat conditions, made using quantile regression random forest models (black bars) versus the capacity required to support contemporary abundance and minimum abundance thresholds (MATs) needed for ESA de-listing (green bars).

General Recommendations and Actions

The general recommendations and actions provided by the IRA are targeted toward Chinook salmon, as steelhead available capacity model results are still preliminary at the time of publication of this document. Steelhead model results will be improved and incorporated into future reach-scale assessments as appropriate.

Further investigation in the MRA step will allow us to more closely link specific life-stage habitat requirements, but for now our investigation suggests that actions aimed at increasing low- to zero-velocity pool habitat with cover, increased interstitial spaces, and improved hyporheic flow should be prioritized, to both improve freshwater population productivity and buffer against changes in stream temperatures due to climate change.

From an implementation standpoint, we recommend actions be implemented in all three focal watersheds focused on increasing summer and winter rearing capacity by reducing width-to-depth ratios, increasing floodplain connectivity and complex habitat structure, increasing low- to zero-velocity pool habitat with cover, providing side channel habitat, and reducing sediment. Additional required actions include moderating water temperatures and instream flows by increasing hyporheic flow and alluvial aquifer connections and improving riparian habitat.

The following conclusions and recommendations apply to the entire Upper Salmon River subbasin as a whole, based on the Generalized Capacity and QRF models, key limiting factors analysis, and local expertise:

- Summer (parr) and overwinter (presmolt) rearing are the key limited life stages for Chinook salmon production throughout all three watersheds (Lemhi River, Pahsimeroi River, and Upper Salmon River). Available capacity for summer (parr) and winter (presmolt) rearing are significantly below levels required to support current adult escapement levels required for MAT and MAT + 25%.
- Limiting PBFs associated with the lack of summer (parr) rearing habitat include limited hydraulic and habitat complexity (i.e., velocity gradients, pool and side channel frequency, etc.).
- Limiting PBFs associated with the lack of winter (presmolt) rearing habitat include lack of concealment cover within low- and zero-velocity areas.
- Concealment cover for all juvenile life stages is lacking due to embedded substrate, a lack of woody debris, a lack of deep complex pools, a lack of undercut banks, and in places, fast water velocities.
- The lack of available juvenile rearing capacity required increased juvenile movement to seek suitable habitat (including to mainstem Salmon River reaches), resulting in increased exposure and survival risk.
- Available spawning habitat (i.e., redd capacity) is not limiting in any of the target watersheds (Lemhi River, Pahsimeroi River, and Upper Salmon River above Redfish Lake Creek). However, providing sufficient adult holding (prespawn) habitat should be considered and would be provided by increased habitat complexity.
- Spawning habitat historically occurred farther upstream than current core areas, especially in the Upper Salmon River headwaters, effectively reducing the area currently available for rearing (i.e., area downstream of spawning).

In addition to the limiting PBFs described in this document, NOAA (2017) identified the following seven tributary habitat limiting factors for Chinook salmon in the Lemhi, Pahsimeroi, and Upper Salmon Rivers:

- Reduced stream complexity and channel structure,
- Excess fine sediment,
- Impaired fish passage,
- Diminished streamflow during critical periods,
- Elevated summer water temperatures,
- Degraded riparian conditions, and
- Reduced floodplain connectivity and function (Upper Salmon only).

Beyond the PBFs identified here and the tributary habitat limiting factors identified by NOAA (2017), the lack of marine-derived nutrients should also be recognized as a potential PBF limiting Chinook salmon vitality throughout the Upper Salmon River subbasin. However, analyses of marine-derived nutrients within watershed are outside of the scope of the IRA.

Below, we describe additional details regarding limiting factors, recommendations, and priority areas for each of the three target watersheds based on the watershed-scale IRA. We expect these recommendations and priority areas will be further refined as part of the future MRA process.

The Lemhi River Watershed

In addition to general conclusions and recommendations listed above, the following are watershed-specific conclusions, priority areas, and recommendations for Chinook salmon in the Lemhi River watershed.

Limiting Physical and Biological Features

The key limiting PBF for population productivity in the Lemhi River is summer and winter juvenile fish rearing habitat downstream of current spawning habitat. Within the Lemhi River, we estimated that roughly twice as much spawning (redd) capacity currently exists than required to achieve MAT + 25%; however, summer juvenile rearing capacity must be increased by approximately four-fold and winter rearing capacity by approximately three-fold, relative to current conditions, to support MAT + 25%.

- Summer (parr) and winter (presmolt) juvenile rearing capacity were each identified as high-priority PBF limiting Chinook salmon production in the Lemhi River.

Priority Areas

Priority enhancement areas within the Lemhi River watershed include the upper and lower Lemhi and Hayden Creek:

- **First priority: mainstem Lemhi River downstream of Hayden Creek.** This section currently does not support Chinook salmon spawning but provides key summer and winter rearing for fish spawned in the upper Lemhi River and Hayden Creek.

- **Second priority: mainstem Lemhi River upstream of Hayden Creek.** This is the section of the Lemhi River watershed where about two-thirds of the spawning occurs on average.
- **Third priority: Hayden Creek.** This is the section where about one-third of the spawning occurs on average.

Recommendations

In the lower Lemhi River and Hayden Creek (characterized as peak-flow dominated), habitat complexity enhancements are preferred, including diversifying the mostly single-thread channel to multi-threaded and island-braided channels with large cottonwood tree recruitment for pool formation and cover. Actions should also maintain and improve tributary stream connections to the mainstem Lemhi River.

In the Upper Lemhi River (characterized as groundwater-influenced), treatments that improve habitat complexity are also preferred, including a return to multi-threaded channels, reduction in width-to-depth ratios, stabilization of stream banks, and increased riparian shrub-dominated habitat to increase both pool area/frequency and associated instream cover.

The following recommended actions can increase habitat quantity and quality in the Lemhi River:

- In the lower mainstem Lemhi River (downstream of Hayden Creek), increase habitat complexity by increasing the sinuosity of the single-thread main channel while creating areas of island braiding with complex instream structure, hydraulic variability, and low-velocity areas with cover. Provide structure with large wood (cottonwood) while accommodating active channel migration. Mediate summer water temperatures and provide low-velocity cover areas for winter rearing.
- In the upper mainstem Lemhi River (upstream of Hayden Creek), increase habitat complexity by creating multi-threaded channels, narrow width-to-depth ratios, stable banks, and willow-dominated riparian areas.
- Maintain and improve instream flow and tributary stream connections to the mainstem Lemhi River.
- Reduce fine sediment inputs to the watershed from upland and instream sources to improve substrate conditions for interstitial spaces, providing overwinter concealment habitat for juvenile fishes.
- Increase seasonal floodplain connection to improve floodwater storage, hyporheic exchange, fine sediment storage, high-flow juvenile refugia, nutrient exchange, and riparian vegetation, and to reduce instream velocities.

Biological and Geomorphic Assessment Integration

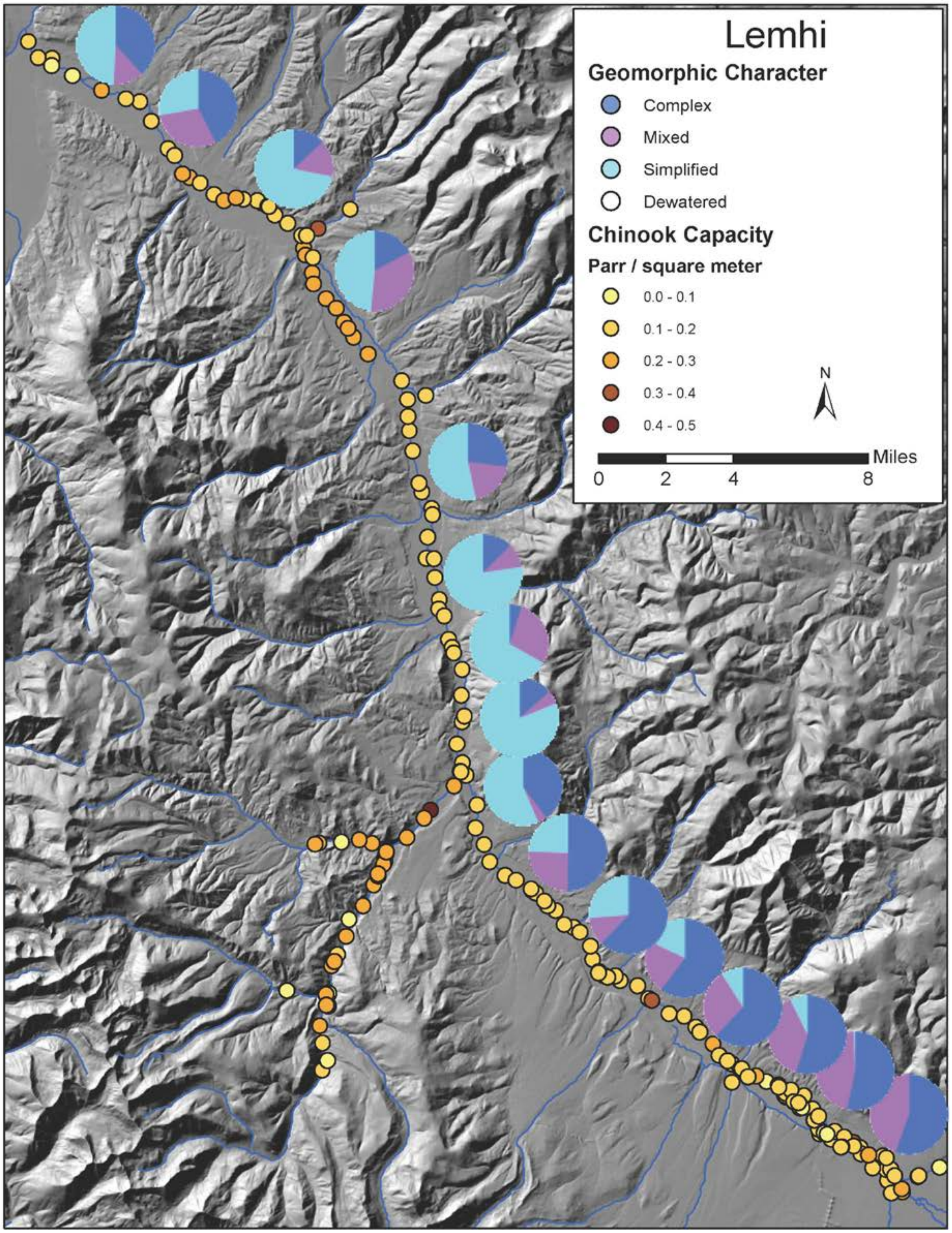

Figure 18. Lemhi River map spatially illustrating geomorphic character per reach (pie charts) and predicted existing capacity for Chinook salmon parr (graded orange to yellow dots).

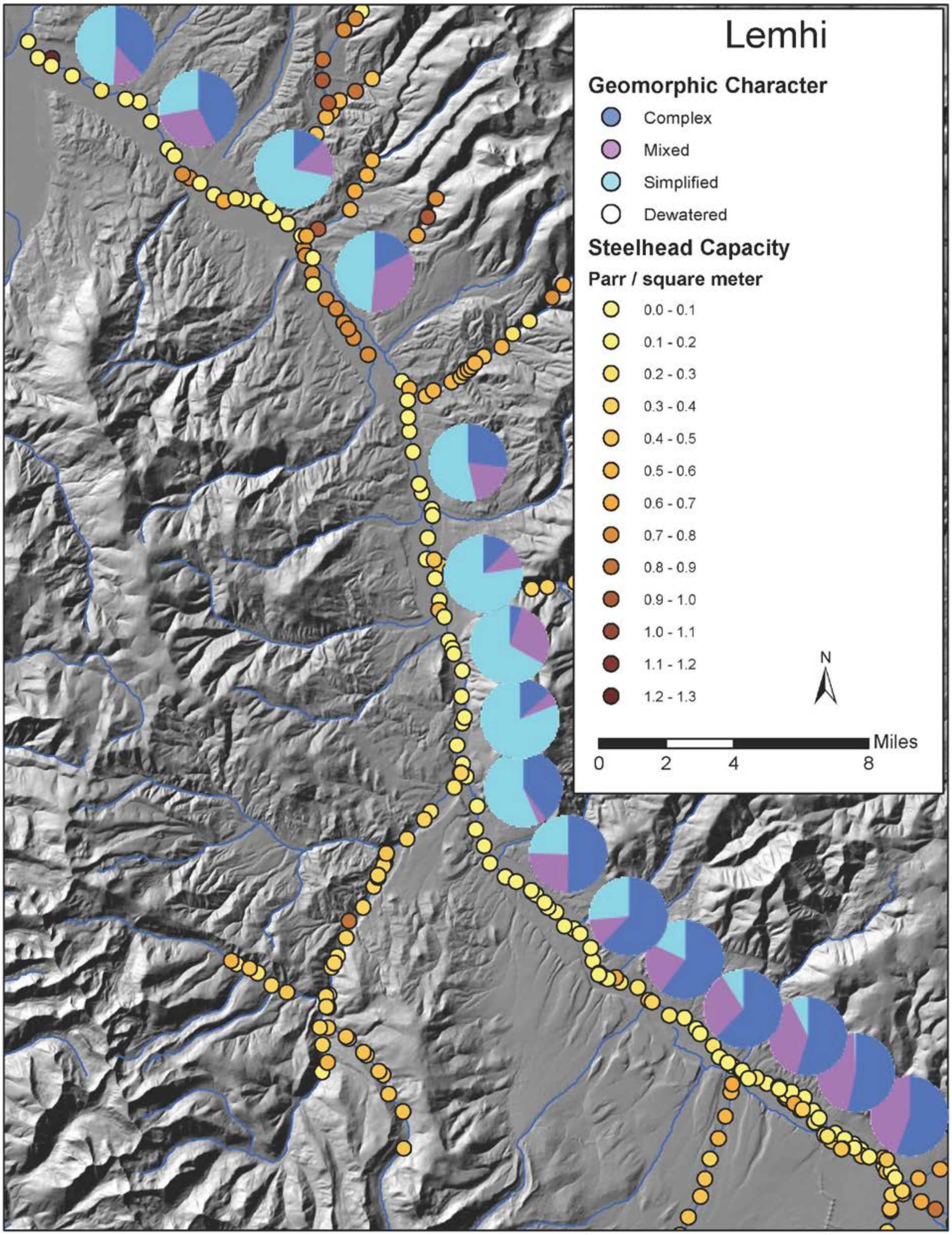

Figure 19. Lemhi River map spatially illustrating geomorphic character per reach (pie charts) and predicted existing capacity for steelhead parr (graded orange to yellow dots).

The Pahsimeroi River Watershed

In addition to general conclusions and recommendations listed above, the following are watershed-specific conclusions, priority areas, and recommendations for Chinook salmon in the Pahsimeroi River watershed.

Limiting Physical and Biological Features

The key limiting PBF for population productivity in the Pahsimeroi River is summer and winter juvenile fish-rearing habitat. Within the Pahsimeroi River, we estimated that roughly twice as much spawning (redd) capacity currently exists than required to achieve MAT + 25%; however, summer juvenile rearing capacity must be approximately doubled and winter rearing capacity must be increased by approximately 2.5 times, relative to current conditions, to support MAT + 25%.

- Summer (parr) and winter (presmolt) juvenile rearing capacity were each identified as high-priority PBF limiting Chinook salmon production in the Pahsimeroi River.

Priority Areas

Priority areas within the Pahsimeroi River watershed include the mainstem Pahsimeroi River and (Patterson) Big Springs Creek.

- **First priority: Pahsimeroi River from the mouth to Hooper Lane.** Hooper Lane is currently the upstream-most extent of Chinook salmon spawning and rearing, except for Big Springs Creek.
- **Second priority: (Patterson) Big Springs Creek.** This is the portion of the creek within the Pahsimeroi valley bottom.

Recommendations

The following recommended actions can increase habitat quantity and quality in the Pahsimeroi River:

- Increase habitat quantity by adding more channels within groundwater-influenced reaches that provide high-quality, complex habitat, including split flows, side channels, spring channels, and alcoves.
    - Reconnecting upstream habitat may be limited in certain areas (e.g., upstream of Goldberg Creek) due to geologic conditions, resulting in significant surface water losses to the aquifer (i.e., dry river).
- Increase stream length by increasing sinuosity, which also increases hyporheic flow.
- Establish a robust, riparian community along the banks and floodplain, increasing shade, improving bank structure and habitat, and providing a buffer from upland and floodplain sediment sources.
- Reduce fine sediment (systemic throughout the Pahsimeroi River basin) by increasing bank stability and decreasing surface water runoff.
- Improve and/or provide tools to landowners and land manager to protect land uses that benefit and maintain fish habitat.

- Increase seasonal floodplain connection to improve flood water storage, hyporheic exchange, fine sediment storage, high-flow juvenile refugia, nutrient exchange, riparian vegetation, and to reduce instream velocities.

Biological and Geomorphic Assessment Integration

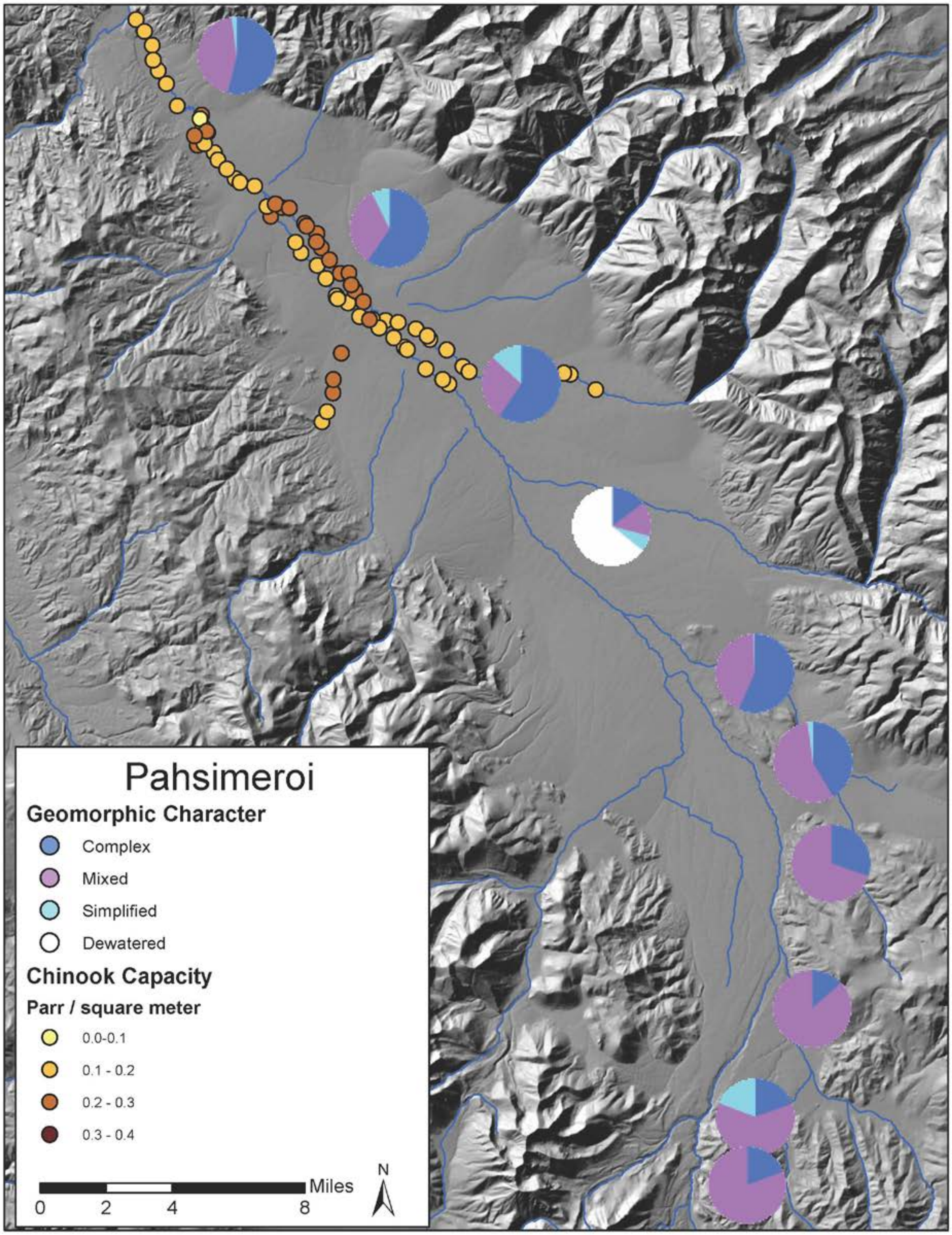

Figure 20. Pahsimeroi River map spatially illustrating geomorphic character per reach (pie charts) and predicted existing capacity for Chinook salmon parr (graded orange to yellow dots).

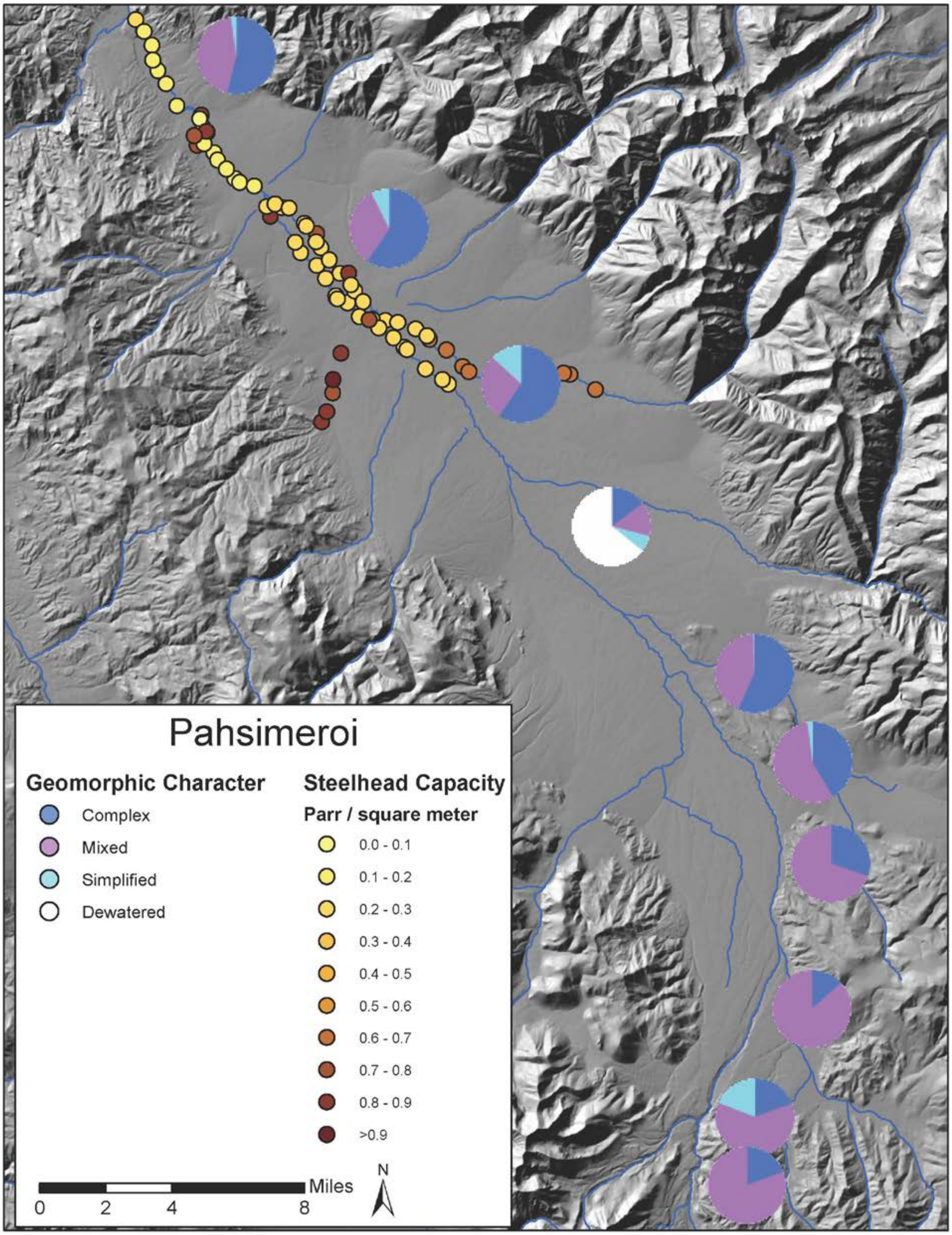

Figure 21. Pahsimeroi River map spatially illustrating geomorphic character per reach (pie charts) and predicted existing capacity for steelhead parr (graded orange to yellow dots).

The Upper Salmon River (Headwaters) Watershed

In addition to general conclusions and recommendations listed above, the following are watershed-specific conclusions, priority areas, and recommendations for Chinook salmon in the Upper Salmon River (headwaters) watershed.

Limiting Physical and Biological Features

Limiting PBFs for population productivity in the Upper Salmon River (above Redfish Lake Creek) include summer and winter juvenile fish-rearing habitat. Within the Upper Salmon River, we estimate that available spawning (redd) capacity is ample to support MAT + 25%; however, summer juvenile rearing capacity must be increased by approximately 30 percent and winter rearing capacity by approximately 70 percent, relative to current conditions, to support MAT + 25%. However, the downstream boundary of juvenile rearing for this sub-population is uncertain. Summer flow is also a limitation in some reaches. Problematically, most of the habitat currently used for spawning and rearing is concentrated in the lower valley just upstream of the Sawtooth fish hatchery, limiting juvenile use of the majority of available upstream habitat.

- Winter (presmolt) juvenile rearing habitat was identified as a high-priority PBF limiting Chinook salmon production in the Upper Salmon River (headwaters).
- Summer (parr) juvenile rearing habitat was identified as a medium-priority PBF limiting Chinook salmon production in the Upper Salmon River (headwaters).

Priority Areas

Priority areas in the upper Salmon River (headwaters) include lower-gradient reaches of the Salmon River around Decker Flats, the Alturas Lake Creek confluence area, and the Pole Creek area.

- **First priority: mainstem Upper Salmon from Alturas Creek to Redfish Lake Creek.** This section is where the majority of the Chinook salmon production currently occurs.
- **Second priority: Alturas Lake Creek and the mainstem Upper Salmon above Alturas Lake Creek, including Pole Creek.**

Recommendations

The following recommended actions can increase habitat quantity and quality in the Upper Salmon River:

- Redistribute spawning to take advantage of available rearing habitat in the upper and middle watershed above currently used spawning habitat. This could potentially be accomplished using current supplementation programs in place in the area, and Venditti et al. (2018) note that there are at least three goals appropriate for supplementation programs, including: (1) maintain smolt production during low escapements, (2) seed unoccupied or restored habitats, and (3) restore or maintain harvest opportunity concurrent with population recovery.
- Increase habitat complexity by creating and/or enhancing multi-threaded channels, narrow width-to-depth ratios, instream structure provided by large woody debris, and willow-dominated riparian areas within groundwater-influenced response areas immediately upstream of geologic controls composed primarily of glacial moraine deposits.

- Maintain and improve instream flow and tributary stream connections to the mainstem Upper Salmon River. Summer flow limitations continue to exist upstream of the Alturas Lake Creek confluence.
- Increase seasonal floodplain connection to improve flood water storage, hyporheic exchange, fine sediment storage, high-flow juvenile refugia, nutrient exchange, and riparian vegetation, and to reduce instream velocities.

Biological and Geomorphic Assessment Integration

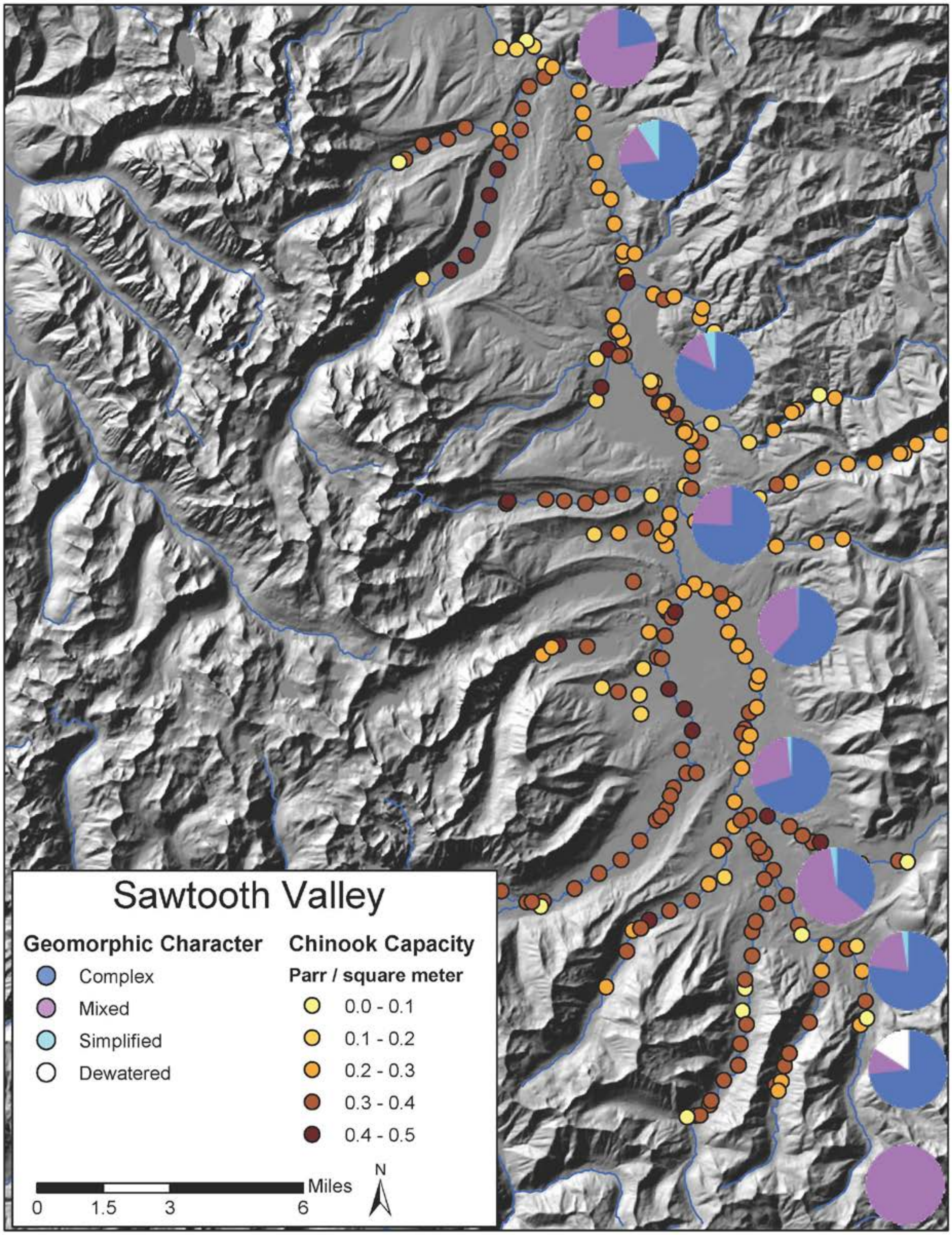

Figure 22. Upper Salmon River headwaters map spatially illustrating geomorphic character per reach (pie charts) and predicted existing capacity for Chinook salmon parr (graded orange to yellow dots).

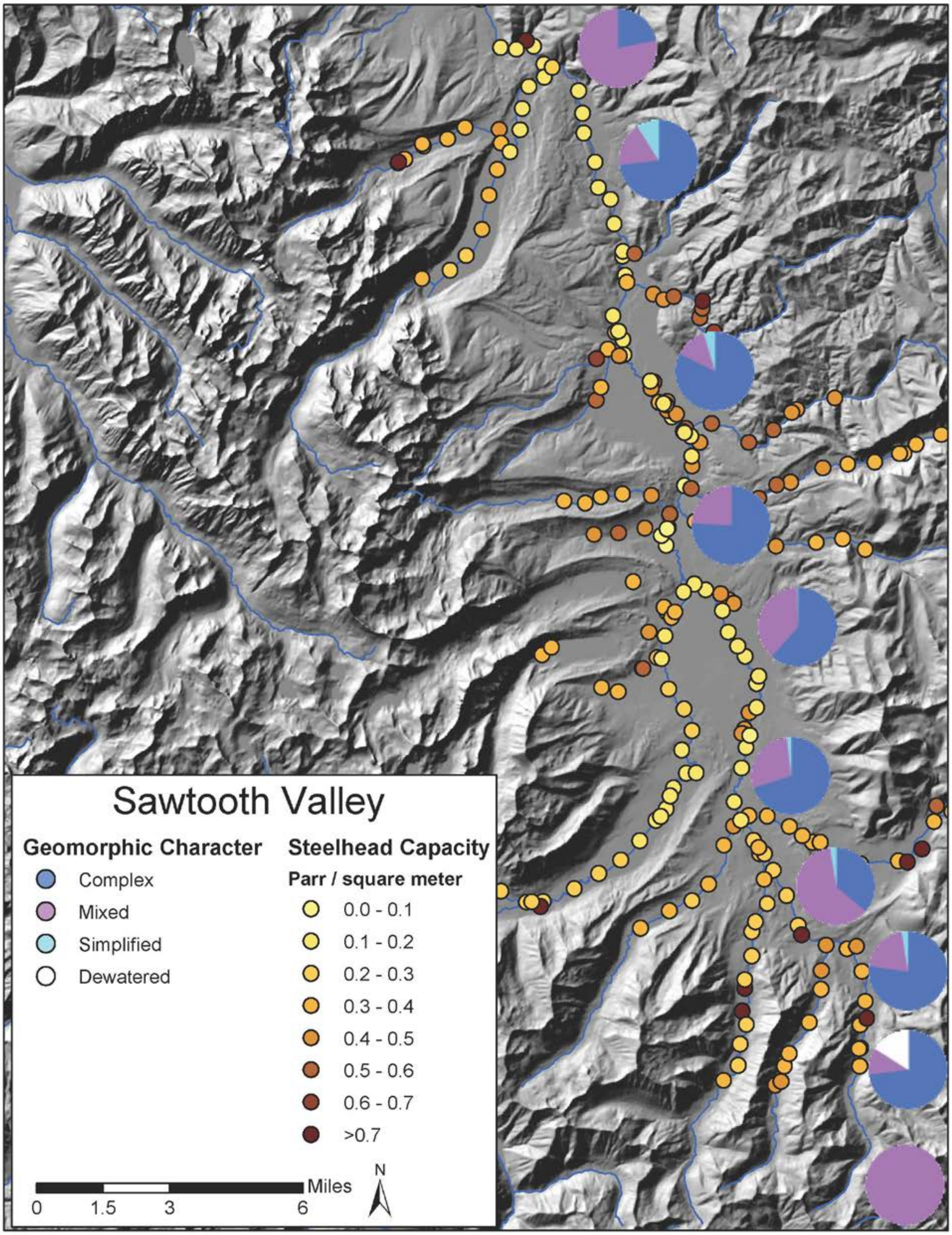

Figure 23. Upper Salmon River headwaters map spatially illustrating geomorphic character per reach (pie charts) and predicted existing capacity for steelhead parr (graded orange to yellow dots).

Sections 1 and 2 References

Breckenridge, R.R., L.R. Stanford, J.F.P. Cotter, J.M. Bloomfield, and E.B. Evenson. 1988. Field Guides to the Quaternary Geology of Central Idaho: Part B., Glacial Geology of the Stanley Basin, *in* P.K. Link, and W.R. Hackett, *eds*. Guidebook to the Geology of Central and Southern Idaho: Idaho Geological Survey Bulletin 27, p. 209-221.

Budy, P. and H. Schaller. 2007. Evaluating Tributary Restoration Potential for Pacific Salmon Recovery. *Ecological Applications*. 17(4): 1068-1086.

Hammar, L. and H.T. Shen. 1995. Anchor Ice Growth in Channels. P 77-92. Full proceedings from the Committee on River Ice Processes and the Environment: 8th Workshop on the Hydraulics of Ice-Covered Rivers. Kamloops, British Columbia, Canada. http://cripe.civil.ualberta.ca/proceedings/cripe-workshop08.html. Accessed on October 27, 2011.

Idaho Soil Conservation Commission. 1995. Model Watershed Plan for Lemhi, Pahsimeroi and East Fork Salmon River.

Johnson, K.M., R.S. Lewis, E.H. Bennett, and T.H. Kiilsgaard. 1988. Cretaceous and Tertiary intrusive rocks of south-central Idaho, *in* P.K. Link, and W.R. Hackett, *eds*. Guidebook to the Geology of Central and Southern Idaho: Idaho Geological Survey Bulletin 27. p. 55-86.

Kyle, R. and T. Brabets. 2001. Water Temperature of Streams in the Cook Inlet Basin, Alaska, and Implications of Climate Change. Water Resources Investigations Report 01-4109. U.S. Geological Survey. Anchorage, Alaska.

Link, P.K. and S.U. Janecke. 1999. Geology of East-Central Idaho: Geologic Roadlogs for the Big and Little Lost River, Lemhi, and Salmon River Valleys. *In* Guidebook to the Geology of Eastern Idaho. S.S. Hughes and G.D. Thackray, *eds*. Idaho Museum of Natural History. Online Link: http://imnh.isu.edu/digitalatlas/geo/gsa/gsafrm.htm

Mantua, N.J., I. Tohver, and A. Hamlet. 2010. Climate change impacts on streamflow extremes and summertime stream temperature and their possible consequences for freshwater salmon habitat in Washington state. *Climate Change* 102: 187–223

McNyset, K., C. Volk, and C. Jordan. 2015. Developing an Effective Model for Predicting Spatially and Temporally Continuous Stream Temperatures from Remotely Sensed Land Surface Temperatures. *Water*. 7: 6827-6846.

Meinzer, O.E. 1924. Ground water in Pahsimeroi Valley, Idaho. Idaho Bureau of Mines and Geology, Pamphlet 9, 36p.

Montgomery, D., and J.M. Buffington, 1988. Channel Processes, Classification, and Response, *in* River Ecology and Management, Chapter 2. R. Naiman, and R. Bilby, *eds*. Springer-Verlag New York, Inc., p. 13-42.

Moye, F.J., W.R. Hackett, J.D. Blakley, and L.G. Snider. 1988. Regional geologic setting and volcanic stratigraphy of the Challis volcanic field, central Idaho. *In* P.K. Link, and W.R. Hackett, *eds*. Guidebook to the Geology of Central and Southern Idaho: Idaho Geological Survey Bulletin 27, p. 87-97.

Nez Perce Tribe. 2013. Department Management Plan 2013-2028. Prepared by the Department of Fisheries Resources Management Strategic Plan Ad Hoc Team. Completed July 17, 2013.

NOAA (National Oceanic and Atmospheric Administration). 2017. Proposed ESA Recovery Plan for Snake River Spring/Summer Chinook Salmon (*Oncorhynchus tshawytscha*) and Snake River Steelhead (*Oncorhynchus mykiss*). U.S. Department of Commerce, National Oceanic and Atmospheric Administration, National Marine Fisheries Service, West Coast Region.

Pierce, K.L. and W.E. Scott. 1982. Pleistocene episodes of alluvial gravel deposition, southeastern Idaho. *In* Cenozoic Geology of Idaho. B. Bonnichsen and R. Breckenridge, *eds*. Idaho Bureau of Mines and Geology Bulletin 26. p. 685-702.

Pierce, K.L., D.G. Despain, L.A. Morgan, and J.M. Good. 2007. The Yellowstone Hotspot, Greater Yellowstone Ecosystem, and Human Geography: U.S. Geological Survey Paper 79, 39 p.

Simpson, D.W. and M.H. Anders. 1992. Tectonics and topography of the western U.S.: An example of digital map making. *GSA Today*. 2: 118-121.

Tang, Chunling, Benjamin T. Crosby, Joseph M. Wheaton, Thomas C. Piechotac. 2012. Assessing Streamflow Sensitivity to Temperature Increases in the Salmon River Basin, Idaho. *Global and Planetary Change* 88-89: 32-44. https://www.sciencedirect.com/science/article/pii/S0921818112000422.

Ungate, C.A. 1998. Neogene – Quaternary Basin – Fill History of the Pahsimeroi Valley. Master's Thesis. Idaho State University, Pocatello, Idaho.

Venditti, D.A., R. N. Kinzer, K. A. Apperson, B. Barnett, M. Belnap, T. Copeland, M. P. Corsi, and K. Tardy. 2018. Effects of hatchery supplementation on abundance and productivity of natural-origin Chinook salmon: two decades of evaluation and implications for conservation programs. *Can. J. Fish. Aquat. Sci*. 75: 1495–1510.

Winston, Don, and P.K. Link. 1993, Middle Proterozoic Rocks of Montana, Idaho, and Washington: The Belt Supergroup. *in* The Geology of North America, Precambrian of the conterminous United States. v. C-3, p. 487-521. J. Reed., P. Simms, R. Houston, D. Rankin, P. Link, R. Van Schmus, and P. Bickford, *eds*., Geological Society of America. Boulder, Colorado.

Section 3: Watershed-Level Results

Chapter 1 – Lemhi River Watershed

Location and Watershed Description

The Lemhi River watershed is located in the Northern Rocky Mountain System physiographic region that comprises extensive parallel mountain ranges, intermontane valleys, and plateaus (Figure 24). Elevations in the watershed range from a low of about 4,000 feet to a high of 11,000 feet, with the lowest elevations along the Lemhi valley floor and the highest elevations along the bounding Beaverhead Mountains to the north and Lemhi Range to the south. The watershed is in the Dry Intermontane Sagebrush Valleys Ecoregion (17AA), characterized by stream terraces, floodplains, saline areas, and alluvial fans. Water availability and potential for cropland agriculture are low because the Ecoregion is in the rain shadow of high mountains, receives little mountain runoff, and is underlain by highly permeable valley fill deposits. Its deep gravels are unlike the basalts of Ecoregion 12. Sagebrush grassland is widespread and contrasts with the open-canopied forests of the more-rugged and higher Ecoregion 17e. Shadscale and greasewood grow on alkaline soils that receive fewer than 8 inches of precipitation annually. Grazing is the dominant land use (McGrath *et. al*. 2002).

The Lemhi River watershed is a hydrologic unit code (HUC) 8th field basin (HUC 8 – 17060204) within the Salmon River Subbasin and the Columbia River Basin. The watershed covers about 1,260 square miles in east-central Idaho and is entirely within Lemhi County, Idaho. About 80 percent of the land is owned by the Federal government and administered by the U.S. Forest Service (USFS) and Bureau of Land Management (BLM). Federal lands are located primarily in the higher elevations, whereas the 20 percent private ownership is predominantly located in lower elevations along the valley bottoms.

The Lemhi River is predominantly an alluvial stream flowing over gravel and cobble originating at the confluence of Hawley, Eighteenmile, and Texas Creeks near the town of Leadore, Idaho. The river flows to the northwest for about 63 miles, where it discharges to the Salmon River near Salmon, Idaho.

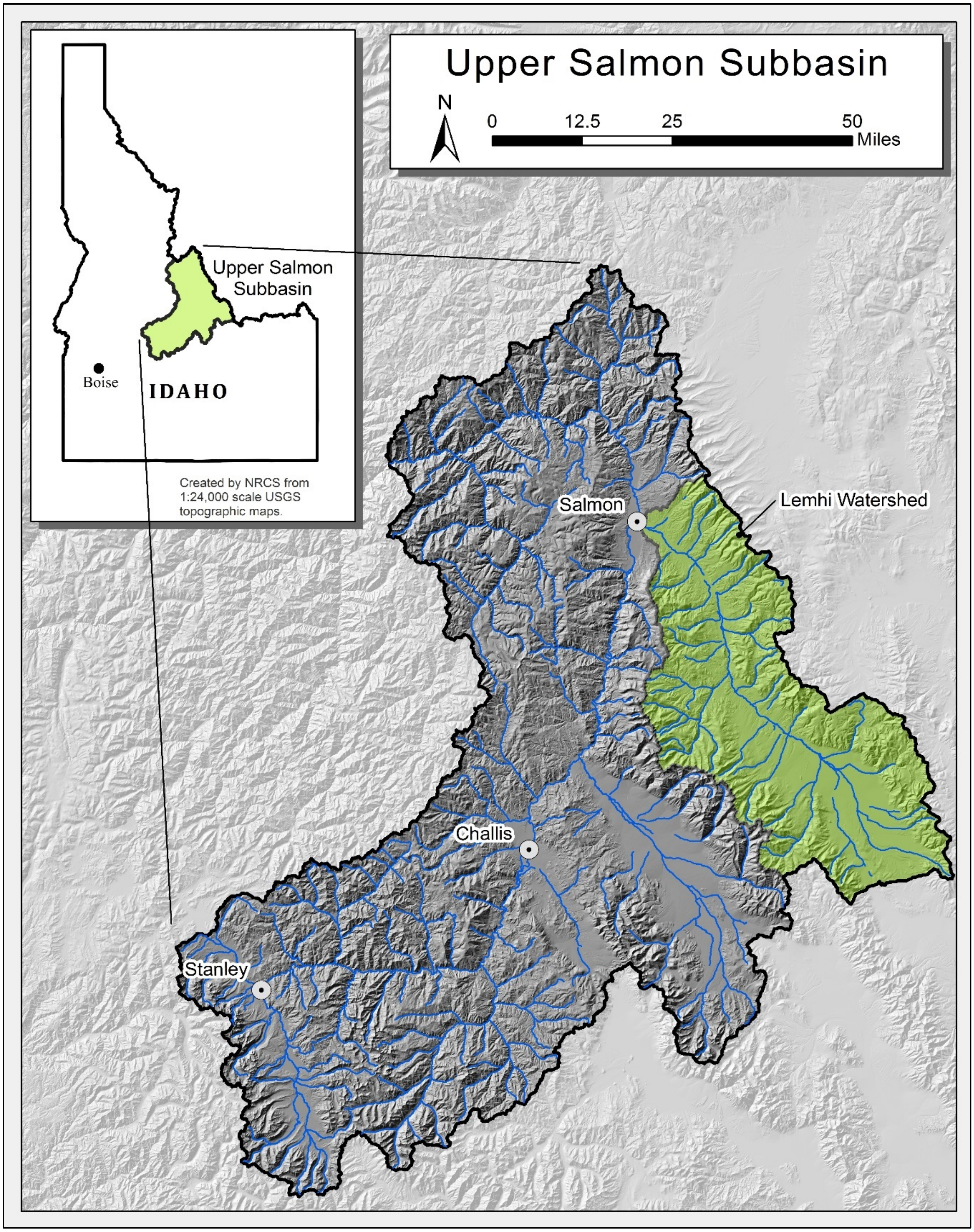

Figure 24. Location of the Lemhi River watershed within the Upper Salmon River subbasin.

Biological Assessment

The Lemhi River maintains populations of three fish species listed under the ESA: Chinook salmon, steelhead, and bull trout. The watershed also supports westslope cutthroat trout (*O. clarki lewisi*), which has been petitioned for listing under the ESA. As described in the journals of Lewis and Clark, the Lemhi Valley was completely overgrown with willows, from valley shoulder to valley shoulder, and the river itself had multiple deep channels, rendering the valley bottom nearly impassable. Early reports of tribal fishing (Walker 1994) estimated Chinook salmon and steelhead harvest at 60,000 pounds per year. However, by 1872, the effects of downstream commercial fishing were apparent as estimated salmon and steelhead harvest in the Lemhi River was reduced to approximately 10,000 pounds (Walker 1994). Historical harvest and abundance estimates support the NOAA (2017) classification of the Lemhi River Chinook salmon population as Very Large and the Lemhi River steelhead population as Intermediate.

In its current form, the Lemhi River is heavily affected by legacy mining impacts, railroad construction, road construction, and agriculture. Of its 31 major tributaries, only Hayden Creek and Big Springs Creek retained a constant hydraulic connection to the mainstem Lemhi until tributary reconnection efforts began in 2001. Diversions and agricultural activity have increased water temperature and fine sediment (IDEQ 2013). These anthropogenic influences, combined with out-of-subbasin sources of mortality, have resulted in a high-risk finding for Lemhi River Chinook salmon (NOAA 2017). Lemhi River steelhead were identified as being maintained (6 to 25 percent risk of extinction, NOAA 2017), but that listing is tentative due to insufficient data for Lemhi River steelhead. Among recent years (2010 through 2015), the Lemhi River has a mean adult escapement of 347 Chinook salmon, with a maximum of 718 in 2015. In those same years, mean adult escapement for steelhead was 337, with a maximum of 417 in 2010. Despite legacy degradation, primary productivity in the Lemhi River remains high relative to other Idaho rivers, and groundwater influence continues to modulate water temperatures (Bjornn 1978).

Habitat Capacity

Chinook salmon

Current Conditions

Contemporary estimates of life-stage-specific capacity requirements were generated based on the mean (347) and maximum (718) adult Chinook salmon escapement observed in the Lemhi River from 2010 to 2015. Those adult escapements were then propagated through to four additional life stages to estimate life-stage-specific capacity requirements for Chinook salmon in the Lemhi River; capacity requirements were then compared to available habitat capacity estimated using QRF models (Table 2).

Table 2. Estimated current life stage specific capacity requirement versus estimated available capacity for Chinook salmon in the Lemhi River.

Life-Stage	Required Capacity		Available Capacity	Capacity Deficit
	Mean	Max		
Escapement	347	718		
Redd	170	352	2,641	0
Eggs	899,027	1,861,128		
Summer Parr	260,718	539,727	550,562	0
Winter Presmolt	105,635	218,681	173,375	45,306

Using contemporary escapement estimates, habitat capacity does not appear to limit the production of redds or summer parr in the Lemhi River under current conditions; however, it does appear that juvenile (presmolt) rearing capacity is limited during the winter months (Table 2). The finding of limited winter hearing habitat is further supported by three lines of evidence:

1. Bjornn (1971) identified winter habitat capacity limitations in Big Springs Creek, a tributary to the Lemhi River, and later confirmed those observations in subsequent experiments in Hayden Creek, the largest tributary to the Lemhi River (Peery and Bjornn 2004).
2. A time-series process model (described in Appendix C) for Chinook salmon in the Lemhi River found density-independent production from the adult-to-parr transition but found evidence of density-dependent production from the presmolt-to-smolt life history transition.
3. The majority of juvenile Chinook salmon emigrate from the Lemhi River as age-0 presmolts prior to the winter (Appendix C). This is consistent with behavior, observed by Bjornn (1971) and Peery and Bjornn (2004), potentially resulting from winter habitat limitations.

We estimate an approximately 20 percent deficit in winter (presmolt) rearing habitat to support even a recent escapement of 718 adult Chinook salmon, which is far below desired escapement. Additionally, on average, 72 percent of juvenile emigrants from the Lemhi River emigrate during the parr (2 percent) or presmolt (70 percent) life stage. This suggests that a substantial increase in winter habitat capacity would be required to support current Chinook salmon productivity in the Lemhi River.

Desired Conditions

NOAA (2017) delisting requirements include a minimum annual escapement (i.e., MAT) of 2,000 Chinook salmon adults to the Lemhi River. Based on this requirement, life-stage-specific capacity requirements were recalculated consistent with 2,000 adults (MAT) and 2,500 adults (MAT + 25%) using the same methods as above. Those capacity requirements were also compared to estimates of currently available habitat capacity to identify potential habitat limitations if delisting is desired (Table 3). Potential limitations (capacity deficit) were calculated as the life stage-specific capacity requirements needed to achieve a MAT of 2,000 plus a 25 percent buffer minus available capacity.

Table 3. Estimated life stage specific capacity requirements to accommodate ESA delisting and estimated available capacity for Chinook salmon in the Lemhi River.

Life-Stage	Required Capacity		Available Capacity	Capacity Deficit
	MAT	MAT + 25%		
Escapement	2,000	2,500		
Redd	980	1,225	3,192	0
Eggs	5,184,200	6,480,250		
Summer Parr	1,503,418	1,879,273	357,948	1,521,325
Winter Presmolt	609,140	761,425	173,375	588,049

There appears to be sufficient redd capacity in the Lemhi River to support 2,500 adult Chinook salmon (Table 3). However, the available juvenile rearing capacity during summer (357,948) and winter (173,375) are far from sufficient to support the potential parr and presmolt production from 2,500 adult Chinook salmon (Table 3). Therefore, to achieve delisting of Chinook salmon in the Lemhi River, both summer and winter juvenile rearing capacity would need to be increased.

Summary

There appears to be sufficient spawning (redd) capacity in the Lemhi River to support both current escapement and additional escapement required to achieve delisting criteria for Chinook salmon (Figure 25). Although available summer and winter juvenile rearing capacity appears sufficient to support recent (2010-2015) mean escapement, juvenile habitat appears to be limiting for recent high escapements and far below juvenile rearing habitat necessary to achieve delisting criteria (NOAA 2017) for Lemhi River Chinook salmon (Figure 26 and Figure 27).

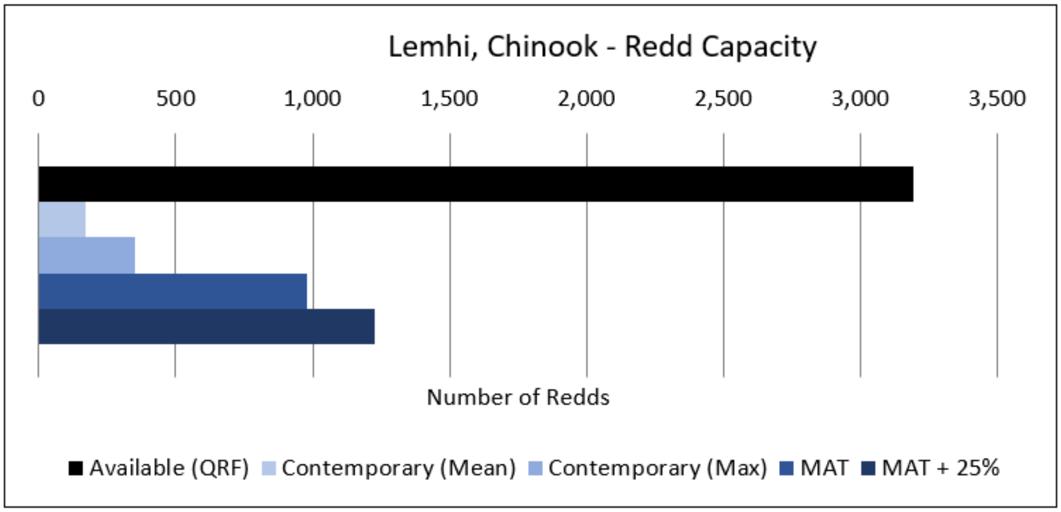

Figure 25. Estimates of available spawning (redd) capacity given current habitat conditions for Chinook salmon in the Lemhi River watershed, made using quantile regression forest models (black bars) versus the capacity required to support contemporary abundance and minimum abundance thresholds (MATs) needed for ESA de-listing (blue bars).

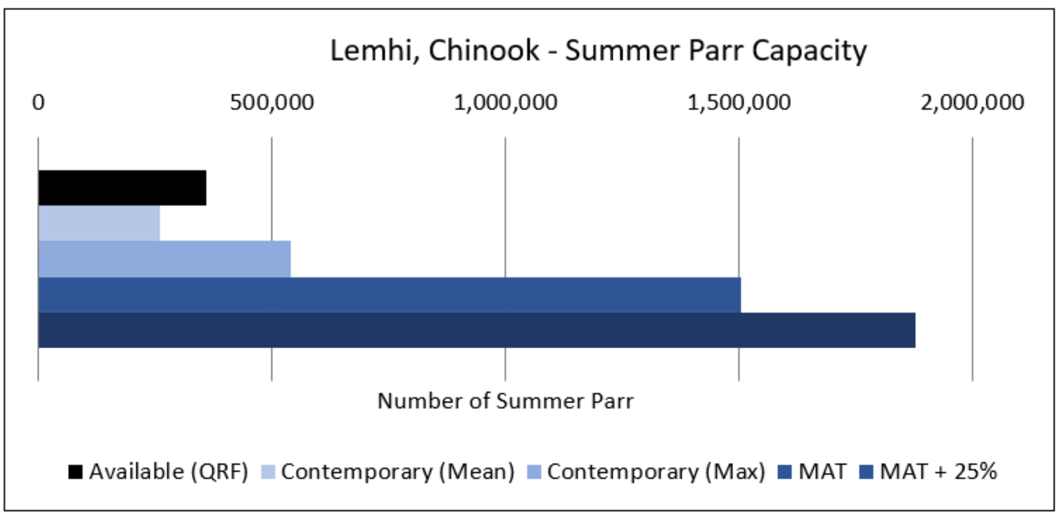

Figure 26. Estimates of available summer juvenile (parr) rearing capacity given current habitat conditions for Chinook salmon in the Lemhi River watershed, made using quantile regression forest models (black bars) versus the capacity required to support contemporary abundance and minimum abundance thresholds (MATs) needed for ESA de-listing (blue bars).

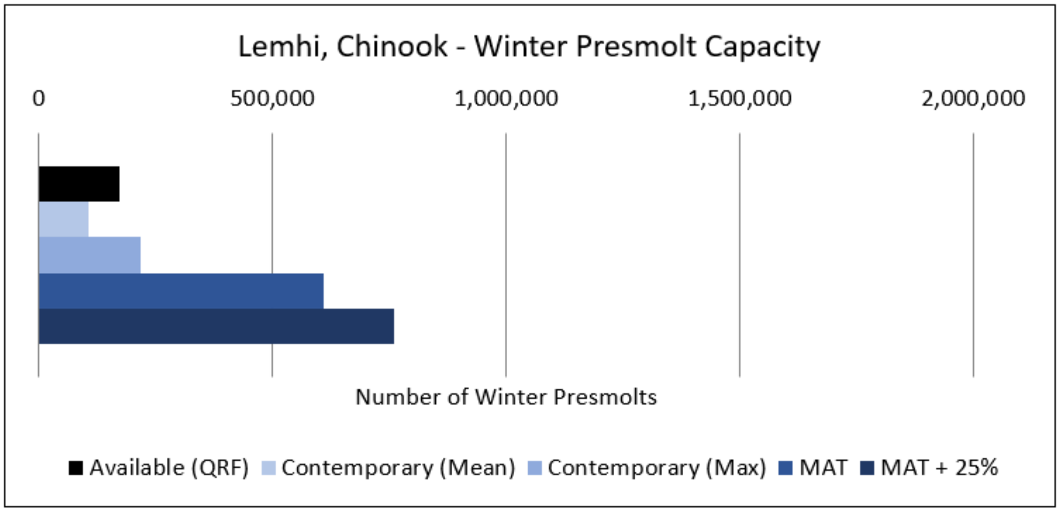

Figure 27. Estimates of available winter juvenile (presmolt) rearing capacity given current habitat conditions for Chinook salmon in the Lemhi River watershed, made using quantile regression forest models (black bars) versus the capacity required to support contemporary abundance and minimum abundance thresholds (MATs) needed for ESA de-listing (blue bars).

Bjornn (1971) identified winter habitat capacity limitations in Big Springs Creek (Lemhi River) and confirmed those observations in subsequent experiments in Hayden Creek, the largest tributary to the Lemhi River (Peery and Bjornn 2004). Hillman et al. (1987) likewise observed winter habitat limitations in the Red River (Clearwater River Subbasin) and confirmed those observations by evaluating habitat improvements.

Steelhead

Available habitat capacity estimates from QRF models are considered preliminary for steelhead in the Lemhi River due to unknown spatial extents of available habitat for steelhead spawning and rearing. The IRA team will work with local biologists and experts to more appropriately identify the extents of habitat in the Lemhi River available to steelhead. Available habitat capacity estimates can be improved in future reach assessments or as needed with local groups.

Current Conditions

Using contemporary escapement estimates, available habitat capacity does not appear to limit spawning (redd) or juvenile rearing for steelhead in the Lemhi River under current conditions (Table 4).

Table 4. Estimated current life-stage-specific capacity requirements versus estimated available capacity for steelhead salmon in the Lemhi River.

Life-Stage	Required Capacity		Available Capacity	Capacity Deficit
	Mean	Max		
Escapement	337	417		
Redd	187	231	3,425	0
Eggs	920,357	1,139,967		
Summer Parr	123,558	153,041	741,594	0
Winter Presmolt	44,311	54,885	583,442	0

Desired Conditions

NOAA (2017) delisting requirements include a minimum annual escapement (i.e., MAT) of 1,000 steelhead adults to the Lemhi River. Based on this requirement, life-stage-specific capacity requirements were recalculated consistent with 1,000 adults (MAT) and 1,250 adults (MAT + 25%) using the same methods as above. Those capacity requirements were also compared to estimates of currently available habitat capacity to identify potential limitations (Table 5). Potential limitations (capacity deficit) were calculated as the life stage-specific capacity requirements needed to achieve a MAT of 1,000 plus a 25 percent buffer minus available capacity.

Table 5. Estimate life-stage-specific capacity requirements to accommodate ESA delisting and estimated available capacity for steelhead in the Lemhi River.

Life-Stage	Required Capacity		Available Capacity	Capacity Deficit
	MAT	MAT + 25%		
Escapement	1,000	1,250		
Redd	555	694	3,425	0
Eggs	2,733,733	3,417,166		
Summer Parr	367,004	458,755	741,594	0
Winter Presmolt	131,618	164,522	583,442	0

There appears to be sufficient redd and juvenile rearing capacity for steelhead to support 1,250 adult steelhead in the Lemhi River (Table 5).

Summary

There appears to be sufficient spawning (redd) and juvenile rearing capacity for steelhead in the Lemhi River to support contemporary escapement and escapement required to achieve delisting criteria for steelhead (Figure 28, Figure 29, and Figure 30).

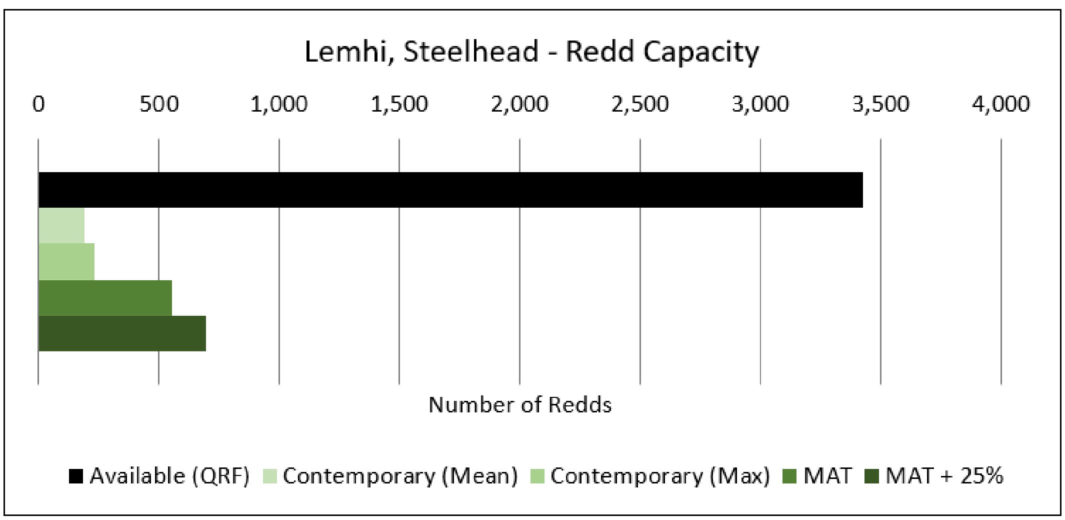

Figure 28. Estimates of available spawning (redd) capacity given current habitat conditions for steelhead in the Lemhi River watershed, made using quantile regression forest models (black bars) versus the capacity required to support contemporary abundance and minimum abundance thresholds (MATs) needed for ESA de-listing (green bars).

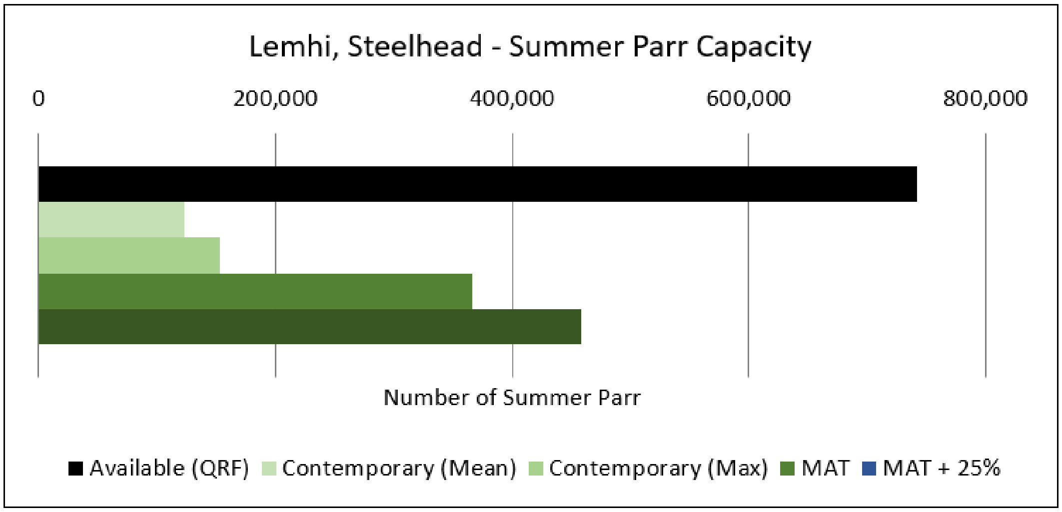

Figure 29. Estimates of available summer juvenile (parr) rearing capacity given current habitat conditions for steelhead in the Lemhi River watershed, made using quantile regression forest models (black bars) versus the capacity required to support contemporary abundance and minimum abundance thresholds (MATs) needed for ESA de-listing (green bars).

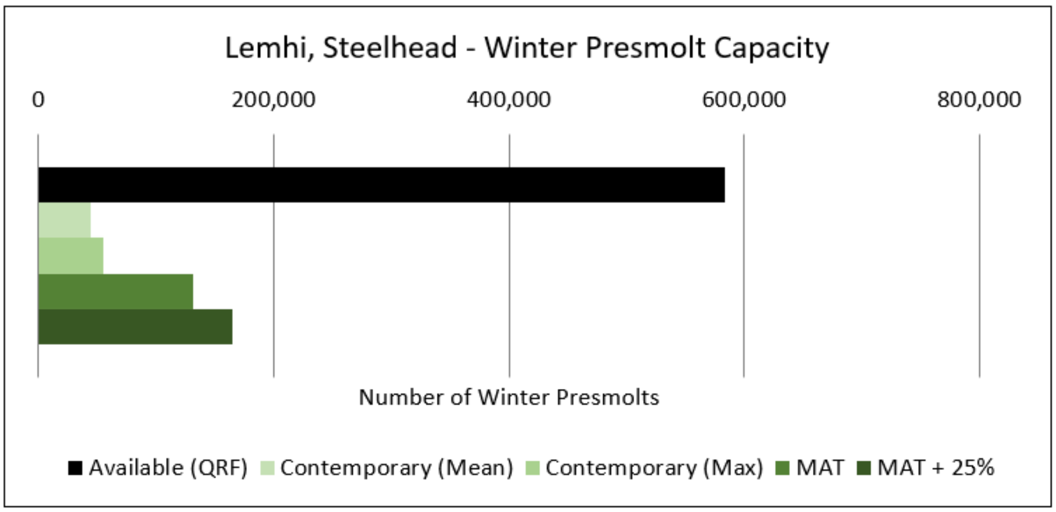

Figure 30. Estimates of available winter juvenile (presmolt) rearing capacity given current habitat conditions for steelhead in the Lemhi River watershed, made using quantile regression forest models (black bars) versus the capacity required to support contemporary abundance and minimum abundance thresholds (MATs) needed for ESA de-listing (green bars).

Geomorphic Assessment

Much of the geomorphic assessment in this report has been compiled in an effort to help paint a better picture of historical and potential target conditions (qualitative), recognizing that detailed (quantitative) target conditions will be generated as part of the MRA for select reaches in the future.

Historical Watershed Conditions

The Lemhi River is located within a northwest-trending valley between the Lemhi Range to the southwest and the Beaverhead Range on the Idaho-Montana border to the northeast. The valley is a block of the northern Rocky Mountain overthrust belt that dropped along basin-and-range normal faults during the past several million years (Link and Janecke 1999). Folded and faulted Precambrian, Paleozoic, and Mesozoic sedimentary rocks are exposed in the mountains on either side of the valley, while the Lemhi Valley itself is composed of deep deposits of valley-fill alluvium accumulated primarily during the warm/dry Pliocene (3 to 5 million years ago; Alt and Hyndman 1989). Beginning with the onset of the cool/moist Pleistocene ice age (2 million years ago), the Lemhi River carved a broad, erosional valley into the thick deposits of alluvium, leaving remnant benches of the original basin-fill surface along the valley margins that persist today.

Thick deposits of unconsolidated alluvium underlain by bedrock permit the presence of an aquifer in the Lemhi basin. A prominent bedrock constriction roughly in the center of the watershed, near the town of Lemhi, Idaho, forces the aquifer to the surface, driving greater groundwater contributions to the system upstream of that point. The bedrock constriction also provides upstream grade control, which has resulted in a lower gradient in the upper half of the valley relative to the lower half. Additionally, the watershed’s largest surface-water tributary (Hayden Creek) enters the Lemhi in this area, further differentiating the upper and lower halves of the basin. Largely as a result of differing hydrologic conditions, the upper half of the Lemhi River likely exhibited traits similar to multi-thread, groundwater-influenced systems, while the lower half exhibited traits more similar to single-thread, snowmelt-dominated systems (Figure 31).

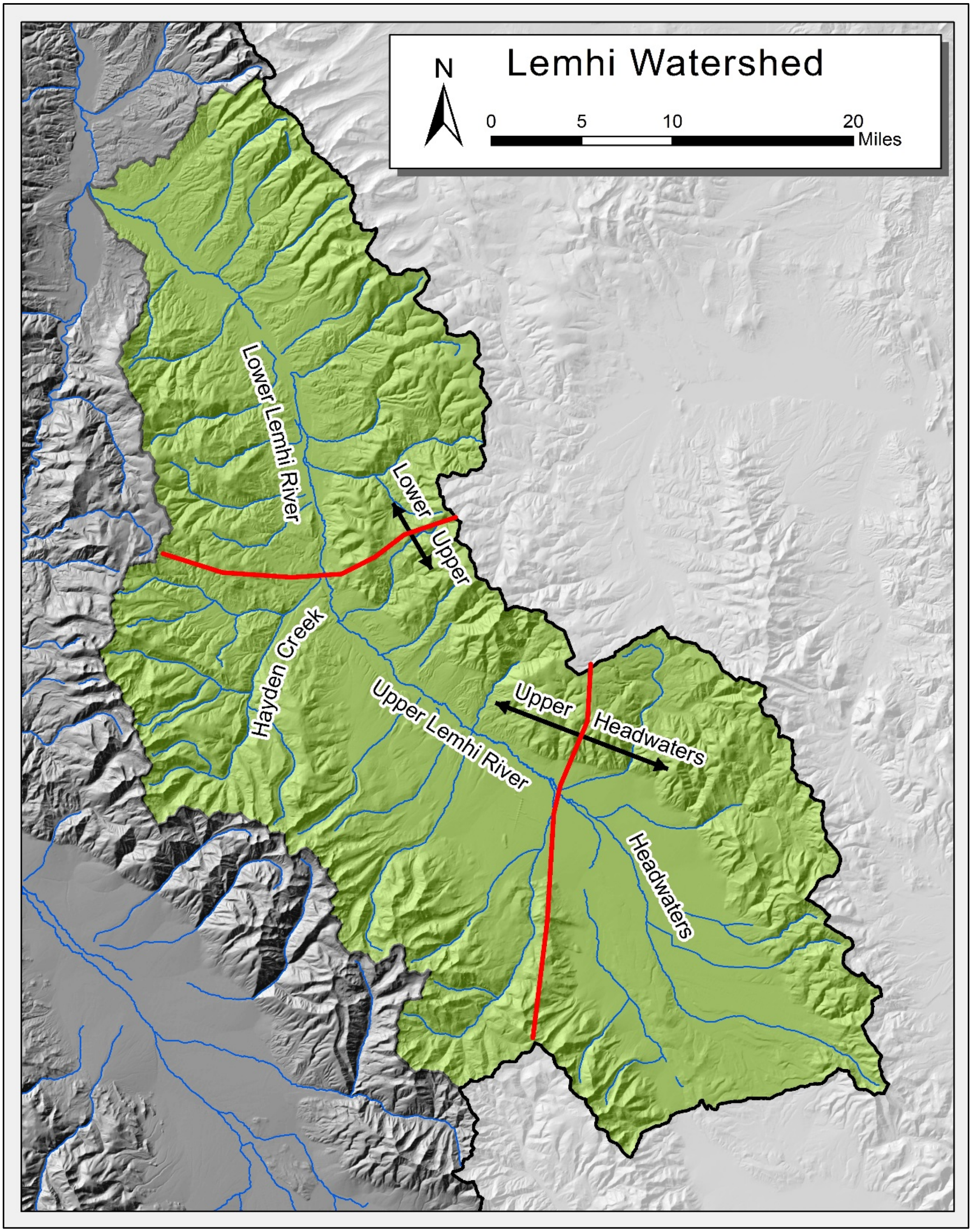

Figure 31. Map showing delineation between the upper and lower Lemhi River.

Historically, the upper Lemhi River (above Hayden Creek) was likely characterized as a fairly stable, multi-threaded (anastomosing), highly sinuous, groundwater-influenced stream with multiple side channels and spring-fed tributary channels all occupying the same floodplain. Observations of reference analogues from Horse Prairie Creek (Montana) and a lack of obvious meander scrolls visible in recent detailed LiDAR topography suggest the channel migration rates were historically low, and channel response tended toward episodic split flow and avulsion.

Beaver and their associated dams likely had a significant impact on the historical geomorphology of the upper Lemhi River. Modern bank exposures reveal 4 to 5 feet of silt and clay sediment overlying coarse gravel and cobble. The extent, depth, and continuity of the fine sediment suggest that widespread slack-water conditions (e.g., beaver dam-influenced wetlands) persisted for long periods of time throughout the valley bottom. The lack of coarse sand and gravel layers in bank exposures suggests that sediment from episodic debris flows and/or catastrophic events were attenuated or arrested at the valley margin, further supporting a broad slack-water environment spanning the majority of the valley bottom. Trapper journals (Ferris 1830-1835) also noted large numbers of beavers, documenting the capture of 50 to 60 beavers per day in the vicinity of the Lemhi River.

Historical riparian conditions in the upper Lemhi River likely reflected a consistent groundwater-influenced hydrology and associated high water table punctuated by periods of extended flooding associated with beaver activity. Relic topographic variation from occasional avulsions, beaver dams, and disturbance from grazing animals (bison, elk, and deer) likely created a mosaic of open water, emergent wetland, floodplain, and upland. The riparian community would have mirrored this diversity with areas of wetland meadow (rushes and sedges), floodplain shrubs (willow) and upland vegetation (sagebrush and grass). Most riparian vegetation had to tolerate fine, poorly draining soils and extended periods of submergence. Few sporadic stands of cottonwood or aspen trees may have established on well-draining soils, particularly near the mouths of snowmelt-dominated tributaries that could occasionally produce the disturbance (i.e., sand and gravel deposition) required for germination and establishment. The lack of coarse sediment inputs to the channel likely severely limited rates of point bar development and channel migration, suggesting the banks were fairly stable and able to maintain mature vegetation.

The lower Lemhi River below Hayden Creek has a slightly steeper gradient, a more snowmelt/surface-flow-dominated hydrology, and greater coarse sediment availability from large tributaries compared to the upper Lemhi River. The historical lower Lemhi River was likely dominated by a single-thread channel with a seasonally active floodplain; localized areas of island braiding were unconfined and in association with in-channel obstructions (i.e., log jams and stands of dense riparian vegetation).

The more-pronounced snowmelt-dominated hydrograph and greater coarse sediment inputs enabled significant portions of the lower Lemhi River to migrate on a year-to-year basis, punctuated by episodic avulsions. From the 2016 Upper Lemhi Riparian Management Plan (Cardno 2016):

> *Although there are no known measurements of channel geometry prior to large-scale settlement and disturbance, there are several anecdotal accounts of the river's form from historic journals and maps as well as ancient channel scars visible on the floodplain from detailed LiDAR topography. From the journals of W. A. Ferris (1830-1835), the lower Lemhi River is described as "forty paces wide, bordered with willows, and birch, and aspen, and flows norwestward fifty miles to Salmon River." It is likely that stream crossings occurred at unobstructed riffles where the water was shallow and wide and the riparian vegetation was limited, suggesting the widest portion of the channel may have been upwards of 80-100-feet on the lower river. Identification of the "principal stream" by W. A. Ferris (1830-1835) also suggests a primary channel with side channels. A true multi-threaded (anabranching) stream does not have a principal thread, while a single-threaded stream with no side channels would not warrant mention of the "principal"*

stream, which implies multiple branches. Additionally, maps from Lewis and Clark (1805) show a single-threaded stream with areas of multiple side channels and many tributaries flowing through the valley bottom further supporting this characterization (Figure 32).

Figure 32. Lewis and Clark map (Moulton 1983) illustrating the lower Lemhi River (called the East Fork of the Lewis River by Lewis and Clark). The modern towns of Tendoy and Salmon are shown for reference.

Although the upper Lemhi River banks were likely somewhat more stable than the lower Lemhi River due to the fairly flat, groundwater-influenced hydrograph and lack of coarse sediment input, both the upper and lower Lemhi were historically characterized by stable banks and a low width-to-depth ratio enabled by dense riparian vegetation (willow shrubs and/or cottonwood) and a low gradient. Mature riparian vegetation provided bank structure along the outside of bends, forcing flow convergence that created pools with associated tail-out riffles. The lack of observed buried wood in bank exposures on the upper Lemhi River and likely beaver-dam-influenced wetland conditions suggest little to no large woody material likely recruited historically in the upper valley. The flashier hydrology and increased coarse sediment load in the lower valley likely created a disturbance regime more suitable for the establishment and propagation of cottonwood and aspen trees, in addition to willows and other shrubs. It is likely that large woody material has been recruited to the lower Lemhi River via local windfall for thousands of years. Large floods and debris torrents from tributaries may have transported large wood from the uplands episodically, but research suggests that wood is unlikely to transport through such small streams with low channel width and meander radius of curvature (Braudrick and Grant 2001). Hayden Creek is likely the only tributary large enough to have consistently transported large woody material to the Lemhi River.

Prior to Euro-American settlement, the Lemhi region was most likely inhabited by a group of Northern Shoshone known as the *Tu'kudeka,*or Sheepeaters, who lived in the area (Rossillon 1980). Reports from Lewis and Clark suggest their impacts on the land were primarily confined to their encampments, where tribes from the region would congregate and trade their goods. Lewis and Clark also reported on the abundance of fur-bearing animals west of the divide, which spurred the business of fur trade. Independent fur trappers, as well as several companies (including the Hudson Bay Company and the American Fur

Company) made their way into the northwest to explore and exploit the region. By the early 1840s, local beaver populations were brought to the brink of extinction and the bison had disappeared from the Salmon River region (Albers et al. 1998).

The discovery of gold in California in 1848 began a western mining craze, leading to an influx of prospectors into Idaho and the discovery of gold there. Mining in the area consisted of placer mining along some tributaries and some hard-rock mining. Miners and other settlers were interested in acquiring the Shoshone Tribe's lands and waterways to support their growing agrarian and mining enterprises, and homesteads sprang up across the lower-elevation lands (Albers et al. 1998). Timber was an important commodity during this time, as lumber and poles were needed for building construction and livestock fencing. Timber harvests and associated management activities affected the watershed during this time and led to increased runoff, erosion, and sedimentation in many of the tributaries that discharge into the Lemhi River.

Beginning in the 1880s, irrigation development and associated water rights were established in the mainstem Lemhi and tributaries (ISCC 1995). Irrigation ditches withdrew water from the river and distributed it across the floodplain. In the mid-1900s, significant stream channeling and straightening was undertaken by the state highway department and local ranchers, which together altered roughly 21 percent of the channel length (Gebhards 1958). Between 1908 and 1954, Idaho Power operated a roughly 6-foot-tall diversion dam that spanned the lower Lemhi River about 1 mile upstream of its confluence with the Salmon River (Figure 33). Historical fisheries reports are unclear regarding the passage of fish at the dam, but they suggest that upstream, adult fish passage must have been possible during high water, "otherwise the salmon run would surely have been eliminated" (Gebhards 1959). The dam likely affected fish migration and impounded sediment. In 1959, approximately 5 percent of the flow (15 cubic feet per second (cfs)) was being discharged at the mouth of the river, while 95 percent (312 cfs) was diverted into the power plant (Gebhards 1959). Anecdotal accounts suggest the lower river was completely dry in other years.

Figure 33. Idaho Power diversion dam on the lower Lemhi River (Source: Oregon State University, downloaded March 14, 2017, from https://oregondigital.org/sets/streamsurvey/oregondigital:df66q392q)

Presently, livestock grazing is the predominant land use activity that occurs on both private and public lands within the Lemhi valley. Grazing on Federal lands provides nearly 30 percent of the feed base for cattle in the Lemhi River watershed (ISCC 1995). Generally, cattle are grazed on higher-elevation Federal lands from May to October and then return to private lands in the valley for the remainder of the year (ISCC 1995). Historical grazing practices resulted in riparian vegetation clearing and associated streambank destabilization, as well as increased surface-water runoff and erosion (Photograph 19).

Photograph 19. Hummocks observed on the floodplain of the upper Lemhi River reveal 2 to 3 feet of fine sediment erosion (area between hummocks) associated with historic cattle grazing. Similar hummocks are common throughout large areas of the Lemhi River floodplain.

Existing Watershed Conditions

Hydrology/floods

The Lemhi River flow regime is predominantly snowmelt-dominated, with numerous diversions that are in operation from April through September. While diversion locations and volumes are regulated, exact withdrawal rates on a seasonal and daily basis are unknown. Groundwater is another important component of the Lemhi River water budget. Groundwater levels are highest from May to September due to snowmelt and irrigation. A natural constriction occurs between river miles (RM) 34 and 25 that divides the upper and lower regions of the basin. Flood-frequency peaks were estimated at two U.S. Geological Survey (USGS) gages and two Idaho Department of Water Resources (IDWR) gages using the PeakFQ program, and at 23 ungaged locations, applying a drainage area ratio (Table 6).

Table 6. Summary of Lemhi River hydrology.

River Mile	Drainage Area (mi^2)	Valley Segment	Estimated Flood-Frequency Values (cfs)						
			1.5	2	5	10	25	50	100
0.1	1,260	4	912	1,223	2,059	2,638	3,371	3,913	4,444
19.1	1,055	3	771	1,018	1,670	2,113	2,666	3,069	3,462
32.7	733	2	463	586	892	1,089	1,326	1,494	1,654
60.4	470	1	197	228	257	292	331	357	381

Irrigation Use and Natural Hydrograph Shape

During the growing season, there are numerous diversions throughout the basin that remove surface water for irrigation. The volume of water removed from the Lemhi during the irrigation season (groundwater and surface water) can impact the peak flow hydrograph, potentially altering the hydrologic regime. Streamflow data from the IDWR gage at Cottom Lane from a heavy-snowpack year (2010) was compared with streamflow data from a low-snowpack year (2014) to assess the variation in the hydrograph at this location. It was assumed that irrigation starts around the beginning of May and ends near the beginning of October upstream of this location. The hydrographs for these 2 years were assessed to estimate the base flow through the irrigation season with and without irrigation. The difference between these two base flows is the approximate loss due to irrigation withdrawals, as seen in Figure 34. This difference for each day was added back into the recorded daily average flow hydrograph to approximate what a natural hydrograph may have resembled without irrigation. The overall shape of the hydrograph doesn't change, but the peak magnitude and the rising and falling limbs of the hydrograph increase, as seen in Figure 35 and Figure 36 for a dry and wet year, respectively.

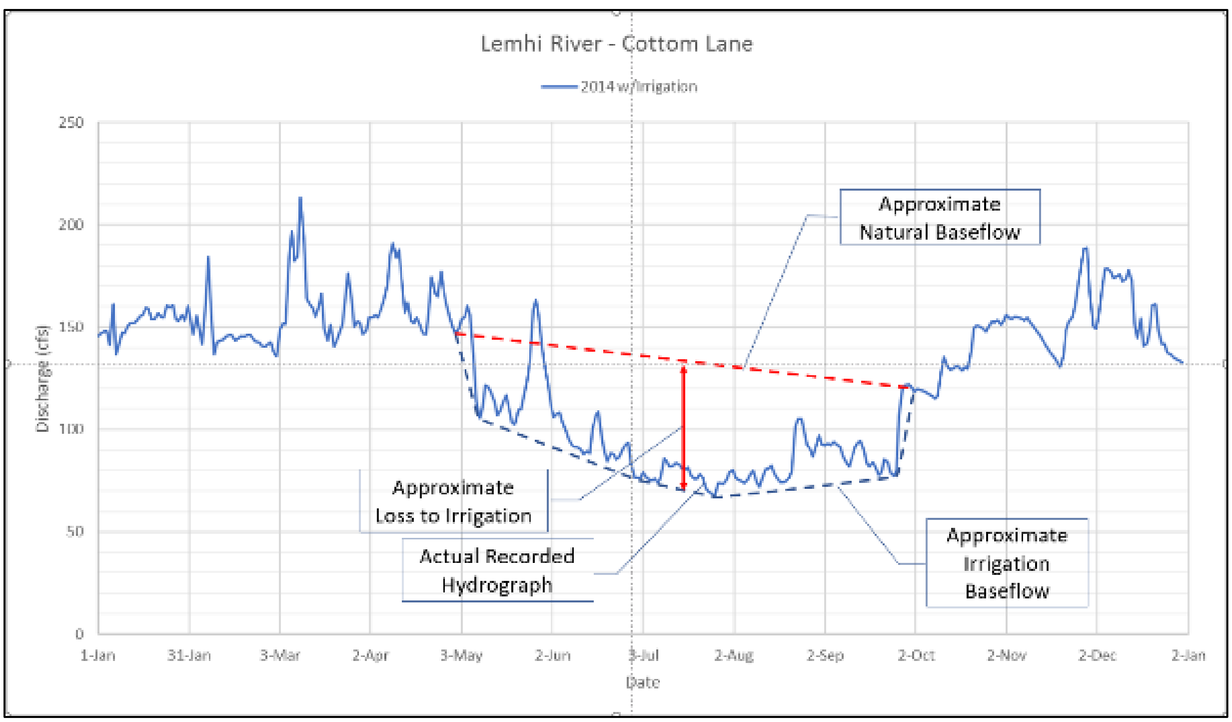

Figure 34. Estimation of discharge lost to irrigation.

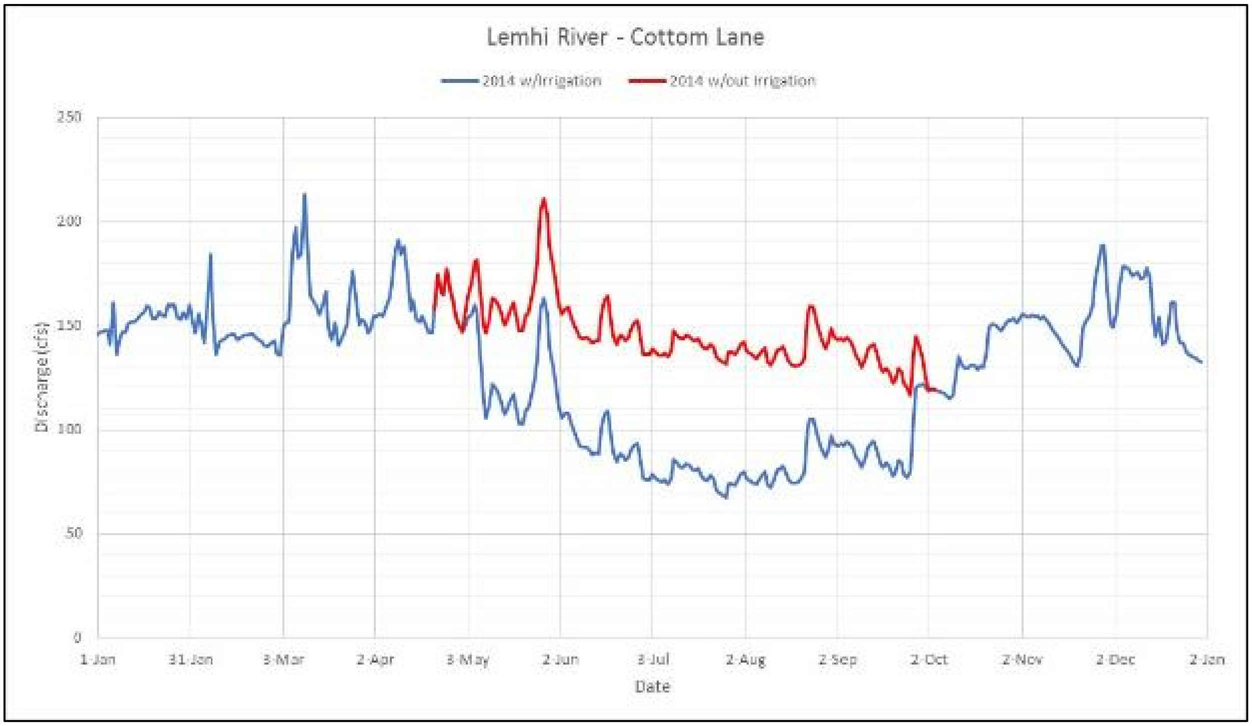

Figure 35. Comparison of actual and natural hydrographs for a dry year on the Lemhi River at Cottom Lane.

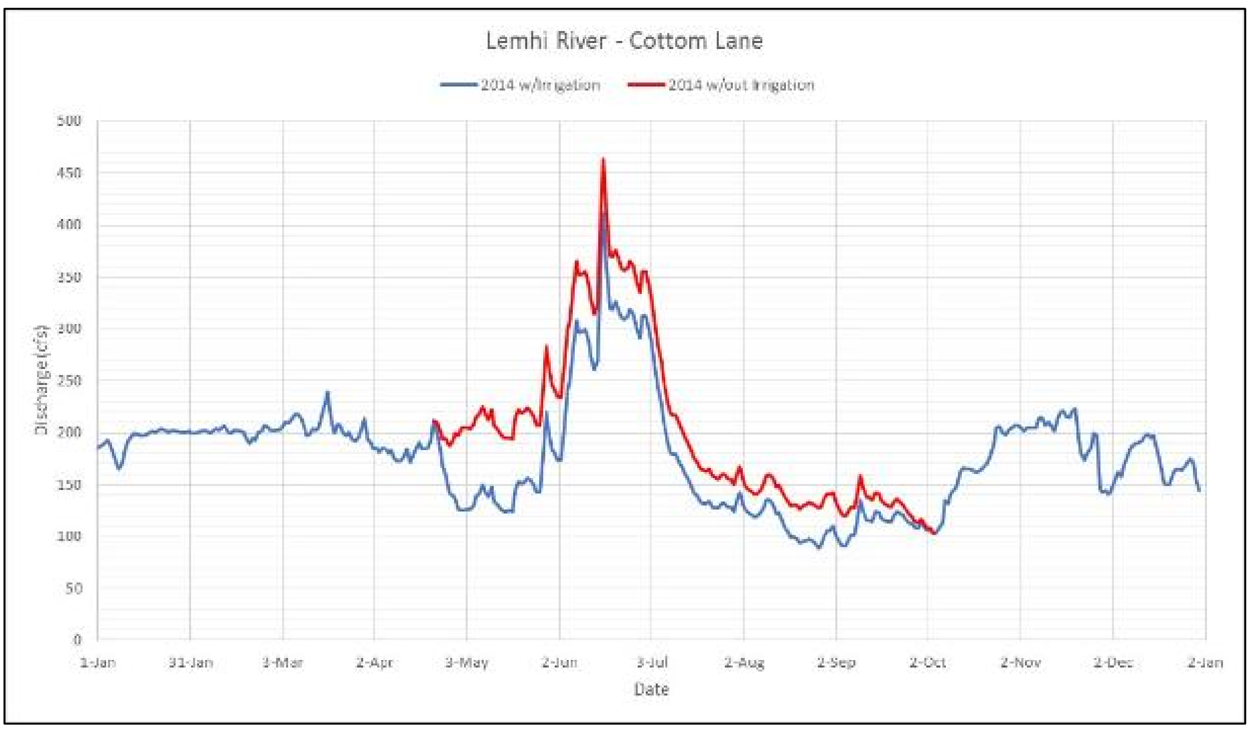

Figure 36. Comparison of actual and natural hydrographs for a wet year on the Lemhi River at Cottom Lane.

This procedure can be refined and completed at all the gages on the Lemhi River or other tributary of interest to develop a theoretical natural flow hydrograph. This can inform water users and regulators of the significance and timing of flushing flows. Irrigation users often begin to divert water earlier in the season during high-flow years, and this could affect the baseflow timing. These variations should be accounted for in future analyses to more accurately estimate the irrigation withdrawals.

Surface and Groundwater Interactions

In the Lemhi River, water consumption is primarily for agricultural and domestic purposes. More than 70 diversions direct water from the Lemhi River and its tributaries to irrigate about 90,000 acres of cropland and to water livestock. The irrigation season starts in early spring and continues through early fall. Much of the diverted water for irrigation returns to the Lemhi River by surface and groundwater flows. The highest measured streamflow in the Lemhi River is from late spring through mid-summer and usually peaks in early June, when the mountain snowmelt occurs. The lowest streamflow generally is in the fall.

Most of the Lemhi River typically gains discharge from groundwater in early August, during the peak of the irrigation season, with the greatest volume of gains in the areas near the towns of Leadore (RM 60), Tendoy (RM 25), and Salmon (RM 1) (Figure 37 and Figure 38; Donato 1998; IDWR 2017). Groundwater contributions to the Lemhi River decrease after the irrigation season in almost all locations, except near RM 11 and RM 34, where groundwater discharge increases slightly, and near Leadore (RM 60), where groundwater discharge remain relatively unchanged.

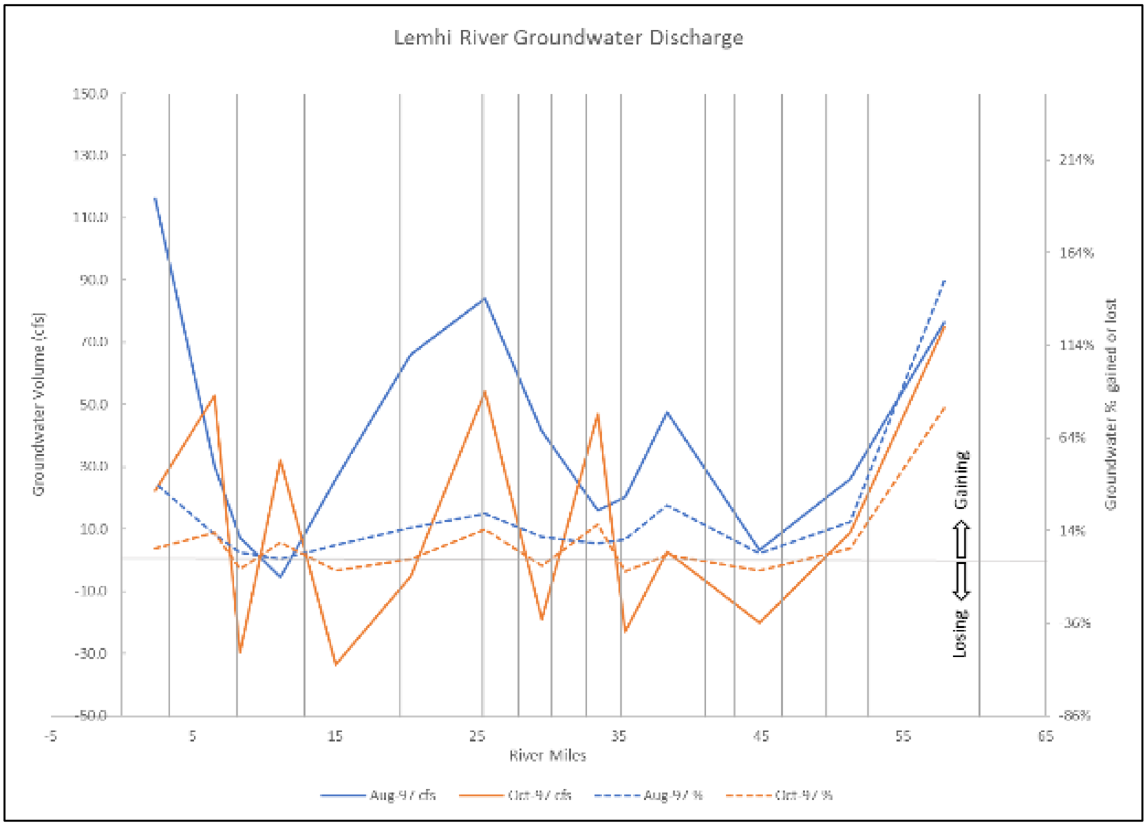

Figure 37. 1997 Lemhi River groundwater discharge graph, illustrating groundwater volume (solid lines) and percent of total discharge (dashed lines) for August during the peak of irrigation (blue lines) and October after irrigation season (orange lines) (interpreted from Donato 1998).

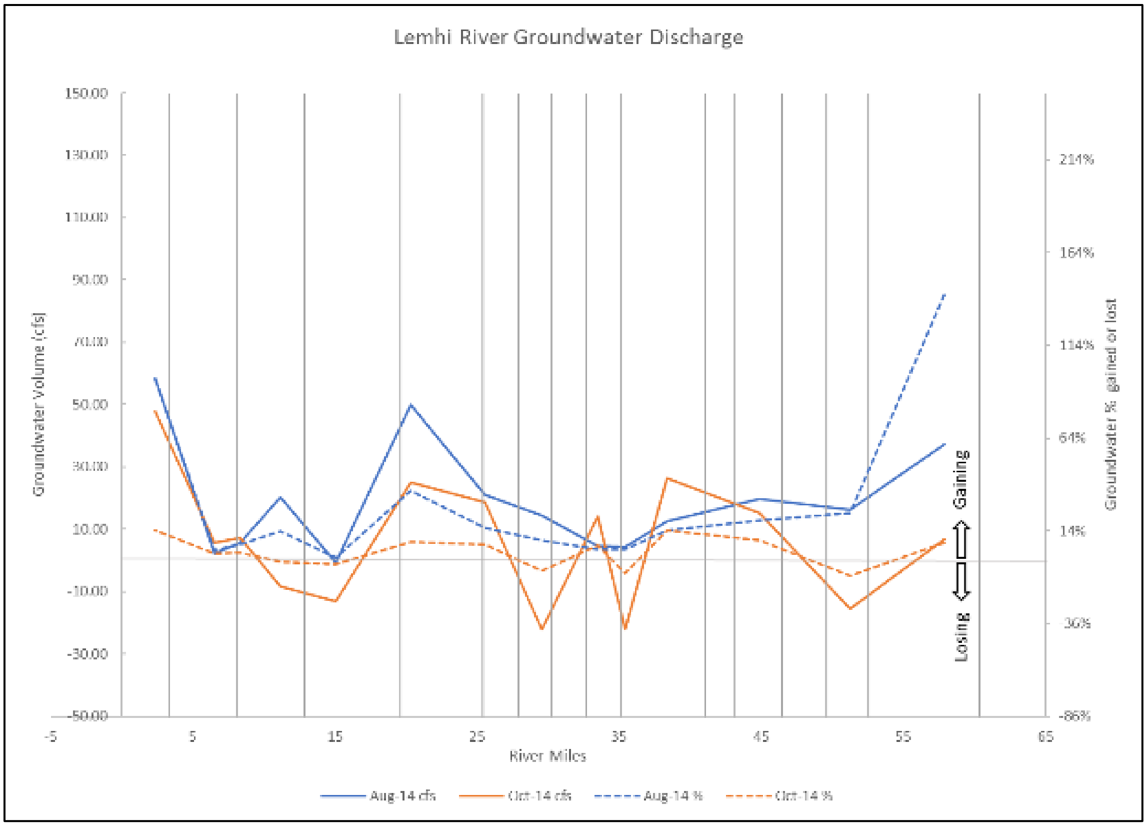

Figure 38. 2014 Lemhi River groundwater discharge graph illustrating groundwater volume (solid lines) and percent of total discharge (dashed lines) for August during the peak of irrigation (blue lines) and October after irrigation season (orange lines) (interpreted from IDWR 2017).

Hydraulics

Coarse, at-a-station hydraulic analyses were completed from three representative locations within the watershed to provide context for the geomorphic conditions discussed below. More-detailed two-dimensional hydraulic modeling will be completed as part of the future MRA process for select reaches. Three typical cross-sections located throughout the Lemhi River watershed were measured and evaluated to assess representative existing hydraulic characteristics and to determine if any generalizations can be inferred from these calculations. Cross-sections were measured at RM 60.4 (Valley Segment 2, Geomorphic Reach 2, Figure 39), RM 35.9 (Valley Segment 2, Geomorphic Reach 7, Figure 40), and RM 9.8 (Valley Segment 4, Geomorphic Reach 14, Figure 41).

At a Station Hydraulic Calculations Summary Sheet

River:	Lemhi
Rivermile:	60.4
Valley Segment:	2
Geomorphic Reach:	2
Reach Slope:	0.0038
Localized Slope:	0.0035
n-value (range):	0.035 - 0.045

Local Sediment Size (mm)

D_{16}: 12 D_{50}: 21 D_{84}: 39

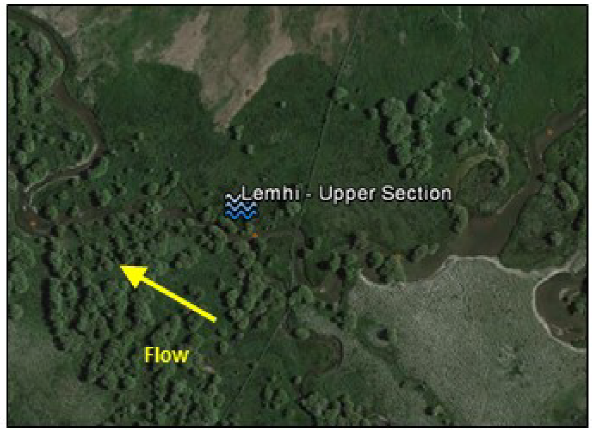

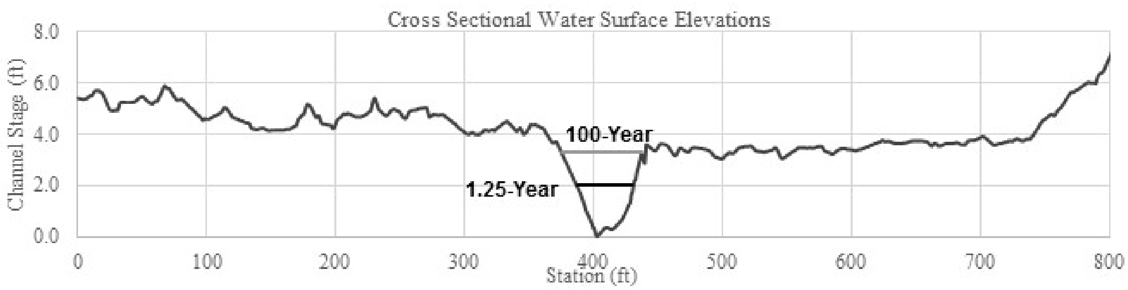

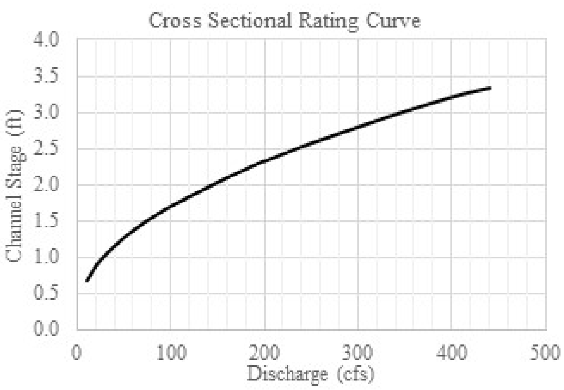

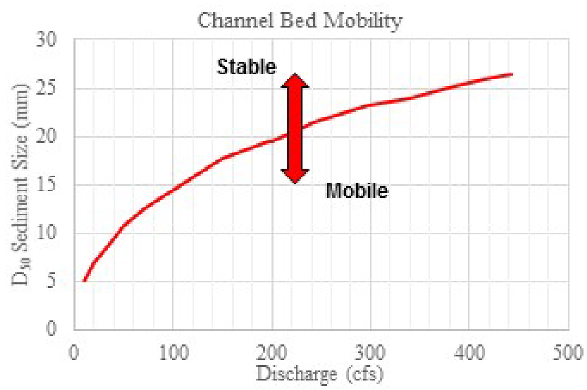

Recurrence Event:	1.25-Year	100-Year
Discharge (cfs):	150	447
Stage (ft):	2.0	3.3
Top Width (ft):	45	66
Ave. Velocity (ft/s):	2.6	3.4
Ave. Shear (lb/ft^2):	0.3	0.4
Ave. St. Power (lb/ft*s):	0.7	1.4
D_{50} Mobilized (mm):	18	26

Entrenchment Ratio (ft/ft):	1.5
Discharge to Mobilize D_{50} (cfs):	228
Bed Armored (yes/no):	No

Lemhi River – Upper Section

Integrated Rehabilitation Assessment

Idaho Governor's Office of Species Conservation Date Exported: 03/23/2017

Figure 39. Summary of representative hydraulic conditions at Site 1.

At a Station Hydraulic Calculations Summary Sheet

River:	Lemhi
Rivermile:	35.9
Valley Segment:	2
Geomorphic Reach:	7
Reach Slope:	0.0061
Localized Slope:	0.0066
n-value (range):	0.035 - 0.045

Local Sediment Size (mm)

D_{16}:	9	D_{50}:	51	D_{84}:	101

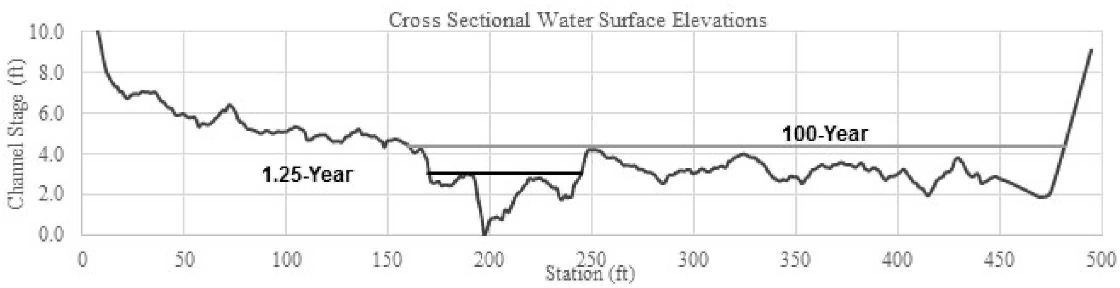

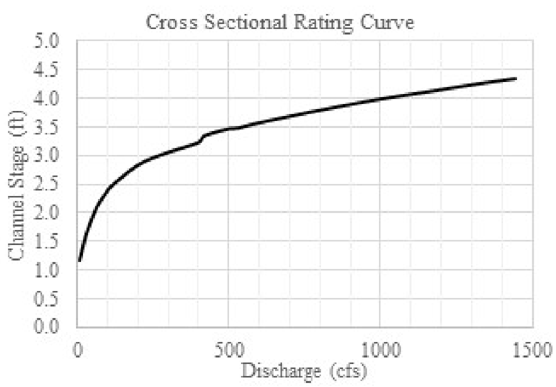

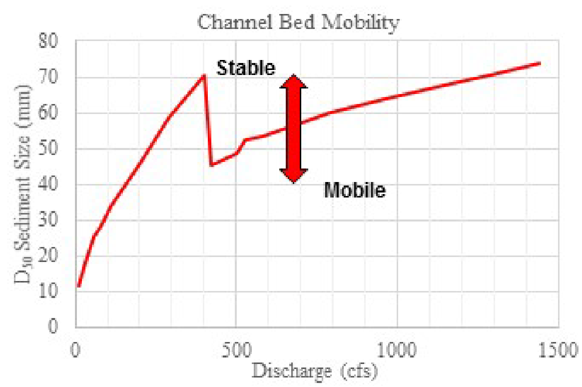

Recurrence Event:	1.25-Year	100-Year
Discharge (cfs):	291	1443
Stage (ft):	3.0	4.4
Top Width (ft):	75	312
Ave. Velocity (ft/s):	4.9	6.1
Ave. Shear (lb/ft^2):	0.9	1.2
Ave. St. Power (lb/ft*s):	4.6	7.1
D_{50} Mobilized (mm):	59	74

Entrenchment Ratio (ft/ft):	4.2[1]
Discharge to Mobilize D_{50} (cfs):	210
Bed Armored (yes/no):	No

Lemhi River – Middle Section

Integrated Rehabilitation Assessment

Notes: 1. Entrenchment Ratio based off main channel width not including side channels.

Idaho Governor's Office of Species Conservation Date Exported: 03/23/2017

Figure 40. Summary of representative hydraulic conditions at Site 2.

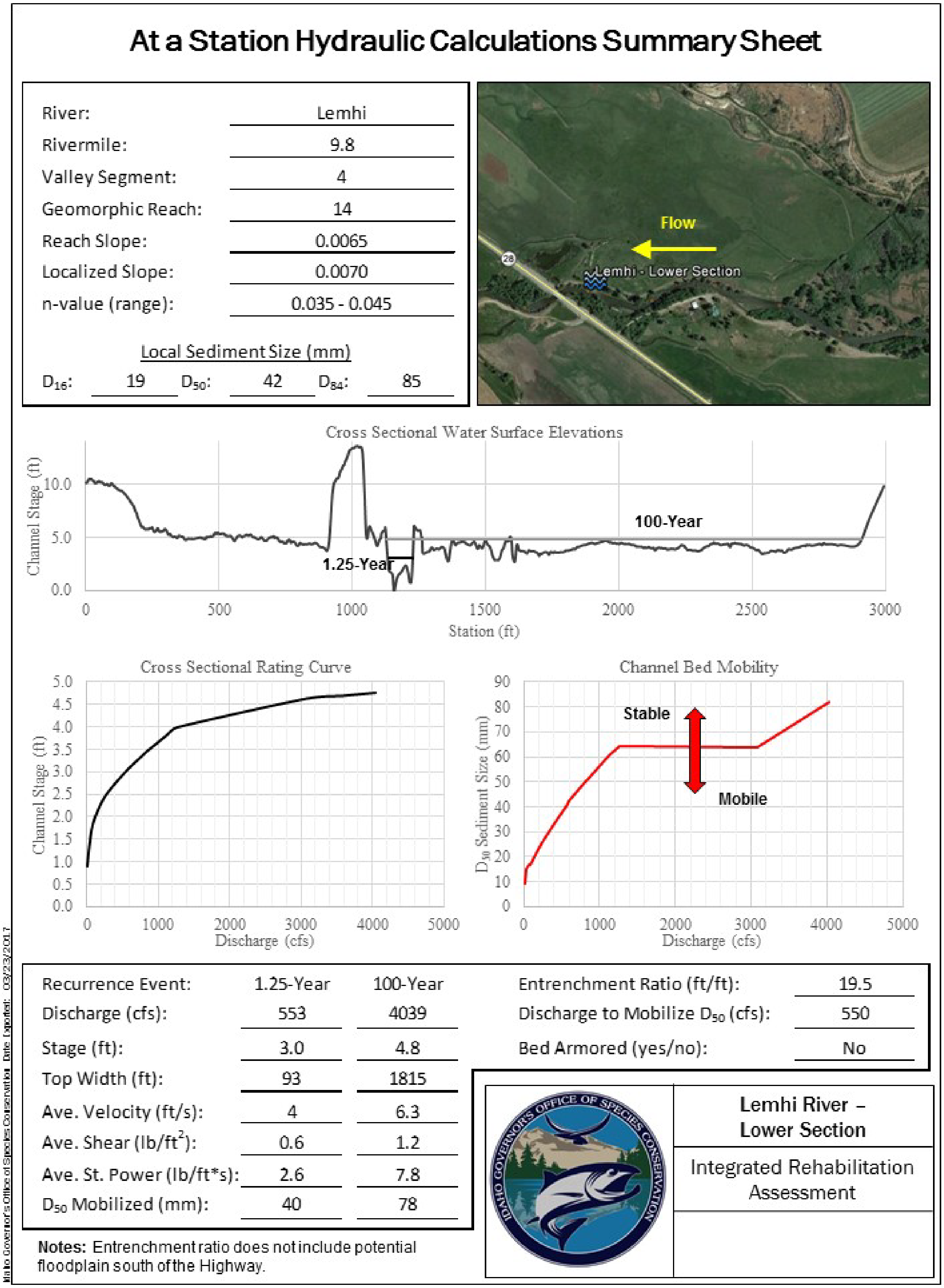

Figure 41. Summary of representative hydraulic conditions at Site 3.

In the groundwater-influenced flow regime of the upper Lemhi River, there is less variation from the 1.25 to the 100-year discharge, which results in a lower entrenchment ratio (1.5). The section modeled shows the 100-year discharge contained primarily within the main channel banks. The sediment size was showing bed mobilization beginning near the 2-year event, which allows the channel to scour and maintain pools. Fine-grained sediment filling interstitial space between larger clasts (embeddedness) may limit bedload mobilization. Channel velocities varied from 2.5 feet per second at the 1.25-year up to 3.5 feet per second at the 100-year event. Shear stresses also had minor variation from 0.3 to 0.4 lb/ft^2 between these two events. The groundwater-dominated hydrology results in fairly uniform and consistent flow patterns through this section.

The middle section is located a short distance upstream of Hayden Creek and is located at the beginning of a gaining reach. There are much larger variations in flow differences between the 1.25-year and 100-year discharge at this location compared to the upper Lemhi River. The channel geometry is such that the 1.25-year event is slightly out of bank and the 100-year event accesses a good portion of its floodplain, which increases the entrenchment ratio to approximately 4.2, assuming that the floodplain actively conveys flow downstream. Local sediment sizes suggest that the bed may begin to mobilize near 200 cfs, which is less than the 1.25-year event, although sediment embeddedness may limit actual bedload mobilization. Channel velocities range from 5 ft/sec. to upwards of 6 ft/sec. Depending on how and when the channel accesses a large portion of its floodplain at this section, there is a lot potential variation in flood hydraulics, and further study would be required to assess those characteristics.

The lower section is located upstream of an existing crossing of Highway 28 and is in the snowmelt-dominated segment of the Lemhi River. The main channel is partially channelized, with discontinuous levees or high ground on each river bank. Assuming that the levees are ineffective at holding back flood flows, the 100-year discharge extends across the valley floor, creating a high entrenchment ratio of 19.5. Channel velocities range between 4 and 6.5 ft/sec for the 1.25- and 100-year discharge events, respectively. Shear stresses vary from 0.6 up to 1.2 lb/ft^2 for the same two flow events. The channel appears to be unarmored through this section of river, beginning to mobilize the D_{50} near the 1.25-year event. Sediment embeddedness may limit bedload mobilization. (Note: the highway cuts off a portion of the accessible floodplain at this location and throughout significant portions of the Lemhi River valley.)

General trends observed between these three cross-sections are that the floodplain becomes more accessible to flood waters in downstream reaches, assuming levees cannot contain all flow. While this is largely due to the gradual shift from groundwater-dominated to snowmelt-dominated hydrology, this trend could be exacerbated by channel widening in the upper region and channelization through the lower region. Incipient motion calculations suggest that the channel bed appears not to be heavily armored and becomes mobilized on a regular basis. To the contrary, field observations, including a lack of gravel bars and vegetative growth on bed material, suggest bedload mobilization does not occur as frequently as the incipient motion calculations predict. This suggests that the bed material is embedded with sand and silt, reducing mobilization frequency. It is likely that areas of flow constriction (outside of bends or adjacent instream structure) exhibit sufficient additional shear stress to overcome the embedded condition of the substrate to develop or create self-sustaining pools and sort of gravels on a regular basis.

A stream power assessment was also completed to investigate the potential sediment transport capacity of each geomorphic reach. Stream power is a function of discharge and slope but does not incorporate channel geometry (i.e., width), which is important in understanding where deposition and scour are likely to occur. More-refined sediment transport analyses will be possible with refined reach-scale analyses that incorporate detailed hydraulic modeling. Results of the stream power analysis show that stream power was primarily dependent on the discharge input; thus, overall stream power increased in the downstream direction with increasing peak discharge.

Basin Geometry

Domains within a watershed can be characterized as zones that are governed by sediment supply, alluvial fan formation, sediment transfer, or deposition (Figure 42). The headwaters streams of the Lemhi River basin are generally classified as sediment supply zones, dominated by weathering and erosion of steep slopes, where tributaries collect and transport sediment downslope to the alluvial fan zone. The alluvial fan zone is where coarse sediment has accumulated across broad alluvial fans and piedmont belts, creating terraces along the valley margins. Here, the basin-fill sediments are porous, and the river commonly loses surface water to the aquifer. Unlike most streams, the Lemhi River exhibits a pronounced deposition zone below the alluvial fan zone before entering a sediment transfer zone.

Below the alluvial fan zone, tributaries flow across the broad, low-gradient valley bottom, where they are unable to transport coarse sediment, creating a pronounced deposition zone characterized by fine sediment and a highly sinuous, multi-threaded channel. A longitudinal profile of the channel from Leadore near RM 63 to Salmon at RM 0 shows a convex profile, with the lowest gradient near Leadore and a generally increasing slope in the downstream direction (Figure 43). These conditions are the result of a prominent mid-valley grade control associated with shallow bedrock near the confluence of Hayden Creek (RM 32.9). The combination of a low gradient and a broad valley promotes coarse sediment deposition on the valley margins in the alluvial fan zone, and fine sediment deposition in the broad floodplain of the deposition zone upstream of Hayden Creek.

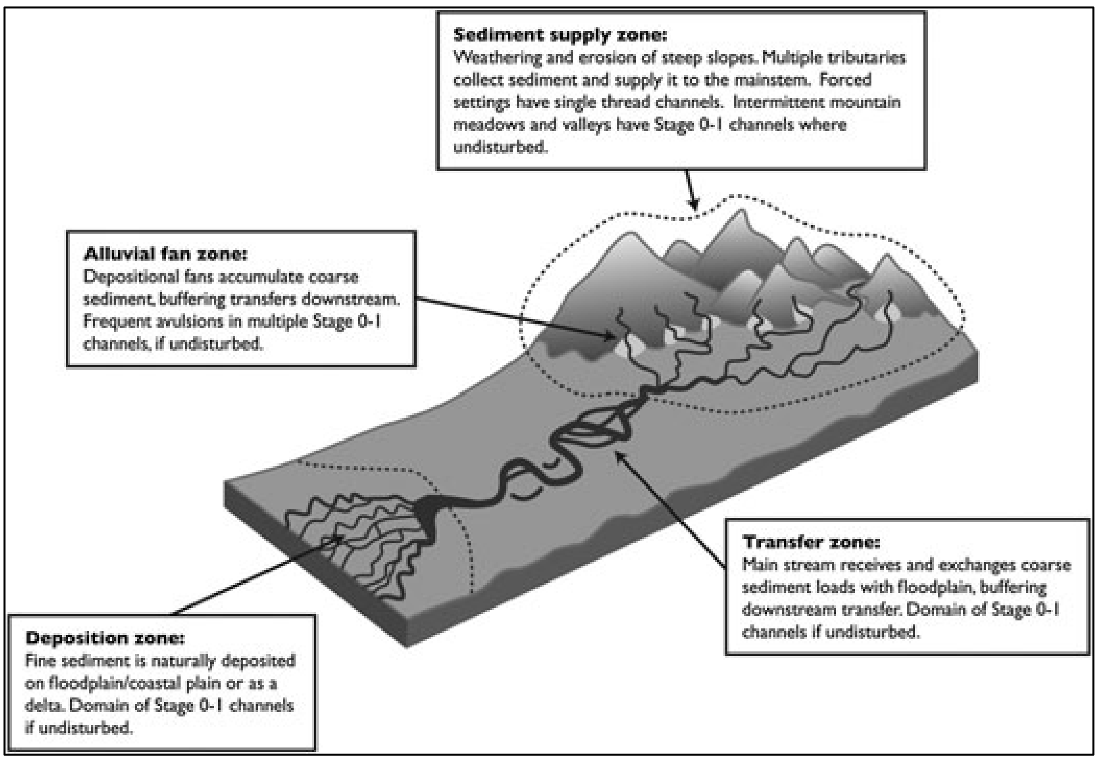

Figure 42. Locations of sediment domains within a typical watershed (Cluer and Thorne 2013). Unlike typical watersheds, a pronounced, low-gradient deposition zone occurs immediately below the alluvial fan zone on the Lemhi River resulting from a mid-valley bedrock grade control near the confluence of Hayden Creek (RM 32.9), followed by a transfer zone characterized by greater sediment availability and transport.

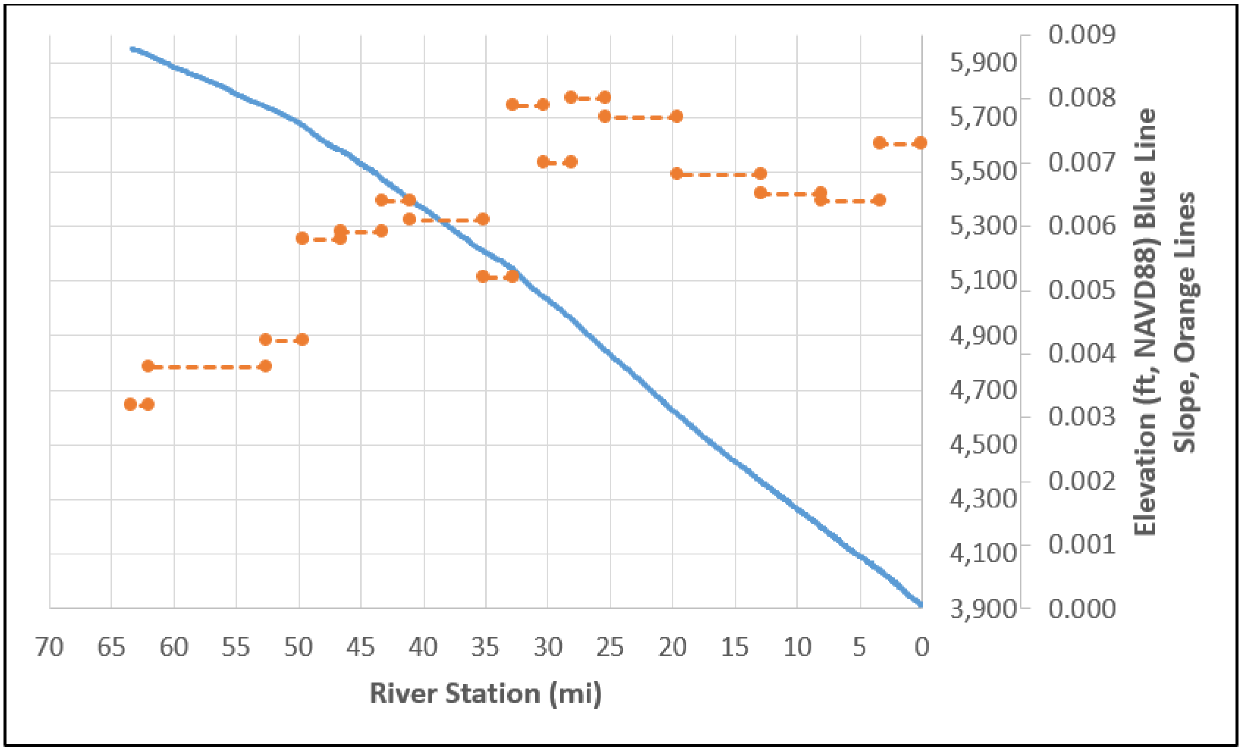

Figure 43. Lemhi River longitudinal profile (blue line) and average reach slope (dashed orange lines) by river mile. The gradient is generally lower upstream of an area of shallow bedrock that coincides with the Hayden Creek confluence near RM 32.9.

The width of the Lemhi River floodplain, as defined by the location of confining terraces and/or valley margin, is generally wide. Dividing the width of the floodplain by the width of the bankfull channel produces a result called the entrenchment ratio. A small entrenchment ratio means the channel has less-accessible floodplain area and therefore less ability to dissipate flood energy on the floodplain, resulting in deeper, higher-velocity, more-forceful flood flows, increasing the potential for erosion and/or incision (i.e., transport reach). Large entrenchment ratios are representative of channels with broadly accessible floodplains that can dissipate flood energy outside the banks of the channel, resulting in less-forceful flood flows and a tendency for deposition (i.e., response reach). The entrenchment ratio on the Lemhi is generally lower in areas of groundwater-influenced hydrology as a result of lower peak flows and possibly minor incision. The entrenchment ratio increases in the lower Lemhi River, where greater peak flows occur due to a more snowmelt-dominated hydrology. Human features such as levees, road embankments, and other obstructions have unnaturally confined the floodplain in several locations, particularly in the middle and lower Lemhi, greatly reducing the local entrenchment ratio in those areas.

Soils

Geomorphic features in the Lemhi valley bottom include the active channel, floodplains, alluvial fans, stream terraces, and outwash fans and fan terraces. Soils that have formed on these features are described in Table 7. Soil descriptions are based on the NRCS detailed soil maps and the Detailed Soil Map Units section in the report (NRCS 2003).

Table 7. Geomorphic features along the valley bottoms and margins, and associated soils.

Geomorphic Feature	Soil Description and Other Information
Active Channel	Water. Soils that have formed adjacent to or in the channel (gravel bars and islands) are described in the Floodplains soil description.
Floodplains	Soil description: a very deep, poorly drained to somewhat excessively drained soil that is dark-colored, silty loam to very cobbly sandy loam, and on floodplains and old stream channels. Slope range: 0 to 4 percent; Elevation range: 3700 to 7400 feet; Average annual precipitation: 8 to 18 inches; Average annual air temperature: 34 to 47° F; Frost-free season: 5 to 90 days; Depth class: very deep; Drainage class: very poorly drained to somewhat excessively drained; Permeability: moderately slow to very rapid; Available water capacity: 1 to 12 inches; Effective rooting depth: 10 inches to more than 60 inches; Runoff: slow; hazard of water erosion: slight; Range site: basin big sagebrush, western wheatgrass, black cottonwoods, willows, and sedges
Alluvial Fans and Stream Terraces	Soil description: a very deep, poorly drained to somewhat excessively drained soil that is light-colored; silt loam over silty clay to very gravely loamy silt, and on alluvial fans and stream terraces Slope range: 1 to 8 percent; Elevation range: 3700 to 6600 feet; Average annual precipitation: 7 to 20 inches; Average annual air temperature: 36 to 46° F; Frost-free season: 30 to 100 days; Depth class: very deep; Drainage class: poorly drained to somewhat excessively drained; Permeability: moderate in the upper part to very rapid in the lower part to moderately slow; Available water capacity: 2 to 11 inches; Effective rooting depth: 10 inches to more than 60 inches; Runoff: slow to medium; Hazard of water erosion: slight to moderate; Range site: Wyoming big sagebrush, bluebunch wheatgrass, threetip sagebrush, and Idaho fescue
Outwash Fans and Fan Terraces	Soil description: a very deep, somewhat poorly drained soil that is a darker-colored, gravely loam, and on outwash fans and fan terraces. Slope range: 2 to 10 percent; Elevation range: 6000 to 7500 feet; Average annual precipitation: 8 to 22 inches; Average annual air temperature: 35 to 42° F; Frost-free season: 30 to 80 days; Depth class: very deep; Drainage class: well drained; Permeability: moderate in upper part and very rapid in lower part to moderately slow; Available water capacity: 3.5 to 5.5 inches; Effective rooting depth: 40 inches to more than 60 inches; Runoff: slow; Hazard of water erosion: slight; Range site: mountain big sagebrush, Idaho fescue, Wyoming big sagebrush, and bluebunch wheatgrass

Water Quality

Surface water quality standards apply to a waterbody, depending on its designated uses and/or existing uses. Pursuant to the Clean Water Act (CWA), Idaho recognizes existing uses, which are uses present or attained in a water body on or after November 28, 1975. When water bodies do not have designated beneficial uses, they are assigned a presumed-use protection. All water bodies are classified for more than one beneficial use and must meet the fishable/swimmable intent of the CWA.

Under Idaho's water quality standards, beneficial uses are categorized as aquatic life, recreation, water supply, wildlife habitat, and aesthetics. For the Lemhi River watershed, beneficial uses that are not fully supported are: (1) aquatic life, which includes salmonid spawning and cold-water aquatic life beneficial uses, and (2) and contact recreation that includes primary and secondary contact recreation.

The Idaho Department of Environmental Quality completed a subbasin assessment for the Lemhi River watershed in 1999 (IDEQ 2012). Total maximum daily loads (TMDLs) were developed for water bodies not supporting their beneficial uses and impaired by a pollutant. In Idaho's 2002 Integrated Report (September 30, 2005), streams were converted from water-quality-limited segments to assessment units (AUs) based on Strahler stream order within a waterbody ID.

Additional AUs identified by IDEQ's Beneficial Use Reconnaissance Program monitoring were added to the 2008 and 2010 Integrated Reports. Further investigation by IDEQ determined that some listed AUs are ephemeral and therefore should not be listed as water-quality limited (Section 5: TMDL needed) but rather placed in Section 4C (impaired but not due to a pollutant). Under the CWA, lack of flow is not considered pollution, and no TMDL can be calculated. The 2012 Addendum updated water bodies and pollutants for which TMDLs have been developed (Table 8).

Table 8. Streams and pollutants listed in the 1999 and 2012 reports with TMDLs

Water Body	1999 TMDL	2012 TMDL Addendum
Lemhi River	Fecal coliform bacteria	Temperature
Bohannon Creek	Sediment	Temperature
Canyon Creek		Bacteria (E. coli)
Eighteenmile Creek	Sediment	Temperature
Geertson Creek	Sediment	
Kirtley Creek	Sediment	Temperature
Little Eightmile Creek		Temperature
McDevitt Creek	Sediment	
Sandy Creek	Sediment	Temperature
Wimpey Creek	Sediment	

Source: IDEQ 2012

Land Use

The Lemhi River watershed covers about 1,260 square miles, and about 80 percent of the land is owned by the Federal government and administered by the U.S. Forest Service (USFS) and Bureau of Land Management (BLM). Private lands are located predominantly along the more-fertile valley bottom. The primary land uses in the watershed are livestock grazing, irrigated pasturelands and hay fields, developed and dispersed recreation, and timber harvests. Livestock grazing occurs on both public and private lands across much of the middle and lower elevations in the watershed. Livestock typically graze on public lands from May to October, and then return to private lands for the remainder of the year. Irrigated pasturelands and hay fields are on private lands along the Lemhi Valley bottom and margins. The effects of irrigation and grazing in the valley bottom include diversion of flows from the mainstem Lemhi River, diversion of tributaries away from the mainstem Lemhi River, stream alterations, native vegetation clearing, increasing sedimentation and water temperatures, and entrainment of juvenile and adult fish in irrigation facilities (NPCC 2004; NOAA 2015).

Developed and dispersed recreation, several small mining claims, and small timber harvests are additional land uses that are believed to have minimal impact on the modern Lemhi River.

Land Cover and Riparian Conditions

The upper Lemhi River has areas of dense, native riparian vegetation comprising several species of willow, birch, and dogwood, with an understory of sedge and grass. About 60 percent of the streambanks have woody riparian vegetation along the stream corridors, and about 40 percent of the streambanks have grassland along the stream corridors (Trapani 2002). Land clearing and livestock grazing have altered the riparian vegetation through consumption and soil compaction, resulting in the replacement of native sedge and willow species with grass and other species that do not have the bank-stabilizing effects that natural woody riparian vegetation provides.

The lower Lemhi has fewer areas of dense, native riparian vegetation compared with the upper Lemhi, and more than 65 percent of the streambanks have a thin (less than 30 feet wide) or discontinuous woody riparian vegetation corridor along the river (Trapani 2002). Livestock grazing has altered the riparian vegetation, resulting in the replacement of native sedge and willow species with grass species, and many of the grass-lined banks have been armored with riprap. Large tracts of floodplains have been converted to grasslands and used for pastures or for hay production. Near the town of Salmon, much of the floodplain areas have been leveed to protect residential areas from flooding.

Most of the tributary drainages exhibit degraded riparian conditions due to livestock grazing and irrigation withdrawals. Riparian corridors have been converted to grassland, with discontinuous woody riparian vegetation resulting in bank instability, sedimentation, and high water temperatures (Trapani 2002).

Channel Migration

Despite channelization and straightening in multiple locations, ancient coarse-grained sediment underlying fine-grained floodplain soils across most of the valley bottom has limited the potential for widespread channel incision. The inability of the system to dissipate energy by mobilizing sediment on the bed has resulted in excess energy forced downstream and onto the river banks. In the absence of dense, riparian vegetation that prevents erosion, bank recession has occurred, resulting in channel widening. Channel widening was observed via aerial photographs throughout the Lemhi River but was more pronounced in the upper Lemhi River, while both widening and channel migration (i.e., erosion on one bank with concurrent deposition on the other) were observed in the lower Lemhi River (Photograph 20). The increased channel width associated with widening increases the cross-sectional area of the channel, allowing greater conveyance between the banks and resulting in less over-bank conveyance during floods (i.e., less frequent floodplain inundation) and less scour potential for forming pools (i.e., more frequent plane-bed morphology).

Photograph 20. Example of significant channel widening in the upper Lemhi River (Reach 2). Photograph is looking upstream, where the channel width exceeds 100 feet. Estimated historic and existing reference widths for this reach are on the order of 20 to 30 feet.

In addition to channel migration and widening, the Lemhi River also exhibits lateral channel movement via abrupt channel relocation (called avulsion). Avulsions generally occur via meander cut-off or channel obstruction. Meander cut-off avulsion typically occurs when high flows bypass a large, looping meander by cutting through the narrow neck on either end of the meander. The shorter flow path rapidly expands to capture most or all of the flow, abandoning the old meander as an oxbow pond or alcove. An avulsion created by an obstruction occurs when the main flow path is blocked sufficiently to force enough flow across the floodplain to scour a new channel. Typical obstructions resulting in avulsion include excessive sediment deposition, debris jams, and/or beaver dams. With less discharge and coarse sediment input, channel migration on the upper Lemhi River was likely heavily influenced by avulsion. Rather than meander bends forming as a result of persistent channel migration in the upper Lemhi River, it is more likely that fairly stable meanders formed each time the stream avulsed around a beaver dam or other obstruction.

The presence or absence of dense, woody riparian vegetation also influences the direction and shape of avulsion channel formation in the Lemhi. A lack of dense riparian vegetation allows the channel to adjust to an obstruction by widening, rather than overtopping, the banks and forming a new channel. Furthermore, without floodplain roughness in the form of dense vegetation, avulsion channels and newly formed side channels are more likely to be straighter and less complex than the original or mainstem channel.

Where channel migration and avulsion occur, channel bedform morphology (i.e., pools and riffles) depends largely on the presence and maturity of riparian vegetation. Where dense riparian vegetation comes in contact with a channel due to either migration or avulsion, the root mass of the vegetation creates a relative hard point in the channel. The structure of the root mat stabilizes the bank, enabling greater local velocity and shear stress capable of scouring the bed and forming a pool. Without the stabilizing function of the riparian root mass, excessive stream velocity and shear would be attenuated on the erosion-prone bank, rather than the bed, resulting in widening rather than localized pool scour.

Channel Planform and Morphology

Channel planform on the Lemhi River is generally sinuous, with several channel segments that have been straightened adjacent to roads or other human features. In an alluvial valley, sinuosity is typically inversely proportional to gradient, with lower sinuosity in areas of steeper gradient. This is the case on the Lemhi, where reach-averaged sinuosity ranges from over 2 in the low-gradient, upper Lemhi River, to as low as 1.1 in the somewhat steeper, lower Lemhi River, where the channel has also been straightened along Highway 28. In the upper Lemhi River, low gradients, high sinuosity, groundwater-influenced hydrology, dense riparian vegetation, and beaver activity likely led to a historically multi-threaded channel system. Over the past 100+ years, the removal of riparian vegetation and loss of beaver, along with irrigation diversions and channel manipulation, have created a largely single-thread system. Where riparian vegetation has been removed, the bankfull width of the channel has increased to 2 to 3 times the width of undisturbed areas. The lower Lemhi River, with lower sinuosity, greater sediment supply, higher gradient, and more pronounced peak flows, was historically a single-threaded system with several island-braided areas likely associated with in-stream obstruction (i.e., log jams) (Photograph 21). Channelization, levees, the removal of riparian vegetation, and other human impacts on the lower Lemhi River have all but eliminated the areas of island braiding and have significantly reduced the sinuosity and entrenchment of the channel. As with the upper Lemhi River, the reduction of riparian vegetation in many areas has led to areas of increased bank erosion.

Photograph 21. Island-braided channel network along the lower Lemhi River within Reach 15 from RM 3.5 to RM 4.5. Although the area has been impacted by land use, irrigation, and other human activities, it represents the best reference condition for an island-braided reach in the lower Lemhi River watershed.

Beaver

The existing influence from beavers has been severely limited as a result of legacy fur trapping. Limited evidence of beaver activity on the Lemhi River was observed during 2016 field work, suggesting population numbers remain extremely low, which is a marked difference from historical conditions. As discussed previously, beaver activity likely played a significant role in modifying and developing the historic Lemhi River morphology. Beavers generally require 40 to 60 percent tree/shrub canopy closure and shrub height greater than 6.6 feet within a broad/intact riparian corridor (Slough and Sadleir 1977). Beavers also require trees less than 6 inches in diameter for food source, preferring aspen, willow, cottonwood, and alder (in that order) (Denney 1952). These conditions are present in discontinuous patches throughout the valley and suggest that beaver reestablishment is possible.

Watershed Impacts

The higher-elevation areas along the Beaverhead Mountains southwest of the Continental Divide and the Lemhi Range are on public lands that are administered by the Salmon-Challis National Forest. The Eighteenmile Creek headwaters are currently being considered for wilderness designation. The middle- and lower-elevation areas along the foothills and piedmont belts are on public lands administered by the BLM Challis Field Office and on private lands. The valley bottoms of the Lemhi Valley are predominantly private lands.

Forested, higher-elevation areas along the Beaverhead Mountains and Lemhi Range have been minimally impacted by human activities. Road density, timber harvests, and dispersed recreation have had minor impacts on the watershed. However, at middle and lower elevations, there are significant, localized human impacts that have negatively affected riverine processes. These impacts include, but are not limited to, flow alteration from irrigation diversions, loss of riparian vegetation, channel and floodplain alteration from roads, and increased fine-sediment deposition.

Irrigation diversions significantly reduce instream flows by diverting tributaries away from and out of the mainstem Lemhi River. The many irrigation diversions have nearly eliminated an important intermittent disturbance regime associated with the spring freshet and channel-forming flows. It also reduces the quantity of instream habitat available through isolation (i.e., disconnected tributaries) and volume (i.e., cubic feet of water in the mainstem). Another effect of the irrigation diversions is an alteration of the timing and spatial distribution of groundwater recharge. Diversions redistribute river water onto the floodplain during the summer months, artificially increasing groundwater levels in those locations. Conversely, many naturally wet meadows have been ditched and drained to lower the groundwater table in those areas.

The loss of dense riparian vegetation (primarily willow in the upper Lemhi River and willow/cottonwood in the lower Lemhi River) has resulted in an over-widened and homogenous channel. Dense riparian vegetation on the outside of bends stabilizes the bank and obstructs flow, forcing contraction and resulting in pool scour and undercut banks. Dense riparian vegetation also promotes channel response via side-channel formation and avulsion around the structure provided by the vegetation, rather than bank erosion and widening when vegetation is lacking. A reduction in the amount of bank structure and instream structure have resulted in a simplified, homogenous channel exemplified by an over-widened, predominantly plane-bed morphology. The over-widened condition also expands the cross-sectional area of the channel between the banks, enabling more water to pass between the banks during floods, reducing floodplain connection frequency and duration. In the lower Lemhi River, the lack of cottonwood vegetation has also limited large woody material recruitment to the stream, resulting in low levels of instream structure, cover, and associated habitat. In all areas where woody riparian vegetation has been lost, the channel is exposed to greater solar radiation and thermal heating from the loss of shade.

Channel and floodplain alterations from roads are most prevalent in the middle to lower Lemhi River valley. Highway 28 significantly constrains the floodplain from near Mill Creek (RM 45) downstream to the area below Geertson Creek (RM 7), where 28 to 67 percent of the floodplain has been disconnected by the highway. County roads and levees further constrain the channel near the town of Salmon, Idaho (RM 0 to RM 3), where 50 to 71 percent of the floodplain has been disconnected. The low entrenchment ratios resulting from road and levee constrictions have concentrated flood flow, increasing depth and velocity and therefore also increasing the potential for bank erosion, channel incision, and bed armoring. Exacerbating the issue is the channelization and straightening of the river adjacent to the highway and levees. The sinuosity of the channel decreases by more than 75 percent, to near 1.0 in several reaches. The loss of channel length associated with the decreased sinuosity also increases the gradient in the lower Lemhi River, which is already high compared to the upper Lemhi River.

Excessive bank erosion, cattle grazing, and runoff from roads, all-terrain vehicle trails, and mining operations have increased fine sediment inputs to the channel through sheet erosion. Dense riparian vegetation had historically stabilized banks composed of fine sand and silt, which are now eroding and contributing sediment to the river on an annual basis. Cattle grazing has disturbed the surface of the floodplain and compacted the soils, both of which lead to more fine sediment runoff. Heavy grazing in some areas has resulted in so much erosion that 2- to 3-foot-tall hummocks have formed from the loss of soil between each hummock (see Photograph 19). Such erosion is plainly visible from aerial photographs. Roads have been located adjacent to many of the tributaries, where they have altered the riparian vegetation composition, compacted soils, and provide conduits for concentrated sheet flows during snowmelt and thunderstorms. Mining operations have included placer mining and exploratory trenches, especially in the foothills and headwater areas along the Beaverhead Mountains from Gilmore to Salmon. The cumulative effects of these impacts have likely increased fine-sediment inputs entering the Lemhi River system, resulting in elevated fine sediment levels and siltation.

Data Gaps

Future analysis could be aided by the collection of additional data currently unavailable, including:

- Hydraulic modeling to confirm floodplain inundation timing and extent, sediment transport character, and appropriate channel geometry (i.e., width-to-depth ratio).
    - Data gaps necessary for hydraulic modeling include bathymetry data, frequent pebble counts, and an improved understanding of diversion withdrawals/returns, tributary inflows, and groundwater contributions.
- Riparian vegetation inventory, including health and successional stages within the low surface that directly influence lateral channel migration, force pool-riffle bedforms, sort and retain gravel, and provide bank stability.

Lemhi Valley Segments and Geomorphic Reaches

Valley segments, geomorphic reaches, and channel units are three hierarchically nested subdivisions of the drainage network (Frissell et al. 1986). Within the hierarchy of spatial scales, valley segments, geomorphic reaches, and channel units represent the largest physical subdivisions that can be directly altered by human activities. As such, it is useful to understand how they respond to anthropogenic disturbance, but to do so requires classification systems and quantitative assessment procedures that facilitate accurate, repeatable descriptions and convey information about biophysical processes that create, maintain, and destroy channel structure (Bisson et al. 2006).

Valley Segments

The Lemhi River occupies an alluvial valley that has varying discharge along its course due to flow and sediment inputs from major tributaries, classified using a 10th-field Hydrologic Unit Code (HUC 10). There are eight HUC 10 sub-watersheds that discharge to the Lemhi River (Table 9). Four valley segments were identified based on where the HUC 10 sub-watersheds interact with or are identified along the Lemhi River (Figure 44). These valley segments include the following:

1) The Lemhi Headwaters Valley Segment includes the Texas Creek, Eighteenmile Creek, and Hawley Creek HUC 10 sub-watersheds to where they combine to form the Lemhi River (Headwaters downstream to RM 63.3)
2) The Upper Lemhi Valley Segment includes the upstream extent of the Lemhi River to its confluence with Hayden Creek, including discharge from the Timber Creek HUC 10 sub-watershed and five other named tributaries (RM 63.3 to RM 32.7). The lower boundary of the Upper Lemhi Valley Segment includes the area of bedrock confinement that separates the upper and lower watershed based on groundwater influence. Upstream of this point, the hydrologic regime is primarily groundwater-influenced. Below this point and the confluence of Hayden Creek, the hydrologic regime is primarily surface-water/snowmelt-dominated.
3) The Middle Lemhi Valley Segment begins at the confluence of the Lemhi River and Hayden Creek, a HUC 10 sub-watershed, and continues downstream to the alluvial fan at the mouth of Kenney Creek. This valley segment includes discharges from four named tributaries (RM 32.7 to RM 19.6).
4) The Lower Lemhi Valley Segment begins at the confluence of the Lemhi River and Kenney Creek and collects discharges from six named tributaries before flowing into the Salmon River (RM 19.6 to RM 0.0).

Table 9. Lemhi River watershed valley segment delineations and sub-watersheds.

Valley Segments and Locations	Sub-watershed	HUC 10	Named Tributaries	River Miles	Square Miles
Lemhi Headwaters Valley Segment	Texas Creek	1706020401	6	Upstream of 63.3	97.38 mi^2
	Eighteenmile Creek	1706020403	9		158.13 mi^2
	Hawley Creek	1706204002	11		63.26 mi^2
Upper Lemhi Valley Segment	Upper Lemhi River	1706020405	31	63.3 – 32.7	333.35 mi^2
	Timber Creek	1706020404	12		81.54 mi^2
Middle Lemhi Valley Segment	Middle Lemhi River	1706020407	13	32.7 – 19.6	179.48 mi^2
	Hayden Creek	1706020406	28		143.55 mi^2
Lower Lemhi Valley Segment	Lower Lemhi River	1706020408	21	19.6 – 0	204.75 mi^2
	Total		**131**	**63.3**	**1261.44**

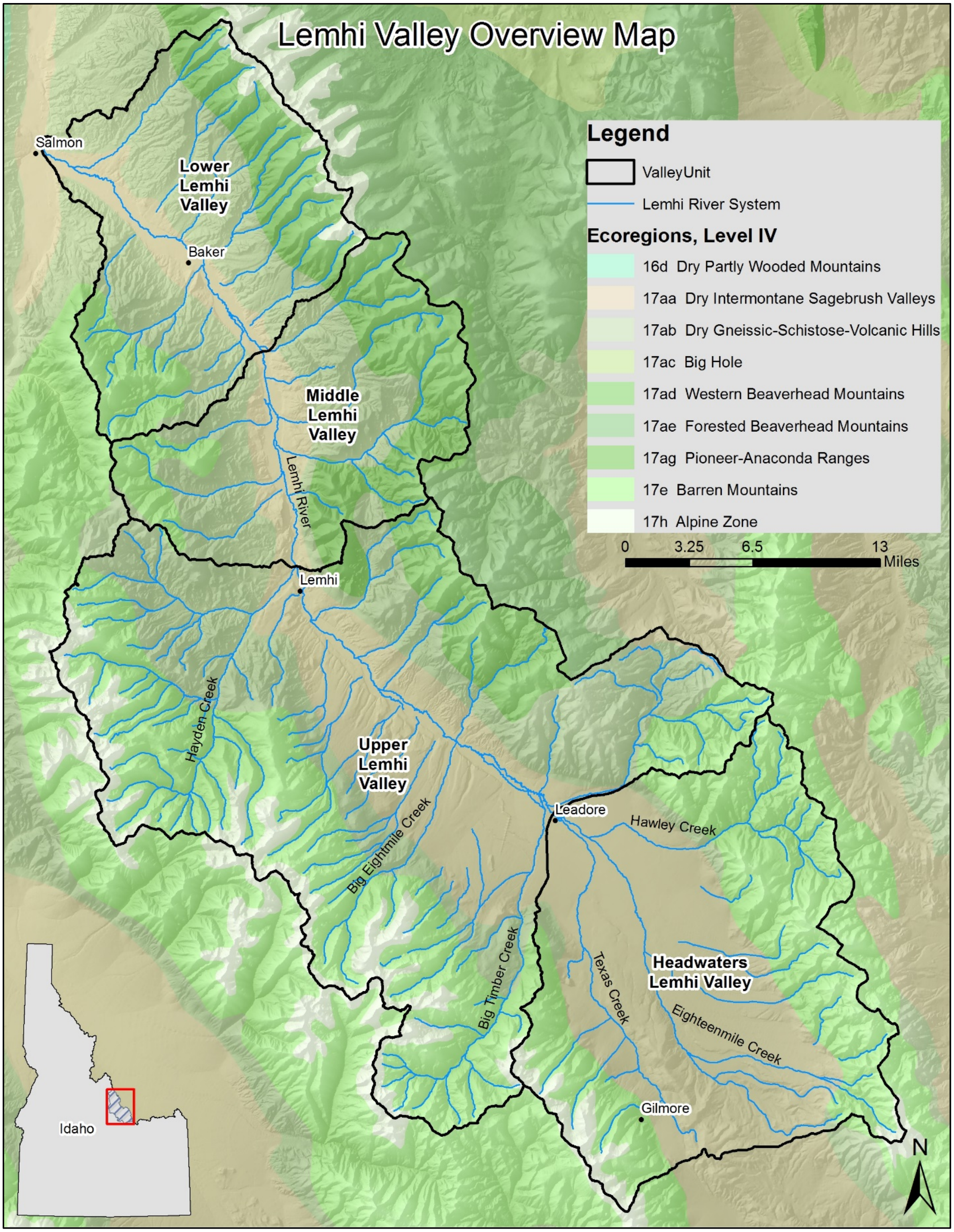

Figure 44. Lemhi River watershed valley segment locations.

Reach Characteristics

Reach characteristics are summarized per reach in Table 10 below.

Table 10. Summary of geomorphic reach characteristics for the Lemhi watershed.

Valley Segment	Reach	River Miles	Valley Slope (ft/ft)	Average Valley Width (ft)	Average Constrained Valley Width (ft)	Channel Slope (ft/ft)	Average Channel Width (ft)	Sinuosity	Entrenchment Ratio (ft/ft)	Constrained Entrenchment Ratio (ft/ft)	Human Disturbance Ratio (%)	Groundwater Characteristics	Geomorphic Characterization "Complex"	Geomorphic Characterization "Mixed"	Geomorphic Characterization "Simplified"
VS-2	GR-1	63.3 - 60.4	0.0075	526	558	0.0038	19	2.0	28	29	0%	Gaining	56%	44%	0%
VS-2	GR-2	60.4 - 52.6	0.0081	2050	2305	0.0038	29	2.2	71	80	6%	Gaining	53%	46%	1%
VS-2	GR-3	52.6 - 49.6	0.0075	1070	1053	0.0044	33	1.7	32	32	11%	Gaining	55%	38%	7%
VS-2	GR-4	49.6 - 46.5	0.0077	1235	1086	0.0057	37	1.4	33	29	7%	Losing	62%	29%	9%
VS-2	GR-5	46.5 - 43.2	0.0086	1675	1197	0.0060	34	1.4	49	35	8%	Losing	60%	22%	18%
VS-2	GR-6	43.2 - 41.1	0.0083	1342	676	0.0064	33	1.3	41	21	23%	Losing	62%	12%	26%
VS-2	GR-7	41.1 - 35.1	0.0080	2127	1338	0.0061	35	1.3	60	38	19%	Neutral	50%	25%	24%
VS-2	GR-8	35.1 - 32.7	0.0073	1393	805	0.0054	36	1.4	39	22	23%	Gaining	40%	4%	56%
VS-3	GR-9	32.7 - 30.3	0.0088	1488	1102	0.0077	54	1.1	28	20	6%	Gaining	13%	5%	81%
VS-3	GR-10	30.3 - 28	0.0093	1273	1063	0.0071	46	1.3	28	23	25%	Neutral	5%	28%	67%
VS-3	GR-11	28 - 25.4	0.0088	1158	518	0.0080	51	1.1	23	10	27%	Gaining	12%	10%	77%
VS-3	GR-12	25.4 - 19.6	0.0088	2813	2015	0.0076	54	1.1	53	38	32%	Gaining	27%	20%	53%
VS-4	GR-13	19.6 - 12.9	0.0084	2813	1492	0.0070	57	1.2	49	26	55%	Neutral	17%	34%	48%
VS-4	GR-14	12.9 - 8.1	0.0080	2217	1407	0.0065	62	1.2	36	23	64%	Neutral	13%	15%	72%
VS-4	GR-15	8.1 - 3.3	0.0080	1995	1657	0.0065	54	1.2	37	31	32%	Gaining	43%	30%	28%
VS-4	GR-16	3.3 - 0	0.0081	2480	1699	0.0072	62	1.1	40	27	20%	Gaining	38%	13%	49%

Lemhi Headwaters Valley Segment (VS-1)

The Lemhi Headwaters Valley Segment includes the headwater region of the Lemhi River watershed, and comprises the Texas Creek, Hawley Creek, and Eighteenmile Creek HUC 10 sub-watersheds (Figure 45). The individual sub-watersheds are described in the following sections.

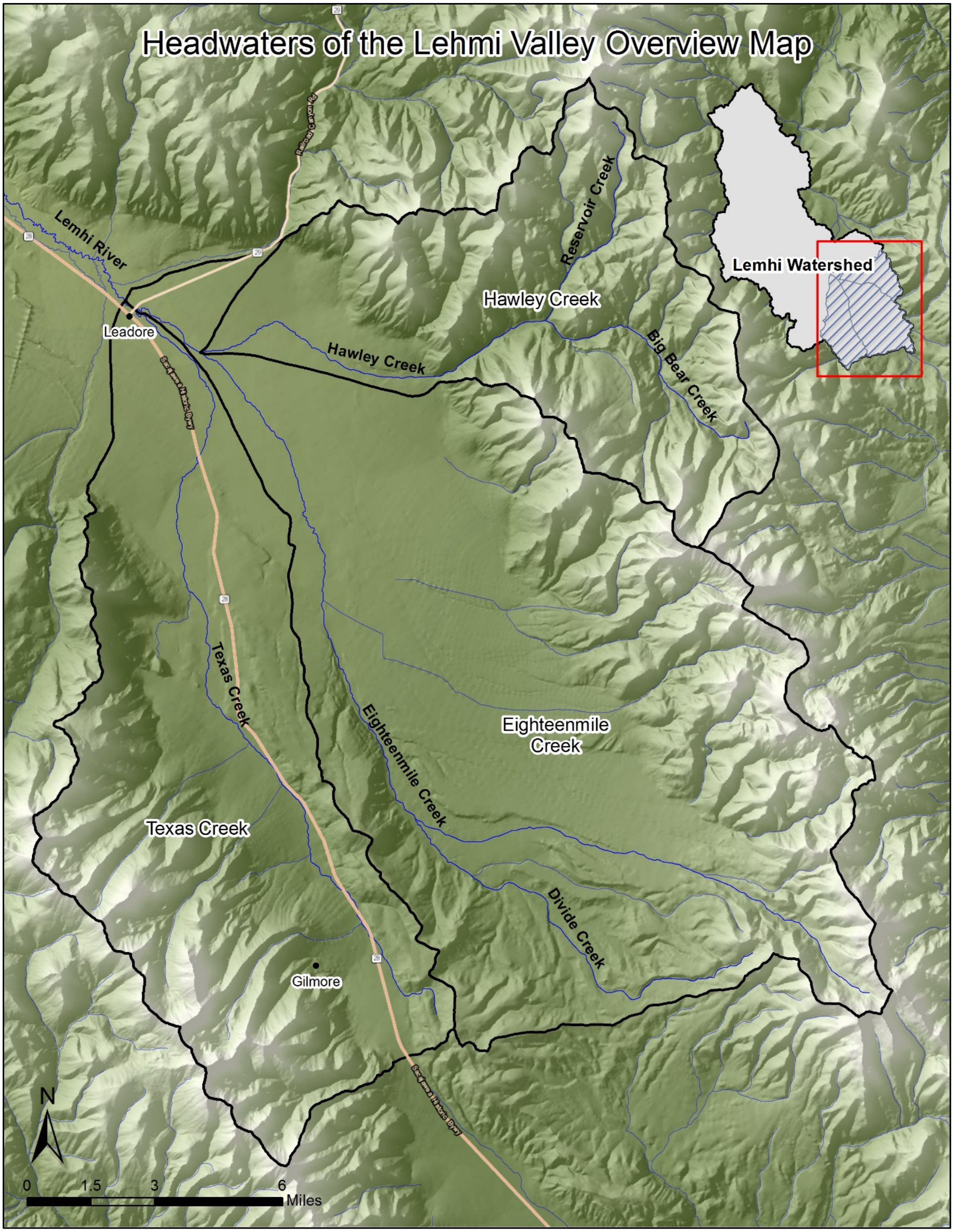

Figure 45. Location of Lemhi Headwaters Valley Segment (VS-1) comprising Hawley Creek, Eighteenmile Creek, and Texas Creek.

Texas Creek Sub-watershed

The Texas Creek sub-watershed (HUC 1706020401) covers 62,321 acres. Elevations range from about 5960 feet at the town of Leadore to more than 10000 feet along the Lemhi Range to the west. Gilmore Summit is an intrabasin divide that separates Texas Creek, which flows northward, from Birch Creek, which flows south. Center Ridge to the east separates the Texas Creek sub-watershed from the Eighteenmile Creek sub-watershed. The drainage pattern within the sub-watershed is dendritic, and the bedrock is predominantly limestone, dolomite, and quartzite. The higher-elevation, timbered lands are administered by the Salmon-Challis National Forest, lower-elevation slopes covered with shrub- and grasslands are administered by the Bureau of Land Management, and private holdings are predominantly located along the valley bottoms, covered with pastures and croplands.

Texas Creek begins as an ephemeral channel along Center Ridge and across an alluvial fan, with intermittent flows during snowmelt and thunderstorms. Allhands Spring, a tributary to Texas Creek, is impounded by an embankment dam. The creek becomes perennial where seeps and springs flowing out of alluvial fans along the foot of the Lemhi Range form wetland areas along an unconfined valley and coalesce to form Texas Creek (Figure 46). Pastureland and wetland meadows are heavily grazed, and livestock have direct access to Texas Creek. Two embankment dams (T14N and R26E) once impounded Texas Creek in the wetlands but have since been breached. Dunkin Lane, Timber Creek, and Eight Mile Roads are topographic highs that bisect the wetland meadows, interfering with surface water connectivity. A diversion at the confluence of Purcell Creek and Texas Creek flows along the base of Leadore Hill, collecting seepage and spring discharges from the alluvial fans. There are three cross-basin drainage diversions that flow from Timber Creek to Texas Creek. Highway 28, the Sacajawea Historic Byway and old railroad grade, crosses Texas Creek and runs south along the base of Middle Ridge, where it does not impact Texas Creek or the wetlands. About 0.6 miles downstream of the Highway 28 bridge crossing, Texas Creek dewaters due to diversions.

Summary

Texas Creek’s flows are over-allocated for irrigation, resulting in dewatering about 0.6 miles downstream of the Highway 28 bridge crossing. The wetland meadows are heavily grazed by livestock, resulting in loss of riparian vegetation along Texas Creek, and thus, reduced shade and bank instability. Livestock have direct access to Texas Creek, resulting in bank erosion, channel widening, sedimentation, and nutrient loading.

The wetlands created by cold-water seeps and springs could provide a cold-water source to the Lemhi River if the wetlands were allowed to function naturally or were managed in a way that reestablishes the riparian vegetation, and flows were not over-allocated to maintain perennial flows along lower Texas Creek to the Lemhi River.

The cross-basin diversions from Timber Creek could have negative impacts to Timber Creek’s flows.

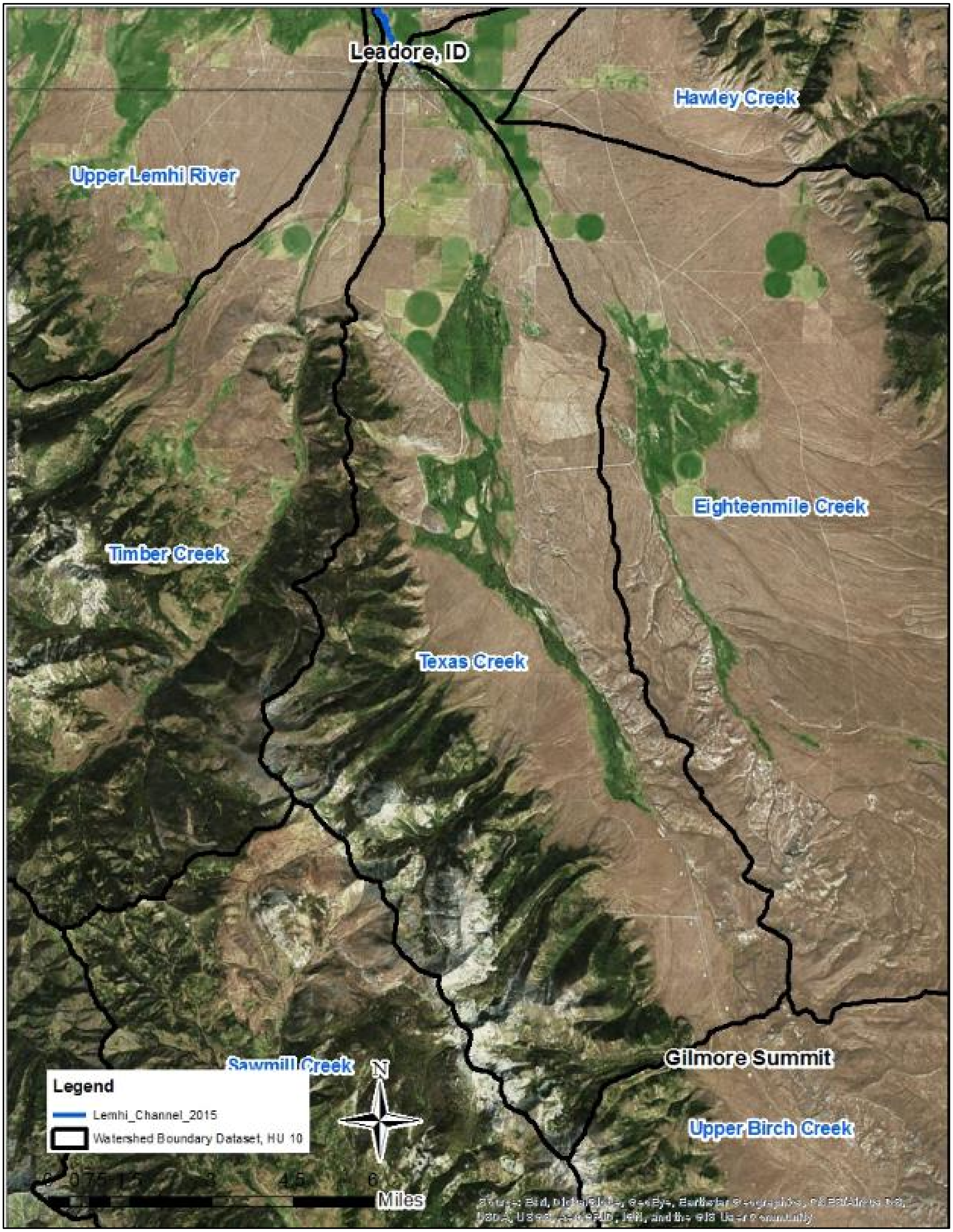

Figure 46. Location of Texas Creek sub-watershed with the Lemhi Range and alluvial fans along the west that have seeps and springs that drain into a wetland complex that maintains perennial flows in Texas Creek.

Hawley Creek Sub-watershed

The Hawley Creek sub-watershed (HUC 1706020402) covers 40,485 acres (Figure 47). Elevations range from about 6000 feet on the Lemhi Valley floor to more than 10000 feet along the Beaverhead Mountains to the east. A high ridge and alluvial fan separates the Hawley Creek sub-watershed from the Eighteenmile Creek sub-watershed. The drainage pattern within the sub-watershed is dendritic, and bedrock is predominantly limestone, dolomite, and quartzite. The higher-elevation, timbered lands are administered by the Salmon-Challis National Forest, lower-elevation slopes covered with shrub- and grasslands are administered by the Bureau of Land Management, and private holdings are predominantly along the valley bottoms, covered with pastures and croplands.

Hawley Creek begins in the Beaverhead Mountains at the confluence of Reservoir Creek and Big Bear Creek (T13S: R28E: Sect. 31). Reservoir Creek has been impounded with an embankment dam near its confluence with Short Creek (T13S: R28E: Sect. 16). Forest Service Road 275 parallels Hawley Creek from its junction with Hawley Creek Road and Forest Service Road 177, downstream about 1.6 miles to its junction with Cedar Canyon Loop Road. There are two irrigation diversions high on the Hawley Creek alluvial fan that divert most of Hawley Creek's flows. Downstream of the irrigation diversions and Cedar Creek Loop Road junction, Hawley Creek flows over its alluvial fan, where there are at least five ford crossings that have widened the channel. There are two additional irrigation diversions about midway down the alluvial fan, and at the base of the fan, Hawley Creek and irrigation return flows are ditched and again diverted, leaving little flow in the channel. Hawley Creek seasonally dewaters downstream of this lowest diversion. Any remaining flows are then discharged into the Eighteenmile Creek ditch, leaving the Hawley Creek and Eighteenmile Creek confluence area highly altered.

Summary

Reservoir Creek Dam and irrigation diversions have resulted in significant flow alterations in the Hawley Creek sub-watershed. Hawley Creek flows are essentially regulated by releases from Reservoir Creek Dam, a major tributary to Hawley Creek. Irrigation diversions along the Hawley Creek alluvial fan divert almost all of Hawley Creek flows, and then Hawley Creek and irrigation return flows are discharged into the Eighteenmile Creek ditch. Additionally, Forest Service roads adjacent to the creek and several ford crossings may increase fine sediment inputs to the Hawley Creek system.

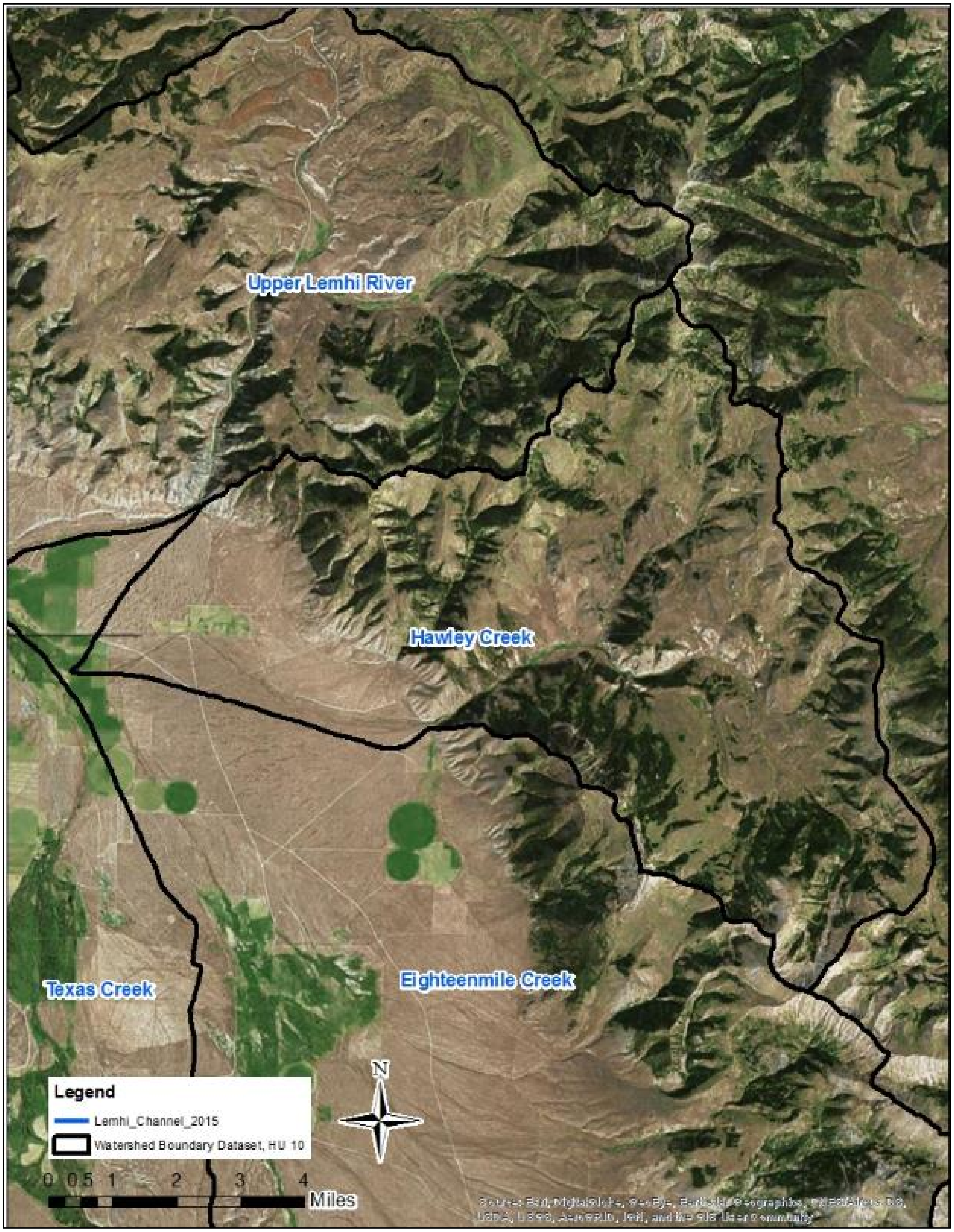

Figure 47. Location of the Hawley Creek sub-watershed.

Eighteenmile Creek Sub-watershed

The Eighteenmile Creek sub-watershed (HUC 1706020403) covers 101,200 acres (Figure 48). Elevations range from about 5960 feet at the town of Leadore to more than 11000 feet along the Beaverhead Mountains to the east. A ridge trending east from Gilmore Summit across Center Ridge to Eighteenmile Peak forms an intrabasin divide that separate the Eighteenmile Creek sub-watershed, which drains northward, from the Upper Birch Creek sub-watershed, which drains southward. The drainage pattern within the sub-watershed is dendritic, and bedrock is predominantly limestone, dolomite, and quartzite. The higher-elevation, timbered lands are administered by the Salmon-Challis National Forest, lower-elevation slopes covered with shrub- and grasslands are administered by the Bureau of Land Management, and private holding are located predominantly along the valley bottoms, covered with pastures and hay fields.

Eighteenmile Creek heads in a glacial cirque and trough on the northern aspect of Eighteenmile Peak (elevation 11142 feet). Several ephemeral tributaries coalesce along the glacial trough to form Eighteenmile Creek at about elevation 8699 feet. Eighteenmile Creek is a single-thread, sinuous channel in confined reaches and a multi-thread, island-braided channel along the unconfined meadows with dense willow species. Several avulsion paths are present through the grass and shrub areas, possibly forced by ice jams and/or beaver dams.

Where Eighteenmile Creek flows across the alluvial fan zone, it (a) loses surface water to groundwater through the porous sediments, (b) has more than a dozen irrigation diversions that divert surface water used to irrigate pastures, and (c) is intercepted by a cross-ditch (R15N: T27E: Sect. 32) that collects and diverts flows. About 4 miles of the historic Eighteenmile Creek was channelized and ditched along the northeast valley wall, where it no longer coalesces with Divide Creek in T15N, R27E, Sect. 29. Essentially, Divide Creek flows through this area, and Eighteenmile Creek no longer exists downstream of it. Below this section, the historic Eighteenmile Creek (now Divide Creek) flows down to T16N, R26E, Sect. 36, where it is ditched around pivot-irrigated crops, and then captures Hawley Creek before flowing into the Lemhi River near Leadore. A placer mining operation appears to be active in the Clear Creek drainage, and Clear Creek is fully diverted near a road crossing at the apex of the Clear Creek alluvial fan. Tenmile Creek and Bull Creek are fully diverted near the apexes of their alluvial fans.

Summary

Most of the tributaries in the Eighteenmile Creek sub-watershed enter the alluvial fan zone at the base of the mountains, where they go subsurface due to the porous alluvial materials. Eighteenmile Creek and Divide Creek (historic Eighteenmile Creek alignment) are the only perennial tributaries along the valley bottom. Irrigation diversions along these tributaries are used to irrigate pasturelands and hay fields. Livestock grazing has changed the native riparian vegetation through alteration and replacement, reducing the overall abundance of native willow and sedge species through consumption and soil compaction. Livestock also have direct access to tributaries resulting in bank instability, channel widening, sedimentation, and nutrient loading. An EPA-approved TMDL has been developed for Eighteenmile Creek for sedimentation and temperature (IDEQ 2011).

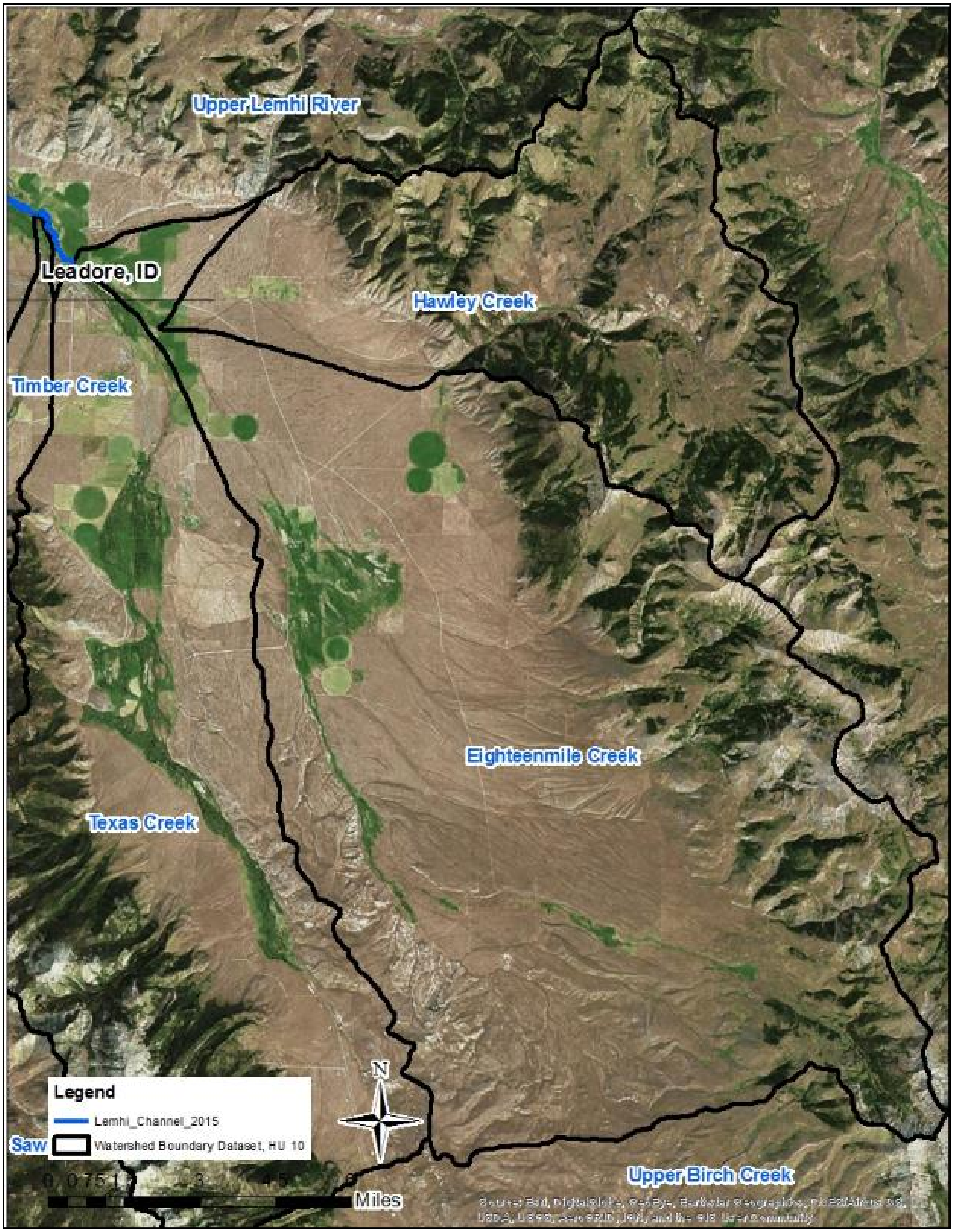

Figure 48. Location of the Eighteenmile Creek sub-watershed.

Upper Lemhi Valley Segment (VS-2)

The Upper Lemhi Valley Segment comprises the Upper Lemhi River watershed from RM 63.3 to RM 32.7. See Table 11 and Figure 49 below.

Table 11. Upper Lemhi Valley Segment watershed hydrologic units and areas.

Sub-watershed	HUC 10	Named Tributaries	Acreage	Square Miles
Upper Lemhi River	1706020405	31	213,346 acres	333.35 mi^2
Timber Creek	1706020404	12	52,188 acres	81.54 mi^2
Total		**43**	**265,534 acres**	**414.89 mi^2**

VS-2 Defining characteristics

Compared to the lower valley segments, VS-2 exhibits a groundwater/baseflow-dominated hydrology characterized by stable flows (consistent annual hydrograph) with significant groundwater inputs. Common characteristics include a low volume of coarse sediment bedload (sand, gravel, and cobble), low gradient, and broad valley/floodplain width.

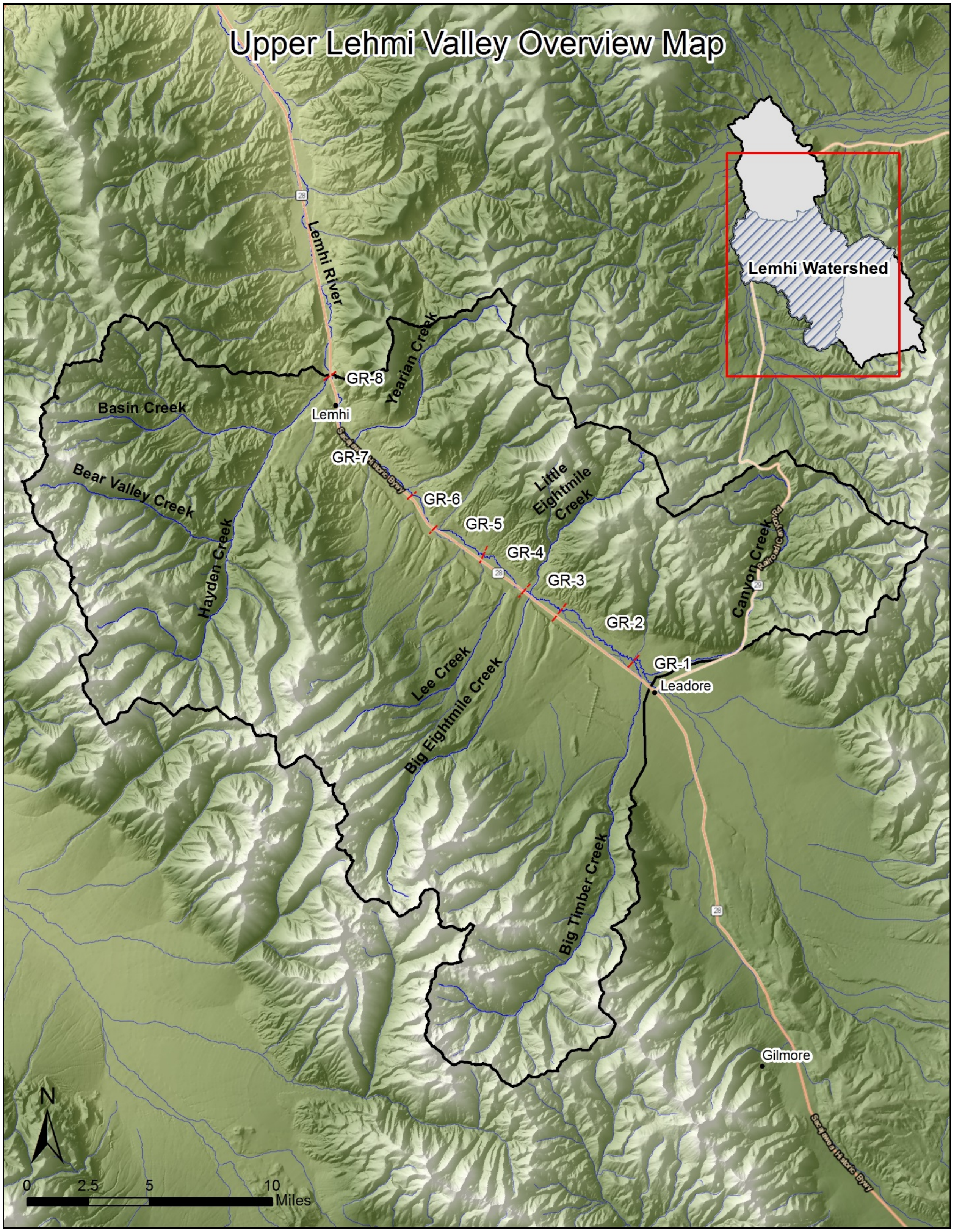

Figure 49. Upper Lemhi Valley Segment (VS-2) and associated geomorphic reaches (GR-2 through GR-8).

Timber Creek (Big Timber Creek) Sub-watershed

The Timber Creek sub-watershed (HUC 1706020404) covers 52,188 acres (Figure 50). Elevations range from about 5854 feet at the Lemhi River and Timber Creek confluence to more than 11000 feet along the Lemhi Range to the west. A ridge trending south from Leadore Hill to Sheephorn Peak separates the Timber Creek sub-watershed from the Texas Creek sub-watershed to the east. The drainage pattern within the sub-watershed is dendritic, and bedrock is predominantly limestone, dolomite, and quartzite. The higher-elevation, timbered lands are administered by the Salmon-Challis National Forest, lower-elevation slopes covered with shrub and grass species are administered by the Bureau of Land Management, and private holdings are predominantly along the valley bottoms, covered with pastures and croplands. The Timber Creek sub-watershed hydrology is snowmelt-dominated, with peak discharges capable of mobilizing and transporting coarse sediment.

Primary tributaries to Big Timber Creek include North Fork Little Timber Creek, Middle Fork Little Timber Creek (impounded to create Timber Creek Reservoir), Little Timber Creek, and Basin Creek.

Timber Creek heads in a glacial cirque and trough, where groundwater flows through glacial debris and colluvium and intermittently daylights at about elevation 9250 feet on the east aspect of the Lemhi Range, near Yellow Peak. From its headwaters to a half-mile downstream of its confluence with Falls Creek, Timber Creek occupies a channelized colluvial valley with a single-thread, fairly straight channel where confined, and a moderately sinuous channel where it is unconfined along wet meadows. Timber Creek then flows through a canyon section that opens up to a moderately confined valley, and instream flows appear to increase in the downstream direction, likely due to seeps and groundwater discharge. The channel is predominantly a single-thread, moderately sinuous to sinuous channel with pool-riffle morphology, likely forced by large woody material recruited through bank erosion and wind throw. Downstream from Trail Creek to Grove Creek, the channel has unconfined sections that have been impounded by beaver complexes in wet meadows with dense riparian vegetation (willow), and in the moderately confined sections between the beaver complexes, the channel reverts back to a single-thread, moderately sinuous channel with pool-riffle morphology. Downstream from Grove Creek, the unconfined sections have less riparian vegetation due to cattle grazing, with minor beaver activity in these sections. Where riparian vegetation is lacking, the channel has widened and shallowed. There is what appears to be a concrete irrigation diversion structure upstream of the junction where Big Timber Creek Road starts ascending the canyon that should be evaluated for fish passage. The structure also diverts surface water out-of-basin from Big Timber Creek to the Texas Creek sub-watershed. Downstream of the irrigation diversion to the Lemhi River confluence, Big Timber Creek has several irrigation diversions along its mainstem that reduce instream flows, and thus, the sediment transport capacity of the stream and the channel becomes moderately sinuous where dense riparian vegetation lines the banks with a predominantly pool-riffle morphology. Conversely, the channel tends to be fairly straight and wide where there is discontinuous or no riparian vegetation.

Summary

Big Timber Creek has a snowmelt-dominated hydrology capable of mobilizing and transporting coarse sediment. Irrigation diversions have attenuated peak flows in the stream, thus reducing the stream power and transport capacity. In addition, flows are impounded on the Middle Fork Little Timber Creek, and on Timber Creek, flows are diverted out-of-basin to the Texas Creek sub-watershed.

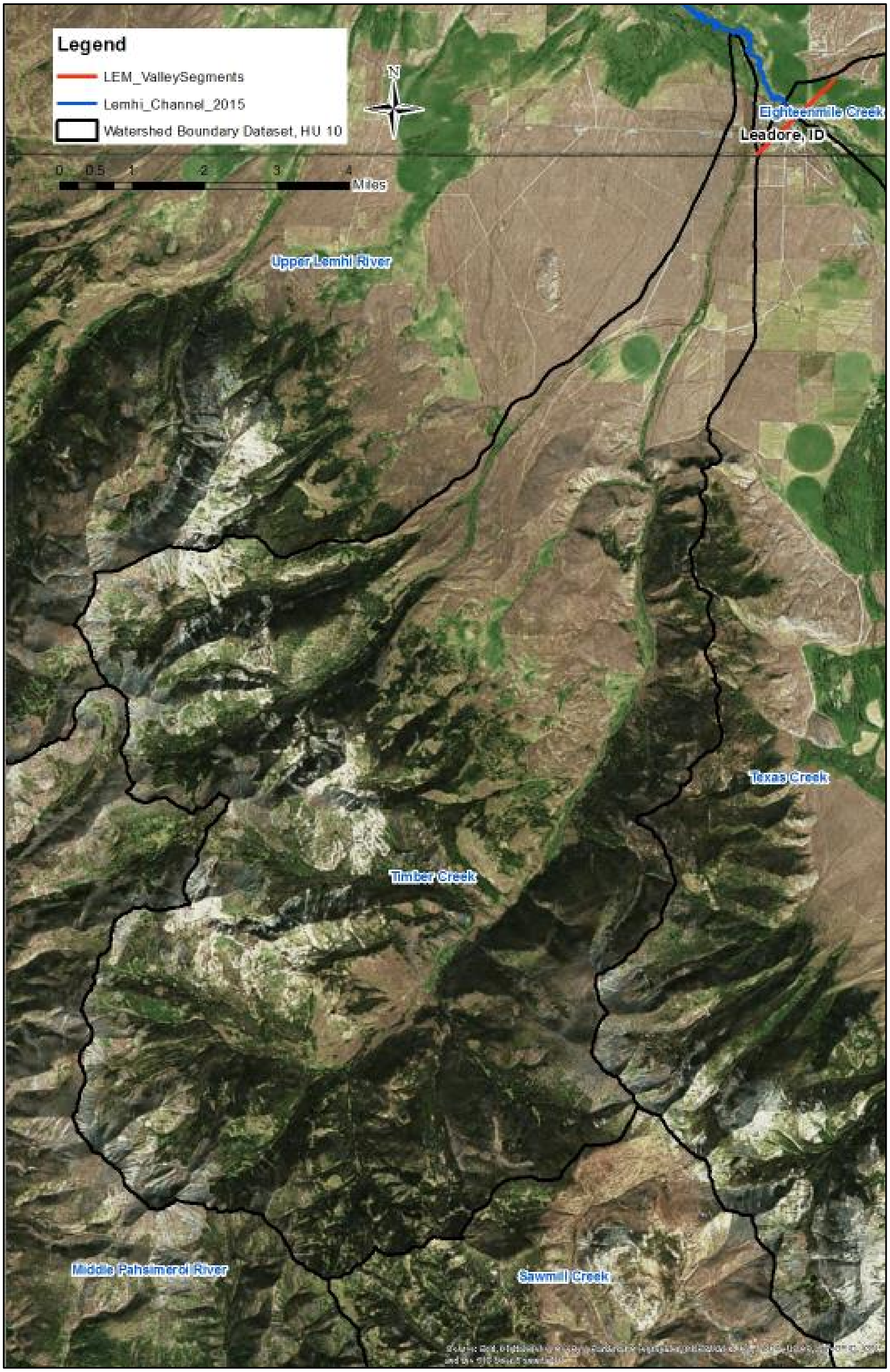

Figure 50. Location of the Timber Creek sub-watershed.

Geomorphic Reach GR-1 (RM 63.3 – 60.4)

Geomorphic Reach GR-1 is located along the Lemhi River between RM 63.3 and RM60.4 in an unconfined valley with minimal valley bottom constraints (Figure 51). Reach characteristics are summarized below in Table 12.

Table 12. Summary of attributes for Geomorphic Reach GR-1.

Valley Segment	Reach	River Miles	Valley Slope (ft/ft)	Avg. Valley Width (ft)	Avg. Constrained Valley Width (ft)	Channel Slope (ft/ft)	Average Channel Width (ft)	Sinuosity	Entrenchment Ratio (ft/ft)	Constrained Entrenchment Ratio (ft/ft)	Human Disturbance Ratio (%)	Groundwater Characteristics	Geomorphic Characterization "Complex"	Geomorphic Characterization "Mixed"	Geomorphic Characterization "Simplified"
VS-2	GR-1	63.3 - 60.4	0.0075	526	526	0.0038	19	2.0	28	28	0%	Gaining	56%	44%	0%

Forms

- Sinuous reach with little evidence of planform alterations not related to flow and sediment transport processes.
- Many banks lacking riparian vegetation.
- Over-widened channel in areas lacking riparian vegetation.
- Although unconfined, GR-1 has the narrowest average floodplain width measured on the Lemhi River.
- One of the lowest valley gradients of the Lemhi reaches.

Processes

- Observable channel widening where riparian vegetation is lacking.
- No point bar deposition suggests very low rates of channel migration (concurrent bank erosion on one bank and deposition on the other).
- Excessive fine sediment contributions resulting from increased erodibility of banks due to degraded riparian vegetation and livestock grazing leading to siltation and substrate embeddedness.

Human Impacts

- Patchy, discontinuous riparian corridor and associated bank instability, channel widening, plane-bed morphology, and lack of shade.
- Excessive fine sediment.
- Irrigation diversions.

Response Potential

- Groundwater-influenced hydrology, gaining reach (Donato 1998). Shallow groundwater supports riparian vegetation regeneration and associated bank stability.
- Channel form (especially width and bedform) and processes are driven by the presence or absence of mature riparian vegetation (primarily willow). Dense riparian vegetation maintains a narrow width-to-depth ratio, stabilizes banks, and promotes scour pool formation versus channel widening.
- Typical response to disturbances includes avulsion, side-channel formation, floodplain activation, and scour pool formation.

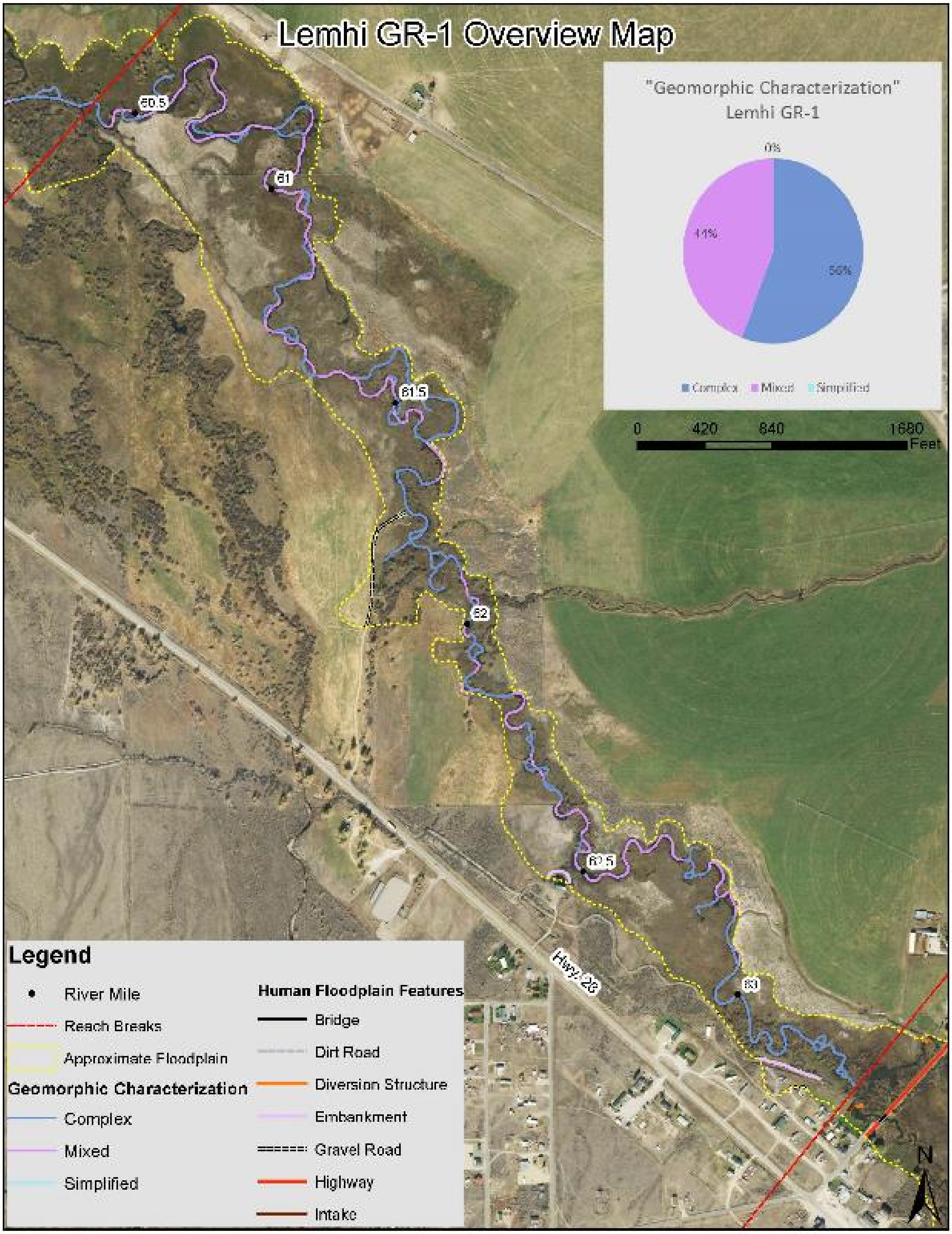

Figure 51. GR-1 overview map illustrating the approximate floodplain, geomorphic characterization, and human alterations to the floodplain.

Geomorphic Reach GR-2 (RM 60.4 – 52.6)

Geomorphic Reach GR-2 is located along the Lemhi River between RM 60.4 and RM 52.5 in an unconfined valley with few valley bottom constraints (Figure 52). The riverine system is geomorphically and hydrologically similar to Geomorphic Reach GR-1. Reach characteristics are summarized below in Table 13.

Table 13. Summary of attributes for Geomorphic Reach GR-2

Valley Segment	Reach	River Miles	Valley Slope (ft/ft)	Average Valley Width (ft)	Average Constrained Valley Width (ft)	Channel Slope (ft/ft)	Average Channel Width (ft)	Sinuosity	Entrenchment Ratio (ft/ft)	Constrained Entrenchment Ratio (ft/ft)	Human Disturbance Ratio (%)	Groundwater Characteristics	Geomorphic Characterization	Geomorphic Characterization "Mixed"	Geomorphic Characterization "Simplified"
VS-2	GR-2	60.4 - 52.6	0.0081	2050	1,785	0.0038	29	2.2	71	62	6%	Gaining	53%	46%	1%

Forms

- Sinuous reach with little evidence of planform alterations not related to flow and sediment transport processes
- Mix of plane-bed and pool-riffle morphology, with pool-riffle generally associated with areas of dense riparian vegetation.
- Many banks lacking riparian vegetation.
- Over-widened channel in areas lacking riparian vegetation.
- Expanded floodplain inundation area relative to upstream GR-1.

Processes

- Observable channel widening where riparian vegetation is lacking.
- No point bar deposition suggests very low rates of channel migration.
- Fine sediment deposition observed in over-widened areas.

Human Impacts

- Little evidence of possible artificial grade control influence
- Patchy, discontinuous riparian corridor and associated bank instability, channel widening, plane-bed morphology, and lack of shade.
- Excessive fine sediment contributions resulting from increased erodibility of banks due to degraded riparian vegetation and livestock grazing leading to siltation
- Irrigation diversions.

Response Potential

- Groundwater-influenced hydrology, gaining reach (Donato 1998). Shallow groundwater supports riparian vegetation regeneration and associated bank stability.
- Channel form (especially width and bedform) and processes are driven by the presence or absence of mature riparian vegetation (primarily willow). Dense riparian vegetation maintains a narrow width-to-depth ratio, stabilizes banks, and promotes scour pool formation versus channel widening.
- Typical response to disturbances includes avulsion, side-channel formation, floodplain activation, and scour pool formation.

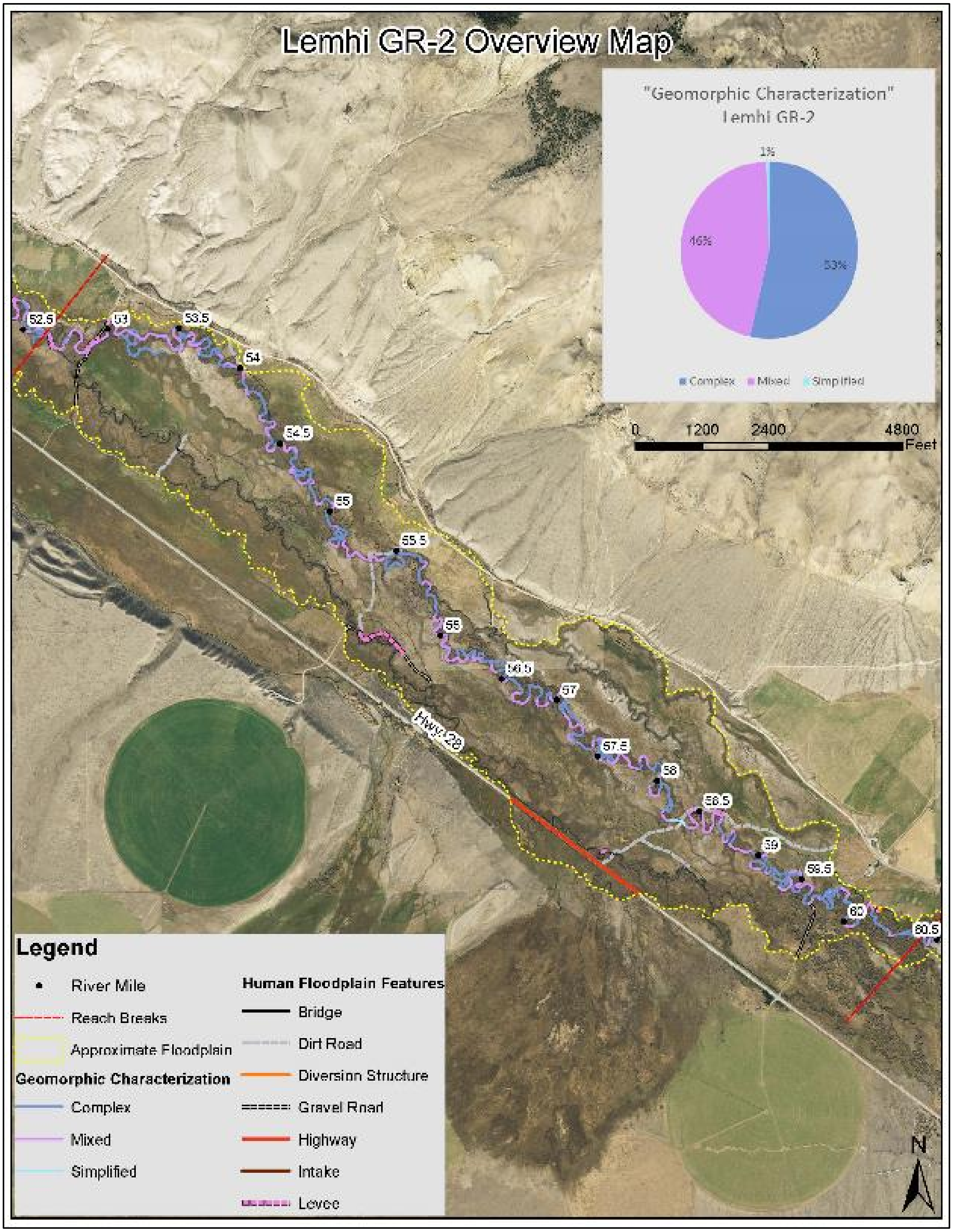

Figure 52. GR-2 overview map illustrating the approximate floodplain, geomorphic characterization, and human alterations to the floodplain

Geomorphic Reach GR-3 (RM 52.6 – 49.6)

Geomorphic Reach GR-3 is located along the Lemhi River between RM 52.6 and RM 49.6 in a mostly unconfined valley setting (Figure 53). The riverine system is beginning to transition to an increasingly simplified structure with less groundwater influence. Reach characteristics are summarized below in Table 14.

Table 14. Summary of attributes for Geomorphic Reach GR-3

Valley Segment	Reach	River Miles	Valley Slope (ft/ft)	Average Valley Width (ft)	Average Constrained Valley Width (ft)	Channel Slope (ft/ft)	Average Channel Width (ft)	Sinuosity	Entrenchment Ratio (ft/ft)	Constrained Entrenchment Ratio (ft/ft)	Human Disturbance Ratio (%)	Groundwater Characteristics	Geomorphic Characterization "Complex"	Geomorphic Characterization "Mixed"	Geomorphic Characterization "Simplified"
VS-2	GR-3	52.6 - 49.6	0.0075	1070	960	0.0044	33	1.7	32	29	11%	Gaining	55%	38%	7%

Forms

- Sinuous, except minor channel straightening associated with roads and bridges in the downstream end of the reach.
- Mix of plane-bed and pool-riffle morphology, with pool-riffle generally associated with areas of dense riparian vegetation in the upper 75 percent of the reach.
- Many banks lacking riparian vegetation.
- Over-widened channel in areas lacking riparian vegetation.

Processes

- Observable channel widening where riparian vegetation is lacking.
- Few point bars suggests low rates of channel migration.
- Fine sediment deposition observed in over-widened areas.

Human Impacts

- Patchy, discontinuous riparian corridor and associated bank instability, channel widening, plane-bed morphology, and lack of shade. Riparian conditions improve toward the downstream end of the reach.
- Areas of channel straightening and bridges may locally concentrate flow, causing incision and/or bed armoring.
- Excessive fine sediment filling interstitial space in the bed.
- Irrigation diversions, road embankments, bridges, and discontinuous levees altering in-channel and floodplain processes.

Response Potential

- Begins to transition from groundwater-influenced hydrology to more heavily peak-flow influenced, gaining reach (Donato 1998). Shallow groundwater supports riparian vegetation regeneration and associated bank stability.
- Channel form (especially width and bedform) and processes are driven by the presence or absence of mature riparian vegetation (primarily willow). Dense riparian vegetation maintains a narrow width-to-depth ratio, stabilizes banks, and promotes scour pool formation versus channel widening.

- Typical response to disturbances includes avulsion, side-channel formation, floodplain activation, and scour pool formation.

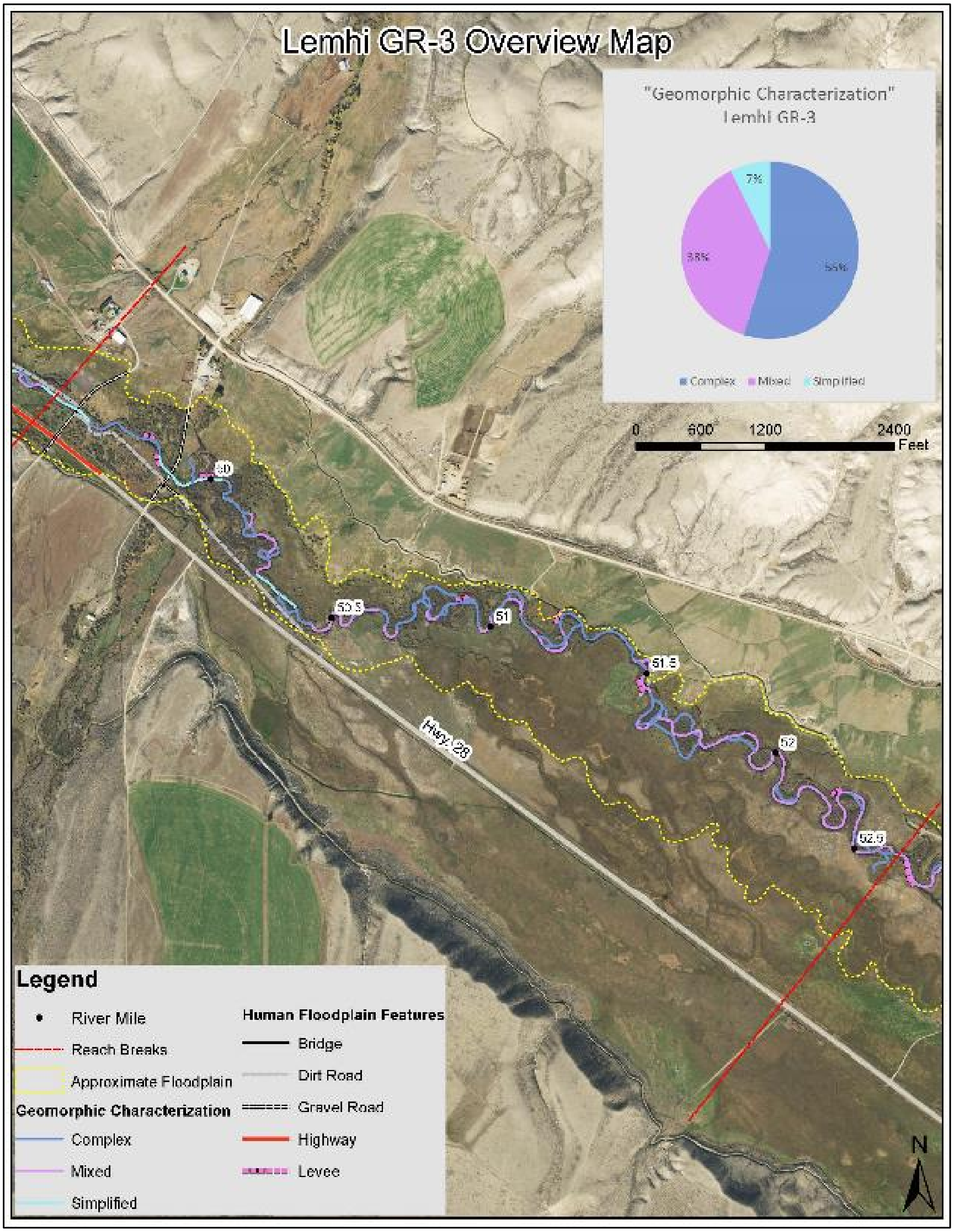

Figure 53. GR-3 overview map illustrating the approximate floodplain, geomorphic characterization, and human alterations to the floodplain.

Geomorphic Reach GR-4 (RM 49.6 – 46.5)

Geomorphic Reach GR-4 is located along the Lemhi River between RM 49.6 and RM 46.5 in an unconfined valley, with some valley bottom constraints resulting in the downstream disruption of flows and channel migration along the floodplain (Figure 54). Reach characteristics are summarized below in Table 15.

Table 15. Summary of attributes for Geomorphic Reach GR-4

Valley Segment	Reach	River Miles	Valley Slope (ft/ft)	Average Valley Width (ft)	Average Constrained Valley Width (ft)	Channel Slope (ft/ft)	Average Channel Width (ft)	Sinuosity	Entrenchment Ratio (ft/ft)	Constrained Entrenchment Ratio (ft/ft)	Human Disturbance Ratio (%)	Groundwater Characteristics	Geomorphic Characterization "Complex"	Geomorphic Characterization "Mixed"	Geomorphic Characterization "Simplified"
VS-2	GR-4	49.6 - 46.5	0.0077	1235	1,236	0.0057	37	1.4	33	33	7%	Losing	62%	29%	9%

Forms

- Sinuous, except channel straightening associated with roads and bridges in the upper third of the reach.
- Multi-threaded form is prevalent in lower reach.
- Mix of plane-bed and pool-riffle morphology, with plane-bed generally associated with channel straightening, and pool-riffle associated with areas of dense riparian vegetation in the lower reach.
- Many banks lacking riparian vegetation.
- Over-widened channel in areas lacking riparian vegetation.

Processes

- Observable, often significant, channel widening where riparian vegetation is lacking.
- Little to no point bar deposition suggests low rates of channel migration.
- Fine sediment deposition observed in over-widened areas.

Human Impacts

- Patchy, discontinuous riparian corridor and associated bank instability leading to channel widening, plane-bed morphology, and lack of shade.
- Channel confinement and straightening in the upper reach may increase local transport capacity, resulting in bed armoring.
- Excessive fine sediment filling interstitial space in the bed.
- Irrigation diversions, road embankments, bridges, and discontinuous levees altering in-channel and floodplain processes.

Response Potential

- Peak-flow-dominated hydrology; after irrigation season, it is a losing reach (Donato 1998). Shallow groundwater during summer months supports riparian vegetation and associated bank stability.
- Channel form (especially width and bedform) and processes are driven by the presence or absence of mature riparian vegetation (primarily willow). Dense riparian vegetation maintains a narrow width-to-depth ratio, stabilizes banks, and promotes scour pool formation versus channel widening.

- Typical response to disturbances includes avulsion, lateral channel migration, side-channel formation, floodplain activation, and scour pool formation.

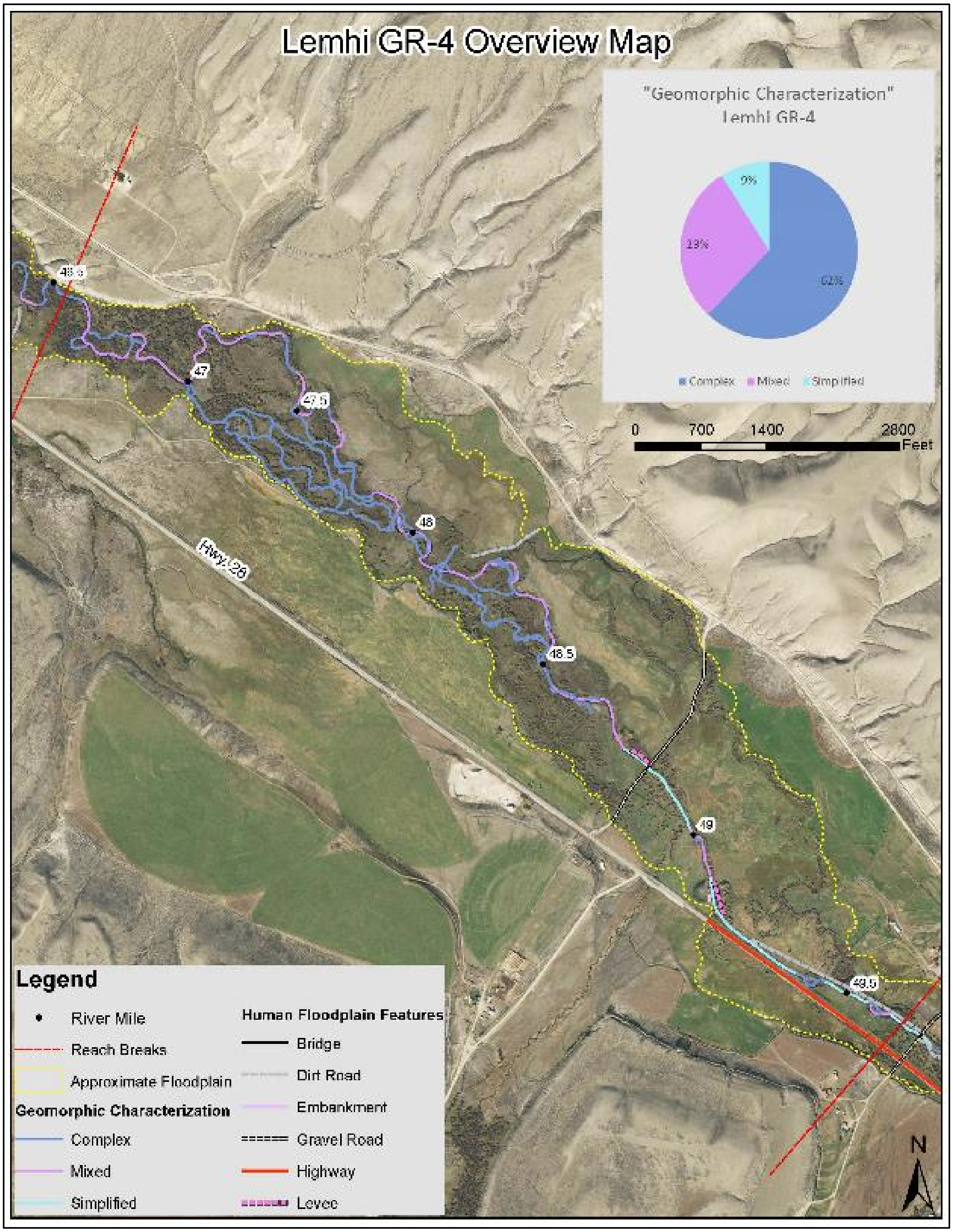

Figure 54. GR-4 overview map illustrating the approximate floodplain, geomorphic characterization, and human alterations to the floodplain.

Geomorphic Reach GR-5 (RM 46.5 – 43.2)

Geomorphic Reach GR-5 is located along the Lemhi River between RM 46.5 and RM 43.2 in an unconfined valley with significant constraints from Highway 28, resulting in the narrowing of the valley bottom by 30 percent and downstream disruption of flows and channel migration along the floodplain (Figure 55). Reach characteristics are summarized below in Table 16.

Table 16. Summary of attributes for Geomorphic Reach GR-5

Valley Segment	Reach	River Miles	Valley Slope (ft/ft)	Average Valley Width (ft)	Average Constrained Valley Width (ft)	Channel Slope (ft/ft)	Average Channel Width (ft)	Sinuosity	Entrenchment Ratio (ft/ft)	Constrained Entrenchment Ratio	Human Disturbance Ratio (%)	Groundwater Characteristics	Geomorphic Characterization	Geomorphic Characterization	Geomorphic Characterization "Simplified"
VS-2	GR-5	46.5 - 43.2	0.0086	1675	1,171	0.0060	34	1.4	49	34	8%	Losing	60%	22%	18%

Forms

- Sinuous, single-thread channel with significant side-channel development in the lower reach.
- Predominantly pool-riffle morphology generally associated with areas of mature riparian vegetation.
- Many banks lacking riparian vegetation.
- Over-widened channel in areas lacking riparian vegetation.
- Relatively high floodplain inundation area and valley gradient (similarities with GR-12 and GR-13)

Processes

- Observable channel widening where riparian vegetation is lacking.
- No point bar deposition suggests very low rates of channel migration.
- Fine sediment deposition observed in over-widened areas.

Human Impacts

- Discontinuous riparian corridor and associated bank instability and channel widening, and lack of shade.
- Highway 28 bisects the floodplain and artificially constrains the channel in the lower third of the reach, and channel confinement and straightening along the lower section may increase local transport capacity armoring the bed.
- Excessive fine sediment contributions resulting from increased erodibility of banks and floodplain due to degraded riparian vegetation and livestock grazing leading to siltation.
- Highway 28 road embankment, irrigation diversions, and bridges.

Response Potential

- Peak-flow-dominated hydrology; after irrigation season, it is a losing reach (Donato 1998). Fairly shallow groundwater during summer months supports riparian vegetation and associated bank stability.
- Channel form (especially width and bedform) and processes are driven by the presence or absence of mature riparian vegetation (primarily willow). Dense riparian vegetation maintains a narrow width-to-depth ratio, stabilizes banks, and promotes scour pool formation versus channel widening.

- Typical response to disturbances includes avulsion, side-channel formation, floodplain activation, and scour pool formation.

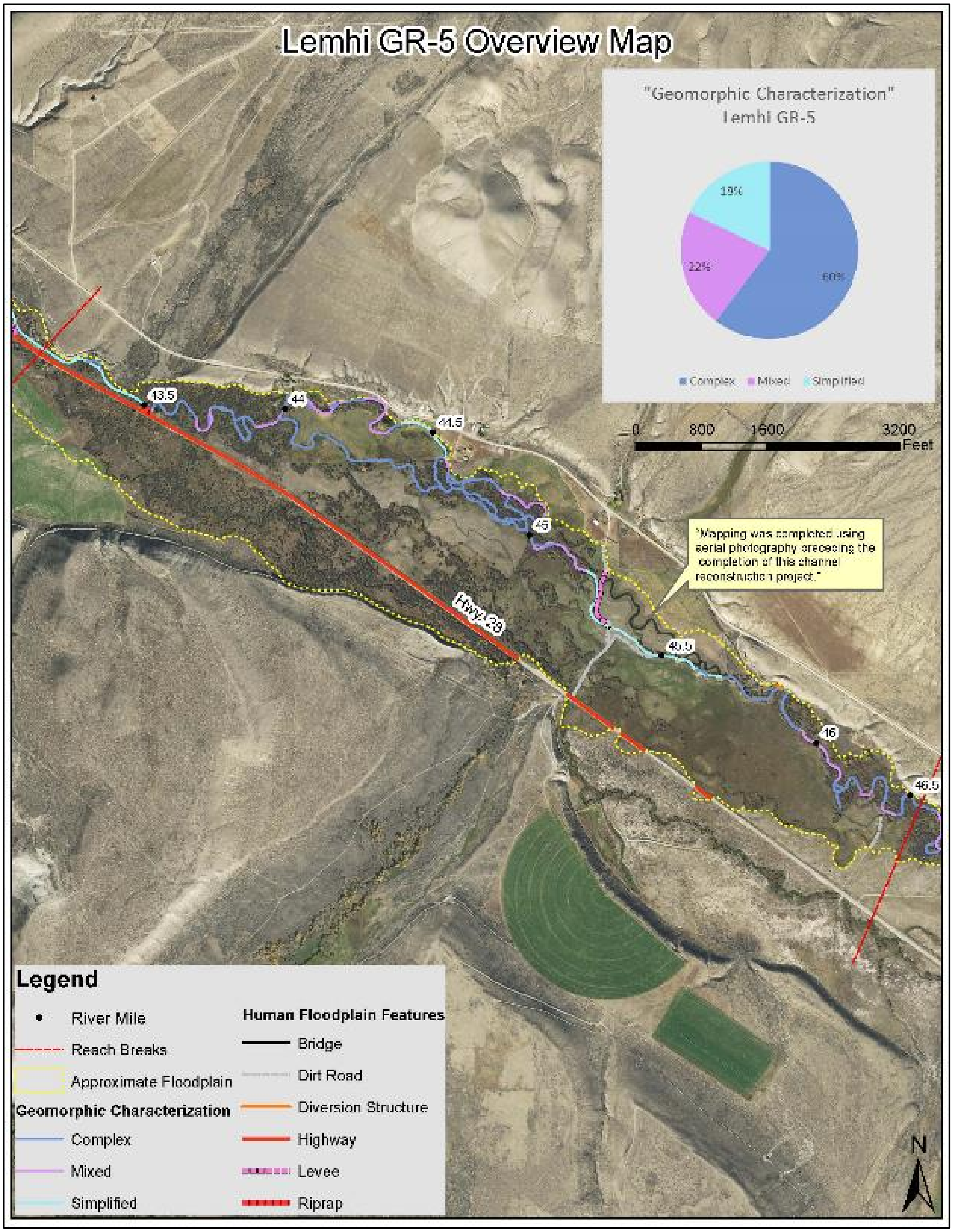

Figure 55. GR-5 overview map illustrating the approximate floodplain, geomorphic characterization, and human alterations to the floodplain.

Geomorphic Reach GR-6 (RM 43.2 – 41.1)

Geomorphic Reach GR-6 is located along the Lemhi River between RM 43.2 and RM 41.1 in an unconfined valley with significant human constraints from Highway 28, resulting in the narrowing of the valley bottom by about 50 percent, disrupting floodplain connection and channel migration (Figure 56). Reach characteristics are summarized below in Table 17.

Table 17. Summary of attributes for Geomorphic Reach GR-6

Valley Segment	Reach	River Miles	Valley Slope (ft/ft)	Average Valley Width (ft)	Average Constrained Valley Width (ft)	Channel Slope (ft/ft)	Average Channel Width (ft)	Sinuosity	Entrenchment Ratio (ft/ft)	Constrained Entrenchment Ratio (ft/ft)	Human Disturbance Ratio (%)	Groundwater Characteristics	Geomorphic Characterization "Complex"	Geomorphic Characterization "Mixed"	Geomorphic Characterization "Simplified"
VS-2	GR-6	43.2 - 41.1	0.0083	1342	663	0.0064	33	1.3	41	20	23%	Losing	62%	12%	26%

Forms

- Sinuous, except minor channel straightening associated with roads and bridges in the upstream and downstream ends of the reach.
- Mix of plane-bed and pool-riffle morphology, with pool-riffle generally associated with areas of dense riparian vegetation in the middle section of the reach.
- Many banks lacking riparian vegetation.
- Over-widened channel in areas lacking riparian vegetation.

Processes

- Observable channel widening where riparian vegetation is lacking.
- No point bar deposition suggests very low rates of channel migration.
- Fine sediment deposition observed in over-widened areas.

Human Impacts

- Patchy, discontinuous riparian corridor and associated bank instability, channel widening, plane-bed morphology, and lack of shade.
- Channel confinement and minor straightening may increase local transport capacity, armoring the bed predominantly in the upstream quarter of the reach.
- Excessive fine sediment filling interstitial space in the bed.
- Highway 28 road embankment, bridges, irrigation diversions, and discontinuous levees.

Response Potential

- Peak-flow-dominated hydrology; after irrigation season, it is a losing reach (Donato 1998). Fairly shallow summer groundwater supports riparian vegetation regeneration and associated bank stability.
- Channel form (especially width and bedform) and processes are driven by the presence or absence of mature riparian vegetation (primarily willow). Dense riparian vegetation maintains a narrow width-to-depth ratio, stabilizes banks, and promotes scour pool formation versus channel widening.
- Typical response to disturbances includes avulsion, side-channel formation, floodplain activation, and scour pool formation.

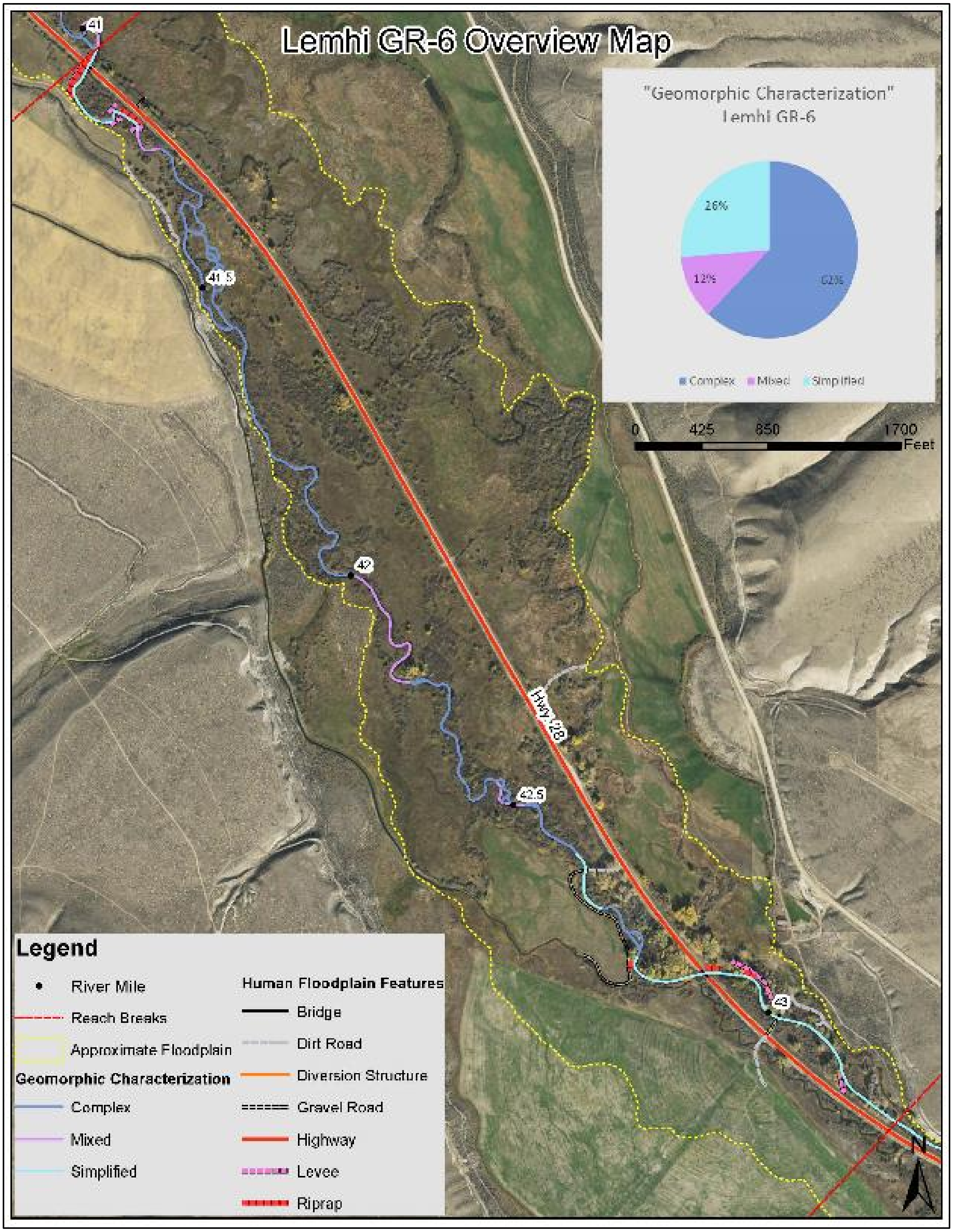

Figure 56. GR-6 overview map illustrating the approximate floodplain, geomorphic characterization, and human alterations to the floodplain.

Geomorphic Reach GR-7 (RM 41.1 – 35.1)

Geomorphic Reach GR-7 is located along the Lemhi River between RM 41.1 and RM 35.1 in an unconfined valley with significant valley bottom constraints, resulting in the narrowing of the valley bottom by about 40 percent (Figure 57). Reach characteristics are summarized below in Table 18.

Table 18. Summary of attributes for Geomorphic Reach GR-7

Valley Segment	Reach	River Miles	Valley Slope (ft/ft)	Average Valley Width (ft)	Average Constrained Valley Width (ft)	Channel Slope (ft/ft)	Average Channel Width (ft)	Sinuosity	Entrenchment Ratio (ft/ft)	Constrained Entrenchment Ratio (ft/ft)	Human Disturbance Ratio (%)	Groundwater Characteristics	Geomorphic Characterization "Complex"	Geomorphic Characterization "Mixed"	Geomorphic Characterization "Simplified"
VS-2	GR-7	41.1 - 35.1	0.0080	2127	1,204	0.0061	35	1.3	60	34	19%	Neutral	50%	25%	24%

Forms

- Sinuous, except major channel straightening associated with roads, bridges, and discontinuous levees primarily in the upstream half of the reach.
- Mix of plane-bed morphology generally associated with channel straightening, and pool-riffle morphology generally associated with areas of dense riparian vegetation.
- Many banks lacking riparian vegetation.
- Over-widened channel in areas lacking riparian vegetation.

Processes

- Observable channel widening where riparian vegetation is lacking.
- Little to no point bar deposition suggests low rates of channel migration.
- Fine sediment deposition observed in over-widened areas.

Human Impacts

- Patchy, discontinuous riparian corridor resulting in bank instability, channel widening, plane-bed morphology, and lack of shade.
- Channel confinement and straightening may increase local transport capacity, armoring the bed.
- Highway 28 artificially constrains the floodplain from RM 37.7 to 36.5.
- Excessive fine sediment filling interstitial space in the bed.
- Road embankments, bridges, irrigation diversions, and discontinuous levees.

Response Potential

- This reach gains from groundwater discharge during the irrigation season and then loses to the aquifer following irrigation season (Donato 1998). Shallow bedrock forces groundwater flows toward the surface at the downstream end of the reach and supports an area of dense, mature riparian vegetation.
- Channel form (especially width and bedform) and processes are driven by the presence or absence of mature riparian vegetation (primarily willow). Dense riparian vegetation maintains a narrow width-to-depth ratio, stabilizes banks, and promotes scour pool formation versus channel widening.
- Typical response to disturbances includes avulsion, side-channel formation, floodplain activation, and scour pool formation.

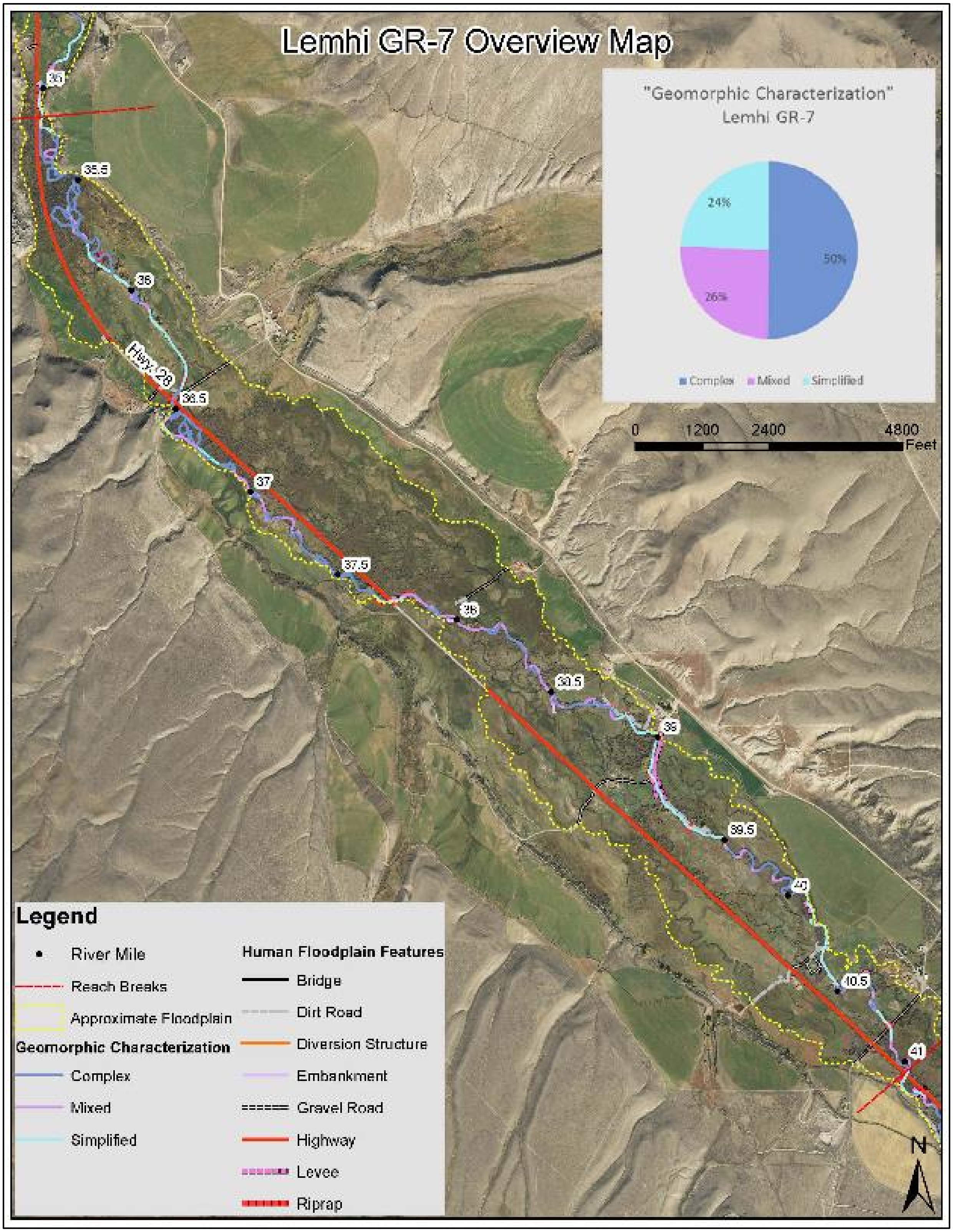

Figure 57. GR-7 overview map illustrating approximate floodplain, geomorphic characterization, and human alterations to floodplain.

Geomorphic Reach GR-8 (RM 35.1 – 32.7)

Geomorphic Reach GR-8 is located along the Lemhi River between RM 35.1 and RM 32.7 in a naturally unconfined valley with significant valley bottom constraints, resulting in narrowing of the valley bottom by about 40 percent due to Highway 28 (Figure 58). The reach is located immediately upstream of the confluence with Hayden Creek. Reach characteristics are summarized below in Table 19.

Table 19. Summary of attributes for Geomorphic Reach GR-8.

Valley Segment	Reach	River Miles	Valley Slope (ft/ft)	Average Valley Width (ft)	Average Constrained Valley Width (ft)	Channel Slope (ft/ft)	Average Channel Width (ft)	Sinuosity	Entrenchment Ratio (ft/ft)	Constrained Entrenchment Ratio (ft/ft)	Human Disturbance Ratio (%)	Groundwater Characteristics	Geomorphic Characterization "Complex"	Geomorphic Characterization "Mixed"	Geomorphic Characterization "Simplified"
VS-2	GR-8	35.1 - 32.7	0.0073	1393	781	0.0054	36	1.4	39	22	23%	Gaining	40%	4%	56%

Forms

- Sinuous, except for major channel straightening along Highway 28 in the downstream third of the reach.
- Predominantly plane-bed morphology generally associated with a lack of instream structure and channel straightening.
- Many banks lacking riparian vegetation.
- Over-widened channel in areas lacking riparian vegetation.

Processes

- Observable channel widening where riparian vegetation is lacking.
- No point bar deposition suggests very low rates of channel migration.
- Fine sediment deposition observed in over-widened areas.

Human Impacts

- Narrow, discontinuous riparian corridor resulting in bank instability, channel widening, plane-bed morphology, and lack of shade.
- Channel confinement and straightening may increase local transport capacity armoring the bed.
- Highway 28 artificially constrains the floodplain throughout the reach.
- Excessive fine sediment filling interstitial space in the bed.
- Road embankments, bridges, irrigation diversions, and discontinuous levees.

Response Potential

- Groundwater/baseflow-dominated hydrology, predominantly a gaining reach (Donato 1998). Shallow bedrock has raised the groundwater table, supporting riparian vegetation and associated bank stability.
- Channel form (especially width and bedform) and processes are driven by the presence or absence of mature riparian vegetation (primarily willow). Dense riparian vegetation maintains a narrow width-to-depth ratio, stabilizes banks, and promotes scour pool formation versus channel widening.
- Typical response to disturbances includes avulsion, side-channel formation, floodplain activation, and scour pool formation. Incision and bed armoring occur in straightened and confined areas.

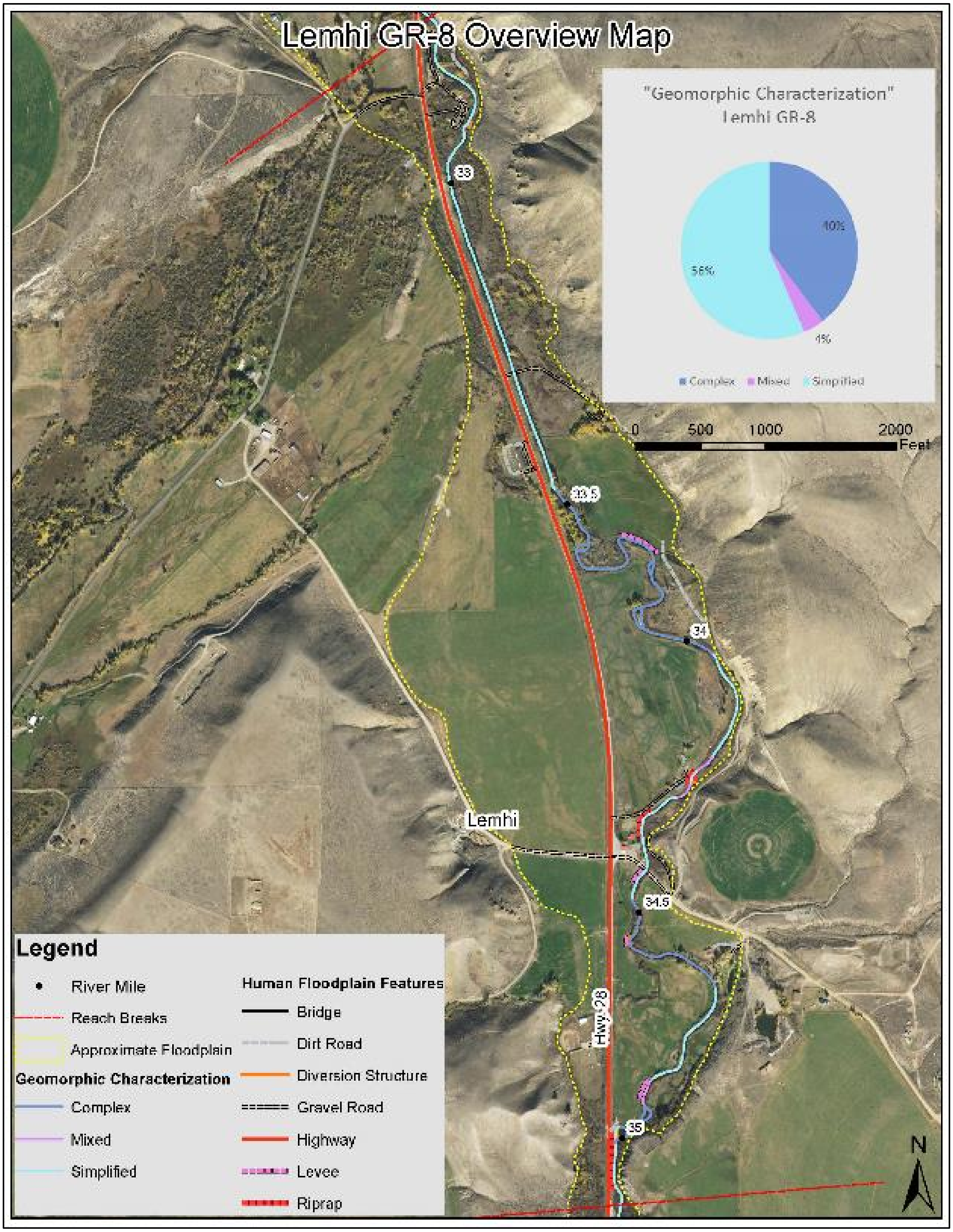

Figure 58. GR-8 overview map illustrating the approximate floodplain, geomorphic characterization, and human alterations to the floodplain.

Middle Lemhi Valley Segment (VS-3)

Middle Lemhi River Valley Segment comprises the Middle Lemhi River watershed and the Hayden Creek watershed (Table 20, Table 21, Figure 59). The Hayden Creek watershed contributions nearly double the flows in the Lemhi River.

RM 32.73– RM 19.55

Table 20. Lemhi watershed hydrologic units and areas

Sub-watershed	HUC 10	Named Tributaries	Acreage	Square Miles
Hayden Creek	1706020406	28	91,873 acres	143.55 mi^2
Middle Lemhi River	1706020407	13	114,868 acres	179.48 mi^2
Total		**41**	**206,741 acres**	**323.03 mi^2**

Table 21. Middle Lemhi sub-watershed tributaries

Tributary	Flow Regime	Drainage	Connectivity	Other
Kenney Creek (RM 19.6)	Perennial	Beaverhead Mountains	Direct connection	EPA-approved TMDL (Category 4a); Tributaries include East Fork Kenney Creek
Pattee Creek (RM 23.22)	Perennial	Beaverhead Mountains	Direct connection	Tributaries include Cherry Creek, High Creek, and Wade Creek
Agency Creek (RM 24.76)	Perennial	Beaverhead Mountains	Direct connection	Blue Bird – Gold Flint Copper Queen Consolidated Lodes, (Mineral Survey #993), Aug. 27, 1892, T19N – R25E, 58.65 acres; Mine T19N – R25E, Sect. 15, Quarry; Mine T19N –R25E, Sect. 9, Quarry; Tributaries include Cow Creek, Sharkey Creek, White Creek, Flume Creek, and Horseshoe Bend Creek; Lewis and Clark Pass
McDevitt Creek (RM 25.85)	Perennial	Lemhi Range	Indirect connection	Dewaters on alluvial fan; EPA-approved TMDL (Category 4)
Muddy Creek (RM 26.75)	Ephemeral	Lemhi Range	Direct connection	Channelized due to railroad/road grade
Hayden Creek (RM 32.66)	Perennial	Lemhi Range	Direct connection	HUC 10 sub-watershed; See Table 20.

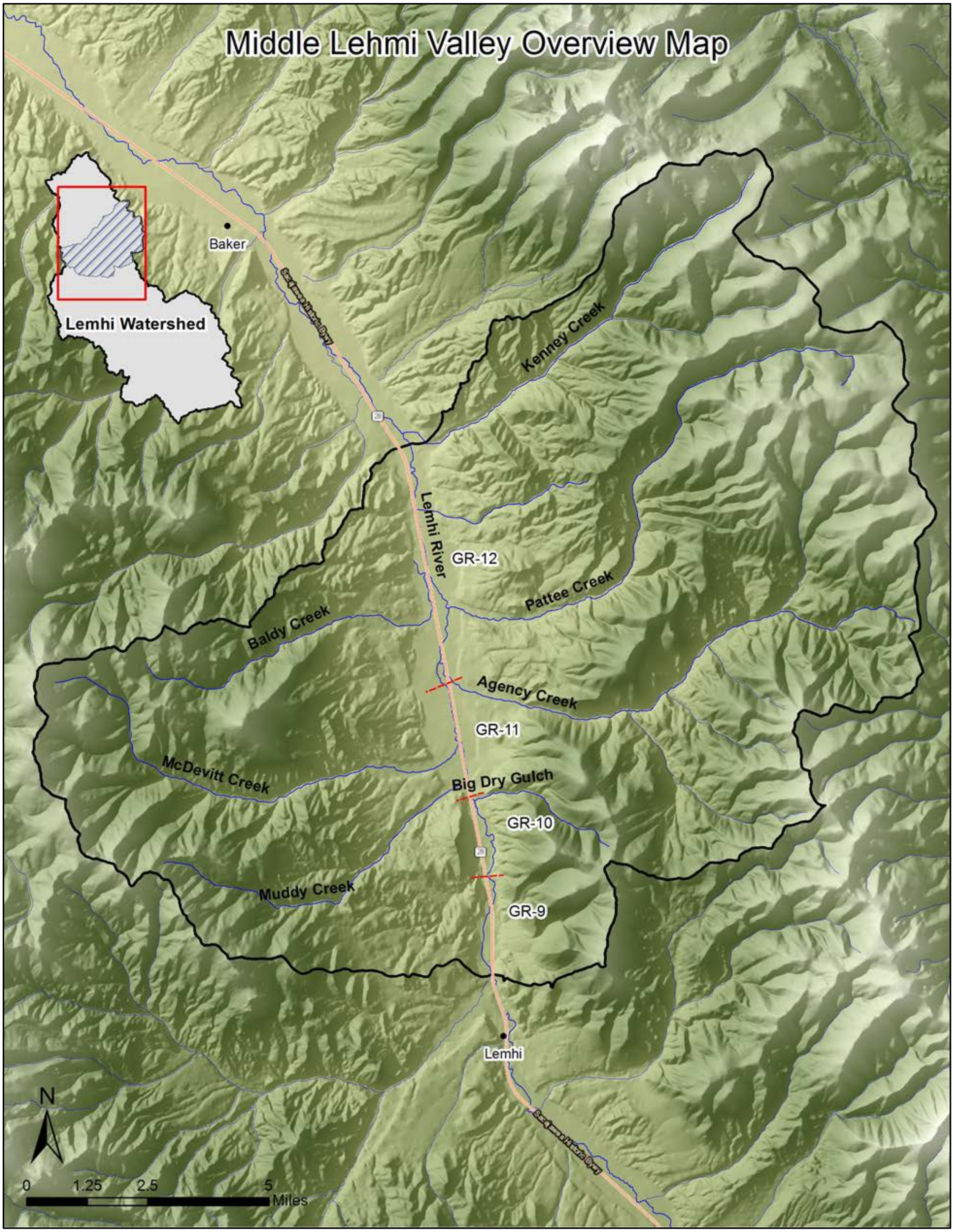

Figure 59. Middle Lemhi Valley Segment (VS-3) and geomorphic reaches (GR-9 through GR-12).

Hayden Creek Sub-watershed

The Hayden Creek sub-watershed (HUC 1706020406) covers 91,873 acres (Figure 60). Elevations range from about 5140 feet at the confluence of the Lemhi River and Hayden Creek to more than 10000 feet along the Lemhi Range. The Lemhi Range has several alpine lakes and tarns within glacial cirques. The drainage pattern within the sub-watershed is dendritic, and bedrock is predominantly limestone, dolomite, and quartzite. The higher-elevation, timbered lands are administered by the Salmon-Challis National Forest, lower-elevation slopes covered with shrub- and grasslands are administered by the BLM, and private holdings are predominantly along the valley bottoms in Hayden Creek and Basin Creek, and at the Hayden Creek and Lemhi River confluence. The Hayden Creek sub-watershed hydrology is snowmelt-dominated, with peak discharges capable of mobilizing and transporting coarse bedload from its confluence with Paradise Creek downstream through the canyon section to the Lemhi River.

Primary tributaries to Hayden Creek include West Fork Hayden Creek, Mogg Creek, East Fork Hayden Creek, Bear Valley Creek, and Basin Creek. Along the base of the Lemhi Range ridge, the West Fork Hayden Creek, Bear Valley Creek, and Basin Creek watersheds head in several alpine lakes and unnamed tarns. Named alpine lakes include Bear Valley Lakes and Buck Lakes in the Bear Valley Creek watershed, and Basin Lake in the Basin Creek watershed.

Hayden Creek heads in a glacial cirque where groundwater flows through glacial debris and colluvium, and intermittently daylights at about elevation 8240 feet on the east aspect of Long Mountain in the Lemhi Range. In the headwaters area to its confluence with Paradise Creek, Hayden Creek has a channelized colluvial valley with a single-thread, moderately sinuous channel with likely step-pool morphology, where forced by instream structure, and possibly multi-thread, island-braided channel where unconfined along wet meadows with dense willow and grass species. Hayden Creek then flows through a canyon section as a single-thread, fairly straight channel with sediment inputs from landslides and debris flows, and significant large wood recruitment that likely forces a step-pool to pool-riffle morphology. As the valley bottom opens up and the channel is no longer confined, log jams begin to accumulate upstream of the Hayden Creek and Meadow Creek confluence, likely forcing a pool-riffle morphology. From about the end of Tonsmeire Ranch Road, several irrigation diversions reduce instream flows, thereby reducing the stream’s transport capacity to move wood downstream. There is a significant reduction in instream wood, likely due to removal from the channel through the populated sections to reduce the threat of flooding. In this area, the channel has adjusted to a single-thread, moderately sinuous channel with a likely pool-riffle morphology. Here, dense riparian vegetation (willows and cottonwoods) and log jams still force flow convergence and bed scour, as well as a likely plane-bed channel in widened areas where riparian vegetation has been replaced with pasturelands for grazing, which is causing bank recession.

Summary

Hayden Creek has a snowmelt-dominated hydrology capable of mobilizing and transporting large wood and coarse sediment. However, peak flows have been attenuated by irrigation diversions taking water out of Hayden Creek and reducing stream power and transport capacity. In addition, the visible reduction of instream wood near populated areas suggests wood has been removed from the system to reduce the threat of flooding.

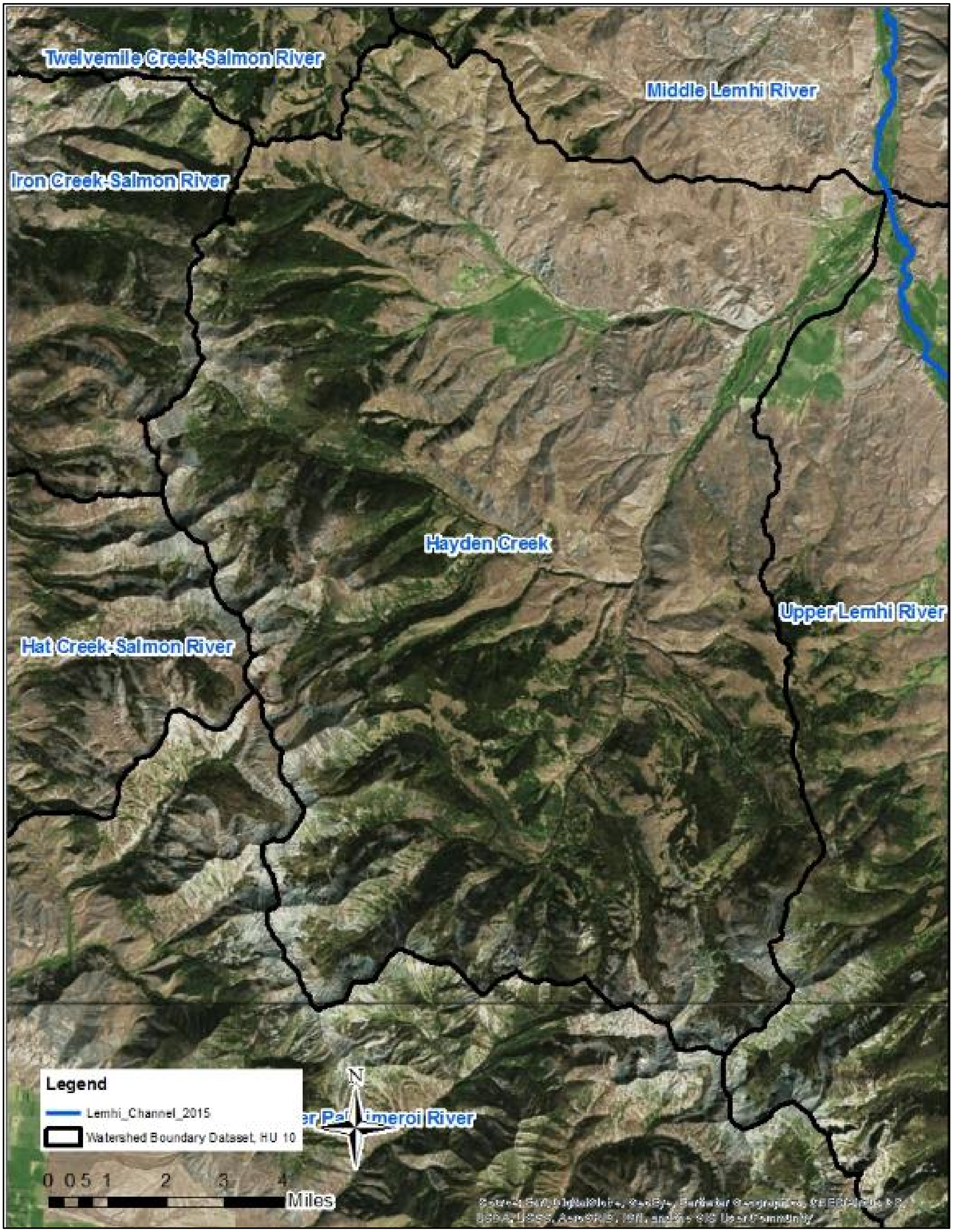

Figure 60. Aerial image of Hayden Creek sub-watershed.

Geomorphic Reach GR-9 (RM 32.7 – 30.3)

Geomorphic Reach GR-9 is located along the Lemhi River between RM 32.7 and RM 30.3, in an unconfined valley with moderate valley bottom constraints resulting in the narrowing of the valley bottom by about 25 percent (Figure 61). The reach is located immediately below the confluence with Hayden Creek and is significantly influenced by the peak-flow hydrology and coarse sediment inputs from Hayden Creek. Reach characteristics are summarized below in Table 22.

Table 22. Summary of attributes for Geomorphic Reach GR-9

Valley Segment	Reach	River Miles	Valley Slope (ft/ft)	Average Valley Width (ft)	Average Constrained Valley Width (ft)	Channel Slope (ft/ft)	Average Channel Width (ft)	Sinuosity	Entrenchment Ratio (ft/ft)	Constrained Entrenchment Ratio (ft/ft)	Human Disturbance Ratio (%)	Groundwater Characteristics	Geomorphic Characterization "Complex"	Geomorphic Characterization "Mixed"	Geomorphic Characterization "Simplified"
VS-3	GR-9	32.7 - 30.3	0.0088	1488	1,074	0.0077	54	1.1	28	20	6%	Gaining	13%	5%	81%

Forms

- Low to moderate sinuosity; much of the channel appears to have been mechanically altered and straightened.
- Predominantly plane-bed morphology generally associated with a lack of instream structure, low sinuosity, and likely channel alteration.
- Many banks lacking riparian vegetation.

Processes

- Possible incision and/or bed armoring associated with channel alterations and straightening.
- No point bar deposition suggests very low rates of channel migration.
- Bank recession and widening observed in areas lacking mature riparian vegetation.
- Disturbance regime supports cottonwood riparian vegetation from this point downstream.

Human Impacts

- Patchy, discontinuous riparian corridor resulting in bank instability, channel widening, plane-bed morphology, and lack of shade.
- Channel confinement and straightening may increase local transport capacity incising and/or armoring the bed.
- Highway 28 artificially constrains the floodplain throughout the reach.
- Road embankments, bridges, and irrigation diversions.

Response Potential

- Snowmelt-dominated hydrology driven by discharge from Hayden Creek with groundwater inputs. Shallow groundwater supports riparian vegetation and associated bank stability.
- Channel form (especially width and bedform) and processes are driven by the presence or absence of mature riparian vegetation (primarily willow and cottonwood) in addition to coarse sediment and large wood inputs from Hayden Creek. Dense riparian vegetation maintains a narrow width-to-depth ratio, stabilizes banks, and promotes scour pool formation versus channel widening.

- Typical response to disturbances includes channel migration, floodplain activation, pool and riffle formation, and island braiding associated with instream obstruction. Incision and bed armoring in straightened and confined areas.

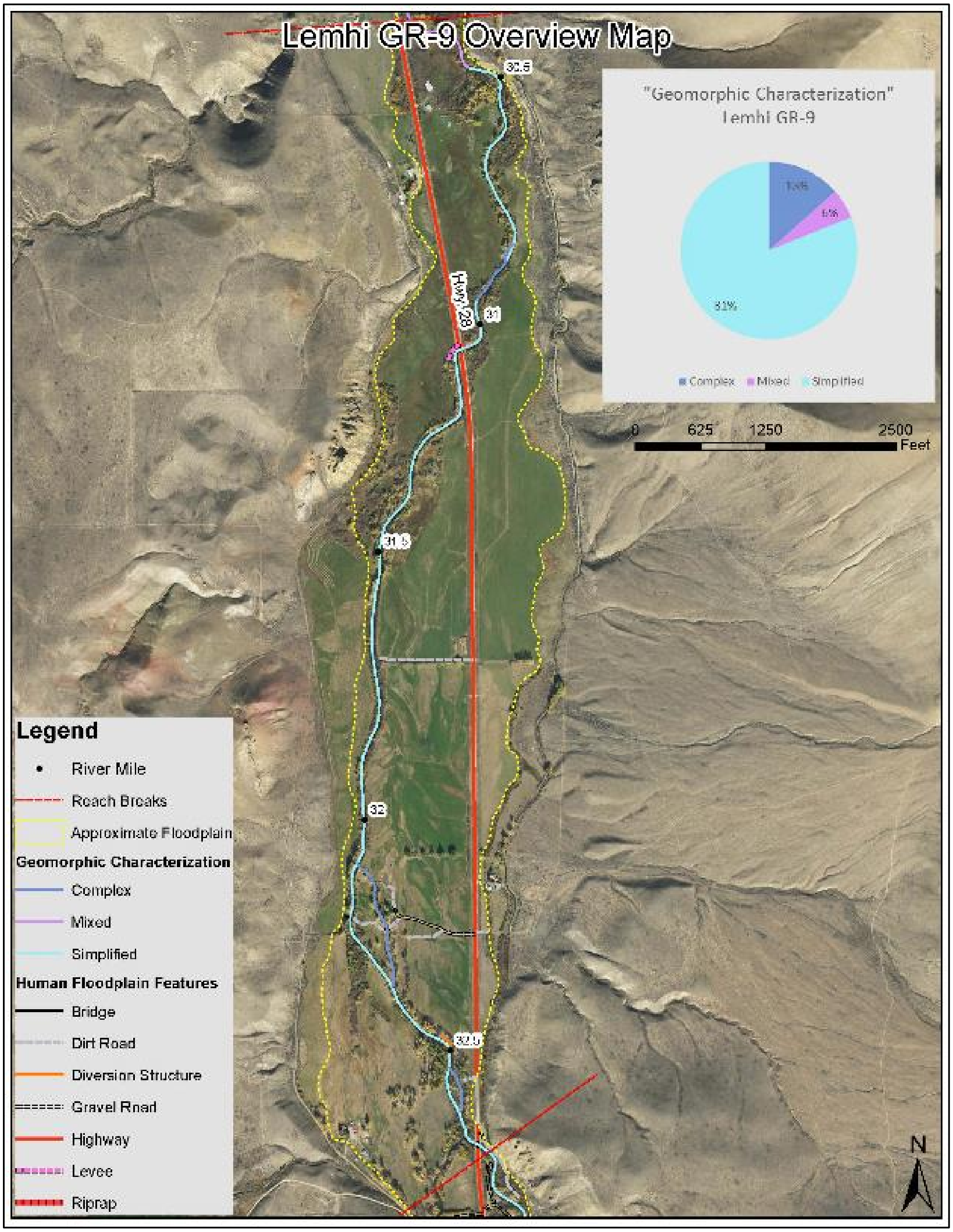

Figure 61. GR-9 overview map illustrating the approximate floodplain, geomorphic characterization, and human alterations to the floodplain.

Geomorphic Reach GR-10 (RM 30.3 – 28)

Geomorphic Reach GR-10 is located along the Lemhi River between RM 30.3 and RM 28.0, in an unconfined valley with moderate valley bottom constraints, resulting in the narrowing of the valley bottom by about 35 percent (Figure 62). Reach characteristics are summarized below in Table 23.

Table 23. Summary of attributes for Geomorphic Reach GR-10.

Valley Segment	Reach	River Miles	Valley Slope (ft/ft)	Average Valley Width (ft)	Average Constrained Valley Width (ft)	Channel Slope (ft/ft)	Average Channel Width (ft)	Sinuosity	Entrenchment Ratio (ft/ft)	Constrained Entrenchment Ratio (ft/ft)	Human Disturbance Ratio (%)	Groundwater Characteristics	Geomorphic Characterization "Complex"	Geomorphic Characterization "Mixed"	Geomorphic Characterization "Simplified"
VS-3	GR-10	30.3 - 28	0.0093	1273	816	0.0071	46	1.3	28	18	25%	Neutral	5%	28%	67%

Forms

- Sinuous channel may have been repositioned along the right valley wall, at least in the upper half of the reach, if not most of the reach.
- Predominantly plane-bed morphology
- Narrow (about 30 feet wide) riparian corridor.
- Many banks lacking riparian vegetation.

Processes

- Possible incision and/or bed armoring associated with channel alterations and straightening.
- No point bar deposition suggests very low rates of channel migration.
- Bank recession and widening observed in areas lacking mature riparian vegetation.

Human Impacts

- Patchy, discontinuous riparian corridor resulting in bank instability, channel widening, plane-bed morphology, and lack of shade.
- Channel confinement and straightening may increase local transport capacity armoring the bed.
- Highway 28 artificially constrains the floodplain, predominantly in the downstream third of the reach.
- Road embankments, bridges, irrigation diversions, discontinuous levees, and riprap.

Response Potential

- Snowmelt surface-water-dominated hydrology driven by discharge from Hayden Creek, with groundwater inputs during irrigation season and losses to aquifer after irrigation season. Shallow groundwater during the summer supports riparian vegetation and associated bank stability.
- Channel form (especially width and bedform) and processes are driven by the presence or absence of mature riparian vegetation (primarily willow and cottonwood) in addition to coarse sediment and large wood inputs from Hayden Creek. Dense riparian vegetation maintains a narrow width-to-depth ratio, stabilizes banks, and promotes scour pool formation versus channel widening.
- Typical response to disturbances includes channel migration, floodplain activation, pool and riffle formation, and island braiding associated with instream obstruction. Incision and bed armoring in straightened and confined areas.

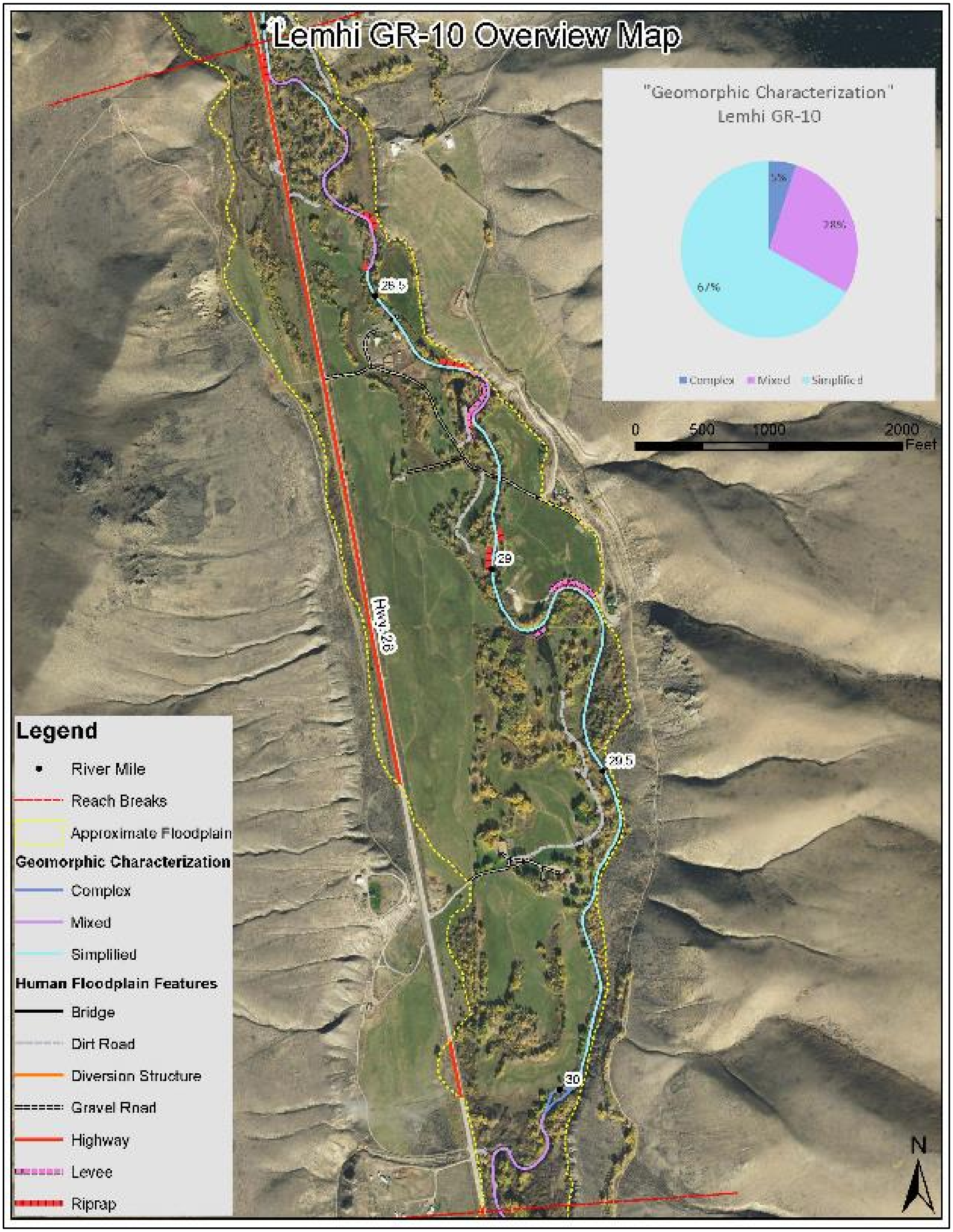

Figure 62. GR-10 overview map illustrating the approximate floodplain, geomorphic characterization, and human alterations to the floodplain.

Geomorphic Reach GR-11 (RM 28 – 25.4)

Geomorphic Reach GR-11 is located along the Lemhi River between RM 28.0 and RM 25.4 in a naturally unconfined valley with significant valley bottom constraints resulting from narrowing of the valley bottom by about 55 percent due to Highway 28 (Figure 63). Reach characteristics are summarized below in Table 24.

Table 24. Summary of attributes for Geomorphic Reach GR-11

Valley Segment	Reach	River Miles	Valley Slope (ft/ft)	Average Valley Width (ft)	Average Constrained Valley Width (ft)	Channel Slope (ft/ft)	Average Channel Width (ft)	Sinuosity	Entrenchment Ratio (ft/ft)	Constrained Entrenchment Ratio (ft/ft)	Human Disturbance Ratio (%)	Groundwater Characteristics	Geomorphic Characterization "Complex"	Geomorphic Characterization "Mixed"	Geomorphic Characterization "Simplified"
VS-3	GR-11	28 - 25.4	0.0088	1158	490	0.0080	51	1.1	23	10	27%	Gaining	12%	10%	77%

Forms

- Sinuous channel may have been repositioned along the right valley wall, at least in the upper half of the reach, if not most of the reach.
- Predominantly plane-bed morphology
- Narrow (about 30 feet wide) riparian corridor.
- Many banks lacking riparian vegetation.

Processes

- Possible incision and/or bed armoring associated with channel alterations and straightening.
- No point bar deposition suggests very low rates of channel migration.
- Bank recession and widening observed in areas lacking mature riparian vegetation.

Human Impacts

- Patchy, discontinuous riparian corridor resulting in bank instability, channel widening, plane-bed morphology, and lack of shade.
- Channel confinement and straightening may increase local transport capacity armoring the bed.
- Highway 28 artificially constrains the floodplain throughout the reach.
- Road embankments, bridges, irrigation diversions, discontinuous levees, and riprap.

Response Potential

- Snowmelt surface-water-dominated hydrology driven by discharge from Hayden Creek with groundwater inputs. Shallow groundwater during the summer supports riparian vegetation and associated bank stability.
- Channel form (especially width and bedform) and processes are driven by the presence or absence of mature riparian vegetation (willow and cottonwood) in addition to coarse sediment and large wood recruitment. Dense riparian vegetation maintains a narrow width-to-depth ratio, stabilizes banks, and promotes scour pool formation versus channel widening.
- Typical response to disturbances includes channel migration, floodplain activation, pool and riffle formation, and island braiding associated with instream obstruction. Incision and bed armoring in straightened and confined areas.

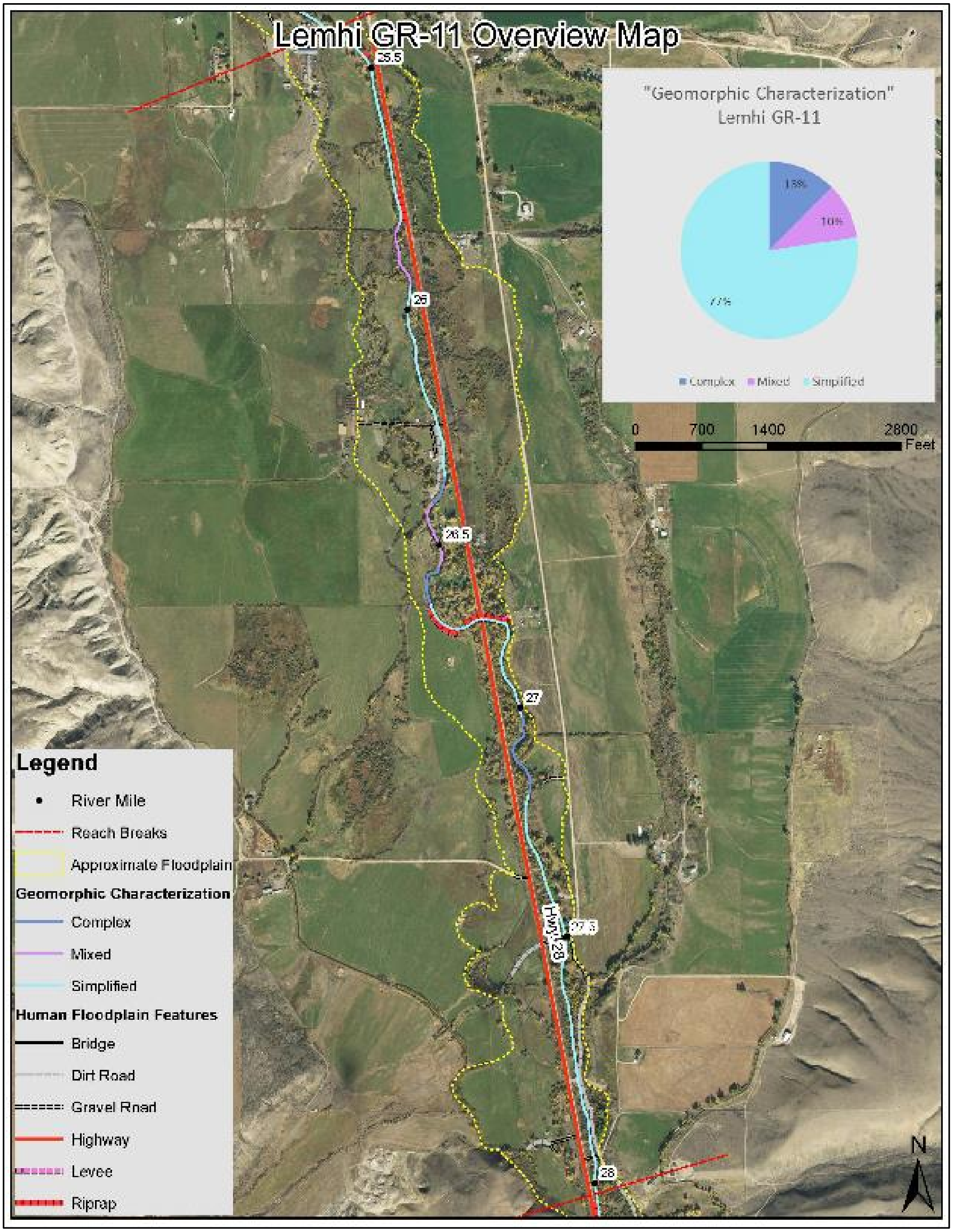

Figure 63. GR-11 overview map illustrating the approximate floodplain, geomorphic characterization, and human alterations to the floodplain.

Geomorphic Reach GR-12 (RM 25.4 – 19.6)

Geomorphic Reach GR-12 is located along the Lemhi River between RM 25.4 and RM 19.6 in a naturally unconfined valley with significant valley bottom constraints associated with Highway 28, resulting in the narrowing of the valley bottom by about 30 percent (Figure 64). Reach characteristics are summarized below in Table 25.

Table 25. Summary of attributes for Geomorphic Reach GR-12.

Valley Segment	Reach	River Miles	Valley Slope (ft/ft)	Average Valley Width (ft)	Average Constrained Valley Width (ft)	Channel Slope (ft/ft)	Average Channel Width (ft)	Sinuosity	Entrenchment Ratio (ft/ft)	Constrained Entrenchment Ratio (ft/ft)	Human Disturbance Ratio (%)	Groundwater Characteristics	Geomorphic Characterization "Complex"	Geomorphic Characterization "Mixed"	Geomorphic Characterization "Simplified"
VS-3	GR-12	25.4 - 19.6	0.0088	2813	1,917	0.0076	54	1.1	53	36	32%	Gaining	27%	20%	53%

Forms

- Low to moderate sinuosity with major channel straightening along Highway 28 and levees in the downstream half of the reach.
- Floodplain constrained by Highway 28 along the entire reach.
- Predominantly plane-bed morphology generally associated with a simplified and straightened channel.
- Many banks lacking riparian vegetation.
- Over-widened channel, primarily where riparian vegetation is lacking.

Processes

- No point bar deposition suggests very low rates of channel migration.
- Evidence of large wood recruitment on bends in lower reach initiating small-scale island braiding (near RM 20.5).

Human Impacts

- Patchy, discontinuous riparian corridor resulting in bank instability, channel widening, plane-bed morphology, and lack of shade.
- Channel confinement and straightening may increase local transport capacity armoring the bed.
- Highway 28 artificially constrains the floodplain throughout the reach.
- Road embankments, bridges, irrigation diversions, discontinuous levees, and riprap.

Response Potential

- Snowmelt surface-water-dominated hydrology with groundwater inputs. Shallow groundwater during the summer supports riparian vegetation and associated bank stability.
- Channel form (especially width and bedform) and processes are driven by the presence or absence of mature riparian vegetation (willow and cottonwood) in addition to coarse sediment and large wood recruitment. Dense riparian vegetation maintains a narrow width-to-depth ratio, stabilizes banks, and promotes scour pool formation.

- Typical response to disturbances includes channel migration, floodplain activation, pool and riffle formation, and island braiding associated with instream obstruction. Incision and bed armoring in straightened and confined areas.

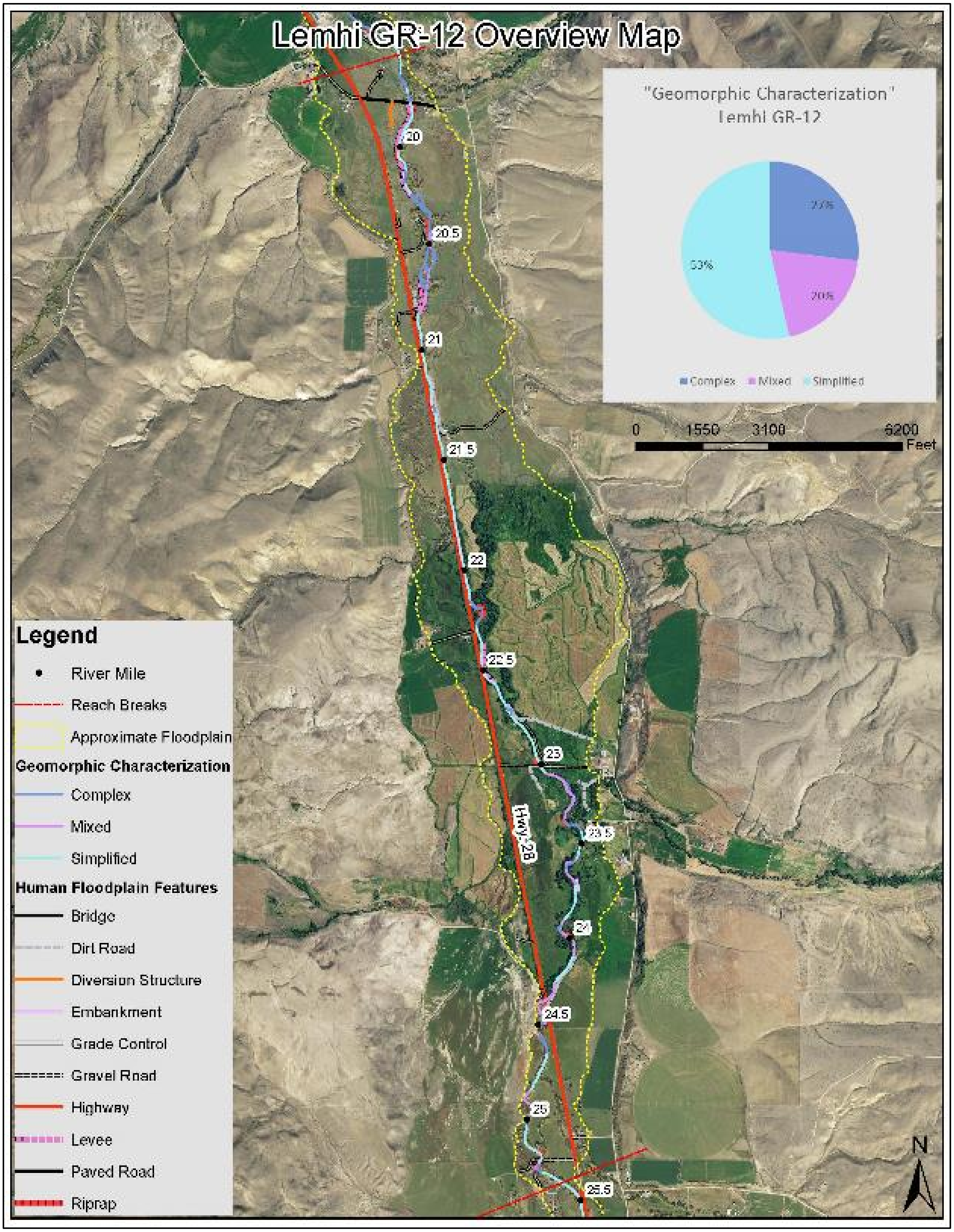

Figure 64. GR-12 overview map illustrating the approximate floodplain, geomorphic characterization, and human alterations to the floodplain.

Lower Lemhi Valley Segment (VS-4)

Includes the mainstem Lemhi River from RM 0 to RM 19.55.

The Lower Lemhi River Valley Segment comprises the Lower Lemhi River watershed (Table 26, Table 27, Figure 65), gaining from groundwater inputs in August and October (Donato 1998).

Table 26. Lemhi watershed hydrologic units and areas.

Sub-watershed	HUC 10	Named Tributaries	Acreage	Square Miles
Lower Lemhi River	1706020408	21	131,037 acres	204.75 mi^2
Total		**21**	**131,037 acres**	**204.75 mi^2**

Table 27. Lower Lemhi sub-watershed tributaries.

Tributary	Flow Regime	Drainage	Connectivity	Other
Kirtley Creek (RM 2.55)	Ephemeral	Beaverhead Mountains	Indirect Connection	Dewaters on alluvial fan; EPA-approved TMDL (Category 4a); Tributaries include North Fork Kirtley Creek, East Fork Kirtley Creek, and four unnamed tributaries; No. 3 Placer, No. 2 Placer, and No. 1 Placer (Mineral Survey #990), approved June 23, 1892, T21N – R22E/T22N – R22E, 3.8 miles of valley bottom.
Geertson Creek (~RM 8.4)	Perennial	Beaverhead Mountains	Indirect connection	Dewaters on alluvial fan; heads in tarn; EPA-approved TMDL (Category 4a); tributaries include Gary Creek
Bohannon Creek (RM 10.9)	Perennial	Beaverhead Mountains	Direct connection	Heads in tarn; EPA-approved TMDL (Category 4a); Marengo, Durango, and Red Bluff Consolidated Placers, (Mineral Survey #1202), Nov. 6, 1896, T21N- R23E, 360 acres; Red Bluff Placer (Mineral Survey #2585), 8/10/1911, T21N – R23E, 70.12 acres; tributaries include East Fork Bohannon Creek; tributaries include East Fork Bohannon Creek, 3 miles of valley bottom.
Wimpey Creek (RM 12.8)	Perennial	Beaverhead Mountains	Direct connection	EPA-approved TMDL (Category 4a); tributaries include East Fork Wimpy Creek, and West Fork Wimpey Creek
Withington Creek (RM 13.15)	Perennial	Lemhi Range	Indirect connection	Disconnected near Old Baker Highway; Harmony Millsite (Mineral Survey #3121B), Nov. 12, 1926, T20N – R22E, 4.44 acres; tributaries include Cheney Creek and Joe Moore Creek; Eli Creek with Pope Shenon Group (Mineral Survey #2952) Cancelled, Sept. 20, 1922, T20N – R22E, NA acres

Tributary	Flow Regime	Drainage	Connectivity	Other
Pratt Creek (~RM 14.3)	Perennial	Beaverhead Mountains	Indirect connection	Dewaters on alluvial fan
Kadletz Creek (RM 14.95)	Ephemeral	Lemhi Range	Direct connection	
Sandy Creek (~RM 17.8)	Perennial	Beaverhead Mountains	Indirect connection	Dewaters on alluvial fan; heads in tarn; Lone Star, Lone Star Extension, and Walcott Consolidated Lodes, (Mineral Survey #1591), Jan. 4, 1901, T21N – R24E, 61.9 acres; Grizzly Bear Group (Mineral Survey #2473A), March 23, 1910, T20N – R24E/T21N – R24E, 61.22 acres; Gem Group (Mineral Survey #2531), July 29, 1910, T21N – R24E, 70.12 acres; Grizzly Bear Millsite (Mineral Survey #2473B), March 23, 1910, T21N – R24E, 4.98 acres; tributaries include West Fork Sandy Creek
Haynes Creek (RM 19.02)	Perennial	Lemhi Range	Direct connection	Dewaters on alluvial fan; Haynes Creek Reservoir (T19S – R23E, Sect. 10)

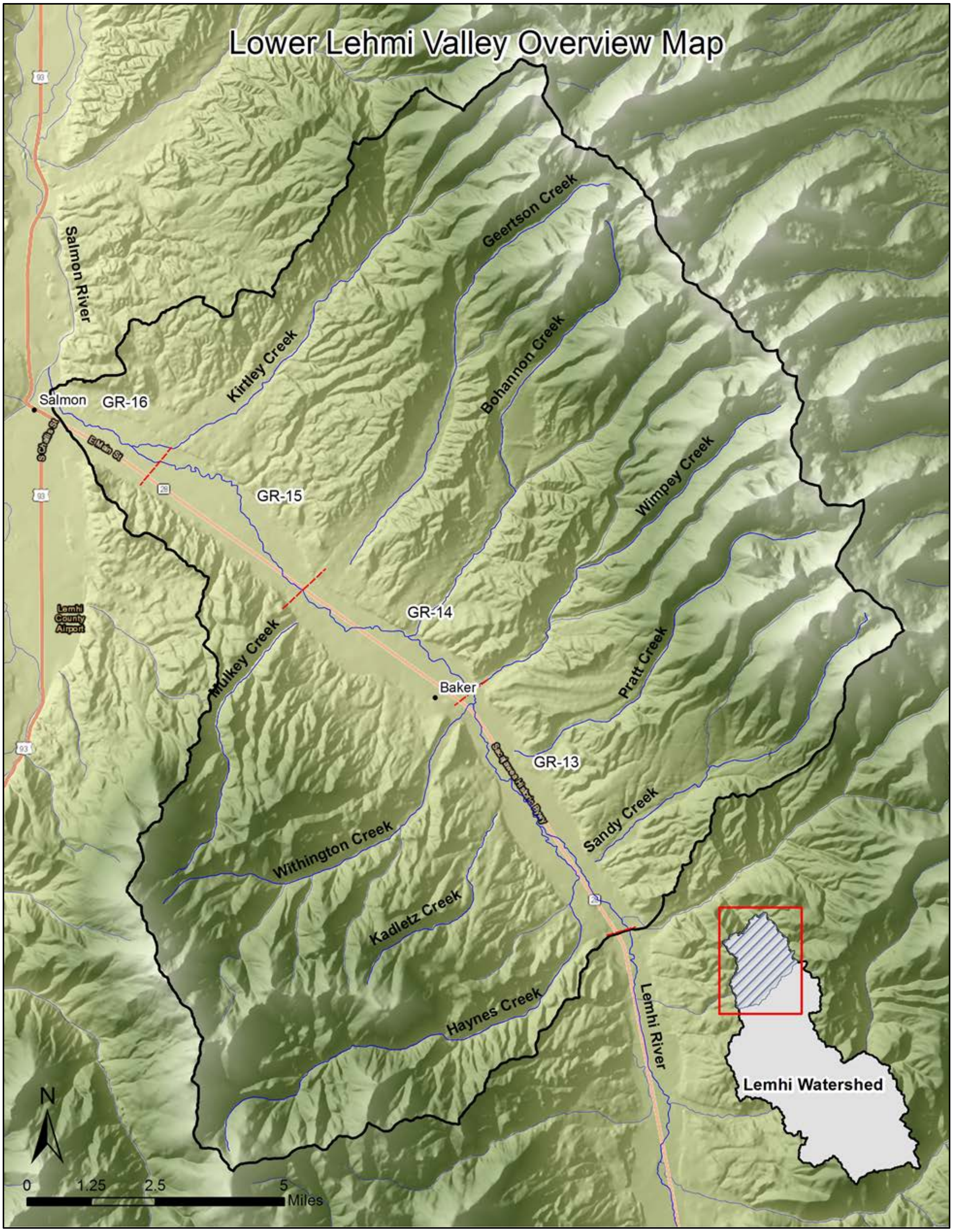

Figure 65. Lower Lemhi Valley Segment (VS-4) and geomorphic reaches (GR-13 through GR-16).

Geomorphic Reach GR-13 (RM 19.6 – 12.9)

Geomorphic Reach GR-13 is located along the Lemhi River between RM 19.6 and RM 12.9 in an unconfined valley with significant valley bottom constraints, resulting in the narrowing of the valley bottom by about 65 percent (Figure 66). Reach characteristics are summarized below in Table 28.

Table 28. Summary of attributes for Geomorphic Reach GR-13.

Valley Segment	Reach	River Miles	Valley Slope (ft/ft)	Average Valley Width (ft)	Average Constrained Valley Width (ft)	Channel Slope (ft/ft)	Average Channel Width (ft)	Sinuosity	Entrenchment Ratio (ft/ft)	Constrained Entrenchment Ratio (ft/ft)	Human Disturbance Ratio (%)	Groundwater Characteristics	Geomorphic Characterization	Geomorphic Characterization "Mixed"	Geomorphic Characterization "Simplified"
VS-4	GR-13	19.6 - 12.9	0.0084	2813	919	0.0070	57	1.2	49	16	55%	Neutral	17%	34%	48%

Forms

- Low to moderate sinuosity; minor channel straightening and alteration, especially near bridges, irrigation diversions, and levees throughout the reach.
- Floodplain constrained by Highway 28 along the entire reach.
- Predominantly plane-bed morphology generally associated with mechanical channel alterations and lack of instream structure.
- Many banks lacking riparian vegetation.
- Over-widened channel in areas lacking riparian vegetation.

Processes

- Observable channel widening where riparian vegetation is lacking.
- Areas of point bar deposition with low to moderate rates of channel migration
- Evidence of large wood recruitment in few places where instream structure is present, including irrigation diversions and at the head of islands.

Human Impacts

- Patchy, discontinuous riparian corridor resulting in bank instability, channel widening, plane-bed morphology, and lack of shade.
- Channel confinement and straightening may increase local transport capacity, causing incision and bed armoring.
- Road embankments, bridges, discontinuous levees, riprap, and irrigation diversions.

Response Potential

- Snowmelt surface-water-dominated hydrology with groundwater inputs during the irrigation season and groundwater losses after the irrigation season. Shallow groundwater during the summer supports riparian vegetation consisting of willow and cottonwood.
- Channel form (especially width and bedform) and processes are driven by the presence or absence of mature riparian vegetation (willow and cottonwood) in addition to coarse sediment and large wood recruitment. Dense riparian vegetation maintains a narrow width-to-depth ratio, stabilizes banks, and promotes scour pool formation.
- Typical response to disturbances includes channel migration, floodplain activation, pool and riffle formation, and island braiding associated with instream obstruction. Incision and bed armoring in straightened and confined areas.

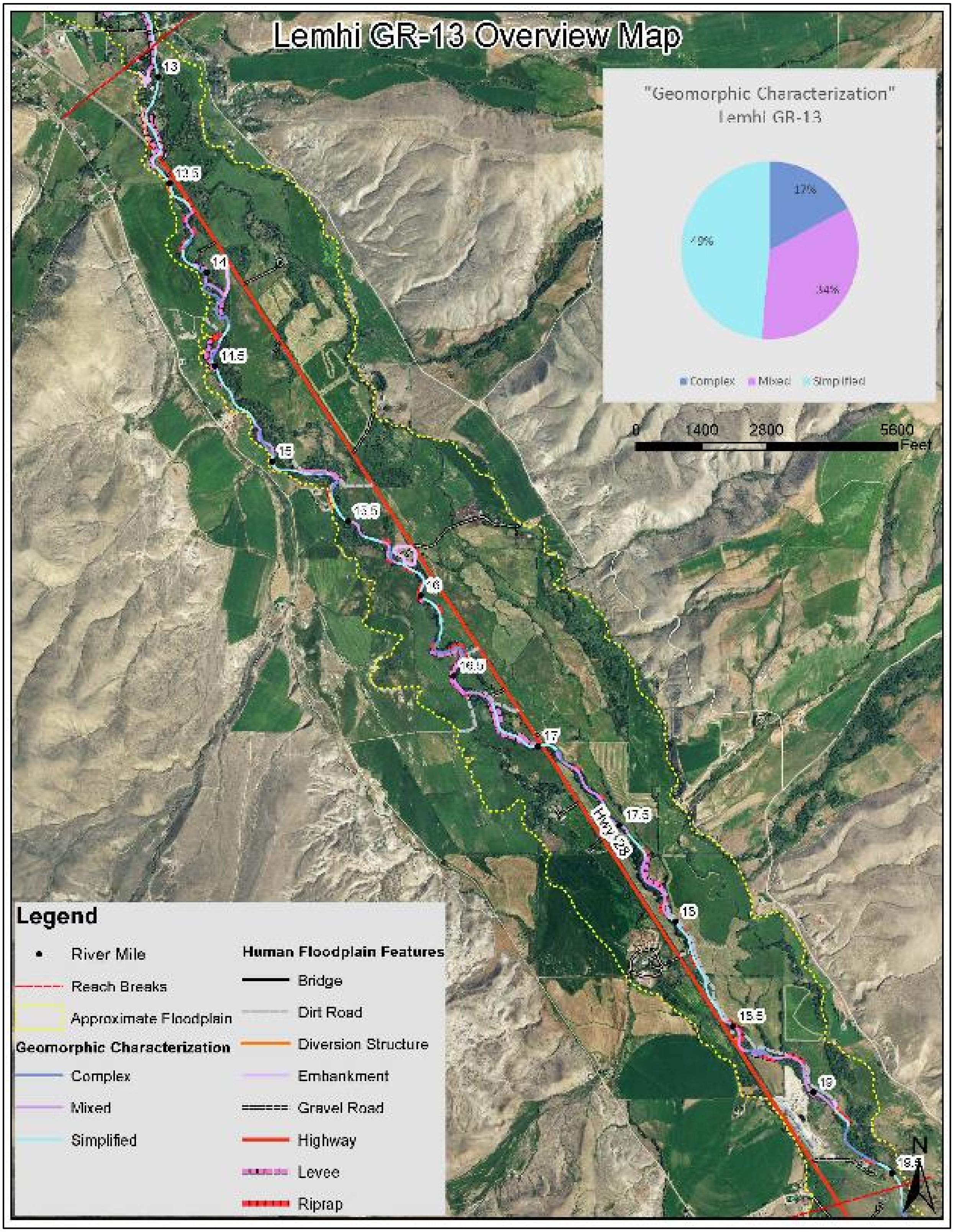

Figure 66. GR-13 overview map illustrating the approximate floodplain, geomorphic characterization, and human alterations to the floodplain.

Geomorphic Reach GR-14 (RM 12.9 – 8.1)

Geomorphic Reach GR-14 is located along the Lemhi River between RM 12.9 and RM 8.1 in an unconfined valley with significant valley bottom constraints, resulting in the narrowing of the valley bottom by about 65 percent (Figure 67). Reach characteristics are summarized below in Table 29.

Table 29. Summary of attributes for Geomorphic Reach GR-14.

Valley Segment	Reach	River Miles	Valley Slope (ft/ft)	Average Valley Width (ft)	Average Constrained Valley Width (ft)	Channel Slope (ft/ft)	Average Channel Width (ft)	Sinuosity	Entrenchment Ratio (ft/ft)	Constrained Entrenchment Ratio (ft/ft)	Human Disturbance Ratio (%)	Groundwater Characteristics	Geomorphic Characterization "Complex"	Geomorphic Characterization "Mixed"	Geomorphic Characterization "Simplified"
VS-4	GR-14	12.9 - 8.1	0.0080	2217	640	0.0065	62	1.2	36	10	64%	Neutral	13%	15%	72%

Forms

- Low to moderate sinuosity.
- Significant channel alterations, simplification, and straightening.
- Floodplain constrained by Highway 28 along the downstream half of the reach.
- Predominantly plane-bed morphology generally associated with channel alterations and lack of instream structure.
- Many banks lacking riparian vegetation.

Processes

- Minimal point bar deposition suggests low rates of channel migration.
- Large wood recruitment associated with limited instream obstructions, including irrigation diversions and islands.

Human Impacts

- Patchy, discontinuous riparian corridor contributing to bank instability, channel widening, plane-bed morphology, and lack of shade.
- Channel confinement and straightening may increase local transport capacity armoring the bed.
- Discontinuous levees, road embankments, bridges, riprap, and irrigation diversions.

Response Potential

- Snowmelt surface-water-dominated hydrology with groundwater inputs during the irrigation season and groundwater losses after the irrigation season. Shallow groundwater during the summer supports riparian vegetation consisting of willow and cottonwood.
- Channel form (especially width and bedform) and processes are driven by the presence or absence of mature riparian vegetation (willow and cottonwood) in addition to coarse sediment and large wood recruitment. Dense riparian vegetation maintains a narrow width-to-depth ratio, stabilizes banks, and promotes scour pool formation.
- Typical response to disturbances includes channel migration, floodplain activation, pool and riffle formation, and island braiding associated with instream obstruction.

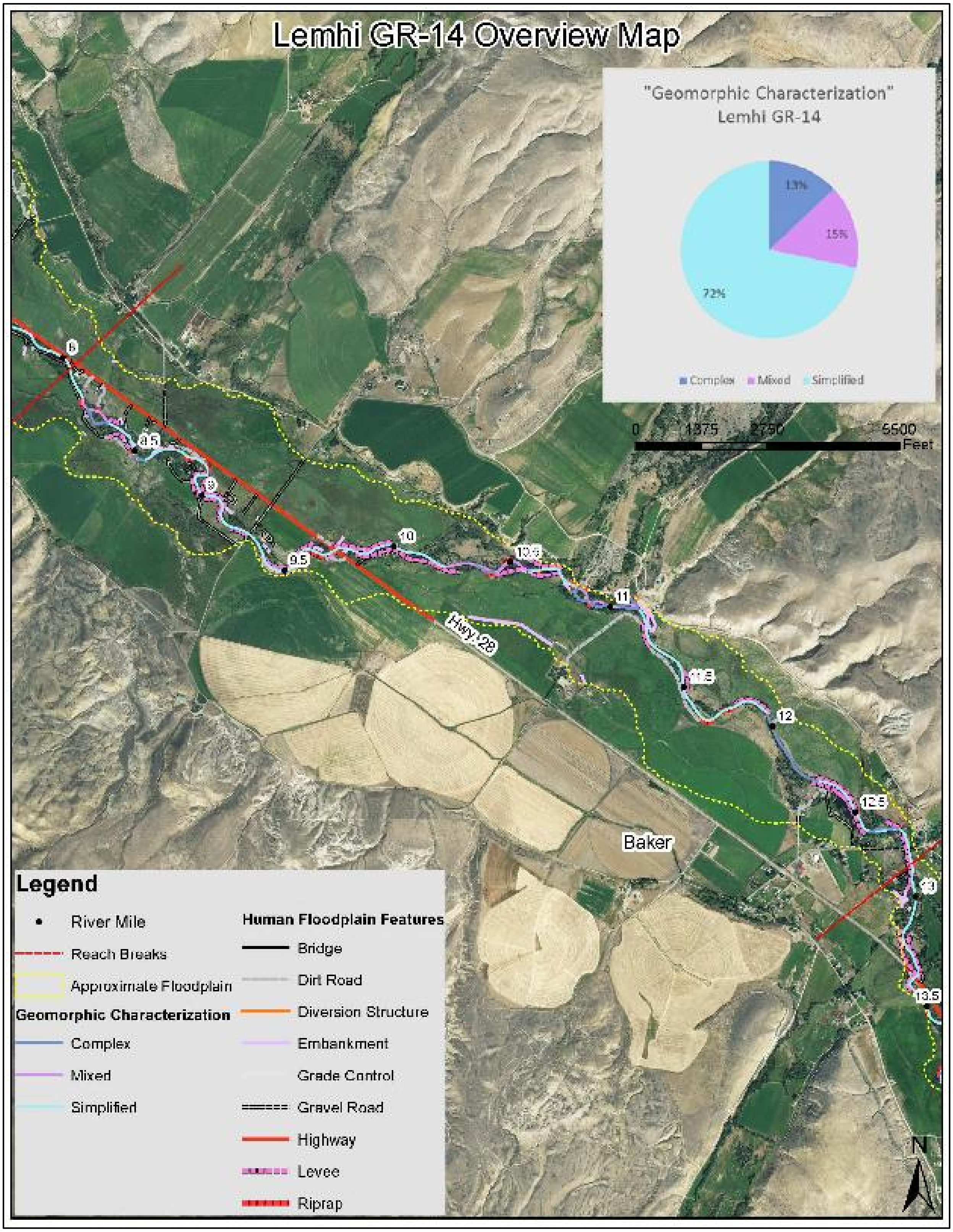

Figure 67. GR-14 overview map illustrating the approximate floodplain, geomorphic characterization, and human alterations to the floodplain.

Geomorphic Reach GR-15 (RM 8.1 – 3.3)

Geomorphic Reach GR-15 is located along the Lemhi River between RM 8.1 and RM 3.3 in an unconfined valley with significant valley bottom constraints, resulting in the narrowing of the valley bottom by about 50 percent (Figure 68). Reach characteristics are summarized below in Table 30.

Table 30. Summary of attributes for Geomorphic Reach GR-15

Valley Segment	Reach	River Miles	Valley Slope (ft/ft)	Average Valley Width (ft)	Average Constrained Valley Width (ft)	Channel Slope (ft/ft)	Average Channel Width (ft)	Sinuosity	Entrenchment Ratio (ft/ft)	Constrained Entrenchment Ratio (ft/ft)	Human Disturbance Ratio (%)	Groundwater Characteristics	Geomorphic Characterization "Complex"	Geomorphic Characterization "Mixed"	Geomorphic Characterization "Simplified"
VS-4	GR-15	8.1 - 3.3	0.0080	1995	991	0.0065	54	1.2	37	18	32%	Gaining	43%	30%	28%

Forms

- Low to moderate sinuosity.
- Minor channel straightening, alterations, and simplification throughout reach.
- Floodplain constrained by Highway 28 along the upstream third of the reach.
- Mixed morphology. Pool-riffle morphology generally associated with higher-sinuosity areas of dense riparian vegetation. Plane-bed morphology generally associated with low-sinuosity, altered areas.
- Many banks lacking riparian vegetation.
- Over-widened channel in areas lacking riparian vegetation.

Processes

- Point bar deposition suggests low to moderate rates of channel migration, increasing where riparian vegetation is lacking.
- Large woody debris recruitment and retention in areas with instream channel obstructions, including islands and irrigation diversions (especially between RM 3.5 and RM 4.6).
- Island braiding and avulsion occurring where unconfined and associated with instream structure (wood recruitment).

Human Impacts

- Patchy, discontinuous riparian corridor contributing to bank instability, channel widening, plane-bed morphology, and lack of shade.
- Channel confinement and straightening may increase local transport capacity armoring the bed.
- Discontinuous levees, road embankments, bridges, riprap, and irrigation diversions.

Response Potential

- Snowmelt surface-water-dominated hydrology with groundwater inputs throughout the year. Shallow groundwater during the summer supports riparian vegetation consisting of willow and cottonwood.
- Channel form (especially width and bedform) and processes are driven by the presence or absence of mature riparian vegetation (willow and cottonwood) in addition to coarse sediment and large wood recruitment. Dense riparian vegetation maintains a narrow width-to-depth ratio, stabilizes banks, and promotes scour pool formation.
- Typical response to disturbances includes channel migration, floodplain activation, pool and riffle formation, and island braiding associated with instream obstruction.

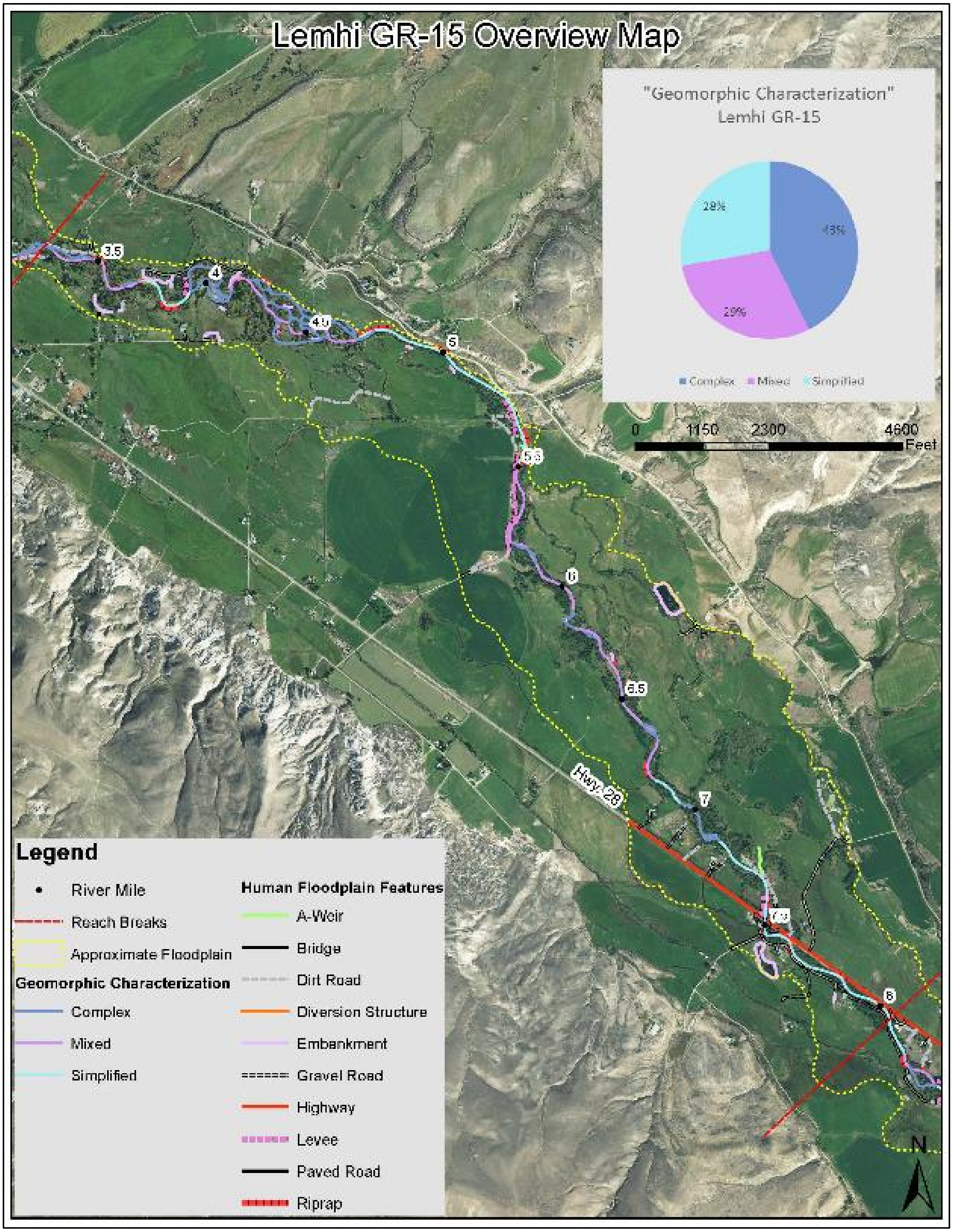

Figure 68. GR-15 overview map illustrating the approximate floodplain, geomorphic characterization, and human alterations to the floodplain.

Geomorphic Reach GR-16 (RM 3.3 – 0)

Geomorphic Reach GR-16 is located along the Lemhi River between RM 3.3 and RM 0 in an unconfined valley with significant valley bottom constraints associated with roads and levees, resulting in the narrowing of the valley bottom by about 65 percent (Figure 69). Reach characteristics are summarized below in Table 31.

Table 31. Summary of attributes for Geomorphic Reach GR-16

Valley Segment	Reach	River Miles	Valley Slope (ft/ft)	Average Valley Width (ft)	Average Constrained Valley Width (ft)	Channel Slope (ft/ft)	Average Channel Width (ft)	Sinuosity	Entrenchment Ratio (ft/ft)	Constrained Entrenchment Ratio (ft/ft)	Human Disturbance Ratio (%)	Groundwater Characteristics	Geomorphic Characterization "Complex"	Geomorphic Characterization "Mixed"	Geomorphic Characterization "Simplified"
VS-4	GR-16	3.3 - 0	0.0081	2480	821	0.0072	62	1.1	40	13	20%	Gaining	38%	13%	49%

Forms

- Low to moderate sinuosity.
- Major channel straightening, alterations, and simplification throughout reach, especially in the lower half.
- Floodplain constrained by levees in the lower reach.
- Mixed morphology. Pool-riffle morphology generally associated with higher-sinuosity areas of dense riparian vegetation. Plane-bed morphology generally associated with low-sinuosity, altered areas.
- Many banks lacking riparian vegetation.
- Over-widened channel in areas lacking riparian vegetation.

Processes

- Point bar deposition in upper reach suggests low to moderate rates of channel migration, increasing where riparian vegetation is lacking. Channel confinement in lower reach prevents deposition.
- Channel straightening, confinement, and bank armoring likely increase sediment transport, resulting in incision and bed armoring.
- Minimal floodplain connection.

Human Impacts

- Patchy, discontinuous riparian corridor contributing to bank instability, channel widening, plane-bed morphology, and lack of shade.
- Channel confinement, straightening, and bank armoring may increase local transport capacity, incision, and bed armoring.
- Discontinuous levees, road embankments, bridges, riprap, and irrigation diversions.

Response Potential

- Snowmelt surface-water-dominated hydrology with groundwater inputs throughout the year. Shallow groundwater during the summer supports riparian vegetation consisting of willow and cottonwood.
- Channel form (especially width and bedform) and processes are driven by the presence or absence of mature riparian vegetation (willow and cottonwood) in addition to coarse sediment and large wood recruitment. Dense riparian vegetation maintains a narrow width-to-depth ratio, stabilizes banks, and promotes scour pool formation.

- Typical response to disturbances includes incision and bed armoring in the lower reach; channel migration and point bar deposition associated with instream obstruction and sinuosity in the upper reach.

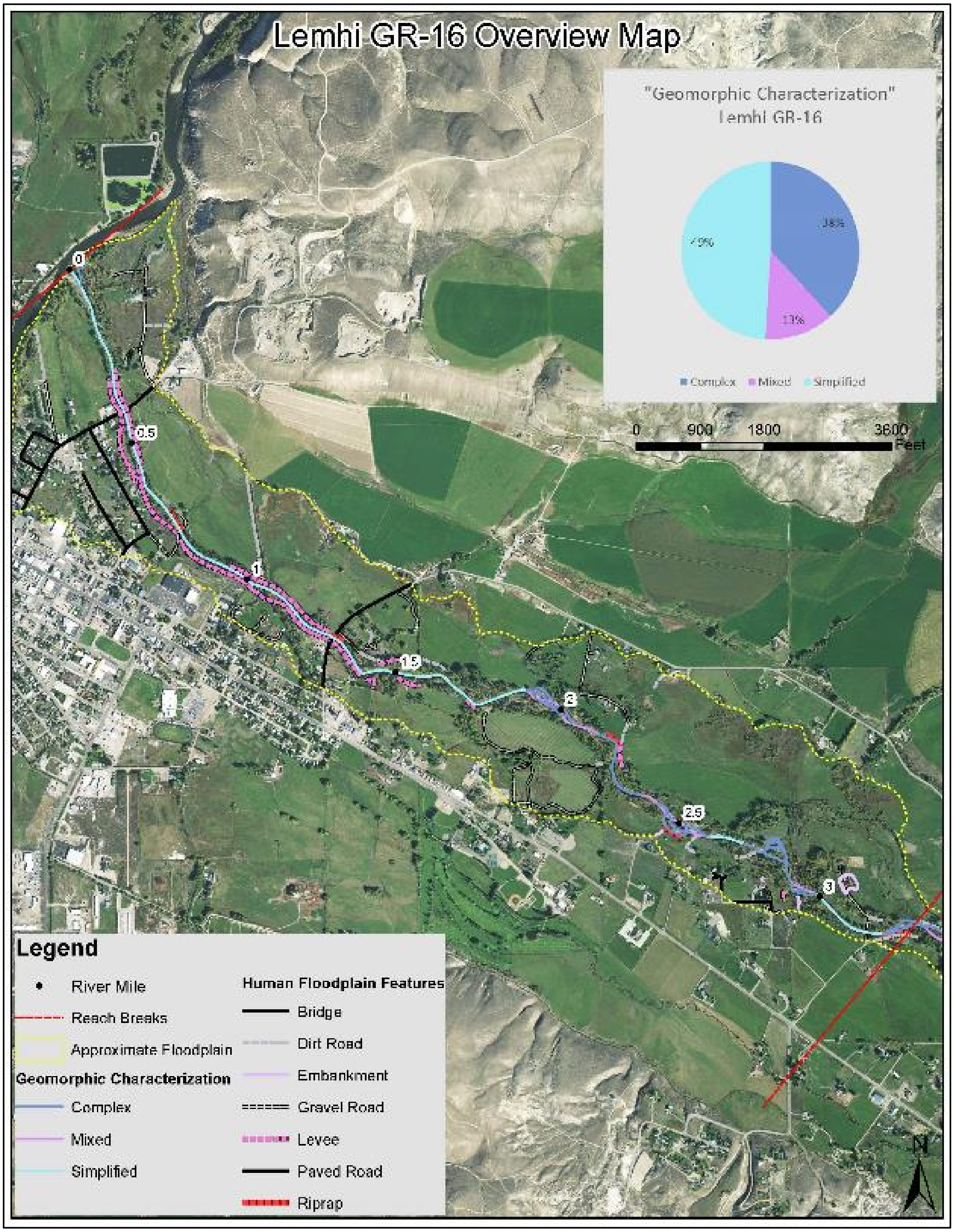

Figure 69. GR-16 overview map illustrating the approximate floodplain, geomorphic characterization, and human alterations to the floodplain.

Temperature and Climate Change Assessment

Chinook salmon

Under current conditions, winter and early-spring modeled water temperatures are generally below optimum values for Chinook salmon for the following life-stages: egg incubation, fry emergence, juvenile winter rearing, and spring smolt emigration (Figure 70). This is likely to reduce or cease presmolt growth during winter months. Modeled spring temperature values vary widely and can include periods of both below-optimum and above-optimum temperature ranges. Alternatively, summer temperatures exceed optimum values at times, potentially increasing spawner stress and elevating food requirements for summer parr. Under an assumed 3° C water temperature increase scenario, conditions improve somewhat for winter and spring life stages (incubation and emergence, winter rearing, spring emigration; Figure 71). Conditions worsen for summer parr and spawners, though, with conditions across much of the watershed exceeding maximum temperature criteria in excess of 50 percent of the time.

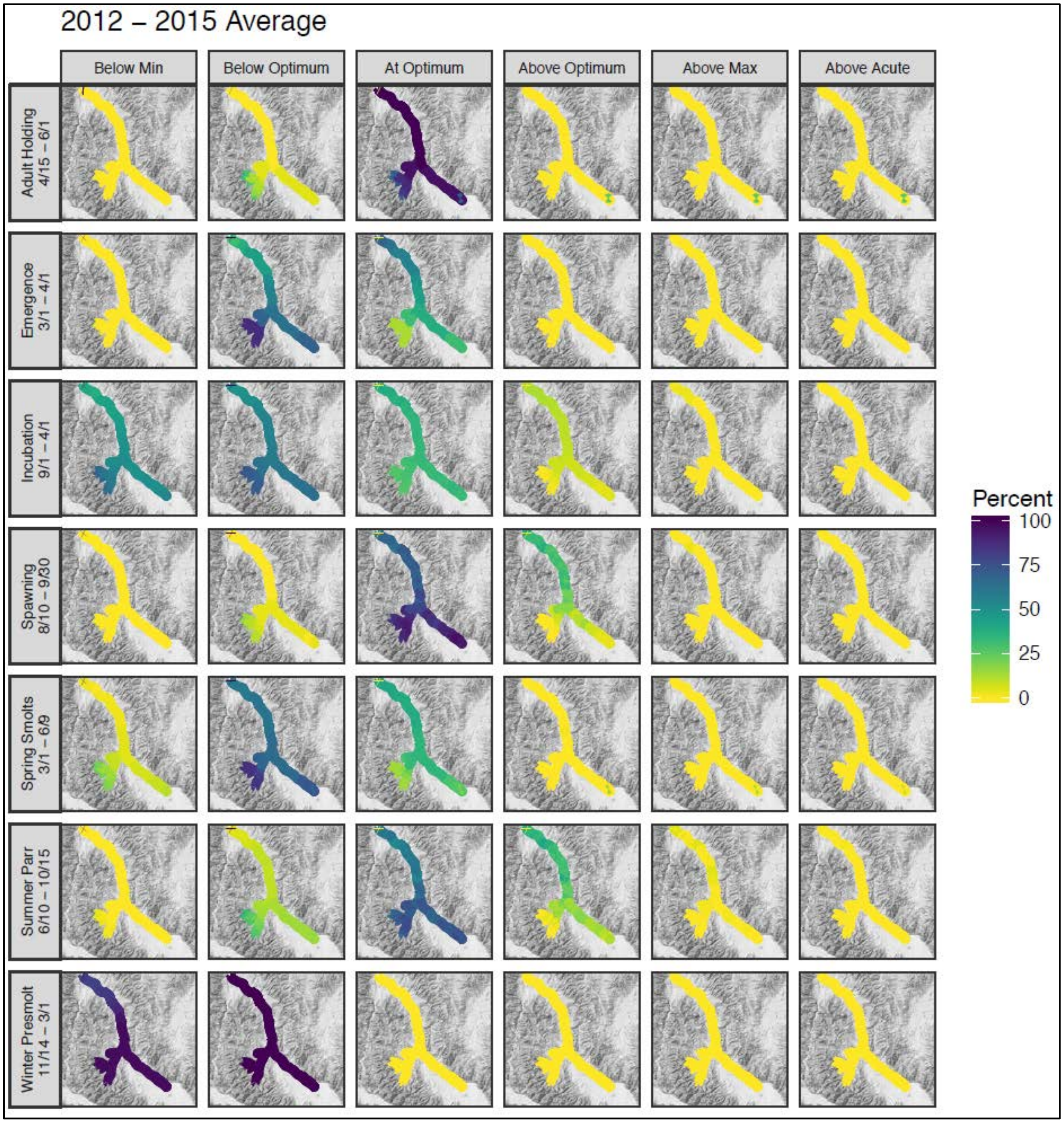

Figure 70. The percentage of time that Lemhi River watershed water temperatures were below, within, or above a given temperature threshold (Carter 2005) for seven Chinook salmon life stages. Water temperatures were averaged across years for which complete modeled temperature data were available (2012-2015).

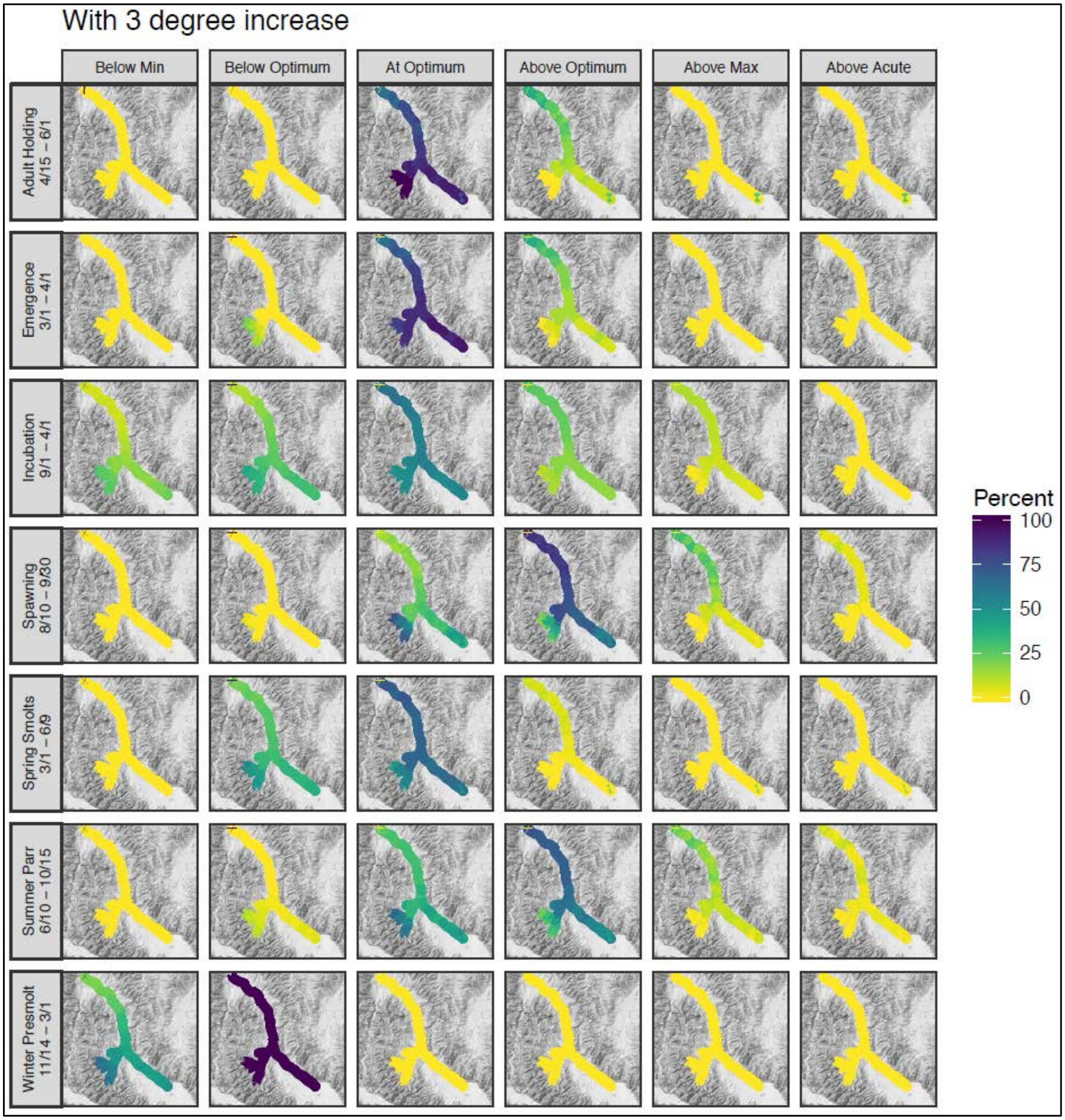

Figure 71. The percentage of time that Lemhi River watershed water temperatures may potentially be below, within, or above a given temperature threshold (Carter 2005) for seven Chinook salmon life stages, assuming a potential climate change scenario.

Steelhead

Under current conditions, winter and early-spring modeled water temperatures are generally below optimum values for steelhead juvenile winter rearing and spring emigration (Figure 72). This is likely to reduce or cease presmolt growth during winter months. Alternatively, summer temperatures exceed optimum values during late incubation and emergence for steelhead; however, it is unclear to what degree late incubation and emergence might overlap with early summer high temperatures in the Lemhi River.

Under an assumed 3° C water temperature increase scenario, conditions improve somewhat for winter and spring life stages (winter rearing and spring emigration; Figure 73). Conditions worsen for late-spring and summer life stages (late spawning, incubation/emergence, summer rearing), though, with conditions exceeding maximum temperature criteria during incubation/emergence and summer juvenile rearing across much of the watershed.

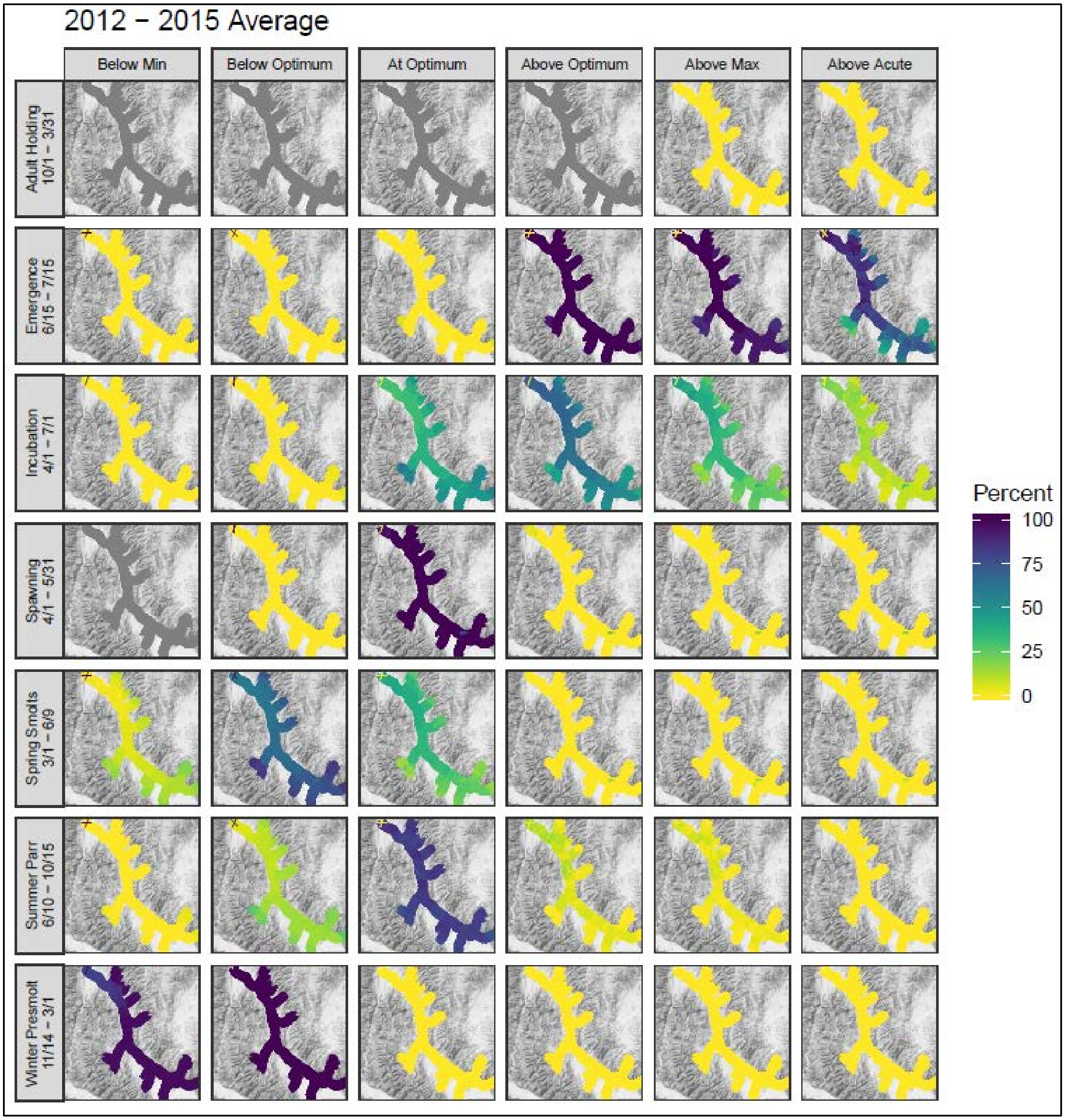

Figure 72. The percentage of time that Lemhi River watershed water temperatures were below, within, or above a given temperature threshold (Carter 2005) for seven steelhead life-stages. Water temperatures were averaged across years for which complete modeled temperature data were available (2012-2015).

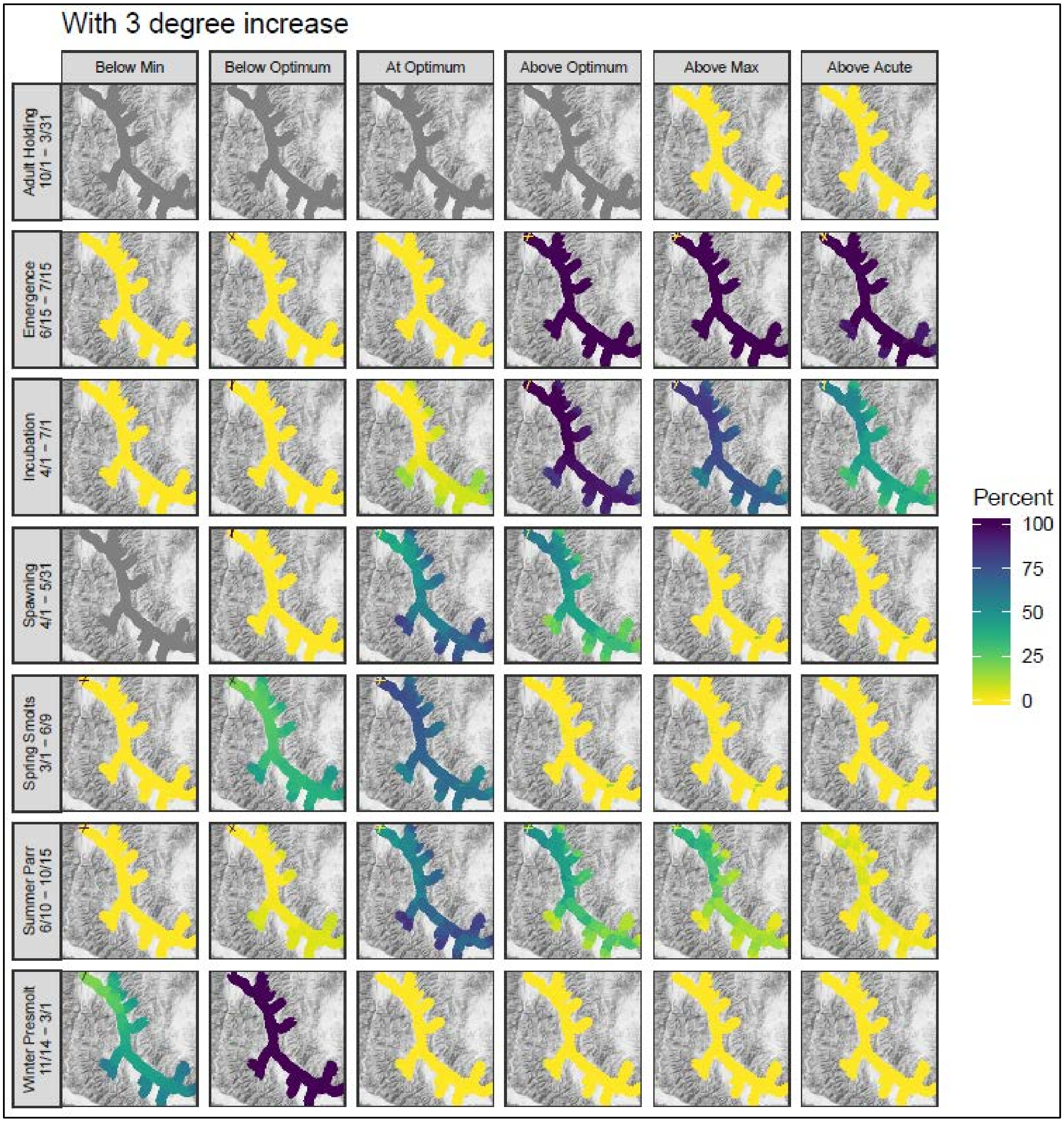

Figure 73. The percentage of time that Lemhi River watershed water temperatures may potentially be below, within, or above a given temperature threshold (Carter 2005) for seven steelhead life stages, assuming a potential climate change scenario.

Results and Discussion

In the Lemhi River Biological Assessment, the lack of quantity and quality juvenile rearing habitat during summer and winter months was identified as the highest-priority limiting PBF for Chinook salmon. Assuming recent mean adult Chinook salmon escapement, habitat capacity does not appear to limit the production of summer parr or winter presmolts (Table 2). However, currently available rearing habitat (summer and winter) is likely not sufficient to support recent high escapements or support escapements necessary for ESA delisting (Table 3). Juvenile rearing habitat during summer and winter does not appear to be a limiting PBF for *O. mykiss* in the Lemhi River. Finally, redd capacity (i.e., available spawning habitat) does not appear to be limiting for Chinook salmon or steelhead in the Lemhi River.

Limiting Physical and Biological Features

The lack of quality juvenile rearing habitat during summer (parr) and winter (presmolt) life stages appears to be the highest-priority PBF limiting Chinook salmon in the Lemhi River. Assuming mean contemporary adult Chinook salmon escapement in the Lemhi River from 2010 to 2015, habitat does not appear to limit the production of summer parr or winter presmolts. However, estimates of carrying capacity given current habitat for summer parr (357,948) and winter presmolts (173,375) fall short of capacity required for adult escapement in 2015 and are approximately one-fourth of the juvenile capacity needed to support an annual escapement of 2,000 adult Chinook salmon required for delisting (Table 2, Table 3). The lack of quantity and quality overwinter rearing habitat is further supported by recent data showing that, on average, 72 percent of juvenile emigrants from the Lemhi River emigrate as parr or presmolts prior to the winter. This suggests that winter rearing habitat is insufficient or unsuitable to support a large portion of juvenile production. The lack of overwinter capacity requires increased juvenile emigration during the critical winter period, which can lead to increased survival risk in mainstem corridor habitats.

- Summer (parr) and winter (presmolt) juvenile rearing capacity were each identified as high-priority PBF limiting Chinook salmon production in the Lemhi River.

Priority Areas

To address both PBFs limiting Chinook salmon production in the Lemhi River (overwinter and summer rearing habitat), rehabilitation to reaches within the Lemhi River should be considered in the following order:

- **First priority: mainstem Lemhi River downstream of Hayden Creek.** This section does not currently support Chinook salmon spawning but provides key summer and winter rearing for fish spawned in the upper Lemhi River and Hayden Creek.
- **Second priority: mainstem Lemhi River upstream of Hayden Creek.** This is the section of the Lemhi River watershed where about two-thirds of the spawning occurs, on average.
- **Third priority: Hayden Creek.** This is the section where about one-third of the spawning occurs, on average.

References

Albers, P.C., J. Lowry, and G.E. Smoak. 1998. The Rivers and Fisheries of the Shoshone-Bannock Peoples: American West Center, University of Utah, published by The Shoshone-Bannock Tribes, 282 p.

Alt, D.D. and D.W. Hyndman. 1989. Roadside Geology of Idaho: Mountain Press Publishing Company, Missoula, Montana.

Bisson, P.A., J.M. Buffington, and D.R. Montgomery. 2006. Chapter 2. Valley Segments, Stream Reaches, and Channel Units, *in* Methods in Stream Ecology, 2nd Edition. Elsevier.

Bjornn, T.C. 1978. Survival, production, and yield of trout and Chinook salmon in the Lemhi River, Idaho. Idaho Cooperative Fish and Wildlife Research Unit. Final Report for Federal Aid to Fish Restoration Project F-49-R. 57pp.

Braudrick, C.A. and G.E. Grant. 2001. Transport and deposition of large woody debris in streams: a flume experiment. *Geomorphology*. (41) 263-283.

Cluer, B. and C. Thorne. 2013. A Stream Evolution Model Integrating Habitat and Ecosystem Benefits. *River Research and Applications*. 30:135-154

Cardno. 2016. Riparian Habitat Management Plan, Upper Lemhi River, Leadore, ID: Prepared for the Lemhi Regional Land Trust by Cardno, Boise, Idaho.

Carter, K. 2005. The effects of temperature on steelhead trout, Coho salmon, and Chinook salmon biology and function by life stage. Implications for Klamath Basin TMDLs. California Regional Water Quality Control Board. North Coast Region. 26pp.

Denney, R. N. 1952. A Summary of North American Beaver Management, 1946-1948. Colorado Game and Fish Department. 58p.

Donato, M.M. 1998. Surface-Water/Ground-Water Relations in the Lemhi River Basin, East-Central Idaho: USGS Water Resources Investigations Report 98-4185.

Ferris, W. A. 1830-1835. Life in the Rocky Mountains: A Diary of Wanderings on the sources of the Rivers Missouri, Columbia, and Colorado from February, 1830, to November, 1835. Full Text downloaded November 15, 2015 from: www.mtmen.org

Frissell, C.A., Liss, W.J., Warren, C.E., and Hurley, M.D., 1986. A Hierarchical Framework for Stream Habitat Classification: Viewing Streams in a Watershed Context. *Environmental Management* 10: 199-214.

Gebhards, S. V. 1958. Stage reduction and channel relocation on the Lemhi River and the effects on fish production. Idaho Fish and Game Department. p41.

Gebhards, S. V. 1959. Preliminary Planning Report: Salmon River. State of Idaho Department of Fish and Game Columbia River Fisheries Development Program. Volume 059, Article 08.

Hillman, T.W., J.S. Griffith, and W.S. Platt. 1987. Summer and winter habitat selection by juvenile Chinook salmon in a highly sedimented Idaho stream. Transactions of the American Fisheries Society. 116:185-195.

Idaho Soil Conservation Commission. 1995. Model Watershed Plan: Lemhi, Pahsimeroi, and East Fork of the Salmon River; Prepared by the Idaho Soil Conservation Commission, 84 p.

Idaho Department of Water Resources. 2017. Cooperative 2014 Lemhi Seepage Run Field Data, conducted by the Idaho Department of Water Resources. Provided by IDWR on April 5, 2017.

Idaho Department of Environmental Quality. 2012. Lemhi River Watershed TMDL. Available at https://www.deq.idaho.gov/water-quality/surface-water/tmdls/table-of-sbas-tmdls/lemhi-river-subbasin/.

Idaho Department of Environmental Quality. 2011. Idaho's 2010 Integrated Report Final. Available at http://www.deq.idaho.gov/media/725927-2010-integrated-report.pdf.

Link, P.K. and S.U. Janecke. 1999. Geology of East-Central Idaho: Geologic Roadlogs for the Big and Little Lost River, Lemhi, and Salmon River Valleys. *In* Guidebook to the Geology of Eastern Idaho. S.S. Hughes and G.D. Thackray, *eds*. Idaho Museum of Natural History. Online Link: http://imnh.isu.edu/digitalatlas/geo/gsa/gsafrm.htm

McGrath, C.L., A.J. Woods, J.M. Omernik, S.A. Bryce, M. Edmondson, J.A. Nesser, J. Shelden, R.C. Crawford, J.A. Comstock, and M.D. Plocher. 2002. Ecoregions of Idaho (color poster with map, descriptive text, summary tables, and photographs). U.S. Geological Survey (map scale 1:1,350,000). Reston, Virginia.

Montgomery, D.R. and J.M. Buffington. 1998. Channel processes, classification, and response. *In* River Ecology and Management. R.J. Naiman and R.E. Bilby, *eds.* Springer-Verlag, New York, pp. 13-42.

Moulton, G, E. 1983. Atlas of the Lewis and Clark Expedition (The Journals of the Lewis and Clark Expedition, Vol 1). University of Nebraska Press.

Northwest Power and Conservation Council. 2004. Salmon Subbasin Management Plan. May 2004. Contracted by Nez Perce Tribe Watershed Division and Shoshone-Bannock Tribes. Written by Ecovista.

National Oceanic and Atmospheric Administration. 2017. ESA Recovery Plan for Snake River Spring/Summer Chinook salmon (*Oncorhynchus tshawytscha*) and Snake River Basin Steelhead (*Oncorhynchus mykiss*). NOAA Fisheries, West Coast Region. U.S. Department of Commerce. National Marine Fisheries Service. November 2017.

Peery, C. and T. Bjornn. 2004. Interactions between natural and hatchery chinook salmon parr in a laboratory stream channel. *Fisheries Research.* 66: 311-324.

Rossillon, M., 1980. An Overview of History in the Drainage Basin of the Middle Fork of the Salmon River: Boise National Forest, Boise, Idaho.

Slough, B.G. and R.M.F.S. Sadleir. 1977. A land capability classification system for beaver (Castor canadensis). Canadian Journal of Zoology 55(8): 1324-1335.

Trapani, J. 2002. 1994 Stream Habitat Inventory Report: Lemhi, Pahsimeroi, and the East Fork Salmon River, ID. Upper Salmon Basin Watershed Project. USBWP-pdf file.

Walker, Jr., D.E. 1994. Lemhi Shoshone-Bannock Reliance on Anadromous and Other Fish Resources. Idaho Bureau of Land Management Technical Bulletin No. 94-4. April 1994.

Chapter 2 – Pahsimeroi River Watershed

Location and Watershed Description

The Pahsimeroi River watershed is located in the Northern Rocky Mountain System physiographic region that comprises extensive parallel mountain ranges, intermontane valleys, and plateaus (Figure 74). Elevations in the watershed range from about 4600 to 12000 feet, with the lowest elevations along the Pahsimeroi valley floor and the highest elevations along the bounding Lemhi Range to the north and Lost River Range to the south. It is in the Dry Intermontane Sagebrush Valleys Ecoregion (17AA), characterized by stream terraces, floodplains, saline areas, and alluvial fans. Water availability and potential for cropland agriculture are low because the Ecoregion is in the rain shadow of high mountains, receives little mountain runoff, and is underlain by highly permeable valley fill deposits. Its deep gravels are unlike the basalts of Ecoregion 12. Sagebrush grassland is widespread and contrasts with the open-canopied forests of the more-rugged and higher Ecoregion 17e. Shadscale and greasewood grow on alkaline soils that receive less than 8 inches of precipitation annually. Grazing is the dominant land use (McGrath et al. 2002).

The Pahismeroi River watershed is a hydrologic unit code (HUC) 8th field basin (HUC 8 – 17060202), within the Salmon River subbasin within the Columbia River Basin. The watershed covers about 839 square miles (536,960 acres) in east-central Idaho and is located in Lemhi and Custer Counties. About 90 percent of the land is owned by the Federal government and administered by the U.S. Forest Service (USFS) and Bureau of Land Management (BLM). Federal lands are located primarily in the higher elevations, whereas private lands are typically located in lower elevations along the valley bottoms.

The Pahsimeroi River is an alluvial stream flowing over gravel and cobble originating at the confluence of the East Fork and West Fork Pahsimeroi Rivers near the base of Leatherman Peak. The river flows generally to the northwest along the Pahsimeroi Valley for about 64 miles, where it discharges into the Salmon River near Ellis, Idaho.

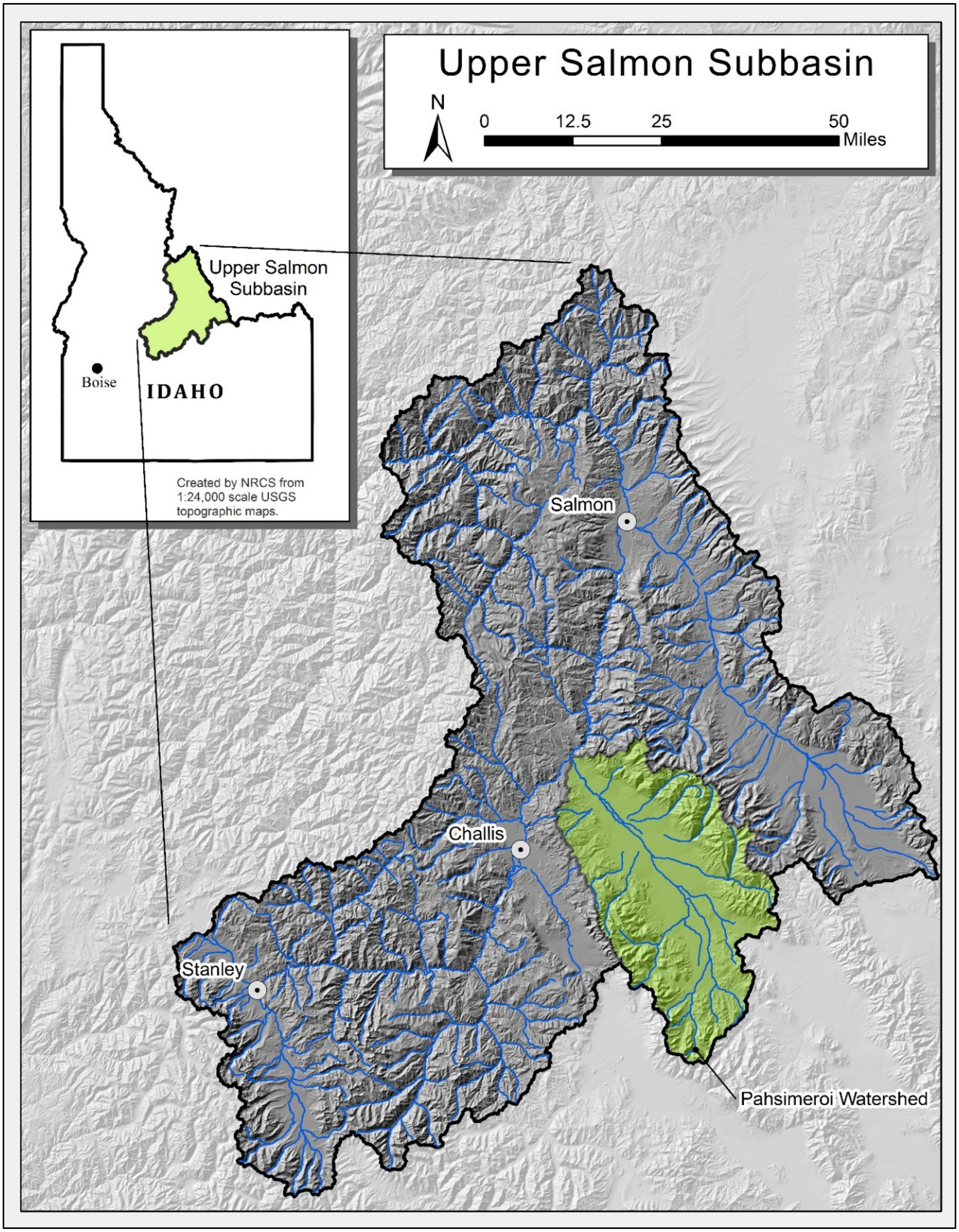

Figure 74. Location map of the Pahsimeroi River watershed.

Biological Assessment

The Pahsimeroi River maintains populations of three fish species listed under the ESA including Chinook salmon, steelhead, and bull trout. The watershed also supports westslope cutthroat trout, which has been petitioned for listing under the ESA. The Pahsimeroi River is a snowmelt-dominated tributary to the mainstem Salmon River, with a drainage area of approximately 840 mi^2. Similar to the Lemhi River, agricultural diversions have significantly reduced the connection of Pahsimeroi River tributaries and have truncated access to the mainstem Pahsimeroi River from RM 26.4 to RM 17.8 (NOAA 2017). The remaining lower mainstem reach available to Chinook salmon and steelhead is a low-gradient, sinuous, groundwater-dominated channel with high primary productivity (Copeland and Venditti 2009). NOAA (2017) classifies the Pahsimeroi River Chinook salmon population as Large and the Pahsimeroi River steelhead population as Intermediate.

Despite the moderate- to high-quality habitat available in the lower mainstem Pahsimeroi River, the Chinook salmon population has declined dramatically from historical escapement estimates (2,500 adults) and is currently considered at high risk of extinction (NOAA 2017). Between 2000 and 2015, the Pahsimeroi River has a mean escapement of 402 adult Chinook salmon, with a maximum escapement of 822 adults in 2003. Pahsimeroi River Chinook salmon are unique for the Upper Salmon River Major Population Group (MPG) because they exhibit a summer run timing. Pahsimeroi River steelhead have been identified as being maintained (i.e., 6 to 25 percent risk of extinction; NOAA 2017), but that listing is tentative due to insufficient data for Pahsimeroi River steelhead. Between 2011 and 2015, the Pahsimeroi River had an estimated mean escapement of 1,156 adult steelhead, with a maximum escapement of 1,614 adults in 2015 (see Stark et al. 2017 and references therein). The Idaho Power Company funds the operation of a production hatchery on the Pahsimeroi River, which is operated by the Idaho Department of Fish and Game; however, no hatchery-origin adults have been placed above the hatchery weir located in the lowermost Pahsimeroi River since 2005.

Habitat Capacity

Chinook salmon

Current Conditions

Contemporary estimates of life-stage-specific capacity requirements were generated based on the mean (402) and maximum (822) adult Chinook salmon escapement observed in the Pahsimeroi River from 2000 to 2015. Those adult escapements were then propagated through to four additional life stages to estimate life-stage-specific capacity requirements for Chinook salmon in the Pahsimeroi River; capacity requirements were then compared to available habitat capacity estimated using QRF models (Table 32).

Table 32. Estimated current life-stage-specific capacity requirements versus estimated available capacity for Chinook salmon in the Pahsimeroi River.

Life-Stage	Required Capacity		Available Capacity	Capacity Deficit
	Mean	Max		
Escapement	402	822		
Redd	197	403	1,886	0
Eggs	1,041,496	2,129,424		
Summer Parr	302,034	617,533	311,530	306,003

Life-Stage	Required Capacity		Available Capacity	Capacity Deficit
	Mean	Max		
Winter Presmolt	122,375	250,206	103,977	146,229

Under current habitat conditions, and using contemporary escapement estimates, habitat capacity does not appear to limit the production of redds in the Pahsimeroi River; however, it does appear that juvenile rearing capacity is limited during both summer (parr) and winter (presmolt) months (Table 32). Given current habitat conditions, it appears that the Pahsimeroi River watershed can support roughly half of the required juvenile capacity, assuming recent maximum escapement. These findings are supported by the fact that, on average, 39 percent of total Chinook salmon juveniles emigrate from the Pahsimeroi River as fry or parr prior to or during the summer rearing period. Further, approximately 48 percent of total Chinook salmon juveniles leave the Pahsimeroi River as presmolts prior to the winter rearing period, suggesting that winter habitat capacity is limited. Only 12 percent of total Chinook salmon juvenile emigrants have left at the spring smolt (age 1) life stage in recent years.

Chinook salmon have lost access to approximately 33 percent of mainstem stream length available prior to agricultural development. Therefore, it is possible that a large fraction of fry emigration from the Pahsimeroi River is partially a function of the proximity of spawning habitat to the mainstem Salmon River.

Desired Conditions

NOAA (2017) delisting requirements include a minimum annual escapement (i.e., MAT) of 1,000 Chinook salmon adults to the Pahsimeroi River. Based on this requirement, life-stage-specific capacity requirements were recalculated consistent with 1,000 adults (MAT) and 1,250 adults (MAT + 25%). Those capacity requirements were also compared to estimates of currently available habitat capacity to identify potential habitat limitations if delisting is desired (Table 33). Potential limitations (capacity deficit) were calculated as the life-stage-specific capacity requirements needed to achieve a MAT of 1,000 plus a 25 percent buffer minus available capacity.

Table 33. Estimated life-stage-specific capacity requirements to accommodate ESA de-listing and estimated available capacity for Chinook salmon in the Pahsimeroi River.

Life-Stage	Required Capacity		Available Capacity	Capacity Deficit
	MAT	MAT + 25%		
Escapement	1,000	1,250		
Redd	490	613	1,886	0
Eggs	2,592,100	3,240,125		
Summer Parr	751,709	939,636	311,530	628,106
Winter Presmolt	304,570	380,712	103,977	276,735

There appears to be sufficient redd capacity in the Pahsimeroi River to support 1,250 adult Chinook salmon. However, the available juvenile rearing capacity during summer (311,530) and winter (103,977) are far from sufficient to support the potential parr and presmolt production from 1,250 adult Chinook salmon (Table 33). Therefore, to achieve delisting of Chinook salmon in the Pahsimeroi River, both summer and winter juvenile rearing capacity would need to be increased.

Summary

There appears to be sufficient spawning (redd) capacity in the Pahsimeroi River to support contemporary escapement and escapement required to achieve delisting criteria for Chinook salmon (Figure 75). However, juvenile rearing habitat appears to be limiting to support both recent escapements and escapements required to achieve delisting (NOAA 2017) for Pahsimeroi River Chinook salmon (Figure 76 and Figure 77).

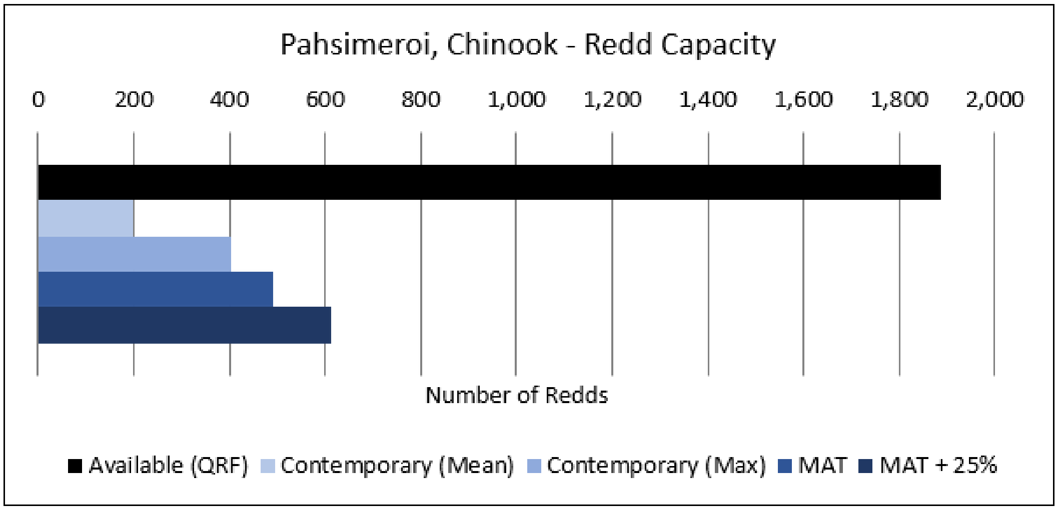

Figure 75. Estimates of available spawning (redd) capacity given current habitat conditions for Chinook salmon in the Pahsimeroi River watershed, made using quantile regression forest models (black bars) versus the capacity required to support contemporary abundance and minimum abundance thresholds (MATs) needed for ESA de-listing (blue bars).

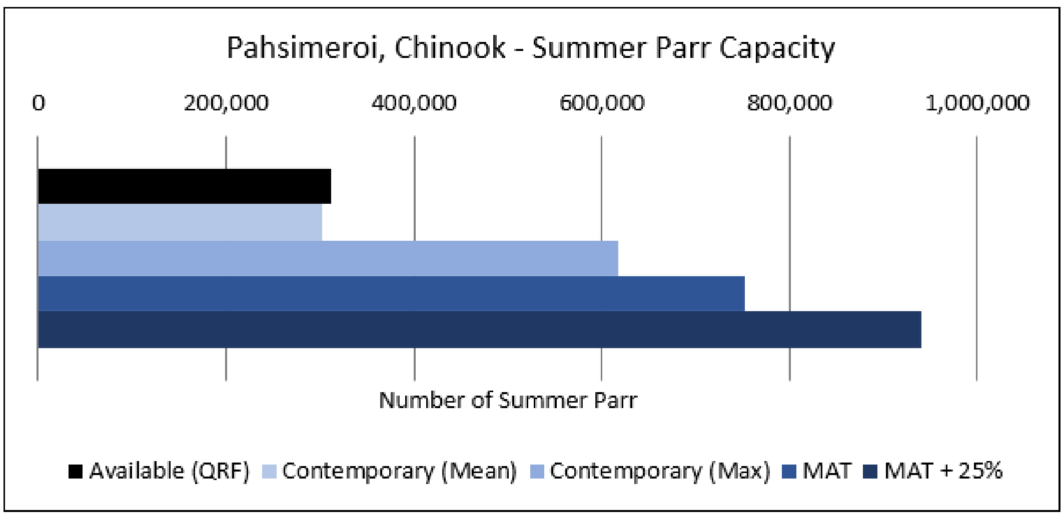

Figure 76. Estimates of available summer juvenile (parr) rearing capacity given current habitat conditions for Chinook salmon in the Pahsimeroi River watershed, made using quantile regression forest models (black bars) versus the capacity required to support contemporary abundance and minimum abundance thresholds (MATs) needed for ESA de-listing (blue bars).

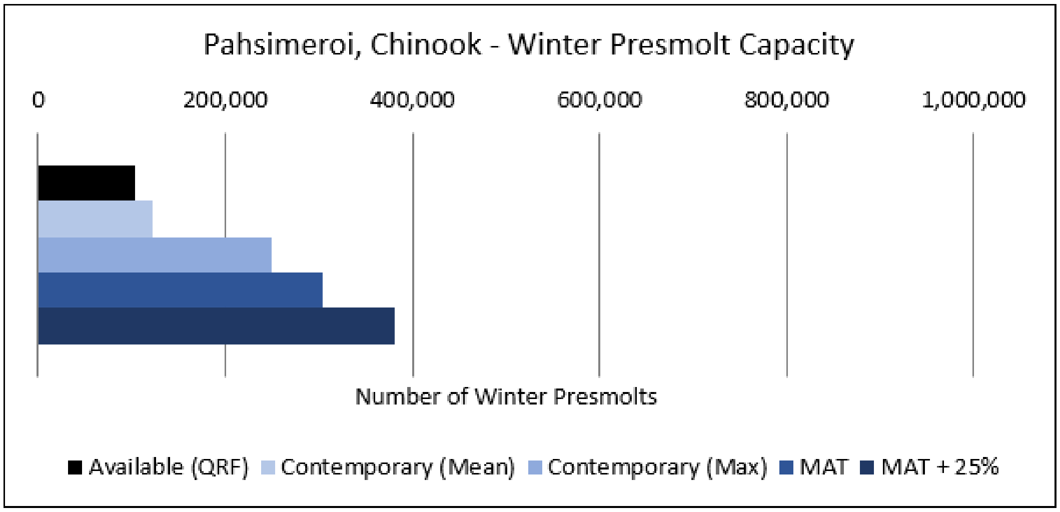

Figure 77. Estimates of available winter juvenile (presmolt) rearing capacity given current habitat conditions for Chinook salmon in the Pahsimeroi River watershed, made using quantile regression forest models (black bars) versus the capacity required to support contemporary abundance and minimum abundance thresholds (MATs) needed for ESA de-listing (blue bars).

Steelhead

Available habitat capacity estimates from QRF are considered preliminary for steelhead in the Pahsimeroi River due to unknown spatial extents of available habitat for steelhead spawning and rearing. The IRA team will work with local biologists and experts to more appropriately identify the extents of habitat in the Pahsimeroi River available to steelhead. Available habitat capacity estimates can be improved in future reach assessments or as needed with local groups.

Current Conditions

Contemporary estimates of life-stage-specific capacity requirements were generated based on the mean (1,156) and maximum (1,614) adult steelhead escapements estimated in the Pahsimeroi River from 2011 to 2015. Those adult escapements were then propagated through to four additional life stages to estimate life-stage-specific capacity requirements for steelhead in the Pahsimeroi River; capacity requirements were then compared to available habitat capacity estimated using QRF models (Table 34).

Table 34. Estimated current life-stage-specific capacity requirements versus estimated available capacity for steelhead in the Pahsimeroi River.

Life-Stage	Required Capacity		Available Capacity	Capacity Deficit
	Mean	Max		
Escapement	1,156	1,614		
Redd	641	896	1,228	0
Eggs	3,159,649	4,412,245		
Summer Parr	424,183	592,344	264,740	327,604
Winter Presmolt	152,124	212,431	166,936	45,495

Under current habitat conditions, and using contemporary escapement estimates (e.g., Stark et al. 2017), habitat capacity does not appear to limit the production of steelhead redds in the Pahsimeroi River; however, it does appear that juvenile rearing capacity is limited during both summer (parr) and winter (presmolt) months (Table 34). Given current habitat conditions, it appears that the Pahsimeroi River watershed can support roughly half of the required juvenile steelhead capacity during summer (parr) rearing months. Available winter (presmolt) capacity is sufficient to support recent mean adult steelhead escapements, but not numbers estimated during recent high escapements.

Desired Conditions

NOAA (2017) delisting requirements include a minimum annual escapement (i.e., MAT) of 1,000 steelhead adults to the Pahsimeroi River. Based on this requirement, life-stage-specific capacity requirements were recalculated consistent with 1,000 adults (MAT) and 1,250 adults (MAT + 25%). Those capacity requirements were also compared to estimates of currently available habitat capacity to identify potential habitat limitations if delisting is desired (Table 35). Potential limitations (capacity deficit) were calculated as the life-stage-specific capacity requirements needed to achieve a MAT of 1,000 plus a 25 percent buffer minus available capacity.

Table 35. Estimated life-stage-specific capacity requirements to accommodate ESA de-listing and estimated available capacity for steelhead in the Pahsimeroi River.

Life-Stage	Required Capacity		Available Capacity	Capacity Deficit
	MAT	MAT + 25%		
Escapement	1,000	1,250		
Redd	555	694	1,228	0
Eggs	2,733,733	3,417,166		
Summer Parr	367,004	458,755	264,740	194,015
Winter Presmolt	131,618	164,522	166,936	0

There appears to be sufficient redd capacity and juvenile rearing capacity during winter months to support 1,250 adult steelhead (Table 35). However, the available juvenile rearing capacity during summer (264,740) is insufficient to support the potential parr production from 1,250 adult steelhead. Therefore, to achieve delisting of steelhead in the Lemhi River, summer juvenile rearing capacity would likely need to be increased.

Summary

There appears to be sufficient spawning (redd) capacity in the Pahsimeroi River to support contemporary escapement and escapement required to achieve delisting criteria for steelhead (Figure 78). Moreover, juvenile rearing capacity during winter (presmolt) months may be sufficient within the Pahsimeroi River to support delisting criteria for steelhead (Figure 80). However, juvenile rearing habitat during summer (parr) months appears to be limiting for recent escapements and for escapements necessary to achieve delisting criteria (NOAA 2017) for Pahsimeroi River steelhead (Figure 79).

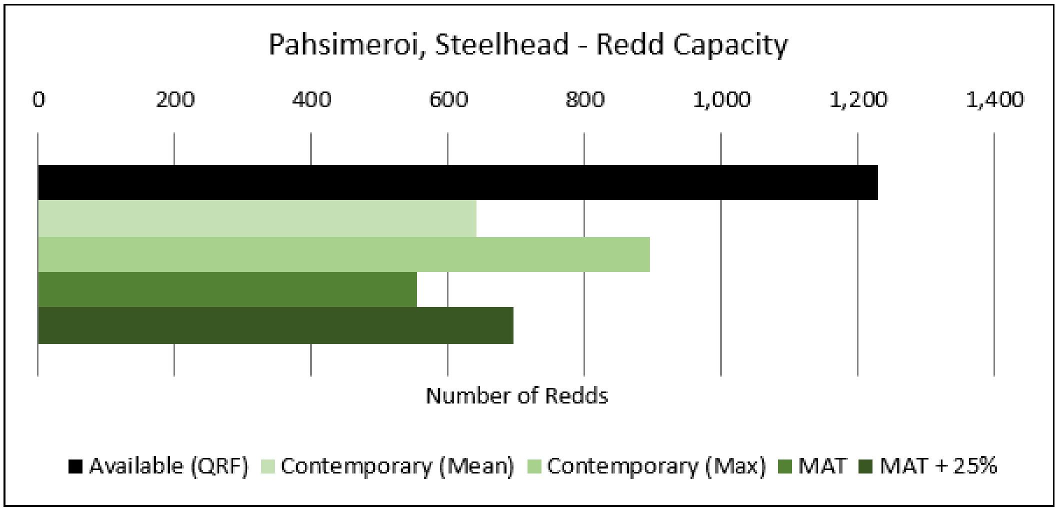

Figure 78. Estimates of available spawning (redd) capacity given current habitat conditions for steelhead in the Pahsimeroi River watershed, made using quantile regression forest models (black bars) versus the capacity required to support contemporary abundance and minimum abundance thresholds (MATs) needed for ESA de-listing (green bars).

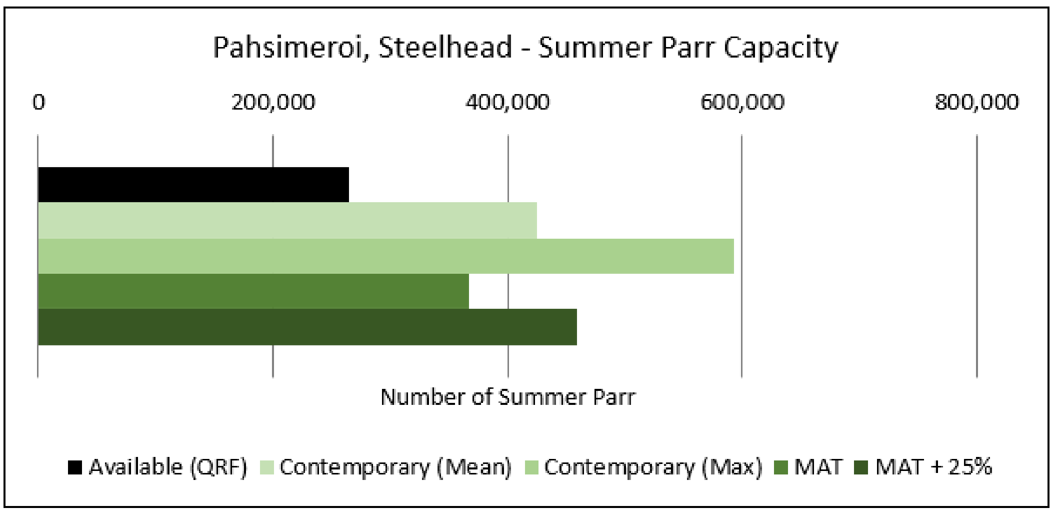

Figure 79. Estimates of available summer juvenile (parr) rearing capacity given current habitat conditions for steelhead in the Pahsimeroi River watershed, made using quantile regression forest models (black bars) versus the capacity required to support contemporary abundance and minimum abundance thresholds (MATs) needed for ESA de-listing (green bars).

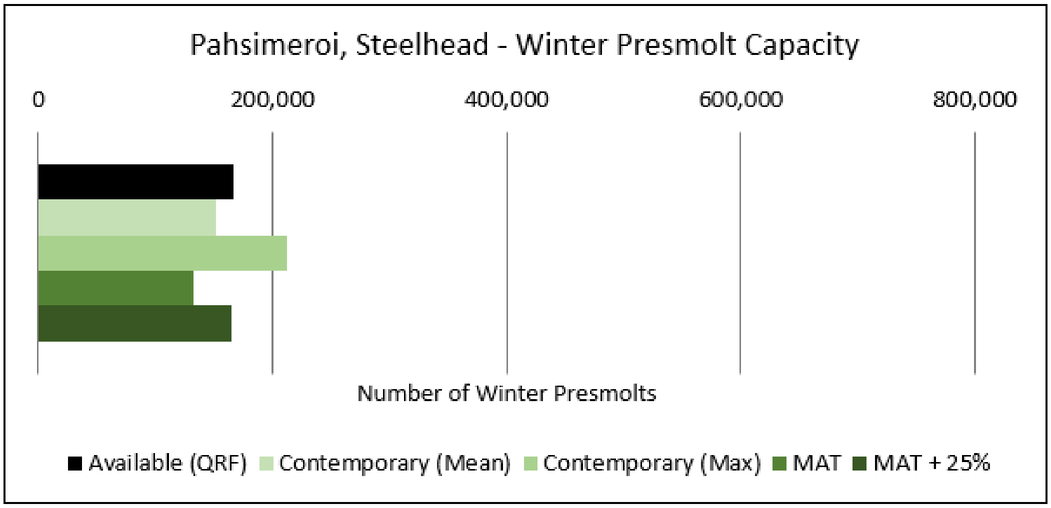

Figure 80. Estimates of available winter juvenile (presmolt) rearing capacity given current habitat conditions for steelhead in the Pahsimeroi River watershed, made using quantile regression forest models (black bars) versus the capacity required to support contemporary abundance and minimum abundance thresholds (MATs) needed for ESA de-listing (green bars).

Geomorphic Assessment

Much of the geomorphic assessment in this report has been compiled in an effort to help paint a better picture of historical and potential target conditions (qualitative), recognizing that detailed (quantitative) target conditions will be generated as part of the MRA for select reaches in the future.

Historical Watershed Conditions

The Pahsimeroi River is located in a north/northwest-trending valley between the Pahsimeroi Mountains and the Lost River Range to the southwest, the Donkey Hills to the south, and the Lemhi Range to the northeast. The mountains consist of volcanic, metamorphic, and marine sedimentary rocks. The oldest metamorphic and sedimentary rocks were thrust up onto the continental crust roughly 60 million years ago during the formation of the ancestral Rocky Mountains (Link and Janecke 1999). The volcanic rocks are part of the Challis Volcanic Group that erupted onto the surface roughly 45 million years ago (Moye et al. 1988). Over the past several million years, the continental crust has expanded in this area due to the nearby Yellowstone hotspot (Simpson and Anders 1992; Pierce et al. 2007). Normal faulting associated with the expansion has lowered some blocks of the crust, creating valleys and raising others, forming mountain ranges. The Pahsimeroi Valley is one of these lowered blocks that has now partially filled with deep deposits of alluvial sediment. Valley fill sediment includes multiple episodes of significant alluvial fan deposition that occurred over several million years (Ungate 1988). During the last ice age (between 1.8 million years and 10,000 years ago), glaciers were present in the Lemhi and Lost River Ranges, contributing additional outwash sediment to the Pahsimeroi Valley, although no glacial ice is believed to have reached the valley bottom (Meinzer 1924; Ungate 1988). Since the last ice age, over-bank river deposits have added a thin additional layer of sediment to the valley bottom.

Geophysical data suggest the valley fill sediment is deepest (approximately 3,000 feet deep) near Furey Lane, between Big Creek and Goldberg Creek, and generally shallows to about 30 feet deep at the northern end of the basin (Young and Harenberg 1973). These sediments were determined to be coarse-grained (Meinzer 1924; Ungate 1988) and capable of sustaining a robust aquifer. Areas where the aquifer intercepts the surface produce reaches that gain flow from groundwater, while areas where the aquifer is below the surface generally lose flow to the aquifer. Although modern measurements of surface/groundwater exchange are influenced by irrigation practices, seepage runs measured after the irrigation season in 2005 provide an estimate of historic groundwater conditions. These measurements suggest that historically, the upper Pahsimeroi River was largely losing flow to groundwater, the lower Pahsimeroi River was largely gaining flow from groundwater, and the middle Pahsimeroi River was mixed (Williams et al. 2006) (Figure 81). The historic conditions of the Pahsimeroi channel and floodplain were influenced greatly based on the spatial variability of surface-to-groundwater interactions in the valley.

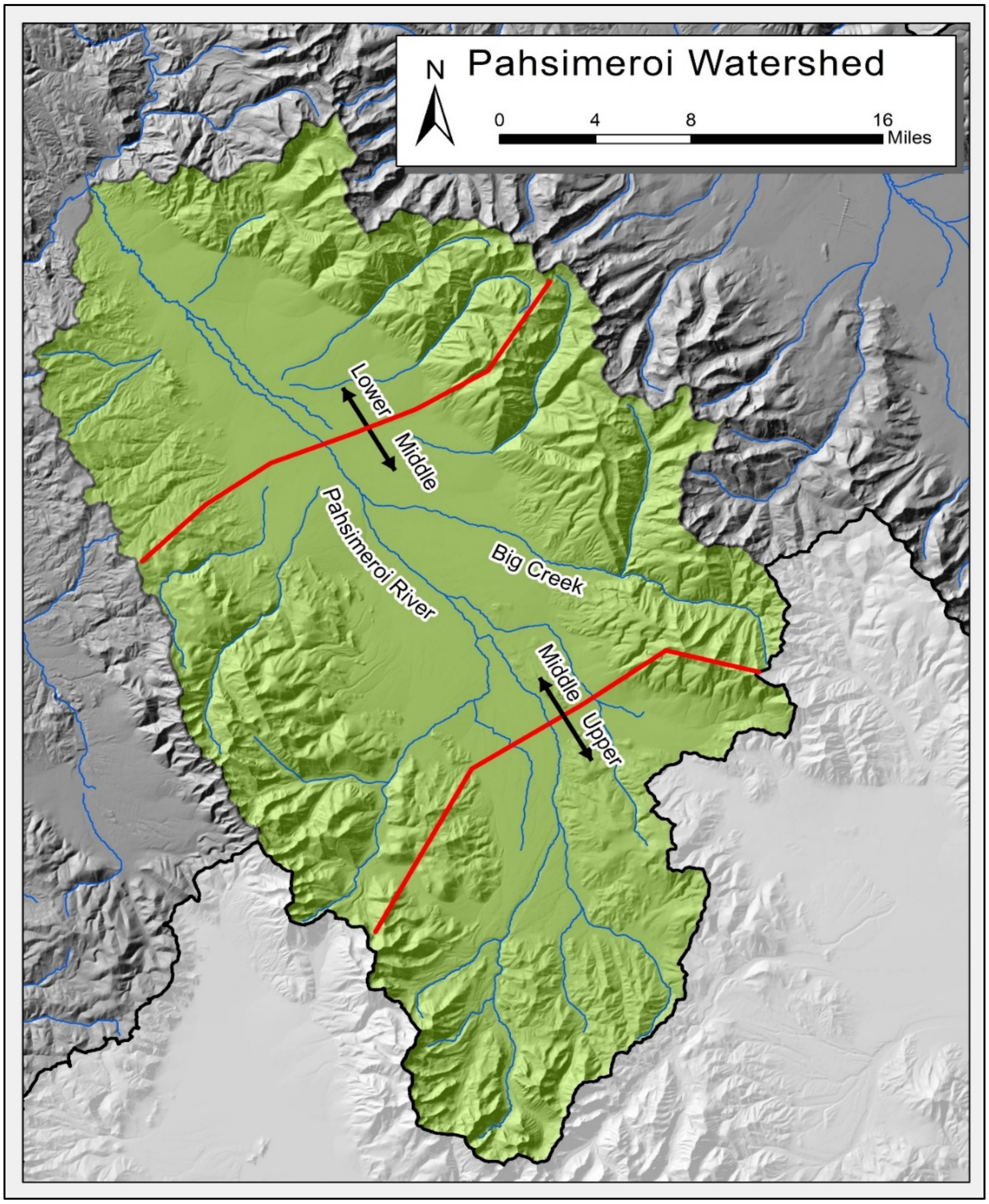

Figure 81. Map of the Pahsimeroi River watershed illustrating the approximate boundary between the upper, middle, and lower valleys.

The character of the upper Pahsimeroi River and other areas that lose flow to groundwater was largely driven by the snowmelt-dominated (i.e., peak-flow) hydrology in those areas. The upper Pahsimeroi River was primarily transport-dominated, with sufficient gradient and discharge to mobilize sediment and slowly incise its bed over thousands of years, creating a narrow, inset floodplain bound by relic terraces. The single-threaded channel within the terraces was characterized by a low sinuosity and a predominantly plane-bed morphology, although a forced pool-riffle morphology may have formed over small areas, given sufficient structure and/or woody debris loading (based on Montgomery and Buffington 1998). The snowmelt-dominated, losing reaches of the middle Pahsimeroi River were lower gradient than the upper Pahsimeroi River and had a depositional character (i.e., transport-limited), enabling the formation of a broad floodplain. The sinuous channel in these areas was likely characterized by a pool-riffle morphology (based on Montgomery and Buffington 1998) driven by abundant coarse-sediment deposition.

Flashy, snowmelt-dominated hydrology provided a disturbance regime suitable for the establishment and propagation of cottonwood and aspen trees, in addition to willow and other shrubs. The roots of the riparian vegetation provided bank stability and instream structure. Bank erosion into densely vegetated riparian areas provided a source of large wood recruitment that likely enhanced and/or forced pool-riffle morphology and may have created localized areas of island braiding. Large floods and debris torrents from tributaries may have transported large wood from the uplands episodically, but research suggests that wood is unlikely to transport through such small streams with low channel width and depth (Braudrick and Grant 2001).

In contrast to the losing reaches, the character of the lower Pahsimeroi River and other areas gaining flow from the groundwater was largely driven by their groundwater-influenced (i.e., baseflow) hydrology. These reaches were characterized by a fairly stable, multi-threaded (anastomosing), highly sinuous channel, with multiple side channels and spring-fed tributary channels all occupying the same broad floodplain. Channel morphology was likely pool-riffle, where sufficient gradient and coarse sediment (gravel) were available, or dune-ripple within low-gradient areas dominated by fine sediment (sand) deposition (Montgomery and Buffington 1998). Although the low gradient and unconfined channel created a depositional character, much of the available incoming sediment was likely deposited within losing/dry reaches and/or alluvial fans prior to reaching the lower Pahsimeroi River, except during large floods, promoting a fairly stable channel with episodic response to large disturbance.

Historical riparian conditions in the lower Pahsimeroi River likely reflected a consistent groundwater-influenced hydrology and associated high water table punctuated by periods of extended flooding associated with beaver activity. Relic topographic variation from occasional avulsions, beaver dams, and disturbance from grazing animals (bison, elk, and deer) likely created a mosaic of open water, emergent wetland, floodplain, and upland. The riparian community would have mirrored this diversity with areas of wetland meadow (rushes and sedges), floodplain shrubs (willow) and upland vegetation (sagebrush and grass). Most riparian vegetation had to tolerate fine, poorly draining soils and extended periods of submergence. Few, sporadic stands of cottonwood or aspen trees may have established on well-draining soils, particularly near the mouth of snowmelt-dominated tributaries that could occasionally produce the disturbance (i.e., sand and gravel deposition) required for germination and establishment. The inconsistent source of coarse sediment to the channel likely severely limited rates of point bar development and channel migration, suggesting the banks were fairly stable and able to maintain a deep/narrow channel. A first-hand account of the historic Pahsimeroi from W. A. Ferris, 1830-1835 (Journal entry taken on June 28, 1831) supports this characterization, stating that the river:

> *…though only ten or twelve feet wide, was yet so deep as to be unfordable, except at occasional points. Some of our men, ignorant of its depth, attempted to ford it, but only escaped drowning, by clinging to the branches which were interlaced and bound together by wild vines, forming a complete canopy over the stream. Their horses were carried some distance down by the impetuosity of the current before we could reach and rescue them.*

Another first-hand account from W. A. Ferris in 1832 states that the Pahsimeroi Valley:

> *…is thirty miles long, and twelve broad; it is intersected by willowed streams, and large bottoms, covered with rich pasturage, hence it is a favourite resort for both deer and buffalo. The only trees are a few orchard-like groves in the head of the valley, and pines of every variety, on the abrupt sides of the surrounding mountains.*

Notably, Ferris and his compatriots were fur trappers, and over the course of 5 years of traversing the region, did not document significant trapping of beaver in the Pahsimeroi River valley, nor did they document passing extended periods of time there, suggesting that beaver populations may have been relatively low in the Pahsimeroi compared to neighboring watersheds. Given the likely vegetation assemblages and physical conditions of the historic river, it is likely that beaver were present, but in lower numbers compared with other areas due to isolation and/or previous trapping. Regardless, it is highly likely that beaver had an impact on the Pahsimeroi River, particularly in the lower-gradient, gaining reaches.

Prior to Euro-American settlement, the Salmon River Mountains region was most likely inhabited by a group of Northern Shoshone known as the *Tu'kudeka*, or Sheepeaters, who wintered in the mountains, where they hunted mountain sheep (Rossillon 1980). Given the Shoshone's subsistence cycles and seasonal movements across central and southern Idaho, their impacts on the land were likely confined to their encampments, where tribes from the region would congregate and trade their goods. Reports from Lewis and Clark and others on the abundance of fur-bearing animals west of the divide spurred the business of fur trade. Independent fur trappers, as well as several companies (including the Hudson Bay Company and the American Fur Company) made their way into the northwest to explore and exploit the region. By the early 1840s, local beaver populations were brought to the brink of extinction, and bison had disappeared from the Salmon River region (Albers et al. 1998).

The discovery of gold in California in 1848 began a western mining craze, leading to an influx of prospectors into Idaho and the discovery of gold there. Mining in the area consisted of placer mining along some tributaries and some hard-rock mining. Miners and other settlers were interested in acquiring the Shoshone Tribe's lands and waterways to support their growing agrarian and mining enterprises, and homesteads sprang up across the lower-elevation lands (Albers et al. 1998). Beginning in the 1880s, irrigation development and associated water rights were established in the mainstem Pahsimeroi River and its tributaries (ISCC 1995). Irrigation ditches withdrew water from the river and drained wetlands, redistributing the captured water across the floodplain. Such a redistribution of water had significant impacts on the hydrology of the river, increasing losses in the upper river and enhancing gains in the lower river.

Presently, irrigated and dryland agriculture and livestock grazing are the major land uses in the valley. Livestock grazing is the predominant ongoing activity that occurs on both private and public lands. Grazing on public lands provides a substantial feed base for cattle in the Pahsimeroi River watershed. Generally, cattle graze on public lands from May to October and then return to private lands along the valley bottoms for the remainder of the year (ISCC 1995). Historical agricultural and grazing practices resulted in riparian vegetation clearing and associated streambank destabilization, as well as increased surface-water runoff and erosion.

Existing Watershed Conditions

The modern Pahsimeroi River has changed as a result of human influence relative to its historical condition. The physical and ecological processes in the Pahsimeroi River have been impacted through irrigation diversions that alter instream flows, reducing the timing and magnitude of seasonal channel-forming flows associated with the spring freshet. Livestock grazing and agriculture along the mainstem Pahsimeroi River and its tributaries have caused a loss of woody riparian vegetation, leading to bank instability, bank erosion, and sedimentation. Road embankments, fine sediment from dirt and gravel roads, and dispersed campsites throughout the drainage network have a cumulative effect on siltation in the mainstem Pahsimeroi River.

Hydrology/floods

The Pahsimeroi River flow regime differs from a traditional snowmelt-dominated stream. The upper basin experiences peak flows in May or June, which is consistent with snowmelt-dominated stream flows. In contrast, the lower Pahsimeroi River experiences peak flows in November, with flow remaining high through the winter, then dropping to lower-than-normal base flow from May through September, indicating a highly modified hydrograph (Arthaud et al. 2010). Overall, the hydrology in the Pahsimeroi River basin is largely driven by groundwater influences (bedrock depth and alluvium) and irrigation practices. Diversions direct water from the Pahsimeroi River and its tributaries to irrigate about 38,000 acres of cropland and to water livestock. While agricultural diversion locations and volumes are regulated by local water authorities and the Idaho Department of Water Resources, exact withdrawal rates on a seasonal and daily basis are unknown.

Flood frequency peaks were estimated at two operational United States Geological Survey (USGS) gages using the PeakFQ program, and at 12 ungaged locations (including two locations in the headwaters), applying methods from Berenbrock (2002). Flow uncertainties are especially high in the middle of the Pahsimeroi River basin (between RM 41.7 and RM 52.4), where sites are located too far away from the gages to adhere to the assumptions of the drainage area ratio method, resulting in a large range of possible discharges. Using the USGS gage data, it appears that discharge does not regularly increase with distance downstream. Discharge decreases from the upper valley to the middle valley, likely due to groundwater influences and irrigation withdrawals (Table 36).

Table 36. Pahsimeroi River hydrology.

River Mile [1]	Drainage area (sq. mi.)	Valley Segment	Estimated Flood-Frequency Values (cfs)						
			1.5	2	5	10	25	50	100
2.1	824	Lower	308	350	459	535	634	712	792
35.7	331	Middle[2]	149	169	221	258	306	343	382
55.9	56	Upper	302	361	506	600	715	798	880

[1]The river mile location is near the downstream end of the valley segment.
[2]High uncertainty exists for flow estimates in the middle of the Pahsimeroi Valley.

Surface and Groundwater Interactions

Irrigation diversions and groundwater pumping have altered the surface water/groundwater interchange along the Pahsimeroi River. Many tributaries are naturally disconnected from the mainstem Pahsimeroi

River during low flow and are disconnected by irrigation diversions at high flow. Surface flow is also ephemeral in many parts of the upper Pahsimeroi River. Water diverted for irrigation or lost to the aquifer returns to the river in many locations as springs along the valley floor, providing the lower river with year-round flow and high connectivity to the Salmon River (NOAA 2017). Detailed seepage runs were conducted in the Pahsimeroi River in 2005 to measure gains and losses to surface flow to and from the local aquifer. Results of the study suggest the upper Pahsimeroi River (upstream of RM 42) is largely losing surface water to the aquifer, while the lower Pahsimeroi River (downstream of RM 23) is largely gaining surface water from the aquifer (Figure 82) (Williams et al. 2006). The middle Pahsimeroi River is mixed, with some areas gaining and some areas losing.

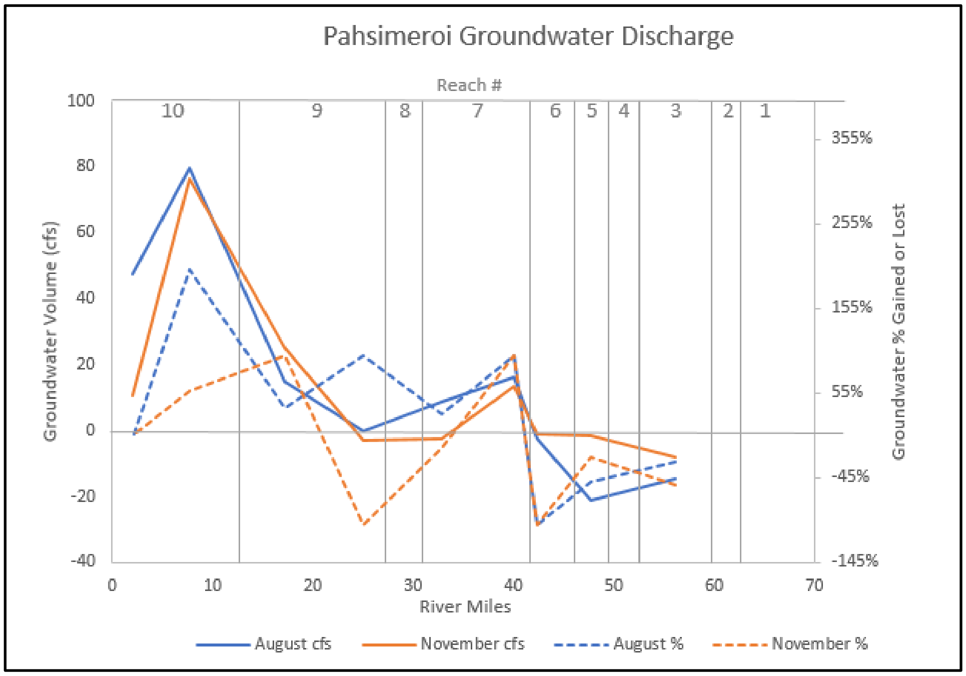

Figure 82. Representative Pahsimeroi River groundwater discharge, as interpreted from Williams et al (2006).

Results represent 1 year of data collected via seepage runs measured in August and November 2005. Surface water flows went dry at the time of measurement in Reaches 5, 6, and the upper portion of Reach 9; therefore, measurements in these areas reflect the minimum volumes lost. Surface water lost to groundwater may be significantly higher in these reaches during years with greater overall discharge. Where discharge increased from 0 cubic feet per second (cfs) to a measurable volume between two reaches, percent gain calculations were not possible (divide by 0). A standard value of 100 percent has been used to graphically represent these gains (RM 40.05 Aug. and Nov.; RM 25.05 Aug.; RM 17.2 Nov.).

A detailed water budget was prepared for the Pahsimeroi River basin by Whittier for water years 2006 and 2007 to calculate where the majority of the groundwater originated (Whittier 2010). The results of the analysis conclude that nearly all of the groundwater contributions to the Pahsimeroi originate from the west (Lost River Range and Pahsimeroi Mountains) and south (Donkey Hills), with negligible contributions from the east (Lemhi Range). The study further concludes that 67 percent of the water discharged at the mouth of the Pahsimeroi River originated from the Lost River Range as a combination of surface water and groundwater.

Icing and Surface Water Interactions

Ice and ice-related channel response may play a minor role in defining the channel morphology in the perennial headwaters of the upper Pahsimeroi River, but the thermal buffering provided by significant groundwater inputs generally prevents large ice accumulations and associated channel response in the gaining reaches of the middle and lower Pahsimeroi River.

Hydraulics

Coarse, at-a-station hydraulic analyses were completed from three representative locations within the watershed to provide context for the geomorphic conditions discussed below. More-detailed two-dimensional hydraulic modeling will be completed as part of the future MRA process for select reaches. Three typical cross-sections located in the lower Pahsimeroi River watershed were measured and evaluated to assess existing hydraulic characteristics and to determine if any generalizations could be inferred from the calculations. Cross-sections were measured at RM 25.6 (Valley Segment 3, Geomorphic Reach 11, Figure 83), RM 11.8 (Valley Segment 3, Geomorphic Reach 12, Figure 84), and RM 2.1 (Valley Segment 3, Geomorphic Reach 12, Figure 85).

At a Station Hydraulic Calculations Summary Sheet

River:	Pahsimeroi
Rivermile:	25.6
Valley Segment:	3
Geomorphic Reach:	11
Reach Slope:	TBD
Localized Slope:	0.0062
n-value (range):	0.035 - 0.045

Local Sediment Size (mm)

D_{16}: 15 D_{50}: 35 D_{84}: 66

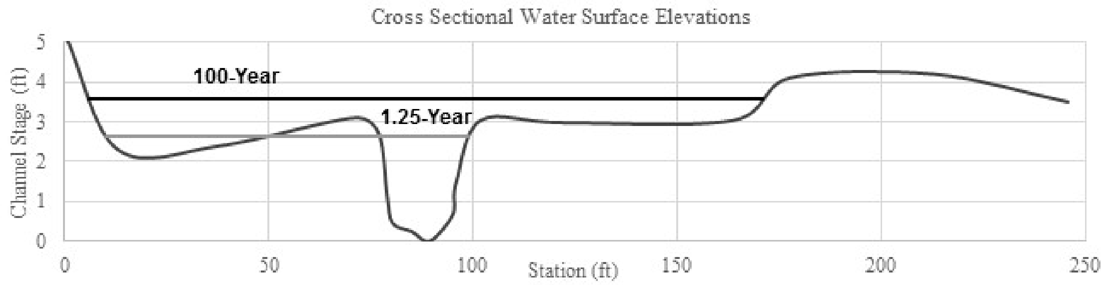

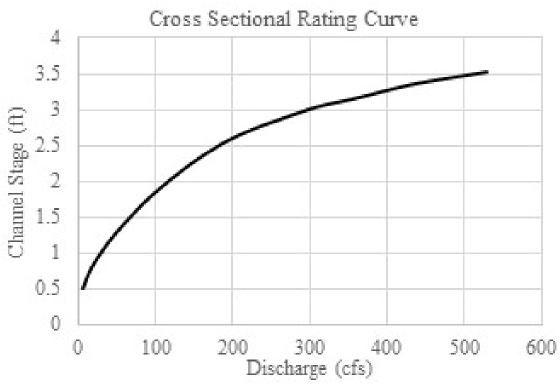

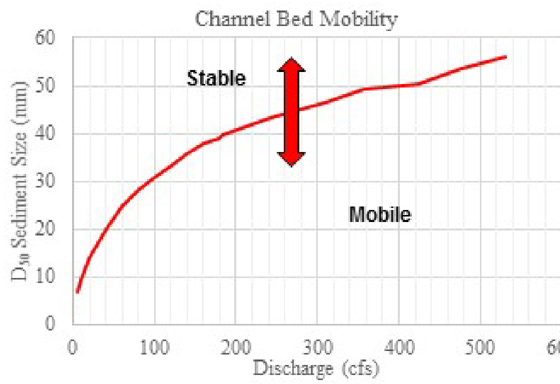

Recurrence Event:	1.25-Year	100-Year
Discharge (cfs):	184	530
Stage (ft):	2.7	3.6
Top Width (ft):	24	164
Ave. Velocity (ft/s):	4.1	5.2
Ave. Shear (lb/ft^2):	0.6	0.9
Ave. St. Power (lb/ft*s):	2.6	4.6
D_{50} Mobilized (mm):	48	69

Entrenchment Ratio (ft/ft):	6.8[1]
Discharge to Mobilize D_{50} (cfs):	> 530
Bed Armored (yes/no):	Yes

Pahsimeroi River– Upper Section

Integrated Rehabilitation Assessment

Notes: 1. Entrenchment Ratio based off main channel width not including side channel.

Idaho Governor's Office of Species Conservation Date Exported: 03/23/2017

Figure 83. Summary of representative hydraulic conditions at Site 1.

At a Station Hydraulic Calculations Summary Sheet

River:	Pahsimeroi
Rivermile:	11.8
Valley Segment:	3
Geomorphic Reach:	12
Reach Slope:	TBD
Localized Slope:	0.0027
n-value (range):	0.035 - 0.045

Local Sediment Size (mm)

D_{16}:	14	D_{50}:	29	D_{84}:	56

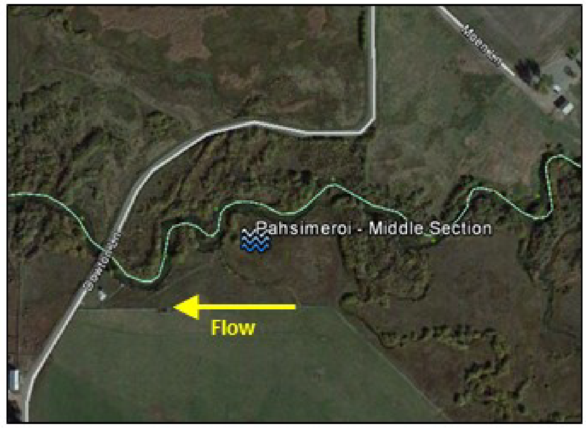

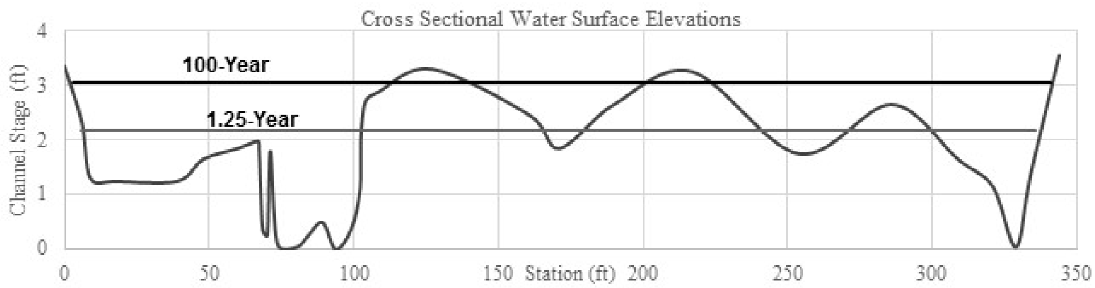

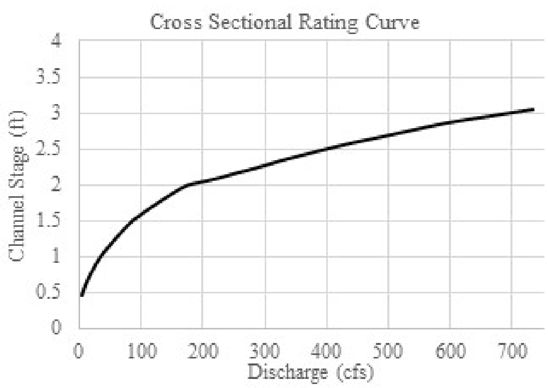

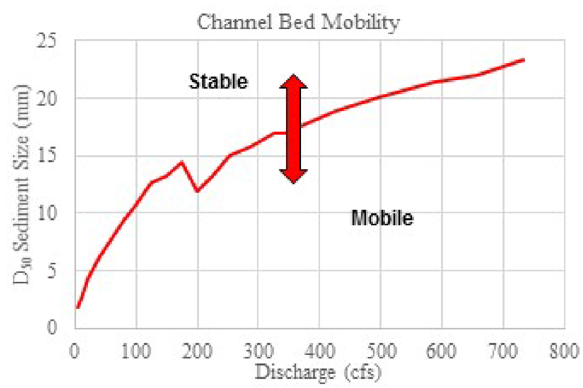

Recurrence Event:	1.25-Year	100-Year
Discharge (cfs):	254	733
Stage (ft):	2.2	3.1
Top Width (ft):	36	306
Ave. Velocity (ft/s):	2.5	3.3
Ave. Shear (lb/ft²):	0.2	0.4
Ave. St. Power (lb/ft*s):	0.6	1.2
D_{50} Mobilized (mm):	15	23

Entrenchment Ratio (ft/ft):	8.5[1]
Discharge to Mobilize D_{50} (cfs):	> 733
Bed Armored (yes/no):	Yes

Pahsimeroi River–Middle Section

Integrated Rehabilitation Assessment

Notes: 1. Entrenchment Ratio based off main channel width not including side channels.

Idaho Governor's Office of Species Conservation Date Exported: 03/23/2017

Figure 84. Summary of representative hydraulic conditions at Site 2.

At a Station Hydraulic Calculations Summary Sheet

River:	Pahsimeroi
Rivermile:	2.1
Valley Segment:	3
Geomorphic Reach:	12
Reach Slope:	TBD
Localized Slope:	0.0075
n-value (range):	0.035 - 0.045

Local Sediment Size (mm)

D_{16}:	2	D_{50}:	18	D_{84}:	32

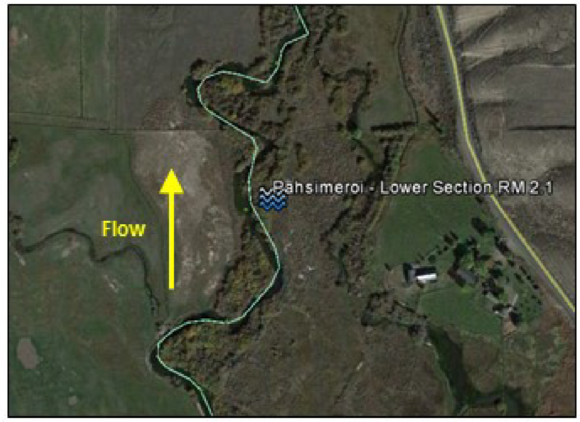

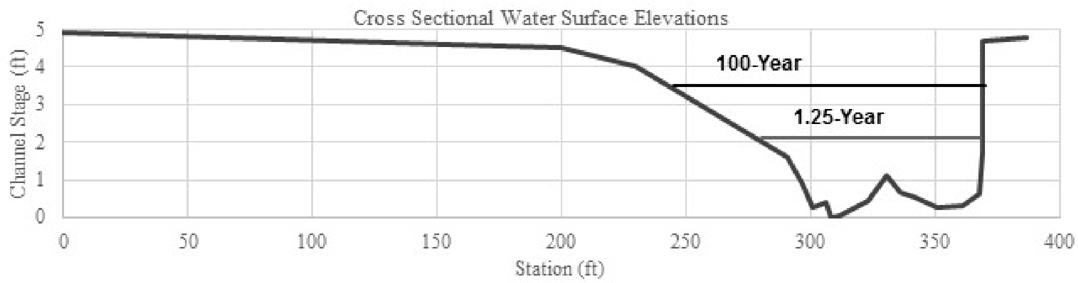

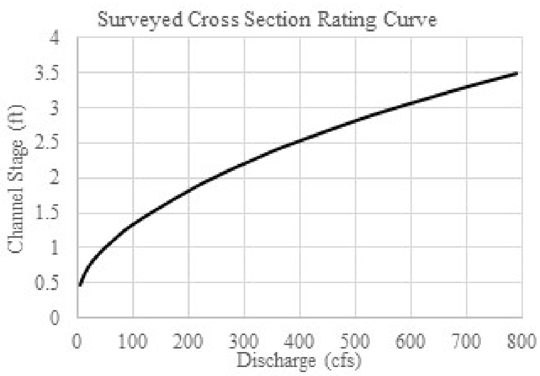

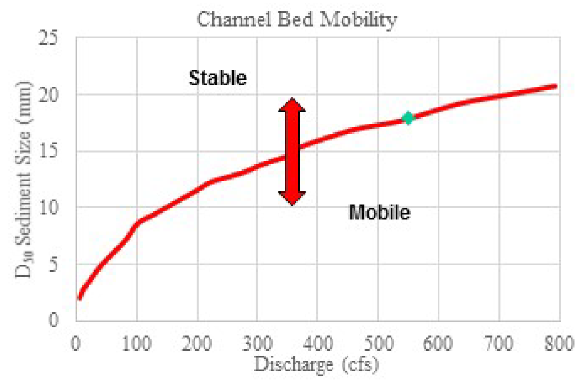

Recurrence Event:	1.25-Year	100-Year
Discharge (cfs):	275	792
Stage (ft):	2.1	3.5
Top Width (ft):	92	127
Ave. Velocity (ft/s):	2.1	2.8
Ave. Shear (lb/ft^2):	0.2	0.3
Ave. St. Power (lb/ft*s):	0.4	0.8
D_{50} Mobilized (mm):	13	21

Entrenchment Ratio (ft/ft):	1.4
Discharge to Mobilize D_{50} (cfs):	550
Bed Armored (yes/no):	Yes

Pahsimeroi River–Lower Section

Integrated Rehabilitation Assessment

Idaho Governor's Office of Species Conservation Date Exported: 03/23/2017

Figure 85. Summary of representative hydraulic conditions at Site 3.

The upstream-most section is located at the upstream end of a gaining area, based on previous groundwater studies. The section modeled shows the 1.25-year discharge contained primarily within the main channel banks, with overtopping occurring near the 1.25-year discharge. The entrenchment ratio is 6.8, which relates to a well-activated floodplain. The sediment size was showing bed mobilization beginning at less than the 1.25-year event, which allows the channel to scour and maintain pools. Average channel velocities varied from 4.1 feet per second at the 1.25-year event up to 5.2 feet per second at the 100-year event. Shear stresses varied from 0.6 to 0.9 lb/ft^2 between these two events. The estimated discharges and resultant hydraulic forces associated with this cross-section result in the potential for bed and bank movement at high-frequency return intervals (yearly).

The middle section is located a short distance upstream of Dowton Lane in a predominantly multi-threaded channel. The channel geometry is such that the 1.25-year event is slightly out of bank, with active, flowing side channels. The 100-year event accesses a good portion of its floodplain, with an entrenchment ratio of approximately 8.5, assuming that the floodplain actively conveys flow downstream. Local sediment sizes show that the bed begins to mobilize at flows higher than 733 cfs, which is greater than the 100-year event, suggesting a heavily armored bed. Channel velocities range from 2.5 ft/sec to upwards of 3.3 ft/sec. Depending on how and when the channel accesses a large portion of its floodplain (side channel network) at this section, there is a lot potential variation in flood hydraulics, and further study would be required to assess those characteristics to determine if all side channels were active. Given the multi-thread pattern of this cross-section, dispersion of flow between these channels could be affecting the armoring of the channel bed. If these side channels are not active and all flows are concentrated toward the main channel bed, armoring might be less than estimated in this analysis.

The lower section is located approximately 1 mile upstream of the lower hatchery. At this section, the waterway is channelized by high ground on each river bank, reducing the entrenchment ratio to 1.4. Channel velocities range between 2 and 3 ft/sec for the 1.25- and 100-year discharge events, respectively. Shear stresses vary from 0.2 to 0.3 lb/ft^2 for the same two flow events. The channel appears to be armored through this section of river, with D_{50} mobilization occurring between the 10- and 25-year events. Upon additional review of LiDAR data, it appears the lower section was taken in a locally confined area with limited floodplain connectivity and likely does not represent the overall reach accurately. It is anticipated that adjacent areas do not contain the 100-year flow, based on similar stage estimates and likely increases in both the entrenchment ratio and the effect of bed armoring.

Among these three cross-sections, the floodplain is accessible to flood waters at the upper two sections, and perhaps artificially limited by the downstream section. The channel bed appears to become more armored farther downstream. This could be caused by distributary and multi-thread channels reducing stream energy in the upper sections or increasing influence of groundwater versus peak-flow hydrology. Armoring could limit potential scour depths and pool development at these locations. Results from the lower Pahsimeroi River cross-section hydraulics do not appear to be representative of the lower valley segment. The cross-section was taken at a location with high ground on the floodplain (approximately 1 to 2 feet higher than surrounding areas), yielding a lower entrenchment ratio than is believed to be representative of the area. Alterations to the peak hydrograph from irrigation withdrawals, and possibly minor channel incision, may also affect the hydraulic calculations, resulting in lower entrenchment ratios than those interpreted from aerial photos. More-detailed hydraulic modeling is required to confirm actual floodplain inundation timing and associated entrenchment.

Water Quality

Surface water quality standards apply to a waterbody depending on its designated uses and/or existing uses. Pursuant to the Clean Water Act (CWA), Idaho recognizes existing uses, which are uses present or attained in a water body on or after November 28, 1975. When water bodies do not have designated beneficial uses, they are assigned a presumed use protection. All water bodies are classified for more than one beneficial use and must meet the fishable/swimmable intent of the CWA.

Under Idaho's water quality standards, beneficial uses are categorized as aquatic life, recreation, water supply, wildlife habitat, and aesthetics. For the Lemhi River watershed, the beneficial uses that are not fully supported are: (1) aquatic life, which includes salmonid spawning and cold-water aquatic life beneficial uses, and (2) and contact recreation that includes primary and secondary contact recreation.

The Idaho Department of Environmental Quality completed a subbasin assessment for the Pahsimeroi River watershed in 1999 (IDEQ 2013). Total maximum daily loads (TMDLs) were developed for water bodies not supporting their beneficial uses and impaired by a pollutant. In Idaho's 2002 Integrated Report (IDEQ 2005), streams were converted from water-quality-limited segments to assessment units (AUs) based on Strahler Stream Order within a Waterbody ID.

Additional AUs identified by IDEQ's Beneficial Use Reconnaissance Program monitoring were added to the 2008 and 2010 Integrated Reports. Further investigation by IDEQ determined that some listed AUs are ephemeral and therefore should not be listed as water-quality-limited (Section 5: TMDL needed) but rather placed in Section 4C (impaired but not due to a pollutant). Under the CWA, lack of flow is not considered pollution, and no TMDL can be calculated. The 2012 Addendum updated water bodies and pollutants for which TMDLs have been developed (Table 37).

Table 37. Streams and pollutants for which TMDLs were developed

Waterbody	2001	2013 Addendum
Pahsimeroi River	Sediment, Temperature	Bacteria
North Fork Lawson Creek		Sediment
East Fork Pahsimeroi River		Temperature
Short Creek		Sediment

Source: IDEQ 2013

Basin Geometry

Domains within a watershed can be characterized as zones that are governed by sediment supply, alluvial fan formation, sediment transfer, or deposition (Figure 86). The headwaters and upper reaches of the Pahsimeroi River are generally classified as sediment supply zones dominated by weathering and erosion of steep slopes, where tributaries collect and transport sediment downslope to the alluvial fan zone. The alluvial fan zone is where coarse sediment has accumulated across broad alluvial fans and piedmont belts at the valley head and margins. Here, the basin-fill sediments are porous and the river loses surface water to the aquifer and commonly goes dry. During high flow, even losing reaches of the Pahsimeroi River convey surface flow, episodically transporting and depositing sediment through the transfer zone.

Below the alluvial fan and ephemeral transfer zones, tributaries flow across the broad, low-gradient valley bottom, where they are unable to consistently transport a coarse sediment load, creating a pronounced deposition zone characterized by fine sediment and a highly sinuous, commonly multi-threaded channel. A longitudinal profile of the channel from RM 60 to the mouth of the river (RM 0) shows a concave profile, with the highest gradient in the upper valley and a generally decreasing slope in the downstream direction (Figure 87).

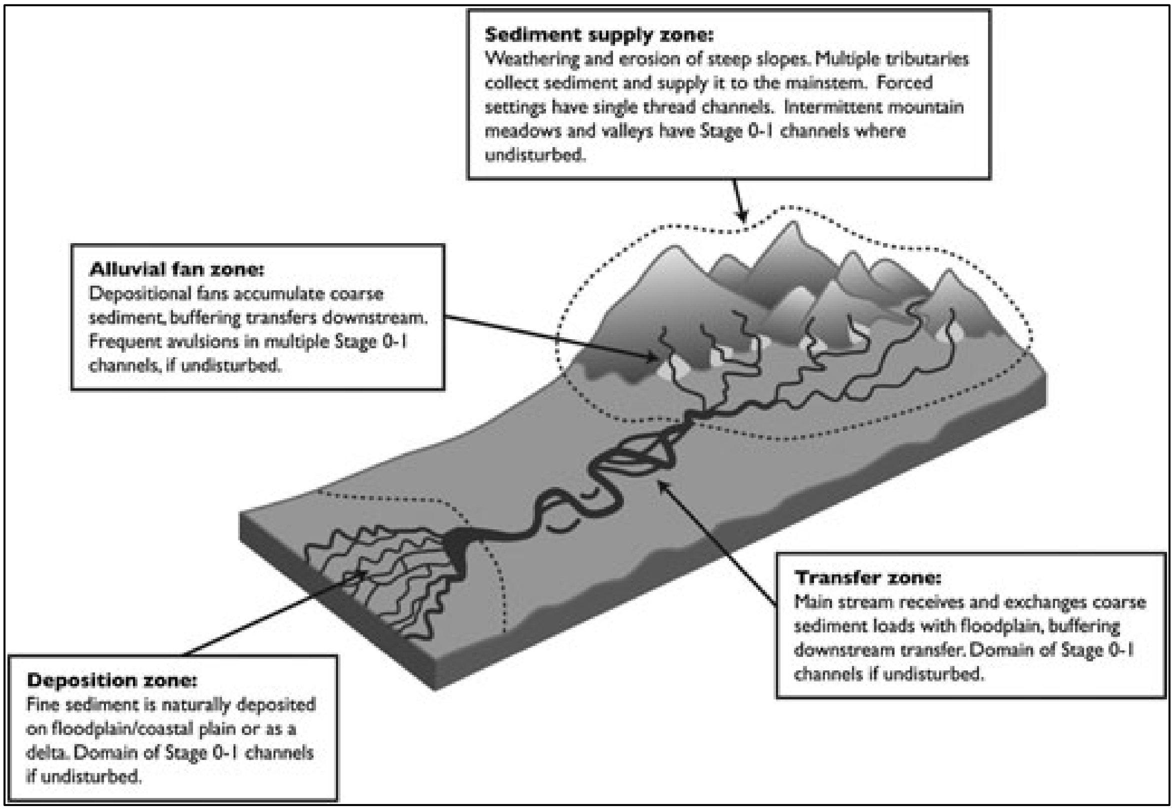

Figure 86. Locations of sediment domains within a typical watershed (Cluer and Thorne 2013).

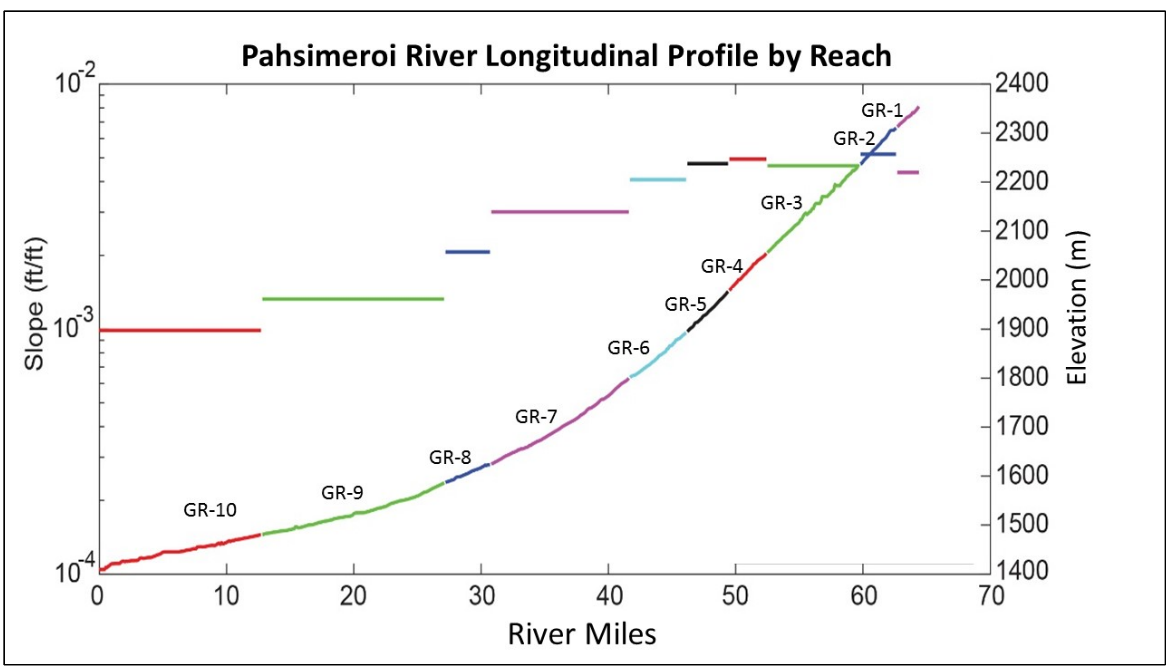

Figure 87. Pahsimeroi River longitudinal profile by geomorphic reach. The channel exhibits a typical concave curve with generally decreasing slopes in the downstream direction.

The width of the Pahsimeroi River floodplain, as defined by the location of confining terraces and/or valley margin, is narrow in the upper valley and wide in the lower valley. Dividing the width of the floodplain by the width of the bankfull channel produces a result called the entrenchment ratio. A small entrenchment ratio means the channel has less accessible floodplain area and therefore less ability to dissipate flood energy on the floodplain. This results in deeper, higher-velocity, more-forceful flood flows, increasing the potential for erosion and/or incision (i.e., transport reach). Large entrenchment ratios are representative of channels with broadly accessible floodplains that can dissipate flood energy outside the banks of the channel, resulting in less-forceful flood flows and a tendency for deposition (i.e., response reach).

Large portions of the upper and middle Pahsimeroi River are naturally confined by terraces and exhibit relatively low entrenchment ratios. Measurements of entrenchment in the lower Pahsimeroi River were highly variable, but lower than expected, possibly due to a highly altered hydrograph from irrigation and/or minor incision and channel widening (i.e., larger cross-sectional area). The middle Pahsimeroi River is mixed, exhibiting both high and low entrenchment ratios. Human features such as levees, road embankments, and other obstructions appear to have had minimal large-scale impact on entrenchment in the Pahsimeroi River. More-detailed hydraulic modeling is required to confirm floodplain inundation timing and extent and associated entrenchment.

Soils

Geomorphic features in the Pahsimeroi River valley bottom include the active channel, floodplains, alluvial fans and stream terraces, and outwash fans and fan terraces. Soils that have formed on these features are described in Table 38. Soil descriptions are based on the NRCS detailed soil maps and the Detailed Soil Map Units section in the report (NRCS 2003).

Table 38. Geomorphic features along the valley bottoms and margins, and associated soils

Geomorphic Feature	Soil Description and Other Information
Active Channel	Water. Soils that have formed adjacent to or in the channel (gravel bars and islands) are described in the Floodplains soil description.
Floodplains	Soil description: a very deep, very poorly drained to moderately well drained soil that is dark-colored, silty loam to very cobbly sandy loam, and on floodplains and old stream channels. Slope range: 0 to 4 percent; Elevation range: 3700 to 7400 feet; Average annual precipitation: 8 to 18 inches; Average annual air temperature: 34 to 45° F; Frost-free season: 5 to 90 days; Depth class: very deep; Drainage class: very poorly drained to moderately well drained; Permeability: moderately slow to very rapid; Available water capacity: 1 to 12 inches; Effective rooting depth: 10 inches to more than 60 inches; Runoff: slow; Hazard of water erosion: slight; Range site: basin big sagebrush, western wheatgrass, black cottonwoods, willows, and sedges
Alluvial Fans and Stream Terraces	Soil description: a very deep, poorly drained to well-drained soil the is light-colored silt loam over silty clay to very gravely loamy silt, and on alluvial fans and stream terraces Slope range: 0 to 6 percent; Elevation range: 3800 to 6600 feet; Average annual precipitation: 8 to 12 inches; Average annual air temperature: 37 to 45° F; Frost-free season: 25 to 100 days; Depth class: very deep; Drainage class: poorly drained to well drained; Permeability: moderate in the upper part to very rapid in the lower part to moderately slow; Available water capacity: 2 to 11 inches; Effective rooting depth: 10 inches to more than 60 inches; Runoff: slow to medium; Hazard of water erosion: slight to moderate; Range site: Wyoming big sagebrush, bluebunch wheatgrass, threetip sagebrush, and Idaho fescue
Outwash Fans and Fan Terraces	Soil description: a very deep, well drained to somewhat excessively drained soil that is a darker-colored, gravely loam, and on outwash fans and fan terraces. Slope range: 1 to 20 percent; Elevation range: 4500 to 7100; Average annual precipitation: 6 to 12 inches; Average annual air temperature: 35 to 44° F; Frost-free season: 30 to 90 days; Depth class: very deep; Drainage class: well drained; Permeability: moderate in upper part and very rapid in lower part to moderately slow; Available water capacity: 3.5 to 5.5 inches; Effective rooting depth: 40 inches to more than 60 inches; Runoff: slow; Hazard of water erosion: slight; Range site: mountain big sagebrush, Idaho fescue, Wyoming big sagebrush, and bluebunch wheatgrass

Land Use

The Pahsimeroi River watershed covers about 839 square miles, and about 90 percent of the land is owned by the Federal government and administered by the USFS and BLM. Private lands are primarily located along the more-fertile valley bottoms. The primary land uses are livestock grazing, irrigated pasturelands and hay fields, developed and dispersed recreation, and timber harvest. Livestock grazing occurs on both public and private lands across much of the middle and lower elevations in the watershed. Livestock are grazed on public lands from May to October and then return to private lands for the remainder of the year. Irrigated pasturelands and hay fields are on private lands along the Pahsimeroi valley bottom and margins. The effects of irrigation and grazing in the valley bottom include diversion of flows from the mainstem Pahsimeroi River, diversion of tributaries away from the mainstem Pahsimeroi River, stream alterations, and native vegetation replacement.

Developed and dispersed recreation, several small mining claims, and small timber harvests are additional land uses that are believed to have minimal impact on the modern Pahsimeroi River.

Land Cover and Riparian Conditions

More than half of the drainages in the Pahsimeroi River watershed have less-than-satisfactory riparian conditions, based on stream functionality and plant community-type assessments. Most of these altered riparian communities are in the lower portions of the watershed (NPCC 2004). Degradation of riparian conditions is due to both livestock grazing and reduced streamflows from irrigation withdrawals (NOAA 2017). Agricultural development and livestock grazing have altered the riparian vegetation through clearing and soil compaction, resulting in the replacement of native sedge and willow species with grass and other species that do not have the bank-stabilizing and shade-providing effects that natural woody riparian vegetation provides.

Channel Migration

Meander bend channel migration involves erosion of the outside bank of a bend, coupled with concurrent deposition of sediment along the inside bank of the same bend, resulting in the lateral movement of the channel while maintaining consistent channel shape and width. This process is driven by and dependent on concurrent deposition and erosion. Bank erosion without deposition results in channel widening. Deposition without bank erosion results in aggradation and possible avulsion. There are very few active depositional point bars within the entire Pahsimeroi River, suggesting that channel migration is not a dominant process. Observable bank erosion and bank recession are common, especially in the lower Pahsimeroi River, where riparian vegetation has been cleared and bank stability compromised (Photograph 22). These areas of bank erosion do not show evidence of deposition on the opposite bank, resulting in channel widening, rather than channel migration. Where bank erosion has occurred in areas with dense riparian vegetation, rates of bank recession are so slow that active point-bar deposition is not readily observable. The sinuous channel pattern observed on the lower Pahsimeroi River is likely the result of episodic avulsion and very low rates of channel migration, largely undetectable over the span of available historical photos for the area.

Photograph 22. Example of eroding bank in the Lower Pahsimeroi. This bank has subsequently been improved with multiple rootwad structures to reduce excessive bank erosion, reduce the over-widened width-to-depth ratio of the channel, and to provide habitat and cover for juvenile salmonids.

Large Wood Recruitment and Retention

Other than a handful of cottonwood trees that appear to have been planted or otherwise associated with human disturbance, no large trees were observed in the lower Pahsimeroi River riparian area (downstream of RM 24), and no buried wood was observed in the banks or bed of the lower Pahsimeroi River during 2016 field work. A high groundwater table and limited coarse sediment disturbance (overbank sand and gravel deposition) suggest few large trees historically occupied the banks of the lower Pahsimeroi River. Additionally, large depositional zones, ephemeral surface flow, and small tributary drainages upstream of the lower Pahsimeroi River likely precluded frequent large wood recruitment from upstream sources. Historically and currently, mature riparian vegetation (willow clumps) provide structure to the lower Pahsimeroi River channel, forcing flow convergence and stabilizing banks where present, providing a function similar to large wood (Photograph 23). Rehabilitation projects may consider using large woody material to emulate willow clumps as a temporary surrogate for mature riparian vegetation on otherwise barren banks until mature vegetation can be established.

Photograph 23. Mature willow clump providing instream structure and splitting flow in a groundwater-influenced channel (Big Springs Creek in the Lemhi watershed).

Historically and currently, most of the upper Pahsimeroi River (upstream of RM 24) had/has a greater influence from snowmelt hydrology and tributary-derived coarse sediment than the lower Pahsimeroi River. These conditions have created a disturbance regime more suitable for the establishment and propagation of cottonwood trees, in addition to willows and other shrubs. It is likely that large woody material has been recruited to the upper Pahsimeroi River via local windfall for thousands of years. It is unlikely that large floods and debris torrents commonly transported large wood from the uplands, given the distance of transport required and the small size of tributaries in the upper Pahsimeroi River. Reports suggest that wood is unlikely to transport through such small streams with low channel width and depth (Braudrick and Grant 2001).

Channel Planform and Morphology

Channel planform on the Pahsimeroi River is moderately to highly sinuous. In an alluvial valley, sinuosity is typically inversely proportional to gradient, with lower sinuosity in areas of steeper gradient. This is the case on the Pahsimeroi River, where reach-averaged sinuosity ranges between 1.1 and 1.3 in the high-gradient upper Pahsimeroi River and between 1.3 and 1.8 in the lower-gradient lower Pahsimeroi River, where the hydrology also tends to be more groundwater-influenced. The upper Pahsimeroi River, with lower sinuosity, greater sediment supply, higher gradient, and more pronounced peak flows, likely has been and remains a predominantly single-threaded system. In the lower Pahsimeroi River, low gradients, high sinuosity, groundwater-influenced hydrology, dense riparian vegetation, and beaver activity likely led to a historically multi-threaded channel system. Over the past 100+ years, the removal of riparian vegetation and loss of beaver, along with irrigation diversions and channel manipulation, have created a largely single-threaded system. Where riparian vegetation has been removed, the bankfull width of the channel has increased significantly.

Channel morphology, as defined by Montgomery and Buffington (1998), is determined by bedform features associated with slope, discharge, sediment supply, bedrock lithology, and disturbance history. The channel morphology of the Pahsimeroi River has not significantly changed since historic times, with the upper Pahsimeroi River characterized by a predominant plane-bed morphology, and the lower Pahsimeroi River characterized by a predominant pool-riffle morphology. Channel obstructions and bank structure-associated riparian vegetation and woody debris may increase areas of flow contraction within the channel, locally driving otherwise plane-bed morphology toward a forced pool-riffle morphology (Photograph 24). Alternatively, where a lack of riparian vegetation has resulted in bank recession and channel widening, flow divergence reduces local transport competence and the development of scour pools, driving a pool-riffle morphology toward a plane-bed morphology (Photograph 25 and Photograph 26). The significant lack of riparian vegetation on the lower mainstem Pahsimeroi River, and to an even larger extent on tributaries within the valley bottom, has likely resulted in many more linear feet of plane-bed as opposed to pool-riffle morphology, relative to historic conditions. Detailed reach-scale mapping will be required to quantify this claim.

Photograph 24. Forced pool-riffle morphology due to riparian plant structure on the bank of the lower Pahsimeroi River.

Photograph 25. Photograph illustrating a straightened channel and plane-bed morphology in the lower Pahsimeroi River.

Photograph 26. Plane-bed morphology in Big Creek in the upper Pahsimeroi River valley.

The upper Pahsimeroi River loses so much flow to groundwater and irrigation withdrawals that near RM 40, the channel not only goes dry but is reduced to such infrequent surface flow that it does not have recognizable banks or a specific morphology. The valley bottom in this area reveals many small, dry channels similar to the surface of an alluvial fan, but no well-defined primary channel, suggesting this condition to be natural, although likely exacerbated by irrigation withdrawals. Many springs originate at the toe of the Doublesprings alluvial fan immediately downstream of this point, reestablishing a multi-thread network of surface channels by RM 38, which have coalesced into a primary single-thread channel by RM 33. Many irrigation ditches and ponds intercept flow, influencing the morphology of the channel(s) in this area.

Beaver

The existing influence from beavers has been severely limited as a result of legacy fur trapping. Limited evidence of beaver activity on the Pahsimeroi River was observed during 2016 field work, suggesting that population numbers remain extremely low. As discussed previously, beaver activity likely played a significant role in modifying and developing the historic Pahsimeroi River morphology. Beavers generally require 40 to 60 percent tree/shrub canopy closure and shrub height greater than 6.6 feet within a broad/intact riparian corridor (Slough and Sadleir 1977). Beavers also require trees less than 6 inches in diameter for food source, preferring aspen, willow, cottonwood, alder (in that order) (Denney 1952). These conditions are present in discontinuous patches throughout the valley and suggest beaver reestablishment is possible.

Watershed Impacts

The higher-elevation areas along the Lemhi Range and the Lost River Range are on public lands that are administered by the Salmon-Challis National Forest. The middle and lower elevation areas along the foothills and piedmont belts are on public lands administered by the BLM Challis Field Office. The valley bottoms of the Pahsimeroi Valley are predominantly private lands.

Forested, higher-elevation areas along the Lemhi Range and Lost River Range have been minimally impacted by human activities. Road density, timber harvests, and dispersed recreation have had minor impacts on the watershed. However, at middle and lower elevations, there are significant, localized human impacts that have negatively affected riverine processes. These impacts include, but are not limited to, flow alteration from irrigation diversions, loss of riparian vegetation on tributaries, channel and floodplain alteration from roads, and increased fine-sediment deposition.

Irrigation diversions significantly reduce instream flows by diverting tributaries away from and out of the mainstem Pahsimeroi River. The many irrigation diversions reduce the frequency and magnitude of peak flows, as well as the quantity of instream habitat available through isolation (i.e., disconnected tributaries) and volume (i.e., linear feet of stream with adequate surface water). Another effect of irrigation diversions is an alteration of the timing and spatial distribution of groundwater recharge. Diversions redistribute river water onto the floodplain during the summer months, artificially increasing groundwater levels in those locations.

The loss of dense riparian vegetation (primarily willow, and especially in the lower Pahsimeroi River) has resulted in an over-widened and homogenous channel. Dense riparian vegetation on the outside of bends stabilizes the bank and obstructs flow, forcing contraction and resulting in pool scour and a narrow width-to-depth ratio, often with undercut banks. Dense riparian vegetation also promotes channel response via side-channel formation and avulsion around the structure provided by the vegetation, rather than bank erosion and widening when vegetation is lacking. A reduction in the amounts of bank structure and instream structure has resulted in a simplified, homogenous channel exemplified by an over-widened, predominantly plane-bed morphology. The over-widened condition also expands the cross-sectional area of the channel between the banks, enabling more water to pass between the banks during floods, reducing floodplain connection frequency and duration. Finally, in all areas where woody riparian vegetation has been lost, the channel is exposed to greater solar radiation and thermal heating from the loss of shade.

Channel and floodplain alterations from roads are most prevalent in the lower Pahsimeroi River valley. Several roads span the valley bottom, with culverts and bridges passing the stream beneath the road, concentrating flow at each crossing location. It is unclear to what extent these crossings have impacted physical and biological conditions on the Pahsimeroi River. Undersized crossings can obstruct flow, promoting upstream flooding and deposition (for better or worse). Crossings often also provide grade control that can impact (positively or negatively) the stream gradient.

Loss of riparian vegetation, cattle grazing, and to a lesser extent, runoff from roads, all-terrain vehicle trails, and mining operations, have increased fine sediment inputs to the channel through sheetwash and wind erosion. Dense riparian vegetation had historically stabilized banks composed of fine sand and silt, which are now eroding and contributing sediment to the river on an annual basis. Cattle grazing has disturbed the surface of the floodplain and compacted the soils, both of which lead to greater fine-sediment runoff. Roads have been located adjacent to or drain into many of the tributaries, where they have altered the riparian vegetation composition, compacted soils, and provided conduits for concentrated sheet flows during snowmelt and thunderstorms. Mining operations have included placer mining and exploratory trenches, especially in the foothills and headwater areas along the Lemhi Range by the Patterson Creek drainage. The cumulative effects of these impacts have likely increased fine sediment inputs entering the Pahsimeroi River system, resulting in elevated fine-sediment levels and siltation.

Data Gaps

Future analysis could be aided by the collection of additional data currently unavailable, including:

- Hydraulic modeling to confirm floodplain inundation timing and extent, sediment transport character, and appropriate channel geometry (i.e., width-to-depth ratio).
    - Data gaps necessary for hydraulic modeling include bathymetry data, frequent pebble counts, and an improved understanding of diversion withdrawals/returns, tributary inflows, and groundwater contributions.
- Riparian vegetation inventory, including health and successional stages within the low surface that directly influence lateral channel migration, force pool-riffle bedforms, sort and retain gravel, and provide bank stability.

LiDAR upstream of RM 30 will aid assessment and design efforts in the mid- and upper Pahsimeroi River if and when regular surface flow can be extended upstream to this area.

Pahsimeroi Valley Segments and Geomorphic Reaches

Valley segments, geomorphic reaches, and channel units are three hierarchically nested subdivisions of the drainage network (Frissell et al. 1986). Within the hierarchy of spatial scales, valley segments, geomorphic reaches, and channel units represent the largest physical subdivisions that can be directly altered by human activities. As such, it is useful to understand how they respond to anthropogenic disturbance, but to do so requires classification systems and quantitative assessment procedures that facilitate accurate, repeatable descriptions and convey information about biophysical processes that create, maintain, and destroy channel structure (Bisson, Buffington, and Montgomery 2006).

Valley Segments

The Pahsimeroi River occupies an alluvial valley that has varying discharge along its course due to flow and sediment inputs from major tributaries classified using a 10th field Hydrologic Unit Code (HUC-10). There are four HUC 10 sub-watersheds that discharge to the Pahsimeroi River (Table 39). Four valley segments were identified based on the location of where the Pahsimeroi River begins and where the HUC 10 sub-watersheds interact with or are identified along the Pahsimeroi River (Figure 88).

(1) The Pahsimeroi Headwaters Valley Segment includes the East and West Forks of the Pahsimeroi River downstream to where they combine to form the Pahsimeroi River (Headwaters to RM 64.4)

(2) The Upper Pahsimeroi Valley Segment includes the upstream extent of the Pahsimeroi River to a point estimated to represent an average location where perennial surface flow becomes ephemeral. The entire Upper Pahsimeroi has been shown to lose significant volumes of flow to the aquifer (Williams et al. 2006)/ (RM 64.4 to 52.5)

(3) The Middle Pahsimeroi Valley Segment includes the majority of the Pahsimeroi River that is considered ephemeral due to surface water losses to groundwater and irrigation. There are sections of the Middle Valley Segment that gain flow from groundwater sources (along the toe of the Doublesprings alluvial fan), but the stream is generally ephemeral above and below these locations. The hydrologic regime is considered mixed, with most of the Middle Valley Segment characterized by surface-water/snowmelt discharge, with the exception of the groundwater-influenced section identified above. (RM 52.5 – 30.9)

(4) The Lower Pahsimeroi Valley Segment includes the majority of the Pahsimeroi River that is considered perennial due in large part to significant groundwater gains throughout this valley segment. (RM 30.9 – 0).

Table 39. Pahsimeroi River watershed valley segments delineations and sub-watersheds

Valley Segments and Locations	Sub-watershed	HUC 10	Named Tributaries	River Miles	Square Miles
Pahsimeroi Headwaters Valley Segment (Headwaters to RM 64.55)	West Fork Pahsimeroi River	Sub-watershed in HUC 1706020201	0	Upstream of 64.5	12.9
	East Fork Pahsimeroi River	Sub-watershed in HUC 1706020201	0		17.5
Upper Pahsimeroi Valley Segment (RM 64.55 to 52.50)	Upper Pahsimeroi River	1706020201	3	64.5 – 52.5	90.1
Middle Pahsimeroi Valley Segment (RM 52.50 to 30.92)	Middle Pahsimeroi River	1706020202	2	52.5 – 30.9	342.7
Lower Pahsimeroi Valley Segment (RM 30.92 to 0)	Lower Pahsimeroi River	1706020203	12	30.9 – 0	367.2
	Total		**15**	**64.5**	**830.4**

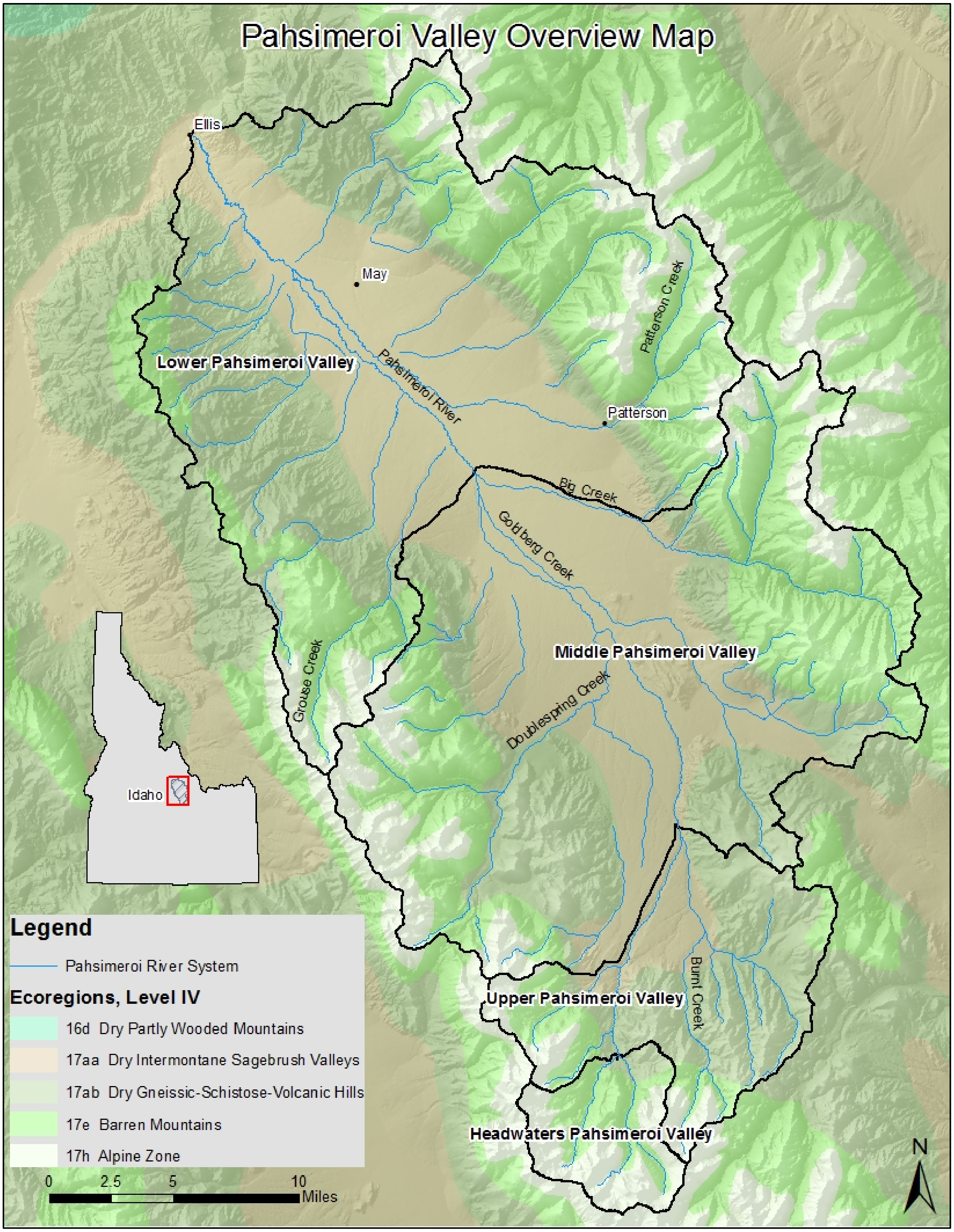

Figure 88. Pahsimeroi River watershed valley segment locations.

Reach Characteristics

Reach characteristics are summarized by reach in Table 40 below.

Table 40. Summary of geomorphic conditions for the Pahsimeroi River watershed

Valley Segment	Reach	River Miles	Valley Slope (ft/ft)	Average Valley Width (ft)	Average Constrained Valley Width (ft)	Channel Slope (ft/ft)	Average Channel Width (ft)	Sinuosity	Entrenchment Ratio (ft/ft)	Constrained Entrenchment Ratio (ft/ft)	Human Disturbance Ratio (%)	Groundwater Characteristics	Geomorphic Characterization "Complex"	Geomorphic Characterization "Mixed"	Geomorphic Characterization "Simplified"
VS-2	GR-1	64.5 - 62.6	0.0185	391	-	0.0145	23	1.3	17	-	0%	-	19%	81%	0%
VS-2	GR-2	62.6 - 59.8	0.0194	204	-	0.0169	23	1.1	9	-	0%	-	20%	61%	19%
VS-2	GR-3	59.8 - 52.5	0.0168	290	-	0.0152	28	1.1	10	-	1%	Losing	13%	87%	0%
VS-3	GR-4	52.5 - 49.5	0.0182	389	-	0.0155	23	1.2	17	-	1%	Losing	30%	70%	0%
VS-3	GR-5	49.5 - 46.1	0.0188	208	-	0.0164	18	1.1	11	-	1%	Losing	41%	56%	2%
VS-3	GR-6	46.1 - 41.6	0.0165	594	-	0.0128	18	1.3	33	-	3%	Losing	57%	43%	0%
VS-3	GR-7	41.6 - 30.9	0.0124	3187	-	0.0098	13	1.3	243	-	3%	Losing	15%	14%	7%
VS-4	GR-8	30.9 - 27.2	0.0089	315	-	0.0069	17	1.3	19	-	3%	Neutral	59%	27%	13%
VS-4	GR-9	27.2 - 12.8	0.0075	3672	-	0.0045	19	1.7	195	-	2%	Gaining	60%	33%	7%
VS-4	GR-10	12.8 - 0	0.0057	1510	-	0.0032	34	1.8	44	-	7%	Gaining	54%	44%	2%

- No constraints exist within the approximated floodplain.

Pahsimeroi Headwaters Valley Segment (VS-1)

The Pahsimeroi Headwaters Valley Segment comprises the West Fork Pahsimeroi River (West Fork) and the East Fork Pahsimeroi River (East Fork) drainages (Figure 89). Both the West Fork and East Fork drain the Lost River Range, an uplifted mountainous region that has been sculpted by alpine glaciers. Along the eastern ridgeline, there are several glacial cirques that are still occupied by lakes (tarns) in which the East Fork and West Fork begin their journeys and then coalesce to form the Pahsimeroi River at RM 64.55. Both the West Fork and East Fork drainages are within the larger Upper Pahsimeroi River sub-watershed (HUC 1706020201). The entire drainage is administered by the Salmon-Challis National Forest.

This valley segment is within the sediment supply zone of the upper Pahsimeroi River watershed. The supply zone provides sediment through the weathering and erosion of bedrock and colluvium that is transported downslope to the mainstem Pahsimeroi River through a dendritic (branching) network of coalescing tributaries. These tributaries generally have single-thread, sinuous channels. Channel segments that are unconfined have evidence of beaver activity where the tributary has been impounded and sediment has accumulated to form mountain meadows. Nearly all beavers have been removed from this region, based on interpretation of 2015 aerial photographs. Livestock grazing occurs along tributaries and has altered the riparian vegetation along some channel segments.

The West Fork drainage includes about 8,275 acres, with elevations ranging from about 7950 feet at the confluence of the West Fork and East Fork to more than 12000 feet along the Lost River Range, between Mount Borah and Leatherman Peak. The historically glaciated Lost River Range has several tarns in the glacial cirques along the eastern slopes. The West Fork begins in Pass Lake at 10600 feet in elevation and has ephemeral flows for about 1 mile until it intercepts several seeps and springs before becoming perennial. About 4 river miles downstream, the West Fork intercepts additional flows from the outlet flows of Merriam Lake at about 9800 feet.

The East Fork drainage includes 11,230 acres, with elevations ranging from about 7950 feet at the confluence of the West Fork and East Fork to more than 12000 feet along the Lost River Range, between Leatherman Peak and Mount Breitenbach. The historically glaciated Lost River Range has several tarns in the glacial cirques along the eastern slopes. The East Fork begins in a glacial cirque and has ephemeral flows into a tarn at 9800 feet in elevation and has perennial flows to the East Fork and West Fork confluence. The East Fork has EPA-approved TMDLs for water temperature and sediment/siltation (IDEQ 2011).

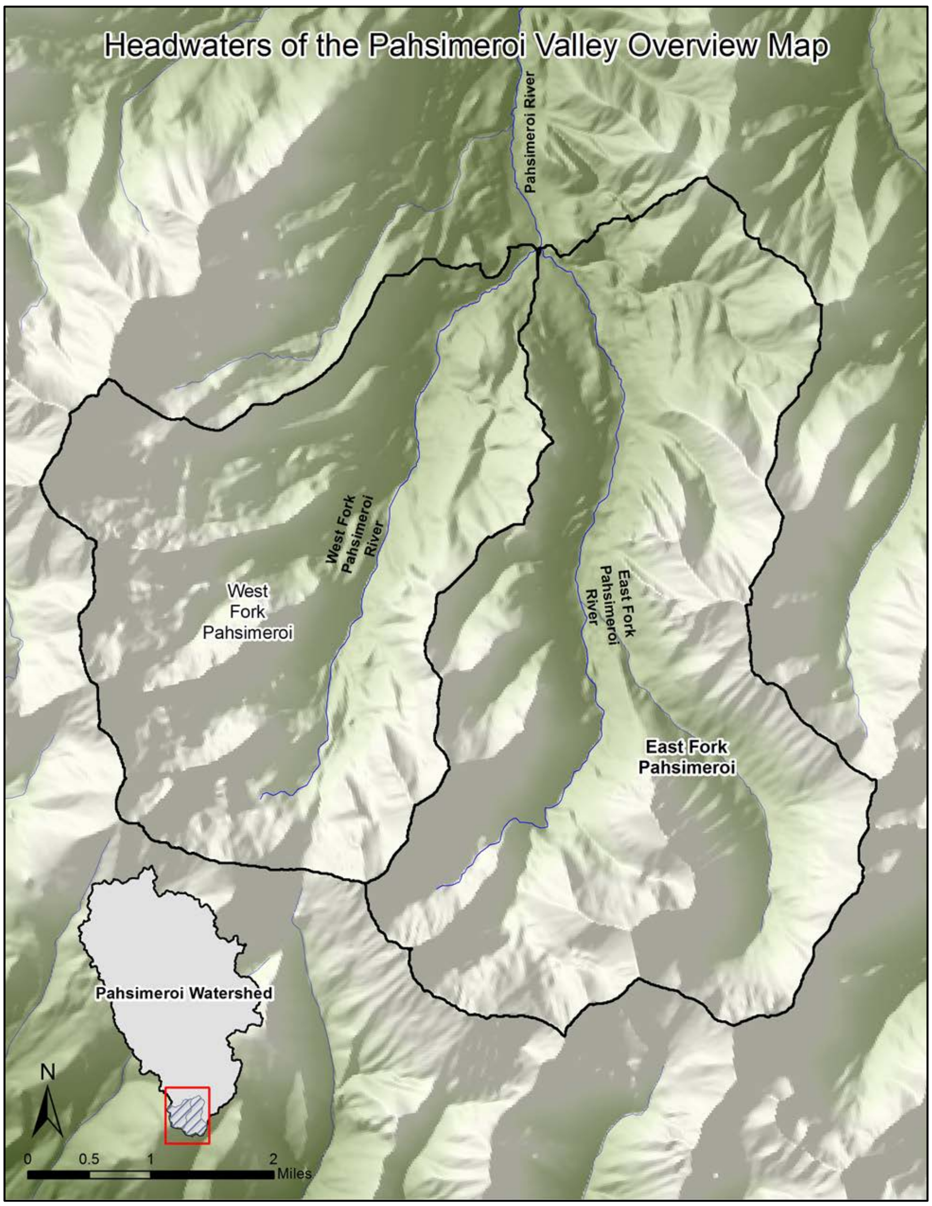

Figure 89. Location of Pahsimeroi Headwaters Valley Segment, comprising the West Fork and the East Fork drainages.

Upper Pahsimeroi Valley Segment (VS-2)

The Upper Pahsimeroi Valley Segment comprises the Upper Pahsimeroi River sub-watershed, excluding the West Fork and East Fork drainages, covering about 57,637 acres (Figure 90). The valley segment is along the Pahsimeroi River from about RM 64.55 to 52.50, and contains Geomorphic Reaches GR-1, GR-2, and GR-3. This valley segment is within the alluvial fan zone, where coarse sediment accumulates across broad alluvial fans and piedmonts before entering the transfer zone. Here, the basin-fill sediments are permeable, and the Pahsimeroi River loses water to the groundwater system.

Groundwater flow from the Lost River Range is an important component to the Pahsimeroi Valley aquifer. Geochemical analysis of underground flow found the Lost River Range to be the largest contributor to the Pahsimeroi Valley aquifer, and that underlying geologic structures influence gaining and losing reaches along the Pahsimeroi River (Whittier 2009). For example, an extension of the Goldburg Fault follows the Pahsimeroi River through this valley segment and could be providing a conduit through permeable, fractured rock, thereby exacerbating the surface water losses to the aquifer.

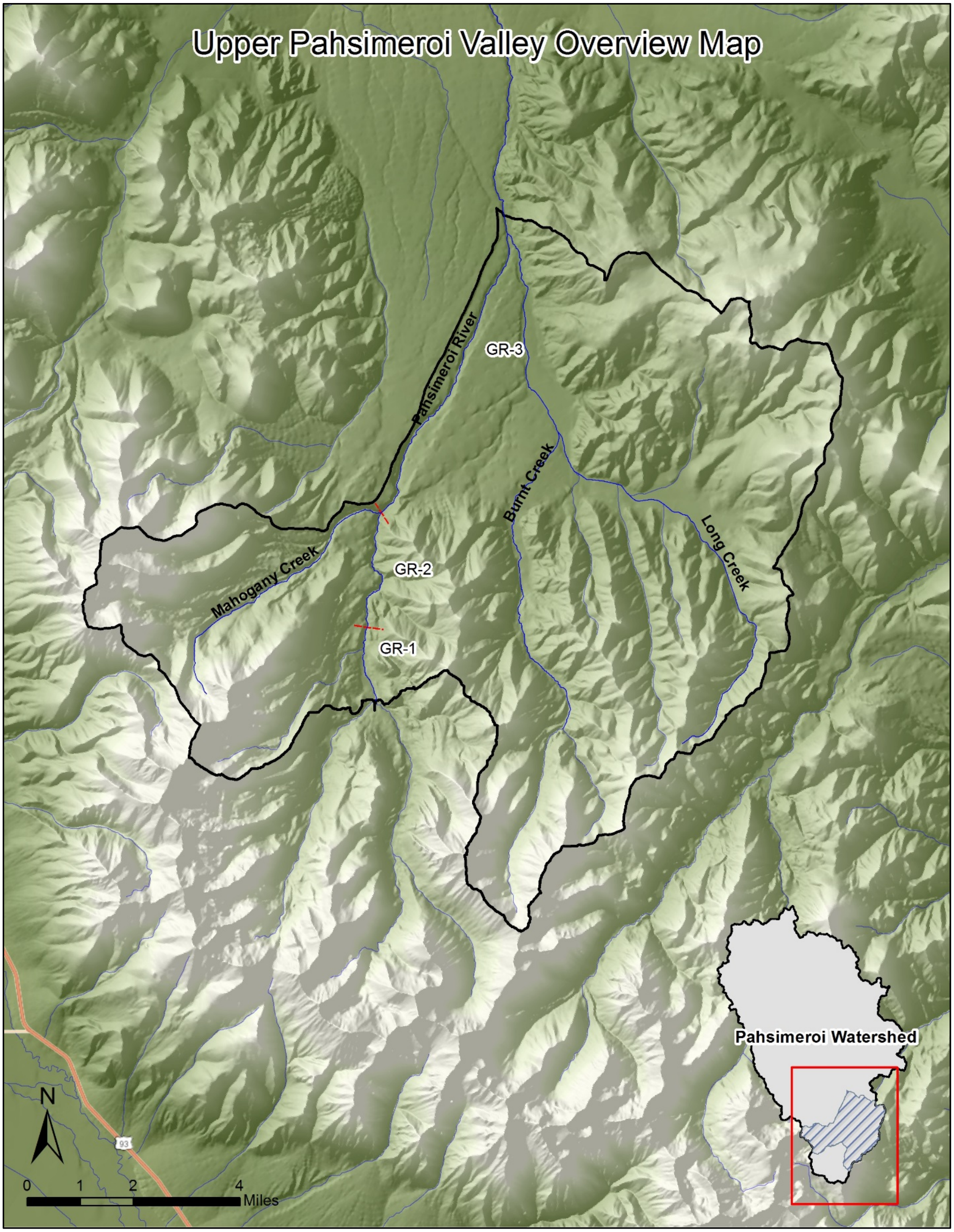

Figure 90. The Upper Pahsimeroi Valley Segment and associated geomorphic reaches (GR-1 through GR-3).

Geomorphic Reach GR-1 (RM 64.5 – 62.6)

Geomorphic Reach GR-1 is located along the Pahsimeroi River between RM 64.5 and RM 62.6 in a moderately confined valley with no valley bottom constraints (Figure 91). Reach characteristics are summarized below in Table 41.

Table 41. Summary of attributes for Geomorphic Reach GR-1.

Valley Segment	Reach	River Miles	Valley Slope (ft/ft)	Average Valley Width (ft)	Average Constrained Valley Width (ft)	Channel Slope (ft/ft)	Average Channel Width (ft)	Sinuosity	Entrenchment Ratio (ft/ft)	Constrained Entrenchment Ratio (ft/ft)	Human Disturbance Ratio (%)	Groundwater Characteristics	Geomorphic Characterization "Complex"	Geomorphic Characterization "Mixed"	Geomorphic Characterization "Simplified"
VS-2	GR-1	64.5 - 62.6	0.0185	391	391	0.0145	23	1.3	17	17	0%	-	19%	81%	0%

Forms

- Moderate sinuosity (little to no channel straightening) single-thread channel.
- Primarily pool-riffle morphology.
- Dense riparian vegetation consisting primarily of willow and other shrubs.
- Areas of bank erosion associated with lost riparian vegetation and cattle grazing.

Processes

- Relatively stable banks; minimal channel migration; some widening observed where riparian vegetation is lacking.
- Historical photos reveal periods of impounded water, suggesting beaver activity.
- Mixed sediment-transport regime, including deposition, temporary storage, and transport.

Human Impact

- Minimal human impact.
- Cattle grazing impacts, including bank erosion and lost riparian vegetation in several locations.
- Fine sediment from roads.

Response Potential

- Increased sinuosity and pool-riffle formation associated with riparian vegetation and instream obstruction (including beaver dams).
- Channel avulsion associated with instream obstruction (beaver dams, debris flows).
- Channel widening and simplification associated with lost bank vegetation and eroding banks.

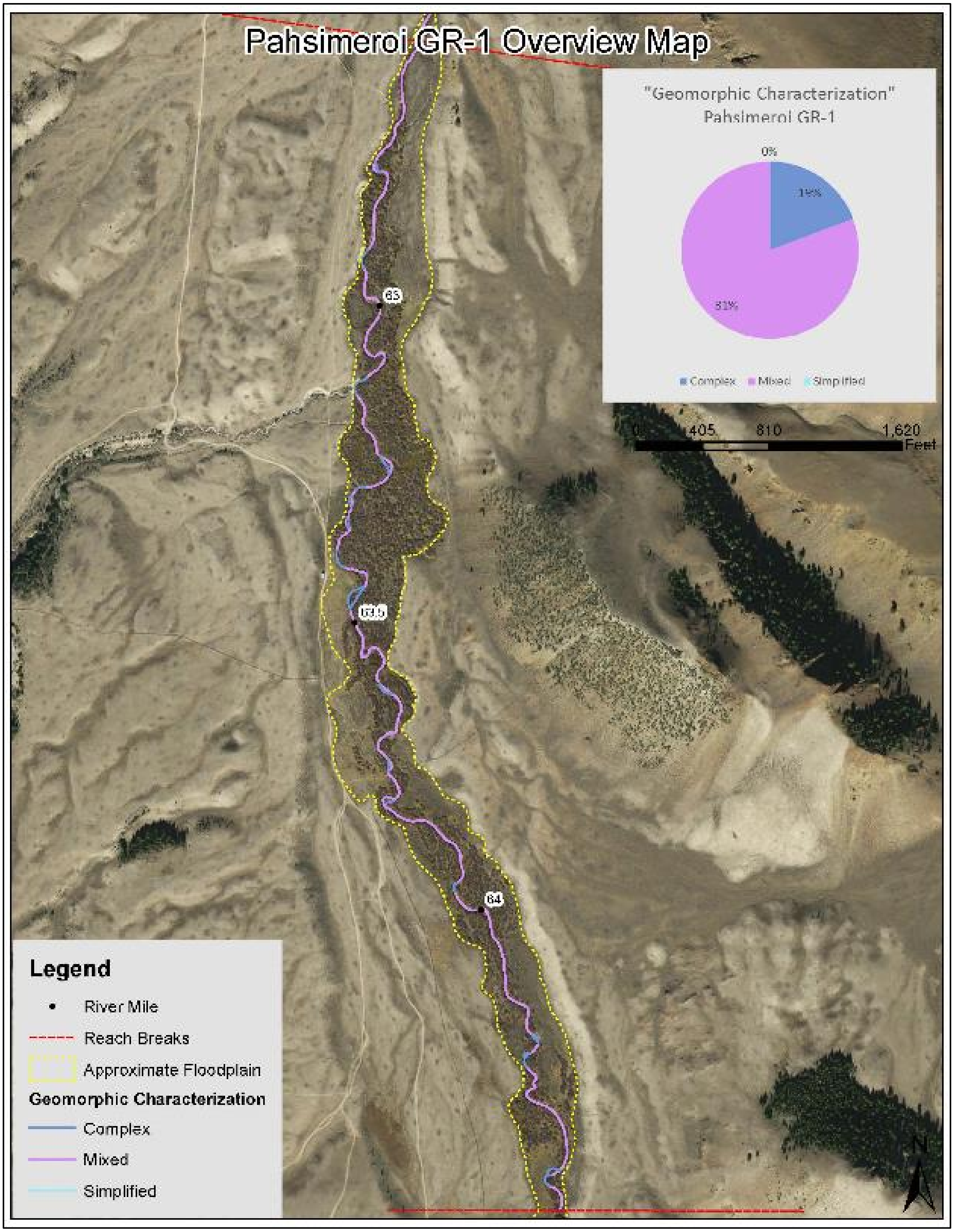

Figure 91. GR-1 overview map illustrating the approximate floodplain, geomorphic characterization, and human alterations to the floodplain.

Geomorphic Reach GR-2 (RM 62.6 – 59.8)

Geomorphic Reach GR-2 is located along the Pahsimeroi River between RM 62.6 and RM 59.8 in an unconfined valley with no valley bottom constraints (Figure 92). Reach characteristics are summarized below in Table 42.

Table 42. Summary of attributes for Geomorphic Reach GR-2.

Valley Segment	Reach	River Miles	Valley Slope (ft/ft)	Average Valley Width (ft)	Average Constrained Valley Width (ft)	Channel Slope (ft/ft)	Average Channel Width (ft)	Sinuosity	Entrenchment Ratio (ft/ft)	Constrained Entrenchment Ratio (ft/ft)	Human Disturbance Ratio (%)	Groundwater Characteristics	Geomorphic Characterization "Complex"	Geomorphic Characterization "Mixed"	Geomorphic Characterization "Simplified"
VS-2	GR-2	62.6 - 59.8	0.0194	204	204	0.0169	23	1.1	9	9	0%	-	20%	61%	19%

Forms

- Moderately sinuous (little to no channel straightening) single-thread channel.
- Primarily pool-riffle morphology.
- Narrow band of dense riparian vegetation consisting primarily of willow and other shrubs.
- Channel is largely confined by bedrock and/or terraces.

Processes

- Relatively stable banks; minimal channel migration.
- Three bedrock channel segments provide vertical grade control.
- Channel migration is limited but appears to be more downstream than lateral where observed.
- Mixed sediment-transport regime, including deposition, temporary storage, and transport.

Human Impacts

- Minimal human impact.
- Fine sediment from roads.

Response Potential

- Increased sinuosity and pool-riffle formation associated with riparian vegetation and instream obstruction (including beaver dams).
- Bed armoring within confined sections.
- Minimal incision anticipated due to bedrock grade controls.

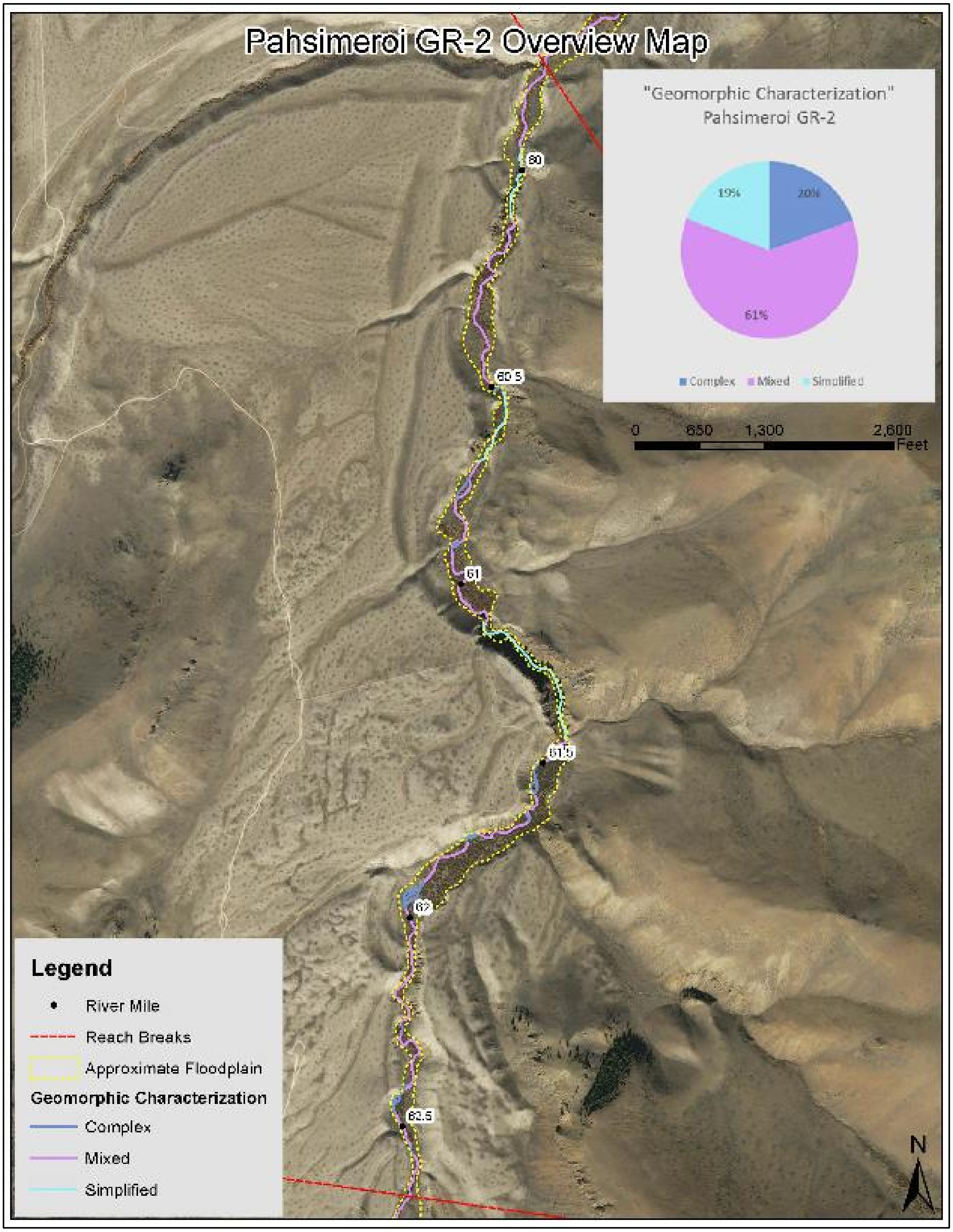

Figure 92. GR-2 overview map illustrating the approximate floodplain, geomorphic characterization, and human alterations to the floodplain.

Geomorphic Reach GR-3 (59.8 – 52.5)

Geomorphic Reach GR-3 is located along the Pahsimeroi River between RM 59.8 and RM 52.5 in an unconfined valley with minimal valley bottom constraints (Figure 93). Reach characteristics are summarized below in Table 43.

Table 43. Summary of attributes for Geomorphic Reach GR-3.

Valley Segment	Reach	River Miles	Valley Slope (ft/ft)	Average Valley Width (ft)	Average Constrained Valley Width (ft)	Channel Slope (ft/ft)	Average Channel Width (ft)	Sinuosity	Entrenchment Ratio (ft/ft)	Constrained Entrenchment Ratio (ft/ft)	Human Disturbance Ratio (%)	Groundwater Characteristics	Geomorphic Characterization "Complex"	Geomorphic Characterization "Mixed"	Geomorphic Characterization "Simplified"
VS-2	GR-3	59.8 - 52.5	0.0168	290	290	0.0152	28	1.1	10	10	1%	Losing	13%	87%	0%

Forms

- Low to moderate sinuosity (little to no channel straightening) single-thread channel.
- Primarily plane-bed morphology with limited pool-riffle associated with instream structure.
- Narrow band of dense riparian vegetation consisting primarily of willow and other shrubs.
- Channel and floodplain naturally confined by relic terraces.

Processes

- Relatively stable banks.
- Little to no channel migration (only in unconfined sections of the upper reach).
- Sediment transport dominated.

Human Impacts

- Minor human impacts from single road crossing with culvert, dispersed campsites, and limited cattle grazing.
- Fine sediment from roads.

Response Potential

- Forced pool-riffle formation associated with instream structure.
- Episodic channel avulsion associated with debris and/or ice jams.
- Surface water flows over porous alluvium and is lost to the groundwater system (losing reach).

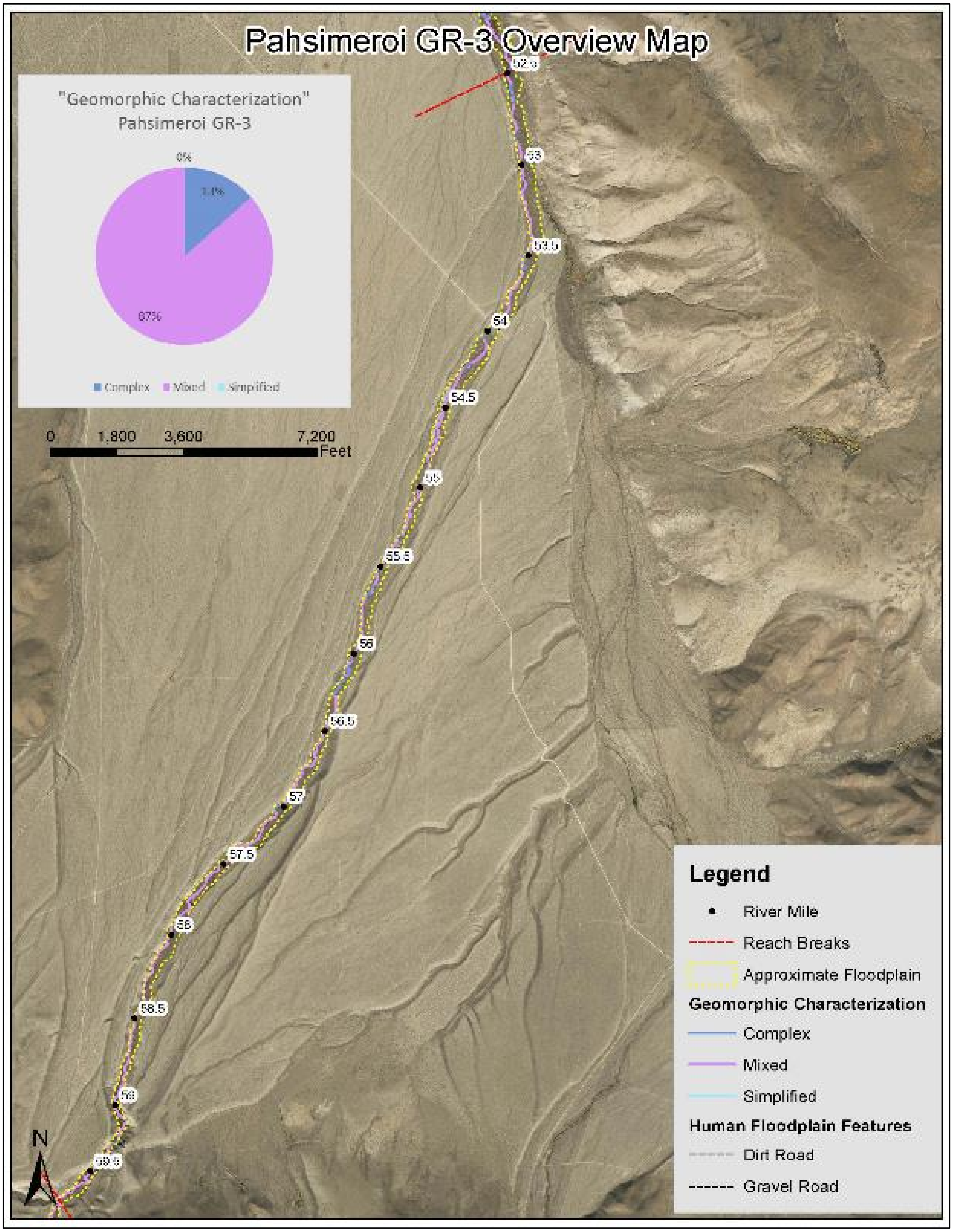

Figure 93. GR-3 overview map illustrating the approximate floodplain, geomorphic characterization, and human alterations to the floodplain.

Middle Pahsimeroi Valley Segment

The Middle Pahsimeroi Valley Segment comprises the Middle Pahsimeroi River sub-watershed (HUC 10 – 1706020202) covering about 219,335 acres (Figure 94). The valley segment is along the Pahsimeroi River from about RM 52.5 to RM 30.9 and contains Geomorphic Reaches GR-4, GR-5, GR-6, and GR-7. This valley segment includes the alluvial fan zone and transfer zone, where coarse sediment accumulates across broad alluvial fans and then is exchanged with the floodplain through channel-floodplain interactions. In the alluvial fan zone, the basin-fill sediments are permeable and the Pahsimeroi River loses water to the groundwater system through GR-6. The Pahsimeroi River is dewatered from about RM 41 to RM 34 in GR-7.

Flows daylight near RM 34 along a poorly defined channel and the Pahsimeroi River continues to gain flows through seeps and springs where a northwest bend along the Goldburg Fault creates a subsurface barrier and forces groundwater to surface (Whittier 2009).

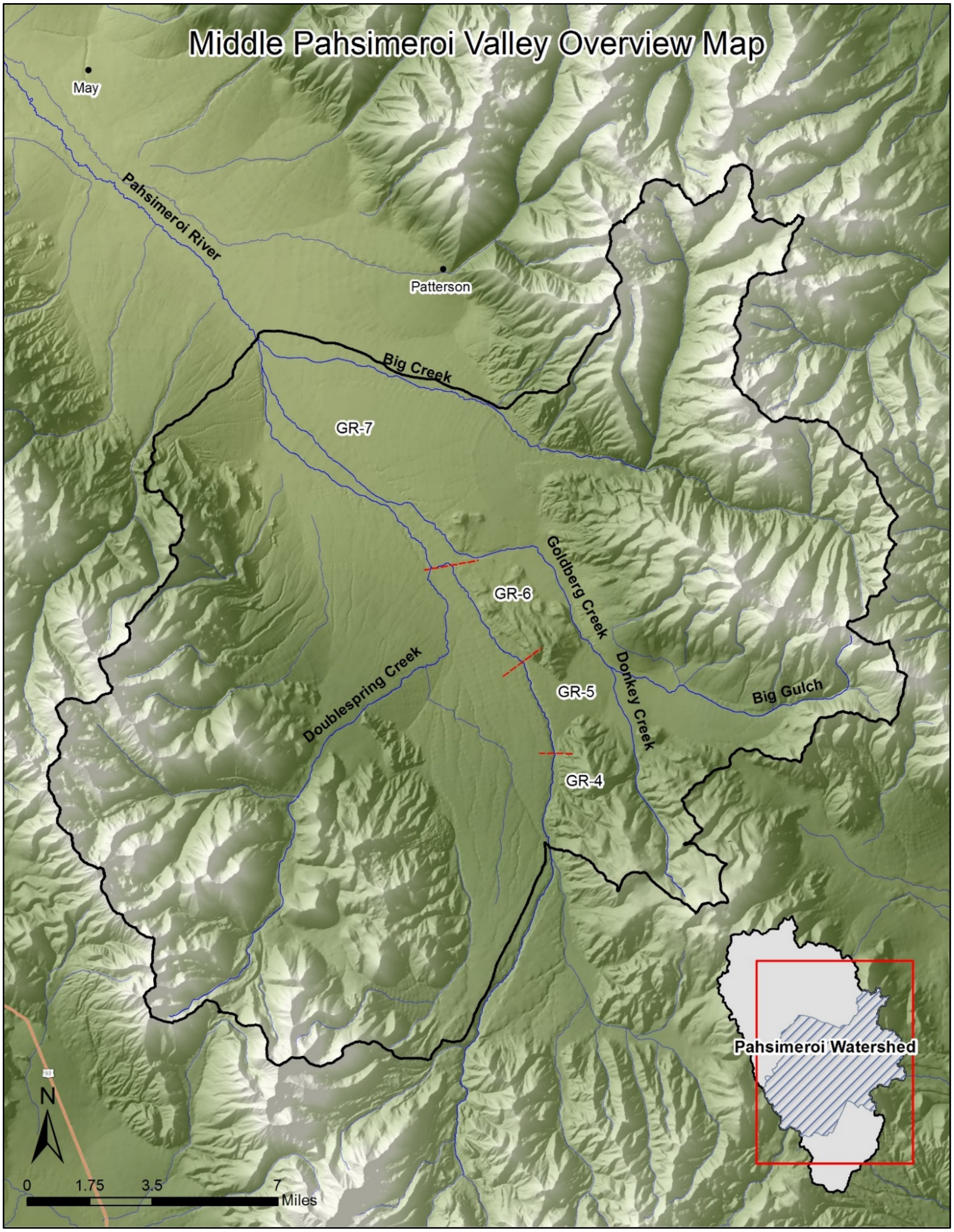

Figure 94. Middle Pahsimeroi Valley Segment and associated geomorphic reaches (GR-4 through GR-7).

Geomorphic Reach GR-4 (52.5 – 49.5)

Geomorphic Reach GR-4 is located along the Pahsimeroi River between RM 52.5 and RM 49.5 in an unconfined valley, with no valley bottom constraints (Figure 95). Reach characteristics are summarized below in Table 44.

Table 44. Summary of attributes for Geomorphic Reach GR-4

Valley Segment	Reach	River Miles	Valley Slope (ft/ft)	Average Valley Width (ft)	Average Constrained Valley Width (ft)	Channel Slope (ft/ft)	Average Channel Width (ft)	Sinuosity	Entrenchment Ratio (ft/ft)	Constrained Entrenchment Ratio (ft/ft)	Human Disturbance Ratio (%)	Groundwater Characteristics	Geomorphic Characterization "Complex"	Geomorphic Characterization "Mixed"	Geomorphic Characterization "Simplified"
VS-3	GR-4	52.5 - 49.5	0.0182	389	389	0.0155	23	1.2	17	17	1%	Losing	30%	70%	0%

Forms

- Low to moderate sinuosity (little to no channel straightening); single-thread channel.
- Primarily pool-riffle morphology with large plane bed sections where sinuosity is low.
- Visible point bars in several locations.
- Narrow band of dense riparian vegetation consisting of willow and other shrubs, with some small patches of cottonwood.
- Several abandoned avulsion channels present within the inset floodplain bound by terraces.

Processes

- Relatively stable banks where vegetation is present.
- Low to moderate occurrence of channel migration in unconfined areas.
- Mixed sediment-transport regime, including deposition, temporary storage, and transport.

Human Impacts

- Significant human impact primarily from three irrigation diversions.
- Channel commonly dewaters due to irrigation withdrawals and natural losses to groundwater.
- Cattle grazing impacts, including bank erosion and lost riparian vegetation in several locations.
- Fine sediment from roads.

Response Potential

- Returning diverted flows to the Pahsimeroi River could seasonally connect the upper Pahsimeroi River to the lower Pahsimeroi River when discharge is greater than 50 cfs (Meinzer 1924).
- Increased sinuosity and pool-riffle formation associated with riparian vegetation and instream obstruction (including beaver dams).
- Channel avulsion associated with instream obstruction (beaver dams, debris and ice jams).
- Channel widening and simplification associated with lost bank vegetation and eroding banks.

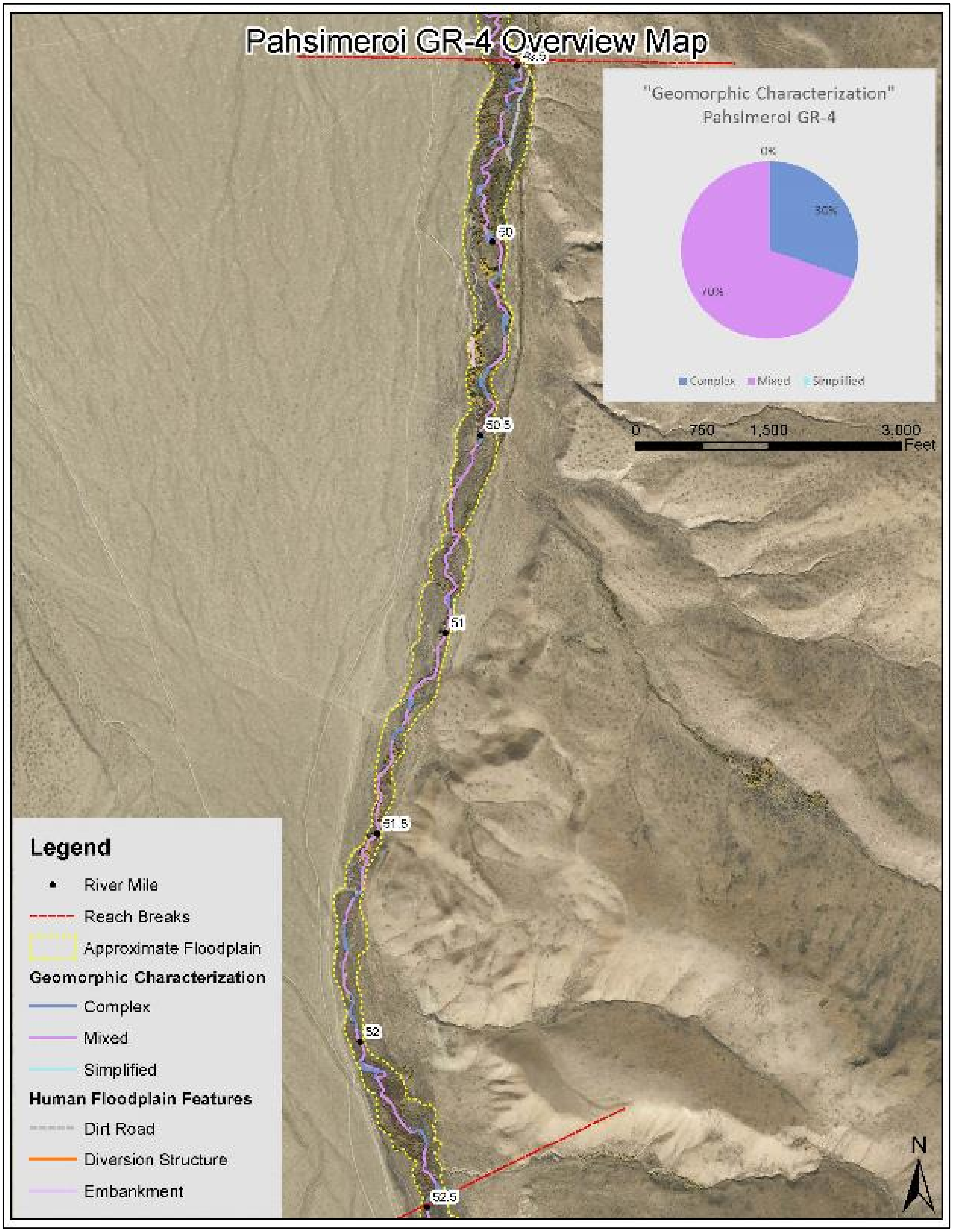

Figure 95. GR-4 overview map illustrating the approximate floodplain, geomorphic characterization, and human alterations to the floodplain.

Geomorphic Reach GR-5 (49.5 – 46.1)

Geomorphic Reach GR-5 is located along the Pahsimeroi River between RM 49.5 and RM 46.1 in an unconfined valley with no significant valley bottom constraints (Figure 96). Reach characteristics are summarized below in Table 45.

Table 45. Summary of attributes for Geomorphic Reach GR-5.

Valley Segment	Reach	River Miles	Valley Slope (ft/ft)	Average Valley Width (ft)	Average Constrained Valley Width (ft)	Channel Slope (ft/ft)	Average Channel Width (ft)	Sinuosity	Entrenchment Ratio (ft/ft)	Constrained Entrenchment Ratio (ft/ft)	Human Disturbance Ratio (%)	Groundwater Characteristics	Geomorphic Characterization "Complex"	Geomorphic Characterization "Mixed"	Geomorphic Characterization "Simplified"
VS-3	GR-5	49.5 - 46.1	0.0188	208	208	0.0164	18	1.1	11	11	1%	Losing	41%	56%	2%

Forms

- Low to moderate sinuosity (little to no channel straightening); single-thread channel.
- Primarily pool-riffle morphology.
- Discontinuous riparian vegetation consisting primarily of willow and other shrubs, with small patches of cottonwood; channel dewatering limits riparian growth.
- Areas of bank erosion associated with areas lacking riparian vegetation.

Processes

- Channel migration and some widening observed where riparian vegetation is lacking.
- Mixed sediment-transport regime, including deposition, temporary storage, and transport.

Human Impacts

- Channel seasonally dewaters or has significantly reduced surface water flows due to upstream irrigation diversions and natural infiltration through porous alluvium.
- Cattle grazing impacts, including bank erosion and lost riparian vegetation in several locations.
- Fine sediment from roads.

Response Potential

- Returning diverted flows to the Pahsimeroi River could provide seasonal surface water flows through this reach.
- Increased sinuosity and pool-riffle formation associated with riparian vegetation and instream obstruction.
- Channel avulsion associated with instream obstruction (debris and ice jams).
- Channel widening and simplification associated with lost bank vegetation and eroding banks.

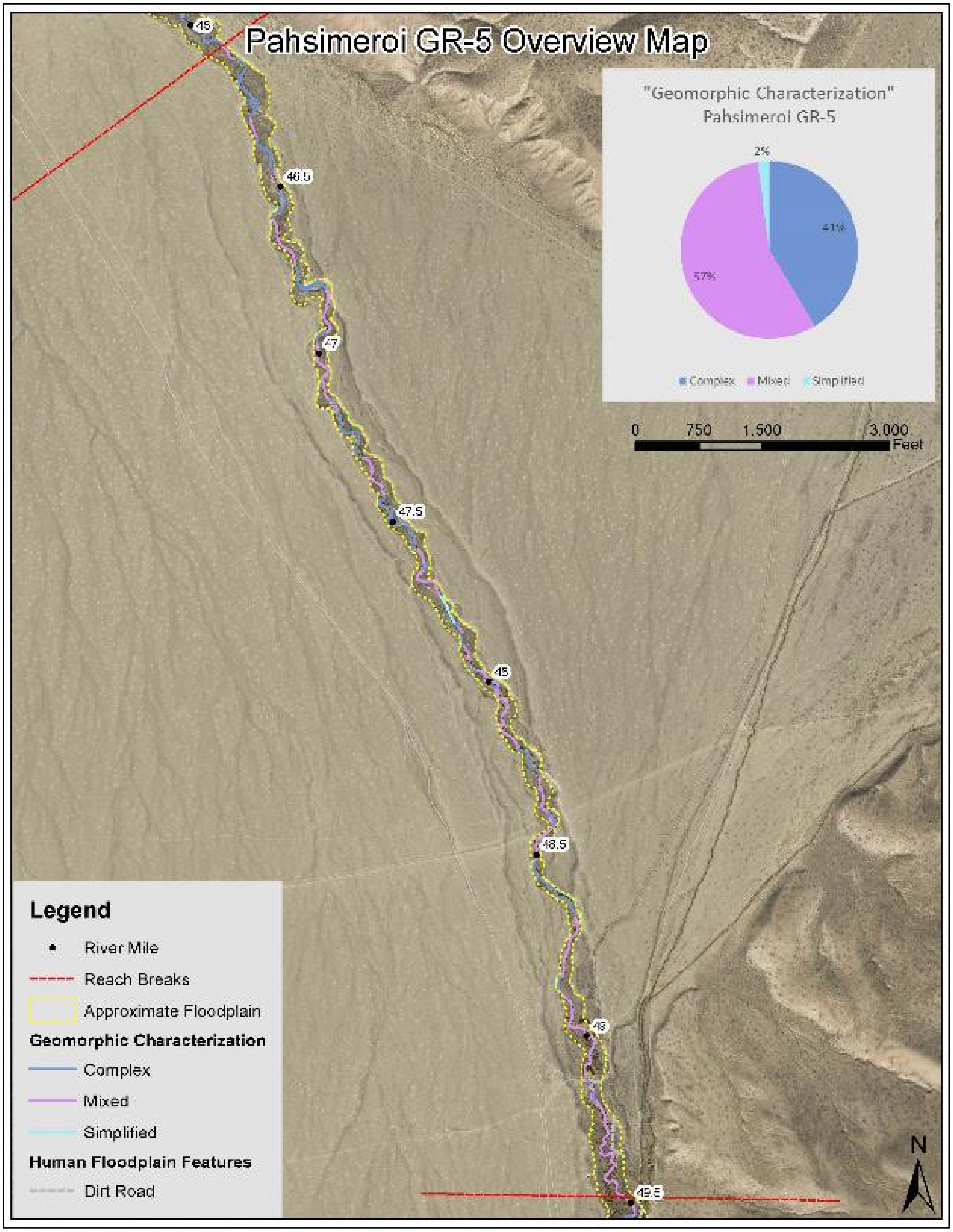

Figure 96. GR-5 overview map illustrating the approximate floodplain, geomorphic characterization, and human alterations to the floodplain.

Geomorphic Reach GR-6 (RM 46.1 – 41.6)

Geomorphic Reach GR-6 is located along the Pahsimeroi River between RM 46.1 and RM 41.6 in an unconfined valley with minimal valley bottom constraints (Figure 97). Reach characteristics are summarized below in Table 46.

Table 46. Summary of attributes for Geomorphic Reach GR-6.

Valley Segment	Reach	River Miles	Valley Slope (ft/ft)	Average Valley Width (ft)	Average Constrained Valley Width (ft)	Channel Slope (ft/ft)	Average Channel Width (ft)	Sinuosity	Entrenchment Ratio (ft/ft)	Constrained Entrenchment Ratio (ft/ft)	Human Disturbance Ratio (%)	Groundwater Characteristics	Geomorphic Characterization "Complex"	Geomorphic Characterization "Mixed"	Geomorphic Characterization "Simplified"
VS-3	GR-6	46.1 - 41.6	0.0165	594	594	0.0128	18	1.3	33	33	3%	Losing	57%	43%	0%

Forms

- Moderately sinuous (little to no channel straightening); primarily single-thread channel.
- Primarily pool-riffle morphology.
- Discontinuous riparian vegetation consisting of primarily willow and other shrubs, with cottonwood patches. Seasonally dry channel limits riparian growth.
- Areas of bank erosion associated with areas lacking riparian vegetation.

Processes

- Channel migration and some widening observed where riparian vegetation is lacking.
- Mixed sediment-transport regime, including deposition, temporary storage, and transport.

Human Impacts

- Channel seasonally dewaters or has significantly reduced surface water flows due to irrigation diversions and natural infiltration through porous alluvium.
- Cattle grazing impacts, including bank erosion and lost riparian vegetation in several locations.
- Fine sediment from roads.

Response Potential

- Returning diverted flows to the Pahsimeroi River could provide seasonal surface water flows through this reach.
- Increased sinuosity and pool-riffle formation associated with riparian vegetation and instream obstruction.
- Channel avulsion associated with instream obstruction (aggradation of coarse sediment, debris, and ice jams).
- Channel widening and simplification where lacking riparian vegetation.

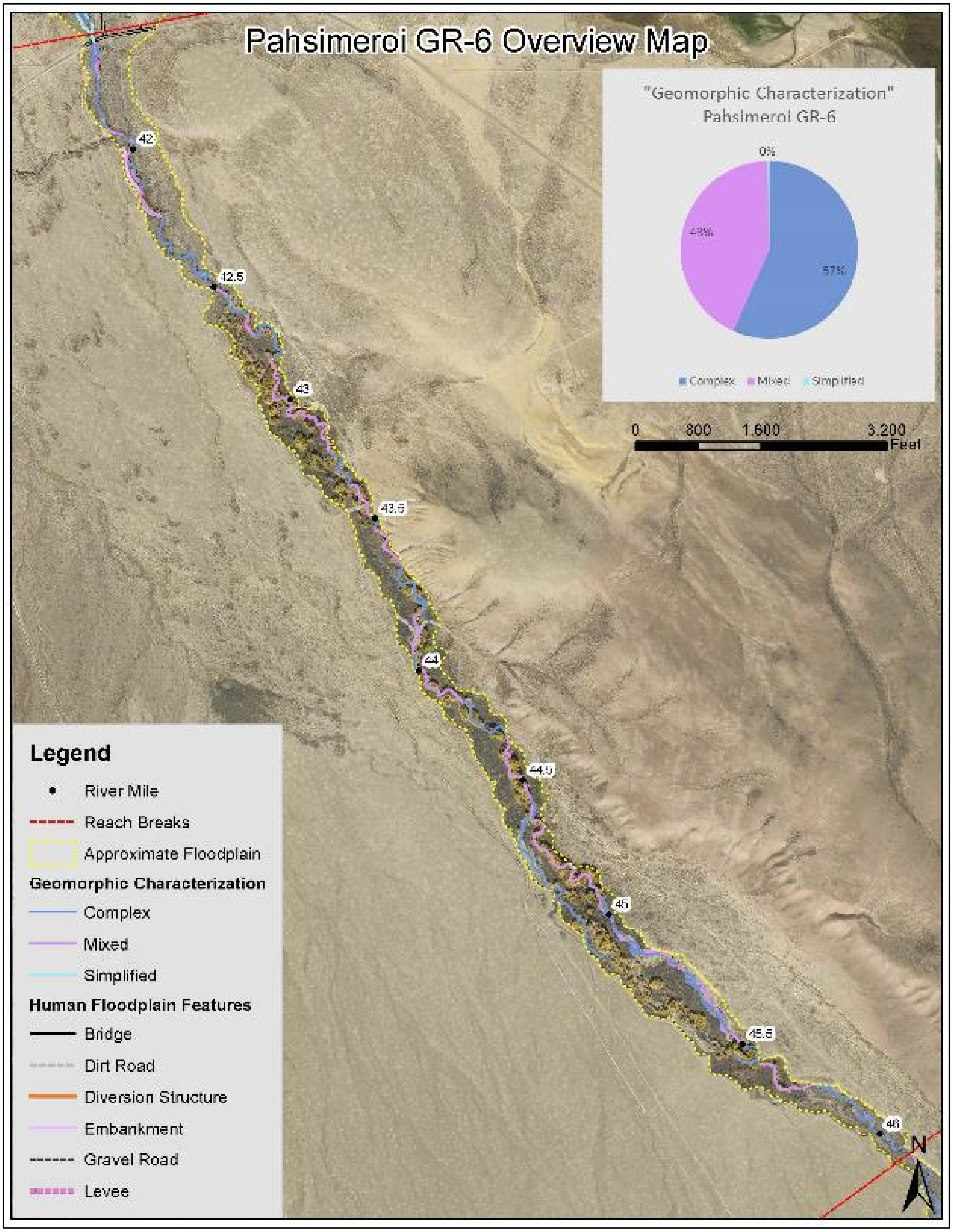

Figure 97. GR-6 overview map illustrating the approximate floodplain, geomorphic characterization, and human alterations to the floodplain.

Geomorphic Reach GR-7 (RM 41.6 – 30.9)

Geomorphic Reach GR-7 is located along the Pahsimeroi River between RM 41.6 and RM 30.9 in a naturally unconfined valley with significant valley bottom constraints associated with roads and irrigation infrastructure (Figure 98). Reach characteristics are summarized below in Table 47.

Table 47. Summary of attributes for Geomorphic Reach GR-7.

Valley Segment	Reach	River Miles	Valley Slope (ft/ft)	Average Valley Width (ft)	Average Constrained Valley Width (ft)	Channel Slope (ft/ft)	Average Channel Width (ft)	Sinuosity	Entrenchment Ratio (ft/ft)	Constrained Entrenchment Ratio (ft/ft)	Human Disturbance Ratio (%)	Groundwater Characteristics	Geomorphic Characterization "Complex"	Geomorphic Characterization "Mixed"	Geomorphic Characterization "Simplified"
VS-3	GR-7	41.6 - 30.9	0.0124	3187	-	0.0098	13	1.3	243	-	3%	Losing	15%	14%	7%

Forms

- Moderate sinuosity (little to no channel straightening); split flow (north and south channel).
- Dewatered from about RM 40.95 to RM 33.75 with no definitive channel morphology.
- Primarily pool-riffle morphology where the channel is well-defined.
- Discontinuous riparian vegetation consisting primarily of willow and other shrubs, with cottonwood patches.
- Areas of bank erosion associated with lost riparian vegetation and cattle grazing.

Processes

- The north channel loses flow while the south channel gains flow from groundwater.
- Springs discharge groundwater to the south channel from the Doublesprings alluvial fan, and the Pahsimeroi River starts flowing intermittently.
- Sediment regime is dominated by deposition with episodic transport during large floods.

Human Impacts

- The Pahsimeroi River dewaters between RM 40.95 and RM 33.75 due to infiltration through porous alluvium and multiple irrigation diversions.
- Cattle grazing impacts downstream of the dewatered section include bank erosion and lost riparian vegetation in several locations.
- Fine sediment from roads.
- Ditching, impoundments, irrigation diversions, airstrip, dirt roads, cattle grazing, and bridges.

Response Potential

- Returning diverted flows could provide seasonal surface water through this reach.
- Increased sinuosity and pool-riffle formation associated with riparian vegetation and instream obstruction.
- Channel avulsion associated with instream obstruction (coarse sediment deposition, debris, and ice jams).
- Channel widening and simplification associated with lost bank vegetation.

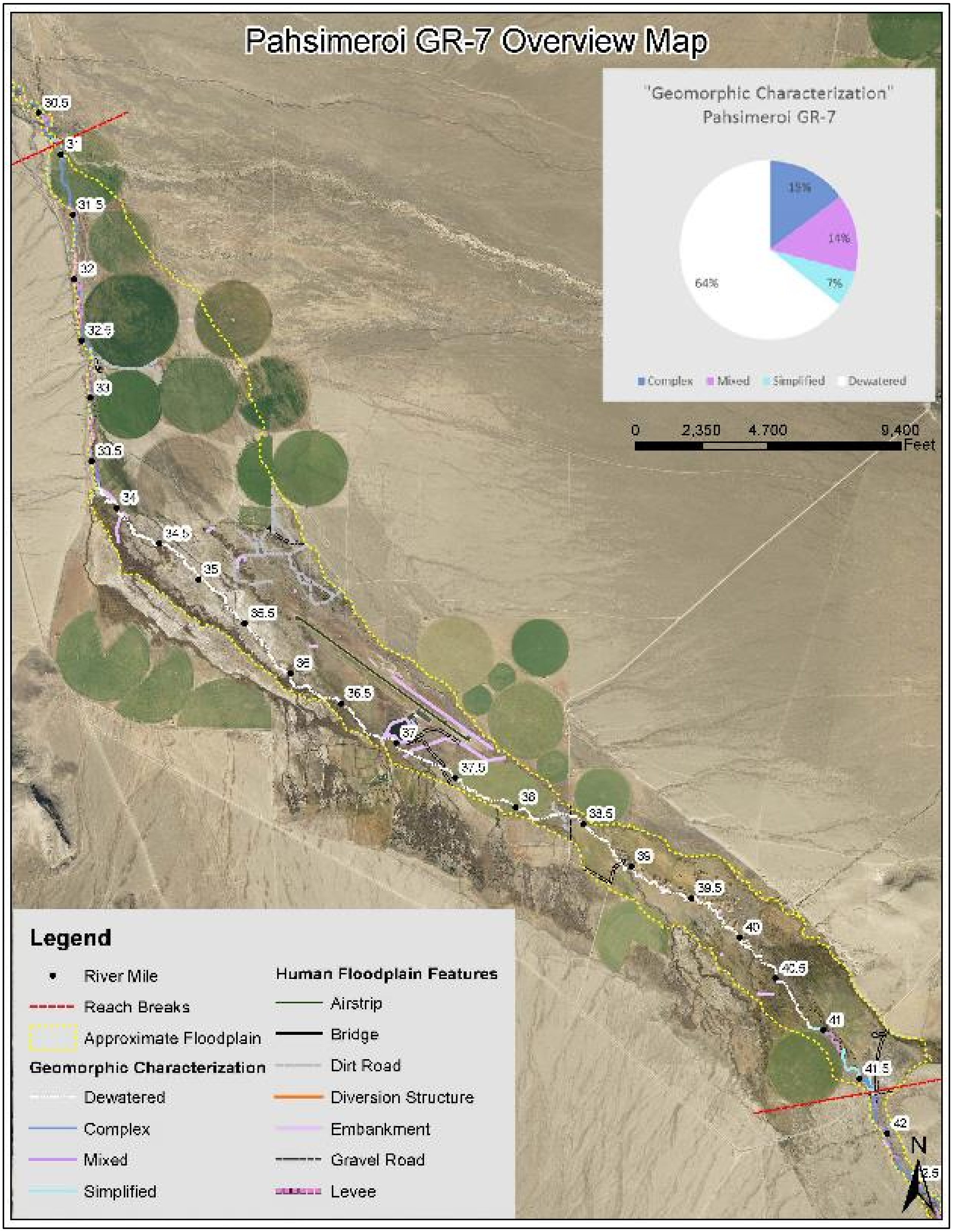

Figure 98. GR-7 overview map illustrating the approximate floodplain, geomorphic characterization, and human alterations to the floodplain.

Lower Pahsimeroi Valley Segment

The Lower Pahsimeroi Valley Segment comprises the Lower Pahsimeroi River sub-watershed (HUC 10 – 1706020203) covering about 234,993 acres (Figure 99). The valley segment is along the Pahsimeroi River from about RM 30.9 to RM 0 and contains Geomorphic Reaches GR-8, GR-9, and GR-10. This valley segment is within the transfer zone and deposition zones, where sediment is exchanged with the floodplain through channel-floodplain interactions and deposited in low-gradient areas.

Along GR-8, the Pahsimeroi River loses water to the groundwater system and can intermittently run dry due to highly porous surficial geology, irrigation diversions, groundwater recharge, or a combination of all three. The Pahsimeroi River gains flows from groundwater through GR-9 and GR-10 as the bedrock shallows near the confluence with the Salmon River. These two lower geomorphic reaches are highly groundwater-influenced and maintain perennial flows (Whittier 2009).

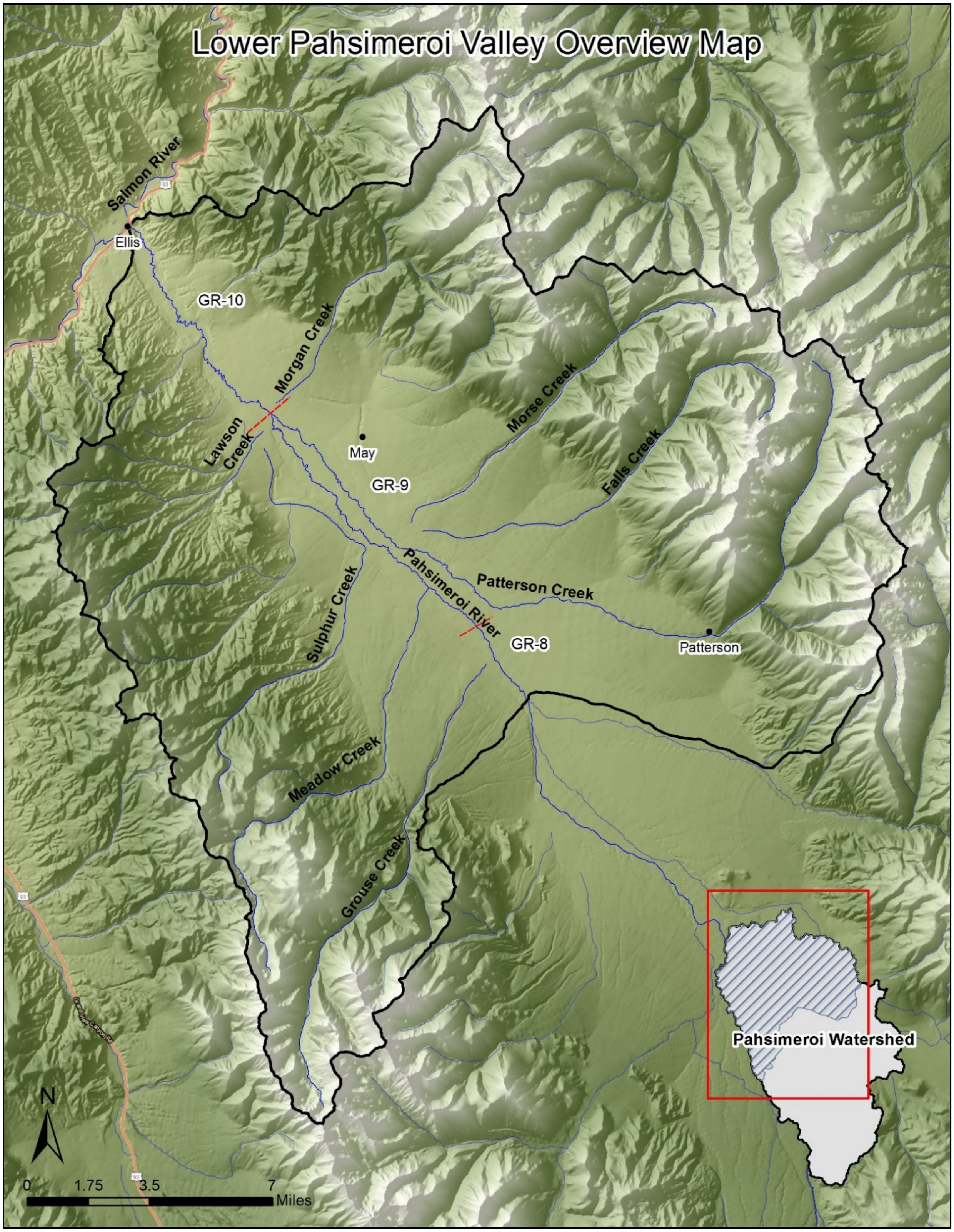

Figure 99. Lower Pahsimeroi Valley Segment and associated geomorphic reaches (GR-8 through GR-10).

Geomorphic Reach GR-8 (RM 30.9 – 27.2)

Geomorphic Reach GR-8 is located along the Pahsimeroi River between RM 30.9 and RM 27.2 in a naturally unconfined valley with some valley bottom constraints associated with human features (Figure 100). Reach characteristics are summarized below in Table 48.

Table 48. Summary of attributes for Geomorphic Reach GR-8.

Valley Segment	Reach	River Miles	Valley Slope (ft/ft)	Average Valley Width (ft)	Average Constrained Valley Width (ft)	Channel Slope (ft/ft)	Average Channel Width (ft)	Sinuosity	Entrenchment Ratio (ft/ft)	Constrained Entrenchment Ratio (ft/ft)	Human Disturbance Ratio (%)	Groundwater Characteristics	Geomorphic Characterization "Complex"	Geomorphic Characterization "Mixed"	Geomorphic Characterization "Simplified"
VS-4	GR-8	30.9 - 27.2	0.0089	315	-	0.0069	17	1.3	19	-	3%	Neutral	59%	27%	13%

Forms

- Moderately sinuous (minor channel straightening) single-thread channel.
- Large portions of the reach are seasonally dry due to irrigation diversions and natural losses to groundwater.
- Primarily pool-riffle morphology.
- Discontinuous riparian vegetation consisting primarily of willow and other shrubs, with some cottonwood; poor riparian growth where the channel is seasonally dry.
- Areas of bank erosion associated with lost riparian vegetation and cattle grazing.

Processes

- Poor bank stability and areas of channel migration/widening where riparian vegetation is lacking.
- Mixed sediment-transport regime, including primarily deposition with periods of transport during large floods.

Human Impacts

- Irrigation diversions contribute to surface water losses and a seasonally dry channel.
- Fine sediment from roads.
- Irrigation diversions, cattle grazing, dirt roads, fords and bridges.

Response Potential

- Increased sinuosity and pool-riffle formation associated with riparian vegetation and instream obstructions, primarily in response to large floods when surface water has sufficient capacity to mobilize sediment.
- Channel avulsion associated with in-stream obstruction (coarse sediment deposition, debris, and ice jams).
- Channel widening and simplification associated with lost bank vegetation.

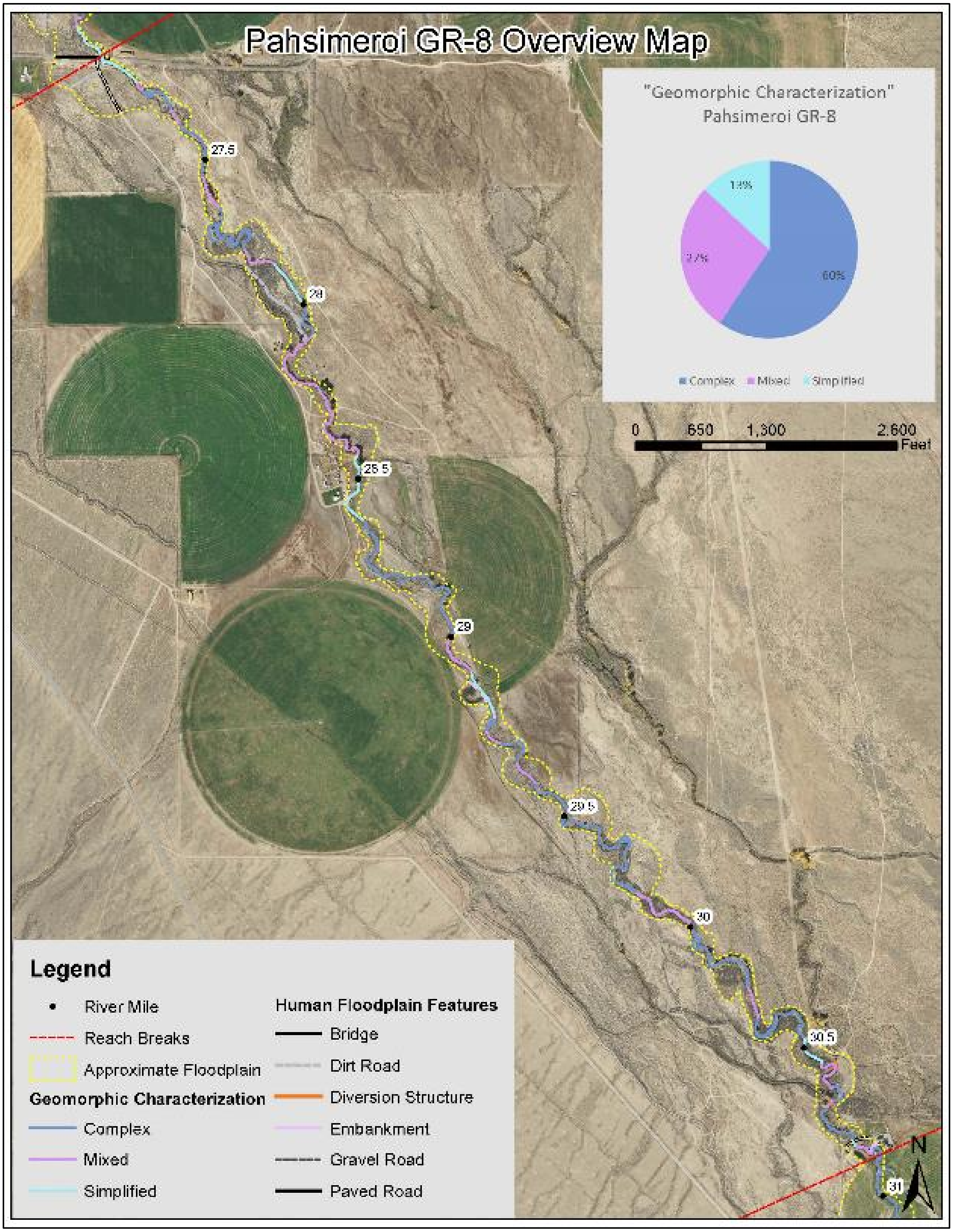

Figure 100. GR-8 overview map illustrating the approximate floodplain, geomorphic characterization, and human alterations to the floodplain.

Geomorphic Reach GR-9 (RM 27.2 – 12.8)

Geomorphic Reach GR-9 is located along the Pahsimeroi River between RM 27.2 and RM 12.8 in a naturally unconfined valley with some valley bottom constraints associated with human features, such as bridges and roads (Figure 101). Reach characteristics are summarized below in Table 49.

Table 49. Summary of attributes for Geomorphic Reach GR-9.

Valley Segment	Reach	River Miles	Valley Slope (ft/ft)	Average Valley Width (ft)	Average Constrained Valley Width (ft)	Channel Slope (ft/ft)	Average Channel Width (ft)	Sinuosity	Entrenchment Ratio (ft/ft)	Constrained Entrenchment Ratio (ft/ft)	Human Disturbance Ratio (%)	Groundwater Characteristics	Geomorphic Characterization "Complex"	Geomorphic Characterization "Mixed"	Geomorphic Characterization "Simplified"
VS-4	GR-9	27.2 - 12.8	0.0075	3672	-	0.0045	19	1.7	195	-	2%	Gaining	60%	33%	7%

Forms

- Moderate to high sinuosity, single-thread channel with many spring-fed tributary channels.
- Primarily pool-riffle morphology.
- Discontinuous riparian vegetation consisting primarily of willow and other shrubs; significant areas of riparian vegetation clearing, especially in the floodplain.
- Areas of bank erosion associated with lost riparian vegetation.

Processes

- Relatively stable banks; minimal channel migration; some widening observed where riparian vegetation is lacking.
- Pools and riffles forced by flow interactions with woody material and riparian vegetation.
- Mixed sediment-transport regime, including deposition, temporary storage, and transport during large floods.

Human Impacts

- Cattle grazing impacts include bank erosion and lost riparian vegetation in several locations.
- Fine sediment from roads, floodplain erosion, and bank erosion.
- Irrigation diversions, ditching, cattle grazing, channel straightening, dirt roads, fords, and bridges.

Response Potential

- Increased sinuosity and pool-riffle formation associated with riparian vegetation and instream obstructions.
- Channel avulsion associated with instream obstruction (sediment deposition especially in the upper reach, beaver dams, and debris).
- Potential for channel incision where confined and/or straightened.
- Channel widening and simplification associated with lost bank vegetation and eroding banks.

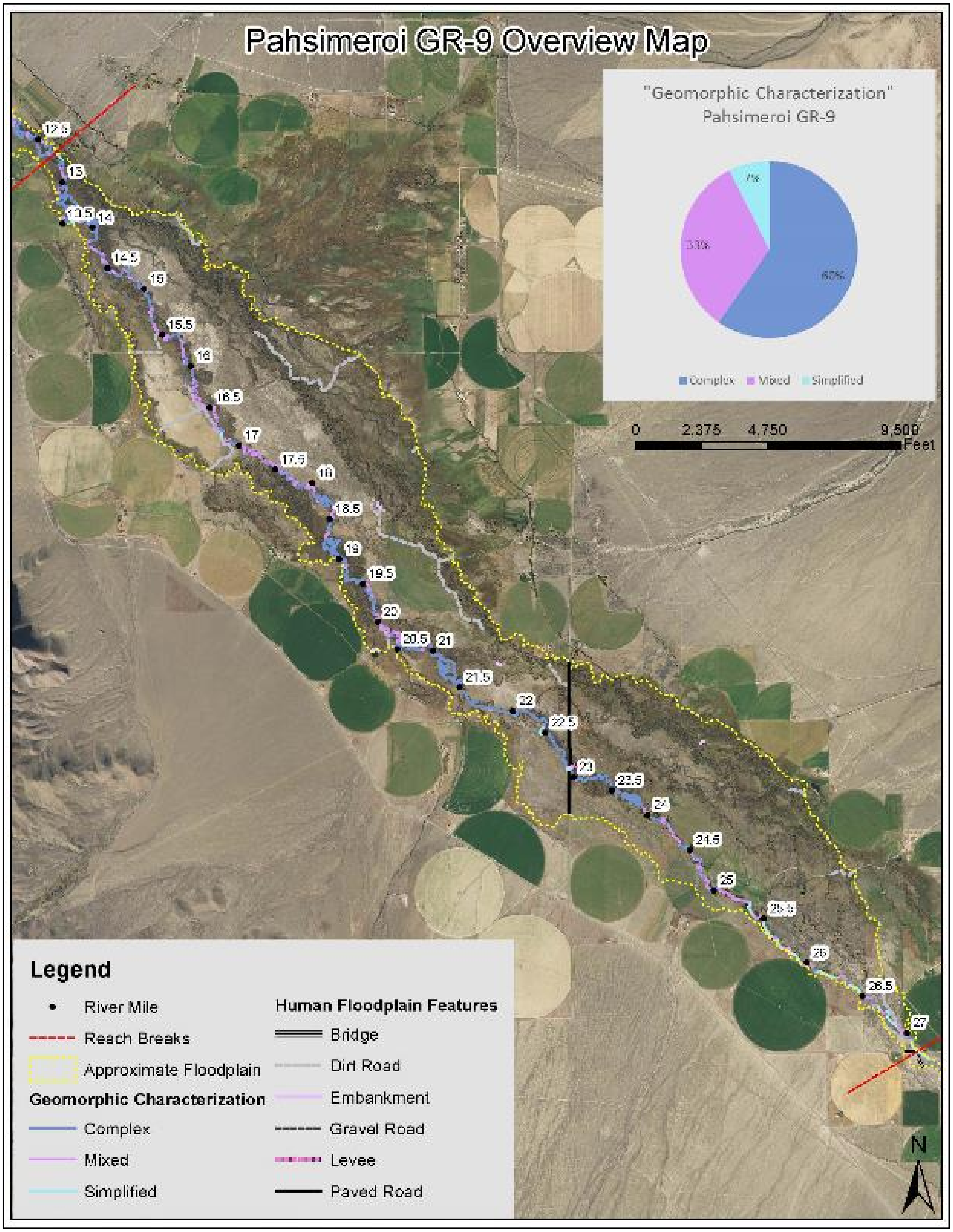

Figure 101. GR-9 overview map illustrating the approximate floodplain, geomorphic characterization, and human alterations to the floodplain.

Geomorphic Reach GR-10 (RM 12.8 – 0)

Geomorphic Reach GR-10 is located along the Pahsimeroi River between RM 12.8 and RM 0.0 in a naturally unconfined valley with some valley bottom constraints associated with human features, such as bridges and roads (Figure 102). Reach characteristics are summarized below in Table 50.

Table 50. Summary of attributes for Geomorphic Reach GR-10.

Valley Segment	Reach	River Miles	Valley Slope (ft/ft)	Average Valley Width (ft)	Average Constrained Valley Width (ft)	Channel Slope (ft/ft)	Average Channel Width (ft)	Sinuosity	Entrenchment Ratio (ft/ft)	Constrained Entrenchment Ratio (ft/ft)	Human Disturbance Ratio (%)	Groundwater Characteristics	Geomorphic Characterization "Complex"	Geomorphic Characterization "Mixed"	Geomorphic Characterization "Simplified"
VS-4	GR-10	12.8 - 0	0.0057	1510	-	0.0032	34	1.8	44	-	7%	Gaining	54%	44%	2%

Forms

- Moderate to high sinuosity, single-thread channel with numerous spring-fed side channels and oxbows.
- Primarily pool-riffle morphology.
- Discontinuous riparian vegetation consisting primarily of willow and other shrubs; significant areas of riparian vegetation clearing, especially in the floodplain.
- Areas of bank erosion associated with lost riparian vegetation.

Processes

- Relatively stable banks; minimal channel migration; some widening observed where riparian vegetation is lacking.
- Pools and riffles forced by flow interactions with woody material and riparian vegetation.
- Mixed sediment-transport regime, including deposition, temporary storage, and transport during large floods.

Human Impacts

- Cattle grazing impacts include bank erosion and lost riparian vegetation in several locations.
- Three roads that bisect the floodplain may inhibit dynamic channel-floodplain interactions.
- Flow diversions to two fish hatcheries.
- Fine sediment from roads, floodplain erosion, and bank erosion.
- Irrigation diversions, ditching, cattle grazing, channel straightening, dirt roads, fords, and bridges.

Response Potential

- Increased sinuosity and pool-riffle formation associated with riparian vegetation and instream obstructions.
- Channel avulsion associated with instream obstruction (beaver dams and debris).
- Spring-fed tributary channel formation or augmentation.
- Potential for channel incision where confined and/or straightened.
- Channel widening and simplification associated with lost bank vegetation and eroding banks.

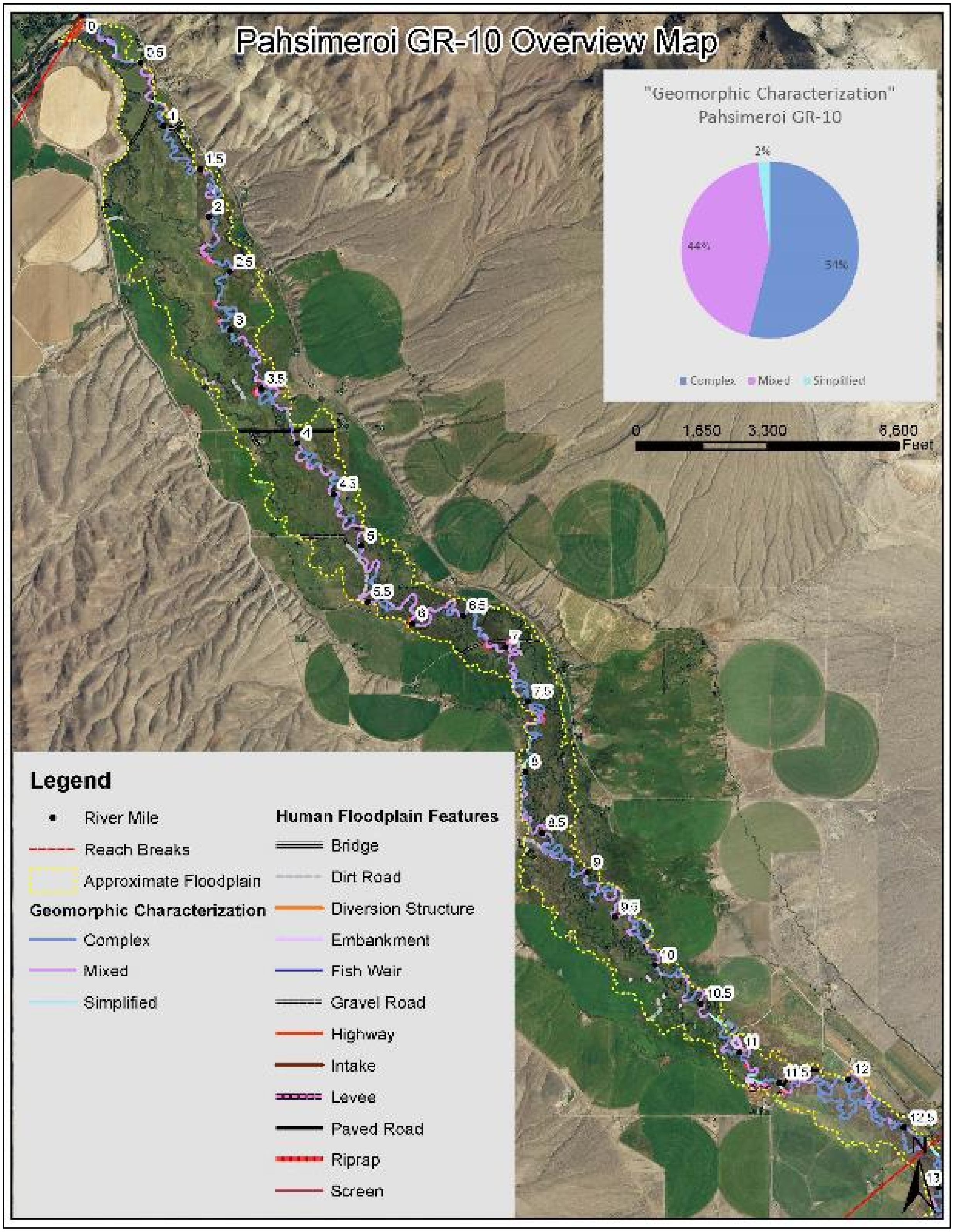

Figure 102. GR-10 overview map illustrating the approximate floodplain, geomorphic characterization, and human alterations to the floodplain.

Temperature and Climate Change Assessment

Chinook salmon

Under current conditions, water temperatures in the Pahsimeroi River are rarely to never below minimum or above maximum values for Chinook salmon (Figure 103). Only in brief periods during the spring (smolts) and summer (parr) are water temperatures below optimum conditions for Chinook salmon. Alternatively, spring and summer temperature tend to exceed optimum values for extended periods. Elevated temperatures potentially increase stress on adults during the staging (holding) and spawning periods, decrease survival during incubation/emergence, and increase food requirements for spring smolts and summer parr. Under an assumed 3° C water temperature increase scenario, conditions worsen for all five life stages evaluated (Figure 104). For both adults (holding and spawning) and juveniles (emergence, summer parr, spring smolts), water temperatures are above optimum for a majority of the time. Moreover, acute (lethal) temperatures may be expected during the summer for both holding and spawning adults.

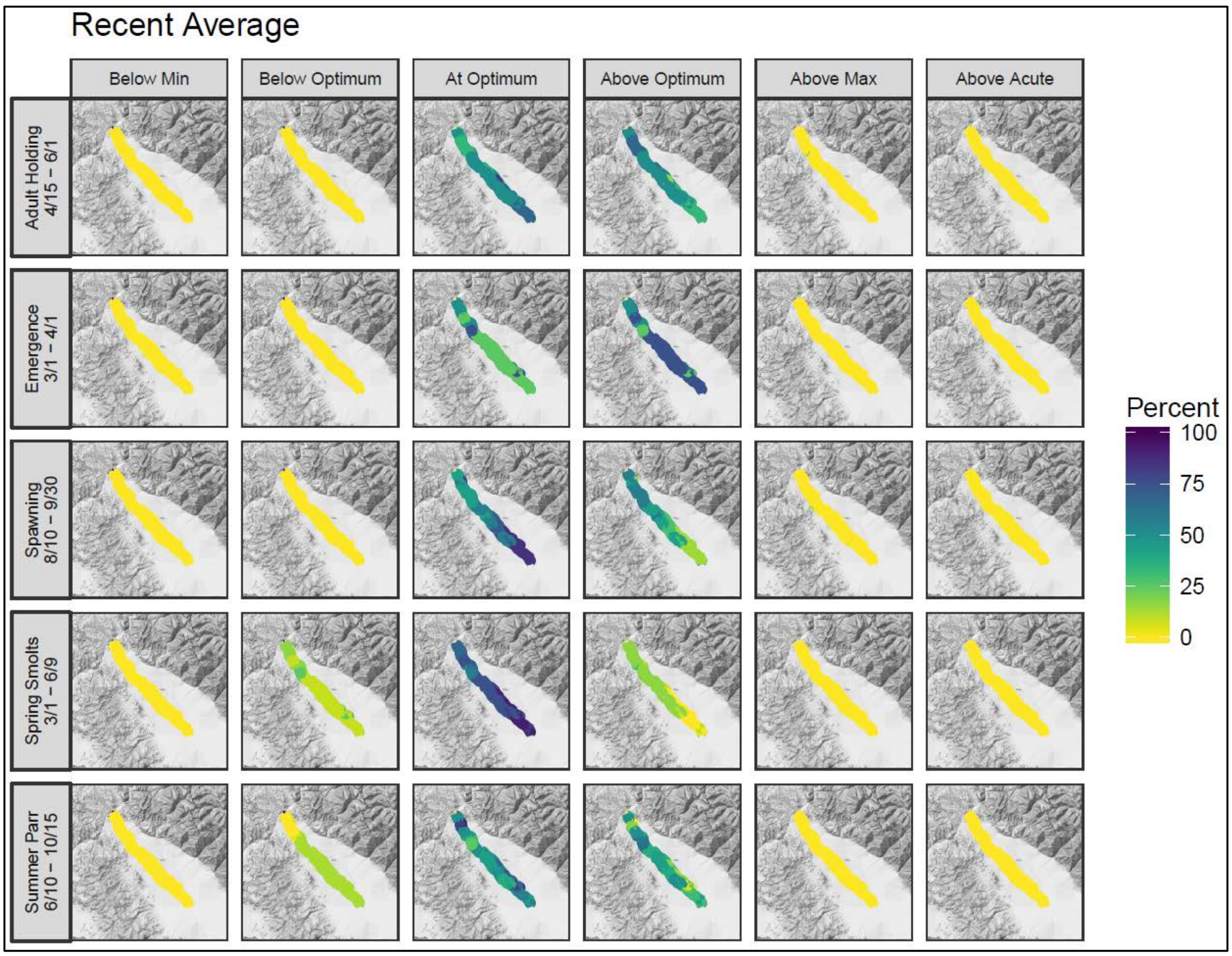

Figure 103. The percentage of time that Pahsimeroi River watershed water temperatures were below, within, or above a given temperature threshold (Carter 2005) for five Chinook salmon life stages. Water temperatures were averaged across years for which complete modeled temperature data were available (2011 and 2013).

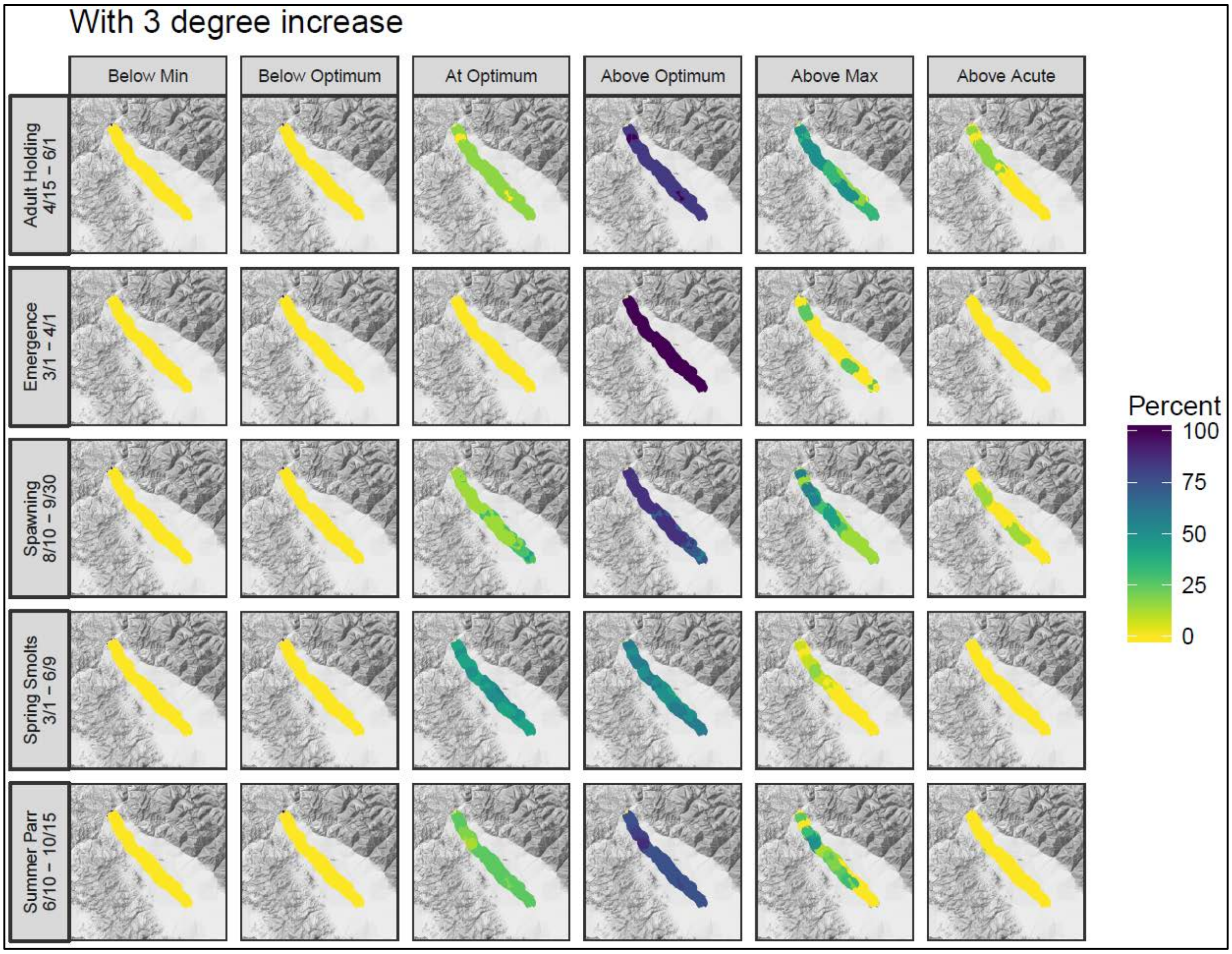

Figure 104. The percentage of time that Pahsimeroi River watershed water temperatures may potentially be below, within, or above a given temperature threshold (Carter 2005) for five Chinook salmon life-stages assuming a potential climate change scenario.

Steelhead

Under current conditions, water temperatures in the Pahsimeroi River are rarely below optimum values for steelhead (Figure 105) except during brief periods in the late spring and early summer. Water temperatures are largely within optimal values during spring and early summer during periods of spawning, spring smolt emigration, and early-summer parr rearing. Alternatively, summer temperatures exceed optimum and acute values during late incubation and emergence for steelhead; however, it is unclear to what degree late incubation and emergence timings might overlap with summer high temperatures in the Pahsimeroi River. Under an assumed 3° C water temperature increase scenario, conditions worsen for all steelhead life stages evaluated (Figure 106). Modeled water temperatures became above optimum, maximum, or acute temperature thresholds for steelhead for the entire duration of the spawning and incubation/emigration life stages. Further, water temperatures tend to move above optimum, and in some cases maximum, temperature thresholds for the summer parr rearing and spring smolt emigration steelhead life stages during portions of the season.

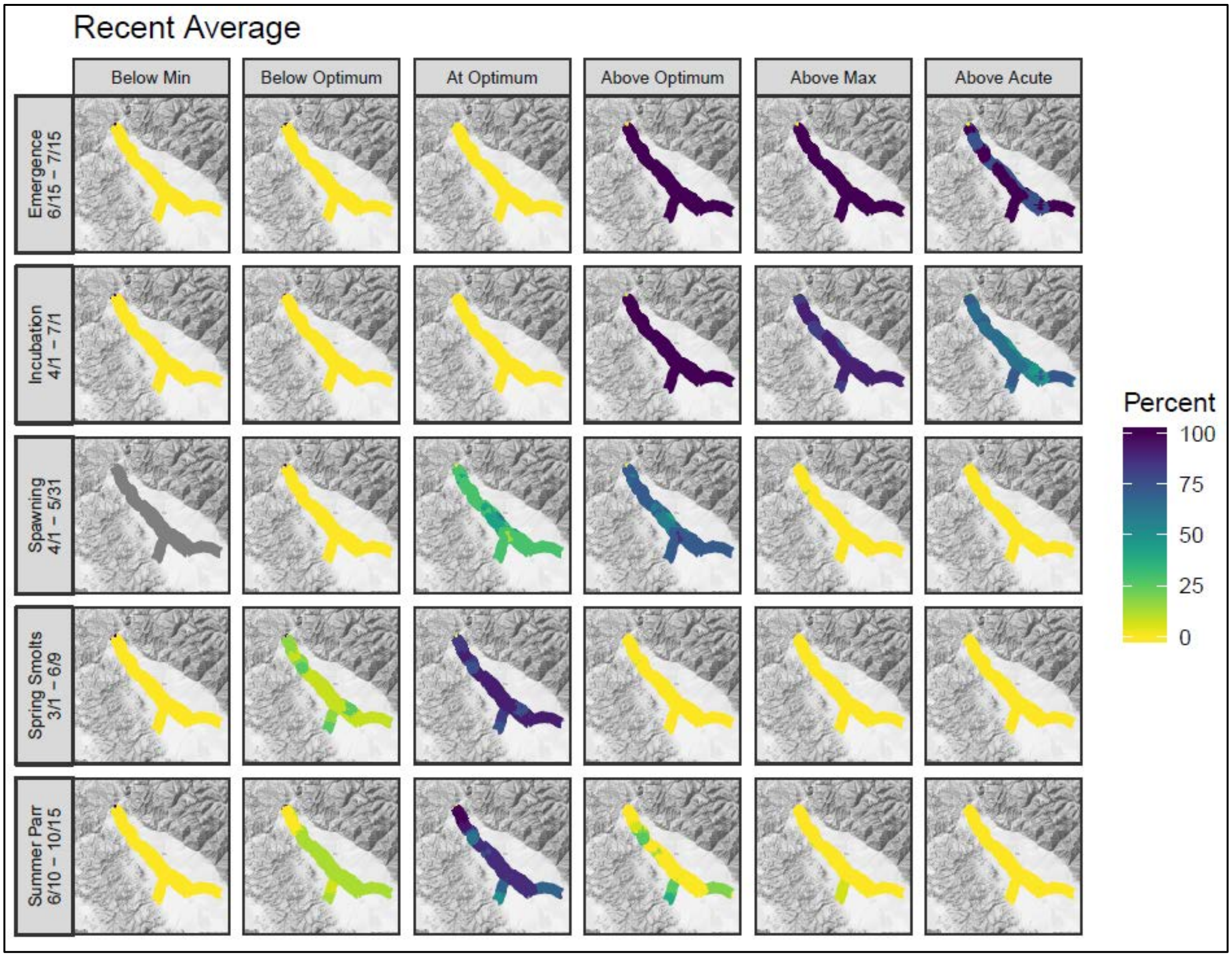

Figure 105. The percentage of time that Pahsimeroi River watershed water temperatures in 2013 were below, within, or above a given temperature threshold (Carter 2005) for five steelhead life stages. Water temperatures were averaged across years for which complete modeled temperature data were available (2011 and 2013).

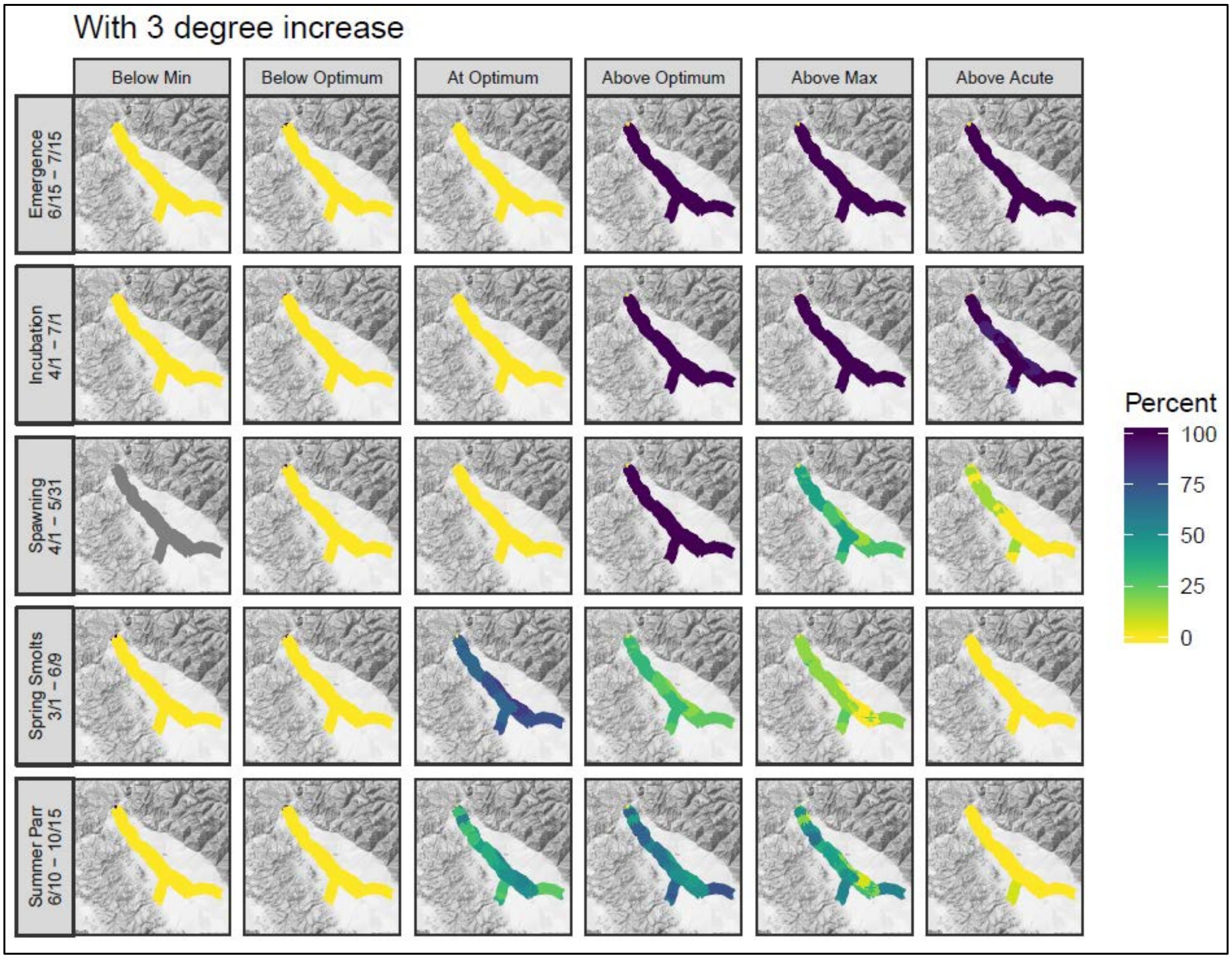

Figure 106. The percentage of time that Pahsimeroi River watershed water temperatures may potentially be below, within, or above a given temperature threshold (Carter 2005) for five steelhead life-stages, assuming a potential climate change scenario.

Results and Discussion

In the Pahsimeroi River Biological Assessment, the lack of quantity and quality juvenile rearing habitat was identified as the highest-priority limiting PBF. Assuming recent mean adult Chinook salmon escapement, habitat capacity does not appear to limit production of summer parr (Table 32). However, currently available juvenile rearing habitat (summer and winter) likely is not sufficient to support recent high escapements or escapements necessary for ESA delisting of Chinook salmon (Table 33). For steelhead in the Pahsimeroi River, winter (presmolt) juvenile rearing habitat may be sufficient to support ESA delisting (Table 34), but available summer (parr) rearing habitat appears to be limiting if ESA delisting is desired (Table 35). Redd capacity (i.e., available spawning habitat) does not appear to be limiting for Chinook salmon or steelhead in the Lemhi River.

Limiting Physical and Biological Features

The lack of quality summer (parr) and overwinter (presmolt) rearing habitat downstream of spawning habitat were identified as high-priority PBFs in the Pahsimeroi River. In recent years, only 12 percent of the total Chinook salmon juvenile production from the Pahsimeroi River have emigrated at the spring smolt (age 1) life stage; the remaining 88 percent have emigrated prior to the spring as fry, parr, or presmolts, suggesting limited rearing habitat. Estimates of currently available summer and winter rearing capacity (via QRF models) suggest that the Pahsimeroi River provides only roughly 50 percent of the juvenile parr or presmolt production required for recent high escapements (Table 32) and is far short of juvenile habitat required for ESA delisting (Table 33). Both summer and winter rearing habitat appear to be insufficient or unsuitable to support a large portion of juvenile production in the Pahsimeroi River. The lack of rearing capacity requires increased juvenile emigration during the critical periods and leads to increased survival risk in mainstem corridor habitats.

The lack of quality summer (parr) rearing habitat downstream of current spawning habitat was also identified as a PBF for steelhead in the Pahsimeroi River. The Pahsimeroi River was the only watershed of the three evaluated in this assessment identified as having PBFs limiting production of steelhead. Estimated available summer rearing habitat for steelhead in the upper Salmon River is approximately 50 percent of that required to support recent high escapements (Table 34) and is short of habitat required to support ESA delisting criteria (Table 35). Estimated available winter (presmolt) rearing habitat in the Upper Salmon River is below required habitat for recent high escapements but appears to be sufficient to support ESA delisting (NOAA 2017).

- Summer (parr) and winter (presmolt) juvenile rearing capacity were each identified as high-priority PBF limiting Chinook salmon production in the Pahsimeroi River.
- Summer (parr) juvenile rearing capacity was identified as a medium-priority PBF limiting steelhead production in the Pahsimeroi River.

Priority Areas

Priority areas within the Pahsimeroi River watershed include the mainstem Pahsimeroi River and (Patterson) Big Springs Creek.

- **First priority: Pahsimeroi River from the mouth to Hooper Lane.** Hooper Lane is currently the upstreammost extent of Chinook salmon spawning and rearing, except for Big Springs Creek.
- **Second priority: (Patterson) Big Springs Creek.** The portion of the creek within the Pahsimeroi valley bottom.

References

Albers, P.C., J. Lowry, and G.E. Smoak. 1998. The Rivers and Fisheries of the Shoshone-Bannock Peoples. American West Center, University of Utah, published by the Shoshone-Bannock Tribes, 282 p.

Arthaud, D., C. Green, K. Guilbault, J. and Morrow. 2010. Contrasting life-cycle impacts of stream flow on two chinook salmon populations. *Hydrobiologia* 655: 171-188.

Bisson, P.A., J.M. Buffington, and D.R. Montgomery. 2006. Chapter 2. Valley Segments, Stream Reaches, and Channel Units, *in* Methods in Stream Ecology, 2nd Edition. Elsevier.

Berenbrock, C. 2002. Estimating the Magnitude of Peak Flows at Selected Recurrence Intervals for Streams in Idaho. Water-Resources Investigations Report 02-4170. United States Geological Survey. Boise, Idaho.

Braudrick, C.A. and G.E. Grant. 2001. Transport and deposition of large woody debris in streams: a flume experiment. *Geomorphology*. 41: 263-283.

Carter, K. 2005. The effects of temperature on steelhead trout, Coho salmon, and Chinook salmon biology and function by life stage. Implications for Klamath Basin TMDLs. California Regional Water Quality Control Board. North Coast Region. 26pp.

Cluer, B. and C. Thorne. 2013. A Stream Evolution Model Integrating Habitat and Ecosystem Benefits. *River Research and Applications*. 30:135-154

Denney, R. N. 1952. A Summary of North American Beaver Management, 1946-1948. Colorado Game and Fish Department. 58p.

Frissell, C.A., W.J. Liss, C.E. Warren, and M.D. Hurley. 1986. A Hierarchical Framework for Stream Habitat Classification: Viewing Streams in a Watershed Context. *Environmental Management* 10(2): 199-214.

Idaho Department of Environmental Quality. 2013. Pahsimeroi River Subbasin Assessment and Total Maximum Daily Load. Available at http://www.deq.idaho.gov/water-quality/surface-water/tmdls/table-of-sbas-tmdls/pahsimeroi-river-subbasin/.

Idaho Department of Environmental Quality. 2005. Principles and Policies for the 2002 Integrated (303(d)/305(b)) Report. Available at http://www.deq.idaho.gov/media/458038-integrated_report_2002_final_entire.pdf.

Idaho Department of Environmental Quality. 2011. Idaho's 2010 Integrated Report Final. Available at http://www.deq.idaho.gov/media/725927-2010-integrated-report.pdf

Idaho Soil Conservation Commission. 1995. Model Watershed Plan, Lemhi, Pahsimeroi, and East Fork of the Salmon River: Idaho Soil Conservation Commission for the Bonneville Power Administration, Portland, Oregon.

Link, P.K. and S.U. Janecke. 1999. Geology of East-Central Idaho: Geologic Roadlogs for the Big and Little Lost River, Lemhi, and Salmon River Valleys. *In* Guidebook to the Geology of Eastern Idaho. S.S. Hughes and G.D. Thackray, *eds*. Idaho Museum of Natural History. Online Link: http://imnh.isu.edu/digitalatlas/geo/gsa/gsafrm.htm

McGrath, C.L., A.J. Woods, J.M. Omernik, S.A. Bryce, M. Edmondson, J.A. Nesser, J. Shelden, R.C. Crawford, J.A. Comstock, and M.D. Plocher. 2002. Ecoregions of Idaho (color poster with map, descriptive text, summary tables, and photographs). U.S. Geological Survey (map scale 1:1,350,000). Reston, Virginia.

Meinzer, O.E. 1924. Ground water in Pahsimeroi Valley, Idaho. Idaho Bureau of Mines and Geology, Pamphlet 9, 36p.

Montgomery, D., and J.M. Buffington, 1998. Channel Processes, Classification, and Response, *in* River Ecology and Management, Chapter 2. R. Naiman and R. Bilby, *eds*. Springer-Verlag New York, Inc., p. 13-42.

Moye, F.J., W.R. Hackett, J.D. Blakley, and L.G. Snider. 1988. Regional geologic setting and volcanic stratigraphy of the Challis volcanic field, central Idaho. *In* P.K. Link, and W.R. Hackett, *eds*. Guidebook to the Geology of Central and Southern Idaho. Idaho Geological Survey Bulletin 27, p. 87-97.

NOAA National Marine Fisheries Service. 2017. Proposed ESA Recovery Plan for Snake River Idaho Spring/Summer Chinook Salmon and Steelhead Populations. NOAA Fisheries, Portland, Oregon, 330 p.

Northwest Power and Conservation Council. 2004. Salmon Subbasin Management Plan. May 2004. Contracted by Nez Perce Tribe Watershed Division and Shoshone-Bannock Tribes. Written by Ecovista.

Natural Resources Conservation Service. 2003. Soil Survey of Custer-Lemhi Area, Idaho, Parts of Blaine, Custer, and Lemhi Counties. USDA Natural Resources Conservation Service, 578 p., online (http://www.nrcs.usda.gov).

Pierce, K.L., D.G. Despain, L.A. Morgan, and J.M. Good. 2007. The Yellowstone Hotspot, Greater Yellowstone Ecosystem, and Human Geography. U.S. Geological Survey Paper 79, 39 p.

Rossillon, M., 1980. An Overview of History in the Drainage Basin of the Middle Fork of the Salmon River. Boise National Forest, Boise, Idaho.

Simpson, D.W. and M.H. Anders. 1992. Tectonics and topography of the western U.S.: An example of digital map making. *GSA Today*. 2: 118-121.

Slough, B.G. and R.M.F.S. Sadleir. 1977. A land capability classification system for beaver (*Castor canadensis*). Canadian Journal of Zoology 55(8): 1324-1335.

Stark, E.J., A. Byrne, P.J. Cleary, T. Copeland, L. Denny, R. Engle, T. Miller, D. Nemeth, S. Rosenberger, E.R. Sedell, G.E. Shippentower, and C. Warren. 2017. Snake River basin steelhead 2014/2015 run reconstruction. Report to Bonneville Power Administration, Portland, Oregon.

Ungate, C.A. 1998. Neogene – Quaternary Basin – Fill History of the Pahsimeroi Valley. Masters Thesis. Idaho State University, Pocatello, ID.

Whittier, R.B. 2009. Geologic Controls on Groundwater/Surface Water Interaction in the Pahsimeroi Valley. Upper Salmon Basin Watershed News, Salmon, Idaho, Fall 2009, p. 2.

Williams, C.J., J.P. McNamara, and R.B. Whittier. 2006. Surface-Water and Ground-Water Interaction in the Pahsimeroi Valley, Idaho, USA: Technical Report BSU CGISS 06-02, November 1, 2006, 67 p.

Young, H. W. and W.J. Harenberg. 1973. Reconnaissance of the water resources in the Pahsimeroi River Basin, Idaho. Idaho Department of Water Administration. Bulletin No. 31, 57p.

Chapter 3 – Upper Salmon River Watershed (Above Redfish Lake Creek)

Location and Watershed Description

The Upper Salmon River watershed is located in the Northern Rocky Mountains System physiographic region that comprises extensive parallel mountain ranges, intermontane valleys, and plateaus (Figure 107). Elevations in the watershed range from a low of about 6190 to a high of 10750 feet. It is also in the High Glacial Drift-Filled Valleys Ecoregion (16G), characterized by terraces, outwash plains, moraines, wetlands, and hills that are much less rugged and less forested than Ecoregion 16k. Originally, sedges and rushes were common on wet soils, bunchgrasses and mountain big sagebrush occurred on drier soils, and lodgepole pine and ponderosa pine grew on valley floors. Winters are cold and snowy. Ecoregion 16g receives large amounts of spring runoff from mountain snowpack. It is summer pasture for large numbers of livestock; cropland and growing residential and recreational developments also occur. Flood irrigation and grazing have raised sediment and phosphorus levels in streams (McGrath et al. 2002).

The Upper Salmon River watershed is defined as the Salmon River and its headwaters upstream from the confluence of Redfish Lake Creek. The watershed includes two hydrologic unit code (HUC) 10^{th} field basins: Pole Creek – Salmon River (HUC 10 – 1706020102) and Alturas Lake Creek (HUC 1706020103). The watershed covers more than 305 square miles in east-central Idaho and is within Blaine and Custer Counties, Idaho. More than 90 percent of the land is owned by the Federal government and administered by the USFS. Federal lands are primarily in the higher elevations, whereas private lands are typically located in lower elevations along the valley bottoms.

The Upper Salmon River is predominantly an alluvial stream that originates high in the Sawtooth Range at about 9800 feet. The river flows about 6 miles through a U-shaped valley eroded by an alpine glacier with steep valley walls. It then flows for another 32 miles across a broad floodplain that has developed within the glacial outwash plain to a canyon section, where it flows about another half-mile to its confluence with Redfish Lake Creek.

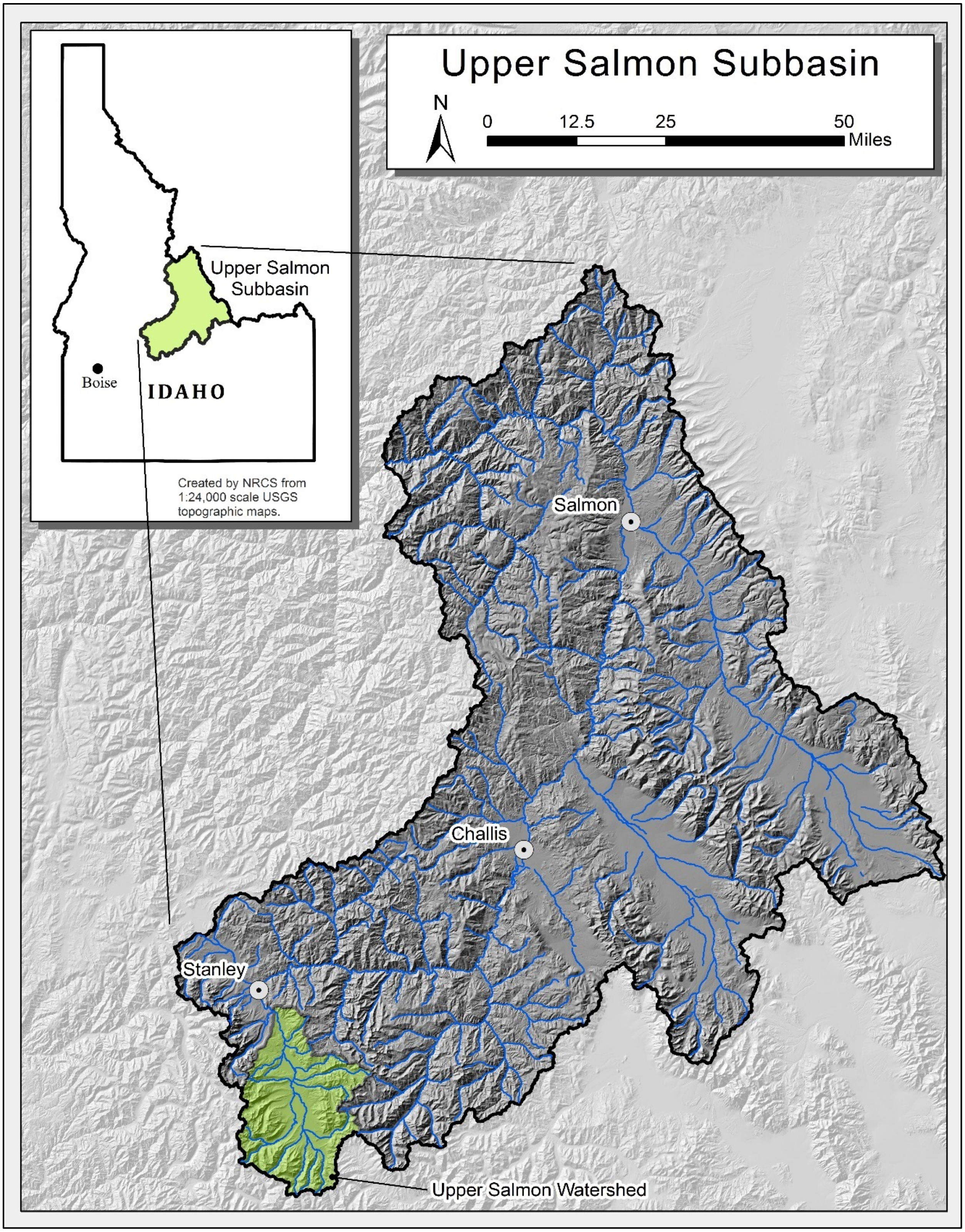

Figure 107. Map of location of the Upper Salmon River subbasin.

Biological Assessment

The Upper Salmon River maintains populations of three fish species listed under the ESA: Chinook salmon, steelhead, and bull trout. The watershed also supports westslope cutthroat trout, which has been petitioned for listing under the ESA. The headwaters of the Upper Salmon River are dominated by roadless wilderness areas, although the valley floor has been developed for agriculture. Timber harvest, grazing, and recreation activities occur within the watershed.

The mainstem Salmon River is estimated to provide 56 percent of the spawning habitat and 34 percent of the rearing habitat for this Chinook salmon population, with the remainder supported by tributary habitat, of which Alturas Lake Creek is the largest contributor (NOAA 2017). The Upper Salmon River Chinook salmon population inhabits the mainstem Salmon River and tributaries upstream from the confluence with Redfish Lake Creek, including Redfish Lake Creek. Since 2000, the Upper Salmon River has a mean escapement of 656 adult Chinook salmon, with a maximum escapement of 1,419 in 2002. NOAA (2017) classifies this population as Large and at a high risk of extinction.

The Upper Salmon River steelhead population includes the mainstem Salmon River and all of its tributaries (including Yankee Fork Salmon, Valley Creek, Upper Salmon) upstream from the confluence of the East Fork Salmon River. In the steelhead section here, we focus on the portion of the population that inhabits the mainstem Salmon River and tributaries upstream from the confluence with Redfish Lake Creek, including Redfish Lake Creek. Since 2010, the Upper Salmon River has a mean escapement of 92 adult steelhead, with a maximum escapement of 154 in 2010. NOAA (2017) classifies the entire Upper Salmon River steelhead population as Intermediate with a maintained (i.e., 6 to 25 percent chance) risk of extinction.

Habitat Capacity

Chinook salmon

Current Conditions

Contemporary estimates of life-stage-specific capacity requirements were generated based on the mean (656) and maximum (1,419) adult Chinook salmon escapement observed in the Upper Salmon River from 2000 to 2016. Those adult escapements were then propagated through to four additional life stages to estimate life-stage-specific capacity requirements for Chinook salmon in the Upper Salmon River; capacity requirements were then compared to available habitat capacity estimated using QRF models (Table 51).

Table 51. Estimated current life-stage-specific capacity requirements versus estimated available capacity for Chinook salmon in the Upper Salmon River.

Life-Stage	Required Capacity		Available Capacity	Capacity Deficit
	Mean	Max		
Escapement	656	1,419		
Redd	321	695	4,909	0
Eggs	1,700,372	3,678,497		
Summer Parr	493,108	1,066,764	721,873	344,891
Winter Presmolt	199,793	432,221	220,838	211,383

Under current habitat conditions and using contemporary escapement estimates, the productivity of the Upper Salmon River Chinook salmon population does not appear to be limited by redd capacity; however, it does appear that juvenile rearing capacity may be limited during both summer (parr) and winter (presmolt) months (Table 51). Available summer and winter juvenile rearing habitat for Chinook salmon seems adequate to support parr and presmolt capacity requirements given contemporary mean escapement, but available habitat may support only roughly 70 percent of summer (parr) and 50 percent of winter (presmolt) production from the recent max escapement in 2002. In other words, considering the mean of recent escapements, it appears that required capacity is below the predicted available capacity, suggesting zero deficit. However, during large escapements, required capacity likely exceeds available capacity during summer and winter months (Table 51). These findings appear to be supported by the fact that 57 percent of total Chinook salmon juvenile production from this reach emigrate as fry (26 percent) or parr (31 percent); however, this could be due, in part, to the fact that the majority of redds are enumerated within roughly 6 river miles upstream of the rotary screw trap. Further, on average, 33 percent of total Chinook salmon juveniles emigrate as presmolts, prior to the winter rearing period, suggesting that winter habitat capacity in upper reaches of the Upper Salmon River is limited.

Desired Conditions

NOAA (2017) delisting requirements include a minimum annual escapement (i.e., MAT) of 1,000 Chinook salmon adults to the Upper Salmon River. Based on this requirement, life-stage-specific capacity requirements were recalculated consistent with 1,000 adults (MAT) and 1,250 adults (MAT + 25%). Those capacity requirements were also compared to estimates of currently available habitat capacity to identify potential habitat limitations if delisting is desired (Table 52). Potential limitations (capacity deficit) were calculated as the life-stage-specific capacity requirements needed to achieve a MAT of 1,000 plus a 25 percent buffer minus available capacity. There appears to be sufficient redd capacity in the Upper Salmon River to support 1,250 adult Chinook salmon. However, the available juvenile rearing capacity during summer (721,873) and winter (220,838) are far from sufficient to support the potential parr and presmolt production from 1,250 adult Chinook salmon (Table 52). Therefore, to achieve delisting of Chinook salmon in the Lemhi River, both summer and winter juvenile rearing capacity would need to be increased.

Table 52. Estimated life-stage-specific capacity requirements to accommodate ESA de-listing and estimated available capacity for Chinook salmon in the Upper Salmon River.

Life-Stage	Required Capacity		Available Capacity	Capacity Deficit
	MAT	MAT + 25%		
Escapement	1,000	1,250		
Redd	490	613	4,909	0
Eggs	2,592,100	3,240,125		
Summer Parr	751,709	939,636	721,873	217,763
Winter Presmolt	304,570	380,712	220,838	159,874

Summary

Sufficient spawning (redd) capacity is available in the Upper Salmon River to support contemporary escapement and escapement required to achieve delisting criteria for Chinook salmon (Figure 108). Predicted available juvenile rearing capacity during summer (parr) and winter (presmolt) months appears sufficient to support recent mean escapements, but perhaps not high escapements in recent years (Figure

109 and Figure 110); juvenile rearing capacity for Chinook salmon in both summer and winter months would likely need to be increased to achieve delisting.

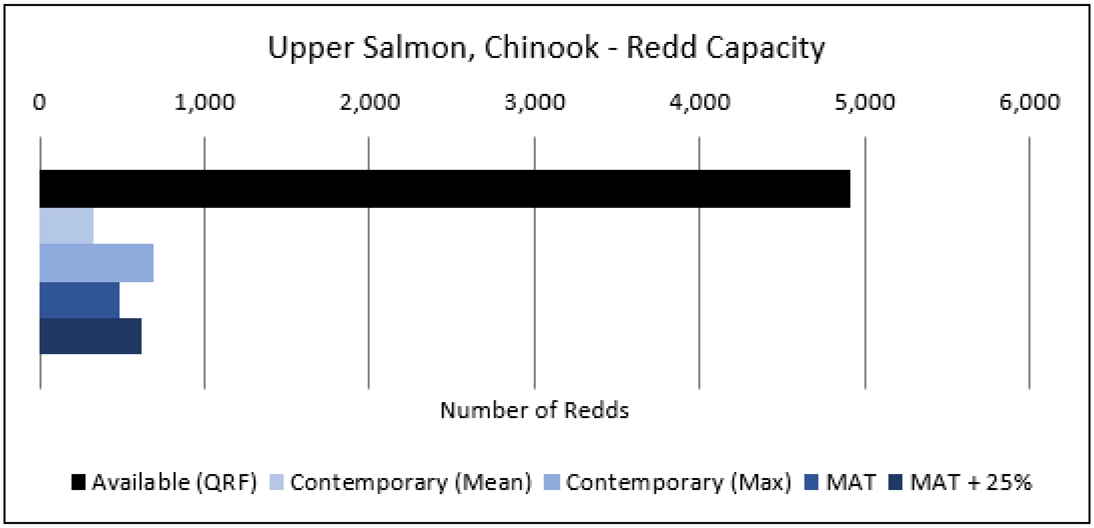

Figure 108. Estimates of available spawning (redd) capacity given current habitat conditions for Chinook salmon in the Upper Salmon River watershed, made using quantile regression forest models (black bars), versus the capacity required to support contemporary abundance and minimum abundance thresholds (MATs) needed for ESA de-listing (blue bars).

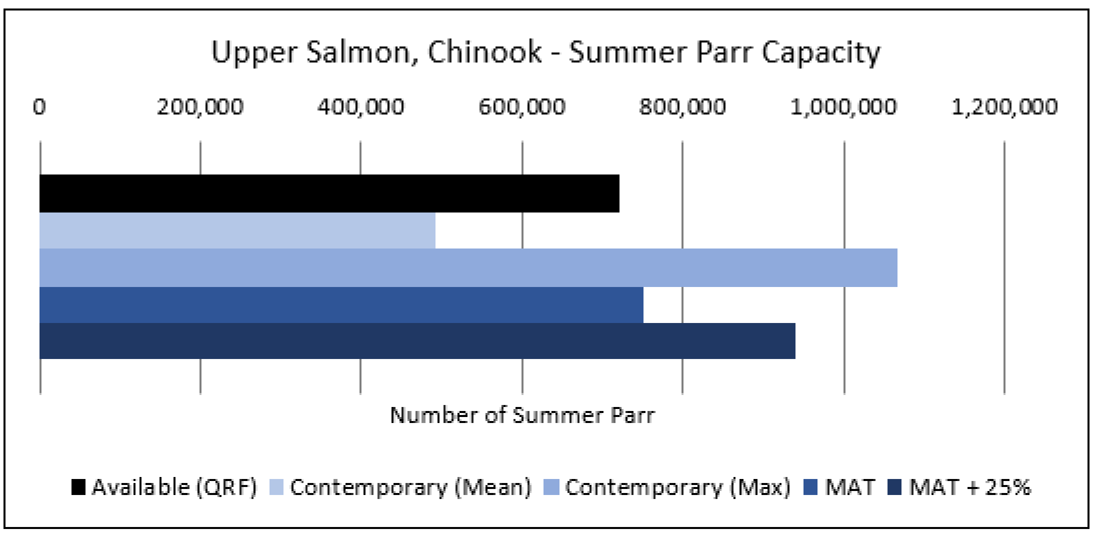

Figure 109. Estimates of available summer juvenile (parr) rearing capacity given current habitat conditions for Chinook salmon in the Pahsimeroi River watershed, made using quantile regression forest models (black bars), versus the capacity required to support contemporary abundance and minimum abundance thresholds (MATs) needed for ESA de-listing (blue bars).

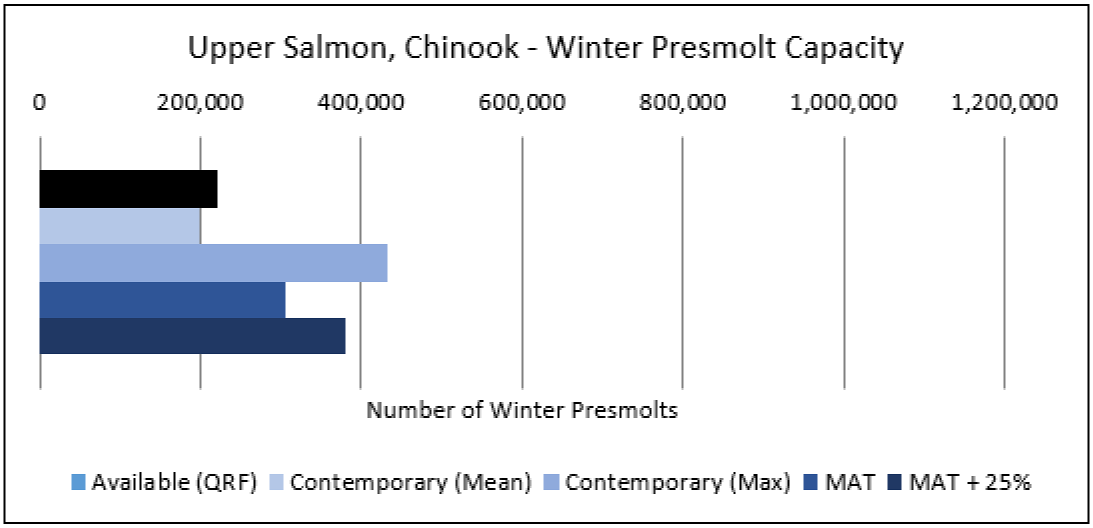

Figure 110. Estimates of available winter juvenile (presmolt) rearing capacity given current habitat conditions for Chinook salmon in the Pahsimeroi River watershed, made using quantile regression forest models (black bars), versus the capacity required to support contemporary abundance and minimum abundance thresholds (MATs) needed for ESA de-listing (blue bars).

Steelhead

Available habitat capacity estimates from QRF models are considered preliminary for steelhead in the Upper Salmon River due to unknown spatial extents of available habitat for steelhead spawning and rearing. The IRA team will work with local biologists and experts to more appropriately identify the extents of habitat in the Upper Salmon River available to steelhead. Available habitat capacity estimates can be improved in future reach assessments or as needed with local groups.

Current Conditions

Contemporary estimates of life stage-specific capacity requirements were generated based on the mean (92) and maximum (154) adult steelhead escapements estimated in the Upper Salmon River from 2010 to 2015. Those adult escapements were then propagated through to four additional life stages to estimate life-stage-specific capacity requirements for steelhead in the Upper Salmon River; capacity requirements were then compared to available habitat capacity estimated using QRF models (Table 53).

Table 53. Estimated current life-stage-specific capacity requirements versus estimated available capacity for steelhead in the Upper Salmon River.

Life-Stage	Required Capacity		Available Capacity	Capacity Deficit
	Mean	Max		
Escapement	92	154		
Redd	51	85	2,475	0
Eggs	251,959	420,995		
Summer Parr	33,826	56,519	470,009	0
Winter Presmolt	12,131	20,269	473,201	0

Under current habitat conditions, and using contemporary escapement estimates, habitat capacity does not appear to limit spawning (redd) or juvenile rearing for steelhead in the Lemhi River.

Desired Conditions

NOAA (2017) delisting requirements include a minimum annual escapement (i.e., MAT) of 1,000 steelhead adults to the Upper Mainstem Salmon River steelhead population that includes the mainstem Salmon River and all tributary habitats upstream of its confluence with the East Fork Salmon River. For this Biological Assessment, we are only interested in the portion of the population that inhabits the mainstem Salmon River and tributaries upstream from the confluence with Redfish Lake Creek, including Redfish Lake Creek. To determine a relative MAT for this portion of the population, we first compared the available stream length within the steelhead domain in the Upper Salmon River above Redfish Lake Creek (195.3 km) to available stream length within the steelhead domain in Valley Creek (99.9 km) and the Yankee Fork Salmon River (111.3 km) and determined that about 48 percent of the available habitat in the Upper Mainstem Salmon River steelhead population lies within our area of interest. Therefore, we multiplied the total MAT (1,000) by 48 percent to establish a relative MAT of 480 adult steelhead. Based on this requirement, life-stage-specific capacity requirements were recalculated consistent with 480 adults (MAT) and 601 adults (MAT + 25%) using the same methods as above. Those capacity requirements were also compared to estimates of currently available habitat capacity to identify potential habitat limitations if delisting is desired (Table 54). Potential limitations (capacity deficit) were calculated as the life-stage-specific capacity requirements needed to achieve an abundance of 601 minus available capacity.

There appears to be sufficient redd and juvenile rearing capacity for steelhead to support 601 adult steelhead in the Upper Salmon River above Redfish Lake (Table 54).

Table 54. Estimated life-stage-specific capacity requirements to accommodate ESA de-listing and estimated available capacity for steelhead in the Upper Salmon River.

Life-Stage	Required Capacity		Available Capacity	Capacity Deficit
	MAT	MAT + 25%		
Escapement	480	601		
Redd	267	333	2,475	0
Eggs	1,313,402	1,641,753		
Summer Parr	176,324	220,405	470,009	0
Winter Presmolt	63,235	79,043	473,201	0

Summary

There appears to be sufficient spawning (redd) and juvenile rearing capacity for steelhead in the Upper Salmon River (above Redfish Lake) to support contemporary escapement and escapement required to achieve delisting criteria for steelhead (Figure 111, Figure 112, Figure 113).

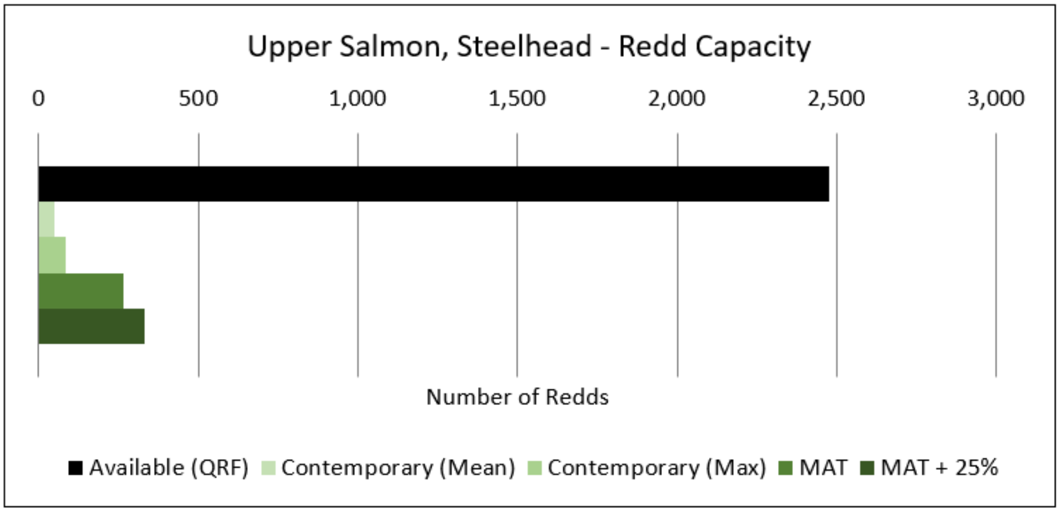

Figure 111. Estimates of available spawning (redd) capacity given current habitat conditions for steelhead in the Upper Salmon River watershed, made using quantile regression forest models (black bars) versus the capacity required to support contemporary abundance and minimum abundance thresholds (MATs) needed for ESA de-listing (green bars).

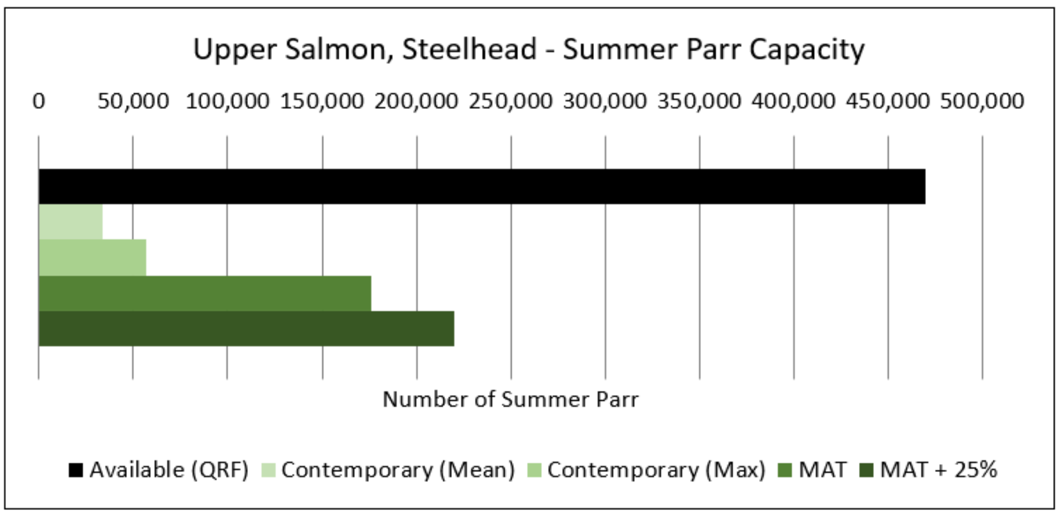

Figure 112. Estimates of available summer juvenile (parr) rearing capacity given current habitat conditions for steelhead in the Upper Salmon River watershed made using quantile regression forest models (black bars) versus the capacity required to support contemporary abundance and minimum abundance thresholds (MATs) needed for ESA de-listing (green bars).

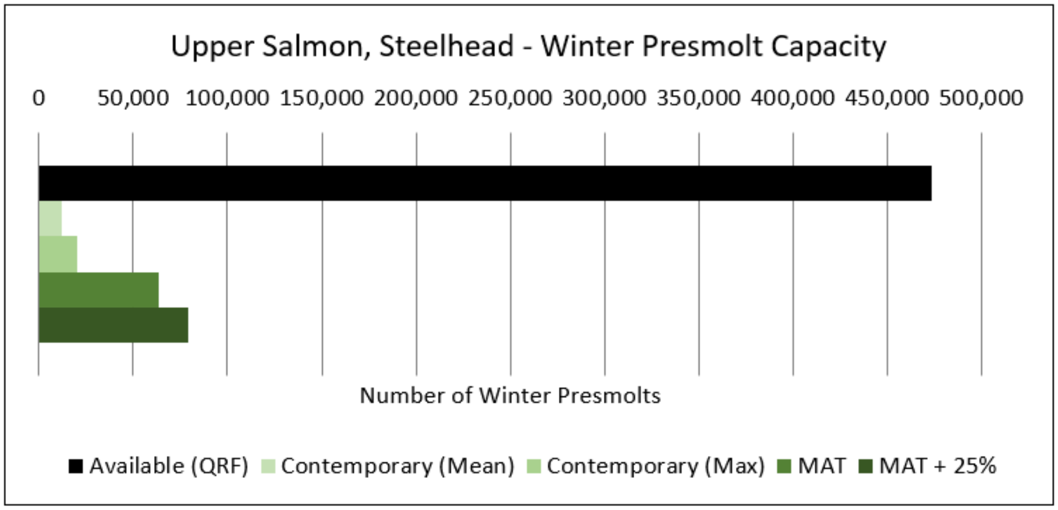

Figure 113. Estimates of available winter juvenile (presmolt) rearing capacity given current habitat conditions for steelhead in the Upper Salmon River watershed made using quantile regression forest models (black bars) versus the capacity required to support contemporary abundance and minimum abundance thresholds (MATs) needed for ESA de-listing (green bars).

Geomorphic Assessment

Much of the geomorphic assessment in this report has been compiled in an effort to help paint a better picture of historical and potential target conditions (qualitative), recognizing that detailed (quantitative) target conditions will be generated as part of the MRA for select reaches in the future.

Historical Watershed Conditions

The Upper Salmon River occupies a broad north/northwest-trending valley bound by the granitic Sawtooth Mountains to the west and the granitic and sedimentary White Cloud Mountains to the east. The valley formed through a sequence of mountain building, faulting, and valley-fill sedimentation over millions of years. Some of the oldest rocks in the area were deposited more than 100 million years ago as marine sediments that were subsequently thrust up onto the continental crust about 60 million years ago, during the formation of the ancestral Rocky Mountains (Link and Janecke 1999). At roughly the same time, the subduction of the ancestral oceanic tectonic plate beneath the continental tectonic plate resulted in the emplacement of the granitic Idaho batholith, a large body of igneous granitic rock that comprises much of central Idaho, including the Sawtooth Mountains and portions of the White Clouds (Johnson et al. 1988). Over the past several million years, the continental crust has expanded in this area due to the nearby Yellowstone hotspot. Normal faulting associated with the expansion has lowered some blocks of the crust, creating valleys and raising others, forming mountain ranges (Pierce et al. 2007). The Idaho batholith was faulted along a roughly northwest-trending normal fault (Sawtooth Fault), forming the Salmon River Valley (lowered block) and Sawtooth Mountains (raised block) (Simpson and Anders 1992).

During the last ice age that ended approximately 10,000 years ago, the temperatures in the area were estimated to be 6 to 10° C colder than today (Pierce and Scott 1982). Lower temperatures resulted in more snow accumulation and less evaporation, which formed glaciers in the Sawtooth and White Cloud Mountains and is estimated to have increased stream flow by at least an order of magnitude relative to modern hydrology (Pierce and Scott 1982). Glaciers and streams with much-higher-than-modern discharge transported large volumes of sediment to the valley bottom, where they were deposited in thick layers. Glacial ice from the Sawtooth Mountains extended onto the Sawtooth Valley, forming substantial moraine deposits grading in sequence to fan and outwash gravels that occupy much of the valley floor (Breckenridge et al. 1988) (Figure 114). Outlet glaciers from the White Cloud Mountains are believed to have reached the margin of the Sawtooth Valley but did not coalesce with glaciers from the Sawtooth Range (Breckenridge et al. 1988). Ten thousand years of subsequent erosion into the glacial sediment has resulted in the formation of large terraces that, along with remnant glacial moraines, confine the otherwise broad valley.

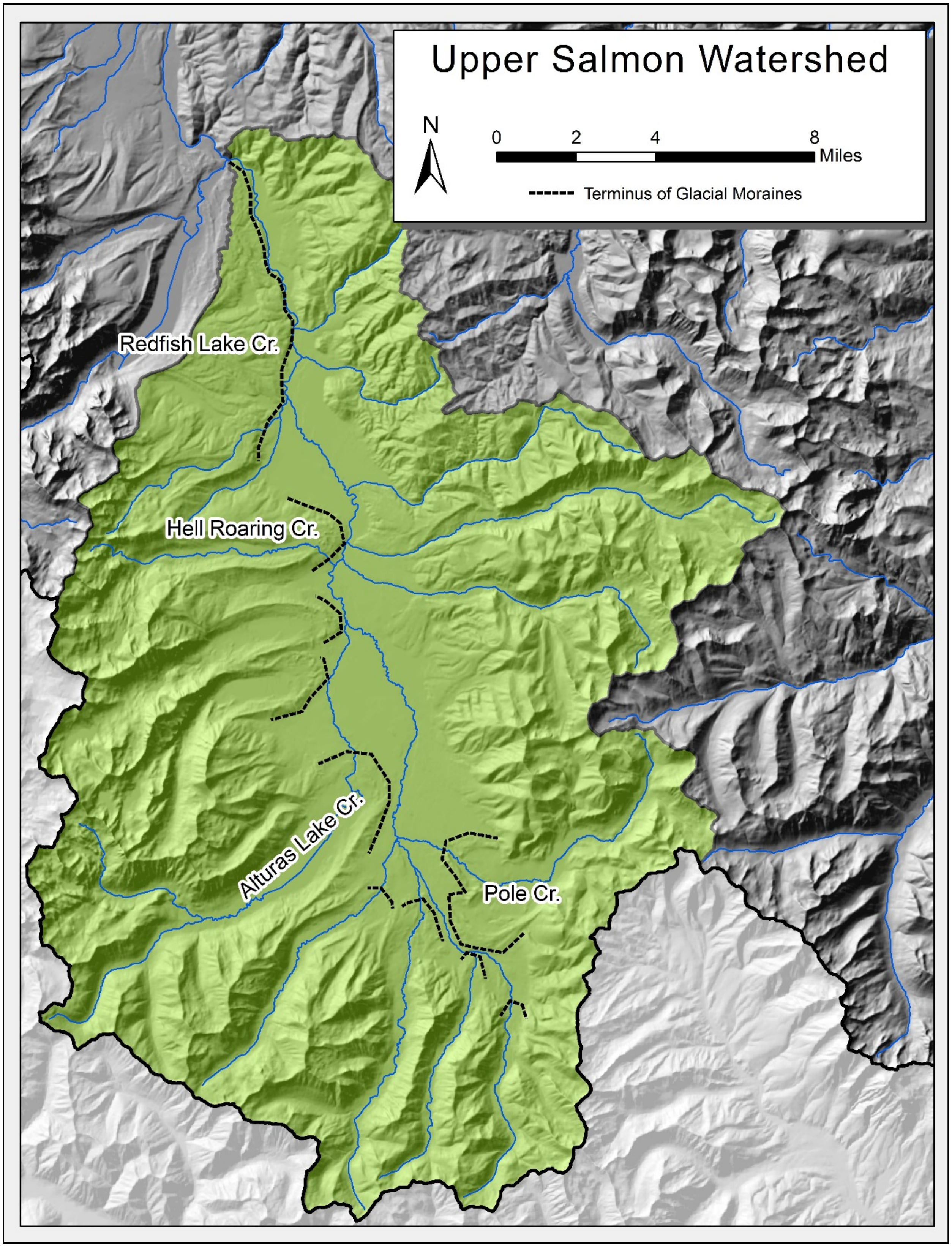

Figure 114. Ten-meter digital elevation model hill shade map illustrating the approximate terminal extent of Pleistocene glacial moraines.

The porous, ice-age alluvial deposits (moraines, fans, and outwash gravels) filling the Sawtooth Valley also enable a local aquifer. Areas where the aquifer intercepts the surface produce reaches that gain flow from groundwater, while areas where the aquifer is below the surface generally lose flow to the aquifer. Although detailed groundwater analyses are not available, aerial photograph observation reveals several locations where the local groundwater table appears to intercept the surface, resulting in visible springs. The historic conditions of the Sawtooth Valley were likely significantly influenced by the spatial variability of surface-to-groundwater interactions in the valley.

The character of the majority of the valley is driven predominantly by snowmelt-dominated (i.e., peak-flow) hydrology. These areas were historically transport-dominated, with sufficient gradient and discharge to mobilize sediment and slowly incise the bed over thousands of years, creating a narrow, inset floodplain bound by relic terraces. The primarily single-threaded channel within the terraces was characterized by a low sinuosity and a predominantly plane-bed morphology, although a forced pool-riffle morphology may have formed over small areas, given sufficient structure and/or woody debris loading (based on Montgomery and Buffington 1998).

Flashy, snowmelt-dominated hydrology provided a disturbance regime suitable for the establishment and propagation of cottonwood trees, but cottonwoods likely did not occupy the riparian areas due to incompatible climate and elevation. Cottonwoods are not currently observed in abundance above roughly 6,500 feet elevation on either the Salmon or neighboring Big Wood Rivers. Willows likely dominated the riparian areas above 7,000 feet, as they do today, providing bank stability and structure. Conifer trees, including lodgepole and whitebark pine, occupied upland areas, especially glacial moraines, which have a greater fine sediment composition and annual precipitation compared with alluvial fans and terraces. Bank erosion into areas vegetated with conifers, primarily along glacial moraines, tributaries, and upstream of Smiley Creek, provided a local source of large wood recruitment that enhanced and/or forced pool-riffle morphology and may have created localized areas of island braiding. Large floods and debris torrents may have transported large wood from the tributaries and upstream areas, but research suggests that large wood is unlikely to transport significant distances through such small streams with low channel width and depth (Braudrick and Grant 2001).

In several locations, valley-spanning grade controls forced the local groundwater table to intercept the surface, resulting in springs; the grade controls also yielded low gradients. These low-gradient, groundwater-influenced areas likely exhibited historical conditions similar to modern references of low-gradient, groundwater-influenced channels characterized by a sinuous channel pattern, frequent split flows, and spring-fed side-channels. Relic topographic variation from channel migration, occasional avulsions, beaver dams, and disturbance from grazing animals (bison, elk, and deer) likely created a mosaic of open water, emergent wetland, floodplain, and upland. The riparian community would have mirrored this diversity with areas of wetland meadow (rushes and sedges), floodplain shrubs (willow) and upland vegetation (sagebrush and grass). The sinuous and multi-threaded channel in these areas likely exhibited a pool-riffle morphology (based on Montgomery and Buffington 1998) driven by sediment deposition, bank structure from willow vegetation, and instream woody structure (including beaver dams), where present. Other natural geomorphic forcing agents likely included winter anchor ice and ice jams that obstructed flow and forced water out of the channel onto the floodplain.

Aerial photograph observation reveals many relic channel scars, oxbows, and meander scrolls visible in the modern floodplain (Photograph 27). Based on interpretation of these relic channels, it is believed that the peak-flow-dominated hydrology and readily available coarse sediment load resulted in frequent, pronounced channel migration and avulsion on all reaches of the Upper Salmon River headwaters. Low-gradient, beaver- and groundwater-influenced areas likely exhibited greater rates of channel response and variability due to their enhanced depositional character relative to the more-confined, higher-gradient, transport-dominated areas.

Photograph 27. Aerial photograph example of relic channel scars, oxbows, and meander scrolls in a response reach of the Upper Salmon River headwaters.

Prior to Euro-American settlement, the Salmon River Mountain region was most likely inhabited by a group of Northern Shoshone known as the *Tu'kudeka,* or Sheepeaters, who wintered in the mountains, where they hunted mountain sheep (Rossillon 1980). Given the Shoshone's subsistence cycles and seasonal movements across central and southern Idaho, their impacts on the land were likely confined to their encampments, where tribes from the region would congregate and trade their goods. Reports from Lewis and Clark and others on the abundance of fur-bearing animals west of the divide spurred the business of fur trade. Independent fur trappers, as well as several companies (including the Hudson Bay Company and the American Fur Company) made their way into the northwest to explore and exploit the region. By the early 1840s, local beaver populations were brought to the brink of extinction and bison had disappeared from the Salmon River region (Albers et al. 1998).

The discovery of gold in California in 1848 began a western mining craze, leading to an influx of prospectors into Idaho and the discovery of gold there. Mining in the area consisted of placer mining along some tributaries and some hard-rock mining in the headwaters. Miners and other settlers were interested in acquiring the Shoshone Tribe's lands and waterways to support their growing agrarian and mining enterprises, and homesteads sprang up across the lower-elevation lands (Albers et al. 1998). Beginning in the 1880s, irrigation development and associated water rights were established in the mainstem Salmon River and its tributaries (ISCC 1995). Irrigation ditches withdrew water from the river and drained wetlands, redistributing the captured water across the floodplain. Such a redistribution of water had significant impacts on the hydrology of the river, causing at least one portion of the channel to run dry during the later summer months of the irrigation season.

Presently, irrigated agriculture and livestock grazing are the predominant land use activities within the valley. Grazing on public lands provides a substantial feed base for cattle in the Sawtooth Valley.

Generally, cattle graze on public lands from May to October and then return to private lands along the valley bottoms for the remainder of the year (ISCC 1995). Historical agricultural and grazing practices resulted in riparian vegetation clearing and associated streambank destabilization, as well as increased surface-water runoff and erosion.

Existing Watershed Conditions

Channel form and process have not changed significantly from historical to existing conditions, but several human-related impacts currently influence the Upper Salmon River. The headwaters are pristine, protected public lands, but along the hillslopes and valley bottom, there are localized areas of disturbances, including irrigation diversions, livestock grazing, roads, and channel alterations. Irrigation diversions have reduced instream flows and altered aquifer recharge by diverting tributaries away from and out of the mainstem Upper Salmon River. Livestock grazing and agriculture along the mainstem Salmon River and its tributaries have caused loss of woody riparian vegetation, impacting bank stability, bank erosion, and sedimentation. Road embankments artificially confine the valley in several locations, and fine sediment from dirt and gravel roads, along with dispersed campsites throughout the drainage network, have a cumulative effect on siltation in the mainstem Salmon River.

Hydrology/Floods

The Main Salmon River flow regime is snowmelt-dominated, with numerous diversions in operation from July through September. Peak snowmelt flows generally occur during May and June. While agricultural diversion locations and volumes are regulated by local water authorities and the Idaho Department of Water Resources, exact withdrawal rates on a seasonal and daily basis are unknown. Mountain lakes are another important component of the Main Salmon River hydrology, as lakes modify water, sediment, and nutrient fluxes. Flood frequency peaks were estimated at four operational USGS gages using the PeakFQ program, and at 12 ungaged locations, applying methods published in Bulletin 17C and Berenbrock (2002). Peak flood frequency values at each valley segment are presented in Table 55.

Table 55. Upper Salmon River hydrology.

River Mile	Drainage Area (mi^2)	Flood Frequency Values (cfs)								
		1	1.5	2	2.33	5	10	25	50	100
0	304	685	1,643	1,919	2,043	2,554	2,936	3,383	3,694	3,987
15.3	177	389	940	1,099	1,170	1,463	1,682	1,937	2,114	2,281
36	3.8		35.1	43.1	45.1	60.7	73.3	88.9	100	114

Surface and Groundwater Interactions

Based on aerial photograph and field observations, there are several areas within the Upper Salmon River basin where the local groundwater aquifer intercepts the surface, resulting in visible springs and spring-fed channels on the floodplain. As discussed by others (USFS 2014), aerial photograph imagery of wide, green floodplains provides the best indication of gaining reaches. These groundwater-influenced areas tend to occur immediately upstream of geologic grade controls that constrict and/or span the valley width, such as converging glacial deposits (i.e., moraines and glacial outwash fans), alluvial fans, and/or possibly resulting from shallow bedrock or other subsurface geologic features (Figure 115).

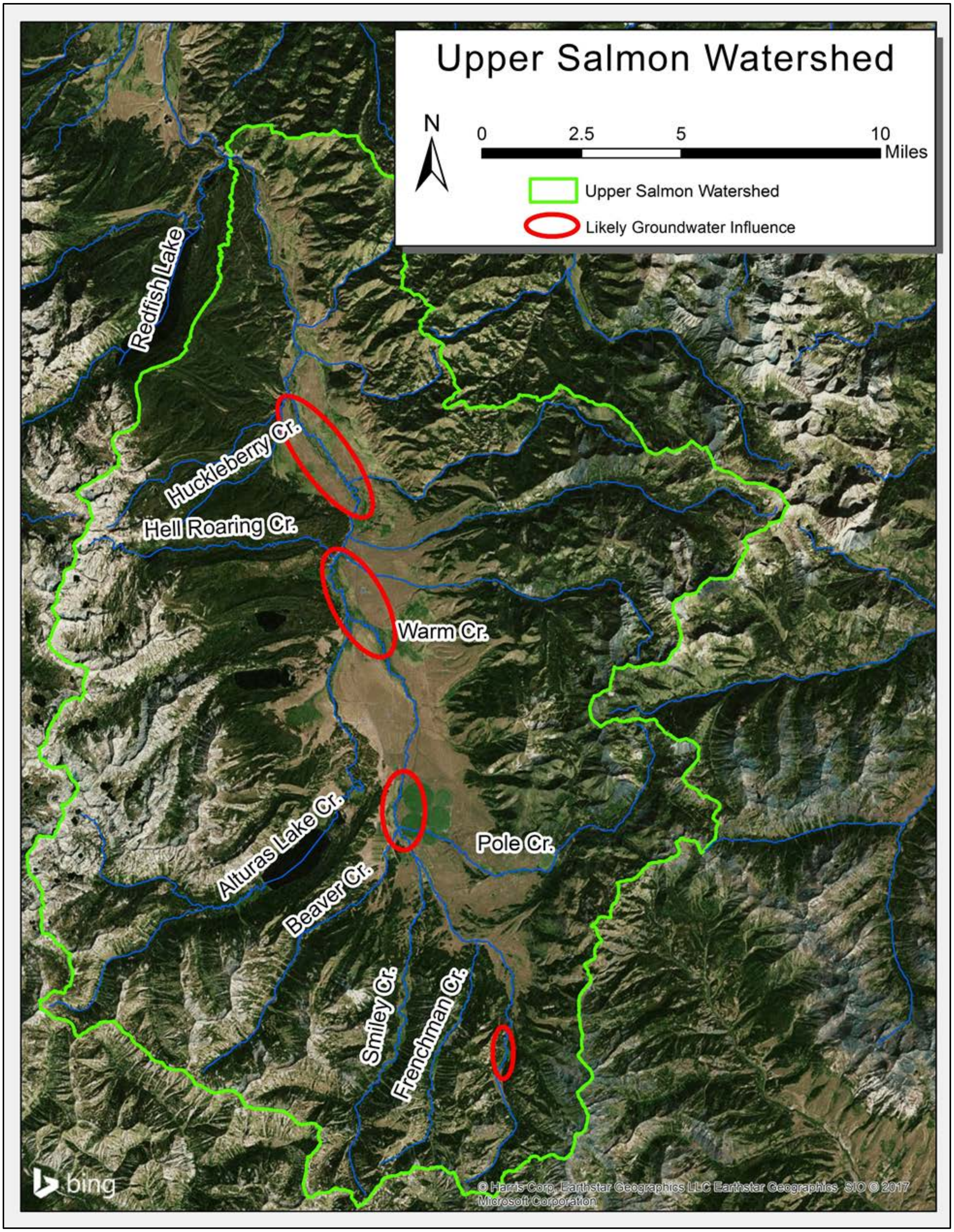

Figure 115. Aerial photo of the Sawtooth Valley identifying areas of known and expected groundwater influence, based on past seepage runs and visible green floodplains relative to surrounding areas.

There are no known groundwater analyses of the Upper Salmon River headwaters to provide comprehensive quantitative information supporting surface and groundwater interactions, but local seepage runs on and near Pole Creek were performed between 2006 and 2013 by the Idaho Department of Water Resources, USGS, and the USFS (USFS 2014). Results from these studies suggest that Pole Creek gains significantly from groundwater upstream of the Pole Creek Diversion and loses between 4 and 27 percent between the diversion and its confluence with the Salmon River. In the vicinity of the Pole Creek confluence, the mainstem Salmon River has both gains and losses from the local aquifer. Seepage runs suggest the mainstem Salmon River gains flow immediately downstream from the Pole Creek confluence (influenced by the Alturas glacial moraine near RM 24.5), then transitions into a losing condition (up to 33 percent loss) by the time it passes the former S45 diversion (i.e., Busterback diversion near RM 22.8). This losing condition persists downstream to near the Warm Creek confluence (RM 16.5), where the channel transitions again to a gaining condition between Warm Creek and roughly Huckleberry Creek (RM 6.6), where the seepage study ended (USFS 2014). These limited seepage runs support the assertion that gaining reaches tend to occur in the areas upstream of geologic grade controls (i.e., glacial moraines and/or glacial outwash fans).

Hydraulics

Coarse, at-a-station hydraulic analyses were completed from three representative locations within the watershed to provide context for the geomorphic conditions discussed below. More-detailed two-dimensional hydraulic modeling will be completed as part of the future MRA process for select reaches. Three typical cross-sections located throughout the Upper Salmon River watershed were measured and evaluated to assess existing hydraulic characteristics and to determine if any generalizations could be inferred from the calculations. Cross-sections were measured at RM 33.2 (Valley Segment 1, Geomorphic Reach 2, Figure 116), RM 13 (Valley Segment 2, Geomorphic Reach 7, Figure 117), and RM 8.2 (Valley Segment 2, Geomorphic Reach 8, Figure 118).

At a Station Hydraulic Calculations Summary Sheet

River:	Salmon
Rivermile:	33.2
Valley Segment:	2
Geomorphic Reach:	8
Reach Slope:	TBD
Localized Slope:	0.0123
n-value (range):	0.045 - 0.055

Local Sediment Size (mm)

D_{16}:	17	D_{50}:	40	D_{84}:	70

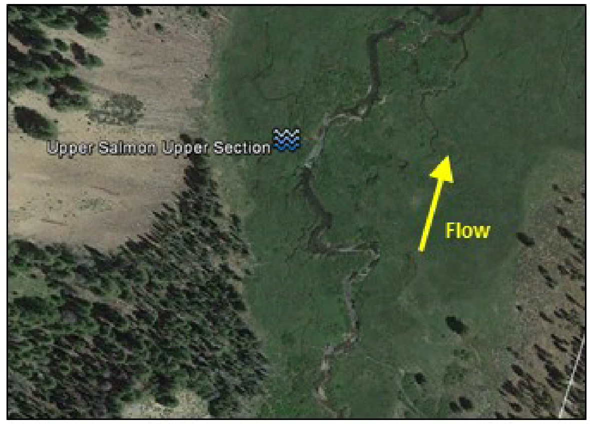

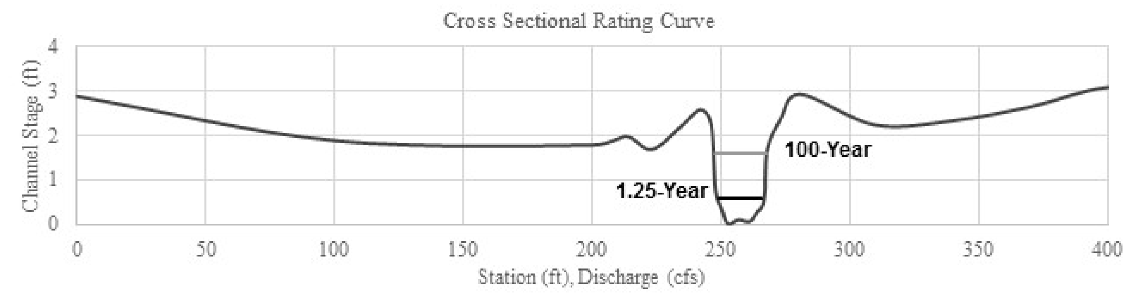

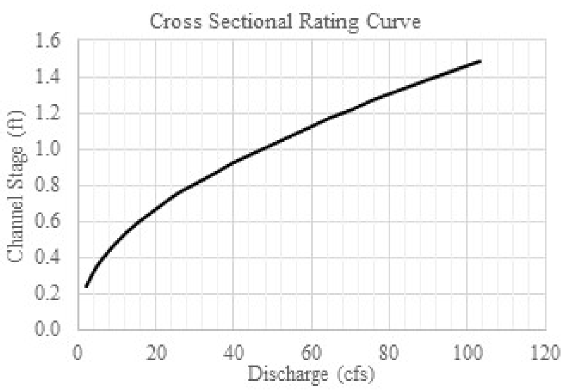

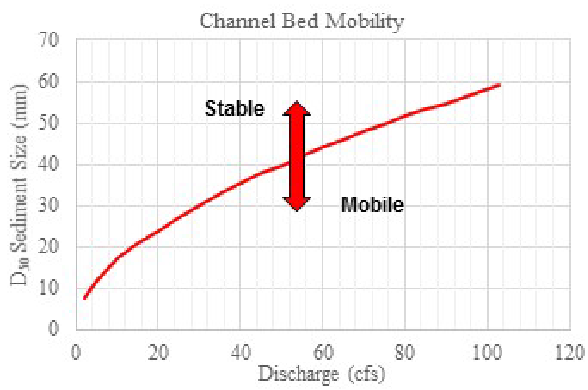

Recurrence Event:	1.25-Year	100-Year
Discharge (cfs):	12	103
Stage (ft):	0.6	1.6
Top Width (ft):	18	21
Ave. Velocity (ft/s):	1.9	3.8
Ave. Shear (lb/ft^2):	0.3	0.9
Ave. St. Power (lb/ft*s):	0.6	3.6
D_{50} Mobilized (mm):	21	103

Entrenchment Ratio (ft/ft):	1.2
Discharge to Mobilize D_{50} (cfs):	35
Bed Armored (yes/no):	Yes

Upper Salmon River– Upper Section

Integrated Rehabilitation Assessment

Idaho Governor's Office of Species Conservation Date Exported: 03/23/2017

Figure 116. Summary of representative hydraulic conditions at Site 1.

At a Station Hydraulic Calculations Summary Sheet

River:	Salmon
Rivermile:	13
Valley Segment:	1
Geomorphic Reach:	3
Reach Slope:	TBD
Localized Slope:	0.0089
n-value (range):	0.035 - 0.045

Local Sediment Size (mm)

D_{16}:	51	D_{50}:	143	D_{84}:	219

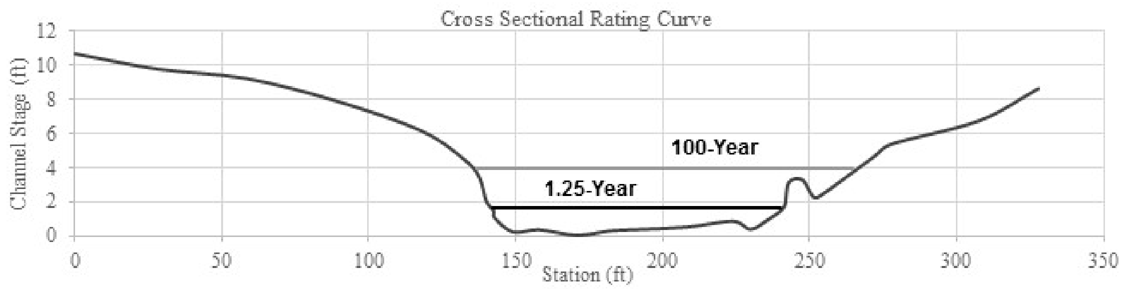

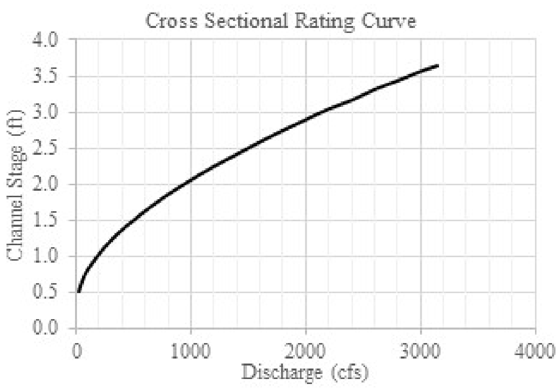

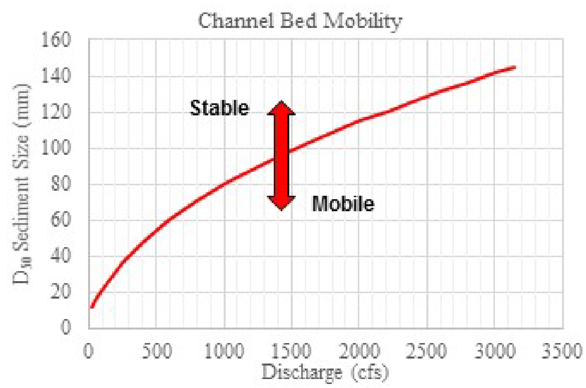

Recurrence Event:	1.25-Year	100-Year
Discharge (cfs):	487	3152
Stage (ft):	1.6	3.9
Top Width (ft):	100	135
Ave. Velocity (ft/s):	4.5	8.7
Ave. Shear (lb/ft^2):	0.9	2.3
Ave. St. Power (lb/ft*s):	3.8	20
D_{50} Mobilized (mm):	54	145

Entrenchment Ratio (ft/ft):	1.4
Discharge to Mobilize D_{50} (cfs):	3050
Bed Armored (yes/no):	Yes

Upper Salmon River – Middle Section

Integrated Rehabilitation Assessment

Idaho Governor's Office of Species Conservation Date Exported: 03/23/2017

Figure 117. Summary of representative hydraulic conditions at Site 1.

At a Station Hydraulic Calculations Summary Sheet

River:	Salmon
Rivermile:	8.2
Valley Segment:	1
Geomorphic Reach:	2
Reach Slope:	TBD
Localized Slope:	0.0064
n-value (range):	0.035 - 0.045

Local Sediment Size (mm)

D_{16}:	34	D_{50}:	73	D_{84}:	138

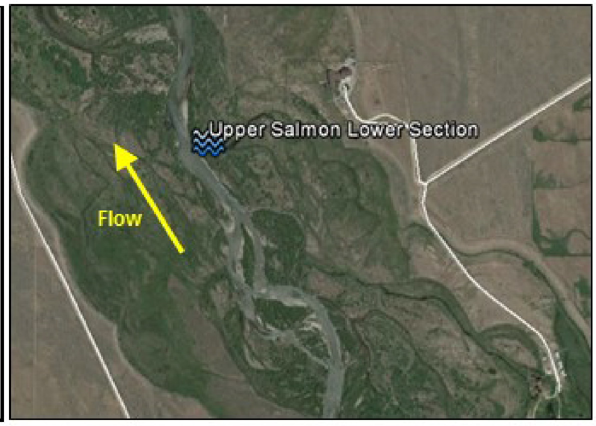

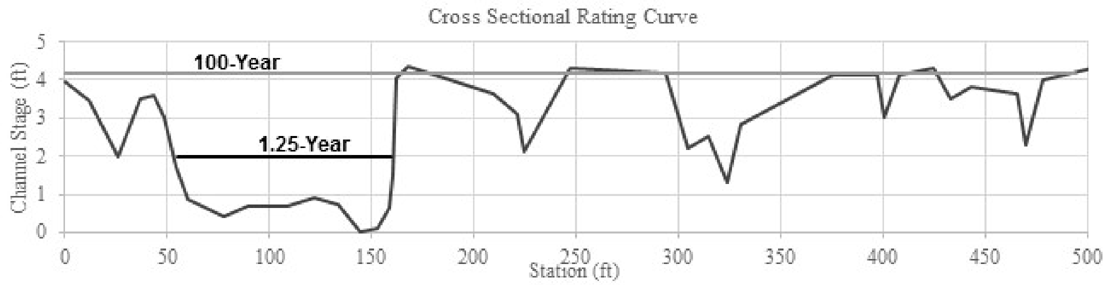

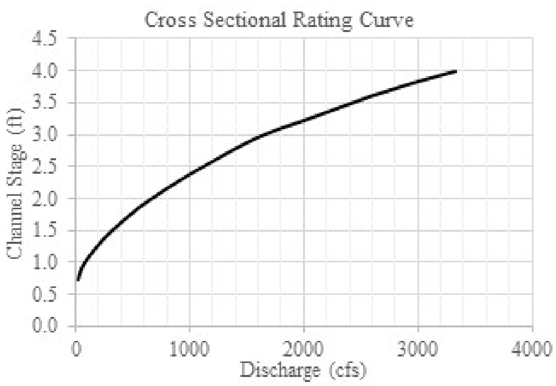

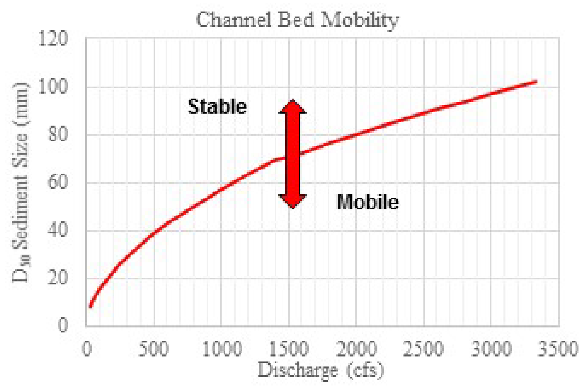

Recurrence Event:	1.25-Year	100-Year
Discharge (cfs):	597	3331
Stage (ft):	2.0	4.2
Top Width (ft):	108	533
Ave. Velocity (ft/s):	4.1	7.3
Ave. Shear (lb/ft^2):	0.7	1.6
Ave. St. Power (lb/ft*s):	2.8	11.9
D_{50} Mobilized (mm):	43	102

Entrenchment Ratio (ft/ft):	4.9[1]
Discharge to Mobilize D_{50} (cfs):	1600
Bed Armored (yes/no):	Yes

Upper Salmon River– Lower Section

Integrated Rehabilitation Assessment

Notes: 1. Entrenchment Ratio based off main channel width not including side channel.

Idaho Governor's Office of Species Conservation Date Exported: 03/23/2017

Figure 118. Summary of representative hydraulic conditions at Site 1.

The upstream-most section is located in a wide meadow with multiple beaver dam complexes. The section was taken a short distance downstream of a beaver dam. The section modeled shows the 1.25-year discharge contained within the main channel banks, with overtopping occurring above the 100-year discharge. The entrenchment ratio is 1.2, which is a completely disconnected floodplain. The sediment size showed bed mobilization beginning at less than the 1.25-year event, which allows the channel to scour and maintain pools. Average channel velocities varied from 1.9 feet per second at the 1.25-year event to 3.8 feet per second at the 100-year event. Shear stresses varied from 0.3 to 0.9 lb/ft^2 between these two events. This cross-section is likely influenced by beaver complexes, which can cause localized backwater effects, reduce sediment transport, and increase stage discharge relationships and associated floodplain activation. As a result, this section may not be representative of the reach as a whole.

The middle section is located a short distance downstream of the Salmon River's confluence with Pettit Creek. The channel is single-threaded in this area, and the section is located upstream of a bridge crossing that could be causing channel confinement. The channel geometry is such that the 1.25-year and 100-year discharge events are predominately confined within the channel, with a low entrenchment ratio of 1.4. Local sediment sizes show that the bed begins to mobilize at flows greater than 3,050 cfs, which is slightly less than the 100-year event. Channel velocities range from 4.5 ft/sec to upwards of 8.5 ft/sec. Local channel confinement and the single-threaded nature of this location have led to channel bed armoring and localized incision. The channel confining structure (bridge) located downstream is likely influencing the channel characteristics at this location.

The lower section is located in what appears to be an unconfined section of the Salmon River. At this section, there is a dominant channel, multiple relic channels, and side-channel features present throughout the section. The 100-year floodplain stage estimates show good floodplain connection through side channels and peripheral flow paths but potentially lack full floodplain width connection. The entrenchment ratio has been estimated at 4.9. Channel velocities range between 4 and 7.3 ft/sec for the 1.25- and 100-year discharge events, respectively. Shear stresses vary from 0.7 to 1.6 lb/ft^2 for the same two flow events. The channel appears to be unarmored through this section of river and begins to mobilize the D_{50} on the channel bed between the 2-year and 5-year event.

General trends observed among these three cross-sections suggest the channel bed is predominately unarmored and becomes more armored near areas confined by hydraulic control structures like bridges. Localized hydraulic controls can create either backwater conditions (i.e., beaver complexes) or localized incision and disconnection of historic floodplain. Overall channel bed material shows potential for formation and maintenance of scour pools and localized zones of deposition and scour.

A stream power assessment was also completed to examine the relative sediment transport capacity of each geomorphic reach and changes in slope. Results showed that the upper mile and lower half of the basin (RM 15.4 to RM 0) have higher stream power compared to the remainder of the basin due to a large increase in discharge from Alturas Lake Creek and slight variation in channel slope.

A two-dimensional hydraulic model is recommended for future hydraulic modeling to quantify hydraulic variables, including inundation extent, flow depth, velocity, and shear stress. A two-dimensional model (rather than a one-dimensional model) will better represent multiple channel networks, geomorphic features, and lateral flow over the floodplain. Additional data necessary for future hydraulic modeling include detailed topography, bathymetry, flow calibration data, and an improved understanding of diversion outflows, tributary inflows, and groundwater contributions.

Water Quality

The USFS reported localized areas of accelerated sediment delivery to streams in the watershed, primarily from livestock grazing, dispersed recreation, and irrigation use (SNF 2003, in NOAA 2017). In 2016, the IDEQ published a list of revisions made on tributaries and the mainstem Upper Salmon River (Table 56). The mainstem Upper Salmon River and its side channels between Decker Creek and Fisher Creek were revised to recommend delisting for sediment/siltation, based on a full-support determination for cold-water aquatic life uses and contact recreation uses. This was also the case for Alturas Lake Creek and Champion Creek. Williams Creek was not supporting cold-water aquatic life use and requires a TMDL. Further analysis will determine the pollutant(s) for the TMDL(s) on Williams Creek.

Table 56. Streams and pollutants listed in the 2016 Addendum (IDEQ 2016).

Water Body	2016 Addendum
Salmon River – Fisher Creek to Decker Creek	Sedimentation/Siltation: Recommended delisting for sediment/siltation due to insufficient information. No TMDL completed.
Alturas Lake Creek	Combined biota/habitat bioassessments: Recommended delisting for sediment/siltation due to insufficient information. No TMDL completed.
Champion Creek	Combined biota/habitat bioassessments: Recommended delisting for sediment/siltation due to insufficient information. No TMDL completed.
William Creek	Combined biota/habitat bioassessments: Recommended retaining for combined biota/habitat bioassessments. Identified as waters that need a TMDL.

Basin Geometry

Domains within a watershed can be characterized as zones that are governed by sediment supply, alluvial fan formation, sediment transfer, or deposition (Figure 119). The headwaters of the Upper Salmon River are generally classified as sediment supply zones dominated by weathering and erosion of steep slopes, where tributaries collect and transport sediment downslope to the alluvial fan zone. The alluvial fan zone is where coarse sediment has accumulated across broad alluvial fans and piedmont belts at the valley head and margins. Below the alluvial fan zone, the valley gradient flattens as the Upper Salmon River flows across the transfer zone, where the river deposits and erodes sediment, driving channel migration and occasional avulsion. Prominent grade controls influence the gradient and groundwater hydrology through the transfer zone, including terminal glacial moraines at the outlet of nearly every tributary flowing from the east face of the Sawtooth Mountains, and from Pole Creek flowing west from the White Cloud Mountains. The largest terminal moraines have impounded water, raising the local groundwater table sufficiently to form lakes on several tributaries. Prominent grade controls affecting basin and channel geometry include the Alturas Lake Creek moraine, the Hell Roaring Creek moraine, and the Redfish Lake Creek moraine (Figure 120 and Figure 121). The channel generally exhibits a typical concave curve, with decreasing slopes in the downstream direction, although several distinct breaks in slope occur as a result of grade controls formed by terminal glacial moraines, including Upper Salmon moraine (RM 33), Hell Roaring moraine (RM 13), and Redfish Lake moraine (RM 0.4). Although not a major break in slope, a moderate slope is maintained for a significant distance as a result of grade control provided by the Alturas Lake moraine (RM 23).

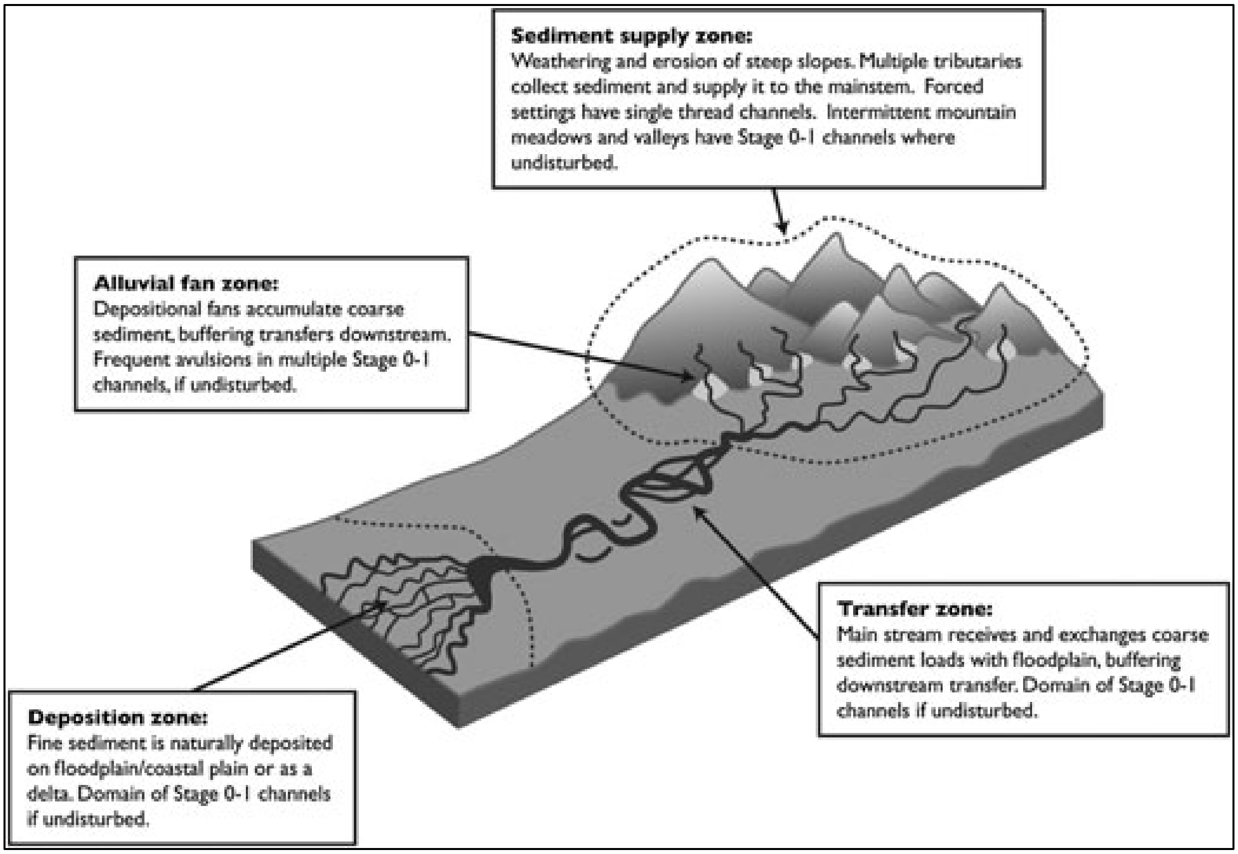

Figure 119. Locations of sediment domains within a typical watershed (Cluer and Thorne 2013).

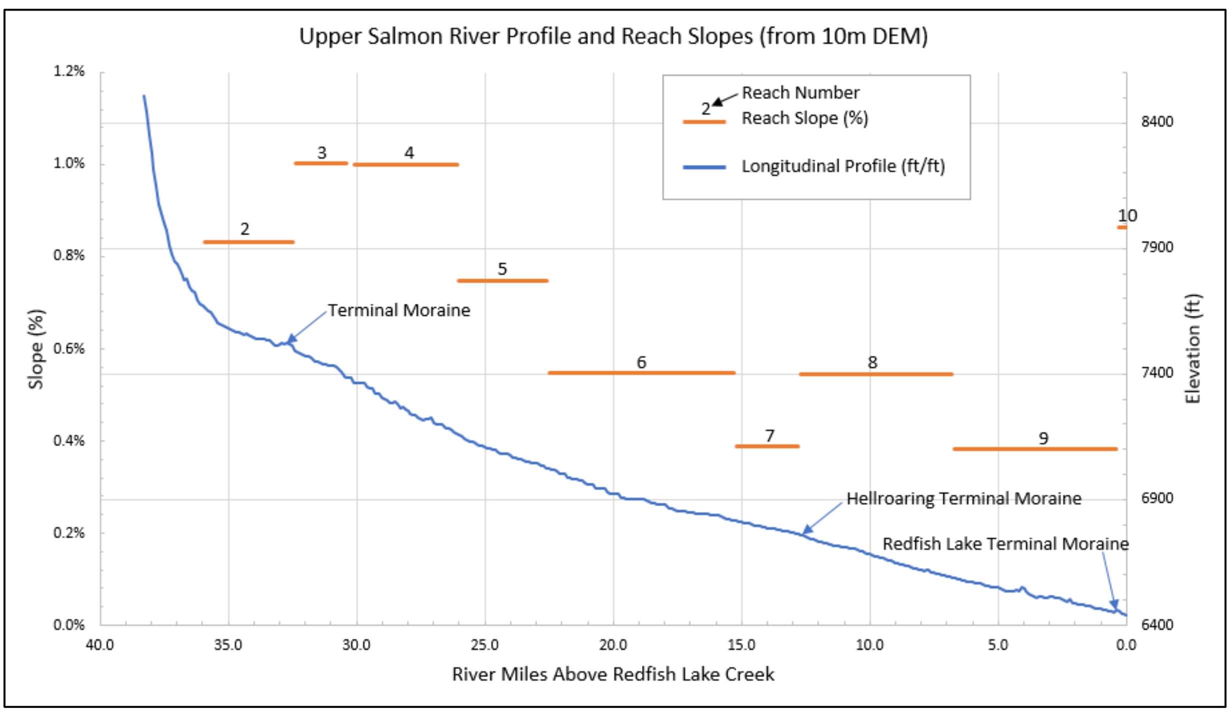

Figure 120. Upper Salmon River longitudinal profile and slope by geomorphic reach (Reach 1 slope is 6.94 percent and has been omitted from the figure to maintain a more legible scale).

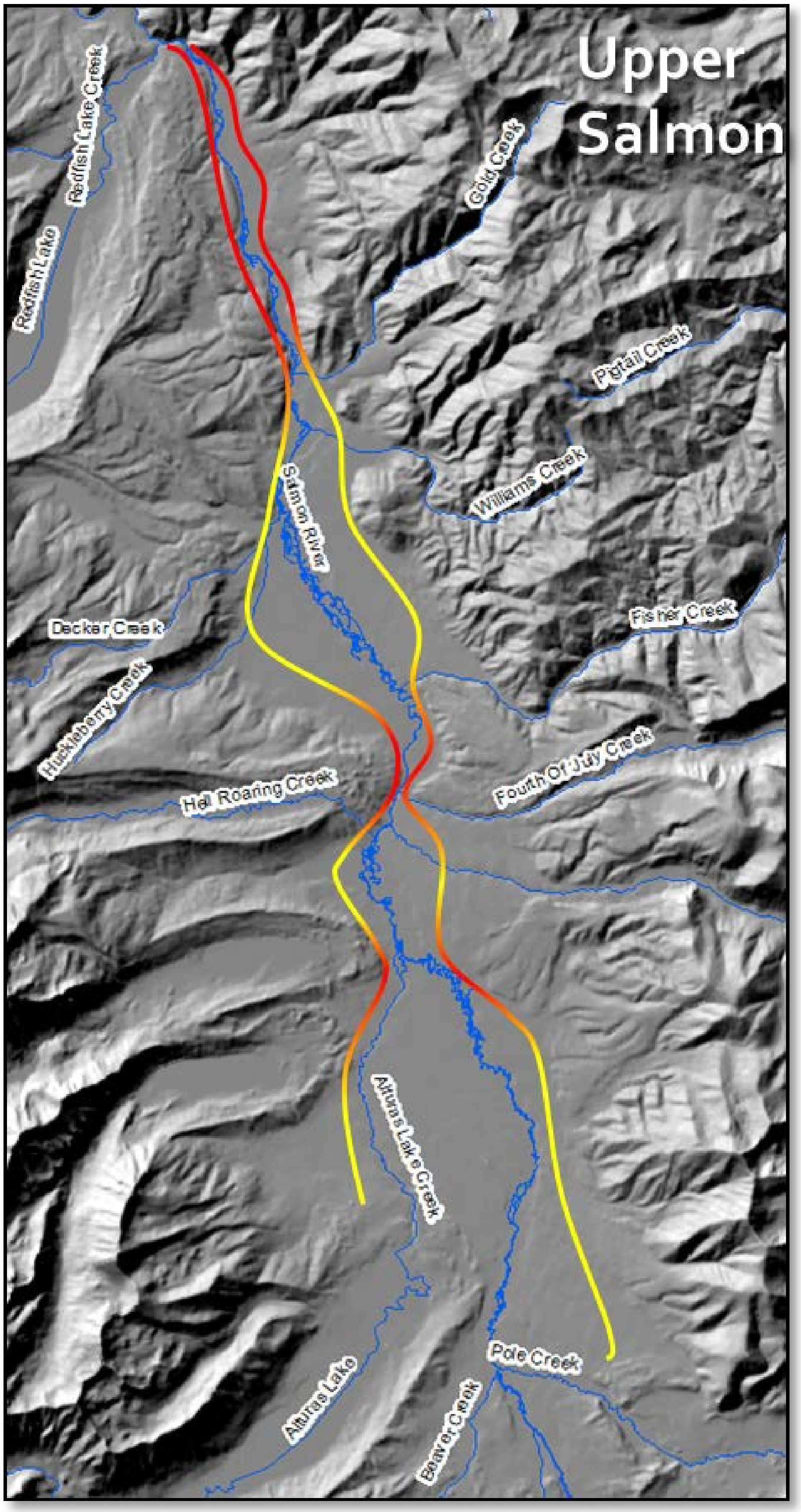

Figure 121. Illustration of valley constrictions and grade controls associated with glacial moraines and glacial outwash in the Upper Salmon River headwaters. The red lines illustrate the approximate edge of valley constrictions formed by glacial deposition on one or both sides of the valley, while the yellow lines illustrate the approximate edge of relatively unconfined valley areas.

The width of the Upper Salmon River floodplain is defined by the location of confining glacial moraines, terraces, outwash fans, and/or the valley margin. Dividing the width of the floodplain by the width of the bankfull channel produces a result called the entrenchment ratio. A small entrenchment ratio means the channel has less-accessible floodplain area and, therefore, less ability to dissipate flood energy on the floodplain, resulting in deeper, higher-velocity, more-forceful flood flows that increase the potential for erosion and/or incision (i.e., transport reach). Large entrenchment ratios are representative of channels with broadly accessible floodplains that can dissipate flood energy outside the banks of the channel, resulting in less-forceful flood flows and a tendency for deposition (i.e., response reach).

The majority of the Upper Salmon River watershed within the study area exhibits a high entrenchment ratio, with several distinct areas of confinement. The upstream-most portion of the watershed is naturally confined by a narrow valley and exhibits a low entrenchment ratio. Additionally, each of the grade controls listed above, along with other converging glacial deposits, also naturally confines the valley. Human features such as levees, road embankments, and other obstructions appear to have had minimal large-scale impact on entrenchment in the Upper Salmon River, although the impacts become more pronounced near the downstream end of the study area, where Highway 75 disconnects a large portion of the floodplain. More-detailed hydraulic modeling is required to confirm floodplain inundation timing and extent of associated entrenchment.

Soils

Geomorphic features in the Upper Salmon River valley bottom include the active channel, floodplains, alluvial fans, stream terraces, and glacial features, including moraines, outwash fans and fan terraces. Soils that have formed on these features are described in Table 57. Soil descriptions are based on the NRCS detailed soil maps and the Detailed Soil Map Units section in the report (NRCS 2003).

Table 57. Geomorphic features along the valley bottoms and margins, and associated soils.

Geomorphic Feature	Soil Description and Other Information
Active Channel	Water. Soils that have formed adjacent to or in the channel (gravel bars and islands) are described in the Floodplains soil description.
Floodplains	Soil description: a very deep, poorly drained to somewhat excessively drained soil that is dark-colored, silty loam to very cobbly sandy loam, and on floodplains and old stream channels. Slope range: 0 to 4 percent; Elevation range: 4500 to 7400 feet; Average annual precipitation: 10 to 18 inches; Average annual air temperature: 34 to 40° F; Frost-free season: 5 to 60 days; Depth class: very deep; Drainage class: very poorly drained to somewhat poorly drained; Permeability: rapid to moderate in upper part and very rapid on lower part; Available water capacity: 2.0 to 5.0 inches; Effective rooting depth: 10 to 30 inches to more than 60 inches; Runoff: slow; Hazard of water erosion: slight; Range site: mountain big sagebrush, willows, and sedges

Geomorphic Feature	Soil Description and Other Information
Alluvial Fans and Stream Terraces	Soil description: a very deep, generally well drained to somewhat excessively drained soil, is light-colored gravely loam formed on alluvial fans and stream terraces. Slope range: 1 to 8 percent; Elevation range: 6200 to 7800 feet; Average annual precipitation: 13 to 19 inches; Average annual air temperature: 33 to 40° F; Frost-free season: 5 to 60 days; Depth class: very deep; Drainage class: well-drained to somewhat excessively drained; Permeability: moderately rapid in the upper part to very rapid in the lower part; Available water capacity: 2 to 3 inches; Effective rooting depth: 10 inches to 18 inches; Runoff: slow; Hazard of water erosion: slight; Range site: mountain big sagebrush, and Idaho fescue
Outwash Fans, Fan Terraces and Moraines	Soil description: a very deep, somewhat poorly drained soil that is a darker-colored, gravely loam on outwash fans and fan terraces; sandy loam on moraines. Slope range: 2 to 10 percent (up to 15 percent on moraines); Elevation range: 6300 to 8000; Average annual precipitation: 12 to 19 inches (up to 25 inches on moraines); Average annual air temperature: 33 to 38° F; Frost-free season: 5 to 30 days; Depth class: very deep; Drainage class: well drained to excessively drained; Permeability: moderately rapid in upper part and very rapid in lower part; Available water capacity: 1 to 3 inches; Effective rooting depth: more than 60 inches; Runoff: slow; Hazard of water erosion: slight; Range site: low sagebrush, Idaho fescue, and mountain big sagebrush

Land Use

The Upper Salmon River watershed covers about 305 square miles, and about 93 percent of land is under Federal ownership. The Sawtooth National Recreation Area (SNRA) encompasses the entire watershed, with most of the upper reaches occurring in inventoried roadless areas of public land, including the Sawtooth Wilderness and the Boulder-White Clouds Wilderness. Private lands are primarily located along the more fertile valley bottoms (NOAA 2017).

The primary land uses are recreation, livestock grazing, and timber harvest. Recreation in both developed and dispersed areas is one of the most common activities. Livestock grazing and hay production are the exclusive agricultural land uses on private lands and occur across much of the middle and lower elevations in the watershed. Some timber harvesting occurs, with small operations for post and pole, personal fuelwood, or commercial saw timber and fuelwood (SNF 2006, in NOAA 2017).

Miners settled the upper Sawtooth Valley in the 1860s in the Smokey Mountains area, around the towns of Vienna and Sawtooth City, and other areas dispersed throughout the headwaters region. On August 22, 1972, Public Law 92-400 was passed, establishing the SNRA, and all lands were withdrawn from additional mineral entry, except those with existing valid claims. Currently, no active mining occurs in the SNRA (SNF 2006, in NOAA 2017).

Land Cover and Riparian Conditions

The Upper Salmon River watershed is covered by rock, water, grassland, shrubland, or meadows, including the Mountain Big Sagebrush, Montane Shrub, Basin Big Sage, Low Sage, and Dry Meadows vegetation groups. The primary forested vegetation groups include Persistent Lodgepole Pine, Warm Dry Subalpine Fir, and High Elevation Subalpine Fir. Aspen is an important component of the Persistent

Lodgepole Pine and Warm Dry Subalpine Fir groups, and whitebark pine is an important component of the High Elevation Subalpine Fir group (SNF 2003).

The riparian vegetation condition varies throughout the watershed, and localized areas have been degraded due to loss of vegetation, stream and floodplain alterations from roads, developed and dispersed recreation, water withdrawals, and livestock grazing. The native sedge and willow species are being replaced by grass species due to livestock grazing in riparian areas. In addition, irrigation diversions have had the cumulative effect of reducing wet meadows, willows, and the overall amount of riparian areas (SNF 2003).

Fire exclusion has altered vegetation succession, leading to older ages dominating structural stages, and has allowed the subalpine fir component to locally out-compete the whitebark pine component. An outbreak of mountain pine beetles and mistletoe led to large-scale mortality of mature lodgepole and whitebark stands in the late 1990s and early 2000s, which increased the fire hazard within the watershed (SNF 2003). On July 27, 2012, the Halstead Fire ignited northwest of Stanley, Idaho, and burned about 182,000 acres in timber that was described as mixed conifers, with the majority of those being dead, standing, bug-killed trees (InciWeb – Incident Information System report dated July 14, 2013).

Some noxious weeds and exotic plants are in the watershed, especially along main road and trail corridors. Plant species of particular concern are spotted knapweed and yellow toadflax that are currently found in small, scattered populations (SNF 2003).

Channel Migration

Channel migration is defined as erosion of the outside bank of a bend, coupled with concurrent deposition of sediment along the inside bank of the same bend. This process results in the lateral movement of the channel, while maintaining consistent channel shape and width (Figure 122). The peak-flow-dominated hydrology and readily available coarse sediment load in the Upper Salmon River enables frequent disturbance via pronounced channel migration throughout the Sawtooth Valley. Aerial photograph observation of active gravel bars, historical channel scars, and relic meander scrolls suggest channel migration is the dominant geomorphic process shaping the planform of the river within all but the most confined, high-gradient reaches of the study area. Low-gradient, beaver- and groundwater-influenced areas appear to exhibit greater rates of channel response and variability due to their enhanced depositional character relative to the more confined, higher-gradient, transport-dominated areas.

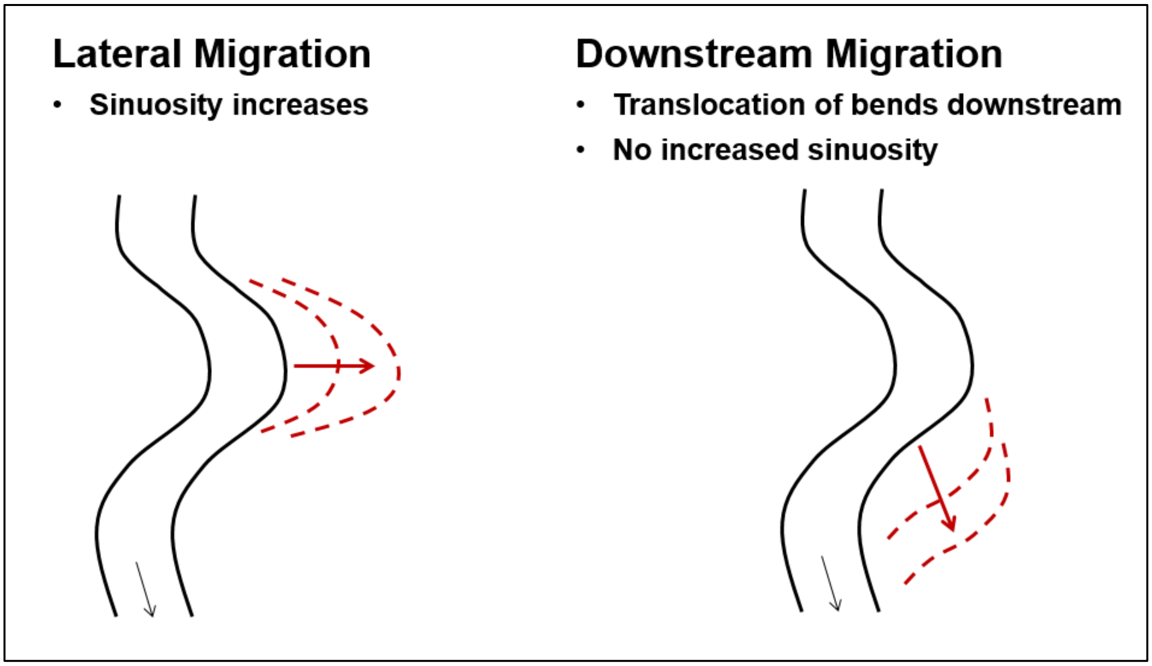

Figure 122. Simplified graphic illustrating the difference between lateral and downstream channel migration.

In areas where bank-stabilizing riparian vegetation has been cleared, bank erosion has occurred more frequently at rates greater than those of more densely vegetated banks. Sufficient coarse sediment is available to deposit gravel point bars opposite the eroding banks, generally maintaining channel geometry and preventing large-scale channel widening. Measured channel widths remain relatively consistent throughout each reach, with expected downstream gains associated with greater discharge. Conversely, where dense, woody riparian vegetation occurs, banks are stable with near-vertical to undercut geometry. The deep root systems and exposed root clumps along the banks force scour and deposition, creating and maintaining pools and riffles.

In addition to channel migration, low-gradient, beaver- and groundwater-influenced reaches also exhibit lateral channel movement via abrupt channel relocation called avulsion. Avulsions generally occur via meander cutoff or channel obstruction. Meander cutoff avulsion typically occurs when high flows bypass a large, looping meander by cutting through the narrow neck on either end of the meander. The shorter flow path rapidly expands to capture most or all of the flow, abandoning the old meander as an oxbow pond or alcove. An avulsion created by an obstruction occurs when the main flow path is blocked sufficiently to force enough flow across the floodplain to scour a new channel. Typical obstructions resulting in avulsion include excessive sediment deposition, debris jams, beaver dams, and/or ice jams.

Large Wood Recruitment and Retention

Cottonwoods are not currently observed in abundance above roughly 6,500 feet elevation on either the Salmon River or neighboring Big Wood River. Willows dominate the riparian areas above 7000 feet, providing bank stability and structure. Conifer trees, including lodgepole and whitebark pine, occupy upland areas, especially glacial moraines, which have a greater fine sediment composition and annual precipitation compared with alluvial fans and terraces. Bank erosion into areas vegetated with conifers, primarily along glacial moraines, tributaries, and upstream of Smiley Creek, provide a local source of large wood recruitment, enhancing and/or forcing channel migration and pool-riffle morphology.

Frequent, scattered pieces of large wood and several log jams are visible in recent aerial imagery of tributaries flowing through glacial moraines, but little to no large wood is visible within the mainstem Salmon River, apart from areas directly adjacent glacial moraines with conifer land cover. Large floods and debris torrents may occasionally transport large wood from the tributaries and upstream areas, but research suggests that large wood is unlikely to transport significant distances through such small streams with low channel width and depth (Braudrick and Grant 2001).

Channel Planform and Morphology

Channel planform on the Upper Salmon River is predominantly single-threaded, with a low to moderate reach-scale sinuosity ranging between 1.03 and 1.54. Sinuosity on the Upper Salmon River is the byproduct of lateral channel migration and avulsion, both of which are driven by coarse sediment deposition, with increasing response in areas of low gradient and high entrenchment ratio. Low gradients reduce overall stream power and sediment-transport capacity, and areas with high entrenchment ratios have active floodplains capable of dissipating flood energy, lowering overall channel depth and velocity. These combined characteristics tend to promote sediment deposition over transport, thereby driving channel response (including migration and avulsion), creating localized areas of high sinuosity and/or multi-threaded channels. Several reaches of the Upper Salmon River exhibit this type of response character, which is commonly enhanced by instream structure, including beaver activity and large wood. Over the past 100+ years, the removal of riparian vegetation and loss of beaver, along with irrigation diversions and channel manipulation, have likely reduced sinuosity and simplified the overall planform of the channel.

Channel morphology, as defined by Montgomery and Buffington (1998), is determined by bedform features associated with slope, discharge, sediment supply, bedrock lithology, and disturbance history. The existing channel morphology on the Upper Salmon River is predominantly characterized by a plane-bed morphology where straight and confined (Photograph 28), and is predominantly characterized by a pool-riffle morphology where sinuous and unconfined (high entrenchment ratio) (Photograph 29). Channel obstructions and bank structure-associated riparian vegetation and woody debris can increase areas of flow contraction within the channel, locally driving otherwise plane-bed morphology toward a forced pool-riffle morphology. Alternatively, where a lack of riparian vegetation has resulted in bank recession and channel widening, flow divergence reduces local transport competence and the development of scour pools driving a pool-riffle morphology toward a plane-bed morphology. Similarly, channel manipulations that have straightened and/or incised the channel tend to reduce the amount of in-stream structure and channel roughness, often creating a relatively homogenous, armored, plane-bed morphology. The significant lack of riparian vegetation and channel manipulations in some areas has likely resulted in many more linear feet of plane-bed, rather than pool-riffle, morphology relative to historic conditions. Detailed reach-scale mapping will be required to quantify this claim.

Photograph 28. Plane-bed stretch of the Upper Salmon River in Geomorphic Reach 8.

Photograph 29. Photograph example from Reach 9 illustrating a sinuous channel segment with deep scour pools along the outside of each bend, with riffles in between and woody debris associated with both.

Beaver

The existing influence from beaver has been severely limited as a result of legacy fur trapping. Evidence of existing beaver activity in several tributaries, headwaters, and small spring-fed side-channels was observed in the field (2016; Photograph 30) and via recent aerial photographs. Limited evidence of beaver activity on the mainstem Salmon River downstream of RM 33 was observed, suggesting population numbers remain fairly low. Beaver activity likely played a significant role in modifying and developing not only the headwaters and smaller tributaries, but also the lower-gradient, multi-threaded reaches of the historic mainstem Upper Salmon River. Beavers generally require 40 to 60 percent tree/shrub canopy closure and shrub height greater than 6.6 feet within a broad/intact riparian corridor (Slough and Sadleir 1997). Beavers also require trees less than 6 inches in diameter for food source, preferring aspen, willow, cottonwood, and alder (in that order) (Denney 1952). These conditions are present in discontinuous patches throughout the valley and suggest increased beaver reestablishment is possible.

Photograph 30. Beaver dam located in a perennial side channel within a multi-threaded, groundwater-influenced portion of Reach 8.

Watershed Impacts

The Upper Salmon River watershed is within the Sawtooth National Recreation Area, and most of its upper tributary reaches occur in inventoried roadless areas of public land that include the Sawtooth Wilderness Area and the Boulder-White Clouds Wilderness. Much of the watershed is pristine and protected from anthropogenic disturbances, and only natural disturbances are allowed to occur (i.e., forest fires). Overall, the physical and ecological processes in the upper tributary reaches are intact and functioning properly. However, there are localized impacts at mid- and lower-elevations that have negatively affected riverine processes. These impacts include, but are not limited to, flow alteration from irrigation diversions, loss of riparian vegetation, excessive fine sediment, and areas of channel and floodplain alteration from roads and infrastructure.

Irrigation diversions historically dewatered (or otherwise made impassible to anadromous fish) many tributaries to the Salmon River during critical anadromous fish life cycles, including Smiley Creek, Beaver Creek, Pole Creek, Champion Creek, and Fourth of July Creek (USFS 1975). The most significant impacts were associated with irrigation diversions on the Busterback Ranch, which historically dewatered both the Salmon River and Alturas Lake Creek during the summer low flows of most years between 1941 and 1992 (USFS 1975) (Photograph 31). This action was estimated to have significantly disrupted more than 32.5 miles of spawning and rearing habitat upstream of the diversions (Moulton 2014). Water rights associated with the ranch included 65.6 cfs from the Salmon River and 37.3 cfs from Alturas Lake Creek. In 1992, the majority of the Busterback Ranch and 96.53 cfs of associated water rights were purchased through a joint effort by the USFS, Bonneville Power Administration, and the Nature Conservancy, restoring consistent, perennial flows to both the Salmon River and Alturas Lake Creek (Wells 1992). An additional roughly 100 cfs of water rights held within the Sawtooth National Recreation Area have been subsequently eliminated or discontinued for instream use since 1992. Nevertheless, substantial irrigation losses continue to adversely impact instream discharge and fish passage. Another effect of irrigation diversions is an alteration of the timing and spatial distribution of groundwater recharge. Diversions redistribute river water onto the floodplain during the summer months, often artificially increasing groundwater levels in those locations.

Photograph 31. Historic oblique aerial photograph of the dewatered section of channel immediately downstream of the Busterback diversion prior to its removal.

Livestock grazing and agricultural land use practices have changed the riparian vegetation in many areas by replacing native woody riparian species (primarily willow) with grasses and other herbaceous species incapable of providing the same level of bank stability and cover. Observations of significant bank erosion generally correspond with areas where willow riparian vegetation has been reduced or lost as a result of relic or modern livestock grazing or agriculture.

Grazing and agricultural practices, as well as dirt roads and trails, have a cumulative effect on fine sediment accumulation in the Upper Salmon River. Sheetwash erosion and excessive bank erosion associated with lost riparian vegetation contribute elevated levels of fine sediment to the system from spring snowmelt and summer rainstorm runoff. Similarly, sheetwash and wind-blown fine sediment from roads and trails adds to the level of fine sediment contribution from the watershed. Fine sediment fills interstitial spaces between gravels and cobbles, eliminating concealment cover for over-wintering juvenile fish and reducing bed and pool scour potential through substrate embeddedness.

Channel and floodplain alterations from roads and infrastructure are prevalent primarily in the lower reaches and near the Sawtooth Fish Hatchery, where the channel has been straightened and confined, and a large portion of the floodplain has been disconnected from channel interactions by roads that function as levees (including Highway 75). Additionally, two channel-spanning weirs associated with the Sawtooth Fish Hatchery obstruct the natural passage of fish and sediment within the reach, contributing to the localized channel alterations of the reach.

Data Gaps

Future analysis could be aided by the collection of additional data currently unavailable, including:

- Hydraulic modeling to confirm floodplain inundation timing and extent, sediment transport character, and appropriate channel geometry (i.e., width-to-depth ratio).
    - Data gaps necessary for hydraulic modeling include detailed topography and bathymetry data, frequent pebble counts, and an improved understanding of diversion withdrawals/returns, tributary inflows, and groundwater contributions.
- Riparian vegetation inventory, including health and successional stages within the low surface that directly influence lateral channel migration, force pool-riffle bedforms, sort and retain gravel, and provide bank stability.

The acquisition of LiDAR will aid hydraulic modeling and riparian vegetation inventories in addition to future assessment and design efforts in the Sawtooth Valley.

Upper Salmon Valley Segments and Geomorphic Reaches

Valley segments, geomorphic reaches, and channel units are three hierarchically nested subdivisions of the drainage network (Frissell et al. 1986). Within the hierarchy of spatial scales, valley segments, geomorphic reaches, and channel units represent the largest physical subdivisions that can be directly altered by human activities. As such, it is useful to understand how they respond to anthropogenic disturbance, but to do so requires classification systems and quantitative assessment procedures that facilitate accurate, repeatable descriptions and convey information about biophysical processes that create, maintain, and destroy channel structure (Bisson, Buffington, and Montgomery 2006).

Valley Segments

The Upper Salmon River has a predominantly alluvial valley and has varying discharge and morphology along its course due to flow and sediment inputs from sub-watersheds (Table 58). Two valley segments were identified based on the location of where the Upper Salmon River begins and where the sub-watersheds interact with or are identified along the mainstem (Figure 123).

Table 58. Upper Salmon River watershed valley segment delineations and sub-watersheds.

Valley Segments and Locations	Sub-watershed	HUC 10	River Miles	Square Miles
Pole Creek Valley Segment (Headwaters to RM 15.3)	Pole Creek – Salmon River	1706020102	Upstream of 15.3	106
	Alturas Lake Creek	1706020103		70
Redfish Lake Creek Valley Segment (RM 15.3 to 0)	Portion of Redfish Lake Creek – Salmon River	1706020104	15.3 - 0	128
Total				**195,200 acres**

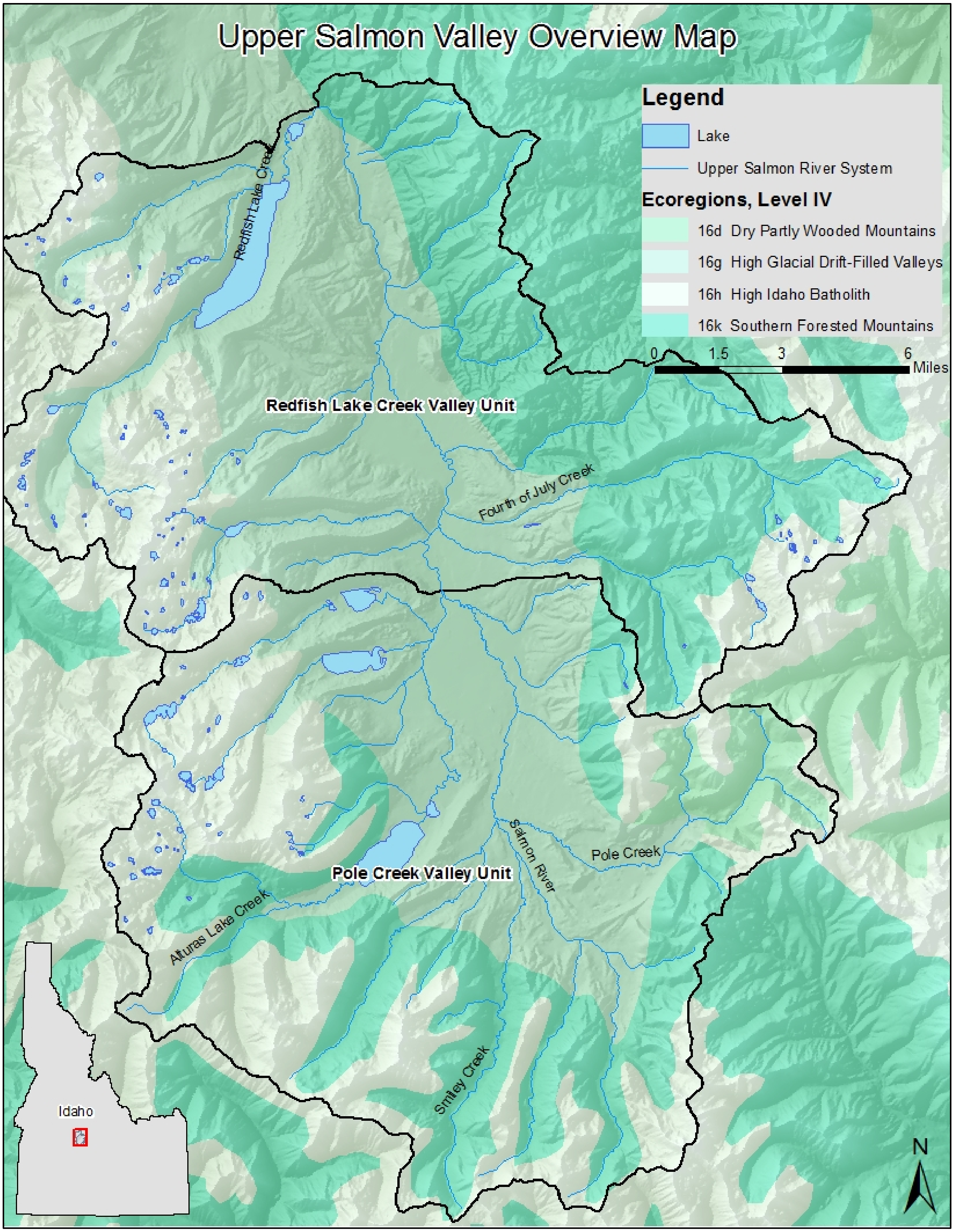

Figure 123. Upper Salmon River watershed valley segment locations.

Reach Characteristics

Reach characteristics are summarized per reach in Table 59 below.

Table 59. Summary of geomorphic reach characteristics for the Upper Salmon watershed.

Valley Segment	Reach	River Miles	Valley Slope (ft/ft)	Average Valley Width (ft)	Average Constrained Valley Width (ft)	Channel Slope (ft/ft)	Average Channel Width (ft)	Sinuosity	Entrenchment Ratio (ft/ft)	Constrained Entrenchment Ratio (ft/ft)	Human Disturbance Ratio (%)	Groundwater Characteristics	Geomorphic Characterization "Complex"	Geomorphic Characterization "Mixed"	Geomorphic Characterization "Simplified"
VS-1	GR-1	38.3 - 36.0	0.0767	97	96	0.0713	11	1.1	9	9	1%	-	0%	100%	0%
VS-1	GR-2	36.0 - 32.5	0.0131	499	501	0.0092	17	1.4	29	29	8%	-	73%	11%	0%
VS-1	GR-3	32.5 - 30.4	0.0121	339	340	0.0091	18	1.3	18	18	2%	-	77%	20%	3%
VS-1	GR-4	30.4 - 26.1	0.0123	252	228	0.0099	17	1.2	15	13	3%	-	36%	62%	3%
VS-1	GR-5	26.1 - 22.6	0.0095	652	650	0.0072	33	1.3	20	20	1%	Gaining	70%	28%	2%
VS-1	GR-6	22.6 - 15.3	0.0083	944	877	0.0054	37	1.5	26	24	1%	Losing	62%	38%	0%
VS-2	GR-7	15.3 - 12.8	0.0050	1584	1,525	0.0038	68	1.3	23	22	1%	Gaining	76%	24%	0%
VS-2	GR-8	12.8 - 6.6	0.0063	1280	1280	0.0048	66	1.3	19	19	6%	Gaining	81%	14%	5%
VS-2	GR-9	6.6 - 0.4	0.0057	1123	903	0.0052	72	1.1	16	13	3%	-	73%	18%	9%
VS-2	GR-10	0.4 - 0.0	0.0020	122	-	0.0020	78	1.0	2	-	0%	-	56%	44%	0%

- No constraints exist within the approximated floodplain.

Pole Creek Valley Segment (VS-1)

The Pole Creek Valley Segment comprises the Pole Creek sub-watershed (HUC 10 – 1706020102) with 106 square miles (68,129 acres), and the Alturas Lake Creek sub-watershed (HUC 10 – 1706020103) with 70 square miles (45,008 acres), for a total of 177 square miles (113,137 acres) (Figure 124). The valley segment is along the Upper Salmon River from the headwaters to about RM 15.3 and contains Geomorphic Reaches GR-1 through GR-6. In the Pole Creek sub-watershed, elevations range from a low of about 6820 feet at the Upper Salmon River and Alturas Lake Creek confluence to a high of about 10100 feet along the ridgeline near Bromaghin Peak. Named tributaries in this valley segment include Beaver Creek, Smiley Creek, Frenchman Creek, Pole Creek, Taylor Creek, Lost Creek, Warm Creek, and Camp Creek. In the Alturas Lake Creek sub-watershed, elevations range from a low of about 6820 feet where Alturas Lake Creek enters the Upper Salmon River to a high of about 10600 feet along the ridgeline near Snowyside Peak. Named waterbodies include Alturas Lake, Perkins Lake, Twin Lakes, Alice Lakes, Toxaway Lake, Pettit Lake, and Yellow Belly Lake. Named tributaries include Alpine Creek, Cabin Creek, Vat Creek, and Alturas Lake Creek.

This valley segment includes portions of the supply, alluvial fan, and transfer zones where coarse sediment is generated in the headwaters, accumulates across broad alluvial fans, and finally enters the mainstem, where it is exchanged with bed, bar, and floodplain deposits through channel/floodplain interactions. The Upper Salmon River is believed to lose water to the groundwater system through geomorphic reaches GR-1 and GR-2 and naturally runs dry during low-flow periods from about RM 35.55 to 34.72.

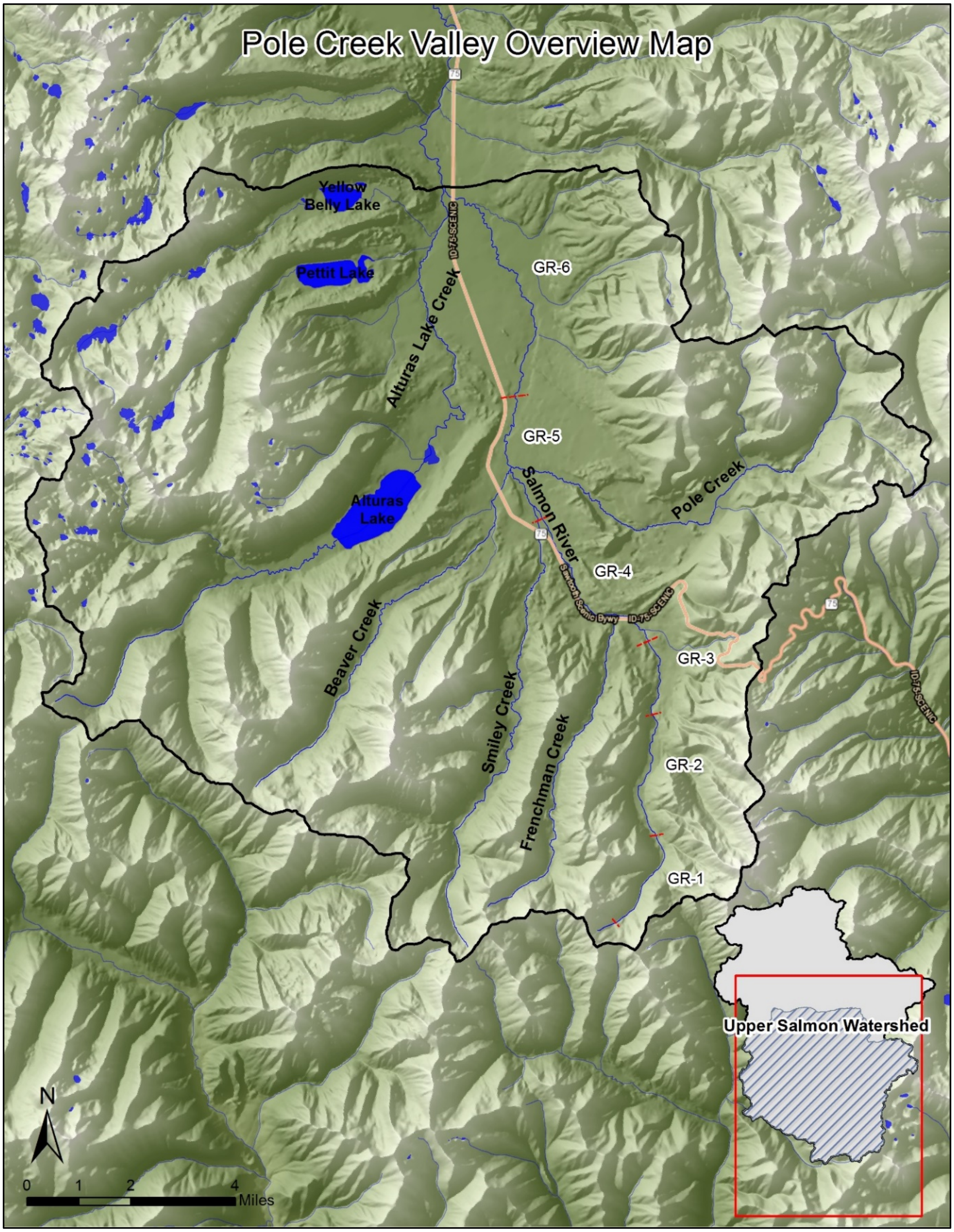

Figure 124. Location of Pole Creek Valley Segment and associated geomorphic reaches (GR-1 through GR-6).

Geomorphic Reach GR-1 (RM 38.3 – 36.0)

Geomorphic Reach GR-1 is located along the Upper Salmon River between RM 38.3 and RM 36.0. The riverine system begins where water flowing through glacial debris and colluvium daylights near RM 38.3 in a channelized colluvial valley. The reach becomes less confined farther downstream, with no valley bottom constraints (Figure 125). The downstream end of the reach is defined by a geological grade control near RM 36.0. Reach characteristics are summarized below in Table 60.

Table 60. Summary of attributes for Geomorphic Reach GR-1.

Valley Segment	Reach	River Miles	Valley Slope (ft/ft)	Average Valley Width (ft)	Average Constrained Valley Width (ft)	Channel Slope (ft/ft)	Average Channel Width (ft)	Sinuosity	Entrenchment Ratio (ft/ft)	Constrained Entrenchment Ratio (ft/ft)	Human Disturbance Ratio (%)	Groundwater Characteristics	Geomorphic Characterization "Complex"	Geomorphic Characterization "Mixed"	Geomorphic Characterization "Simplified"
VS-1	GR-1	38.3 - 36.0	0.0767	97	97	0.0713	11	1.1	9	9	1%	-	0%	100%	0%

Forms

- Relatively straight, single-thread, headwater channel confined by the valley margins.
- Primarily step-pool (or forced step-pool) morphology.
- Significant volume of individual pieces of large wood (no log jams).
- Geologic grade control associated with ancient glacial activity enables the establishment of a relatively low-gradient, wet meadow at the downstream end of the otherwise high-gradient reach.

Processes

- Dominated by sediment transport.
- Presumed to be primarily losing flow to groundwater, with the exception of the wet meadow at the downstream end of the reach, where a geologic grade control enables what appears to be a small gaining area.
- Large wood recruitment via avalanches, mass wasting, and wind throw; little to no large wood transport due to the small width and shallow depth of the channel.
- Probable beaver activity in the wet meadow.

Human Impact

- Minimal human impact.
- Fine sediment from an abandoned road (recently closed and converted to a trail).

Response Potential

- Minimal.
- Sediment transport and incision.
- Bank erosion and localized large wood recruitment.

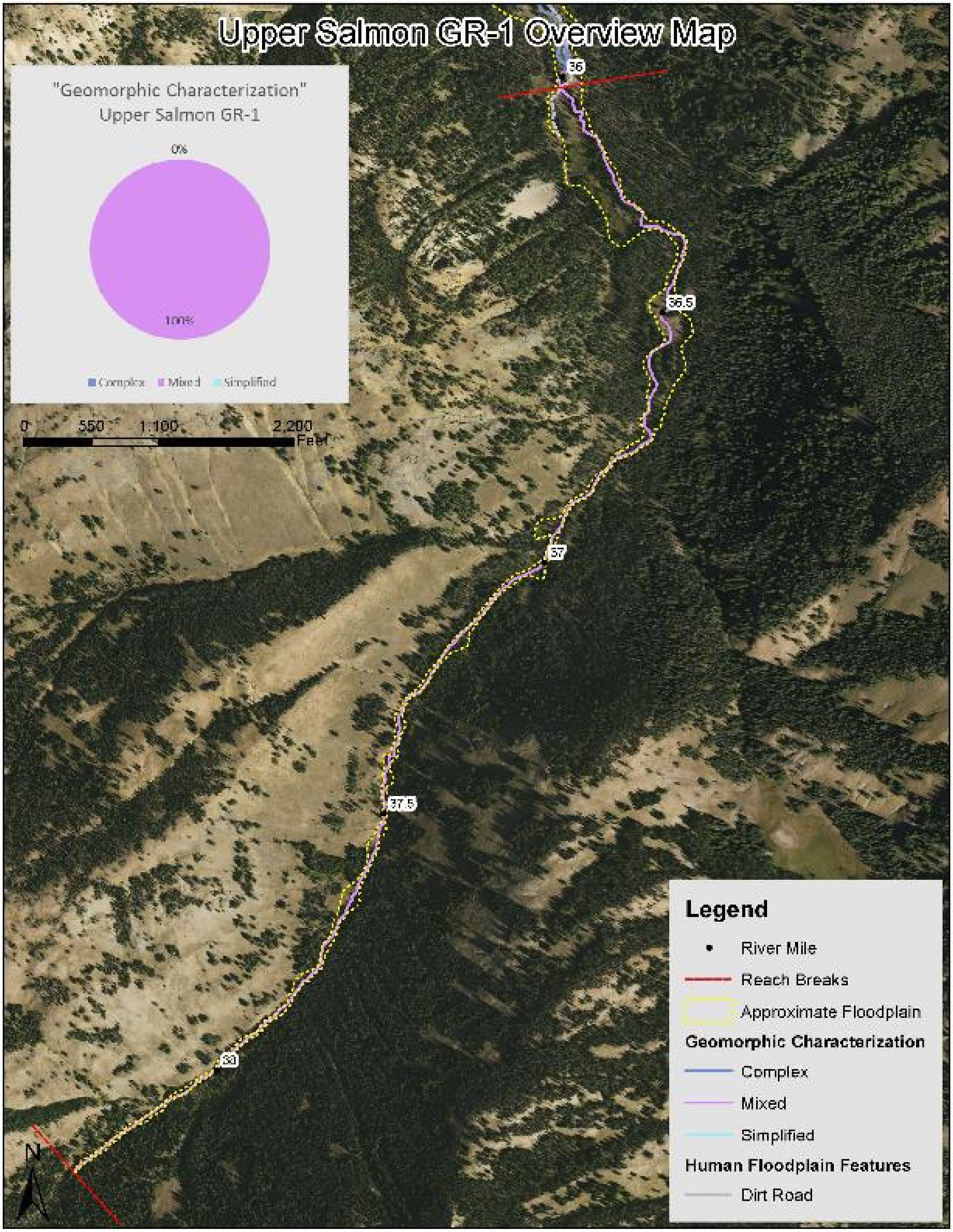

Figure 125. GR-1 overview map illustrating the approximate floodplain, geomorphic characterization, and human alterations to the floodplain.

Geomorphic Reach GR-2 (RM 36.0 – 32.5)

Geomorphic Reach GR-2 is located along the Upper Salmon River between RM 36.0 and RM 32.5 in a naturally unconfined valley, with no human features constraining valley or channel width (Figure 126). Reach characteristics are summarized below in Table 61.

Table 61. Summary of attributes for Geomorphic Reach GR-2.

Valley Segment	Reach	River Miles	Valley Slope (ft/ft)	Average Valley Width (ft)	Average Constrained Valley Width (ft)	Channel Slope (ft/ft)	Average Channel Width (ft)	Sinuosity	Entrenchment Ratio (ft/ft)	Constrained Entrenchment Ratio (ft/ft)	Human Disturbance Ratio (%)	Groundwater Characteristics	Geomorphic Characterization "Complex"	Geomorphic Characterization "Mixed"	Geomorphic Characterization "Simplified"
VS-1	GR-2	36.0 - 32.5	0.0131	499	499	0.0092	17	1.4	29	29	8%	-	73%	11%	0%

Forms

- Moderate sinuosity, single-thread channel with numerous side channels and ponds.
- Upper reach is naturally dewatered during low-flow periods (RM 35.55 to RM 34.72).
- Primarily grass and shrub species in the dewatered section; dense riparian vegetation consisting primarily of willow and other shrubs downstream of dewatered section.
- Dry upper reach has unstable banks and a braided morphology.
- Groundwater-influenced lower reach has well-vegetated, stable banks with a pool-riffle morphology.

Processes

- Mixed sediment-transport regime, including deposition, temporary storage, and transport.
- Beaver activity in the wet meadows visible in aerial photography.

Human Impact

- Minimal human impact; an access road to the upper section has been decommissioned and is now a trail. There is a developed campsite and dispersed campsites in the lower section.
- Cattle grazing impacts, including bank erosion and lost riparian vegetation in several locations. The historical cattle grazing allotment in this area may have been closed in conjunction with the decommissioning of the access road.

Response Potential

- Increased sinuosity and pool-riffle formation associated with riparian vegetation and instream obstruction (including beaver dams).
- Channel avulsion associated with instream obstruction (coarse sediment deposition, beaver dams, debris flows).
- Channel widening and simplification associated with lost bank vegetation and eroding banks.

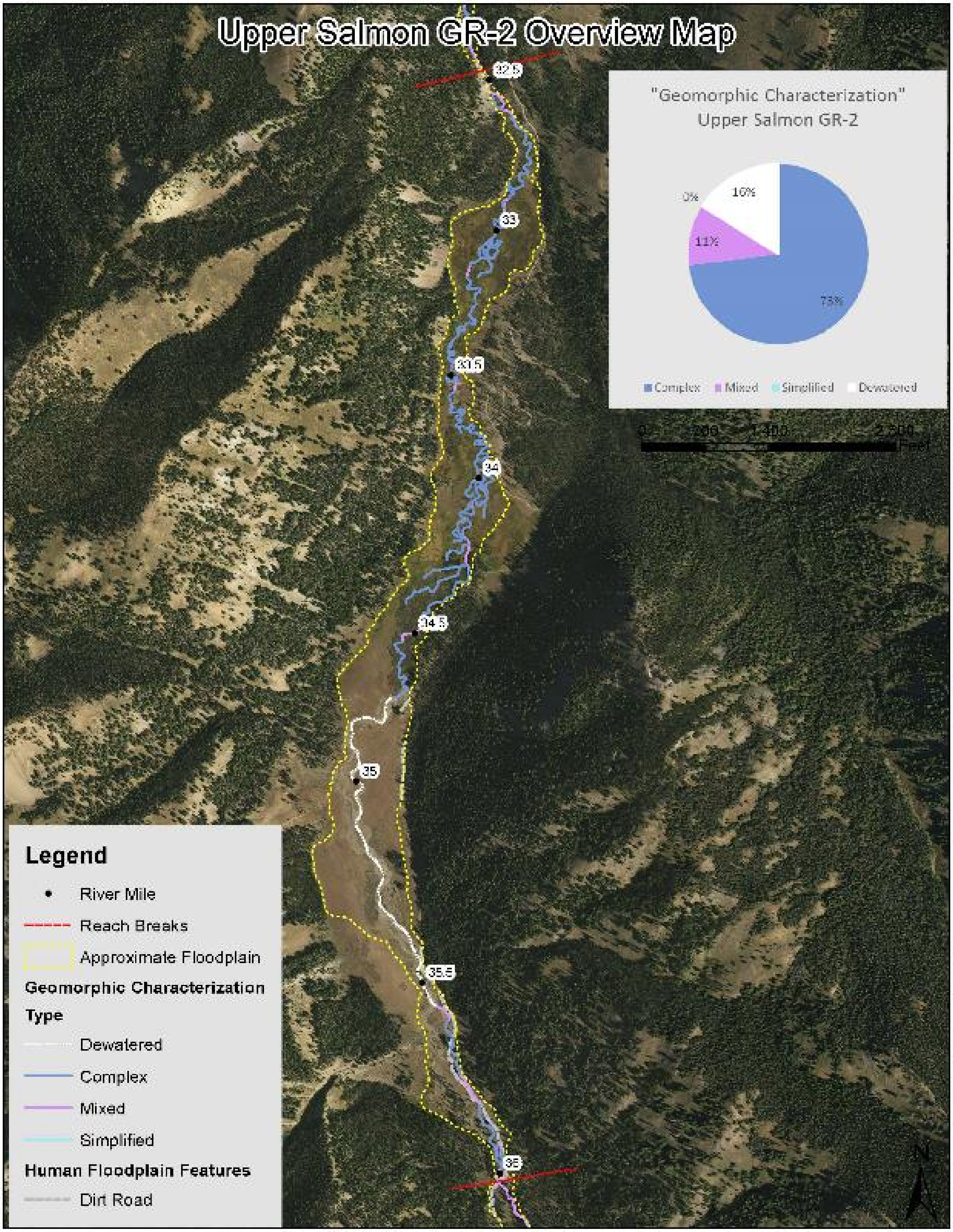

Figure 126. GR-2 overview map illustrating the approximate floodplain, geomorphic characterization, and human alterations to the floodplain.

Geomorphic Reach GR-3 (RM 32.5 – 30.4)

Geomorphic Reach GR-3 is located along the Upper Salmon River between RM 32.5 and RM30.4 in an unconfined valley, with no human features constraining the valley bottom (Figure 127). The upper end of the reach is defined by a glacial moraine that constricts the valley width. Much of the reach flows through variable glacial terrain, providing apparent areas of groundwater gains and losses. Reach characteristics are summarized below in Table 62.

Table 62. Summary of attributes for Geomorphic Reach GR-3.

Valley Segment	Reach	River Miles	Valley Slope (ft/ft)	Average Valley Width (ft)	Average Constrained Valley Width (ft)	Channel Slope (ft/ft)	Average Channel Width (ft)	Sinuosity	Entrenchment Ratio (ft/ft)	Constrained Entrenchment Ratio (ft/ft)	Human Disturbance Ratio (%)	Groundwater Characteristics	Geomorphic Characterization "Complex"	Geomorphic Characterization "Mixed"	Geomorphic Characterization "Simplified"
VS-1	GR-3	32.5 - 30.4	0.0121	339	339	0.0091	18	1.3	18	18	2%	-	77%	20%	3%

Forms

- Moderate sinuosity, single-thread channel with occasional side channels and ponds.
- Primarily pool-riffle morphology.
- Significant volume of individual pieces of large wood with a few log jams.
- Continuous dense riparian vegetation consisting primarily of willow and pine trees with sections of grass and shrubs.

Processes

- Relatively stable banks; minimal channel migration; some widening observed upstream of beaver dams.
- Mixed sediment-transport regime, including deposition, temporary storage, and transport.
- Observable beaver activity in the wet meadows.

Human Impact

- Minimal human impacts.
- Several dispersed campsites along the river.

Response Potential

- Increased sinuosity and pool-riffle formation associated with riparian vegetation and instream obstruction.
- Channel avulsion associated with instream obstruction (debris jams and beaver dams).

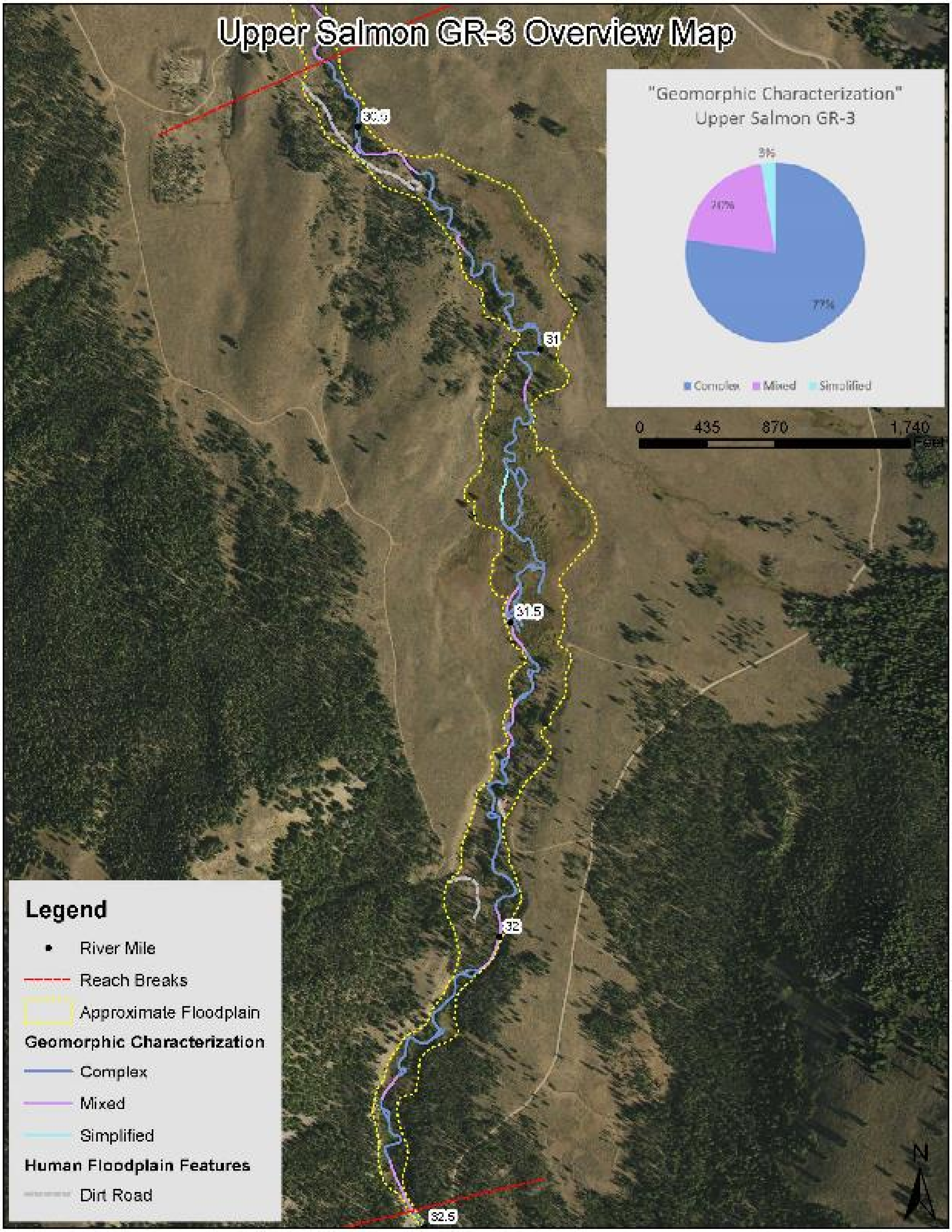

Figure 127. GR-3 overview map illustrating the approximate floodplain, geomorphic characterization, and human alterations to the floodplain.

Geomorphic Reach GR-4 (RM 30.4 – 26.1)

Geomorphic Reach GR-4 is located along the Upper Salmon River between RM 30.4 and RM 26.1 and is naturally confined by glacial terraces, with minor valley-bottom constraints associated with Highway 75 (Figure 128). Reach characteristics are summarized below in Table 63.

Table 63. Summary of attributes for Geomorphic Reach GR-4.

Valley Segment	Reach	River Miles	Valley Slope (ft/ft)	Average Valley Width (ft)	Average Constrained Valley Width (ft)	Channel Slope (ft/ft)	Average Channel Width (ft)	Sinuosity	Entrenchment Ratio (ft/ft)	Constrained Entrenchment Ratio (ft/ft)	Human Disturbance Ratio (%)	Groundwater Characteristics	Geomorphic Characterization "Complex"	Geomorphic Characterization "Mixed"	Geomorphic Characterization "Simplified"
VS-1	GR-4	30.4 - 26.1	0.0123	252	218	0.0099	17	1.2	15	13	3%	-	36%	62%	3%

Forms

- Low to moderate sinuosity, single-thread channel with occasional side channels.
- Primarily pool-riffle morphology.
- Discontinuous riparian vegetation consisting primarily of willow and other shrubs.

Processes

- Relatively stable banks; minimal channel migration; some widening observed where riparian vegetation is lacking.
- Mixed sediment-transport regime, including deposition, temporary storage, and transport.

Human Impact

- Minor human impacts.
- Cattle grazing impacts including bank erosion and lost riparian vegetation in several locations.
- Minimal valley confinement associated with Highway 75.
- Cattle grazing, dirt roads, bridges and irrigation diversion.

Response Potential

- Increased sinuosity and pool-riffle formation associated with riparian vegetation and instream obstruction (including beaver dams).
- Channel avulsion associated with instream obstruction (coarse sediment deposition, debris, and ice jams).
- Channel widening and simplification associated with lost bank vegetation.

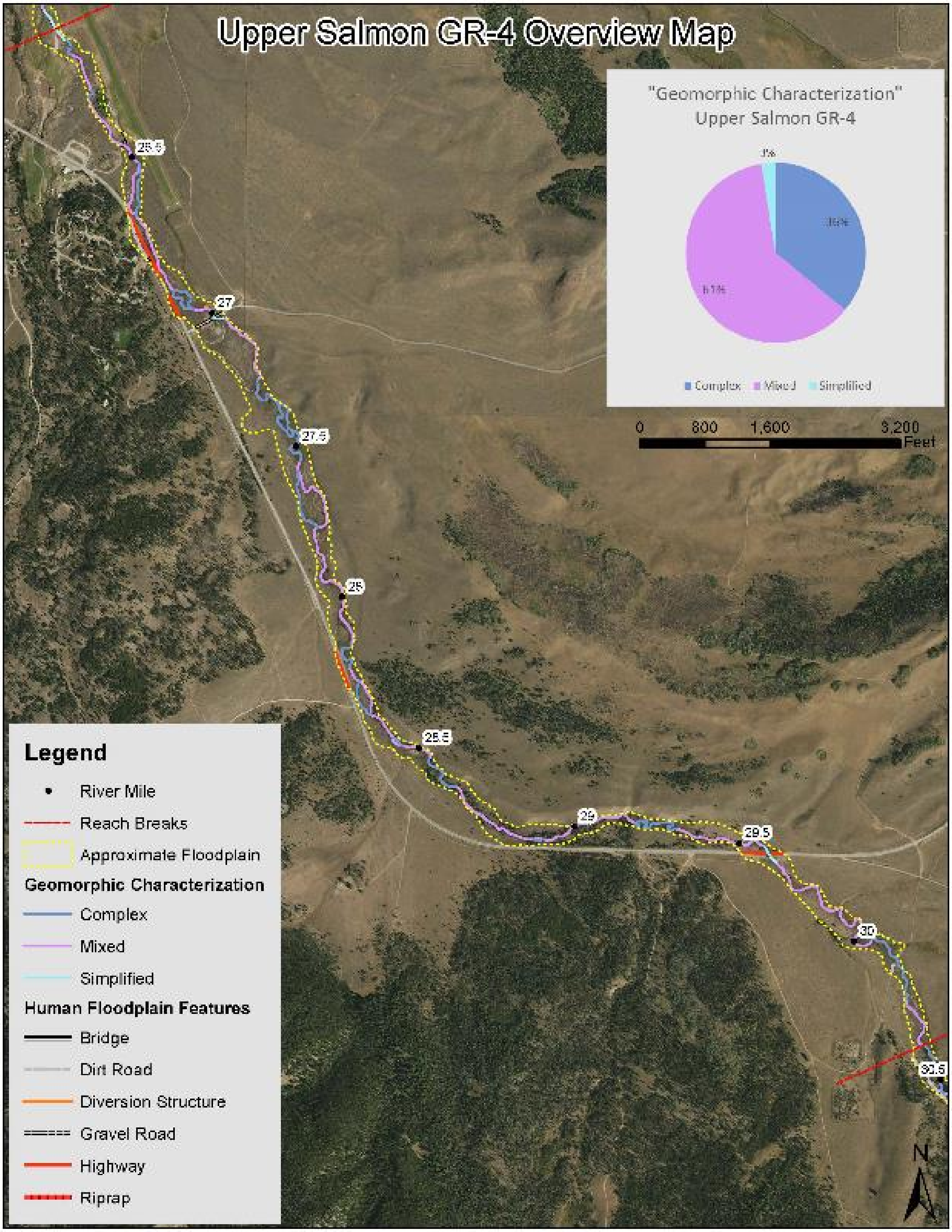

Figure 128. GR-4 overview map illustrating the approximate floodplain, geomorphic characterization, and human alterations to the floodplain.

Geomorphic Reach GR-5 (RM 26.1 – 22.6)

Geomorphic Reach GR-5 is located along the Upper Salmon River between RM 26.1 and RM 22.6 in an unconfined valley, with no significant valley-bottom constraints (Figure 129). Reach characteristics are summarized below in Table 64.

Table 64. Summary of attributes for Geomorphic Reach GR-5.

Valley Segment	Reach	River Miles	Valley Slope (ft/ft)	Average Valley Width (ft)	Average Constrained Valley Width (ft)	Channel Slope (ft/ft)	Average Channel Width (ft)	Sinuosity	Entrenchment Ratio (ft/ft)	Constrained Entrenchment Ratio (ft/ft)	Human Disturbance Ratio (%)	Groundwater Characteristics	Geomorphic Characterization "Complex"	Geomorphic Characterization "Mixed"	Geomorphic Characterization "Simplified"
VS-1	GR-5	26.1 - 22.6	0.0095	652	652	0.0072	33	1.3	20	20	1%	Gaining	70%	28%	2%

Forms

- Moderate sinuosity, single-thread channel with numerous side channels and ponds.
- Primarily pool-riffle morphology.
- Discontinuous riparian vegetation consisting primarily of willow and other shrubs. Greater riparian density in multi-threaded areas.
- Gaining reach associated with geologic control formed by the Alturas glacial moraine.

Processes

- Relatively stable banks; minimal channel migration; some widening observed where riparian vegetation is lacking.
- Mixed sediment-transport regime, including deposition, temporary storage, and transport.
- Beaver activity in the wet meadows visible in aerial photography.

Human Impact

- Minor human impacts.
- Cattle grazing impacts, including bank erosion and lost riparian vegetation in several locations.
- Cattle grazing, dirt roads, and bridges.

Response Potential

- Increased sinuosity and pool-riffle formation associated with riparian vegetation and instream obstruction (including beaver dams).
- Channel avulsion associated with instream obstruction (coarse sediment deposition, beaver dams, debris, and ice jams).
- Channel widening and simplification associated with lost bank vegetation and eroding banks.

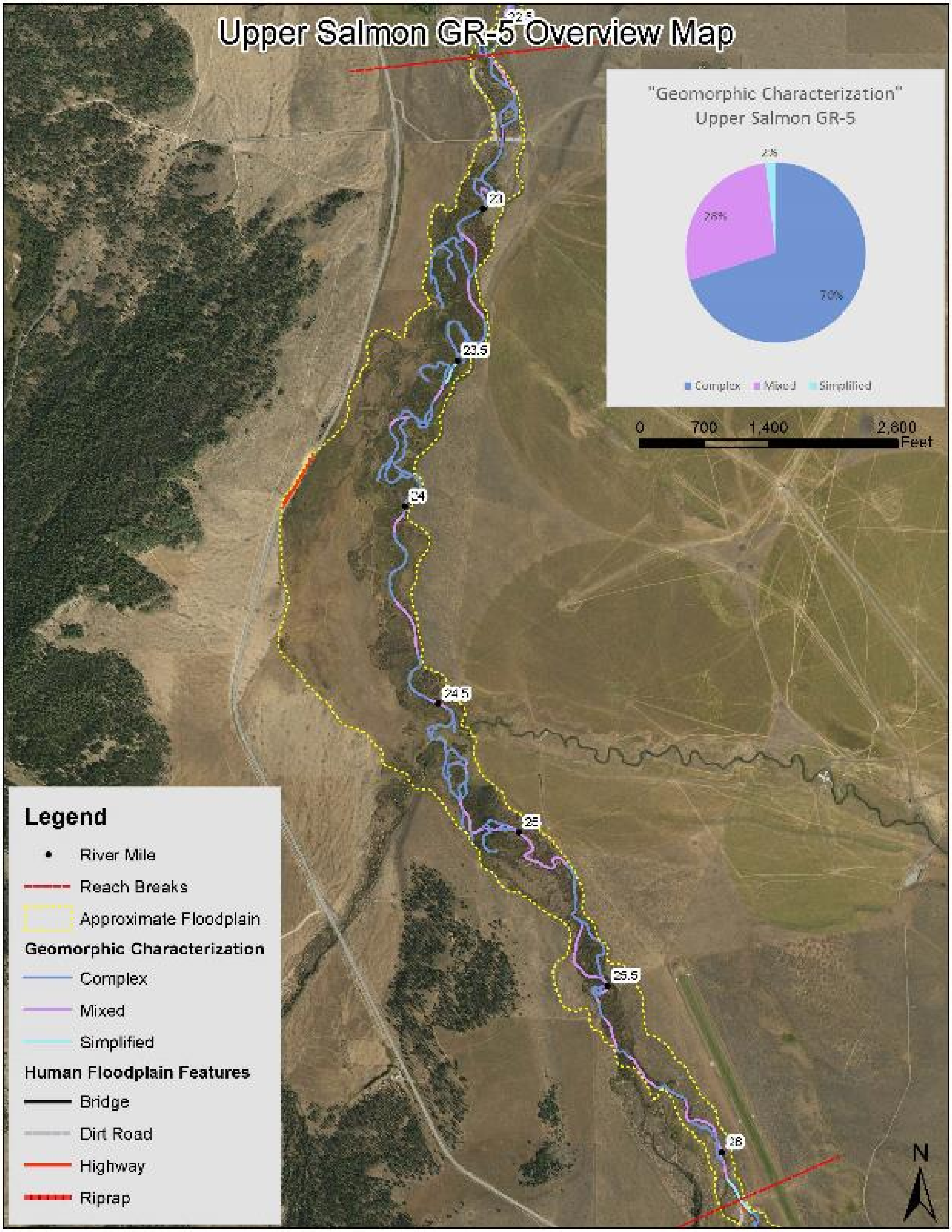

Figure 129. GR-5 overview map illustrating the approximate floodplain, geomorphic characterization, and human alterations to the floodplain.

Geomorphic Reach GR-6 (RM 22.6 – 15.3)

Geomorphic Reach GR-6 is located along the Upper Salmon River between RM 22.6 and RM 15.3 in a naturally unconfined valley, with minimal valley-bottom constraints associated with human infrastructure (Figure 130). Reach characteristics are summarized below in Table 65.

Table 65. Summary of attributes for Geomorphic Reach GR-6.

Valley Segment	Reach	River Miles	Valley Slope (ft/ft)	Average Valley Width (ft)	Average Constrained Valley Width (ft)	Channel Slope (ft/ft)	Average Channel Width (ft)	Sinuosity	Entrenchment Ratio (ft/ft)	Constrained Entrenchment Ratio (ft/ft)	Human Disturbance Ratio (%)	Groundwater Characteristics	Geomorphic Characterization "Complex"	Geomorphic Characterization "Mixed"	Geomorphic Characterization "Simplified"
VS-1	GR-6	22.6 - 15.3	0.0083	944	877	0.0054	37	1.5	26	24	1%	Losing	62%	38%	0%

Forms

- Sinuous, single-thread channel with numerous side channels and ponds.
- Primarily plane-bed morphology in areas of low sinuosity and pool-riffle morphology in more sinuous sub-reaches.
- Thin ribbon of riparian vegetation consisting primarily of willow and other shrubs throughout the majority of the reach; more continuous and densely vegetated riparian area within the downstream, groundwater-influenced portion of reach.
- Active point bars throughout the middle portion of the reach.

Processes

- Losing to groundwater throughout the majority of the reach; gaining from groundwater below RM 17.
- Increasing evidence of channel migration, especially where riparian vegetation is lacking.
- Complex sediment-transport regime, including deposition, temporary storage, and transport.
- Island braiding around densely vegetated patches primarily in groundwater-influenced area.
- Beaver activity in the wet meadows visible in aerial photography.

Human Impact

- Cattle grazing impacts, including bank erosion and lost riparian vegetation in several locations.
- Irrigation diversions, bridge and dirt roads.

Response Potential

- Increased sinuosity, island braiding, and pool-riffle formation associated with riparian vegetation and instream obstruction (including beaver dams).
- Channel avulsion associated with instream obstruction (coarse sediment deposition, beaver dams, debris jams).
- Channel widening and simplification associated with lost bank vegetation and eroding banks.

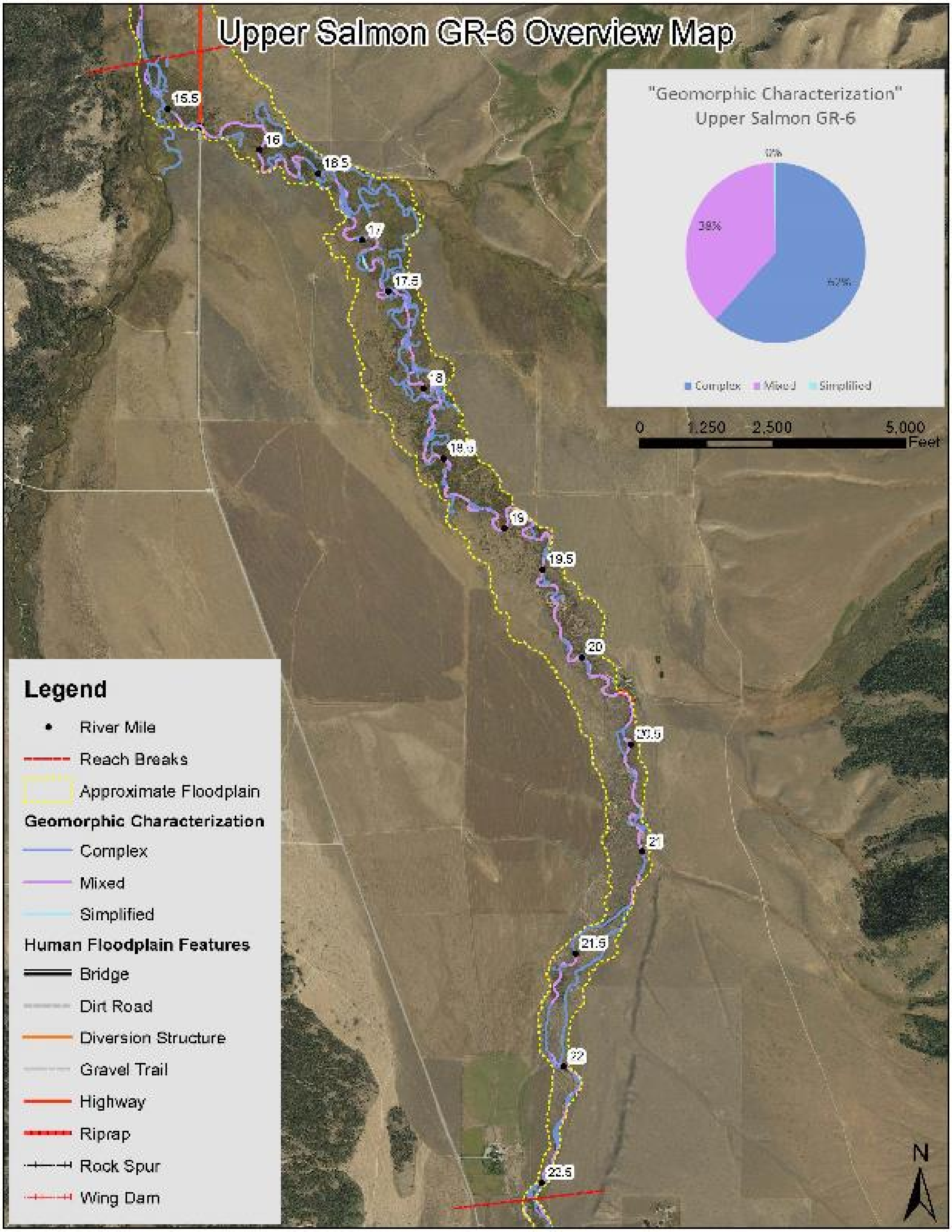

Figure 130. GR-6 overview map illustrating the approximate floodplain, geomorphic characterization, and human alterations to the floodplain.

Redfish Lake Creek Valley Segment (VS-2)

The Redfish Lake Creek Valley Segment comprises the Upper Salmon River upstream of Redfish Lake Creek from about RM 15.3 to RM 0.0 and contains Geomorphic Reaches GR-7 through GR-10 (Figure 131). Elevations range from a low of about 6440 feet at the Upper Salmon River and Redfish Lake Creek confluence to a high of about 10700 feet in the Sawtooth Mountains. This valley segment is in the transfer zone where coarse sediment is exchanged with the bed, bars, and floodplain through channel/floodplain interactions. Named waterbodies in this valley segment include Imogene Lake, Hell Roaring Lake, Upper Cramer Lake, Redfish Lake, Little Redfish Lake, Heart Lake, and Fourth of July Lake. Named tributaries in this valley segment include Fishhook Creek, Decker Creek, Huckleberry Creek, Hell Roaring Creek, Mays Creek, Champion Creek, Fourth of July Creek, Fisher Creek, Williams Creek, and Gold Creek.

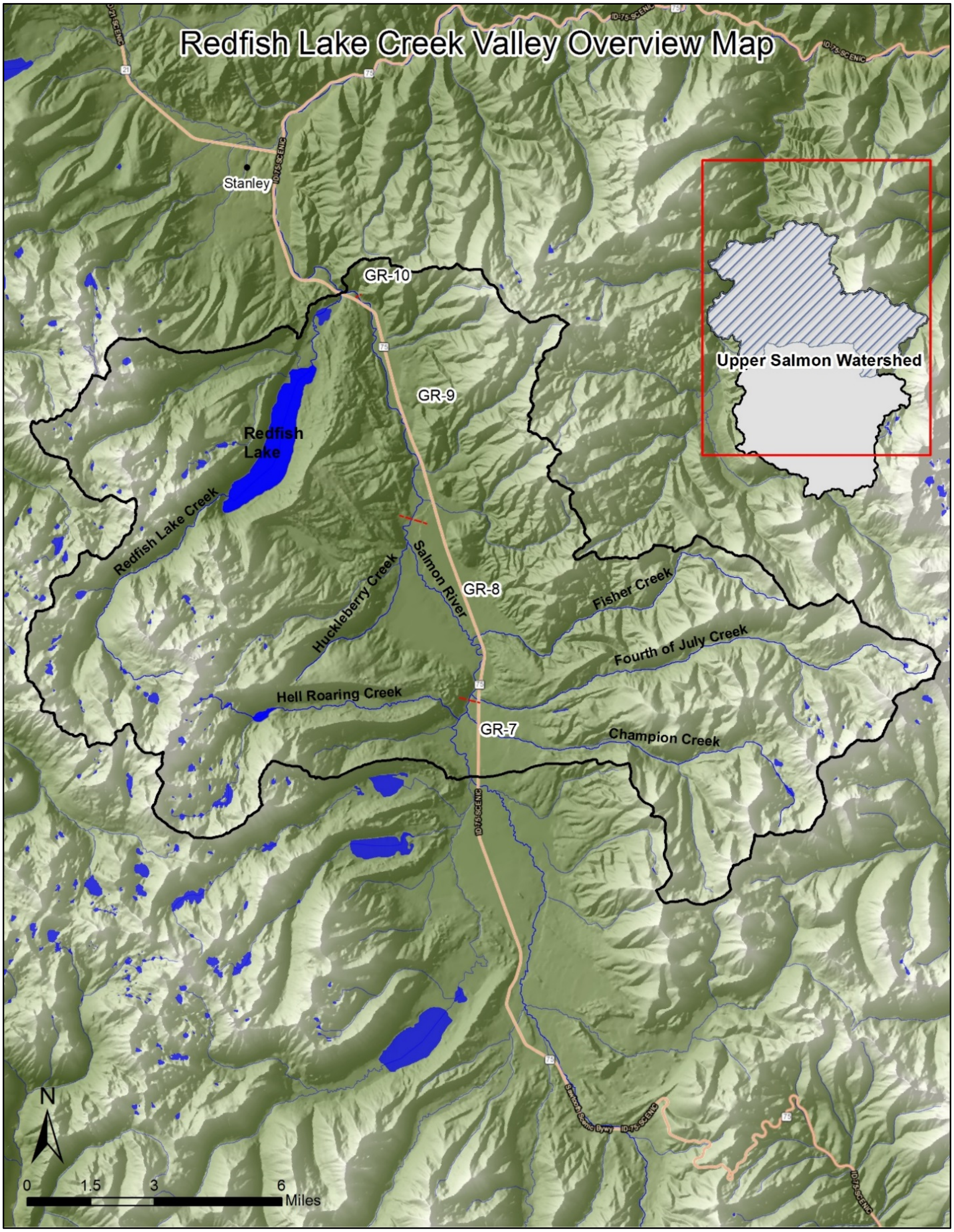

Figure 131. Location of Redfish Lake Creek Valley Segment and associated geomorphic reaches (GR-7 through GR-10).

Geomorphic Reach GR-7 (RM 15.3 – 12.8)

Geomorphic Reach GR-7 is located along the Upper Salmon River between RM 15.3 and RM 12.8 in a naturally unconfined valley, with no major valley-bottom constraints associated with human features (Figure 132). Reach characteristics are summarized below in Table 66.

Table 66. Summary of attributes for Geomorphic Reach GR-7.

Valley Segment	Reach	River Miles	Valley Slope (ft/ft)	Average Valley Width (ft)	Average Constrained Valley Width (ft)	Channel Slope (ft/ft)	Average Channel Width (ft)	Sinuosity	Entrenchment Ratio (ft/ft)	Constrained Entrenchment Ratio (ft/ft)	Human Disturbance Ratio (%)	Groundwater Characteristics	Geomorphic Characterization "Complex"	Geomorphic Characterization "Mixed"	Geomorphic Characterization "Simplified"
VS-2	GR-7	15.3 - 12.8	0.0050	1584	1,584	0.0038	68	1.3	23	23	1%	Gaining	76%	24%	0%

Forms

- Moderate sinuosity, single-thread channel with numerous side channel and ponds.
- Primarily pool-riffle morphology.
- Little to no observed instream structure.
- Discontinuous riparian vegetation consisting primarily of grass, willow, and other shrubs.
- Active gravel bars and observable meander scrolls in the floodplain.
- Gaining reach associated with geologic control from Hell Roaring glacial moraine.

Processes

- Lateral channel migration.
- Relatively stable banks where well-vegetated.
- Complex sediment-transport regime, including deposition, temporary storage, and transport.
- Beaver activity in the wet meadows and spring-fed tributaries visible in aerial photography.

Human Impact

- Minor human impacts.
- Cattle grazing, dirt roads, dispersed campsites, and bridge.

Response Potential

- Increased sinuosity, island braiding, and pool-riffle formation associated with riparian vegetation and instream obstruction (including beaver dams in side channels and spring-fed tributaries).
- Channel avulsion associated with instream obstruction (coarse sediment deposition, debris, and ice jams).
- Channel simplification associated with lost bank vegetation.

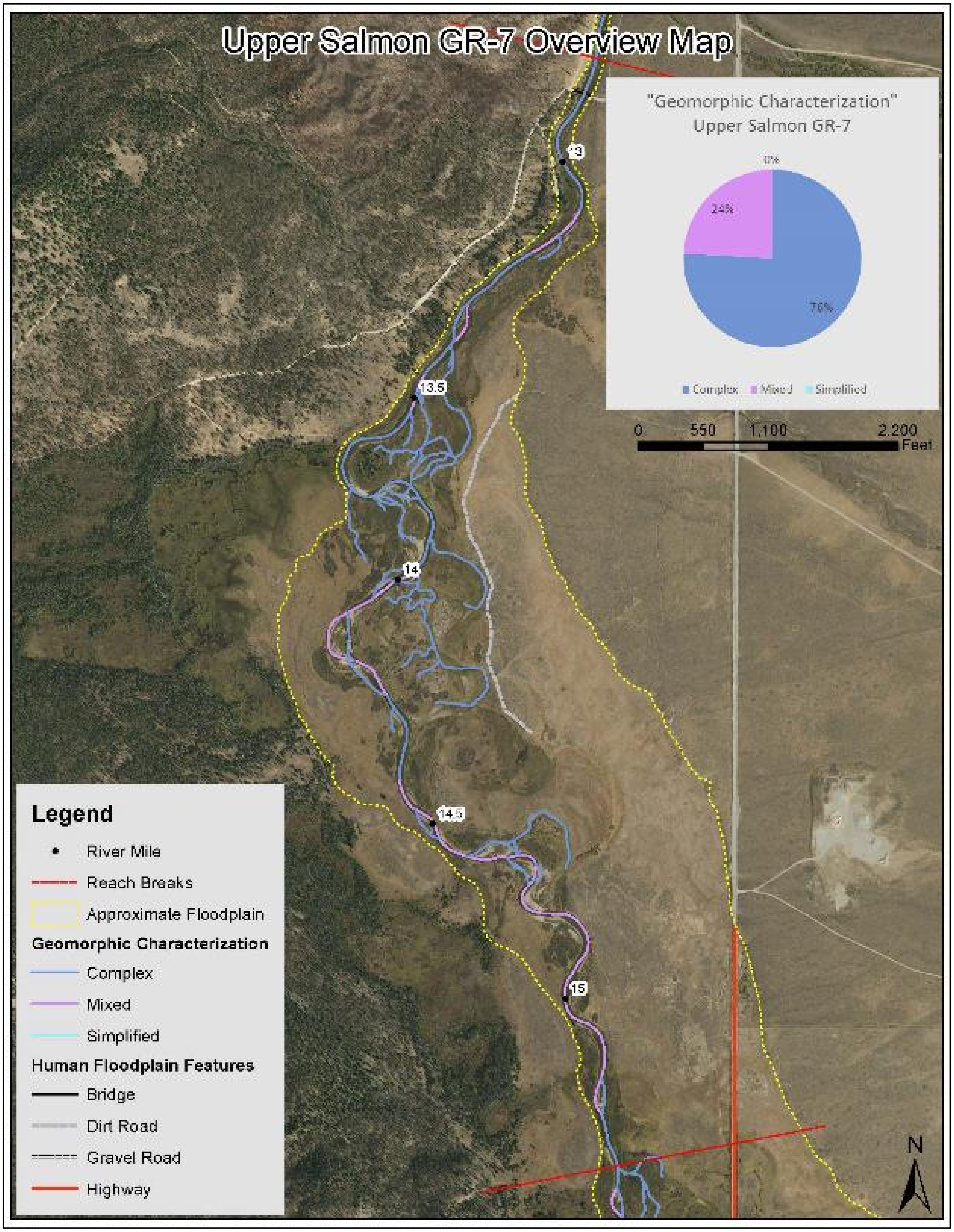

Figure 132. GR-7 overview map illustrating the approximate floodplain, geomorphic characterization, and human alterations to the floodplain.

Geomorphic Reach GR-8 (RM 12.8 – 6.6)

Geomorphic Reach GR-8 is located along the Upper Salmon River between RM 12.8 and RM 6.6 in a naturally unconfined valley, with no significant valley-bottom constraints associated with human features (Figure 133). The downstream reach break is defined by constriction from the Redfish Lake glacial moraine. Reach characteristics are summarized below in Table 67.

Table 67. Summary of attributes for Geomorphic Reach GR-8.

Valley Segment	Reach	River Miles	Valley Slope (ft/ft)	Average Valley Width (ft)	Average Constrained Valley Width (ft)	Channel Slope (ft/ft)	Average Channel Width (ft)	Sinuosity	Entrenchment Ratio (ft/ft)	Constrained Entrenchment Ratio (ft/ft)	Human Disturbance Ratio (%)	Groundwater Characteristics	Geomorphic Characterization "Complex"	Geomorphic Characterization "Mixed"	Geomorphic Characterization "Simplified"
VS-2	GR-8	12.8 - 6.6	0.0063	1280	1280	0.0048	66	1.3	19	19	6%	Gaining	81%	14%	5%

Forms

- Moderate sinuosity, single-thread channel with numerous side channels and ponds.
- Primarily pool-riffle morphology associated with meander bends.
- Active point bars and visible meander scrolls in the floodplain.
- Relatively continuous riparian vegetation consisting primarily of willow and other shrubs; poor riparian vegetation on elevated terraces.

Processes

- Channel migration and avulsion, including side-channel formation.
- Complex sediment-transport regime, including deposition, temporary storage, and transport.
- Beaver activity in side channels and spring-fed tributaries visible in aerial photography.

Human Impact

- Series of weirs for irrigation diversions in the upper reach.
- Cattle grazing impacts, including bank erosion and lost riparian vegetation.
- Irrigation diversions, dirt roads, and dispersed campsites.

Response Potential

- Increased sinuosity, island braiding, and pool-riffle formation associated with riparian vegetation and instream obstruction.
- Channel avulsion associated with instream obstruction (coarse sediment deposition, debris, and ice jams).
- Channel simplification associated with lost bank vegetation.

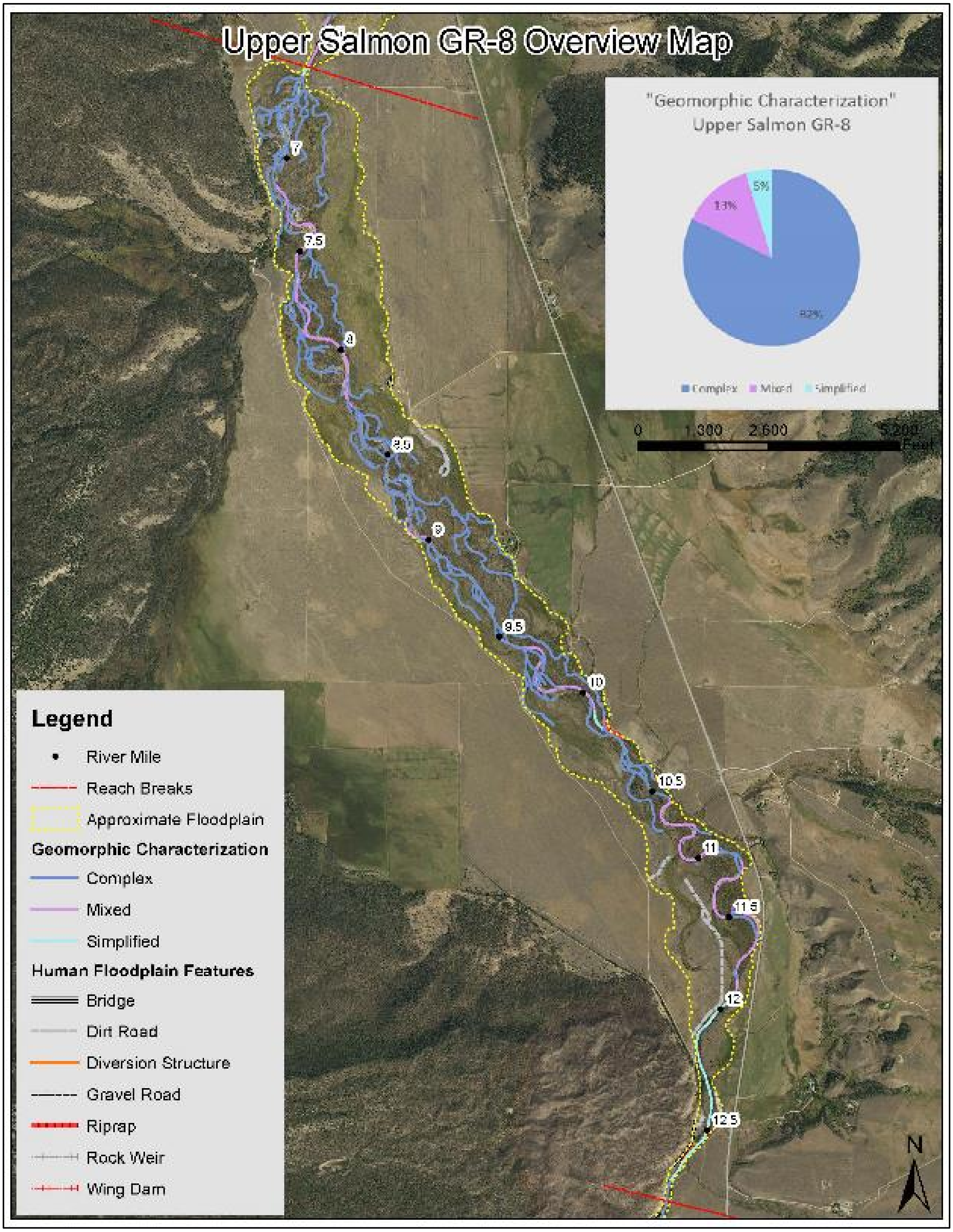

Figure 133. GR-8 overview map illustrating the approximate floodplain, geomorphic characterization, and human alterations to the floodplain.

Geomorphic Reach GR-9 (RM 6.6 – 0.4)

Geomorphic Reach GR-9 is located along the Upper Salmon River between RM 6.6 and RM 0.4 in a naturally unconfined valley with several valley-bottom constraints associated with human features (Figure 134). The western valley margin is defined by the Redfish Lake glacial moraine. Reach characteristics are summarized below in Table 68.

Table 68. Summary of attributes for Geomorphic Reach GR-9.

Valley Segment	Reach	River Miles	Valley Slope (ft/ft)	Average Valley Width (ft)	Average Constrained Valley Width (ft)	Channel Slope (ft/ft)	Average Channel Width (ft)	Sinuosity	Entrenchment Ratio (ft/ft)	Constrained Entrenchment Ratio (ft/ft)	Human Disturbance Ratio (%)	Groundwater Characteristics	Geomorphic Characterization "Complex"	Geomorphic Characterization "Mixed"	Geomorphic Characterization "Simplified"
VS-2	GR-9	6.6 - 0.4	0.0057	1123	868	0.0052	72	1.1	16	12	3%	-	73%	18%	9%

Forms

- Relatively low sinuosity, single-thread channel with numerous side channels.
- Mixed morphology. Plane-bed where relatively straight; pool-riffle where relatively sinuous.
- Many active point bars; visible meander scrolls and abandoned channel scars in the floodplain extending well beyond the existing meander belt width.
- Discontinuous riparian vegetation consisting primarily of willow and other shrubs.

Processes

- Active channel migration and avulsion; side channel and alcove creation.
- Mixed sediment-transport regime, including deposition, temporary storage, and transport; appears to become more transport-dominant in the lower reach.
- Beaver activity visible in downstream wetland area in aerial photography.

Human Impact

- Channel and floodplain confined by road embankments along the hatchery and Highway 75.
- Channel confinement and straightening may increase local transport capacity, armoring the bed.
- Cattle grazing impacts, including bank erosion and lost riparian vegetation in several locations.
- Road embankments, the fish hatchery’s permanent intake and weir structures, dispersed campsites, dirt roads, cattle grazing, discontinuous levees, rock weirs, riprap, and bridge.

Response Potential

- Increased sinuosity and pool-riffle formation associated with riparian vegetation and instream structure.
- Channel avulsion associated with instream obstruction (coarse sediment deposition; debris and ice jams).
- Channel simplification associated with lost bank vegetation and confinement.

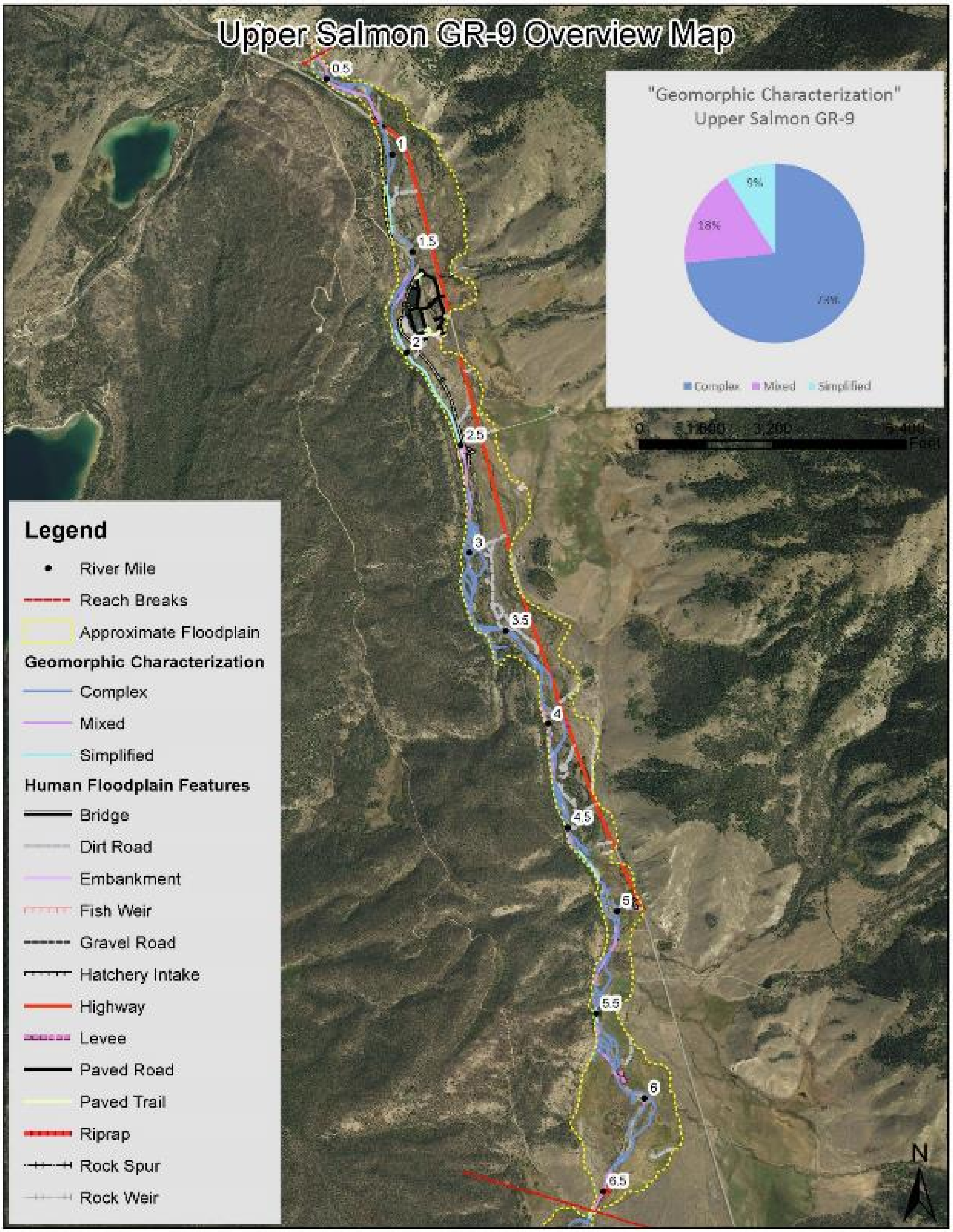

Figure 134. GR-9 overview map illustrating the approximate floodplain, geomorphic characterization, and human alterations to the floodplain.

Geomorphic Reach GR-10 (RM 0.4 – 0.0)

Geomorphic Reach GR-10 is located along the Upper Salmon River between RM 0.4 and RM 0 in a confined valley, with no additional valley-bottom constraints associated with human features (Figure 135). Reach characteristics are summarized below in Table 69.

Table 69. Summary of attributes for Geomorphic Reach GR-10.

Valley Segment	Reach	River Miles	Valley Slope (ft/ft)	Average Valley Width (ft)	Average Constrained Valley Width (ft)	Channel Slope (ft/ft)	Average Channel Width (ft)	Sinuosity	Entrenchment Ratio (ft/ft)	Constrained Entrenchment Ratio (ft/ft)	Human Disturbance Ratio (%)	Groundwater Characteristics	Geomorphic Characterization "Complex"	Geomorphic Characterization "Mixed"	Geomorphic Characterization "Simplified"
VS-2	GR-10	0.4 - 0.0	0.0020	122	122	0.0020	78	1.0	2	2	0%	-	56%	44%	0%

Forms

- Relatively straight, single-thread channel.
- Primarily plane-bed morphology.
- Primarily grass, shrub, and coniferous tree species along stream corridor.

Processes

- Confined channel; stable banks; continual sediment inputs from a slide area along river right
- Transport-dominated sediment regime.

Human Impact

- Minimal human impacts.
- Dispersed campsites.

Response Potential

- Sediment transport, incision, bed armoring.
- Bank erosion and localized large wood recruitment.

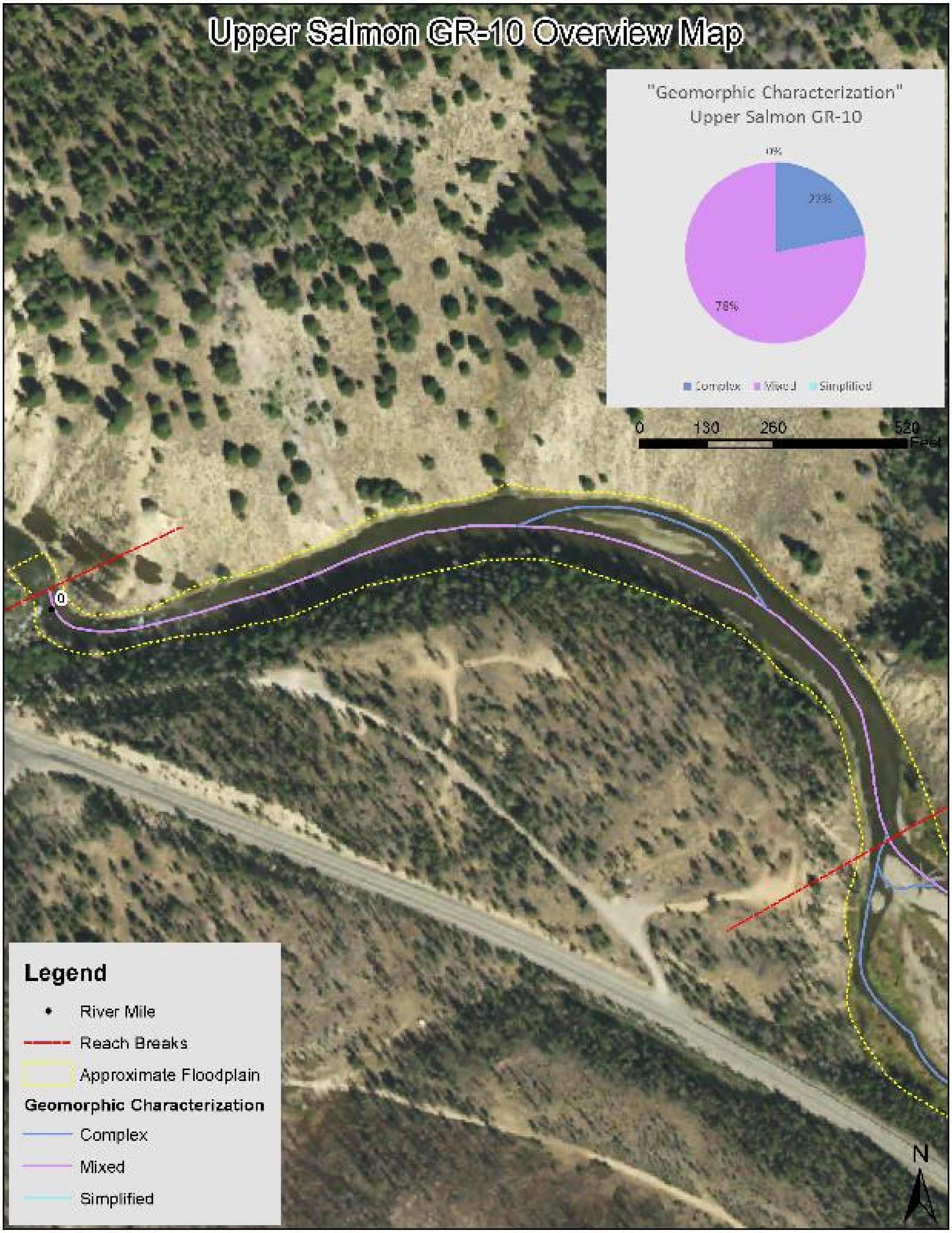

Figure 135. GR-10 overview map illustrating the approximate floodplain, geomorphic characterization, and human alterations to the floodplain.

Temperature and Climate Change Assessment

Chinook salmon

Under current conditions, spring water temperatures are generally below minimum or optimum values for Chinook salmon smolts. Alternatively, summer water temperatures can be above maximum or optimum values for a portion of the adult spawning and summer parr rearing life stages. Under current conditions, however, water temperatures in the Upper Salmon River are often within optimum temperatures for each of the five life stages evaluated (Figure 136). Under an assumed 3° C water temperature increase scenario (Figure 137), conditions improve during the spring (emergence, spring smolt emigration) but notably worsen for summer life stages (adult holding and spawning, parr rearing). Summer water temperatures potentially increase to above maximum (adult spawning, parr rearing) or above acute (summer spawning) during portions of the summer life stages.

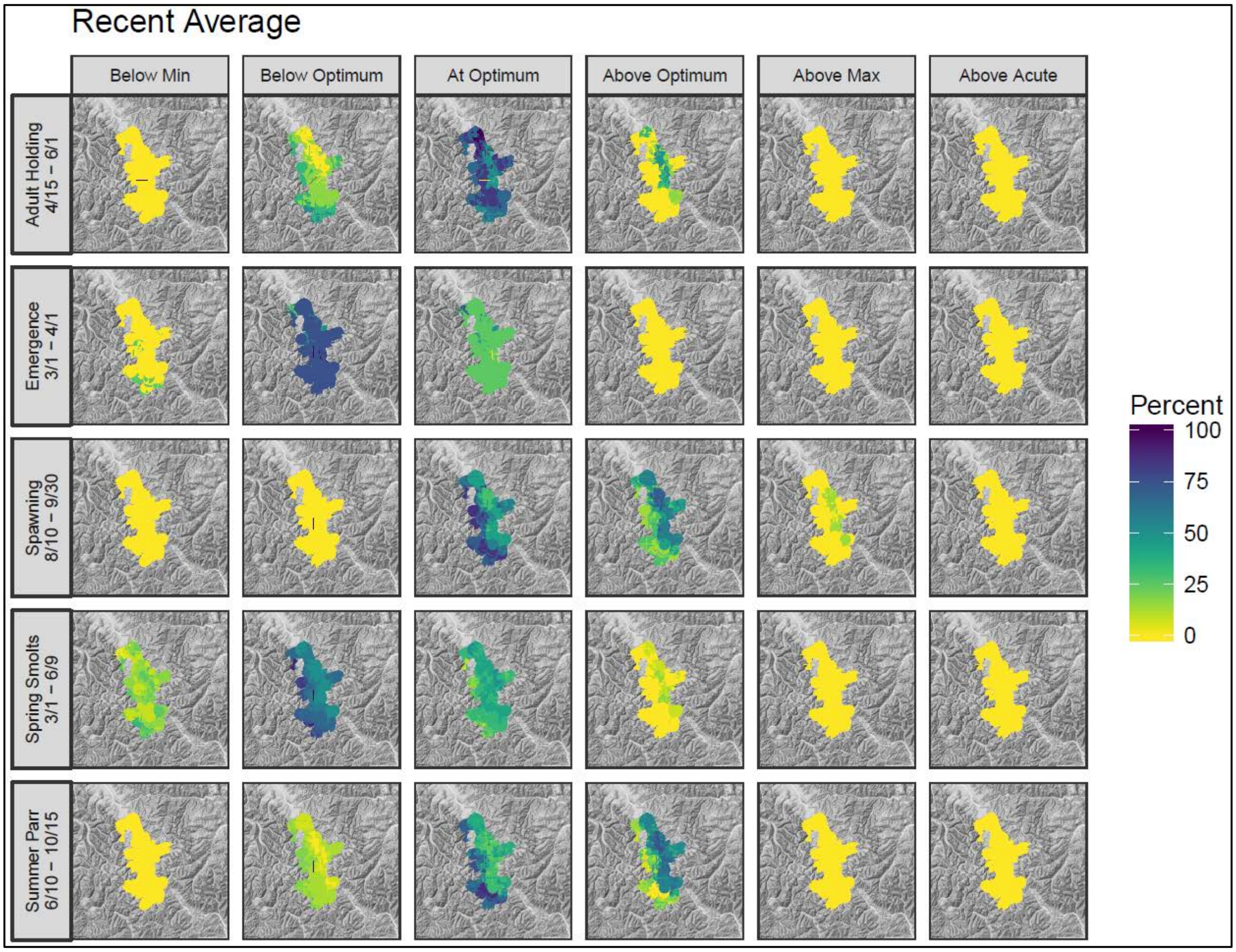

Figure 136. The percentage of time that Upper Salmon River watershed water temperatures were below, within, or above a given temperature threshold (Carter 2005) for five Chinook salmon life stages. Water temperatures were averaged across years for which complete modeled temperature data were available (2011 and 2013).

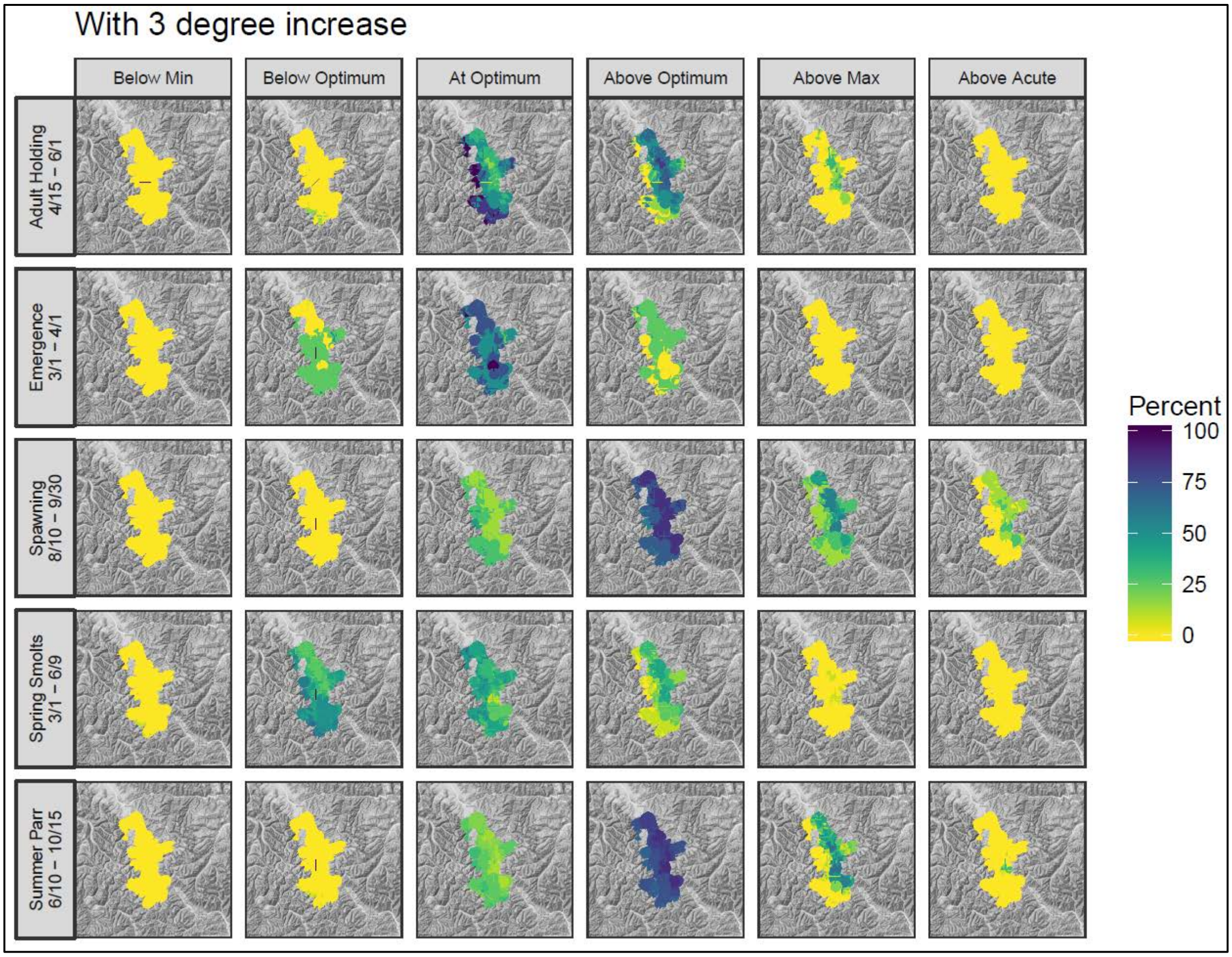

Figure 137. The percentage of time that Upper Salmon River watershed water temperatures may potentially be below, within, or above a given temperature threshold (Carter 2005) for five Chinook salmon life stages, assuming a potential climate change scenario.

Steelhead

Under current conditions, spring water temperatures are below optimum values for steelhead for portions of the spring smolt emigration. Alternatively, summer water temperatures can be above optimum or maximum values for a portion of the egg incubation and fry emergence life stages. Under current conditions, however, water temperatures in the Upper Salmon River are often within optimum temperatures for three (spawning, incubation, summer parr rearing) of the life stages evaluated (Figure 138). Under an assumed 3° C water temperature increase scenario (Figure 139), water temperature conditions improve during the spring smolt emigration but notably worsen for late-spring and summer life stages (incubation/emergence, spawning, parr rearing). Summer water temperatures potentially increase to above maximum during portions of the spawning or summer parr rearing stages. It is unclear to what degree late incubation and emergence timings might overlap with summer high temperatures in the Upper Salmon River.

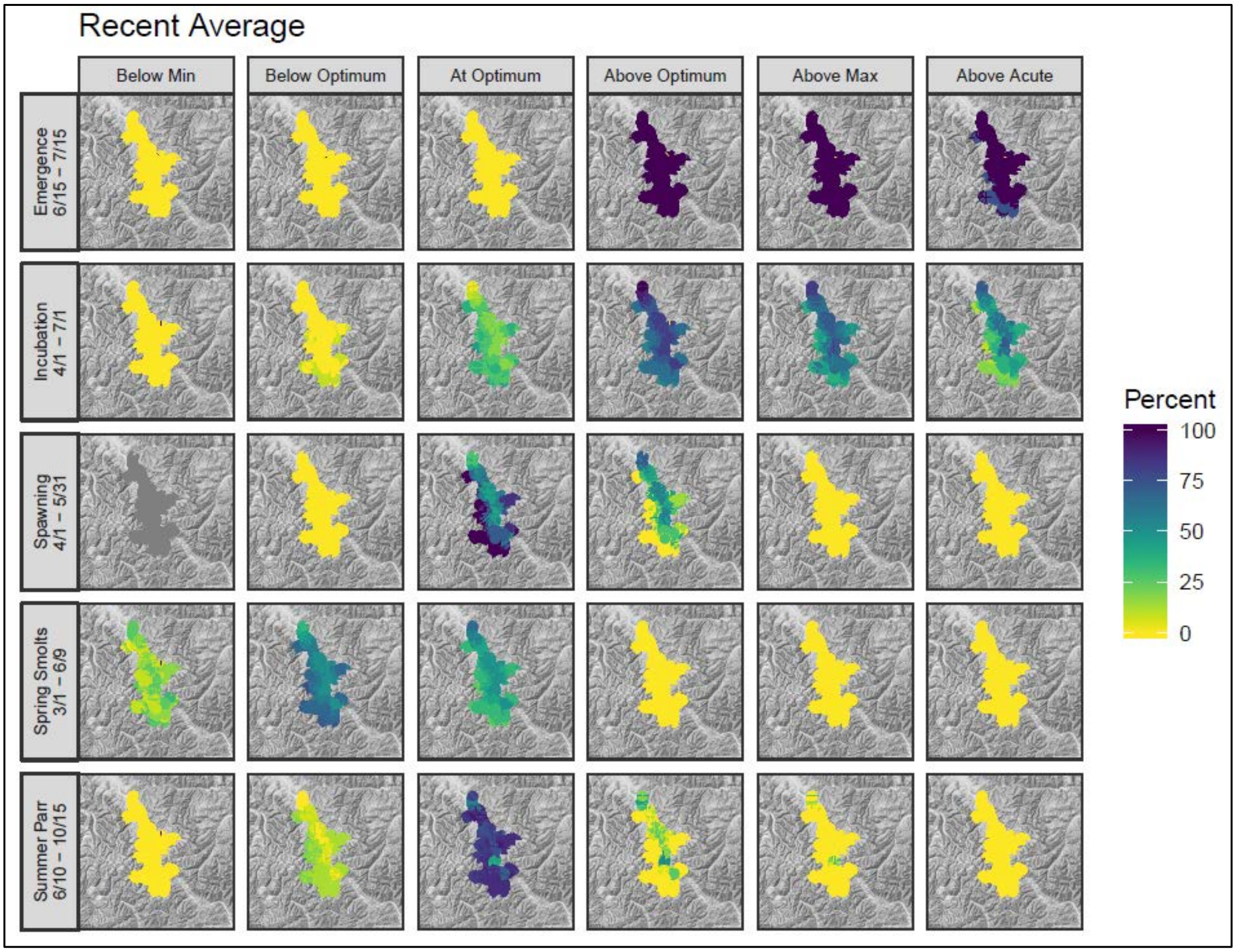

Figure 138. The percentage of time that Upper Salmon River watershed water temperatures were below, within, or above a given temperature threshold (Carter 2005) for five steelhead life stages. Water temperatures were averaged across years for which complete modeled temperature data were available (2011 and 2013).

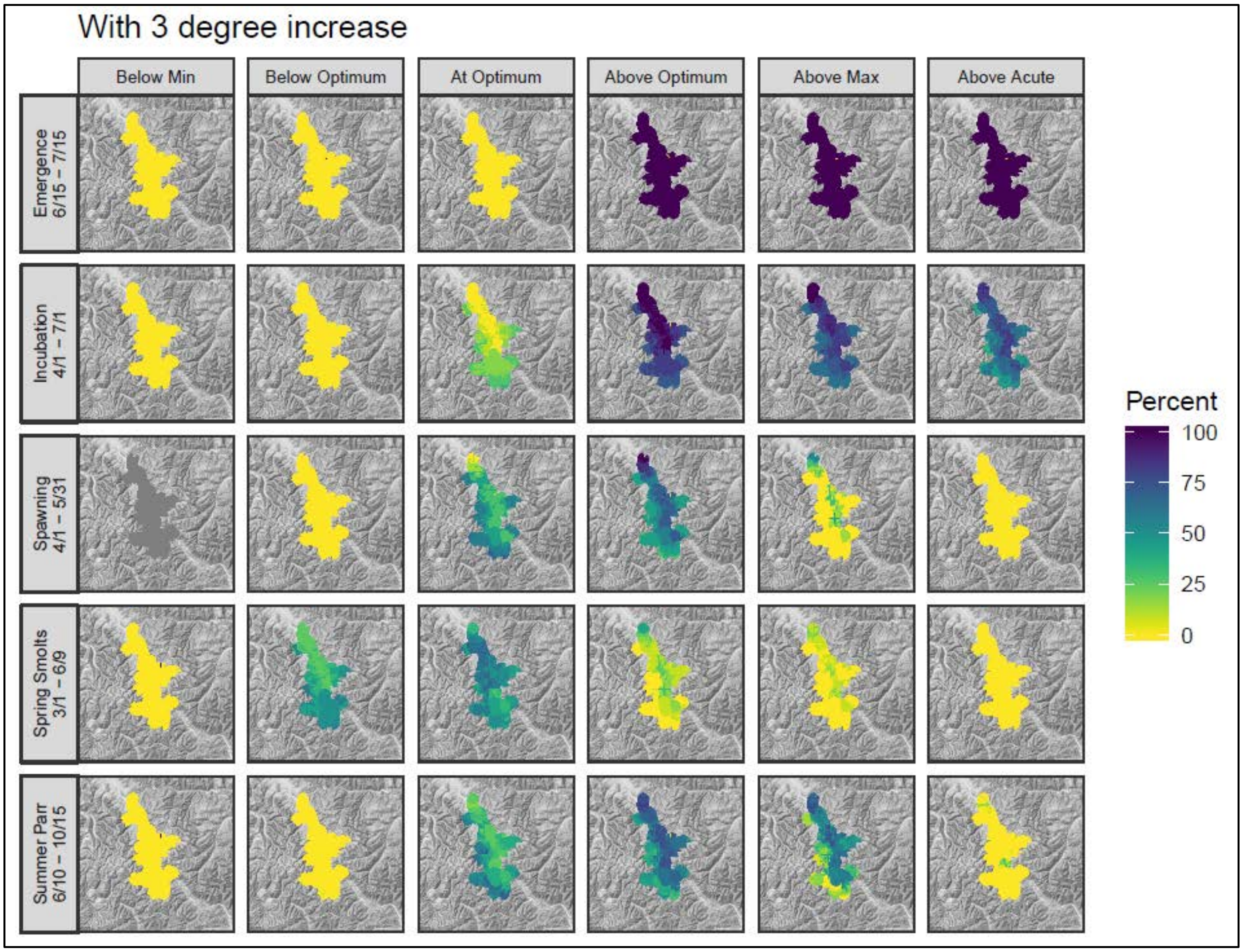

Figure 139. The percentage of time that Upper Salmon River watershed water temperatures may potentially be below, within, or above a given temperature threshold (Carter 2005) for five steelhead life stages, assuming a potential climate change scenario.

Results and Discussion

In the Upper Salmon River Biological Assessment, the lack of quantity and quality juvenile rearing habitat during summer and winter months was identified as the highest-priority limiting PBF for Chinook salmon. Assuming recent mean adult Chinook salmon escapement, habitat capacity does not appear to limit production of summer parr or winter presmolts (Table 51). However, currently available rearing habitat (summer and winter) is likely not sufficient to support recent high escapements or support escapements necessary for ESA delisting. Juvenile rearing habitat during summer and winter does not appear to be a limiting PBF for steelhead in the Upper Salmon River. Finally, redd capacity (i.e., available spawning habitat) does not appear to be limiting Chinook salmon or steelhead in the Upper Salmon River.

Limiting Physical and Biological Features

The lack of quantity and quality summer (parr) and overwinter (presmolt) rearing habitat downstream of current spawning habitat were identified as high-priority PBFs for Chinook salmon in the Upper Salmon River. During typical recent adult escapements for Chinook salmon in the Upper Salmon River, available summer and winter rearing capacity appears sufficient to support juvenile productions. However, the available capacity is below values required to support parr and/or premolts during high escapement years (Table 51) or to sustain adult Chinook salmon escapement required to achieve ESA delisting goals (Table 52). This finding is supported by the fact that roughly 90 percent of total Chinook salmon production from this reach emigrate past the Sawtooth Hatchery rotary screw trap as fry, parr, or presmolts prior to the winter rearing season, suggesting that summer and winter rearing capacity is limited. Redd capacity does not appear to be a PBF limiting Chinook salmon in the Upper Salmon River.

Available juvenile rearing and spawning habitat in the upper Salmon River do not appear to be limiting PBFs for steelhead in the Upper Salmon River.

- Winter (presmolt) juvenile rearing habitat was identified as a high-priority PBF limiting Chinook salmon production in the Upper Salmon River (headwaters).
- Summer (parr) juvenile rearing habitat was identified as a medium-priority PBF limiting Chinook salmon production in the Upper Salmon River (headwaters).

Priority Areas

To address both PBFs limiting Chinook salmon production in the Upper Salmon River (overwinter and summer rearing habitat), rehabilitation to reaches within the Upper Salmon should be considered in the following order:

- **First priority: mainstem Upper Salmon from Alturas Creek to Redfish Lake Creek.** This section is where the majority of the Chinook salmon production currently occurs.
- **Second priority: Alturas Lake Creek and the mainstem Upper Salmon above Alturas Lake Creek including Pole Creek.**
- Summer flow limitations at the Busterback Ranch Diversion area.

References

Albers, P.C., J. Lowry, and G.E. Smoak. 1998. The Rivers and Fisheries of the Shoshone-Bannock Peoples: American West Center, University of Utah, published by the Shoshone-Bannock Tribes, 282 p.

Berenbrock, C. 2002. Estimating the Magnitude of Peak Flows at Selected Recurrence Intervals for Streams in Idaho. Water-Resources Investigations Report 02-4170. U.S. Geological Survey. Boise, Idaho.

Bisson, P.A., J.M. Buffington, and D.R. Montgomery. 2006. Chapter 2. Valley Segments, Stream Reaches, and Channel Units, *in* Methods in Stream Ecology, 2nd Edition. Elsevier.

Braudrick, C.A. and G.E. Grant. 2001. Transport and deposition of large woody debris in streams: a flume experiment. *Geomorphology* 41: 263-283.

Breckenridge, R.R., L.R. Stanford, J.F.P. Cotter, J.M. Bloomfield, and E.B. Evenson. 1988. Field Guides to the Quaternary Geology of Central Idaho: Part B., Glacial Geology of the Stanley Basin, *in* P.K. Link, and W.R. Hackett, *eds*. Guidebook to the Geology of Central and Southern Idaho: Idaho Geological Survey Bulletin 27, p. 209-221.

Carter, K. 2005. The effects of temperature on steelhead trout, Coho salmon, and Chinook salmon biology and function by life stage. Implications for Klamath Basin TMDLs. California Regional Water Quality Control Board. North Coast Region. 26pp.

Cluer, B. and C. Thorne. 2013. A Stream Evolution Model Integrating Habitat and Ecosystem Benefits. *River Research and Applications*. 30:135-154

Denney, R. N. 1952. A Summary of North American Beaver Management, 1946-1948. Colorado Game and Fish Department. 58p.

Frissell, C.A., W.J. Liss, C.E. Warren, and M.D. Hurley. 1986. A Hierarchical Framework for Stream Habitat Classification: Viewing Streams in a Watershed Context. *Environmental Management* 10(2): 199-214.

Idaho Department of Environmental Quality. 2016. Upper Salmon River Subbasin Assessment and TMDL, 2016 Addendum and Five-Year Review, Hydrologic Unit Code 17060201, 114 p.

InciWeb – Information System 2017. Halstead Fire, access online https://inciweb.nwcg.gov/incident/3062/

Idaho Soil Conservation Commission. 1995. Model Watershed Plan, Lemhi, Pahsimeroi, and East Fork of the Salmon River. Idaho Soil Conservation Commission for the Bonneville Power Administration, Portland, Oregon.

Johnson, K.M., R.S. Lewis, E.H. Bennett, and T.H. Kiilsgaard. 1988. Cretaceous and Tertiary intrusive rocks of south-central Idaho, *in* P.K. Link, and W.R. Hackett, *eds*. Guidebook to the Geology of Central and Southern Idaho: Idaho Geological Survey Bulletin 27. p. 55-86.

Link, P.K. and S.U. Janecke. 1999. Geology of East-Central Idaho: Geologic Roadlogs for the Big and Little Lost River, Lemhi, and Salmon River Valleys. *In* Guidebook to the Geology of Eastern Idaho. S.S. Hughes and G.D. Thackray, *eds*. Idaho Museum of Natural History. Online Link: http://imnh.isu.edu/digitalatlas/geo/gsa/gsafrm.htm

McGrath, C.L., A.J. Woods, J.M. Omernik, S.A. Bryce, M. Edmondson, J.A. Nesser, J. Shelden, R.C. Crawford, J.A. Comstock, and M.D. Plocher. 2002. Ecoregions of Idaho (color poster with map, descriptive text, summary tables, and photographs). U.S. Geological Survey (map scale 1:1,350,000). Reston, Virginia.

Montgomery, D., and J.M. Buffington, 1998. Channel Processes, Classification, and Response, *in* River Ecology and Management, Chapter 2. R. Naiman and R. Bilby, *eds*. Springer-Verlag New York, Inc., p. 13-42.

Moulton, M. 2014. Pole Creek Diversion Authorization. As included within: Biological Assessment of Effects of Ongoing and Proposed Federal Actions on the Sawtooth Valley Subpopulation of listed Snake River Sockeye, Snake River Spring/Summer Chinook Salmon, Snake River Steelhead, and Columbia River Bull Trout and sensitive Westslope Cutthroat Trout. On File, Sawtooth National Recreation Area. Accessed via PDF provided by USFS on April 13, 2017.

Natural Resources Conservation Service. 2003. Soil Survey of Custer-Lemhi Area, Idaho, Parts of Blaine, Custer, and Lemhi Counties. USDA Natural Resources Conservation Service, 578 p., online (http://www.nrcs.usda.gov).

NOAA National Marine Fisheries Service. 2017. Proposed ESA Recovery Plan for Snake River Idaho Spring/Summer Chinook Salmon and Steelhead Populations: NOAA Fisheries, Portland, Oregon, 330 p.

Pierce, K.L. and W.E. Scott. 1982. Pleistocene episodes of alluvial gravel deposition, southeastern Idaho. *In* Cenozoic Geology of Idaho. B. Bonnichsen and R. Breckenridge, *eds*. Idaho Bureau of Mines and Geology Bulletin 26. p. 685-702.

Pierce, K.L., D.G. Despain, L.A. Morgan, and J.M. Good. 2007. The Yellowstone Hotspot, Greater Yellowstone Ecosystem, and Human Geography. U.S. Geological Survey Paper 79, 39 p.

Rossillon, M., 1980. An Overview of History in the Drainage Basin of the Middle Fork of the Salmon River: Boise National Forest, Boise, Idaho.

Simpson, D.W. and Anders, M.H. 1992. Tectonics and topography of the western U.S.: An example of digital map making, GSA Today, 2, 118-121.

Slough, B.G. and R.M.F.S. Sadleir. 1977. A land capability classification system for beaver (Castor canadensis). Canadian Journal of Zoology 55(8): 1324-1335.

Sawtooth National Forest. 2003. Sawtooth National Forest Final Forest Plan Revision. U.S. Forest Service, Sawtooth National Forest.

Sawtooth National Forest. 2006. Biological Assessment of Effects on Ongoing and Proposed Federal Actions on the Sawtooth Valley Subpopulation of listed Snake River Sockeye, Snake River Spring/Summer Chinook Salmon, Snake River Steelhead, and Columbia River Bull Trout and sensitive Westslope Cutthroat Trout. Sawtooth National Recreation Area, July 26, 2006.

USFS 1975. Fishery Effects of Irrigation Diversion and Related Structures: An interim fisheries management plan for the Sawtooth National Recreation Area. Prepared by Greg Munther, Fisheries Biologist.

Wells, D. E. 1992. Busterback Ranch Case (a summary to 5/15/92) Sawtooth National Recreational Area. PDF copy provided by USFS on April 13, 2017.

Appendices

Appendix A – Temperature Modeling and Climate Change

This section describes a spatially and temporally continuous temperature model and how it was applied to the Upper Salmon, Pahsimeroi, and Lemhi River watersheds. A combination of modeled temperature predictions and life-stage-specific temperature thresholds are used to evaluate whether current water temperatures might limit the ability of spring-summer run Chinook salmon (hereafter Chinook salmon) and summer run steelhead (hereafter steelhead) to use available habitat. A simple warming scenario is then presented that describes potential increases in stream temperature expected to result from climate change to assess whether the implementation of restoration actions to reduce temperatures may be necessary. With that said, caution must be taken because climate change is likely to impose changes in freshwater habitat beyond simple potential increases in water temperature, including (NOAA 2017):

- Winter flooding, which may scour redds;
- Increases in the frequency of wildfire and insect infestation, which may influence bank stability, upland sediment contribution, and riparian corridors;
- Reduction in summer flow; and
- Changes to mainstem migratory corridors.

Life-Stage-Specific Temperature Thresholds

Life-stage-specific temperature criteria were adopted from Carter (2005) in addition to the transition timing of local Chinook salmon and steelhead life stages (USBWP 2004; Personal Communication, Jude Trapani, Bureau of Reclamation; Personal Communication, Mike Edmondson, Idaho Office of Species Conservation; and Personal Communication, Mike Ackerman, Biomark ABS) to identify minimum, maximum, and acute temperature criteria for various life stages of Chinook salmon (Table A-1) and steelhead (Table A-2). A 7-day Maximum Weekly Maximum Temperature (MWMT) was adopted as the temperature metric, because it is informative for identifying both chronic and acute temperature effects (Carter 2005).

Table A-1. Life stage timing, and minimum, optimum, maximum, and acute temperature (Celsius) thresholds for Chinook salmon, adopted from Carter (2005). All temperatures are expressed as the 7-day Maximum Weekly Maximum Temperature (MWMT).

Life Stage	Timing	Minimum	Optimum	Maximum	Acute
Adult Holding	4/15 - 6/1	3.3	7.2-14.5	18	20
Spawning	8/10 - 9/30	3.3	7.2-14.5	18	20
Incubation	9/1 - 4/1	4	5-11	14	17.5
Emergence	3/1 - 4/1	2	6-10	16.7	17.5
Summer Parr	6/10 - 10/15	4.5	10-16	20	22
Winter Presmolt	11/14 - 3/1	4.5	10-16	20	22
Spring Smolt	3/1 - 6/9	4.5	10-16	20	22

Table A-2. Life stage timing, and minimum, optimum, maximum, and acute temperature (Celsius) thresholds for steelhead, adopted from Carter (2005). All temperatures are expressed as the 7-day Maximum Weekly Maximum Temperature (MWMT).

Life Stage	Timing	Minimum	Optimum	Maximum	Acute
Adult Holding	10/1 – 3/31	NA	NA	18	20
Spawning	4/1 – 5/31	NA	3.9-12.8	18	20
Incubation	4/1 – 7/1	2	5-10	12	14
Emergence	6/15 – 7/15	2	5-10	12	14
Summer Parr	6/10 – 10/15	4.5	10-18	19	22
Winter Presmolt	11/14 – 3/1	4.5	10-18	19	22
Spring Smolt	3/1 – 6/9	4.5	10-18	19	22

Temperature Model

A temperature model described by McNyset et al. (2015) was used to define existing temperature conditions for the Upper Salmon, Pahsimeroi, and Lemhi River watersheds. The model uses land surface temperature (LST) data obtained from the U.S. National Aeronautics and Space Administration’s (NASA) Moderate Resolution Imaging Spectroradiometer (MODIS) satellite sensor. The LST data are available daily at a resolution of 1 square kilometer and were summarized over an 8-day NASA “week”. McNyset et al. (2015) used LST data as a covariate in a linear model to predict stream water temperatures in a spatially and temporally continuous manner.

Summarization of temperature data was done by Chinook salmon and steelhead life stages for each year and basin for which modeled temperature data were available. The Supplementary Figures to Appendix A contains a series of maps showing the percentage of time for each basin and year that water temperatures were below, within, or above a given temperature threshold (Carter 2005) for seven Chinook salmon and steelhead life stages (winter presmolt, summer parr, spring smolt, spawning, incubation, emergence, adult holding). For the Lemhi River, modeled temperature data were available for 2011 to 2015. For the Pahsimeroi River, modeled temperature data were available for 2011 and 2013. For the Upper Salmon River, modeled temperature data were available for 2011 and 2013.

The main document provides a summary by averaging temperature data across years for which complete modeled data were available and a simple climate change scenario by adding 3° C, a median value based on a series of climate change scenarios (Kyle and Brabets 2001). Because only 2 years of modeled temperature data are available for the Pahsimeroi and Upper Salmon River watersheds, only data from 2013 (and a +3° C scenario) are presented.

Literature Cited

Carter, K. 2005. The effects of temperature on steelhead trout, Coho salmon, and Chinook salmon biology and function by life stage. Implications for Klamath Basin TMDLs. California Regional Water Quality Control Board. North Coast Region. 26pp.

Kyle, R.E. and T.P. Brabets. 2001. Water temperature of streams in the Cook Inlet Basin, Alaska, and Implications of Climate Change. Water-Resources Investigations Report 01-4109. U.S. Department of the Interior. U.S. Geological Survey. 32pp.

McNyset, K.M., C.J. Volk, and C.E. Jordan. 2015. Developing an effective model for predicting spatially and temporally continuous stream temperatures from remotely sensed land surface temperatures. Water. 7:6827-6846.

NOAA Fisheries. 2017. ESA Recovery Plan for Snake River Spring/Summer Chinook Salmon (*Oncorhynchus tshawytscha*) & Snake River Basin Steelhead (*Oncorhynchus mykiss*). U.S. Department of Commerce. National Oceanic and Atmospheric Administration. National Marine Fisheries Service. West Coast Region. November 2017.

USBWP (Upper Salmon Basin Watershed Project). 2004. Upper Salmon River recommended instream work windows and fish periodicity. 29pp.

This page intentionally left blank.

Supplementary Figures to Appendix A – Chinook Salmon Temperature Criteria and Contemporary Water Temperature Maps

Chinook salmon

Lemhi River

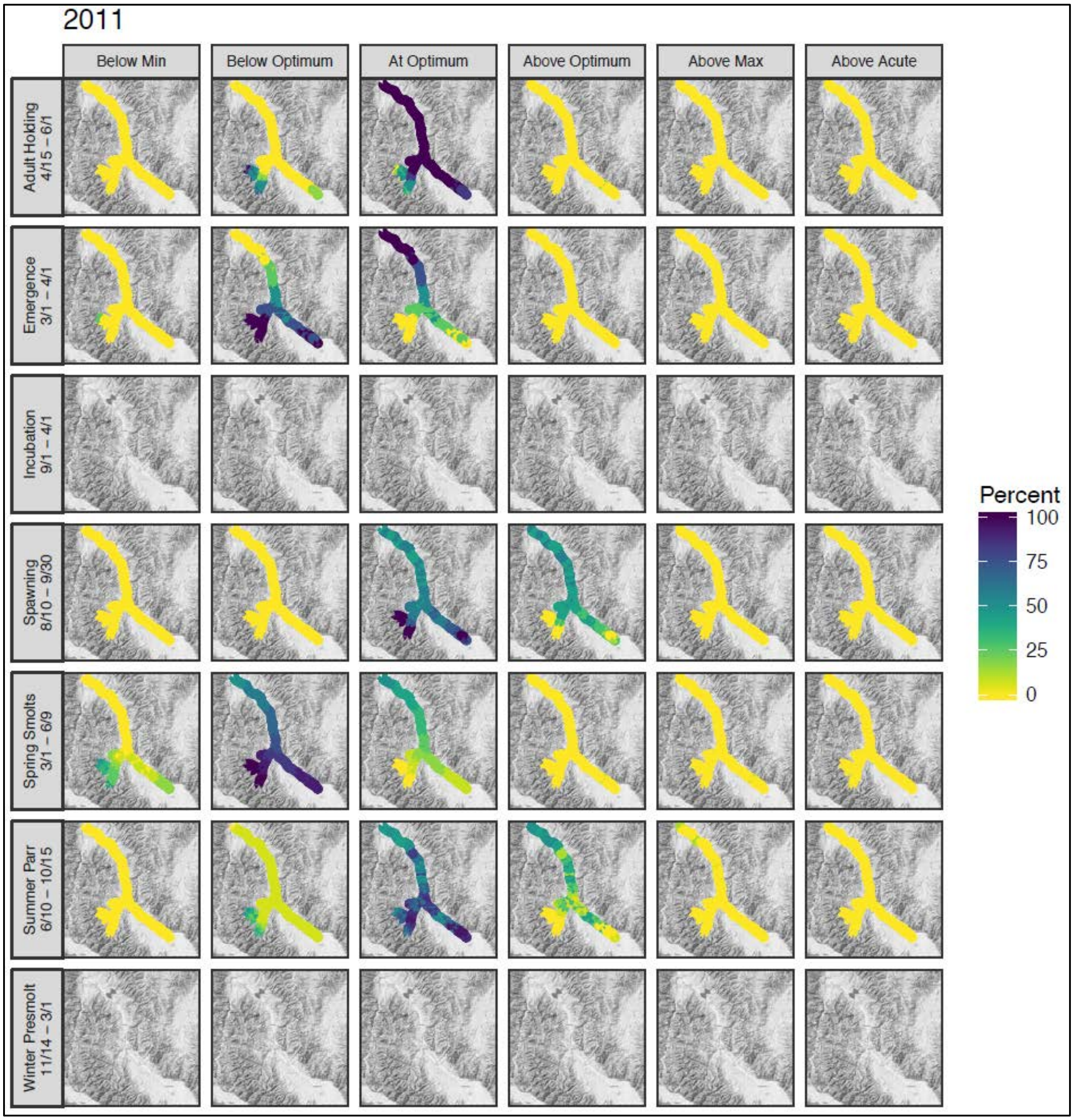

Supplemental Figure A-1. The percentage of time that 2011 water temperatures in the Lemhi River were below, within, or above a given temperature threshold (Carter 2005) for seven Chinook salmon life stages. For facets with no data, modeled temperature data were unattainable for that timespan.

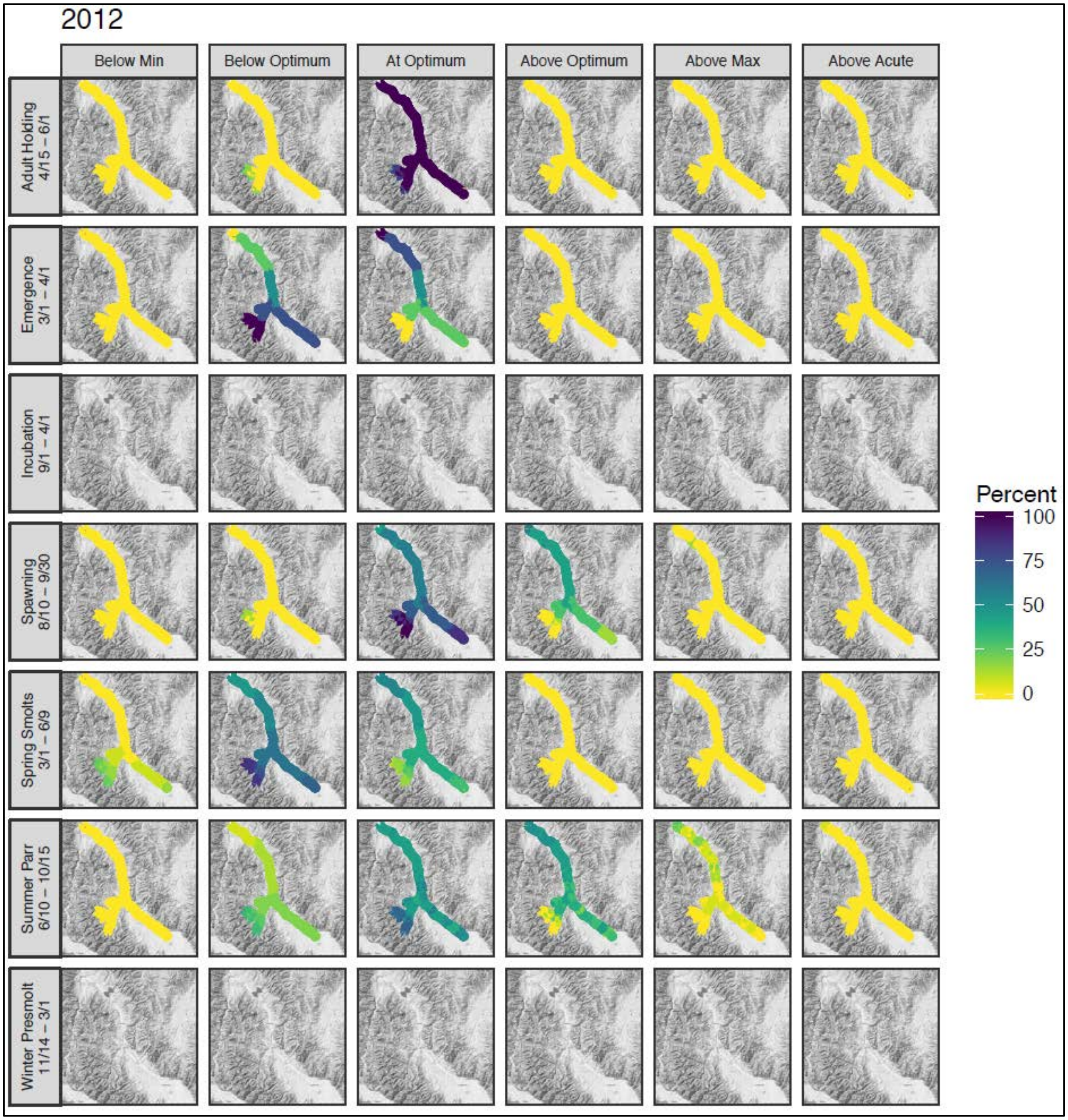

Supplemental Figure A-2. The percentage of time that 2012 water temperatures in the Lemhi River were below, within, or above a given temperature threshold (Carter 2005) for seven Chinook salmon life stages. For facets with no data, modeled temperature data were unattainable for that timespan.

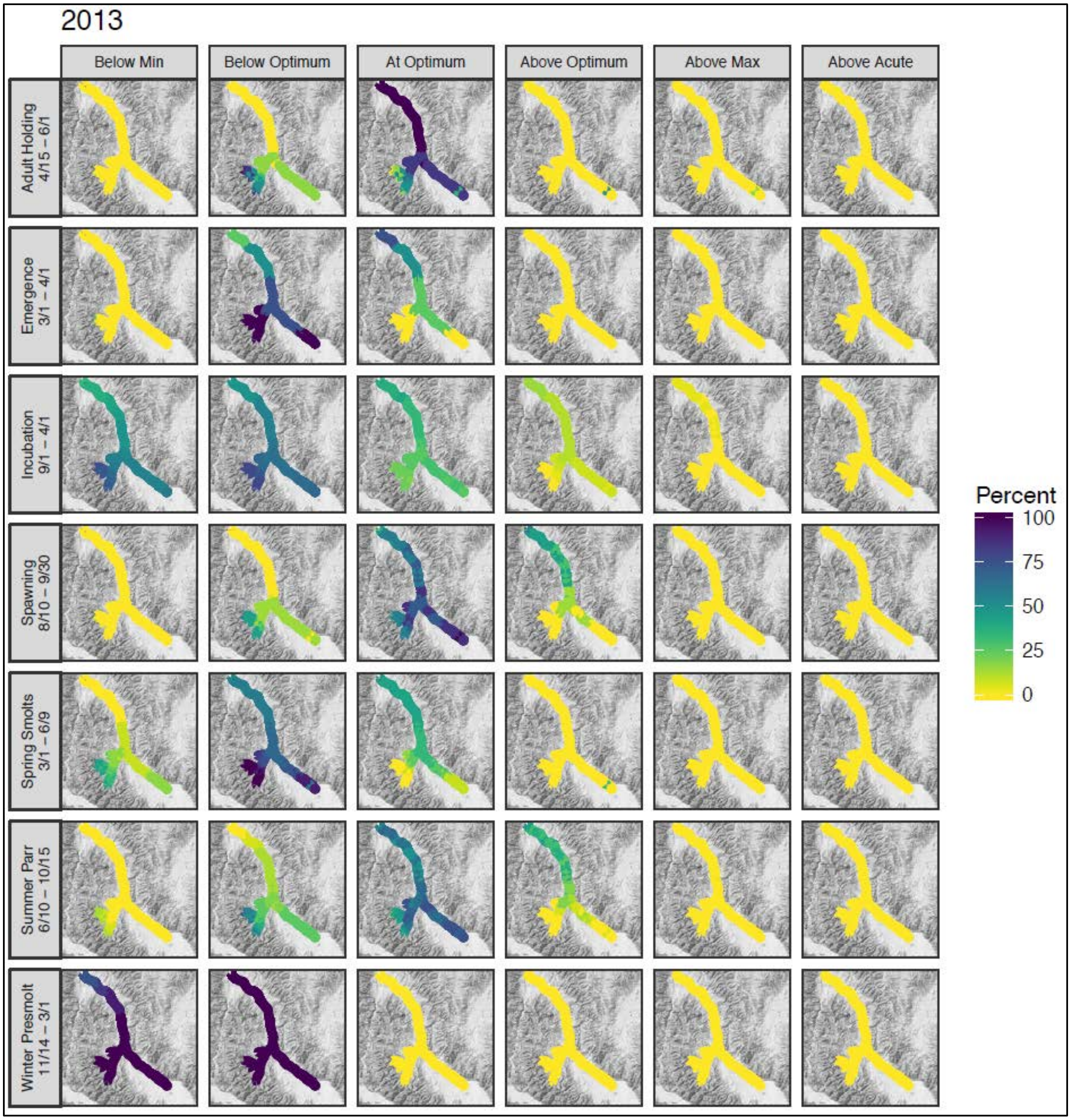

Supplemental Figure A-3. The percentage of time that 2013 water temperatures in the Lemhi River were below, within, or above a given temperature threshold (Carter 2005) for seven Chinook salmon life stages.

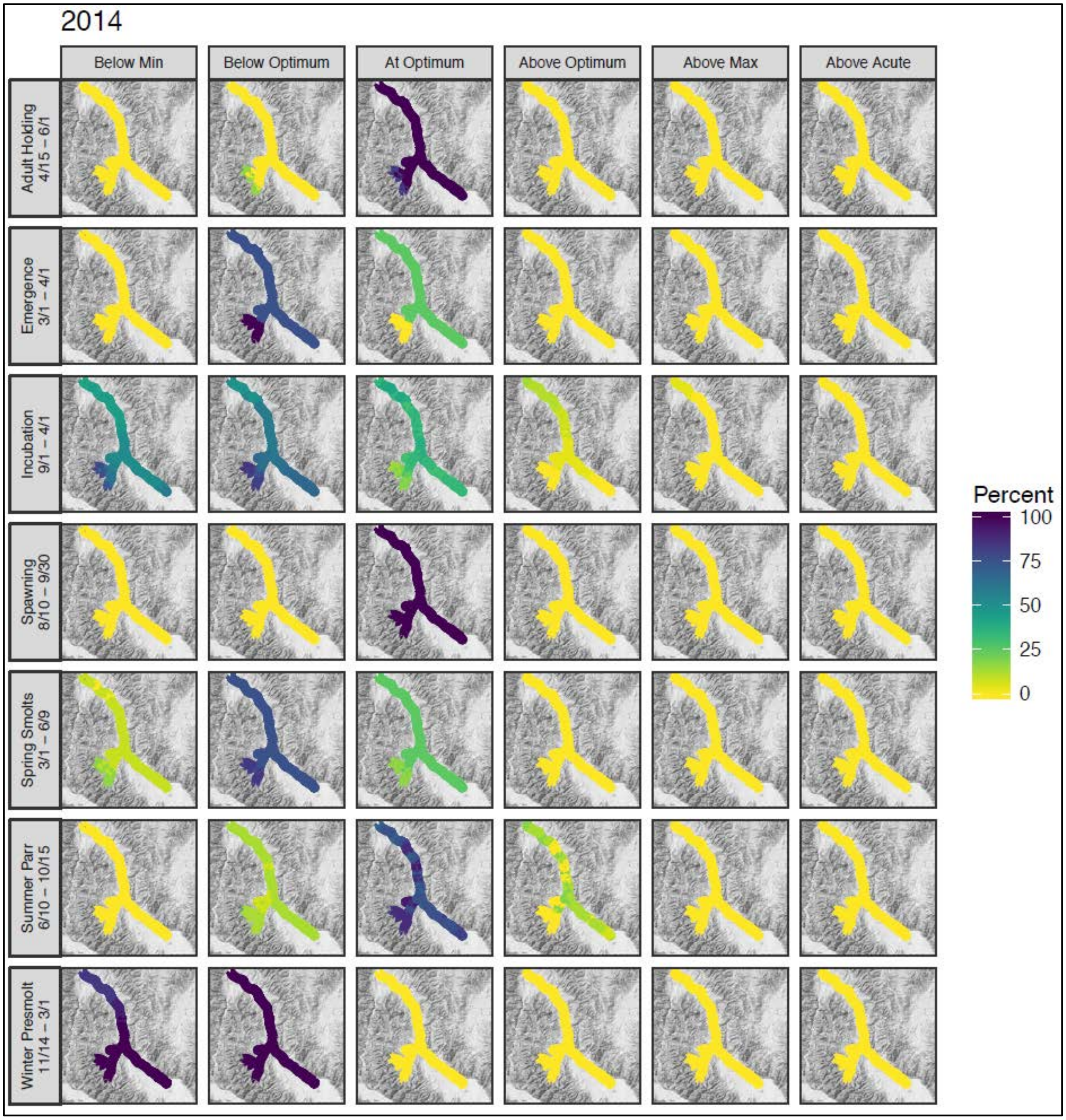

Supplemental Figure A-4. The percentage of time that 2014 water temperatures in the Lemhi River were below, within, or above a given temperature threshold (Carter 2005) for seven Chinook salmon life stages.

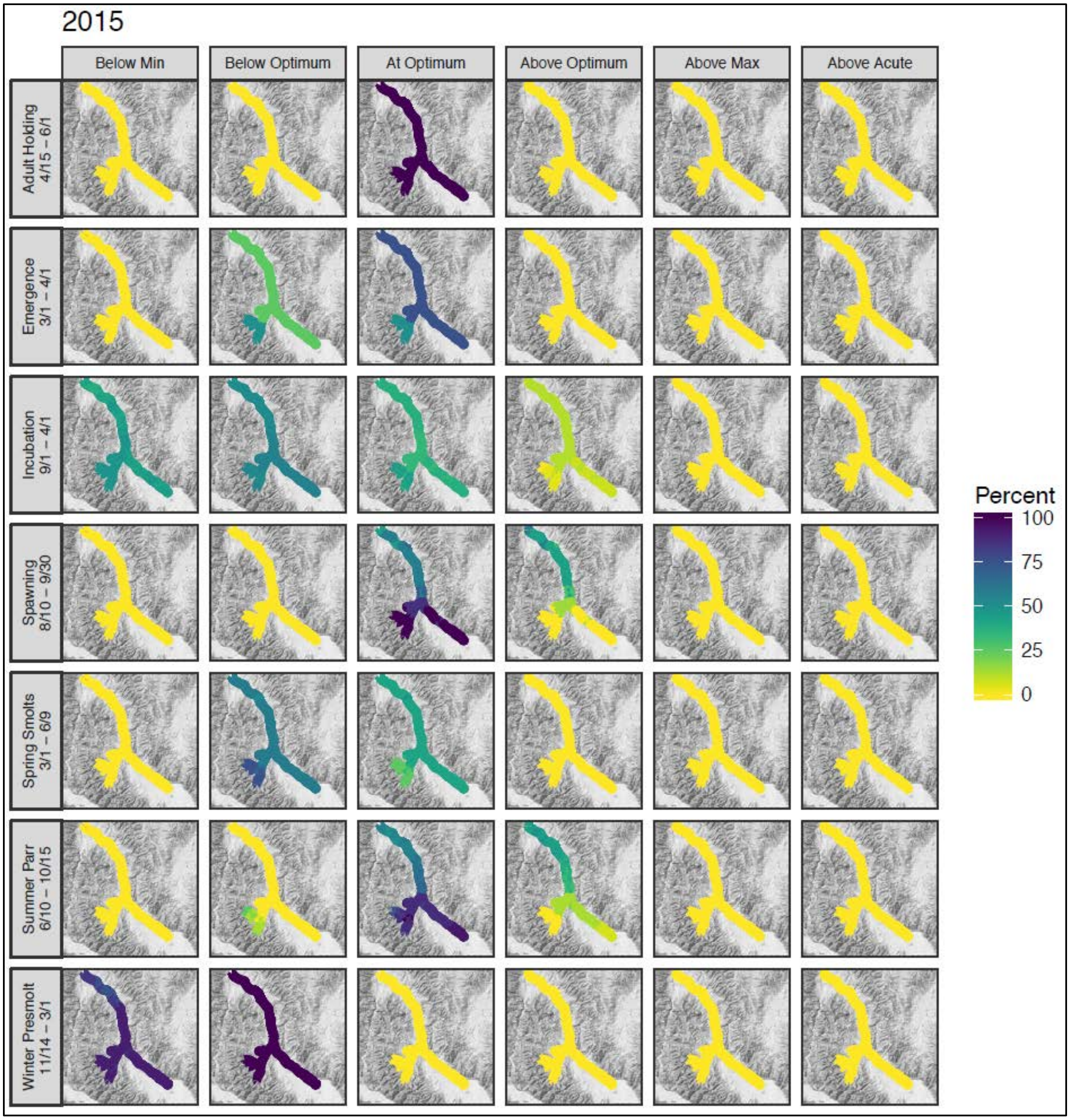

Supplemental Figure A-5. The percentage of time that 2015 water temperatures in the Lemhi River were below, within, or above a given temperature threshold (Carter 2005) for seven Chinook salmon life stages.

Pahsimeroi River

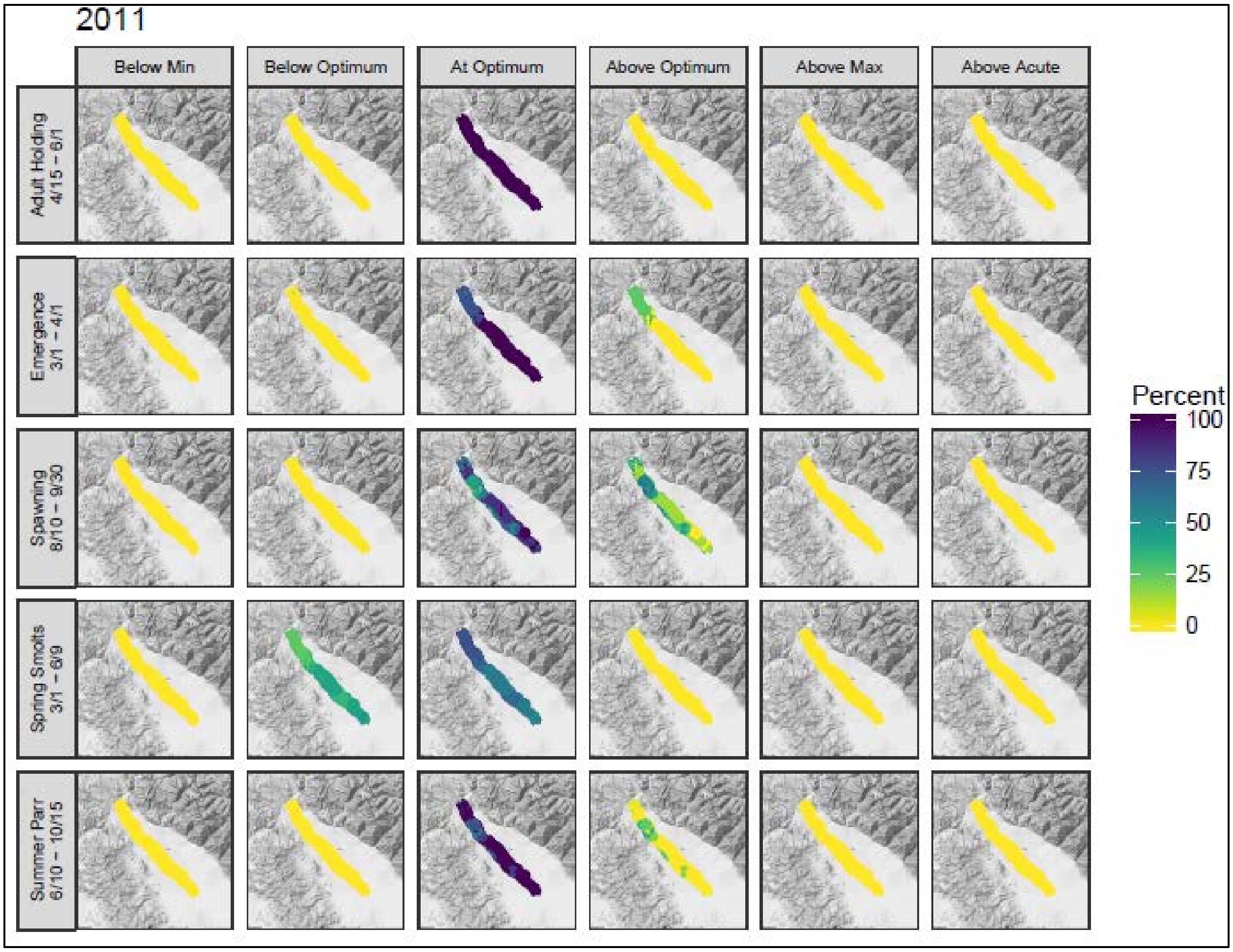

Supplemental Figure A-6. The percentage of time that 2011 water temperatures in the Pahsimeroi River were below, within, or above a given temperature threshold (Carter 2005) for five Chinook salmon life stages. Modeled temperature data for the winter time periods (incubation and winter presmolt life stages) were unattainable.

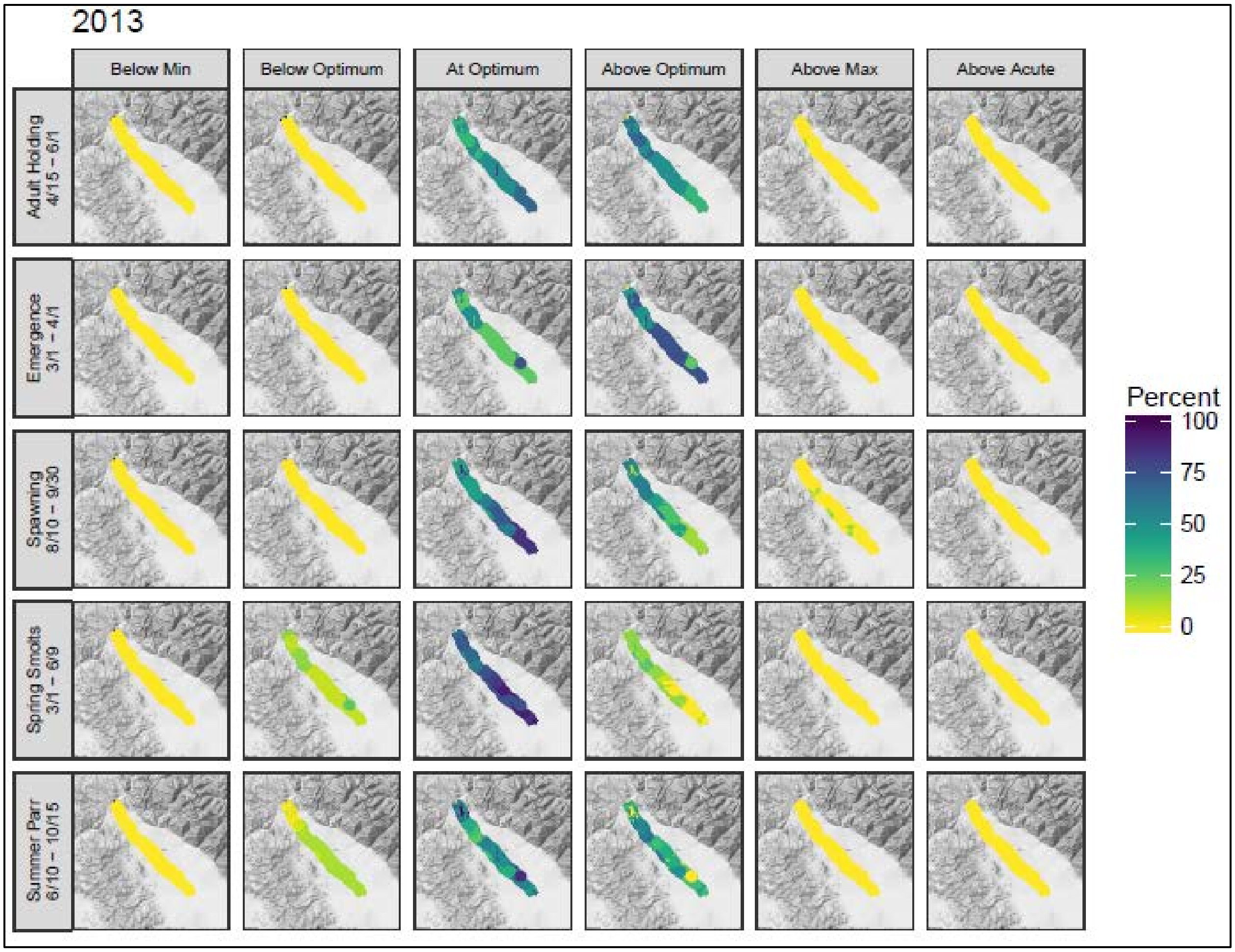

Supplemental Figure A-7. The percentage of time that 2013 water temperatures in the Pahsimeroi River were below, within, or above a given temperature threshold (Carter 2005) for five Chinook salmon life-stages. Modeled temperature data for the winter time periods (incubation and winter presmolt life stages) were unattainable.

Upper Salmon River

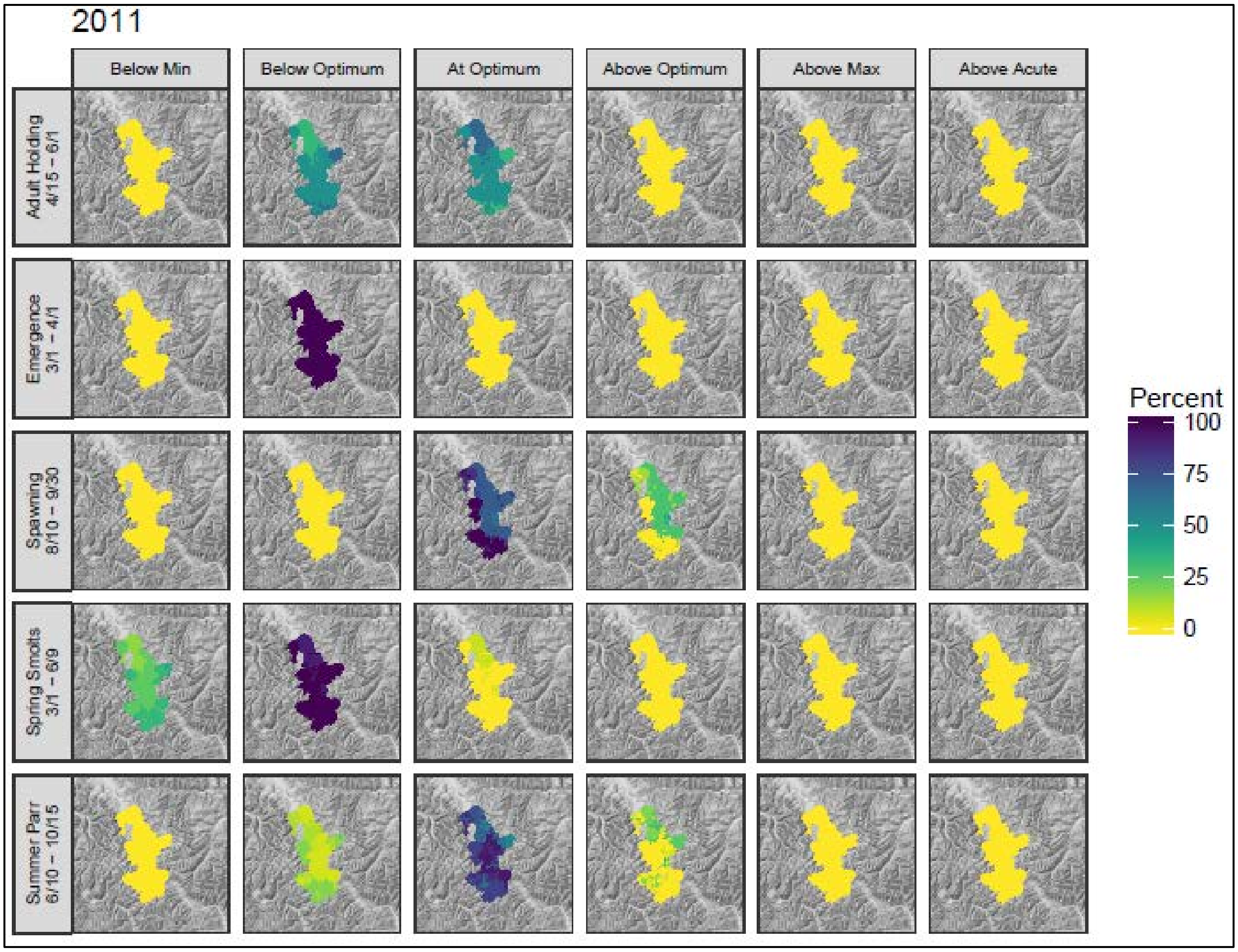

Supplemental Figure A-8. The percentage of time that 2011 water temperatures in the Upper Salmon River were below, within, or above a given temperature threshold (Carter 2005) for five Chinook salmon life-stages. Modeled temperate data for the winter time periods (incubation and winter presmolt life stages) were unattainable.

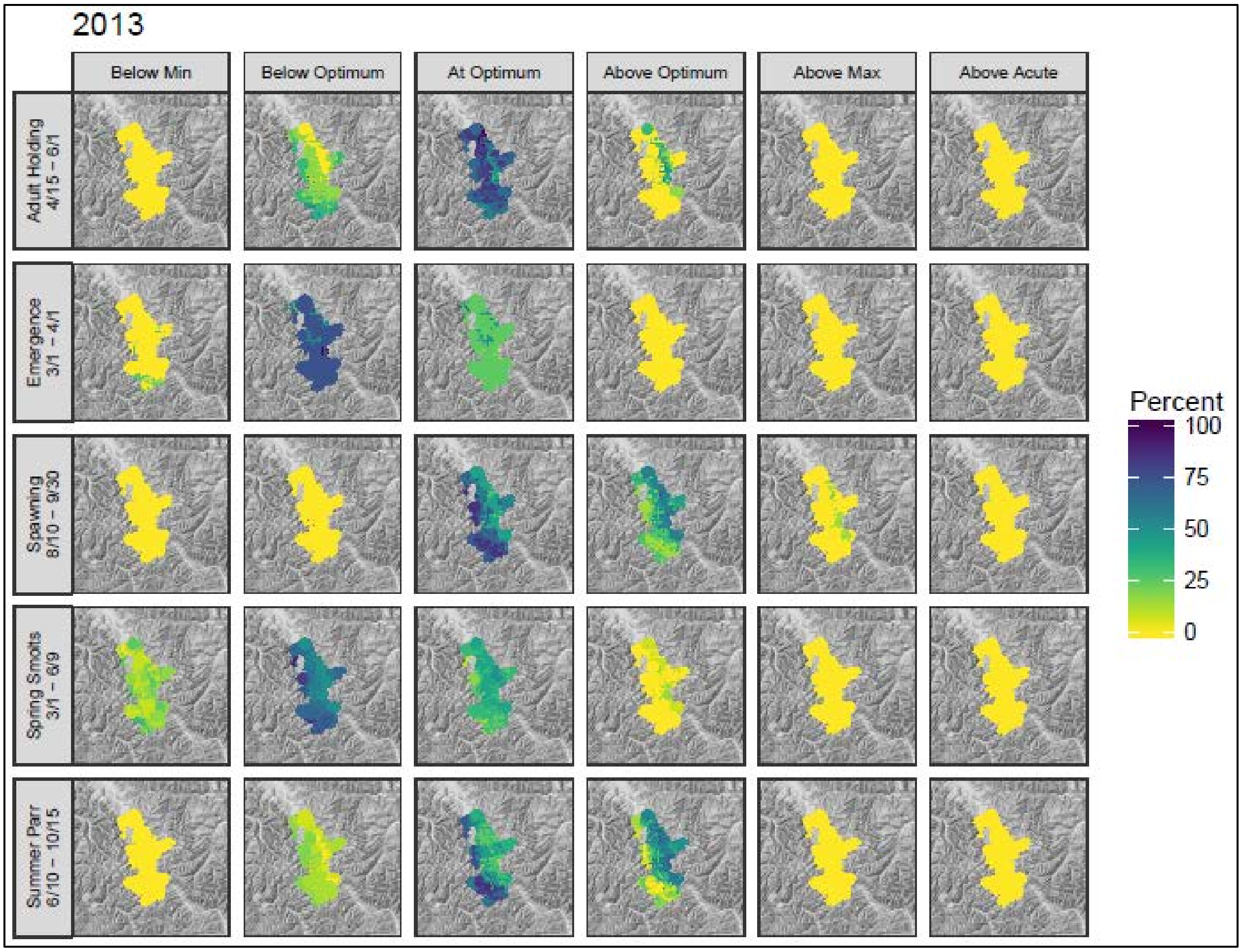

Supplemental Figure A-9. The percentage of time that 2013 water temperatures in the Upper Salmon River were below, within, or above a given temperature threshold (Carter 2005) for five Chinook salmon life-stages. Modeled temperate data for the winter time periods (incubation and winter presmolt life stages) were unattainable.

Steelhead

Lemhi River

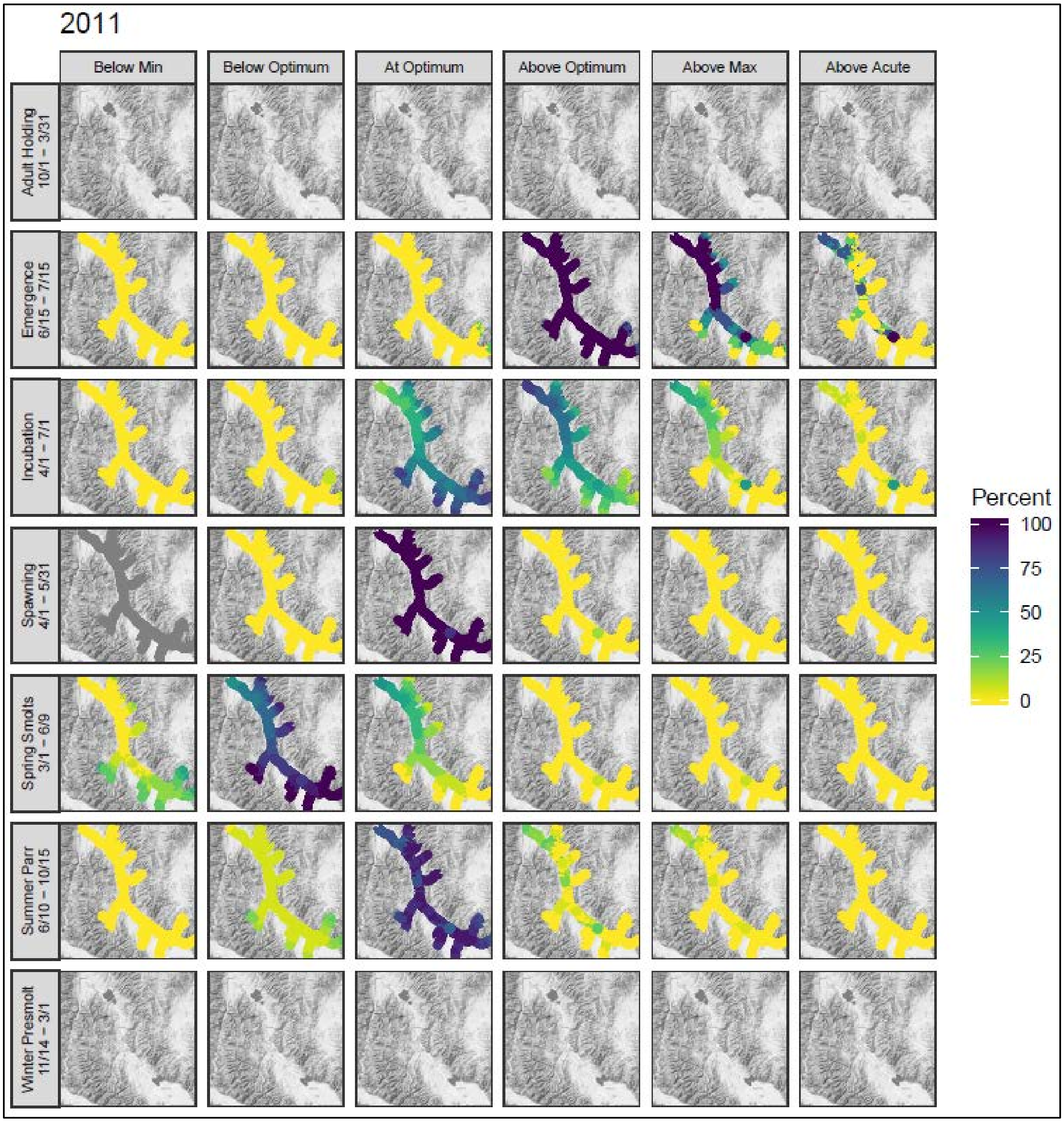

Supplemental Figure A-10. The percentage of time that 2011 water temperatures in the Lemhi River were below, within, or above a given temperature threshold (Carter 2005) for seven steelhead life stages. For facets with no data, modeled temperature data were unattainable for that timespan.

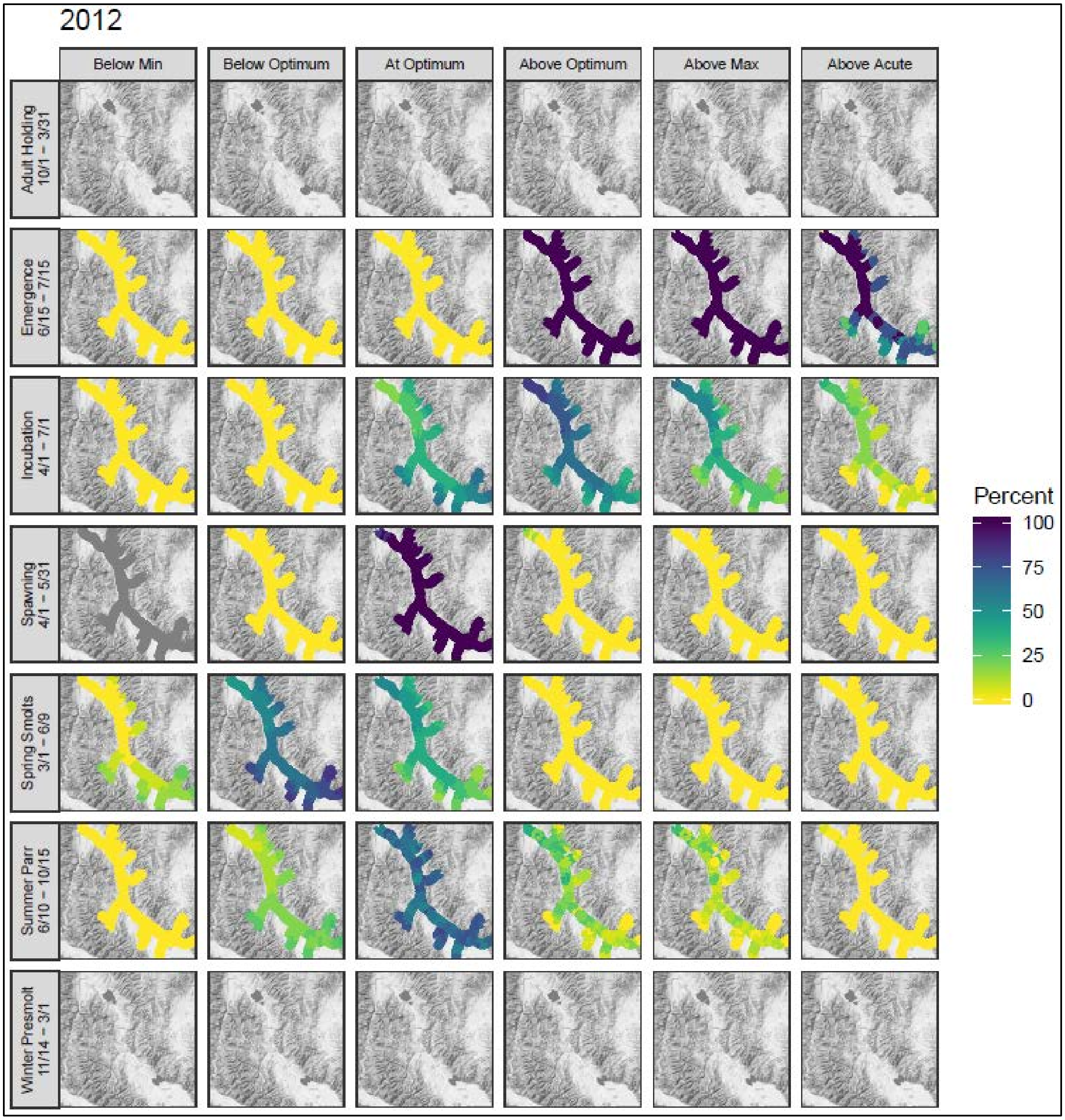

Supplemental Figure A-11. The percentage of time that 2012 water temperatures in the Lemhi River were below, within, or above a given temperature threshold (Carter 2005) for seven steelhead life stages. For facets with no data, modeled temperature data were unattainable for that timespan.

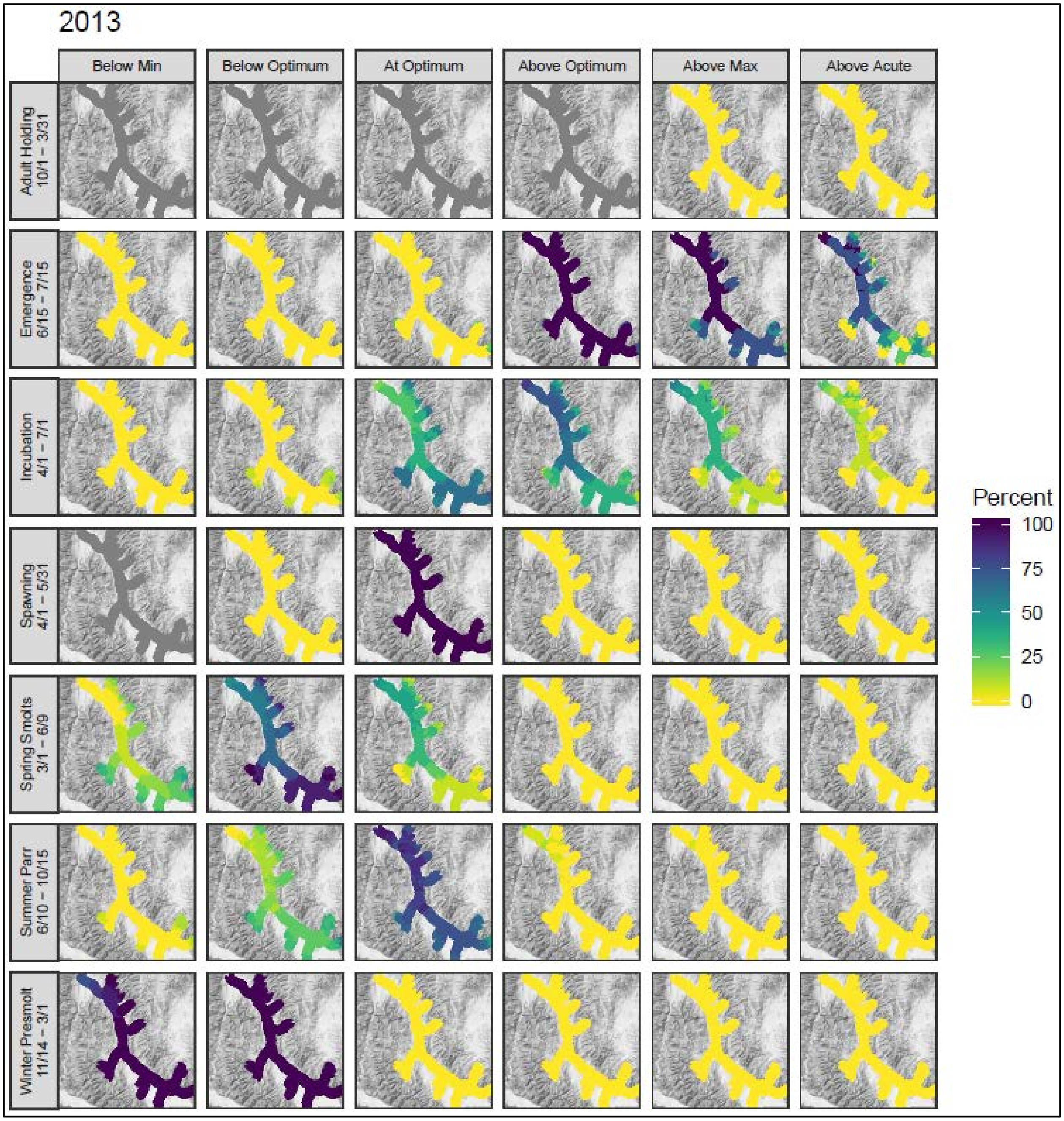

Supplemental Figure A-12. The percentage of time that 2013 water temperatures in the Lemhi River were below, within, or above a given temperature threshold (Carter 2005) for seven steelhead life stages.

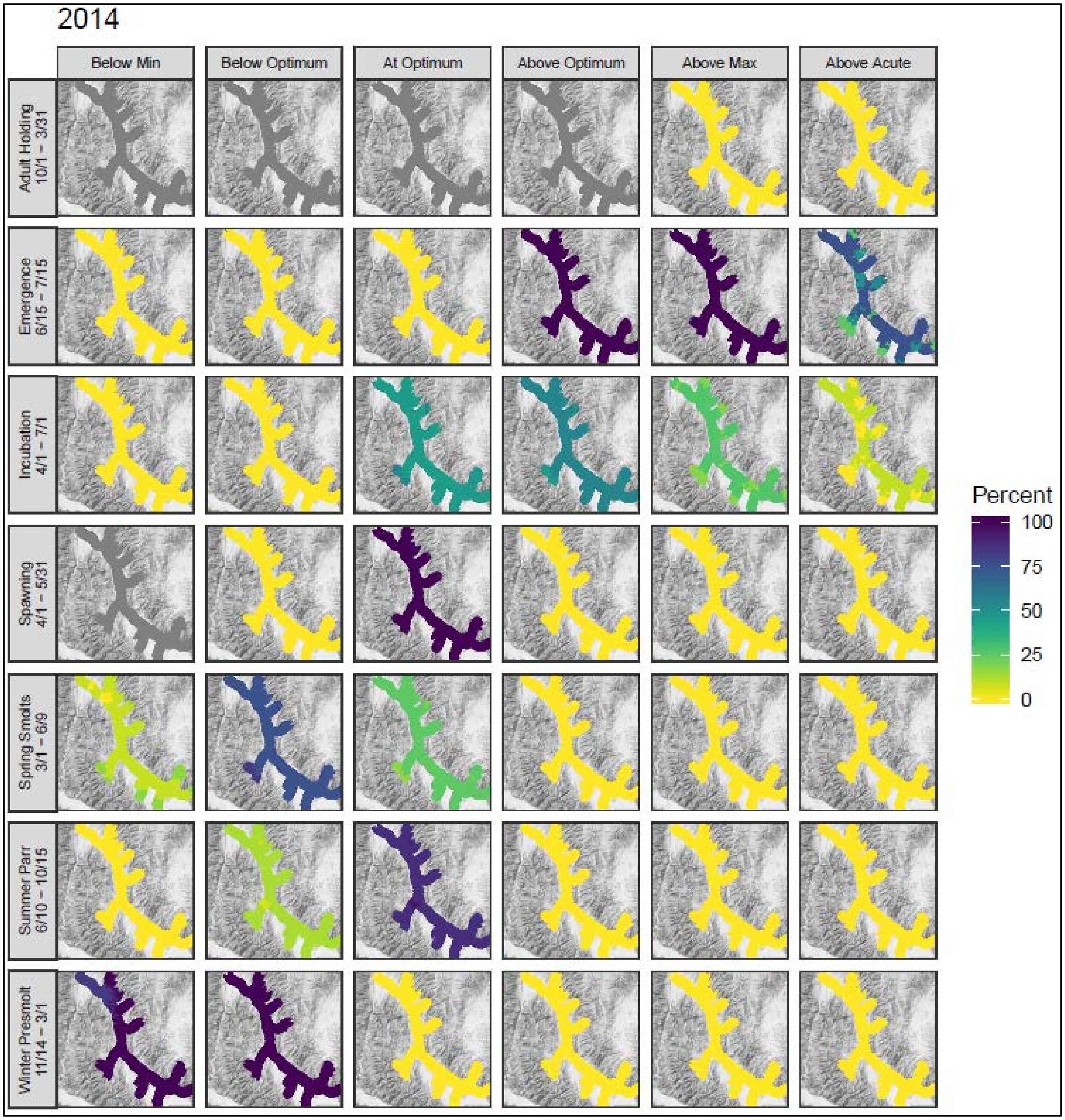

Supplemental Figure A-13. The percentage of time that 2014 water temperatures in the Lemhi River were below, within, or above a given temperature threshold (Carter 2005) for seven steelhead life stages.

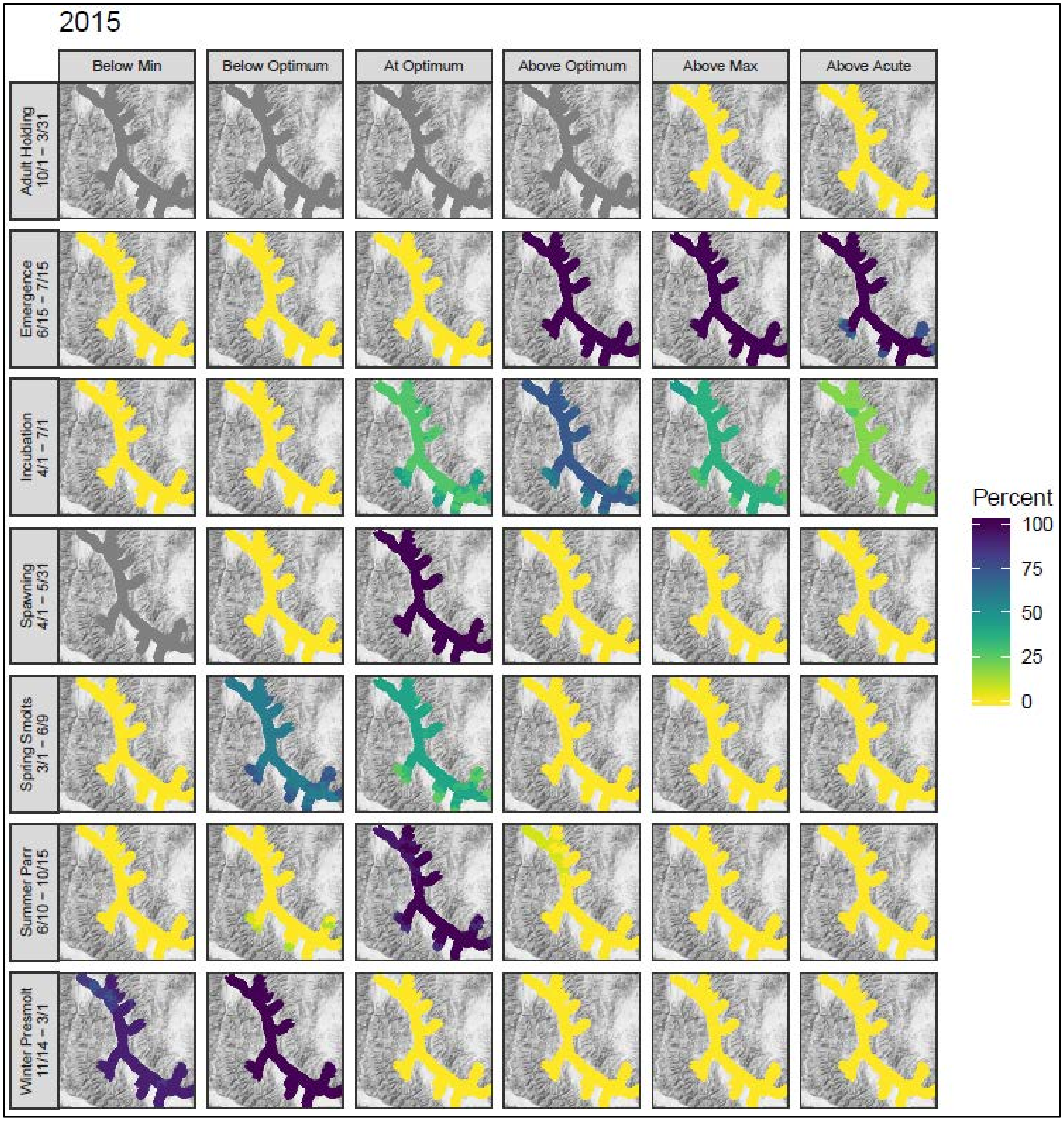

Supplemental Figure A-14. The percentage of time that 2015 water temperatures in the Lemhi River were below, within, or above a given temperature threshold (Carter 2005) for seven steelhead life stages.

Pahsimeroi River

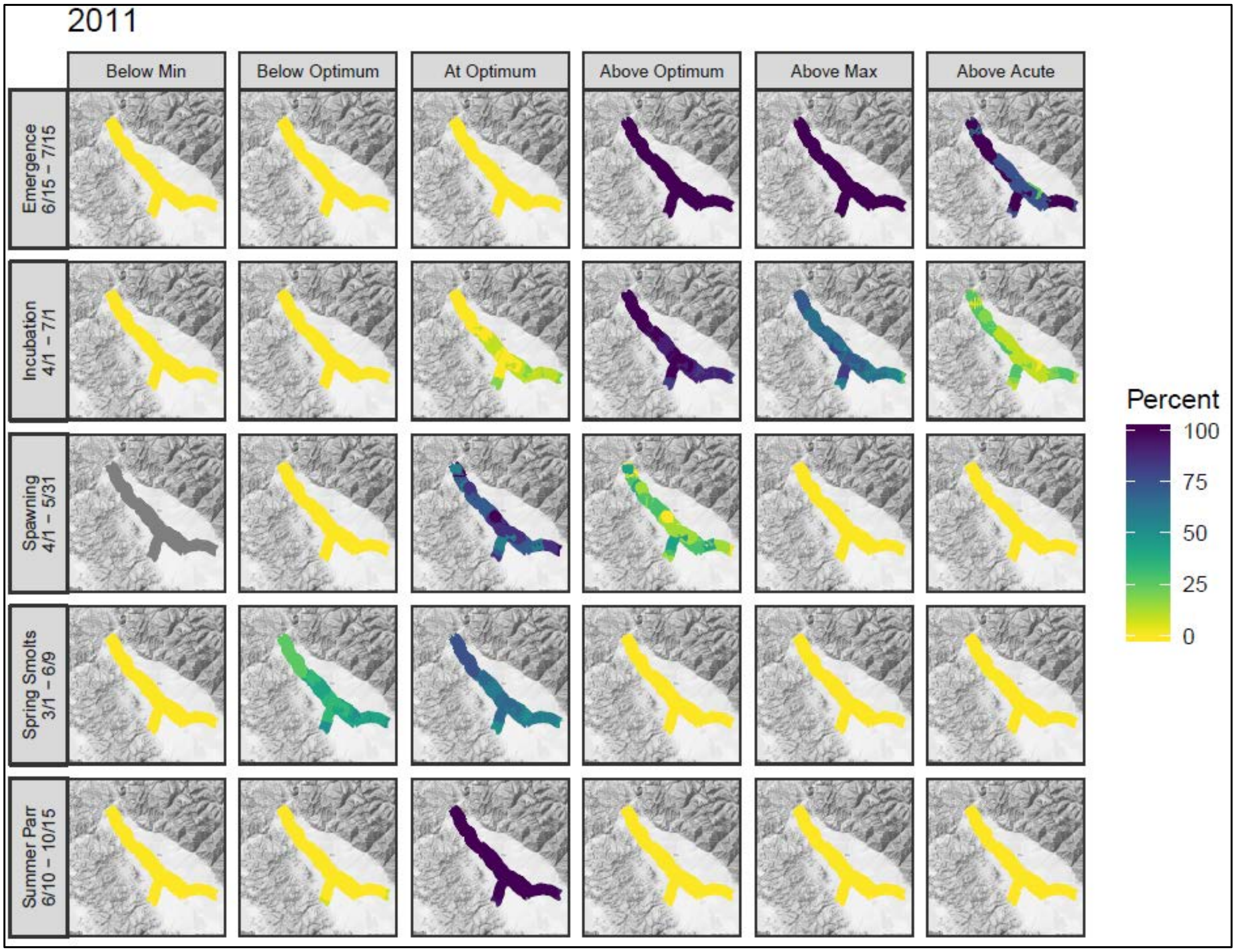

Supplemental Figure A-15. The percentage of time that 2011 water temperatures in the Pahsimeroi River were below, within, or above a given temperature threshold (Carter 2005) for five steelhead life stages. Modeled temperature data for the winter time periods (incubation and winter presmolt life stages) were unattainable.

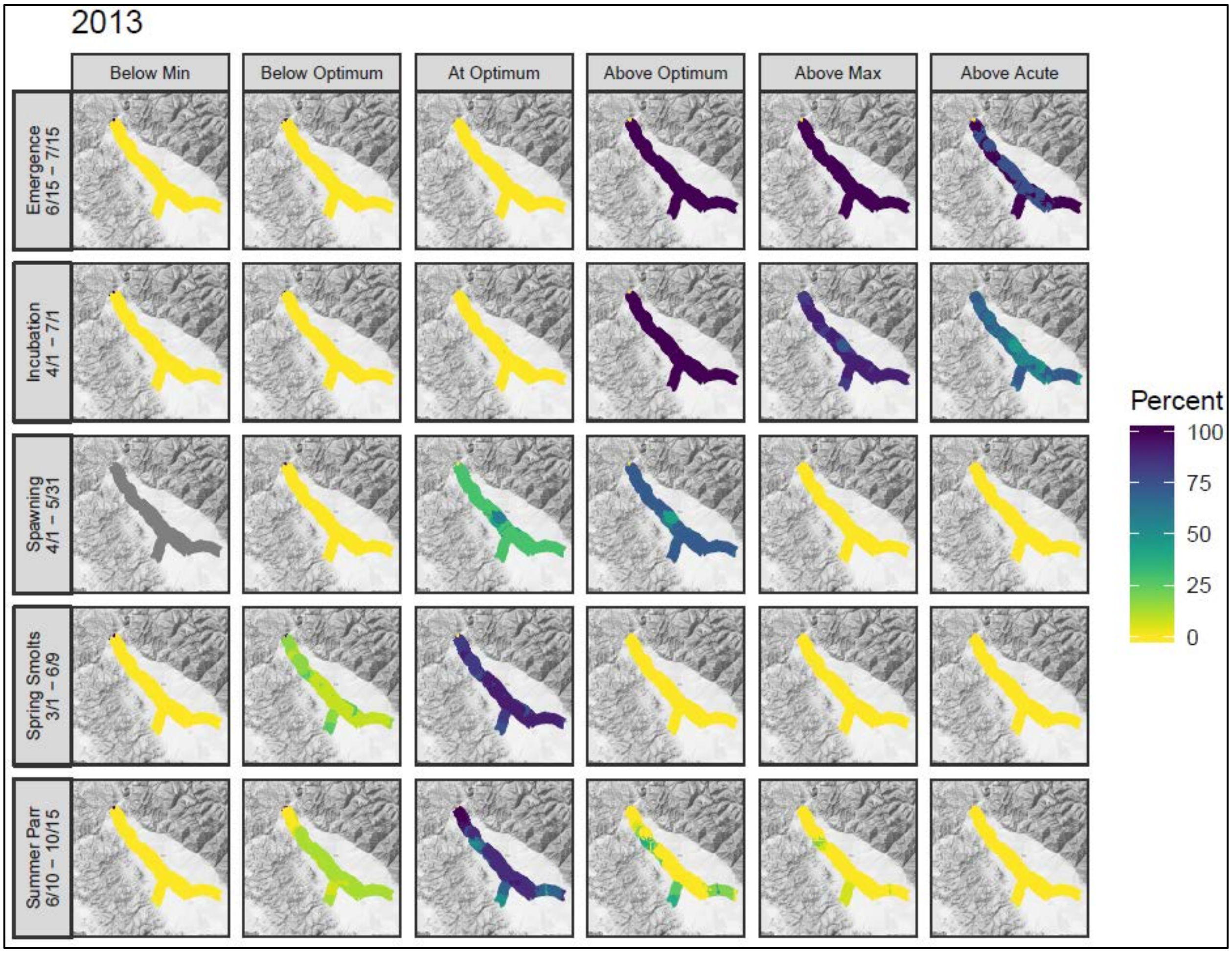

Supplemental Figure A-16. The percentage of time that 2013 water temperatures in the Pahsimeroi River were below, within, or above a given temperature threshold (Carter 2005) for five steelhead life stages. Modeled temperature data for the winter time periods (incubation and winter presmolt life stages) were unattainable.

Upper Salmon River

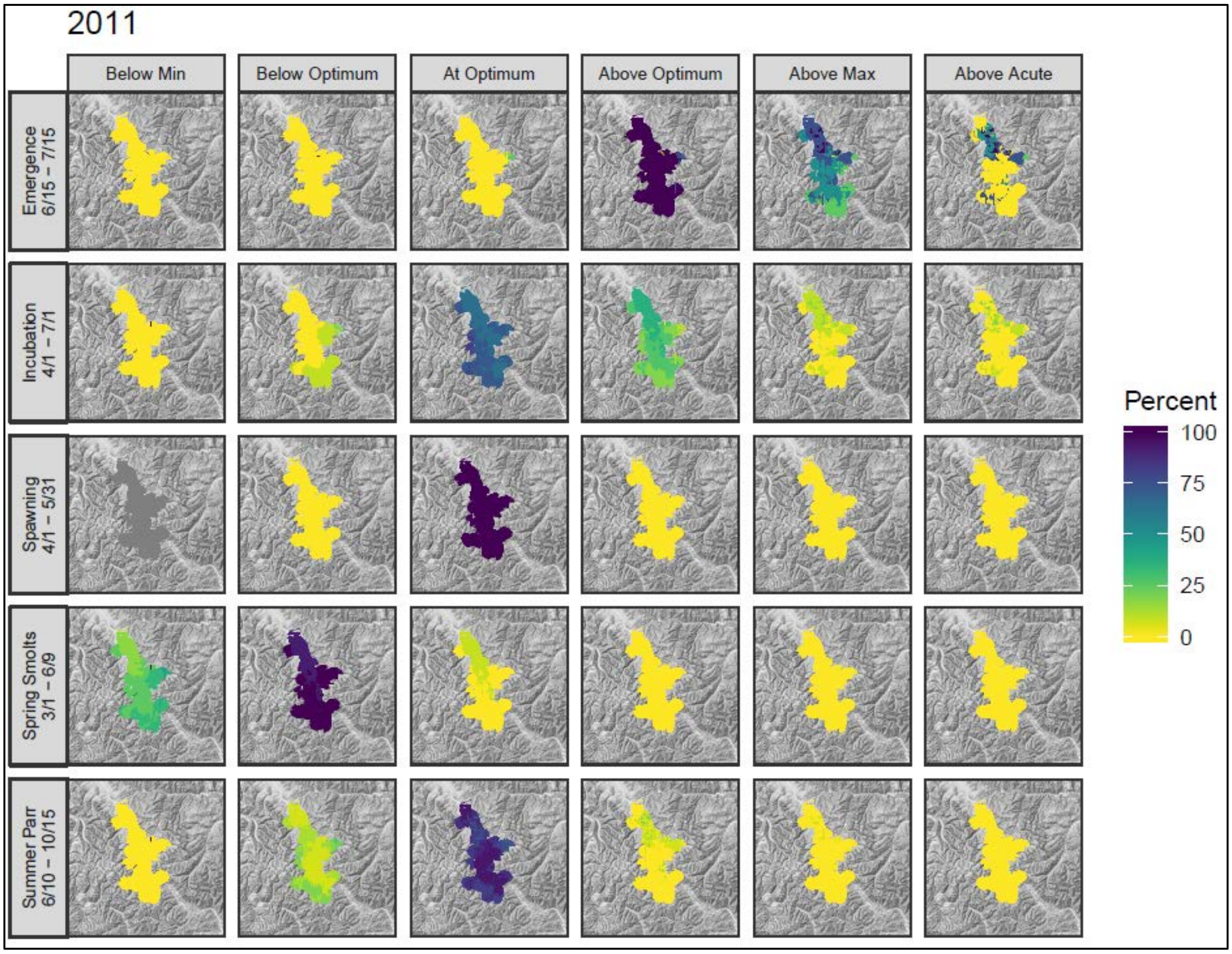

Supplemental Figure A-17. The percentage of time that 2011 water temperatures in the Upper Salmon River were below, within, or above a given temperature threshold (Carter 2005) for five steelhead life stages. Modeled temperate data for the winter time periods (incubation and winter presmolt life stages) were unattainable.

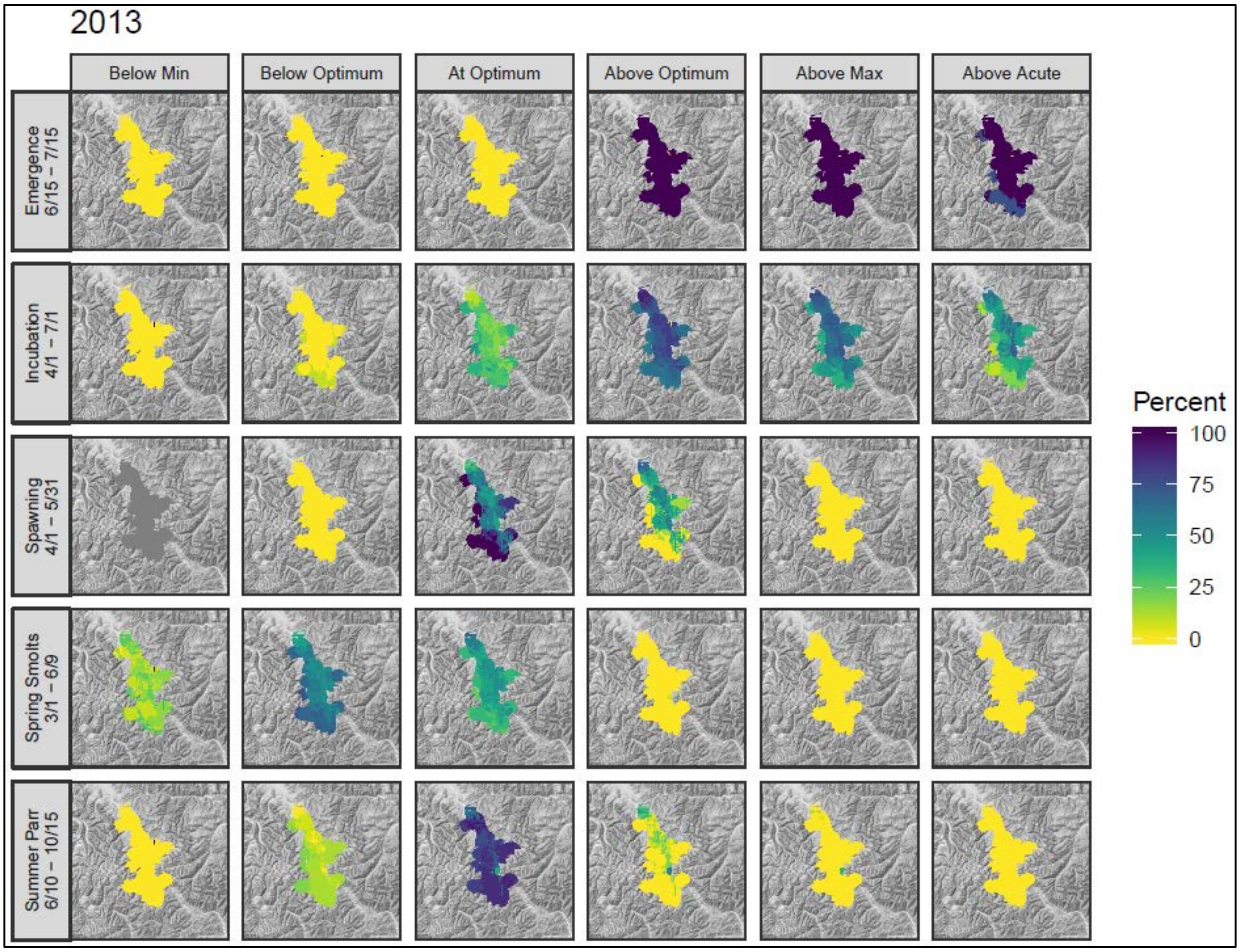

Supplemental Figure A-18. The percentage of time that 2013 water temperatures in the Upper Salmon River were below, within, or above a given temperature threshold (Carter 2005) for five steelhead life stages. Modeled temperate data for the winter time periods (incubation and winter presmolt life stages) were unattainable.

Appendix B – Habitat Capacity Estimation

Introduction

The decline of anadromous Pacific salmonids (*Oncorhynchus* spp.) across the Pacific Northwest has prompted numerous actions aimed at reversing that trend. These actions are often categorized into four Hs – harvest modification, habitat rehabilitation, hydroelectric operations, and hatchery practices. Substantial uncertainty remains regarding the degree of change to salmon populations that can be exerted across and within these categories, and what combination of changes might most cost-effectively and sustainably reduce mortality and recover depleted populations. Recently released delisting criteria (NOAA 2017) identified adult escapement targets at the population scale, providing a quantitative metric useful for evaluating the magnitude of survival improvements (across life stages) required. These abundance targets provide a benchmark against which habitat rehabilitation actions can be measured. In Appendix B, we describe a novel approach for estimating life stage-specific habitat capacity that can be used to quantitatively identify the magnitude of tributary habitat restoration needed to support Endangered Species Act (ESA) delisting. For perhaps the first time, the necessity of tributary habitat restoration actions can be demonstrated, and the magnitude of required change can be placed in context with the other Hs.

We define habitat (carrying) capacity as the maximal abundance or load the habitat can support for a given species and life stage given current resources and habitat quantity and quality. Within fisheries research and management, it has long been recognized that biotic and abiotic factors limit productivity within and across life stages. However, we assume that observed fish density is a poor predictor of habitat capacity owing to both a paucity of individuals and the existence of unmeasured biotic or abiotic variables that may serve to limit capacity. To address this, we have developed a novel approach to estimate the carrying capacity of wadeable streams to support spawning and rearing spring-summer run Chinook salmon (*O. tshawytscha*; hereafter Chinook salmon) and summer run steelhead (*O. mykiss*; hereafter steelhead) using quantile regression forest models (QRF; Meinshausen 2006).

We describe the development and implementation of QRF models to 1) better elicit fish-habitat relationships, and 2) predict habitat carrying capacity for juvenile and adult Chinook salmon and steelhead using paired measurements of fish abundance/density and habitat. The juvenile models pertain to juveniles rearing in wadeable streams during both summer (parr) and winter (presmolt) months; the adult model is to elicit fish-habitat relationships for spawning areas and predict habitat capacity to support redds. The habitat data are from the Columbia Habitat Monitoring Program (CHaMP; https://www.champmonitoring.org). Fish and habitat data were paired at CHaMP sites (200 to 500 meters) where fish survey data were available. The QRF model places no constraints on possible fish-habitat relationships; instead, relationships are estimated from the data regardless of being positive, negative, linear, non-linear, etc. Based on the observed fish-habitat relationships, we then predict habitat capacity at any location using measurements of the same habitat covariates used to populate the model (e.g., at all CHaMP sites). Finally, we extrapolate capacity predictions at CHaMP sites across larger scales (e.g., watershed, population) using globally available attribute data.

In summary, our objectives in Appendix B include:

1. Identify measured habitat characteristics that are most strongly associated with observed Chinook salmon and steelhead juvenile and redd abundance/density. This objective will use fish and habitat data from CHaMP sites from across the Columbia River Basin.
2. Use paired fish and habitat measurements to elicit fish-habitat relationships for those habitat characteristics identified as most important for determining juvenile or redd abundance/density. Again, this objective will use fish and habitat data from CHaMP sites across the Columbia River Basin.
3. Predict contemporary habitat carrying capacity at all sites in the Upper Salmon River Subbasin where CHaMP habitat characteristics are measured. This includes predictions for both species (Chinook salmon and steelhead) and three life stages (summer parr, winter presmolts, redds).
4. Extrapolate capacity predictions from CHaMP sites across larger scales (e.g., watershed, population) in the Upper Salmon River Subbasin using globally available attribute data to estimate Chinook salmon and steelhead juvenile and redd capacity at those larger scales. Watersheds include: Upper Salmon River (above Redfish Lake Creek), Valley Creek, Yankee Fork Salmon River, East Fork Salmon River, Pahsimeroi River, Lemhi River, North Fork Salmon River, and Panther Creek.

For summer parr capacity models, we predict capacity at the reach (200- to 500-meter) scale. For overwintering presmolt capacity, we modeled capacity at the channel unit scale, but then combined channel units up to the reach scale. For the redd model, we predict capacity at a slightly larger reach (1 river kilometer [rkm]) scale. In doing so, we elicit data-driven fish-habitat relationships from the data. Moreover, we describe a method to extrapolate capacity estimates to larger spatial scales (e.g., basin, population). Estimates of available habitat capacity for a given life stage (e.g., summer parr, winter presmolt, redds) at any given scale (e.g., watershed, population) can then be compared to estimates of life-stage-specific abundance necessary to achieve delisting or recovery goals (described in Appendix C). Doing so provides a quantitative means to elucidate the relative amount of habitat rehabilitation needed to provide sufficient habitat (quantity and quality) for recovery. Carrying capacity models based on QRF and habitat data, like those presented here, provide managers with a framework to guide the identification, prioritization, and development of habitat rehabilitation actions to recover salmon populations.

Methods

Study Site

Fish and habitat data used in the QRF models were collected from 11 watersheds within the interior Columbia River Basin: Asotin, Entiat, Grande Ronde (upper), John Day, Lemhi, Methow, Minam (tributary of Grande Ronde), Secesh, Tucannon, Wenatchee and Yankee Fork. Juvenile fish and redd data collected at CHaMP survey sites were provided by several collaborators and projects and included the Integrated Status and Effectiveness Monitoring Program (ISEMP).

Data

Habitat Data

The habitat data were collected by CHaMP (ISEMP/CHaMP 2017) and were downloaded from the CHaMP website. CHaMP sites are 200- to 500-meter reaches within wadeable streams across select watersheds within the interior Columbia River Basin and were selected based on a spatially balanced Generalized Random Tesselation Stratified (GRTS) sample selection algorithm (Stevens and Olsen 1999, 2004). Habitat data within CHaMP sites are collected using the CHaMP protocol (CHaMP 2016), which calls for field data collection during the low-flow period, typically from June through October. CHaMP habitat data include, but are not limited to, measurements describing channel complexity, channel units, disturbance, fish cover, large woody debris, riparian cover, size (depth, width, discharge), substrate, temperature, and water quality.

Temperature data collected using in-stream temperature loggers were only available for a small portion of CHaMP survey sites over appropriate time intervals. Therefore, modeled temperature data (McNyset et al. 2015) was provided by South Fork Research, Inc. Modeled temperature data summarizing the mean of 8-day means and the maximum of 8-day means for CHaMP sites during summer months (August and September) were available for the years 2011 through 2014.

Juvenile Fish Data

Juvenile fish surveys were conducted for Chinook salmon and steelhead during the summer and winter low-flow seasons at many of the same sites that were surveyed for habitat using the CHaMP protocol. Juvenile fish data included in this analysis were collected during summers of 2011 to 2014, and in the winter of 2017-2018. Fish survey methods to estimate juvenile abundance included mark-recapture, three-pass removal, two-pass removal, and single-pass electrofishing, as well as snorkeling. Survey data were used to estimate juvenile abundance at all sites where data were available. See et al. (2018) provide further detail on methods used to generate juvenile abundance estimates. Summer sampling and data collection were conducted at the site scale, whereas winter sampling was conducted at the channel unit scale, primarily using snorkel surveys.

Juvenile abundance estimates at all sites were translated into linear fish densities (parr/m) for the summer, and areal densities (parr/m^2) in the winter, and density estimates were paired with the associated CHaMP habitat data. For sites that were sampled in multiple years, only the fish and habitat data from the year with the highest observed fish density were retained to avoid possible pseudo-replication.

Redd Data

Chinook salmon and steelhead redd data were graciously provided by the Idaho Department of Fish and Game, Nez Perce Tribe Department of Fisheries Resources, Oregon Department of Fish and Wildlife, U.S. Fish and Wildlife Service, and the Washington Department of Fish and Wildlife and span the years 1995 to 2016. Redd data were available for the following CHaMP watersheds: Asotin, Entiat, John Day, Lemhi, Methow, Minam, Secesh, Tucannon, upper Grande Ronde, Wenatchee, and Yankee Fork.

To pair the redd and habitat data, the number of redds that occurred within a 1 rkm buffer of the central point (i.e., x-site) for each CHaMP site were tallied. The latitude and longitude of each CHaMP site and each redd were snapped to a route in ArcGIS and the number of redds that occurred within 500 meters upstream or downstream of each CHaMP site for each year in which redds were observed were counted and transformed into linear densities (redds/m). For each CHaMP site, we identified the year in which the maximum number of redds were observed because we are ultimately interested in redd capacity, and therefore used the highest observed redd density at each CHaMP site.

Habitat Covariate Selection

A crucial step in developing a QRF model to predict habitat capacity to support juveniles or redds is selecting the habitat covariates to include in the model. Random forest models naturally incorporate interactions between correlated covariates, which is essential because nearly all CHaMP habitat variables are correlated to one degree or another. However, we aimed to avoid including redundant variables (i.e., variables that measure similar aspects of the habitat). Including too many habitat covariates can result in overfitting of the model (e.g., including as many covariates as data points).

The CHaMP protocol produces more than 100 metrics describing the quantity and quality of fish habitat for each survey site, as well as number of metrics at the channel unit scale. To decide which habitat metrics to use in each QRF model, we considered first the association between the habitat metric and observed juvenile or redd densities and second the correlation among habitat metrics. We used the Maximal Information-Based Nonparametric Exploration (MINE) class of statistics (Reshef et al. 2011) to determine those habitat characteristics most highly associated with observed juvenile or redd densities. MINE statistics were employed using the R package *minerva* (Albanese et al. 2013). Within the MINE statistics, we used the maximal information coefficient (MIC) to measure the strength of the linear or non-linear association between fish density and each habitat characteristic (Reshef et al. 2011). The MIC value was used to inform decisions on which habitat covariates to include in the model. Habitat metrics were grouped into broad categories that include channel unit, complexity, cover, disturbance, riparian, size, substrate, temperature, water quality, and woody debris. Within each category, metrics were ranked according to their MIC value. Our strategy was to select one or two variables with high MIC scores within each category so that covariates describe different aspects of the spawning and juvenile rearing habitat. Additionally, we measured pairwise correlations among all habitat metrics and attempted to avoid covariates that were highly correlated and include covariates that describe potentially meaningful fish-habitat relationships. Table B-1 provides a summary of habitat covariates used in each of the QRF models.

QRF Model Fitting

In total, six QRF models were fit including combinations of two species (Chinook salmon and steelhead) and three life stages (summer parr, winter presmolt, redd). Each of the QRF models were fit using the selected habitat covariates and using the *quantregForest* function from the *quantregForest* package (Meinshausen 2016) in R software (R Core Team 2015). The individual predictions from each tree, viewed collectively, describe the entire distribution of the predicted response. Therefore, the random forest model can be used in the same way as other quantile regression methods to predict any quantile of the response. The 90th quantile of the predicted distribution was used as a proxy for habitat carrying capacity. We chose to use the 90th quantile, instead of something higher, to avoid using predictions that are aimed at the very upper tails of observed fish density, which may be influenced by sampling issues.

Chinook salmon and steelhead summer parr, winter presmolt, and redd densities and associated habitat data were paired by site and year; this habitat data contained some missing values. Within each dataset, any site visit with more than three missing covariates was dropped from the dataset; the remaining missing habitat values were imputed using the *missForest* R package (Stekhoven and Buehlmann 2012; Stekhoven 2013).

After model fitting, each QRF model can then be used to predict Chinook salmon or steelhead summer parr, winter presmolt, or redd capacity using measurements of the habitat covariates used to fit each model. In our case, this includes all sites in the Columbia River Basin surveyed using the CHaMP protocol (CHaMP 2016). For CHaMP sites surveyed in multiple years, we first calculated the mean among years prior to making predictions. For overwintering capacity, QRF predictions were made at the channel unit scale, and then combined to estimate capacity at the CHaMP site scale.

Results

Habitat Covariate Selection

We categorized 150 habitat measurements collected using the CHaMP habitat protocol (CHaMP 2016) into 11 habitat groups. For each model, an MIC value was calculated for each habitat covariate based on the strength of association between the habitat covariate and the response variable (fish or redd density). Covariates were then ranked within each habitat group, and we selected one or two covariates within each habitat group, taking into consideration their MIC rank and number of missing values. Our strategy was to 1) consider pairwise correlations among habitat covariates to minimize redundant covariates measuring similar aspects of habitat, and 2) select covariates that describe habitat characteristics likely important towards spawning or rearing.

We focused on each life stage in turn, examining the MIC statistics of each habitat covariates for both Chinook and steelhead. We selected between eight and 14 metrics to use in each life stage. Table B-1 shows the CHaMP habitat covariates used to fit each of the QRF models.

Table B-1. Habitat metrics and descriptions of metrics included in each of the QRF capacity models. Numbers indicate where each metric ranked in relative importance for each model. Dashes indicate a metric was not used for a given model.

Metric Category	Metric	Description	Chinook Sum. Juv.	Chinook Win. Juv.	Chinook Redd	Steelhead Sum. Juv.	Steelhead Win. Juv.	Steelhead Redd
Channel Unit	Channel Unit Frequency	Number of channel units per 100 meters.	8	2	–	12	3	–
Channel Unit	Fast Turbulent Frequency	Number of Fast Water Turbulent channel units per 100 meters.	–	–	13	–	–	6
Channel Unit	Fast Turbulent Percent	Percent of wetted area identified as Fast Water Turbulent channel units.	–	–	11	–	–	8
Channel Unit	Tier1	Tier 1 channel unit type.	–	8	–	–	8	–
Complexity	Sinuosity	Ratio of the thalweg length to the straight-line distance between the start and end points of the thalweg.	–	4	–	–	6	–
Complexity	Thalweg Depth CV	Coefficient of Variation (CV) of thalweg depths at a site.	9	–	–	7	–	–
Complexity	Wetted Width To Depth Ratio Avg	Average width to depth ratio of the wetted channel measured from cross-sections. Depths represent an average of depths along each cross-section.	4	–	12	5	–	2
Complexity	Wetted Width To Depth Ratio CV	Retired. Coefficient of Variation of wetted width to depth ratios derived from cross-sections.	–	–	9	–	–	14
Cover	Fish Cover: LW	Percent of wetted area that has woody debris as fish cover.	–	6	–	–	4	–
Cover	Fish Cover: Total	Percent of wetted area with the following types of cover: aquatic vegetation, artificial, woody debris, and terrestrial vegetation.	5	–	–	9	–	–
Land Classification	Disturbance Index	Disturbance index that includes measures of % urban, % agricultural, % impervious surface and road density (Whittier et al. 2011).	14	–	6	4	–	3
Land Classification	Natural PC 1	A natural index that describes watershed slope, precipitation, growing season (growing degree day), and low-gradient streams (Whittier et al. 2011).	–	–	3	–	–	7
Riparian	Riparian Cover: Ground	Percent of groundcover vegetation.	6	–	–	14	–	–

Metric Category	Metric	Description	Chinook			Steelhead		
			Sum. Juv.	**Win. Juv.**	**Redd**	**Sum. Juv.**	**Win. Juv.**	**Redd**
Riparian	Riparian Cover: No Canopy	Percent of riparian canopy devoid of vegetation.	–	–	8	–	–	13
Size	Discharge	The sum of station discharge across all stations. Station discharge is calculated as depth x velocity x station increment for all stations except first and last. Station discharge for first and last station is 0.5 x station width x depth x velocity.	–	–	7	–	–	1
Size	Discharge - Fish	Discharge at time of fish survey	–	1	–	–	1	–
Size	Gradient	Site water surface gradient is calculated as the difference between the top of site (upstream) and bottom of site (downstream) water surface elevations divided by thalweg length.	–	–	2	–	–	4
Size	Thalweg Depth Avg	Average thalweg depth of the wetted channel.	1	–	–	2	–	–
Size	Thalweg Exit Depth	Depth of the thalweg at the downstream edge of the channel unit.	–	3	–	–	2	–
Substrate	Substrate < 6mm	Average percentage of pool tail substrates comprised of sediment <6 mm.	11	–	–	13	–	–
Substrate	Substrate Est: Boulders	Percent of boulders (256-4000 mm) within the wetted site area.	–	–	4	–	–	5
Substrate	Substrate Est: Coarse and Fine Gravel	Percent of coarse and fine gravel (2-64 mm) within the wetted site area.	10	7	5	10	5	11
Substrate	Substrate: D50	Diameter of the 50th percentile particle derived from pebble counts.	12	5	–	8	7	–
Temperature	Max7dAM	Highest 7-day average of daily maximum (7dAM) value between July 15th - August 31st.	7	–	10	6	–	12
Temperature	Summer Hourly Average Temp	Average of all hourly temperature measurements collected July 15th - August 31st.	2	–	–	3	–	–
Water Quality	Conductivity	Measure of the concentration of ionized materials in water, or the ability of water to conduct electrical current.	3	–	1	1	–	9

Metric Category	Metric	Description	Chinook			Steelhead		
			Sum. Juv.	Win. Juv.	Redd	Sum. Juv.	Win. Juv.	Redd
Wood	Large Wood Frequency: Wetted	Number of large wood pieces per 100 meters within the wetted channel.	13	–	14	11	–	10

QRF Model Fitting

QRF models were fit for each of the species and life stages using the chosen habitat covariates (Table B-1) and the *quantregForest* package (Meinshausen 2016) in R (R Core Team 2015). Table B-1 provides the relative importance of each habitat covariate included in each of the QRF models, after model fit. Additionally, QRF models allow one to visually examine the marginal effect of each habitat covariate on the quantile of interest using partial dependence plots. These plots show the marginal effect of changing a single covariate on the response variable while maintaining all other covariates at their mean values (see Supplemental Figure B-1 to Supplemental Figure B-6).

Model Extrapolation

After model fitting, QRF models can be used to predict capacity for a given species and life stage at all CHaMP sites within the interior Columbia River Basin, using the 90th quantile of the predicted distribution as a proxy for carrying capacity. CHaMP site carrying capacity predictions from each of the six QRF models (Chinook salmon/steelhead; summer parr, overwinter presmolt, and redds) were extrapolated to larger scales (e.g., watershed, population) using GAA covariate data. In the Supplementary Tables and Figures to Appendix B, we provide estimates of habitat capacity, by life stage and species, for tributaries and mainstem habitats in eight watersheds of the Upper Salmon River Subbasin. Watersheds include the Upper Salmon River (above Redfish Lake), Valley Creek, Yankee Fork Salmon River, East Fork Salmon River, Pahsimeroi River, Lemhi River, North Fork Salmon River, and Panther Creek (see Supplementary Tables and Figures). Moreover, we provide maps to visualize predictions of parr and redd capacity at all master sample points in these watersheds using the extrapolation model. These capacity tables and maps provide an example of outputs available from our current QRF and extrapolation models.

Discussion

We have described a novel approach to estimate the capacity of habitat in wadeable streams to support Chinook salmon and steelhead juveniles (during summer and winter months) and redds in the interior Columbia River Basin. We have built QRF models for three different life stages (summer parr, overwintering juveniles, and redds) for two different species. The approach is entirely empirical, allowing fish-habitat relationships to emerge from the input data, even if they are non-linear in nature (as most ecological relationships are). For these species and life stages, we have generated estimates of capacity where similar habitat data are available (i.e., at all CHaMP sites). In this appendix, we further extrapolated those predictions to larger spatial scales using globally available attribute data and have provided estimates of habitat capacity and capacity maps for eight watersheds in the Upper Salmon River Subbasin. The habitat capacity predictions for each of the watersheds can then be compared to estimates of habitat capacity necessary to support ESA delisting (described in Appendix C) to identify life-stage-specific capacity limitations. To date, we have validated the QRF estimates of Chinook summer parr with spawner-recruit curves from a variety of watersheds in the Columbia River Basin and found them to match up very well, despite being based on entirely different data (See et al. 2018). Additionally, QRF predictions of capacity can be built on habitat sampling conducted over a handful of years (or a single year with enough effort), whereas spawner-recruit curves, while often considered a gold standard for estimating capacity, require many years of data with plenty of contrast to be considered valid.

There are potential limitations to our approach that should be considered when interpreting results. First, we assume that at least some sites in our empirical dataset are at or near carrying capacity at the site level.

Having at least some sites near capacity allows the random forest model to more accurately provide classification and regression trees, which, in turn, allows better approximation of quantiles and capacity. However, this assumption may not be true in this case, especially since juvenile fish abundance/density and redd data used in the model have been collected during recent years of low escapement. If this assumption is not met, the QRF models will likely produce conservative (low) estimates of capacity (but the framework of the model is not wrong). To address this limitation, we hope to add paired fish-habitat data in the future from areas of increased escapement or that are likely near rearing or spawning capacity (e.g., Secesh River, Idaho, or regions outside of the Columbia River [e.g., Alaska]) to provide more accurate estimates of capacity. Adding fish-habitat data from additional areas has the benefit of providing additional contrast in habitat data to the model, which can improve model predictions and extrapolation.

Our QRF models are populated using CHaMP habitat data and juvenile fish or redd abundance and density information collected within those CHaMP sites. Predictions of habitat capacity can then be made at locations where similar habitat data are available (i.e., all CHaMP sites) and then extrapolated to larger spatial scales using globally available attributes or similar. However, there are a few issues related to the extrapolation of QRF estimates of capacity to larger spatial scales that should be noted. For example, determining the downstream extent of wadeable streams can be a challenge, and whether all the master sample points we include meet that definition is unclear. Fish-habitat relationships may change in deeper rivers, and these QRF models should currently only be applied to wadeable areas of a watershed. In the future, we hope to explore the ability to apply QRF models to larger river systems where desired.

We recognize that, occasionally, estimates of winter capacity for a particular stream or watershed are higher for winter juveniles than summer parr (e.g., upper Grande Ronde steelhead), which was contrary to our expectations. Although this may be true, there are other alternative potential expectations for these results. First, we assumed that the spatial extent for rearing during summer and winter months was the same. In reality, the winter extent for each species is likely not as broad as the summer rearing extent, so even if more fish could be supported at some sites during winter, there may be extents of the watershed not available to overwintering fish. However, without knowing the true winter distributional extent, it is difficult to correct for varying summer/winter extents. To date, our winter fish sampling has focused on areas within the domain of Chinook salmon, so we do not have the observational data to restrict a species' winter range appropriately, and such data would be difficult to obtain.

Next Steps

The QRF models presented here are currently populated using habitat data collected by CHaMP (CHaMP 2016). However, with the reduction in effort of on-the-ground habitat data collection (i.e., CHaMP), habitat data and covariates used in the model may become outdated as habitat evolves year-to-year via natural and/or anthropogenic changes. As a result, the need for a broader, watershed-scale, cost-effective approach to sampling riverine habitat to populate fish-habitat models has become apparent. Remote sensing techniques paired with minimal, streamlined, on-the-ground sampling may allow for more rapid habitat data collection, at increased scale, and in a more cost-effective manner. Fish-habitat models, including QRF, would benefit by incorporating habitat data collected via remotely sensed platforms and at a greater spatial scale. Emerging techniques, such as multi-spectral analysis, bathymetric LiDAR, and high-resolution RGB cameras are becoming more affordable and attainable for watershed-scale habitat data collection. Further, if data availability via remotely sensed habitat information is adequate in detail and spatial scale, the need for extrapolation models may be removed completely. Use of continuous, remotely sensed habitat data at the watershed scale would provide accurate habitat data that can be used in QRF and similar fish-habitat models, while decreasing costs and potentially removing the need for extrapolation models where remotely sensed data are available.

Habitat rehabilitation groups have requested further guidance on identification of limiting factors for Chinook salmon and steelhead and paths to address those limiting factors. Currently, fish and habitat data metrics used in our QRF models are collected at the reach (200- to 500-meters) scale. However, fish and habitat can be heterogeneous within that scale, and thus, identifying fine-scale (channel unit) fish-habitat relationships within the data can be difficult. Ideally, we would like to better understand fish-habitat relationships within individual channel units (e.g., pools, riffles, runs). Understanding relationships within individual channel units would allow us to identify what characteristics provide a high-capacity pool, riffle, or similar, and further, would provide information on appropriate configuration of channel units to increase habitat capacity. We hope to build QRF models for estimating summer parr rearing capacity at the channel-unit scale, similar to the winter presmolt capacity model we present here. A channel-unit-scale model would help to better translate fish-habitat relationships and allow for a more applicable assessment of restoration evaluation at a finer spatial scale. The channel-unit-scale is closer to the biological patches that fish occupy. Therefore, we hope to collect fish and habitat data at the channel unit scale in the future, and data can be lumped to larger scales if desired. Channel-unit-scale information can be directly applied to restoration design and evaluation and assist engineers and geomorphologists.

Conclusions

In this appendix, we provide estimates (and maps) of contemporary habitat capacity for two species (Chinook salmon, steelhead), three life stages (summer parr, winter juveniles, redds), and eight watersheds in the Upper Salmon River Subbasin. Estimates of available habitat capacity from QRF models can then be compared to estimates of habitat necessary to support ESA delisting goals. Carrying capacity models based on QRF and habitat data, like those presented here, provide managers a framework to guide the identification, prioritization, and development of habitat rehabilitation actions to recover salmon populations. For perhaps the first time, the necessity of tributary habitat restoration actions can be demonstrated, and the magnitude of required change can be placed in context with the other Hs.

Acknowledgements

QRF development efforts have been funded by the Bonneville Power Administration (BPA) through their ISEMP and CHaMP projects and by the Bureau of Reclamation (Reclamation). Fish sampling work in the Lemhi River was also funded through the State of Idaho Office of Species Conservation (OSC) Pacific Coast Salmon Recovery Fund. Redd QRF model development was funded by BPA and through the OSC through a cooperative agreement with Reclamation. Special thanks to staff from the following agencies for providing spatial redd data: Idaho Department of Fish and Game, Nez Perce Tribe Department of Fisheries Resources, Oregon Department of Fish and Wildlife, U.S. Fish and Wildlife Service, and Washington Department of Fish and Wildlife. Special thanks to staff from the following agencies for providing data to calculate juvenile fish abundance and density estimates: Columbia River Inter-Tribal Fish Commission, Oregon Department of Fish and Wildlife, Washington Department of Fish and Wildlife and U.S. Fish and Wildlife Service. The models described in this study were improved by conversations with Eric Buhle.

Literature Cited

Albanese, D., M. Filosi, R. Visintainer, G. Jurman, and C. Furlanello. 2013. Minerva and minepy: a C engine for the MINE suite and its R, Python, and MATLAB wrappers. Bioinformatics. 29(3):407-408.

Carle, F.L. and M.R. Strub. 1978. A new method for estimating population size from removal data. Biometrics. 34:621-630.

CHaMP (Columbia Habitat Monitoring Program). 2016. Scientific protocol for salmonid habitat surveys within the Columbia Habitat Monitoring Program. Prepared by CHaMP for the Bonneville Power Administration. Available at https://www.monitoringresources.org/Document/Protocol/Details/416.

Chapman, D.G. 1951. Some properties of the hypergeometric distribution with applications to zoological sample censuses. University of California Press.

Hedger, R.D., E. De Eyto, M. Dillane., O.H. Diserud, K. Hindar, P. McGinnity, R. Poole, and G. Rogan. 2013. Improving abundance estimates from electrofishing removal sampling. Fisheries Research. 137:104-115.

ISEMP/CHaMP. 2017. Integrated Status and Effectiveness Monitoring Program (ISEMP) and Columbia Habitat Monitoring Program (CHaMP) Annual Combined Technical Report, January – December 2016. BPA Projects 2003-017-00 and 2011-006-00, 93 Electronic Pages.

McNyset, K.M., C.J. Volk, and C.E. Jordan. 2015. Developing an Effective Model for Predicting Spatially and Temporally Continuous Stream Temperatures from Remotely Sensed Land Surface Temperatures. Water. 7:6827-6846.

Meinshausen, N. 2016. quantregForest: Quantile Regression Forests. R package version 1.3-5. https://CRAN.R-project.org/package=quantregForest

Meinshausen, N. 2006. Quantile regression forests. Journal of Machine Learning Research. 7:983-999.

Ogle, D.H, P. Wheeler, and A. Dinno. 2018. FSA: Fisheries Stock Analysis. R package version 0.8.22, https://github.com/droglenc/FSA

NOAA Fisheries. 2017. ESA Recovery Plan for Snake River Spring/Summer Chinook Salmon (*Oncorhynchus tshawytscha*) & Snake River Basin Steelhead (*Oncorhynchus mykiss*). U.S. Department of Commerce. National Oceanic and Atmospheric Administration. National Marine Fisheries Service. West Coast Region. November 2017.

R Core Team. 2015. R: A language and environment for statistical computing. R Foundation for Statistical Computing, Vienna, Austria.

Reshef, D.N., Y.A. Reshef, H.K. Finucane, S.R. Grossman, G. McVean, P.J. Turnbaugh, E.S. Lander, M. Mitzenbacher, and P.C. Sabeti. 2011. Detecting Novel Associations in Large Data Sets. Science. 334:1518-1524.

Rivest, L.P. and S. Baillargeon. 2014. Rcapture: Loglinear models for capture-recapture experiments. R package version 1.4-2.

Robson, D. and H. Regier. 1964. Sample size in Peterson mark-recapture experiments. Transactions of the American Fisheries Society. 93:215-226.

Seber, G. 2002. The estimation of animal abundance and related parameters. Blackburn Press Caldwell, New Jersey.

See, K., M.W. Ackerman, R. Carmichael, B. Lott, and C. Beasley. 2018. Quantile Regression Forest Models to Estimate Habitat Capacity for Spring-Summer Chinook and Steelhead. December 2017 – November 2018, BPA Project 2003-017-00, pp:1-37.

Stekhoven, D.J. 2013. missForest: Nonparametric Missing Value Imputation using Random Forest. R package version 1.4.

Stekhoven, D.J. and P. Buehlmann. 2012. MissForest – non-parametric missing value imputation for mixed-type data. Bioinformatics. 28(1):112-118.

Stevens, D. and A. Olsen. 2004. Spatially balanced sampling of natural resources. Journal of the American Statistical Association. 99:262-278.

Stevens, D.L., Jr., and A.R. Olsen. 1999. Spatially Restricted Surveys Over Time for Aquatic Resources. Journal of Aquatic, Biological, and Environmental Statistics. 4:415-428.

Whittier, T., A. Herlihy, C. Jordan, and C. Volk. 2011. Landscape classification of Pacific Northwest hydrologic units based on natural features and human disturbance to support salmonid research and management. NOAA, National Marine Fisheries Service. NOAA Contract #AB1133F10SE2464. Pp. 39.

This page intentionally left blank.

Supplementary Tables and Figures to Appendix B

Partial Dependence Plots

Chinook salmon

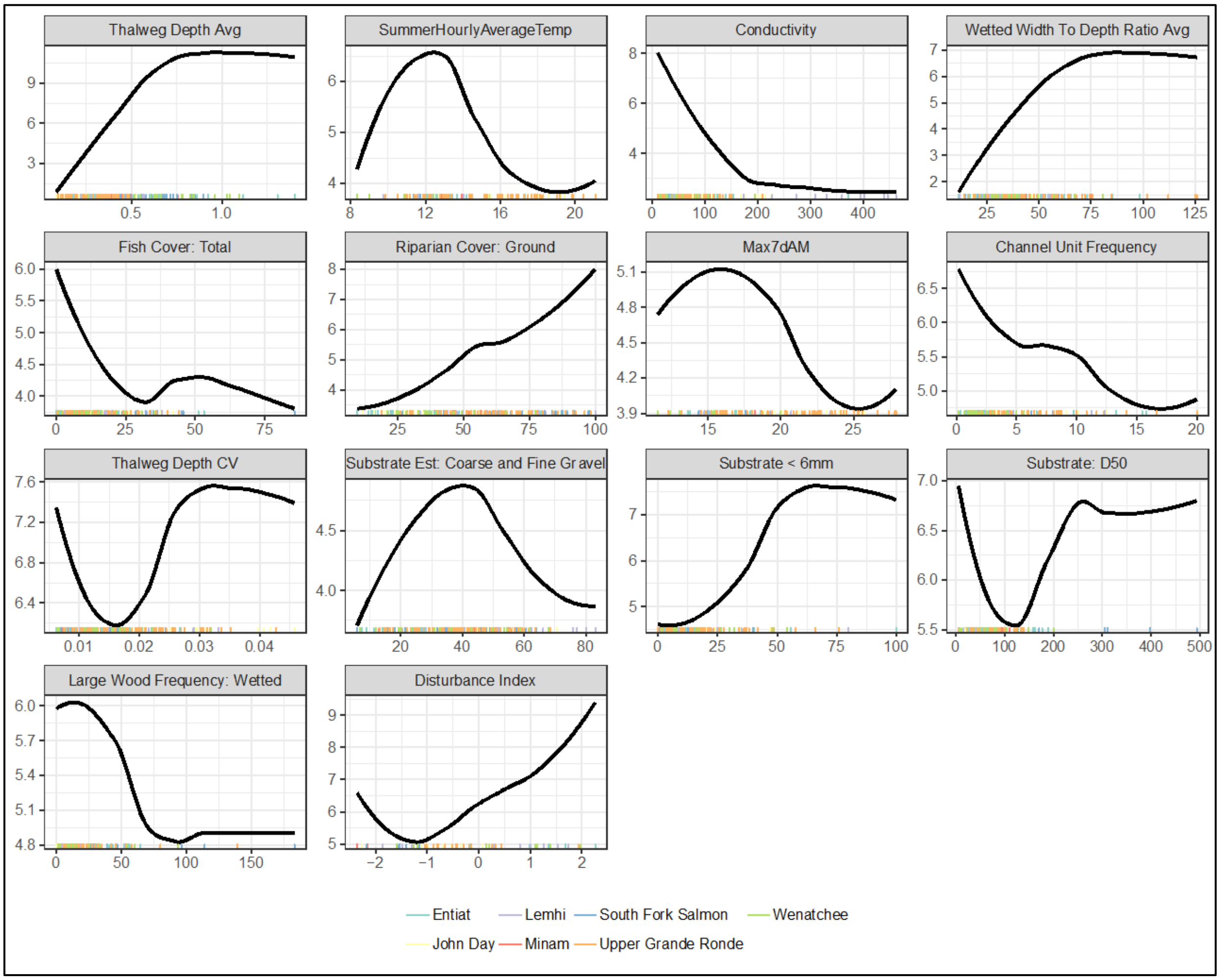

Supplemental Figure B-1. Partial dependence plots from the Chinook salmon parr (summer) capacity quantile regression forest (QRF) model, depicting how parr capacity shifts as each habitat metric changes, assuming all other habitat metrics remain at their mean values. Tick marks along the X-axis depict observed values, and the subbasin they came from.

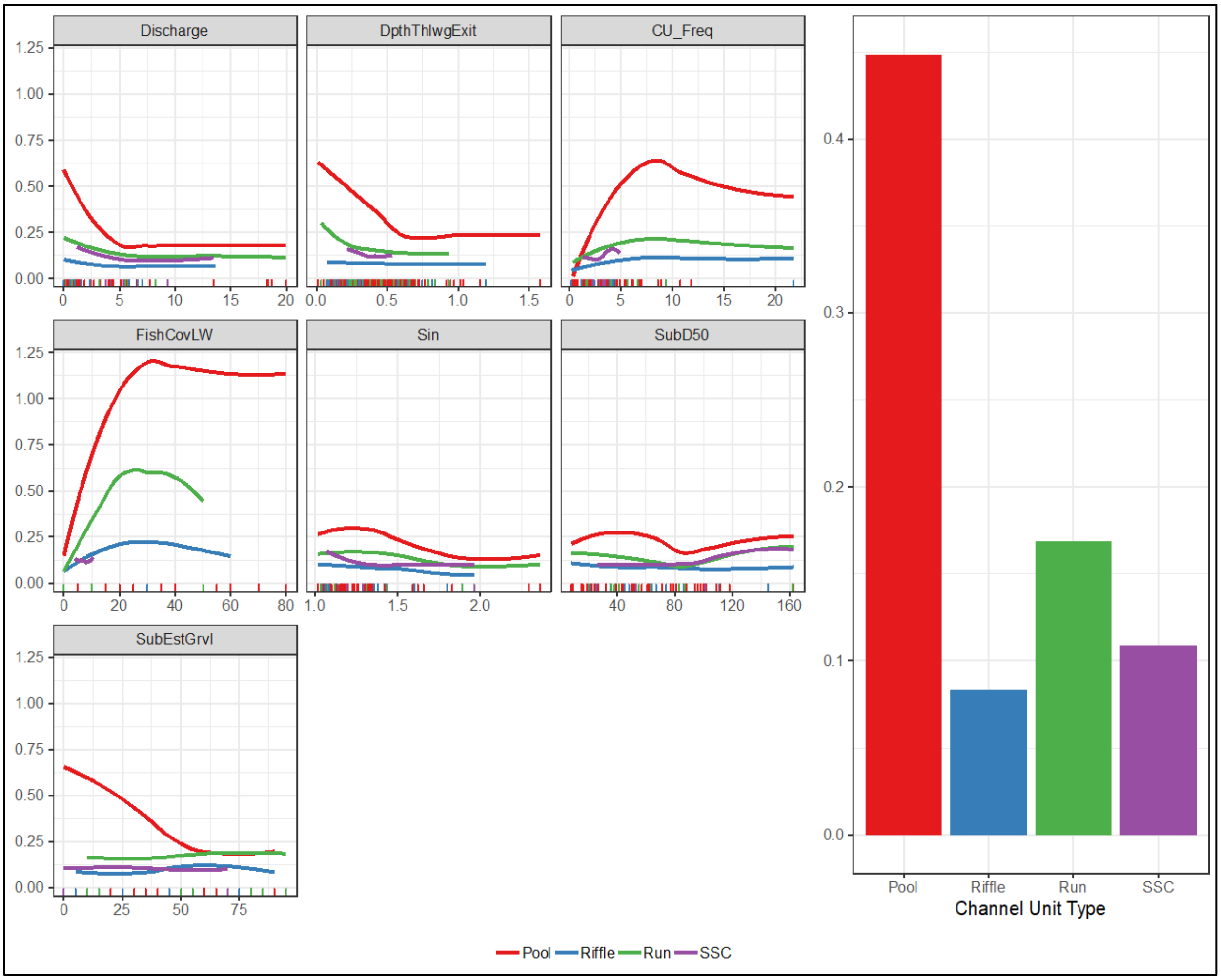

Supplemental Figure B-2. Partial dependence plots from the Chinook salmon parr (winter) capacity quantile regression forest (QRF) model, depicting how parr capacity shifts as each habitat metric changes, assuming all other habitat metrics remain at their mean values. Tick marks along the X-axis depict observed values. Colors correspond to the type of channel unit (pool, riffle, run or small side channel).

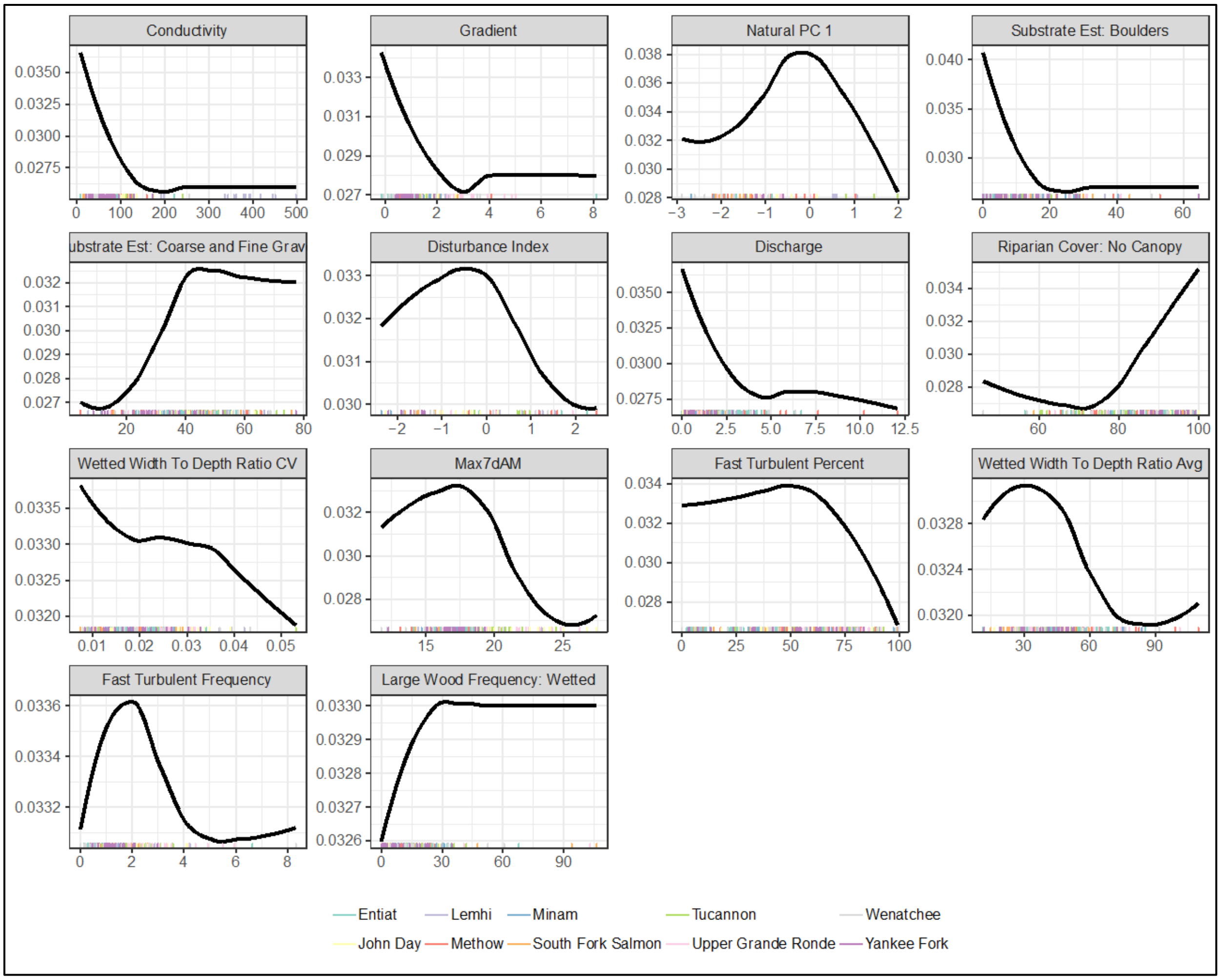

Supplemental Figure B-3. Partial dependence plots from the Chinook salmon redd capacity quantile regression forest (QRF) model, depicting how redd capacity shifts as each habitat metric changes, assuming all other habitat metrics remain at their mean values. Tick marks along the X-axis depict observed values, and the subbasin they came from.

Steelhead

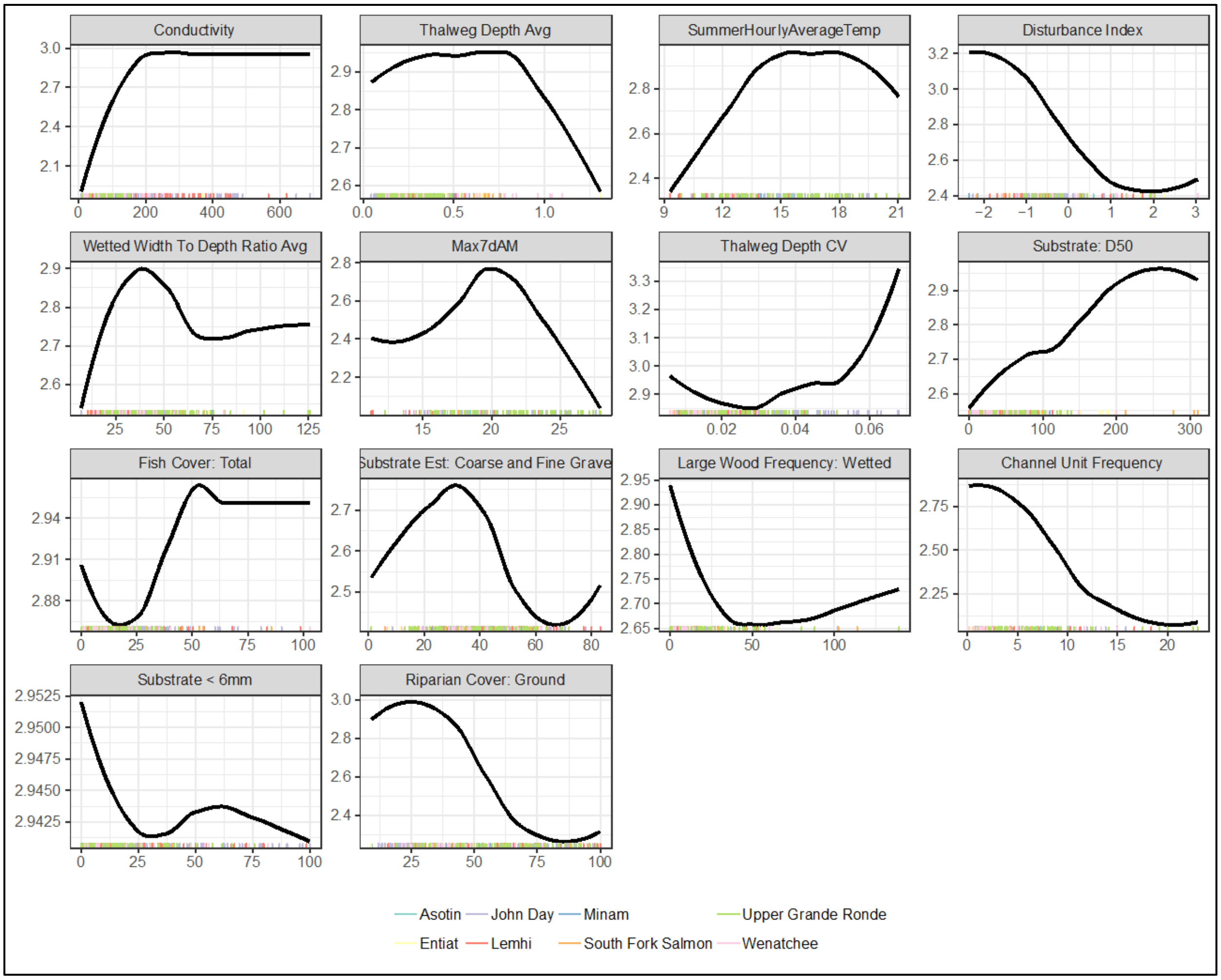

Supplemental Figure B-4. Partial dependence plots from the steelhead juvenile (summer) capacity quantile regression forest (QRF) model, depicting how juvenile capacity shifts as each habitat metric changes, assuming all other habitat metrics remain at their mean values. Tick marks along the X-axis depict observed values, and the subbasin they came from.

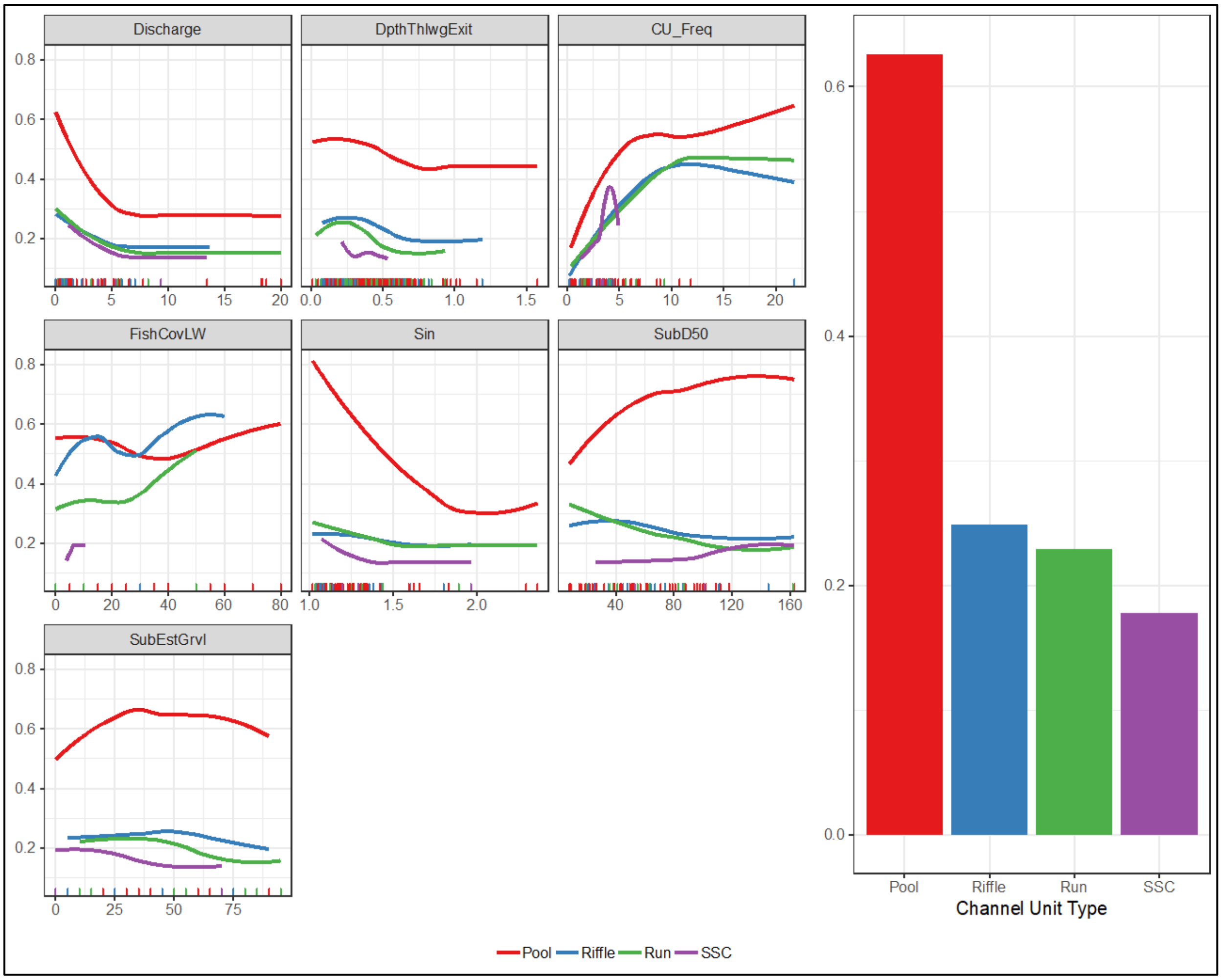

Supplemental Figure B-5. Partial dependence plots from the steelhead juvenile (winter) capacity quantile regression forest (QRF) model, depicting how juvenile capacity shifts as each habitat metric changes, assuming all other habitat metrics remain at their mean values. Tick marks along the X-axis depict observed values. Colors correspond to the type of channel unit (pool, riffle, run or small side channel).

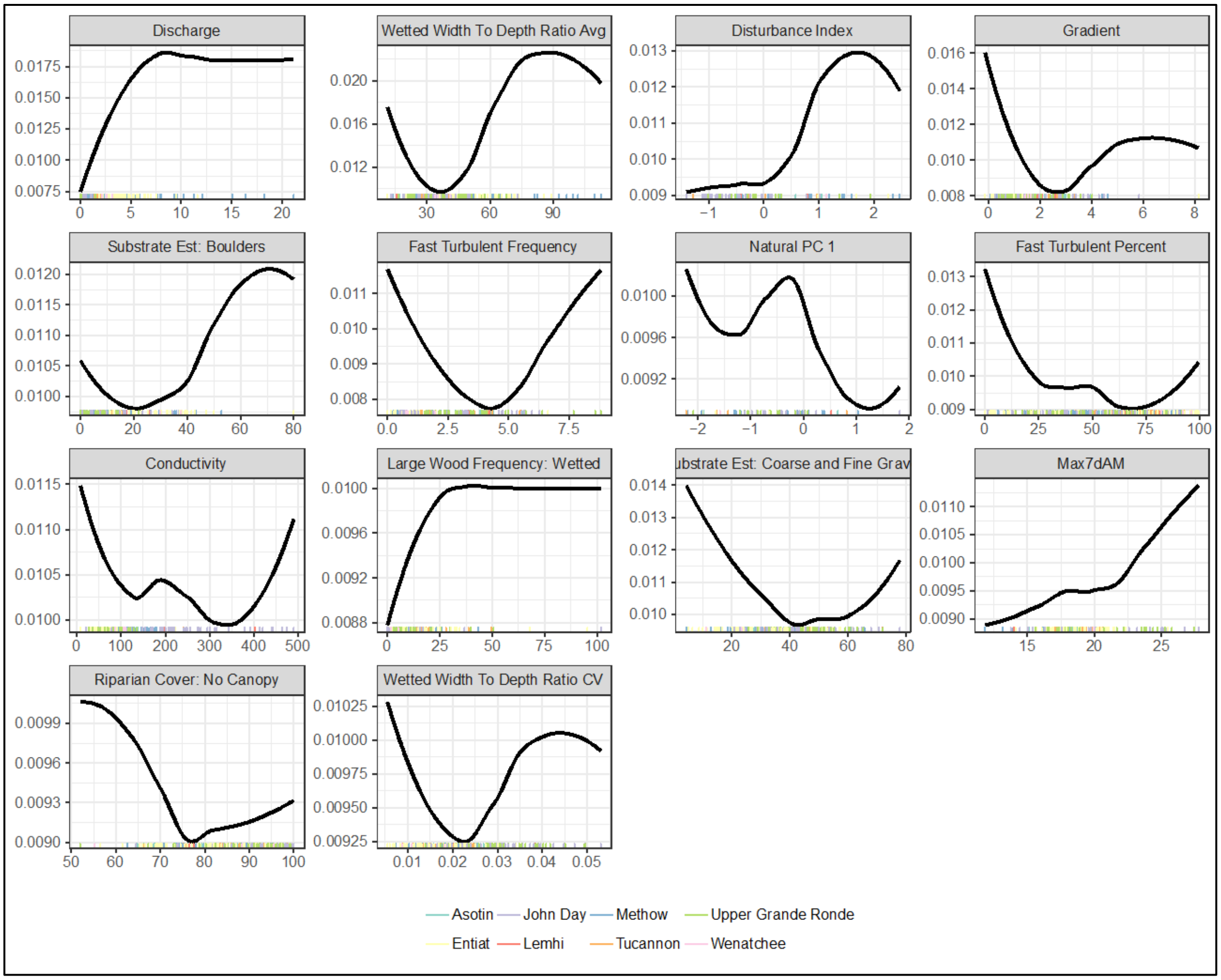

Supplemental Figure B-6. Partial dependence plots from the steelhead redd capacity quantile regression forest (QRF) model, depicting how redd capacity shifts as each habitat metric changes, assuming all other habitat metrics remain at their mean values. Tick marks along the X-axis depict observed values, and the subbasin they came from.

Habitat Capacity Estimates

Chinook salmon

Supplemental Table B-1. Estimates of total Chinook salmon summer parr, overwintering parr, and redd capacity for the Upper Salmon River, with standard error (SE).

Stream	Stream length		Summer Parr		Winter Parr		Redd	
	km	mi	Capacity	SE	Capacity	SE	Capacity	SE
Alpine Creek	1.6	1.0	7,474	1,461	1,854	244	44	2
Alturas Lake Creek	17.4	10.8	61,223	10,516	23,051	3,555	618	36
Beaver Creek	10.2	6.4	46,018	9,423	12,762	1,730	281	11
Champion Creek	7.3	4.5	11,026	2,848	7,890	1,122	185	10
Decker Creek	0.9	0.6	1,142	423	631	132	22	1
Fisher Creek	6.2	3.9	7,233	2,566	6,524	985	155	9
Fishhook Creek	5.7	3.5	26,636	5,359	6,146	1,007	145	7
Fourth of July Creek	12.5	7.7	20,123	5,533	13,273	1,962	337	17
Frenchman Creek	5.4	3.4	24,055	5,007	6,692	914	150	6
Gold Creek	1.7	1.1	7,145	1,597	1,749	295	44	2
Hell Roaring Creek	8.3	5.2	39,280	7,917	9,648	1,475	221	10
Huckleberry Creek	2.9	1.8	13,007	2,703	3,305	524	73	3
Pettit Lake Creek	2.2	1.3	9,859	2,042	2,395	366	60	2
Pole Creek	10.5	6.5	47,350	9,747	12,503	1,697	279	12
Redfish Lake Creek	4.1	2.6	14,945	2,604	4,762	859	138	9
Salmon River	59.3	36.8	265,251	24,534	75,726	10,895	1,438	85
Smiley Creek	14.7	9.1	66,076	13,551	18,038	2,364	404	16
Vat Creek	1.1	0.7	4,817	1,024	1,164	189	30	1
Williams Creek	4.5	2.8	18,275	4,131	4,609	744	113	5
Yellowbelly Creek	6.6	4.1	30,938	6,117	8,117	1,073	172	7
Total	**183.1**	**113.8**	**721,873**	**119,101**	**220,838**	**12,488**	**4,909**	**250**

Supplemental Table B-2. Estimates of total Chinook salmon summer parr, overwintering parr, and redd capacity for Valley Creek, with standard error (SE).

Stream	Stream length		Summer Parr		Winter Parr		Redd	
	km	mi	Capacity	SE	Capacity	SE	Capacity	SE
Crooked Creek	2.4	1.5	9,851	2,161	2,629	389	60	3
East Fork Valley Creek	1.8	1.1	8,125	1,707	2,003	283	47	2
Elk Creek	9.8	6.1	45,978	9,306	12,659	1,769	244	12
Goat Creek	3.1	1.9	12,741	2,855	2,979	514	76	4
Iron Creek	3.6	2.2	15,346	3,297	3,832	605	89	4
Job Creek	2.3	1.4	5,427	1,602	1,796	381	57	3

Stream	Stream length		Summer Parr		Winter Parr		Redd	
	km	mi	Capacity	SE	Capacity	SE	Capacity	SE
Meadow Creek	7.0	4.3	30,964	6,422	8,772	1,184	173	8
Park Creek	2.9	1.8	2,571	1,229	2,631	462	68	4
Stanley Creek	3.2	2.0	13,286	2,887	4,044	596	78	4
Stanley Lake Creek	4.9	3.0	22,357	4,558	6,244	832	122	6
Valley Creek	40.5	25.2	142,654	25,815	49,859	7,853	1,197	71
Total	**81.5**	**50.5**	**309,300**	**61,840**	**97,449**	**8,275**	**2,211**	**121**

Supplemental Table B-3. Estimates of total Chinook salmon summer parr, overwintering parr, and redd capacity for the Yankee Fork Salmon River, with standard error (SE).

Stream	Stream length		Summer Parr		Winter Parr		Redd	
	km	mi	Capacity	SE	Capacity	SE	Capacity	SE
Cabin Creek	2.8	1.7	5,626	1,772	2,912	501	63	5
Eightmile Creek	3.3	2.1	14,655	3,289	4,743	688	79	5
Elevenmile Creek	1.2	0.7	440	539	689	160	28	2
Fivemile Creek	1.9	1.2	4,082	1,167	1,486	259	42	3
Jordan Creek	4.0	2.5	9,684	2,488	3,813	627	89	7
Lightning Creek	5.0	3.1	10,605	3,263	4,840	732	111	9
McKay Creek	1.9	1.2	3,463	1,165	2,544	449	43	3
Ninemile Creek	1.5	0.9	318	797	574	174	35	3
Sevenmile Creek	1.0	0.6	576	522	419	123	25	2
Sixmile Creek	2.1	1.3	1,821	1,001	1,432	252	49	3
Tenmile Creek	2.1	1.3	3,723	1,348	1,813	413	50	4
West Fork Yankee Fork	16.4	10.2	58,308	11,213	20,956	2,855	376	26
Yankee Fork	42.2	26.2	161,831	27,286	56,609	8,478	954	68
Total	**85.4**	**53.0**	**275,132**	**55,850**	**102,830**	**9,069**	**1,944**	**140**

Supplemental Table B-4. Estimates of total Chinook salmon summer parr, overwintering parr, and redd capacity for the East Fork Salmon River, with standard error (SE).

Stream	Stream length		Summer Parr		Winter Parr		Redd	
	km	mi	Capacity	SE	Capacity	SE	Capacity	SE
Big Boulder Creek	8.2	5.1	16,629	6,767	7,260	1,216	210	11
Big Lake Creek	2.6	1.6	4,179	1,064	2,148	370	62	3
East Fork Herd Creek	3.7	2.3	5,403	1,648	2,890	514	92	5
East Fork Salmon River	59.1	36.7	301,555	19,510	78,875	13,118	1,385	84
East Pass Creek	14.3	8.9	23,977	5,783	13,942	2,236	369	19
Germania Creek	7.8	4.8	34,673	3,235	7,422	1,135	197	9
Herd Creek	15.3	9.5	67,829	6,106	18,892	3,038	341	20
Lake Creek	2.3	1.4	6,752	1,495	2,291	345	57	3

Stream	Stream length		Summer Parr		Winter Parr		Redd	
	km	mi	Capacity	SE	Capacity	SE	Capacity	SE
South Fork East Fork Salmon River	3.3	2.0	5,647	1,319	3,467	571	87	5
Taylor Creek	2.3	1.4	2,603	1,704	1,196	229	56	3
West Fork East Fork Salmon River	1.8	1.1	2,967	1,397	1,149	199	47	3
West Fork Herd Creek	3.4	2.1	5,312	1,339	3,303	522	86	5
West Pass Creek	10.0	6.2	17,338	4,112	9,404	1,521	259	14
Total	**134.1**	**83.1**	**494,864**	**55,479**	**152,240**	**13,878**	**3,248**	**184**

Supplemental Table B-5. Estimates of total Chinook salmon summer parr, overwintering parr, and redd capacity for the Pahsimeroi River, with standard error (SE).

Stream	Stream length		Summer Parr		Winter Parr		Redd	
	km	mi	Capacity	SE	Capacity	SE	Capacity	SE
Pahsimeroi River	37.5	23.3	173,435	13,803	52,332	7,773	668	49
Patterson Creek	30.2	18.8	104,074	19,318	36,493	7,521	863	72
PattersonSideChannel1	8.3	5.2	26,506	5,631	10,029	2,325	241	21
Sulphur Creek	5.5	3.4	7,515	2,300	5,123	999	114	9
Pahsimeroi River	37.5	23.3	173,435	13,803	52,332	7,773	668	49
Total	**81.5**	**50.7**	**311,530**	**41,052**	**103,977**	**11,108**	**1,886**	**151**

Supplemental Table B-6. Estimates of total Chinook salmon summer parr, overwintering parr, and redd capacity for the Lemhi River, with standard error (SE).

Stream	Stream length		Summer Parr		Winter Parr		Redd	
	km	mi	Capacity	SE	Capacity	SE	Capacity	SE
Bear Valley Creek	2.3	1.4	0	0	1,897	449	55	5
Big Eightmile Creek	0.9	0.6	0	0	653	170	20	2
Big Springs Creek	6.8	4.2	15,159	4,293	5,381	1,308	156	9
Big TImber Creek	2.0	1.2	11,012	0	1,886	180	66	0
Bohannon Creek	1.4	0.9	3,950	892	789	121	30	2
Canyon Creek	6.2	3.9	17,946	4,281	5,054	1,045	144	9
Hayden Creek	19.9	12.3	24,123	11,789	21,518	3,331	422	36
Kenney Creek	1.5	0.9	3,176	0	1,533	170	39	0
Lemhi River	99.8	62.0	265,739	47,828	127,672	18,574	2,097	163
Little Springs Creek	5.0	3.1	13,323	2,209	4,510	742	106	8
Wimpey Creek	2.8	1.7	3,520	1,282	2,484	403	57	5
Total	**148.6**	**92.2**	**357,948**	**74,837**	**173,375**	**18,971**	**3,192**	**239**

Supplemental Table B-7. Estimates of total Chinook salmon summer parr, overwintering parr, and redd capacity for the North Fork Salmon River, with standard error (SE).

Stream	Stream length		Summer Parr		Winter Parr		Redd	
	km	mi	Capacity	SE	Capacity	SE	Capacity	SE
Dahlonega Creek	4.0	2.5	6,089	1,544	4,418	640	94	5
Hughes Creek	4.8	3.0	17,425	2,824	4,930	750	100	8
Hull Creek	2.1	1.3	2,891	921	1,593	291	44	3
Moose Creek	5.4	3.4	4,888	4,191	3,407	665	130	7
North Fork Salmon River	39.9	24.8	152,269	14,473	38,545	5,178	868	51
Sheep Creek	10.9	6.8	18,644	4,613	9,784	1,594	263	15
Twin Creek	2.5	1.5	4,218	1,917	1,531	266	53	3
Total	**69.6**	**43.3**	**206,424**	**30,483**	**64,209**	**5,561**	**1,552**	**93**

Supplemental Table B-8. Estimates of total Chinook salmon summer parr, overwintering parr, and redd capacity for Panther Creek, with standard error (SE).

Stream	Stream length		Summer Parr		Winter Parr		Redd	
	km	mi	Capacity	SE	Capacity	SE	Capacity	SE
Big Deer Creek	9.2	5.7	44,878	8,819	8,906	1,539	206	12
Blackbird Creek	3.5	2.2	4,632	2,230	3,259	557	80	5
Clear Creek	10.7	6.7	44,396	5,415	10,223	1,760	198	16
Moyer Creek	5.3	3.3	8,146	2,080	4,787	777	125	7
Musgrove Creek	9.8	6.1	44,242	8,969	10,130	1,608	229	11
Napias Creek	2.1	1.3	8,964	1,117	1,516	343	46	3
Panther Creek	66.4	41.3	284,387	26,699	78,552	10,734	1,434	86
Total	**107.0**	**66.6**	**439,645**	**55,329**	**117,372**	**11,150**	**2,318**	**141**

Steelhead

Supplemental Table B-9. Estimates of total Steelhead summer parr, overwintering parr, and redd capacity for the Upper Salmon River, with standard error (SE).

Stream	Stream length		Summer Parr		Winter Parr		Redd	
	km	mi	Capacity	SE	Capacity	SE	Capacity	SE
Alpine Creek	1.6	1.0	3,140	241	4,108	205	19	1
Alturas Lake Creek	17.4	10.8	47,811	8,719	40,100	4,701	259	16
Beaver Creek	6.6	4.1	13,593	959	17,597	1,015	79	4
Champion Creek	10.6	6.6	23,881	2,089	26,742	1,523	120	7
Decker Creek	0.9	0.6	2,093	212	1,941	168	8	1
Fisher Creek	7.9	4.9	18,052	1,896	18,708	1,048	77	6
Fishhook Creek	5.7	3.5	12,422	968	14,797	1,408	70	4
Fourth of July Creek	13.4	8.3	28,671	2,674	33,070	1,954	137	9
Frenchman Creek	5.4	3.4	10,882	785	14,390	853	63	3
Gold Creek	1.7	1.1	4,069	328	4,190	281	21	1
Hell Roaring Creek	5.8	3.6	12,532	924	15,597	1,253	71	4
Huckleberry Creek	2.9	1.8	6,394	459	8,353	613	35	2
Mays Creek	3.0	1.9	6,672	490	7,622	722	31	2
Pettit Lake Creek	2.2	1.3	4,391	344	5,233	300	26	2
Pole Creek	14.1	8.7	29,831	2,122	36,609	2,217	174	9
Redfish Lake Creek	3.8	2.4	11,387	2,036	8,107	1,328	60	4
Salmon River	61.0	37.9	166,401	11,013	137,274	12,399	846	42
Smiley Creek	11.8	7.3	24,214	1,707	30,209	1,931	143	7
Twin Creek	1.4	0.9	3,060	273	2,974	286	17	1
Vat Creek	3.0	1.9	6,325	431	7,598	550	35	2
Warm Creek	2.0	1.2	4,315	328	5,192	299	24	1
Williams Creek	6.5	4.0	15,217	1,237	15,043	1,124	78	5
Yellowbelly Creek	6.6	4.1	14,656	981	17,749	1,035	82	4
Total	**195.3**	**121.3**	**470,009**	**41,217**	**473,201**	**14,239**	**2,475**	**137**

Supplemental Table B-10. Estimates of total Steelhead summer parr, overwintering parr, and redd capacity for Valley Creek, with standard error (SE).

Stream	Stream length		Summer Parr		Winter Parr		Redd	
	km	mi	Capacity	SE	Capacity	SE	Capacity	SE
Crooked Creek	2.4	1.5	5,519	443	5,960	368	29	2
East Fork Valley Creek	1.8	1.1	4,219	306	4,739	262	23	1
Elk Creek	9.8	6.1	22,452	1,671	28,287	2,143	124	7
Goat Creek	6.2	3.8	14,729	1,245	14,238	1,598	75	5
Iron Creek	5.1	3.2	12,187	1,162	12,334	769	57	4
Job Creek	2.3	1.4	5,415	529	4,889	370	24	2

Stream	Stream length		Summer Parr		Winter Parr		Redd	
	km	mi	Capacity	SE	Capacity	SE	Capacity	SE
Meadow Creek	12.2	7.6	28,302	2,188	30,331	1,807	148	9
Park Creek	2.9	1.8	7,010	789	6,589	436	27	3
Stanley Creek	7.0	4.4	17,026	1,482	18,700	1,262	87	6
Stanley Lake Creek	4.9	3.0	11,499	851	13,615	753	63	3
Trap Creek	4.8	3.0	11,078	788	13,041	734	59	3
Valley Creek	40.5	25.2	106,860	15,970	93,125	9,418	578	33
Total	**99.9**	**62.1**	**246,296**	**27,424**	**245,849**	**10,146**	**1,294**	**77**

Supplemental Table B-11. Estimates of total Steelhead summer parr, overwintering parr, and redd capacity for the Yankee Fork Salmon River, with standard error (SE).

Stream	Stream length		Summer Parr		Winter Parr		Redd	
	km	mi	Capacity	SE	Capacity	SE	Capacity	SE
Cabin Creek	2.8	1.7	7,021	447	7,589	597	30	3
Deadwood Creek	2.6	1.6	6,622	395	5,744	741	28	2
Eightmile Creek	3.3	2.1	7,889	536	9,521	502	43	3
Elevenmile Creek	2.5	1.5	5,457	391	5,056	553	27	2
Fivemile Creek	5.2	3.3	12,630	784	11,497	1,013	56	4
Jordan Creek	6.6	4.1	17,038	1,057	16,484	1,188	71	7
Lightning Creek	5.8	3.6	14,565	909	15,188	1,129	63	6
McKay Creek	2.9	1.8	6,402	522	7,989	685	33	4
Ninemile Creek	1.5	0.9	3,218	258	2,559	285	16	1
Ramey Creek	3.8	2.3	9,733	611	8,788	593	40	4
Sawmill Creek	1.5	0.9	3,875	248	2,886	409	16	1
Sevenmile Creek	1.0	0.6	2,367	177	1,797	217	11	1
Sixmile Creek	3.2	2.0	7,723	484	6,895	669	34	3
Tenmile Creek	3.8	2.4	8,755	603	9,517	874	48	4
Twelvemile Creek	2.6	1.6	5,560	436	6,066	656	30	2
West Fork Yankee Fork	16.1	10.0	42,932	2,608	42,540	3,844	204	15
Yankee Fork	44.0	27.3	113,388	7,356	107,459	9,341	558	45
Unnamed	2.1	1.3	4,467	392	4,483	530	24	2
Total	**111.3**	**69.0**	**279,642**	**18,213**	**272,057**	**10,499**	**1,332**	**109**

Supplemental Table B-12. Estimates of total Steelhead summer parr, overwintering parr, and redd capacity for the East Fork Salmon River, with standard error (SE).

Stream	Stream length		Summer Parr		Winter Parr		Redd	
	km	mi	Capacity	SE	Capacity	SE	Capacity	SE
Big Boulder Creek	8.2	5.1	16,979	1,511	19,243	2,020	91	6
Big Lake Creek	2.6	1.6	6,078	596	6,071	592	25	2
East Fork Herd Creek	3.7	2.3	8,631	872	8,608	844	36	3

Stream	Stream length		Summer Parr		Winter Parr		Redd	
	km	mi	Capacity	SE	Capacity	SE	Capacity	SE
East Fork Salmon River	59.1	36.7	157,910	8,695	138,357	18,229	804	39
East Pass Creek	14.3	8.9	31,448	2,954	35,407	3,096	140	10
Germania Creek	7.8	4.8	18,999	1,331	16,041	1,863	73	6
Herd Creek	15.3	9.5	41,657	2,586	37,722	4,513	188	10
Lake Creek	5.8	3.6	13,315	942	13,548	913	66	4
Little Boulder Creek	5.5	3.4	10,740	1,396	11,882	2,158	73	5
McDonald Creek	2.2	1.3	4,689	347	4,765	496	23	1
Pine Creek	0.8	0.5	1,656	124	1,750	184	8	1
Road Creek	2.6	1.6	7,733	612	5,992	568	31	2
South Fork East Fork Salmon River	3.3	2.0	6,917	712	8,331	814	33	3
Taylor Creek	5.3	3.3	10,699	837	10,520	1,497	54	3
West Fork East Fork Salmon River	1.8	1.1	3,450	286	3,916	427	20	1
West Fork Herd Creek	3.4	2.1	7,739	764	8,442	748	33	2
West Pass Creek	10.0	6.2	21,548	2,142	24,443	2,310	101	7
Total	**151.7**	**94.0**	**370,188**	**26,708**	**355,039**	**19,645**	**1,799**	**106**

Supplemental Table B-13. Estimates of total Steelhead summer parr, overwintering parr, and redd capacity for the Pahsimeroi River, with standard error (SE).

Stream	Stream length		Summer Parr		Winter Parr		Redd	
	km	mi	Capacity	SE	Capacity	SE	Capacity	SE
Pahsimeroi River	37.5	23.3	120,049	7,953	76,645	7,610	556	26
Patterson Creek	30.2	18.8	101,791	17,108	62,729	9,019	484	29
Patterson Side Channel	8.3	5.2	28,107	5,022	14,806	2,918	133	9
Sulphur Creek	5.5	3.4	14,793	1,125	12,756	822	55	4
Total	**81.5**	**50.7**	**264,740**	**31,209**	**166,936**	**12,184**	**1,228**	**69**

Supplemental Table B-14. Estimates of total Steelhead summer parr, overwintering parr, and redd capacity for the Lemhi River, with standard error (SE).

Stream	Stream length		Summer Parr		Winter Parr		Redd	
	km	mi	Capacity	SE	Capacity	SE	Capacity	SE
Agency Creek	14.4	8.9	40,302	4,670	39,807	1,699	171	12
Bear Valley Creek	6.2	3.8	14,615	1,735	14,354	971	66	6
Big Eightmile Creek	11.5	7.1	32,723	3,790	29,809	1,745	120	10
Big Springs Creek	6.8	4.2	20,428	2,442	17,594	1,470	80	6
Big Timber Creek	22.7	14.1	63,252	7,490	56,256	4,039	273	20
Bohannon Creek	12.2	7.6	34,454	4,054	24,230	1,786	129	10
Canyon Creek	17.9	11.1	49,159	6,750	40,720	3,079	221	15

Stream	Stream length		Summer Parr		Winter Parr		Redd	
	km	mi	Capacity	SE	Capacity	SE	Capacity	SE
Cruikshank Creek	2.2	1.3	5,388	646	4,388	210	22	2
East Fork Bohannon Creek	2.7	1.7	7,602	981	3,760	305	25	3
Eighteenmile Creek	4.4	2.7	13,385	2,118	7,245	738	68	5
Hawley Creek	17.4	10.8	47,711	5,744	41,928	2,919	216	15
Hayden Creek	19.9	12.3	52,785	6,256	43,626	3,290	219	19
Kenney Creek	8.7	5.4	24,784	2,877	20,388	999	90	7
Lemhi River	99.8	62.0	295,988	32,307	211,151	17,965	1,572	79
Pratt Creek	7.0	4.3	19,331	2,308	13,981	1,128	75	7
Reservoir Creek	1.5	0.9	3,508	437	1,876	0	15	1
Wimpey Creek	5.7	3.5	16,179	1,878	12,328	802	63	5
Total	**261.0**	**161.7**	**741,594**	**86,484**	**583,442**	**19,588**	**3,425**	**222**

Supplemental Table B-15. Estimates of total Steelhead summer parr, overwintering parr, and redd capacity for the North Fork Salmon River, with standard error (SE).

Stream	Stream length		Summer Parr		Winter Parr		Redd	
	km	mi	Capacity	SE	Capacity	SE	Capacity	SE
Anderson Creek	2.5	1.6	6,201	608	5,553	363	23	2
Dahlonega Creek	8.4	5.2	20,131	1,997	20,586	1,376	85	6
Hughes Creek	7.8	4.8	19,616	1,589	18,558	1,271	79	5
Hull Creek	4.2	2.6	10,856	923	9,272	666	41	3
Moose Creek	2.4	1.5	5,094	389	4,560	421	25	2
North Fork Salmon River	39.9	24.8	110,778	7,549	83,526	6,753	421	27
Pierce Creek	2.7	1.7	6,576	559	5,986	306	26	2
Sheep Creek	10.9	6.8	26,445	2,791	25,416	1,996	115	9
Twin Creek	5.7	3.6	12,688	952	12,715	1,395	63	4
Total	**84.5**	**52.6**	**218,385**	**17,356**	**186,170**	**7,476**	**878**	**60**

Supplemental Table B-16. Estimates of total Steelhead summer parr, overwintering parr, and redd capacity for Panther Creek, with standard error (SE).

Stream	Stream length		Summer Parr		Winter Parr		Redd	
	km	mi	Capacity	SE	Capacity	SE	Capacity	SE
Beaver Creek	2.8	1.8	7,274	556	6,421	576	34	2
Big Deer Creek	12.3	7.6	31,433	2,535	30,537	2,390	159	9
Blackbird Creek	3.5	2.2	8,768	776	8,498	644	38	3
Clear Creek	17.9	11.2	49,104	5,015	41,188	4,453	197	16
Deep Creek	4.0	2.5	9,002	743	9,009	877	46	3
Garden Creek	6.9	4.3	18,128	2,202	13,571	2,264	89	8
Moyer Creek	8.4	5.2	20,053	1,994	19,568	1,350	87	6
Musgrove Creek	4.1	2.6	10,074	709	10,195	684	52	3
Napias Creek	7.7	4.8	21,836	1,664	14,380	1,343	76	7
Panther Creek	66.4	41.3	186,821	13,609	154,660	13,136	791	54

Stream	Stream length		Summer Parr		Winter Parr		Redd	
	km	mi	Capacity	SE	Capacity	SE	Capacity	SE
Trail Creek	5.2	3.3	12,822	1,041	10,854	1,548	59	4
Woodtick Creek	2.2	1.4	5,279	500	4,825	418	23	2
Total	**141.4**	**88.2**	**380,594**	**31,344**	**323,705**	**14,540**	**1,651**	**117**

Habitat Capacity Maps

Chinook salmon

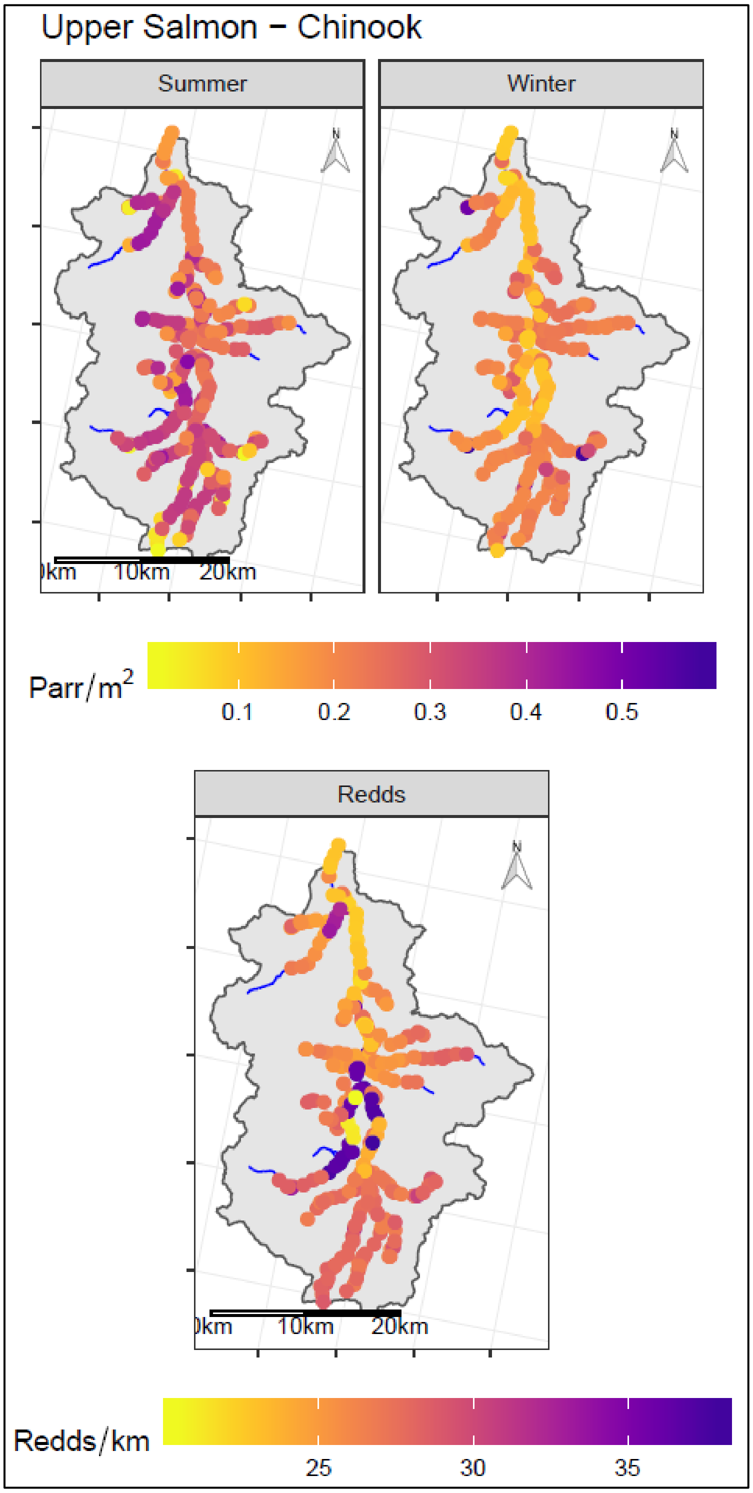

Supplemental Figure B-7. Map showing predictions of Chinook salmon carrying capacity for three life stages (summer juveniles, winter juveniles, redds) at master sample points in the Upper Salmon River.

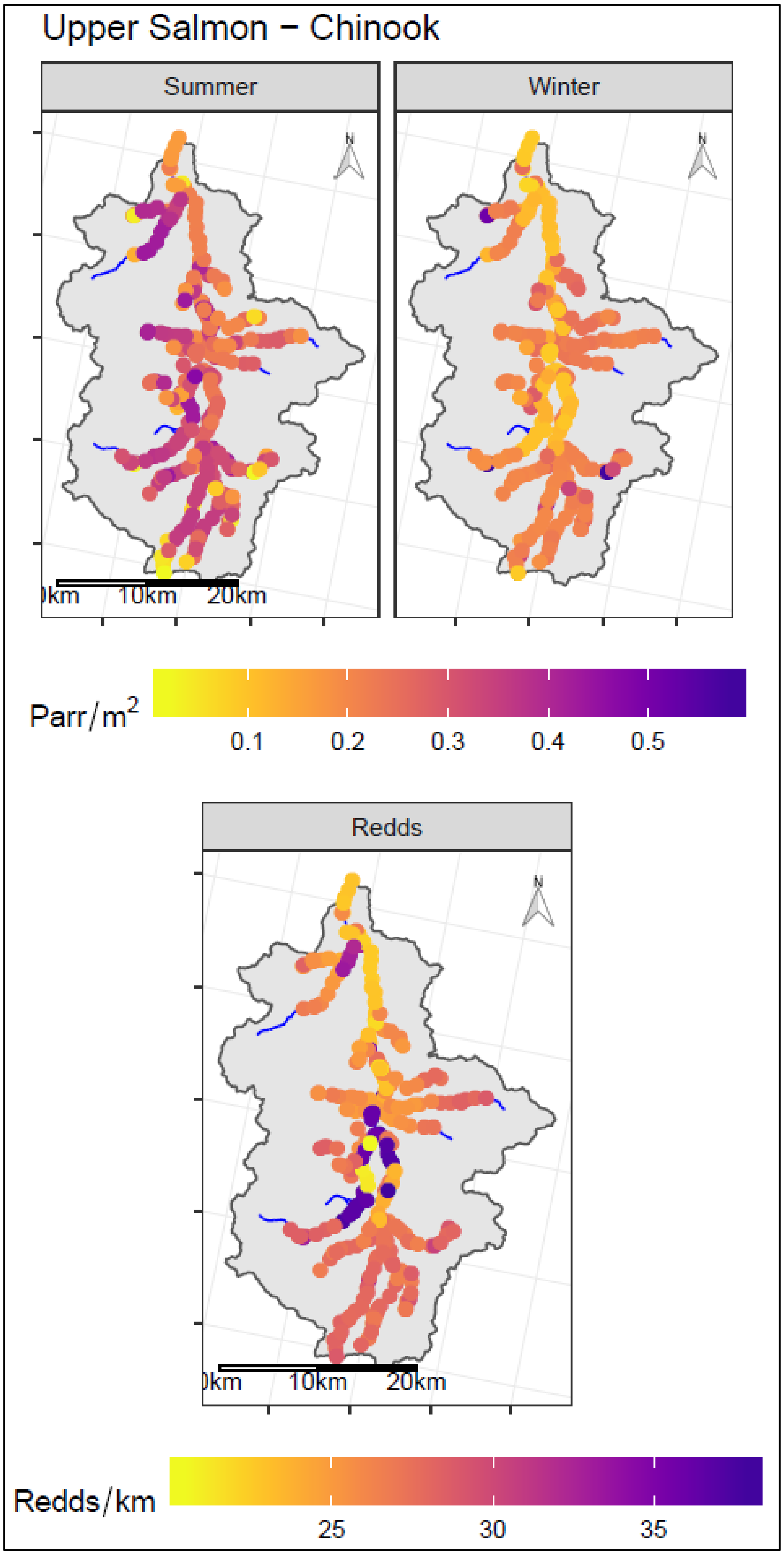

Supplemental Figure B-8. Map showing predictions of Chinook salmon carrying capacity for three life stages (summer juveniles, winter juveniles, redds) at master sample points in the Upper Salmon River.

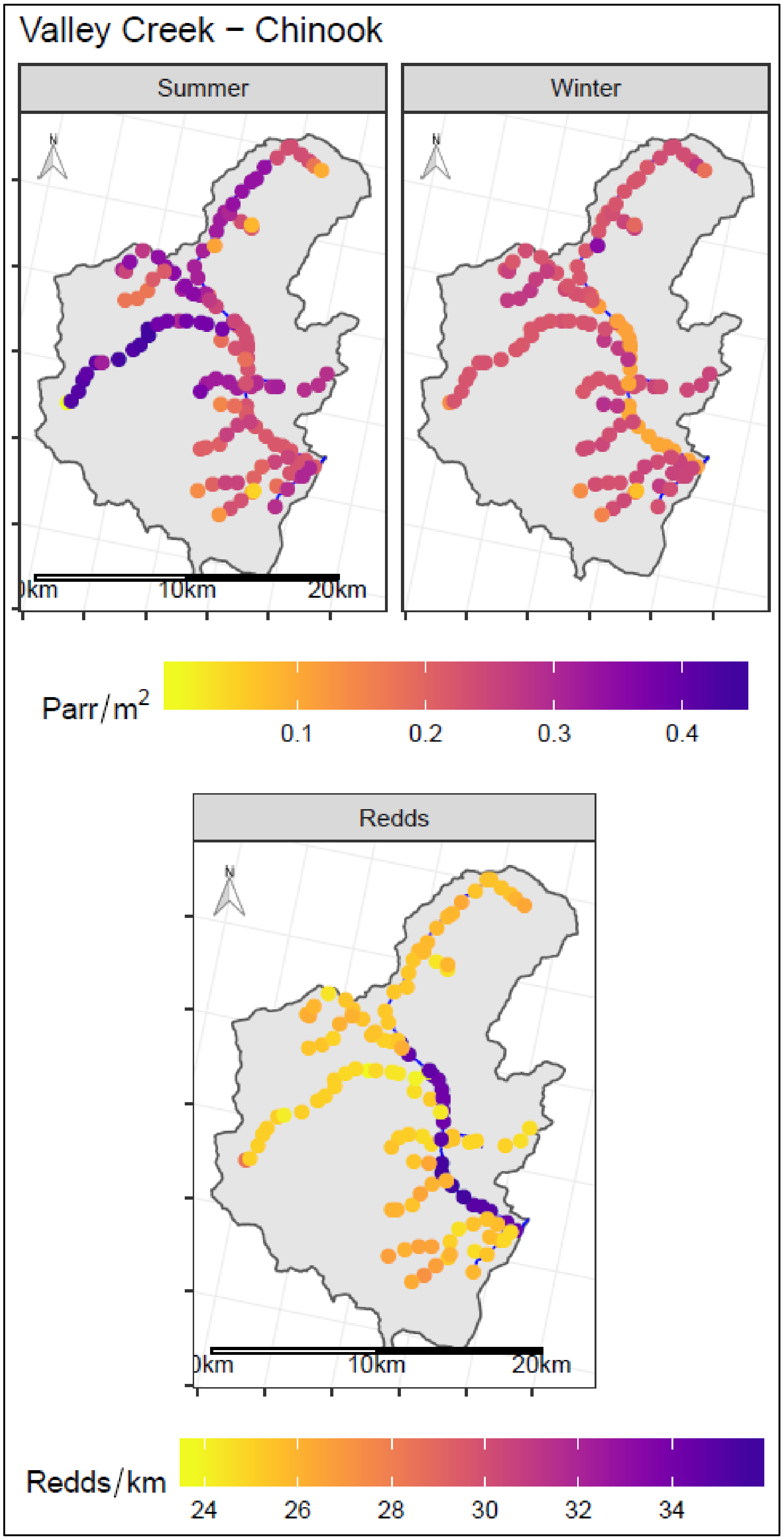

Supplemental Figure B-9. Map showing predictions of Chinook salmon carrying capacity for three life stages (summer juveniles, winter juveniles, redds) at master sample points in Valley Creek.

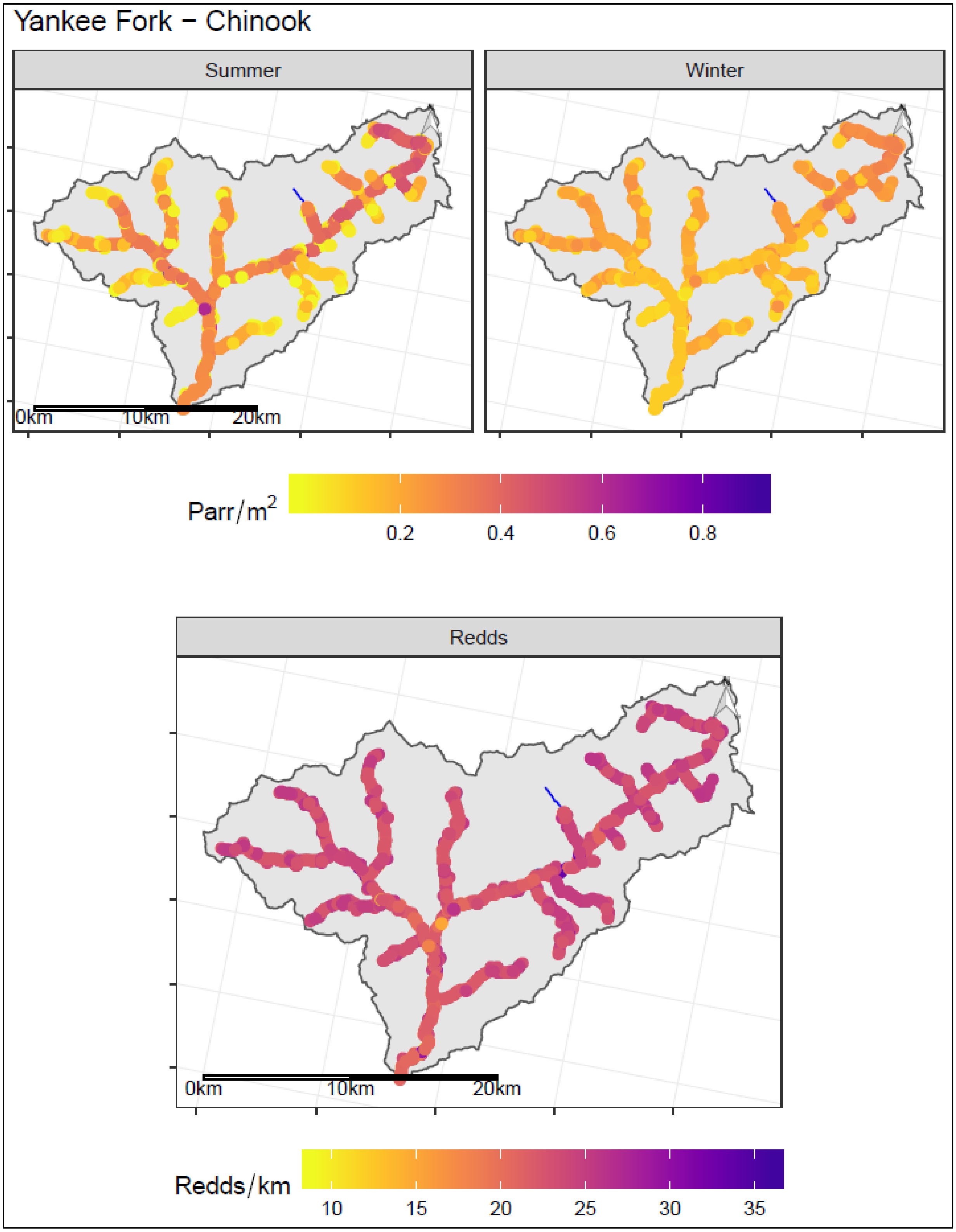

Supplemental Figure B-10. Map showing predictions of Chinook salmon carrying capacity for three life stages (summer juveniles, winter juveniles, redds) at master sample points in the Yankee Fork Salmon River.

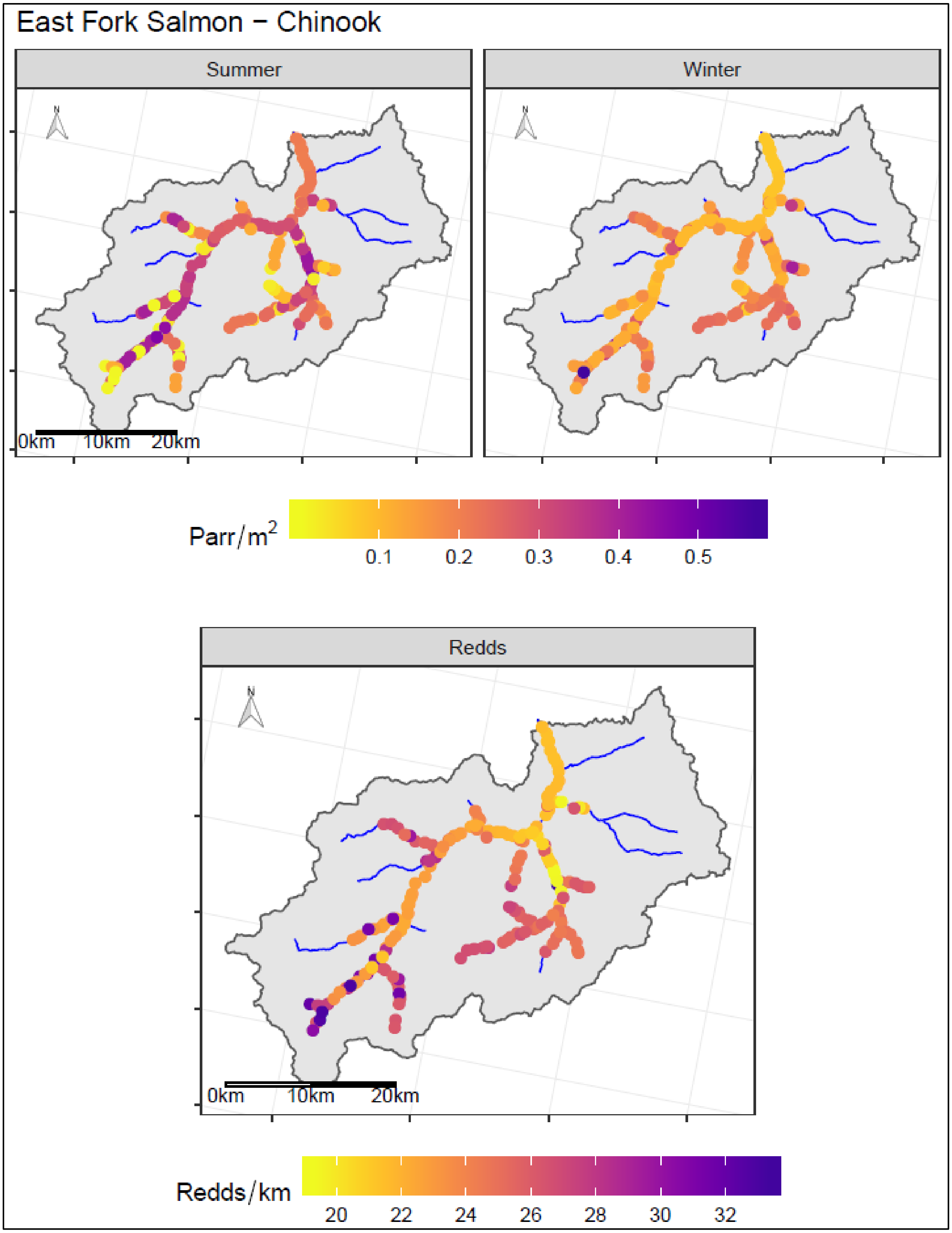

Supplemental Figure B-11. Map showing predictions of Chinook salmon carrying capacity for three life stages (summer juveniles, winter juveniles, redds) at master sample points in the East Fork Salmon River.

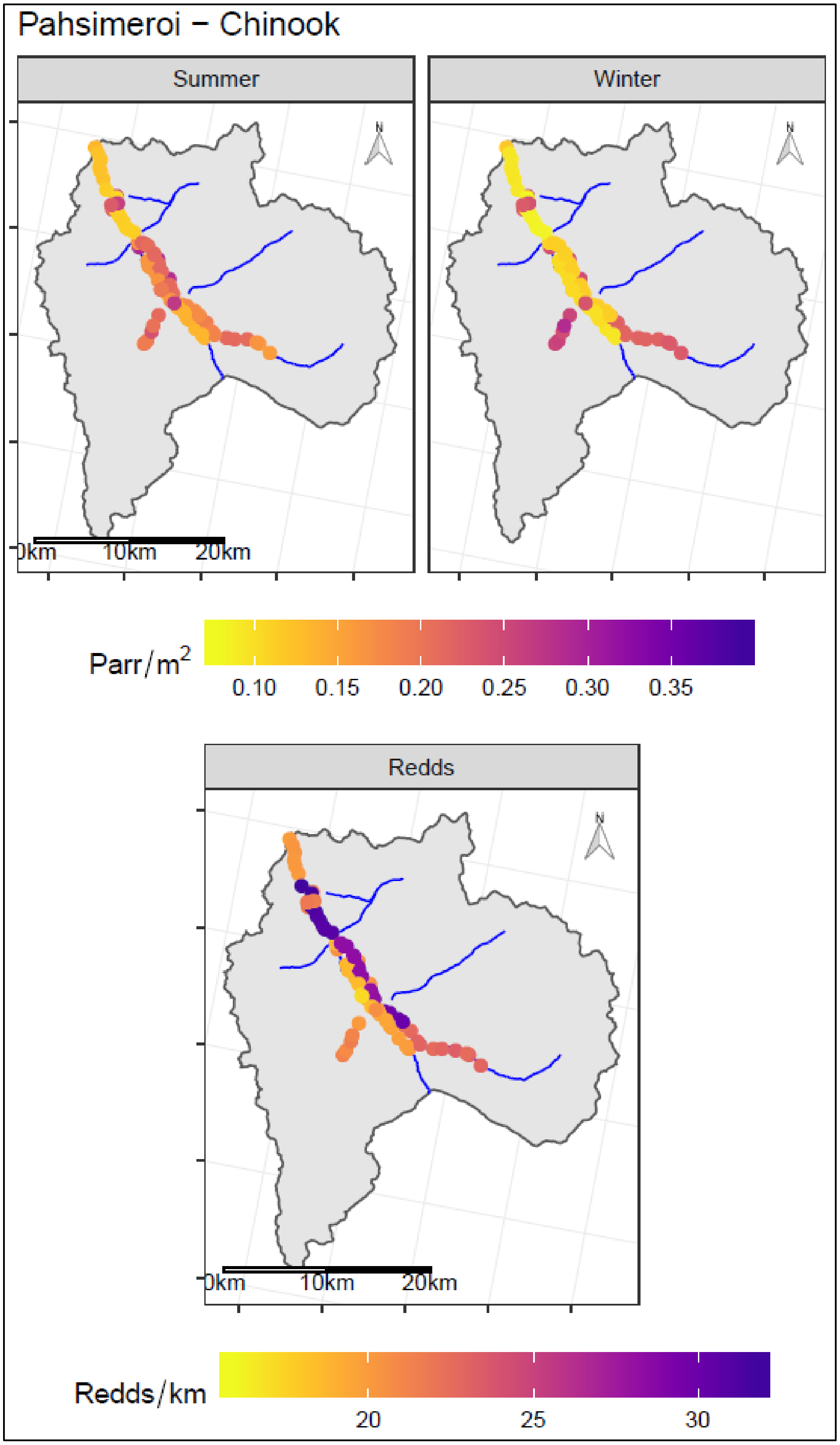

Supplemental Figure B-12. Map showing predictions of Chinook salmon carrying capacity for three life stages (summer juveniles, winter juveniles, redds) at master sample points in the Pahsimeroi River.

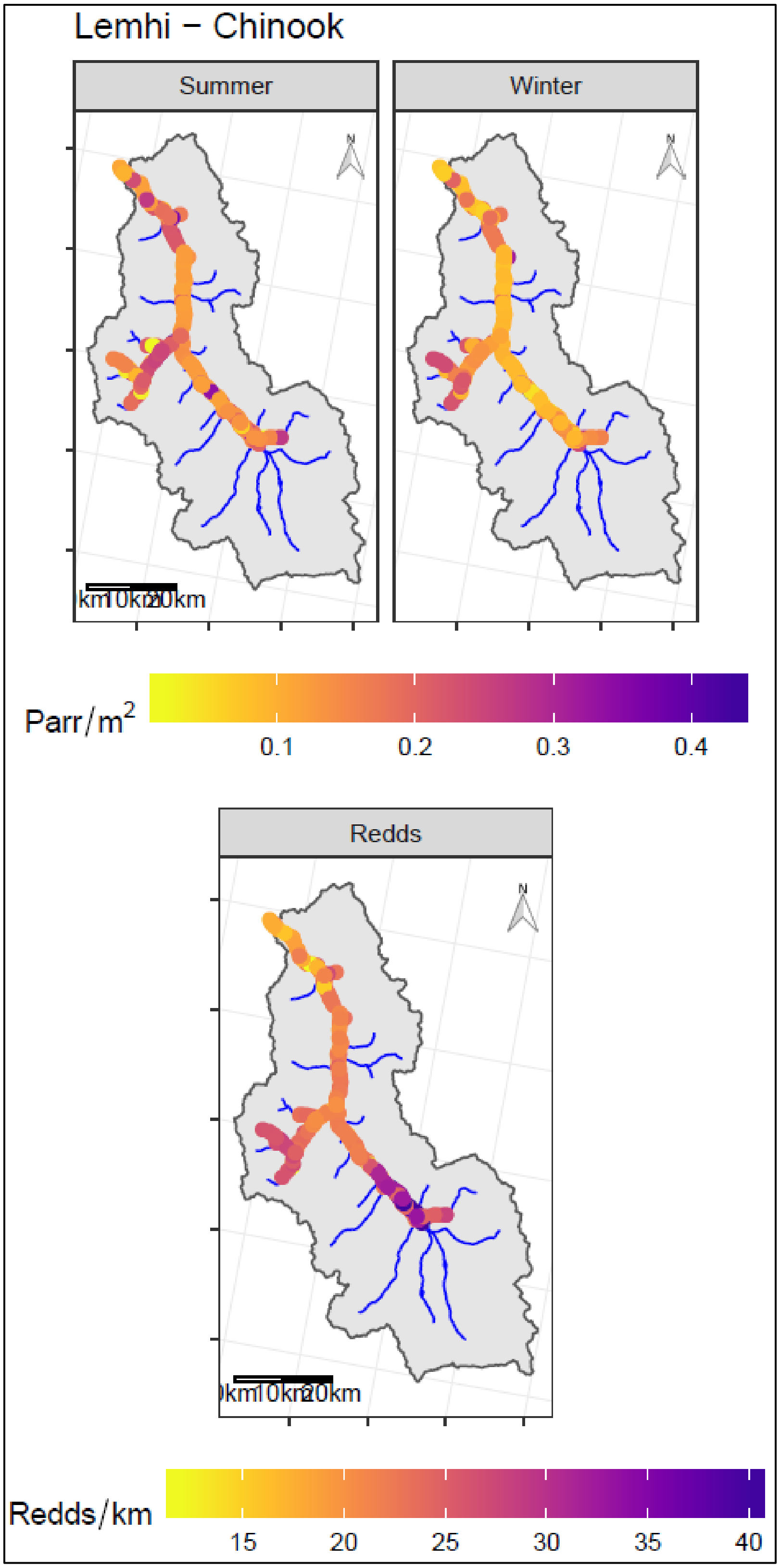

Supplemental Figure B-13. Map showing predictions of Chinook salmon carrying capacity for three life stages (summer juveniles, winter juveniles, redds) at master sample points in the Lemhi River.

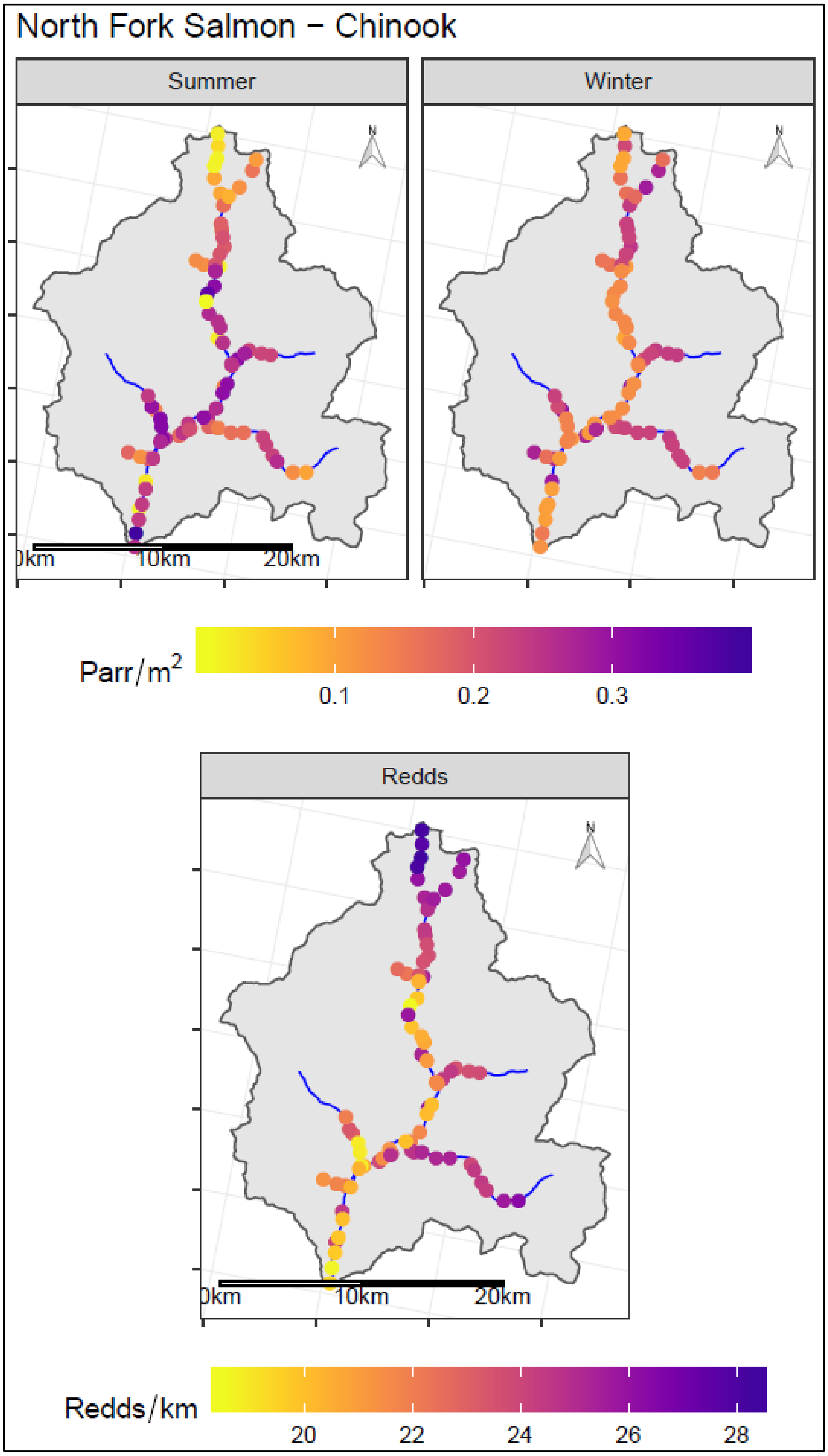

Supplemental Figure B-14. Map showing predictions of Chinook salmon carrying capacity for three life stages (summer juveniles, winter juveniles, redds) at master sample points in the North Fork Salmon River.

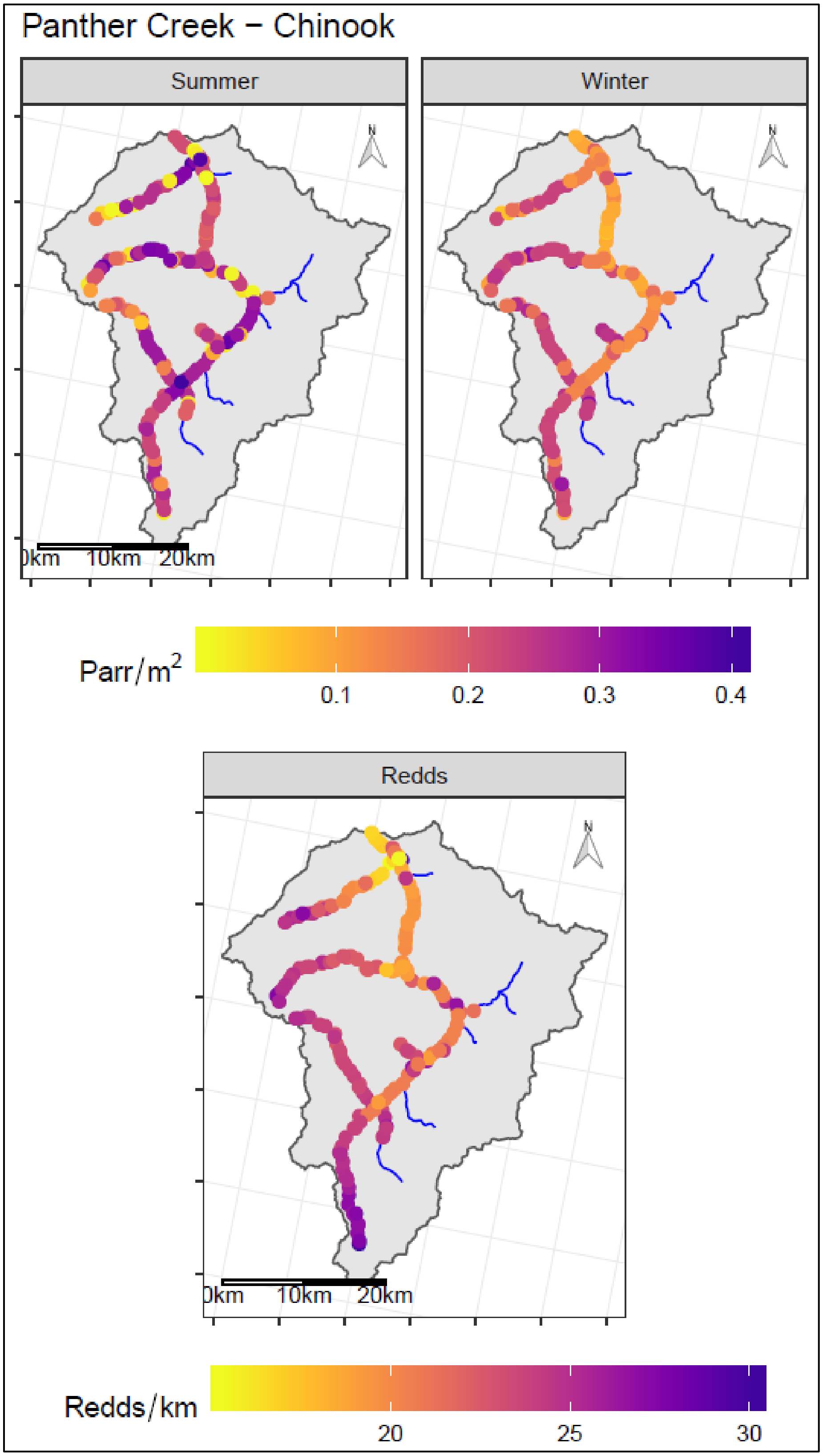

Supplemental Figure B-15. Map showing predictions of Chinook salmon carrying capacity for three life stages (summer juveniles, winter juveniles, redds) at master sample points in Panther Creek.

Steelhead

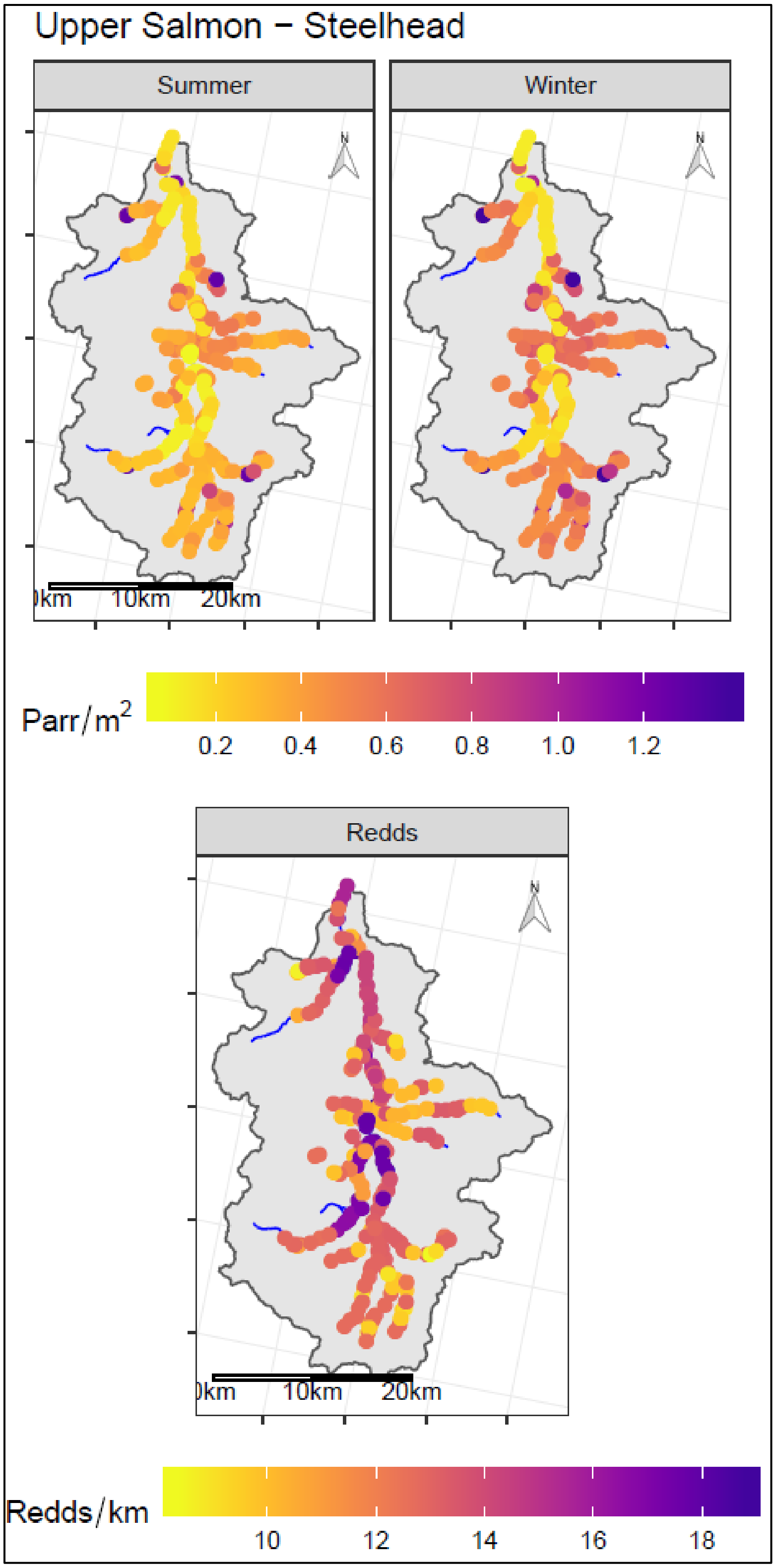

Supplemental Figure B-16. Map showing predictions of steelhead carrying capacity for three life stages (summer juveniles, winter juveniles, redds) at master sample points in the Upper Salmon River.

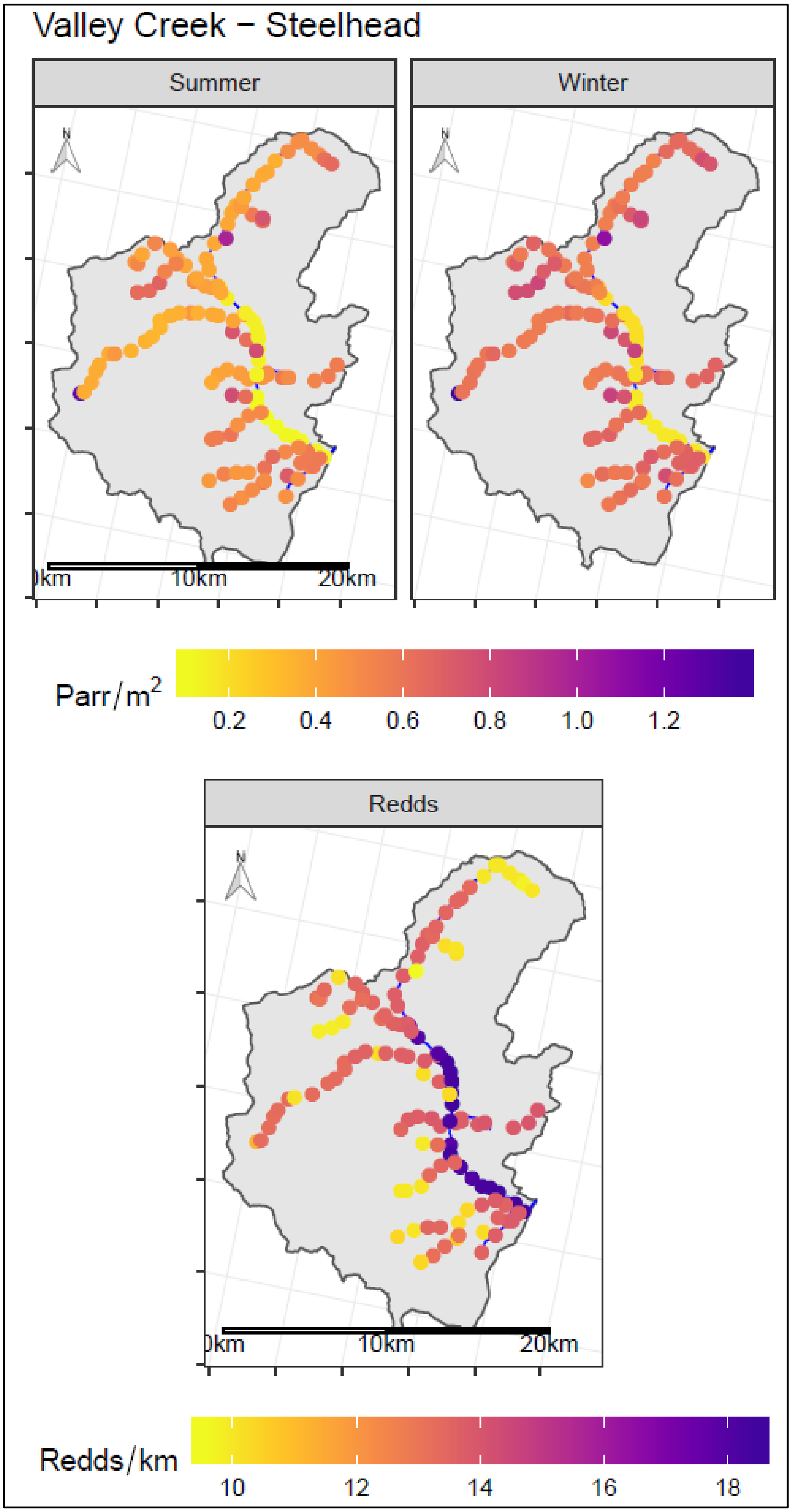

Supplemental Figure B-17. Map showing predictions of steelhead carrying capacity for three life stages (summer juveniles, winter juveniles, redds) at master sample points in Valley Creek.

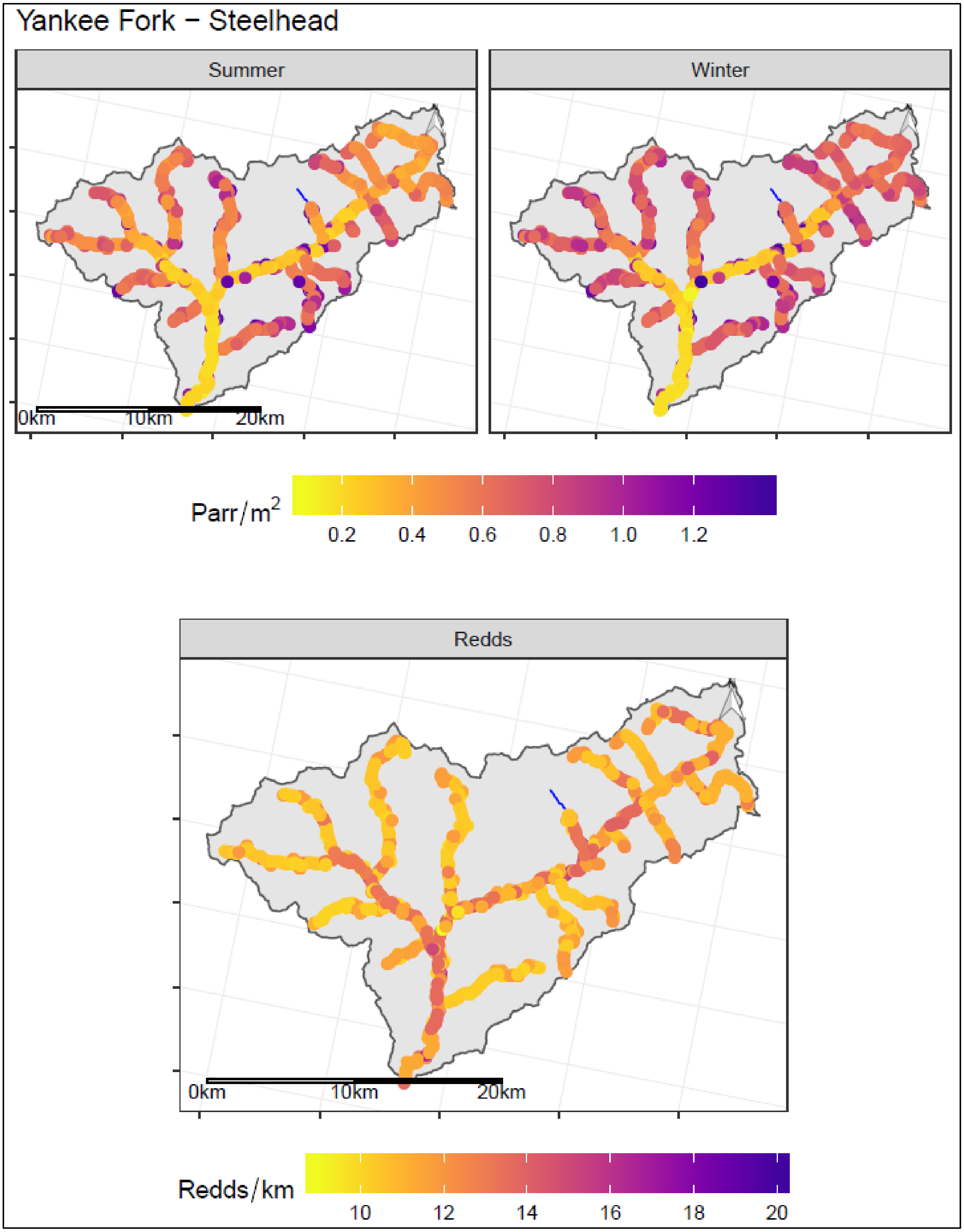

Supplemental Figure B-18. Map showing predictions of steelhead carrying capacity for three life stages (summer juveniles, winter juveniles, redds) at master sample points in the Yankee Fork Salmon River.

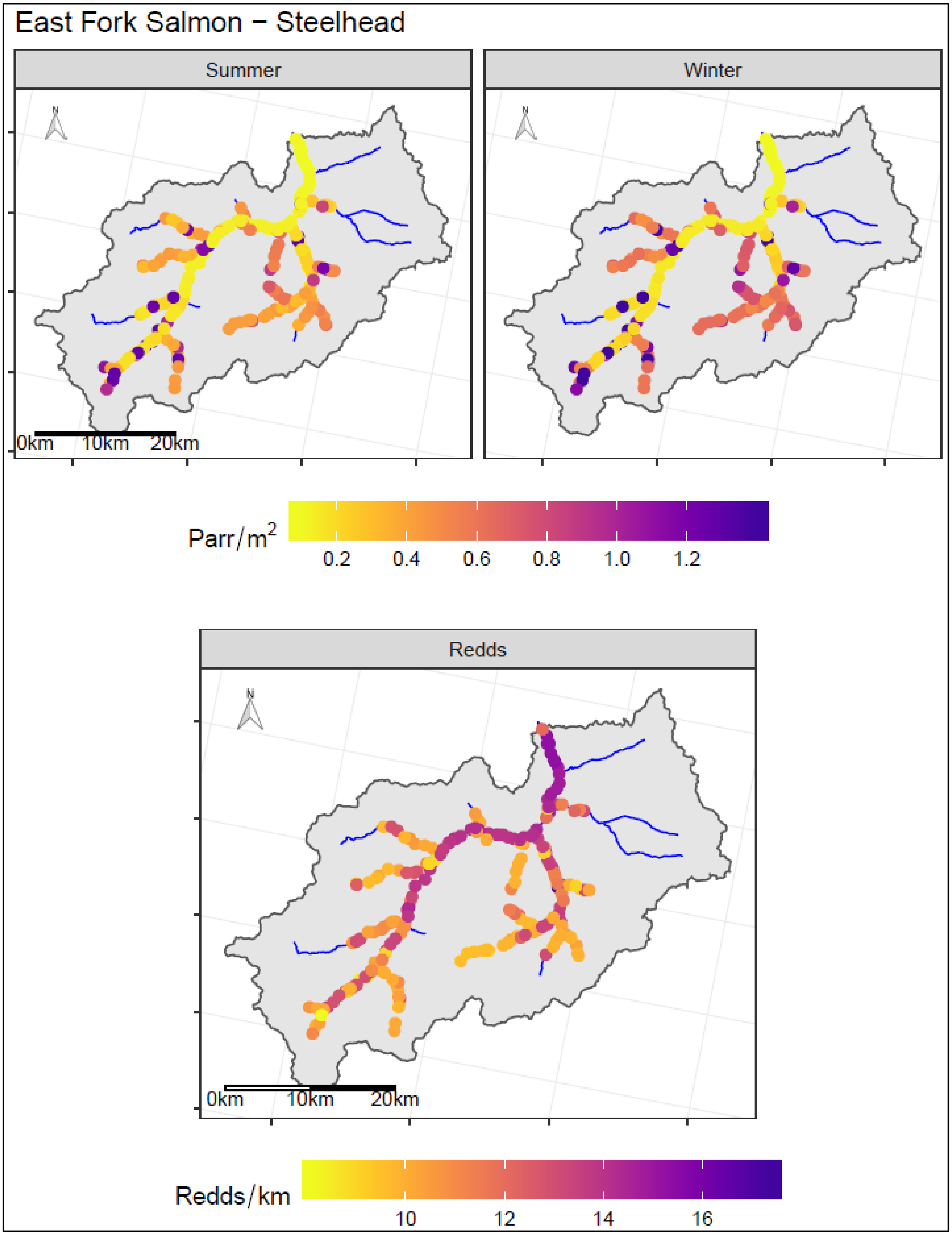

Supplemental Figure B-19. Map showing predictions of steelhead carrying capacity for three life stages (summer juveniles, winter juveniles, redds) at master sample points in the East Fork Salmon River.

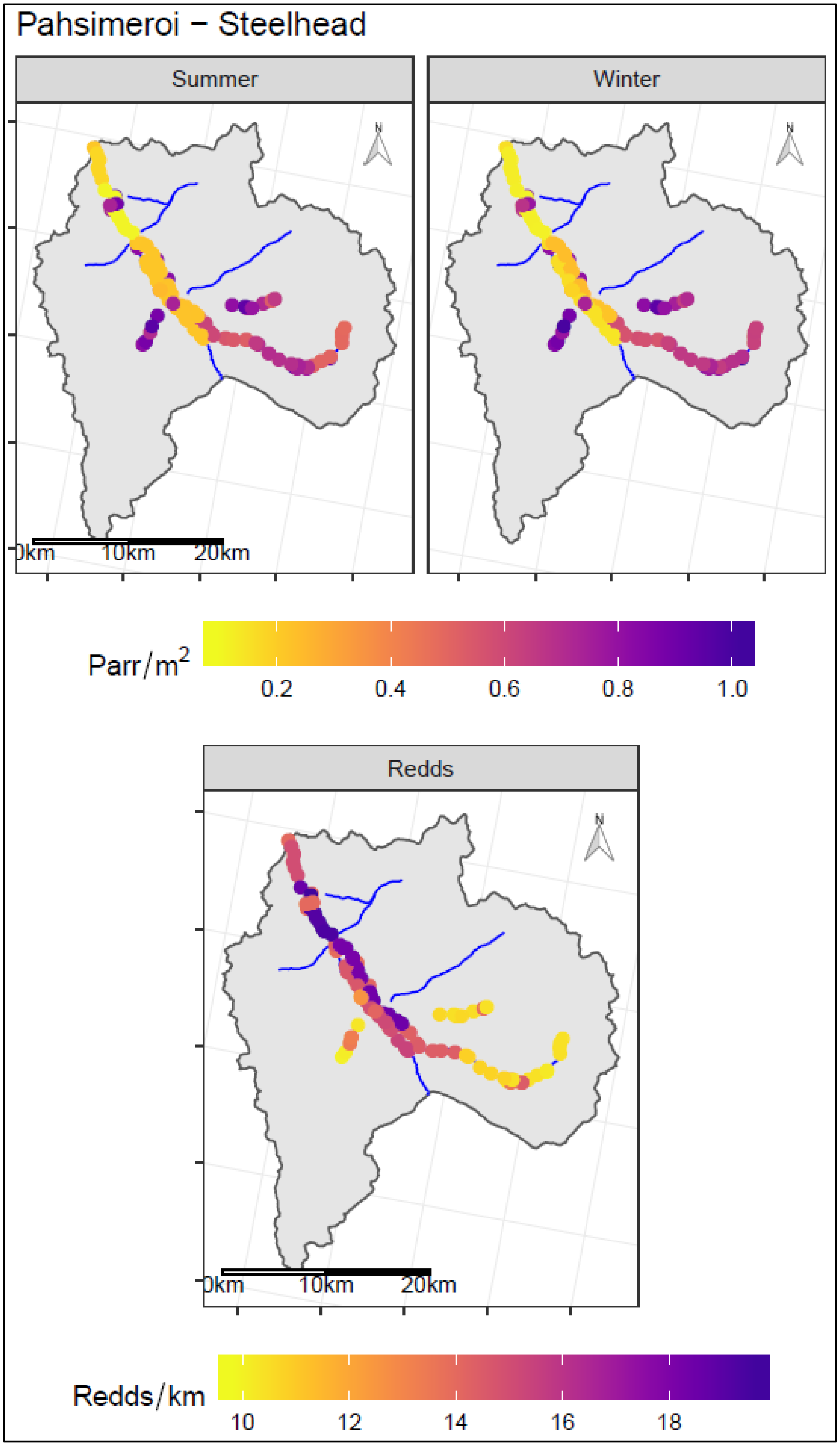

Supplemental Figure B-20. Map showing predictions of steelhead carrying capacity for three life stages (summer juveniles, winter juveniles, redds) at master sample points in the Pahsimeroi River.

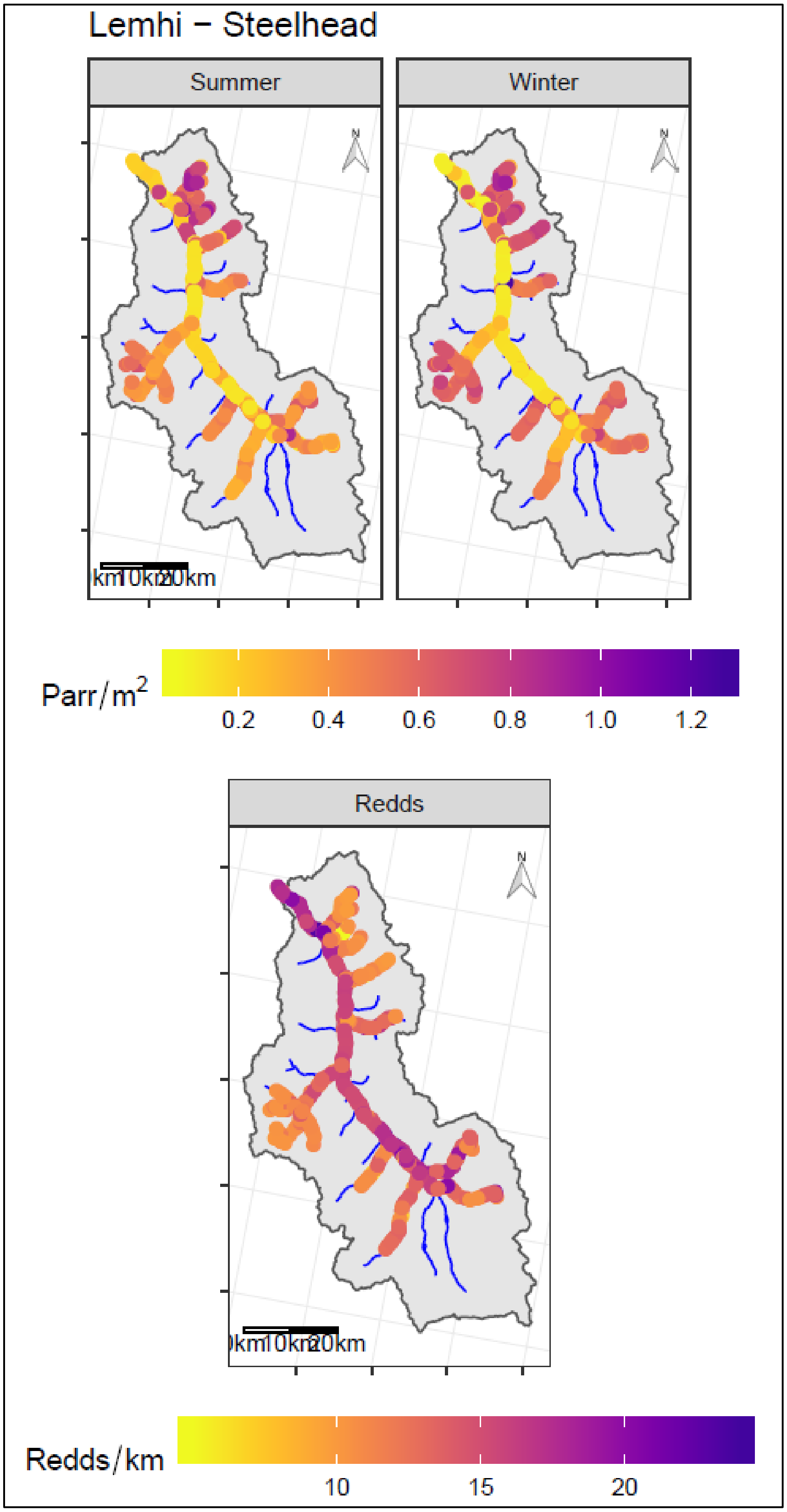

Supplemental Figure B-21. Map showing predictions of steelhead carrying capacity for three life stages (summer juveniles, winter juveniles, redds) at master sample points in the Lemhi River.

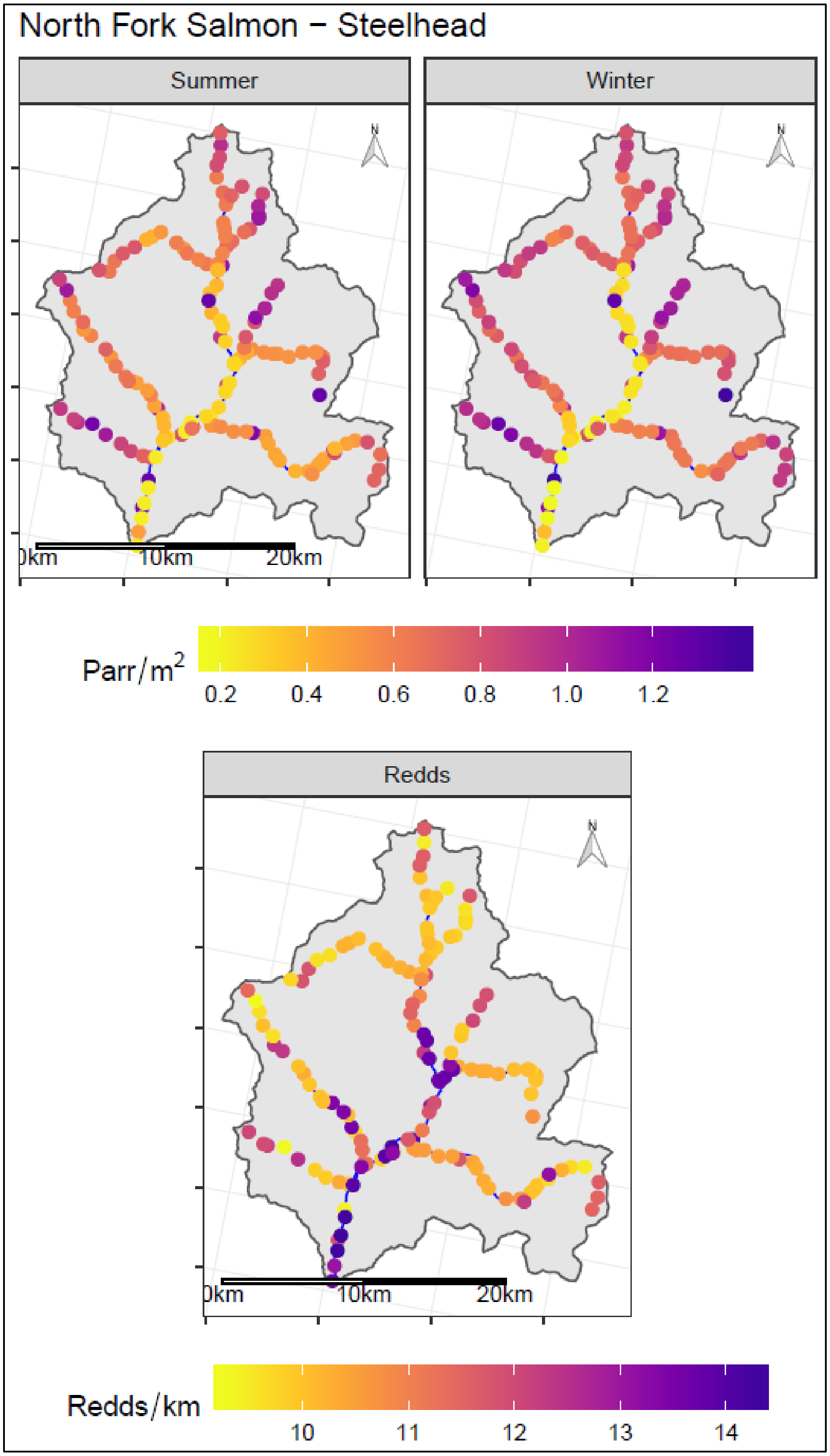

Supplemental Figure B-22. Map showing predictions of steelhead carrying capacity for three life stages (summer juveniles, winter juveniles, redds) at master sample points in the North Fork Salmon River.

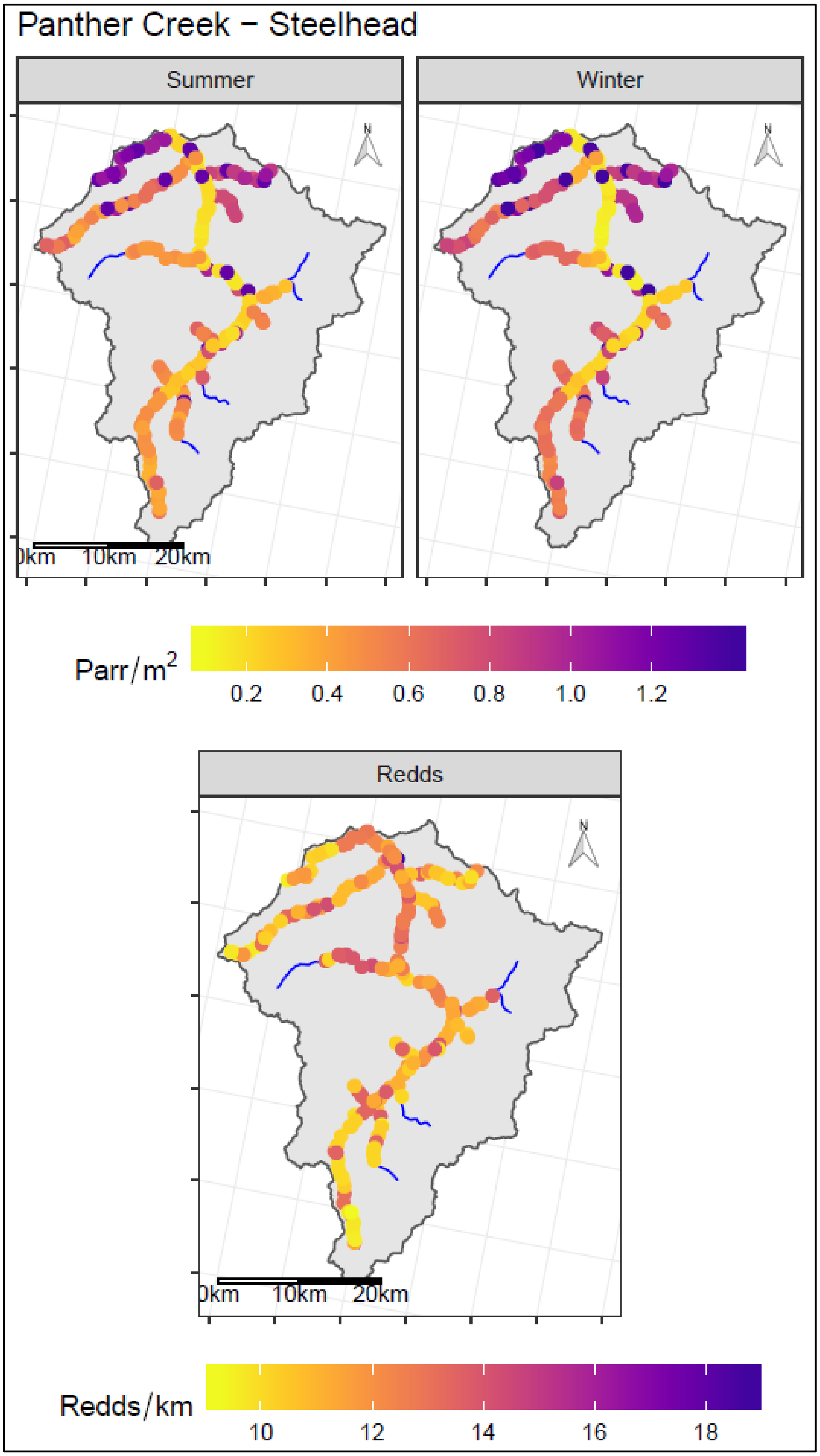

Supplemental Figure B-23. Map showing predictions of steelhead carrying capacity for three life stages (summer juveniles, winter juveniles, redds) at master sample points in Panther Creek.

Appendix C – Habitat Capacity Requirements

Introduction

Appendix C describes a series of approaches to determine life-stage-specific capacity requirements for spring-summer run Chinook salmon (hereafter Chinook salmon) and summer-run steelhead (hereafter steelhead) under two conditions: 1) contemporary adult escapement and 2) adult escapement accompanying proposed de-listing criteria (NOAA 2017). The goal is to estimate the maximum redd capacity, summer parr rearing capacity, and over-winter presmolt capacity necessary to support both conditions. The primary challenge associated with this initiative arises from the fact that observations of productivity and survival from one life stage to the next are only recently available and are therefore the product of heavily modified habitat and management actions, such as hatchery production. Additionally, data availability varies among the three targeted watersheds.

The following options to estimate capacity requirements were considered:

1. Using empirical observations of adult escapement, redd production, and life-stage-specific juvenile abundance.
2. Applying a time-series process model to estimate and remove sampling error from productivity estimates.
3. Applying a generalized model of survival combining empirical data and literature values.

Initially, each of the three options (Empirical Observation Model, Time-Series Process Model, and Generalized Capacity Model) were explored for Chinook salmon in the Upper Salmon, Pahsimeroi, and Lemhi Rivers to evaluate their utility. Ultimately, we chose to use the third approach, the Generalized Capacity Model, and that model was then applied to both species, and further, to all eight watersheds in the Upper Salmon River Subbasin (Upper Salmon River, Valley Creek, Yankee Fork Salmon River, East Fork Salmon River, Pahsimeroi River, Lemhi River, North Fork Salmon River, Panther Creek).

Empirical Observation Model

A time series of Chinook salmon adult escapement and juvenile production data are available for the Upper Salmon, Pahsimeroi, and Lemhi Rivers. The Sawtooth Hatchery, located on the Upper Salmon River, operates an adult weir for broodstock collection, enabling a precise estimate of adults released upstream to spawn. Similarly, the Pahsimeroi Hatchery operates an adult weir for broodstock collection on the lower Pahsimeroi River, also enabling a precise estimate of adults released upstream to spawn. Further, the Idaho Department of Fish and Game operates one rotary screw trap (RST) in the Upper Salmon River, one RST in the lower Pahsimeroi River, and three RSTs within the Lemhi River to estimate juvenile productions. The adult escapement data and juvenile production data can be combined to monitor productivity in those areas. We queried the Idaho Fish and Wildlife Information System (IFWIS) to compile data from the year 2000 onward at these facilities (Supplemental Table C-1 and Supplemental Table C-2).

A shorter time series of data are available for Lemhi River Chinook salmon at the population level. Adult escapement estimates are generated by tagging natural-origin adult Chinook salmon with passive integrated transponder (PIT) tags as they migrate past Lower Granite Dam and then subsequent detection of those adults as they pass in-stream PIT tag detection systems (IPTDS) located in the lower Lemhi River (ISEMP/CHaMP 2017). These data are available since 2010. We paired adult escapement data with juvenile abundance data generated from the three RSTs operated in the Lemhi River watershed, beginning in 2008 (Supplemental Table C-3).

These data summaries illuminate differences among the Upper Salmon, Pahsimeroi, and Lemhi River Chinook salmon populations. First, adult escapement into the Upper Salmon and Pahsimeroi Rivers is managed, manifesting in a lower percentage of female escapement relative to the Lemhi River (Table C-1). Second, most Chinook salmon juveniles pass RSTs in the Upper Salmon and Pahsimeroi Rivers as fry and parr, whereas most juvenile production in the Lemhi passes the lowest RST (L3A0) as presmolts and smolts (Table C-1). Differences in the observed emigration timing between the Upper Salmon and Pahsimeroi Rivers relative to the Lemhi River are likely a function of the proximity of the RSTs to Chinook salmon spawning areas. Lastly, the average number of redds per female spawner (Table C-1) differs among the three locations. It is unclear whether these differences are a result of observation error or a function of larger differences in pre-spawning mortality.

Table C-1. Mean percentage of total escapement composed of females and subsequent mean productivity for the Upper Salmon, Pahsimeroi, and Lemhi Rivers

Location	% Female	Redds/Female	% Fry	% Parr	% Presmolt	% Smolt
Upper Salmon	36%	0.7	26%	31%	33%	10%
Pahsimeroi	45%	0.9	32%	7%	48%	12%
Lemhi	49%	1.5	0%	2%	70%	28%

Given the uncertainty about the mechanisms underlying productivity differences among the three populations, we did not attempt to develop a joint model of capacity requirements based on empirical data.

Time-Series Process Model

As described in the prior section, productivity data differ among Chinook salmon in the Upper Salmon, Pahsimeroi, and Lemhi Rivers. One of the most obvious differences among the three locations is the timing of juvenile emigration. Given the earlier relative age of juvenile Chinook salmon emigrants in the Upper Salmon and Pahsimeroi Rivers (i.e., juveniles tend to emigrate as fry and parr), estimating juvenile abundance in natal habitat is difficult. Here, we describe a simple model of the freshwater portion of the life cycle for Chinook salmon and fit the model using data from the Lemhi River basin. This is a minimal, empirical model, including only those life stages for which abundance or survival can be directly observed: spawners, parr, and smolts (operationally defined as juvenile emigrants passing Lower Granite Dam). It is assumed that all juveniles that survive to the smolt stage emigrate past Lower Granite Dam as yearlings. The spatial scale is the entire Lemhi River basin; we do not distinguish among subbasins or reaches, and thus there is no dispersal or movement beyond the direct migration implicit in the parr-to-smolt transition.

Transitions between successive life stages within the time-series process model are described by a Beverton-Holt model fit using data from the Lemhi River basin. Specifically, the Beverton-Holt model provides information regarding life-stage-specific abundance, intrinsic productivity, and the life-stage-specific required capacity (not to be confused with carrying capacity). Required capacity is the life-stage-specific capacity required to support a given level of adult escapement, whereas carrying capacity is the life-stage-specific abundance that the habitat can support. To estimate the parameters in the spawner-to-parr and parr-to-smolt Beverton-Holt functions, we require observations of abundance (spawner or parr), transition probabilities (e.g., survival), or both, along with estimates of observation uncertainty.

Estimates of smolt emigration abundance in the model do not rely directly on empirical estimates from the Lemhi River, because a large fraction of total juvenile emigration in the Lemhi occurs during the fall at the presmolt life stage. Instead, survival estimates of parr tagged during the summer prior to outmigration and until passing Lower Granite Dam the following spring are used, regardless of whether they reared within or outside of the Lemhi River watershed. These overall parr-to-Lower Granite Dam survival estimates and associated standard errors are produced using TribPIT (Lady et al. 2014), which models a cohort of juveniles following the same migration route, albeit potentially at different times. In this case, cohorts consist of parr tagged in Hayden Creek and in the upper Lemhi River, respectively.

Total parr abundance is defined as the sum of abundance estimates from Hayden Creek and the mainstem Lemhi River. Basin-wide parr-to-smolt survival is estimated by resampling distributions describing annual survival in Hayden Creek and the upper mainstem Lemhi River. Note that temporally comprehensive estimates of parr abundance in the upper and lower mainstem Lemhi River are not available, nor do we have cohorts of PIT-tagged parr residing in the lower mainstem. In the absence of such information, we assume the survival of parr from the upper mainstem Lemhi River is representative of those throughout the mainstem. Finally, we use independent estimates of parr capacity as an informative prior to help constrain the model fits. These estimates are derived from the quantile regression forest (QRF) models described in Appendix B that predict parr capacity as a function of habitat covariates.

Results

Model diagnostics suggested a reasonable model fit. Figure C-1 shows the posterior distributions of stage-specific intrinsic productivity and capacity, and Figure C-2 and Figure C-3 show the Beverton-Holt spawner-to-parr and parr-to-smolt relationships.

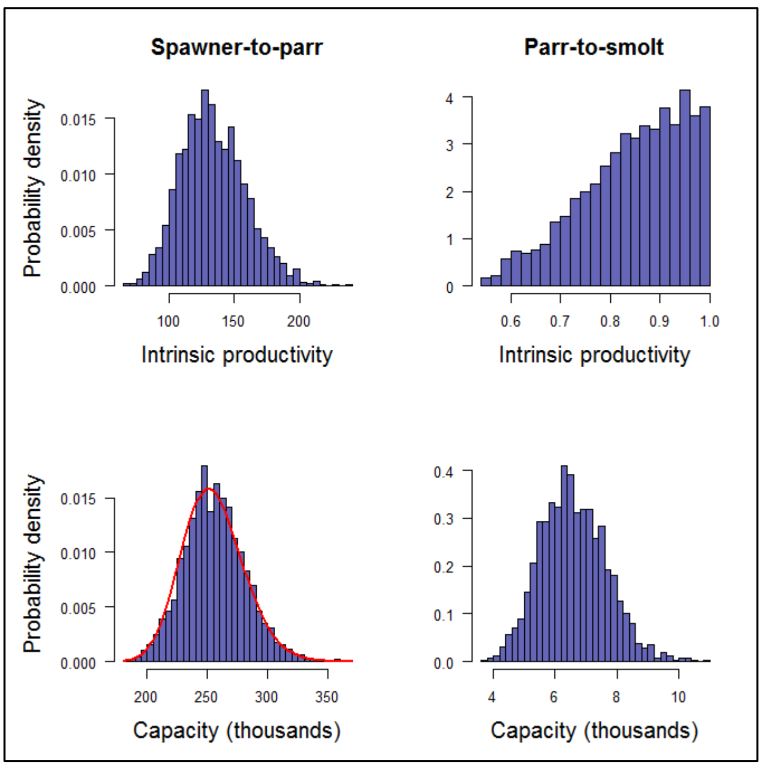

Figure C-1. Spawner to parr, parr to smolt, intrinsic productivity and capacity

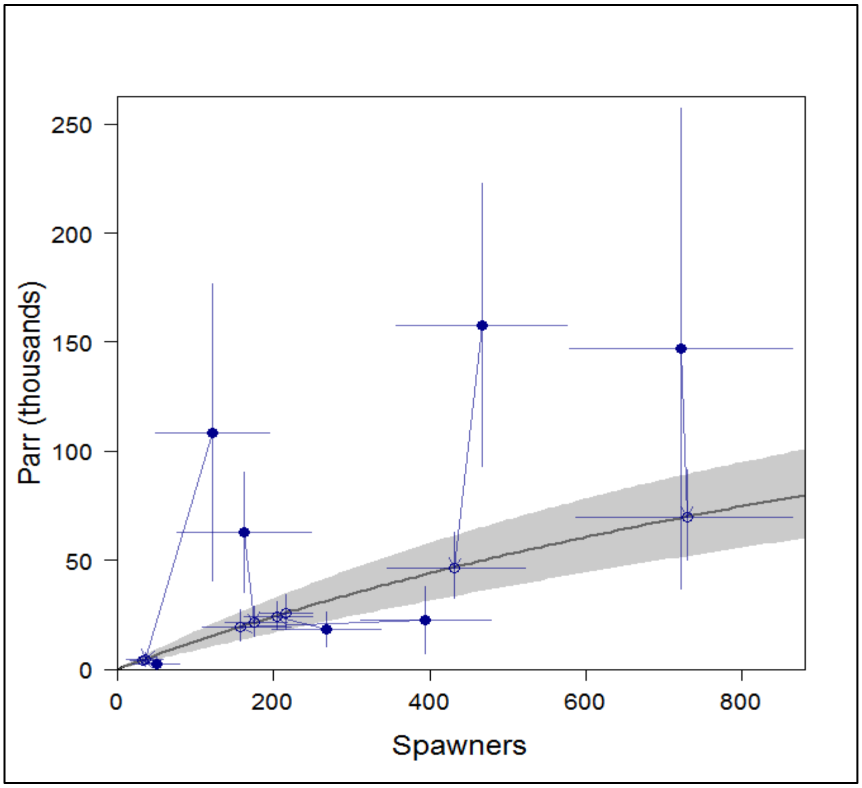

Figure C-2. Beverton-Holt spawner to parr productivity

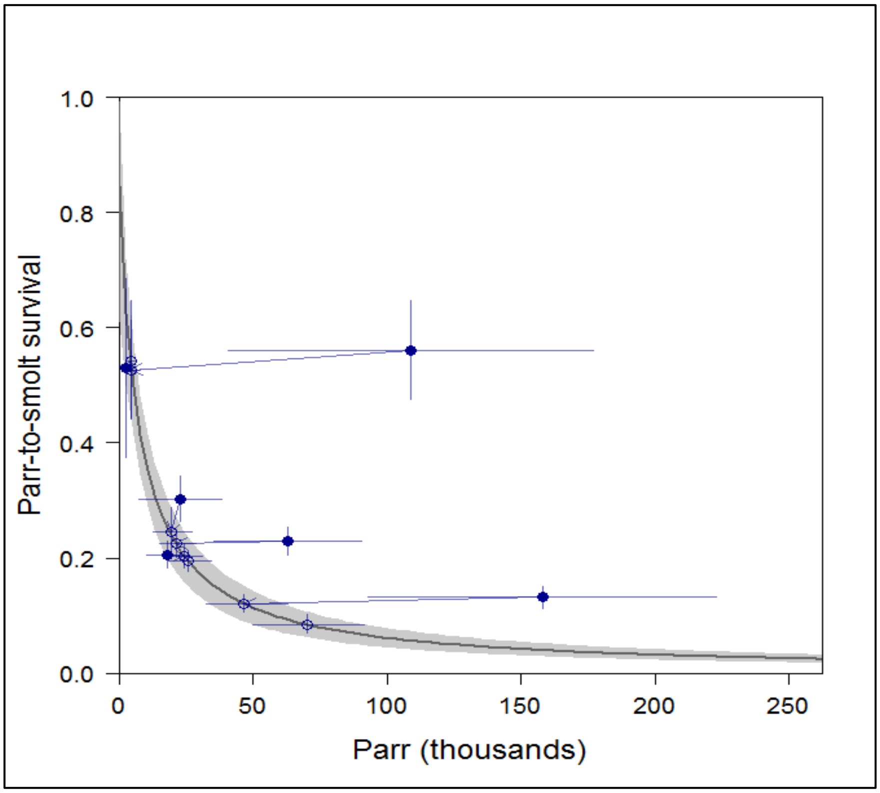

Figure C-3. Beverton-Holt parr to smolt relationship

In Figure C-1, the informative prior for capacity is shown in red; clearly, the posterior is determined entirely by the prior. Given that the posterior estimates of capacity are so closely related to the prior, we tested the sensitivity of other parameter estimates to starting values for capacity. Results suggest that the remaining parameters are quite robust to variations in capacity. In Figure C-2 and Figure C-3, data are shown as filled circles with approximate 95 percent confidence intervals, based on the observation error variances. Arrows connect each observation to the corresponding estimated “true” value (open circle) show with 95 percent posterior credible intervals.

Clearly, the largest deviations between observed and fitted values are in parr abundance (Figure C-2), which has the largest relative observation uncertainty. The model attributes three exceptionally high values to measurement error, producing a much more conservative estimate of the slope of the spawner-to-parr relationship at low spawner abundance (i.e., intrinsic productivity). It is also clear why the prior on parr capacity is so informative; the model does not think any of the observed escapements have come close to saturating the system with parr.

The same downward shift in the observed parr abundances is also evident in the parr-to-smolt survival plot (Figure C-3). Because the models for the two-stage transitions are coupled, they use the same estimated “true” parr values. This ensures internal consistency through the entire spawner-to-smolt model. In contrast to the spawner-to-parr relationship, there is not much evidence of density dependence in the parr-to-smolt transition, based on the raw data. After shrinkage of the measurement errors, however, a relationship emerges with intrinsic productivity (i.e., maximum survival) around 0.84. This seems reasonable by comparison with the range of realized parr-to-smolt survival.

Conclusions

Although the time-series process model offers a statistically rigorous means to model density-dependent productivity, the data necessary to populate the model are limited to Chinook salmon in the Lemhi River and are only available for 8 years. Given uncertainty about the transferability of this model to Chinook salmon populations in the Upper Salmon River and Pahsimeroi River populations (and populations elsewhere in the Upper Salmon River subbasin), and further, to steelhead populations, we are hesitant to use this approach.

Generalized Capacity Model

A combination of empirical and literature-based abundance and survival estimates were used as a final approach for estimating life-stage specific capacity requirements.

Chinook salmon

The Chinook salmon model operated under the assumption that, in the absence of weirs, sex ratios in the Upper Salmon and Pahsimeroi Rivers would approximate those observed in the Lemhi River. Further, the model assumed that, on average, each escaping female would produce one redd, based on observations by Bjornn (1978), and corresponding to the combined mean number of redds constructed by females averaged across the Upper Salmon, Pahsimeroi, and Lemhi Rivers (Table C-2). Chinook salmon fecundity values in the model approximated those observed at Sawtooth Hatchery (Snider et al. 2005), and egg-to-parr survival reflected those reported by Petrosky et al. (1989). Finally, the weighted mean transition probability of parr-to-presmolt were generated from empirical data in the Lemhi River (ISEMP/CHaMP 2017).

Table C-2. Parameter values used to estimate life-stage specific capacity requirements for the Upper Salmon, Pahsimeroi, and Lemhi Rivers

Parameter	Value	Source
Female Ratio	0.49	IDFG/ISEMP
Redds/Female	1	Bjornn (1978)
Fecundity	5,290	Snider et al. (2005)
Egg:Parr	0.29	Petrosky, Everson, and Holubetz (1989)
Parr: Presmolt	0.41	Lemhi Empirical

Life-stage-specific habitat capacity requirements cannot be estimated without making assumptions regarding the fraction of juvenile Chinook salmon expected to emigrate from natal habitat as fry and parr. Many of the habitat changes that influence capacity and behavior existed prior to the time series of juvenile observation data. It is therefore unclear whether fry and parr emigration rates observed in recent years for the Upper Salmon and Pahsimeroi Rivers are a natural condition. For the purposes of calculating capacity requirement, the model assumed that natural rates of fry or parr emigration were historically negligible. Further, it is assumed that when habitat capacity is sufficient, rates of presmolt emigration are negligible, as observed by Bjornn (1971). They reported fall presmolt emigration rates as low as 6.7 percent. Taken together, these parameters and assumptions (Table C-2) can be used to estimate the expected number of redds, summer parr, and presmolts expected given a specified adult escapement and negligible density-dependence.

Expected parr (summer) and presmolt (winter) abundances were calculated based on both the mean and maximum observed adult escapement among recent (contemporary) data to estimate current capacity requirements. For the Upper Salmon and Pahsimeroi Rivers, the mean and maximum escapement was based on observed adult escapement since 2010. For the Lemhi River, parr and presmolt abundance estimates were calculated based on the mean and maximum observed adult escapement since 2010. Further, using the parameters in Table C-2, we applied the generalized capacity model to the remaining five populations in the Upper Salmon River Subbasin. Mean and maximum observed adult escapement in Valley Creek (2010 to 2015), Yankee Fork Salmon River (2012 to 2015), and East Fork Salmon River (2010 to 2015) were based on IPTDS located in those rivers. For the North Fork Salmon River (1991 to 2017) and Panther Creek (2001- to 2017), mean and maximum adult escapement estimates were based on redd counts and estimates of fish-per-redd for those systems (Personal Communication, Matt Belnap, Idaho Department of Fish and Game). We then calculated expected capacity requirements to support adult escapement targets identified in NOAA (2017) de-listing criteria (Supplemental Table C-4 to Supplemental Table C-11).

Steelhead

We used the generalized capacity model framework that was first developed for Chinook salmon in the Upper Salmon River Subbasin and applied that framework to steelhead in the subbasin. For steelhead, sex ratios were estimated from all adult steelhead that were PIT-tagged at Lower Granite Dam and later detected at IPTDS in the Upper Salmon River Subbasin (Powell et al. 2017). IPTDS used to estimate sex ratios were located in the following areas: Upper Salmon River (above Redfish Lake), Valley Creek, Yankee Fork Salmon River, upper mainstem Salmon River, East Fork Salmon River, Pahsimeroi River, Lemhi River, and Carmen Creek. Further, the model assumed that, on average, each escaping female would produce 0.89 redds based on observations by Jonasson et al. (2016) for steelhead in Deer Creek, Grande Ronde River, Oregon. Steelhead fecundity values in the model approximated those observed at the Sawtooth and Pahsimeroi hatcheries (Personal Communication, Steve Pomerleau and Todd Garlie, Idaho Department of Fish and Game). Finally, egg-to-parr survival and parr-to-smolt survival were derived from McHugh et al. (2017). Parameters used in the steelhead generalized capacity model are summarized in Table C-3.

Table C-3. Parameter values used to estimate life-stage specific capacity requirements for the Upper Salmon, Pahsimeroi, and Lemhi Rivers

Parameter	Value	Source
Female Ratio	0.62	Powell et al. (2017)
Redds/Female	0.89	Jonasson et al. (2016)
Fecundity	4,926	IDFG, Personal Communication
Egg:Parr	0.13	McHugh et al. 2017
Parr: Presmolt	0.36	McHugh et al. 2017

Similar to the Chinook generalized capacity model, expected summer parr and winter juvenile abundances were calculated based on both the mean and maximum observed adult escapement among recent (contemporary) data to estimate current capacity requirements. For Valley Creek (2010- to 2015) and Lemhi River (2010 to 2015), mean and maximum observed adult escapement were based on IPTDS located in those rivers. Escapement data for Panther Creek, North Fork Salmon River, and Pahsimeroi River were all available from 2011 to 2015 from run reconstruction efforts across the Snake River Basin (e.g., Stark et al. 2017). For the East Fork Salmon River (2012 to 2015) and Upper Salmon River (2010 to 2015), escapement estimates were from weirs at hatchery facilities in those locations. Escapement estimates in the Yankee Fork Salmon River (2012 to 2015) were based on a weir and IPTDS located in the lower river. We then calculated expected capacity requirements to support adult escapement targets identified in NOAA (2017) de-listing criteria (Supplemental Table C-12 to Supplemental Table C-19). Note that for steelhead, the Upper Salmon (above Redfish Lake), Valley Creek, and Yankee Fork Salmon groups are all located within the Upper Salmon mainstem Technical Recovery Team (TRT) population (NOAA 2017). To calculate expected capacity requirements for those watersheds, we multiplied the total adult escapement target for that population (1,000) by the percentage of available stream length within the steelhead domain in those watersheds (Table C-4).

Table C-4. Available stream length within the steelhead domain for the Upper Salmon (above Redfish Lake), Valley Creek, and Yankee Fork watersheds within the Upper Salmon mainstem

Watershed	Stream Length (km)	Stream Length (%)
Upper Salmon (above Redfish Lake)	195.3	48.0%
Valley Creek	99.9	24.6%
Yankee Fork	111.3	27.4%

Literature Cited

Bjornn, T.C. 1978. Survival, production, and yield of trout and Chinook salmon in the Lemhi River, Idaho. Idaho Cooperative Fish and Wildlife Research Unit. Final Report for Federal Aid to Fish Restoration Project F-49-R. 57pp.

Bjornn, T.C. 1971. Trout and Salmon Movements in Two Idaho Streams as Related to Temperature, Food, Stream Flow, Cover, and Population Density. Transactions of the American Fisheries Society. 100(3):423-438.

ISEMP/CHaMP. 2017. Integrated Status and Effectiveness Monitoring Program (ISEMP) and Columbia Habitat Monitoring Program (CHaMP) Annual Combined Technical Report, January – December 2016. BPA Projects 2003-017-00 and 2011-006-00, 93 Electronic Pages.

Jonasson, B., et al. 2016. Investigations into the Life History of Naturally Produced Spring Chinook Salmon and Summer Steelhead in the Grande Ronde River Subbasin. Annual Report for BPA Project #1992-026-04.

Lady, J. J.R. Skalski, and R. Buchanan. 2014. Program tribPIT. USDOE. BPA. http://www.cbr.washington.edu/sites/default/files/manuals/TribPit%20User%27s%20Manual.pdf.

McHugh, P.A, W.C. Saunders, N. Bouwes, C.E. Wall, S. Bangen, J.M. Wheaton, M. Nahorniak, J.R. Ruzycki, I.A. Tattam, and C.E. Jordan. 2017. Linking models across scales to assess the viability and restoration potential of a threatened population of steelhead (*Oncorhynchus mykiss*) in the Middle Fork John Day River, Oregon, USA. Ecological Modelling. 355:24-38.

NOAA. 2017. Proposed ESA r4ecovery plan for Snake River spring/summer Chinook salmon (*Oncorhynchus tshawytscha*) and Snake River steelhead (*Oncorhynchus mykiss*). http://www.nmfs.noaa.gov/pr/recovery/plans/proposed_snake_roll_up_10.25.16_draft_.pdf

Petrosky, C.E., T.B. Holubetz. And L.B. Everson. 1989. Idaho habitat evaluation for off-site mitigation record. 1987 Annual Report. Contract DE-A179-84BP13381. Project 83-7. 46pp.

Powell, J.H., N. Vu, J. McCane, M.W. Ackerman, M.R. Campbell, D.J. Hasselman, and S.R. Narum. 2017. Chinook and Steelhead Genotyping for Genetic Stock Identification at Lower Granite Dam. Idaho Department of Fish and Game Report 17-02. Annual Report, BPA Project 2010-026-00.

Snider, B.R., R. Elmore, M. Hughes, H. Smith, and D. Munson. 2005. Sawtooth fish hatchery and East Fork satellite 2003 spring Chinook brood year report 2004 steelhead brood year report. IDFG 05-53. 54pp.

Stark, E.J., A. Byrne, P.J. Cleary, T. Copeland, L. Denny, R. Engle, T. Miller, D. Nemeth., S. Rosenberger, E.R. Sedell, G.E. Shippentower, and C. Warren. 2017. Snake River basin steelhead 2014/2015 run reconstruction. Report to Bonneville Power Administration, Portland, Oregon.

Supplementary Tables to Appendix C

Empirical Observation Model

Supplemental Table C-1. Adult escapement, redd counts, and juvenile production data for Chinook salmon in the Upper Salmon River (Sawtooth Weir and Rotary Screw Trap).

Year	Escapement	Females	Redds	Females/Redd	Redds/Female	Fry	Parr	Presmolt	Smolt
2000	553	168	126	1.33	0.75	18,674	24,538	35,289	28,096
2001	1304	484	275	1.76	0.57	158,479	120,538	44,452	28,182
2002	1419	663	378	1.75	0.57	213,696	74,005	119,332	34,049
2003	775	400	227	1.76	0.57	50,533	62,877	74,409	47,435
2004	748	267	139	1.92	0.52	41,511	79,575	98,146	17,682
2005	457	186	144	1.29	0.77	25,713	121,373	136,300	12,010
2006	441	128	93	1.38	0.73	12,959	16,293	96,331	9,964
2007	215	64	48	1.33	0.75	N/A	27,500	47,483	5,728
2008	592	118	99	1.20	0.84	11,640	41,787	29,245	12,015
2009	447	166	103	1.61	0.62	45,619	31,640	58,200	15,270
2010	771	189	164	1.15	0.87	5,662	96,413	34,307	8,386
2011	657	228	118	1.93	0.52	N/A	76,712	62,954	13,481
2012	816	284	215	1.32	0.76	20,425	36,377	48,528	29,701
2013	413	73	58	1.26	0.79	5,289	12,106	7,719	5,240
2014	705	268	141	1.90	0.53	17,546	18,872	14,717	5,904
2015	399	121	73	1.66	0.60	14,908	30,451	23,907	N/A
2016	438	229	125	1.83	0.55	N/A	N/A	N/A	N/A
Mean	656	237	149	1.6	0.7	45,904	54,441	58,207	18,210
Maximum	1,419	663	378	1.9	0.9	213,696	121,373	136,300	47,435

Supplemental Table C-2. Adult escapement, redd counts, and juvenile production data for Chinook salmon in the Pahsimeroi River (Pahsimeroi Weir and Rotary Screw Trap).

Year	Escapement	Females	Redds	Females/Redd	Redds/Female	Fry	Parr	Presmolt	Smolt
2000	105	48	51	0.95	1.05	7,595	336	5,274	4,083
2001	329	168	173	0.97	1.03	20,202	8,904	27,272	6,189
2002	322	174	125	1.39	0.72	12,681	162	26,232	3,433
2003	822	439	354	1.24	0.81	28,560	1,069	36,908	6,187
2004	517	251	235	1.07	0.94	16,229	1,003	13,026	6,731
2005	681	356	273	1.30	0.77	26,449	446	45,619	6,595
2006	186	94	64	1.46	0.68	4,995	338	6,069	1,853
2007	166	72	77	0.94	1.07	2,443	747	9,863	1,080
2008	224	92	82	1.13	0.89	5,034	N/A	13,217	4,090
2009	338	159	199	0.80	1.25	15,543	2,747	24,672	7,934
2010	328	147	100	1.47	0.68	3,531	12,060	20,978	7,678
2011	436	209	113	1.85	0.54	15,946	5,513	22,001	8,253
2012	234	89	78	1.14	0.88	5,931	N/A	37,374	6,693
2013	387	74	56	1.32	0.76	6,377	2,209	5,991	3,486
2014	776	327	291	1.12	0.89	33,672	5,290	18,806	3,679
2015	580	186	172	1.08	0.92	11,578	2,426	11,226	N/A
Mean	402	180	153	1.2	0.9	13,548	3,089	20,283	5,198
Maximum	822	439	354	1.8	1.2	33,672	12,060	45,619	8,253

Supplemental Table C-3. Adult escapement, redd counts, and juvenile production data for Chinook salmon in the Lemhi River (Lower Lemhi IPTDS [LLR] and L3A0, LRW, and HYC Rotary Screw Traps).

Year	Escapement	Females	Redds	Females/ Redd	Redds/ Female	L3A0				LRW				HYC			
						Fry	Parr	Presmolt	Smolt	Fry	Parr	Presmolt	Smolt	Fry	Parr	Presmolt	Smolt
2008	N/A	N/A	N/A	N/A	N/A	N/A	N/A	N/A	N/A	0	15	5,905	1,143	N/A	22	10,590	1,172
2009	N/A	N/A	N/A	N/A	N/A	N/A	N/A	N/A	N/A	3,796	4444	39,634	3,710	7,468	1,953	8,053	983
2010	156	51	126	0.4	2.4	N/A	N/A	N/A	N/A	799	783	18,818	2,654	13,763	1,657	16,739	826
2011	267	101	184	0.6	1.8	N/A	N/A	N/A	16,842	1,372	354	26,858	5,387	15,507	1,571	17,501	947
2012	83	N/A	98	N/A	N/A	0	0	15,307	6,519	445	461	6,128	5,167	16,447	665	9,476	1,468
2013	393	98	131	0.8	1.3	0	0	17,056	14,440	0	160	12,330	6,288	N/A	536	6,164	1,160
2014	464	269	288	0.9	1.1	0	2,878	56,436	19,816	21,971	2,428	40,978	15,226	59,431	1,617	15,178	732
2015	718	337	310	1.1	0.9	0	862	52,523	N/A	19,965	1,334	21,549	N/A	35,473	2,195	24,196	N/A
Mean	347	172	190	0.7	1.5	0	935	35,330	14,404	6,044	747	21,525	5,653	24,682	1,277	1,041	13,487
Max.	718	337	310	1.1	2.4	0	2,878	56,436	19,816	21,971	2,428	40,978	15,226	59,431	2,195	1,468	24,196

Generalized Capacity Model

Chinook salmon

Supplemental Table C-4. Estimated redds, eggs, summer parr, and winter presmolt capacity requirements for Chinook salmon in the Upper Salmon River. Recent capacity requirements are based on the mean and maximum estimated escapement to the Upper Salmon River, 2000-2016. De-listing capacity requirements are based on NOAA de-listing adult escapement targets.

Life Stage	Recent		De-listing
	Mean	Maximum	
Escapement	656	1,419	1,000
Redd	321	695	490
Eggs	1,700,372	3,678,497	2,592,100
Parr	493,108	1,066,764	751,709
Presmolt	199,793	432,221	304,570

Supplemental Table C-5. Estimated redds, eggs, summer parr, and winter presmolt capacity requirements for Chinook salmon in Valley Creek. Recent capacity requirements are based on the mean and maximum estimated escapement to Valley Creek, 2010-2015. De-listing capacity requirements are based on NOAA de-listing adult escapement targets.

Life Stage	Recent		De-listing
	Mean	Maximum	
Escapement	506	739	500
Redd	248	362	245
Eggs	1,311,603	1,915,562	1,296,050
Parr	308,365	555,513	375,855
Presmolt	154,112	225,077	152,285

Supplemental Table C-6. Estimated redds, eggs, summer parr, and winter presmolt capacity requirements for Chinook salmon in the Yankee Fork Salmon River. Recent capacity requirements are based on the mean and maximum estimated escapement the Yankee Fork Salmon River, 2012-2015. De-listing capacity requirements are based on NOAA de-listing adult escapement targets.

Life Stage	Recent		De-listing
	Mean	Maximum	
Escapement	248	343	500
Redd	121	168	245
Eggs	641,545	889,090	1,296,050
Parr	186,048	257,836	375,855
Presmolt	75,381	104,467	152,285

Supplemental Table C-7. Estimated redds, eggs, summer parr, and winter presmolt capacity requirements for Chinook salmon in the East Fork Salmon River. Recent capacity requirements are based on the mean and maximum estimated escapement to the East Fork Salmon River, 2010-2015. De-listing capacity requirements are based on NOAA de-listing adult escapement targets.

Life Stage	Recent		De-listing
	Mean	Maximum	
Escapement	283	343	1,000
Redd	139	168	490
Eggs	733,046	889,090	2,592,100
Parr	212,583	257,836	751,709
Presmolt	86,132	104,467	304,570

Supplemental Table C-8. Estimated redds, eggs, summer parr, and winter presmolt capacity requirements for Chinook salmon in the Pahsimeroi River. Recent capacity requirements are based on the mean and maximum estimated escapement to the Pahsimeroi River, 2000-2015. De-listing capacity requirements are based on NOAA de-listing adult escapement targets.

Life Stage	Recent		De-listing
	Mean	Maximum	
Escapement	402	822	1,000
Redd	197	403	490
Eggs	1,042,496	2,129,424	2,592,100
Parr	302,034	617,533	751,709
Presmolt	122,375	250,206	304,570

Supplemental Table C-9. Estimated redds, eggs, summer parr, and winter presmolt capacity requirements for Chinook salmon in the Lemhi River. Recent capacity requirements are based on the mean and maximum estimated escapement to the Lemhi River, 2010-2015. De-listing capacity requirements are based on NOAA de-listing adult escapement targets.

Life Stage	Recent		De-listing
	Mean	Maximum	
Escapement	347	718	2,000
Redd	170	352	980
Eggs	899,027	1,861,128	5,184,200
Parr	260,718	539,727	1,503,418
Presmolt	105,635	218,681	609,140

Supplemental Table C-10. Estimated redds, eggs, summer parr, and winter presmolt capacity requirements for Chinook salmon in the North Fork Salmon River. Recent capacity requirements are based on the mean and maximum estimated escapement for the North Fork Salmon River, 1991-2017. De-listing capacity requirements are based on NOAA de-listing adult escapement targets.

Life Stage	Recent		De-listing
	Mean	Maximum	
Escapement	55	208	500
Redd	27	102	245
Eggs	142,486	540,297	1,296,050
Parr	41,321	156,686	375,855
Presmolt	16,742	63,485	152,285

Supplemental Table C-11. Estimated redds, eggs, summer parr, and winter presmolt capacity requirements for Chinook salmon in Panther Creek. Recent capacity requirements are based on the mean and maximum estimated escapement for Panther Creek, 2001-2017. De-listing capacity requirements are based on NOAA de-listing adult escapement targets.

Life Stage	Recent		De-listing
	Mean	Maximum	
Escapement	20	115	750
Redd	10	56	368
Eggs	51,616	297,210	1,944,075
Parr	14,969	86,191	563,782
Presmolt	6,065	34,922	228,427

Steelhead

Supplemental Table C-12. Estimated redds, eggs, summer parr, and winter presmolt capacity requirements for steelhead in the Upper Salmon River. Recent capacity requirements are based on the mean and maximum estimated escapement to the Upper Salmon River, 2010-2015. De-listing capacity requirements are based on NOAA de-listing adult escapement targets.

Life Stage	Recent		De-listing
	Mean	Maximum	
Escapement	92	154	480[1]
Redd	51	85	267
Eggs	251,959	420,995	1,313,402
Parr	33,826	56,519	176,324
Presmolt	12,131	20,269	63,235

[1]The de-listing escapement for the Upper Salmon River was determined by multiplying the de-listing goal for the entire upper mainstem Salmon River TRT population by the amount of available stream habitat in the Upper Salmon River relative to Valley Creek and the Yankee Fork Salmon River (Table C-4).

Supplemental Table C-13. Estimated redds, eggs, summer parr, and winter presmolt capacity requirements for steelhead in Valley Creek. Recent capacity requirements are based on the mean and maximum estimated escapement to Valley Creek, 2010-2015. De-listing capacity requirements are based on NOAA de-listing adult escapement targets.

Life Stage	Recent		De-listing
	Mean	Maximum	
Escapement	193	278	246
Redd	107	154	136
Eggs	526,244	759,978	671,833
Parr	70,648	102,027	90,194
Presmolt	25,336	36,590	32,346

[1]The de-listing escapement for Valley Creek was determined by multiplying the de-listing goal for the entire upper mainstem Salmon River TRT population by the amount of available stream habitat in Valley Creek relative to the Upper Salmon River and the Yankee Fork Salmon River (Table C-4).

Supplemental Table C-14. Estimated redds, eggs, summer parr, and winter presmolt capacity requirements for steelhead in the Yankee Fork Salmon River. Recent capacity requirements are based on the mean and maximum estimated escapement the Yankee Fork Salmon River, 2012-2015. De-listing capacity requirements are based on NOAA de-listing adult escapement targets.

Life Stage	Recent		De-listing
	Mean	Maximum	
Escapement	95	213	274
Redd	53	118	152
Eggs	260,388	582,285	748,498
Parr	34,957	78,172	100,486
Presmolt	12,537	28,035	36,037

[1]The de-listing escapement for the Yankee Fork Salmon River was determined by multiplying the de-listing goal for the entire upper mainstem Salmon River TRT population by the amount of available stream habitat in the Yankee Fork Salmon River relative to the Upper Salmon River and Valley Creek (Table C-4).

Supplemental Table C-15. Estimated redds, eggs, summer parr, and winter presmolt capacity requirements for steelhead in the East Fork Salmon River. Recent capacity requirements are based on the mean and maximum estimated escapement to the East Fork Salmon River, 2012-2015. De-listing capacity requirements are based on NOAA de-listing adult escapement targets.

Life Stage	Recent		De-listing
	Mean	Maximum	
Escapement	30	54	1,000
Redd	17	30	555
Eggs	82,695	147,622	2,733,733
Parr	11,102	19,818	367,004
Presmolt	3,981	7,107	131,618

Supplemental Table C-16. Estimated redds, eggs, summer parr, and winter presmolt capacity requirements for steelhead in the Pahsimeroi River. Recent capacity requirements are based on the mean and maximum estimated escapement to the Pahsimeroi River, 2011-2015. De-listing capacity requirements are based on NOAA de-listing adult escapement targets.

Life Stage	Recent		De-listing
	Mean	Maximum	
Escapement	1,156	1,614	1,000
Redd	641	896	555
Eggs	3,159,649	4,412,245	2,733,733
Parr	424,183	592,344	367,004
Presmolt	152,124	212,431	131,618

Supplemental Table C-17. Estimated redds, eggs, summer parr, and winter presmolt capacity requirements for steelhead in the Lemhi River. Recent capacity requirements are based on the mean and maximum estimated escapement to the Lemhi River, 2010-2015. De-listing capacity requirements are based on NOAA de-listing adult escapement targets.

Life Stage	Recent		De-listing
	Mean	Maximum	
Escapement	337	417	1,000
Redd	187	231	555
Eggs	920,357	1,139,967	2,733,733
Parr	123,558	153,041	367,004
Presmolt	44,311	54,885	131,618

Supplemental Table C-18. Estimated redds, eggs, summer parr, and winter presmolt capacity requirements for steelhead in the North Fork Salmon River. Recent capacity requirements are based on the mean and maximum estimated escapement for the North Fork Salmon River, 2011-2015. De-listing capacity requirements are based on NOAA de-listing adult escapement targets.

Life Stage	Recent		De-listing
	Mean	Maximum	
Escapement	252	349	500
Redd	140	194	277
Eggs	688,354	954,073	1,366,867
Parr	92,412	128,084	183,502
Presmolt	33,141	45,935	65,809

Supplemental Table C-19. Estimated redds, eggs, summer parr, and winter presmolt capacity requirements for steelhead in Panther Creek. Recent capacity requirements are based on the mean and maximum estimated escapement for Panther Creek, 2011-2015. De-listing capacity requirements are based on NOAA de-listing adult escapement targets.

Life Stage	Recent		De-listing
	Mean	Maximum	
Escapement	449	650	500
Redd	249	361	277
Eggs	1,226,353	1,776,927	1,366,867
Parr	164,638	238,552	183,502
Presmolt	59,044	85,551	65,809

Appendix D – Hydraulics and Hydrologic Assessments (Lemhi, Pahsimeroi, and Upper Salmon Rivers)

RECLAMATION
Managing Water in the West

Technical Report No. SRH-2017-17

Lemhi River Hydraulics & Hydrologic Assessment

Columbia-Snake Salmon Recovery Office
Pacific Northwest Region

U.S. Department of the Interior
Bureau of Reclamation
Technical Service Center
Denver, Colorado

April 2017

Mission Statements

The Department of the Interior protects and manages the Nation's natural resources and cultural heritage; provides scientific and other information about those resources; and honors its trust responsibilities or special commitments to American Indians, Alaska Natives, and affiliated island communities.

The mission of the Bureau of Reclamation is to manage, develop, and protect water and related resources in an environmentally and economically sound manner in the interest of the American public.

Technical Report No. SRH-2017-17

Lemhi River Hydraulics & Hydrologic Assessment

Columbia-Snake Salmon Recovery Office
Pacific Northwest Region

U.S. Department of the Interior
Bureau of Reclamation
Technical Service Center
Denver, Colorado

April 2017

Bureau of Reclamation
Technical Service Center, Denver, Colorado
Sedimentation and River Hydraulics Group, 86-68240

Technical Report SRH-2017-17

Lemhi River Hydraulic and Hydrologic Assessment

Columbia-Snake Salmon Recovery Office
Pacific Northwest Region

Caroline Ubing	4/17/17

Prepared by:	Date
Caroline Ubing, M.S., E.I.T., Hydraulic Engineer
Sedimentation and River Hydraulics Group

Sean Kimbrel	4/21/17

Peer Reviewed by:	Date
Sean Kimbrel, M.S., P.E., Hydraulic Engineer
Sedimentation and River Hydraulics Group

4-21-17

Peer Reviewed by:	Date
Amanda Stone, M.S., P.E., Hydrologic Engineer
Flood Hydrology and Meteorology Group

Peer Review Certification: *This document has been peer reviewed and is believed to be in accordance with the service agreement and standards of the profession.*

Table of Contents

page

1 Purpose and Scope 3

2 Lemhi Subbasin Characteristics..4

2.1 Available Discharge Data 6
2.2 Hydrologic Influences...7
2.3 Gaged Flow Characteristics 9

3 Methods..16

3.1 Hydrologic Assessment 16
3.1.1 Peak Flow Calculations at Gaged Locations 19
3.1.2 Peak Flow Calculations at Ungaged Locations 19
3.2 Stream Power Analysis 20
3.3 Data Collection 22
3.3.1 Instrumentation 22
3.3.2 Data Collection Methodology.. 22
3.3.3 Post-Processing Methodology 26
3.3.4 Discharge Uncertainty Discussion... 28

4 Results 30

4.1 Hydrologic Assessment Results...30
4.1.1 Peak Flow Calculations at Gaged Locations 30
4.1.2 Peak Flow Calculations at Ungaged Locations 34
4.2 Stream Power Analysis Results 36
4.3 Discharge Measurement Results..39
4.3.1 High Flow Discharge Measurements... 39
4.3.2 Low Flow Discharge Measurements 43
4.3.3 Discharge Measurement Comparison.. 46
4.4 Water Surface Elevation Measurements.......................................47
4.5 Pebble Count Measurement Results 48

5 Data Gaps and Recommendations 52

5.1 Existing Data for the Lemhi River Basin.......................................53
5.2 Bathymetric Data Collection Options..56
5.3 Hydrologic Data Gaps...57
5.4 Stream Power Assessment Recommendations 57
5.5 Field Data Recommendations...58

6 Conclusion 61

7 References..62

8 Appendix A – Annual Hydrographs 64

9 Appendix B – Annual Peak Streamflow 76

10 Appendix C – ADCP Discharge Measurements.........................79

11 Appendix D – Survey Data...80

12 Appendix E – Pebble Count Data 95

Tables

page
Table 1.–USGS and IWRB stream gage information for gages on the Lemhi River with more than 10 years of record. 6
Table 2.–Low flow discharge values 14
Table 3.–Coverage factors to determine variability in transect discharges 28
Table 4.–Gage and flood frequency results, in cfs, from USGS stream gage locations. 30
Table 5.–Recommended Peak Discharge Values along the Lemhi River. 36
Table 6.–Stream Power Analysis Results 39
Table 7.–Discharge measurements along the Lemhi River during high flows..... 40
Table 8.–Discharge measurements of contributing tributaries. 40
Table 9.–Comparison of discharge measurements and gage record..................... 40
Table 9.–Discharge measurements along the Lemhi River and contributing tributaries during the low flow season. 44
Table 10.–Discharge measurements in contributing tributaries during the low flow seasons 44
Table 12.–Comparison of discharge measurements and gage record................... 44
Table 11.–Discharge measurement comparison 46
Table 12.–Water Surface Profile Measurement Comparison. Elevation values are in NAVD88 ft. 48
Table 13.–Pebble count results 49
Table 14.–Discharge upper and lower limits for high flow measurements. 59
Table 15.–Discharge upper and lower limits for low flow measurements. All discharge measurements were taken with a velocity meter during the low flow season. 59

Figures

page
Figure 1.–USGS, IWRB, and SNOTEL Gage Locations 5
Figure 2.–Map of Lemhi Basin including points of diversion with the legal diversion rates (m^3/s). The triangle represents USGS gage 13305310 and the star identifies the Lower Granite Dam located far downstream on the Lower Snake River. Figure source: Walters et al., 2013. 8
Figure 3.–A hydrologic constriction divides the basin between RM 34 and 25..... 9
Figure 4.–Mean and median daily discharge values for the entire period of record for the DS USGS Gage (13305310), near Salmon, ID. Day-of-Year numbers the days of the year with January 1st and December 31st represented as 1 and 366, respectively. 10

Figure 5.–Mean and median daily discharge values for the entire period of record for US USGS Gage (13305000), near Lemhi, ID. 11
Figure 6.–2003 Annual hydrograph for the Lemhi River. The discharge data is denoted by the thin orange and blue lines, which align with discharge on the primary (left) y-axis. Snow Water Equivelent (SWE) is denoted by the thick gray line and values correspond with the secondary (right) y-axis. SWE data was downloaded from the Snow Telemetry (SNOTEL) data set developed by the Nationl Resources Conservation Service (NRCS) from site ID620. 12
Figure 7.–Comparison of annual peak events over the two gages. Dots next to the year indicate years were the annual peaks between gages occurred during different events. Diagonally hatched data points indicate events that occurred outside of the snowmelt runoff period. 13
Figure 8.–Theil-Sen line at the DS gage (13305000) with 60 years of record. 14
Figure 9.–Daily discharge for 1994. Notice that flows approach zero at the DS gage (RM 7.3), but fluctuate between 50 and 100cfs at the US gage at RM 26.7. 15
Figure 10.–Valley segments and geomorphic reaches labeled by river mile. 16
Figure 11.–Peak Flow estimation locations. River miles of flow estimation sites are labeled in black along the Lemhi River. Drainage area values are labeled in blue along the edges of the drainage basins. 18
Figure 12.– Example of average reach slope determination using a trendline fit to topographic data. Figure represents geomorphic reach 1 from the confluence to RM 3.3. The average slope for this reach is 0.0073 ft/ft. 21
Figure 13.–The site at RM 33 was an ideal discharge measurement location. The site featured a straight run, with little to no vegetation, and a flat water surface with no eddies. 23
Figure 14.–Base station located over staked control point. 25
Figure 15.–Pebble axis measurement (Harrelson, Rawlins, & Potyondy, 1994) . 26
Figure 16.–Mid-section method for computing discharge (HACH, 2012). 27
Figure 17.–Peak discharge values plotted across annual exceedance probability (AEP) 31
Figure 18.–Annual Exceedance Curve for USGS Gage 13305310 below L5 Diversion (RM 7.25). Potentially influential low flows (PILF) are plotted with x's while systematic peaks are plotted with circles. 32
Figure 19.–Annual Exceedance Curve for USGS Gage 13305000 near Lemhi (RM 26.7) 32
Figure 20.–Annual Exceedance Curve for IWRB Gage on the Lemhi River at Cottom Lane (RM 48.8).. 33
Figure 21.–Annual Exceedance Curve for IWRB Gage on the Lemhi River above Big Springs (RM 52.9)... 33
Figure 22.–Estimated peak discharge values at RM 19.1. 34
Figure 23.–Estimated discharge values for the 100-yr event............................... 35
Figure 24.–Estimated discharge values along the Lemhi River. 37
Figure 25.–Lemhi River longitudinal profile and slope by river mile. 38
Figure 26.–Total stream power results by river mile. 38
Figure 27.–High flow discharge measurement locations. USGS and IWRB gages are included on the map and compared to the measured discharge. A comparison

was not conducted on the DS USGS gage as a tributary flows into the Lemhi in between the gage and measurement location, making the value incompatible. ... 41
Figure 28.–Examples of challenging discharge measurement transects at RM 36.4 (left) and on Hayden Creek (right). Notice that both measurements have high error values. 42
Figure 29.–Acoustic Doppler current profiler transducer beam pattern and regions of unmeasured velocity in each profile (from Simpson, 2002). 43
Figure 30.–Low flow discharge measurement locations. USGS and IWRB gages are included on the map and compared to the measured discharge. 45
Figure 31.–Split channel with missing flow at RM 40.8. 47
Figure 32.–Median and most frequent (mode) grain sizes in run or riffle features with respect to river miles. 49
Figure 33.–Sediment grain size distribution for RM 36.4 and RM 0.4 50
Figure 34.–Exposed channel bed photos at RM 40.8 (left) and RM 0.4 (right). Boot toe is approximately 95mm for scale. 51
Figure 35.–Well graded sediment beneath the armor layer at RM 24.3. The pen provides relative scale. 51
Figure 36.–Topographic LiDAR Extent 53
Figure 37.–2013 topographic and bathymetric LiDAR extent 55

Acronyms and Abbreviations

%	percent
°C	degrees Celsius
°F	degrees Fahrenheit
°N	latitude degrees north
°N	longitude degrees west
2D	two-dimensional
AEP	Annual Exceedance Probability
ADCP	Acoustic Doppler Current Profiler
cfs	cubic feet per second
CORS	Continuously Operating Reference Station
COV	Coefficient of Variance
D_n	Sediment particle diameter size at n% passing
DS	Downstream
EMA	Expected moments algorithm
Eq	Equation
ESA	Endangered Species Act
Ft	foot/feet
GIS	Geographic Information System
GNSS	Global Navigation Satellite Systems
GPS	Global Positioning System
HSI	Habitat Suitability Index
IACWD	Interagency Advisory Committee on Water Data
IDEQ	Idaho Department of Environmental Quality
IDWR	Idaho Department of Water Resources
IWRB	Idaho Water Resources Board
Km	kilometer
LiDAR	Laser Imaging, Detection and Ranging
MGBT	Multiple Grubbs-Beck test
Mi	mile(s)
Mm	millimeter

NAD	North American Datum
NAVD	North American Vertical Datum
NRCS	National Resources Conservation Service
No.	number
OPUS	Online Position User Service
PILF	Potential influential low flows
PN	Pacific Northwest
Reclamation	Bureau of Reclamation
RM	River mile
RMS	Root Mean Square
RTK	Real Time Kinematic
RTS	Resource and Technical Services
SNOTEL	Snow Telemetry
SRH	Sedimentation and River Hydraulics Group
SWE	Snow water equivalent
TSC	Technical Service Center
U.S.	United States
US	Upstream
USACE	U.S. Army Corps of Engineers
USGS	U.S. Geological Survey
USFS	U.S. Forest Service
WSE	Water Surface (Elevation)

Symbols

DA_u	Contributing drainage area at the ungaged site (mi^2)
DA_g	Contributing area at the gaged site (mi^2)
DA_{g1}	Contributing area at the upstream gaged site (mi^2)
DA_{g2}	Contributing area at the downstream gaged site (mi^2)
Q	Flow discharge or rate (ft^3/s)
Q_u	discharge at an ungaged site (ft^3/s)
Q_g	discharge at the gaged site (ft^3/s)
Q_{g1}	discharge at the upstream gaged site (ft^3/s)
Q_{g1}	discharge at the downstream gaged site (ft^3/s)
S	slope (ft/ft)
γ	specific weight of water (lb/ft^3)
Ω	total stream power (lb/s)

Executive Summary

The information provided in this report is intended to advise an Integrated Rehabilitation Assessment of the Lemhi River Basin, where the goal is to characterize watershed conditions within the river basin while providing context for future analyses and potential rehabilitation projects. The objectives of this report include: peak flow frequency estimates, a stream power assessment, discharge and water surface elevation measurements, and bottom sediment characteristics. These data were then combined to develop a list of data needs for future hydraulic modeling analyses.

The Lemhi River flow regime is snowmelt dominated with numerous diversions which are in operation from April through September. While diversion locations and volumes are regulated, exact withdrawal rates on a seasonal and daily basis are unknown. Groundwater is another important component of the Lemhi River water budget. Groundwater levels are highest from May to September due to snowmelt and irrigation. A natural constriction occurs between river mile (RM) 34 and 25 that divides the upper and lower regions of the basin. Flood frequency peaks were estimated at two United States Geological Survey (USGS) gages and two Idaho Water Resources Board (IWRB) gages using the PeakFQ program and at 23 ungaged locations applying a drainage area ratio.

River Mile	DA (mi^2)	Valley Segment	Estimated Flood-Frequency Values (cfs)						
			1.5	2	5	10	25	50	100
0.1	1260	4	912	1,223	2,059	2,638	3,371	3,913	4,444
19.1	1055	3	771	1,018	1,670	2,113	2,666	3,069	3,462
32.7	733	2	463	586	892	1,089	1,326	1,494	1,654
60.4	470	1	197	228	257	292	331	357	381

A stream power assessment was completed to investigate the potential sediment transport capacity of each geomorphic reach. Results show that stream power was primarily dependent on the discharge input; thus, stream power increased in the downstream direction with increasing peak discharge.

Discharge and water surface elevation measurements were collected during the high flow (May) and low flow (August) seasons. These data were collected with the intension of calibrating a future hydraulic model. Pebble counts were collected during the low flow season to characterize the bed material. Results show that the coarsest sediment was observed from RM 33 to RM 21.

The information necessary to build a hydraulic model is dependent on the level of detail and the questions being asked. For future project-based hydraulic modeling analyses to assess habitat uplift along the Lemhi River, a two-dimensional (2D) hydraulic model is recommended. Data gaps necessary for hydraulic modeling include bathymetry data and an improved understanding of diversion outflows, tributary inflows, and groundwater contributions.

1 Purpose and Scope

The Bureau of Reclamation's (Reclamation) Resource and Technical Services (RTS) in the Pacific Northwest (PN) Regional Office tasked Reclamation's Sedimentation and River Hydraulics (SRH) Group at the Technical Service Center (TSC) with supporting a coarse level Integrated Rehabilitation Assessment of the Lemhi River Basin. The Lemhi River extends 63.3 river miles (RM) from the headwaters in Leadore, ID (RM 63.3) to the confluence with the Salmon River in Salmon, ID (RM 0).

The primary objective was to conduct analyses and field assessments to inform hydrology, hydraulics, and sediment trends in support of the coarse-scale Integrated Rehabilitation Assessment. This study focuses on summarizing available hydraulic, streamflow, and sediment data that can be utilized in future reach or project scale hydraulic modeling. Key elements of this report are:

1. Description of hydrologic characteristics in the basin,
2. Regional regression hydrologic assessment of flood-frequency events at multiple locations,
3. Stream power analysis at geomorphic reaches to inform sediment transport capacity,
4. Discharge measurements and surveyed water surface profiles during high flow and low flow seasons,
5. Channel bottom sediment characteristics, and
6. Data gaps for future numerical hydraulic modeling.

The analyses from this report will feed into a watershed-scale geomorphic and fish production model, intended to identify a reach with the most potential for on-the-ground habitat rehabilitation projects for steelhead and spring Chinook. The model develops a fish population and habitat relationship which incorporates twelve different metrics including: average annual discharge, substrate (D_{84}), slow water area, wetted depth, etc. (outlined in Zabel, et al., 2016). Average annual discharge is the primary indicator for population and habitat capacity. Future hydraulic modeling can provide information regarding slow water area and wetted depth. The field data collected in this study can be used to calibrate future hydraulic models, depending on the project location. Finally, the population and habitat relationship can be used to predict fish capacity based on existing physical habitat. The results can then be used to identify locations where future rehabilitation projects could have the greatest benefit.

2 Lemhi Subbasin Characteristics

The Lemhi Subbasin is located in Lemhi County, Idaho. The Lemhi River is a fourth-order stream flowing northwest from its headwaters near Leadore, ID to its outlet into the Salmon River in Salmon, ID. Eighteen Mile and Texas Creeks are headwater sources to the Lemhi River, which then flows through a valley between the Beaverhead Mountains and the Lemhi Range. There are many tributaries from the surrounding canyons in the valley as the river approaches the Salmon River, the largest being Hayden Creek (11% of the Lemhi River Basin). The total watershed area measured from the confluence with the Salmon River is 1,260.5 square miles.

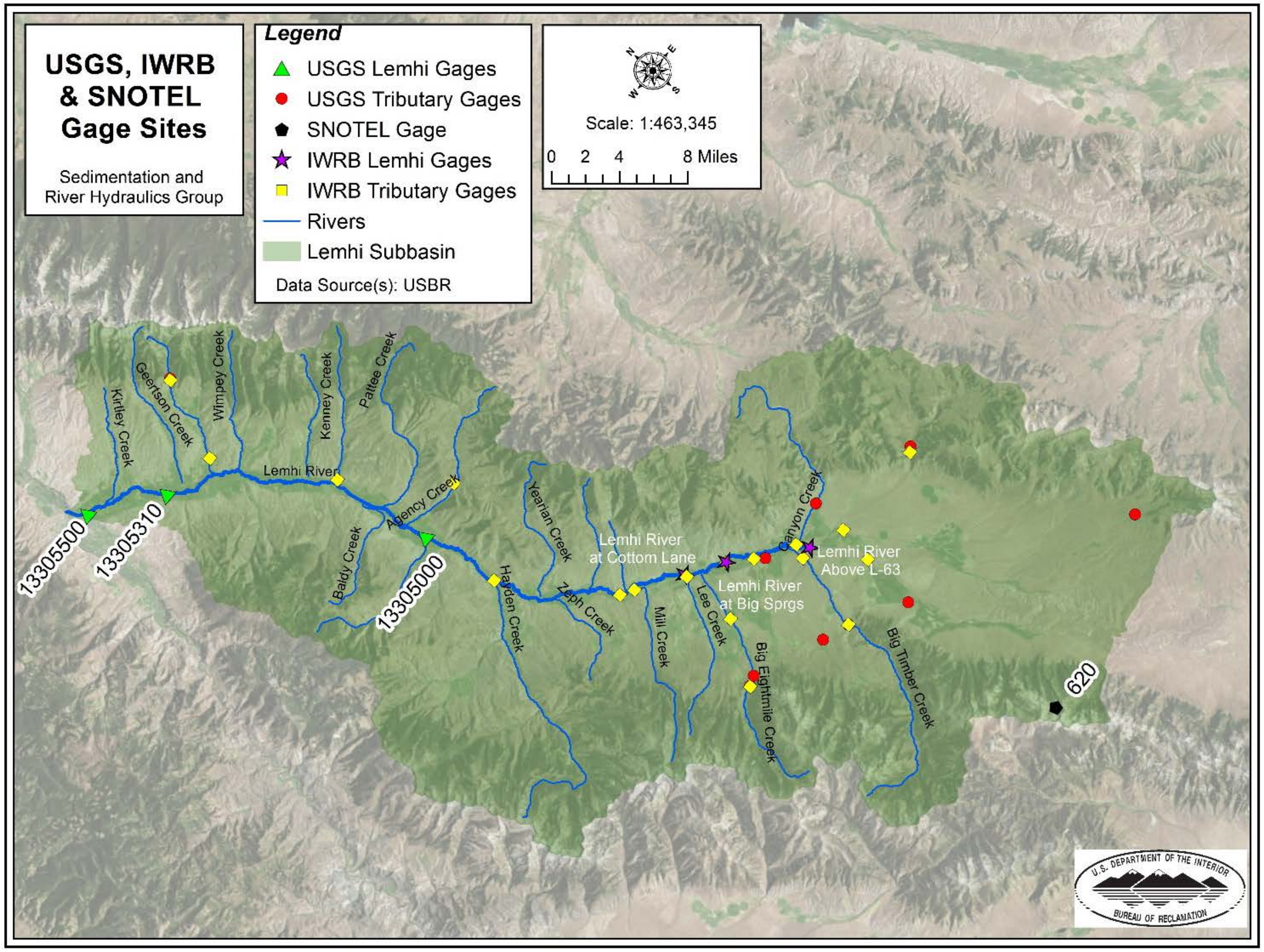

Figure 1.–USGS, IWRB, and SNOTEL Gage Locations

2.1 Available Discharge Data

There are several USGS stream gage stations within the Lemhi Subbasin. Three key gages measure flow on the main stem of the Lemhi River (Figure 1, Table 1). USGS gages with short periods of record were also located along several of the contributing tributaries but were not included in this analysis. A minimum of 10 years for record is recommended for peak flood-frequency analyes (Interagency Avisory Committee on Water Data, 1981).

Idaho Water Resources Board (IWRB) also operates several stream gages within the basin. The period of record on the IWRB gages goes back to 1997, at the earliest. Three of the gages are located on the Lemhi River, and the remaining eighteen are located on tributaries. The gages report mean daily discharge, although 15-minute interval data may be available upon request.

USGS gages selected for this analysis were on the main stem of the Lemhi River with over 10 years of record: 13305000, 13305500, and 13305310. The records from gages 13305500 and 13305310 were combined. There is no overlap in the period of record, and the gages are located approximately 6 river miles apart. It is likely that gage 13305500 was removed and replaced with gage 13305310. Gage 13305000 will be referred to as the upstream (US) USGS gage, while the combined records of gages 13305500 and 13305310 are referred to as the downstream (DS) USGS gages.

Table 1.–USGS and IWRB stream gage information for gages on the Lemhi River with more than 10 years of record.

					Daily Streamflow (cfs)		
Agency	**Gage No.**	**Description**	**Drainage Area (mi^2)**	**Period of Record**	**Min.**	**Mean**	**Max.**
USGS	13305000	Lemhi River near Lemhi ID	907[1]	1938 - 2017[2]	34	256	2100
USGS	13305310	Lemhi River Below L5 Diversion near Salmon, ID	1,216[1]	1992 - 2017	1	253	2610
USGS	13305500	Lemhi River at Salmon, ID	1,258	1928 - 1943	14	246	2300
IWRB	13304400	Lemhi River at Cottom Lane	577	2006-2017	43	144	609
IWRB	13304160	Lemhi River above Big Springs	486	2006-2017	30	89	371

[1]Drainage area for these two gages contradicted between two sources. The USGS website assigns a drainage area of 897mi^2 and 1,256mi^2 to gages 13305000 and 13305310, respectively. Berenbrock (2002) recorded the drainage area as 907.1, and 1,216. The values from Berenbrock (2002) were utilized for consistency with the analysis. Gage 13305000 will be refered to as the upstream (US) USGS gage and gages 13305310 and 13305500 will be refered to as the downstream (DS) USGS gages.

[2]Annual peaks begin in 1956 and end in 2015.

2.2 Hydrologic Influences

Discharge values along the Lemhi River are impacted by irrigation withdrawals, groundwater flows, and tributaries. Over 250 diversions exist along the Lemhi River, primarily for irrigation (IDWR, 2006), which impacts flow rates during the irrigation season (typically April through September). Legal diversion rates were mapped in a study by Walters et al, published in 2013, presented in Figure 2. While diversion locations and volumes are regulated, exact withdrawal rates on a seasonal and daily basis are unknown.

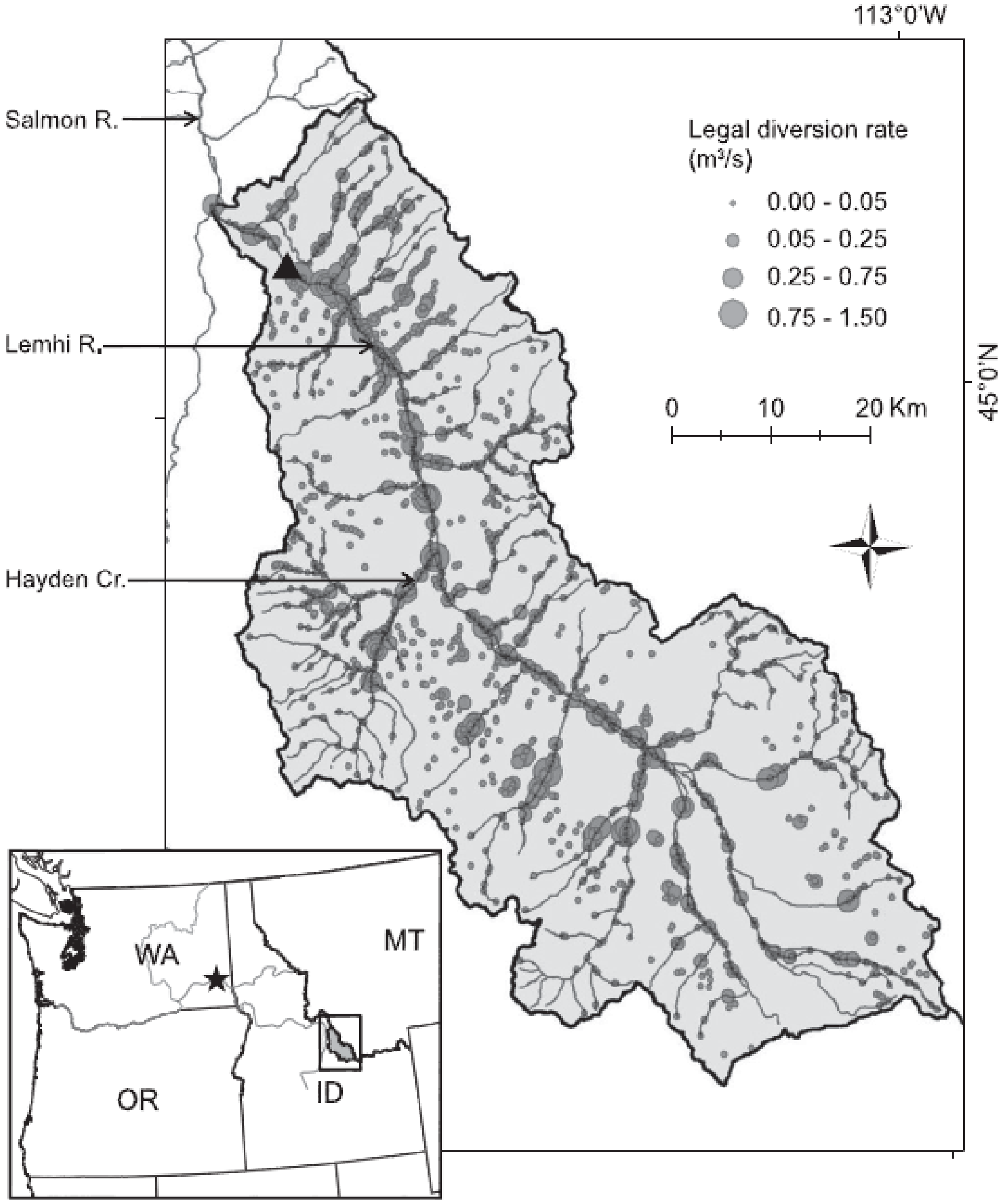

Figure 2.–Map of Lemhi Basin including points of diversion with the legal diversion rates (m^3/s). The triangle represents USGS gage 13305310 and the star identifies the Lower Granite Dam located far downstream on the Lower Snake River. Figure source: Walters et al., 2013.

The USGS published an investigation of the relationship between surface water and ground water in the Lemhi River basin in 1998 demonstrating that groundwater underflow is an important component of the basin's annual water budget. The study described a hydrologic groundwater constriction between RM 34 and RM 25 that divides the upper and lower regions of the basin, Figure 3. The alluvial layer in the upper basin averages 200 feet thick, which allows groundwater to be rapidly and broadly transmitted. Downstream of RM 34, the alluvium is less than 20 ft thick and approximately 3,300 feet wide. The rise in bedrock and thin alluvial layer contracts the aquifer, creating this natural hydrologic groundwater constriction. Groundwater levels are highest from May to September due to snowmelt and irrigation. The application water to nearby agricultural fields during the summer months increases the water table (Donato, 1998). Idaho Department of Water Resources (IDWR) confirmed the influence of groundwater through a seepage study performed in 2008. IDWR measured streamflows, diversion rates, and return flows to quantify gaining and returning flows.

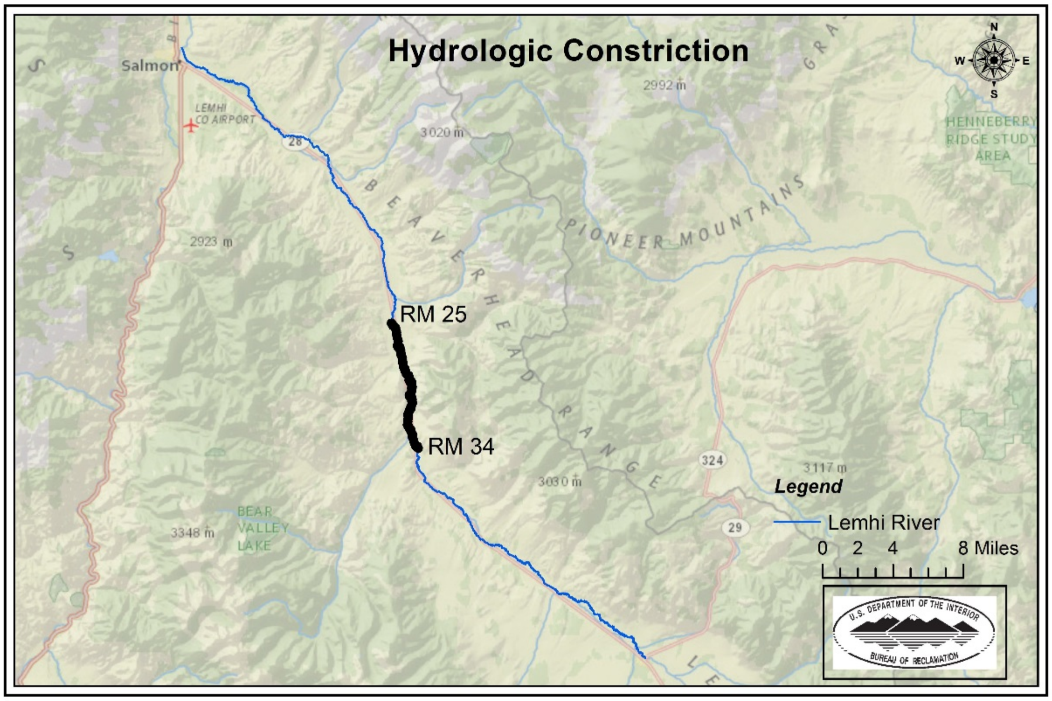

Figure 3.–A hydrologic constriction divides the basin between RM 34 and 25.

2.3 Gaged Flow Characteristics

Most peak flows on the Lemhi River occur during the snowmelt runoff period (typically May to June) and minimum flows typically occur in August and September (Figure 4 and Figure 5). The irrigation season and associated irrigation in the basin typically starts around April 1. Diversions are shut off at the end of the irrigation season (typically October 1st), and streamflows increase to natural winter flow volumes, approximately 200 cfs at both gages, which is maintained through April (Day 91; IDEQ, 2012). Hayden Creek is a reasonable, preliminary estimation of the natural hydrograph shape to be expected in the basin as there are eleven small diversions upstream of the IDWR gage (R. Sager, personal communication, 4/26/2017; Figure 6).

Annual hydrographs plotting snow water equlivalent and daily discharge values for USGS gages 13305000 and 13305310 are included in Appendix A – Annual Hydrographs. Figure 7 illustrates the typical annual flow pattern on the Lemhi River. Annual peak streamflow in the Lemhi River is typically associated with peak spring runoff. Flows steadily decrease until the irrigation season when the discharge falls below 100cfs. Withdrawals result in lower flows at the DS gage (13305310, RM 7.25) compared to the US gage (13305000, RM 26.7) from late July through October (Figure 7).

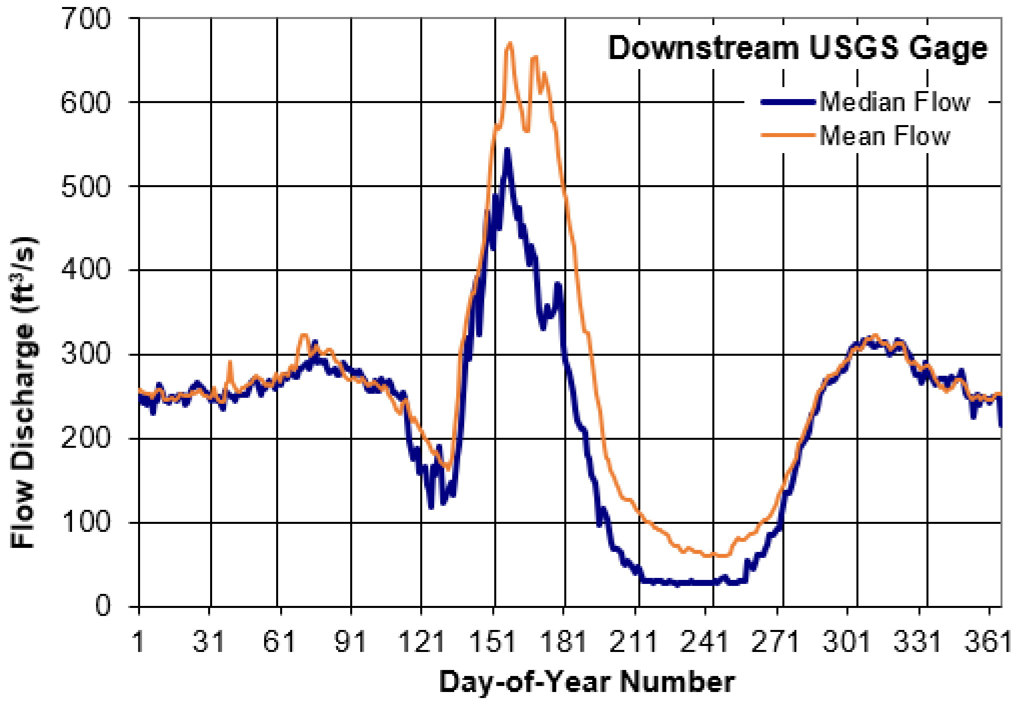

Figure 4.–Mean and median daily discharge values for the entire period of record for the DS USGS Gage (13305310), near Salmon, ID. Day-of-Year numbers the days of the year with January 1st and December 31st represented as 1 and 366, respectively.

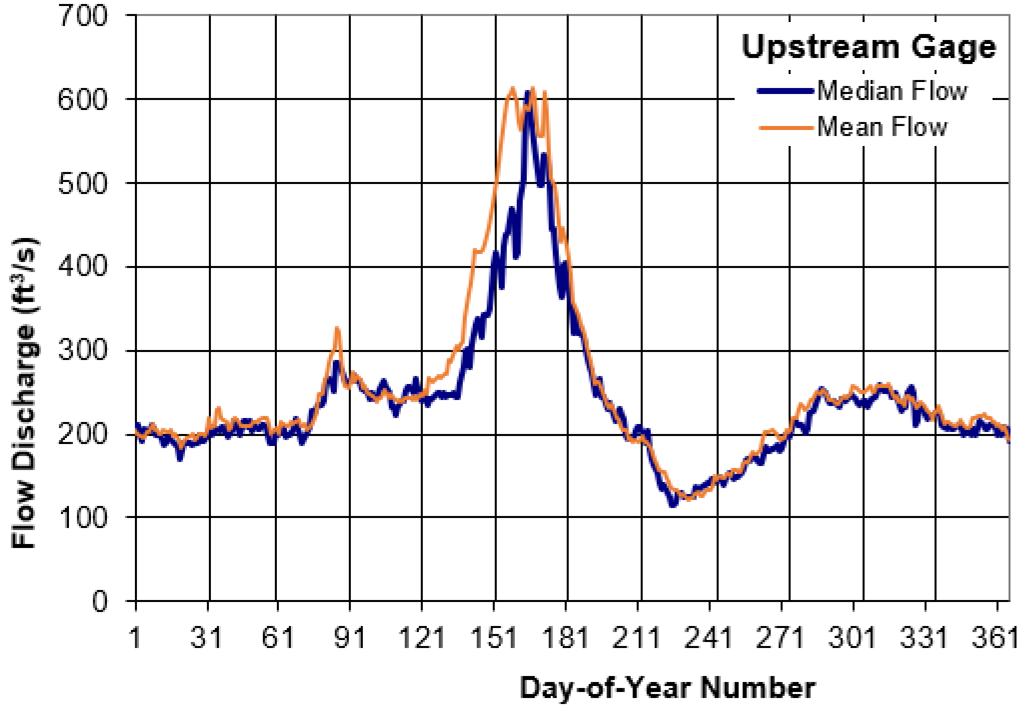

Figure 5.–Mean and median daily discharge values for the entire period of record for US USGS Gage (13305000), near Lemhi, ID.

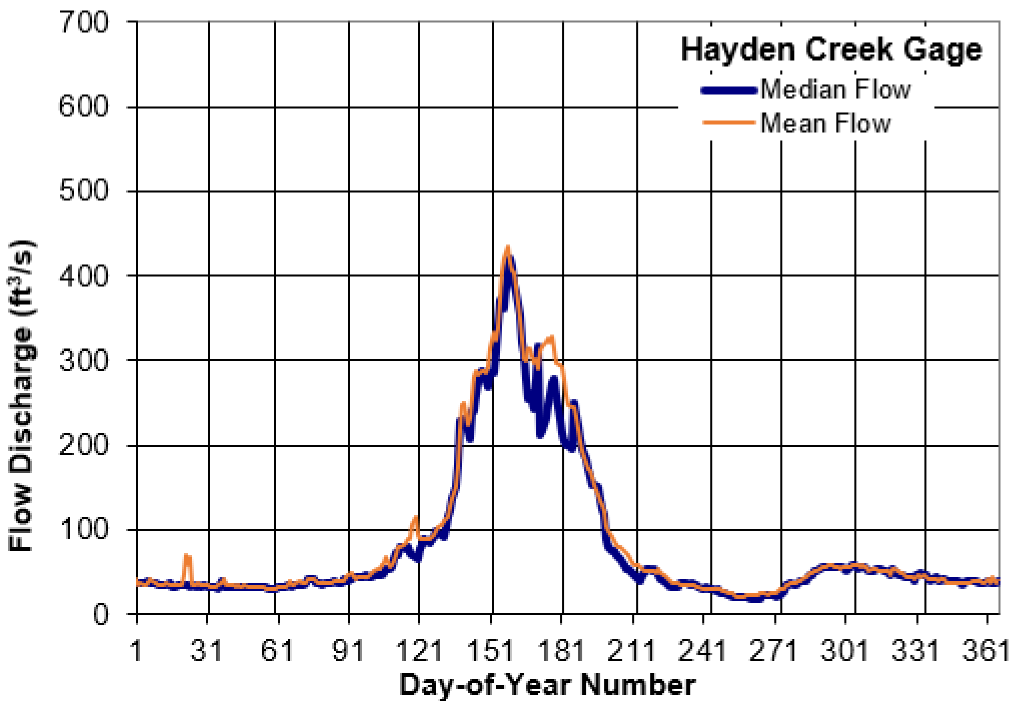

Figure 6.–Mean and median daily discharge values for the entire period of record for the IDWR gage on Hayden Creek.

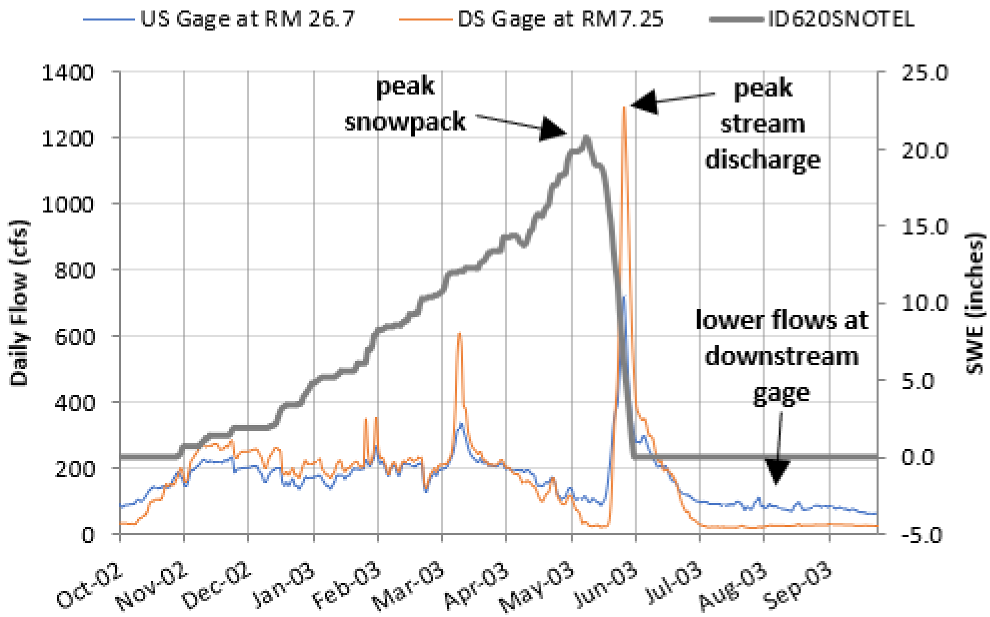

Figure 7.–2003 Annual hydrograph for the Lemhi River. The discharge data is denoted by the thin orange and blue lines, which align with discharge on the primary (left) y-axis. Snow Water Equivelent (SWE) is denoted by the thick gray line and values correspond with the secondary (right) y-axis. SWE data was downloaded from the Snow Telemetry (SNOTEL) data set developed by the Nationl Resources Conservation Service (NRCS) from site ID620.

The annual peak discharge values for both gages are presented in Appendix B – Annual Peak Streamflow. Comparing the two gages, 13 of the 23 overlapping peak annual discharge values occurred during the same event (the same day or the day after). The majority of the annual peak flows occurred during the period of snowmelt runoff (87%). Annual peaks outside of the snowmelt runoff period were more frequent near the confluence, with 11 events in 38 years at the DS gage (13305500 and 13305310) versus three events over 60 years of record at the US gage (13305000). Annual peaks were higher at the DS gage than the US gage for 20 out of the 23 overlapping years of gage record (Figure 8). Larger peaks are expected at the DS gage due to the larger contributing drainage area.

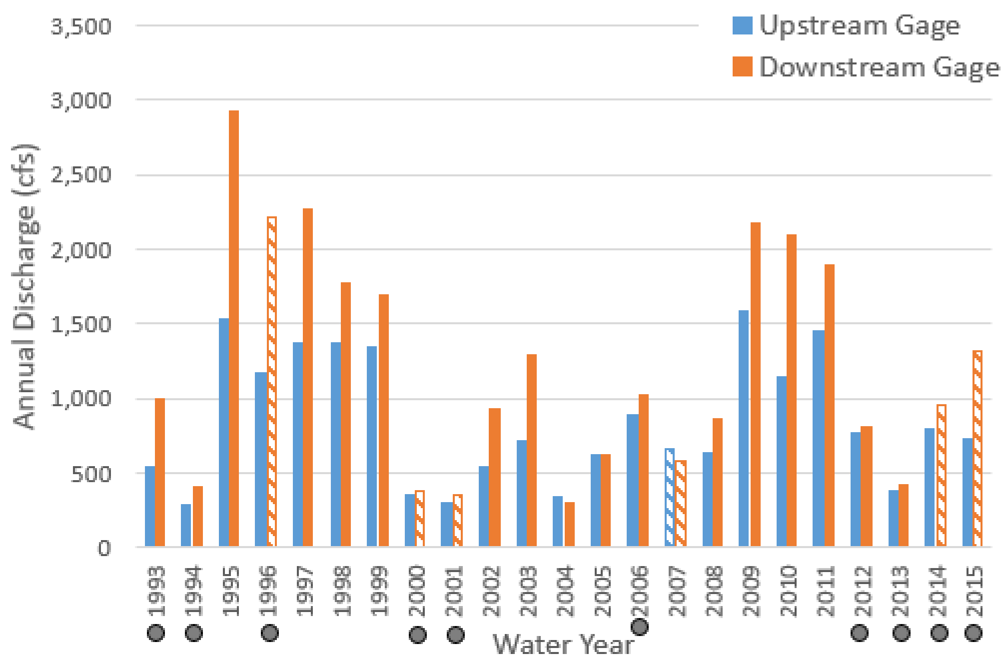

Figure 8.–Comparison of annual peak events over the two gages. Dots next to the year indicate years were the annual peaks between gages occurred during different events. Diagonally hatched data points indicate events that occurred outside of the snowmelt runoff period.

A Theil-Sen slope line (Helsel & Hirsh, 1992) was fit to the annual peaks of the US gage (13305000) to foresee trends in the annual peaks, Figure 9. The annual peaks are decreasing at a rate of 5.6 cfs per year, likely due to an increase in irrigation withdrawals.

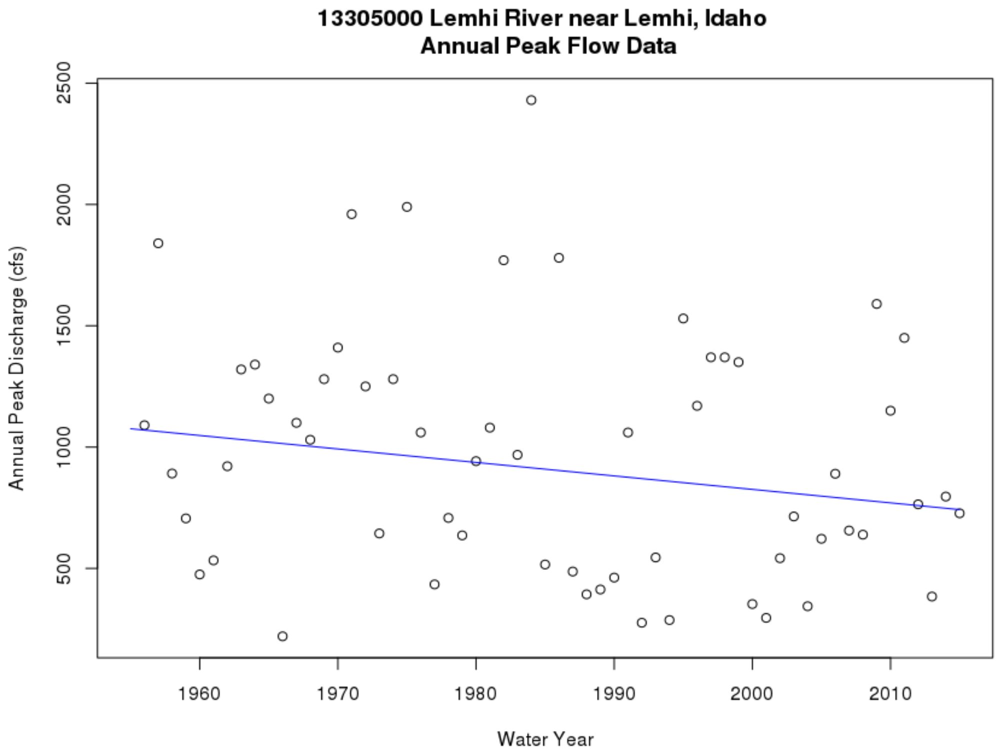

Figure 9.–Theil-Sen line at the DS gage (13305000) with 60 years of record.

A low flow analysis was performed to identify the lowest 7-day average flow that occurs every 10 years (7Q10) at the gage sites using the methods described in Hortness (2006). While estimates for peak flow frequencies were extended throughout the basin, low flow values were not extrapolated to other locations given the highly variable nature of irrigation withdrawals and groundwater influences throughout the watershed. The relative impact of groundwater and irrigation on low flows is likely much larger than the impact on annual peaks. The results are presented in Table 2. The 7Q10 for the DS gage (13305310), near Salmon, ID was significantly lower than the results at the US gage. During the summer of 1994, withdrawals from the Lemhi River resulted in reduction of flows from the upstream to the downstream gage from approximately 80 cfs to nearly zero (Figure 10). Low flow values are lower at the downstream end due to irrigation withdrawals during. Fish passage and water temperature may become an issue during the irrigation season when flow is diverted from the river.

Table 2.–Low flow discharge values

Gage	Period of Record	7Q10 (cfs)
DS - 13305310	1992 - 2016	8
US - 13305000	1938 - 2016	55

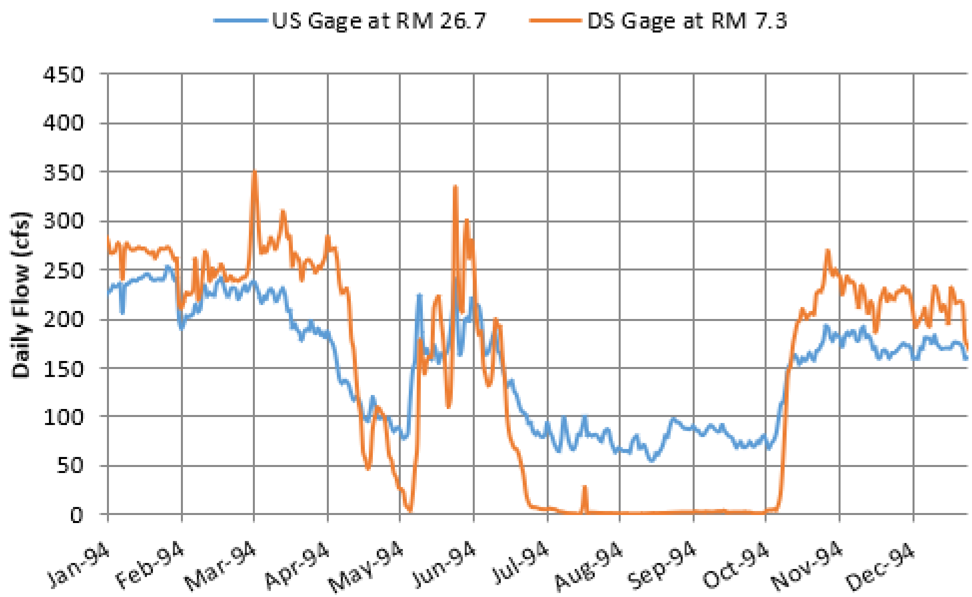

Figure 10.–Daily discharge for 1994. Notice that flows approach zero at the DS gage (RM 7.3), but fluctuate between 50 and 100cfs at the US gage at RM 26.7.

3 Methods

The following sections provide detail on the methodology applied to the hydrologic assessment, stream power analysis, and data collection effort. Valley segments and geomorphic reaches were developed by the PN region and given to TSC to establish consistent locations for the several analyses included in the Integrated Rehabilitation Assessment (Figure 11).

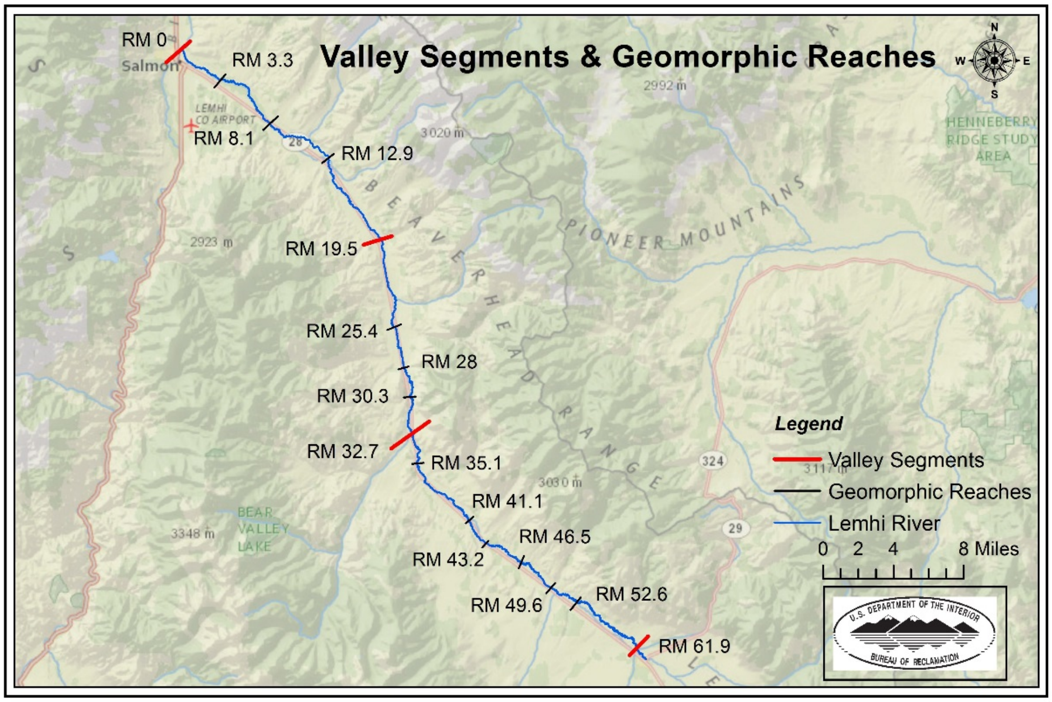

Figure 11.–Valley segments and geomorphic reaches labeled by river mile.

3.1 Hydrologic Assessment

Peak flood frequency estimates were generated at multiple locations along the Lemhi River for a range of recurrence intervals. Flood-frequency peak flow values were calculated at the two USGS gage locations (DS at 13305500 and 13305310, and US at 13305000) and two IWRB gages (at Cottom Lane and above Big Springs) utilizing methods described in Bulletin 17C (England, et al., 2015) and applying software, PeakFQ (Flynn, Kirby, & Hummel, 2006). The drainage-area ratio method was applied to ungaged locations, as described in Berenbrock (2002). Flood-frequency peak flows were estimated at a total of 23 locations along the Lemhi River for 1-, 1.5-, 2-, 2.33-, 5-, 10-, 25-, 50-, and 100-year recurrence intervals. Flow estimate locations (labeled by river mile) and associated contributing area are presented in Figure 12.

Mean daily data, available from the IWRB gages, were utilized to develop peak flood-frequency flow values; however, literature cautions against it as it often underestimates the peak (e.g., Ellis & Gray 1966, Fill & Steiner 2003, etc.). Project success relies on fully quantifying the actual peak flow for flood planning and design purposes. However, 28% of the USGS annual peak values are maximum daily averages. While use of the IWRB daily data is reasonable in this instance, instantaneous peak flow data is preferred.

In areas where wetlands attenuate floods and groundwater becomes influential, hydrologic modeling (HEC-HMS, SWMM, MIKE, SHE, etc.) may be beneficial. Given the purpose of the Integrated Rehabilitation Assessment, peak flood-frequency values were calculated utilizing the USGS and IWRB gage data and methods published by England et al. (2015) and Berenbrock (2002).

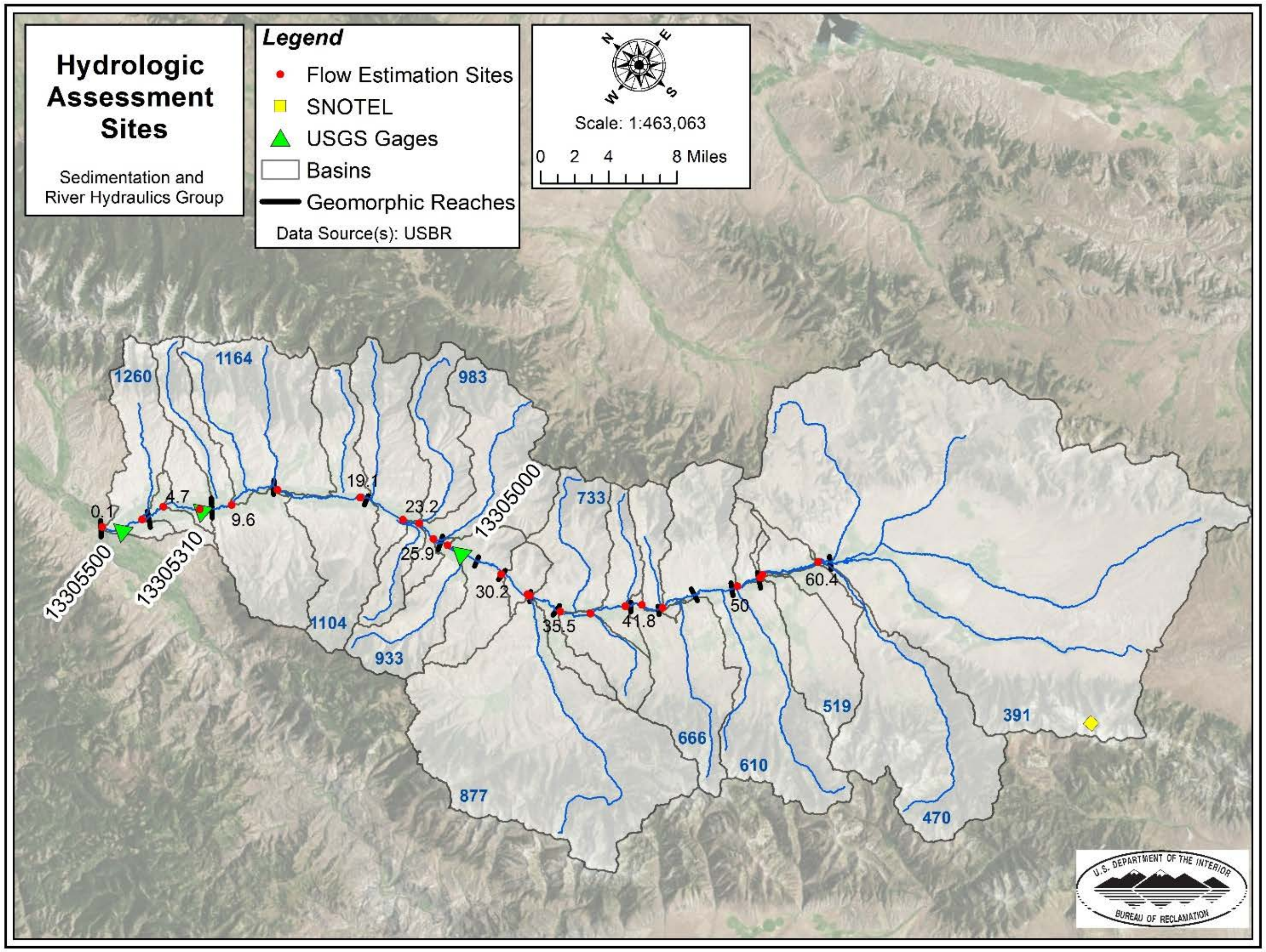

Figure 12.–Peak Flow estimation locations. River miles of flow estimation sites are labeled in black along the Lemhi River. Drainage area values are labeled in blue along the edges of the drainage basins.

3.1.1 Peak Flow Calculations at Gaged Locations

The annual peak flow data was acquired for the four USGS and IWRB gages (Table 1). The longest period of record was located at the US USGS gage (13305000). This record was utilized to extend the period of record for the other three gages to 60 years by applying the MOVE.4 method. MOVE.4 technique extends a period of record by developing regression equations to estimate the mean and variance of flows at short-record gages by employing the cross-correlation between a long and short gage record. Four MOVE techniques are documented in literature. The MOVE.4 method was selected as it has the lowest mean square error and is the current recommended method (Vogel & Stedinger, 1958)

The annual peak discharge values were then analyzed utilizing PeakFQ, a program developed by USGS, which analyzes peak annual discharge measurements in accordance with Bulletin 17C guidelines (England, et al., 2015). Bulletin 17C recommends the Expected Moments Algorithm (EMA), which provides a direct fit of the Log-Pearson III distribution, which includes an estimate of variance. As recommended in Bulletin 17C, the Multiple Grubbs-Beck test (MGBT) was performed to remove potentially-influential low flood (PILF) values. PILFs are data points which are significantly lower than the trend of the remaining data. Low outliers can be caused by different processes than the larger floods in the basin. Therefore, including these floods can significantly affect the frequency distribution at the high end of the data, especially for small samples (England, et al., 2015). Peak discharge probabilities were estimated using the Cunnane's plotting position (0.4) for the following events: 1-, 1.5-, 2-, 2.33-, 5-, 10-, 25-, 50-, 100-, 200-, and 500-year (Flynn et al., 2006). The method does not directly account for irrigation losses. However, many of the peaks were recorded during the irrigation season and the peak streamflow may be lower if water is being withdrawn during that time. Furthermore, the use of daily data may also under estimate the peaks.

3.1.2 Peak Flow Calculations at Ungaged Locations

The USGS guidelines for Idaho streams in Region 6 (Berenbrock, 2002) recommends applying the drainage area ratio method to ungaged locations (Eq. 1 and 2). Equation 1 was applied to areas downstream of the downstream USGS gage (combined 13305500 and 13305310) and upstream of the IWRB gage above Big Springs. Equation 2 was applied to areas located in between two gaged sites.

Drainage areas were estimated using StreamStats, a web-based Geographic Information Systems (GIS) tool that can be applied to water-resources engineering and design purposes. Among many other applications, StreamStats can obtain a drainage-basin boundary and area based on a user-identified point and USGS digital elevation model.

Equations 1 and 2 are presented below:

$$Q_u = Q_g \left(\frac{DA_u}{DA_g}\right)^{0.80} \quad (1)$$

Where:

- Q_u is the peak discharge (cfs) for a specific recurrence interval at the ungaged site,
- Q_g is the peak discharge (cfs) for a specific recurrence interval at the gaged site,
- DA_u is the contributing drainage area (mi^2) for the ungaged site, and
- DA_g is the contributing drainage area (mi^2) for the gaged site.
- The exponent value of 0.80 is based on a regression analysis for Idaho, Region 6 (Berenbrock, 2002)

$$Q_u = \frac{Q_{g1}(DA_{g2}-DA_u)+Q_{g2}(DA_u-DA_{g1})}{DA_{g2}-DA_{g1}} \quad (2)$$

Where:

- Q_u is the peak discharge (cfs) for a specific recurrence interval at the ungaged site,
- Q_{g1} is the peak discharge (cfs) for a specific recurrence interval at the upstream gaged site,
- Q_{g2} is the peak discharge (cfs) for a specific recurrence interval at the downstream gaged site,
- DA_u is the contributing drainage area (mi^2) for the ungaged site,
- DA_{g1} is the contributing drainage area (mi^2) for the upstream gaged site, and
- DA_{g2} is the contributing drainage area (mi^2) for the downstream gaged site.

The results of these analyses are presented in Section 4.1 – Hydrologic Assessment Results.

3.2 Stream Power Analysis

A stream power analysis was performed to investigate the potential sediment transport capacity of each geologic reach along the Lemhi River. Stream power is the river’s rate of energy dissipation against the wetted perimeter (bed and banks) per unit of downstream length, as show in Equation 3. It is often used to indicate and compare the relative magnitude of sediment transport capacity between reaches. It does not provide quantitative information regarding quantities or size of sediment transported. In addition to flow characteristics (e.g. depth, velocity, shear stress), sediment transport is also dependent on sediment supply and grain size, which were not included in this study. If total stream power increases, the sediment transport capacity would be expected to increase as well. Relative stream power values can also indicate whether a reach is more likely to be degrading (incising) or aggrading (depositional).

(3)

$$\Omega = \gamma\, Q\, S \quad (3)$$

Where Ω is stream power (lb/s), γ is the specific weight of water (62.4 lb/ft^3), Q is flow discharge (cfs), and S is the terrain slope (ft/ft). Discharge generally increases in the downstream direction in river basins as tributaries contribute more flow. For the same given slope, this increase in discharge provides more energy to transport sediment and debris.

Stream power calculations were performed for the 1.0-, 2-, 10-, and 100-year flow events. Flow discharge was estimated using the methods described in Section 3.1 – Hydrologic Assessment. When the flow estimation sites did not perfectly align with geomorphic reaches, the discharge value for a given return period was linearly interpolated. Reach/segment slope was estimated using the compiled topographic LiDAR data from 2008, 2010, and 2011. Topography was extrapolated for each of the sixteen geomorphic reaches. A trendline was then fit to the data to determine an average slope (Figure 13).

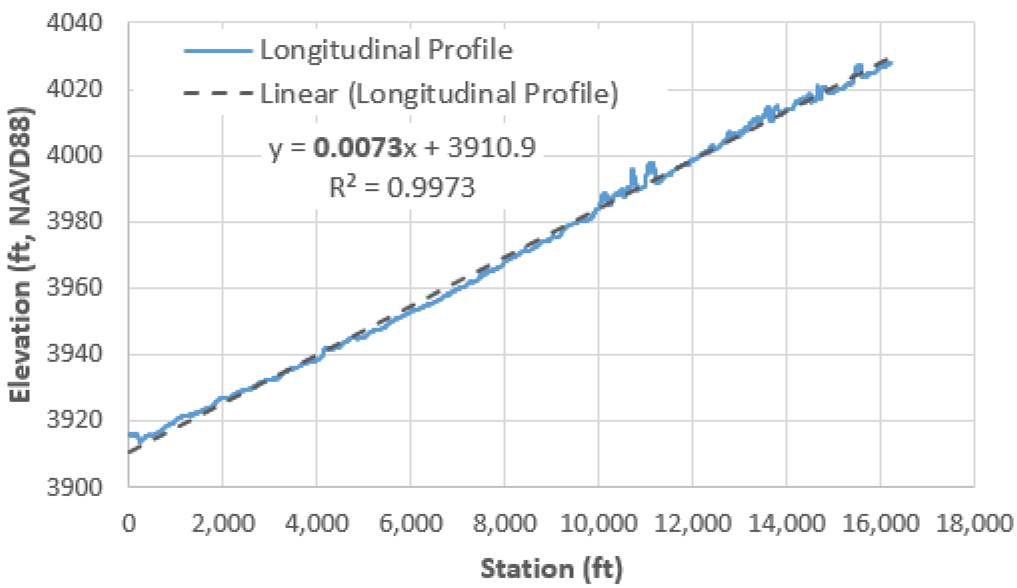

Figure 13.– Example of average reach slope determination using a trendline fit to topographic data. Figure represents geomorphic reach 1 from the confluence to RM 3.3. The average slope for this reach is 0.0073 ft/ft.

3.3 Data Collection

3.3.1 Instrumentation

The following sections will describe the process of selecting a site for discharge measurements and the equipment used for collecting a water surface profile and discharge measurements.

3.3.1.1 Discharge

Discharge measurements were collected along the Lemhi River during high flow and low flow periods. Samples were collected from May 23 – 26 and August 22 – 25, 2016 during the high and low flow seasons, respectively. Discharge measurements were collected by two teams from TSC. Site selection for discharge measurements was determined based on significant flow change locations and access to features that allowed easy river crossing. Due to time restrictions, 15 and 12 sites were selected for the high and low flow season, respectively. Discharge data collection equipment included:

- An Acoustic Doppler Current Profiler (ADCP), a Xylem brand Sontek M9 unit mounted to a hydroboard, and
- A portable velocity meter, a HACH FH950.

The ADCP was utilized during the high flow season when flow depths were greater than 2 ft. The velocity meter was utilized during the low flow season as depths were primarily below 2 ft.

3.3.1.2 Water Surface Elevation

Water surface elevations were collected at each discharge measurement location by the TSC teams. Real Time Kinematic (RTK) Trimble R10 Global Navigation Satellite Systems (GNSS) with Global Positioning System (GPS) receivers were utilized. All survey data reported in this document is tied to the U.S. State Plane Idaho Central (FIPS 1102) Coordinate System in U.S. Survey Feet. Elevations are in NAVD88 orthometric heights calculated using Geoid12A (Conus). Positional accuracies for R10s and this survey are ± 0.03 feet (± 1 cm) horizontally and ± 0.06 feet (± 2 cm) vertically (Trimble, 2014).

3.3.2 Data Collection Methodology

3.3.2.1 ADCP Data Collection Methods

Measurement quality and accuracy was ensured through a three-step process. The first step was to select an area with the best hydraulic conditions where the river had a uniform cross section geometry, a minimum depth of 2 feet, and minimal aquatic and bank vegetation. Locations to be avoided included rapidly expanding or contracting widths, sections that steepen in slope (glides/riffles), local hydraulic influence from inline structures, or tight curvature along the river planform. An example of an ideal location is pictured in Figure 14. In addition, the site must also be accessible. As much of the property in the basin is privately owned, river access was only possible at public and limited private bridges. Discharge measurement efforts were focused at public bridges.

The second step was collecting the flow measurements. The ADCP was deployed back and forth across the river on a tag line or tow rope off a bridge to measure discharge a minimum of four times. If the difference between the raw discharge measurements was outside of 5% of the mean, the measurement was thrown out and another pass (left and right pair) was completed. The third step in the process was to analyze the speed of the boat traversing the river. The transverse boat velocity had to be less than or equal to the depth-averaged downstream flow velocity otherwise the measurement was thrown out.

Figure 14.–The site at RM 33 was an ideal discharge measurement location. The site featured a straight run, with little to no vegetation, and a flat water surface with no eddies.

3.3.2.2 Velocity Meter Data Collection Methods

Collecting discharge measurements with the velocity meter requires measuring the velocity at various points across the cross section. The first step was selecting a river cross section with uniform and steady flow. Minimal aquatic and bank vegetation was also desirable with depths greater than 0.1 ft (3 cm). The stream channel cross section was then divided into numerous vertical subsections. Area was calculated in each subsection based on the width and flow depth. Water velocity was measured using the velocity meter and assumed to be uniform within each subsection. The total discharge was then computed by multiplying the area by the velocity for a given subsection and then summing the values of each subsection (Buchanan & Somers, 1969).

Velocity measurements were taken with a HACH FH950 velocity meter mounted to standard top-setting wading rod. Measurements were taken approximately every 1 to 2 feet depending on channel width. For this study, all velocity measurements were taken at 60% depth due to average cross section depths measuring below 2.5 feet. A minimum of two transects were taken at each location. If the change in discharge between the two measurements was greater than 10%, the cross section was measured a third time.

3.3.2.3 Water Surface Elevation Data Collection Methods

Water surface elevation measurements were taken at each discharge. Individual base station assemblies were required at each site in the 63.3 mile project reach. Guidelines recommend remaining within 6.2 miles (10 km) of the base station with the rover receiver. An example base station set up in shown in Figure 15. Twelve sites did not have previously established control points. Therefore, wooden stakes with “X” markings were installed at each site during the first site visit. An approximate coordinate was estimated by the base R10 to establish a starting location. An exact location of the base requires post-processing, which is discussed later in this section. Water surface elevations, along with pertinent features (bridge deck, riffle location, etc.) were then measured by the TSC team. During the second data collection effort, base stations were set up at a known coordinate, derived from post-processing of the data from the first data collection effort, for the same wooden stakes. At three sites, the original wooden stake could not be found and replacement stakes were installed.

Figure 15.–Base station located over staked control point.

3.3.2.4 Pebble Count Collection Methods

Pebble counts were performed during the low flow field trip to characterize the bed material. Seventeen pebble counts were completed according to the Wolman Pebble Count Procedure (Wolman, 1954). The technique requires the user to measure the b-axis axis (Figure 16) of 100 random sediment particles using a gravelometer. This study focused on riffle and run geomorphic features. One measurement was taken at a pool to compare the size distribution between geomorphic features. Pebble counts were taken at all the low flow discharge measurement locations (Figure 31). In addition, one pebble count was performed on Hayden Creek.

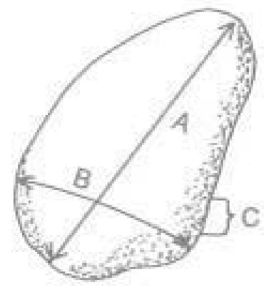

Figure 16.–Pebble axis measurement (Harrelson, Rawlins, & Potyondy, 1994)

3.3.3 Post-Processing Methodology

The methodology for post-processing all field collected data are included in the sections below.

3.3.3.1 ADCP Post-Processing

Discharge measurements can be impacted by weather. During sampling, the weather consisted of air temperatures ranging between 37˚F-69˚F during the high flow season and 36˚F-84˚F during the low flow season. No precipitation occurred during either measurement time period. Weather data were obtained from Weather Underground at station KSMN in Salmon, ID located at 44.52°N, 114.21°W, and 5,072 feet elevation (Weather Underground, 2016). Weather data are collected with a Davis Vantage Pro 2.

The ADCP must compute the speed of sound correctly to accurately measure velocities, depths, and compute discharge. Temperature is the most important variable in the equation used to compute the speed of sound (Urick, 1983). An error of 5 degrees Celsius (°C) in the water temperature measurement could cause a 2-percent bias error in the measured discharge (Oberg, Morlock, & Caldwell, 2005). Thus, the temperature measured by the ADCP should be compared with an independent temperature measurement. Because the Lemhi River is known to be shallow, changes in ambient air temperature can influence changes in water temperature. Furthermore, the shallow depths are likely to decrease the 2-percent error bias.

SonTek RiverSurveyor Live version 3.6 software in conjunction with USGS QRev, version 2.80 (Mueller, 2016) was used to collect and post-process discharge data on the SonTek M9 (SonTek/YSI, 2013). QRev is a Matlab program to aid discharge measurement post-processing. QRev automates filtering and quality checking of the collected data. Quality control checks include: system test, compass test, temperature, moving-bed test, bottom tracking, GPS filtering (if applicable), depth filtering, water track filtering, extrapolation, and edges. The user control comes primarily from measurement location selection and the choice of an appropriate top and bottom discharge extrapolation methods in the unmeasured portion of the cross-section. The software uses an automatic algorithm to evaluate the data and suggest a fit, but the user can manually change the fit. In this study, the appropriate extrapolation fit were selected based on the data curves.

3.3.3.2 Velocity Meter Post-Processing

The discharge associated with the velocity meter measurements was calculated using the mid-section method. Vertical segments are defined as half the distance to the neighboring measurements. The discharge was calculated using the equation defined in Figure 17.

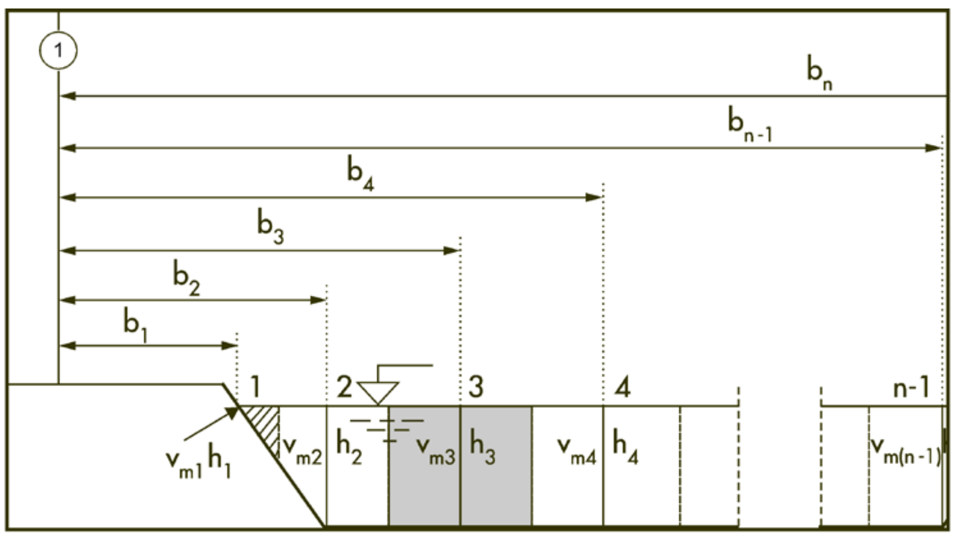

$$q_3 = V_{m3} \times \left(\frac{(b_3 - b_2) + (b_4 - b_3)}{2} \right) \times h_3$$

Figure 17.–Mid-section method for computing discharge (HACH, 2012).

3.3.3.3 Water Surface Elevation Post-Processing

Water surface elevation and other survey data were post-processed using the Online Position User Service (OPUS) and Trimble Business Center Software. OPUS is an online tool developed by the National Oceanic and Atmospheric Administration (NOAA). OPUS computes base station coordinates relative to the National Geodetic Survey's Continuously Operating Reference Station (CORS) Network with a specific base station file. Once each base station point location was post-processed, all corresponding rover point survey data were shifted in Trimble Business Center based on the recalculated base station location.

3.3.4 Discharge Uncertainty Discussion

Although care was taken while discharge measurements were made, there is still inherent uncertainty in the measurements. Factors that can affect the uncertainty in measurements are the transect discharge accuracy, percentage of unmeasured areas, quality of boat navigation reference, sample random error in the discharge measurement, and extrapolation of the discharge curve in top and bottom unsampled areas (Mueller D. S., 2012). The variability of transect discharge can be affected by pulsing flows and/or aquatic vegetation in the channel, and is typically observed in patterns of difference between transects. Directional bias as a result of variable channel bottom geometry can affect measurements in a given transect. A transect was thrown out if there were observable discrepancies between transect flows combined with notable measurement challenges.

The variability in transect discharge can also be attributed to random error, which was represented by the coefficient of variation (COV) and is calculated by:

$$\text{COV} = (\text{Standard Deviation}) / (\text{Mean discharge of the transects})$$

To determine the 95% uncertainty of random error the COV is multiplied a coverage factor, described in Table 3. To scale the components of uncertainty consistently, or a combined uncertainty, one can rescale the results. The combined standard uncertainty can be thought of as an equivalent to one standard deviation but since 95% is the desired deviation, re-scaling of the uncertainty can be done through a coverage factor, *k* (Bell, 1999).

Table 3.–Coverage factors to determine variability in transect discharges

Number of Transects	*k Coefficient*
4	1.6
6	1.0
8	0.8
10	0.7
12 or more	0.6

3.3.4.1 ADCP Uncertainty

Uncertainty associated with ADCP measurements stems largely from extrapolation and the quality of the collected bottom tracking data. The accuracy and percentage of unmeasured area are related to the top and bottom extrapolation, edge extrapolation, and quantity and distribution of missing and/or invalid data. The percentage of measured area for each discharge measurement is documented in Appendix C – ADCP Discharge Measurements.

The quality of boat navigation reference is dependent upon the bias or noise in bottom tracking data. Noise in bottom tracking can be the result of a moving bed condition (from either aquatic vegetation or a mobile bed such as during high flow conditions). In this study, a "moving bed" test was completed at RM 40.8 with the Sontek M9. A moving bed was not detected during the test.

3.3.4.2 Velocity Meter Uncertainty

Sources of uncertainty for velocity meter measurements include: accuracy and resolution of the instrument, spatial resolution of the measurement, and the skill of the operator (Fulford, n.d.). The accuracy of the instrument depends on the velocities being measured. Between 0 and 10 ft/s the accuracy is ±2% of reading. Between 10 and 16 ft/s the accuracy is ±4% of measurement. The zero stability of the instrument is ±0.05 ft/s (HACH, 2012).

4 Results

The following sections describe the results of each of the analyses described in Section 3 – Methods.

4.1 Hydrologic Assessment Results

The results of the flood-frequency estimates are presented in the following sections.

4.1.1 Peak Flow Calculations at Gaged Locations

Table 4 and Figure 18 illustrate the results of the PeakFQ analysis at the four gages along the Lemhi River. Utilizing the MOVE.4 technique, each of the gages contained 60+ years of record. The results from PeakFQ with uncertainty bounds are shown in Figure 19 through Figure 22. Irrigation diversion volumes were not directly incorporated into this assessment, as specific volumes and locations are unknown. Many of the peaks occurred during irrigation season, and the analysis at the IWRB gages included daily data instead of peak annual flows. Therefore, it is likely that the annual peak vales are underestimated.

Table 4.–Gage and flood frequency results, in cfs, from USGS stream gage locations.

Gage No.		13305500 & 13305310 (DS Gages) RM 7.25	13305000 (US Gage) RM 26.7	Cottom Lane (IWRB Gage) RM 48.8	Above Big Springs (IWRB Gage) RM 52.9
Recurrence Interval (years)	% AEP	PeakFQ Results (cfs)			
1.0	**99.5**	157	141	93	84
1.5	**66.7**	886	664	282	202
2	**50**	1,188	861	339	235
2.33	**42.9**	1,334	954	364	249
5	**20**	2,001	1,365	468	306
10	**10**	2,563	1,697	544	348
25	**4**	3,276	2,102	630	394
50	**2**	3,802	2,393	688	426
100	**1**	4,318	2,672	742	454

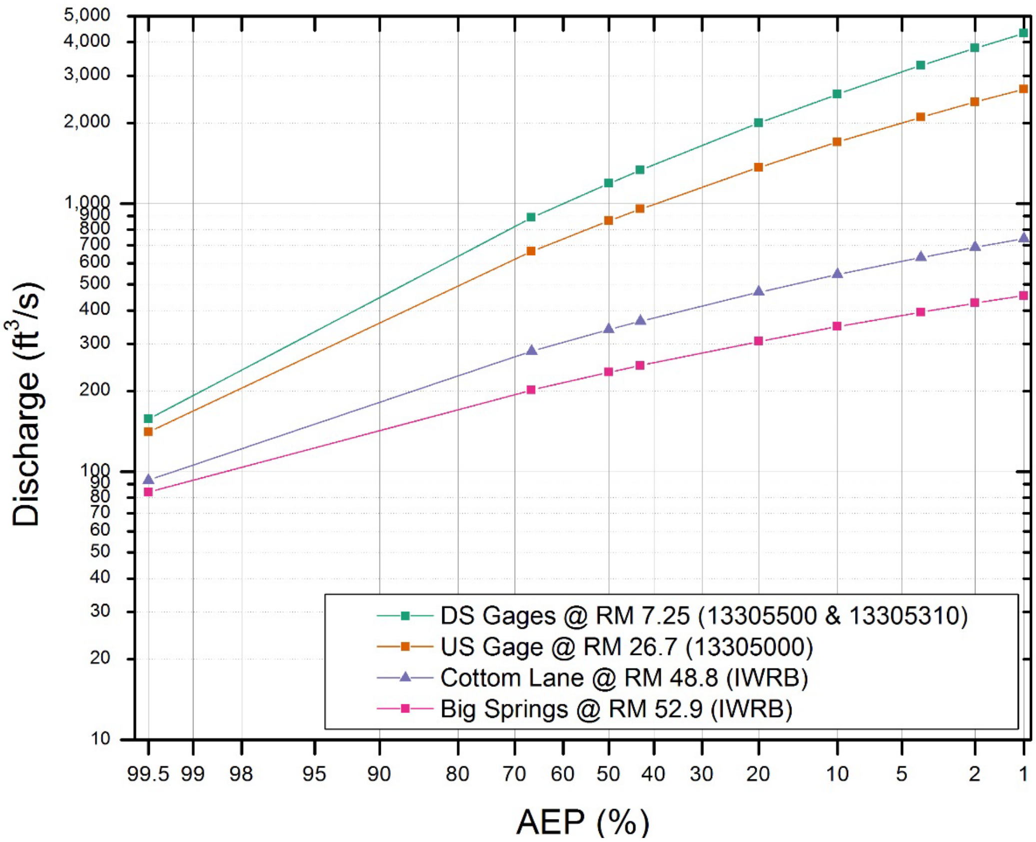

Figure 18.–Peak discharge values plotted across annual exceedance probability (AEP)

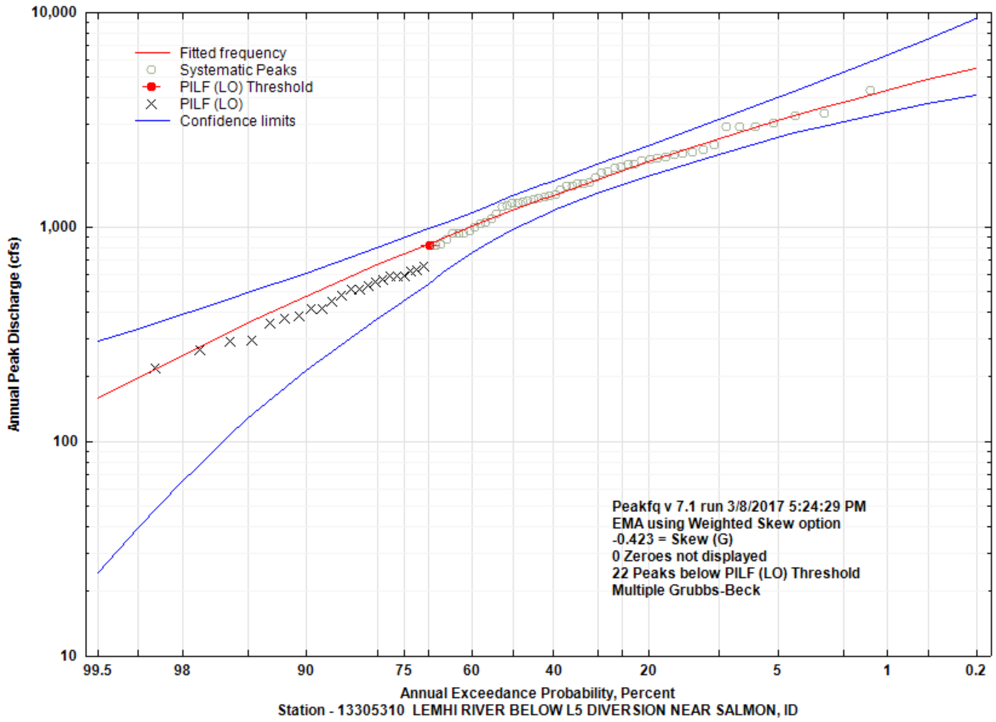

Figure 19.–Annual Exceedance Curve for USGS Gage 13305310 below L5 Diversion (RM 7.25). Potentially influential low flows (PILF) are plotted with x's while systematic peaks are plotted with circles.

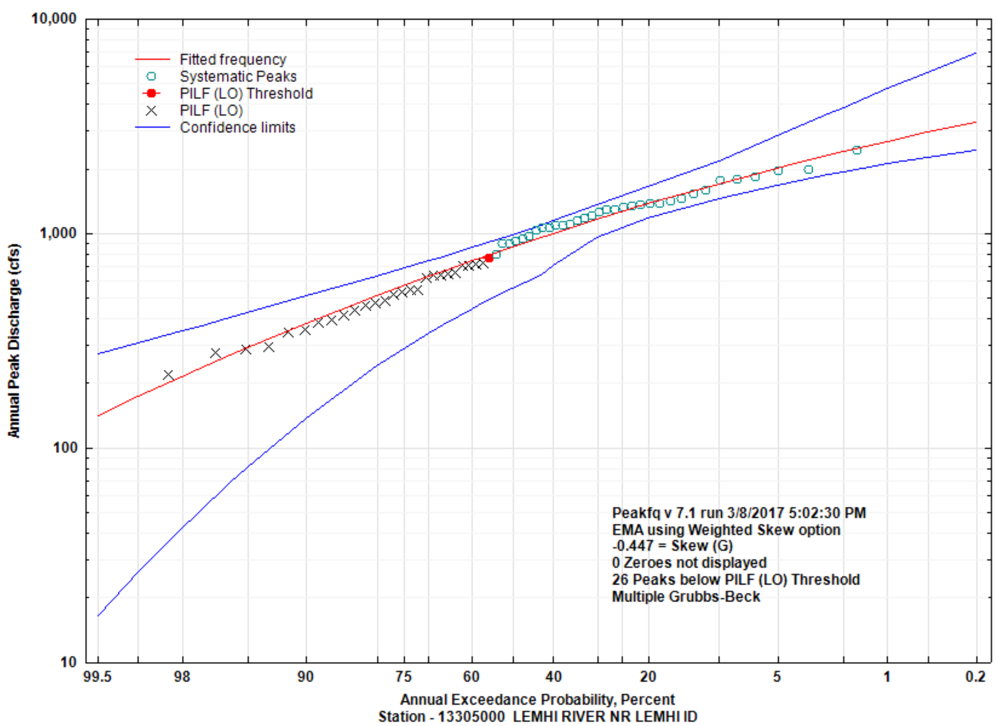

Figure 20.–Annual Exceedance Curve for USGS Gage 13305000 near Lemhi (RM 26.7)

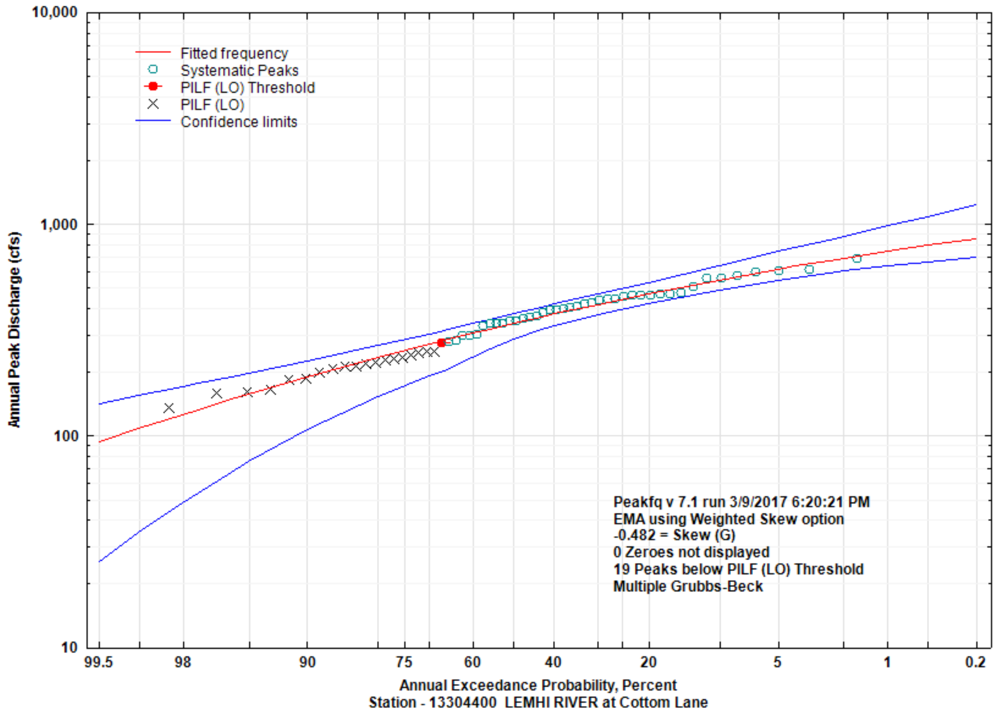

Figure 21.–Annual Exceedance Curve for IWRB Gage on the Lemhi River at Cottom Lane (RM 48.8)

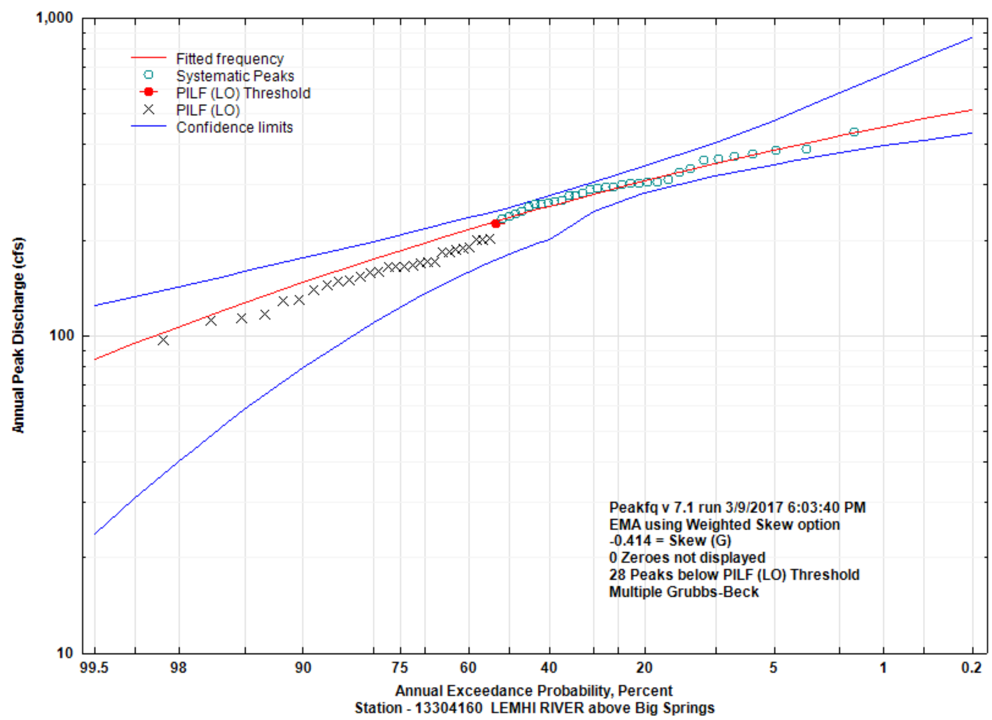

Figure 22.–Annual Exceedance Curve for IWRB Gage on the Lemhi River above Big Springs (RM 52.9)

4.1.2 Peak Flow Calculations at Ungaged Locations

Equations 1 and 2 were applied to ungaged locations based on their location relative to the USGS and IWRB gages. 1) For reaches upstream of the IWRB gage above Big Springs, Equation 1 was applied, 2) For reaches downstream of the DS USGS gages (13305500 and 13305310), Equation 1 was applied using the DS gage data, and 3) Equation 2 was applied to locations between two gages. The tabular results are presented in Table 5. The cell colors indicate the equation and gages applied for each location. Figure 24 plots the estimated peak discharge values with respect to river miles for the 100-year event.

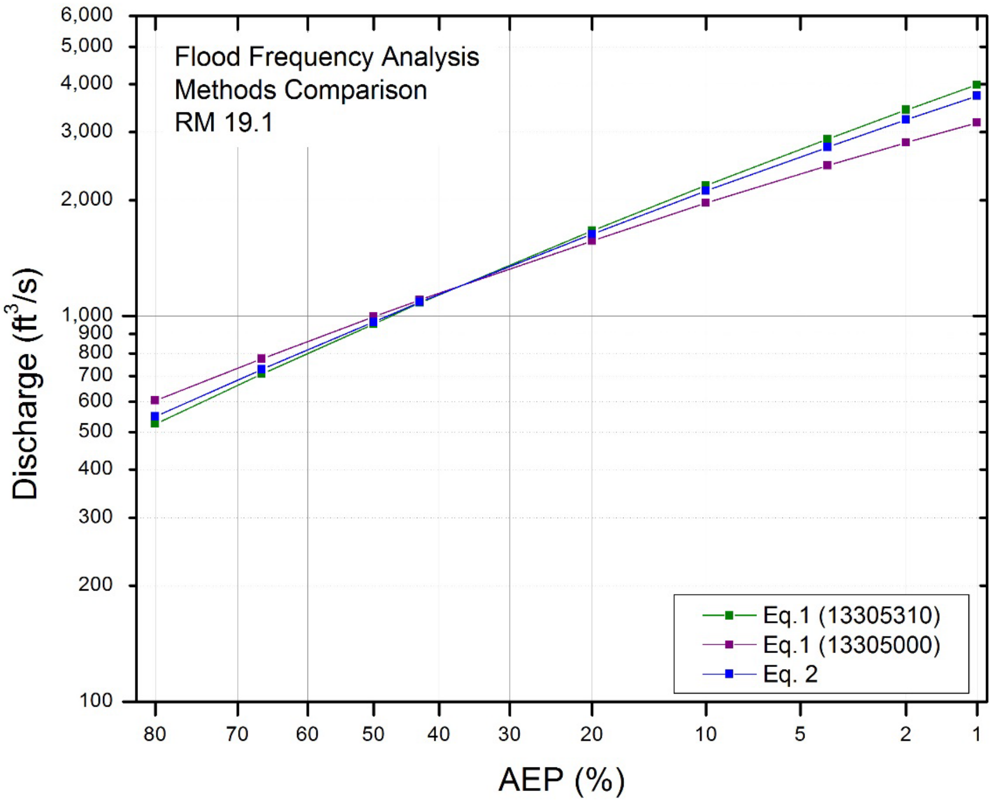

Figure 23.–Estimated peak discharge values at RM 19.1.

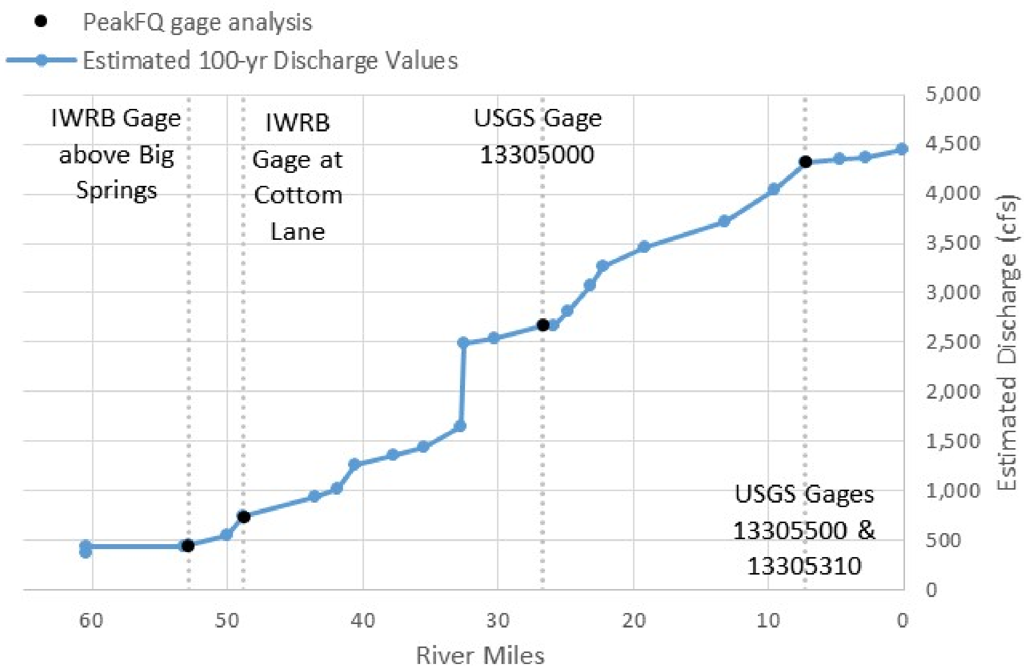

Figure 24.–Estimated discharge values for the 100-yr event.

Table 5.–Recommended Peak Discharge Values along the Lemhi River.

River Mile	Drainage Area (mi2)	Geomorphic Reach	Discharge values (cfs)								
			1	1.5	2	2.33	5	10	25	50	100
0.1	1,260	GR 15	162	912	1,223	1,373	2,059	2,638	3,371	3,913	4,444
2.8	1,231	GR 15	159	895	1,200	1,347	2,021	2,589	3,309	3,840	4,361
4.7	1,226	GR 14	158	892	1,196	1,343	2,014	2,579	3,297	3,826	4,346
7.3	**1,216**	**GR 14**	**157**	**886**	**1,188**	**1,334**	**2,001**	**2,563**	**3,276**	**3,802**	**4,318**
7.2	1,216	GR 14	157	886	1,187	1,333	2,000	2,562	3,274	3,800	4,315
9.6	1,164	GR 13	155	849	1,133	1,270	1,893	2,416	3,077	3,563	4,039
13.2	1,104	GR 12	151	806	1,069	1,196	1,770	2,249	2,850	3,291	3,721
19.1	1,055	GR 12	149	771	1,018	1,137	1,670	2,113	2,666	3,069	3,462
22.2	1,018	GR 11	147	744	979	1,091	1,594	2,009	2,525	2,901	3,265
23.2	983	GR 11	145	719	942	1,048	1,522	1,910	2,391	2,740	3,077
24.8	933	GR 11	142	683	888	986	1,418	1,769	2,200	2,510	2,809
25.9	908	GR 10	141	664	862	955	1,366	1,698	2,104	2,395	2,675
26.7	**907**	**GR 10**	**141**	**664**	**861**	**954**	**1,365**	**1,697**	**2,102**	**2,393**	**2,672**
30.2	884	GR 9	138	637	824	912	1,301	1,615	1,997	2,272	2,535
32.5	877	GR 8	137	629	813	900	1,282	1,591	1,966	2,236	2,494
32.7	733	GR 8	116	463	586	643	892	1,089	1,326	1,494	1,654
35.5	697	GR 6	111	421	529	578	794	963	1,165	1,308	1,443
37.7	681	GR 6	108	403	504	551	751	908	1,096	1,228	1,353
40.6	666	GR 6	106	385	480	523	710	855	1,027	1,148	1,263
41.8	623	GR 5	100	336	412	447	594	706	837	928	1,014
43.5	610	GR 4	98	321	392	424	559	660	779	861	938
48.8	**577**	**GR 3**	**93**	**282**	**339**	**364**	**468**	**544**	**630**	**688**	**742**
50.0	519	GR 2	87	231	272	291	365	419	480	521	559
52.9	**486**	**GR 1**	**84**	**202**	**235**	**249**	**306**	**348**	**394**	**426**	**454**
53.2	477	GR 1	83	199	231	245	302	342	388	419	447
60.4	470	GR 1	82	197	228	242	298	339	384	414	442
60.4	390	GR 1	70	169	197	209	257	292	331	357	381

Eq. 1 utilizing the DS USGS gage (13305500 &13305310)
PeakFQ gage analysis
Eq. 2 utilizing the US and DS USGS gages
Eq. 2 utilizing the US USGS gage and IWRB gage at Cottom Lane
Eq. 2 utilizing the IWRB gage at Cottom Lane and above Big Springs
Eq. 1 utilizing the IWRB gage above Big Springs

4.2 Stream Power Analysis Results

Stream power was calculated for four flow events (1.0-, 2-, 10-, and 100-year recurrence intervals) within 16 geomorphic reaches along the Lemhi River. Only the USGS gage data was applied to this analysis. If the discharge values were calculated based on the IWRB flow data, the stream power values would be significantly reduced in the upper basin. Discharge increases in the downstream direction, as shown in Figure 25. A significant increase is seen at RM 32.7, where Hayden Creek flows into the Lemhi River. Moving downstream, peak flow increases at a higher rate for less frequent events relative to more frequent smaller events. Figure 26 shows the longitudinal profile and average geologic reach slope. In general, the slope is lower in the upstream, less altered reaches. The downstream reaches show a higher slope, which could be a result of the historic channelization and straightening of the Lemhi River for flood conveyance. A decrease in slope is observed downstream of Hayden Creek at RM 35.1. This break in slope could be a result of sediment load from Hayden Creek depositing in the reach downstream of the confluence. The slope remains relatively high, between 0.006 and 0.008 ft/ft, to the confluence with the Salmon River.

Total stream power results increase in the downstream direction along the Lemhi River as shown in Figure 27. The tabular results are presented in Table 6. A steady increase in stream power demonstrates that discharge is more influential than slope on sediment transport. The only exception occurs at RM 35.1, downstream of the Hayden Creek confluence. Discharge is increasing steadily at this location, but the slope significantly decreases. Therefore, slope becomes the control for sediment transport along this reach. The decrease in stream power suggests a depositional zone. Stream power is highest at the downstream reach near the confluence, implying a high transport zone, which may be prone to erosion.

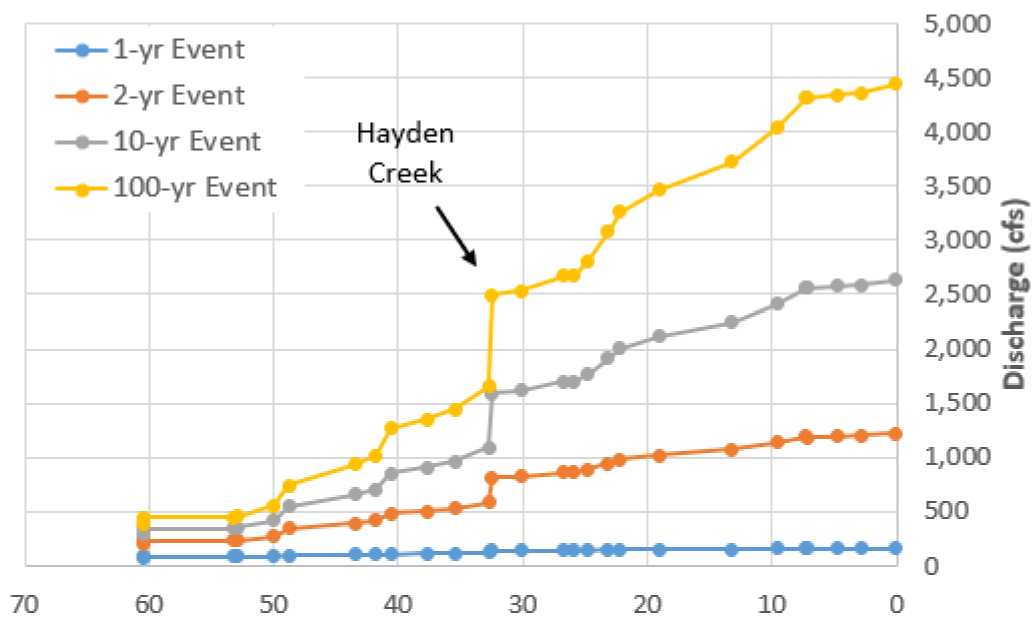

Figure 25.–Estimated discharge values along the Lemhi River.

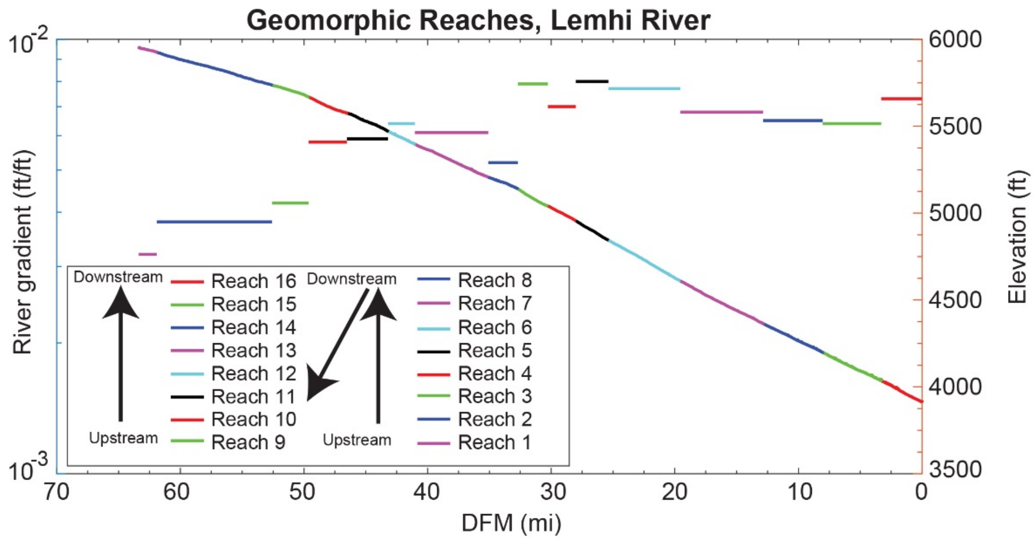

Figure 26.–Lemhi River longitudinal profile and slope by river mile.

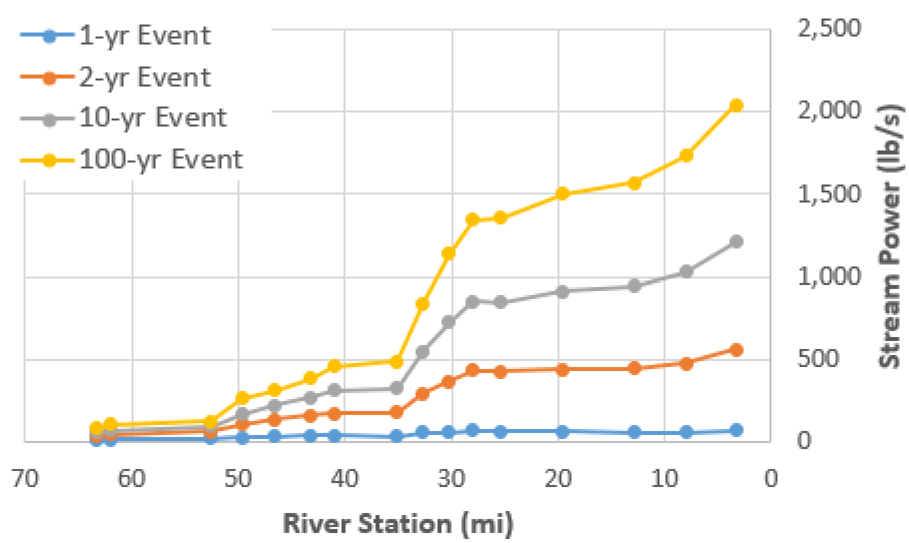

Figure 27.–Total stream power results by river mile.

Table 6.–Stream Power Analysis Results

			1-yr Event		2-yr Event		10-yr Event		100-yr Event	
Geo. Reach No.	River Mile	Slope	Q (cfs)	Ω (lb/s)	Q (cfs)	Ω (lb/s)	Q (cfs)	Ω (lb/s)	Q (cfs)	Ω (lb/s)
16	3.3	0.0073	159	74	1,199	562	2,586	1,212	4,357	2,042
15	8.0	0.0064	156	64	1,168	480	2,511	1,032	4,218	1,733
14	12.9	0.0065	151	63	1,075	449	2,265	945	3,752	1,566
13	19.6	0.0068	149	65	1,012	442	2,098	916	3,433	1,499
12	25.4	0.0077	141	70	869	429	1,719	850	2,739	1,354
11	28.0	0.0080	140	72	847	435	1,666	856	2,621	1,346
10	30.3	0.0070	138	62	824	370	1,614	725	2,534	1,139
9	32.7	0.0079	116	59	586	297	1,089	552	1,654	839
8	35.1	0.0052	112	37	537	179	981	328	1,473	492
7	41.0	0.0061	104	41	455	178	801	314	1,173	459
6	43.2	0.0064	98	40	395	163	668	274	951	391
5	46.5	0.0059	95	36	362	137	594	225	826	313
4	49.6	0.0058	89	33	293	109	458	170	711	265
3	52.6	0.0042	84	23	239	64	356	96	466	126
2	61.9	0.0038	70	17	197	48	292	71	447	109
1	63.4	0.0032	70	14	197	40	292	60	447	92

4.3 Discharge Measurement Results

4.3.1 High Flow Discharge Measurements

Fifteen discharge measurements were collected during the high flow season. Twelve measurements were collected along the Lemhi River, two were collected at the headwaters in Eighteen Mile and Texas Creek, and one measurement was collected at Hayden Creek near the confluence with Lemhi River (Figure 28). The tabular results are presented in Table 7 and Table 8. Detailed tabular results are presented in Appendix C – ADCP Discharge Measurements.

One USGS and four IWRB gages are located near high flow discharge measurement sites (Table 9). The IWRB gages only provide daily data; therefore, the percent difference is expected to be greater at these locations. In general, the discharge measurements compare well with the gage data, except the discharge measurement RM 55.5 and the gage at RM 52.9. It is likely that the difference in discharge is a result of a tributary confluence in between the gage and measurement site.

Table 7.–Discharge measurements along the Lemhi River during high flows.

River Mile	Discharge (cfs)	Error	Instrument	Date & Time
55.5	47.1	2.3%	Velocity Meter	5/26/16 15:40
48.8	189	5.7%	ADCP	5/23/16 15:35
40.8	74.1	10.2%	ADCP	5/24/16 10:06
36.4	220	8.6%	ADCP	5/24/16 15:14
33	180	4.1%	ADCP	5/24/16 17:02
31.1	469	6.7%	ADCP	5/25/16 12:25
27.5	338	5.9%	ADCP	5/25/16 15:17
24.3	369	4.7%	ADCP	5/25/16 16:41
21.4	404	4.8%	ADCP	5/26/16 13:52
17.2	392	5.9%	ADCP	5/26/16 16:20
9.3	510	4.3%	ADCP	5/26/16 18:32
0.4	535	4.0%	ADCP	5/26/16 15:40

Table 8.–Discharge measurements of contributing tributaries.

Tributary	Discharge (cfs)	Error	Instrument	Date & Time
Texas Creek	19.2	3.9%	Velocity Meter	5/23/16 10:00
Eighteen Mile Creek	16.3	0.6%	Velocity Meter	5/23/16 12:30
Hayden Creek	181	10.6%	ADCP	5/24/16 12:00

Table 9.–Comparison of discharge measurements and gage record

Discharge Location	Measured Discharge (cfs)	Gage River Mile	Gage Name	Gage Discharge (cfs)	% Difference
Texas Creek	19.2	Texas Creek	IWRB Gage above L-63	16[2]	20%
RM 55.5	47.1	RM 52.9	IWRB Gage on Lemhi River above Big Spings	94[2]	-50%
RM 48.8	189	RM 48.8	IWRB Gage on Lemhi River at Cottom Lane	185[2]	2%
Hayden Creek	181	Hayden Creek	Hayden Creek	215[2]	-16%
RM 27.5	338	RM 26.7	USGS Gage on Lemhi River at Lemhi, ID	337[1]	0%

[1]15-minute interval data
[2]Mean daily value

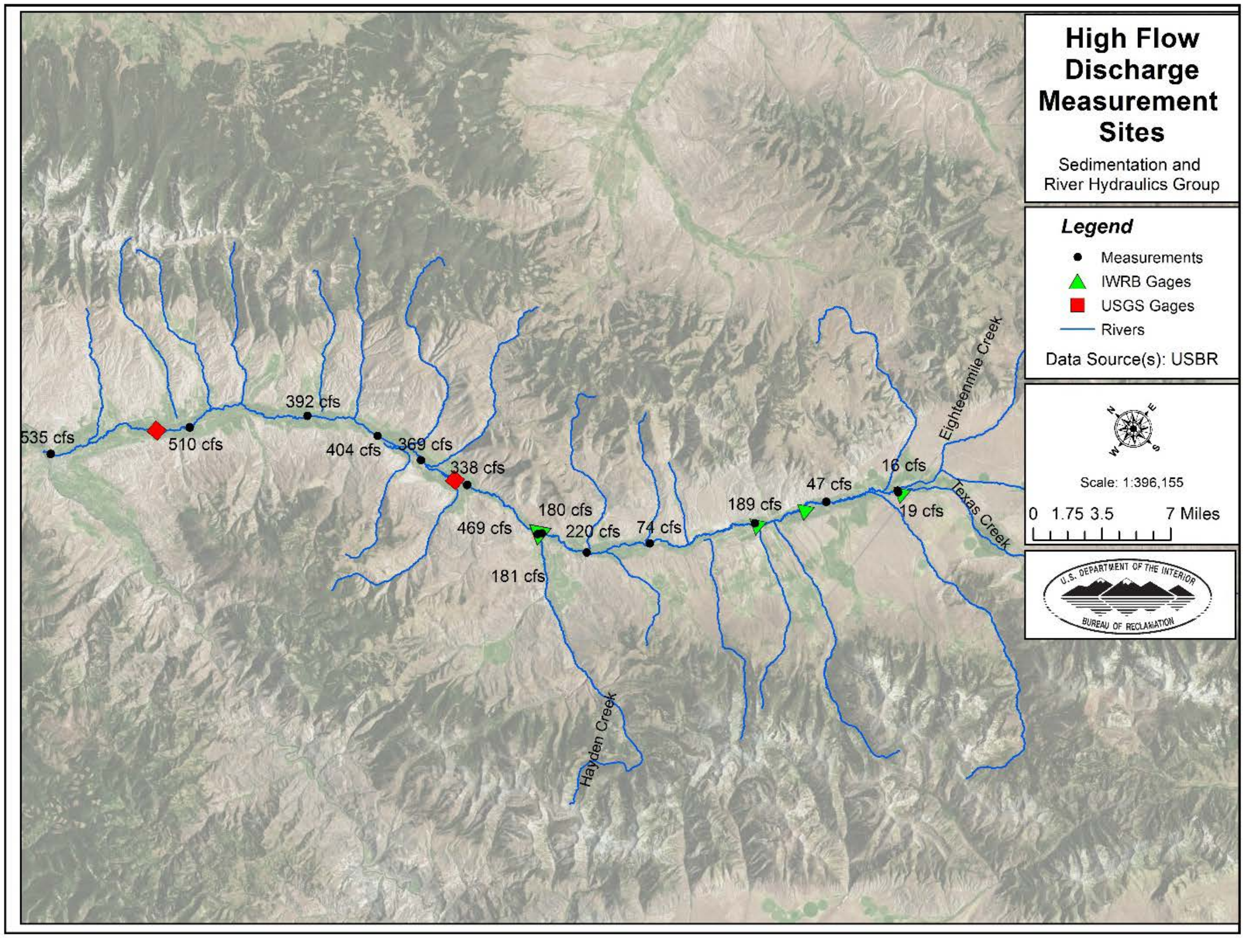

Figure 28.–High flow discharge measurement locations. USGS and IWRB gages are included on the map and compared to the measured discharge. A comparison was not conducted on the DS USGS gage as a tributary flows into the Lemhi in between the gage and measurement location, making the value incompatible.

Discharge measurements were challenging during the high flow season due to limited access and physical characteristics of the channel. The majority of the land along the Lemhi River and associated tributaries is privately owned, making access challenging. Therefore, discharge measurement efforts were focused near public bridges. When public bridges were spaced too far apart, private land owners were contacted. Private access was only granted at three locations, RM 55.5, 33, and 21.4. Limited access to the river made it more challenging to find ideal hydraulic locations.

At many sites, the best transect on public land was selected, but it was necessary to compromise hydraulic components ideal for measuring discharge. Sites with high error values often had challenging hydraulic conditions such as vegetation, eddies, or shallow depths. Examples of tough measurement locations are presented in Figure 29. The transect location at RM 36.4 (left photo) was vegetated on the left bank. Vegetation can result in non-uniform flow causing eddies and backwater effects, which adds noise to the ADCP readings. The site on Hayden Creek (right photo) did not have a smooth water surface due to high velocities (3.0 ft/s), low depths (1.7 ft), coarse bed material (median grain size > 64 mm). An uneven water surface will result in more noise in the depth and velocity readings on the ADCP. It will also make it more difficult to move the ADCP steadily across the transect.

Figure 29.–Examples of challenging discharge measurement transects at RM 36.4 (left) and on Hayden Creek (right). Notice that both measurements have high error values.

The wide and shallow physical characteristic of the Lemhi River make discharge measurements during the high flow season difficult. The average flow depths during the high flow season ranged from 0.6 ft to 2.7 ft. The ADCP cannot measure near the water surface due to instrument draft and the required blanking distance, nor can it collect data near the bed due to side-lobe interference, explained in Figure 30. The instrument draft necessary for the M9 and hydroboard was 0.3 ft for this project. The recommended blanking distance for shallow water is 0.52 ft (Mueller et al., 2013). The depth of the water column impacted by side-lobe interference can be as high ast 13%, and is dependent on the distance between the transducer and the streambed and the angle of the transducers from the vertical. Given the three factors, in a 2.5 ft deep river, the instrument can only measure 1.47 ft of depth. Velocities in the remainder of the transect must be extrapolated, potentially increasing the error of the measurement. Shallow flow depths and high velocities over coarse sediment often results in rough hydraulic conditions with a noisy water surface profile, which increases the beam scatter, resulting in a larger error. High velocities made wading dangerous at most sites; therefore, measurement with the velocity meter was not an option.

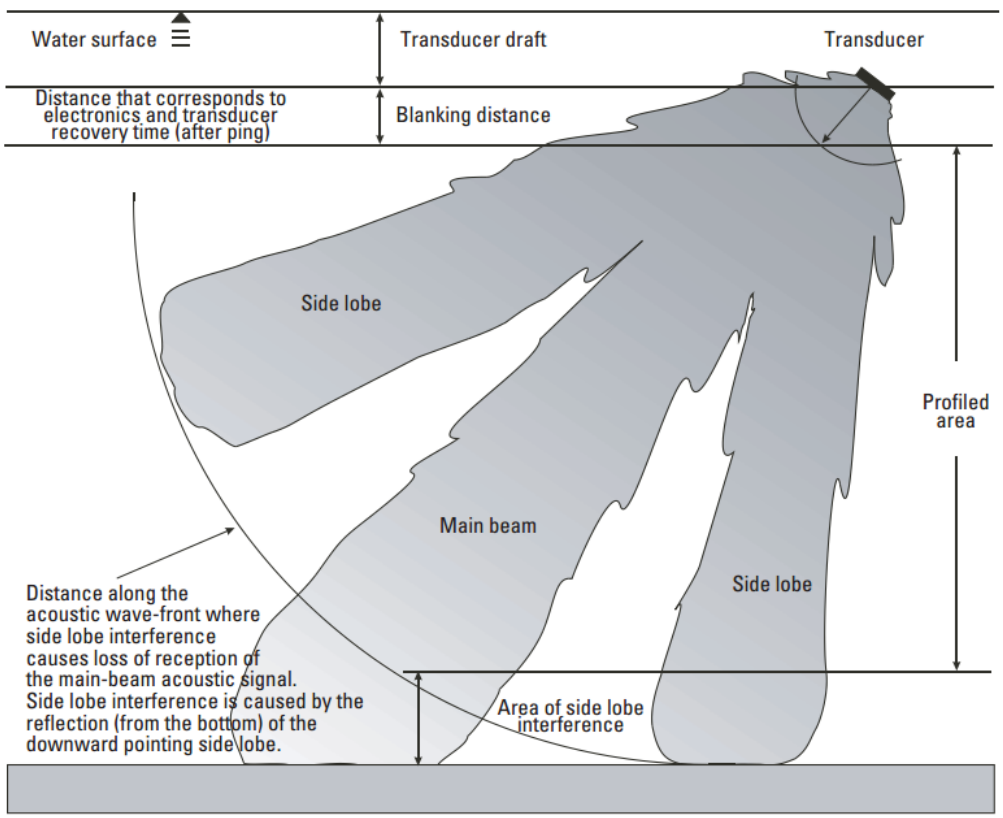

Figure 30.–Acoustic Doppler current profiler transducer beam pattern and regions of unmeasured velocity in each profile (from Simpson, 2002).

4.3.2 Low Flow Discharge Measurements

Twelve discharge measurements were taken during the low flow site visit: ten measurements along the Lemhi River and two measurements at contributing tributaries, Figure 31. Due to low flow depths, the velocity meter was used for all twelve measurements. Tabular results are presented in Table 10 and Table 11.

One USGS and three IWRB gages are located near low flow discharge measurement sites (Table 12). The IWRB gages only provide daily data; therefore, the percent difference is expected to be greater at these locations. In general, the discharge measurements compare well with the gage data (<22%). The highest difference is at Texas Creek. While the percent difference (21%) appears to be relatively high, the absolute difference was less than 1 cfs.

Table 10.–Discharge measurements along the Lemhi River and contributing tributaries during the low flow season.

River Mile	Discharge (cfs)	Error	Date & Time
55.5	39.6	1.8%	8/22/16 18:00
48.8	73.9	7.4%	8/23/16 10:38
40.8	57.0	4.0%	8/23/16 13:54
36.4	82.6	4.2%	8/23/16 16:59
27.5	109	4.7%	8/24/16 11:50
24.3	93.4	4.0%	8/24/16 13:54
21.4	91.7	2.8%	8/24/16 16:18
17.2	87.9	1.7%	8/25/16 9:32
9.3	78.1	2.7%	8/25/16 11:00
0.4	57.5	2.4%	8/25/16 14:31

Table 11.–Discharge measurements in contributing tributaries during the low flow seasons

Tributary	Discharge (cfs)	Error	Date & Time
Texas Creek	5.58	4.60%	8/22/16 12:00
Eighteen Mile Creek	1.54	6.80%	8/22/16 15:00

Table 12.–Comparison of discharge measurements and gage record

Discharge Location	Measured Discharge (cfs)	Gage River Mile	Gage Name	Gage Discharge (cfs)	% Difference
Texas Creek	5.58	Texas Creek	IWRB Gage above L-63	4.63[2]	21%
RM 55.5	39.6	RM 52.9	IWRB Gage on Lemhi River above Big Spings	42.7[2]	-7%
RM 48.8	73.9	RM 48.8	IWRB Gage on Lemhi River at Cottom Lane	78.3[2]	-6%
RM 27.5	109	RM 26.7	USGS Gage on Lemhi River at Lemhi, ID	107[1]	2%

[1]15-minute interval data
[2]Mean daily value

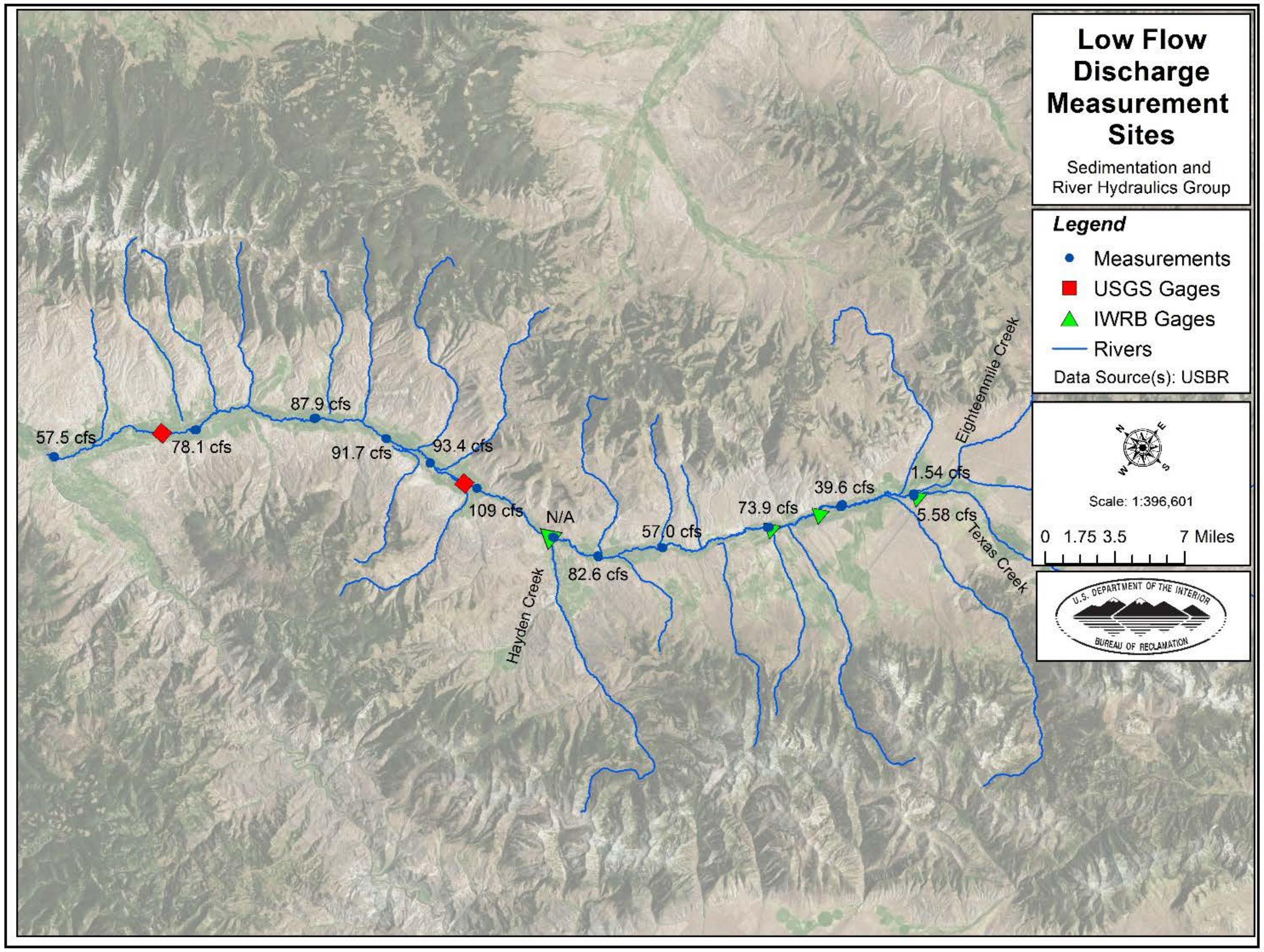

Figure 31.–Low flow discharge measurement locations. USGS and IWRB gages are included on the map and compared to the measured discharge.

Compared to the high flow measurements, the error associated with the low flow measurements was significantly less. Lower flows resulted in smoother water surfaces, producing higher quality measurements. The lower flow rates made it safe to wade the river, making it easier to select an appropriate transect location.

The results from both the high flow and low flow measurements show that the discharge does not steadily increase in the downstream. An increasing trend occurs from RM 55.5 to RM 27.5. From RM 27.5 to RM 0.4, the discharge steadily decreases as more water is diverted to the surrounding lands for irrigation. Typically, a mass balance would be performed to verify measurements. However, a mass balance check cannot be performed when diversion rates and locations are unknown.

4.3.3 Discharge Measurement Comparison

Table 13 compares the discharge measurements from both collection efforts at the same location. The general trend shows that the change in discharge increases in the downstream direction, as drainage area increases. The percent change also increases in the downstream direction. The dramatic decrease in discharge from high to low flow season is largely due to flow diversions and the seasonal precipitation of the region. Groundwater recharge may also contribute to the percentage increase in the downstream direction. The headwaters and upper reaches of the Lemhi River are also groundwater fed. Therefore, the percent change in discharge is expected to decrease further upstream as groundwater influx is relatively higher upstream of RM 34 and groundwater flux is less dynamic than surface water gains and losses.

The only exception to the trend is at RM 40.8. The error associated with the high flow measurement was 10.2%. While it is the highest error in the data set, that does not account for the entire discrepancy. Both discharge values at this site are significantly lower than the upstream and downstream sites. After reviewing aerial photography, it is likely that the Lemhi is split into two channels at RM 40.8, see Figure 32. Thus, only a portion of the flow was measured. The authors would not recommend utilizing this data point for future model calibration.

Table 13.–Discharge measurement comparison

River Mile	High flow discharge (cfs)	Low flow discharge (cfs)	Discharge Difference (cfs)	% Change
55.5	47	40	7	15%
48.8	189	74	115	61%
40.8	74	57	17	23%
36.4	220	83	137	62%
27.5	338	109	229	68%
24.3	369	93	276	75%
21.4	404	92	312	77%

River Mile	High flow discharge (cfs)	Low flow discharge (cfs)	Discharge Difference (cfs)	% Change
17.2	392	88	304	78%
9.3	510	78	432	85%
0.4	535	58	477	89%

Figure 32.–Split channel with missing flow at RM 40.8.

4.4 Water Surface Elevation Measurements

Water surface elevations were measured at each discharge measurement location. It was safe to wade the river during the low flow season; therefore, a water surface elevation and thalweg channel bottom profile was measured at each site. The tabular data are presented in Table 14. The base location stakes were located for eight sites. At three of the twelve sites, the original stake could not be located, requiring a new stake to be installed and a new OPUS solution submission.

Table 14.–Water Surface Profile Measurement Comparison. Elevation values are in NAVD88 ft.

River Mile	WSE during high flow (ft)	WSE during low flow (ft)	WSE Difference (ft)
55.5[1]	5796.7	5796.9	-0.2
48.8[1]	5640.5	5640.8	-0.2
40.8	5389.5	5389.0	0.5
36.4	5249.2	5248.7	0.5
33	5152.0	5151.6	0.4
27.5	4932.5	4931.7	0.8
24.3	4804.7	4803.6	1.1
21.4	4685.4	4684.4	1.0
17.2	4517.7	4516.4	1.3
9.3	4242.9	4241.9	1.1
0.4[1]	3929.7	3927.8	1.9

[1]Indicates a replacement base station monument.

The difference in water surface elevation followed similar trends to the difference in discharge values. The change in water surface elevation increased in the downstream direction, with the highest difference being 1.9 ft near the confluence with the Salmon River, RM 0.4.

At RM 55.5 and 48.8 the water surface slightly increased, 0.2 ft, from high flow to low flow season. It is likely that the water surface elevations were very similar between the two sites and the negative change could be a result of a variety of factors. The negative change in elevation could be an artifact of two separate base station locations rather than a drop in water surface elevation. Downstream hydraulic control (riffles or diversion crests) may have changed between measurement periods. Thirdly, an increase in seasonal roughness due to macrophytes and other vegetation could reduce channel capacity and result in an increase in water surface elevation.

4.5 Pebble Count Measurement Results

During the August trip (low flow) pebble counts were taken at each site to characterize the bed material. Tabular results are presented in Table 15, graphical results with respect to river mile are presented in Figure 33. The raw pebble count data is presented in Appendix E – Pebble Count Data. Much of the sediment could be classified as very coarse gravel (32 – 64 mm); however, the full range of particle sizes was observed, from a diameter of 512 mm to fines (< 2 mm).

Figure 33 shows that the coarsest sediment was observed along the middle portion of the river. Sediment at the far downstream and upstream reaches was slightly finer. The fine sediment observed at the downstream end of the Lemhi River is largely due to backwater effects creating a depositional zone as the Lemhi River approaches the Salmon River.

Table 15.–Pebble count results

Location	Geomorphic Feature	D_{84} (mm)	D_{50} (mm)	D_{16} (mm)	Mode (mm)
RM 55.5	Riffle	39	17	5	32
RM 55.5	Pool	39	20	9	27
RM 55.5	Riffle	40	22	11	32
RM 48.8	Riffle	100	41	21	32
RM 40.8	Run	98	36	10	32
RM 36.4		101	51	9	32
RM 33	Run	67	32	10	45
RM 27.5	Run	88	42	18	64
RM 24.3	Riffle	150	58	23	64
RM 21.4	Riffle	151	62	31	64
RM 17.2		105	46	19	45
RM 9.3	Riffle	85	42	19	45
RM 0.4	Riffle	96	41	16	23
Texas Creek	bar	14	8	3	11
Texas Creek		30	30	5	0
Eighteen Mile Creek	Riffle	8	5	0	7
Hayden Creek	Riffle	132	69	22	90

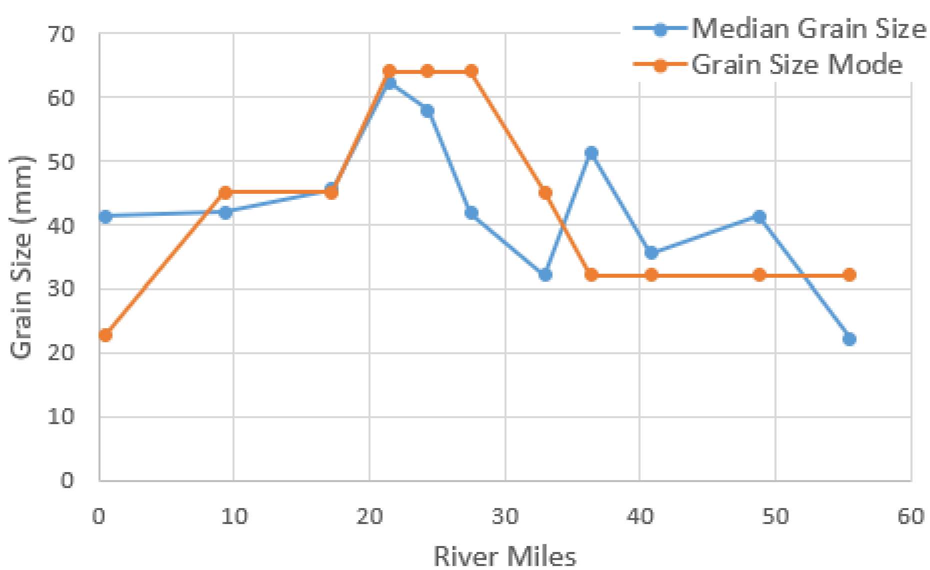

Figure 33.–Median and most frequent (mode) grain sizes in run or riffle features with respect to river miles.

Example sediment curves are presented in Figure 34. The steep slope indicates that the bed material is relatively uniform, or poorly graded. The bed was armored at each site on the Lemhi River and Hayden Creek. Often sediment was highly embedded and difficult to remove from the armored layer. Examples of the channel beds at two sites are presented in Figure 35. The particles are very angular and "plate-like" in shape. Underneath the armored layer, the sediment was well graded with a wide range of sands, gravels, and cobbles. An example photo is presented in Figure 36. No analyses were performed for the sublayer.

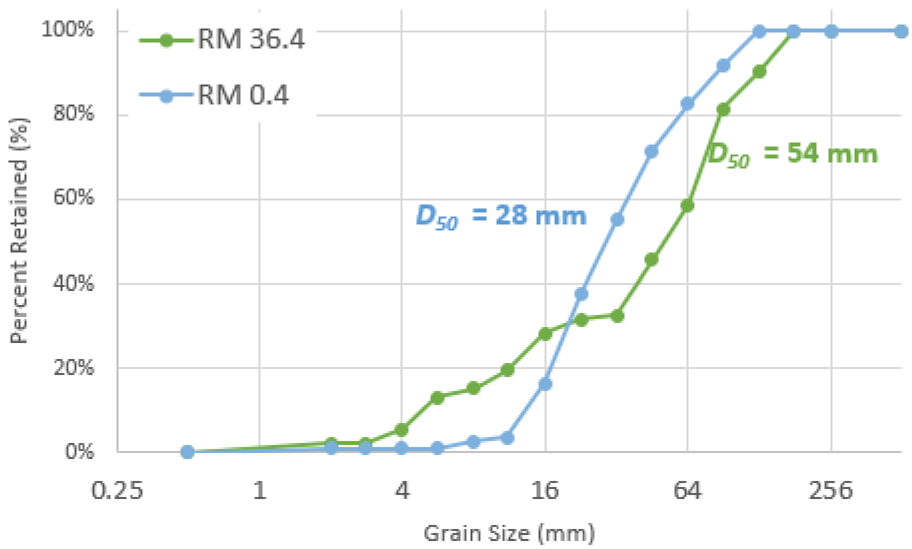

Figure 34.–Sediment grain size distribution for RM 36.4 and RM 0.4

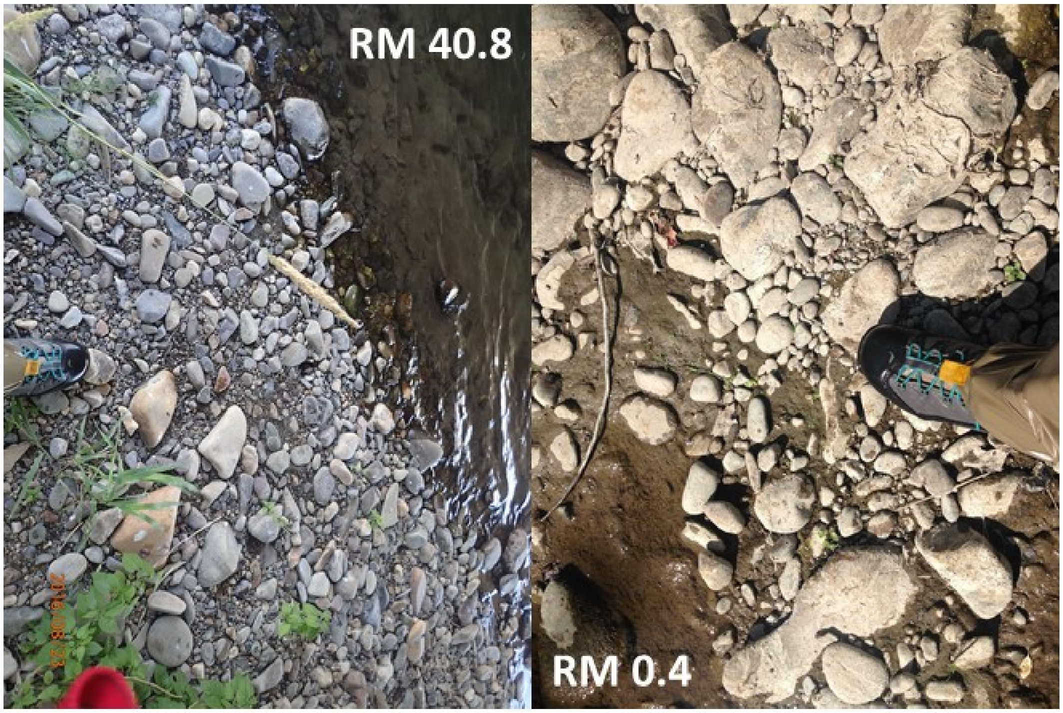

Figure 35.–Exposed channel bed photos at RM 40.8 (left) and RM 0.4 (right). Boot toe is approximately 95mm for scale.

Figure 36.–Well graded sediment beneath the armor layer at RM 24.3. The pen provides relative scale.

5 Data Gaps and Recommendations

This study utilized a combination of measurement data, field observations, and surrogate parameters to inform an Integrated Rehabilitation Assessment. The assessment is intended to identify watershed-scale characteristics and select optimal project locations for further study and channel/floodplain rehabilitation. The recommendations provided in this section are geared towards future hydraulic modeling at the reach or project scale.

Flow depth and velocity are often key parameters to analyze the quality of fish habitat in a river reach. Hydraulic modeling informs potential habitat improvement projects and provides important tools for project planning. Hydraulic model results can provide a detailed understanding of the existing conditions with regards to Endangered Species Act (ESA) listed salmonid physical habitat conditions. The hydraulic model results for depth, velocity, and shear stress can provide input data for Habitat Suitability Index (HSI) modeling.

The information necessary to build a hydraulic model is dependent on the level of detail and the questions being asked. For the Lemhi River, a steady two-dimensional (2D) hydraulic model is recommended. A 2D model (as compared to a one-dimensional, 1D, model) better informs parameters necessary for habitat improvement such as: velocity, depth, and floodplain connectivity. A 1D model is limited when calculating the above parameters, a 2D model better captures floodplain connectivity and provides the data in a much higher longitudinal and lateral resolution. The Lemhi River has many multi-threaded and anastomosing reaches, which are difficult to represent in a one-dimensional model. Data collection effort necessary to inform both a 1D and 2D model are very similar. The additional cost of a 2D model is minimal in comparison to the information gained. Data necessary for a 2D model include:

1. Topographic data,
2. **Bathymetric data,**
3. Flow values of interest (typically includes low flow values and peak flow events)
4. **Flow change locations and quantities (diversions, returns, etc.),**
5. Sediment data to inform channel roughness and potential mobility,
6. Photos of the project site to inform modeling efforts, and
7. **Measured water surface elevation for a known discharge event for model calibration.**

The **bold** values remaining are data gaps. The following section discusses the available data. Reclamation's in-house 2D model, SRH-2D, a depth-averaged hydraulic model, specifically focused on the flow hydraulics of river systems and is recommended by TSC staff for future project and reach scale assessments.

5.1 Existing Data for the Lemhi River Basin

This study populates the data for four items numerated above: discharge values, sediment data, photos, and calibration data. There are existing topographic and bathymetric data sets. Furthermore, the University of Idaho is currently developing a 2D model of the upper Lemhi Basin.

Topographic LiDAR was collected in 2008, 2010, and 2011. The data sets were combined to produce one terrain surface, as shown in Figure 37. These data only contain topographic values. Data within the river reflects the water surface elevation of the day the LiDAR was flown, rather than the channel bottom.

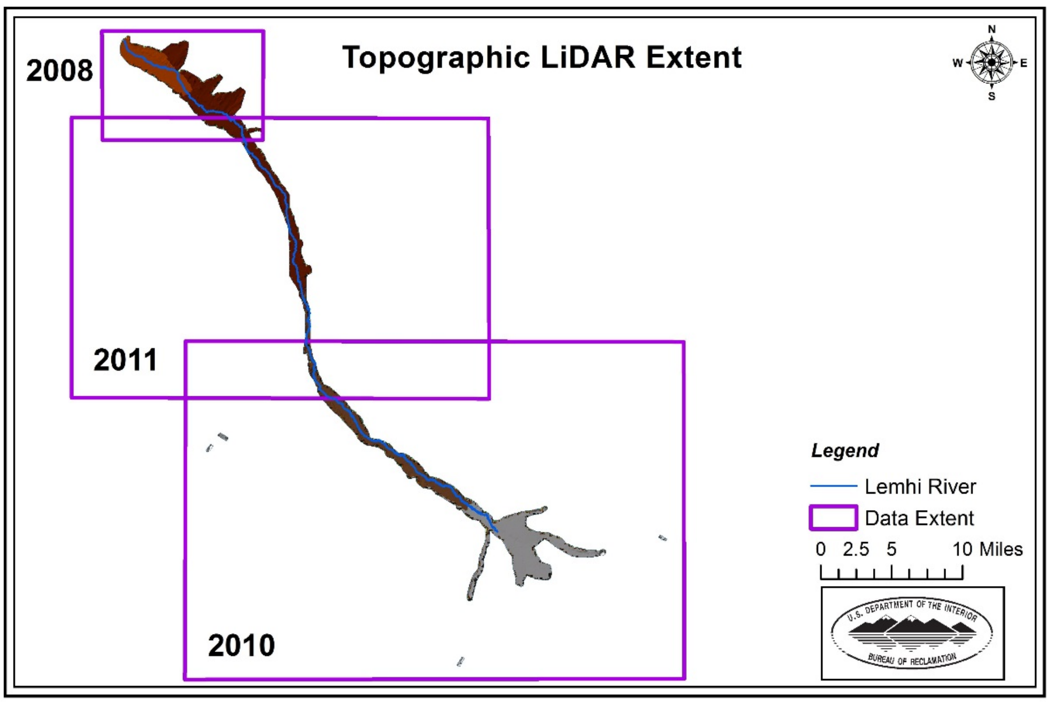

Figure 37.–Topographic LiDAR Extent

Bathymetric LiDAR was collected by the U.S. Forest Service (USFS) during a three day mission in October of 2013. University of Idaho Civil Engineering Department post-processed the data set. The data set is EAARL-B data, which is a narrow beam (20cm diameter at the ground) fast pulse Green LiDAR. Its nominal resolution is meter scale flying approximately 300 m from the ground, with a 200 m wide swap. The EAARL-B splits the laser pulse into three beamlets, which stagger to provide a denser resolution. A fourth receiver was added to maximize energy return for deep water conditions.

The data extends from RM 31.0 past 63.3. The width ranges from approximately 3,000 ft to 4,500 ft, perpendicular to the channel (Figure 38). The resolution of the LiDAR is approximately 1 m (3.28 ft). There is a gap in the LiDAR between RM

34 and RM 37. Reclamation should consider collecting their own bathymetric LiDAR in the downstream half of the basin (RM 0 through RM 31). The Lemhi River is relatively shallow with clear water. While the banks are vegetated, the vegetation is rarely thick enough to create a scenario with 100% canopy cover. A discussion of bathymetric data collection options is discussed in the following section.

The University of Idaho’s Civil Engineering Department is building a MIKE 21, 2D model for the upper portion of the basin from approximately Leadore to Lemhi (RM 63.3 to RM 34.4). The purpose of the modeling effort is to prove the application of bathymetric LiDAR, which was flown by USFS. As previously mentioned, model results could be used to inform habitat suitability metrics, if results are published within the project timeframe. MIKE 21 and Reclamation’s SRH-2D have very different mesh formats and file systems. Therefore, the level of effort required to convert between the two is not compatible. It would be more advantageous to build a new model utilizing the same input data.

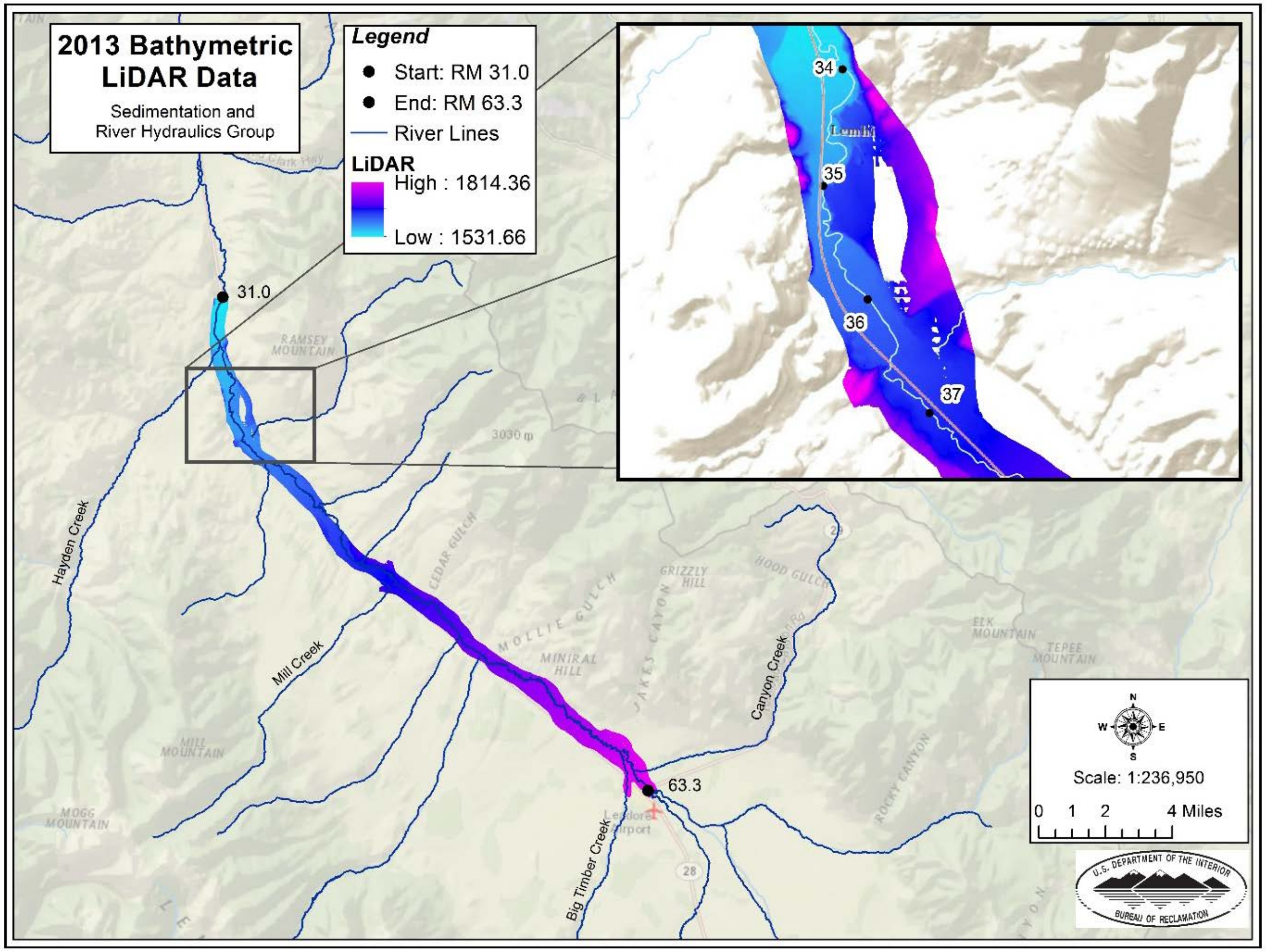

Figure 38.–2013 topographic and bathymetric LiDAR extent

5.2 Bathymetric Data Collection Options

Flying bathymetric LiDAR is a newer technology, which determines the water depth by measuring a time delay between a transmission pulse and return signal. Laser pulses operate at two frequencies, a lower frequency which reflects off the water surface and a higher frequency which can penetrate the water column, reflecting off the bottom. Limiting factors of airborne bathymetric LiDAR include: water clarity/turbulence, water depth, vegetation, bottom material, weather, and background light (Muirhead & Cracknell, 1986). The Lemhi River is relatively shallow with clear water, which can be measured at a vertical accuracy level of up to 15cm (Gao, 2009). LiDAR should be flown in the fall/winter season, once the trees/shrubs have shed their leaves and before significant snow fall. However, it would be most economical to fly LiDAR for all basins (Main Salmon, Pahsimeroi, and Lemhi Rivers) at the same time. The recommended time for the Pahsimeroi River Basins are when river stage is the lowest, late-July and August. The canopy will be in leaf-on conditions. None of the three basins are heavily vegetated; therefore, the majority of the landscape will not be obstructed by leaf cover. For vegetated areas in the basins, a dense point cloud can capture the ground elevation through the canopy. A minimum point density of 7 points per square meter (pts/m^2) is recommended. An optimal collection density would be 12 pts/m^2. LiDAR data can be converted into a surface by linearly interpolating between measurement points.

Boat or manual surveys are two alternatives for collecting bathymetric data. A boat survey involves floating the project area with an acoustic Doppler current profiler (ADCP) mounted to the boat. The boat would float cross sections and profiles (at minimum the centerline) of the project reach collecting bathymetric data. A surface can be created from the data set by linearly interpolating between surveyed points. A boat survey would need to occur during the high flow season, when flow depths are high enough for the instrument operation and boat access. A manual survey would require a crew to survey several cross sections along the project reach and a longitudinal profile. This method may be cost prohibitive depending on the size and resolution of the desired data set. Manual surveys should take place during the low flow season for the safety of the crew.

With a boat or manual survey, it is impractical to sample with as fine of a resolution as a LiDAR data set. Therefore, the measured point cloud will be coarse and the majority of the surface will be estimated via linear interpolation. This methodology increases uncertainty in the results. Both the boat bathymetric survey and manual survey could be tied into the existing LiDAR data. However, if the river has significantly shifted vertically or horizontally, the combined surface will be inconsistent.

5.3 Hydrologic Data Gaps

The purpose of the hydrologic assessment was to identify available gage data and provide appropriate discharge values to inform existing and future assessment efforts including hydraulic modeling. Low flow discharges drive habitat suitability analyses and fish use. The only low flow discharge estimated in this study was the 7Q10. Therefore, monthly and fish passage and moderate flow discharge values should be estimated throughout the basin in future phases of work.

The hydrologic assessment did not directly account for irrigation losses and returns. One of the hydrology data gaps is an understanding of the locations, volume, and timing of many diversions along the Lemhi River. Hydraulic modeling without this information would not accurately reflect existing conditions. Another data gap is the incoming flow rates from each tributary. IWRB provides gages on many of the Lemhi tributaries, but many are still ungaged. If the hydraulic model were to include one of the ungaged tributaries, its flow contribution would be a data gap.

Groundwater interactions and wetlands play a large role in the hydrology of the Lemhi River Basin, particularly in the upper basin. Groundwater and wetland interaction will impact both the timing and magnitude of the peak flows spatially within the study area. The quantitative role of groundwater interactions was not assessed in this study. Local knowledge suggests that the basin upstream of Hayden Creek deviates from the typical snow melt hydrologic regime due to both groundwater interactions and irrigation diversions (L. Johnson, personal communication, 2/27/2017; J. Trapani, 3/15/2017). Therefore, the IWRB gages were included in the hydrologic analysis to represent the upper basin. However, these annual peaks were developed utilizing mean daily data, which adds additional uncertainty to the analysis.

5.4 Stream Power Assessment Recommendations

The purpose of the stream power assessment was to gain a general understanding of the relative sediment transport capacity of each geomorphic reach. Sediment supply and size as well as channel geometry are necessary to better understand the actual trends in sediment transport within the Lemhi River. Although high stream power results were observed in the downstream reaches, signs of recent incision were not observed at the site. Furthermore, the pebble count data yielded smaller grain sizes in the downstream end Lemhi River, which suggests a lower sediment transport competency zone, or depositional zone.

The discrepancy between the stream power and a combination of pebble count data and site observations could be a result of several factors explained in the paragraphs below. The first major factor is channel width. Given that the channel flows through generally unconfined valley reaches, the Lemhi River likely widens as additional tributary flows join the system during spring snowmelt. Knowing average reach channel width may help explain the discrepancy by calculating the unit-width stream power moving downstream. The unit-width stream power was not calculated during this study as the channel width for a given flow rate was unknown. The second factor is the difference between the estimated discharge values and the actual discharge values. The estimated discharge values are based on drainage area ratios between gaged and ungaged sites. The estimated values do not directly account for irrigation losses. Therefore, the depositional zone observed at RM 0.4 is likely an artificial result of irrigation diversions. If water was not diverted out of the Lemhi River, signs of incision or meandering would be more likely in this area, rather than deposition.

Other reaches that reported high stream power did not show signs of incision. It is likely that incision was avoided by the heavily armored bed layer. The energy would then be applied to the stream banks, possibly eroding the banks, which would slowly widen the channel, increasing the width-to-depth ratio. This phenomena is especially apparent where the river has been straightened and channelized. Other factors that could explain the difference between the stream power estimates and pebble count observations are increased channel roughness, greater floodplain connection, and/or channel geometry (i.e.: higher width-to-depth ratios).

5.5 Field Data Recommendations

Field data was collected during this study to inform the Integrated Rehabilitation Assessment and to populate and calibrate ongoing and future hydraulic modeling efforts. Both high and low flow calibration can be useful in better understanding the hydraulics at a site. During high flow events, form roughness dominates resulting in a lower roughness value, on average. Particle roughness dominates at low flow events, likely resulting in a higher roughness value. If form-dominant roughness were to be applied in low flow conditions, it is likely that flow depths would be underestimated, velocities over-estimated, resulting in a gross underestimation of fish habitat.

The error associated with each discharge measurement was greater than the suggested 5%, due to many challenges associated with collecting high flow measurements on the Lemhi River. Furthermore, the lack of diversion/tributary flow rates and locations prevents a mass balance analysis. A mass balance analysis involves a discharge measurement upstream, downstream, and within a tributary/diversion. The upstream minus the diversion values (or upstream plus the inflowing tributary values) should be equal to the downstream value. If they are not equal and the groundwater flux is negligible, one of, or multiple measurements may be incorrect.

The high error and inability to perform a mass balance analysis decreases the confidence in calibrating a model to the measured data set. Therefore, it is recommended to provide a range of values by assuming an upper and lower limit to the discharge measurement. This can be done by adding and subtracting the error from each of the measurements. The values are presented in Table 16 for high flow measurements and in Table 17 for low flow measurements. The goal when calibrating a model would be to fit the water surface elevation measurement within the two modeled water surface profiles of different discharges.

Measured water surface elevation for a known discharge event for model calibration was listed as a potential data gap in Section 5 as the data provided in this study are coarse in resolution. Depending on the location of the next phase of work, it may be necessary to collect additional discharge and water surface elevation measurements, specific to the modeled reach. Furthermore, water surface elevation data, associated with a known discharge value, are necessary when calibrating a hydraulic model. It is recommended to collect water surface elevation data along the entire modeled reach.

Table 16.–Discharge upper and lower limits for high flow measurements.

Measurement Location	Measured Discharge (cfs)	Error	Discharge Upper Limit	Discharge Lower Limit	Instrument
55.5	47.1	2.3%	48.1	46.0	Velocity Meter
48.8	189	5.7%	200	178	ADCP
40.8	74.1	10.2%	81.6	66.5	ADCP
36.4	220	8.6%	239	201	ADCP
33	180	4.1%	188	173	ADCP
31.1	469	6.7%	500	437	ADCP
27.5	338	5.9%	358	318	ADCP
24.3	369	4.7%	386	352	ADCP
21.4	404	4.8%	423	385	ADCP
17.2	392	5.9%	415	369	ADCP
9.3	510	4.3%	532	488	ADCP
0.4	535	4.0%	557	514	ADCP
Texas Creek	19.2	3.9%	20.0	18.5	Velocity Meter
Eighteen Mile Creek	16.3	0.6%	16.4	16.2	Velocity Meter
Hayden Creek	181	10.6%	200	162	ADCP

Table 17.–Discharge upper and lower limits for low flow measurements. All discharge measurements were taken with a velocity meter during the low flow season.

Measurement Location	Measured Discharge (cfs)	Error	Discharge Upper Limit	Discharge Lower Limit
55.5	39.6	1.8%	40.3	38.9
48.8	73.9	7.4%	79.4	68.5
40.8	57.0	4.0%	59.4	54.7
36.4	82.6	4.2%	86.1	79.2

Measurement Location	Measured Discharge (cfs)	Error	Discharge Upper Limit	Discharge Lower Limit
27.5	109	4.7%	114	103
24.3	93.4	4.0%	97.1	89.7
21.4	91.7	2.8%	94.3	89.2
17.2	87.9	1.7%	89.4	86.4
9.3	78.1	2.7%	80.2	76.0
0.4	57.5	2.4%	58.8	56.1
Texas Creek	5.58	4.6%	5.83	5.32
Eighteen Mile Creek	1.54	6.8%	1.64	1.43

6 Conclusion

The information provided in this report is intended to advise an Integrated Rehabilitation Assessment of the Lemhi River Basin, whose goal is to characterize watershed-conditions within the river basin while providing context for future analyses and potential rehabilitation projects. The objectives of this report include: peak flow estimations, a stream power assessment, discharge and water surface elevation measurements, and bottom sediment characteristics. These data were then combined to develop a list of data needs for future hydraulic modeling analyses.

The Lemhi River flow regime is snowmelt dominated and is highly altered due to numerous diversions along the entire 63.3 miles. The locations and volumes of water being diverted is currently not well understood. Groundwater is also an important contributor to the Lemhi River, especially in the upper half of the basin. Flood-frequency peak flows were estimated at twenty-seven sites along the Lemhi River using a drainage area ratio method and did not directly account for any diversions.

The stream power assessment indicated that the lower half of the basin is high energy and has a higher capacity to transport sediment compared to the upper half. Both the slope and discharge values are lower in the upper half, decreasing the capacity for sediment transport. The reach downstream of Hayden Creek is likely a depositional zone as both stream power and slope significantly decrease. More information is needed to verify sediment transport trends.

The pebble count results show that the finest particles were seen in the upper portion of the basin, especially in the headwaters. Finer particles were also observed at RM 33, near the Hayden Creek confluence, which corroborates the depositional zone hypothesis noted in the stream power analysis. The coarsest bed material was found at RM 21.4 and RM 24.3. Sediment sizes were smaller as the Lemhi River approached the confluence with the Salmon River. Armoring and embedded particles were observed at all sites on the Lemhi River and Hayden Creek, which could be a result of a variety of historical factors including: grazing, irrigation, channel straightening, etc.

Two sets of discharge and water surface elevation measurements were performed during high and low flow seasons. These data were collected with the intention of calibrating a future hydraulic model. A 2D hydraulic model will estimate the spatial distribution of depth, velocity, and shear stress. Recommendations were provided on what data are necessary to build a 2D hydraulic model. The primary data input missing is bathymetric data, although an improved understanding of diversion outflows, tributary inflows, and groundwater contributions will increase the accuracy of a 2D hydraulic model for this area. Furthermore, additional field data may be necessary depending on the location of future phases of work.

7 References

Bell, S. (1999). *A Beginner's Guide to Uncertainty of Measurement.* Teddington, Misslesex, United Kingdom: National Physical Laboratory.

Berenbrock, C. (2002). *Estimating the magnitude of peak flows at selected recurrence intervals for streams in Idaho: US Geological Survey Water-Resources Investigation Report.*

Buchanan, T., & Somers, W. (1969). *Discharge Measurements at Gaging Stations.* Washington D.C.: U.S. Geological Survey.

Donato, M. (1998). *Surface-water/ground-water relations in the Lemhi River basin, east-central Idaho.* Boise, ID: US Geological Survey Water-resources investigations.

England, J., Cohn, T., Faber, B., Stedinger, J., Thomas, W., Veilleux, A., . . . Mason, R. (2015). *Guidelines for determining flood flow frequency Bulletin 17C.* Reston, VA: U.S. Geological Survey.

Flynn, K., Kirby, W., & Hummel, P. (2006). *User's Manual for Program PeakFQ, Annual Flood-Frequency Analysis Using Bulletin 17B Guidelines.* U.S. Geological Survey.

Fulford, J. (n.d.). *Discharge Uncertainty Example: Wading Measurements of Discharge Using a Point Velocity Meter and the Velocity-Area Method.* World Meteorological Organization.

Gao, J. (2009). Bathymetric mapping by means of remote sensing: methods, accuracy and limitations. *Progress in Physical Geography, 33*(1), 103-116.

HACH. (2012). *FH950 User Manual, Edition 3.*

Harrelson, C., Rawlins, C., & Potyondy, J. (1994). *Stream channel reference sites: an illustrated guide to field technique.* Fort Collins, CO: USDA Forest Service, Rocky Mountain Forest and RAnge Experiment Station.

Helsel, D., & Hirsh, R. (1992). *Statistical Methods in Water Resources* (Vol. 49). Elsevier.

Hortness, J. (2006). *Estimating Low-Flow Frequency Statistics for Unregulated Streams in Idaho.* Reston, VA: U.S. Department of the Interior, U.S. Geological Survey.

Idaho Department of Environmental Quality. (2012). *Lemhi River Subbasin Total Maximum Daily Loads and Five-Year Review*. Boise, ID.

Idaho Department of Water Resources. (2006). Points of diversion inventoried in existing water districts in the Lemhi basin. *shapefile 2001 - 2002*. Boise, ID: IDWR.

Idaho Department of Water Resources. (2008). *Upper Lemhi River seepage study.* Boise, ID.

Interagency Avisory Committee on Water Data. (1981). Guidelines for Determining Flood Flow Frequency, Bulletin #17B of the Hydrology Committee. US Department of Interior.

Mueller, D. (2012, September). Review and Rating of Moving-Boat ADCP Discharge Measurements. U.S. Geological Survey.

Mueller, D. (2016). *QRev - Software for Computation and Quality Assurance of Acoustic Doppler Current Profiler Moving-Boat Streamflow Measurements*

- *User's Manual (ver.2.80).* U.S. Geological Survey. Retrieved from http://dx.doi.org/10.31133/ofr20161056

Mueller, D., Wagner, C., Rehmel, M., Oberg, K., & Rainville, F. (2013). *Measuring discharge with acoustic Doppler current profilers from a moving boat (ver. 2.0, December 2013.* U.S. Geological Survey. Retrieved from http://pubs.usgs.gov/tm/3a22/

Muirhead, K., & Cracknell, A. (1986). Airborne lidar bathymetry. *International Journal of Remote Sensing, 7*, 597-614.

Oberg, K., Morlock, S., & Caldwell, W. (2005). *Quality-assurance plan for discharge measurements using acoustic Doppler current profilers.* Reston, VA: U.S. Geological Survey.

Simpson, M. (2002). *Discharge measurements using a broad-band acoustic Doppler current profiler.* U.S. Geological Survey.

SonTek/YSI. (2013). *RiverSurvyor S5/M9 Version 9.00.* San Diego, CA: Xylem Brand.

Trimble. (2014). *Trimble R10 GNSS System.* Retrieved from Trimble: http://trl.trimble.com/docushare/dsweb/Get/Document-625158/022543-544E_TrimbleR10_DS_1014_LR.pdf

Urick, R. (1983). *Principles of underwater sound* (3rd. ed.). McGraw-Hill.

Vogel, R., & Stedinger, J. (1958). Minimum variance streamflow record augmentation procedures. *Water Resources Research*, *21*(5), 715-723.

Walters, A., Bartz, K., & McClure, M. (2013). Interactive Effects of Water Diversion and Climate Change for Juvenile Chinook Salmon in the Lemhi River Basin (USA). *Conservation Biology*, *27*(6), 1179-1189. doi:10.1111/cobi.12170

Weather underground PWS data. (n.d.). *Salmon, ID (83467) Forecast*. Retrieved from Weather Underground: https://www.wunderground.com/us/id/salmon/zmw:83467.1.99999

Wolman, M. (1954). A method of smapling coarse river-bed material. *EOS, Transactions American Geophysical Union, 35*(6), 951-956.

Zabel, R., Cooney, T., Jordan, C., Carmichael, R., Jonasson, B., Sedell, E., . . . Scheuerell, M. (2016). *Life-Cycle models of salmonid populations in the interior Columbia River Basin.*

8 Appendix A – Annual Hydrographs

Appendix A – Annual Hydrographs includes hydrographs of the Lemhi River from water years 1993 through 2015. Only water years with complete data from both the US (USGS gages 13305000) and DS (13305310) gages were included.

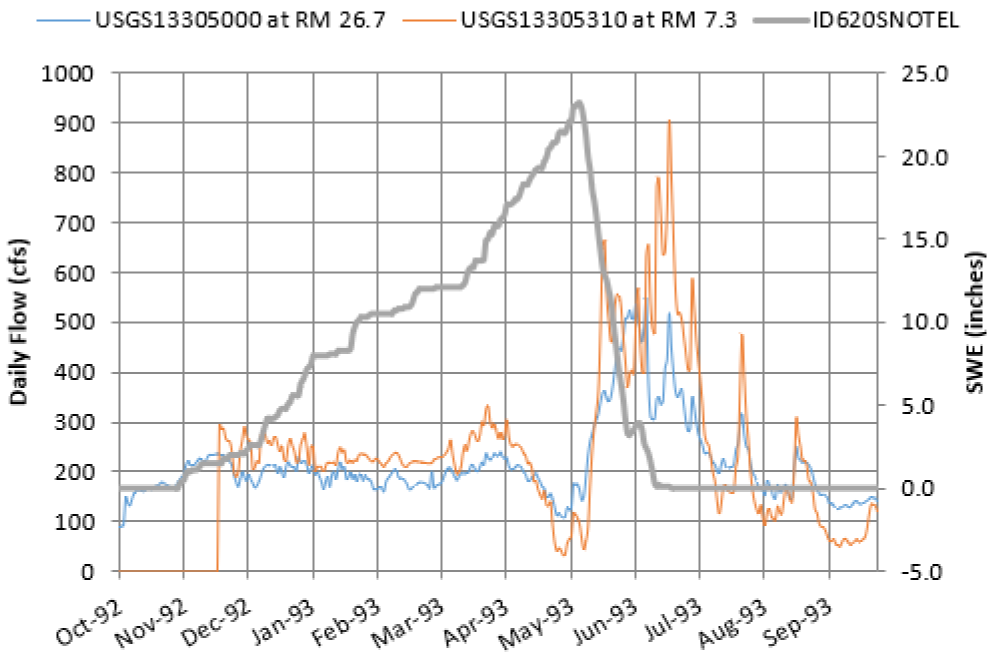

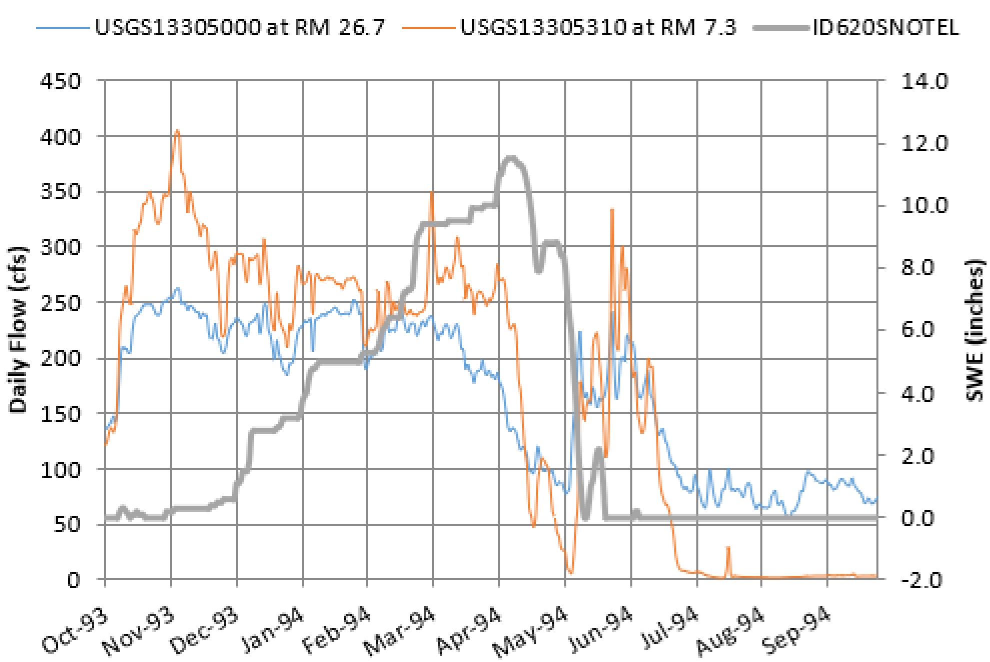

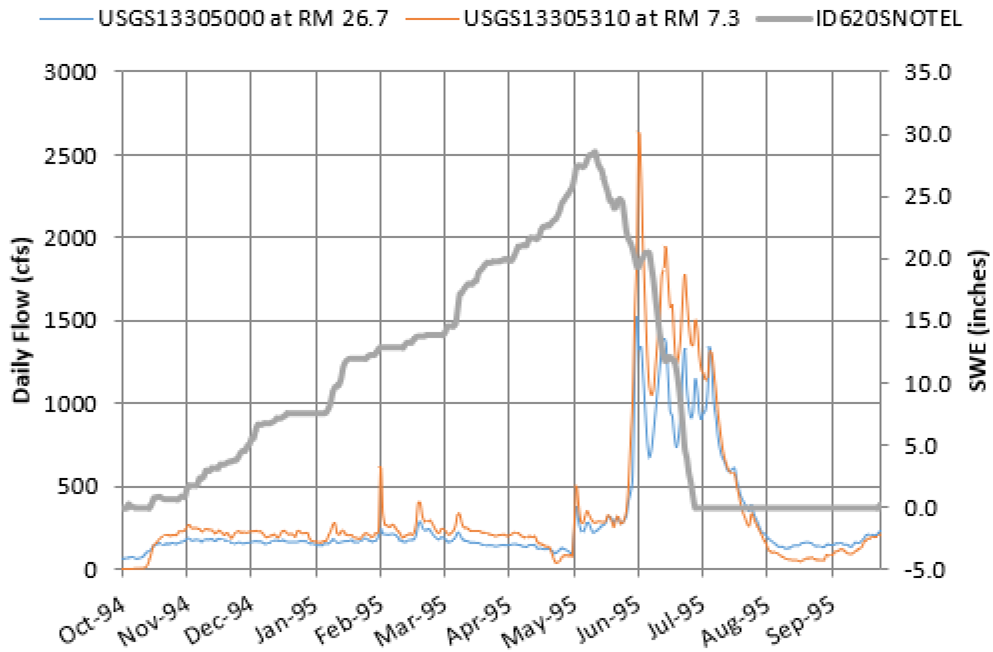

USGS13305000 at RM 26.7
USGS13305310 at RM 7.3
ID620SNOTEL
Daily Flow (cfs)
SWE (inches)
3000
2500
2000
1500
1000
500
0
35.0
30.0
25.0
20.0
15.0
10.0
5.0
0.0
-5.0
Oct-94
Nov-94
Dec-94
Jan-95
Feb-95
Mar-95
Apr-95
May-95
Jun-95
Jul-95
Aug-95
Sep-95

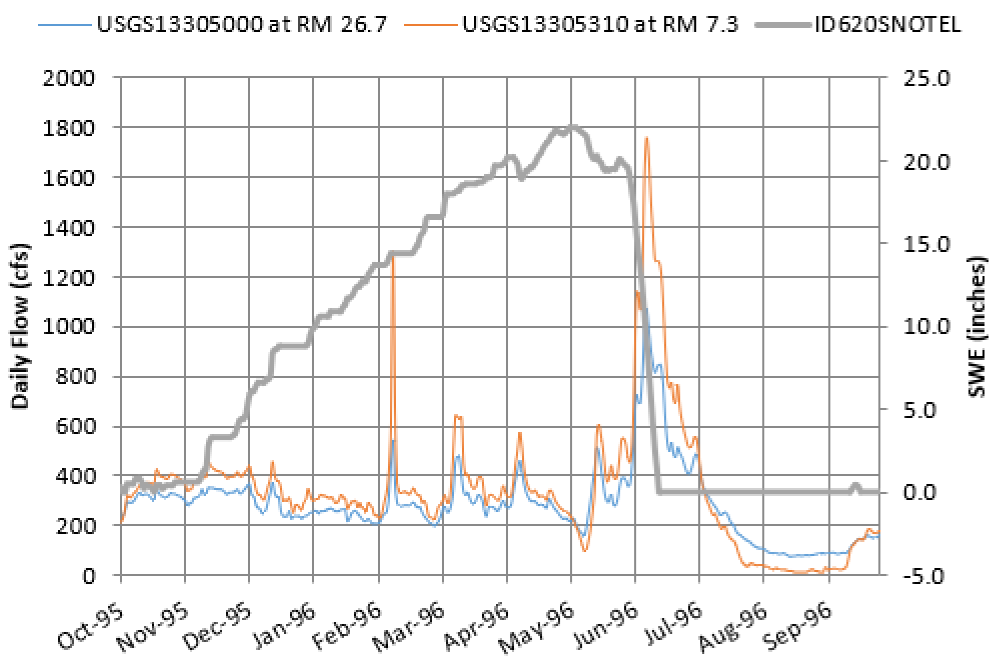

USGS13305000 at RM 26.7
USGS13305310 at RM 7.3
ID620SNOTEL
Daily Flow (cfs)
SWE (inches)
2000
1800
1600
1400
1200
1000
800
600
400
200
0
25.0
20.0
15.0
10.0
5.0
0.0
-5.0
Oct-95
Nov-95
Dec-95
Jan-96
Feb-96
Mar-96
Apr-96
May-96
Jun-96
Jul-96
Aug-96
Sep-96

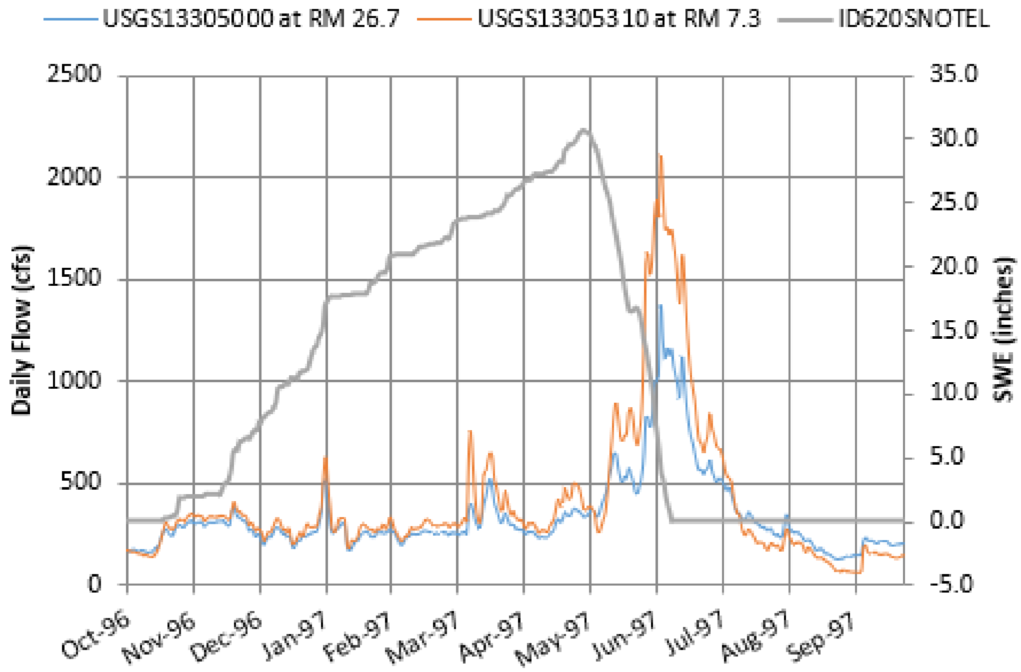
USGS13305000 at RM 26.7
USGS13305310 at RM 7.3
ID620SNOTEL
Daily Flow (cfs)
SWE (inches)
2500
2000
1500
1000
500
0
35.0
30.0
25.0
20.0
15.0
10.0
5.0
0.0
-5.0
Oct-96
Nov-96
Dec-96
Jan-97
Feb-97
Mar-97
Apr-97
May-97
Jun-97
Jul-97
Aug-97
Sep-97

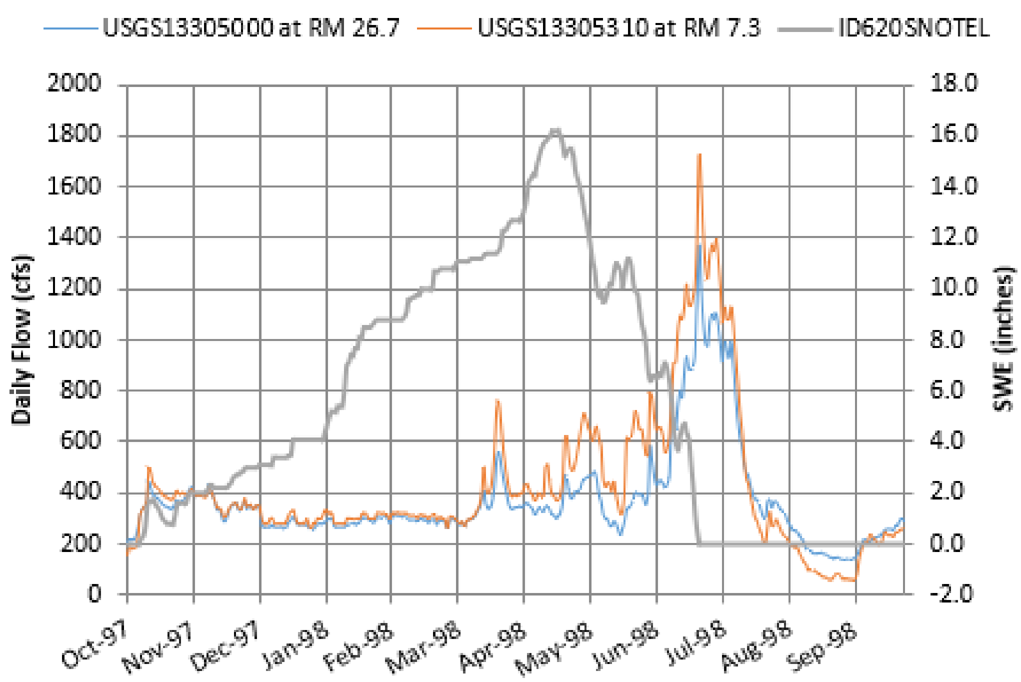
USGS13305000 at RM 26.7
USGS13305310 at RM 7.3
ID620SNOTEL
Daily Flow (cfs)
SWE (inches)
2000
1800
1600
1400
1200
1000
800
600
400
200
0
18.0
16.0
14.0
12.0
10.0
8.0
6.0
4.0
2.0
0.0
-2.0
Oct-97
Nov-97
Dec-97
Jan-98
Feb-98
Mar-98
Apr-98
May-98
Jun-98
Jul-98
Aug-98
Sep-98

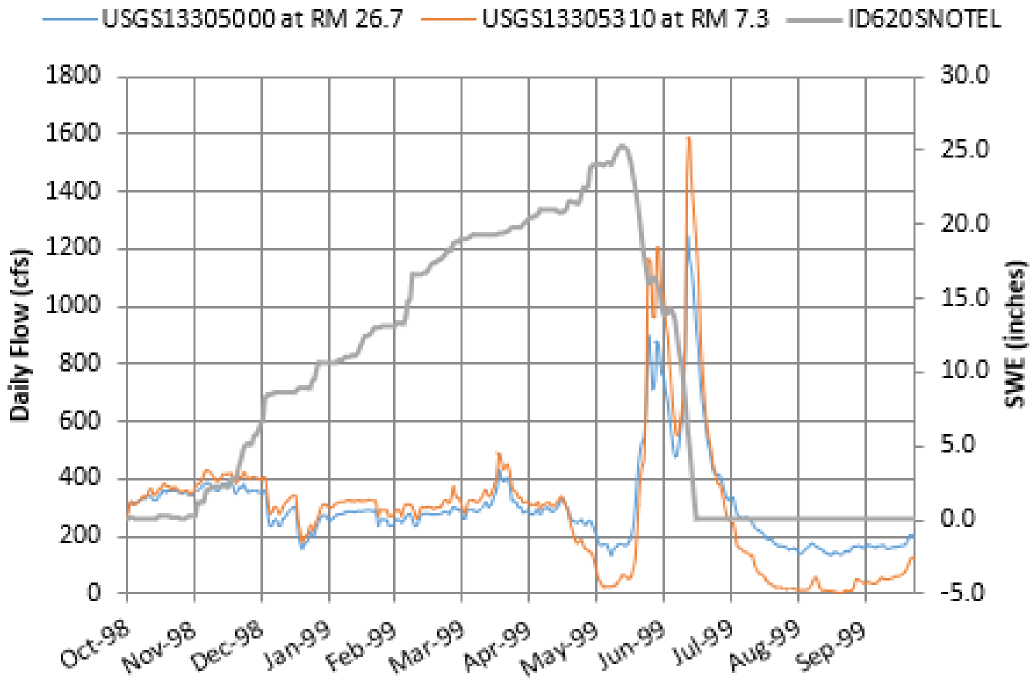

USGS13305000 at RM 26.7
USGS13305310 at RM 7.3
ID620SNOTEL
Daily Flow (cfs)
SWE (inches)
1800
1600
1400
1200
1000
800
600
400
200
0
30.0
25.0
20.0
15.0
10.0
5.0
0.0
-5.0
Oct-98
Nov-98
Dec-98
Jan-99
Feb-99
Mar-99
Apr-99
May-99
Jun-99
Jul-99
Aug-99
Sep-99

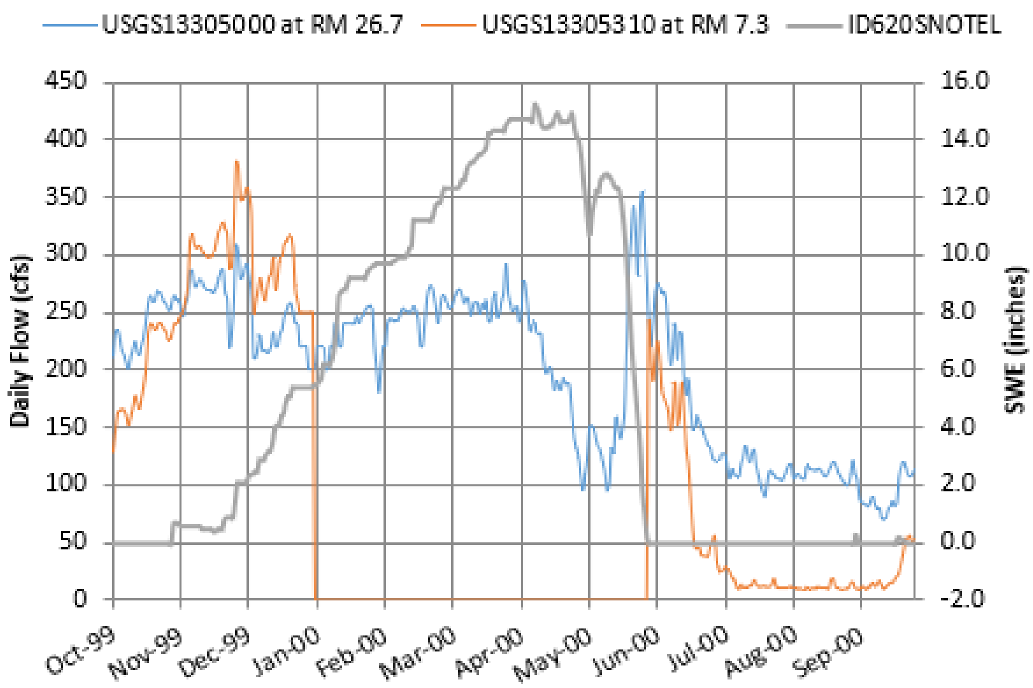

USGS13305000 at RM 26.7
USGS13305310 at RM 7.3
ID620SNOTEL
Daily Flow (cfs)
SWE (inches)
450
400
350
300
250
200
150
100
50
0
16.0
14.0
12.0
10.0
8.0
6.0
4.0
2.0
0.0
-2.0
Oct-99
Nov-99
Dec-99
Jan-00
Feb-00
Mar-00
Apr-00
May-00
Jun-00
Jul-00
Aug-00
Sep-00

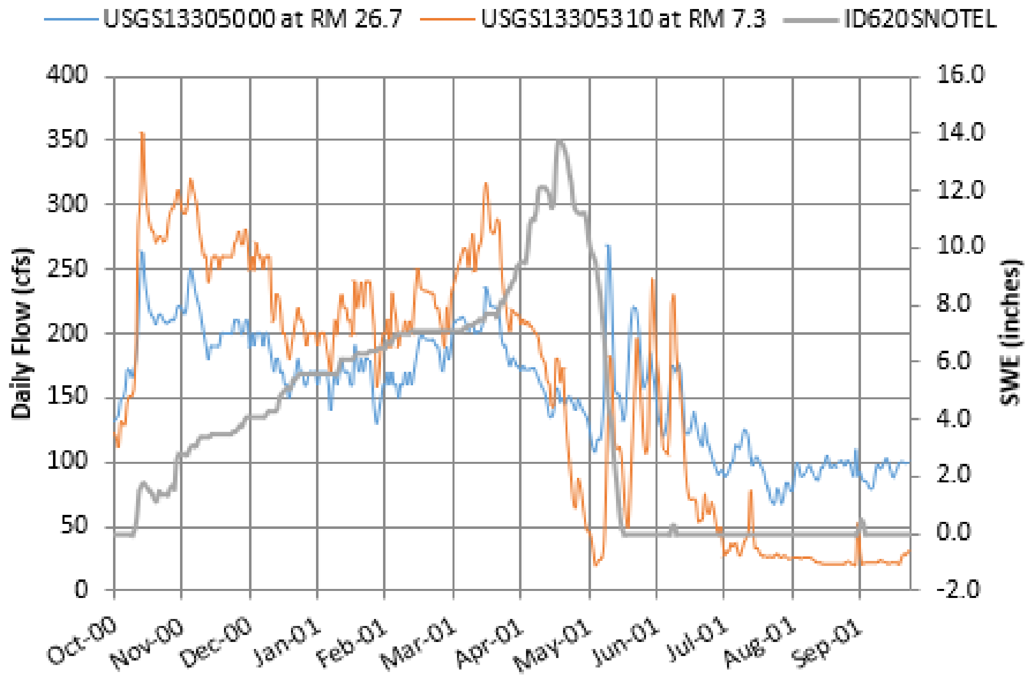
USGS13305000 at RM 26.7
USGS13305310 at RM 7.3
ID620 SNOTEL
Daily Flow (cfs)
SWE (inches)
400
350
300
250
200
150
100
50
0
16.0
14.0
12.0
10.0
8.0
6.0
4.0
2.0
0.0
-2.0
Oct-00
Nov-00
Dec-00
Jan-01
Feb-01
Mar-01
Apr-01
May-01
Jun-01
Jul-01
Aug-01
Sep-01

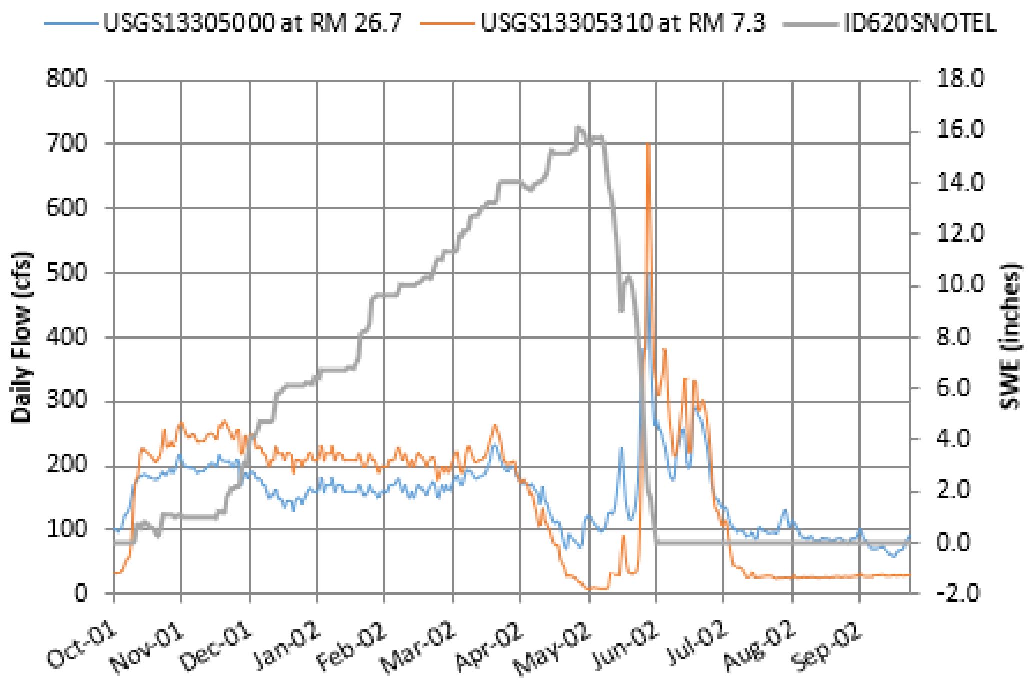
USGS13305000 at RM 26.7
USGS13305310 at RM 7.3
ID620 SNOTEL
Daily Flow (cfs)
SWE (inches)
800
700
600
500
400
300
200
100
0
18.0
16.0
14.0
12.0
10.0
8.0
6.0
4.0
2.0
0.0
-2.0
Oct-01
Nov-01
Dec-01
Jan-02
Feb-02
Mar-02
Apr-02
May-02
Jun-02
Jul-02
Aug-02
Sep-02

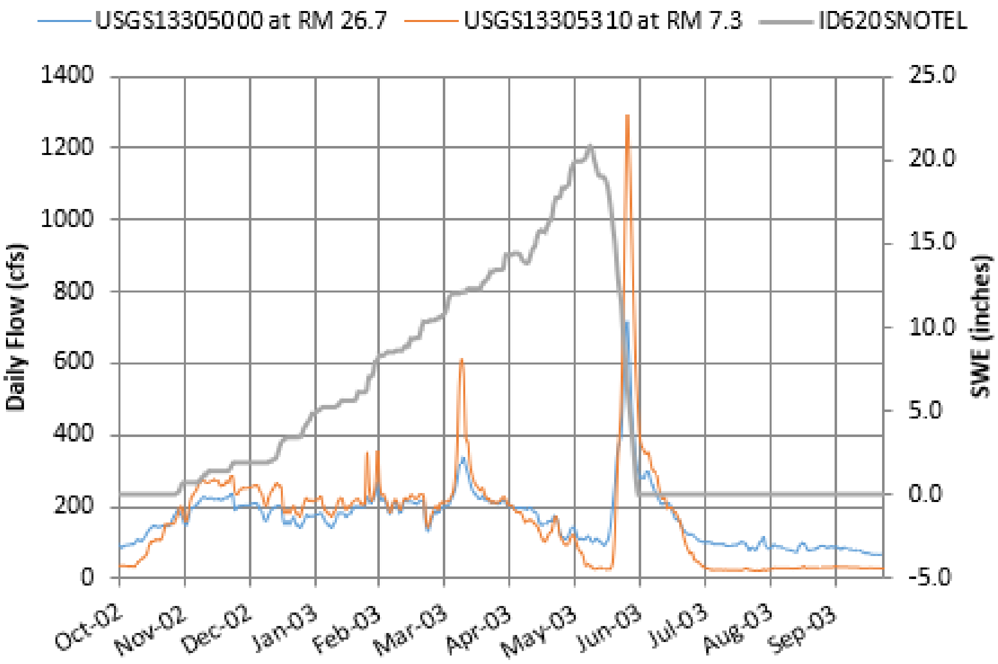
USGS13305000 at RM 26.7
USGS13305310 at RM 7.3
ID620 SNOTEL
Daily Flow (cfs)
SWE (inches)
1400
1200
1000
800
600
400
200
0
25.0
20.0
15.0
10.0
5.0
0.0
-5.0
Oct-02
Nov-02
Dec-02
Jan-03
Feb-03
Mar-03
Apr-03
May-03
Jun-03
Jul-03
Aug-03
Sep-03

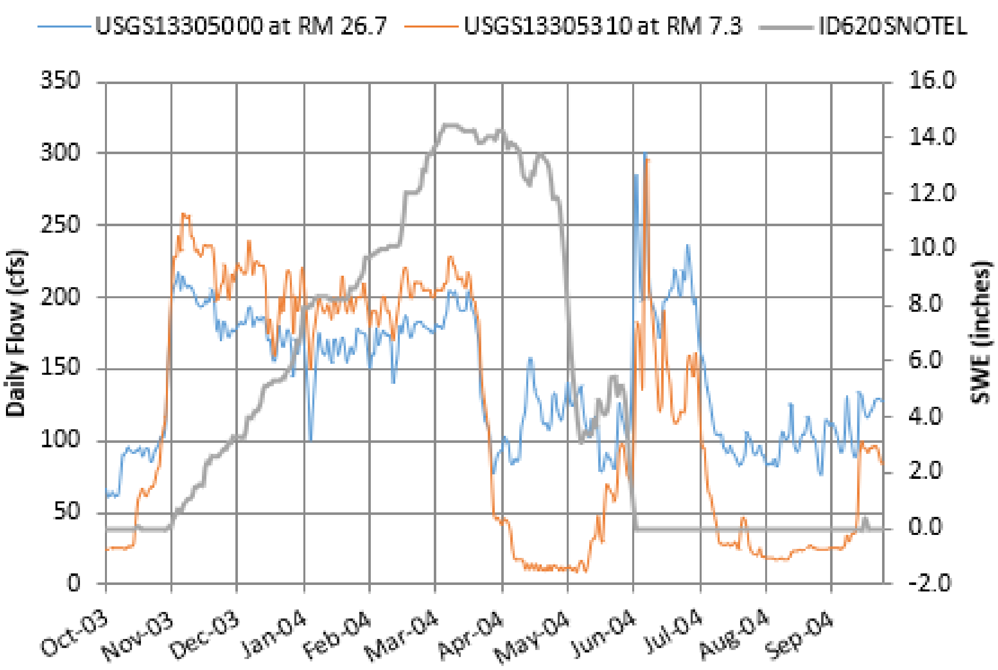
USGS13305000 at RM 26.7
USGS13305310 at RM 7.3
ID620 SNOTEL
Daily Flow (cfs)
SWE (inches)
350
300
250
200
150
100
50
0
16.0
14.0
12.0
10.0
8.0
6.0
4.0
2.0
0.0
-2.0
Oct-03
Nov-03
Dec-03
Jan-04
Feb-04
Mar-04
Apr-04
May-04
Jun-04
Jul-04
Aug-04
Sep-04

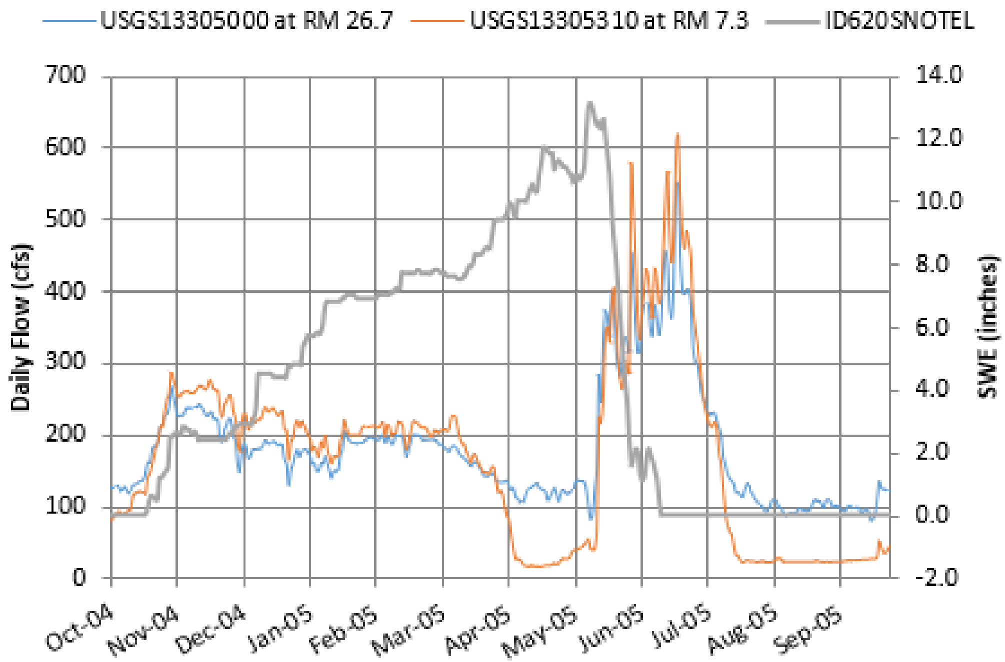
USGS13305000 at RM 26.7
USGS13305310 at RM 7.3
ID620 SNOTEL
Daily Flow (cfs)
SWE (inches)
700
600
500
400
300
200
100
0
14.0
12.0
10.0
8.0
6.0
4.0
2.0
0.0
-2.0
Oct-04
Nov-04
Dec-04
Jan-05
Feb-05
Mar-05
Apr-05
May-05
Jun-05
Jul-05
Aug-05
Sep-05

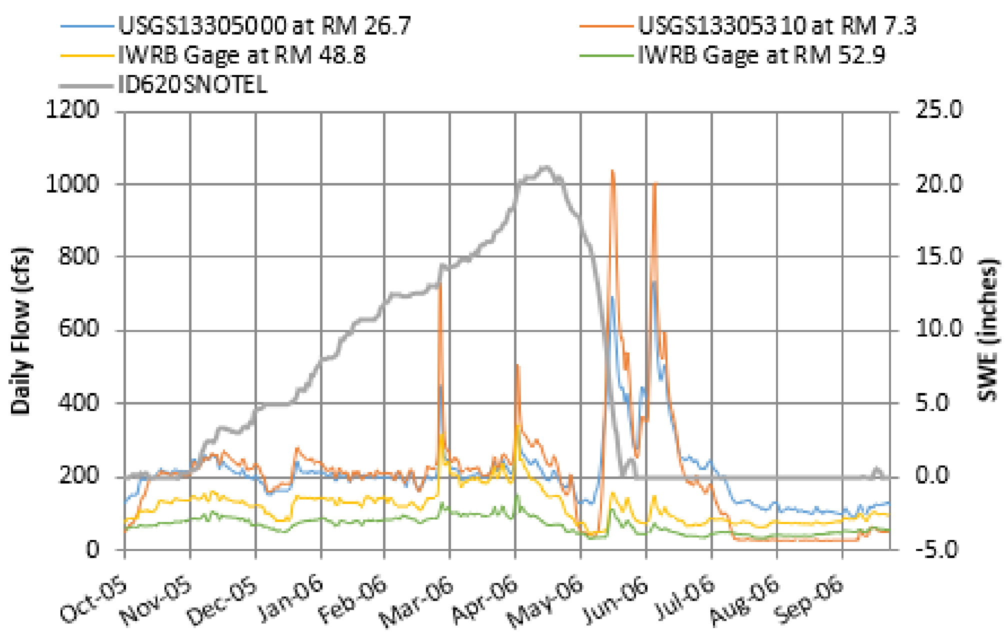
USGS13305000 at RM 26.7
USGS13305310 at RM 7.3
IWRB Gage at RM 48.8
IWRB Gage at RM 52.9
ID620 SNOTEL
Daily Flow (cfs)
SWE (inches)
1200
1000
800
600
400
200
0
25.0
20.0
15.0
10.0
5.0
0.0
-5.0
Oct-05
Nov-05
Dec-05
Jan-06
Feb-06
Mar-06
Apr-06
May-06
Jun-06
Jul-06
Aug-06
Sep-06

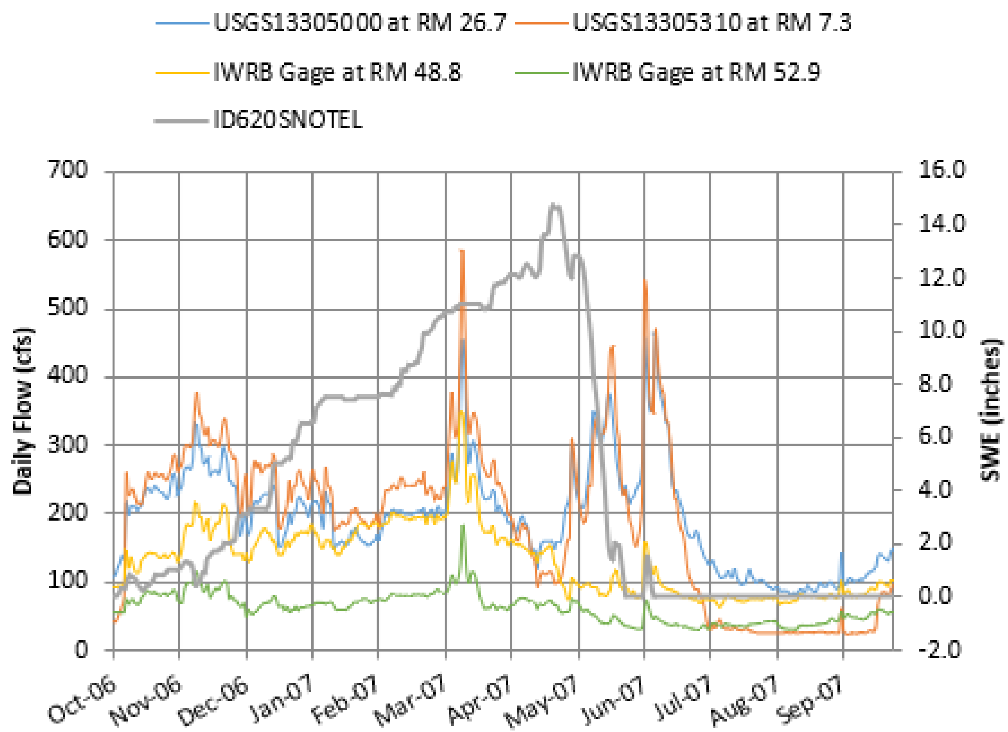
USGS13305000 at RM 26.7
USGS13305310 at RM 7.3
IWRB Gage at RM 48.8
IWRB Gage at RM 52.9
ID620SNOTEL
Daily Flow (cfs)
SWE (inches)
0
100
200
300
400
500
600
700
-2.0
0.0
2.0
4.0
6.0
8.0
10.0
12.0
14.0
16.0
Oct-06
Nov-06
Dec-06
Jan-07
Feb-07
Mar-07
Apr-07
May-07
Jun-07
Jul-07
Aug-07
Sep-07

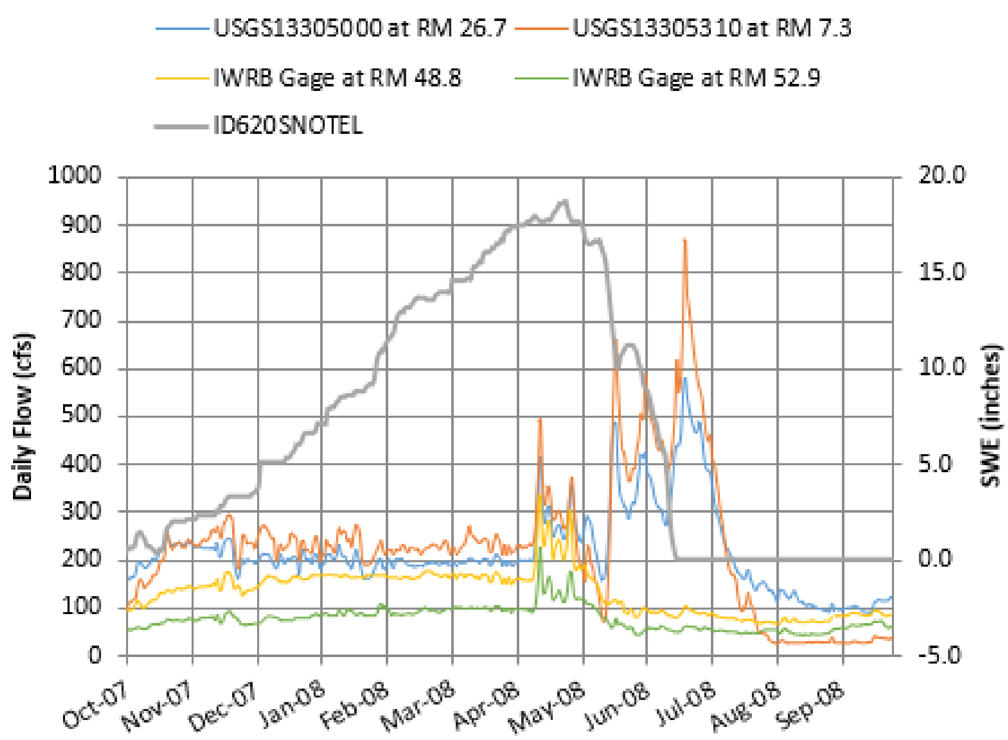
USGS13305000 at RM 26.7
USGS13305310 at RM 7.3
IWRB Gage at RM 48.8
IWRB Gage at RM 52.9
ID620SNOTEL
Daily Flow (cfs)
SWE (inches)
0
100
200
300
400
500
600
700
800
900
1000
-5.0
0.0
5.0
10.0
15.0
20.0
Oct-07
Nov-07
Dec-07
Jan-08
Feb-08
Mar-08
Apr-08
May-08
Jun-08
Jul-08
Aug-08
Sep-08

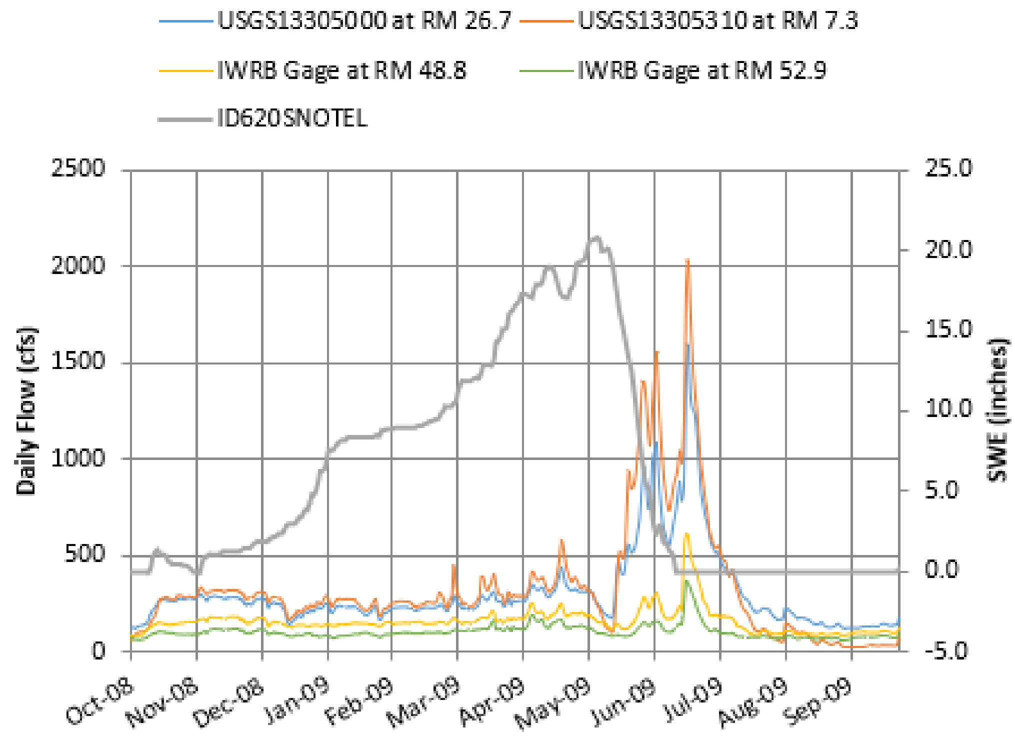
USGS13305000 at RM 26.7
USGS13305310 at RM 7.3
IWRB Gage at RM 48.8
IWRB Gage at RM 52.9
ID620SNOTEL
Daily Flow (cfs)
SWE (inches)
2500
2000
1500
1000
500
0
25.0
20.0
15.0
10.0
5.0
0.0
-5.0
Oct-08
Nov-08
Dec-08
Jan-09
Feb-09
Mar-09
Apr-09
May-09
Jun-09
Jul-09
Aug-09
Sep-09

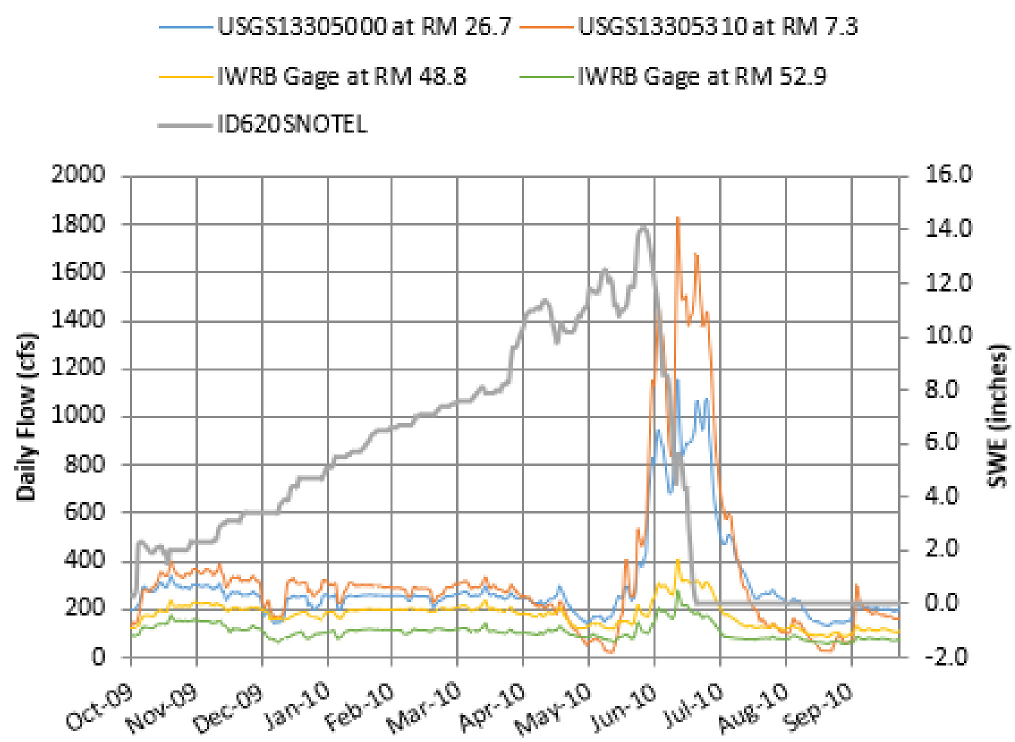
USGS13305000 at RM 26.7
USGS13305310 at RM 7.3
IWRB Gage at RM 48.8
IWRB Gage at RM 52.9
ID620SNOTEL
Daily Flow (cfs)
SWE (inches)
2000
1800
1600
1400
1200
1000
800
600
400
200
0
16.0
14.0
12.0
10.0
8.0
6.0
4.0
2.0
0.0
-2.0
Oct-09
Nov-09
Dec-09
Jan-10
Feb-10
Mar-10
Apr-10
May-10
Jun-10
Jul-10
Aug-10
Sep-10

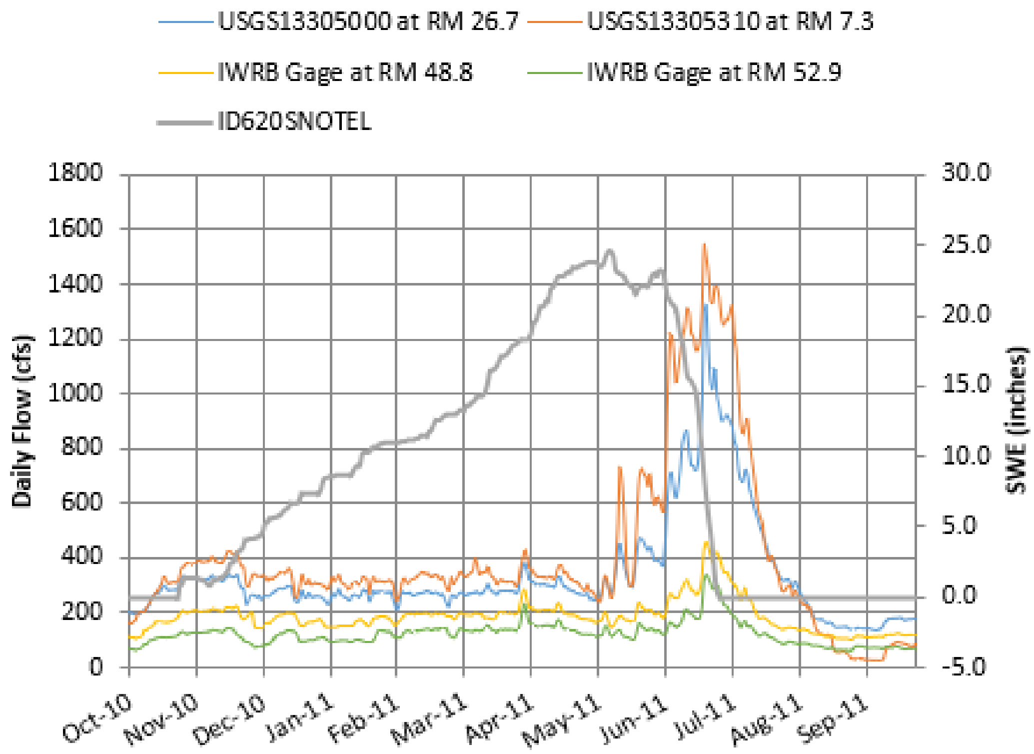
USGS13305000 at RM 26.7
USGS13305310 at RM 7.3
IWRB Gage at RM 48.8
IWRB Gage at RM 52.9
ID620SNOTEL
Daily Flow (cfs)
SWE (inches)
1800
1600
1400
1200
1000
800
600
400
200
0
30.0
25.0
20.0
15.0
10.0
5.0
0.0
-5.0
Oct-10
Nov-10
Dec-10
Jan-11
Feb-11
Mar-11
Apr-11
May-11
Jun-11
Jul-11
Aug-11
Sep-11

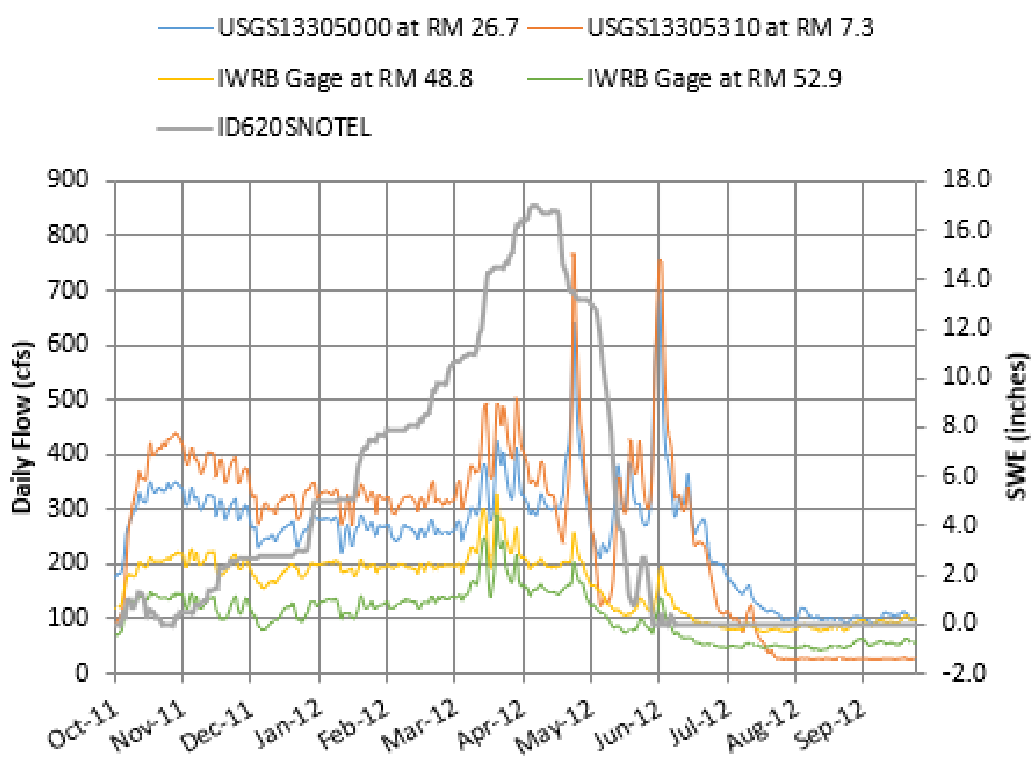
USGS13305000 at RM 26.7
USGS13305310 at RM 7.3
IWRB Gage at RM 48.8
IWRB Gage at RM 52.9
ID620SNOTEL
Daily Flow (cfs)
SWE (inches)
900
800
700
600
500
400
300
200
100
0
18.0
16.0
14.0
12.0
10.0
8.0
6.0
4.0
2.0
0.0
-2.0
Oct-11
Nov-11
Dec-11
Jan-12
Feb-12
Mar-12
Apr-12
May-12
Jun-12
Jul-12
Aug-12
Sep-12

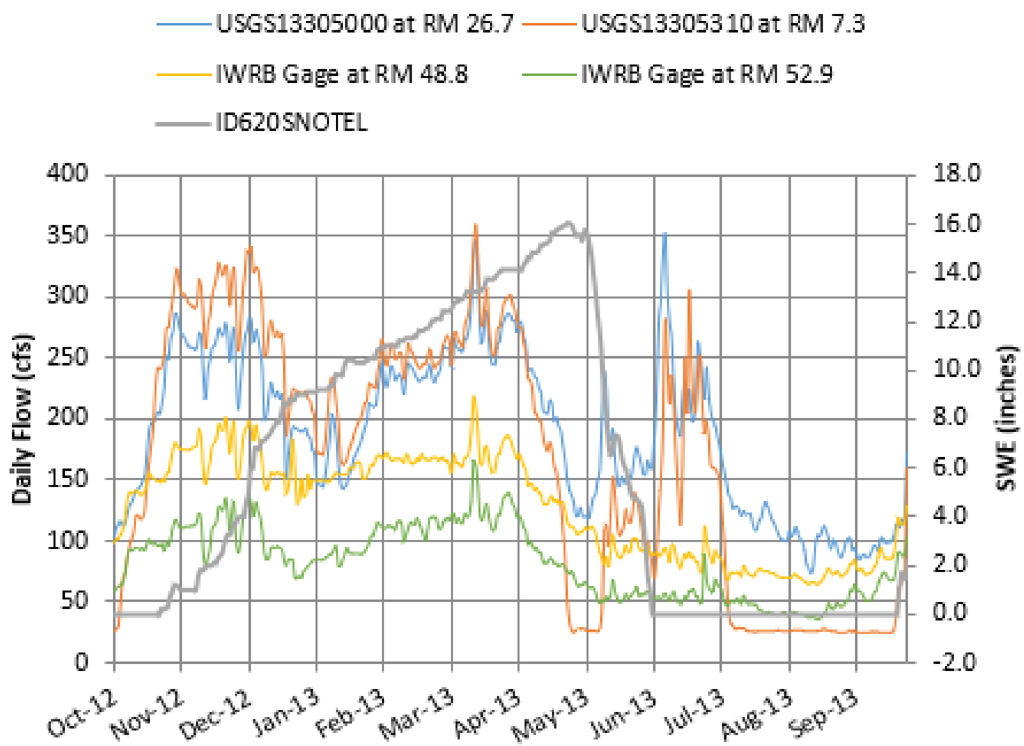
USGS13305000 at RM 26.7
USGS13305310 at RM 7.3
IWRB Gage at RM 48.8
IWRB Gage at RM 52.9
ID620 SNOTEL
Daily Flow (cfs)
SWE (inches)
400
350
300
250
200
150
100
50
0
18.0
16.0
14.0
12.0
10.0
8.0
6.0
4.0
2.0
0.0
-2.0
Oct-12
Nov-12
Dec-12
Jan-13
Feb-13
Mar-13
Apr-13
May-13
Jun-13
Jul-13
Aug-13
Sep-13

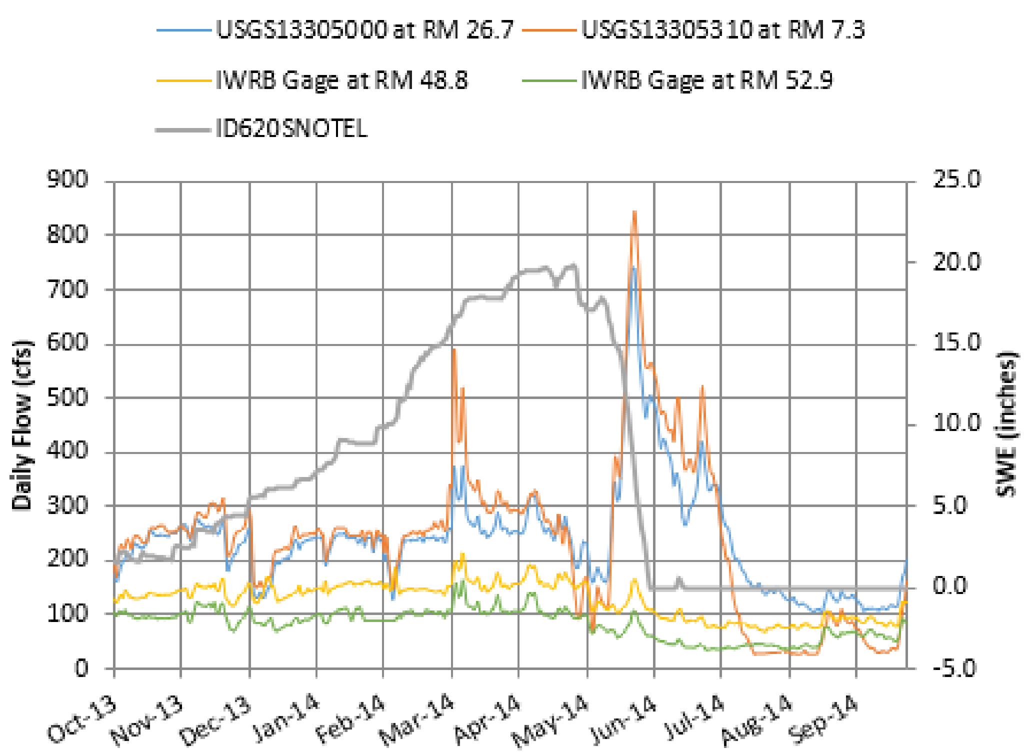
USGS13305000 at RM 26.7
USGS13305310 at RM 7.3
IWRB Gage at RM 48.8
IWRB Gage at RM 52.9
ID620 SNOTEL
Daily Flow (cfs)
SWE (inches)
900
800
700
600
500
400
300
200
100
0
25.0
20.0
15.0
10.0
5.0
0.0
-5.0
Oct-13
Nov-13
Dec-13
Jan-14
Feb-14
Mar-14
Apr-14
May-14
Jun-14
Jul-14
Aug-14
Sep-14

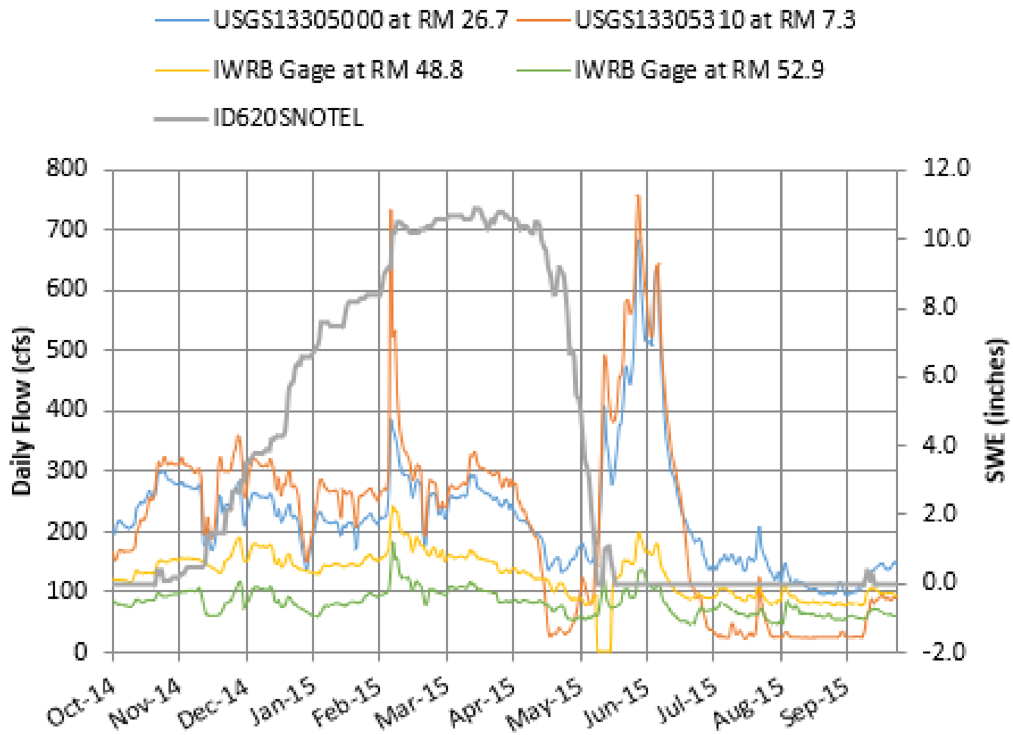
USGS13305000 at RM 26.7
USGS13305310 at RM 7.3
IWRB Gage at RM 48.8
IWRB Gage at RM 52.9
ID620 SNOTEL
Daily Flow (cfs)
SWE (inches)
800
700
600
500
400
300
200
100
0
12.0
10.0
8.0
6.0
4.0
2.0
0.0
-2.0
Oct-14
Nov-14
Dec-14
Jan-15
Feb-15
Mar-15
Apr-15
May-15
Jun-15
Jul-15
Aug-15
Sep-15

9 Appendix B – Annual Peak Streamflow

Annual peak streamflow data are provided in the tables below. Gray cells represent events that occurred outside of the snowmelt runoff season. . Values *italicized* and shaded in blue without dates are the artificially generated annual peaks, developed utilizing the MOVE.4 methodology.

	US USGS Gage		DS USGS Gages		Cottom Lane		Above Big Springs	
Water Year	Date	Annual Max. Q (cfs)	Date	Annual Max. Q (cfs)	Date	Annual Max. Q (cfs)	Date	Annual Max. Q (cfs)
1929			6/16/1929	1,402				
1930			2/8/1930	373				
1931			6/3/1931	531				
1932			6/17/1932	1,312				
1933			6/14/1933	1,091				
1934			11/1/1933	509				
1935			6/14/1935	1,041				
1936			6/3/1936	2,403				
1937			4/2/1937	267				
1938			7/4/1938	1,262				
1939			3/20/1939	1,141				
1940			9/28/1940	587				
1941			6/8/1941	1,352				
1942			6/9/1942	2,113				
1943			6/19/1943	1,412				
1956	6/1/1956	1,090		*1,593*		*399*		*264*
1957	6/7/1957	1,840		*3,048*		*570*		*366*
1958	5/26/1958	891		*1,241*		*348*		*232*
1959	6/26/1959	706		*930*		*298*		*201*
1960	6/4/1960	475		*569*		*228*		*157*
1961	6/8/1961	533		*657*		*246*		*169*
1962	6/18/1962	921		*1,293*		*356*		*237*
1963	6/21/1963	1,320		*2,020*		*455*		*297*
1964	6/27/1964	1,340		*2,058*		*460*		*300*
1965	6/12/1965	1,200		*1,795*		*426*		*280*
1966	5/30/1966	220		*219*		*135*		*97*
1967	6/22/1967	1,100		*1,611*		*402*		*265*
1968	6/13/1968	1,030		*1,485*		*384*		*255*
1969	3/30/1969	1,280		*1,944*		*445*		*292*
1970	6/28/1970	1,410		*2,192*		*476*		*310*
1971	6/27/1971	1,960		*3,297*		*595*		*381*
1972	6/9/1972	1,250		*1,888*		*438*		*287*
Shaded cells indicate peaks that occur outside of the snowmelt runoff season.								

	US USGS Gage		DS USGS Gages		Cottom Lane		Above Big Springs	
Water Year	Date	Annual Max. Q (cfs)	Date	Annual Max. Q (cfs)	Date	Annual Max. Q (cfs)	Date	Annual Max. Q (cfs)
1973	6/15/1973	644		*830*		*280*		*190*
1974	6/18/1974	1,280		*1,944*		*445*		*292*
1975	7/6/1975	1,990		*3,359*		*601*		*384*
1976	5/28/1976	1,060		*1,539*		*392*		*259*
1977	6/9/1977	434		*509*		*214*		*148*
1978	6/11/1978	708		*933*		*298*		*201*
1979	5/27/1979	636		*817*		*277*		*188*
1980	5/25/1980	942		*1,330*		*362*		*241*
1981	5/31/1981	1,080		*1,575*		*397*		*262*
1982	6/24/1982	1,770		*2,905*		*555*		*357*
1983	6/11/1983	968		*1,375*		*369*		*245*
1984	6/21/1984	2,430		*4,303*		*688*		*436*
1985	5/4/1985	516		*631*		*241*		*165*
1986	6/2/1986	1,780		*2,926*		*557*		*358*
1987	5/17/1987	487		*587*		*231*		*159*
1988	6/6/1988	393		*450*		*200*		*139*
1989	6/16/1989	413		*479*		*207*		*144*
1990	6/11/1990	462		*550*		*223*		*154*
1991	6/12/1991	1,060		*1,539*		*392*		*259*
1992	11/13/1991	276		*290*		*158*		*112*
1993	6/11/1993	545	6/22/1993	992		*250*		*171*
1994	5/28/1994	287	11/4/1993	412		*162*		*114*
1995	6/5/1995	1,530	6/6/1995	2,920		*503*		*326*
1996	6/10/1996	1,170	2/9/1996	2,210		*419*		*276*
1997	6/8/1997	1,370	6/8/1997	2,270		*466*		*304*
1998	6/26/1998	1,370	6/26/1998	1,780		*466*		*304*
1999	6/17/1999	1,350	6/18/1999	1,700		*462*		*301*
2000	5/29/2000	353	11/26/1999	381		*186*		*130*
2001	5/15/2001	296	10/14/2000	356		*165*		*117*
2002	6/2/2002	542	6/2/2002	927		*249*		*170*
2003	5/31/2003	714	5/31/2003	1,290		*300*		*202*
2004	6/10/2004	344	6/11/2004	295		*183*		*128*
2005	6/23/2005	622	6/23/2005	617		*273*		*186*
2006	6/9/2006	890	5/21/2006	1,030	4/6/2006	341	4/6/2006	149
2007	3/12/2007	656	3/13/2007	586	3/12/2007	347	3/13/2007	183
2008	6/23/2008	639	6/23/2008	867	4/15/2008	338	4/15/2008	225
2009	6/22/2009	1,590	6/22/2009	2,170	6/21/2009	609	6/21/2009	371
2010	6/17/2010	1,150	6/17/2010	2,090	6/17/2010	411	6/17/2010	276
Shaded cells indicate peaks that occur outside of the snowmelt runoff season.								

	US USGS Gage		DS USGS Gages		Cottom Lane		Above Big Springs	
Water Year	Date	Annual Max. Q (cfs)	Date	Annual Max. Q (cfs)	Date	Annual Max. Q (cfs)	Date	Annual Max. Q (cfs)
2011	6/24/2011	1,450	6/24/2011	1,890	6/25/2011	461	6/25/2011	335
2012	6/5/2012	764	4/27/2012	813	3/23/2012	329	3/23/2012	290
2013	6/11/2013	384	6/22/2013	416	3/15/2013	218	3/15/2013	166
2014	5/27/2014	796	3/6/2014	958	3/10/2014	213	3/10/2014	164
2015	6/1/2015	727	2/7/2015	1,320	2/8/2015	241	2/8/2015	183
2016							3/13/2016	165
Shaded cells indicate peaks that occur outside of the snowmelt runoff season.								

10 Appendix C – ADCP Discharge Measurements

Details regarding the discharge measurements taken with the ADCP are provided in the table below:

Location	Discharge (cfs)	95% Error	Random Error	Invalid Data Error	Extrapolation Error	% Measured	Measurement Duration (sec)	# of Transects	Time Collected
RM 48.8	189	5.7%	4.7%	0.0%	0.7%	47%	459	4	5/26/2016 15:40
RM 40.8	74	10.2%	9.7%	0.1%	0.1%	36%	844	10	5/23/2016 0:00
RM 36.4	220	8.6%	7.1%	2.1%	0.4%	53%	739	8	5/24/2016 10:06
RM 33	180	4.1%	2.5%	2.0%	0.6%	46%	1123	10	5/24/2016 15:14
RM 31.1	469	6.7%	4.3%	4.0%	0.7%	53%	850	8	5/24/2016 17:02
RM 27.5	338	5.9%	4.9%	0.6%	0.6%	44%	806	8	5/25/2016 12:25
RM 24.3	369	4.7%	3.5%	0.1%	0.2%	43%	1550	10	5/25/2016 15:17
RM 21.4	404	4.8%	3.5%	0.1%	0.7%	45%	990	10	5/25/2016 16:41
RM 17.2	392	5.9%	4.9%	1.0%	0.4%	58%	1643	16	5/26/2016 13:52
RM 9.3	510	4.3%	2.8%	0.1%	0.3%	45%	1033	8	5/26/2016 16:20
RM 0.4	535	4.0%	2.3%	0.0%	0.4%	39%	1237	10	5/26/2016 18:32
Hayden Creek	181	10.6%	7.0%	7.2%	1.0%	39%	761	10	5/24/2016 12:00

11 Appendix D – Survey Data

All survey points measured during the high flow site visit are presented in the following tables:

ID	Point Name	Code	Easting	Northing	Elevation	Date
0	Opus_Base14_may	base	1668993.949	1281130.606	3933.656	5/26/2016
1	14000	deck	1669078.143	1281143.786	3935.886	5/26/2016
2	14001	deck	1669134.941	1281173.497	3935.707	5/26/2016
3	14002	tagline	1669167.021	1281120.732	3942.938	5/26/2016
4	14003	tagline	1669086.928	1281105.226	3931.335	5/26/2016
5	14004	wse	1669088.351	1281105.501	3929.702	5/26/2016
6	14005	lowchord	1669077.835	1281139.557	3933.481	5/26/2016
7	9000	deck	1734670.687	1189888.293	4940.849	5/25/2016
8	9001	deck	1734675.934	1189873.626	4940.895	5/25/2016
9	9002	deck	1734744.809	1189899.564	4940.873	5/25/2016
10	9003	deck	1734739.087	1189915.121	4940.725	5/25/2016
11	9004	deck	1734716.212	1189898.657	4941.227	5/25/2016
12	9005	top_rail	1734719.308	1189908.315	4941.478	5/25/2016
13	9006	top_rail	1734716.820	1189888.275	4941.529	5/25/2016
14	9007	wse	1734689.241	1189903.283	4932.509	5/25/2016
15	9008	low_chord	1734724.239	1189890.934	4938.735	5/25/2016
16	10000	deck	1731847.489	1203729.942	4812.41	5/25/2016
17	10001	wse10	1731857.428	1203722.840	4804.65	5/25/2016
18	10002	lowchord	1731850.790	1203733.510	4808.429	5/25/2016
19	10003	wingwall	1731851.172	1203732.238	4807.695	5/25/2016
20	10004	wingwall	1731865.146	1203674.673	4806.488	5/25/2016
21	11000	deck	1729328.402	1216864.740	4693.261	5/25/2016
22	11001	deck	1729388.857	1216864.283	4693.343	5/25/2016
23	11002	top_rail	1729366.187	1216873.127	4694.087	5/25/2016
24	11003	wse	1729329.874	1216888.081	4685.448	5/25/2016
25	11004	wse	1729329.172	1216891.138	4685.42	5/25/2016
26	11005	low_chord	1729366.031	1216873.501	4691.119	5/25/2016
27	Opus_base10_may	base10	1731787.866	1203790.619	4808.632	5/25/2016
28	Opus_Base09_may	base09	1734833.368	1189918.489	4941.896	5/25/2016
29	108b_opus	base08b	1793345.277	1112922.488	5797.561	5/26/2016
30	112_opus	base12	1721316.271	1234834.257	4519.954	5/26/2016
31	8000	wse	1793388.599	1112919.255	5796.071	5/26/2016
32	8001	wse	1793379.054	1112910.578	5795.919	5/26/2016

ID	Point Name	Code	Easting	Northing	Elevation	Date
33	8002	wse	1793365.603	1112892.553	5795.681	5/26/2016
34	8003	wse	1793348.254	1112876.562	5795.548	5/26/2016
35	8004	wse	1793393.79	1112933.584	5796.065	5/26/2016
36	8005	wse	1793408.532	1112962.933	5796.247	5/26/2016
37	8006	wse	1793427.256	1112996.267	5796.745	5/26/2016
38	8007	line rt endpt gnd	1793387.957	1112920.522	5796.938	5/26/2016
39	8008	line left endpt gnd	1793411.649	1112904.908	5796.984	5/26/2016
40	12000	wse	1721315.867	1234806.46	4517.602	5/26/2016
41	12001	wse	1721332.542	1234800.846	4517.749	5/26/2016
42	12002	tagline	1721325.259	1234802.956	4518.695	5/26/2016
43	12003	fence_opening	1721351.44	1234827.361	4519.62	5/26/2016
44	113_opus	base13	1698545.792	1257013.588	4251.991	5/26/2016
45	13000	deck	1698583.51	1257077.189	4253.191	5/26/2016
46	13001	deck	1698612.814	1257111.191	4253.463	5/26/2016
47	13002	deck	1698638.502	1257143.056	4253.38	5/26/2016
48	13003	wse	1698646.784	1257124.509	4242.88	5/26/2016
49	13004	tagline	1698647.75	1257129.335	4244.649	5/26/2016
50	13005	lowchord	1698643.116	1257143.695	4249.527	5/26/2016
51	13006	wingwall	1698643.634	1257143.903	4249.35	5/26/2016
52	13007	usgs_gage_pt	1698643.157	1257142.062	4249.337	5/26/2016
53	13008	cp	1698561.433	1257034.841	4251.717	5/26/2016
54	13009	wingwall	1698587.527	1257073.257	4249.111	5/26/2016
55	13010	tagline	1698604.865	1257073.08	4243.471	5/26/2016
56	13011	wse	1698606.345	1257075.078	4243.004	5/26/2016
57	106_opus	base06	1737725.402	1166100.19	5155.722	5/24/2016
58	500	deck_west	1807794.378	1099687.716	5958.27	5/23/2016
59	501	deck_west	1807827.559	1099724.661	5957.864	5/23/2016
60	502	deck_east	1807858.766	1099720.694	5958.034	5/23/2016
61	503	deck_east	1807826.203	1099683.534	5958.149	5/23/2016
62	504	wse0	1807790.806	1099702.679	5952.116	5/23/2016
63	505	wse0	1807813.21	1099720.926	5952.197	5/23/2016
64	506	lowchord0	1807803.597	1099701.637	5956.837	5/23/2016
65	507	Lwingwall0	1807802.455	1099698.09	5958.296	5/23/2016
66	508	Rwingwall0	1807818.008	1099715.342	5958.124	5/23/2016
67	509	topwallup0	1807843.31	1099699.169	5960.122	5/23/2016
68	510	topwalldown0	1807808.653	1099706.557	5960.23	5/23/2016
69	511	Lwingwall0	1807835.955	1099692.498	5958.117	5/23/2016
70	512	Rwingwall0	1807851.245	1099709.829	5958.047	5/23/2016

ID	Point Name	Code	Easting	Northing	Elevation	Date
71	513	lowchord0	1807848.453	1099703.842	5956.636	5/23/2016
72	1000	wse01	1808086.027	1100156.318	5953.468	5/23/2016
73	1001	wse01	1808084.649	1100152.992	5953.452	5/23/2016
74	1002	wse01	1808070.802	1100161.281	5953.46	5/23/2016
75	2000	deck	1776608.861	1123907.886	5648.435	5/23/2016
76	2001	deck	1776586.691	1123881.993	5648.238	5/23/2016
77	2002	deck	1776601.785	1123865.314	5648.31	5/23/2016
78	2003	deck	1776622.107	1123888.732	5648.365	5/23/2016
79	2004	wse02	1776597.778	1123913.469	5640.538	5/23/2016
80	2005	wse02	1776597.813	1123913.676	5640.546	5/23/2016
81	3000	wse03	1754255.673	1142104.679	5389.573	5/23/2016
82	3001	wse03	1754255.687	1142104.652	5389.557	5/23/2016
83	3002	wse03	1754256.681	1142103.804	5389.524	5/23/2016
84	3003	deck	1754259.663	1142099.636	5397.825	5/23/2016
85	3004	deck	1754277.66	1142117.382	5397.599	5/23/2016
86	3005	lowchord	1754274.751	1142117.372	5396.318	5/23/2016
87	3006	lowchord	1754275.012	1142117.622	5396.334	5/23/2016
88	3007	lowchord	1754274.582	1142117.224	5396.362	5/23/2016
89	3008	wingwall	1754276.94	1142117.195	5397.653	5/23/2016
90	3009	wingwall	1754257.168	1142097.635	5397.8	5/23/2016
91	3010	wingwall	1754274.516	1142079.839	5397.92	5/23/2016
92	3011	wingwall	1754294.613	1142099.629	5397.712	5/23/2016
93	3012	topwall	1754298.311	1142101.661	5400.234	5/23/2016
94	100_opus	base0	1807779.474	1099684.407	5957.141	5/23/2016
95	102_opus	base02	1776628.159	1123947.814	5642.25	5/23/2016
96	4000	wse04	1741496.938	1153515.716	5249.234	5/24/2016
97	4001	bridgedeck04	1741489.827	1153499.905	5253.373	5/24/2016
98	4002	bridgedeck04	1741456.139	1153515.976	5253.116	5/24/2016
99	4003	bridgedeck04	1741460.82	1153525.022	5253.383	5/24/2016
100	4004	bridgedeck04	1741494.089	1153508.818	5253.039	5/24/2016
101	4005	bridgerail04	1741471.249	1153508.322	5253.677	5/24/2016
102	4006	bridgerail04	1741479.128	1153516.447	5253.61	5/24/2016
103	4007	lowchord04	1741480.332	1153516.125	5251.079	5/24/2016
104	5000	deck	1736828.699	1166870.494	5163.775	5/24/2016
105	5001	deck	1736819.755	1166836.745	5164.04	5/24/2016
106	5002	top_rail	1736835.191	1166854.671	5164.672	5/24/2016
107	5003	wse	1736850.337	1166874.974	5157.802	5/24/2016
108	5004	low_chord	1736835.951	1166853.363	5161.224	5/24/2016
109	6000	wse	1737737.617	1166122.488	5151.989	5/24/2016
110	104_opus	base04	1741556.862	1153555.228	5252.278	5/24/2016

ID	Point Name	Code	Easting	Northing	Elevation	Date
111	105_opus	base05	1736763.236	1166931.269	5163.582	5/24/2016
112	103_opus	base03	1754343.563	1142136.564	5395.614	5/23/2016

All survey points measured during the low flow site visit are presented in the following table:

ID	Point Name	Code	Easting	Northing	Elevation	Date
0	Opus_base03_aug		1754343.563	1142136.563	5395.603	
1	103	base03	1754343.563	1142136.563	5395.614	8/23/2016
2	3000	Q03_ws	1754254.540	1142112.038	5388.953	8/23/2016
3	3001	s03_1	1754252.590	1142109.674	5389.545	8/23/2016
4	3002	s03_2	1754270.029	1142129.234	5389.070	8/23/2016
5	3003	pc03	1754294.478	1142056.960	5388.469	8/23/2016
6	3004	pc03	1754298.766	1142025.378	5389.135	8/23/2016
7	3005	ws	1754312.395	1141976.933	5390.595	8/23/2016
8	3006	ws	1754313.910	1141949.812	5390.633	8/23/2016
9	3007	ws	1754312.447	1141990.053	5390.473	8/23/2016
10	3008	ws	1754311.116	1142011.100	5390.373	8/23/2016
11	3009	ws	1754309.271	1142030.013	5390.070	8/23/2016
12	3010	ws	1754308.285	1142044.781	5389.857	8/23/2016
13	3011	ws	1754306.524	1142060.529	5389.711	8/23/2016
14	3012	ws	1754305.005	1142082.201	5389.554	8/23/2016
15	3013	ws	1754305.085	1142082.307	5389.573	8/23/2016
16	3014	scour hole	1754297.919	1142079.047	5387.464	8/23/2016
17	3015	ws	1754299.802	1142089.779	5389.410	8/23/2016
18	3016	ws	1754258.952	1142107.115	5389.007	8/23/2016
19	3017	ws	1754250.838	1142115.060	5388.907	8/23/2016
20	3018	ws	1754233.694	1142135.438	5388.806	8/23/2016
21	3019	ws	1754225.148	1142156.023	5388.331	8/23/2016
22	3020	ws	1754209.740	1142168.249	5388.208	8/23/2016
23	3021	ws	1754194.560	1142174.906	5388.119	8/23/2016
24	3022	ws	1754267.805	1142130.400	5388.808	8/23/2016
25	106	basecp6	1737725.402	1166100.190	5155.722	8/24/2016
26	6000	topo	1737834.578	1165765.456	5157.465	8/24/2016
27	6001	tb	1737845.774	1165768.879	5157.065	8/24/2016
28	6002	bb	1737849.291	1165770.829	5154.547	8/24/2016
29	6003	we	1737850.936	1165771.521	5153.762	8/24/2016
30	6004	cb	1737852.257	1165771.529	5153.322	8/24/2016

ID	Point Name	Code	Easting	Northing	Elevation	Date
31	6005	cb	1737856.218	1165772.910	5152.591	8/24/2016
32	6006	cb	1737863.502	1165774.113	5152.553	8/24/2016
33	6007	cb	1737870.940	1165774.770	5152.576	8/24/2016
34	6008	cb	1737877.636	1165776.068	5152.604	8/24/2016
35	6009	cb	1737885.067	1165777.979	5152.449	8/24/2016
36	6010	cb	1737892.156	1165779.277	5152.465	8/24/2016
37	6011	cb	1737896.675	1165781.233	5152.577	8/24/2016
38	6012	we	1737901.583	1165782.997	5153.624	8/24/2016
39	6013	tb	1737906.898	1165784.398	5158.116	8/24/2016
40	6014	topo	1737925.197	1165788.814	5158.713	8/24/2016
41	6015	cb	1737871.782	1165789.275	5152.417	8/24/2016
42	6016	ws	1737871.923	1165789.127	5153.802	8/24/2016
43	6017	ws	1737861.086	1165814.949	5153.578	8/24/2016
44	6018	cb	1737860.792	1165815.253	5152.421	8/24/2016
45	6019	cb	1737851.209	1165842.430	5152.196	8/24/2016
46	6020	ws	1737851.154	1165842.106	5153.348	8/24/2016
47	6021	cb	1737828.439	1165915.371	5151.624	8/24/2016
48	6022	ws	1737828.291	1165915.059	5152.836	8/24/2016
49	6023	cb	1737808.371	1165982.677	5150.954	8/24/2016
50	6024	ws	1737808.320	1165982.648	5152.266	8/24/2016
51	6025	cb	1737787.172	1166042.862	5150.833	8/24/2016
52	6026	ws	1737787.164	1166042.520	5152.082	8/24/2016
53	6027	cb	1737766.326	1166105.684	5150.158	8/24/2016
54	6028	ws	1737766.352	1166105.138	5151.571	8/24/2016
55	6029	ws	1737766.401	1166105.074	5151.576	8/24/2016
56	6030	cb	1737751.169	1166153.318	5149.962	8/24/2016
57	6031	ws	1737751.379	1166152.956	5151.445	8/24/2016
58	6032	cb	1737732.202	1166226.245	5149.922	8/24/2016
59	6033	ws	1737732.237	1166225.876	5151.102	8/24/2016
60	6034	cb	1737722.267	1166278.848	5149.359	8/24/2016
61	6035	ws	1737722.707	1166277.814	5150.533	8/24/2016
62	109	basecp	1734833.367	1189918.490	4941.906	8/24/2016
63	9000	ws	1734678.605	1189999.080	4931.112	8/24/2016
64	9001	cb	1734678.639	1189998.976	4930.028	8/24/2016
65	9002	pebblecount-site9	1734681.862	1189987.160	4930.109	8/24/2016
66	9003	cb	1734686.745	1189970.916	4930.187	8/24/2016
67	9004	ws	1734686.271	1189971.225	4931.471	8/24/2016
68	9005	cb	1734704.165	1189926.814	4930.526	8/24/2016
69	9006	ws	1734702.470	1189926.895	4931.700	8/24/2016

ID	Point Name	Code	Easting	Northing	Elevation	Date
70	test7	q9_wse	1734706.538	1189914.383	4931.773	8/24/2016
71	9007	q9_wse	1734706.565	1189914.476	4931.680	8/24/2016
72	9008	cb	1734704.875	1189912.834	4930.774	8/24/2016
73	9009	ws	1734717.294	1189860.438	4932.188	8/24/2016
74	9010	cb	1734721.911	1189861.179	4930.699	8/24/2016
75	110	base10	1731787.865	1203790.620	4808.642	8/24/2016
76	10000	test	1731788.268	1203793.297	4808.553	8/24/2016
77	10001	test	1731842.856	1203820.506	4809.554	8/24/2016
78	10002	ws	1731963.722	1203772.626	4802.074	8/24/2016
79	10003	ws	1731956.201	1203762.204	4802.717	8/24/2016
80	10004	ws	1731939.740	1203752.066	4802.854	8/24/2016
81	10005	ws	1731939.715	1203752.052	4802.832	8/24/2016
82	10006	ws	1731920.476	1203743.669	4803.425	8/24/2016
83	10007	ws	1731899.184	1203727.474	4803.460	8/24/2016
84	10008	Q10_ws	1731898.422	1203693.315	4803.538	8/24/2016
85	10009	ws	1731875.657	1203684.843	4803.575	8/24/2016
86	10010	pc10	1731902.072	1203748.438	4802.977	8/24/2016
87	10011	pc10	1731935.716	1203762.877	4802.532	8/24/2016
88	10012	pc10	1731819.658	1203689.401	4803.631	8/24/2016
89	11000	topo	1731790.835	1203790.777	4806.861	8/24/2016
90	11001	topo	1731791.244	1203789.458	4807.957	8/24/2016
91	11002	pebblecount-site11	1729331.042	1216951.223	4682.889	8/24/2016
92	11003	wse	1729409.248	1216719.241	4685.515	8/24/2016
93	11005	wse	1729357.838	1216744.165	4685.101	8/24/2016
94	11006	wse	1729353.417	1216763.411	4685.203	8/24/2016
95	11007	wse	1729355.254	1216762.441	4685.174	8/24/2016
96	11008	wse	1729346.301	1216806.855	4684.756	8/24/2016
97	11009	wse	1729343.766	1216820.937	4684.646	8/24/2016
98	11010	Q11_WSE	1729330.879	1216891.236	4684.442	8/24/2016
99	11011	WSE	1729327.087	1216903.957	4684.263	8/24/2016
100	11012	WSE	1729324.053	1216918.808	4684.256	8/24/2016
101	11013	WSE	1729318.192	1216936.414	4684.295	8/24/2016
102	11014	WSE	1729314.217	1216954.101	4684.114	8/24/2016
103	11015	WSE	1729309.266	1216971.250	4683.253	8/24/2016
104	11004	wse	1729403.049	1216718.353	4688.917	
106	100	base0	1807779.474	1099684.407	5957.106	8/22/2016
107	500	Q0-1	1807796.443	1099706.036	5951.741	8/22/2016
108	501	WSE	1807863.200	1099691.439	5952.092	8/22/2016
109	502	WSE	1807855.925	1099701.302	5952.175	8/22/2016

ID	Point Name	Code	Easting	Northing	Elevation	Date
110	503	WSE	1807853.370	1099704.233	5952.192	8/22/2016
111	504	WSE	1807793.848	1099729.709	5951.757	8/22/2016
112	505	WSE	1807755.525	1099720.475	5951.698	8/22/2016
113	506	WSE	1807723.709	1099714.368	5951.559	8/22/2016
114	507	WSE	1807699.757	1099732.805	5951.471	8/22/2016
115	508	WSE	1807676.421	1099758.196	5951.473	8/22/2016
116	509	SPC1	1807685.512	1099734.465	5950.450	8/22/2016
117	510	EPC1	1807705.193	1099729.693	5951.026	8/22/2016
118	511	QS1	1807795.991	1099706.014	5951.810	8/22/2016
119	512	S0-1	1807796.034	1099705.980	5951.814	8/22/2016
120	513	S0-2	1807809.213	1099722.300	5952.482	8/22/2016
121	1000	wse	1808172.692	1100132.710	5953.487	8/22/2016
122	1001	wse	1808164.473	1100149.660	5953.449	8/22/2016
123	1002	wse	1808161.392	1100174.027	5953.353	8/22/2016
124	1003	wse	1808140.903	1100182.714	5953.316	8/22/2016
125	1004	wse	1808096.166	1100208.891	5953.272	8/22/2016
126	1005	wse	1808079.353	1100177.567	5953.148	8/22/2016
127	1006	wse	1808069.279	1100134.336	5953.028	8/22/2016
128	1007	wse	1808061.490	1100100.342	5952.944	8/22/2016
129	1008	wse	1808024.595	1100055.517	5952.899	8/22/2016
130	1009	wse	1807984.451	1100042.475	5952.768	8/22/2016
131	1010	wse	1807942.429	1100033.539	5952.433	8/22/2016
132	1011	wse	1807857.770	1100024.915	5952.365	8/22/2016
133	1012	wse	1808200.289	1100089.136	5953.800	8/22/2016
134	1013	wse	1808205.945	1100079.618	5954.871	8/22/2016
135	1014	wse	1808209.082	1100064.663	5954.906	8/22/2016
136	1015	wse	1808219.603	1100040.031	5955.011	8/22/2016
137	1016	wse	1808232.970	1100034.777	5955.029	8/22/2016
138	1017	Q1b	1808156.173	1100148.651	5953.418	8/22/2016
139	1018	s1b-1	1808156.170	1100148.995	5953.547	8/22/2016
140	1019	s1b-2	1808164.115	1100150.666	5953.265	8/22/2016
141	1020	SPC1b	1808159.636	1100152.298	5952.934	8/22/2016
142	1021	EPC1b	1808160.684	1100163.668	5952.905	8/22/2016
143	8000	wse	1793557.942	1112933.138	5798.617	8/22/2016
144	8001	wse	1793518.152	1112962.192	5798.208	8/22/2016
145	8002	wse	1793494.611	1112982.872	5797.903	8/22/2016
146	8003	wse	1793466.743	1112991.019	5797.800	8/22/2016
147	8004	wse	1793456.751	1112993.603	5797.592	8/22/2016
148	8005	wse	1793424.972	1112984.946	5796.890	8/22/2016
149	8006	wse	1793393.761	1112932.972	5796.613	8/22/2016

ID	Point Name	Code	Easting	Northing	Elevation	Date
150	8007	wse	1793373.280	1112903.646	5796.291	8/22/2016
151	8008	wse	1793351.685	1112877.618	5795.922	8/22/2016
152	8009	wse	1793327.884	1112872.932	5795.911	8/22/2016
153	8010	wse	1793309.567	1112882.576	5795.914	8/22/2016
154	8011	wse	1793276.547	1112860.246	5795.630	8/22/2016
155	8012	wse	1793224.524	1112829.064	5795.361	8/22/2016
156	8013	wse	1793192.695	1112812.959	5795.281	8/22/2016
157	8014	wse	1793152.397	1112787.741	5795.001	8/22/2016
158	8015	wse	1793104.642	1112813.711	5794.769	8/22/2016
159	8016	wse	1793085.348	1112824.838	5794.480	8/22/2016
160	8017	wse	1793067.798	1112855.551	5794.407	8/22/2016
161	8018	wse	1793009.270	1112858.526	5794.073	8/22/2016
162	8019	wse	1792967.753	1112836.977	5793.964	8/22/2016
163	8020	wse	1793237.204	1112828.978	5795.511	8/22/2016
164	8021	wse	1793247.932	1112810.167	5795.540	8/22/2016
165	8022	wse	1793251.062	1112786.795	5795.578	8/22/2016
166	8023	wse	1793258.379	1112748.025	5795.690	8/22/2016
167	8024	wse	1793246.088	1112703.655	5795.792	8/22/2016
168	8025	wse	1793242.316	1112657.903	5795.993	8/22/2016
169	8026	wse	1793267.563	1112646.785	5796.165	8/22/2016
170	8027	wse	1793308.266	1112672.527	5796.410	8/22/2016
171	8028	wse	1793365.722	1112703.883	5796.705	8/22/2016
172	8029	wse	1793387.007	1112736.558	5796.777	8/22/2016
173	8030	wse	1793411.265	1112758.177	5796.796	8/22/2016
174	8031	wse	1793447.818	1112752.550	5796.901	8/22/2016
175	8032	wse	1793495.832	1112736.779	5797.134	8/22/2016
176	8033	wse	1793529.102	1112708.918	5797.268	8/22/2016
177	8034	wse	1793566.868	1112711.097	5797.325	8/22/2016
178	8035	wse	1793568.043	1112758.036	5797.517	8/22/2016
179	8036	wse	1793549.574	1112804.555	5797.849	8/22/2016
180	8037	wse	1793522.275	1112849.722	5797.996	8/22/2016
181	8038	wse	1793511.425	1112871.779	5798.082	8/22/2016
182	8039	wse	1793515.460	1112883.157	5798.227	8/22/2016
183	8040	wse	1793584.477	1112930.534	5798.699	8/22/2016
184	8041	wse	1793627.333	1112912.279	5798.740	8/22/2016
185	8042	wse	1793667.154	1112921.453	5798.953	8/22/2016
186	8043	wse	1793706.691	1112908.015	5798.981	8/22/2016
187	8044	wse	1793752.758	1112883.422	5799.322	8/22/2016
188	8045	wse	1793835.811	1112869.094	5799.867	8/22/2016
189	8046	q_8	1793370.202	1112899.222	5796.275	8/22/2016

ID	Point Name	Code	Easting	Northing	Elevation	Date
190	8047	s8_1	1793367.928	1112901.240	5797.822	8/22/2016
191	8048	s8_2	1793390.098	1112879.065	5797.424	8/22/2016
192	8049	8_pc	1793348.486	1112866.807	5794.886	8/22/2016
193	8050	8_pc	1793304.452	1112870.501	5794.811	8/22/2016
194	8051	8_pc	1793401.031	1112924.415	5796.081	8/22/2016
195	8052	8_pc	1793415.998	1112946.347	5796.309	8/22/2016
196	8053	8_pc	1793172.626	1112824.897	5794.698	8/22/2016
197	8054	8_pc	1793153.079	1112816.175	5794.561	8/22/2016
198	8055	Q8-3RBWSE-DS-CONFLUENCE	1793196.639	1112814.787	5795.227	8/22/2016
199	8056	Q8-3LBWSE-DS-CONFLUENCE	1793181.392	1112856.826	5795.353	8/22/2016
200	8057	THALWEG	1793042.705	1112871.132	5793.027	8/22/2016
201	8058	THALWEG	1793049.268	1112870.271	5792.838	8/22/2016
202	8059	THALWEG	1793055.973	1112866.716	5793.158	8/22/2016
203	8060	THALWEG	1793060.821	1112860.523	5793.643	8/22/2016
204	8061	THALWEG	1793055.313	1112841.295	5793.245	8/22/2016
205	8062	THALWEG	1793057.999	1112837.545	5793.160	8/22/2016
206	8063	THALWEG	1793062.838	1112833.344	5792.784	8/22/2016
207	8064	THALWEG	1793066.482	1112828.186	5792.484	8/22/2016
208	8065	THALWEG	1793070.611	1112823.759	5792.686	8/22/2016
209	8066	THALWEG	1793076.408	1112818.342	5793.021	8/22/2016
210	8067	THALWEG	1793081.047	1112811.822	5793.870	8/22/2016
211	8068	THALWEG	1793087.763	1112806.444	5794.001	8/22/2016
212	8069	THALWEG	1793096.269	1112802.970	5793.910	8/22/2016
213	8070	THALWEG	1793104.626	1112800.405	5793.798	8/22/2016
214	8071	THALWEG	1793114.741	1112800.545	5793.728	8/22/2016
215	8072	THALWEG	1793124.833	1112801.932	5793.944	8/22/2016
216	8073	THALWEG	1793134.325	1112806.602	5794.163	8/22/2016
217	8074	THALWEG	1793142.536	1112810.679	5794.343	8/22/2016
218	8075	THALWEG	1793154.316	1112815.330	5794.514	8/22/2016
219	8076	THALWEG	1793162.193	1112818.914	5794.432	8/22/2016
220	8077	THALWEG	1793171.220	1112823.426	5794.621	8/22/2016
221	8078	THALWEG	1793178.941	1112826.981	5794.668	8/22/2016
222	8079	THALWEG	1793187.339	1112830.559	5794.489	8/22/2016
223	8080	THALWEG	1793198.023	1112833.233	5794.543	8/22/2016
224	8081	THALWEG	1793208.259	1112836.263	5794.359	8/22/2016
225	8082	THALWEG	1793215.813	1112841.234	5794.131	8/22/2016

ID	Point Name	Code	Easting	Northing	Elevation	Date
226	8083	THALWEG	1793222.865	1112843.583	5794.139	8/22/2016
227	8084	THALWEG	1793231.355	1112845.315	5794.249	8/22/2016
228	8085	THALWEG	1793239.018	1112846.545	5794.536	8/22/2016
229	8086	THALWEG	1793249.530	1112848.129	5794.978	8/22/2016
230	8087	THALWEG	1793255.433	1112853.308	5794.538	8/22/2016
231	8088	THALWEG	1793258.443	1112859.184	5793.945	8/22/2016
232	8089	THALWEG	1793263.291	1112861.266	5794.054	8/22/2016
233	8090	THALWEG	1793268.110	1112871.158	5793.927	8/22/2016
234	8091	THALWEG	1793275.546	1112873.977	5794.114	8/22/2016
235	8092	THALWEG	1793290.148	1112877.168	5795.244	8/22/2016
236	8093	THALWEG	1793300.657	1112873.546	5795.137	8/22/2016
237	8094	THALWEG	1793308.807	1112871.029	5794.652	8/22/2016
238	8095	THALWEG	1793316.975	1112868.462	5794.242	8/22/2016
239	8096	THALWEG	1793324.898	1112865.207	5794.417	8/22/2016
240	8097	THALWEG	1793334.919	1112861.438	5794.627	8/22/2016
241	8098	THALWEG	1793345.266	1112862.298	5794.293	8/22/2016
242	8099	THALWEG	1793354.880	1112865.770	5794.590	8/22/2016
243	8100	THALWEG	1793364.096	1112870.649	5794.944	8/22/2016
244	8101	THALWEG	1793371.033	1112874.983	5795.110	8/22/2016
245	8102	THALWEG	1793380.137	1112882.955	5795.542	8/22/2016
246	8103	THALWEG	1793386.952	1112891.046	5795.678	8/22/2016
247	8104	THALWEG	1793392.516	1112903.239	5795.913	8/22/2016
248	8105	THALWEG	1793393.464	1112916.089	5795.318	8/22/2016
249	8106	THALWEG	1793407.409	1112918.074	5795.590	8/22/2016
250	8107	THALWEG	1793409.454	1112931.781	5795.809	8/22/2016
251	8108	THALWEG	1793409.556	1112941.454	5795.995	8/22/2016
252	8109	THALWEG	1793410.502	1112951.870	5795.182	8/22/2016
253	8110	THALWEG	1793412.539	1112957.982	5794.951	8/22/2016
254	8111	THALWEG	1793416.320	1112965.326	5795.120	8/22/2016
255	8112	THALWEG	1793426.025	1112972.920	5795.733	8/22/2016
256	8113	THALWEG	1793430.230	1112982.787	5796.035	8/22/2016
257	8114	THALWEG	1793440.024	1112991.242	5796.736	8/22/2016
258	8115	THALWEG	1793448.749	1112994.206	5796.530	8/22/2016
259	8116	THALWEG	1793458.104	1112994.228	5796.555	8/22/2016
260	8117	THALWEG	1793463.438	1112993.418	5795.996	8/22/2016
261	8118	THALWEG	1793470.750	1112993.148	5796.274	8/22/2016
262	8119	THALWEG	1793478.056	1112991.684	5797.355	8/22/2016
263	8120	THALWEG	1793490.223	1112992.226	5797.100	8/22/2016
264	8121	THALWEG	1793501.432	1112989.884	5797.133	8/22/2016
265	8122	THALWEG	1793511.935	1112984.792	5797.232	8/22/2016

ID	Point Name	Code	Easting	Northing	Elevation	Date
266	8123	THALWEG	1793519.677	1112978.099	5797.017	8/22/2016
267	8124	THALWEG	1793527.420	1112969.997	5797.194	8/22/2016
268	8125	THALWEG	1793532.362	1112958.531	5797.824	8/22/2016
269	8126	THALWEG	1793539.234	1112946.113	5797.985	8/22/2016
270	8127	THALWEG	1793545.467	1112934.200	5798.035	8/22/2016
271	8128	THALWEG	1793553.990	1112921.857	5797.489	8/22/2016
272	8129	THALWEG	1793565.026	1112920.801	5797.008	8/22/2016
273	8130	THALWEG	1793574.609	1112917.725	5797.049	8/22/2016
274	8131	THALWEG	1793584.856	1112918.264	5797.106	8/22/2016
275	8132	THALWEG	1793598.769	1112919.413	5797.257	8/22/2016
276	8133	THALWEG	1793611.870	1112921.272	5797.147	8/22/2016
277	8134	THALWEG	1793623.883	1112921.932	5797.131	8/22/2016
278	8135	THALWEG	1793633.466	1112923.251	5797.678	8/22/2016
279	8136	THALWEG	1793646.850	1112922.157	5798.150	8/22/2016
280	8137	THALWEG	1793657.604	1112917.084	5797.647	8/22/2016
281	8138	THALWEG	1793668.682	1112913.418	5797.334	8/22/2016
282	8139	THALWEG	1793680.091	1112908.944	5796.949	8/22/2016
283	8140	THALWEG	1793690.163	1112904.893	5796.441	8/22/2016
284	8141	THALWEG	1793700.344	1112898.643	5795.975	8/22/2016
285	102	base02	1776622.156	1123952.389	5645.334	
287	8143	topo	1776623.007	1123944.419	5642.800	8/23/2016
288	8144	QSR_2	1776598.588	1123913.282	5641.502	8/23/2016
289	8145	Q2-3wse	1776585.938	1123885.853	5640.827	8/23/2016
290	8146	WSE	1776730.798	1123761.120	5641.546	8/23/2016
291	8147	WSE	1776730.645	1123761.174	5641.527	8/23/2016
292	8148	WSE	1776720.989	1123772.899	5641.574	8/23/2016
293	8149	WSE	1776712.449	1123785.725	5641.415	8/23/2016
294	8150	WSE	1776712.590	1123785.774	5641.405	8/23/2016
295	8151	WSE	1776700.424	1123798.091	5641.281	8/23/2016
296	8152	WSE	1776684.071	1123806.091	5641.362	8/23/2016
297	8153	WSE	1776659.169	1123810.769	5641.029	8/23/2016
298	8154	WSE	1776653.566	1123814.840	5640.970	8/23/2016
299	8155	WSE	1776644.572	1123820.677	5640.966	8/23/2016
300	8156	WSE	1776628.036	1123826.884	5640.929	8/23/2016
301	8157	WSE	1776608.973	1123859.781	5640.941	8/23/2016
302	8158	WSE	1776593.531	1123919.888	5640.772	8/23/2016
303	8159	WSE	1776593.635	1123920.006	5640.770	8/23/2016
304	8160	WSE	1776571.166	1123944.188	5640.556	8/23/2016
305	8161	WSE	1776535.225	1123974.269	5640.093	8/23/2016
306	8162	WSE	1776521.818	1123986.308	5640.066	8/23/2016

ID	Point Name	Code	Easting	Northing	Elevation	Date
307	8163	WSE	1776502.273	1124003.582	5639.924	8/23/2016
308	8164	WSE	1776435.115	1124046.240	5639.317	8/23/2016
309	8165	WSE	1776356.958	1124048.427	5638.875	8/23/2016
310	8166	WSE	1776324.190	1124075.155	5638.559	8/23/2016
311	8167	WSE	1776331.839	1124121.811	5638.035	8/23/2016
312	8168	WSE	1776300.533	1124186.595	5637.792	8/23/2016
313	8169	RSQ2-2	1776451.225	1124039.936	5642.920	8/23/2016
314	8170	LSQ2-2	1776429.706	1124003.624	5640.250	8/23/2016
315	8171	Q2-2WSE	1776427.809	1124007.290	5639.343	8/23/2016
316	8172	PC2-1	1776574.185	1123939.674	5640.172	8/23/2016
317	104	basept	1741556.862	1153555.228	5252.278	8/23/2016
318	4000	topo	1741554.510	1153551.057	5252.190	8/23/2016
319	4001	PC4-1	1741536.047	1153641.426	5247.635	8/23/2016
320	4002	WSE	1741525.011	1153535.895	5248.726	8/23/2016
321	4003	WSE	1741549.984	1153569.179	5248.529	8/23/2016
322	4004	WSE	1741559.148	1153587.355	5248.536	8/23/2016
323	4005	WSE	1741559.162	1153587.421	5248.561	8/23/2016
324	4006	WSE	1741526.886	1153647.821	5248.042	8/23/2016
325	4007	WSE	1741544.237	1153668.324	5247.302	8/23/2016
326	4008	WSE	1741557.102	1153700.144	5246.933	8/23/2016
327	4009	WSE	1741562.092	1153718.835	5246.942	8/23/2016
328	4010	WSE	1741573.346	1153760.140	5246.771	8/23/2016
329	4011	WSE	1741579.123	1153784.123	5246.568	8/23/2016
330	4012	WSE	1741582.075	1153796.125	5246.420	8/23/2016
331	4013	WSE	1741627.050	1153826.662	5246.118	8/23/2016
332	4014	WSE	1741630.251	1153862.964	5246.204	8/23/2016
333	4015	thweg	1741612.561	1153842.820	5244.691	8/23/2016
334	4016	thweg	1741612.609	1153835.242	5245.016	8/23/2016
335	4017	thweg	1741610.419	1153823.968	5245.250	8/23/2016
336	4018	thweg	1741616.689	1153808.225	5245.029	8/23/2016
337	4019	thweg	1741616.724	1153808.165	5245.019	8/23/2016
338	4020	thweg	1741615.382	1153797.866	5245.154	8/23/2016
339	4021	thweg	1741608.044	1153791.206	5245.372	8/23/2016
340	4022	thweg	1741606.378	1153780.228	5245.244	8/23/2016
341	4023	thweg	1741606.545	1153771.735	5245.241	8/23/2016
342	4024	thweg	1741606.876	1153765.555	5244.913	8/23/2016
343	4025	thweg	1741603.335	1153757.097	5244.892	8/23/2016
344	4026	thweg	1741602.122	1153751.534	5245.234	8/23/2016
345	4027	thweg	1741596.570	1153741.198	5245.274	8/23/2016
346	4028	thweg	1741596.266	1153732.248	5245.112	8/23/2016

ID	Point Name	Code	Easting	Northing	Elevation	Date
347	4029	thweg	1741590.961	1153720.329	5245.600	8/23/2016
348	4030	thweg	1741584.747	1153713.476	5245.641	8/23/2016
349	4031	thweg	1741582.142	1153707.873	5245.795	8/23/2016
350	4032	thweg	1741580.146	1153706.987	5245.588	8/23/2016
351	4033	thweg	1741575.835	1153700.396	5245.446	8/23/2016
352	4034	thweg	1741573.444	1153693.150	5245.570	8/23/2016
353	4035	cb	1741576.996	1153673.968	5245.377	8/23/2016
354	4036	thlwg	1741562.614	1153665.927	5246.412734	8/23/2016
355	4037	thlwg	1741558.17	1153655.086	5246.56262	8/23/2016
356	4038	thlwg	1741552.883	1153644.701	5246.886367	8/23/2016
357	4039	thlwg	1741547.36	1153633.883	5246.98577	8/23/2016
358	4040	thlwg	1741541.833	1153622.167	5247.210382	8/23/2016
359	4041	thlwg	1741540.059	1153613.176	5247.088874	8/23/2016
360	4042	thlwg	1741536.842	1153601.02	5247.354057	8/23/2016
361	4043	thlwg	1741534.07	1153592.179	5247.455067	8/23/2016
362	4044	thlwg	1741528.962	1153579.103	5247.364682	8/23/2016
363	4045	thlwg	1741521.022	1153567.091	5247.644976	8/23/2016
364	4046	thlwg	1741513.027	1153557.099	5247.54476	8/23/2016
365	4047	thlwg	1741503.721	1153545.774	5247.157939	8/23/2016
366	4048	thlwg	1741495.245	1153533.289	5246.986071	8/23/2016
367	4049	thlwg	1741485.08	1153523.209	5246.039559	8/23/2016
368	4050	ws	1741470.371	1153508.431	5248.58626	8/23/2016
369	112	basecp	1721316.271	1234834.257	4519.9544	8/25/2016
370	12000	topo	1721312.152	1234834.06	4524.153002	8/25/2016
371	12001	cb	1721540.631	1234627.243	4523.773433	8/25/2016
372	12002	wse	1721529.174	1234620.945	4525.089845	8/25/2016
373	12003	pc12	1721506.96	1234650.457	4524.625286	8/25/2016
374	12004	cb	1721518.399	1234666.212	4516.670696	8/25/2016
375	12005	wse	1721476.878	1234670.472	4517.83953	8/25/2016
376	12006	channelbottom	1721491.124	1234693.177	4515.844584	8/25/2016
377	12007	wse	1721441.186	1234688.257	4517.469489	8/25/2016
378	12008	channelbottom	1721453.377	1234711.919	4516.176466	8/25/2016
379	12009	wse	1721393.4	1234716.653	4517.286015	8/25/2016
380	12010	wse	1721371.017	1234732.391	4516.956125	8/25/2016
381	12011	wse	1721343.331	1234749.661	4516.281136	8/25/2016
382	12012	wse	1721299.99	1234769.069	4516.385554	8/25/2016
383	12013	channelbottom	1721310.07	1234796.397	4513.50468	8/25/2016
384	12014	wse	1721247.248	1234786.83	4516.356271	8/25/2016
386	12016	channelbottom	1721248.567	1234790.903	4515.062088	8/25/2016
387	12017	wse	1721250.214	1234835.831	4516.175178	8/25/2016

ID	Point Name	Code	Easting	Northing	Elevation	Date
387	12017	wse	1721250.214	1234835.831	4516.175178	8/25/2016
388	12018	channelbottom	1721238.892	1234821.596	4514.924221	8/25/2016
389	12019	channelbottom	1721208.174	1234841.924	4514.323263	8/25/2016
390	12020	wse	1721222.947	1234856.457	4516.143896	8/25/2016
391	12021	wse	1721196.354	1234885.403	4516.121904	8/25/2016
392	12022	chanelbottom	1721180.4	1234868.772	4514.734834	8/25/2016
393	12023	chanelbottom	1721141.44	1234886.963	4514.044488	8/25/2016
394	12024	wse	1721163.407	1234909.857	4515.96184	8/25/2016
395	12025	wse	1721135.284	1234945.232	4515.7678	8/25/2016
396	12026	wse	1721095.719	1234998.241	4514.688031	8/25/2016
397	12027	wse	1721077.27	1235025.536	4514.112002	8/25/2016
398	12028	Q12	1721281.676	1234807.94	4516.438368	8/25/2016
399	12029	channbottom	1721281.53	1234808.174	4514.62009	8/25/2016
400	113	base13	1698545.792	1257013.588	4251.990521	8/25/2016
401	13000	pc13	1698512.407	1257155.731	4240.717803	8/25/2016
402	13001	wse	1698503.739	1257147.98	4241.502659	8/25/2016
403	13002	wse	1698530.36	1257133.749	4241.674917	8/25/2016
404	13003	wse	1698577.163	1257105.138	4241.851947	8/25/2016
405	13004	wse	1698624.515	1257069.794	4241.862894	8/25/2016
406	13005	wse	1698646.81	1257054.374	4241.770153	8/25/2016
407	13006	wse	1698671.084	1257036.686	4241.985289	8/25/2016
408	13007	wse	1698689.718	1257022.016	4242.253702	8/25/2016
409	13008	wse	1698713.873	1257003.035	4242.253196	8/25/2016
410	13009	wse	1698741.266	1256973.525	4242.234086	8/25/2016
411	13010	wse	1698757.633	1256958.383	4242.151217	8/25/2016
412	13011	wse	1698763.444	1256944.61	4242.397903	8/25/2016
413	13012	cb	1698781.421	1256955.343	4241.329523	8/25/2016
414	13013	channelbottom	1698778.05	1256970.82	4241.133972	8/25/2016
415	13014	channelbottom	1698765.772	1256985.831	4240.383409	8/25/2016
416	13015	channelbottom	1698758.872	1256994.391	4240.054074	8/25/2016
417	13016	channelbottom	1698751.011	1257003.363	4240.274116	8/25/2016
418	13017	channelbottom	1698740.539	1257012.021	4240.324258	8/25/2016
419	13018	channelbottom	1698727.968	1257028.126	4240.148059	8/25/2016
420	13019	channelbottom	1698718.793	1257042.824	4240.225491	8/25/2016
421	13020	channelbottom	1698710.054	1257055.727	4240.722364	8/25/2016
422	13021	channelbottom	1698698.638	1257064.93	4240.539169	8/25/2016
423	13022	channelbottom	1698680.706	1257077.015	4240.769872	8/25/2016
424	13023	channelbottom	1698666.009	1257085.102	4241.005578	8/25/2016
425	13024	channelbottom	1698648.85	1257090.265	4240.770676	8/25/2016
426	13025	channelbottom	1698633.128	1257099.054	4240.897992	8/25/2016

ID	Point Name	Code	Easting	Northing	Elevation	Date
427	13026	channelbottom	1698587.624	1257131.512	4240.587362	8/25/2016
428	13027	channelbottom	1698577.043	1257141.484	4240.61181	8/25/2016
429	13028	channelbottom	1698563.25	1257155.633	4240.921314	8/25/2016
430	13029	channelbottom	1698547.732	1257166.475	4240.824115	8/25/2016
431	13030	channelbottom	1698538.229	1257180.895	4240.858788	8/25/2016
432	13031	channelbottom	1698531.238	1257187.502	4240.729829	8/25/2016
433	13032	channelbottom	1698524.036	1257193.842	4240.547788	8/25/2016
434	13033	channelbottom	1698506.581	1257205.434	4240.023617	8/25/2016
435	13034	channelbottom	1698481.003	1257217.389	4245.148234	8/25/2016
436	13035	channelbottom	1698467.405	1257213.237	4240.817547	8/25/2016
437	13036	channelbottom	1698444.225	1257221.348	4240.498397	8/25/2016
438	13037	wse	1698428.262	1257203.675	4241.081053	8/25/2016
439	13038	wse	1698461.374	1257178.231	4241.254046	8/25/2016
440	13039	wse	1698479.556	1257168.673	4241.387445	8/25/2016
441	13040	wse	1698487.088	1257164.981	4241.387082	8/25/2016
442	14000	topo	1668970.704	1281117.637	3934.013741	8/25/2016
443	14001	channelbottom	1668962.753	1281407.395	3927.247223	8/25/2016
444	14002	wse	1668962.544	1281408.183	3928.149971	8/25/2016
445	14003	wse	1669005.641	1281367.186	3927.610769	8/25/2016
446	14004	wse	1669018.33	1281338.335	3927.744163	8/25/2016
447	14005	wse	1669030.265	1281310.076	3927.912846	8/25/2016
448	14006	wse	1669047.051	1281281.054	3927.776704	8/25/2016
449	14007	q14	1669048.866	1281274.234	3927.778426	8/25/2016
450	14008	wse	1669060.879	1281247.288	3927.867485	8/25/2016
451	14009	wse	1669068.213	1281235.852	3927.868915	8/25/2016
452	14010	wse	1669077.905	1281218.954	3927.843381	8/25/2016
453	14011	channelbottom	1669062.205	1281213.541	3926.098614	8/25/2016
454	14012	channelbottom	1669050.483	1281234.905	3926.037677	8/25/2016
455	14013	channelbottom	1669035.323	1281259.754	3926.141401	8/25/2016
456	14014	channelbottom	1669029.35	1281273.111	3926.281418	8/25/2016
457	14015	channelbottom	1669025.668	1281285.202	3926.329112	8/25/2016
458	14016	channelbottom	1669010.667	1281309.803	3926.426412	8/25/2016
459	14017	pc14	1668971.887	1281446.514	3926.778339	8/25/2016
460	114_opus	basecp	1668975.701	1281115.995	3933.764044	8/25/2016
461	108_opus	base08	1793350.893	1112908.111	5798.375787	8/22/2016
462	102b_opus	base02b	1776626.112	1123946.74	5643.013434	8/23/2016

12 Appendix E – Pebble Count Data

The raw pebble count data is presented in the following table:

RM	Description	512	256	180	128	90	64	45	32	22.6	16	11	8	5.6	4	2.8	2	Fines
Texas Creek	Bar						1	1	3	6	12	32	15	8	5	3		14
Texas Creek					3	3	6	3	4	3	4	10	9	14	4	5	1	31
Eighteen Mile Creek	Riffle									3	3	9	21	21	14	6	4	19
55.5	Riffle					5	9	6	20	14	13	12	4	9	5			7
55.5	Pool				1	4	4	13	18	18	12	14	3	2	3	1		1
55.5	Riffle				2	1	7	17	25	21	18	9	3	1	1	2		
48.8	Riffle			8	12	11	17	18	20	10	4	3	1		1		1	
40.8	Run			7	12	8	15	13	17	8	5	5	4	1	4	2		2
36.4				9	8	21	12	12	1	3	8	4	2	7	3		2	
Hayden Creek	Run			16	11	26	28	24	20	13	3	3	3	4				
33	Run			1	6	18	19	27	18	10	19	6	2	7	1			8
27.5	Riffle			9	6	14	18	16	16	9	4	6	2			1		1
24.3	Riffle	2	9	9	11	14	17	15	8	7	2	3	3	1				
21.4		5	3	14	10	16	23	12	10	4	2	0	1					
17.2	Riffle		3	6	13	15	16	19	10	10	2	3	2	2		2	2	
9.3	Riffle			4	13	18	24	25	19	11	3	1	3	2	3	2	2	
0.4	Riffle				9	10	12	18	19	23	14	1	2				1	

RECLAMATION
Managing Water in the West

Technical Report No. SRH-2017-15

Pahsimeroi River Hydraulics & Hydrologic Assessment

Columbia-Snake Salmon Recovery Office
Pacific Northwest Region

U.S. Department of the Interior
Bureau of Reclamation
Technical Service Center
Denver, Colorado

March 2017

Mission Statements

The Department of the Interior protects and manages the Nation's natural resources and cultural heritage; provides scientific and other information about those resources; and honors its trust responsibilities or special commitments to American Indians, Alaska Natives, and affiliated island communities.

The mission of the Bureau of Reclamation is to manage, develop, and protect water and related resources in an environmentally and economically sound manner in the interest of the American public.

Bureau of Reclamation
Technical Service Center, Denver, Colorado
Sedimentation and River Hydraulics Group, 86-68240

Technical Report SRH-2017-15

Pahsimeroi River Hydraulics and Hydrologic Assessment

Columbia-Snake Salmon Recovery Office
Pacific Northwest Region

MELISSA FOSTER Digitally signed by MELISSA FOSTER
Date: 2017.04.21 13:14:22 -06'00'

Prepared by:
Melissa Foster, Ph.D., Physical Scientist
Sedimentation and River Hydraulics Group

AMANDA STONE Digitally signed by AMANDA STONE
Date: 2017.04.21 13:36:51 -06'00'

Prepared by:
Amanda Stone, M.S., P.E., Hydrologic Engineer
Flood Hydrology and Meteorology Group

CAROLINE UBING Digitally signed by CAROLINE UBING
Date: 2017.04.21 13:51:14 -06'00'

Prepared by:
Caroline Ubing, M.S., Hydraulic Engineer
Flood Hydrology and Meteorology Group

MICHAEL SIXTA Digitally signed by MICHAEL SIXTA
Date: 2017.04.21 13:56:23 -06'00'

Peer Reviewed by:
Mike Sixta, M.S., P.E., Hydraulic Engineer
Sedimentation and River Hydraulics Group

Peer Review Certification: *This document has been peer reviewed and is believed to be in accordance with the service agreement and standards of the profession.*

Table of Contents

page

1. Purpose and Scope 2

2. Pahsimeroi River Basin Characteristics 3

2.1 Hydrologic Influences...7
2.2 Gaged Flow Characteristics 8
3. Methods..12

3.1 Hydrologic Assessment 14
3.1.1 Peak Flow Calculations at Gaged Locations.. 14
3.1.2 Peak Flow Calculations at Ungaged Locations.................................... 14
3.2 Stream Power Analysis...16
3.3 Field Data Collection 17
3.3.1 Data Collection Methodology... 17
3.4 At-a-Station Hydraulic Calculations...18
3.4.1 At-a-Station Hydraulic Calculation Methods 18
3.4.2 Uncertainty associated with at-a-station hydraulics............................. 20
4. Results 21

4.1 Hydrologic Assessment Results...21
4.1.1 Peak Flow Calculations at Gaged Locations.. 21
4.1.2 Peak Flow Calculations at Ungaged Locations.................................... 23
4.2 Stream Power Analysis Results 26
4.3 Pebble Count Results..29
4.4 At-a-Station Hydraulic Results...30
5. Data Gaps and Recommendations 33

5.1 Existing Data for the Project Area 35
5.3 Topographic and Bathymetric Data Collection Options.....................................35
5.4 Hydrologic Data Gaps and Recommendations 36
5.5 Sediment Data Gaps and Discussion 37
5.6 Model Calibration Data Gaps 39
7. Conclusion 39

8. References...40

Appendix A – Annual Peak Streamflow 44

Appendix B – Additional Hydrology Plots 47

Appendix C – Drainage Area Ratio 48

Appendix D – Regional Regression Analysis..49

U.S. Department of the Interior
Bureau of Reclamation
Technical Service Center
Denver, Colorado

March 2017

Tables

page
Table 1. USGS stream gage information for gages within the Pahsimeroi River basin utilized for analysis........ 5
Table 2. Major ditches in Pahsimeroi Basin (DHI, 2004) 7
Table 3. Low flow discharge values 11
Table 4. Manning's roughness (*n*) values 19
Table 5. Summary of PeakFQ model results. 23
Table 6. Summary of flow frequency assessment at select locations on the Pahsimeroi River........ 25
Table 7. Stream Power Analysis Results 29
Table 8. Pebble Count Results 29
Table 9. At-a-station hydraulic calculation results 31
Table 10. At-a-station bed mobility calculation results 32

Figures

page
Figure 1. Location map of the Pahsimeroi basin. 4
Figure 2. Key gage locations within the Pahsimeroi basin. 6
Figure 3. Pahsimeroi River basin with tributary creeks........ 8
Figure 4. Mean and median daily discharge values for the record from 1984 to present (USGS gage 13302005) for the Pahsimeroi River near the confluence with the Salmon River. This plot is representative of the recent hydrology. Discharge plots for gage 13302000 and gages 13302000 and 13302005 (combined) are in Appendix B. 9
Figure 5. Example of a high snowpack year (1995) and associated daily flow patterns at USGS gage 13302005. 10
Figure 6. Example of a low snowpack year (2015) and associated daily flow patterns at USGS gage 13302005. 10
Figure 7. Frequency of annual peak flows by month for the Pahsimeroi River near the confluence with the Salmon River (USGS gages 13302000 and 13302005). 11
Figure 8. Valley segments and geomorphic reaches labeled by approximate river mile. 12
Figure 9. Flow frequency assessment locations and gages used for analysis....... 15
Figure 10. Example of first-order polynomial fit for river elevations along a geomorphic reach. Distance from the river mouth (DFM) is shown in river miles, but the linear fit equation is shown in units of ft (y=mx+b, where x [=] ft, y [=] ft, m [=] 0.00494 ft/ft. 17

Figure 11. Locations of cross section surveys and pebble counts performed by Trout Unlimited. 18
Figure 12. Pebble axis measurement (from Harrelson et al., 1994, their Figure 60). 18
Figure 13. PeakFQ results for Pahsimeroi River gage near confluence (USGS 13302000 and 13302005) 22
Figure 14. PeakFQ results for Morse Creek gage (USGS 13301700). 22
Figure 15. Peak discharge values summarized for both gaged locations 23
Figure 16. Illustration of different hydrologic reaches of the Pahsimeroi River .. 26
Figure 17. Estimated discharge values along the main Pahsimeroi River. Both high and low discharge estimates are shown for GR 6-8 (see Table 6 and section 4.1). 27
Figure 18. Pahsimeroi River longitudinal profile and slope, delineated by geomorphic reaches. Note that the slope is plotted on a logarithmic scale. 28
Figure 19. Stream power results; both high and low estimates are shown for GR 6-8. 28
Figure 20. Pebble count cumulative frequency results for the three cross sections along the Pahsimeroi River. Particles smaller than 2 mm are not plotted. 30
Figure 21. Water surface elevation for 1.25- and 100-yr events, assuming normal (Table 4) Manning's n value, at RM 2.1. Cross-section elevations and water-surface elevations are arbitrary. Note that the y and x-axes are consistent on Figures 21, 22, and 23. 32
Figure 22. Water surface elevation for 1.25- and 100-yr events, assuming normal (Table 4) Manning's n value, at RM 11.7. 33
Figure 23. Water surface elevation for 1.25- and 100-yr events, assuming normal (Table 4) Manning's n value, at RM 25.6. 33
Figure 24. Stream power and pebble count results. The median grain size (D50) is plotted on the right vertical. Stream power is presented on the left vertical axis for four flood events. ....**Error! Bookmark not defined.**
Figure 25. Mean and median daily discharge values for the record from 1984 to present (USGS gages 13302000 and 13302005 combined) for the Pahsimeroi River near the confluence with the Salmon River. 47
Figure 26. Mean and median daily discharge values for the record from 1984 to present (USGS gage 13302000) for the Pahsimeroi River near the confluence with the Salmon River. 47

Abbreviations

%	percent
°C	degrees Celsius
°F	degrees Fahrenheit
°N	latitude degrees north
°W	longitude degrees west
2D	two-dimensional
ADCP	Acoustic Doppler Current Profiler
AEP	Annual Exceedance Probability
cfs	cubic feet per second
CORS	Continuously Operating Reference Station
COV	Coefficient of Variance
DFM	Distance From Mouth
DS	Downstream
Eq	Equation
ESA	Endangered Species Act
ft	foot/feet
GIS	Geographic Information System
GNSS	Global Navigation Satellite Systems
GPS	Global Positioning System
HSI	Habitat Suitability Index
IACWD	Interagency Advisory Committee and Water Data
IDEQ	Idaho Department of Environmental Quality
IDWR	Idaho Department of Water Resources
km	kilometer(s)
LiDAR	Laser Imaging, Detection and Ranging
mi	mile(s)
mm	millimeter(s)
NAD	North American Datum
NAVD	North American Vertical Datum
NRCS	National Resources Conservation Service

No.	Number
OPUS	Online Position User Service
PN	Pacific Northwest
Reclamation	Bureau of Reclamation
RM	River mile
RMS	Root Mean Square
RTK	Real Time Kinematic
RTS	Resource and Technical Services
SNOTEL	Snow Telemetry
SRH	Sedimentation and River Hydraulics Group
SWE	Snow Water Equivalent
TSC	Technical Service Center
U.S.	United States
US	Upstream
USACE	U.S. Army Corps of Engineers
USGS	U.S. Geological Survey
USFS	U.S. Forest Service
WSE	Water Surface Elevation

Symbols

D_n	Sediment particle diameter size at n% passing
DA_u	Contributing drainage area at the ungaged site (mi^2)
DA_g	Contributing area at the gaged site (mi^2)
DA_{g1}	Contributing area at the upstream gaged site (mi^2)
DA_{g2}	Contributing area at the downstream gaged site (mi^2)
Q	Flow discharge or rate (ft^3/s)
Q_u	Discharge at an ungaged site (ft^3/s)
Q_g	Discharge at the gaged site (ft^3/s)
Q_{g1}	Discharge at the upstream gaged site (ft^3/s)
Q_{g2}	Discharge at the downstream gaged site (ft^3/s)
S	Slope (ft/ft)
γ	Specific weight of water (lb/ft^3)
Ω	Total stream power (lb/s)

Executive Summary

The Bureau of Reclamation is conducting an Integrated Rehabilitation Assessment of 64 river miles of the Pahsimeroi River Basin by characterizing general watershed conditions. This assessment, along with assessments of the Lemhi and Upper Salmon River Basins, will provide information used to select reaches with the greatest potential for steelhead and spring Chinook rehabilitation projects. The objectives of this hydraulics and hydrologic assessment include: (1) estimating peak flows; (2) assessing stream power; (3) calculating at-a-station hydraulics at three cross sections, which include survey data and pebble counts; and, (4) identifying data needs for future hydraulic modeling analyses. Analyses from this report will feed into a watershed-scale geomorphic and fish production model.

The Pahsimeroi River flow regime differs from a traditional snowmelt dominated stream. The upper basin experiences peak flows in May or June, which is consistent with snowmelt dominated stream flows. However, the remainder of the basin experiences peak flows in November, with flows remaining steady and high between October and April. Overall, the hydrology in the Pahsimeroi River Basin is largely driven by groundwater (influenced by depth to bedrock and thickness of alluvium), as well as irrigation practices. While agricultural diversion locations and volumes are regulated by local water authorities and the Idaho Department of Water Resources, exact withdrawal rates on a seasonal and daily basis are unknown. Flood frequency peaks were estimated at two operational United States Geological Survey (USGS) gages using the PeakFQ program, and at 12 ungaged locations (including 2 locations in the headwaters) applying methods from Berenbrock (2002). Flow uncertainties are especially high in the middle of the Pahsimeroi Basin (between River Mile 41.7 and 52.4), where sites are located too far away from the gages to adhere to the assumptions of the drainage area ratio method, resulting in a large range of possible discharges. Using the USGS gage data, it appears that discharge does not regularly increase with distance downstream. Discharge decreases from the upper valley to the middle valley, likely due to groundwater influences and irrigation withdrawals (Table ES1).

Table ES1.

River Mile [1]	DA (mi^2)	Valley Segment	Estimated Flood-Frequency Values (cfs)						
			1.5	2	5	10	25	50	100
2.1	824	Lower	308	350	459	535	634	712	792
35.7	331	Middle[2]	149	169	221	258	306	343	382
55.9	56	Upper	302	361	506	600	715	798	880

[1]The river mile location is near the downstream end of the valley segment.
[2]High uncertainty exists for flow estimates in the middle of the Pahsimeroi Valley.

Valley and geomorphic reaches were identified to distinguish confinement, sediment transport trends, and provide consistent locations for discussion throughout the Integrated Rehabilitation Assessment. A stream power assessment was completed to investigate the relative sediment transport capacity of each geomorphic reach. Stream power is a function of discharge and slope; therefore, the results should indicate locations of significant tributaries and changes in slope. Results indicated that in general the upper basin has higher stream power than the lower portion of the basin. The upper basin has relatively high flows and higher slopes. The middle basin could potentially have the highest stream power; however, there is a large range in the stream power estimates due to the uncertainty in discharge. Therefore stream power results were not conclusive in the middle basin. The lower basin exhibited lower stream power, indicating the low slopes are the dominate variable in calculating stream power in this portion of the basin.

A two-dimensional (2D) hydraulic model is recommended for future hydraulic modeling to quantify habitat improvement for proposed alternatives along the Pahsimeroi River. A 2D hydraulic model, as opposed to a one-dimensional (1D) model, will better represent multiple channel networks, geomorphic features, and lateral flow over the floodplain. Existing data gaps that need to be acquired for hydraulic modeling include: (1) high-resolution topography; (2) bathymetry; (3) calibration data, including channel roughness and water surface elevations for high and low flows; and, (5) an improved understanding of diversion outflows, tributary inflows, and groundwater contributions (quantitative data, if possible).

1. Purpose and Scope

The Bureau of Reclamation's (Reclamation) Resource and Technical Services (RTS) in the Pacific Northwest (PN) Regional Office tasked Reclamation's Sedimentation and River Hydraulics (SRH) Group at the Technical Service Center (TSC) with supporting a coarse-level Integrated Rehabilitation Assessment of the Pahsimeroi River Basin. The Pahsimeroi River extends over 64 river miles (RM) from the headwaters (RM 64.4) to the confluence with Salmon River (RM 0).

The primary objective of this project was to conduct analyses and field assessments to inform hydrology, hydraulics, and sediment trends in support of the coarse-scale Integrated Rehabilitation Assessment. This study focuses on summarizing available hydraulic, streamflow, and sediment data that can be utilized in future reach or project scale hydraulic modeling. Five key elements of this report are:

1. The description of hydrologic characteristics in the basin.
2. A regional regression hydrologic assessment of flood-frequency events at multiple locations.
3. A stream power analysis at geomorphic reaches to qualitatively assess relative sediment transport potential.
4. Characterizing cross-section and grain size analysis at three locations.
5. Determining data gaps for future hydraulic modeling.

These five elements will feed into a watershed-scale geomorphic and fish production model, intended to identify reaches with the most potential for on-the-ground habitat rehabilitation projects targeting steelhead and spring chinook. The model develops a fish population and habitat relationship which incorporates twelve different metrics, including: average annual discharge, substrate (D_{84}), slow water area, wetted depth, etc. (outlined in Zabel, et al., 2016). Average annual discharge is the primary indicator for population capacity. A stream power analysis was performed to provide an indication of the relative sediment transport capacity of each geomorphic reach along the main Pahsimeroi River. Cross-sections and a grain size analysis were completed to assess hydraulic properties and bed grain size mobility at a single cross section for a given range of discharge values. More detailed, future hydraulic modeling can provide information regarding slow water areas and wetted depth. The field data collected in this study will be used to calibrate future hydraulic models. Finally, the population and habitat relationship can be used to predict fish capacity based on existing physical habitat. The results can then be used to identify locations where rehabilitation projects could have the greatest benefit.

2. Pahsimeroi River Basin Characteristics

The Pahsimeroi River Basin (Figure 1) is a fourth-order river basin located in Lemhi and Custer counties in Idaho. The Pahsimeroi River flows north to northwest from its headwaters in the Lost River and Lemhi Ranges to its confluence with the main stem Salmon River. The highest peak in the basin is Mount Borah at 12,667 feet and the lowest point near the main stem of the Salmon is approximately 4,600 feet. The project area ends at the confluence with the Salmon River, with a basin drainage area of 830 mi^2. In the headwaters, the Pahsimeroi River is confined, flowing through a canyon (above RM 59.8). Downstream of the canyon, the basin is characterized by broad, alluvial valleys (up to 10 mi wide) surrounded by steep mountains. Many of the basin tributaries exit the mountain front onto broad alluvial fans and only contribute surface water to the main stem Pahsimeroi River during high-flow conditions (Young and Harenberg, 1973); small, discontinuous ephemeral streams are mapped across the alluvial fans. The Pahsimeroi River is at times braided and the flow goes subsurface for ~5 mi through the upper portion of the alluvial valley. River gradient typically decreases with distance downstream, with reach-scale (>1 mi of river length) gradients approximately between 0.005 and 0.001ft/ft.

To better constrain the hydrology of the basin, a MIKE basin model of the Pahsimeroi River was constructed in 2004. However, due to insufficient stream and diversion flow data, the model could not be calibrated. At the time the model was developed, there were not data for tributaries within the area. A short duration of daily discharge data at Big Creek was scaled by drainage area and applied to other tributaries. To further develop the model, the following data are recommended: (1)

daily inflow rates for all tributaries; (2) stream gaging upstream and downstream of sensitive areas (e.g., groundwater influenced areas); and, (3) daily diversion discharges. In addition, further analysis of precipitation, groundwater data, and seepage simulations would increase the understanding of water movement within the basin (see DHI, 2004 for detailed results and recommendations).

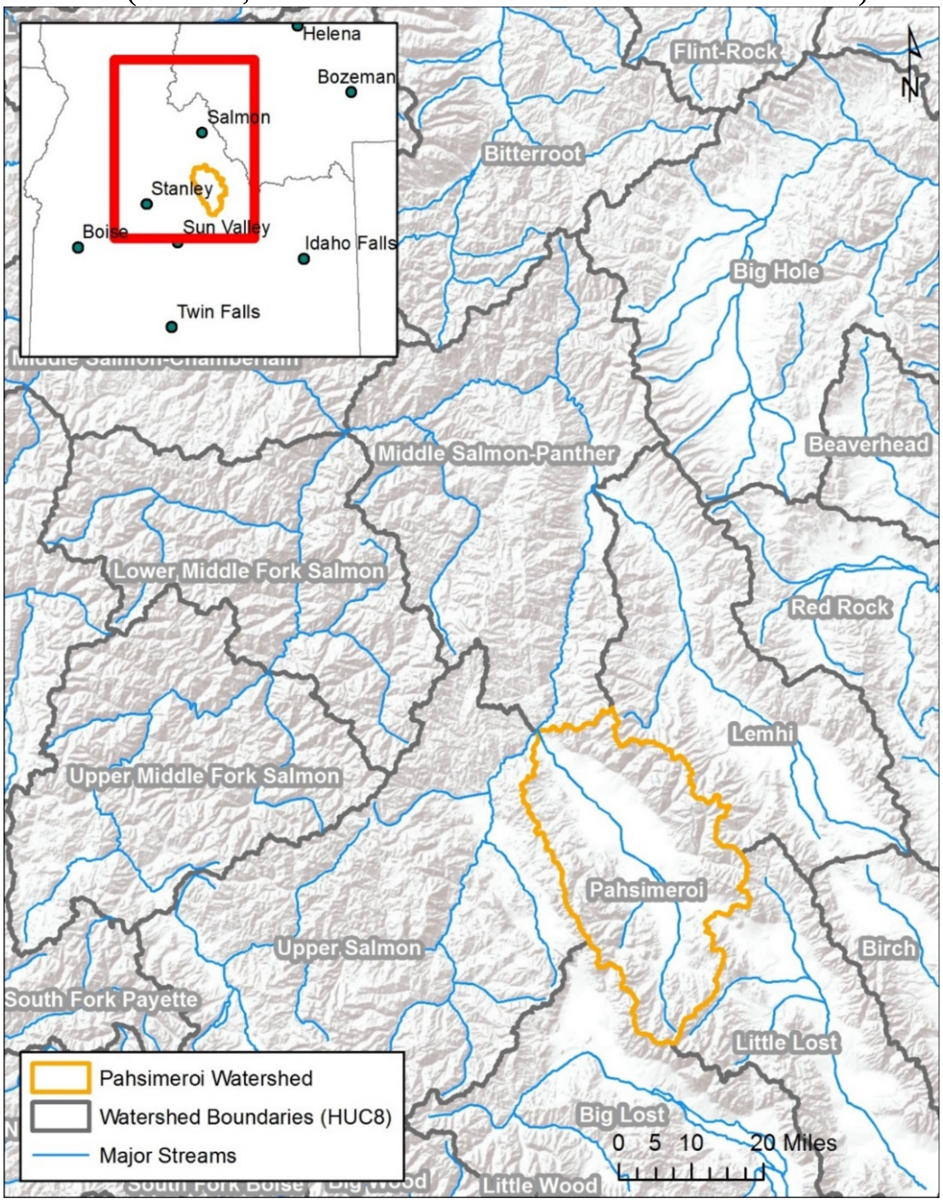

Figure 1. Location map of the Pahsimeroi basin.

There are few locations of flow measurement within the Pahsimeroi basin (**Error! Reference source not found.**). The USGS has maintained a gage on the Pahsimeroi near the confluence with the Salmon River since 1929, with the exception of a break in the record from 1972 to 1984 (13302000 and 13302005; see Table 1). These gages record 15-minute interval data; however, during many large flow events, only maximum average daily flows are recorded. This record includes both annual peak flow values as well as daily flows.

In addition to the gage on the main stem of the Pahsimeroi, two gage locations on Morse Creek (a tributary near RM 18) have at least 10 years of annual peak record (Table 1). Gage 13301700 (Morse Creek above diversions near May, ID) is near the steeper portion of the basin and has 17 annual peaks from 1962 to 1980. Gage 13301800 (Morse Creek near May, ID) is downstream from the previous gage, located more in the alluvial valley. There are 10 annual peak values from 1962 to 1971 at this location with three of them being zero flows.

The Idaho Department of Water Resources (IDWR) currently maintains one gage on the main stem of the Pahsimeroi (at Furey Lane, RM 27.2) and one on Patterson Creek (https://www.idwr.idaho.gov/waterboard/WaterPlanning/Water%20Transaction%20Program/streamgages/stream_gages.htm); Idaho Power maintains one gage along the main stem of the Pahsimeroi (below P9, RM 15.4; see Fig. 2); these data are hosted by the IDWR website (therefore this is referred to as an IDWR gage throughout the text). These gages report only daily flows, do not record annual peaks. The gages on the Pahsimeroi (RM 15.4 and 27.2) started in 2004 and 2005 while the Patterson Creek gage started in 2009.

Table 1. USGS stream gage information for gages within the Pahsimeroi River basin utilized for analysis.

				Daily Streamflow (cfs)		
USGS Gage No.	Description	Drainage Area (mi^2)	Period of Record	Min.	Average	Max.
13302000	Pahsimeroi River near May, ID	830	1930-1959, 1972*	74	214	840
13302005	Pahsimeroi River at Ellis, ID	830	1985-2015	87	229	710
13301700	Morse Creek above diversions near May, ID	18	1962-1980	Only peak flows available		
* There is a gap in the annual peak data from 1959-1971. There is only 1 year of data after the gap, which is not a full water year (1972). The gage was decommissioned in 1972.						

For the purpose of flow frequency and low-flow analysis, gages with reported values for annual peaks and daily measurements for 10 or more years were chosen for analysis (i.e., the USGS gages near the mouth of the Pahsimeroi and at Morse Creek). These gages were chosen based on their period of record, availability of annual peak values, and representative nature of the basin (see Appendix A for annual peaks). The upstream gage on Morse Creek (13301700) is representative of drainages in the basin with steeper slopes. However, Morse Creek is a south-facing tributary basin. There are undoubtedly differences in insolation between north- and south-facing slopes, which likely result in a different hydrologic response to snowmelt.

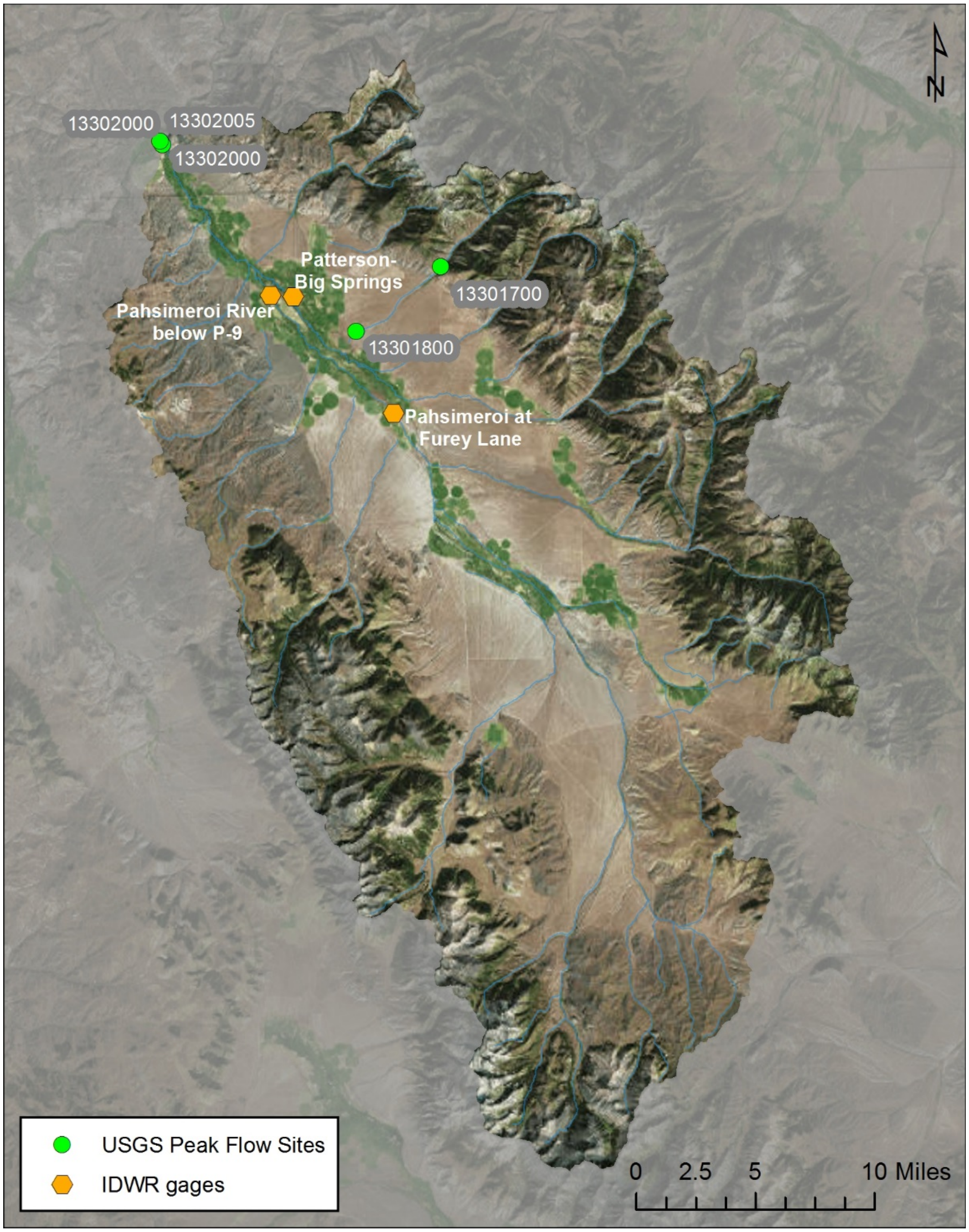

Figure 2. Key gage locations within the Pahsimeroi basin.

The annual peaks at the Pahsimeroi River gage location are impacted by diversion. In the 1970s, the USGS determined that 24,500 acres of surface water were diverted for irrigation. As a result of these diversions from upstream tributaries, only 27% of the yearly annual in-stream flow occurs during April to July (NRCS, 2008), which is uncharacteristic of a snowmelt dominated basin. However, groundwater infiltration likely also plays a role in controlling the volume of in-stream flows. While the flow record near the confluence with the Salmon (13302000 and 13302005) is influenced by diversion and groundwater infiltration, it is a continuous record representative of the main stem of the Pahsimeroi.

2.1 Hydrologic Influences

The hydrology in the Pahsimeroi River basin is driven by permeable alluvium in the valley floor, steep mountain slopes, snowpack, and irrigation withdrawals. The main stem of the Pahsimeroi has numerous gaining and losing reaches due to variations in the alluvium, bedrock depth, and irrigation withdrawals (Meinzer, 1924; Liberty et al., 2006). Bedrock becomes shallow and narrows north of Furey Lane (near RM 27.2), which likely functions as an impermeable barrier forcing groundwater to the surface along the downstream reach of the basin (Liberty et al., 2006). However, Meinzer (1924) noted that cavernous limestone bedrock in the region would readily absorb infiltrating groundwater. Irrigated land covers a large portion of the valley surrounding the main stem of the river. Total irrigated adjudicated water rights include 1,747 cfs of surface water, 102 cfs of groundwater for a total of 1,849 cfs. (NRCS, 2008). There are several large ditches used to convey streamflow from one stream system to another (Table 2; DHI, 2004). Main tributary creeks are shown in Figure 3.

Table 2. Major ditches in Pahsimeroi Basin (DHI, 2004)

Ditch Name	Source of Diversion	Receiving Stream
Alger Ditch	Pahsimeroi River (upper reach)	Goldburg Creek
California Ditch	Big Creek	Goldburg Creek
Goldburg Cross Ditch	Goldburg Creek	Pahsimeroi River (middle reach)
Mulvania Ditch	Big Springs Creek	Pahsimeroi River (lower Reach)
Ellis Cross Ditch	Big Springs Creek	Pahsimeroi River (lower reach)

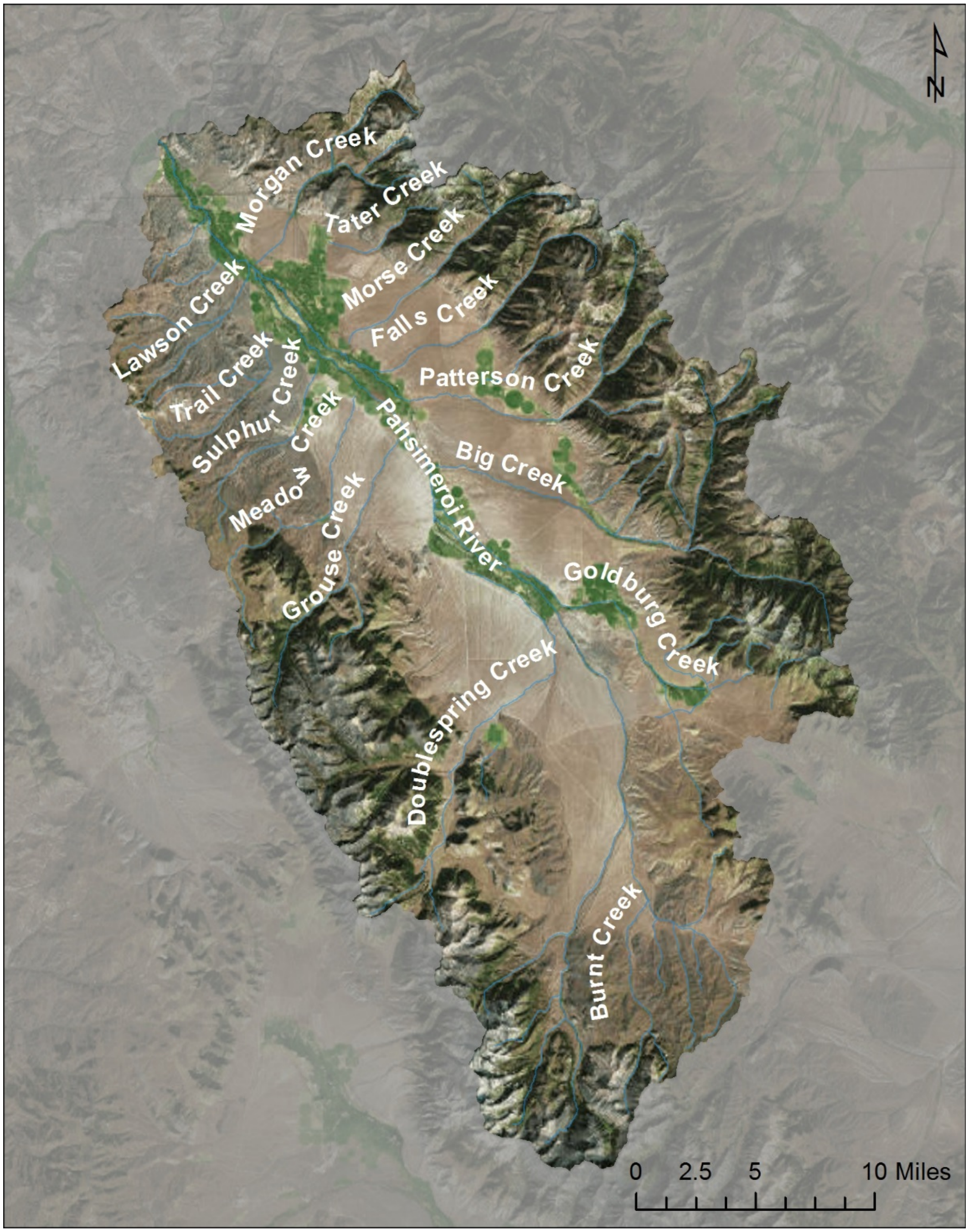

Figure 3. Pahsimeroi River basin with tributary creeks.

2.2 Gaged Flow Characteristics

Annual flow patterns in the Pahsimeroi River are unique for the region and do not reflect a typical mountain west snowmelt pattern. The mean and median daily flows at the USGS gage since 1984 are shown in Figure 4. Starting in October, the flows remain fairly steady and high. There is a reduction in flows starting in April and lasting through the summer, likely due to irrigation withdrawals. During some years, there is a flow increase in June into part of July. The nature of this increase is unknown, but it may be associated with decreases in irrigation relative to the early growing season or excess flows associated with a larger than average snowpack. For comparison, an example of a large snowpack seasonal pattern is shown in Figure 5 and a lower snowpack shown in Figure 6.

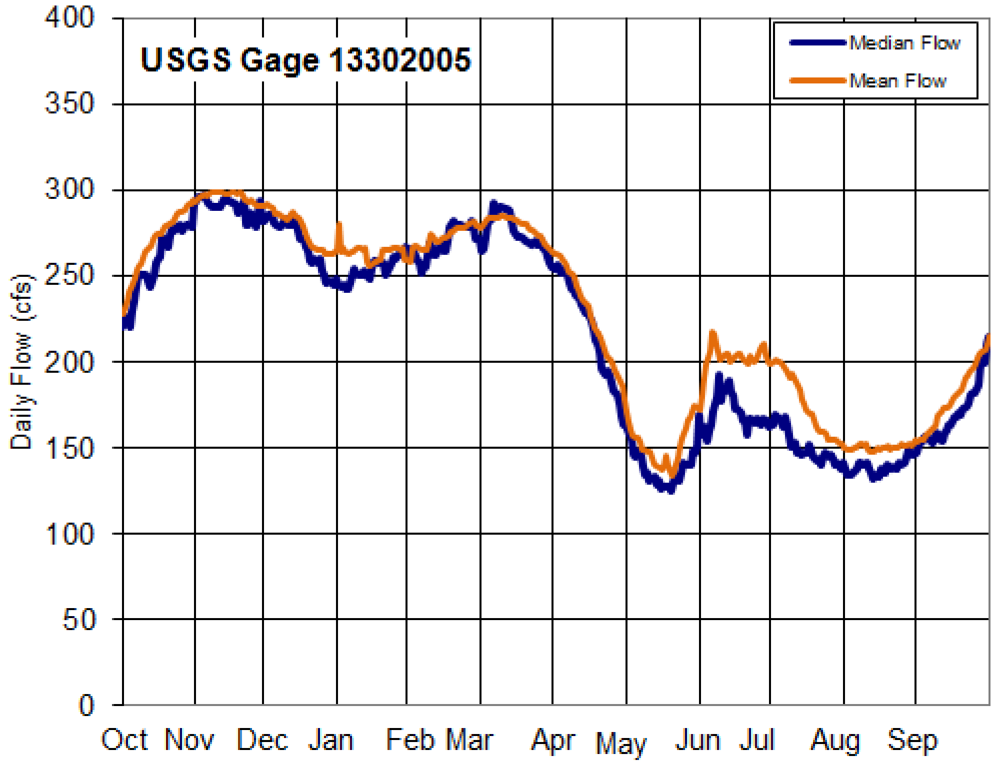

Figure 4. Mean and median daily discharge values for the record from 1984 to present (USGS gage 13302005) for the Pahsimeroi River near the confluence with the Salmon River. This plot is representative of the recent hydrology. Discharge plots for gage 13302000 and gages 13302000 and 13302005 (combined) are in Appendix B.

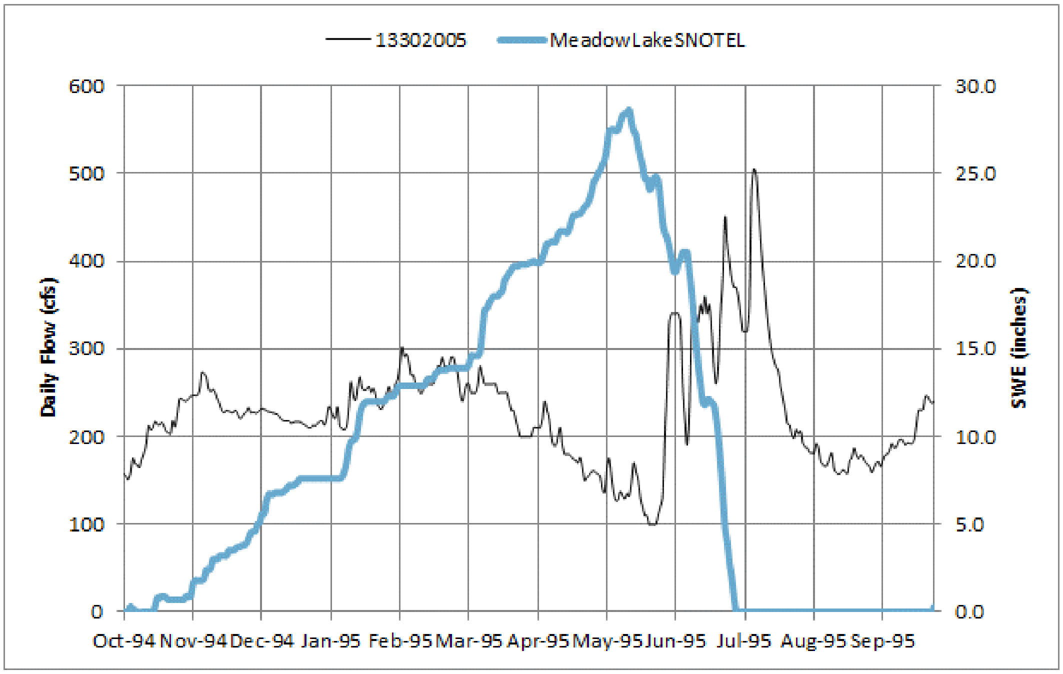

Figure 5. Example of a high snowpack year (1995) and associated daily flow patterns at USGS gage 13302005.

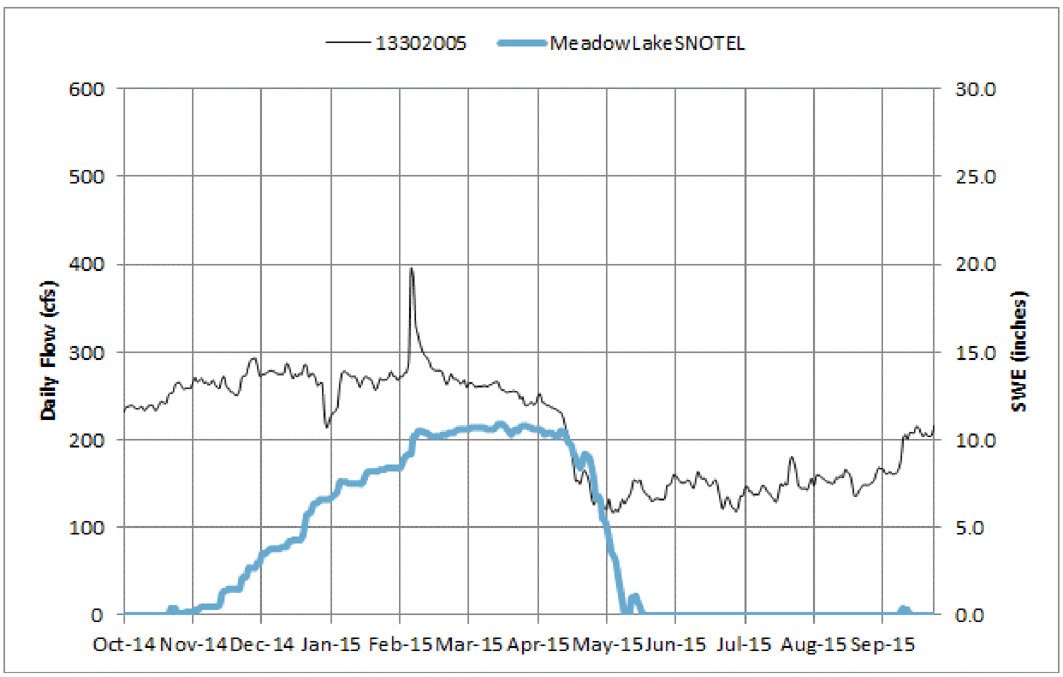

Figure 6. Example of a low snowpack year (2015) and associated daily flow patterns at USGS gage 13302005.

A low flow analysis was performed to identify the lowest 7-day average flow that occurs every 10 years (7Q10) using the methods described in Hortness (2006). The results are presented in Table 3. The 7Q10 values were computed separately for the two gages and then on the combined record for the two gages. There were no other gages within the basin with sufficient records to compute 7Q10 values elsewhere.

Table 3. Low flow discharge values

Gage	Period of Record	Drainage Area (mi^2)	7Q10 (cfs)
Pahsimeroi River at May ID (13302000)	1930- 1959,1972	830	83.5
Pahsimeroi River at Ellis ID (13302005)	1985 - 2015	830	98.5
Combined Record (13302000 & 13302005)	1929 – 1959, 1972, 1984 - 2016	830	89.3

The frequency of annual maximum flows by month are presented in Figure 7. Most peaks occur in November followed by equal frequencies of October and June peaks. This pattern also set the Pahsimeroi apart from other basins in the area as most snowmelt systems experience peak flows in late spring to early summer. This pattern is likely driven by groundwater influences and irrigation practices in the basin. The Morse Creek gage exhibits annual peaks in May or June, which better mimics snowmelt-driven peak flows (see Appendix A for all annual peak data).

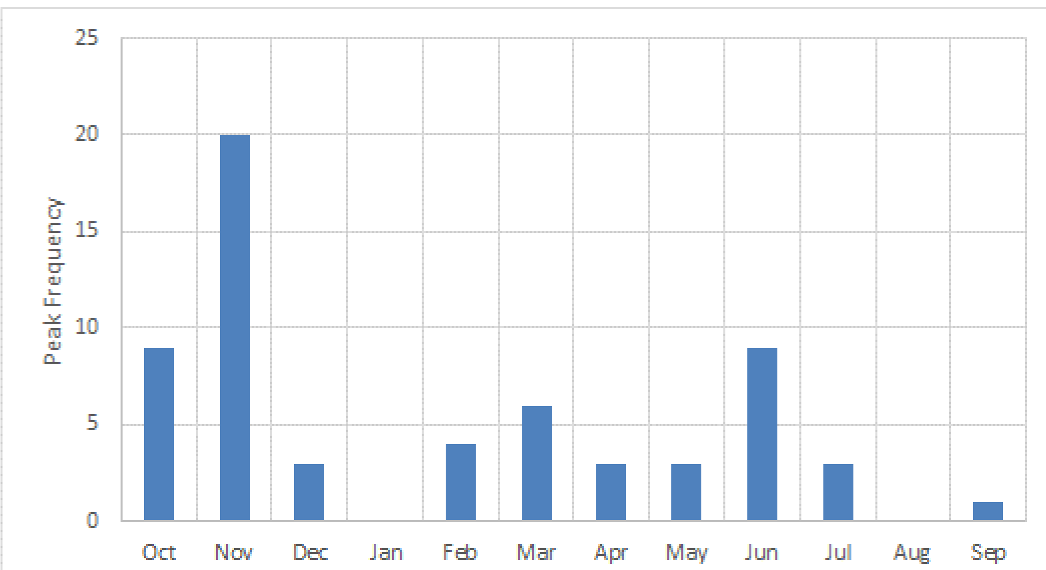

Figure 7. Frequency of annual peak flows by month for the Pahsimeroi River near the confluence with the Salmon River (USGS gages 13302000 and 13302005).

3. Methods

The following sections provide detail on the methodology applied to the hydrologic assessment, stream power analysis, and data collection effort. Valley segments and geomorphic reaches were developed by the PN region and given to TSC to establish consistent locations for the several analyses included in the Integrated Rehabilitation Assessment (**Error! Reference source not found.**).

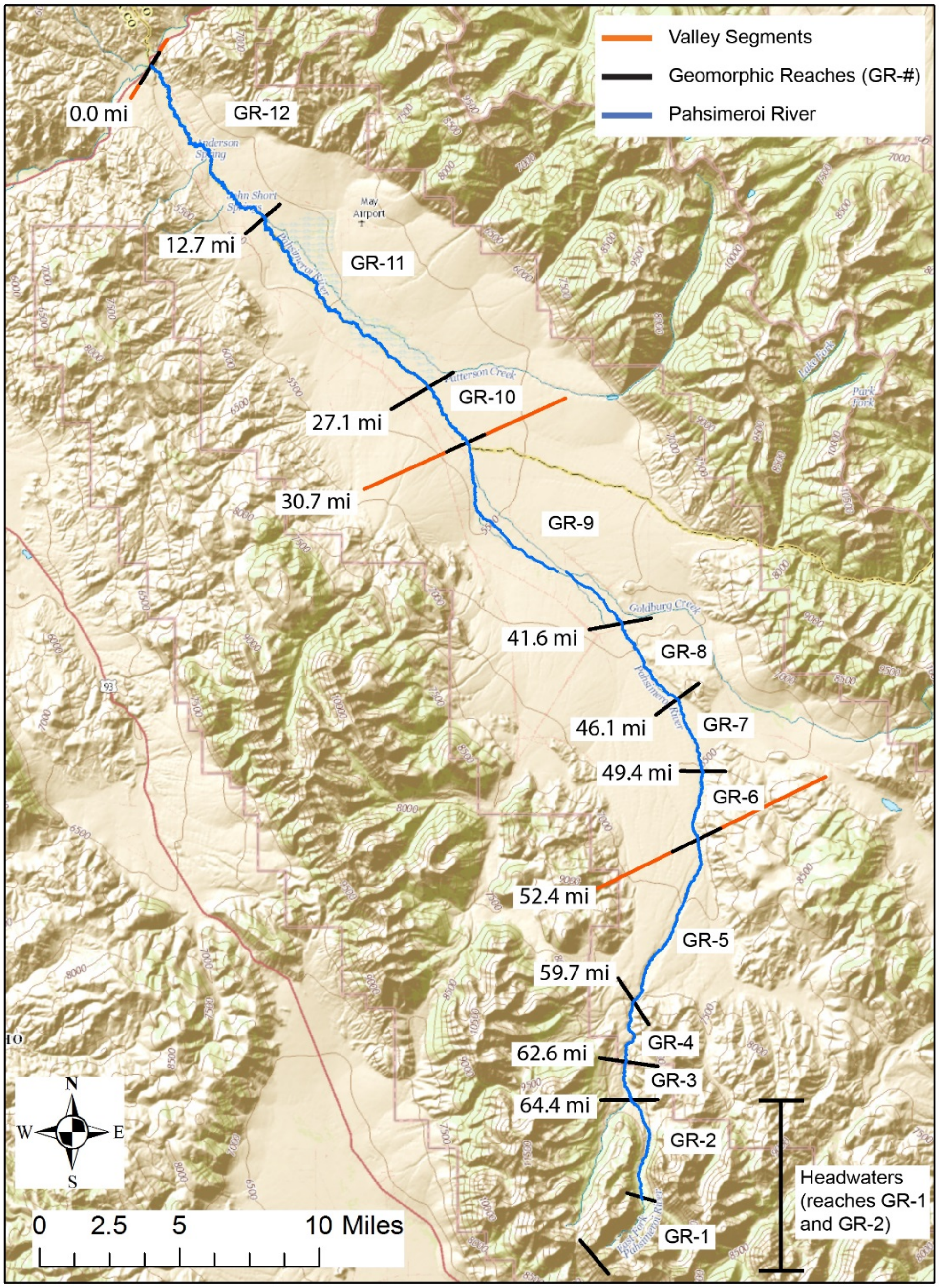

Figure 8. Valley segments and geomorphic reaches labeled by approximate river mile.

In addition to two USGS gages along the main stem Pahsimeroi River, three gages report data hosted by the Idaho Department of Water Resources (Figure 2). The periods of record for the IDWR gages are between 6 and 11 years. The IDWR gages report mean daily discharge, although 15-minute interval data may be available upon request. While mean daily data can be utilized to develop peak flood-frequency flow values, literature cautions against it, as it often underestimates the peak (e.g., Ellis & Gray 1966; Fill & Steiner 2003). Project success relies on fully quantifying the actual peak flow for flood planning and design purposes, so 15-minute interval data are optimal. The USGS gages report 15-minute interval data, but unfortunately for many large flow events, only average maximum daily flows were recorded. Approximately 75% of the annual peaks reported at the USGS gages were based on average maximum daily flows, and therefore these annual peaks likely underestimate the true peak flow.

The USGS gage data were utilized because of two reasons: (1) 15-minute interval data were available (although some of the peaks only represent the average maximum daily flow, as previously stated), and (2) the periods of record for the annual peaks are 17 and 61 years, at the Morse Creek and Pahsimeroi gages, respectively. IDWR gages were not utilized for this study, largely because of the short periods of record. The IDWR gage on the Pahsimeroi River at Furey Lane has a drainage area of 470 mi^2, and an 11 year period of record. However, this record exhibits numerous data gaps and long periods of 0.0 cfs flows (in both summer and winter); due to the numerous data gaps and no flow days, these data should not be used for a peak flow analysis. The IDWR gage located along Patterson Creek and has a drainage area of 141 mi^2. The Patterson Creek gage only represents flow from south-facing basins, similar to the USGS gage at Morse Creek. Based on the drainage area, this gage could provide flow frequencies for geomorphic reaches 6-8. However, as the period of record at this gage is less than 10 years, this gage record should not be used to conduct a peak flow analysis (IACWD, 1981). The IDWR gage at RM 15.7 (labeled ‘below P-9,’ see Figure 2), has a drainage area of 561 mi^2. The period of record at this site now includes 11 full water years (October 1- Sept. 30). For future phases of work, the record at this gage could be extended to conduct a peak flow analysis. Based on drainage area, this IDWR gage could provide flow frequencies for ungaged sites at geomorphic reaches 9-12. Due to differences in drainage area, the USGS Pahsimeroi River gage was not optimal for providing flow frequencies at geomorphic reach 9.

Following the guidelines outlined in Bulletin 17B, the IDWR gages should not be utilized to provide flow frequency estimates in the middle of the Pahsimeroi basin (geomorphic reaches 6-8). However, none of the basin gages (including USGS gages) adhere to the assumptions for estimating flow frequencies in the middle basin. Further analysis of the mean daily data at the IDWR gages and USGS gages, including methods to utilize short periods of record, may refine and better inform the middle basin hydrology. If additional gage data are used to estimate flow frequencies, an analysis of how well these data adhere to the assumptions underlying the methods used to extract peak values should also be included. In the upper basin where there are not any gaged sites, and in areas where wetlands attenuate floods and groundwater becomes influential, additional hydrologic modeling (HEC-HMS, SWMM, MIKE 11, etc.) should be conducted. For the purpose of the Integrated Rehabilitation Assessment, we have utilized the most complete and detailed data available (USGS gage data), estimating peak flood-frequency values based on published methodology by Berenbrock (2002; methods described in greater detail below).

3.1 Hydrologic Assessment

Peak flow frequency estimates were computed at multiple location along the main stem of the Pahsimeroi River for a range of recurrence intervals. Flow-frequency peak flow values were calculated at two USGS gage locations, near the confluence with the Salmon River (13302000 and 13302005) and Morse Creek (13301700), and then scaled to select locations along the Pahsimeroi River. Estimates for the 1.25-, 1.5-, 2-, 2.33-, 5-, 10-, 25-, 50-, and 100-year recurrence intervals were generated at two gaged locations and 16 ungaged locations (see Figure 9).

3.1.1 Peak Flow Calculations at Gaged Locations

Flow-frequency estimates for the two gaged locations were developed using methods described in Bulletin 17B using the USGS software package PeakFQ (Flynn, Kirby, & Hummel, 2006). Bulletin 17B recommends fitting a Log-Pearson III distribution to the gaged record of annual peak flow data, adjusting for outliers, historic peaks, and generalized skew (IACWD, 1981). PeakFQ estimates instantaneous annual maximum peak flows associated with recurrence intervals of the following events: 1.25-, 1.5-, 2-, 2.33-, 5-, 10-, 25-, 50-, 100-, 200-, and 500-year (Flynn et al., 2006). The method does not directly account for irrigation losses.

3.1.2 Peak Flow Calculations at Ungaged Locations

USGS guidelines for Idaho streams in region 6 (Berenbrock, 2002) were applied to compute discharge for ungagged sites along the Pahsimeroi River. Guidelines suggest the drainage-area ratio should be between 0.5 and 1.5 for applicability of this analysis. Drainage areas were estimated using StreamStats, a web-based Geographic Information Systems (GIS) tool that can be applied to water-resources engineering and design purposes (https://water.usgs.gov/osw/streamstats/). Among many other applications, StreamStats can obtain a drainage-basin boundary and area based on a user-identified point and USGS digital elevation model. Flow frequencies for ungaged sites were estimated using a ratio of drainage area as shown in the following equation:

$$Q_u = Q_g \left(\frac{DA_u}{DA_g}\right)^{0.80} \quad (3)$$

Where:

- Q_u is the peak discharge (cfs) for a specific recurrence interval at the ungaged site,
- Q_g is the peak discharge (cfs) for a specific recurrence interval at the gaged site,

- DA_u is the contributing drainage area (mi^2) for the ungaged site, and
- DA_g is the contributing drainage area (mi^2) for the gaged site.
- An exponent value of 0.80 is based on a regression analysis for Idaho, Region 6 (Berenbrock, 2002).

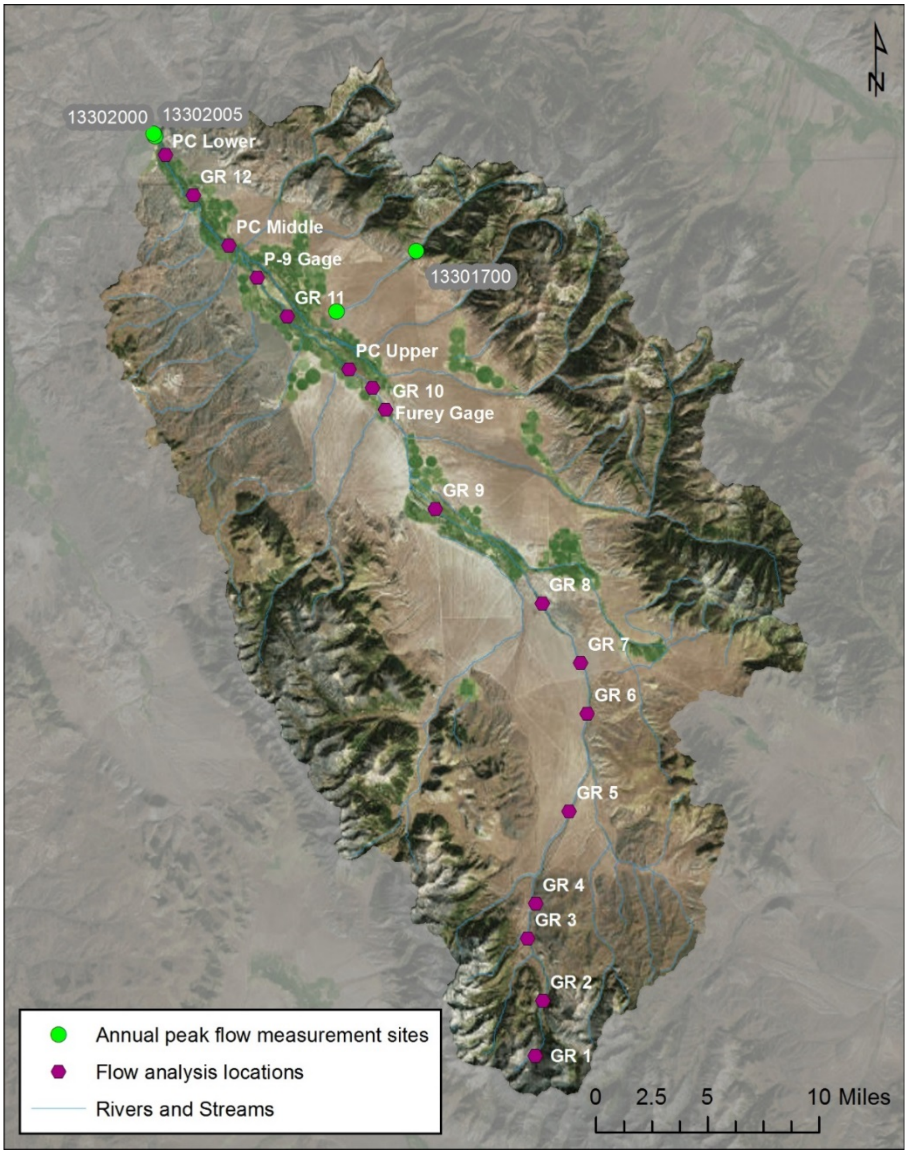

Figure 9. Flow frequency assessment locations and gages used for analysis

Regional regression analysis (Berenbrock, 2002) is an additional option for estimating peak flows. For region 6, equations are based on drainage area and mean annual precipitation. This method was reviewed for the Pahsimeroi River using precipitation estimates from StreamStats. Results indicated much higher flows using this method (see Appendix D). Because of the unique nature of the Pahsimeroi basin relative to other watersheds in the region (meandering channel in alluvial sediments with a high level of groundwater interaction), these analyses were not used in the final assessment. We instead used the drainage area ratio method to estimate flow frequencies based on the best available gage data in the watershed.

The results of the drainage area ratio analyses are presented in Section 4.1 Hydrologic Assessment Results.

3.2 Stream Power Analysis

A stream power analysis was performed to investigate the relative potential sediment transport ability of each geomorphic reach along the Pahsimeroi. Stream power (Ω) is a measure, per unit of downstream length, of the main driving forces acting in a channel and determines a river's ability to transport sediment and perform geomorphic work (Eqn. 4).

$$\Omega = \gamma\ Q\ S \quad (4)$$

where Ω is stream power (lb/s), γ is the specific weight of water (62.4 lb/ft^3), Q is flow discharge (cfs), and S is the river gradient (ft/ft). For the same given slope, an increase in discharge provides more energy to transport sediment and debris. Discharge generally increases in the downstream direction in river basins as the contributing drainage area increases.

Stream power is often used to indicate and compare the relative magnitude of sediment transport ability between reaches. It does not provide quantitative information regarding quantities or size of sediment being transported. In addition to flow characteristics (e.g. depth, velocity, shear stress), sediment transport is also dependent on sediment supply and grain size, which were not included in this study. If total stream power increases, the sediment transport ability would be expected to increase as well. Relative stream power values can also indicate whether a reach is more likely to be degrading (incising) or aggrading (depositional).

Stream power calculations were performed for the 1.25-, 2-, 10-, and 100-year flow events. The headwaters (geomorphic reaches 1 and 2) were excluded from this analysis. Flow discharge was estimated using the methods described in Section 3.1 (Hydrologic Assessment); discharge estimates are for the midpoint of each geomorphic reach. Reach/segment slope was estimated using 10-m (1/3 arc second) digital elevation model (DEM) data from the USGS National Elevation Data (NED) Set. Elevation values were extracted along the channel centerline at 0.1 mi increments and a 1st order polynomial was fit to the data (see **Error! Reference source not found.**).

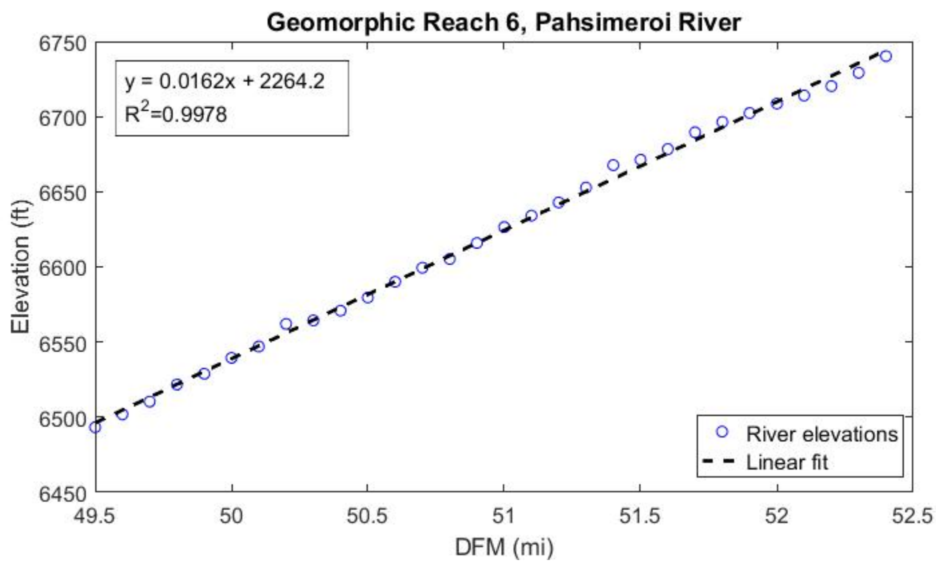

Figure 10. Example of first-order polynomial fit for river elevations along a geomorphic reach. Distance from the river mouth (DFM) is shown in river miles, but the linear-fit equation is shown in units of ft (y=mx+b, where x [=] ft, y [=] ft, m [=] 0.0162 ft/ft).

3.3 Field Data Collection

3.3.1 Data Collection Methodology

Cross section surveys and pebble counts were conducted by Trout Unlimited on November 22, 2016. Three cross sections were surveyed and a pebble count was performed at each site (see locations in Figure 12).

Cross Section and Profile Survey

At the surveyed cross sections, Trout Unlimited measured relative elevations using a LASERMARK LM800 Series electronic self-leveling rotary laser; from these data they report water surface elevations and channel slopes. Stations were measured using an engineer's tape. Station and elevation were recorded at slope breaks with each transect. Water's edge and water surface elevation were also noted. Transects extended across the valley on both sides of the river to the low terrace, where possible. Transects did not extend to the low terrace when vegetation hindered the use of the laser or when the valley was wide. When the valley was wide, the distance to low terrace was estimated. The channel slope was estimated at each site by measuring the channel bottom elevation 150 ft upstream and 150 ft downstream of the site. The slope was then calculated based on the difference in elevation upstream and downstream of the site over the 300 ft segment. It is unknown whether the water surface or channel bottom slope was measured.

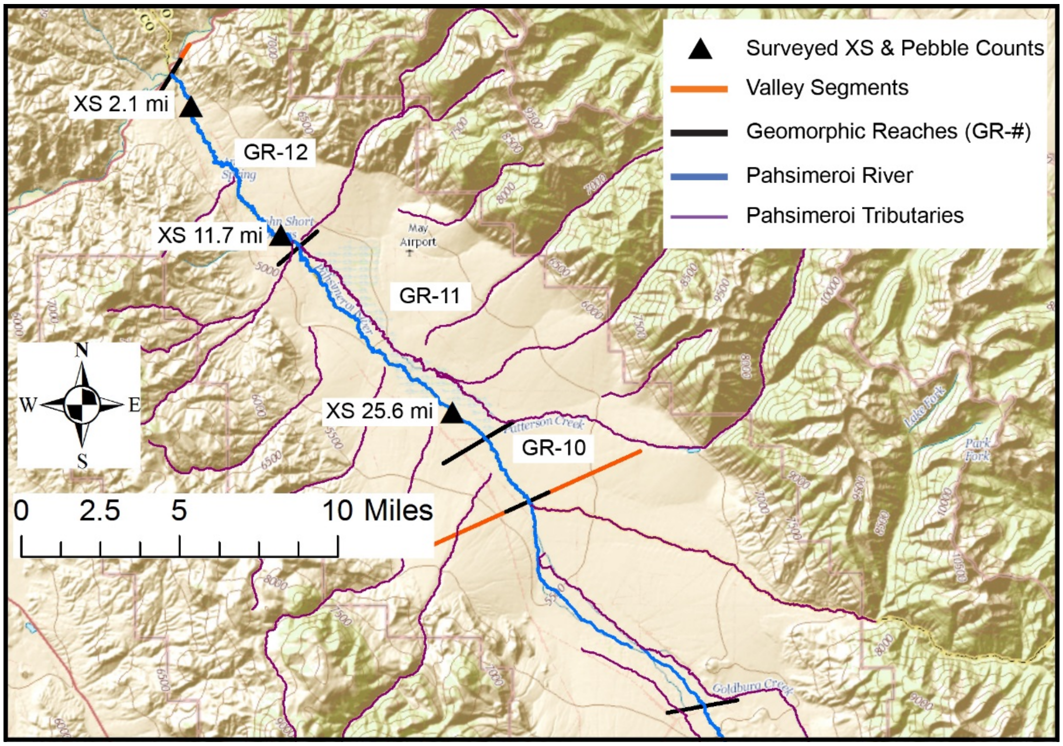

Figure 12. Locations of cross section surveys and pebble counts performed by Trout Unlimited.

Pebble Count Collection Methods
Pebble counts were performed to characterize the bed material. Three pebble counts were completed according to the Wolman Pebble Count Procedure (Wolman, 1954). The technique requires the user to measure the b-axis axis (Figure 11) of 100 random sediment particles within a geomorphic feature of interest (e.g. riffle, bar, etc.).

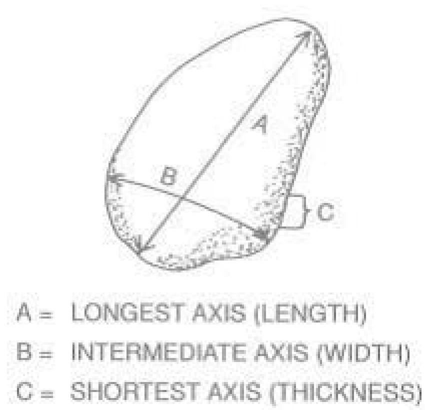

Figure 11. Pebble axis measurement (from Harrelson et al., 1994, their Figure 60).

3.4 At-a-Station Hydraulic Calculations

3.4.1 At-a-Station Hydraulic Calculation Methods

At-a-station hydraulics were calculated at three cross sections mapped in Figure 12 in the Pahsimeroi River Basin. Calculations were made for two flow conditions: 1.25-yr and 100-yr events. Many assumptions are made when performing at-a-station hydraulic calculations which are identified in the following section.

Hydraulic properties were calculated utilizing Manning's equation Eq. (5) and the field data.

$$Q = \frac{1.49}{n} A R^{2/3} \sqrt{S} \quad (5)$$

Where:

- Q is the known discharge (cfs) for a specific flow event,
- n is the assumed Manning's roughness based on aerial imagery (Chow, 1959),
- A is the calculated cross sectional area (sq. ft),
- R is the calculated normal hydraulic radius (ft), and
- S is the channel slope (ft/ft) measured in the field.

Manning's roughness values (*n*) for the main channel and floodplains were estimated separately based on aerial imagery mapping and published values for similar site conditions (i.e., floodplain vegetation or channel features). A sensitivity analysis was performed by utilizing a minimum, normal, and maximum Manning's roughness for the main channel. The roughness values and theoretical channel descriptions are presented in

Table 4. Manning's roughness (*n*) values

River Mile	Description	Minimum *n*	Normal *n*	Maximum *n*
2.1, 11.7, 25.6	Main channel – clean, winding, some pools and shoals	0.033	0.040	0.045
2.1, 11.7 (LB only), 26.5 (LB only)	Floodplain- light brush and trees in summer		0.05	
11.7 (RB only), 26.5 (RB only)	Floodplain- high grass		0.06	
* Only the normal *n*-values were used for the floodplains.				

Table 4. Manning's roughness (*n*) values

River Mile	Description	Minimum *n*	Normal *n*	Maximum *n*
2.1, 11.7, 25.6	Main channel – clean, winding, some pools and shoals	0.033	0.040	0.045
2.1, 11.7 (LB only), 26.5 (LB only)	Floodplain- light brush and trees in summer		0.05	
11.7 (RB only), 26.5 (RB only)	Floodplain- high grass		0.06	
* Only the normal *n*-values were used for the floodplains.				

Based on the hydraulic properties, critical grain size Eq. (6) can be calculated to estimate and compare with the measured median grain size to predict what flow magnitude is capable of mobilizing the bed-material at the cross section locations.

All particles smaller than the estimated critical grain size, D_c, were predicted to be mobile at that flow rate.

$$D_c = \frac{\gamma\ R\ S}{\gamma\ (s-1)\tau_c^*} \quad (6)$$

where γ = specific weight of water; s = relative specific density of sediment (2.65), τ_c^* = critical dimensionless Shield's number, assumed to be 0.05 and D_c = critical sediment size.

3.4.2 Uncertainty associated with at-a-station hydraulics

At-a-station hydraulic calculations are a useful tool to calculate hydraulic properties at a single cross section for a given range of discharge values. However, it is not appropriate to spatially interpolate or extrapolate calculated values. Therefore, these cross sections do not represent the various reaches, they only represent three unique locations in the basin. Discharge values at the cross sections were not measured; therefore, the analysis could not be calibrated. The lack of calibration data increases the uncertainty of the analysis. The calculated water stage may be higher or lower than the stage that would occur at the cross section for a given flow event.

Three key assumptions are made when calculating at-a-station hydraulics. First, the Manning's equation assumes uniform flow. Uniform flow is defined as flow velocity at a given instant of time that does not vary within a given length of channel (Chaudhry, 2008). This means that flow velocity does not change in space or in time. Furthermore, Manning's equation assumes normal depth conditions. Normal depth is a hydraulic term that assumes the slope of the water surface elevation is equal to the slope of the channel bottom. A water surface profile was not measured in the field; therefore, it is not known if this assumption is valid. The methodology is valid, but the lack of calibration data increases the uncertainty of the analysis. Normal depth and uniform flow are assumed hydraulic conditions that do not occur in natural systems, but these assumptions are often made for the purpose of calculations.

Second, Manning's equation is contingent on an assumed Manning's roughness value. The roughness value is typically calibrated so that the model or calculations best reflect existing conditions. However, no calibration data were available for this study. A roughness value was assumed based on literature (Chow, 1959), aerial imagery, and sediment gradation information. To provide a sensitivity analysis, calculations were made utilizing a minimum, normal, and maximum Manning's roughness based on literature values for similar site conditions.

Lastly, grain size mobility is only based on the calculated critical grain size compared against the measured grain size (D_{50} and D_{84}). Often, there is a specific value of the dimensionless shear stress above which initiation of bed motion is assumed to begin. However, sediment motion is better thought of as a probabilistic process with the probability of motion increasing directly with shear stress (or dimensionless shear stress). These criteria are used as opposed to one reference dimensionless shear stress value, which can vary by grain size, shape, sorting, packing (Buffington and Montgomery, 1997), channel slope (Lamb et al., 2008; Mueller et al., 2005), and sand fraction (Curran & Wilcock, 2005). For the critical grain size at incipient motion analysis, a critical dimensionless shear stress (Shield's number) of 0.05 was selected, which corresponds to a coarse to very coarse gravel (see Pebble Count Results, section 4.3).

4. Results

4.1 Hydrologic Assessment Results

4.1.1 Peak Flow Calculations at Gaged Locations

The computer program PeakFQ was used to compute flow frequency estimates at two gaged locations within the Pahsimeroi basin that were deemed as having adequate periods (years) of record. The first location was near the confluence of the Salmon River with a drainage area of 830 square miles. This location has two gage numbers corresponding to two separate time periods: 13302000 for 1929 through 1972 and 13302005 for 1985 through 2015. A combined total of 61 annual peak observations from these two periods were used for the frequency analysis. All peak flows at this location are impacted to an unknown degree by regulation or diversion, many peaks are a maximum daily average. The second gaged location used for analysis was a USGS gage on Morse Creek (13301700) above diversions. This location has a drainage area of 18 square miles with 17 annual peak observations. Results for the two locations including confidence limits are shown in Figure 13 and Figure 14. A summary of the two is provided in Table 5 and Figure 15. Flow frequency estimates are reported in both return period (in years) and annual exceedance probability (AEP) (where the 100 year event corresponds to the 1% AEP).

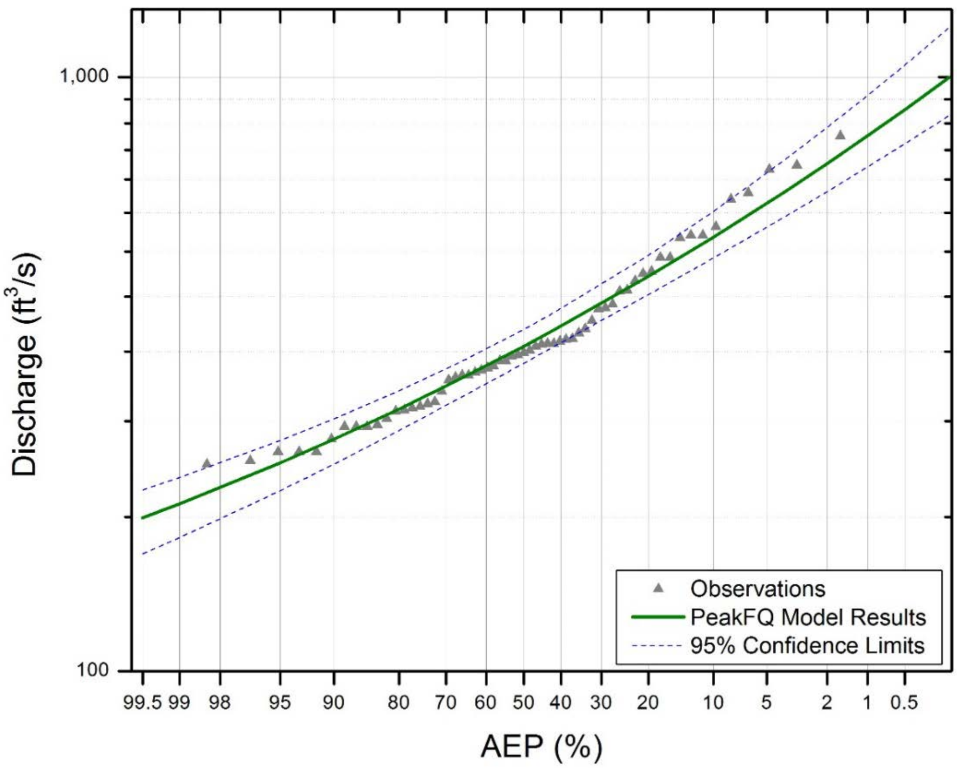

Figure 13. PeakFQ results for Pahsimeroi River gage near confluence (USGS 13302000 and 13302005)

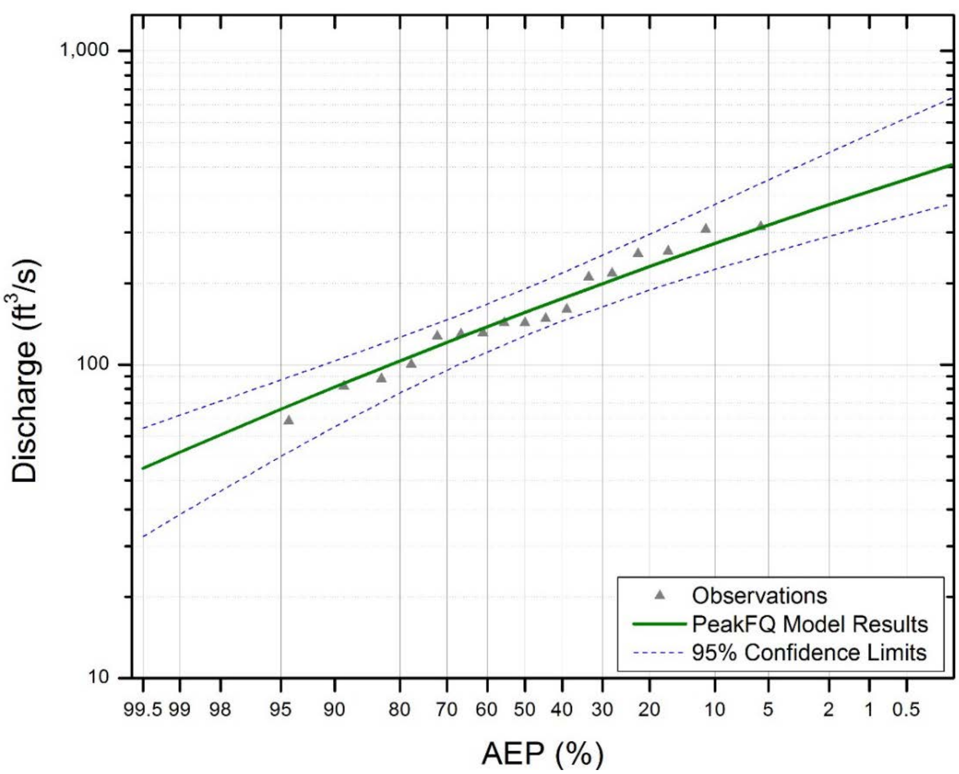

Figure 14. PeakFQ results for Morse Creek gage (USGS 13301700).

Table 5. Summary of PeakFQ model results.

Gage Number		Pahsimeroi River (13302000/13302005)	Morse Creek above diversion near May, ID (13301700)
Recurrence Interval (years)	**AEP (%)**	**PeakFQ Flow Frequency Results (cfs)**	
1.25	**80**	276	103
1.5	**66.7**	310	133
2	**50**	353	147
2.33	**42.9**	372	158
5	**20**	462	205
10	**10**	538	243
25	**4**	638	290
50	**2**	716	324
100	**1**	797	357

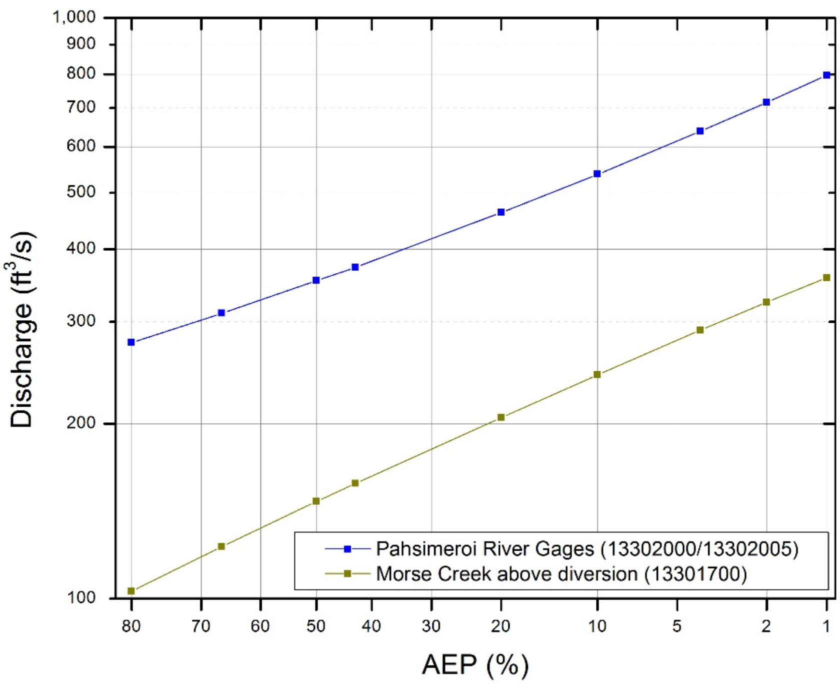

Figure 15. Peak discharge values summarized for both gaged locations

4.1.2 Peak Flow Calculations at Ungaged Locations

Flow frequency estimates were completed using the methods described in Section 0 for 16 ungaged locations along the main stem of the Pahsimeroi River (Figure 9). These 16 sites represent different geomorphic reaches for the study as well as additional points of interest. Drainage areas were estimated at each site using StreamStats (Section 0). Table 6 summarizes the results of this analysis. For the sites from the confluence of the Salmon to GR 9, flow frequency estimates were scaled from the Pahsimeroi gage PeakFQ analysis (13302000 and 13302005). Locations on the upstream end (GR 5 to GR 2) were scaled from the PeakFQ analysis on Morse Creek (13301700). The Morse Creek gage was used because while it is not on the main stem of the Pahsimeroi River, it is still within the basin and assumed to be driven by similar hydrologic characteristics. While some sites fell slightly outside of the valid range for this assessment (DA_u/DA_g = 0.5-1.5), those applied were considered close enough to be utilized for this analysis (see Appendix C for DA_u/DA_g values). Several reaches yielded drainage area ratios just outside of the acceptable range (GR 1; GR 3-5; GR9; see Appendix B); however, these but were included in the analysis because there is no better data source available. Three sites, GR 6 through GR 8, clearly fall far outside of the applicable range for the drainage area ratio method. The drainage area for GR 6-8 fall between the drainage areas of the Morse Creek and Pahsimeroi gages; therefore, both values were reported. The values presented in Table 6 for these three sites represent estimates scaled from both USGS gage sites, yielding an estimate range.

The results in Table 6 show a shift from higher peak flows relative to drainage area in the steeper regions of the basin to lower values at the locations within the valley floor. This pattern is a reflection of some key basin properties to note when reviewing results of the frequency analysis, shown in Figure 16. First is that the USGS gage on Morse Creek (13301700) is representative of the steep, mountainous portions of the basin and is not known to be impacted by diversions or irrigation. Scaling these results is appropriate for similar physiography portions of the basin. Flows in these areas are likely to be flashier due to the steep slopes and thinner soils in the mountains. They may also reflect more of a typical snowmelt driven as all observed peaks at the Morse Creek gage occurred in May or June. Second is that the USGS gage on the main branch of the Pahsimeroi (13302000 and 13302005) will have peak flow attenuation both due to both stream geomorphology and groundwater interactions as well as irrigation practices. Finally, the portion of the main reach that spans from GR 8 to GR 5 is still within the alluvium of the valley but with less irrigation than the downstream reaches. The highly variable physiographic characteristics of the basin mean it is not unreasonable to observe smaller peaks relative to drainage area in the valley floor.

Table 6. Summary of flow frequency assessment at select locations on the Pahsimeroi River

Location	RM	DA (mi^2)	Scaling Location	Flow Frequency Values								
				1.25	1.5	2	2.33	5	10	25	50	100
PC Lower	2.1	824	Pahsimeroi	275	308	350	370	459	535	634	712	792
GR 12	6.6	816	Pahsimeroi	273	306	348	367	456	531	629	706	786
PC Middle	11.8	748	Pahsimeroi	254	285	324	343	425	495	587	659	733
IDWR Gage P-9	15.4	561	Pahsimeroi	202	227	258	272	338	393	467	524	583
GR 11	19.4	559	Pahsimeroi	202	226	257	272	337	392	465	522	581
PC Upper	25.6	499	Pahsimeroi	184	206	234	248	307	358	424	476	530
IDWR Gage Furey	27.2	470	Pahsimeroi	175	197	224	236	293	341	405	454	505
GR 10	28.8	470	Pahsimeroi	175	197	223	236	293	341	404	454	505
GR 9	35.7	331	*Pahsimeroi	132	149	169	178	221	258	306	343	382
GR 8	43.6	134	**	(512, 64)	(610, 72)	(730, 82)	(785, 87)	(1023, 107)	(1212, 125)	(1444, 148)	(1612, 166)	(1778, 185)
GR 7	47.8	128	**	(494, 62)	(589, 70)	(705, 79)	(758, 84)	(987, 104)	(1169, 121)	(1394, 143)	(1556, 161)	(1716, 179)
GR 6	50.7	124	**	(480, 60)	(572, 68)	(685, 77)	(737, 81)	(960, 101)	(1137, 117)	(1355, 139)	(1513, 156)	(1668, 174)
GR 5	55.9	56	*Morse Cr.	253	302	361	389	506	600	715	798	880
GR 4	61.4	40	Morse Cr.	195	233	278	299	390	462	551	615	678
GR 3	63.5	32	*Morse Cr.	162	193	231	248	323	383	456	509	562
GR 2		12	Morse Cr.	75	89	106	115	149	177	211	235	259
GR 1		3	*Morse Cr.	25	29	35	38	49	58	69	77	85

*Sites fall outside of the drainage area ratio that is valid for the method (valid ratios of DA_u/DA_g are between 0.5 and 1.5).GR 6- 8 fall well outside of the valid ratio; results at these sites represent high (Morse Creek gage) and low (Pahsimeroi gage) estimates. See Appendix C for DA_u/DA_g values.

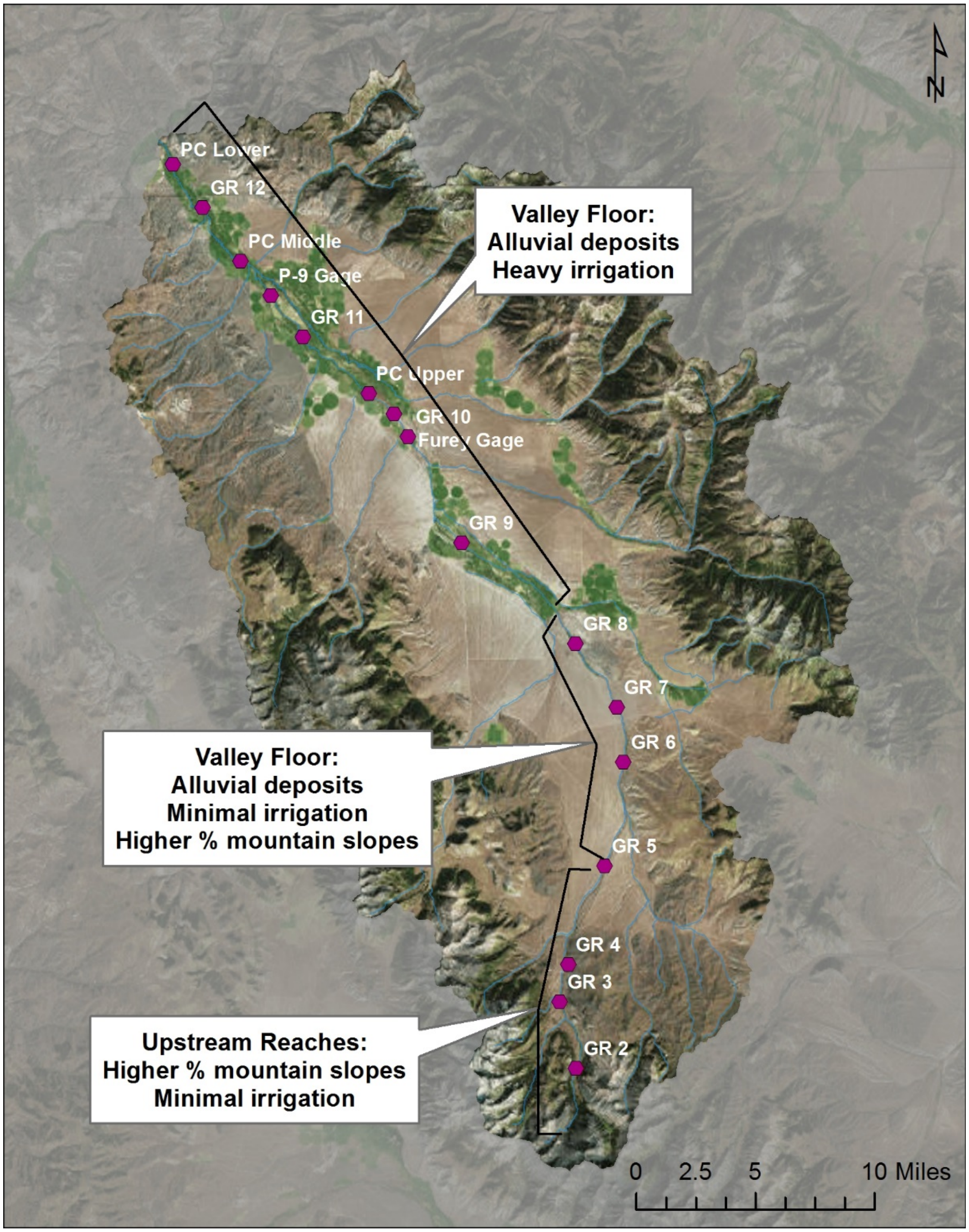

Figure 16. Illustration of different hydrologic reaches of the Pahsimeroi River

4.2 Stream Power Analysis Results

Stream power is a function of discharge and river gradient (slope). Discharge in the Pahsimeroi does not always increase with distance downstream (Figure 17). GR 6-8 fall outside of the applicable range for the drainage area ratio method; estimates from both the upstream and downstream gage for these reaches are shown (Figure 17). As portion of GR-9 flows subsurface, it is likely that the lower discharge estimates for GR 6-8 are more representative of field conditions. Decreasing discharge is likely the result of flow infiltrating into the alluvium-filled valley, as well as withdrawals for irrigation. The impact of water diversions and irrigations has not been quantified for the basin.

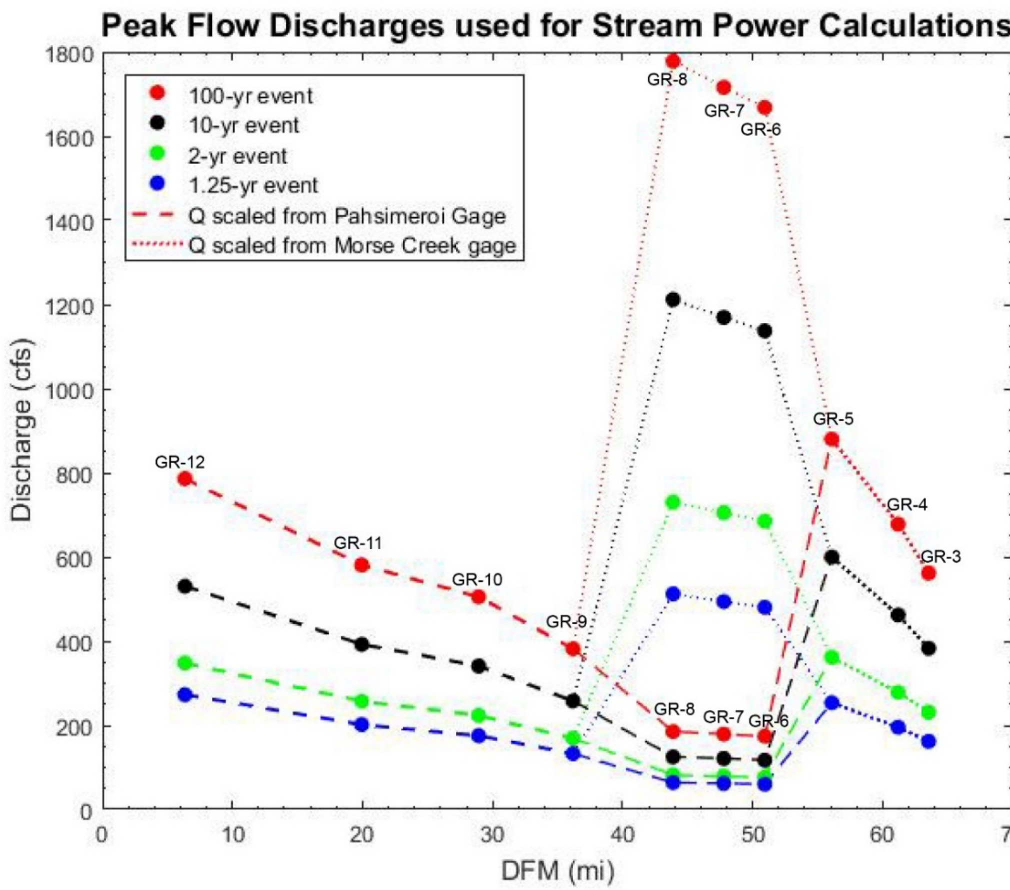

Figure 17. Estimated discharge values along the main Pahsimeroi River. Both high and low discharge estimates are shown for GR 6-8 (see Table 6 and section 4.1).

The stream gradients for geomorphic reaches along the Pahsimeroi (excluding headwaters) are between 0.003 and 0.017 (Figure 18). River gradients typically decrease with distance downstream, particularly below GR-8. The highest gradient is found at GR-4 (near the headwaters) and the lowest gradient is found at GR-12 (near the mouth).

Using these discharges and river gradients, stream power was calculated for four flow events (1.25-, 2-, 10-, and 100-year recurrence intervals) for ten reaches along the Pahsimeroi River. Total stream power increases and then decreases along the

Pahsimeroi River (**Error! Reference source not found.**; Table 7). In the upper reaches, the higher slopes and moderate discharges yield higher stream power values, which may indicate zones of sediment transport. In geomorphic reaches 6-8, the effect of discharge is readily apparent; the high and low discharge estimates control the stream power values. In the lowest reaches, the stream power values remain low, even though discharge again increases (Figure 17 and 19). Here, the low slopes are the dominate variable, resulting in low stream power (**Error! Reference source not found.** and 19). These low values may indicate zones of deposition. However, there are not enough data to definitively identify zones of deposition or transport.

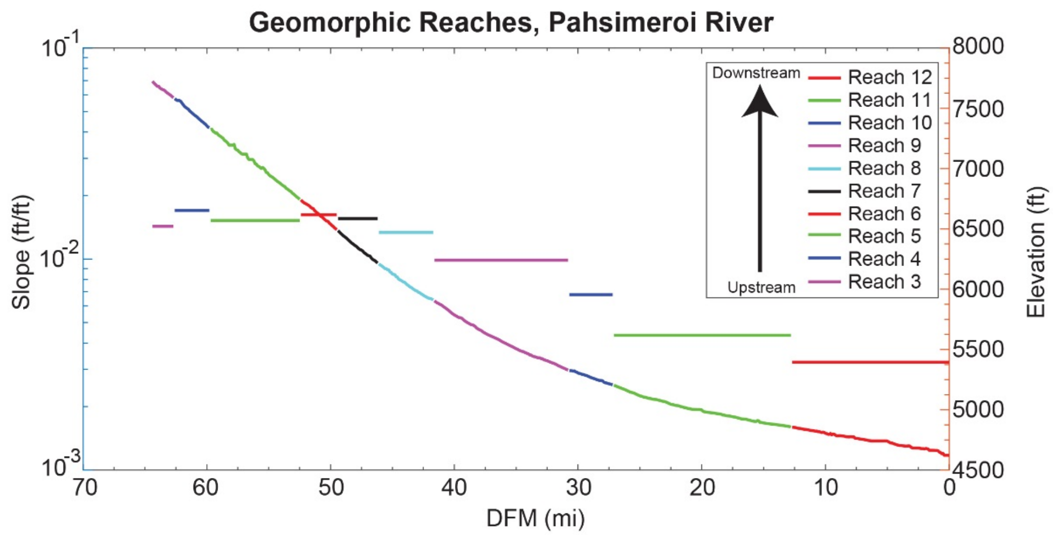

Figure 18. Pahsimeroi River longitudinal profile and slope, delineated by geomorphic reaches. Note that the slope is plotted on a logarithmic scale.

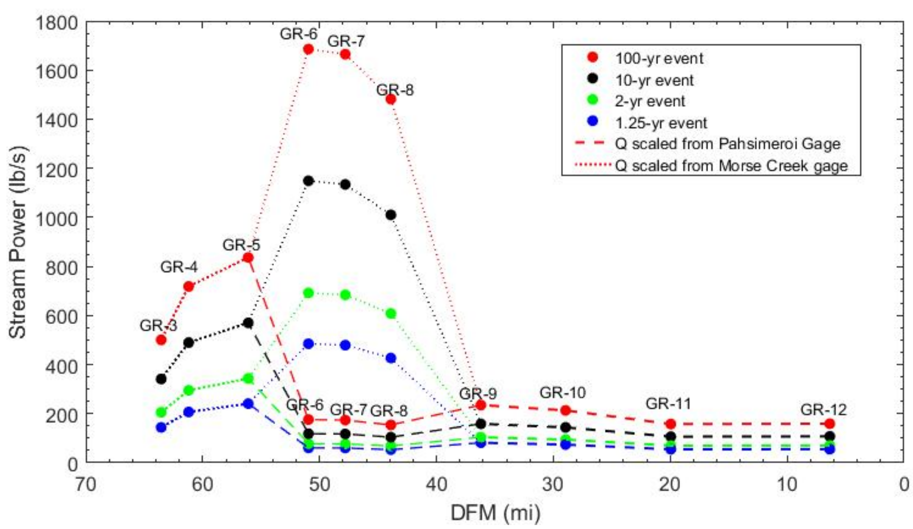

Figure 19. Stream power results; both high and low estimates are shown for GR 6-8.

Table 7. Stream Power Analysis Results

GR	Approx. mid-point (mi)	Slope	1.25-yr Event Q (cfs)	1.25-yr Event Ω (lb/s)	2-yr Event Q (cfs)	2-yr Event Ω (lb/s)	10-yr Event Q (cfs)	10-yr Event Ω (lb/s)	100-yr Event Q (cfs)	100-yr Event Ω (lb/s)
3	63.55	0.0143	162	144	231	206	383	341	562	501
4	61.20	0.0170	195	207	278	295	462	490	678	718
5	56.10	0.0152	253	241	361	344	600	570	880	837
6	50.95	0.0162	480	485	685	692	1137	1149	1668	1685
			60	61	77	78	117	118	174	176
7	47.80	0.0155	494	479	705	684	1169	1134	1716	1665
			62	60	79	77	121	117	179	174
8	43.90	0.0134	512	427	730	608	1212	1010	1778	1482
			64	53	82	68	125	104	185	154
9	36.20	0.0099	132	82	169	104	258	159	382	235
10	28.95	0.0068	175	74	132	94	169	144	258	213
11	19.95	0.0043	202	55	257	70	392	106	581	158
12	6.35	0.0032	273	55	348	70	531	107	786	159

4.3 Pebble Count Results

The D_{84}, D_{50}, and D_{16} were calculated at three cross sections in order to characterize the bed material (Table 8). The D_{50} is the median grain size; D_{84} and D_{16} are the 84th and 16th percentile, which represent the coarse and fine sediment fraction, respectively. The majority of the sediment could be classified as gravel (2 – 64 mm). Particles ranging from silt (< 1 mm) to cobbles (109 mm max) in diameter were observed.

The cross section at RM 25.6 was the coarsest, located within geomorphic reach 11 and fairly low in the basin (Table 8; see Figure 12 for location). The pebble count at the most downstream reach (RM 2.1) yielded the finest sediment.

Table 8. Pebble Count Results

Location	D_{84} (mm)	D_{50} (mm)	D_{16} (mm)
RM 2.1	32.0	18.2	2
RM 11.7	55.7	29.0	14
RM 25.6	65.9	34.6	15

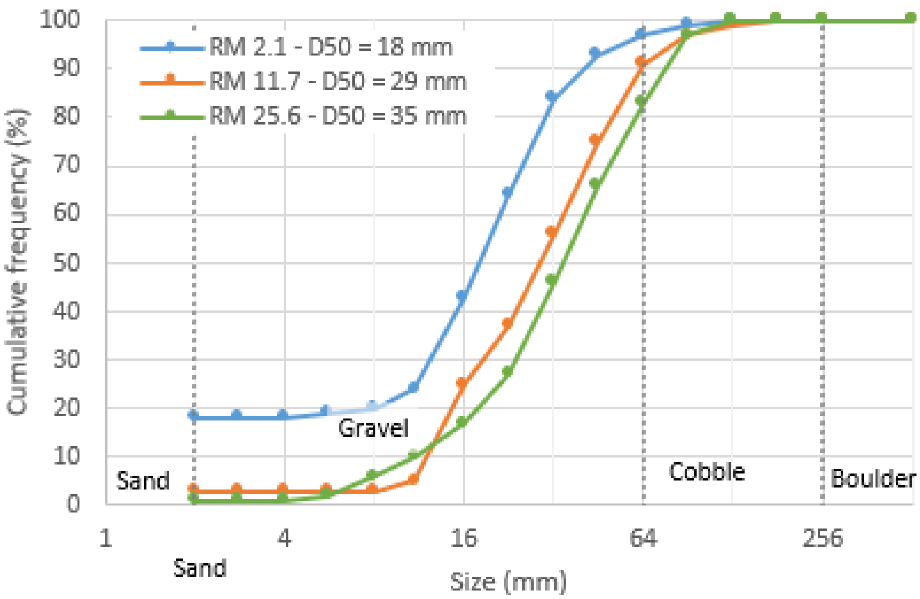

Figure 20. Pebble count cumulative frequency results for the three cross sections along the Pahsimeroi River. Particles smaller than 2 mm are not plotted.

4.4 At-a-Station Hydraulic Results

At-a-station hydraulic computations were completed at three cross sections for the 1.25- and 100-yr recurrence events to estimate what magnitude discharge is needed to mobilize bed-material and overtop into the floodplain. This includes a hydraulic analysis (Table 9) and bed mobility calculations (Table 10).

The lower cross section shows that the channel is confined and the 100-yr event does not inundate the floodplain (Figure 21). At RM 11.7 and 25.6, flood inundation occurs at the 1.25-yr event (Figure 22 and Figure 23). In the cross section at RM 11.7, there are several low points in the topography that may represent smaller channels within the floodplain. These channels are inundated at the 100-yr flow. However, if these channels are hydrologically connected to the main channel farther upstream, smaller flows may also inundate this area (Figure 22).

The analysis did not show sediment mobility for the D_{50} or D_{84} grain sizes at any of the cross-sections (Table 10). The grain sizes are identified as mobile if they are smaller than the critical grain size for a given discharge. Results indicate that the median grain size is stable for the remaining analyzed flow events and locations.

Table 9. At-a-station hydraulic calculation results

	Input Data			Calculated Hydraulic Parameters									
River Mile	*n*	Channel Slope (ft/ft)	Discharge (ft^3/s)	Flow Area (ft^2)	Wetted Perimeter (ft)	Hydraulic Radius (ft)	Top Width (ft)	Normal Depth (ft)	Critical Depth (ft)	Critical Slope (ft/ft)	Velocity (ft/s)	Froude Number	Flow Type
RM 2.1	0.033	0.0020	270	119	90	1.3	89	2.0	1.2	0.020	2.3	0.34	Subcritical
RM 2.1	0.040	0.0020	270	134	94	1.4	93	2.2	1.2	0.028	2.0	0.30	Subcritical
RM 2.1	0.045	0.0020	270	144	97	1.5	96	2.3	1.2	0.034	1.9	0.27	Subcritical
RM 2.1	0.033	0.0020	790	285	130	2.2	128	3.5	2.0	0.022	2.8	0.33	Subcritical
RM 2.1	0.040	0.0020	790	305	134	2.3	132	3.7	2.0	0.026	2.6	0.30	Subcritical
RM 2.1	0.045	0.0020	790	319	137	2.3	134	3.8	2.0	0.030	2.5	0.28	Subcritical
RM 11.7	0.033	0.0027	250	185	206	0.9	202	2.4	1.4	0.049	1.4	0.25	Subcritical
RM 11.7	0.040	0.0027	250	187	208	0.9	204	2.4	1.4	0.051	1.3	0.25	Subcritical
RM 11.7	0.045	0.0027	250	189	209	0.9	206	2.4	1.4	0.053	1.3	0.24	Subcritical
RM 11.7	0.033	0.0027	730	446	347	1.3	343	3.3	2.1	0.050	1.6	0.25	Subcritical
RM 11.7	0.040	0.0027	730	448	347	1.3	343	3.3	2.1	0.050	1.6	0.25	Subcritical
RM 11.7	0.045	0.0027	730	450	347	1.3	343	3.3	2.1	0.051	1.6	0.25	Subcritical
RM 25.6	0.033	0.0062	180	75	85	0.9	83	3.0	1.9	0.028	2.4	0.45	Subcritical
RM 25.6	0.040	0.0062	180	106	158	0.7	157	3.2	1.9	0.038	1.7	0.37	Subcritical
RM 25.6	0.045	0.0062	180	107	158	0.7	157	3.2	1.9	0.040	1.7	0.36	Subcritical
RM 25.6	0.033	0.0062	530	217	187	1.2	185	3.8	3.2	0.046	2.5	0.40	Subcritical
RM 25.6	0.040	0.0062	530	219	188	1.2	186	3.9	3.2	0.048	2.4	0.39	Subcritical
RM 25.6	0.045	0.0062	530	221	189	1.2	187	3.9	3.2	0.049	2.4	0.39	Subcritical

Table 10. At-a-station bed mobility calculation results

	Input Data						Bed Mobility Calculations			
River Mile	*n*	Channel Slope (ft/ft)	Flow Event	Discharge (ft^3/s)	D_{50} (mm)	D_{84} (mm)	Shear Stress (lb/ft^2)	Critical Diameter (mm)	Is D_{50} mobile?	Is D_{84} mobile?
RM 2.1	0.033	0.0020	1.25 - yr	270	18.2	32.0	0.17	10	no	no
RM 2.1	0.04	0.0020	1.25 – yr	270	18.2	32.0	0.18	10	no	no
RM 2.1	0.045	0.0020	1.25 – yr	270	18.2	32.0	0.18	11	no	no
RM 2.1	0.033	0.0020	100 - yr	790	18.2	32.0	0.27	16	no	no
RM 2.1	0.04	0.0020	100 - yr	790	18.2	32.0	0.28	17	no	no
RM 2.1	0.045	0.0020	100 - yr	790	18.2	32.0	0.29	17	no	no
RM 11.7	0.033	0.0027	1.25 - yr	250	29.0	55.7	0.15	9	no	no
RM 11.7	0.04	0.0027	1.25 – yr	250	29.0	55.7	0.15	9	no	no
RM 11.7	0.045	0.0027	1.25 – yr	250	29.0	55.7	0.15	9	no	no
RM 11.7	0.033	0.0027	100 - yr	730	29.0	55.7	0.22	13	no	no
RM 11.7	0.04	0.0027	100 - yr	730	29.0	55.7	0.22	13	no	no
RM 11.7	0.045	0.0027	100 - yr	730	29.0	55.7	0.22	13	no	no
RM 25.6	0.033	0.0062	1.25 - yr	180	34.6	65.9	0.34	20	no	no
RM 25.6	0.04	0.0062	1.25 – yr	180	34.6	65.9	0.26	15	no	no
RM 25.6	0.045	0.0062	1.25 – yr	180	34.6	65.9	0.26	15	no	no
RM 25.6	0.033	0.0062	100 - yr	530	34.6	65.9	0.45	27	no	no
RM 25.6	0.04	0.0062	100 - yr	530	34.6	65.9	0.45	27	no	no
RM 25.6	0.045	0.0062	100 - yr	530	34.6	65.9	0.45	27	no	no

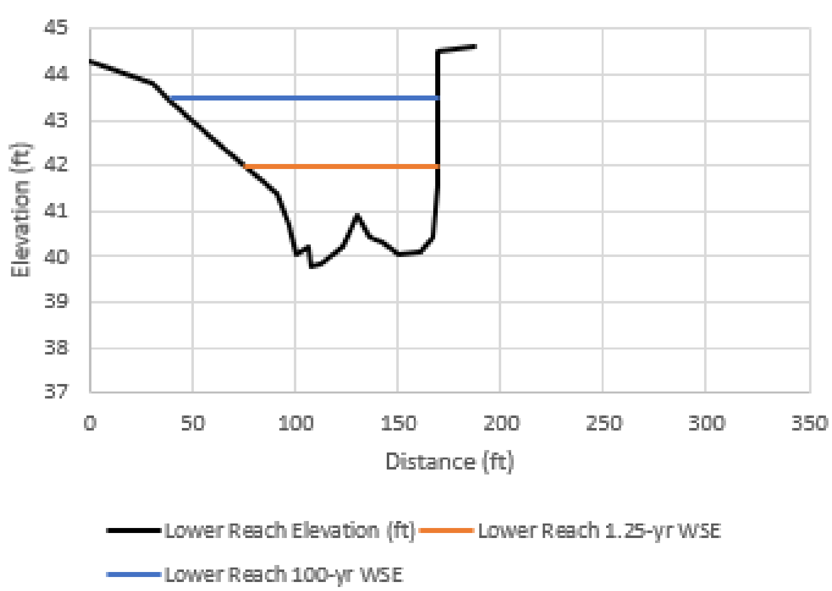

Figure 21. Water surface elevation for 1.25- and 100-yr events, assuming normal (Table 4) Manning's n value, at RM 2.1. Cross-section elevations and water-surface elevations are arbitrary. Note that the y and x-axes are consistent on Figures 21, 22, and 23.

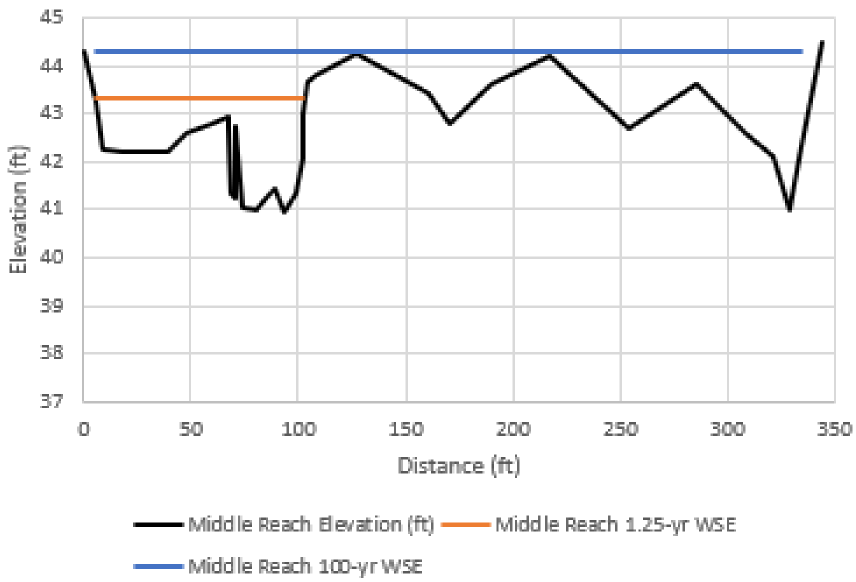

Figure 22. Water surface elevation for 1.25- and 100-yr events, assuming normal (Table 4) Manning's n value, at RM 11.7.

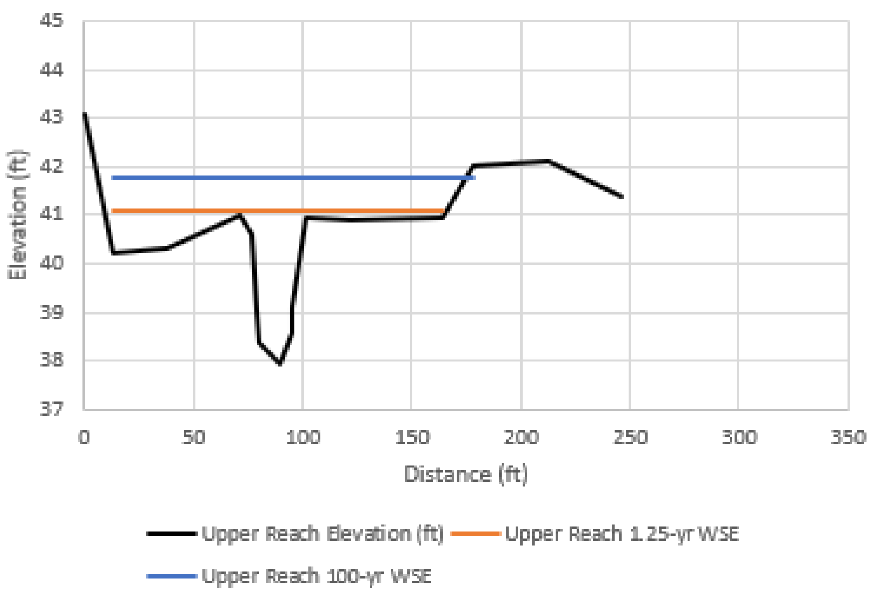

Figure 23. Water surface elevation for 1.25- and 100-yr events, assuming normal (Table 4) Manning's n value, at RM 25.6.

5. Data Gaps and Recommendations

This study utilized a combination of measurement data, field observations, and surrogate parameters to inform an Integrated Rehabilitation Assessment. The assessment is intended to identify watershed-scale characteristics and identify data gaps in order to select optimal project locations for further study and rehabilitation. The recommendations provided in this section are geared towards future hydraulic modeling at the reach and project scales.

Hydraulic models help constrain flow depth and velocity, which are often key parameters used to analyze the quality of fish habitat in a river reach. Hydraulic modeling informs potential habitat improvement projects and provides important tools for project planning. Hydraulic model results can provide an understanding of the existing conditions in regard to Endangered Species Act (ESA) listed salmonid physical habitat conditions. The hydraulic model results for depth, velocity, and shear stress can provide input data for Habitat Suitability Index (HSI) modeling.

The selection of a hydraulic model is dependent on the data available, the complexity of the channel and floodplain terrain, and the study questions that need to be addressed. For the Pahsimeroi River Basin Integrated Rehabilitation Assessment, a steady two-dimensional (2D) hydraulic model is recommended. A 2D model (as compared to a one-dimensional (1D) model) better informs parameters necessary for habitat improvement such as: lateral differences in velocity, depth, and floodplain connectivity. A 1D is limited when calculating the above parameters. 1D calculations can be sufficient in uniform, single-threaded channels. It is also advantageous to apply a 1D model to evaluate the hydraulics of large flood events, where the influence of geomorphic features and channel complexity is not of interest. A 2D model better captures floodplain connectivity and provides data with much higher longitudinal and lateral resolution. This is important to habitat rehabilitation within the project basin as the Pahsimeroi River is often multi-threaded. Furthermore, side channels, large wood, and pools are often incorporated into rehabilitation efforts, and these features would be poorly represented in 1D model. Therefore, a 2D model is recommended for future analysis of the habitat rehabilitation effort. Furthermore, the data collection effort necessary to inform both a 1D and 2D model are very similar. Data necessary for numerical modeling include:

1. **Topographic data (LiDAR),**
2. **Bathymetric (under water) data,**
3. **Flow values of interest (typically includes low flow values, mean monthly flows, and peak flow events).** *(obtained for the lower basin)
4. **Flow change locations and quantities (changes in main channel flow, tributary inputs, diversions, returns, etc.),**
5. **Sediment data to inform channel roughness and potential mobility,**
6. **Field reconnaissance and documentation of reach site conditions**, and
7. **Measured water surface elevations for known discharge events for model calibration.**
8. **Calibrated hydrologic model with updated tributary flows.**

Bold values remain data gaps and each are discussed in more detail in the following sections.

5.1 Existing Data for the Project Area

Of the eight items listed above, this study produced one portion of a necessary data set: flow values of interest for the lower basin and very upper basin. A partial field reconnaissance was conducted, which allowed for the collection of some site photos. However, not all of the geomorphic reaches were visited. The data sets will need to be obtained during future phases of the study. Existing data sets include the 10-m (1/3 arc-second; 25 ft x 25 ft) DEM topographic data. Interferometric Synthetic Aperture Radar (IfSAR) is available for purchase for the project basin. The resolution is 16.4 ft by 16.4 ft (5 m by 5 m) cells. These data sets would provide surfaces too coarse for the 2D hydraulic modeling recommended for reach-scale habitat rehabilitation studies. Therefore, LiDAR data acquisition is recommended for topographic representation.

5.3 Topographic and Bathymetric Data Collection Options

Bathymetric LiDAR is a newer technology, which determines the water depth by measuring a time delay between a transmission pulse and return signal. Laser pulses operate at two frequencies, a lower frequency which reflects off the water surface and a higher frequency which can penetrate the water column, reflecting off the bottom. Limiting factors of airborne bathymetric LiDAR include: water clarity, water depth, water turbulence, vegetation, bottom material, weather, and background light (Muirhead & Cracknell, 1986). The Pahsimeroi River is relatively shallow with clear water, which can be measured at a vertical accuracy level of up to 15cm (Gao, 2009).

If bathymetric LiDAR data are not flown, boat or manual surveys are two alternatives for collecting bathymetric data. A boat survey involves floating the project area with a mounted Acoustic Doppler Current Profiler (ADCP). The boat would float cross sections and longitudinal profiles of the project reach collecting bathymetric data. A surface can be created from the data set by interpolating between surveyed points. A boat survey would need to occur during the high flow season, when flow depths are high enough for the instrument operation and boat access. A minimum of 1ft water depth is required for the ADCP to operate. If depths are approximately 1 ft in the entire project area, a manual survey may be more efficient. The Pahsimeroi River flows peak in October when the irrigation diversions are turned off and groundwater recharge returns to the river.

A manual survey would require a crew to survey cross sections and a longitudinal profile along the project reaches. However, this method is likely impractical for 60+ mi or river, prohibiting its practice.

With a boat survey, it is impractical to sample with as fine of a resolution as a LiDAR data set. Therefore, the measured point cloud will be coarse and the majority of the surface will be estimated via interpolation. This increases uncertainty in the results. A boat bathymetric survey could be tied into topographic LiDAR data.

5.4 Hydrologic Data Gaps and Recommendations

- The purpose of the hydrologic assessment was to identify available gage data and provide appropriate discharge values to inform existing and future assessment efforts, including hydraulic modeling. Existing data gaps and uncertainties were identified through this assessment. A notable data gap in the hydrology exists in the middle Pahsimeroi Basin. None of the existing gages in the Pahsimeroi Basin adhere to the guidelines for estimating flow frequencies in the middle basin. Future phases of work could further explore how the short gage records at IDWR gages could be utilized. This should include a thorough analysis of uncertainty and any potential statistical skew that could be introduced from utilizing short records.
- The Morse Creek gage was able to provide flow values of interest in the very upper portion of the Pahsimeroi Basin; however it would have been more ideal to have a gage in the upper basin that collected flow from both south- and north-facing tributaries.
- Adding additional river gages in the middle and upper basin would be beneficial for long-term restoration or monitoring projects within the basin. The section of the Pahsimeroi River from GR 8 to GR 6 is in the valley bottom and impacted by alluvium (i.e. groundwater infiltration) and subject to a lesser degree by irrigation than downstream reaches. Flow frequency estimates for this reach are highly uncertain; flow measurement through these reaches will aid our understanding of daily and annual peak flows.
- All annual peak flows are influenced to an unknown degree by withdrawal and diversions (Appendix A). Without a comprehensive time series of all withdrawals, the natural peak flows of the system are unknown. The flow frequency assessment presented here was completed using the regulated flow series and may not reflect the true nature of the system in its natural state.
- Many of the annual peak flow measurements from the USGS are the maximum daily average rather an instantaneous peak flow. This results in slightly lower flows used for frequency analysis and impacts the final results. For future analyses, we recommend a more detailed analysis that will relate maximum daily flows to instantaneous peak flows, similar to the methodology used in the Lemhi Basin (also see section 3.1 for background in utilizing maximum daily flows).
- Groundwater interactions play a large role in the hydrology of the Pahsimeroi basin. There are gaining and losing reaches within the study area which will impact both the timing and magnitude of peak flows spatially

within the study area. The quantitative role of groundwater interactions was not assessed for this study.

- Groundwater fluxes driven by the depth to bedrock and the permeable alluvium in the valley floor, as well as irrigation practices, influence flows throughout the year. Groundwater monitoring is recommended for future work.
- An updated and calibrated hydrologic model is recommended to constrain flows within the upper and middle basin, and to also constrain the effects for groundwater infiltration and irrigation withdrawals. The previous MIKE basin model was not calibrated and utilized tributary gage data from Big Creek, which had a short period of record.
- An integrated 2D model of surface and groundwater flows should be considered. One such model is currently under development by Reclamation at TSC, which links MODFLOW (groundwater model) to the SRH 2D (surface flow) model.
- Irrigation plays a large role in the flow patterns of the Pahsimeroi River. Quantifying withdrawal volumes as well as time and duration is key to understanding flows in the Pahsimeroi.
- Low flow discharges drive habitat suitability analyses and fish use. The only low flow discharge estimated in this study was the 7Q10. Monthly minimum flows, fish passage, and moderate flow discharge values should be estimated throughout the basin in future phases of work to better estimate habitat suitability.

5.5 Sediment Data Gaps and Discussion

The purpose of the stream power assessment and at-a-station hydraulics was to gain a general understanding of the sediment transport regime in the Pahsimeroi River Basin. Stream power calculates the capacity of each geomorphic reach based on hydrology and valley slope. The sediment transport regime is also a function of sediment supply, grain size distribution, channel geometry, and water surface slope. A better knowledge of these unknown variables is necessary to better understand the actual trends in sediment transport within the Pahsimeroi River.

To compare the stream power with the results from the pebble counts, D_{50} is plotted along with stream power (**Error! Reference source not found.**). The median grain size increases at both RM 11.7 and 25.6 without a corresponding increase in stream power. Theory states that for a given system an increase in either slope or discharge (stream power) will increase the sediment grain size (Lane, 1955). Therefore, one would expect the stream power to increase at both RM 11.7 and 25.6.

The discrepancy between the stream power and pebble count data could be a result of several factors. The most likely factor is that there are not enough data to determine if grain size and stream power are related. RM 11.7 is between two of the geomorphic reach midpoints where stream power was calculated; RM 25.6 is close to the midpoint of geomorphic reach 10. Stream power was calculated using the overall river gradient for a particular geomorphic reach; stream gradient is more variable at a finer resolution.

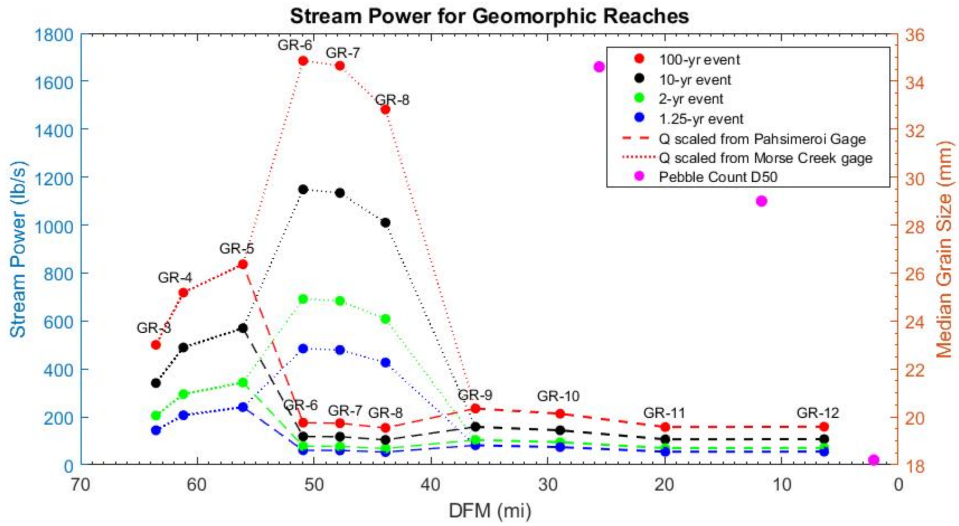

Figure 24. Stream power and pebble count results. The median grain size (D50) is plotted on the right vertical. Stream power is presented on the left vertical axis for four flood events.

Another factor is the difference between the estimated discharge values and the actual discharge values. The estimated discharge values are based on drainage area ratios between gaged and ungaged sites. The estimated values do not directly account for irrigation losses. Therefore, the stream power may not reflect existing conditions due to decreased discharge values. In addition, sediment supply greatly impacts the relationship between stream power and median grain size. High stream power can correlate to small particle sizes when the sediment supply is high (Lane, 1955).

Other factors that could explain the difference between the stream power estimation and pebble count data include increased roughness, greater floodplain connection, and/or channel geometry (i.e.: higher width-to-depth ratios). Finally, the mismatch between stream power and pebble count data could be related to changes in the flow regime due to irrigation. It is possible that sediment transport was higher during pre-irrigation discharges, and that the pebble counts are more reflective of pre-irrigation discharges.

Based on the available data, results regarding the sediment transport regime were inconclusive. More data are necessary to identify supply, transport, and depositional reaches. 1D or 2D modeling can inform sediment transport regimes. Utilizing the model results, dimensionless shear stress and critical grain diameter can assist in assessing the potential geomorphic change (erosion/deposition) and the stability of existing features in the project area.

5.6 Model Calibration Data Gaps

Field data will need to be collected from the project site to calibrate future hydraulic modeling. To calibrate a hydraulic model, discharge measurements and series of longitudinal water surface elevation measurements are required. One discharge measurement is required if there are no tributaries or diversions within the project area. If there are tributary confluences or diversions, flow measurements are required at the upstream model extent and at each confluence/diversion. In addition, Pahsimeroi River flows may go subsurface due to thick alluvial fills. In this case, discharge data should be collected above and below these reaches as well. In general, multiple measurements can inform gains/losses within the project reach. Multiple measurements are highly recommended if groundwater fluxes are high within the project area as is possible in the Pahsimeroi River Basin. Data are typically collected during two events: high flow (during spring runoff) and low flow (during peak irrigation season). These data are used to inform Manning's roughness in the channel, which is a typical model calibration parameter.

Both high and low flow calibration can be useful in better understanding the hydraulics at a site. During high flow events, form roughness dominates, resulting in a lower roughness value, on average. Particle roughness dominates at low flow events, likely resulting in a higher roughness value. If form-dominant roughness were to be applied in low flow conditions, it is likely that flow depths would be underestimated and velocities over-estimated, resulting in an underestimation of fish habitat.

A detailed photo album is also helpful to inform hydraulic modeling. Ground photos are utilized to inform roughness delineation and values, infrastructure locations and hydraulic impacts, and topographic characteristics of the floodplain and channel.

7. Conclusion

The information provided in this report is intended to advise an Integrated Rehabilitation Assessment of the Pahsimeroi River Basin, whose goal is to characterize watershed-conditions within the river basin while providing context for future analyses and potential rehabilitation projects. The objectives of this report include: peak flow estimations, stream power assessment, and at-a-station hydraulic calculations. These data were then combined to develop a list of data needs for future hydraulic modeling analyses.

The Pahsimeroi River flow regime appears to be snowmelt dominated in the upper basin, with flows that peak in May or June at the Morse Creek gage. Otherwise, the Pahsimeroi River exhibits a unique hydrograph when compared to the Salmon or Lemhi Basins. Most of the peaks occur in November. During June and July of some years, there are increases in flow, which may be related to large snowpack years.

Overall, the hydrology in the Pahsimeroi River Basin appears to be driven by groundwater influences (bedrock depth and alluvium), as well as irrigation practices. The locations and volumes of water being diverted is currently not well understood.

Flood-frequency peak flows were estimated at twelve sites within the project area utilizing a drainage area ratio method and assuming all diversions were not operational. Additional uncertainty in flood-frequency exists at geomorphic reaches 6-8, which were located too far away from the gages to adhere to the assumptions of the drainage area ratio method; this resulted in a large range of possible discharges.

The stream power assessment concluded that the upper portion of the basin is high energy and has a higher capacity to transport sediment as compared to the lower basin; the wide range of results was inconclusive for the middle basin. The slope is higher for geomorphic reaches 3-8 (upstream of RM 41.7) resulting in high stream power; this does not hold true for reaches 6-8 if the low discharge estimate is used (see Figures 17-19).

At-a-station hydraulic results were calculated at three individual cross sections. While these results can predict floodplain inundation and sediment mobility at that specific location, it is not appropriate to apply the results to the remainder of the reach. Results generally show a more confined channel in the lower part of the basin as floodplain inundation does not occur at the surveyed cross section at RM 2.1, but the floodplain is inundated at RM 11.7 and 25.6. The 100-yr flood results in a much larger area of inundation at RM 11.7; the area of inundation at RM 25.6 is similar to that of the 1.25–yr flood. Sediment mobility results show that the bed (both D_{50} and D_{84}) is stationary during the 1.25-yr and 100-yr events.

8. References

Arp, C., Gooseff, M., Baker, M., & Wurtsbaugh, W. (2006). Surface-water hydrodynamics and regimes of a small mountain stream-lake ecosystem. Journal of Hydrology, 329, 500-513. doi:10.1016/j.jhydrol.2006.03.006

Arp, C., Schmidt, J., Baker, M., & Myers, A. (2007). Stream geomorphology in a mountain lake district: hydraulic geometry, sediment sources and sinks, and downstream lake effects. Earth Surface Processes and Landforms, 32, 525-543. doi:10.1002/esp.1421

Bell, S. (1999). A Beginner's Guide to Uncertainty of Measurement. Teddington, Misslesex, United Kingdom: National Physical Laboratory.

Berenbrock, C. (2002). Estimating the magnitude of peak flows at selected recurrence intervals for streams in Idaho: US Geological Survey Water-Resources Investigation Report.

Buchanan, T., & Somers, W. (1969). Discharge Measurements at Gaging Stations. Washington D.C.: U.S. Geological Survey.

Dirszowsky, R., & Desloges, J. (2004). Evolution of the Moose Lake delta, British Columbia: implications for Holocene environment change in the Canadian Rocky Mountains. Geomorphology, 57, 75-93.

Donato, M. (1998). Surface-water/ground-water relations in the Lemhi River basin, east-central Idaho. Boise, ID: US Geological Survey Water-resources investigations.

Ellis, W., & Gray, D. (1966). Interrelationships between the peak instantaneous and average daily discharges of small prairie streams. Canadian Agricultural Engineering (2), 1-3, 18.

Fill, H., & Steiner, A. (2003). Estimating Instantaneous Peak Flow from Mean Daily Flow Data. Journal of Hydrologic Engineering, 8(6), 365-369.

Flynn, K., Kirby, W., & Hummel, P. (2006). User's Manual for Program PeakFQ, Annual Flood-Frequency Analysis Using Bulletin 17B Guidelines. U.S. Geological Survey.

Fuller, W. (1914). Flood Flows. Transactions of the American Society of Civil Engineers, 77, 564-617.

Gao, J. (2009). Bathymetric mapping by means of remote sensing: methods, accuracy and limitations. Progress in Physical Geography, 33(1), 103-116.

Goodman, K., Baker, M., & Wurtsbaugh, W. (2011). Lakes as buffers of stream dissolved organic matter (DOM) variability: Temporal patterns of DOM characteristics in mountain stream-lake systems. Journal of Geophysical Research, 116. doi:10.1029/2011JG001709.

HACH. (2012). FH950 User Manual, Edition 3.

Harrelson, C., Rawlins, C., & Potyondy, J. (1994). Stream channel reference sites: an illustrated guide to field technique. Fort Collins, CO: USDA Forest Service, Rocky Mountain Forest and Range Experiment Station

Hortness, J. (2006). Estimating Low-Flow Frequency Statistics for Unregulated Streams in Idaho. Reston, VA: U.S. Department of the Interior, U.S. Geological Survey.

Idaho Department of Environmental Quality. (2012). Lemhi River Subbasin Total Maximum Daily Loads and Five-Year Review. Boise, ID.

Idaho Department of Water Resources. (2006). Points of diversion inventoried in existing water districts in the Lemhi basin. Shapefile 2001 - 2002. Boise, ID: IDWR.

Idaho Department of Water Resources. (2008). Upper Lemhi River see page study. Boise, ID.

Interagency Advisory Committee on Water Data. (1981). Guidelines for Determining Flood Flow Frequency, Bulletin #17B of the Hydrology Committee. US Department of Interior.

Kiefer, R., & Lockhard, J. (1994). Intensive evaluation and monitoring of Chinook salmon and steelhead trout production, crooked river and upper Salmon River sites. Portland, OR: U.S. Department of Energy - Bonneville Power Administration.

Lai, Y. (2000). Unstructured grid arbitrarily shaped element method for fluid flow simulation. AIAA Journal, 38(12), 2246-2252.

Liberty, L.M., Hess, S., Beukelmann, G. (2006). Stratigraphic and structural controls of ground water flow in the Pahsimeroi Basin, Idaho: Insights from geophysical data. Technical Report BSU CGISS 06-01, Boise State University, Boise, Idaho.

Maret, T., Hortness, J., & Ott, D. (2006). Instream flow characterization of Upper Salmon River Basin Streams, Central Idaho, 2005. Reston, Virginia: U.S. Geological Survey.

Meinzer, O.E. (1924).Ground water in Pahsimeroi Valley, Idaho. Pamphlet No. 9, Bureau of Mines and Geology.

Mueller, D. (2012, September). Review and Rating of Moving-Boat ADCP Discharge Measurements. U.S. Geological Survey.

Mueller, D. (2016). QRev - Software for Computation and Quality Assurance of Acoustic Doppler Current Profiler Moving-Boat Streamflow Measurements - User's Manual (ver.2.80). U.S. Geological Survey. Retrieved from http://dx.doi.org/10.31133/ofr20161056

Mueller, D., Wagner, C., Rehmel, M., Oberg, K., & Rainville, F. (2013). Measuring discharge with acoustic Doppler current profilers from a moving boat (ver. 2.0, December 2013. U.S. Geological Survey. Retrieved from http://pubs.usgs.gov/tm/3a22/

Muirhead, K., & Cracknell, A. (1986). Airborne LiDAR bathymetry. International Journal of Remote Sensing, 7, 597-614.

Natural Resources Conservation Service (NRCS) (2008). Pahsimeroi-17060202 8 Digit Hydrologic Unit Profile, Idaho, March 2008.

Oberg, K., Morlock, S., & Caldwell, W. (2005). Quality-assurance plan for discharge measurements using acoustic Doppler current profilers. Reston, VA: U.S. Geological Survey.

Rantz, S. (1982). Measurement and Computation of Streamflow: Volume 1. Measurement of Stage and Discharge. Washington D.C.: U.G. Geological Survey.

Simpson, M. (2002). Discharge measurements using a broad-band acoustic Doppler current profiler. U.S. Geological Survey.

SonTek/YSI. (2013). RiverSurveyor S5/M9 Version 9.00. San Diego, CA: Xylem Brand.

Taguas, E., Ayuso, J., Pena, A., Yuan, Y., Sanchez, M., Giraldez, J., & Pérez, R. (2008). Testing the relationship between instantaneous peak flow and mean daily flow in a Mediterranean Area Southeast Spain. Catena, 75(2), 129-137.

Trimble. (2014). Trimble R10 GNSS System. Retrieved from Trimble: http://trl.trimble.com/docushare/dsweb/Get/Document-625158/022543-544E_TrimbleR10_DS_1014_LR.pdf

Urick, R. (1983). Principles of underwater sound (3rd. ed.). McGraw-Hill.

Walters, A., Bartz, K., & McClure, M. (2013). Interactive Effects of Water Diversion and Climate Change for Juvenile Chinook Salmon in the Lemhi River Basin (USA). Conservation Biology, 27(6), 1179-1189. doi:10.1111/cobi.12170

Weather underground PWS data. (n.d.). Salmon, ID (83467) Forecast. Retrieved from Weather Underground: https://www.wunderground.com/us/id/salmon/zmw:83467.1.99999

Wolman, M. (1954). A method of sampling coarse river-bed material. EOS, Transactions American Geophysical Union, 35(6), 951-956.

Zabel, R., Cooney, T., Jordan, C., Carmichael, R., Jonasson, B., Sedell, E., . . . Scheuerell, M. (2016). Life-Cycle models of salmonid populations in the interior Columbia River Basin, NOAA Report.

Appendix A – Annual Peak Streamflow

Pahsimeroi River gages					
WY	Month	Gage	Date	Peak Flow (cfs)	Code
1930	12	13302000	12/10/1929	279	1,5
1931	11	13302000	11/5/1930	266	1,5
1932	11	13302000	11/20/1931	246	1,5
1933	3	13302000	3/12/1933	223	1,5
1934	10	13302000	10/30/1933	282	1,5
1935	11	13302000	11/30/1934	234	1,5
1936	11	13302000	11/10/1935	234	1,5
1937	11	13302000	11/22/1936	234	1,5
1938	7	13302000	7/4/1938	258	1,5
1939	11	13302000	11/21/1938	258	1,5
1940	2	13302000	2/27/1940	277	1,5
1941	11	13302000	11/6/1940	258	1,5
1943	5	13302000	5/30/1943	454	1,5
1944	10	13302000	10/29/1943	363	1,5
1945	11	13302000	11/17/1944	333	1,5
1946	9	13302000	9/17/1946	356	1,5
1947	11	13302000	11/29/1946	341	1,5
1948	6	13302000	6/21/1948	438	1,5
1949	11	13302000	11/18/1948	371	1,5
1950	10	13302000	10/25/1949	344	1,5
1951	11	13302000	11/20/1950	333	1,5
1952	3	13302000	3/28/1952	352	1,5
1953	11	13302000	11/16/1952	356	1,5
1954	11	13302000	11/24/1953	362	1,5
1955	4	13302000	4/3/1955	296	1,5
1956	12	13302000	12/23/1955	409	1,5
1957	6	13302000	6/8/1957	796	1,5
1958	5	13302000	5/28/1958	415	1,5
1959	12	13302000	12/12/1958	436	1,5
1972	2	13302000	2/29/1972	407	1,5
1985	11	13302005	11/3/1984	536	5
1986	6	13302005	6/4/1986	710	1,5
1987	10	13302005	10/4/1986	377	5
1988	10	13302005	10/24/1987	355	5
1989	5	13302005	5/11/1989	347	5
1990	11	13302005	11/6/1989	274	5,B
1991	6	13302005	6/12/1991	467	5

Pahsimeroi River gages					
WY	**Month**	**Gage**	**Date**	**Peak Flow (cfs)**	**Code**
1992	11	13302005	11/13/1991	315	1,5
1993	3	13302005	3/26/1993	309	1,5
1994	3	13302005	3/3/1994	318	5,B
1995	7	13302005	7/11/1995	542	5
1996	2	13302005	2/9/1996	623	5
1997	6	13302005	6/11/1997	497	1,5
1998	6	13302005	6/26/1998	471	1,5
1999	6	13302005	6/17/1999	560	1,5
2000	11	13302005	11/18/1999	389	5,B
2001	3	13302005	3/9/2001	359	5,B
2002	3	13302005	3/13/2002	312	5
2003	11	13302005	11/23/2002	284	5,B
2004	11	13302005	11/20/2003	226	1,5
2005	10	13302005	10/29/2004	275	1,5
2006	4	13302005	4/6/2006	321	1,5
2007	10	13302005	10/7/2006	315	1,5
2008	6	13302005	6/21/2008	260	1,5
2009	6	13302005	6/22/2009	699	1,5
2010	11	13302005	11/12/2009	324	1,5
2011	7	13302005	7/2/2011	639	1,5
2012	4	13302005	4/27/2012	542	1,5
2013	10	13302005	10/29/2012	339	5
2014	10	13302005	10/3/2013	326	5
2015	2	13302005	2/7/2015	497	5

1 ... Discharge is a Maximum Daily Average
5 ... Discharge affected to unknown degree by regulation or diversion
B ... Month or Day of occurrence is unknown or not exact

Morse Creek gage					
WY	**Month**	**Gage**	**Date**	**Peak Flow (cfs)**	**Code**
1962	6	13301700	6/17/1962	90	
1963	6	13301700	6/9/1963	136	
1964	5	13301700	5/31/1964	126	
1965	6	13301700	6/12/1965	190	
1966	5	13301700	5/30/1966	66	
1967	5	13301700	5/24/1967	225	
1968	6	13301700	6/6/1968	125	
1969	5	13301700	5/15/1969	85	

Morse Creek gage					
WY	Month	Gage	Date	Peak Flow (cfs)	Code
1970	5	13301700	5/26/1970	230	
		13301700	1971	123	B
1973	5	13301700	5/19/1973	140	
1974	6	13301700	6/18/1974	150	
1975	6	13301700	6/16/1975	270	
1976	5	13301700	5/26/1976	136	
1978	6	13301700	6/9/1978	275	
1979	5	13301700	5/27/1979	195	
1980	6	13301700	6/20/1980	100	2

2 ... Discharge is an estimate

B ... Month or Day of occurrence is unknown or not exact

Appendix B – Additional Hydrology Plots

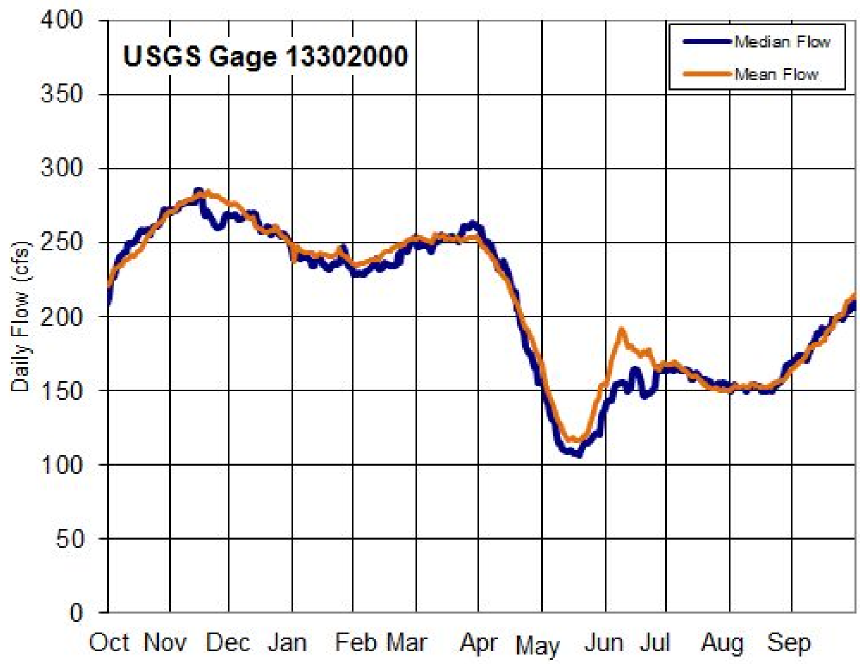

Figure B1. Mean and median daily discharge values for the record from 1984 to present (USGS gage 13302000) for the Pahsimeroi River near the confluence with the Salmon River.

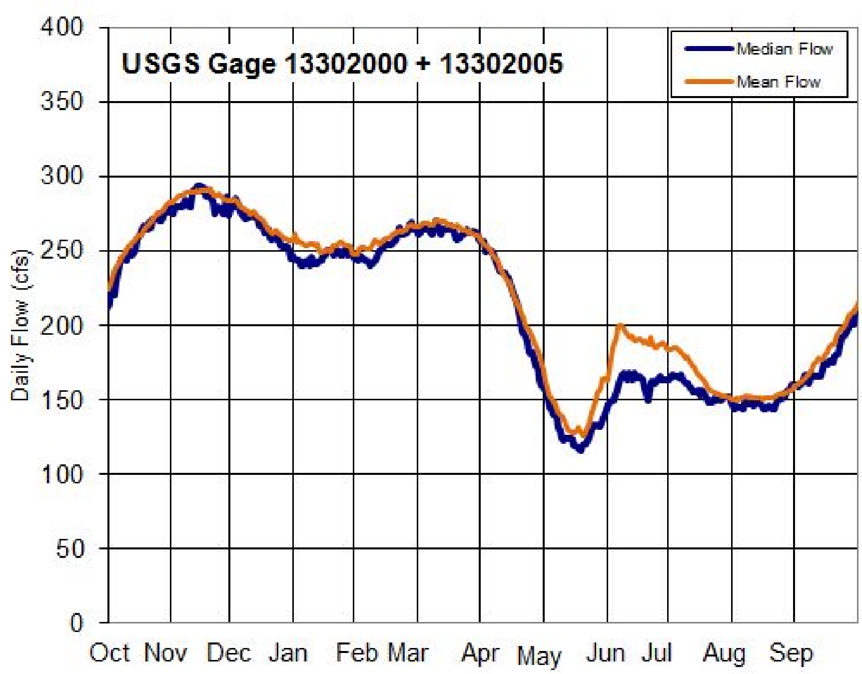

Figure B2. Mean and median daily discharge values for the record from 1984 to present (USGS gages 13302000 and 13302005 combined) for the Pahsimeroi River near the confluence with the Salmon River.

Appendix C – Drainage Area Ratio

Location	Drainage Area (mi^2)	Scaling Location	Drainage Area Ratio (DA_u/DA_g)
PC Lower	824	Pahsimeroi	0.99
GR 12	816	Pahsimeroi	0.98
PC Middle	748	Pahsimeroi	0.90
IDWR Gage P-9	561	Pahsimeroi	0.68
GR 11	559	Pahsimeroi	0.67
PC Upper	499	Pahsimeroi	0.60
IDWR Gage Furey	470	Pahsimeroi	0.57
GR 10	470	Pahsimeroi	0.57
GR 9	331	Pahsimeroi	0.40
GR 8	134	Pahsimeroi, Morse Creek	0.16,7.44
GR 7	128	Pahsimeroi, Morse Creek	0.15,7.11
GR 6	124	Pahsimeroi, Morse Creek	0.15,6.89
GR 5	56	Morse Creek	3.11
GR 4	40	Morse Creek	2.22
GR 3	32	Morse Creek	1.78
GR 2	12	Morse Creek	0.67
GR 1	3	Morse Creek	0.17

Appendix D – Regional Regression Analysis

Location	Drainage Area (mi^2)	P (annual precip, in)**	2	5	10	25	50	100
USGS Gage/Mouth	830	19.9	1287	1990	2445	3015	3451	3901
PC Lower	824	19.9	1279	1977	2430	2997	3431	3879
GR 12	816	20	1288	1988	2441	3008	3442	3889
PC Middle	748	20.5	1288	1973	2413	2963	3382	3814
IDWR Gage P-9	561	21.5	1158	1758	2141	2617	2980	3353
GR 11	559	21.5	1154	1753	2134	2609	2971	3343
PC Upper	499	21.6	1057	1610	1963	2404	2740	3086
IDWR Gage Furey	470	21.2	946	1457	1787	2200	2516	2842
GR 10	470	21.2	945	1456	1785	2198	2514	2840
GR 9	331	21.9	765	1181	1448	1785	2042	2307
GR 8	134	25.7	565	844	1017	1234	1398	1566
GR 7	128	26.4	591	873	1048	1264	1428	1596
GR 6	124	26.7	594	874	1046	1260	1422	1587
GR 5	56	31.4	484	686	806	952	1062	1174
GR 4	40	33.3	436	610	711	835	928	1023
GR 3	32	35.1	417	575	666	778	861	945
GR 2	12	39	245	337	389	453	501	550
GR 1	3	38.4	68	100	119	144	163	182

**Annual precipitation from Streamstats

RECLAMATION

Managing Water in the West

Technical Report No. SRH-2017-18

Upper Salmon River (Upstream of Redfish Lake Creek) Hydraulics & Hydrologic Assessment

Columbia-Snake Salmon Recovery Office
Pacific Northwest Region

U.S. Department of the Interior
Bureau of Reclamation
Technical Service Center
Denver, Colorado

April 2017

Mission Statements

The Department of the Interior protects and manages the Nation's natural resources and cultural heritage; provides scientific and other information about those resources; and honors its trust responsibilities or special commitments to American Indians, Alaska Natives, and affiliated island communities.

The mission of the Bureau of Reclamation is to manage, develop, and protect water and related resources in an environmentally and economically sound manner in the interest of the American public.

Technical Report No. SRH-2017-18

Upper Salmon River (Upstream of Redfish Lake Creek) Hydraulics & Hydrologic Assessment

Columbia-Snake Salmon Recovery Office
Pacific Northwest Region

U.S. Department of the Interior
Bureau of Reclamation
Technical Service Center
Denver, Colorado

April 2017

Bureau of Reclamation
Technical Service Center, Denver, Colorado
Sedimentation and River Hydraulics Group, 86-68240

Technical Report SRH-2017-18

Main Salmon River (Upstream of Redfish Lake Creek) Hydraulic and Hydrologic Assessment

Columbia-Snake Salmon Recovery Office
Pacific Northwest Region

CAROLINE UBING Digitally signed by CAROLINE UBING
Date: 2017.04.21 13:01:42 -06'00'

Prepared by:
Caroline Ubing, M.S., E.I.T., Hydraulic Engineer
Sedimentation and River Hydraulics Group

MELISSA FOSTER Digitally signed by MELISSA FOSTER
Date: 2017.04.21 13:03:25 -06'00'

Prepared by:
Melissa Foster, Ph.D., Physical Scientist
Sedimentation and River Hydraulics Group

JENNIFER BOUNTRY Digitally signed by JENNIFER BOUNTRY
Date: 2017.04.21 14:53:50 -06'00'

Peer Reviewed by:
Jennifer Bountry, M.S., P.E., Hydraulic Engineer
Sedimentation and River Hydraulics Group

AMANDA STONE Digitally signed by AMANDA STONE
Date: 2017.04.21 13:34:10 -06'00'

Peer Reviewed by:
Amanda Stone, M.S., P.E., Hydrologic Engineer
Flood Hydrology and Meteorology Group

Peer Review Certification: *This document has been peer reviewed and is believed to be in accordance with the service agreement and standards of the profession.*

Table of Contents

page

1 Purpose and Scope 10

2 Upper Salmon River Subbasin (Above Redfish Lake Creek) Characteristics..11

2.1 Hydrologic Influences..13
2.2 Gaged Flow Characteristics..14

3 Methods..19

3.1 Hydrologic Assessment 20
3.1.1 Peak Flow Calculations at Gaged Locations 22
3.1.2 Peak Flow Calculations at Ungaged Locations 23
3.2 Stream Power Analysis..25
3.3 Field Data Collection 26
3.3.1 Data Collection Methodology.. 26
3.4 At-a-Station Hydraulic Calculations..28
3.4.1 At-a-Station Hydraulic Calculation Methods 28
3.4.2 At-a-Station Hydraulic Calculation Uncertainty Discussion.......... 29

4 Results 30

4.1 Hydrologic Assessment Results..31
4.1.1 Peak Flow Calculations at Gaged Locations 31
4.1.2 Peak Flow Calculations at Ungaged Locations 35
4.2 Stream Power Analysis Results 36
4.3 Pebble Count Results..39
4.4 At-a-Station Hydraulic Results..40

5 Data Needs for Future Hydraulic Modeling and Recommendations......45

5.1 Topographic and Bathymetric Data 46
5.2 Hydrologic Data Gaps..47
5.3 Sediment Data Gaps & Discussion 47
5.4 Data Needs for Hydraulic Model Calibration..48

6 Conclusions..48

7 References..50

Appendix A – Annual Hydrographs and Snowtel Data 52

Appendix B – Annual Peak Streamflow 58

Tables

page

Table 1.–USGS stream gage information for gages within the Upper Salmon River basin utilized for analysis within this report. 11
Table 2.–Low flow discharge values 19
Table 3.–Manning's *n* values 29
Table 4.–Gage and flood frequency results, in cfs, from USGS stream gage locations. 31
Table 5.–Recommended Peak Discharge Values along the Main Salmon River. Cells are color coded based on calculation method. 36
Table 6.–Stream Power Analysis Results 39
Table 7.–Pebble Count Results 39
Table 8.–At-a-station hydraulic calculation results 42
Table 9.–At-a-station bed mobility calculation results 43

Figures

page

Figure 1.–USGS, IDWR, and SNOTEL gage locations. Gages utilized in the frequency analysis are emphasized with white circles and black, bold text. All inactive gages are black in color. 12
Figure 2.–Lakes in the Main Salmon River Basin. 14
Figure 3.–Mean and median daily discharge values for the entire period of record for the USGS gage on the Upper Salmon River at RM 27.0. Day-of-Year numbers are days of the year with January 1st and December 31st represented as 1 and 366, respectively. 15
Figure 4.–Mean and median daily discharge values for the entire period of record for the USGS gage on Pole Creek. 15
Figure 5.–Mean and median daily discharge values for the entire period of record for the USGS gage on Valley Creek. 16
Figure 6.–Mean and median daily discharge values for the entire period of record for the USGS gage on Salmon River below Valley Creek. 16
Figure 7.–2003 Annual hydrograph of streams in the Upper Salmon River Basin. SWE data was downloaded from the SNOTEL data set developed by the Nationl Resources Conservation Service (NRCS) from site ID490 and ID845. 17
Figure 8.–Frequency of peak flows by month by gage. 18
Figure 9.–Comparison of annual peak events over three gages. The annual peaks that occurred during the same event are outlined (2003 and 2011). Events that occurred during April and September are diagonally hatched (2012 and 2013). 18
Figure 10.–Valley segments and geomorphic reaches labeled by river mile. 20
Figure 11.–Peak plow estimation locations. River miles of flow estimation sites are labeled in black along the flow centerline. Drainage area values are labeled in blue along the edges of the drainage basins. 22
Figure 12.–Example of average reach slope determination using a trendline fit to topographic data. Figure represents geomorphic reach 2 from RM 36.0 to RM 32.5. The average slope for this reach is 0.0024 ft/ft. 26

Figure 13.–Locations of cross section surveys and pebble counts performed by Trout Unlimited. 27
Figure 14.–Pebble axis measurement (Harrelson et al., 1994 Fig. 60)................. 28
Figure 15.–Peak discharge values plotted across annual exceedance probability (AEP). 32
Figure 16.–Annual Exceedance Curve for USGS gage on Pole Creek (13292380). 33
Figure 17.–Annual Exceedance Curve for USGS gage on Salmon River at RM 27.0 (13292280). Potentially influential low flows (PILF) are plotted with x's while systematic peaks are plotted with circles. 33
Figure 18.–Annual Exceedance Curve for USGS gage on Valley Creek (13295000). 34
Figure 19.–Annual Exceedance Curve for USGS gage on Salmon River below Valley Creek (13295500)... 34
Figure 20.–Estimated discharge values for the 2-yr and 100-yr event. Geomorphic reaches are labeled at the top. 35
Figure 21.–Estimated discharge values along the Upper Salmon River.............. 37
Figure 22.–Upper Salmon River longitudinal profile (blue solid line) and slope (orange dotted lines) by river mile. Note: slope is plotted on a logarithmic scale. 38
Figure 23.–Stream power and pebble count results. The median grain size (D_{50}) is plotted on the left vertical axis applying a log base 2 scale. Stream power is presented on the right vertical axis for four flood events. 38
Figure 24.–Pebble count results at all three sites... 40
Figure 25.–Aerial imagery at RM 8.2.. 41
Figure 26.–Water surface elevation for each event, assuming normal Manning's *n* values, at RM 8.2. As the survey does not cover the 100-yr flood extent, vertical walls were assumed at the edges of the cross section.. 43
Figure 27.–Water surface elevation for each event, assuming normal Manning's *n* values, at RM 13.0. 44
Figure 28.–Water surface elevation for each event, assuming normal Manning's *n* values, at RM 33.2. 44

Acronyms and Abbreviations

%	Percent
°C	Degrees Celsius
°F	Degrees Fahrenheit
°N	Latitude degrees north
°W	Longitude degrees west
2D	Two-dimensional
ADCP	Acoustic Doppler Current Profiler
AEP	Annual Exceedance Probabilty
cfs	Cubic feet per second
CORS	Continuously Operating Reference Station
COV	Coefficient of Variance
D_n	Sediment particle diameter size at n% passing
DS	Downstream
Eq	Equation
ESA	Endangered Species Act
Ft	Foot/feet
GIS	Geographic Information System
GNSS	Global Navigation Satellite Systems
GPS	Global Positioning System
HSI	Habitat Suitability Index
IACWD	Interagency Advisory Committee and Water Data
IDWR	Idaho Department of Water Resources
InSAR	Interferometric Synthetic Aperture Radar
Km	Kilometer
LiDAR	Laser Imaging, Detection and Ranging
mi	Mile(s)
mm	Millimeter
NAD	North American Datum
NAVD	North American Vertical Datum
NRCS	National Resources Conservation Service

No.	Number
OPUS	Online Position User Service
PILF	Potential influential low flows
PN	Pacific Northwest
Reclamation	Bureau of Reclamation
RM	River mile
RMS	Root Mean Square
RTK	Real Time Kinematic
RTS	Resource and Technical Services
SNOTEL	Snow Telemetry
SRH	Sedimentation and River Hydraulics Group
SWE	Snow water equivalent
TSC	Technical Service Center
U.S.	United States
US	Upstream
USACE	U.S. Army Corps of Engineers
USGS	U.S. Geological Survey
USFS	U.S. Forest Service
WSE	Water Surface (Elevation)

Symbols

DA_u	Contributing drainage area at the ungaged site (mi^2)
DA_g	Contributing area at the gaged site (mi^2)
DA_{g1}	Contributing area at the upstream gaged site (mi^2)
DA_{g2}	Contributing area at the downstream gaged site (mi^2)
Q	Flow discharge or rate (ft^3/s)
Q_u	discharge at an ungaged site (ft^3/s)
Q_g	discharge at the gaged site (ft^3/s)
Q_{g1}	discharge at the upstream gaged site (ft^3/s)
Q_{g2}	discharge at the downstream gaged site (ft^3/s)
S	slope (ft/ft)
γ	specific weight of water (lb/ft^3)
Ω	total stream power (lb/s)

Executive Summary

Reclamation is conducting an Integrated Rehabilitation Assessment of 38 river miles of the Upper Salmon River (upstream of Redfish Lake Creek) Basin, to characterize general watershed conditions within the river basin. The goal of this assessment is to identify reaches for more detailed study with potential for steelhead and spring Chinook rehabilitation. The objectives of this hydraulics and hydrologic assessment include: peak flow estimations, stream power assessment, at-a-station hydraulic calculations at three cross sections, and identification of data needs for future hydraulic modeling analyses. Analyses from this report will feed into a watershed-scale geomorphic and fish production model. Valley segments and geologic reaches were identified to distinguish confinement, sediment transport trends, and provide a means of consistent locations for discussion throughout the Integrated Rehabilitation Assessment.

The Upper Salmon River flow regime is snowmelt dominated with numerous diversions which are in operation from July to through September. Peak snowmelt flows generally occur between the months of May and June. While agricultural diversion locations and volumes are regulated by local water authorities and the Idaho Department of Water Resources. Exact withdrawal rates on a seasonal and daily basis are unknown. Mountain lakes are another important component of the Upper Salmon River hydrology, as lakes modify water, sediment, and nutrient fluxes. Flood frequency peaks were estimated at four operational United States Geological Survey (USGS) gages using the PeakFQ program, and at 12 ungaged locations applying methods published in Bulletin 17C and Berenbrock (2002). Peak flood frequency values at each valley segment are presented in the table below. An improved understanding of diversion outflows, tributary inflows, and groundwater contributions is recommended for future work.

River Mile	DA (mi^2)	Flood Frequency Values (cfs)								
		1	1.5	2	2.33	5	10	25	50	100
0	304	685	1,643	1,919	2,043	2,554	2,936	3,383	3,694	3,987
15.3	177	389	940	1,099	1,170	1,463	1,682	1,937	2,114	2,281
36	3.8		35.1	43.1	45.1	60.7	73.3	88.9	100	114

A stream power assessment was completed to understand relative sediment transport capacity of each geomorphic reach and identify areas of significant tributaries and changes in slope. Results concluded that the upper mile and lower half (RM 15.4 to RM 0) of the basin have higher stream power compared to the remainder of the basin due to a large increase in discharge from Alturas Lake Creek and slight variation in channel slope.

A two-dimensional (2D) hydraulic model is recommended for future hydraulic modeling to quantify habitat improvement for proposed alternatives along the

Upper Salmon River. A 2D model (as opposed to a one-dimensional (1D) model) will better represent multiple channel networks, geomorphic features, and lateral flow over the floodplain. Additional data necessary for future hydraulic modeling include topography, bathymetry, calibration data, and an improved understanding of diversion outflows, tributary inflows, and groundwater contributions.

1 Purpose and Scope

The Bureau of Reclamation's (Reclamation) Resource and Technical Services (RTS) in the Pacific Northwest (PN) Regional Office tasked Reclamation's Sedimentation and River Hydraulics (SRH) Group at the Technical Service Center (TSC) with supporting a coarse level Integrated Rehabilitation Assessment of the Upper Salmon River Basin, above Redfish Lake Creek. The Upper Salmon River (above Redfish Lake Creek) extends 38.3 river miles (RM) from the headwaters (RM 38.3) to the confluence with Redfish Lake Creek near Stanley, ID (RM 0).

The primary objective was to conduct analyses and field assessments to inform hydrology, hydraulics, and sediment trends in support of the coarse-scale Integrated Rehabilitation Assessment. This study focuses on summarizing available hydraulic, streamflow, and sediment data that can be utilized in future reach or project scale hydraulic modeling. Key elements of this report are:

1. Description of hydrologic characteristics in the basin,
2. Hydrologic assessment of flood-frequency events at multiple locations utilizing the available gage data,
3. Stream power analysis at geomorphic reaches to qualitatively assess relative sediment transport capacity,
4. Cross-section and grain size analysis at three locations, and
5. Data gaps for future hydraulic modeling.

These five analyses from this report will feed into a watershed-scale geomorphic and fish production model, intended to identify a reach with the most potential for on-the-ground habitat rehabilitation projects for steelhead and spring chinook. The model develops a fish population and habitat relationship which incorporates twelve different metrics including: average annual discharge, substrate (D_{84}), slow water area, wetted depth, etc. (outlined in Zabel, et al., 2016). Average annual discharge is the primary indicator for population capacity. A stream power analysis was performed to provide an indication of the relative sediment transport capacity of each geomorphic reach along the Upper Salmon River. Cross-sections and a grain size analysis were completed to assess hydraulic properties and bed grain size mobility at a single cross section for a given range of discharge values. Future hydraulic modeling can provide information regarding slow water areas and wetted depth. Finally, the population and habitat relationship can be used to predict fish capacity based on existing physical habitat. The results can then be used to identify locations where rehabilitation projects could have the greatest benefit.

2 Upper Salmon River Subbasin (Above Redfish Lake Creek) Characteristics

The Upper Salmon River Subbasin (above Redfish Lake Creek), referred to as the Upper Salmon River Subbasin, is located in Custer and Blaine counties in Idaho. The Upper Salmon River is a fourth-order stream flowing north from its headwaters in the Sawtooth Mountains to the Salmon River. The project area ends at the confluence with Redfish Lake Creek, a drainage area of 305 square miles. Within the project area, there are many small tributaries, many of which are connected to mountain lakes formed behind terminal moraines (Goodman, Baker, & Wurtsbaugh, 2011). The largest tributary is at RM 15.3, Alturas Lake Creek, which has a drainage basin of 70 mi^2 (23% of Upper Salmon River Subbasin).

There are several gages operated by USGS and Idaho Department of Water Resources (IDWR) within the Upper Salmon River Subbasin, (Figure 1). IDWR operates five gages in the project area, which only report average daily streamflow values, although 15-minute interval data may be available upon request. One of the gages is located on the Salmon River, and the last recording was in 2009. The other four gages are positioned on tributaries and are still in operation. These gages were not used for the hydrologic analysis, which is discussed in 3.1 – Hydrologic Assessment. There are many USGS gages within the study area, including some with short periods of record. Those with longer records appropriate for flood frequency analysis, including annual peak flow measurements, are presented in Table 1. Two of the gages (13292280 and 13292380) do not record during the winter months due to ice. Annual peak streamflow occurs during the snowmelt in April, May, or June and will not be impacted by the missing data in the winter months. Snow Telemetry (SNOTEL) data provides snowpack information including snow water equivalent (SWE), which is the amount of water contained within the snowpack. Two gages are located within the project area and are mapped in Figure 1.

Table 1.–USGS stream gage information for gages within the Upper Salmon River basin utilized for analysis within this report.

				Daily Streamflow (cfs)		
USGS Gage No.	Description	Drainage Area (mi^2)	Period of Record	Min.	Average	Max.
13292280[1]	Salmon River at Pole Creek Road above diversion near Obsidian, ID	29.1	2003 - 2013	4	35.0	250
13292380[1]	Pole Creek below Pole Creek ranger station near Obsidian, ID	18.5	2003 - 2015	12	30.2	133
13295000	Valley Creek at Stanley, ID	147	1911 - 2017	34	202	1,900
13295500	Salmon River below Valley Creek at Stanley, ID	507	1925 - 1960	100	663	4,970

[1]These gages do not record during the winter months.

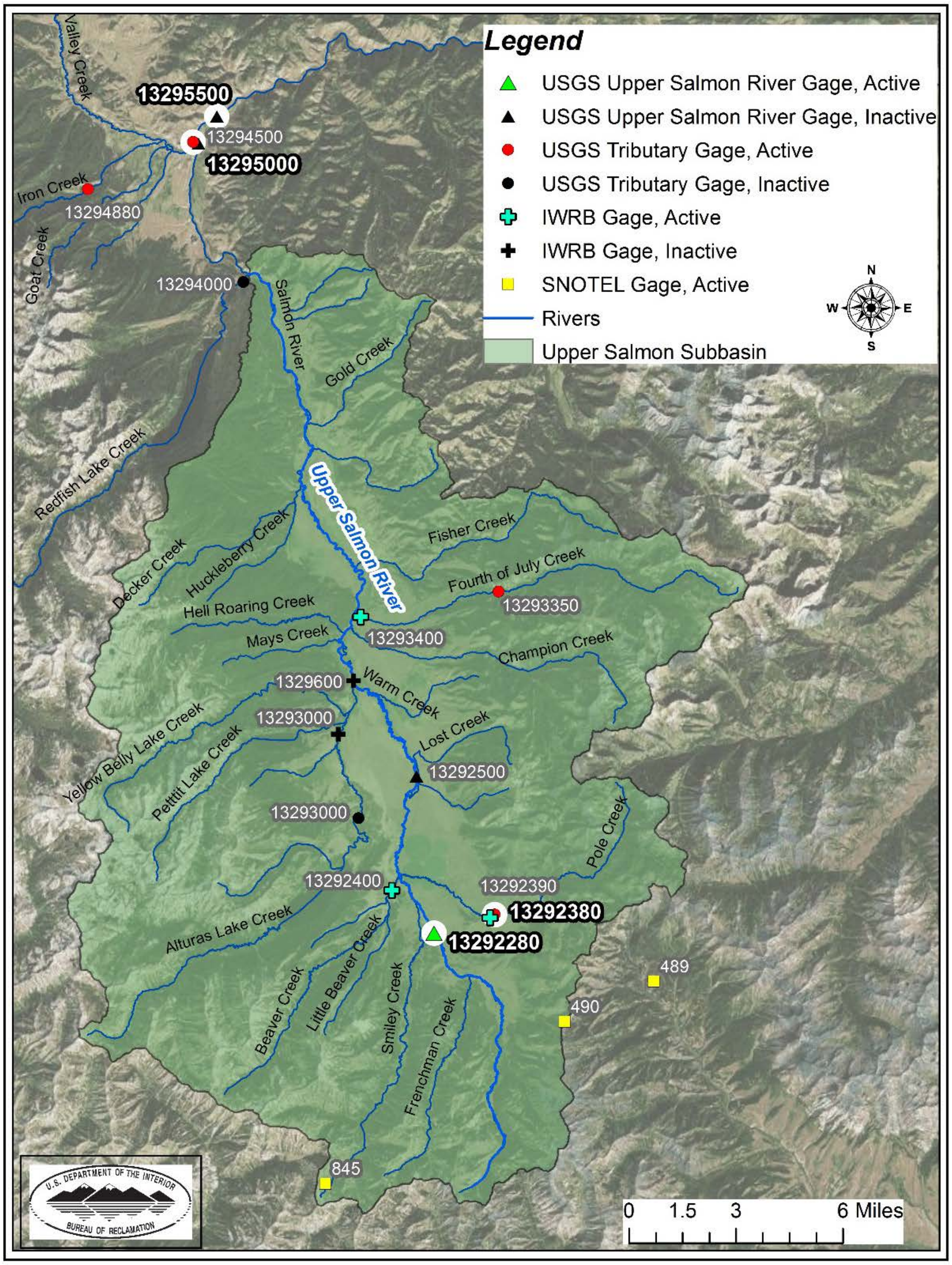

Figure 1.–USGS, IDWR, and SNOTEL gage locations. Gages utilized in the frequency analysis are emphasized with white circles and black, bold text. All inactive gages are black in color.

2.1 Hydrologic Influences

The hydrology in the Upper Salmon River Basin is impacted by irrigation withdrawals, lakes, and tributaries. There are several tributaries to the Upper Salmon River, the largest being Altus Lake Creek and Pole Creek.

The growing season in the Upper Salmon River Basin is relatively short (about 80 days) due to the high elevation (>7,000 ft). Water is diverted for agriculture from July through September (Maret, Hortness, & Ott, 2006). An unknown number of diversions draw water from the Upper Salmon River and its tributaries. There are some key diversions that have dewatered the Upper Salmon River and tributaries. The Busterback diversion, located between Alturas Lake Creek and Pole Creek (Figure 2), has historically drained the river for approximately 2 miles from July through September. Fourth of July, Champion, Fisher, and Beaver creeks are completely dewatered near their confluences with the Upper Salmon River during the irrigation season (Kiefer & Lockhard, 1994).

Several lakes are located within the project area, Figure 2. Lakes modify water, sediment, and nutrient fluxes. A detailed hydrograph analysis found that lakes modified rainfall flood peaks, but had minimal impacts on annual snowmelt peaks (Arp et al., 2006). The altered hydrologic regime can influence channel form and fluvial processes. A study performed in the Upper Salmon River Basin found that the river at the lake inlet was deep and narrow with fine bed sediments (Arp, Schmidt, Baker, & Myers, 2007). The gradient flattens approximately 0.6 miles above the lake. The deltas create slightly convex lateral surfaces (Dirszowsky & Desloges, 2004), which prompts subsurface flow (Arp, Gooseff, Baker, & Wurtsbaugh, 2006). Lake outlets were wide and shallow with coarse bed sediment, which may be a result of the end moraine geology. After initial incision through the end moraine, the stream bed will likely become armored and be relatively stable (Arp, Schmidt, Baker, & Myers, 2007).

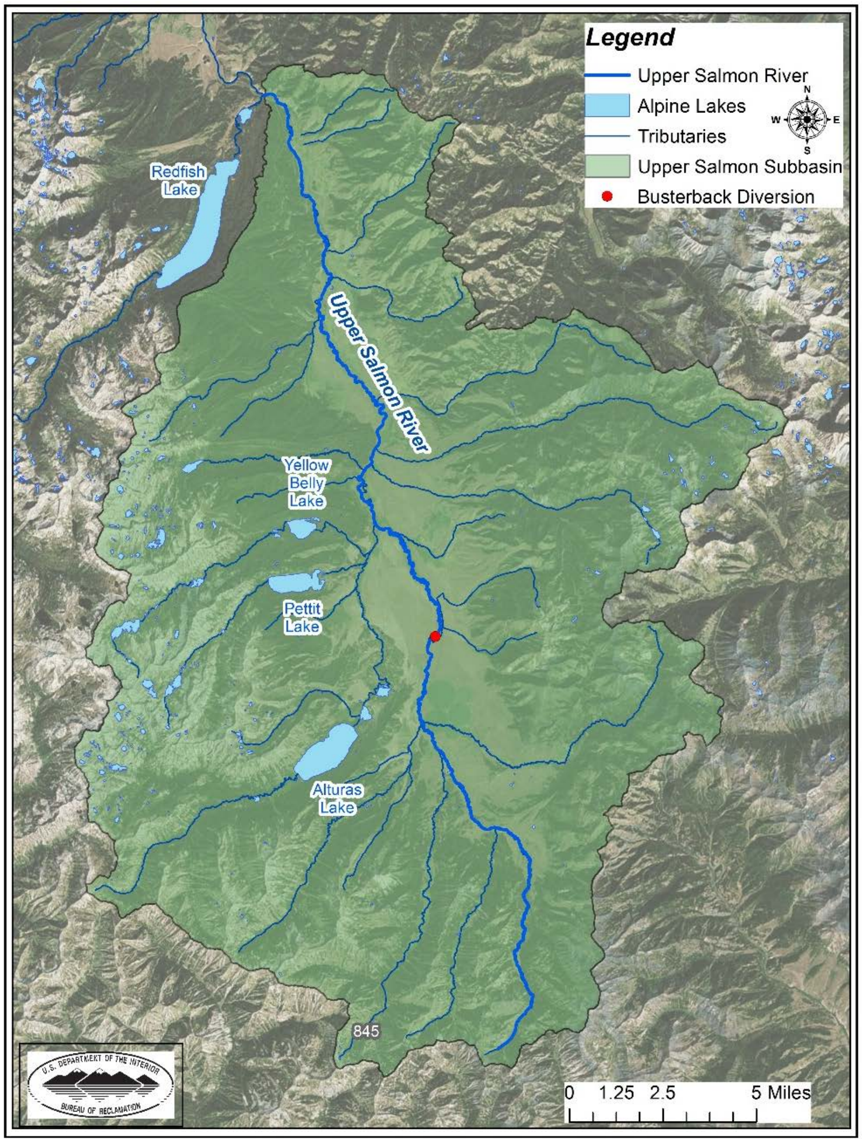

Figure 2.–Lakes in the Main Salmon River Basin.

2.2 Gaged Flow Characteristics

Almost all the peak flows within the Main Salmon River Basin occur during the snowmelt runoff period (typically April to June) and minimum flows typically occur in August and September (Figure 3 through Figure 6). Flows in the channel are affected by diversions during the growing season (typically April 1 to October 1) and unaltered during the winter months. While irrigation is still prevalent within the Main Salmon River Basin, the impact on the natural flow patterns is not nearly as prominent as the other basins (for example, the Pahsimeroi). Figure 7 illustrates the typical annual flow pattern in the Main Salmon River Basin. Annual hydrographs plotting snow water equlivalent and daily discharge values for USGS gages with a peroid of record that overlaps with the SNOTEL gages are included in Appendix A – Annual Hydrographs.

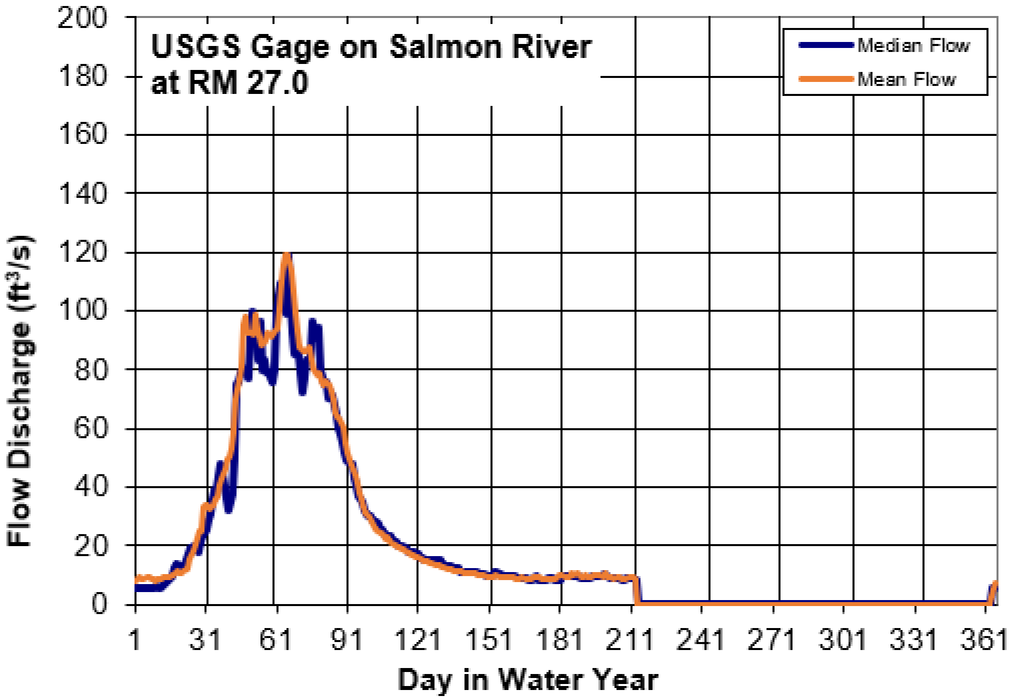

Figure 3.–Mean and median daily discharge values for the entire period of record for the USGS gage on the Upper Salmon River at RM 27.0. Day-of-Year numbers are days of the year with January 1st and December 31st represented as 1 and 366, respectively.

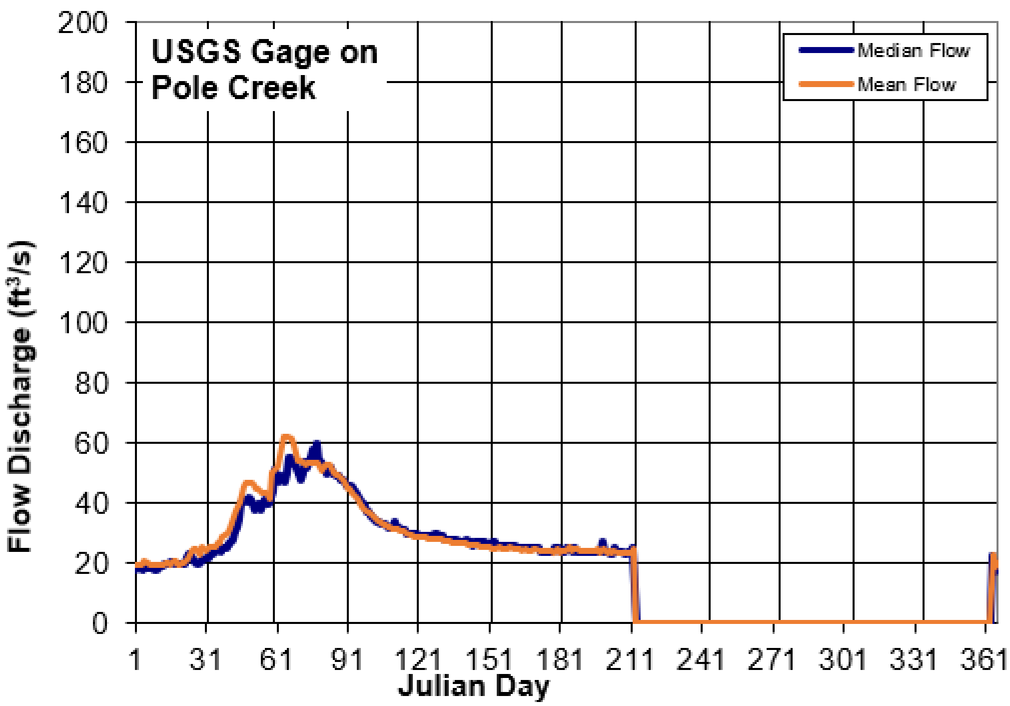

Figure 4.–Mean and median daily discharge values for the entire period of record for the USGS gage on Pole Creek.

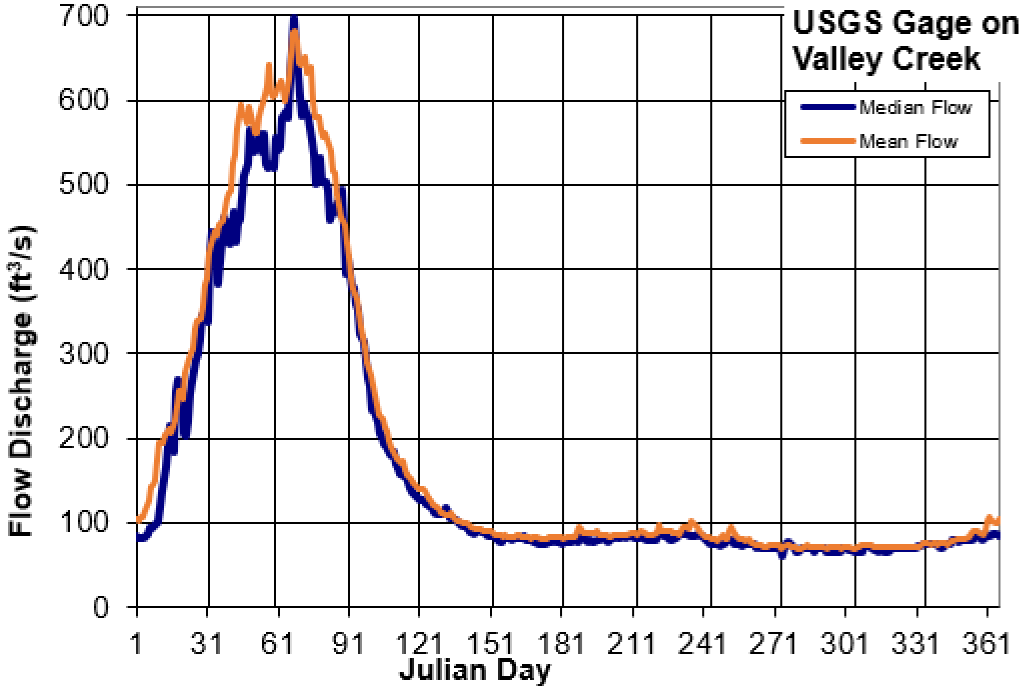

Figure 5.–Mean and median daily discharge values for the entire period of record for the USGS gage on Valley Creek.

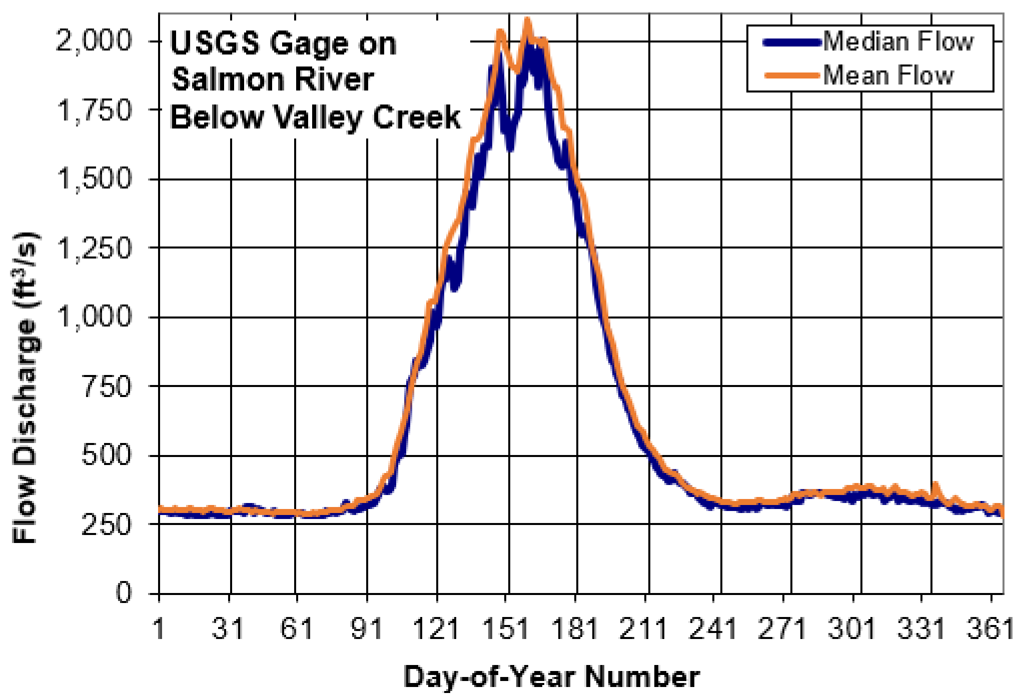

Figure 6.–Mean and median daily discharge values for the entire period of record for the USGS gage on Salmon River below Valley Creek.

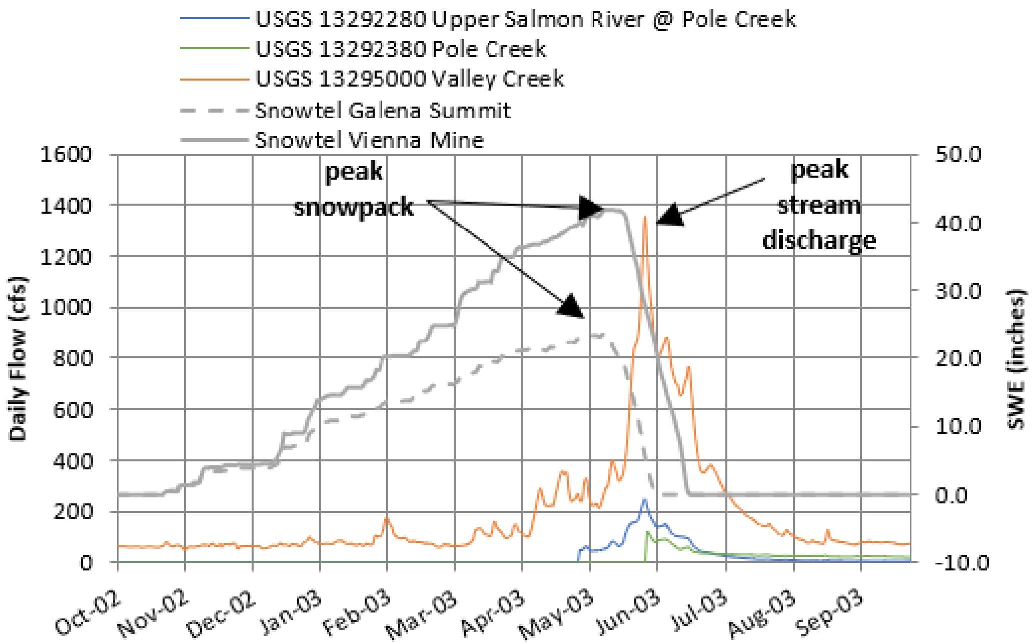

Figure 7.–2003 Annual hydrograph of streams in the Upper Salmon River Basin. SWE data was downloaded from the SNOTEL data set developed by the Nationl Resources Conservation Service (NRCS) from site ID490 and ID845.

The majority of historical annual peak flows occurred during the months of May (41%) and June (56%), Figure 8. The annual peak discharge values for all four gages are presented in Appendix B – Annual Peak Streamflow. While all four gages were not operational at the same time, the peaks were reviewed to identify overlapping events (those that occur due to the same snowmelt or rain event). From 2003 to 2013, three USGS gages were in operation: Valley Creek, Salmon River at RM 27.0, and Pole Creek (Figure 9). Two of the eleven overlapping peak annual discharge values occurred during the same event on all three gages. Both gages near Valley Creek (gage on Valley Creek and on the Salmon River below Valley Creek) were in operation from 1926 – 1941 and again from 1942 – 1960. During these 34 years, 23 of the peaks occurred during the same event.

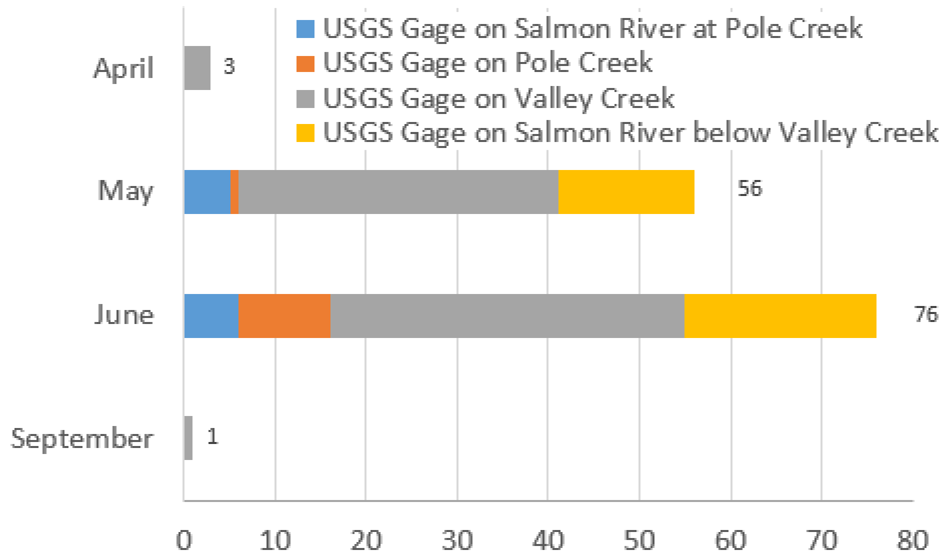

Figure 8.–Frequency of peak flows by month by gage.

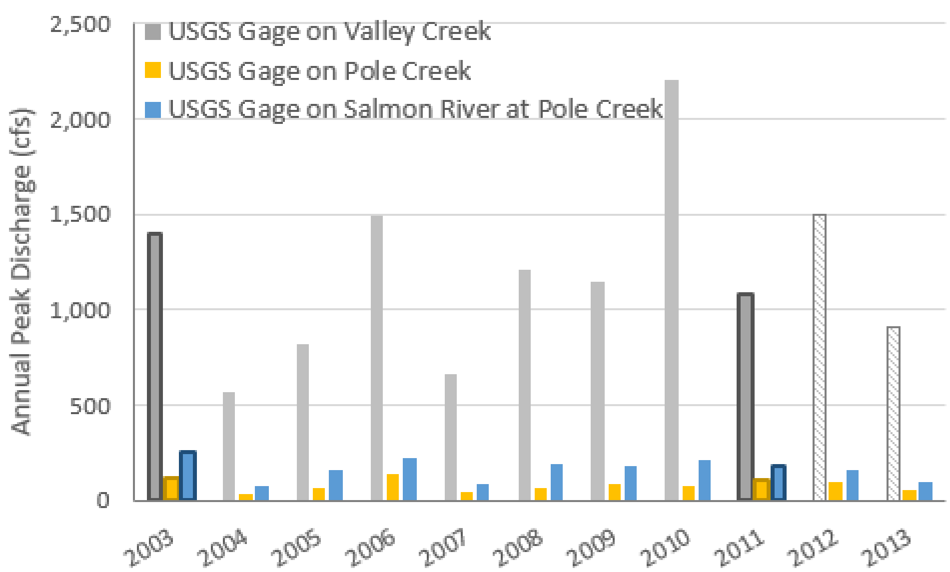

Figure 9.–Comparison of annual peak events over three gages. The annual peaks that occurred during the same event are outlined (2003 and 2011). Events that occurred during April and September are diagonally hatched (2012 and 2013).

A low flow analysis was performed to identify the lowest 7-day average flow that occurs every 10 years (7Q10) using the methods described in Hortness (2006). The results are presented in Table 2. The 7Q10 value for the Salmon River gage at RM 27.0 is less certain, as it is based on only 10 years of data.

Table 2.–Low flow discharge values

Gage	Period of Record	Drainage Area (mi^2)	7Q10 (cfs)
Salmon River below Valley Creek (13295500)	1925 – 1960	507	196
Valley Creek (13295000)	1911 - 2017	147	40.5
Salmon River at RM 27.0 (13292280)	2003 – 2013	29.1	4.08
Pole Creek (13292380)	2003 – 2015	18.5	13.1

3 Methods

The following sections provide detail on the methodology applied to the hydrologic assessment, stream power analysis, and data collection effort. Valley segments and geomorphic reaches (Figure 10) were developed by the PN region and given to TSC to establish consistent locations for the several analyses included in the Integrated Rehabilitation Assessment.

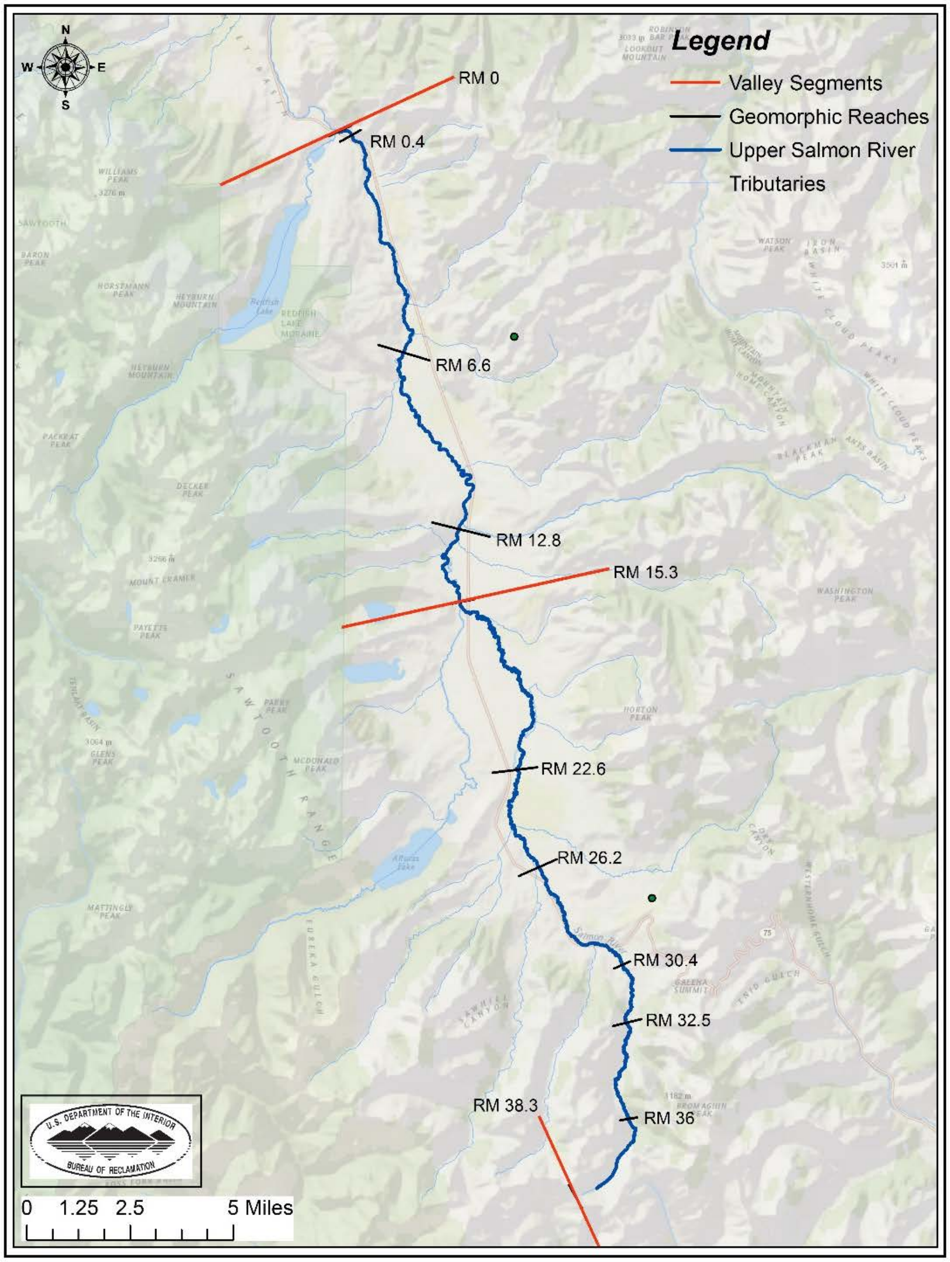

Figure 10.–Valley segments and geomorphic reaches labeled by river mile.

3.1 Hydrologic Assessment

Peak flood frequency estimates were generated at multiple locations along the Upper Salmon River for a range of recurrence intervals. Flood-frequency peak flow values were calculated at four gages (Salmon River below Valley Creek, Valley Creek, Salmon River at Pole Creek, and Pole Creek) using methods described in Bulletin 17C employing the software PeakFQ (Flynn, Kirby, & Hummel, 2006). The drainage-area ratio method with an exponent of 0.94, corresponding to Region

5 from Berenbrock (2002), was applied to estimate peak discharges at ungaged locations along the Upper Salmon River. Five IDWR gages are located in the project area. Only one of these gages is located on the Upper Salmon River, and tabular daily discharge values were not available. The remaining four are located on tributaries. Based on locations and availability, these data were not included in the analysis.

Given the purpose of the Integrated Rehabilitation Assessment, peak flood-frequency values were calculated utilizing the USGS gage data and methods published by Berenbrock in 2002. Flood-frequency peak flows were estimated at a total of 10 locations along the Upper Salmon River for 1-, 1.5-, 2-, 2.33-, 5-, 10, 25-, 50-, and 100-year recurrence intervals. Estimate locations (labeled by river mile) and associated contributing area are presented in Figure 11.

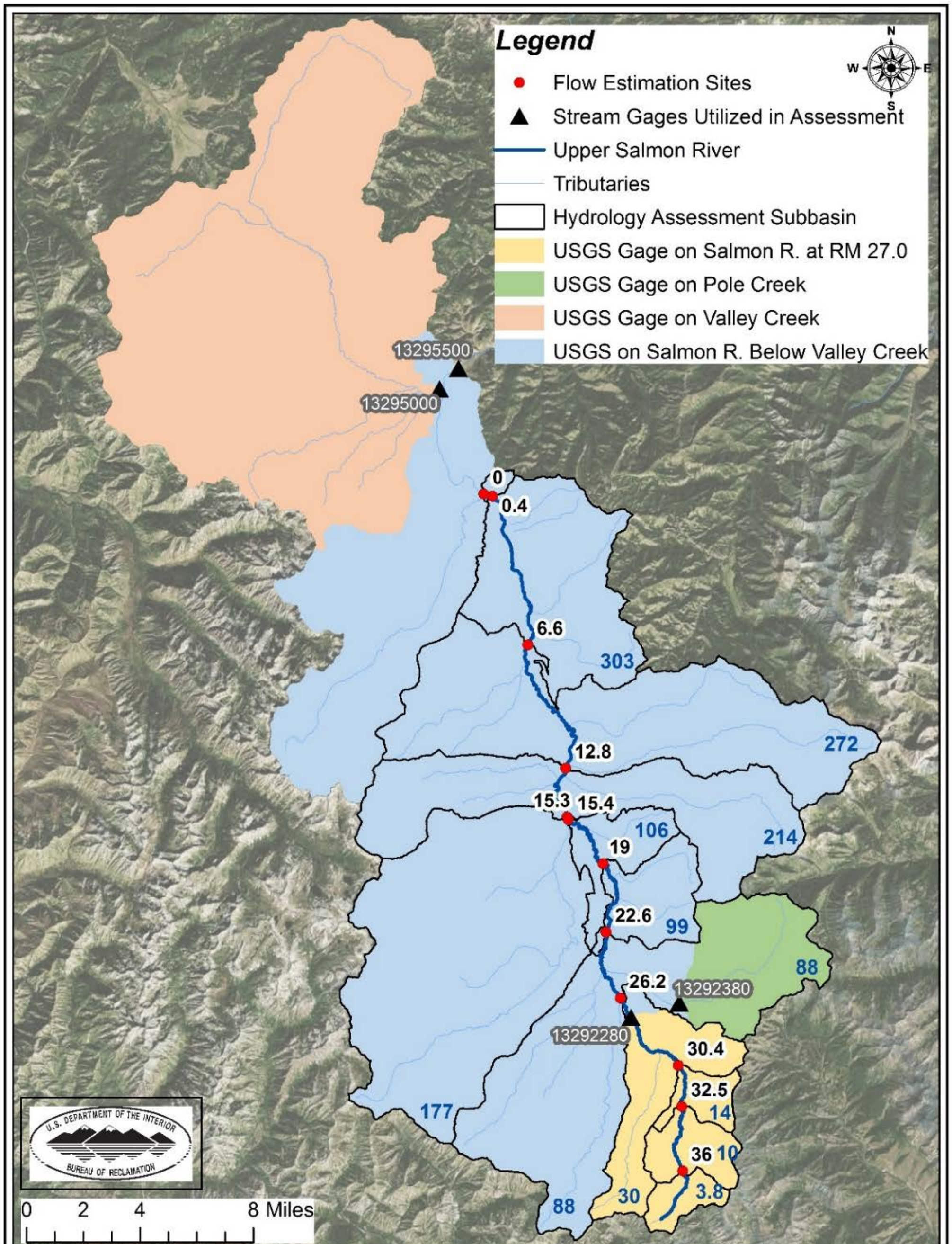

Figure 11.–Peak plow estimation locations. River miles of flow estimation sites are labeled in black along the flow centerline. Drainage area values are labeled in blue along the edges of the drainage basins.

3.1.1 Peak Flow Calculations at Gaged Locations

The annual peak flow data for the four USGS gages mapped in Figure 11 were analyzed for the flood frequency analysis. The longest period of record was gage 13295000 on Valley Creek. The MOVE.4 method was applied to extend the record of the other three gages to 78+ years. MOVE.4 technique extends a period of record by developing regression equations to estimate the mean and variance of flows at short-record gages by employing the cross-correlation between a long and short gage record. Four MOVE techniques are documented in literature. The MOVE.4 method was selected as it has the lowest mean square error and is the current recommended method (Vogel & Stedinger, 1958).

The annual peak discharge values were then analyzed utilizing PeakFQ (Flynn, Kirby, & Hummel, 2006). The program was developed by USGS and analyzes peak annual discharge measurements in accordance with Bulletin 17C recommends the Expected Moments Algorithm (EMA), which provides a direct fit of the Log-Pearson III distribution, which includes an estimate of variance. As recommended in Bulletin 17C, the Multiple Grubbs-Beck test (MGBT) was performed to remove potentially-influential low flood values. Peak discharge probabilities were estimated using the Cunnane’s plotting position (0.4) for 1-, 1.5-, 2-, 2.33-, 5-, 10-, 25-, 50-, 100-, 200-, and 500-year events (Flynn et al., 2006). The method does not directly account for irrigation losses. Most peak flows in the study basin occur during irrigation season (April – October), so the peak values may be impacted to an unknown degree by diversions.

3.1.2 Peak Flow Calculations at Ungaged Locations

USGS guidelines for Idaho streams in region 5 (Berenbrock, 2002) were applied to compute discharge for ungaged sites along the Upper Salmon. Equation 1 was applied between gages 13295000 (Salmon River below Valley Creek) and 13292280 (Salmon River at RM 27.0). Equation 2 was applied upstream of gage 13292280 (Salmon River at RM 27.0). At RM 36.0, regional regression equations were applied (Eq. 3). These equations assume that the flow is unregulated with no unnatural withdrawals/inputs. While this is not necessarily true, it is a reasonably good estimation of peak-flow values.

The guidelines recommend that when applying Eq. 2, the drainage area at the ungaged location must not exceed ±50% of the gaged watershed area. Drainage areas were estimated using StreamStats, a web-based Geographic Information Systems (GIS) tool that can be applied to water-resources engineering and design purposes. Among many other applications, StreamStats can obtain a drainage-basin boundary and area based on a user-identified point and USGS digital elevation model. At RM 36.0, the drainage area of 3.8 was less than 50% of the drainage area of the USGS gage on Pole Creek (gage no. 13292380); therefore, Eq. 2 was not applicable. At this location, predictive regional regression equations defined by Berenbrock (2002) for region 5 were employed (Eq. 3).

Equations 1, 2, and 3 are presented below:

$$Q_u = \frac{Q_{g1}\left(DA_{g2} - DA_u\right) + Q_{g2}\left(DA_u - DA_{g1}\right)}{DA_{g2} - DA_{g1}} \quad (1)$$

Where:
- Q_u is the peak discharge (cfs) for a specific recurrence interval at the ungaged site,
- Q_{g1} is the peak discharge (cfs) for a specific recurrence interval at the upstream gaged site,
- Q_{g2} is the peak discharge (cfs) for a specific recurrence interval at the downstream gaged site,
- DA_u is the contributing drainage area (mi^2) for the ungaged site,
- DA_{g1} is the contributing drainage area (mi^2) for the upstream gaged site, and
- DA_{g2} is the contributing drainage area (mi^2) for the downstream gaged site.

$$Q_u = Q_g\left(\frac{DA_u}{DA_g}\right)^{0.94} \quad (2)$$

Where:
- Q_u is the peak discharge (cfs) for a specific recurrence interval at the ungaged site,
- Q_g is the peak discharge (cfs) for a specific recurrence interval at the gaged site,
- DA_u is the contributing drainage area (mi^2) for the ungaged site, and
- DA_g is the contributing drainage area (mi^2) for the gaged site.
- An exponent value of 0.94 is based on a regression analysis for Idaho, Region 5 (Berenbrock, 2002)

$$Q_2 = 0.0297\, DA^{0.995}\, P^{2.20}\, (NF30 + 1)^{-0.664} \quad (3a)$$

$$Q_5 = 0.0992\, DA^{0.970}\, P^{1.92}\, (NF30 + 1)^{-0.602} \quad (3b)$$

$$Q_{10} = 0.178\, DA^{0.957}\, P^{1.79}\, (NF30 + 1)^{-0.571} \quad (3c)$$

$$Q_{25} = 0.319\, DA^{0.943}\, P^{1.66}\, (NF30 + 1)^{-0.538} \quad (3d)$$

$$Q_{50} = 0.456\, DA^{0.934}\, P^{1.58}\, (NF30 + 1)^{-0.517} \quad (3e)$$

$$Q_{100} = 0.620\, DA^{0.926}\, P^{1.52}\, (NF30 + 1)^{-0.499} \quad (3f)$$

Where:
- Q_n is the peak discharge (cfs) for a specific recurrence interval, n, at the ungaged site,
- DA is the contributing drainage area (mi^2) for the ungaged site,
- P is mean annual precipitation (in) for the ungaged site. , and
- $NF30$ is the percentage of north-facing slopes greater than 30 percent.

The results of these analyses are presented in Section 4.1 – Hydrologic Assessment Results.

3.2 Stream Power Analysis

A stream power analysis was performed to provide an indication of the relative sediment transport capacity of each geomorphic reach along the Upper Salmon River. Stream power is the river's rate of energy dissipation against the wetted perimeter (bed and banks) per unit of downstream length, as show in Equation 4. It is often used to indicate and compare the relative magnitude of sediment transport capacity between reaches. It does not provide quantitative information regarding the mass or size of sediment transported. In addition to flow characteristics (e.g. depth, velocity, shear stress), sediment transport capacity is also dependent on sediment supply and grain size, which were not included in this study. If total stream power increases, the sediment transport capacity would be expected to increase as well.

$$\Omega = \gamma \, Q \, S \qquad (4)$$

Where Ω is stream power (lb/s), γ is the specific weight of water (62.4 lb/ft^3), Q is flow discharge (cfs), and S is the terrain slope (ft/ft). Discharge generally increases in the downstream direction in river basins as tributaries contribute more flow. For the same given slope, this increase in discharge provides more energy to transport sediment and debris.

Stream power calculations were performed for the 1-, 2-, 10-, and 100-year flow events. Flow discharge was estimated using the methods described in Section 3.1 – Hydrologic Assessment. Reach/segment slope was estimated using the compiled topographic DEM data from the USGS National Elevation Data set (NED). The data was collected in 2013 at 1/3 arc-second (approximately 10 m) resolution. Elevation values were extrapolated for each of the sixteen geomorphic reaches. A trendline was then fit to the data to determine an average slope, as demonstrated in Figure 12.

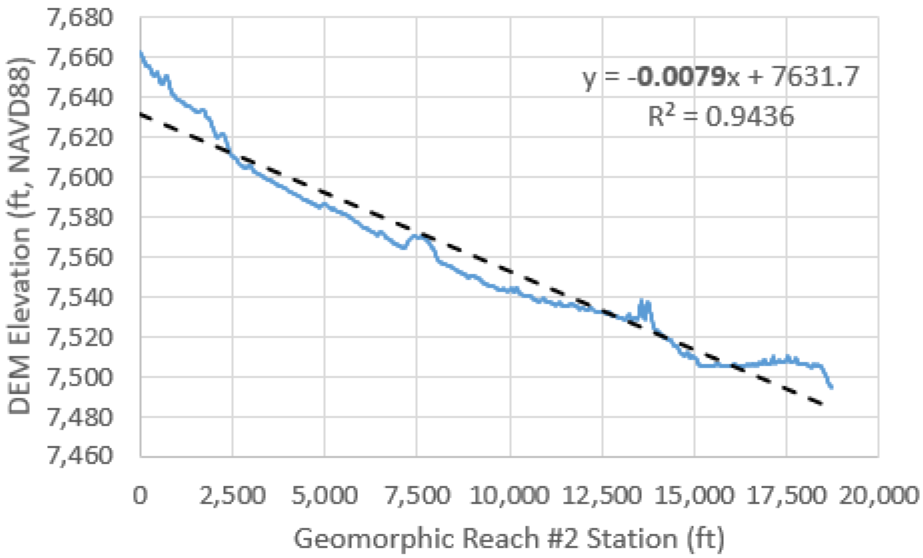

Figure 12.–Example of average reach slope determination using a trendline fit to topographic data. Figure represents geomorphic reach 2 from RM 36.0 to RM 32.5. The average slope for this reach is 0.0024 ft/ft.

3.3 Field Data Collection

Cross sections and pebble counts were measured at three locations within the Upper Salmon River Basin. These cross sections were intended to be representative of the lower, middle, and upper portions of the basins.

3.3.1 Data Collection Methodology

Cross section surveys and pebble counts were conducted by Trout Unlimited on November 16, 2016. Due to access and schedule restrictions, three cross sections were surveyed, mapped in Figure 13.

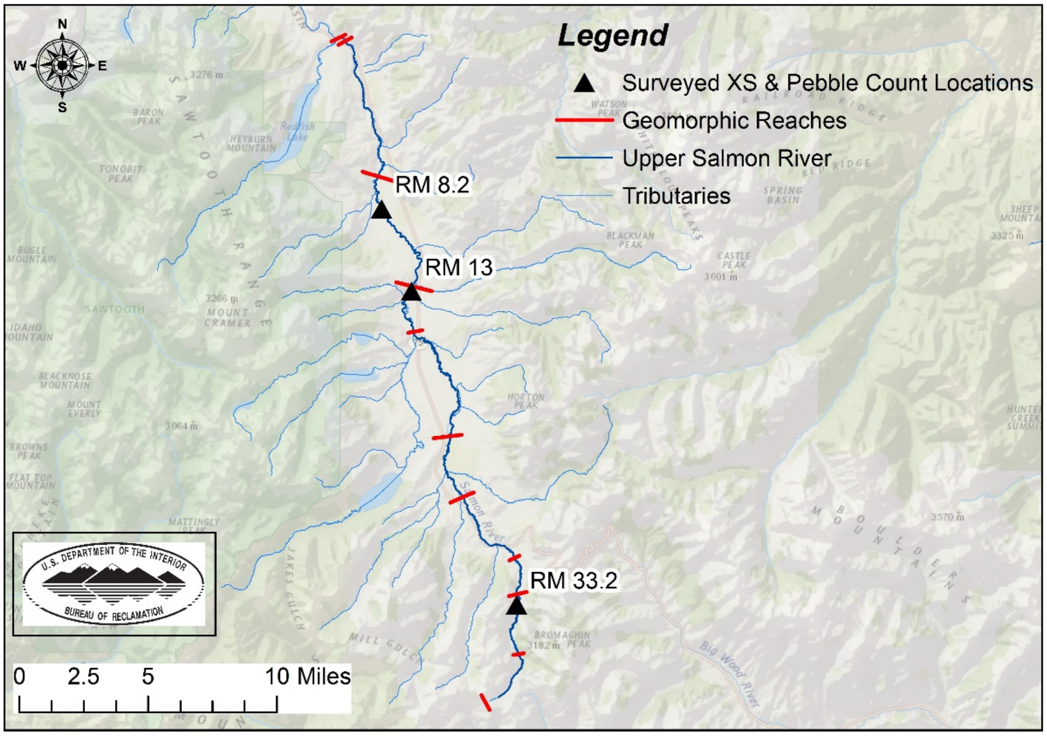

Figure 13.–Locations of cross section surveys and pebble counts performed by Trout Unlimited.

3.3.1.1 Cross Section and Profile Survey

At the surveyed cross sections, Trout Unlimited measured relative elevations using a LASERMARK LM800 Series electronic self-leveling rotary laser; from these data they report water surface elevations and channel slopes. An engineer's tape was utilized to measure station. Station and elevation were recorded at slope breaks with each transect. Water's edge and water surface elevation were also noted. Transects extended across the valley on both sides of the river to the low terrace, if possible. Transects did not extend to the low terrace when vegetation hindered the use of the laser or when the valley was wide. When the valley was wide, the distance to low terrace was estimated.

The channel slope was estimated at each site by measuring the elevation 150 ft upstream and 150 ft downstream of the site. The slope was then calculated based on the difference in elevation upstream and downstream of the site over the 300 ft segment. It is unknown whether the water surface or channel bottom slope was measured. . At RM 33.2 the channel slope was based on two measurements as beaver dams were located upstream and downstream of the cross section. One measurement was at the cross section, the second measurement 53 ft downstream.

3.3.1.2 Pebble Count Collection Methods

Pebble counts were performed to characterize the bed material. Three pebble counts were completed according to the Wolman Pebble Count Procedure (Wolman, 1954). The technique requires the user to measure the b-axis axis (Figure 14) of 100 random sediment particles within a geomorphic feature of interest (e.g. riffle, bar, etc.).

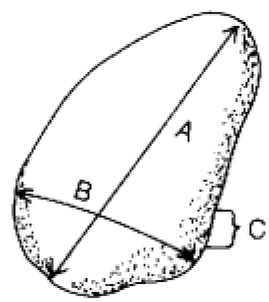

A = LONGEST AXIS (LENGTH)

B = INTERMEDIATE AXIS (WIDTH)

C = SHORTEST AXIS (THICKNESS)

Figure 14.–Pebble axis measurement (Harrelson et al., 1994 Fig. 60)

3.4 At-a-Station Hydraulic Calculations

3.4.1 At-a-Station Hydraulic Calculation Methods

At-a-station hydraulics were calculated at three cross sections mapped in Figure 13 in the Upper Salmon River Basin. Calculations were made for two flow conditions: 1-yr and 100-yr events. Many assumptions are made when performing at-a-station hydraulic calculations which are identified in the following section. Hydraulic properties were calculated utilizing Manning's equation Eq. (5) and the field data.

$$Q = \frac{1.49}{n} A R^{2/3} \sqrt{S} \tag{5}$$

Where:

- Q is the known discharge (cfs) for a specific flow event,
- n is the assumed Manning's roughness based on aerial imagery and (Chow, 1959),
- A is the calculated cross sectional area (sq. ft),
- R is the calculated normal hydraulic radius (ft), and
- S is the channel slope (ft/ft) measured in the field.

Manning's roughness was estimated based on aerial imagery and values documented in literature for similar site conditions. A sensitivity analysis was performed utilizing a minimum, normal, and maximum Manning's roughness in the main channel. Only the normal roughness were applied to the floodplain. The roughness values and theoretical channel descriptions are presented in Table 3.

Table 3.–Manning's *n* values

River Mile	Description	Minimum *n*	Normal *n*	Maximum *n*
8.2 13.0	Main channel – clean, winding, some pools and shoals, with weeds and stones	0.045	0.050	0.060
33.2	Main channel – clean, winding, some pools and shoals	0.033	0.040	0.045
8.2 (RB & LB) 13.0 (LB)	Floodplains – light brush and trees, in summer		0.060	
13.0 (RB)	Floodplains – high grass		0.035	
33.2 (RB & LB)	Floodplains – scattered brush, heavy weeds		0.050	

Based on the hydraulic properties, calculating critical grain size, Eq. (6), can estimate and compare to the measured median grain size to predict what flow magnitude is capable of mobilizing the bed-material at the cross section locations. All particles larger than the estimated critical grain size, D_c, were predicted to be mobile at that flow rate.

$$D_c = \frac{\gamma\, R\, S}{\gamma\, (s-1)\tau_c^*} \tag{6}$$

where γ = specific weight of water; *s* = relative specific density of sediment (2.65), τ_c^* = critical dimensionless Shield's number, assumed to be 0.04 and D_c = critical sediment size.

3.4.2 At-a-Station Hydraulic Calculation Uncertainty Discussion

At-a-station hydraulic calculations are a useful tool to calculate hydraulic properties at a single cross section for a given range of discharge values. However, it is not appropriate to spatially interpolate or extrapolate calculated values. Therefore, these cross sections do not represent the various reaches, they represent three unique locations in the basin. Discharge values at the cross sections were not measured; therefore, the analysis could not be calibrated. The lack of calibration data increases the uncertainty of the analysis. The calculated water stage may be higher or lower than the stage that would occur in the cross section for a given flow event.

Three key assumptions are made when calculating at-a-station hydraulics. First, the Manning's equation assumes uniform flow. Uniform flow is defined as flow velocity at a given instant of time that does not vary within a given length of channel (Chaudhry, 2008). This means that flow velocity does not change in space or in time. Furthermore, Manning's equation assumes normal depth conditions. Normal depth is a hydraulic term that assumes the slope of the water surface elevation is equal to the slope of the channel bottom. Both the water surface profile and channel bed profile were not measured in the field; therefore, we cannot verify if this assumption is valid. The methodology is valid, but the lack of calibration data increase the uncertainty of the analysis. The assumption of uniform flow and normal depth are hydraulic conditions that do not occur in natural systems, but are often assumed for calculation purposes.

Second, Manning's equation is contingent on an assumed Manning's roughness value. The roughness value is typically calibrated so that the model or calculations best reflect existing conditions. However, no calibration data was available for this study. A roughness value was assumed based on literature (Chow, 1959), aerial imagery, and sediment gradation information. A sensitivity analysis was performed. Calculations were made utilizing a minimum, normal, and maximum Manning's in-channel roughness based on literature values for similar site conditions.

Lastly, grain size mobility is only based on the critical grain size and the measured grain size (D_{50} and D_{84}). Often, there is a specific value of the dimensionless shear stress above which initiation of bed motion is assumed to begin. However, sediment motion is better thought of as a probabilistic process with the probability of motion increasing directly with shear stress (or dimensionless shear stress). Dimensionless shear stress value can vary by grain size, shape, sorting, packing (Buffington and Montgomery, 1997), channel slope (Lamb et al., 2008; Mueller et al., 2005), and sand fraction (Curran & Wilcock, 2005). For the critical grain size at incipient motion analysis, a critical dimensionless shear stress (Shield's number) of 0.05 was selected (Julien, 2010).

4 Results

The following sections describe the results of each of the following four analyses described in Section 3 – Methods:

- Flood-frequency estimates,
- Stream power calculations,
- Pebble counts distributions, and
- At-a-station hydraulic calculations.

4.1 Hydrologic Assessment Results

The results of the flood-frequency estimates are presented in the following sections.

4.1.1 Peak Flow Calculations at Gaged Locations

Table 4 and Figure 15 illustrate the results of the PeakFQ analysis at the four USGS gages within the Upper Salmon River Basin. The results from PeakFQ with uncertainty bounds are shown in Figure 16 through Figure 19. Irrigation diversion volumes were not incorporated into this assessment, as specific volumes and locations are unknown. However, many of the peaks occurred during irrigation season. Therefore, it is possible that the annual peak values are reduced.

Table 4.–Gage and flood frequency results, in cfs, from USGS stream gage locations.

Gage No.		Pole Creek (13292380)	Salmon River at RM 27.0 (13292280)	Valley Creek (13295000)	Salmon River below Valley Creek (13295500)
Recurrence Interval (years)	**% AEP**	**PeakFQ Flood Frequency Results (cfs)**			
1	**99.5**	21.4	45.9	342	1,157
1.5	**66.7**	58.9	127	846	2,761
2	**50**	70.8	150	998	3,224
2.33	**42.9**	76.2	160	1,067	3,432
5	**20**	99.2	202	1,356	4,288
10	**10**	117	232	1,578	4,930
25	**4**	139	266	1,843	5,682
50	**2**	154	288	2,032	6,205
100	**1**	169	309	2,212	6,700

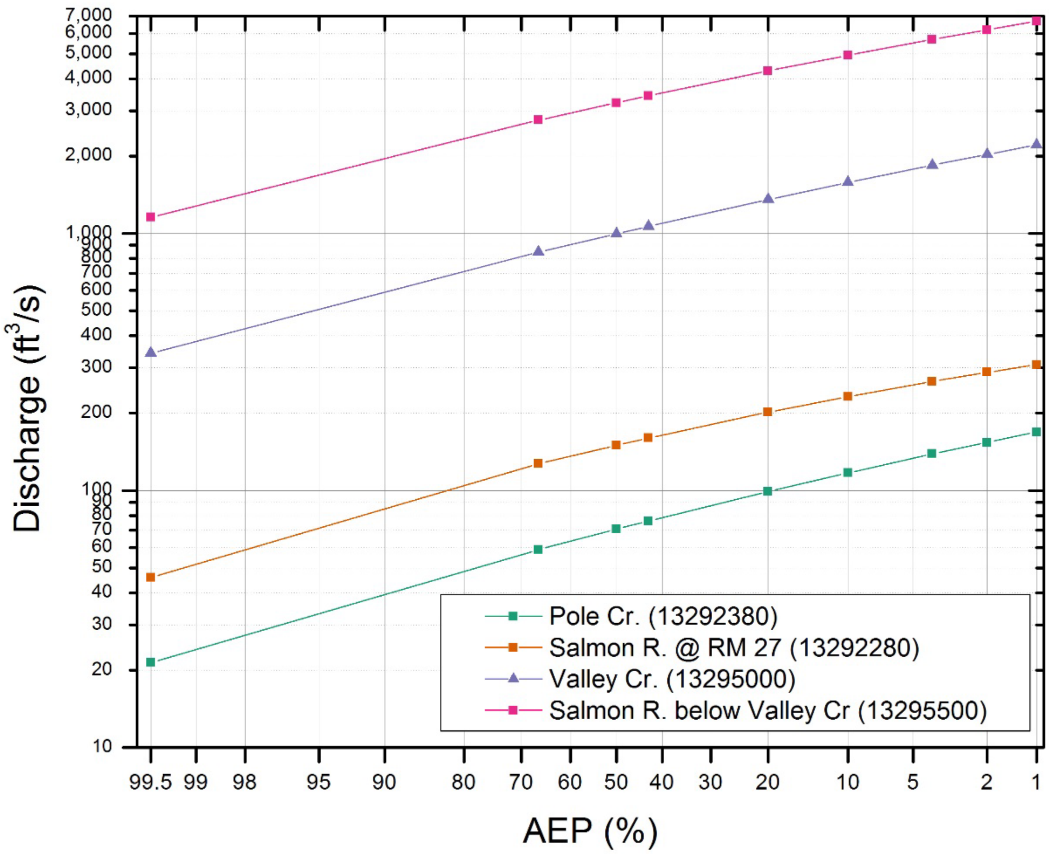

Figure 15.–Peak discharge values plotted across annual exceedance probability (AEP).

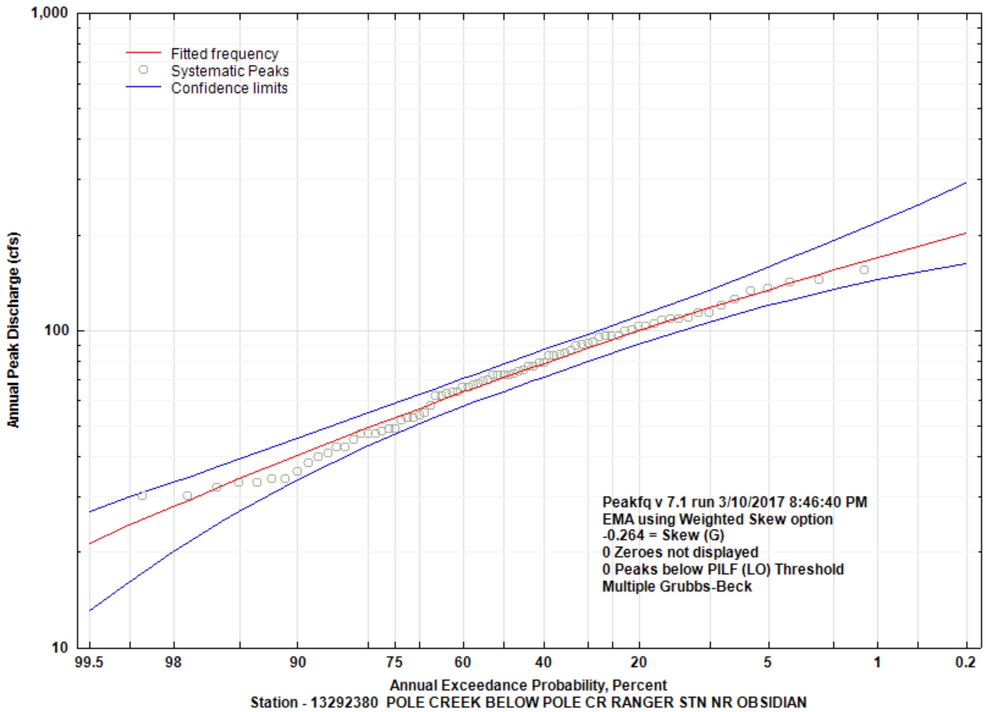

Figure 16.–Annual Exceedance Curve for USGS gage on Pole Creek (13292380).

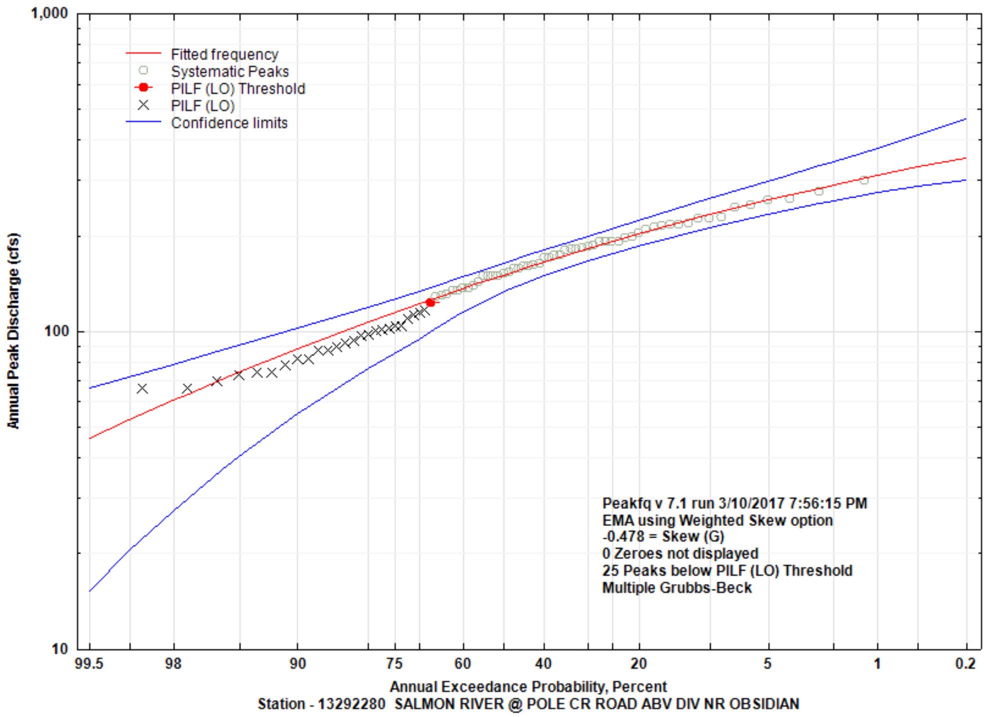

Figure 17.–Annual Exceedance Curve for USGS gage on Salmon River at RM 27.0 (13292280). Potentially influential low flows (PILF) are plotted with x's while systematic peaks are plotted with circles.

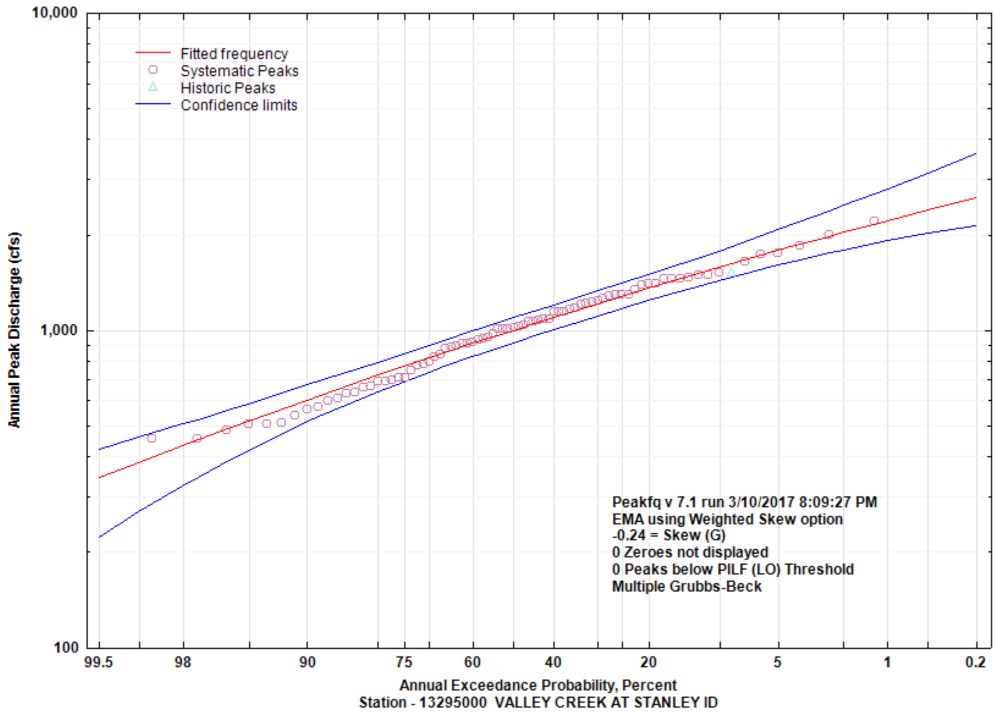

Figure 18.–Annual Exceedance Curve for USGS gage on Valley Creek (13295000).

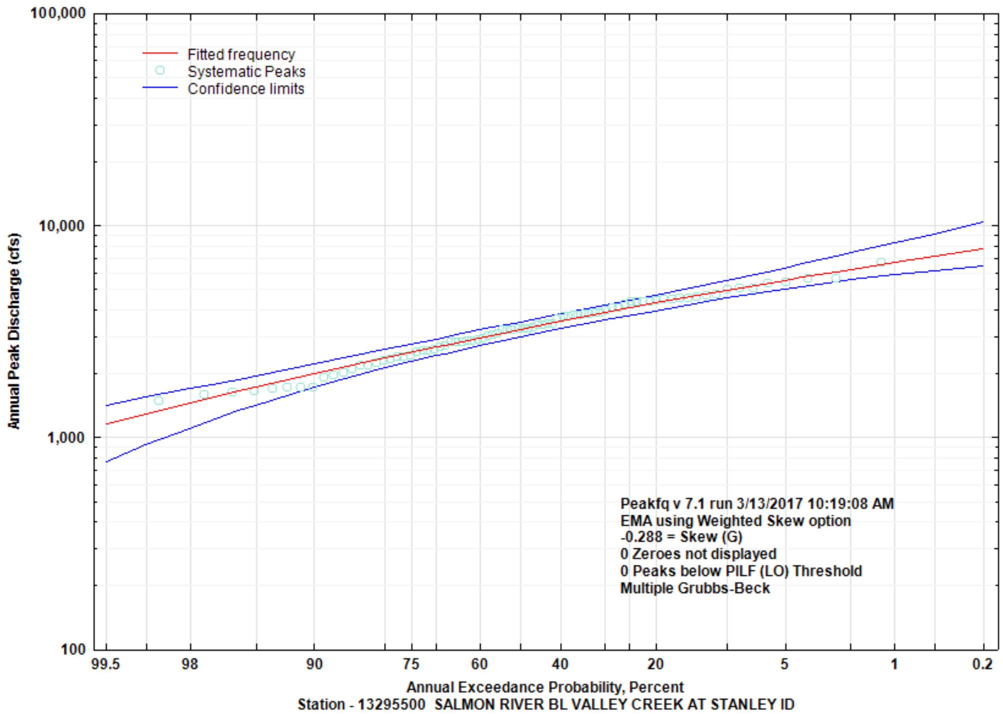

Figure 19.–Annual Exceedance Curve for USGS gage on Salmon River below Valley Creek (13295500).

4.1.2 Peak Flow Calculations at Ungaged Locations

Equations 1, 2, and 3 were applied to ungaged locations based on their location relative to the three USGS gages. 1) For locations in between gages 13295000 (Salmon River below Valley Creek) and 13292280 (Salmon River at Pole Creek), Eq. 1 was applied; 2) Eq. 2 was applied upstream of gage 13292280; 3) Equation 3 was only applied to the one location at RM 36.0. Results are presented in Figure 20 and Table 5. The values estimated utilizing Eq. 3, the regional regression equations, are slightly larger than the values seen downstream at RM 32.5. This is not necessarily realistic, and further investigation in the hydrology in geomorphic reach 1 would be required during future phases of work. The largest increase in flood frequency discharge values is seen at RM 15.3, where Alturas Lake Creek flows into the Upper Salmon River. It is the largest contributing tributary with a drainage area of 70 mi^2.

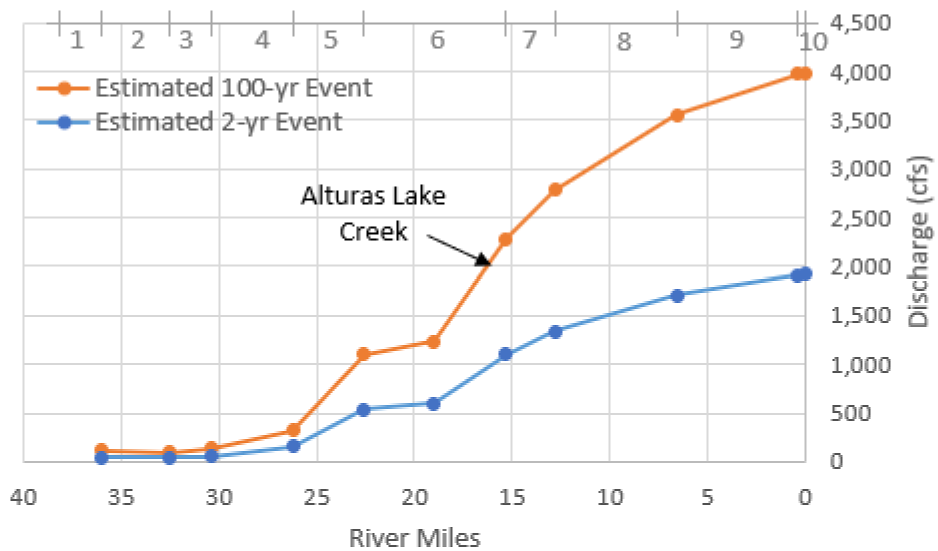

Figure 20.–Estimated discharge values for the 2-yr and 100-yr event. Geomorphic reaches are labeled at the top.

Table 5.–Recommended Peak Discharge Values along the Main Salmon River. Cells are color coded based on calculation method.

RM	DA (mi²)	Reach	Flood Frequency Values (cfs)								
			1	1.5	2	2.33	5	10	25	50	100
0	304	10	685	1,643	1,919	2,043	2,554	2,936	3,383	3,694	3,987
0.4	303	9	684	1,639	1,914	2,038	2,547	2,928	3,374	3,684	3,977
6.6	272	8	610	1,464	1,711	1,821	2,276	2,617	3,015	3,292	3,553
12.8	214	7	477	1,148	1,342	1,428	1,786	2,053	2,365	2,582	2,786
15.3	177	6	389	940	1,099	1,170	1,463	1,682	1,937	2,114	2,281
19	99	6	207	510	597	636	796	915	1,053	1,148	1,238
22.6	88	5	184	453	531	566	708	814	937	1,022	1,101
26.2	30	4	48.1	132	156	167	210	241	276	300	321
30.4	14	3	16.6	45.8	55.0	59.2	77.1	91.0	108	120	132
32.5	10	2	12.3	33.9	40.8	43.9	57.1	67.5	80.0	88.9	97.5
36	3.8	1		35	43	45	61	73	89	100	114

Eq. 1 – Interpolation between Salmon River gages

Eq. 2 - Pole Creek (13292380)

Eq. 3 - Predictive Regression Equations

4.2 Stream Power Analysis Results

Stream power was calculated for four flow events (1-, 2-, 10-, and 100-year recurrence intervals) for twelve reaches along the Upper Salmon River. Discharge increases with increasing drainage area in the downstream direction as shown in Figure 21. A significant increase is seen at RM 15.4, where Alturas Lake Creek flows into the Upper Salmon River. Moving downstream, peak flow increases at a higher rate for less frequent events relative to more frequent, smaller events. Figure 22 shows the longitudinal profiles and average reach slope. The slope is significantly higher for the upstream-most 2.3 miles (RM 36.0 – RM 38.3) and decreases to an average of 0.0019 ft/ft for the remaining 36 miles. The slope within the downstream river reaches varies from a maximum slope of 0.0030 for geomorphic reach 4 to a minimum slope 0.0012 for geomorphic reach 7 and 9.

In general, total stream power decreases between RM 37.0 and 32.5 and then increases between RM 32.5 and RM 6.6 along the Upper Salmon River as shown in Figure 23 and Table 6. The irregular trend in stream power demonstrates that neither slope nor discharge consistently dictate sediment transport capacity. Slope is relatively high in the upstream reaches where the contributing drainage area is small; therefore, slope controls stream power in the headwaters. The high stream power values relative to low discharge values suggests that this may be a high sediment transport zone. Stream power reaches a low at RM 32.5 and 30.4 as slope decreases and discharge values remain low. The decrease in stream power suggests a depositional zone. Beginning at RM 26.2, stream power increases irregularly.

Dips in stream power are observed at RM 19.0 and 0.4, when the decrease in slope is greater than the increase in discharge.

The D_{50} for the three cross-section locations where data was available was overlaid on the stream power plot. For a given system an increase in either slope or discharge (stream power) will increase the sediment grain size (Lane, 1955). The particle size at RM 33.2 is relatively smaller than at RM 8.2 and 13, which corresponds to the lower stream power calculated at that site than higher in the study area. To further analyze sediment transport capacity additional data would be needed on sediment sample sizes to capture variability within and among reaches, refined analysis on discharge peaks, diversions affects during periods of sediment transport, and higher accuracy channel slope data could be incorporated

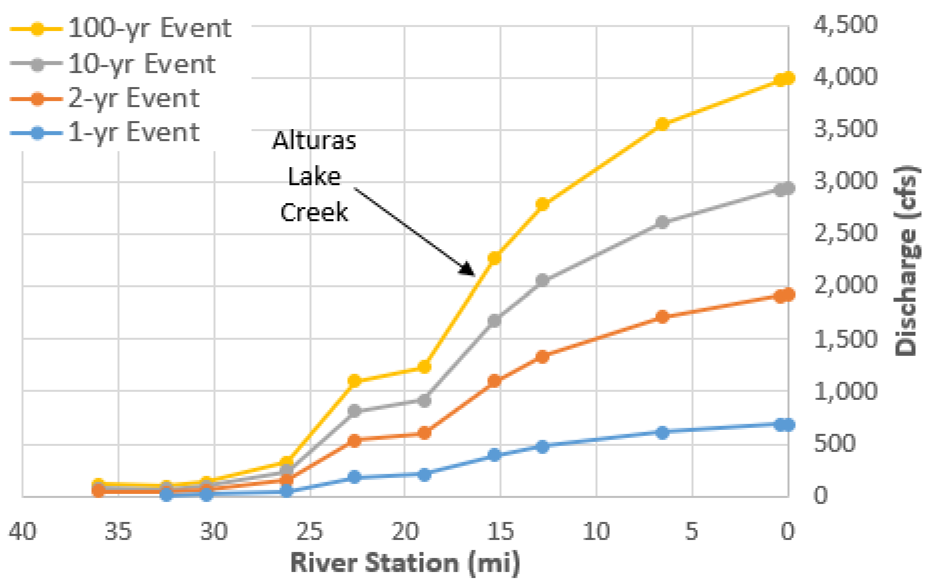

Figure 21.–Estimated discharge values along the Upper Salmon River.

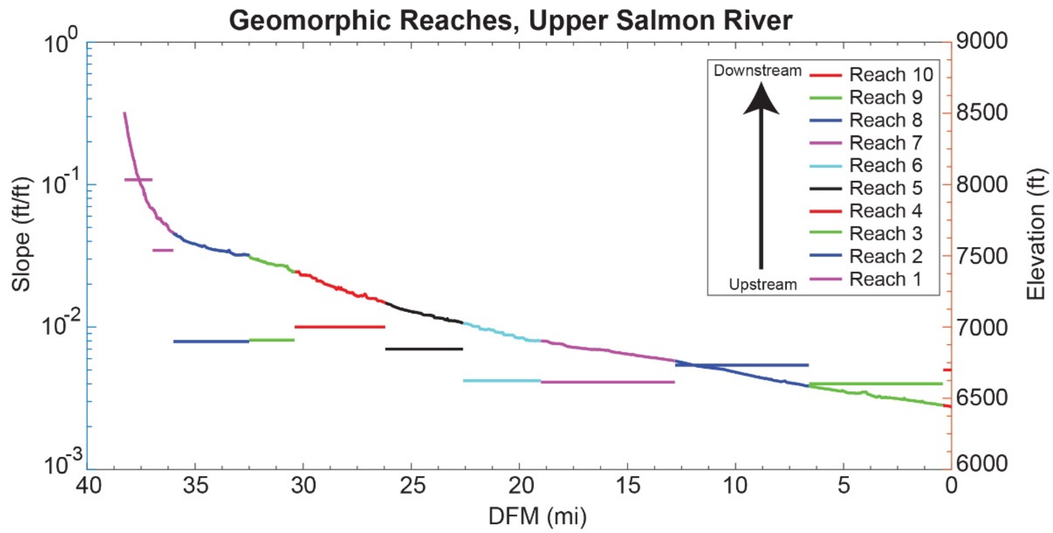

Figure 22.–Upper Salmon River longitudinal profile (blue solid line) and slope (orange dotted lines) by river mile. Note: slope is plotted on a logarithmic scale.

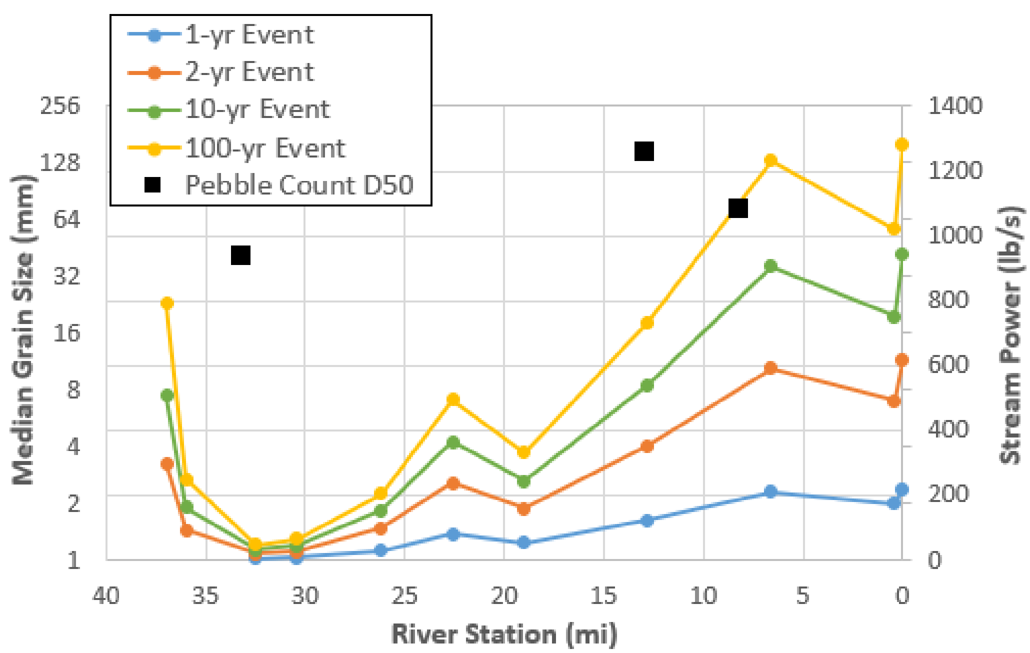

Figure 23.–Stream power and pebble count results. The median grain size (*D_{50}*) is plotted on the left vertical axis applying a log base 2 scale. Stream power is presented on the right vertical axis for four flood events.

Table 6.–Stream Power Analysis Results

			1-yr Event		2-yr Event		10-yr Event		100-yr Event	
Geo. Reach No.	Station (mi)	Slope	Q (cfs)	Ω (lb/s)	Q (cfs)	Ω (lb/s)	Q (cfs)	Ω (lb/s)	Q (cfs)	Ω (lb/s)
1	37.0	0.1080			43	299	73	508	114	790
1	36.0	0.0345			43	95	73	162	114	252
2	32.5	0.0079	12	6	41	21	67	34	97	49
3	30.4	0.0081	17	9	55	29	91	47	132	68
4	26.2	0.0100	48	31	156	100	241	155	321	206
5	22.6	0.0070	184	83	531	239	814	366	1,101	495
6	19.0	0.0042	207	56	597	161	915	247	1,238	334
7	12.8	0.0054	477	125	1,342	353	2,053	540	2,786	733
8	6.6	0.0040	610	211	1,711	593	2,617	907	3,553	1,232
9	0.4	0.0050	684	176	1,914	492	2,928	752	3,977	1,021
10	0.0	0.1080	685	220	1,919	616	2,936	942	3,987	1,280

4.3 Pebble Count Results

Pebble counts were completed at three cross sections to characterize the bed material. Tabular results are presented in Table 7, graphical cumulative frequency results are presented in Figure 24. The D_{84}, D_{50}, D_{16}, and mode were calculated for this analysis. The D_{50} is the median grain size and the D_{84} and D_{16} are the 84th, and 16th percentile utilized to represent the coarse and fine sediment fraction, respectively. The majority of the sediment could be classified as cobble (64 – 256 mm) or boulders (> 256 mm). Particles ranging from silt (< 1 mm) to boulders 325 mm in diameter were observed.

Like the Lemhi River Basin, the coarsest particles were observed within the middle reach (RM 13.0). The pebble count at the upstream reach (RM 33.2) produced the finest sediment.

Table 7.–Pebble Count Results

Location	D_{84} (mm)	D_{50} (mm)	D_{16} (mm)
RM 8.2	138	73	34
RM 13.0	219	143	51
RM 33.2	70	40	17

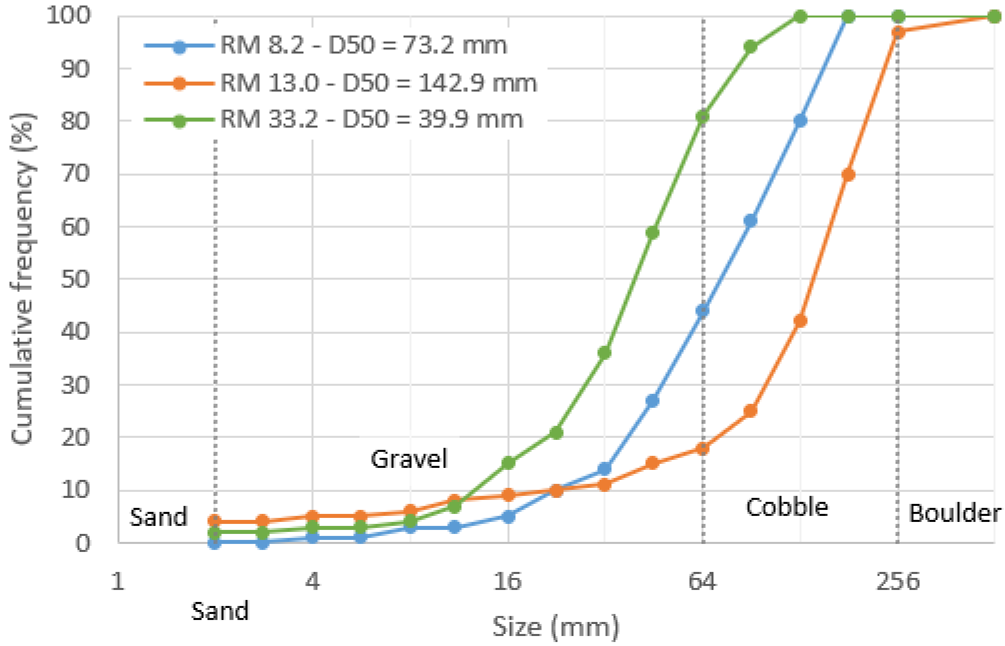

Figure 24.–Pebble count results at all three sites.

4.4 At-a-Station Hydraulic Results

At-a-station hydraulic computations were completed at three cross sections to estimate what magnitude discharge is needed to mobilize bed-material and overtop into the floodplain. The results are presented in Table 8 and Table 9 for the hydraulic analysis and bed mobility calculations, respectively. Water surface elevation for the two flow events at each cross section are presented in Figure 26 through Figure 28.

The results show the channel is confined and the 100-yr event does not inundate the floodplain at RM 13.0 and RM 33.2. At RM 8.2, flood inundation occurs during the 100-yr event. As shown in Figure 26, the topography does not include the entire 100-yr flood width. Given these conditions, at-a-station hydraulic calculations were performed assuming vertical walls at the edges of the cross section. This assumption may result in an overestimation of shear stress and velocity. There are several points in the floodplain at RM 8.2 that are 1 to 3 feet lower than the floodplain (at approximately 44.3 ft). Based on aerial imagery (Figure 25), the low points appear to be smaller channels within the floodplain. Assuming that these smaller channels are hydraulically connected to the main channel, the 1-yr event would not be contained within the channel.

Sediment mobility results are presented in Table 9. The grain sizes are identified as mobile if they are smaller than the critical grain size for a given discharge. The last two columns of Table 9 indicate when the critical grain size is larger than the measured D_{50} and D_{84}. Sediment mobility only occurs during the 100-yr event at

RM 33.2. Results indicate that the median grain size is stable for the remaining analyzed locations and flow events. D_{84} is not mobilized at any of the three cross sections.

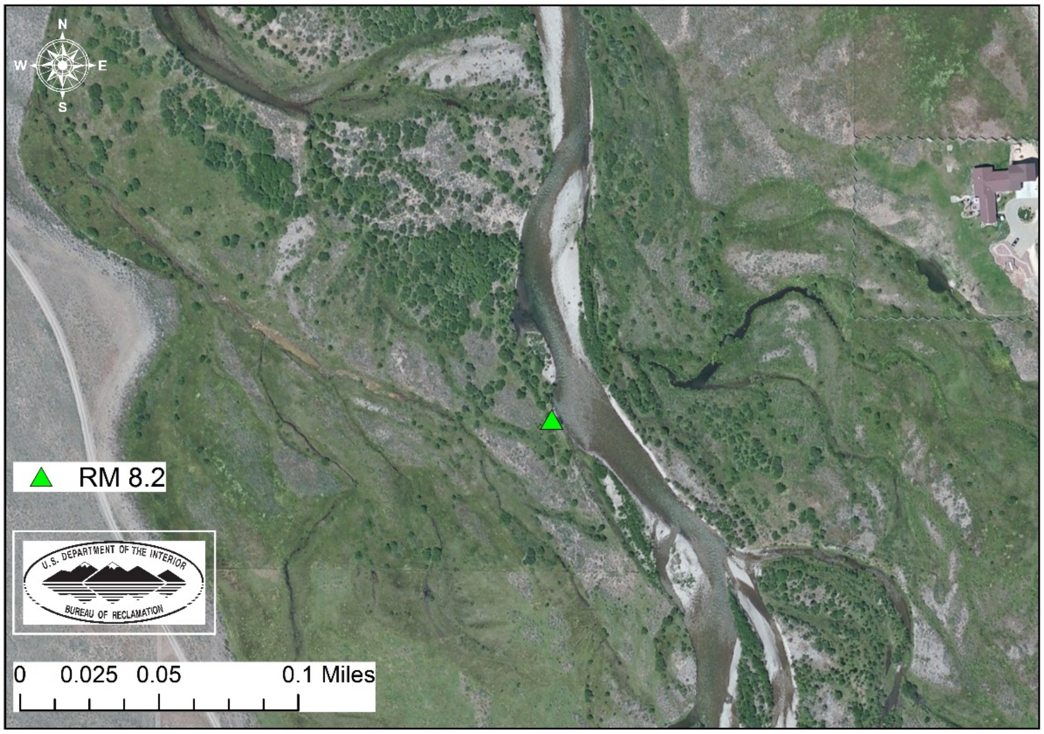

Figure 25.–Aerial imagery at RM 8.2.

Table 8.–At-a-station hydraulic calculation results

	Input Data			Calculated Hydraulic Parameters									
River Mile	*n*	Channel Slope (ft/ft)	Discharge (ft^3/s)	Flow Area (ft^2)	Wetted Perimeter (ft)	Hydraulic Radius (ft)	Top Width (ft)	Normal Depth (ft)	Critical Depth (ft)	Critical Slope (ft/ft)	Velocity (ft/s)	Froude Number	Flow Type
RM 8.2	0.045	0.0064	597	271	231	1.2	228	2.7	1.6	0.053	2.2	0.36	Subcritical
RM 8.2	0.050	0.0064	597	254	221	1.2	219	2.6	1.6	0.045	2.4	0.38	Subcritical
RM 8.2	0.060	0.0064	597	245	216	1.1	214	2.6	1.6	0.042	2.4	0.40	Subcritical
RM 8.2	0.045	0.0064	3,457	1230	727	1.7	720	4.8	3.5	0.048	2.8	0.38	Subcritical
RM 8.2	0.050	0.0064	3,457	1213	727	1.7	720	4.7	3.5	0.046	2.9	0.39	Subcritical
RM 8.2	0.060	0.0064	3,457	1205	727	1.7	720	4.7	3.5	0.045	2.9	0.39	Subcritical
RM 13.0	0.045	0.0089	487	131	101	1.3	101	1.8	1.4	0.030	3.7	0.57	Subcritical
RM 13.0	0.050	0.0089	487	140	102	1.4	101	1.9	1.4	0.038	3.5	0.52	Subcritical
RM 13.0	0.060	0.0089	487	157	103	1.5	102	2.0	1.4	0.054	3.1	0.44	Subcritical
RM 13.0	0.045	0.0089	3,152	460	142	3.3	140	4.5	3.6	0.022	6.9	0.67	Subcritical
RM 13.0	0.050	0.0089	3,152	495	146	3.4	144	4.8	3.6	0.026	6.4	0.61	Subcritical
RM 13.0	0.060	0.0089	3,152	559	153	3.7	151	5.2	3.6	0.037	5.6	0.52	Subcritical
RM 33.2	0.033	0.012	12.0	5.2	16.9	0.3	17	0.5	0.4	0.025	2.3	0.72	Subcritical
RM 33.2	0.040	0.012	12.0	5.9	17.2	0.3	17	0.5	0.4	0.037	2.0	0.61	Subcritical
RM 33.2	0.045	0.012	12.0	6.4	17.5	0.4	17	0.5	0.4	0.046	1.9	0.55	Subcritical
RM 33.2	0.033	0.012	94.7	19.6	20.6	1.0	20	1.2	1.1	0.017	4.8	0.86	Subcritical
RM 33.2	0.040	0.012	94.7	22.2	21.0	1.1	20	1.4	1.1	0.025	4.3	0.72	Subcritical
RM 33.2	0.045	0.012	94.7	23.9	21.2	1.1	21	1.4	1.1	0.032	4.0	0.65	Subcritical

Table 9.–At-a-station bed mobility calculation results

	Input Data						Bed Mobility Calculations			
River Mile	*n*	Channel Slope (ft/ft)	Flow Event	Discharge (ft^3/s)	D_{50} (mm)	D_{84} (mm)	Shear Stress (lb/sq.ft)	Critical Diameter (mm)	Is D_{50} mobile?	Is D_{84} mobile?
RM 8.2	0.045	0.0064	1 - yr	597	73	138	0.47	28	no	no
RM 8.2	0.050	0.0064	1 – yr	597	73	138	0.46	27	no	no
RM 8.2	0.060	0.0064	1 – yr	597	73	138	0.46	27	no	no
RM 8.2	0.045	0.0064	100 - yr	3,457	73	138	0.67	40	no	no
RM 8.2	0.050	0.0064	100 - yr	3,457	73	138	0.67	39	no	no
RM 8.2	0.060	0.0064	100 - yr	3,457	73	138	0.66	39	no	no
RM 13.0	0.045	0.0089	1 - yr	487	143	219	0.72	43	no	no
RM 13.0	0.050	0.0089	1 – yr	487	143	219	0.77	45	no	no
RM 13.0	0.060	0.0089	1 – yr	487	143	219	0.85	50	no	no
RM 13.0	0.045	0.0089	100 - yr	3,152	143	219	1.80	107	no	no
RM 13.0	0.050	0.0089	100 - yr	3,152	143	219	1.89	112	no	no
RM 13.0	0.060	0.0089	100 - yr	3,152	143	219	2.03	120	no	no
RM 33.2	0.033	0.0123	1 - yr	12.0	40	70	0.24	14	no	no
RM 33.2	0.040	0.0123	1 – yr	12.0	40	70	0.26	15	no	no
RM 33.2	0.045	0.0123	1 – yr	12.0	40	70	0.28	17	no	no
RM 33.2	0.033	0.0123	100 - yr	94.7	40	70	0.73	43	yes	no
RM 33.2	0.040	0.0123	100 - yr	94.7	40	70	0.81	48	yes	no
RM 33.2	0.045	0.0123	100 - yr	94.7	40	70	0.87	51	yes	no

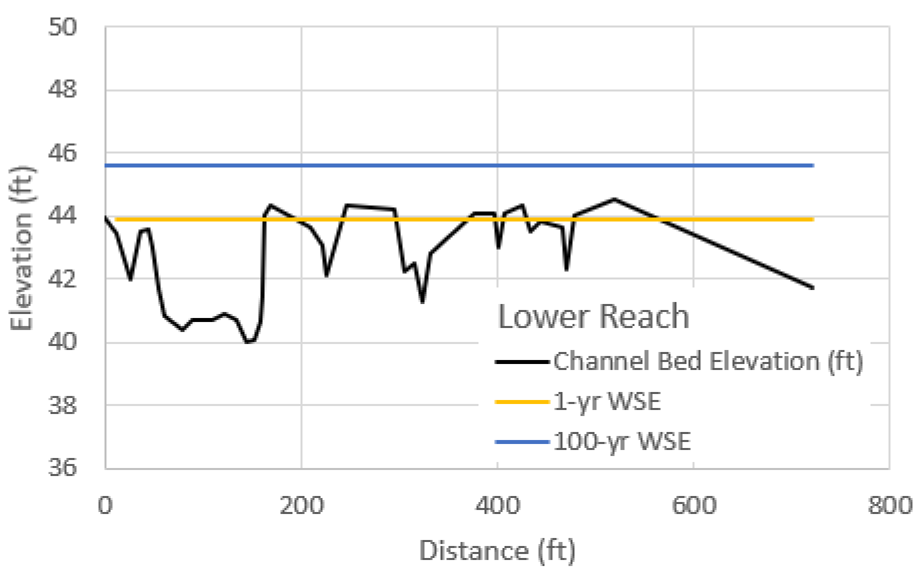

Figure 26.–Water surface elevation for each event, assuming normal Manning's *n* values, at RM 8.2. As the survey does not cover the 100-yr flood extent, vertical walls were assumed at the edges of the cross section.

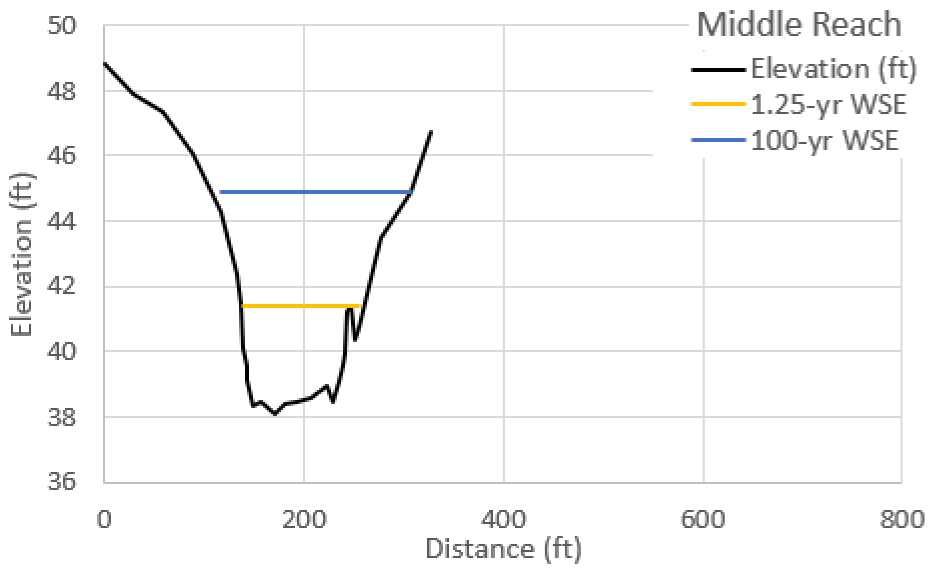

Figure 27.–Water surface elevation for each event, assuming normal Manning's *n* values, at RM 13.0.

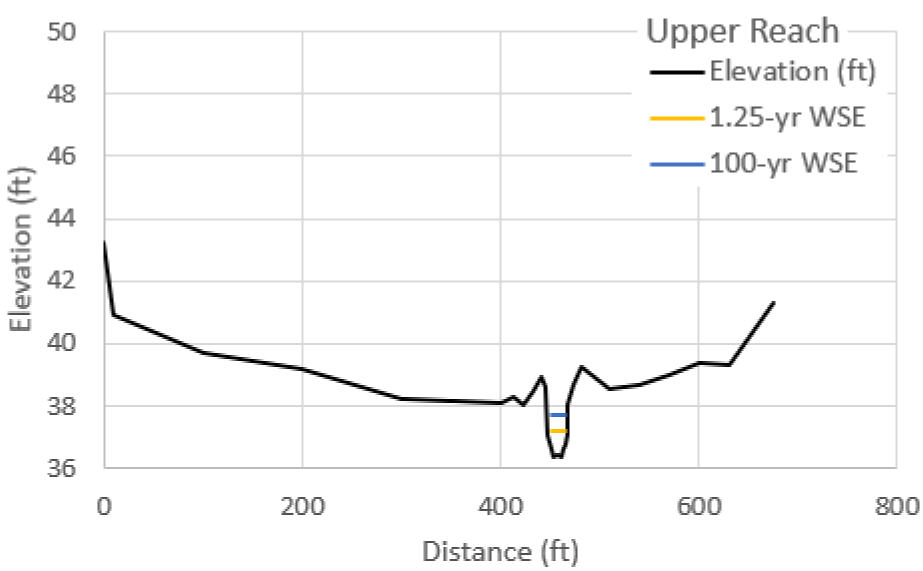

Figure 28.–Water surface elevation for each event, assuming normal Manning's *n* values, at RM 33.2.

5 Data Needs for Future Hydraulic Modeling and Recommendations

This study utilized a combination of measured data, field observations, and surrogate parameters to inform an Integrated Rehabilitation Assessment. The assessment is intended to identify watershed-scale characteristics and select optimal project locations for further study and channel rehabilitation. The recommendations provided in this section are geared towards hydraulic modeling at the reach or project scale.

Flow depth and velocity are often key parameters to analyze the quality of fish habitat in a river reach. Hydraulic modeling informs potential habitat improvement projects and provides important tools for project planning. Hydraulic model results can provide a detailed understanding of the existing conditions in regard to Endangered Species Act (ESA) listed salmonid physical habitat conditions. The hydraulic model results for depth, velocity, and shear stress can provide input data for Habitat Suitability Index (HSI) modeling.

The selection of a hydraulic model is dependent on the data available, the complexity of the channel and floodplain terrain, and the study questions that need to be addressed with the model. For the Upper Salmon River Basin Integrated Rehabilitation Assessment, a steady two-dimensional (2D) hydraulic model is recommended. A 2D model (as compared to a one-dimensional, 1D, model) better informs parameters necessary for habitat improvement such as: lateral differences in velocity and depth, multi-threaded channels, and floodplain connectivity. A 1D is limited when calculating the above parameters. 1D calculations are sufficient in uniform, single-threaded channels. It may be sufficient to apply a 1D model to evaluate the hydraulics of large flood events, where the influence of geomorphic features and channel complexity is not significant. A 2D model better captures floodplain connectivity in channels with multiple flow paths and complex landforms. This is important to habitat rehabilitation within the project basin as the Upper Salmon River is often multi-threaded with geomorphic features. Furthermore, side channels, large wood, and pools are often incorporated into rehabilitation efforts. These features would be poorly represented in 1D model. Furthermore, the data collection effort necessary to inform both a 1D and 2D model are very similar. Therefore, a 2D model is recommended for future analysis for habitat rehabilitation effort. Data necessary for numerical modeling include:

1. **Topographic and bathymetric data (Section 5.1),**
2. Flow values of interest (typically includes low flow values, mean monthly flows, and peak flow events) and **Flow change locations and quantities (changes in main channel flow, tributary inputs, diversions, returns, etc. , Section 5.2),**

3. **Field reconnaissance and documentation of reach site conditions including sediment data to inform channel roughness and potential mobility (Section 5.3),**
4. **Measured water surface elevation for known discharge events for model calibration (Section 5.4).**

Bold values remain data gaps and each are discussed in more detail in the following sections.

5.1 Topographic and Bathymetric Data

Existing data sets include free 1/3 arc-second DEM topographic data. The resolution is 25 ft by 25 ft cells. Interferometric Synthetic Aperture Radar (InSAR) is available for purchase for the project basin. The resolution is 16.4 ft by 16.4 ft cells. These data sets would provide surfaces too coarse for hydraulic modeling recommended for reach-scale habitat rehabilitation studies.

Flying bathymetric LiDAR (Green LiDAR) is a newer technology, which determines the water depth by measuring a time delay between a transmission pulse and return signal. Laser pulses operate at two frequencies, a lower frequency which reflects off the water surface and a higher frequency which can penetrate the water column, reflecting off the bottom. Limiting factors of airborne bathymetric LiDAR include: water clarity, water depth, water turbulence, vegetation, bottom material, weather, and background light (Muirhead & Cracknell, 1986). The Upper Salmon River is relatively shallow with clear water, which can be measured at a vertical accuracy level of up to 15 cm (Gao, 2009).

Topographic LiDAR, bathymetric LiDAR, or a combination should be flown in the fall/winter season in the Upper Salmon River Basin. At this time the trees/shrubs have shed their leaves and snowpack has not yet formed. However, it would be most economical to fly LiDAR for all basins (Upper Salmon, Pahsimeroi, and Lemhi Rivers) at the same time. The recommended time for the Pahsimeroi River Basins are when river stage is the lowest, late-July and August. The canopy will be in leaf-on conditions. None of the three basins are heavily vegetated; therefore, the majority of the landscape will not be obstructed by leaf cover. For vegetated areas in the basins, a dense point cloud can capture the ground elevation through the canopy. A minimum point density of 7 points per square meter (pts/m^2) is recommended. An optimal collection density would be 12 pts/m^2. LiDAR data can be converted into a surface by linearly interpolating between measurement points.

If bathymetric LiDAR is not flown, boat or manual surveys are two alternatives for collecting bathymetric data. A boat survey involves floating the project area with an acoustic Doppler current profiler (ADCP) mounted to the boat. The boat would float cross sections and longitudinal profiles of the project reach collecting bathymetric data. Several longitudinal profiles are preferred, but not always possible based on site conditions. If conditions do not allow for multiple longitudinal profiles, cross sections should be surveyed every 5-7 channel widths. A surface can be created from the data set by linearly interpolating between surveyed points. A boat survey would need to occur during the high flow season, when flow depths are high enough for the instrument operation and boat access. A minimum of 1ft water depth is required for the ADCP to operate. If depths are approximately 1 ft in the entire project area, a manual survey may be more efficient.

A manual survey would require a crew to survey several cross sections along the project reach (every 5-7 channel widths) and a longitudinal profile. This method may be cost prohibitive depending on the size and resolution of the desired data set. Manual surveys should take place during the low flow season for the safety of the crew.

With a boat or manual survey, it is impractical to sample with as fine of a resolution as a LiDAR data set. Therefore, the measured point cloud will be coarse and the majority of the surface will be estimated via linear interpolation. This methodology increases uncertainty in the results. Both the boat bathymetric survey and manual survey could be tied into topographic LiDAR data.

5.2 Hydrologic Data Gaps

The purpose of the hydrologic assessment was to identify available gage data and provide appropriate flood frequency discharge values to inform existing and future assessment efforts including hydraulic modeling. However, low flow discharges drive habitat suitability analyses and fish use. The only low flow discharge estimated in this study was the 7Q10. Monthly minimum flows, fish passage and moderate flow discharge values should be estimated throughout the basin in future phases of work to better estimate habitat suitability.

The hydrologic assessment did not directly compensate for irrigation losses. If the diversions are in operation, it is possible the flood-frequency discharge values calculated in this report are overestimated. One of the hydrology data gaps is an understanding of the locations, volume, and timing of many diversions along the Upper Salmon River. Hydraulic modeling without this information would not reflect current conditions. Another data gap is the incoming flow rates from each tributary. IDWR provides gages on many of the Upper Salmon River tributaries, but many are still ungaged. If the hydraulic model were to include one of the ungaged tributaries, its flow contribution would be a data gap. In areas where wetlands and lakes attenuate floods and groundwater becomes influential, hydrologic modeling (HEC-HMS, SWMM, MIKE SHE, etc.) may be beneficial.

5.3 Sediment Data Gaps & Discussion

The purpose of the stream power assessment and at-a-station hydraulics was to gain a basin scale understanding of the sediment transport capacity in the Upper Salmon

River Basin. Stream power calculates the capacity of each geomorphic reach based on calculated hydrology and approximate channel slope. The sediment transport regime is a function of sediment supply, grain size distribution, channel geometry, and water surface slope. Knowledge of these unknown variables is necessary to better understand the actual trends in sediment transport within the Upper Salmon River. Other factors that could inform sediment transport capacity include roughness changes, floodplain connectivity or lack thereof, and/or channel geometry (i.e.: higher width-to-depth ratios).

Based on the available data, results regarding the sediment transport regime were inconclusive. More data are necessary to identify supply, transport, and depositional reaches. Numerical modeling can inform sediment transport analysis. Utilizing the model results, dimensionless shear stress and critical grain diameter can assist in assess the potential geomorphic change (erosion/deposition) and identify areas of minimal and vigorous sediment transport.

5.4 Data Needs for Hydraulic Model Calibration

If hydraulic models are developed in future studies, correlated discharge and water surface elevation data should be collected to allow calibration, which reduces model uncertainty and improves accuracy. The number of discharge measurements is dependent on the project area. One discharge measurement is required if there are no tributaries or diversions within the project area. If there are tributary confluences or diversions, flow measurements are required at the upstream model extent and at each confluence/diversion. However, multiple measurements can inform gains/losses within the project reach. Data are typically collected during two events: high flow (during spring runoff) and low flow (during peak irrigation season). These data are used to inform Manning’s roughness in the channel.

Both high and low flow calibration can be useful in better understanding the hydraulics at a site. During high flow events, form roughness dominates resulting in a lower roughness value, on average. Particle roughness dominates at low flow events, likely resulting in a higher roughness value.

Documentation of site conditions with ground photos could be utilized to inform model roughness delineation and values. Infrastructure locations and impacts on channel geometry that could affect hydraulics and floodplain connectivity need to be recorded. Topographic characteristics of the floodplain and channel must also be mapped. Examples of these features include terraces, pools, riffles, etc.

6 Conclusions

The information provided in this report is intended to inform an Integrated Rehabilitation Assessment of the Upper Salmon River Basin, whose goal is to characterize watershed-conditions within the river basin while providing context for future analyses and potential rehabilitation projects. Peak flow estimations, stream power assessment, and hydraulic calculations at three cross-sections were accomplished to provide a coarse level understanding of the relative characteristics between geomorphic reaches.

The Upper Salmon River flow regime is snowmelt dominated and contains mountain lakes that modify water, sediment, and nutrient fluxes in the basin. Diversions are located along the entire 38.3 miles of the study area, but locations and volumes of water being diverted is currently not documented in this study. Flood-frequency peak flows were estimated at thirteen sites within the project area utilizing a drainage area ratio method and assuming all diversions were not operational.

The stream power assessment concluded that the upper mile and lower half of the basin has a relatively higher energy compared to remainder of the basin, which could indicate a higher capacity to transport sediment. There is insufficient data to compare this analysis with sediment measurements in the basin. The slope for RM 36 – 38.3 is much higher than the rest of the basin but discharge is low because of the limited drainage area, resulting in a relatively higher stream power. The slope remains between 0.108 ft/ft and 0.004 ft/ft within the remaining downstream 36 miles of the study area. However, discharge increases within increasing drainage area, resulting in higher stream power values downstream of Alturas Lake Creek inlet.

The at-a-station hydraulic results were calculated for three individual cross sections. While these results can predict floodplain inundation and sediment mobility at that specific location, it is not appropriate to apply the results to the remainder of the reach. Results show that floodplain inundation does not occur at the surveyed cross sections at RM 13.0 and 33.2. At RM 8.2, the floodplain is inundated at the 100-yr event, but results are inconclusive for the 1 yr event. Sediment mobility results show that the bed (both D_{50} and D_{84}) is stationary during the 1-yr events. The bed is also stationary during the 100-yr event at RM 8.2 and 13.0. At RM 33.2, the D_{50} is mobilized during the 100-yr event.

7 References

Arp, C., Gooseff, M., Baker, M., & Wurtsbaugh, W. (2006). Surface-water hydrodynamics and regimes of a small mountain stream-lake ecosystem. *Journal of Hydrology, 329*, 500-513. doi:10.1016/j.jhydrol.2006.03.006

Arp, C., Schmidt, J., Baker, M., & Myers, A. (2007). Stream geomorphology in a mountain lake district: hydraulic geometry, sediment sources and sinks, and downstream lake effects. *Earth Surface Processes and Landforms, 32*, 525-543. doi:10.1002/esp.1421

Berenbrock, C. (2002). *Estimating the magnitude of peak flows at selected recurrence intervals for streams in Idaho: US Geological Survey Water-Resources Investigation Report.*

Chaudhry, M. (2008). *Open-Channel Flow* (2nd ed.). New York, NY: Springer Science.

Chow, V. (1959). *Open-Channel Hydraulics.* New York: McGraw-Hill Book Company, Inc.

Curran, J., & Wilcock, P. (2005). Effect of sand supply on transport rates in a gravel-bed channel. *Journal of Hydraulic Engineering, 131*(11), 961-967.

Dirszowsky, R., & Desloges, J. (2004). Evolution of the Moose Lake delta, British Columbia: implications for Holocene environment change in the Canadian Rocky Mountains. *Geomorphology, 57*, 75-93.

Ellis, W., & Gray, D. (1966). Interrelationships between the peak instantaneous and average daily discharges of small prarie streams. *Canadian Agricultural Engineering, 2*, 1-3, 18.

England, J., Cohn, T., Faber, B., Stedinger, J., Thomas, W., Veilleux, A., . . . Mason, R. (2015). *Guidelines for determining flood flow frequency Bulletin 17C.* Reston, VA: U.S. Geological Survey.

Fill, H., & Steiner, A. (2003). Estimating instantaneous peak flow from mean daily flow data. *Journal of Hydrologic Engineering, 8*(6), 365-369.

Flynn, K., Kirby, W., & Hummel, P. (2006). *User's Manual for Program PeakFQ, Annual Flood-Frequency Analysis Using Bulletin 17B Guidelines.* U.S. Geological Survey.

Gao, J. (2009). Bathymetric mapping by means of remote sensing: methods, accuracy and limitations. *Progress in Physical Geography, 33*(1), 103-116.

Goodman, K., Baker, M., & Wurtsbaugh, W. (2011). Lakes as buffers of stream dissolved organic matter (DOM) variability: Temporal patterns of DOM characteristics in mountain stream-lake systems. *Journal of Geophysical Research, 116*. doi:10.1029/2011JG001709

Harrelson, C., Rawlins, C., & Potyondy, J. (1994). *Stream channel reference sites: an illustrated guide to field technique.* Fort Collins, CO: USDA Forest Service, Rocky Mountain Forest and Range Experiment Station.

Hortness, J. (2006). *Estimating Low-Flow Frequency Statistics for Unregulated Streams in Idaho.* Reston, VA: U.S. Department of the Interior, U.S. Geological Survey.

Julien, P. (2010). *Erosion and Sedimentation* (2nd ed.). Cambridge, UK: Cambridge University Press.

Kiefer, R., & Lockhard, J. (1994). *Intensive evaluation and monitoring of Chinook salmon and steelhead trout production, Crooked River and Upper Salmon River sites.* Portland, OR: U.S. Department of Energy - Bonnevile Power Administration.

Lamb, M., Dietrich, W., & Veditti, J. (2008). Is the critical Shields stress for incipient sediment motion dependent on channel-bed slope? *Journal of Geophysical Research: Earth Surface, 113*(F2).

Lane, E. (1955). The importance of fluvial morphology in hydraulic engineering. *American Society of Civil Engineers*, *81*, pp. 1-17.

Maret, T., Hortness, J., & Ott, D. (2006). *Instream flow characterization of Upper Salmon River Basin Streams, Central Idaho, 2005.* Reston, Virginia: U.S. Geological Survey.

Montgomery, D., & Buffington, J. (1997). Channel-reach morphology in mountain drainage basins. *Geological Society of America Bulletin, 109*(5), 596-611.

Mueller, E., Pitlick, J., & Nelson, J. (2005). Variation in the reference Shields stress for bed load transport in gravel-bed streams and rivers. *Water Resources Research, 41*(4).

Muirhead, K., & Cracknell, A. (1986). Airborne lidar bathymetry. *International Journal of Remote Sensing*, *7*, 597-614.

Vogel, R., & Stedinger, J. (1958). Minimum variance streamflow record augmentation procedures. *Water Resources Research*, *21*(5), 715-723.

Wolman, M. (1954). A method of sampling coarse river-bed material. *EOS, Transactions American Geophysical Union, 35*(6), 951-956.

Appendix A – Annual Hydrographs and Snowtel Data

Appendix A – Annual Hydrographs includes hydrographs of the Upper Salmon River and Valley Creek from water years 1993 through 2015. Only water years with complete data from both the upstream (USGS gages 13305000) and downstream (13305310) gages were included.

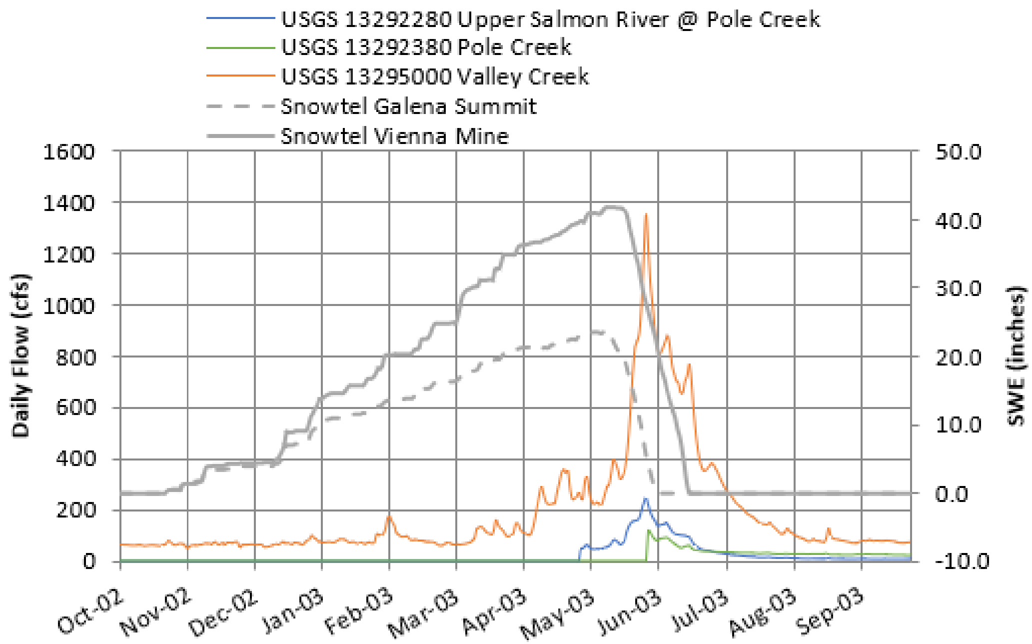

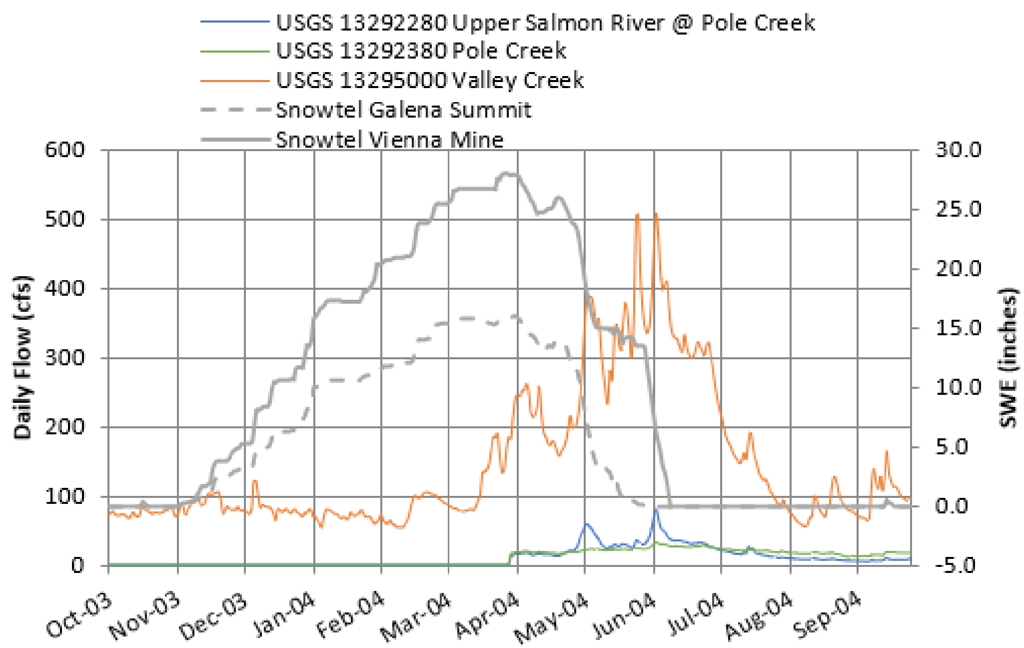

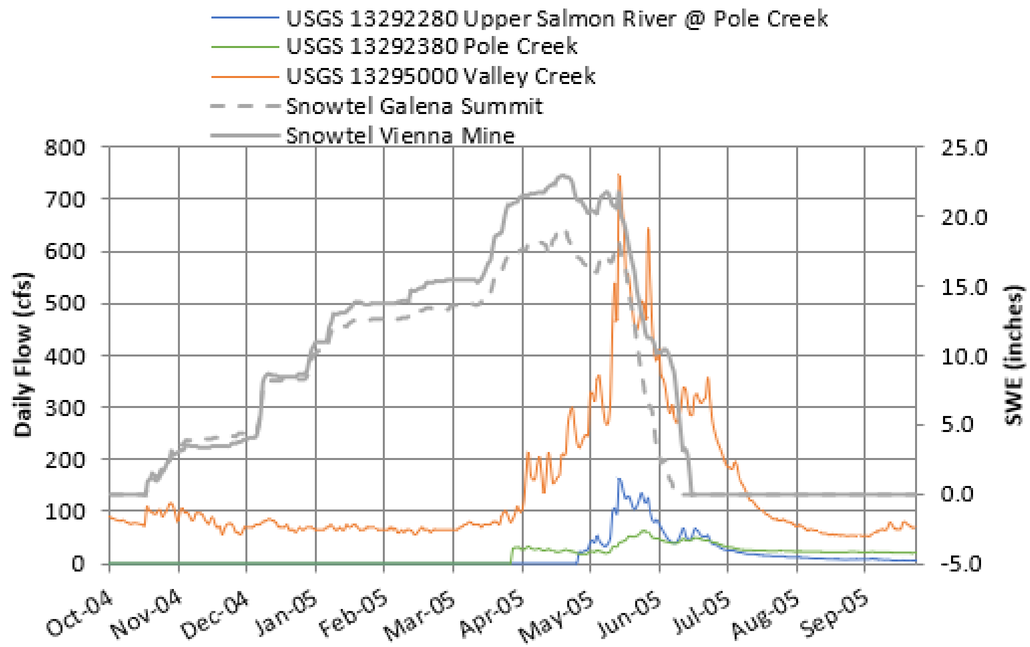
USGS 13292280 Upper Salmon River @ Pole Creek
USGS 13292380 Pole Creek
USGS 13295000 Valley Creek
Snowtel Galena Summit
Snowtel Vienna Mine
Daily Flow (cfs)
SWE (inches)
800
700
600
500
400
300
200
100
0
25.0
20.0
15.0
10.0
5.0
0.0
-5.0
Oct-04
Nov-04
Dec-04
Jan-05
Feb-05
Mar-05
Apr-05
May-05
Jun-05
Jul-05
Aug-05
Sep-05

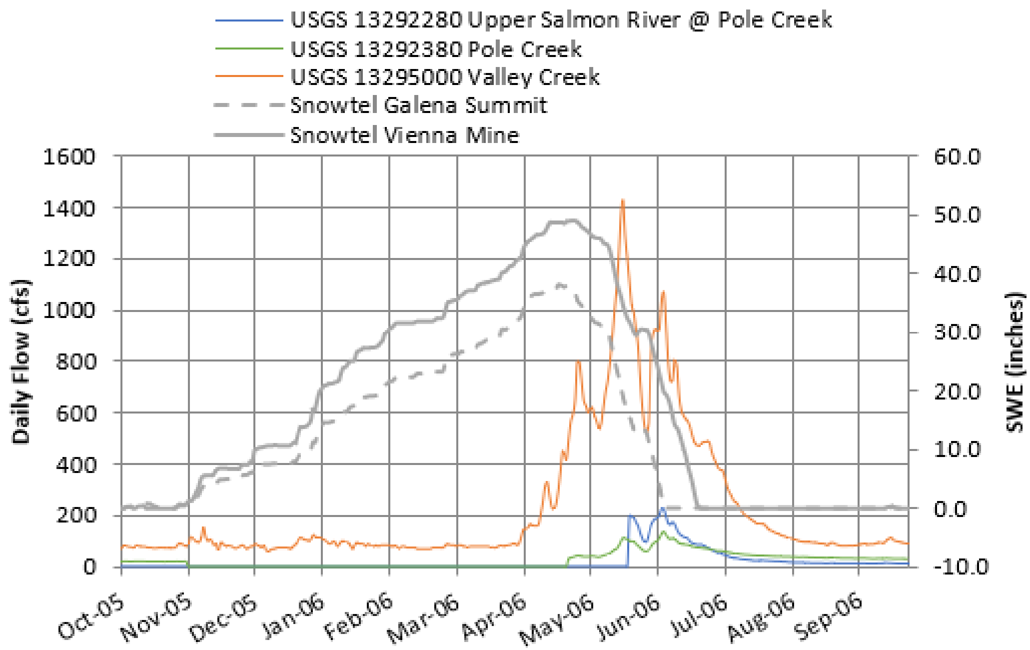
USGS 13292280 Upper Salmon River @ Pole Creek
USGS 13292380 Pole Creek
USGS 13295000 Valley Creek
Snowtel Galena Summit
Snowtel Vienna Mine
Daily Flow (cfs)
SWE (inches)
1600
1400
1200
1000
800
600
400
200
0
60.0
50.0
40.0
30.0
20.0
10.0
0.0
-10.0
Oct-05
Nov-05
Dec-05
Jan-06
Feb-06
Mar-06
Apr-06
May-06
Jun-06
Jul-06
Aug-06
Sep-06

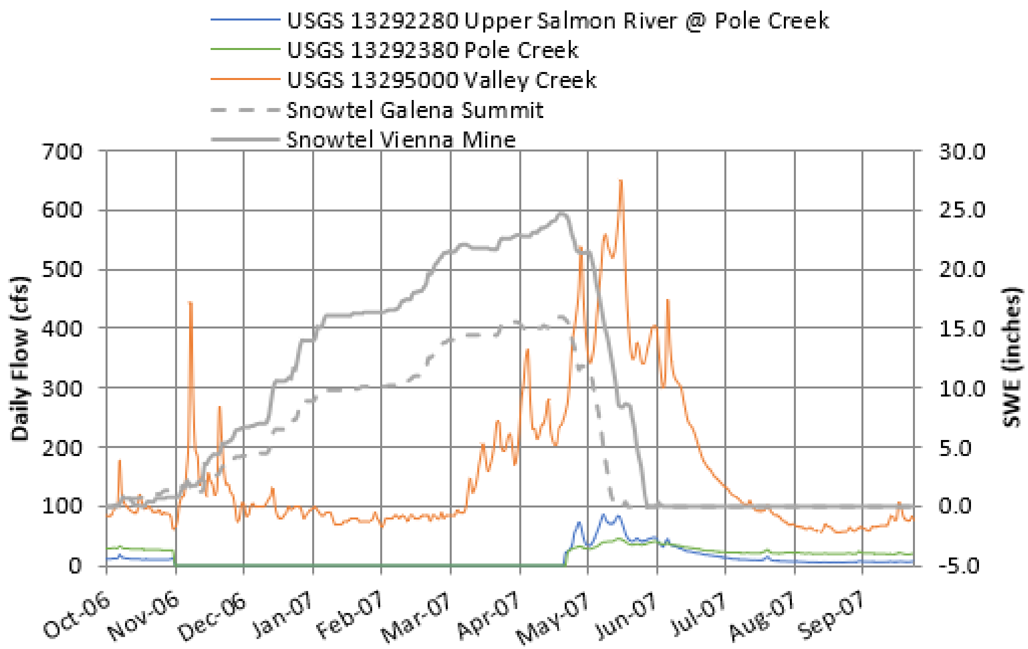
USGS 13292280 Upper Salmon River @ Pole Creek
USGS 13292380 Pole Creek
USGS 13295000 Valley Creek
Snowtel Galena Summit
Snowtel Vienna Mine
Daily Flow (cfs)
SWE (inches)
0
100
200
300
400
500
600
700
-5.0
0.0
5.0
10.0
15.0
20.0
25.0
30.0
Oct-06
Nov-06
Dec-06
Jan-07
Feb-07
Mar-07
Apr-07
May-07
Jun-07
Jul-07
Aug-07
Sep-07

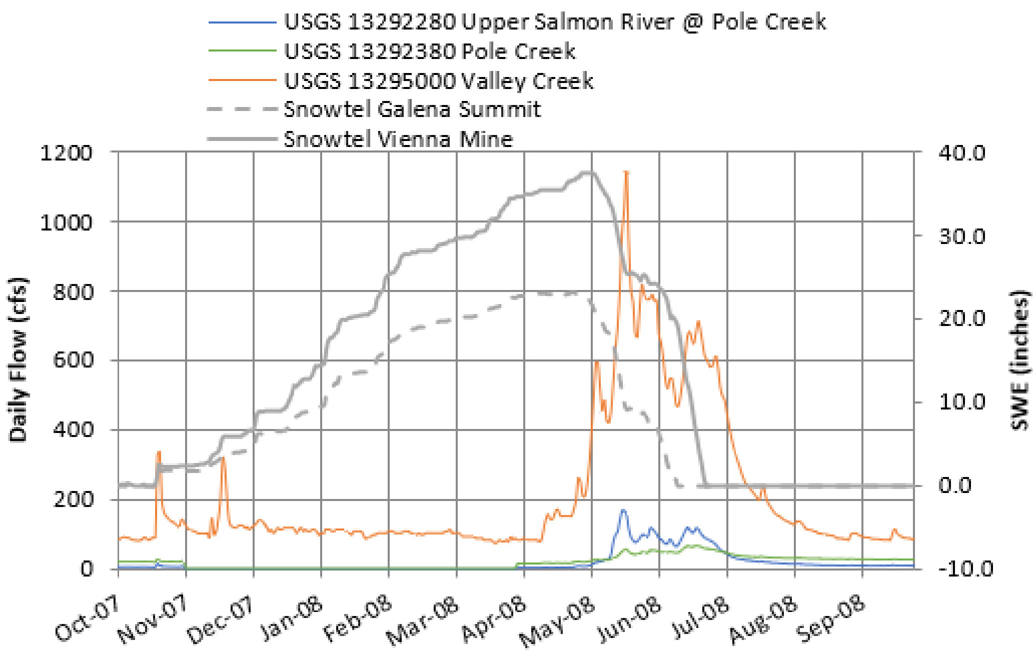
USGS 13292280 Upper Salmon River @ Pole Creek
USGS 13292380 Pole Creek
USGS 13295000 Valley Creek
Snowtel Galena Summit
Snowtel Vienna Mine
Daily Flow (cfs)
SWE (inches)
0
200
400
600
800
1000
1200
-10.0
0.0
10.0
20.0
30.0
40.0
Oct-07
Nov-07
Dec-07
Jan-08
Feb-08
Mar-08
Apr-08
May-08
Jun-08
Jul-08
Aug-08
Sep-08

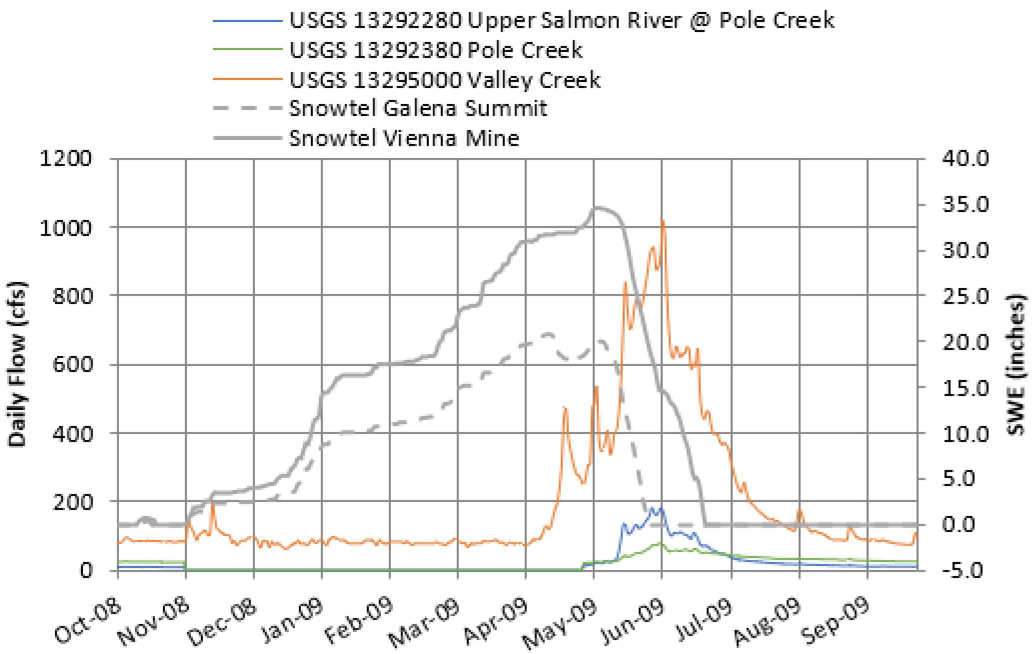

USGS 13292280 Upper Salmon River @ Pole Creek
USGS 13292380 Pole Creek
USGS 13295000 Valley Creek
Snowtel Galena Summit
Snowtel Vienna Mine
Daily Flow (cfs)
SWE (inches)
1200
1000
800
600
400
200
0
40.0
35.0
30.0
25.0
20.0
15.0
10.0
5.0
0.0
-5.0
Oct-08
Nov-08
Dec-08
Jan-09
Feb-09
Mar-09
Apr-09
May-09
Jun-09
Jul-09
Aug-09
Sep-09

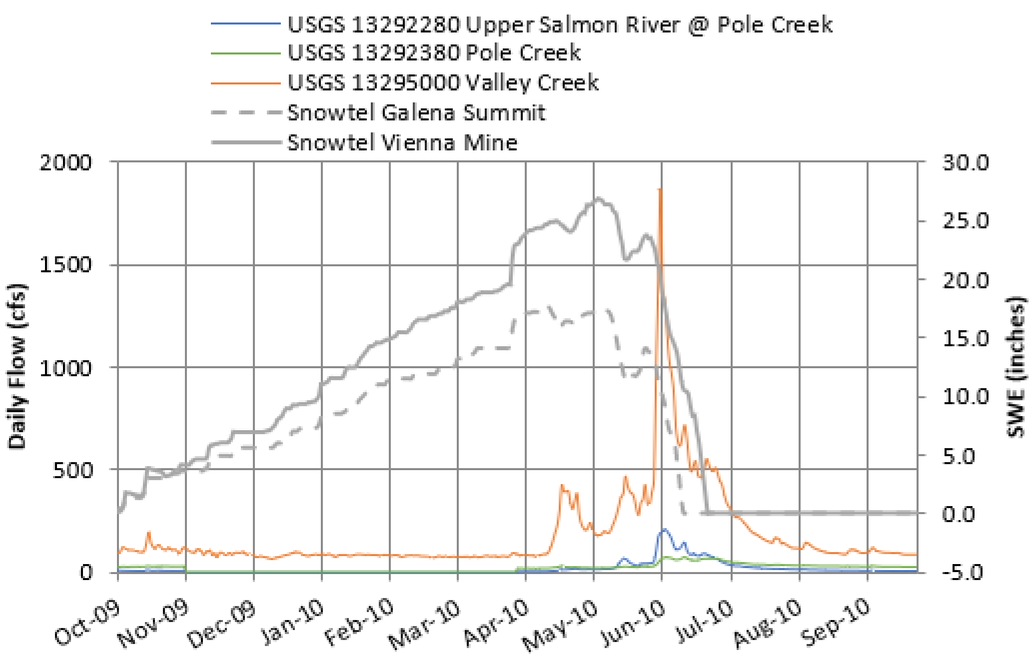

USGS 13292280 Upper Salmon River @ Pole Creek
USGS 13292380 Pole Creek
USGS 13295000 Valley Creek
Snowtel Galena Summit
Snowtel Vienna Mine
Daily Flow (cfs)
SWE (inches)
2000
1500
1000
500
0
30.0
25.0
20.0
15.0
10.0
5.0
0.0
-5.0
Oct-09
Nov-09
Dec-09
Jan-10
Feb-10
Mar-10
Apr-10
May-10
Jun-10
Jul-10
Aug-10
Sep-10

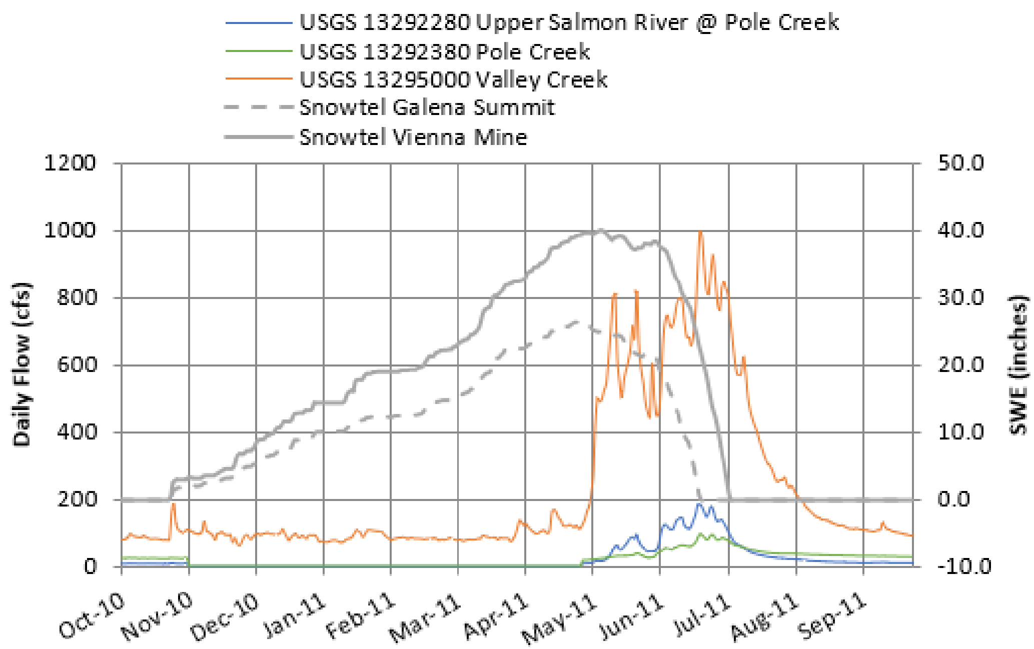
USGS 13292280 Upper Salmon River @ Pole Creek
USGS 13292380 Pole Creek
USGS 13295000 Valley Creek
Snowtel Galena Summit
Snowtel Vienna Mine
Daily Flow (cfs)
SWE (inches)
1200
1000
800
600
400
200
0
50.0
40.0
30.0
20.0
10.0
0.0
-10.0
Oct-10
Nov-10
Dec-10
Jan-11
Feb-11
Mar-11
Apr-11
May-11
Jun-11
Jul-11
Aug-11
Sep-11

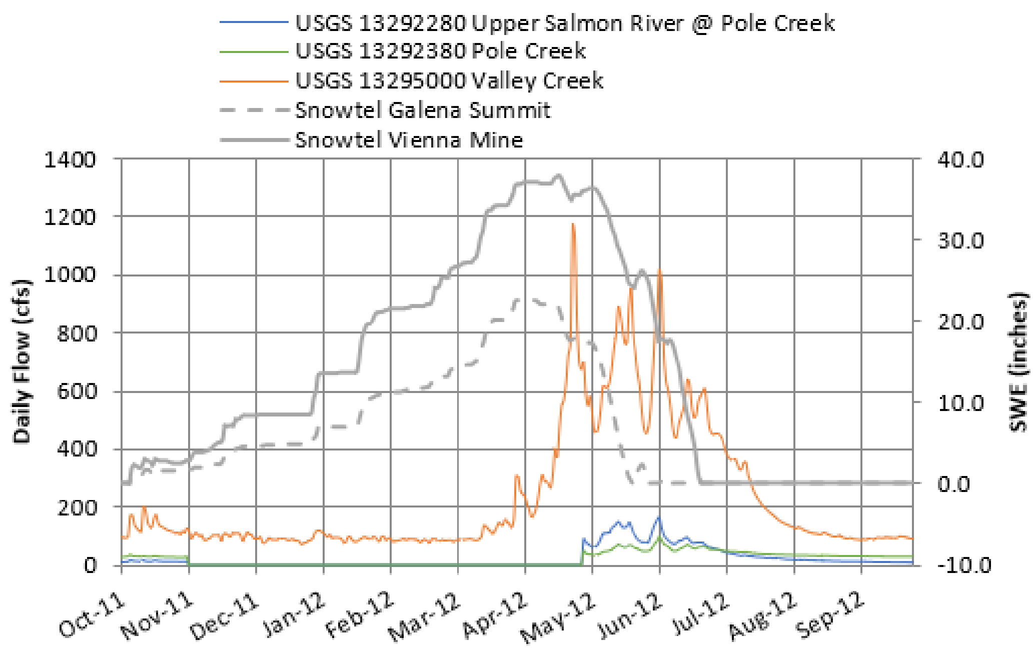
USGS 13292280 Upper Salmon River @ Pole Creek
USGS 13292380 Pole Creek
USGS 13295000 Valley Creek
Snowtel Galena Summit
Snowtel Vienna Mine
Daily Flow (cfs)
SWE (inches)
1400
1200
1000
800
600
400
200
0
40.0
30.0
20.0
10.0
0.0
-10.0
Oct-11
Nov-11
Dec-11
Jan-12
Feb-12
Mar-12
Apr-12
May-12
Jun-12
Jul-12
Aug-12
Sep-12

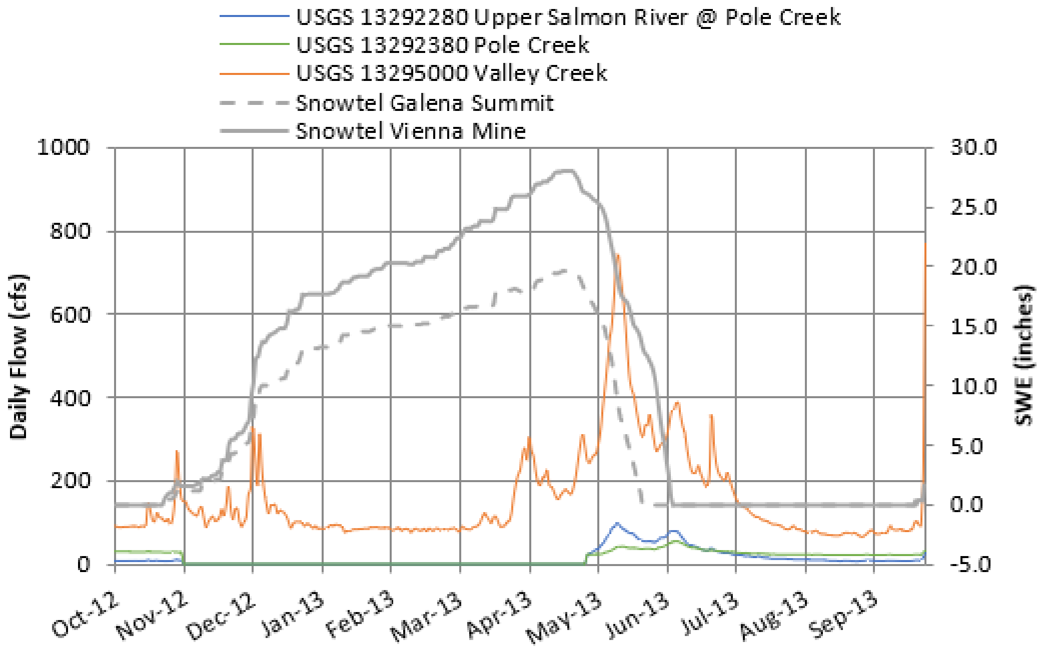
USGS 13292280 Upper Salmon River @ Pole Creek
USGS 13292380 Pole Creek
USGS 13295000 Valley Creek
Snowtel Galena Summit
Snowtel Vienna Mine
Daily Flow (cfs)
SWE (inches)
1000
800
600
400
200
0
30.0
25.0
20.0
15.0
10.0
5.0
0.0
-5.0
Oct-12
Nov-12
Dec-12
Jan-13
Feb-13
Mar-13
Apr-13
May-13
Jun-13
Jul-13
Aug-13
Sep-13

Appendix B – Annual Peak Streamflow

Annual peak streamflow data are provided in the tables below. All peak storms occurred during the snowmelt runoff season. Values *italicized* and shaded in blue without dates are the artificially generated annual peaks, developed utilizing the MOVE.4 methodology.

	USGS Gage on Salmon River at Pole Creek		USGS Gage on Pole Creek		USGS Gage on Valley Creek		USGS Gage on Salmon River below Valley Creek	
Water Year	Date	Annual Max. Q (cfs)	Date	Annual Max. Q (cfs)	Date	Annual Max. Q (cfs))	Date	Annual Max. Q (cfs)
1911		*215*		*108*	6/16/1911	1,450		*4,507*
1912		*161*		*79*	5/17/1912	1,090		*3,456*
1913		*153*		*75*	5/29/1913	1,040		*3,309*
1921		*276*		*142*	5/29/1921	1,850		*5,652*
1922		*180*		*89*	6/15/1922	1,220		*3,838*
1923		*130*		*62*	6/12/1923	886		*2,850*
1924		*70*		*32*	5/18/1924	485		*1,628*
1925		*138*		*66*	5/21/1925	939		*3,009*
1926		*74*		*33*	5/5/1926	507	5/5/1926	1,970
1927		*206*		*103*	6/26/1927	1,390	6/27/1927	5,020
1928		*192*		*96*	5/27/1928	1,300	5/27/1928	4,380
1929		*101*		*47*	6/16/1929	689	6/16/1929	2,340
1930		*92*		*43*	5/30/1930	631	6/11/1930	2,580
1931		*66*		*30*	5/16/1931	457	6/2/1931	1,480
1932		*123*		*58*	6/15/1932	838	6/16/1932	3,230
1933		*226*		*114*	6/9/1933	1,520	6/16/1933	4,400
1934		*82*		*38*	5/8/1934	565	5/8/1934	1,660
1935		*104*		*49*	6/9/1935	710	6/9/1935	2,550
1936		*173*		*85*	6/1/1936	1,170	6/2/1936	3,700
1937		*78*		*36*	5/3/1937	538	5/29/1937	1,720
1938		*161*		*79*	6/8/1938	1,090	6/8/1938	3,790
1939		*66*		*30*	5/1/1939	457	5/19/1939	1,580
1940		*104*		*49*	5/26/1940	710	5/26/1940	2,390
1941		*102*		*48*	5/27/1941	700	5/27/1941	2,320
1942		*149*		*72*			5/26/1942	2,720
1943		*192*		*96*	5/30/1943	1,300	5/30/1943	3,850
1944		*87*		*40*	6/3/1944	598	5/17/1944	1,720
1945		*97*		*45*	5/10/1945	664	6/23/1945	2,200
1946		*131*		*63*	6/6/1946	891	6/6/1946	2,830
1947		*170*		*83*	5/9/1947	1,150	5/9/1947	3,270
1948		*191*		*95*	6/3/1948	1,290	6/9/1948	4,090
1949		*139*		*67*	5/16/1949	947	5/16/1949	2,840
1950		*158*		*77*	6/7/1950	1,070	6/22/1950	3,400
1951		*198*		*99*	5/28/1951	1,340	5/28/1951	4,090
1952		*170*		*83*	6/7/1952	1,150	6/7/1952	3,750

	USGS Gage on Salmon River at Pole Creek		USGS Gage on Pole Creek		USGS Gage on Valley Creek		USGS Gage on Salmon River below Valley Creek	
Water Year	Date	Annual Max. Q (cfs)	Date	Annual Max. Q (cfs)	Date	Annual Max. Q (cfs))	Date	Annual Max. Q (cfs)
1953		*149*		*72*	6/19/1953	1,010	6/19/1953	3,200
1954		*183*		*91*	6/27/1954	1,240	6/27/1954	4,280
1955		*137*		*66*	6/13/1955	930	6/13/1955	3,070
1956		*299*		*155*	5/24/1956	2,000	5/27/1956	5,070
1957		*217*		*109*	6/6/1957	1,460	6/6/1957	4,480
1958		*192*		*96*	5/28/1958	1,300	5/28/1958	4,360
1959		*134*		*64*	6/7/1959	910	6/22/1959	2,800
1960		*113*		*53*	6/5/1960	773	6/5/1960	2,410
1961		*117*		*55*	5/30/1961	798		*2,586*
1962		*101*		*47*	6/14/1962	689		*2,256*
1963		*150*		*73*	6/21/1963	1,020		*3,249*
1964		*129*		*62*	6/8/1964	878		*2,827*
1965		*209*		*105*	6/13/1965	1,410		*4,391*
1966		*93*		*43*	5/30/1966	636		*2,094*
1967		*182*		*90*	6/22/1967	1,230		*3,867*
1968		*115*		*54*	6/6/1968	784		*2,544*
1969		*174*		*86*	5/14/1969	1,180		*3,721*
1970		*218*		*110*	6/29/1970	1,470		*4,564*
1971		*245*		*125*	6/26/1971	1,650		*5,082*
1972		*217*		*109*	6/8/1972	1,460		*4,535*
1974		*226*		*114*	6/17/1974	1,520	6/17/1974	5,650
1993		*152*		*74*	5/21/1993	1,030		*3,279*
1994		*74*		*34*	4/18/1994	513		*1,715*
1995		*158*		*77*	6/6/1995	1,070		*3,397*
1996		*259*		*133*	5/18/1996	1,740		*5,339*
1997		*262*		*135*	6/10/1997	1,760		*5,396*
1998		*134*		*64*	6/26/1998	914		*2,934*
1999		*186*		*92*	5/29/1999	1,260		*3,955*
2000		*110*		*52*	6/13/2000	750		*2,441*
2001		*89*		*41*	5/16/2001	608		*2,008*
2002		*143*		*69*	4/14/2002	973		*3,110*
2003	5/31/2003	250	6/1/2003	120	5/31/2003	1,400		*4,362*
2004	6/6/2004	82	6/6/2004	34	5/28/2004	574		*1,904*
2005	5/19/2005	163	6/1/2005	70	5/19/2005	823		*2,662*
2006	6/8/2006	228	6/9/2006	144	5/21/2006	1,490		*4,622*
2007	5/13/2007	87	5/19/2007	47	5/21/2007	662		*2,174*
2008	5/19/2008	196	6/23/2008	68	5/21/2008	1,210		*3,809*
2009	6/1/2009	182	6/6/2009	84	6/6/2009	1,150		*3,633*
2010	6/7/2010	213	6/16/2010	72	6/5/2010	2,210		*6,668*
2011	6/24/2011	185	6/24/2011	103	6/24/2011	1,080		*3,427*
2012	6/5/2012	162	6/5/2012	100	4/26/2012	1,500		*4,651*
2013	5/14/2013	98	6/10/2013	53	9/30/2013	906		*2,910*
2014		*149*		*72*	5/27/2014	1,010		*3,220*
2015		*73*		*33*	6/2/2015	505		*1,690*